INTRODUCTION TO VOLUME 9: ENABLING TECHNOLOGIES FOR ORGANIC SYNTHESIS

Progress in organic synthesis has always relied on new enabling technologies that expand the frontiers of what is possible. Just as the commercial availability of mass-produced Pyrex glassware and ceramic laboratory equipment a century ago provided a stimulus to the nascent field of organic synthesis, an assortment of new technologies are today transforming and expanding synthetic organic chemistry in exciting new ways. In this volume, we have asked experts from a number of these important new fields to explain the relevance of recent progress in their area to the larger field of organic synthesis and to provide a glimpse of what chemists can look forward to in the next few years. The resulting volume is exciting and inspiring, providing both an entry point for newcomers and a useful resource for current practitioners.

In addition to some outstanding contributions from world-renowned researchers in academia, we have a healthy mix of contributions from researchers from industry, many of whom are engaged full time in practicing the techniques and procedures they here report on. We are deeply grateful for each of our contributing authors' hard work, excellent science, and willingness to share their knowledge.

The volume begins with a chapter from Jeff Aube, Steven Rogers, and Conrad Santini from the University of Kansas on the general topic of 'Enabling Technologies in High Throughput Chemistry (9.01).' Jeff's group has been at the forefront of bringing the parallel and high-throughput synthesis techniques originally pioneered in the pharmaceutical industry into the academic environment, and the group does an exceptional job of explaining key concepts to the uninitiated while conveying a very exciting sense of where this important and exciting field is headed – a good choice for required reading for first year graduate students in organic chemistry.

Wes Schafer and colleagues, Xiaodong Bu, Xiaoyi Gong, Leo Joyce, and Chris Welch from Merck's Process and Analytical Chemistry group in Rahway, NJ next contribute an important chapter on 'High-Throughput Analysis for High-Throughput Experimentation in Organic Chemistry (9.02).' A mastery of analytical techniques has always been an important enabler of organic synthesis, but as chemists delve into new parallel and high-throughput synthesis techniques, they often find that experimental progress is critically dependent on the speedy acquisition and analysis of analytical data. Wes and his coworkers, expert practitioners in this important new field, describe the pros and cons of different strategies that have been developed for dealing with this bottleneck and at the same time provide a vision of where the field is heading.

No work on enabling technologies for organic synthesis could possibly be complete without a chapter on how flow chemistry is revolutionizing the field; there could be no better author to describe these exciting recent developments than MIT's Klavs Jensen. Jensen and coworkers, Stephen Born and Everett O'Neal, brilliantly describe recent progress and emerging trends in flow chemistry in 'Organic Synthesis in Small Scale Continuous Flow: Flow Chemistry (9.03).'

Continuing with the flow theme, Oliver Trapp from the University of Heidelberg reviews some exciting progress involving the use and study of immobilized catalysts in microcapillary systems: 'Microcapillary Catalysis (9.04).' Drawing on a considerable expertise in the analytical chemistry of dynamic systems, Oliver opens a window revealing astonishing detail of what is going on in these reactions. He also champions the concept of 'catalyst by the meter,' in which capillaries coated with different catalysts and reagents can be easily dispensed by cutting a piece of the required length from a larger spool – a great idea that certainly can be of use in creating more complex-flow-based systems.

Nicole L. Snyder and coworkers, George T. Mukosera and Elise Held from Davidson College, along with Peter Seeberger, from the Max Planck Institute for Colloids and Interfaces and the University of Berlin next describe recent advances in 'Technology-Enabled Synthesis of Carbohydrates (9.05).' Although automated solid phase synthesis of peptides and oligonucleotides has been in place for decades, it is only within the past few years that similar techniques for solid phase oligosaccharide synthesis have developed a similar position. Snyder and Seeberger clearly illustrate recent developments in this field, highlighting the solid phase synthesis of some incredibly complex oligosaccharides and giving a sense of the exciting directions that this field will take in the next few years.

Although not all enabling technologies for organic chemistry involve plumbing, flowing systems are indeed very important, especially for purification technologies. In the first of three chapters dedicated to various aspects of preparative chromatography, Chris Welch, from Merck's Process & Analytical Chemistry group, describes 'The Use of Preparative Chiral Chromatography for Accessing Enantiopurity in Pharmaceutical Discovery and Development (9.06).' Chris has been involved in chromatographic separation of enantiomers for more than 30 years and shares his experience on the recent growth of the use of preparative chiral chromatography to support drug discovery and early development and his perspective on the potential for a more widespread adoption of synthetic strategies involving preparative chromatography.

Ray McClain and Eric Streckfuss from Merck's Automated Synthesis and Purification group have contributed an outstanding chapter on 'High-Throughput Purification in Support of Pharmaceutical Discovery (9.07).' Both Ray and Eric run laboratories for high-throughput mass-directed purification to support medicinal chemistry – Ray at the Merck site in West Point, PA and Eric at the Rahway, NJ site. Automated high-throughput mass-directed purification now enables rapid workup of small scale organic reactions, with MS detection allowing convenient isolation of the desired product with very fast turnaround time. In the past

decade, medicinal chemists have embraced the approach, and hundreds of new compounds are purified by this approach every day. In recent years, the technique has begun to be adopted outside the pharmaceutical industry, and there is little doubt about the transformational potential of this technology when it becomes widespread in academia.

Rounding out the chromatographic contributions, Olivier Dapremont's 'Use of Industrial Scale Multiton Continuous Chromatography in Pharmaceutical Manufacturing (9.08)' does an excellent job of introducing the reader to the use of industrial scale chromatographic resolution in the large-scale manufacturing of pharmaceuticals and how this powerful technology can be integrated with organic synthesis. Olivier, who is in charge of preparative separations of pharmaceuticals at AMPAC Fine Chemicals, has considerable expertise in working with industry to develop and implement chromatographic solutions at scale. For the synthetic chemist who thinks that the use of chromatography in organic synthesis is too impractical, take a close look at Olivier's examples currently being performed on the multiton scale.

When beginning a career in the chemical industry, many synthetic chemists are surprised to learn of the huge importance of crystallization, which remains the preferred purification technique for industrial scale synthesis and also plays an important role in modulating the form and properties of organic compounds. The recent emergence of high-throughput techniques to rapidly explore crystallization at small scale is an interesting story that is not well known outside of the pharmaceutical industry. In their chapter, 'High-Throughput Screening to Enable Salt and Polymorph Screening, Chemical Purification, and Chiral Resolution (9.09),' Nara Variankaval and coworkers, Mike McNevin, Scott Shultz, and Scott Trzaska from Merck's Molecular and Materials Characterization group in Summit, NJ, do an excellent job of introducing the reader to key concepts and current workflows in this exciting and rapidly evolving area.

Even though the use of microwave heating in organic synthesis has been widely used for more than a decade, there is still considerable misunderstanding about how and when to use this approach. In 'Organic Synthesis Using Microwave Heating (9.10),' the University of Connecticut's Nicholas Leadbeater, one of the leading practitioners in this field, does a great job of surveying the current state and future prospects for this important and growing field.

Green chemistry advocates have long championed the reduction of solvent use in organic synthesis, and some researchers have pushed this concept to the limit, eliminating reaction solvent altogether. In their review of this important emerging area, 'Useful Chemical Activation Alternatives in Solvent-Free Organic Reactions (9.11),' Eusebio Juaristi and coworkers, José G. Hernández and C. Gabriela Avila-Ortiz, from the Center for Research and Advanced Studies of the National Polytechnic Institute (CINVESTAV) in Mexico City introduce key concepts and recent examples from this growing new area.

The use of fluorous tag and fluorous phase technology has grown considerably in recent years, providing useful tools for a number of different problems in synthetic chemistry. In the chapter, 'Fluorous Linker-Enabled Organic Synthesis (9.12),' Wei Zhang from the University of Massachusetts, Boston explains the origins, principles, and future direction of this powerful approach.

In his chapter, 'Organic Photochemistry (9.13),' Christian Bochet, from University of Fribourg, does a great job of introducing key concepts and recent trends in this resurgent area. Many working organic chemists today studied photochemistry at some point during their training and still have vague recollections of 2+2 photocycloadditions, Norish Type-II reactions, and Rayonet reactors. The recent resurgence of interest in photochemistry, be it LED photocatalysis or study of solar cell technologies, makes it clear that it is high time for chemists to either brush up their previous knowledge or learn for the first time about some of the exciting recent developments in this field.

Preparative Electrochemistry for Organic Synthesis (9.14) is another area of synthetic chemistry that was previously viewed as old fashioned, but that is now enjoying a resurgence of popularity. From a green chemistry perspective, the idea of using an electron as a reagent is hard to beat, and Gerardine Botte and colleagues, Damilola Daramola and Madhivanan Muthuvel from the Center for Electrochemical Engineering Research at Ohio University, do an excellent job of surveying industrial uses of electrochemical synthesis and suggesting where the field may be heading.

Synthetic biology has recently caught the attention of the lay press, and although it is clear that progress in synthetic biology will dramatically impact the future of synthetic chemistry, it is somewhat difficult for practising chemists to untangle the hyperbole from the facts. CalTech's Frances Arnold, one of the pioneers in the field, along with coworkers Pedro Coelho (CalTech) and Jared Lewis (University of Chicago), skillfully presents in 'Synthetic Biology Approaches for Organic Synthesis (9.15)' a wonderful and inspiring introduction to key concepts and strategies for what will undoubtedly be a transformative enabling technology for organic synthesis – another good choice for required reading for first year graduate students in organic chemistry.

Continuing with the biological theme, Gjalt Huisman from Codexis describes in 'Enzyme Evolution as a Tool for Creating Improved Catalysts for Large-Scale Organic Synthesis (9.16)' some of the amazing recent developments in the evolution of highly optimized enzymes for use in industrial processes and how this technology is causing major shifts in synthetic strategies of industrial chemists.

As the worlds of biotechnology and synthetic chemistry continue to merge, synthetic strategies that span the interface will become more important. In the chapter on 'Chemistry of Antibody–Small Molecule Drug Conjugates (9.17),' Merck's Rob Garbaccio brings the synthetic and medicinal chemistry perspective to this exciting topic, convincing one that it is just synthetic chemistry where one of the reactants happens to have a molecule weight of 150 000 Da!

Finally, Yu Yuan, from U. Central Florida, and Weimin Wang, from Merck's RNAi group in West Point, PA, report on 'Post-Synthetic Chemical Functionalization of Oligonucleotides (9.18),' providing a valuable update on this exciting

new area and giving a glimpse of the complexity that awaits one as the areas of synthetic chemistry and biotechnology continue to merge.

We are very pleased and excited with these excellent contributions to the new 'Enabling Technologies' volume to the updated Comprehensive Organic Synthesis series, and we sincerely hope that both beginning and currently practicing organic chemists will find this a valuable resource that will help to open new realms of research possibilities.

CJ Welch
Merck Research Laboratories, Rahway, NJ, USA

9.01 Enabling Technologies in High Throughput Chemistry

J Aubé, SA Rogers, and C Santini, University of Kansas, Lawrence, KS, USA

© 2014 Elsevier Ltd. All rights reserved.

9.01.1	**Introduction – Emergence of Parallel Synthesis with Brief Technical Timeline**	1
9.01.2	**Comparison of the Combinatorial and Parallel Approach**	2
9.01.3	**Solid and Liquid-Phase Parallel Synthesis**	4
9.01.3.1	Solid-Phase Synthesis	4
9.01.3.1.1	Introduction to solid-phase synthesis	4
9.01.3.1.2	Bead types and linkers	4
9.01.3.1.3	Nonbead solid supports	5
9.01.3.2	Liquid-Phase Parallel Synthesis: PEG and Linear Polystyrene (LPS) Support	7
9.01.3.3	Preparation and Deconvolution of Encoded Combinatorial Libraries	8
9.01.3.3.1	Preparing a chemically encoded combinatorial library	9
9.01.3.3.2	Encoding by Rf tagging	12
9.01.3.3.3	Encoding by position within an array	13
9.01.3.3.4	Locating active compounds contained within combinatorial libraries	13
9.01.4	**Solution-Phase Technologies in Parallel Synthesis**	14
9.01.4.1	Solid-Supported Reagents, Catalysts, and Scavengers	14
9.01.4.1.1	Reagents and catalysts	14
9.01.4.1.2	Extractions and scavengers	16
9.01.4.2	Solution-Phase Synthesis Enabling Equipment and Strategies	18
9.01.4.2.1	Automated molecular assembly plant	18
9.01.4.2.2	First automated parallel synthesizer	19
9.01.4.2.3	Fully automated platforms	19
9.01.4.2.4	Semiautomated platforms	19
9.01.4.2.5	Microwave technologies	21
9.01.4.3	Fluorous-Phase Parallel Synthesis	21
9.01.5	**High Throughput Purification and Automated Sample Handling Methods and Protocol**	24
9.01.6	**Parallel Synthesis in Flow**	24
9.01.7	**Summary**	26
References		27

Glossary

Combinatorial synthesis Synthesis in which multiple reactions are run in a tandem fashion in grouped reaction vessels.

High throughput synthesis Chemical synthesis that is performed in parallel with the aim of developing tens to tens of thousands of compounds, typically for the purposes of screening the compounds for desired characteristics.

Liquid-phase synthesis Synthesis that is performed on solvent miscible polymer supports.

Parallel synthesis Synthesis in which multiple reactions are run in a tandem fashion in separate reaction vessels.

Polymer supports Polymer constructs that support solid-phase synthesis, solid-supported scavengers, and/or catalysts.

Solid-phase synthesis Synthesis that is performed on solid supports. Typically, one end of the molecule is attached to the solid construct whereas the molecules are built stepwise from another end.

Solution-phase synthesis Synthesis that is not performed on a polymer or solid support of any kind.

9.01.1 Introduction – Emergence of Parallel Synthesis with Brief Technical Timeline

Modern organic chemistry emerged from 'pharmacie' during the early nineteenth century. At first the focus was on isolation and characterization of biologically derived substances. Early workers learned how to manipulate these materials in a way that afforded insight into their purity and composition. Their accumulated knowledge led to the idea that these substances had unique molecular structures that could be artificially altered in ways that could be understood and therefore planned.[1] Thus, by the third quarter of the nineteenth century the science of organic synthesis appeared. Those workers discovered the implements and techniques that enabled them to transform natural substances into artificial ones. Further progress enabled them to derive one artificial substance from another, the capability that defines contemporary organic synthesis.

For decades afterward synthesis was practiced using the methods from those times suitably updated to reflect advances in ancillary technologies such as separation, spectroscopy, and other techniques. Inevitably the limitations of those early methods became obstacles. In particular, syntheses using linear or even convergent sequences performed on individual substrates became

more burdensome as progress in related fields placed greater demands on the chemist to produce larger numbers of new compounds. By the mid-twentieth century traditional synthesis was lagging behind the escalating needs of the larger research enterprise. This led to the birth of high throughput chemistry, with technological advances that have expedited scientific progress in fields ranging from materials sciences related to coatings and electronics to organic chemical sciences such as reaction discovery, catalyst screening, and pharmaceutical development. A brief timeline highlights significant events in the story of high throughput synthesis during the latter half of the twentieth century (Figure 1).[2]

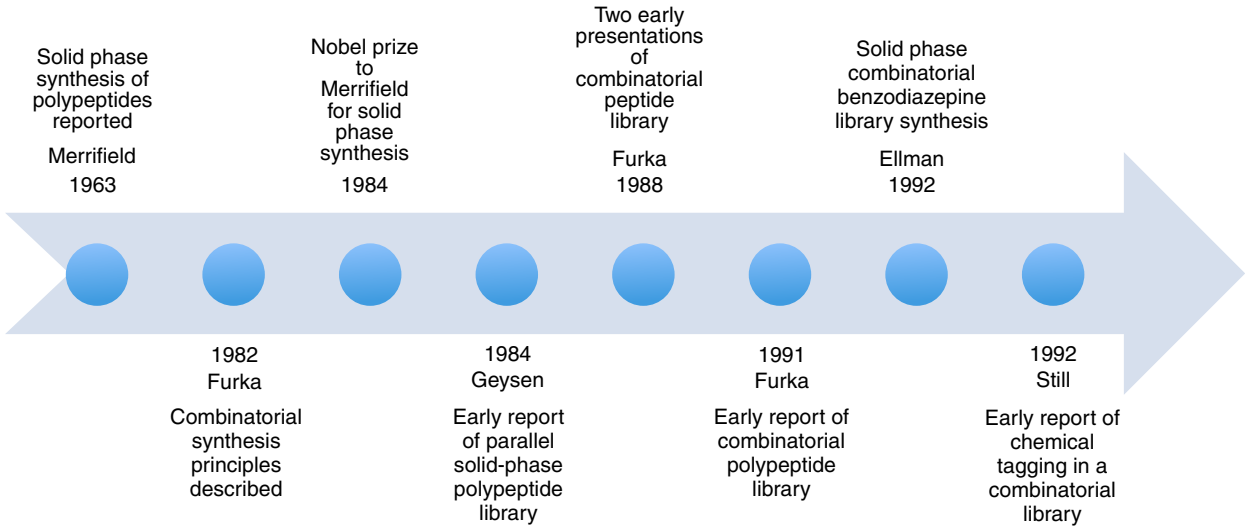


Figure 1 Highlights in the early development of high throughput synthesis.[2]

The purpose of this chapter is to survey the basic concepts and practical aspects of high throughput chemistry. This area can be roughly divided into two branches: combinatorial and parallel. Both types of synthetic methods are designed to surmount the limitations of traditional methods and increase the productivity of organic synthesis in the service of discovery.

9.01.2 Comparison of the Combinatorial and Parallel Approach

Both combinatorial and parallel syntheses provide multiple synthetic analogs that can be employed in research endeavors. However, the two techniques differ dramatically relative to when they are generally used, how they are executed, and the state in which final products exist. Table 1 summarizes the major characteristics of these two types of high throughput syntheses.

Table 1 Comparison of parallel and combinatorial syntheses

Feature	*Parallel*	*Combinatorial*
Types of products	Individual compounds	Mixtures of compounds
Numbers of compounds	Limited by number of available reactor vessels (hundreds)	Less limited (up to millions)
Method	Can use many synthetic methodologies	Generally use solid-phase or tethered synthesis
Synthetic flow	Linear	Split/mix
Product identity	Generally known	Mixtures must be deconvoluted
Compound tracking	Usually by physical position within parallel platform or vessel	Encoding/tagging; chemical, radio, color or bar coding, computer tracked physical position
When to use	Property screening or optimization	Property screening

Abbreviations: AIBN, azobisisobutyronitrile; DCE, dichloroethane; DDQ, 2,3-dichloro-5,6-dicyano-1,4-benzoquinone; DIEA, diisopropylethylamine; EDT, 1,2-ethanedithiol; SASRIN, super acid sensitive resin; TBAC, tertiary-butyl acetate; TFA, trifluoroacetic acid; THF, tetrahydrofuran.

Parallel synthesis uses linear sequences on individual substrates to provide single end products. Instead of converting one starting material into a final product a set of related starting materials are processed simultaneously. The syntheses are separated in space with a unique physical process path for each compound and the final compounds purified individually. This is illustrated schematically using a $3 \times 3 \times 2$ library (Figure 2).

In this scenario every pathway is clearly identified and tracked. Using specialized parallel synthesis hardware, each product's history is known solely by its position within the platform. Reaction sequences are carefully designed to minimize byproduct formation while allowing adequate generation of diversity.

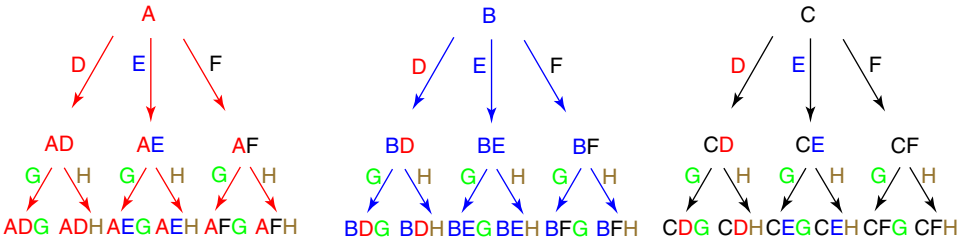


Figure 2 Parallel synthesis of a $3 \times 3 \times 2$ library.

In a parallel synthesis, compound numbers are limited by the capacity of the synthesis hardware. Figure 2 shows that the number of reaction vessels rapidly increases as diversity elements are introduced. Most parallel synthesis platforms contain fewer than 200 reaction sites (with units of 6–96 being most common) that can accommodate only a tiny fraction of what is synthetically possible. Accordingly, much effort has been expended to consider specific chemical design principles that maximize usable chemical diversity in a given library generated by parallel synthesis. The pioneering work of Merrifield[3] in the area of solid-phase synthesis addressed this problem. By covalently attaching a substrate to a solid-phase support, purification of product from byproducts and excess reagents is accomplished by simply washing them away from the resin. This allows for free use of reagents in excess often resulting in increased yields for individual steps. Merrifield's work is discussed in greater detail in Section 9.01.3.1.1.

Solid-phase synthesis was a prominent feature of early approaches to combinatorial chemistry.[4,5] Furka used solid-supported synthesis to expand the number of compounds that can be prepared in a given number of vessels.[6,7] Figure 3 illustrates how this works. At the outset, equimolar quantities of each initial component are tethered to the support. Once the first component is tethered the surrounding solution is removed and the support, in this case beads, is washed and dried.

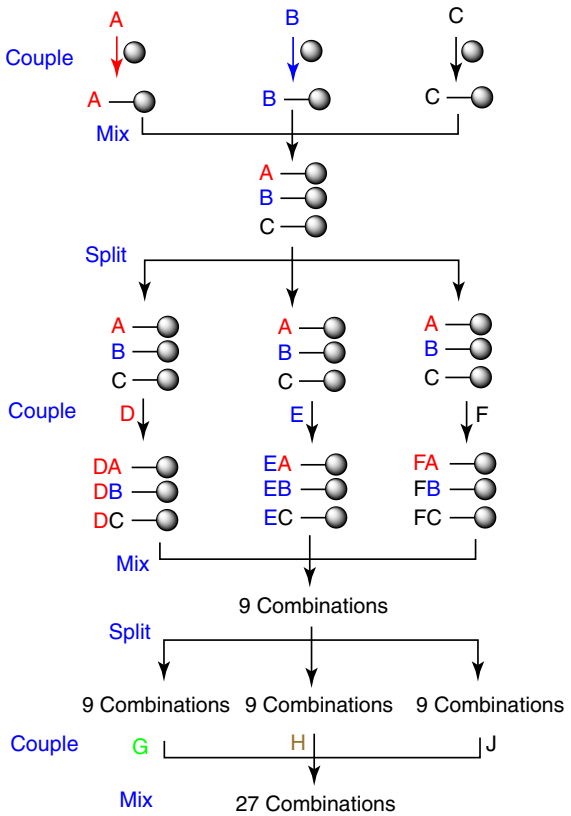


Figure 3 A split/mix combinatorial synthesis using nine diversity components.

This is where parallel and combinatorial synthesis diverge. In parallel synthesis the three batches of beads would be kept separate. The next step would be to divide each batch of beads into three giving nine reaction vessels (Figure 2). They would be individually coupled to any of the second three components giving all nine possible iterations as single compounds. The total number of vessels used is 12, 3 for the coupling of the first three components and 9 for the second.

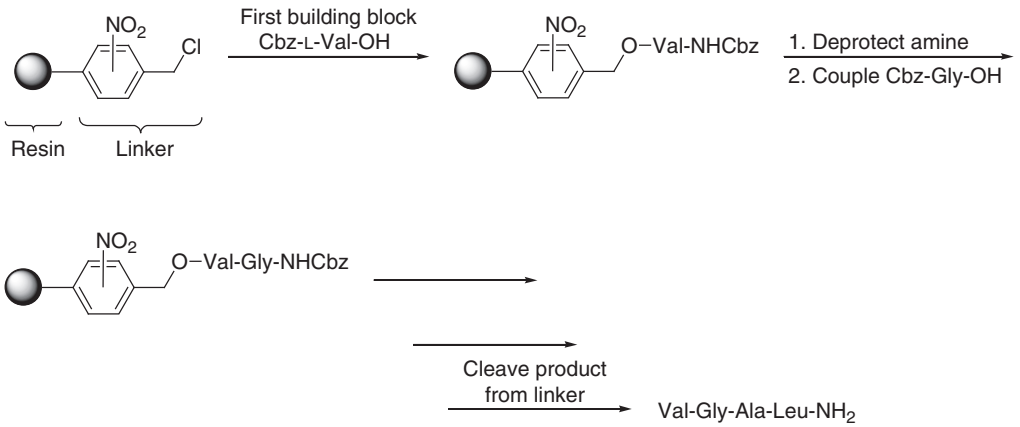
In a split/mix combinatorial synthesis the beads are mixed together. Because all three batches of coupled beads were prepared in equimolar amounts the 'concentration' of all three in the mixture are equal. The mixture of beads is then split into three. Each vessel holds a 1:1:1 mixture of coupled beads and is treated with a second diversity component. Assuming that the coupling of the second component goes to completion, the two-component product is present in a 1:1:1 ratio. Importantly, we now have all nine possible combinations but in only three vessels, six vessels in total having been used. Thus is illustrated the power of split/mix combinatorial synthesis. The act of mixing and splitting means that, unlike in parallel synthesis, as diversity elements are added the number of compounds increases exponentially in each step, whereas the number of vessels used accumulates linearly. As shown in Figure 3, if the three batches of two-component beads are combined, mixed, split, and then again exposed to a diversity component the number of three-component compounds increases to 27 (3^3) using nine vessels in total. Turning the wheel once more would give 81 (3^4) 4-component compounds using 12 vessels in total but with all combinations again contained in only three vessels. This allows one to increase the number of compounds that can be prepared using a limited number of reactors. The products are mixtures of beads each bearing a different immobilized compound.

9.01.3 Solid and Liquid-Phase Parallel Synthesis

9.01.3.1 Solid-Phase Synthesis

9.01.3.1.1 Introduction to solid-phase synthesis

In its original form, solid-phase synthesis was directed at the efficient production of peptides.[3] Within Merrifield's seminal work, an amino acid residue was attached to a resin (200-mesh polymer beads), allowing the free end to undergo reaction following appropriate activation (Scheme 1). In this scenario, the attached end is effectively blocked, whereas the reactive chain is extended via series of peptide bond coupling steps, following the final product is cleaved from the resin. Since the introduction of the technique, solid-phase methods have been extended to an ever-increasing range of chemical structures.



Scheme 1

The advantages of solid-phase synthesis included 'purification' by simply washing away excess reagents, the concomitant enhancements in yield made possible by using excess reagents, and control over the location of reactions. All of these made solid-phase chemistry attractive to practitioners of combinatorial chemistry, whereas peptides, in particular, offered the additional advantage of permitting diversity by adding modular building blocks ('pearls on a string').

This section will review the basic principles and techniques of solid-phase chemistry that have been used in combinatorial chemistry and parallel synthesis.

9.01.3.1.2 Bead types and linkers

The basic requirements of a solid-support bead is that it should be insoluble in the solvents used during synthesis and chemically inert to reaction conditions. Most solid-phase supports are composed of cross-linked polystyrene. They are synthesized by polymerizing divinylbenzene and styrene in different ratios depending on the desired mechanical properties. Solid supports with higher cross-link densities will have increased mechanical stability with decreased solvent-swelling coefficients. Since reactions take place at the surface both on and inside the polymer resin, swelling is necessary to allow reagent access to reactive sites. Most solid supports are commercially available in different mesh sizes that reflect these mechanical properties. Mesh size is inversely proportional to bead diameter. A 200–400 mesh is composed of 35–75 μm diameter beads, whereas a 100×200 mesh is composed of 75–150 μm diameter beads. This can factor into resin loading which is important to consider when calculating reagent needs and theoretical yields.

Other solid supports that are commonly employed include polyethylene glycol (PEG), silica, and functionalized ceramics. However, inorganic supports such as silica or ceramics do not typically swell in solvents, which can be considered a disadvantage, but they surpass organic solid supports in mechanical stability.

Substrates are not generally attached directly to solid-phase beads, but are tethered to the polymer support by a linker. The linker is typically irreversibly covalently linked to the resin while being reversibly attached to the first building block of the synthetic product. Linkers can also be thought of as a protecting group for a specific functional group of the first building block in a multistep synthesis. In fact, linkers are usually chosen strategically so that the reaction conditions needed to build the molecules are orthogonal to those needed to cleave the molecule from the resin. This allows the experimentalist temporal control over product cleavage from the resin, which is usually performed in the final step.

A common solid-phase/linker strategy is to use linkers that are cleaved by acid (entries 1–10, Table 2) with building blocks that have base labile protecting groups (e.g., fluorenylmethyloxycarbonyl (FMOC)).[8] Other common linker cleavage mechanisms are through photochemical, base labile, reductive, or oxidative means for which examples are shown in Table 2. Different cleavage mechanisms also can mean that whatever functional group is attached to the resin may not be the same functional group that results in the cleavage from the resin. An example of this is the Rink amide resin (entry 8, Table 2), in which a carboxylic acid is attached to the resin but a carboxamide results from cleavage. Some strategies use nucleophiles to promote cleavage (entry 13, Table 2), which produces final products that include the nucleophile. In some cases, termed 'safety catch' linkers, the reactivity of the linker is enhanced by chemical modification before the cleavage event (e.g., entry 14).[9]

9.01.3.1.3 Nonbead solid supports

Even though resin-bound synthesis affords mechanical advantages during the purification process when contained in an appropriate reaction vessel, physical manipulation of the resin can be inconvenient, especially in a high throughput setting. Although the beads are separate entities, their direct handling can be likened to that of wet sand. To overcome some of these limitations, methods have been developed that either immobilize or sequester solid supports.

A multipin parallel synthetic apparatus is a microtiter plate that has polyethylene rods (pins) coated with a reactive tether for solid-phase synthesis (Figure 4). In 1984, Geysen et al. reported this method for the synthesis of peptide epitopes.[10] The coupling reagents and amino acid building blocks were dissolved in the well-plates. The coated pins were immersed into solution until the reactions were completed. After the coupling steps, the pins were rinsed in wash well-plates and then transferred to well-plates with reagents that would deprotect the newly tethered amino acids to complete the first cycle. The cycle could be repeated using wells with different coupling partners to create diversity until the desired peptides were developed. Biological screening could be performed without cleavage from the pins.

Advances in pin technology have focused on replacing the coated head of the rods with structures with greater surface area. For example, Mimetopes has developed a commercially available line of Synphase™ Lanterns and Crowns that are radiation-grafted polymer surfaces on which to build small molecules. The lanterns and crowns are named from their respective shapes and offer an increased surface area to volume ratio over traditional pin design (15–36 μmol per unit for lanterns, 18 μmol per unit for crowns). Marcaurelle and coworkers used the Synphase™ Lanterns to synthesize 16 000 medium-sized lactams and sultams via aldol-based build/couple/pair strategy (Scheme 2).[11] Each lactam/sultam set contained eight stereoisomers that were produced individually. To increase diversity, each scaffold contained both a handle of which to *N*-functionalize as well as a site for cross-coupling.

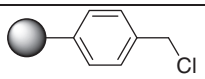
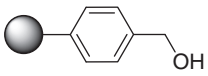
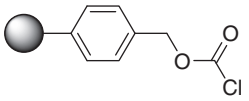
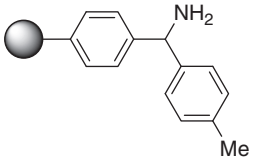
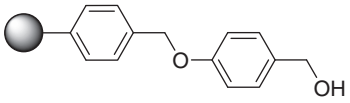
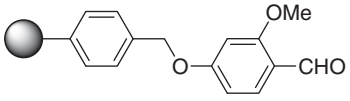
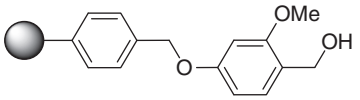
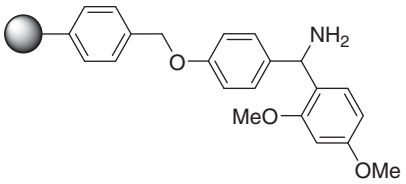
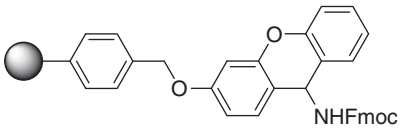
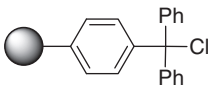
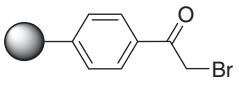
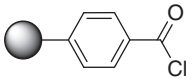
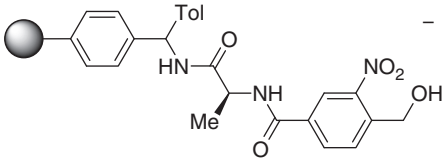
In cellulose synthesis on continuous cellulose membranes (SPOT) synthesis, reagents in a solvent of low volatility are spotted onto a planar support of pure cellulose chromatography paper that has been pretreated with an appropriate linker. This linker is often simply a free amine. Germeroth and coworkers demonstrated the usefulness of this solid support in the synthesis of 8000 triazine derivatives in 20×20 arrays on cellulose membranes (Scheme 3).[12] Beginning with the step-wise attachment of the first two peptides onto the amine tethered cellulose, they used cyanuric chloride to form the dichlorotriazines. These were then substituted with various amines and then finally piperidine. The SPOTs were punched out and then chemically cleaved to provide the target library in 65–95% conversion. SPOT synthesis is relatively economical, adaptable to automated technologies, and can be used with microwave chemistry to reduce reaction times. Also, in cases where polystyrene bead-supported compounds do not perform well in biological screening, cellulose membrane supported compounds may be more compatible with on-support screening methods such as enzyme linked immunosorbent assays (ELISA), protein-binding assays, and agar overlay techniques.

Another method in which to add convenience to solid-phase resin handling came in an early form of macroscopic solid support used for polypeptides, the 'meshed bag or tea-bag' introduced by Houghten.[13,14] As the name implies, these were porous flexible containers, resembling tea bags that were filled with fixed amounts of various beaded resins. The bags were immersed in reactive chemical media and used in split/mix combinatorial fashion with tracking done by label. This technique has been applied mostly to peptide libraries although it has also been adapted for the construction of a carbohydrate library.[15]

MicroKans and MicroTubes are containers that can enclose a reactive resin and also equipped with an Rf or 2D bar code tag. They are discussed in greater detail in Section 9.01.3.3.2.

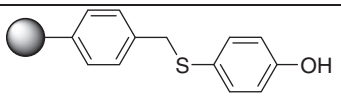
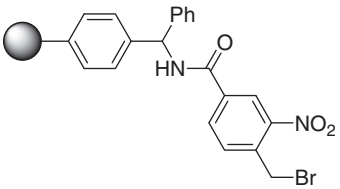
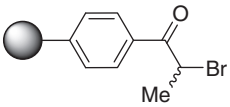
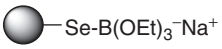
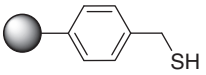
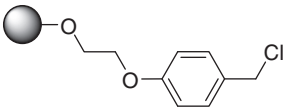
Photolithography is another approach to spatially differentiate parallel synthesis that uses a series of masks that shield the solid support from photodeprotection in predesigned high-density arrays. To direct product development, various mask patterns are used during illumination to control the sequence of reactant addition. An added benefit of this strategy is that a high level of miniaturization can be attained. In their synthesis of 1024 peptides, Pirrung and coworkers used nitroveratryloxycarbon (NVOC) as a photocleavable protecting group (Scheme 4), but Xiaolian Gao and coworkers have recently developed a series of photo-generated acids to remove acid-labile protecting groups.[12,16,17]

Table 2 Solid-phase linker and cleavage strategies

Entry	*Type*	*Linker*	*Resin name*	*Functional groups to attach*	*Cleavage conditions*
1	Electrophilically cleaved (strong acid)		Merrifield	Carboxylic acids	HBr/TFA or HF
2	Electrophilically cleaved (strong acid)		–	Carboxylic acids	HBr/TFA or HF
3	Electrophilically cleaved (strong acid)		–	Amines, alcohols	HF/anisole
4	Electrophilically cleaved (strong acid)		4-Methyl benzhydrylamine Polystyrene (MBHA)	Carboxylic acids	HF/anisole (cleaved as carboxamide)
5	Electrophilically cleaved (mild acid)		Wang	Carboxylic acid	50–95% TFA
6	Electrophilically cleaved (mild acid)		Acid sensitive methoxy benzaldehyde (AMEBA)	Amines via reductive amination	5% TFA/CH_2Cl_2
7	Electrophilically cleaved (mild acid)		SASRIN	Carboxylic acids	1% TFA
8	Electrophilically cleaved (mild acid)		Rink amide	Carboxylic acids	20–95%/2.5% trimethylsilane (cleaved as carboxamide)
9	Electrophilically cleaved (mild acid)		Sieber	Carboxylic acids	2% TFA/98% DCE/ 0.1% EDT (cleaved as carboxamide)
10	Electrophilically cleaved (mild acid)		–	Carboxylic acids, alcohols, phenols, amines, thiols	2–50% TFA or 0.3 M anhydrous HCl in dioxane
11	Nucleophilically cleaved (saponification)		–	Carboxylic acid	Basic aqueous dioxane, sodium thiophenoxide in DMF, methanolic ammonia, hydrazine hydrate in methanol
12	Nucleophilically cleaved		–	Alcohols	TBAC, KOH, H_2O/THF 48 h or MeONa, MeOH, THF 4 h (cleaved as alcohol)
13	Nucleophilically cleaved		–	Carboxylic acids	H_2O/TBAF (cleavage as carboxylic acids), ROH, DIEA (cleavage as esters), Amine, 2-propanol (cleavage as amides)

(*Continued*)

Table 2 Continued

Entry	*Type*	*Linker*	*Resin name*	*Functional groups to attach*	*Cleavage conditions*
14	Nucleophilically cleaved (“Safety-Catch”, “Oxi-dize-cleave”)		–	Carboxylic acids	30% H_2O_2 in CH_3CO_2H (oxidize to sulfone), then RNH_2 in DMF (cleavage as amide)
15	Photocleavable		–	Carboxylic acids	Photolysis
16	Photocleavable		–	Carboxylic acids	Photolysis
17	Reductive cleavage		–	Alkyl halide	Bu_3SnH, AIBN, $PhCH_3$ (cleavage as alkane)
18	Reductive cleavage		–	Carboxylic acids	$LiBH_4$
19	Oxidative cleavage		–	Alcohols	DDQ, mixed-bed DDQ scavenger resin

Abbreviations: AIBN, azobisisobutyronitrile; DCE, dichloroethane; DDQ, 2,3-dichloro-5,6-dicyano-1,4-benzoquinone; DIEA, diisopropylethylamine; EDT, 1,2-ethanedithiol; SASRIN, super acid sensitive resin; TBAC, tertiary-butyl acetate; TFA, trifluoroacetic acid; THF, tetrahydrofuran.

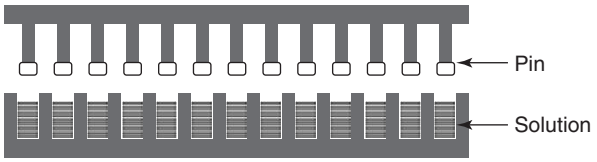


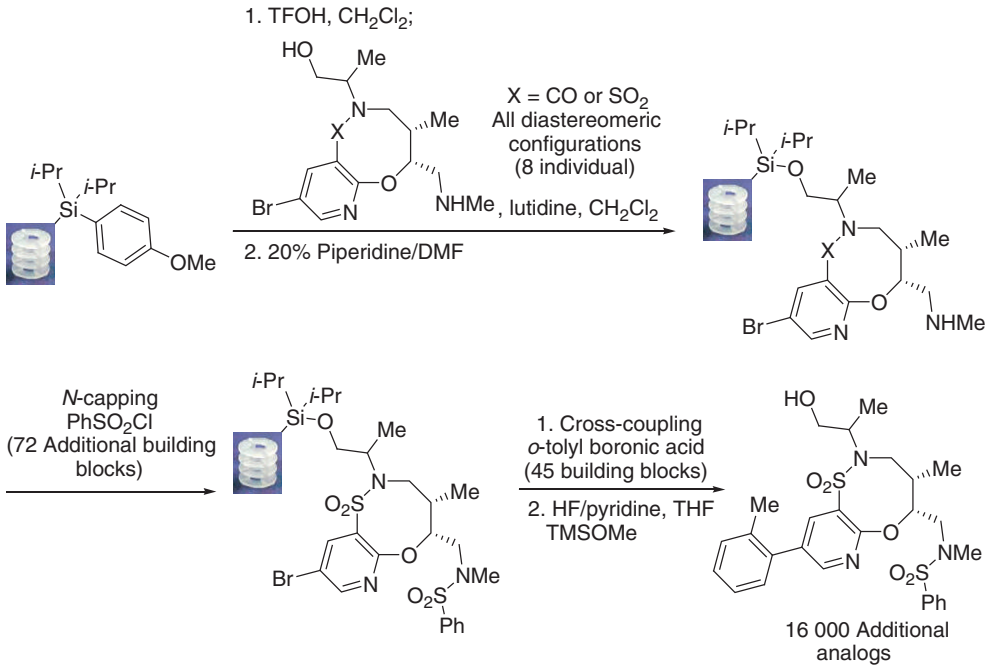
Figure 4 Multipin apparatus.

9.01.3.2 Liquid-Phase Parallel Synthesis: PEG and Linear Polystyrene (LPS) Support

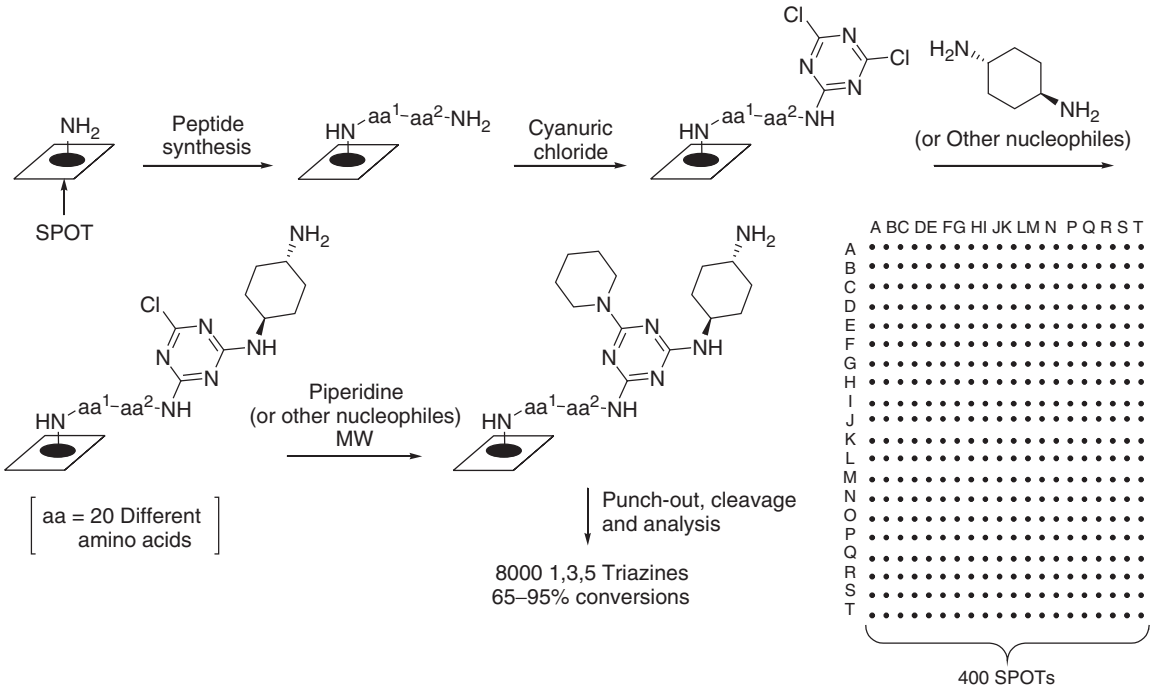
Despite its advantages, solid-phase synthesis has drawbacks that limit its utility in both combinatorial chemistry and parallel synthesis. For example, polymer effects can significantly affect reaction kinetics by chemical or physical means.[18] In contrast to solid-phase synthesis that is performed on insoluble polymer supports, liquid-phase synthesis is defined by the use of soluble polymer supports. Such supports may regain the advantage of solution-phase chemical methods, solution-phase analytical techniques (i.e., NMR spectroscopy and thin layer chromatography (TLC)), and automated liquid handling capabilities.

PEG or LPS polymers have been utilized as supports for parallel synthesis. In these systems, standard solution-phase chemistry can be carried out on the support-linked substrates. However, the polymer’s physical properties allow the linked compound to be selectively precipitated from reaction mixtures. The products may be then cleaved from the support. Alternatively, polymer-supported reagents or scavengers can be precipitated and then discarded.

Janda and coworkers synthesized a small library of prostanoid analogs displaying antiviral activity through a multistep approach on an LPS support (Scheme 5(a)).[19] The LPS support was used because of its solubility in THF, which enabled conventional organometallic chemistry as shown in the first step of the prostanoid synthesis. Janda’s ability to control the sense of enantioselectivity in the Sharpless asymmetric epoxidation reaction by varying the molecular weight of an L-tartrate bound PEG provided a demonstration of polymer effects on molecular reactivity (Scheme 5(b)).[20]



Scheme 2

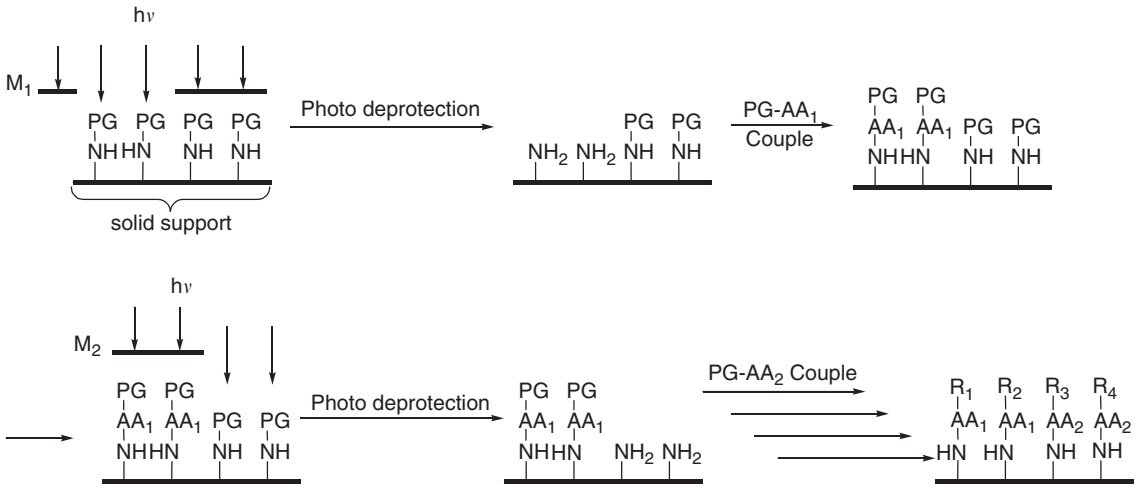


Scheme 3

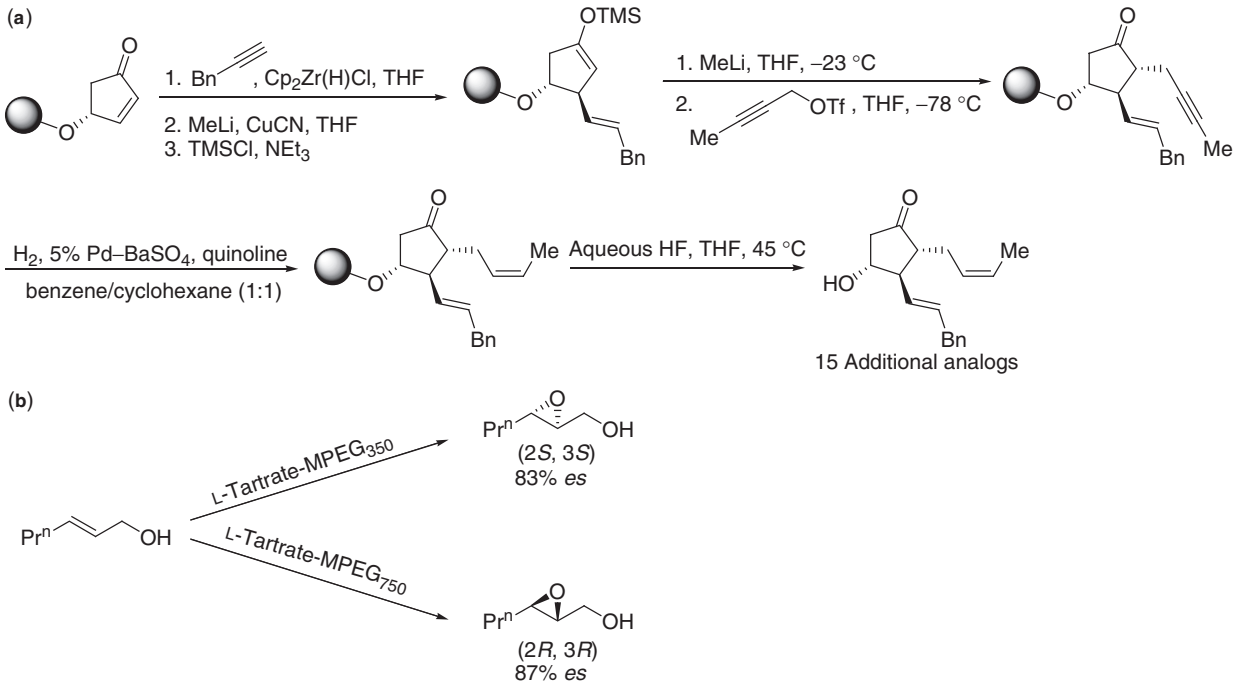
9.01.3.3 Preparation and Deconvolution of Encoded Combinatorial Libraries

Combinatorial library synthesis is designed to produce mixtures containing large numbers of compounds in a limited number of reactors. In order for the combinatorial technique to be useful, there must be a way to both locate and identify an active compound within the library. Locating and identifying a compound of interest from a mixture is called deconvolution.[21]

Deconvolution can be performed by segregating a unit of solid support such as a bead, isolating the attached compound, and characterizing it. Alternatively, one could resynthesize each member of a mixture in pure form and identify the compound of interest by remeasuring the property of interest (e.g., biological activity). One may also incorporate some kind of code, or tag, which when



Scheme 4



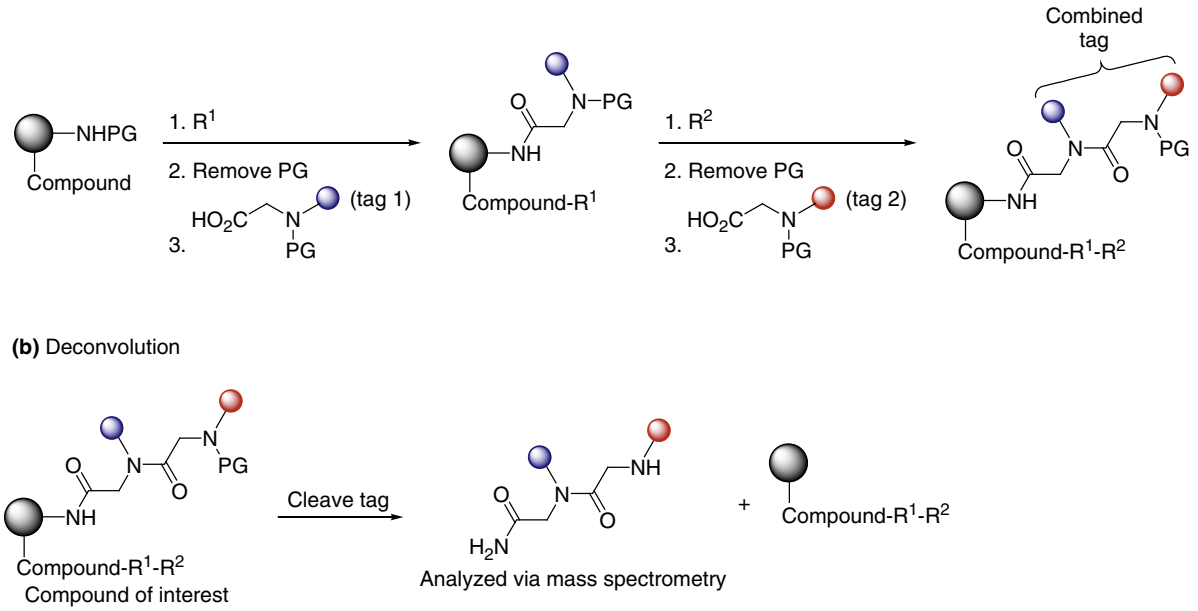
Scheme 5

read reveals the synthetic history of the bead. To be useful, coding should be easier to decipher than characterizing the individual compound itself. Prestandardized coding can be reused for many different libraries, making the deciphering routine.

9.01.3.3.1 Preparing a chemically encoded combinatorial library

One way to encode a combinatorial library is through chemical tagging, in which small molecules are introduced onto a unit of solid support during the library synthesis. These molecules would each have a unique structure that would be correlated to a specific event in the synthesis, generally the introduction of a diversity element. As diversity is introduced, the small molecule tags are each attached in a separate step. A linear tagging sequence illustrates the concept and is depicted in Scheme 6. The starting point is a bead with both an attached library compound and a protected amine site that can be selectively unmasked. Each introduction of a diversity element is recorded by the attachment of a corresponding tag.

The synthesis of a chemically coded combinatorial library of benzimidazoles using beads and a linear tagging method is shown in Scheme 7.[22] There are three points of diversity with 36 components for each making a total of 36^3 compounds (46 656), a number that would be a challenge using only parallel synthesis.



Scheme 6

The number of tags required depends on the number of components at each step and the number of complete split/mix events. In this case there are 36 components in the first diversification followed by a split/mix and 36 components in the second diversification again followed by a split/mix. There are 36 components in the third diversification, followed by a split but no mix. A total of 72 tags are therefore required; 36 for the first step, 36 for the second, and none for the third.

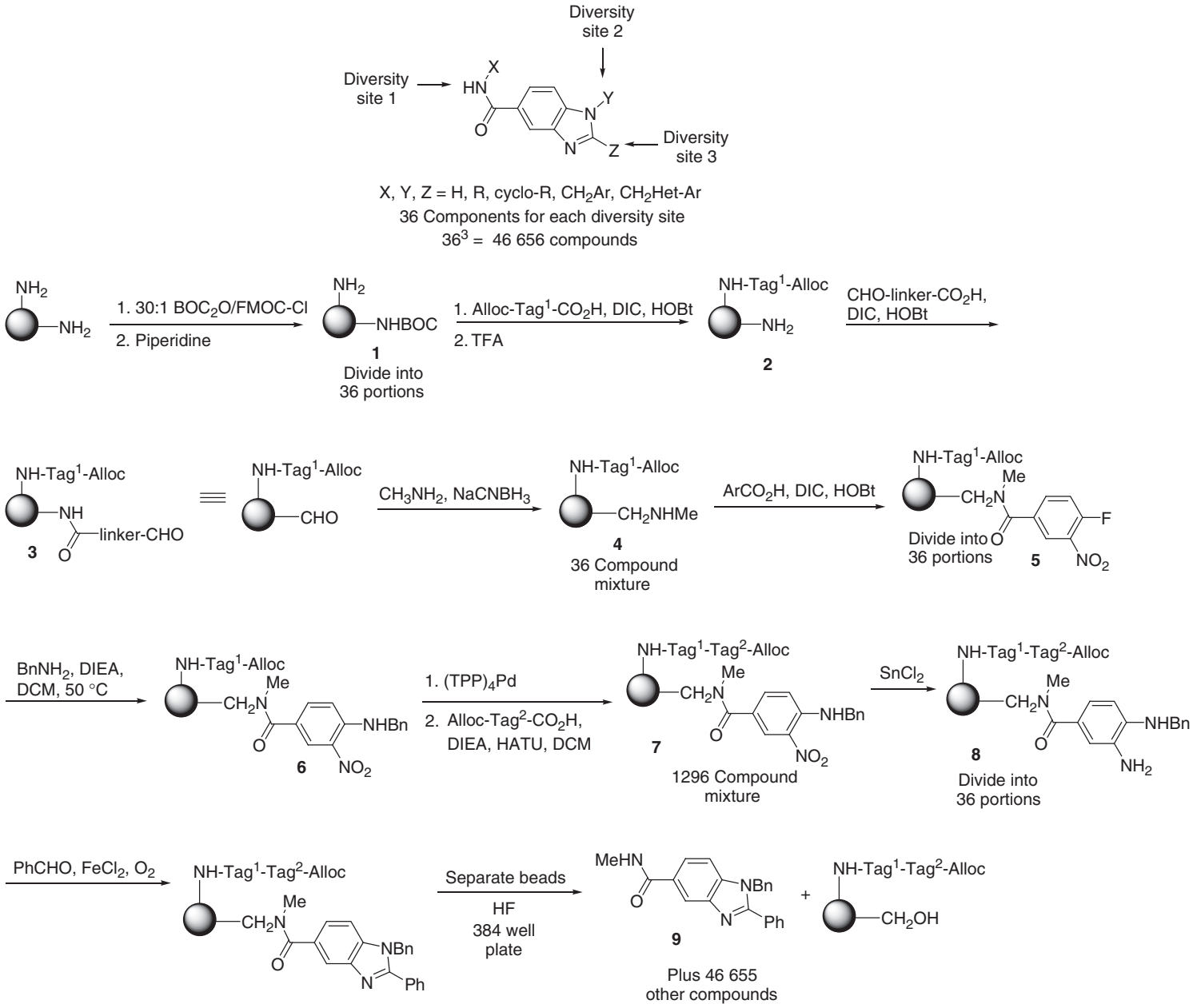
The authors used orthogonal protecting groups to selectively access different sites on the support. The surface amines were protected using a *t*-Butyloxycarbonyl (BOC) or an FMOC group allowing for selective unmasking of alternate sites using acid or base (Scheme 7). The bis-protected support was generated using a mixture of BOC anhydride and FMOC chloride. Most of the sites are BOC protected with a smaller number FMOC protected. Treatment with piperidine gave the BOC protected resin **1**. The resin was divided into 36 equal portions for the diversity site 1 components and the appropriate tag, with an Alloc-protecting group, was attached. TFA treatment gave the tagged resin **2** with the BOC sites unmasked for attachment of a linker giving intermediate **3**. This linker incorporated an electron-rich aromatic ring (not shown) that stabilizes a cation at the point of attachment. The final library benzimidazole could be cleaved via S_N1 dissociation from the support by treatment with acid.

The first diversity components (in this example methylamine) were introduced by reductive amination giving intermediate **4**. The 36 reactions were mixed and acylated with a scaffold affording intermediate **5**. The mixed acylated compounds were split into 36 reactors. At this point each individual bead carried one acylated diversity component and its associated tag, but in each reactor all 36 were present. The second diversity components (in this example benzylamine) were introduced by nucleophilic aromatic substitution giving intermediate **6**. The Alloc-protecting group was removed, exposing an amine on the tag to which the second Alloc-protected tag was attached, giving intermediate **7**. The 36 reactions were mixed. Reduction to diamine **8** was followed by splitting into 36 reactions. Now each individual bead contained two diversity components and their associated tags but each reactor contained 36^2 (1296) compounds. Introduction of the third diversity components as an aldehyde (in this example benzaldehyde) under oxidative conditions completed the synthesis. Since the reaction products were not mixed following this step, incorporation of another tag was unnecessary.

Deconvolution was effected by physically separating the beads and individually subjecting them to acid solvolysis to liberate the library compound **9**. The library compounds were used for screening and the tagged beads were retained in the plates. A biologically active library compound is identified by liberating the tag under more forcing conditions (6N HCl, heat). The recovered tag is derivatized and identified using a preset high performance liquid chromatography (HPLC) protocol. This identifies the compound without having to do structure determination. This example produced 46 656 compounds using only 111 vessels.

An alternative nonlinear chemical tagging method using a series of polychloroaryl ethers (Figure 5) was described by Still.[23–25] The method is depicted in Scheme 8. The tags are not attached to each other but instead individually to the support surface. The combination of tags provides the synthetic history. These can be analyzed using capillary GC with electron-capture detection, a technique that is very sensitive to the presence of these compounds. Because the analytical method is so sensitive very little material is required, typically occupying only 1% of the support surface sites for each tag.

Other means of allowing scientists to track and identify compounds from large mixtures following biological screening have been developed. They include a variety of means for correlating a compound's identity with its physical location in a container or in an array. Representative examples are provided below.


Diversity site 2
Diversity site 1
Diversity site 3
X, Y, Z = H, R, cyclo-R, CH2Ar, CH2Het-Ar
36 Components for each diversity site
36^3 = 46 656 compounds
1. 30:1 BOC2O/FMOC-Cl
2. Piperidine
1
Divide into 36 portions
1. Alloc-Tag1-CO2H, DIC, HOBt
2. TFA
2
CHO-linker-CO2H, DIC, HOBt
3
CH3NH2, NaCNBH3
4
36 Compound mixture
ArCO2H, DIC, HOBt
Divide into 36 portions
5
BnNH2, DIEA, DCM, 50 °C
6
1. (TPP)4Pd
2. Alloc-Tag2-CO2H, DIEA, HATU, DCM
7
1296 Compound mixture
SnCl2
8
Divide into 36 portions
PhCHO, FeCl2, O2
Separate beads
HF
384 well plate
9
Plus 46 655 other compounds

Scheme 7

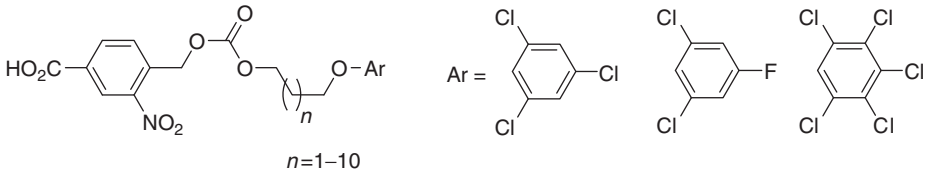
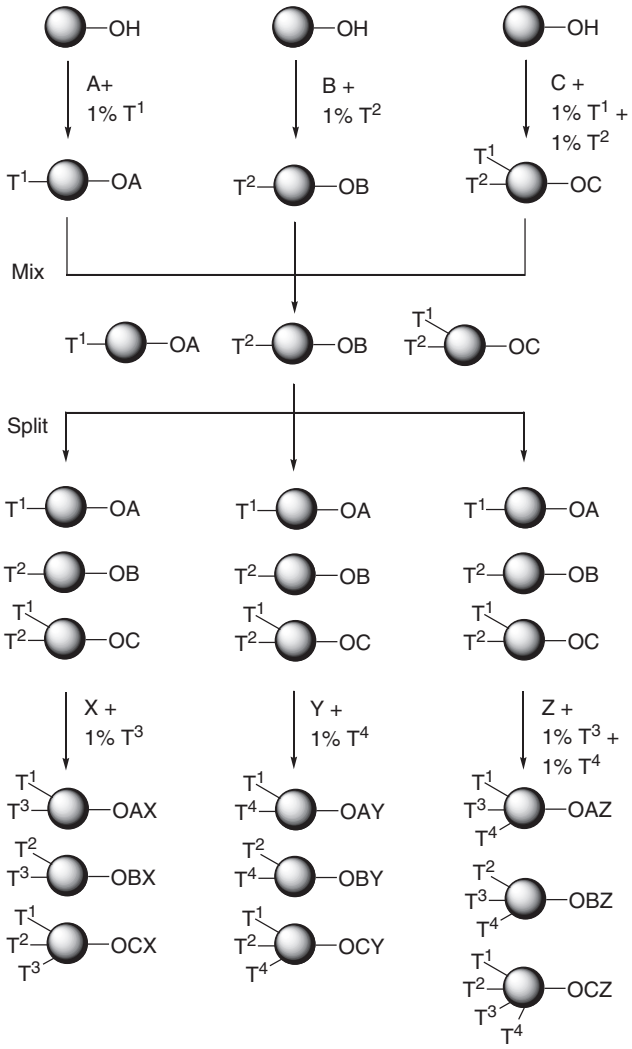


Figure 5 Polychloroaryl ethers used as nonlinear tags.



Scheme 8

9.01.3.3.2 Encoding by Rf tagging

One approach for combinatorial synthesis using macroscopic support was reported in the mid-1990s.[26,27] MicroKans and MicroTubes are permeable, rigid, cylindrical polypropylene capsules that contain resin along with a microelectronic radio frequency (Rf) transponder (Figure 6). Each transponder emits a unique signal when placed in an external Rf field. Later versions used 2D bar codes in lieu of the Rf tags. Either technology allows the individual reaction vessels ('Kans') to be tracked automatically, allowing the chemist to carry out mix/split synthetic sequences, whereas retaining a record of the history of each Kan, and therefore the identity of the compound inside it. Thus, they are large enough to be easily handled but small enough to use for synthesis of library quantities of compounds. MicroKans and MicroTubes hold up to 30 mg of resin that affords 25–30 μmol of library compound. The porous containers permit contact of the support with the surrounding solution. Once the reaction sequence is complete the containers are drained and rinsed.

Each synthetic operation is recorded using the transponder response in an Rf field. Rigid cylindrical containers can be subjected to the split/mix process like beaded resin. For relatively small libraries (< 1000 compounds) this can be done manually by scanning and sorting each container. For larger libraries, automated sorting hardware designed to handle specific containers mixes and distributes them into the next reaction while recording each container's history.

As noted above, synthetic history can be also tracked by bar code scanning. In a related application, the support is deposited and affixed to a plate bearing a bar code (Figure 6).[28] The plates are used in groups like the MicroKans immersed in a reactive medium then washed, mixed, sorted, and recorded by specialized equipment. Another method uses a series of colored rings (Figure 6) to tag crowns and lanterns that are affixed to stems not containing Rf transponders. Sorting and tracking is performed manually.[29]

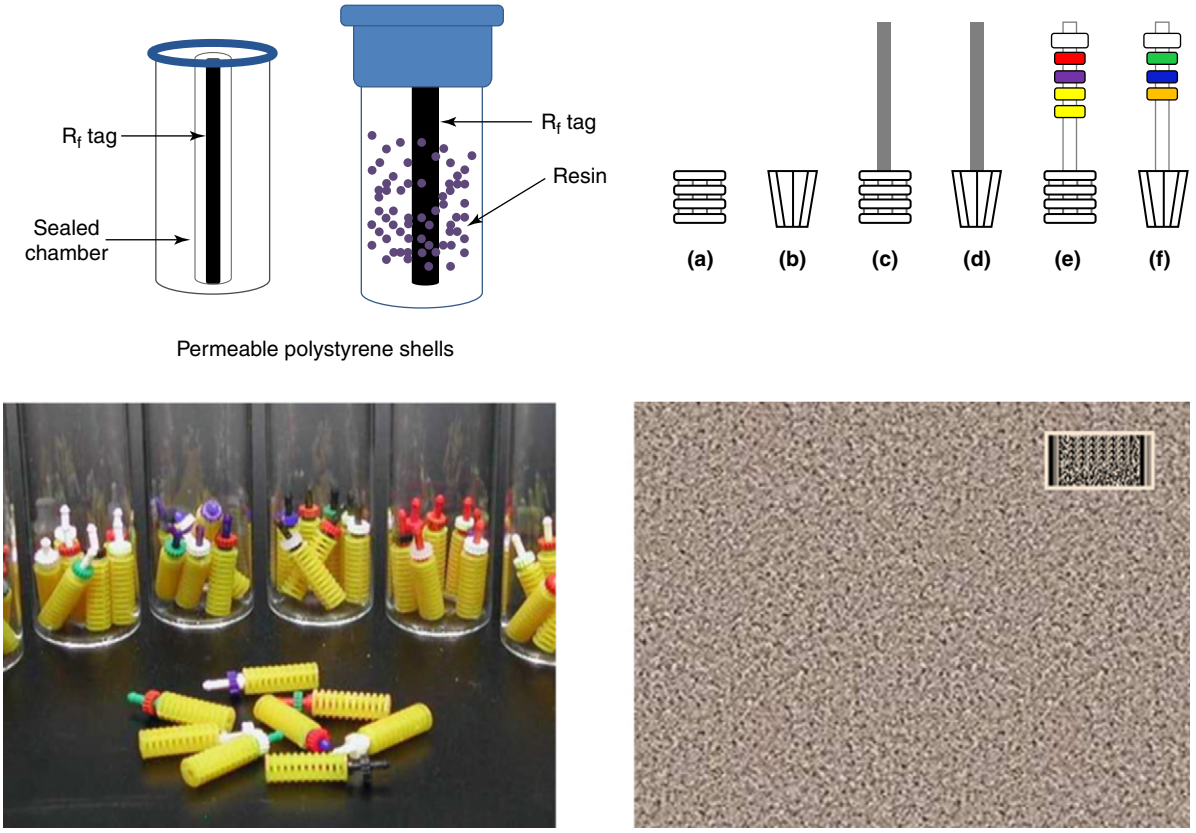


Figure 6 Top left and 2nd left: MicroTubes, MicroKans with R_f transponders. 6(a) Synphase crown; 6(b) Synphase lantern; 6(c,d): crowns and lanterns with R_f stem tags; 6(e,f) crowns and lanterns configured for color code. Photo: color coded 75μmol Synphase lanterns in reactors. Lower right: representation of solid support on plate with 2D bar code. Photographs courtesy of Perer Senake, Mimotopes Ltd.

9.01.3.3.3 Encoding by position within an array

Another technique called 'string synthesis' or 'necklace synthesis' uses unlabeled support units tracked only by position. A polypropylene string is used to form an ordered group of supports with markers to identify the string and to distinguish the two ends. The stringed supports are exposed to the first diversity element. Once the couplings are complete the strings are retrieved and washed. Sorting is done using slotted trays into which the strings of supports are placed in order. The strings are removed and the support units transferred from a source tray to a destination tray, making new strings. These are reattached and exposed to the next diversity element. A more detailed description of this technique can be found in the literature.[30–32]

9.01.3.3.4 Locating active compounds contained within combinatorial libraries

Combinatorial library compounds emerge from synthesis as mixtures that can be screened for desired properties. Strategy options to achieve this are represented in Figure 7. When beads are used the compounds emerge as a tethered mixture in a small number of vessels. The mixture can be assayed with provision for marking the active bead. Examples of this are colorimetric,[33,34] fluorescent,[35,36] or thermal[37] readouts, the latter relying on the enthalpy of reaction when a target interacts with an active compound. Alternatively, the beads can be separated and then assayed while tethered.[21] The library compounds can also be cleaved from the support and assayed in solution but they must be correlated with the tagged bead. Macro forms of support

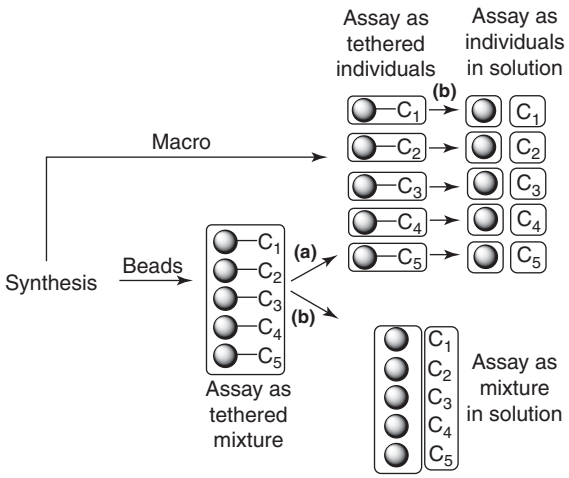


Figure 7 Locating an active compound in a combinatorial library: (a) physical separation; (b) cleavage. Beads = 200 or 400 mesh polymeric spheres. Macro = pins, crowns, lanterns, tea bags, MicroKans, MicroTubes.

eliminate the need for tedious physical separation and provide options for nonchemical tagging. This advantage has contributed to their widespread adoption.

In some special cases deconvolution of the mixture in solution is an option. Part or all of the tethered library is cleaved and released into solution. The compounds are assayed as a group, and if an active is detected deconvolution begins. Strategies for deconvolution of combinatorial libraries in solution can be complex, requiring changes in the way the library is produced. The reader can find these described in several literature reports.[38–40]

9.01.4 Solution-Phase Technologies in Parallel Synthesis

Even though solid and liquid-phase parallel synthesis techniques have seen major technological advances in the past 50 years, solution-phase parallel synthesis has also been the focus of development. Automated equipment, liquid handling technologies, and analytical instrumentation for solution-phase parallel synthesis that was only accessible to larger companies has advanced to a stage that they are becoming more commonplace in smaller companies as well as academic institutions.

9.01.4.1 Solid-Supported Reagents, Catalysts, and Scavengers

In addition, various strategies for streamlining the purification of solution-phase libraries have been developed. The most impactful of these have been the various types of solid-phase reagents and scavengers that have been introduced for this purpose. Doing parallel synthesis in a traditional solution-phase format has the advantages of permitting the direct application of many more well-established reactions in comparison to solid phase and the avoidance of kinetic barriers imposed by chemistry on resins.

Some common solid-phase scavengers are shown in Table 3, exhibiting functional groups such as aldehydes and hydrazines to scavenge excess amines and ketones, respectively. Standard reagents such as oxidizing, reducing, and coupling agents are also exhibited. A thorough list of solid-phase reagents and scavengers can be found in a review by Ley and coworkers.[41]

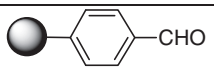
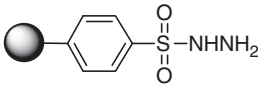
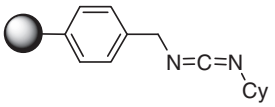
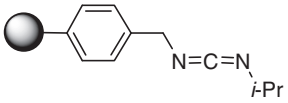
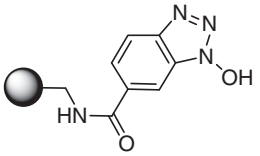
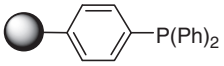
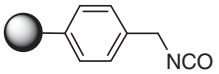
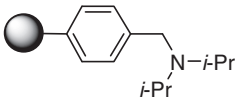
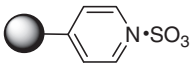
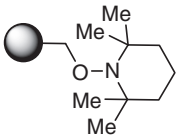
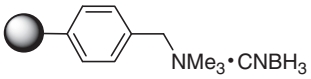
9.01.4.1.1 Reagents and catalysts

A solid-supported reagent is simply a reagent that has been covalently or ionically attached to a polymer resin. This allows a solution of a building block(s) to be added to a reaction vessel containing the solid-supported reagent and then drained away easily after the reaction is completed (Figure 8). Instead of washing unwanted impurities away as in solid-phase synthesis, the impurities are left behind. Solid-supported reagents are very useful when excess reagents are needed to drive a reaction because they are easily separated. The concept of simple separation of polymer-bound reagents is also useful in reactions that generate waste products that can make product isolation difficult (i.e., triphenylphosphine oxide in the Mitsunobu or Appel reactions). In many cases, solid-phase reagents can be regenerated and/or reused, reducing waste. Also, when reagents are noxious or otherwise hazardous because of volatility, immobilizing them onto solid-phase resin provides a method of safe handling.

An interesting example of the utility of solid-supported reagents was demonstrated by Ley and coworkers in the synthesis of the potent analgesic (±)-epimaritidine over a ten-step sequence with >90% purity and a 32% overall yield (Scheme 9).[42]

Polymer-bound catalysts can aid library synthesis as cross-coupling and amine based arylations are staples of diversification. Furthermore, the immobilized metal catalysts are less likely to leach trace amounts of the metal being present in chemical samples

Table 3 Common solid-phase scavengers and reagents

Entry	*Structure*	*Function*
1		Scavenger for primary amines, hydrazines, Meldrum's acid, and organometallic reagents
2		Aldehyde and α-halo ketone scavenger
3		Coupling reagent
4		Coupling reagent
5		Coupling reagent
6		Ligand, reagent
7		Nucleophile scavenger
8		Base
9		Oxidizing agent
10		Oxidizing agent
11		Reducing agent

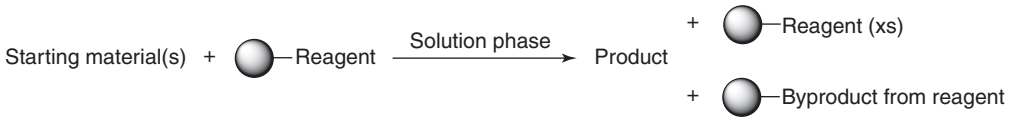
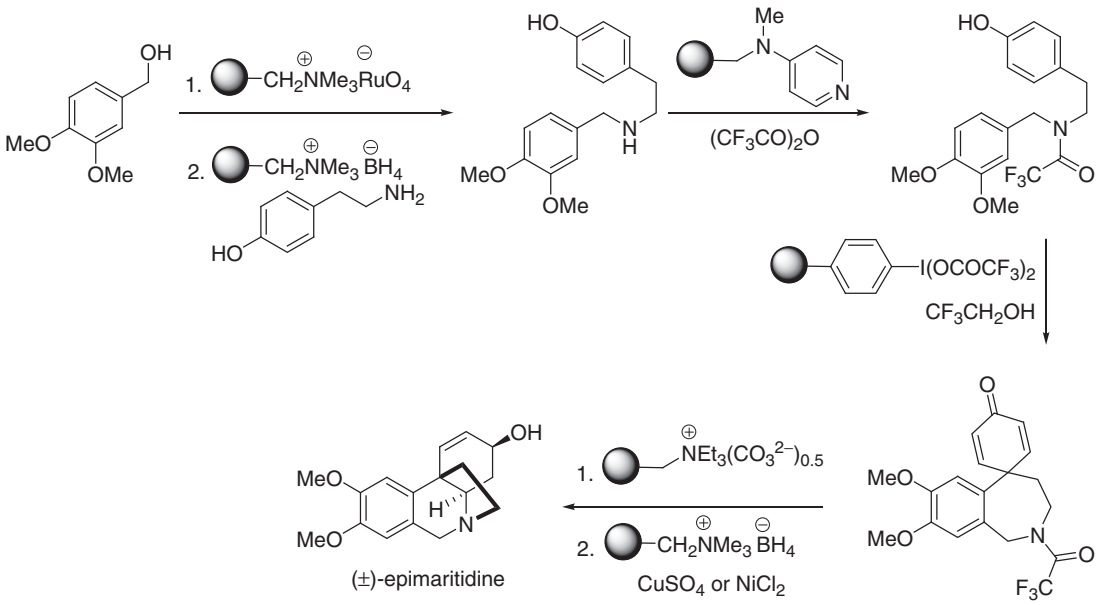


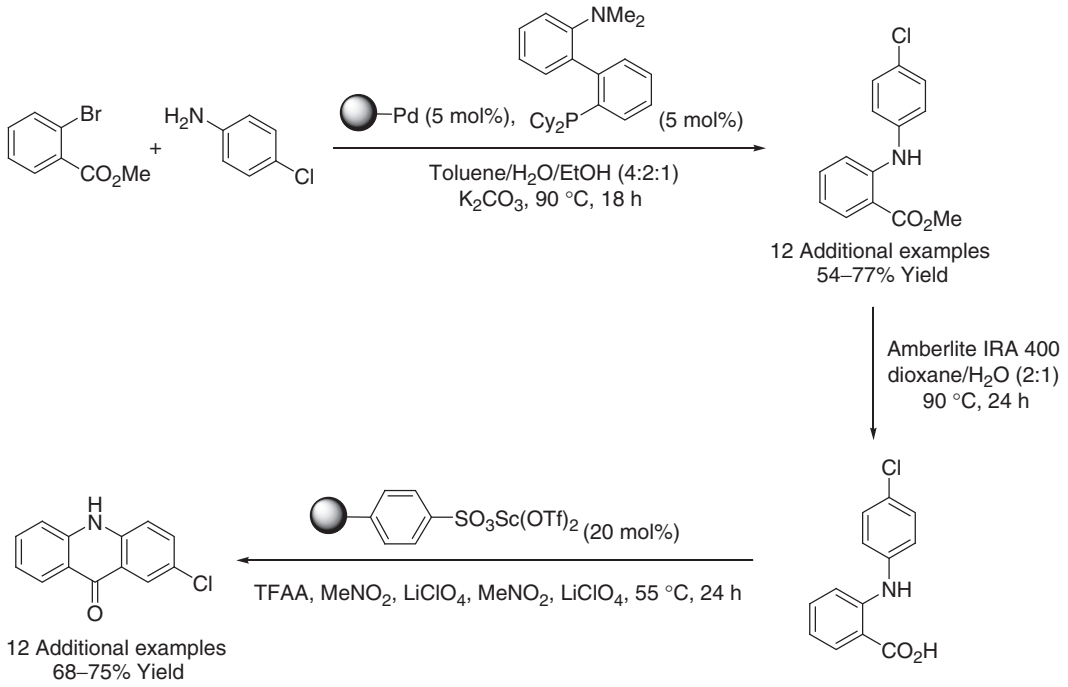
Figure 8 Using a solid-supported reagent in a liquid-phase synthesis.

during biological testing that could result in toxicity or false results. Kobayashi et al. employed both resin-bound metal and Lewis acid catalysts in the synthesis of acridone derivatives to simplify product purification (Scheme 10).[43] To demonstrate the cost effectiveness of these catalysts they repeatedly recycled them after simply washing with solvent. Thus, Kobayashi used 5 mol% of a polymer-supported palladium to facilitate a Buchwald–Hartwig coupling in a 4:2:1 ratio of toluene, water, and ethanol solvent system, chosen because it prevented the leaching of palladium to levels not detectable by fluorescence X-ray analysis. After an Amberlite IRA 400 mediated saponification, a Friedel–Crafts acylation catalyzed by 20 mol% polymer-bound scandium was used to give a small library of acridones.

Hanson and Reiser have developed a nanomagnetic Co/C surface on which catalysts can be attached. The ferromagnetic nature of the solid support allows catalysts to be easily recycled by holding a magnet to the reaction vessel and then decanting the



Scheme 9

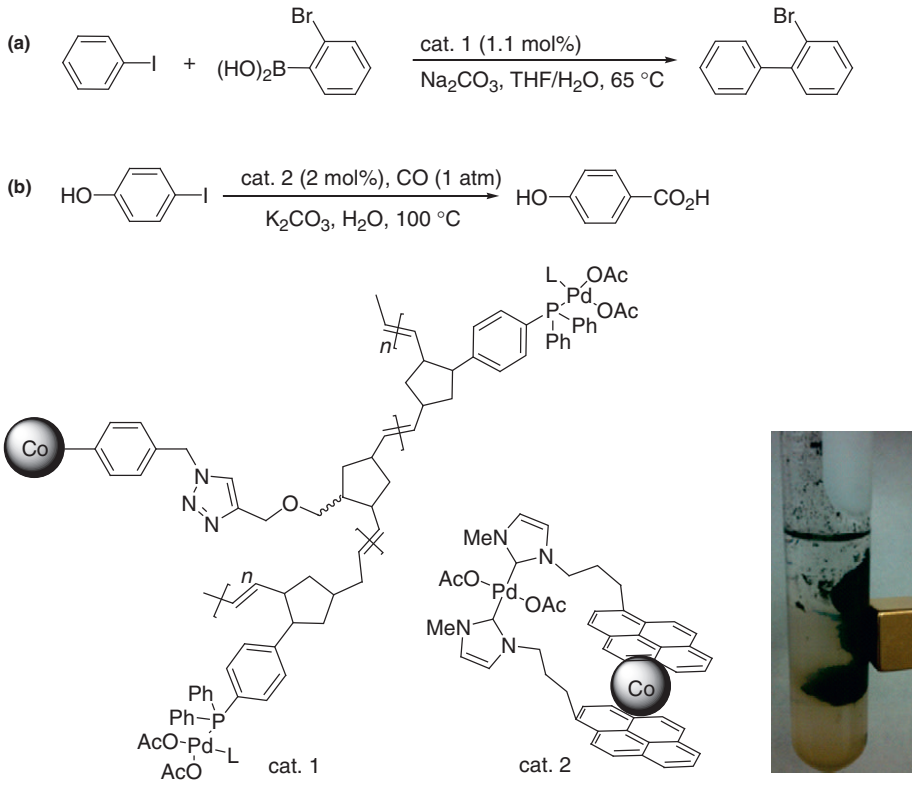


Scheme 10

reaction mixture (Scheme 11). A heterogenous palladium complex on triphenylphosphine functionalized Co/C-ROMP gel was used to facilitate a series of Suzuki–Miyaura cross-coupling reactions (Scheme 11(a)).[44] Reiser and coworkers also reported a similar strategy for the palladium-mediated carbonylation of aryl iodides (Scheme 11(b)).[45]

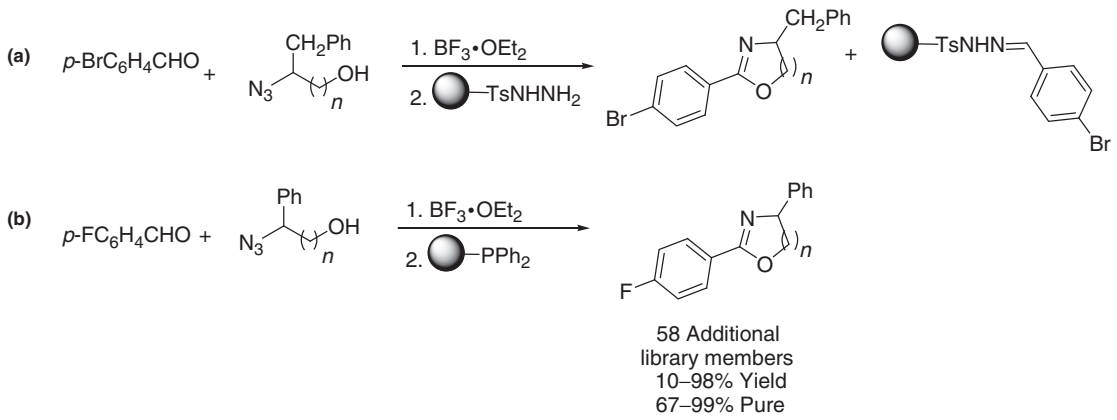
9.01.4.1.2 Extractions and scavengers

Solid-phase scavengers are polymer-supported reagents used to covalently or ionically bind to excess reagents. They offer a means of solution-phase reaction purification while avoiding chromatography or recrystallization. This technique involves passing the crude reaction mixtures over the solid-phase scavenger (usually contained in a solid-phase extractor (SPE) cartridge) and then washing the purified product into a collection tube, leaving behind both unreacted reagent and the scavenger. They are particularly



Scheme 11

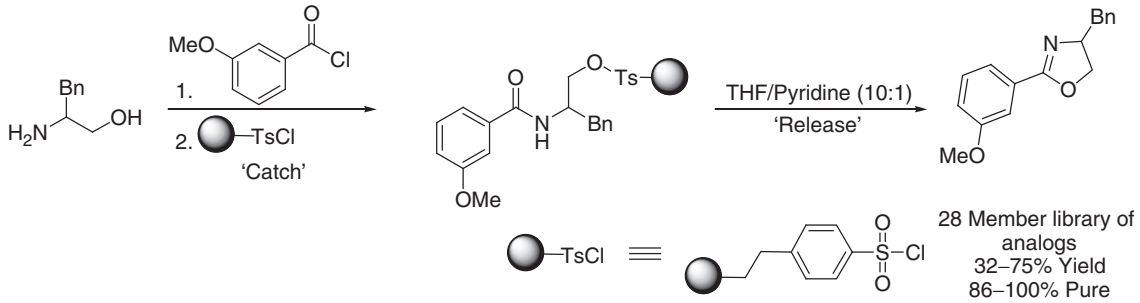
useful in reactions that can be driven to completion through an excess of one of the reacting partners. Aubé and coworkers explored different solid-phase scavenging strategies based on the complementary reactivity of excess reagents and a reciprocally functionalized polymer.[46] In the parallel one-step synthesis of medicinally relevant oxazoline and dihydrooxazine analogs, aldehydes were reacted with 1,2- and 1,3-hydroxyalkyl azides in the presence of $BF_3 \cdot OEt_2$, which resulted in the formation of oxazolines and dihydrooxazines, respectively (**Scheme 12**). Initially, the aldehydes were used in excess in the presence of a polymer-bound tosyl hydrazine to scavenge the unreacted aldehyde, whereas the second involved using excess hydroxyalkyl azide with polymer-bound diphenylphosphine to scavenge the unreacted azide. In this case, the latter scavenging strategy provided better isolated yields of generally $\geq$50%, whereas the former case gave isolated yields of 5–24%.



Scheme 12

As a complementary approach to using solid-phase scavengers, a 'catch-and-release' strategy is widely used. In this operation, crude reaction mixtures are passed over a solid-supported reagent that selectively binds the desired product, while impurities are flushed away. Then, the product is subsequently released from the resin-bound reagent into solution through a second transformation (often involving acid/base chemistry and an ion exchange resin). A form of this is commonly used to purify

recombinant proteins that contain a His-tag in many biotechnology labs where proteins with His-tags (6–8 histidine residues on the N or C-terminus) are bound strongly onto a nickel column, from which impurities may be washed away and the purified protein eluted from the column with high concentrations of imidazole. The concept is also useful in small molecule synthesis. Pirrung and coworkers applied 'catch-and-release' to a synthesis of oxazolines, in which various 1,2-aminoalcohols were reacted with a series of acylating agents (Scheme 13).[12] The crude reaction mixture was then passed through peptide synthesis vessel containing the (polystyrene)tosyl chloride resin which was then washed. Treatment with a 10:1 mixture of THF/pyridine affected both the cyclization to the oxazoline and released the purified product from the resin. Overall, 32–75% yield of products were obtained that were 86–100% pure.



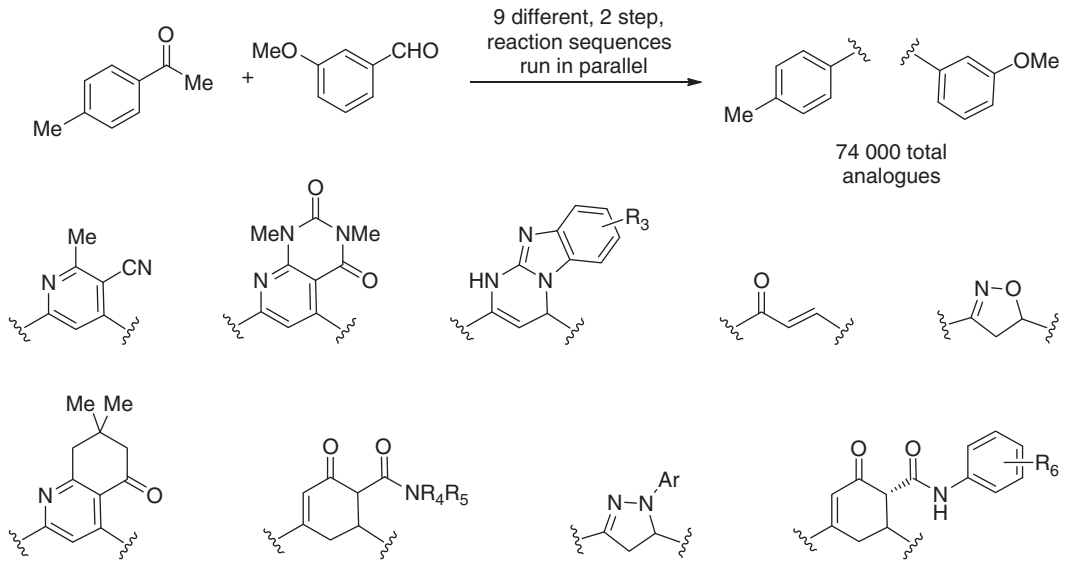
Scheme 13

9.01.4.2 Solution-Phase Synthesis Enabling Equipment and Strategies

Specialized equipment may be needed when synthesizing tens to sometimes thousands of compounds through solution-phase parallel synthesis. This equipment needs to enable the experimentalist to control the temperature, atmosphere, spatial arrangement, and temporal status of multiple reactions simultaneously.

9.01.4.2.1 Automated molecular assembly plant

One of the first major solution-phase parallel synthesis projects was reported by Powers et al., from ArQule in 1998.[47] An Automated Molecular Assembly Plant (AMAP™) was a comprehensive platform for fluid handling, array production, array layout, automated reaction workup, and quality control. Using it, ArQule researchers synthesized 74 000 chalcone and advanced analogs in parallel (Scheme 14). In total, nine combinatorial arrays were used to effect a series of condensations and cyclizations to make large collections of pyrazolines, pyrazoles, flavones, acetoacetanilides, aminobenzimidazoles, and pyridines.



Scheme 14

9.01.4.2.2 First automated parallel synthesizer

In an early report of parallel organic chemistry being run by an automated system, Fuchs reported a microcomputer-driven reaction protocol used to execute nine simultaneous robot performed reactions with an automated workup (aliquot quenching, plug filtration, and extraction) that also implemented automated HPLC yield analysis.[48] This system was used to determine optimal conditions for vinyl sulfone synthesis via a parallel reaction screen (Figure 9). The automated setup included a robotic arm for material transport, a remote dispenser, an aliquot archive station, biphasic workup capabilities, a syringe and needle wash station, a turntable for filtering into an HPLC injector, an HP3390A reporting integrator, and a reagent station (Figure 9). Altogether, they screened 16 reactions (eight bases with one solvent and a set of two bases with four solvents) that were analyzed by HPLC, generating 240 HPLC analyses over the course of a 50-hour period. In the end, the reaction was indeed optimized with a DBU/methylene chloride system that produced a 67% yield of the vinyl sulfones.

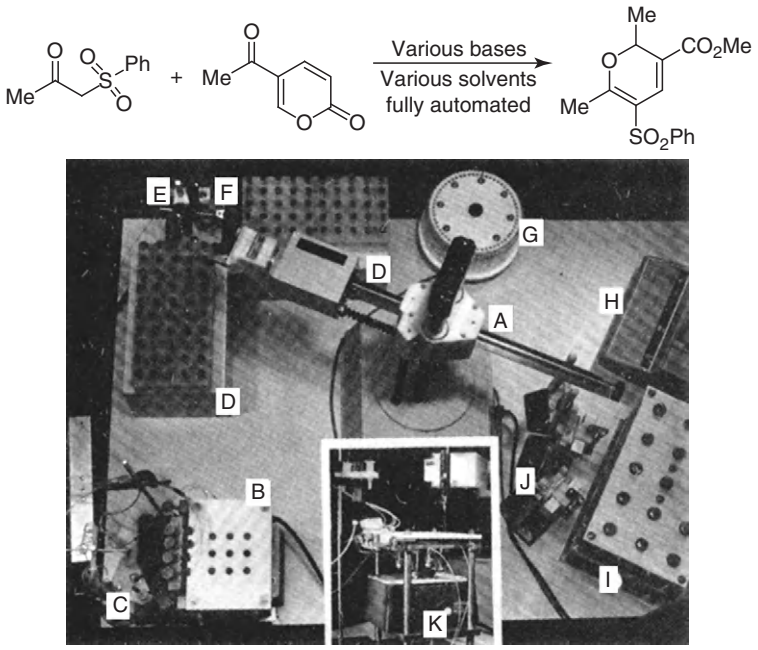


Figure 9 Automated synthetic setup of vinyl sulfone: (A) robotic arm, (B) reactor station, (C) remote dispenser, (D) aliquot archive station, (E) biphasic workup station, (F) syringe and needle wash station, (G) turntable for plug filtering into HPLC injector collection tubes, (H) HP3390A reporting integrator, (I) reagent station, (J) hand parking station, (K) front view of reactor station. Photographs courtesy of Philip Fuchs and Douglas Lantrip.

9.01.4.2.3 Fully automated platforms

Additional examples of commercially available automated parallel synthesis technology have continued to appear. For example, the Chemspeed Accelerator SLT-100 or the Zinsserna automated platforms are capable of performing multistep library synthesis, catalyst preparation and screening, formulation screening, reaction discovery, sample preparation as well as solubility, stability, and compatibility testing with complete automation through a computer interface. The Chemspeed automated synthesizer can handle both solid and liquid dispensing with high degrees of accuracy, control reaction temperatures from -70 to 180 °C, provide a large inert atmosphere for up to 192 parallel reactors and even perform automated workups that include evaporation, filtration, liquid–liquid extraction. and solid-phase extraction (SPE) purification (Figure 10). Zinsserna has introduced automated platforms that similarly incorporate liquid handling systems, resin dispensers, powder handlers, vortexes, and SPEs.

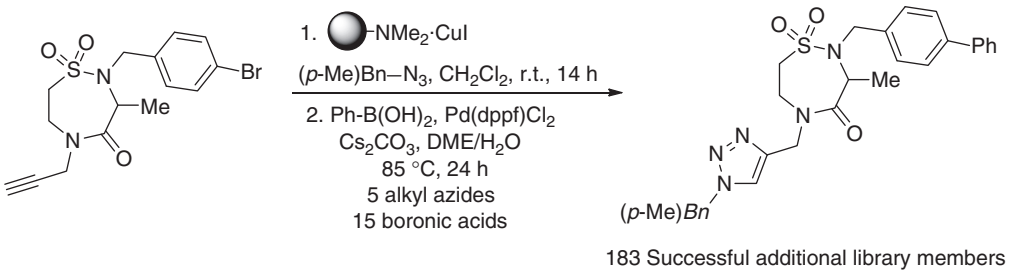
A Chemspeed platform has been used to synthesize a 184 member library of thiadiazepan-1,1-dioxide-4-ones in parallel (Scheme 15).[49] Three sultam core scaffolds were diversified in an automated fashion via two-step [3 + 2] Huisgen cycloaddition/Pd-catalyzed Suzuki–Miyaura coupling sequence. In the first step, the alkynes were reacted separately with an excess of azide in the presence of an immobilized Amberlyst A-21·CuI catalyst. After the reaction was completed, the catalyst was filtered away and the crude reaction was concentrated to give the triazole sultam adducts. The triazole were then reacted with various boronic acids in the presence of solid $Pd(dppf)Cl_2$, Cs_2CO_3 in a mixture of DME/water at 85 °C. After a basic workup to remove the unreacted boronic acid and Cs_2CO_3 a silica SPE filtration to remove the Pd(0), the crude compound mixtures were purified via mass-directed HPLC giving 82% of the expected products in >87% purity.

9.01.4.2.4 Semiautomated platforms

The essential functions that a parallel synthesizer needs to provide are the ability to control fundamental reaction conditions such as mixing, temperature, and atmosphere for multiple chemical reactions simultaneously. A few products that serve these



Figure 10 Chemspeed accelerator SLT-100® automated synthesizer.



Scheme 15

requirements are the Mettler–Toledo Autochem Bohdan MiniBlocks™ and the reaction carrousels by Radleys Discovery Technologies (Figure 11). Miniblocks™ are a commonly used platform in solid and solution-phase parallel synthesis because they function as an affordable and user-friendly technological option. Reactions are run in various parallel arrays (from 3×2 to 6×8 per block) in either plastic or glass reaction vessels that can be heated and cooled under an inert atmosphere. Blocks are paired with an orbital shaker that facilitates reaction mixing. The blocks can also be coupled with a number of automated liquid and solid-dispensing stations. Also, reactions can be purified in parallel because the reaction block can be stacked on top of and drained into a purification block that is outfitted with either a number of solution-phase separating products, solid-phase

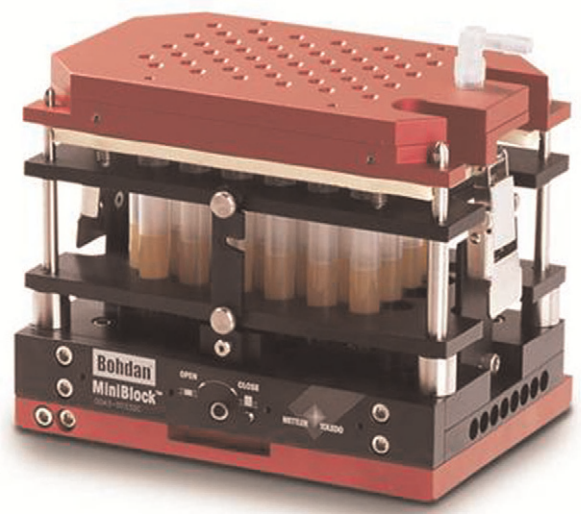


Figure 11 Bohdan Miniblock™. Photograph courtesy of Mettler–Toledo Autochem.

extraction or reaction tubes with solid-supported scavengers. Once parallel purification is complete, the products can be drained simultaneously into collection tubes and then concentrated in parallel in an automatic sample concentrator. Radleys Discovery Technologies products offer similar functionality by turning a single stir/hot-plate into a parallel synthetic platform. A carrousel system houses multiple reactions for heating, cooling, managing reagents and solvents, distributing gas or vacuum, and stirring (overhead, magnetic, and shaking) in both small and large volumes. A carrousel parallel workup station is also available.

Bohdan Miniblocks™ were used by Guy and coworkers to develop antimalarial agents against chloroquine-resistant *Plasmodium falciparum* (Scheme 16).[50] In a two-step parallel one-pot process, various chloroacridines were converted into their respective 9-phenoxyacridine, which serves as an activated intermediate to be reacted with various diamines to produce the 9-aminoacridine analogs. This synthesis demonstrated the utility of this tool by avoiding individual purification of final products. First, various 9-chloroacridines were placed into miniblock reaction vessels in a 48-position block. Phenol, cesium carbonate, and dimethylsulfoxide (DMSO) were also added. The reaction mixtures were heated at 100 °C in an orbital shaker. In the second step, 4 equivalents of various diamines were added separately to the different reaction vessels and then heated and shaken as before. Following conversion to the desired 9-aminoacridines formed, polystyrene-supported methyl isocyanate was added as a scavenger for the unreacted diamines. These crude reaction mixtures were then drained from the reaction vessels onto silica containing SPE tubes. The tubes were then washed to elute purified products into individual collection vessels.

9.01.4.2.5 Microwave technologies

Microwave heating enhances the efficiency of a range of chemical reactions, often affording reduced reaction times along with increased reaction yields and purities. However, most of the >4000 articles published on microwave-assisted organic chemistry have focused on using single-mode microwave reactors to perform single chemical reaction methods. Employing microwave technology in library or parallel synthesis was first augmented with auto-sampling robotics. Later, with the development of commercially available multimode microwave reactors, parallel microwave synthetic strategies have been introduced. One example is a multisample reactor platform composed of silicon carbide, a chemically inert and high melting (2700 °C) solid.[51] The material has a large heat capacity ($1.09\ J\ (molK)^{-1}$) and high thermal conductivity ($350\ W\ (mK)^{-1}$), which allows the platform to balance field inhomogeneities from within the microwave. In fact, temperature gradients were presumably not detectable by infrared thermal imaging (Figure 12).

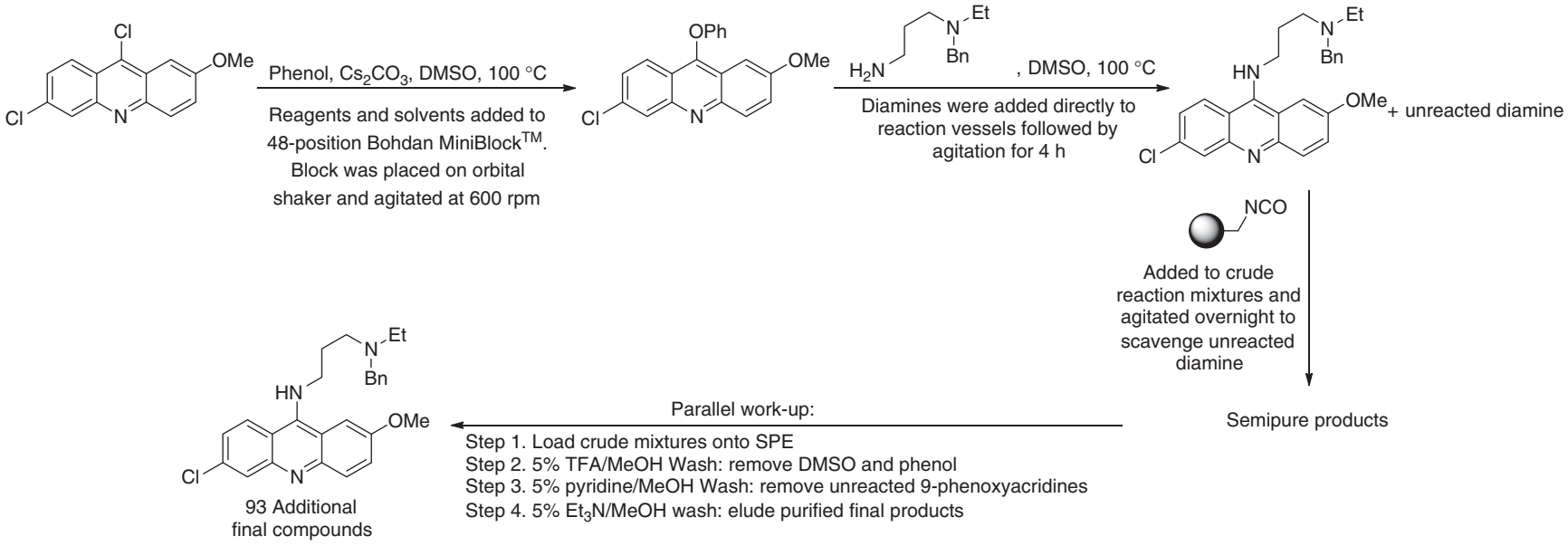
Kappe and coworkers employed a parallel multimode reactor in a microwave synthesis involving esterifications as well as metal-catalyzed dehydrative C–C couplings to test the efficiency of the strongly microwave-absorbing silicon carbide reaction platform (Scheme 17).[51] Their study which showed the capacity of silicon carbide to uniformly conduct heat (Figure 12) also demonstrated a new method in which 20 various methyl esters could be synthesized in ≤1 min with all reactions proceeding in ≥97% conversions. Parallel reaction screening efforts were also demonstrated by Kappe and coworkers in the C–C coupling of diphenylmethanol with dibenzoyl methane in a 5×4 array screen of both solvents and catalysts with 0.5–3 mol% catalyst loading and 110 °C microwave-assisted heating for 10 min. Nitromethane was found to be the best solvent with the four catalyst choices of $Sc(OTf)_3$, $Cu(OTf)_2$, $Zn(OTf)_2$, and $FeCl_3$ all performing similarly in that solvent. More significant effects were observed while changing the catalyst in other solvents.

9.01.4.3 Fluorous-Phase Parallel Synthesis

The fluorous phase was defined by Horváth and Rábei as a fluorocarbon-rich phase of a biphasic system (usually perfluorinated ethers, alkanes, and tertiary amines).[52] In their report, the utility of a fluorous biphase system (FBS) was demonstrated by first performing a hydroformylation of an olefin with the fluorinated rhodium complex $HRh(CO)[P[CH_2CH_2(CF_2)_5CF_3]_3$. After the reaction was completed, the fluorinated rhodium complex could be separated from the toluene crude reaction medium by extracting with perfluoromethylcyclohexane. Horváth and Rábei established the viability of using FBS as a tool to separate reagents, catalysts, or reactants from a reaction medium and in so doing created a new enabling technology for synthetic organic chemistry.

Fluorous-phase chemistry has been further developed as a tool for parallel synthesis.[53] Many fluorous-phase chemistry techniques mirror those of solid-phase synthesis. Fluorous reagents, ligands, catalysts, scavengers, tags, and protecting groups have all been developed and are employable to automated parallel synthesis. A major advantage of fluorous-phase chemistry over solid-phase chemistry is that it is compatible with solution-phase literature procedures, requiring little to no modification of the protocol until the purification step, which can be simplified by FBS. Analytical techniques such as HPLC, IR, NMR, and TLC are all employable. Also, products do not necessarily have to be isolated by using FBS because fluorous-labeled compounds are stable to regular and reverse-phase chromatography. Fluoro*Flash*TM silica gel packed columns have also been developed in which molecules with longer fluorine chains are retained longer on the column. Fluorinated samples are typically eluted by water with increasing methanol, whereas nonfluorous compounds are eluted out with the solvent front because of their low affinity for the stationary phase.

As example, to avoid the toxicity associated with tin contaminants, Curran used a triphasic solvent separation system to purify a series of Stille coupling products in parallel (Scheme 18).[54] Fluorous aryl stannanes were coupled with benzyl and aryl halides and triflates in the presence of lithium chloride and $PdCl_2(PPh_3)_2$ in DMF at 80 °C. The Stille coupled products were isolated in the organic phase, the salts were removed in the aqueous phase, and the tin was sequestered into the fluorous phase.


Cl
OMe
Cl
N
Phenol, Cs2CO3, DMSO, 100 °C
Reagents and solvents added to 48-position Bohdan MiniBlock™. Block was placed on orbital shaker and agitated at 600 rpm
OPh
OMe
Cl
N
H2N
N
Et
Bn
, DMSO, 100 °C
Diamines were added directly to reaction vessels followed by agitation for 4 h
HN
N
Et
Bn
OMe
Cl
N
+ unreacted diamine
NCO
Added to crude reaction mixtures and agitated overnight to scavenge unreacted diamine
Semipure products
Parallel work-up:
Step 1. Load crude mixtures onto SPE
Step 2. 5% TFA/MeOH Wash: remove DMSO and phenol
Step 3. 5% pyridine/MeOH Wash: remove unreacted 9-phenoxyacridines
Step 4. 5% Et3N/MeOH wash: elude purified final products
93 Additional final compounds

Scheme 16

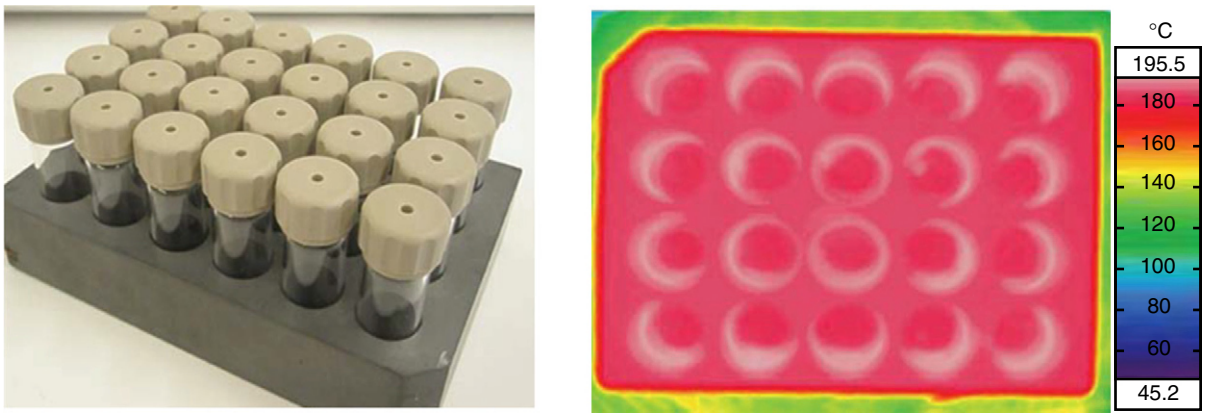
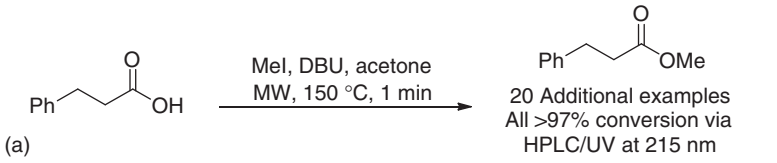
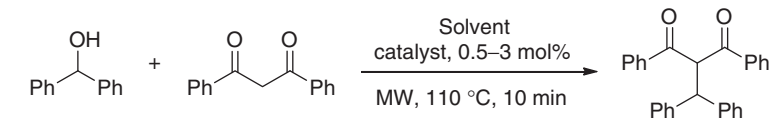


Figure 12 (a) Silicon carbide reactor platforms for parallel microwave chemistry. (b) Infrared thermal image. Photograph courtesy of Christian Oliver Kappe.





Yields (%) in indicated solvent

Catalyst	DCM	$MeNO_2$	MeCN	THF	Toluene
$Sc(OTf)_3$	95	98	82	84	94
$Cu(OTf)_2$	94	98	71	94	93
$Zn(OTf)_2$	53	97	89	37	25
$FeCl_3$	97	95	82	30	69

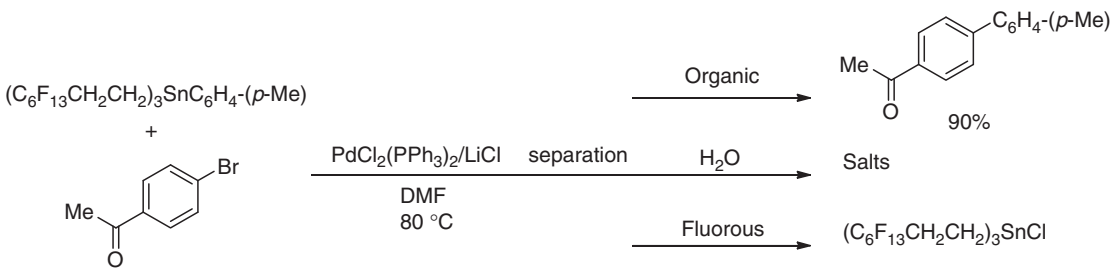
(b)

Scheme 17

Another use of fluorous-tagged substrates permits purification to be carried out where the property driving the separation is the number of linked F atoms rather than the chemical nature of the target molecule. Initial efforts into this strategy were encumbered because to obtain substrates with useful partition coefficients for the fluorous phase, large tags with anywhere from 60 to 120 fluorines were needed. Substrates with highly fluorinated tags proved to have poor solubility profiles that made finding effective reaction conditions difficult. This type of fluorous-phase chemistry is referred to as 'heavy' fluorous.

To overcome these limitations, Curran and coworkers developed a 'light' fluorous synthesis method.[55] The hallmark of light fluorous synthesis is a solid–liquid extraction over fluorous reverse-phase silica gel instead of the liquid–liquid extraction used in heavy fluorous synthesis. Also, a modest number of fluorines can be used in the lighter tags (from 9 to 21 fluorines). These display much better solubility in organic solvents and have been found to be benign to many synthetic sequences. Interestingly, with a 'light' fluorous tag, compounds do not partition to the fluorous phase FC-72 (perfluorohexane, Fluorinert FC-72) as does the 'heavy' tag. The solid–liquid extraction process is tunable by simply adding additional CF_2 groups that increase retention time incrementally (approximately adding 4 min to the retention time per CF_2 group on a Fluofix 120E column).

An example of 'light' fluorous-phase synthesis reported by Curran and coworkers took four carboxylic acids with light tags and simply coupled them with four amines using EDCI, HOBt, and triethylamine in dichloromethane (Scheme 19). The crude reaction mixtures were then loaded onto fluorous silica gel. The fluorous solid phase extraction was flushed with 80% methanol to elute the unwanted waste products and then washed with acetonitrile to obtain the desired products in a 21–100% yield. To remove the light fluorous tags, various conditions were used with varying success (0–85% yield).



Scheme 18

9.01.5 High Throughput Purification and Automated Sample Handling Methods and Protocol

Parallel synthesis provides libraries of crude compounds that must be purified in an appropriately high throughput manner. This requires automated or semiautomated systems designed to provide rapid analysis and preparative processing. Libraries of compounds usually emerge from the synthesis laboratory as crude oils or solids that have been concentrated in parallel using pretared bar-coded vessels. This immediately provides the crude weight and the means to track the compound's progress through the process. The processing system adds solvent, usually DMSO, to the crude compounds to afford a solution at a preset weight/volume concentration. A well-designed system provides an easily accessible array of options for both analytical and preparative HPLC. Different stationary and mobile phases are used to optimize an analytical method that can be transferred to preparative scale. An LCMS analysis is performed on each solution to determine both the approximate amount of target compound present and a preferred method for preparative purification. Those deemed suitable for purification move forward through the process.

Reverse-phase High-Resolution Mass-Directed Fractionation (HR-MDF) is well suited for HT applications. Since HR-MDF collects only when the target mass is detected many fewer fractions are generated per compound. This increases the capacity for multiple injections without having to remove blank fractions. Greater numbers and weights of crude compounds can be processed. The system pools the appropriate fractions into pretared vessels and they are evaporated in parallel. An LCMS analysis to a predetermined area percent completes the purification process. Contemporary electronic compound management software can track many thousands of compounds with less labor and fewer errors relative to traditional notebooks.

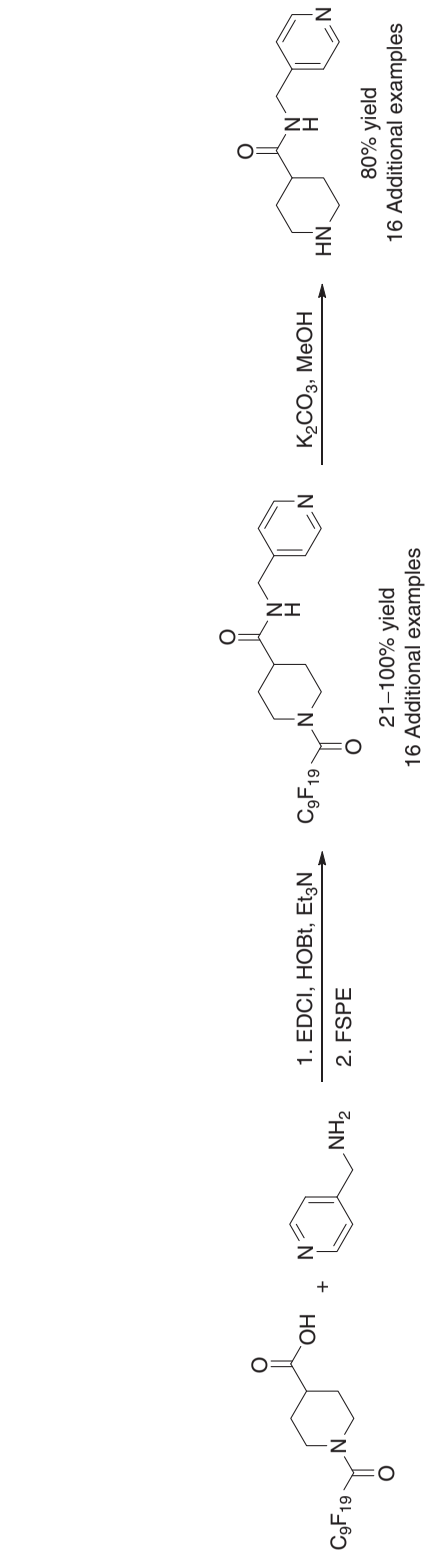
9.01.6 Parallel Synthesis in Flow

Flow chemistry is a handling technique where reaction components in solution are pumped through conduits and combined by mixing of the streams.[56] The combined components can react at the point of mixing spontaneously or with heating. They can be combined with another stream containing a reagent that initiates reaction. They can be fed into a chamber where an immobilized reagent initiates reaction. The effect is to produce a moving stream containing an intermediate. Flow can be used to work with intermediates whose large scale batch preparation is undesirable because of unsafe or noxious properties.

The stream of intermediate can be combined with another reagent converting it to a final product that is collected as it emerges from the conduit. If done in serial fashion, a segmented stream can be created with plugs of solvent in between packets of reacting solution, like a banded snake. This produces a series of small-scale batch reactions that are separated in time within the flow path. Early applications of flow synthesis to the production of compound libraries have used this method. However, the main stream can be partitioned into substreams separated in space. The substreams can each contact a different reagent and convert the intermediate to a different final product. The array could produce many more compounds than otherwise.

The Curtius rearrangement of benzoyl chloride illustrates the method (**Figure 13**). A DCM solution of benzoyl chloride is combined with a stream of aqueous NaN_3 within a chip and is converted to benzoyl azide. Passage of the two-phase segmented stream through a microseparator shunts the aqueous to waste and directs the DCM solution of benzoyl azide into a second reactor where the rearrangement is effected thermally. The stream, now gas/liquid segmented, is passed through a second microseparator membrane. The liquid passes through the microseparator membrane, whereas the gas is repelled by surface tension and passes out of the system. At this point the stream consists of the isocyanate. The isocyanate stream is subdivided before being fed into several microfluidic reactors, each with its input stream containing a nucleophile, and the derived products collected three at a time.

Early workers in this area often fabricated their own devices. An example of this was reported in a discovery-to-production effort that centered on nickel-catalyzed cross-coupling of aryl Grignard reagents with aryl halides.[57] Styring and Parracho were investigating various catalysts for the large-scale production of biphenyls, looking for one that would work for extended periods at ambient temperatures without contaminating the product with trace metals. For discovery purposes they used a 30 mm × 3 mm reusable stainless steel column that could be packed with various experimental catalysts for rapid preliminary screening. On identifying a promising catalyst, they demonstrated its performance in a laboratory scale parallel reactor as a prelude to larger scale use. A parallel flow reactor device was fabricated to hold 120 of the same columns as was used in screening (**Figure 14**).


1. EDCI, HOBt, Et3N
2. FSPE
21–100% yield
16 Additional examples
K2CO3, MeOH
80% yield
16 Additional examples

Scheme 19

These were filled with the catalyst and fed premixed solutions of the reactants at a flow rate equal to 120 times the flow rate used for the screening column. The assumption was that this array would reproduce the screening conditions in each column. This was used to 'scale-out' the reaction. Scaling out is the term used for producing large amounts of products in flow by running a process for a longer time as opposed to 'scaling-up' in which larger volumes and quantities of materials are used. They obtained the desired increased throughput.

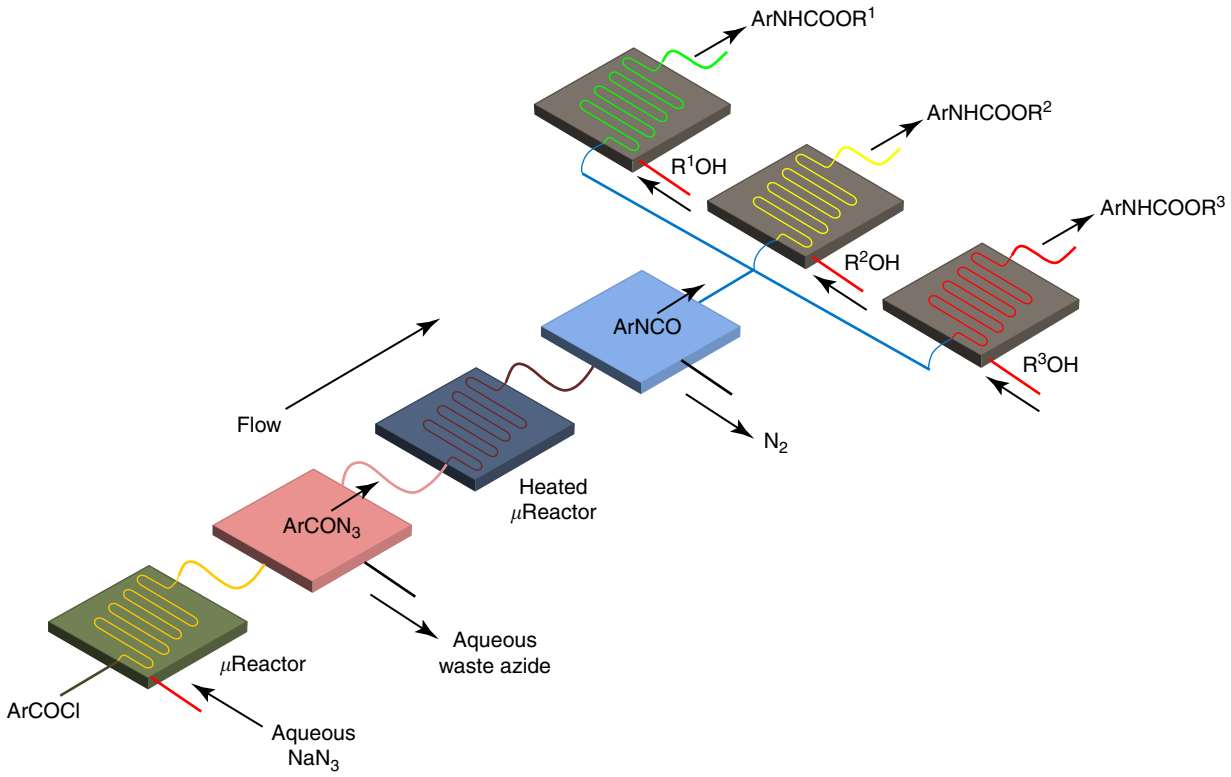


Figure 13 Flow system for Curtius reaction.

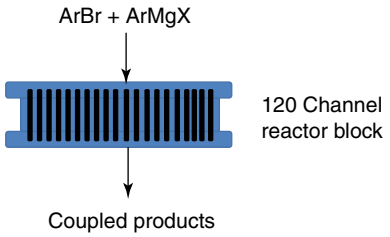


Figure 14 Schematic representation of parallel flow reactor block.

Some commercial flow reactors are available. The Thales Nano H-Cube® is a continuous flow system that allows for continuous hydrogenation reactions through *in situ* generated hydrogen from the electrolysis of water. The reactor can be heated to 100 °C and pressurized to 1450 psi. Catalysts are introduced through a disposable cartridge that is placed in-line with the flow system. The H-Cube® can be set up for relative high throughput hydrogenations through the use of liquid handlers. For flow reactions other than hydrogenations, Vapourtec Ltd provides a series of robust and highly adjustable flow reactors that can handle strong acids, gases, air and moisture sensitive reagents, and light suspensions. Vapourtec Ltd systems allow reactions to be heated to 250 °C as well as cooled to −70 °C in a series of modular reactors that vary in size and type.

9.01.7 Summary

As noted at the outset of this chapter, organic chemistry laboratory techniques have remained largely unchanged since the birth of the field in the eighteenth century. This is now changing, largely driven by the need of chemists to produce ever-larger numbers of

compounds of specific utility in either biology, materials science, or other fields. We have sought to summarize some of the most important new technologies, focusing on those that we think will continue to play a role in the laboratory for years to come. Although many of these techniques arose specifically out of the field of combinatorial chemistry as applied to the synthesis of bioactive molecules, we agree with Lindsley's assessment that 'combinatorial chemistry science' is likely to have an impact that continues apart from the fortunes of that very specific field of inquiry.[58]

References

1. Couper, A. S. *Liebigs Ann. Chem.* **1859**, *34*, 46–51.
2. Marshall, G. R. *J. Pept. Sci.* **2003**, *9*, 534–544.
3. Merrifield, R. B. *J. Am. Chem. Soc.* **1963**, *85*, 2149–2154.
4. Furka, A.; Sebestyen, F.; Asgedom, M.; Dibo, G. *Int. J. Pept. Protein Res.* **1991**, *37*, 487–493.
5. Furka, A. *Drug Discov. Today* **2002**, *7*, 1–4.
6. Furka, A.; Sebestyen, F.; Asgedom, M.; Dibo, G. *Abstracts of the 10th International Symposium on Medicinal Chemistry*; Budapest, Hungary, Aug 15–19, 1988; Elsevier: Amsterdam, **1989**, p 288.
7. Furka, A.; Sebestyen, F.; Asgedom, M.; Dibo, G. *Abstracts of the 14th International Congress on Biochemistry*; Prague, Czechoslaovakia, July 10–15, 1988; W, de Gruyter: Berlin, **1989**, Vol 5; p 47.
8. Guillier, F.; Orain, D.; Bradley, M. *Chem. Rev.* **2000**, *100*, 2091–2158.
9. Lebl, M. *Biopolymers (Peptide Sci.)* **1998**, *47*, 353–363.
10. Geysen, H. M.; Meloen, R. H.; Barteling, S. J. *Proc. Natl. Acad. Sci. USA* **1984**, *81*, 3998–4002.
11. Gerard, B.; Duvall, J. R.; Lowe, J. T.; *et al. ACS Comb. Sci.* **2011**, *13*, 365–374.
12. Scharn, D.; Wenschuh, H.; Reineke, U.; Schneider-Mergener, J.; Germeroth, L. *J. Comb. Chem.* **2000**, *2*, 361–369.
13. Houghten, R. A. *Proc. Natl. Acad. Sci. USA* **1985**, *82*, 5131–5135.
14. Pinilla, C.; Appel, J. R.; Houghten, R. A. *Meth. Mol. Biol.* **1996**, *66*, 171–179.
15. Zhang, S.-D.; Liu, G.; Xia, S.-Q.; Wu, P.; Zhang, L. *J. Comb. Chem.* **2002**, *4*, 131–137.
16. Gao, X.; Zhou, X.; Gulari, E. *Proteomics* **2003**, *3*, 2135–2141.
17. LeProust, E.; Pellois, J. P.; Yu, P.; *et al. J. Comb. Chem.* **2000**, *2*, 349–354.
18. Li, W.; Yan, B. *J. Org. Chem.* **1998**, *63*, 4092–4097.
19. Lee, K. J.; Angulo, A.; Ghazal, P.; Janda, K. D. *Org. Lett.* **1999**, *1*, 1859–1862.
20. Reed, N. N.; Dickerson, T. J.; Boldt, G. E.; Janda, K. D. *J. Org. Chem.* **2005**, *70*, 1728–1731.
21. Lam, K. S.; Lebl, M.; Krchňák, V. *Chem. Rev.* **1997**, *97*, 411–448.
22. Wilson, S. R.; Reinard, K. Techniques and Strategies for Producing Compound Libraries for Biological Screening. In *High-throughput Synthesis: Principles and Practices*; Sucholeiki, I., Ed.; Marcel Dekker: New York, **2001**, pp 55–128.
23. Ohlmeyer, M. H. J.; Swanson, R. N.; Dillard, L.; *et al. Proc. Natl. Acad. Sci. USA* **1993**, *90*, 10922–10926.
24. Still, W. C. *Acc. Chem. Res.* **1996**, *29*, 155–163.
25. Nestler, H. P.; Bartlett, P. A.; Still, W. C. *J. Org. Chem.* **1994**, *59*, 4723–4724.
26. Moran, E. J.; Sarshar, S.; Cargill, J. F.; *et al. J. Am. Chem. Soc.* **1995**, *117*, 10787–10788.
27. Nicolaou, K. C.; Xiao, X.-Y.; Parandoosh, Z.; Senyei, A.; Nova, M. P. *Angew. Chem. Int. Ed. Engl.* **1995**, *34*, 2289–2291.
28. Xiao, X.-Y.; Zhao, C.; Potash, H.; Nova, M. P. *Angew. Chem. Int. Ed. Engl.* **1997**, *36*, 780–782.
29. Guiles, J. W.; Lanter, C. L.; Rivero, R. A. *Angew. Chem. Int. Ed.* **1998**, *37*, 926–928.
30. Furka, A.; Dibo, G.; Gombosuren, N. *Curr. Drug Discov. Technol.* **2005**, *2*, 23–27.
31. Furka, A.; Christensen, J. W.; Healy, E.; Tanner, H. R.; Saneii, H. *J. Comb. Chem.* **2000**, *2*, 220–223.
32. Furka, A. *Magy. Kem. Lapja* **2003**, *58*, 5–10.
33. Lam, K. S.; Salmon, S. E.; Hersh, E. M.; *et al. Nature* **1991**, *354*, 82–84.
34. Vázquez, J.; Qushair, G.; Albericio, F. Combinatorial Chemistry, Part B. In *Methods in Enzymology*; Guillermo, A. M., Barry, A. B., Eds.; Academic Press: San Diego, **2003**, Vol. 369; pp 21–35.
35. Meldal, M. *Biopolymers* **2002**, *66*, 93–100.
36. Bacsa, B.; Gombosuren, N.; Lajos, L.; Furka, A.; Dibo, G. *Pept. Sci.* **2005**, *41*, 209–210.
37. Taylor, S. J.; Morken, J. P. *Science* **1998**, *280*, 267–270.
38. Houghten, R. A.; Pinilla, C.; Blondelle, S. E.; *et al. Nature* **1991**, *354*, 84–86.
39. Janda, K. D. *Proc. Natl. Acad. Sci. USA* **1994**, *91*, 10779–10785.
40. Carell, T.; Wintner, E. A.; Sutherland, A. J.; *et al. Chem. Biol.* **1995**, *2*, 171–183.
41. Ley, S. V.; Baxendale, I. R.; Bream, R. N.; *et al. J. Chem. Soc. Perkin Trans. 1* **2000**, 3815–4195.
42. Ley, S. V.; Schucht, O.; Thomas, A. W.; Murray, P. J. *J. Chem. Soc. Perkin Trans. 1* **1999**, 1251–1252.
43. Nishio, R.; Wessely, S.; Sugiura, M.; Kobayashi, S. *J. Comb. Chem.* **2006**, *8*, 459–461.
44. Schätz, A.; Long, T. R.; Grass, R. N.; *et al. Adv. Functional Mat.* **2010**, *20*, 4323–4328.
45. Wittmann, S.; Schätz, A.; Grass, R. N.; Stark, W. J.; Reiser, O. *Angew. Chem. Int. Ed.* **2010**, *49*, 1867–1870.
46. Chaudhry, P.; Schoenen, F.; Neuenswander, B.; Lushington, G. H.; Aubé, J. *J. Comb. Chem.* **2007**, *9*, 473–476.
47. Powers, D. G.; Casebier, D. S.; Fokas, D.; *et al. Tetrahedron* **1998**, *54*, 4085–4096.
48. Frisbee, A. R.; Nantz, M. H.; Kramer, G. W.; Fuchs, P. L. *J. Am. Chem. Soc.* **1984**, *106*, 7143–7145.
49. Fenster, E.; Long, T. R.; Zang, Q.; *et al. ACS Comb. Sci.* **2011**, *13*, 244.
50. Anderson, M. O.; Sherrill, J.; Madrid, P. B.; *et al. Bioorg. Med. Chem.* **2006**, *14*, 334–343.
51. Damm, M.; Kappe, C. *Mol. Divers.* **2009**, *13*, 529–543.
52. Horváth, I. T.; Rábai, J. *Science* **1994**, *266*(5182), 72–75.
53. Zhang, W. *Tetrahedron* **2003**, *59*, 4475–4489.
54. Hoshino, M.; Degenkolb, P.; Curran, D. P. *J. Org. Chem.* **1997**, *62*, 8341–8349.
55. Curran, D. P.; Luo, Z. *J. Am. Chem. Soc.* **1999**, *121*, 9069–9072.
56. Sahoo, H. R.; Kralji, J. G.; Jensen, K. F. *Angew. Chem. Int. Ed.* **2007**, *46*, 5704–5708.
57. Styring, P.; Parracho, A. I. R. *Beilstein J. Org. Chem.* **2009**, 5, No. 29.
58. Kennedy, J. P.; Williams, L.; Bridges, T. M.; *et al. J. Comb. Chem.* **2008**, *10*, 345–354.

9.02 High-Throughput Analysis for High-Throughput Experimentation in Organic Chemistry

W Schafer, X Bu, X Gong, LA Joyce, and CJ Welch, Merck Research Laboratories, Rahway, NJ, USA

© 2014 Elsevier Ltd. All rights reserved.

9.02.1	**Introduction**	28
9.02.2	**A Variety of Approaches for Fast Analysis**	28
9.02.3	**Chromatography**	29
9.02.3.1	High-Performance Liquid Chromatography	30
9.02.3.2	High Temperature Chromatography	31
9.02.3.3	Supercritical Fluid Chromatography	32
9.02.3.4	Gas Chromatography	32
9.02.3.5	Monolithic Columns for HTA Chromatography	34
9.02.3.6	Mass Spectrometry Detection for Fast Chromatographic Separations	34
9.02.3.7	Multiple Injections in a Single Experimental Run	36
9.02.3.8	Practical Considerations for HTA Chromatography	36
9.02.4	**Parallel Chromatography Approaches for HTA**	40
9.02.5	**Parallel Electrophoresis Approaches for HTA**	45
9.02.6	**Nonchromatographic Approaches to HTA: Mass Spectrometry**	45
9.02.7	**Sensor Technologies for HTA**	48
9.02.8	**Conclusion and Future Prospects**	51
References		51

9.02.1 Introduction

In recent years high-throughput experimentation (HTE) has emerged as an important enabling technology in the field of organic synthesis.[1–10] The principal advantage of the HTE approach is the ability of a single worker to perform dozens or even hundreds of experiments in a single day. This increased rate of experimentation requires a concomitant increase in the rate of analytical measurements relative to methods traditionally employed by synthetic chemists. Although the collection of 10 NMR spectra or 10 high performance liquid chromatography (HPLC) chromatograms in a single day is fairly straightforward, the daily analysis of hundreds or thousands of samples using these approaches would lead to a significant bottleneck. Consequently, high-throughput analysis (HTA) tools are becoming essential for enabling the smooth functioning of newly emerging HTE workflows in organic chemistry.[11] Indeed, HTA is now increasingly becoming an integral component in newly introduced HTE platforms.

In the past, the inexpensive and straightforward technique of thin-layer chromatography, in combination with NMR spectroscopy, dominated the analytical support of synthetic chemistry. Beginning in the 1980s, the superior resolving power of HPLC led to the emergence of HPLC and related chromatographic techniques, like supercritical fluid chromatography (SFC), as the preferred techniques for analytical support of synthetic chemistry. Over the past 20 years, synthetic chemists have become comfortable with the use of these techniques for reaction progress monitoring, the assessment of product purity and the evaluation of enantioenrichment. Researchers have grown accustomed to a typical analysis time of 15–30 min per sample; perfectly reasonable for the analysis of a few samples per day, but completely inappropriate for the analysis of 96-well microplates coming from HTE investigations. Decreasing assay cycle time from 15 to 5 min per sample decreases the 'plate time' (time required to analyze a single 96-well microplate) from 24 h to only 8 h. Further reduction of the analysis cycle time to 2 min, 1 min, or even less can afford the highly desirable outcome of obtaining HTA experimental results in the same day in which the HTE experiments are performed.

In this review, the authors survey the rapidly growing field of HTA for supporting synthetic chemistry, covering well-established analytical techniques such as multiparallel thin-layer chromatography as well as a plethora of recently introduced chromatographic and spectroscopic techniques. Finally, the authors survey recently introduced chemical sensor-based approaches for HTE that offer the promise of ultrafast analysis, potentially enabling the next generation of HTE speed and productivity improvements. Overall, the authors seek to provide interested researchers with a background on the emerging field of HTA than can facilitate a more widespread adoption of HTE in organic synthesis.

9.02.2 A Variety of Approaches for Fast Analysis

A variety of techniques can potentially be used for HTA support of organic chemistry investigations. **Figure 1** summarizes some of the pros and cons of these various approaches for providing HTA support for HTE organic chemistry investigations.

 doi:10.1016/B978-0-08-097742-3.00921-6

	Universality	Quantitation	Mixtures	Speed
Optical spectroscopy	*	*	*	****
Mass spectrometry	**	**	*	***
NMR spectroscopy	***	****	**	*
Chromatography	****	***	****	**
Sensors	*	*	*	****

Figure 1 Assessment of suitability of various analytical techniques for HTA.

The term 'universality' refers to the relative ability of the technique to work for any possible analysis problem. Chromatography and NMR are the most universal techniques, with the edge going to chromatography because of a superior ability to perform trace analysis and assessment of enantiopurity.

The term 'quantitation' refers to the relative ability of the technique to measure absolute concentration of compounds of interest. Chromatography is generally superior to MS and optical spectroscopy approaches in terms of quantitation, although calibration with authentic standards of known concentration is required, and 'response factors' are compound-specific. NMR is the preferred technique for quantitation, as relative concentrations can be determined without the use of standards and absolute concentrations of all components within a mixture can be determined with a single standard.

The term 'mixtures' refers to the relative ability of the technique to handle complex mixtures. Chromatography is particularly good at this task, as the separation of the individual components in space and time aids in accurate quantitation and analysis. In contrast, spectroscopic measurements of complex mixtures are more vulnerable to signal overlap and interference problems.

Finally, the term 'speed' refers to typical sample analysis cycle time for the technique, as currently configured. It is here that the optical spectroscopy and sensor technologies show an edge, with incredibly fast analysis cycle times that hold considerable promise for HTA, if the other shortcomings noted above can be overcome. In contrast, cycle time for NMR analysis is typically several minutes, although subminute cycle times may become possible at some point in the future. Current cycle times for HTA chromatography often break the 1-min barrier.

9.02.3 Chromatography

Overall, chromatography shows an advantage over other analytical techniques for general use in HTA in support of organic synthesis investigations, so it is not surprising that many researchers have focused on applying routinely used chromatography tools to the problem of HTA. A major focus of recent chromatographic research has centered on different approaches for speeding chromatographic resolution and cycle time. Chromatography involves the selective adsorption of analyte molecules by a chromatographic stationary phase. This stationary phase is packed into a chromatographic column, and compounds of interest are swept through the column by a flow of eluent or mobile phase, with the time-based detection of compounds eluting from the column providing a chromatogram, a graphical record of the separation (Figure 2).

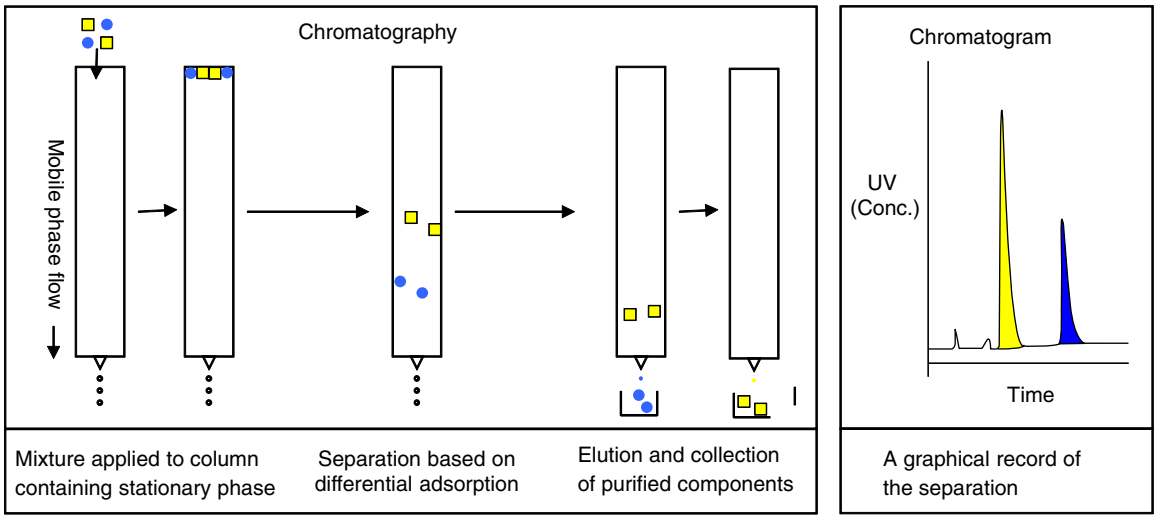


Figure 2 Principles of chromatographic separation. Application of a mixture of compounds to a column containing a chromatographic stationary phase and elution with mobile phase leads to chromatographic resolution of compounds having differing adsorption on the stationary phase. Time-based detection of compounds eluting from the column providing a chromatogram, a graphical record of the separation.

A variety of factors influence the speed with which a chromatographic separation can be carried out, as described in the fundamental chromatographic theory worked out decades ago. Contributions by pioneers such as Giddings,[12] Guichon,[13] and Katz and Scott[14] led to the derivation of equations that define the minimum separation time and maximum resolving power for a given chromatographic system. For a given column size under isocratic (nongradient) conditions, the relationship can be expressed as:

$$\left(\frac{t}{N}\right)_{\lim} \propto \frac{(1+k')}{D_{\mathrm{m}}} d_p^2 \tag{1}$$

where t is the time required to elute the analyte of interest, N is the efficiency (number of theoretical plates) of the chromatographic system, D_{m} is the diffusion rate constant of the analyte in the mobile phase, k' is a measure of how well the analyte is retained (retention factor), and d_{p} is the particle size of the column packing. This equation immediately suggests the following several factors that will be helpful for achieving faster separations:

- 'Factors that tend to increase the rate of diffusion of the analyte in solution are preferred for faster separations.' Chromatography is a diffusion-limited process and factors that increase the rate at which the analytes can enter and exit the stationary phase facilitate fast and efficient chromatographic separations. Factors that influence the rate of diffusion of a molecule in solution include the viscosity of the solvent used in the mobile phase, the thickness of the adsorbent, and the temperature of the chromatographic system. In general, less viscous solvents afford increased compound diffusion and better chromatographic peak shape (assuming otherwise similar solvating properties). Consequently, methanol is generally preferred to ethanol as an eluent for reversed phase chromatography, and acetonitrile is generally preferred to both of these alcohols.[15] Similarly, the increased diffusion obtained at higher temperatures can lead to improved chromatographic performance, although temperature-induced changes in chromatographic adsorption equilibria also come into play.
- 'In general, smaller particles are preferred for faster separations.' The exponential relationship between particle size and separation time makes decreasing particle size an obvious priority in developing faster chromatographic assays. Considerable recent efforts by researchers and manufacturers have gone into the reduction of particle size from the traditional 5 μm diameter (or larger) particles to an emerging standard of less than 2 μm. By decreasing the particle size from 5 to 1.8 μm, the same resolution can be obtained in one-third of the time. It should be noted that the use of smaller particles affords greater resistance to flow, leading to increased backpressure for a column of a given size operating at a given flow rate ($\Delta P = 1000\, F\eta L/(\pi r^2 {d_{\mathrm{p}}}^2)$ where F is the volumetric flow rate, η is the viscosity, L the column length, r the internal radius, and d_{p} the particle size of the packing). A number of vendors have introduced instruments in recent years capable of operating at these substantially higher backpressures.[16] Research aimed at the development of extremely small 'nanoparticle' stationary phases is beginning to produce some interesting results.[17]
- 'Higher chromatographic efficiency (N, theoretical plates) generally leads to faster separations.' More efficient columns afford narrower peaks, which allow greater resolution between peaks of interest. This 'surplus' resolution can allow the adjustment of other factors such as eluent composition, flow rate, temperature or column length to afford faster chromatographic separations.
- 'Shorter chromatographic retention (k) generally leads to faster separations.' This observation is to some degree self-explanatory, but it is important to grasp the concept that for a given chromatographic separation system (column, mobile phase, flow rate, temperature) there is a minimum retention factor at which the compounds of interest are resolved. Retention below this value will lead to incomplete resolution, and, importantly, 'retention greater than this value will lead to surplus resolution,' which amounts to wasted time. Therefore, decreasing retention to near the minimum required for the required resolution is important for minimizing analysis time.

9.02.3.1 High-Performance Liquid Chromatography

A number of strategies for obtaining faster chromatographic separations have emerged in recent years, and the field is still in considerable flux. The relationship between the resolving power and the speed of analysis is a complicated one[18] and judicious choices of columns and equipment are important for maximizing throughput. Typical approaches today involve the use of smaller particle columns operating at higher pressures, often at elevated temperature, and using shorter columns. An example is shown in Figure 3, in which a conventional HPLC method of 15 min has been reduced to less than 2 min while maintaining the same resolution (R_{av}).[19]

As detailed above, one of the disadvantages of using smaller particles is the dramatic increase in column backpressure experienced as particle size is reduced. An innovative strategy to counteract this pitfall is the development of fused core particles.[20] By fusing a porous silica layer onto a solid silica core it is possible to obtain 85% of the efficiency of a sub-2 μm particle column at the optimal flow rate with half the back pressure and only a modest decrease in sample loading capacity.[21] As fused particles are bigger, a larger pore column frit may be used which reduces clogging issues sometimes associated with the use of small particle size columns. Figure 4 shows a comparison between chromatography carried out with either sub-2 μm particles or core–shell particles. The lower backpressure obtained with the core–shell particle columns allows greatly reduced separation speed on

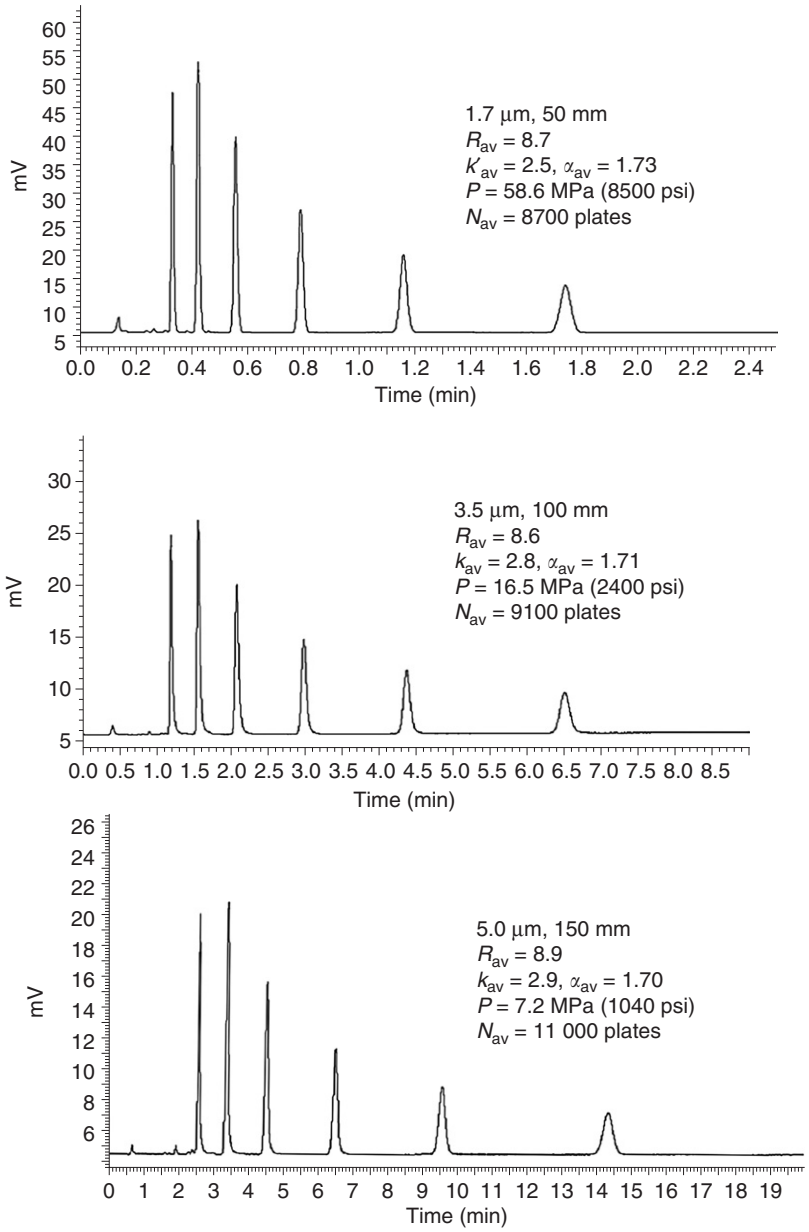


Figure 3 Analysis cycle time of conventional HPLC separations can often be improved 3–5 × by the use of smaller particles, faster flow rates, shorter columns, and increased pressure. Reprinted with permission from Abrahim, A.; Al-Sayah, M.; Skrdla, P.; *et al. J. Pharm. Biomed. Anal.* **2010**, *51*, 131–137.

conventional HPLC instruments, or even faster separations on next generation instruments with the ability to operate at higher pressures.

9.02.3.2 High Temperature Chromatography

As previously noted, temperature has a beneficial effect on the separation speed by decreasing the viscosity of the mobile phase and consequently increasing the diffusion rate of analytes in the mobile phase. Decreasing the viscosity of the mobile phase also has the added practical advantage of lowering the operating pressure at a given flow rate ($\Delta P = 1000\, F\, \eta\, L/(\pi r^2 d_p^2)$, where F is the volumetric flow rate, η is the viscosity, L the column length, r the internal radius, and d_p the particle size of the packing) as well as allowing higher flow rates without a loss in column efficiency.[22] Temperature can also alter chromatographic retention and selectivity[23] and indeed can be used as an independent parameter for optimization in chromatographic method development.

The advantages of performing chromatography at elevated temperatures have been extensively studied and developed as a fast chromatographic technique[24,25] with temperatures up to 200 °C being employed to afford a 3–5 × reduction in assay times.

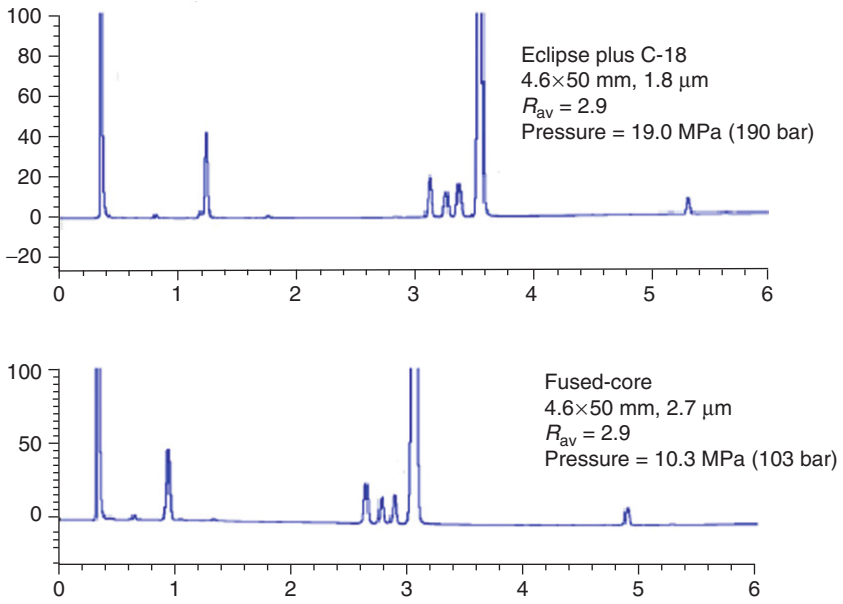


Figure 4 Comparison of backpressure obtained by sub-2 μm vs. fused core particle columns. Reprinted with permission from Wu, Naijun; Clausen, A. M. *J. Sep. Sci.* **2007**, 30, 1167–1182.

Owing to the poor stability of conventional stationary phase materials at such temperatures, high temperature Liquid Chromatography (HTLC) generally requires silica-based columns containing hybrid or modified silica, metal oxide phases (zirconia based), porous graphite carbon phases, and organic polymer-based phases. In addition, conventional chromatography columns are sometimes used at temperatures in excess of 100 °C. HTLC is frequently used in two-dimensional liquid chromatography,[26] where speed in the second chromatographic dimension is critical.[27]

9.02.3.3 Supercritical Fluid Chromatography

Previously, it is seen how the diffusion rate of the analyte in the mobile phase is a critical parameter for achieving fast chromatographic separations. In SFC pressurized carbon dioxide in supercritical or subcritical form replaces hydrocarbon solvents such as heptane that are typically used in normal phase chromatographic separations.[28] Owing to the much faster diffusion rates obtained with supercritical CO_2 relative to hydrocarbon solvents, the resulting chromatographic separations, in addition to being 'greener,'[29] generally show improved peak shape. The lower viscosity of supercritical CO_2 relative to hydrocarbon solvents leads to a reduction in backpressure, allowing flow rates to be increased considerably. Combined, both of these factors result in significant speed advantages for SFC over normal phase HPLC, which helps to explain the increasing popularity of the technique, especially for the chromatographic separation of enantiomers using chiral stationary phases.

Figure 5 illustrates the steps taken in converting a typical chiral SFC screening result to a fast separation method. In this study, a number of different analytical methods were compared to determine best approaches for HTA of the Soai reaction.[30] The separation obtained in the initial column screen takes approximately 20 min, but considerable excess resolution is available, making the conversion to a faster 5 min isocratic separation using a stronger eluent (40% MeOH/CO_2) straightforward (Figure 5(b)). Further increase in speed was obtained by increasing flow rate from 1.5 to 3.5 ml min^{-1} (Figure 5(c)). At this point, system backpressure is at a maximum, however considerable excess resolution is apparent, allowing the use of a shorter column, with fewer theoretical plates, to afford a dramatically shorter separation time of only 0.6 min (Figure 5(d)).

9.02.3.4 Gas Chromatography

Analysis cycle time for gas chromatography (GC) has historically been rather slow; yet the technique of GC offers some strong advantages for fast chromatography. Owing to the excellent diffusion rate of compounds in the gas phase, chromatographic peak shapes in GC can be extremely sharp. Although limited to samples that can be volatilized, fast GC is often useful for analysis of low molecular weight starting materials or early synthetic intermediates. Figure 6 illustrates how a conventional 20 min GC screening result for a chiral separation can be converted to a fast GC separation.[31] In the first step, the gradient temperature ramp is replaced with an isothermal method at 105 °C (Figure 6(a)). Not only does this reduce the chromatographic run time to less than 3 min, but the time required to wait for oven cooling between injections is eliminated. Although further increase in temperature is possible, this approach would lead to coelution of the peaks of interest with the large solvent peak at the beginning of the chromatogram. Consequently, a change to a shorter column (4.7 vs. 30 m) and operation at the slightly lower temperature

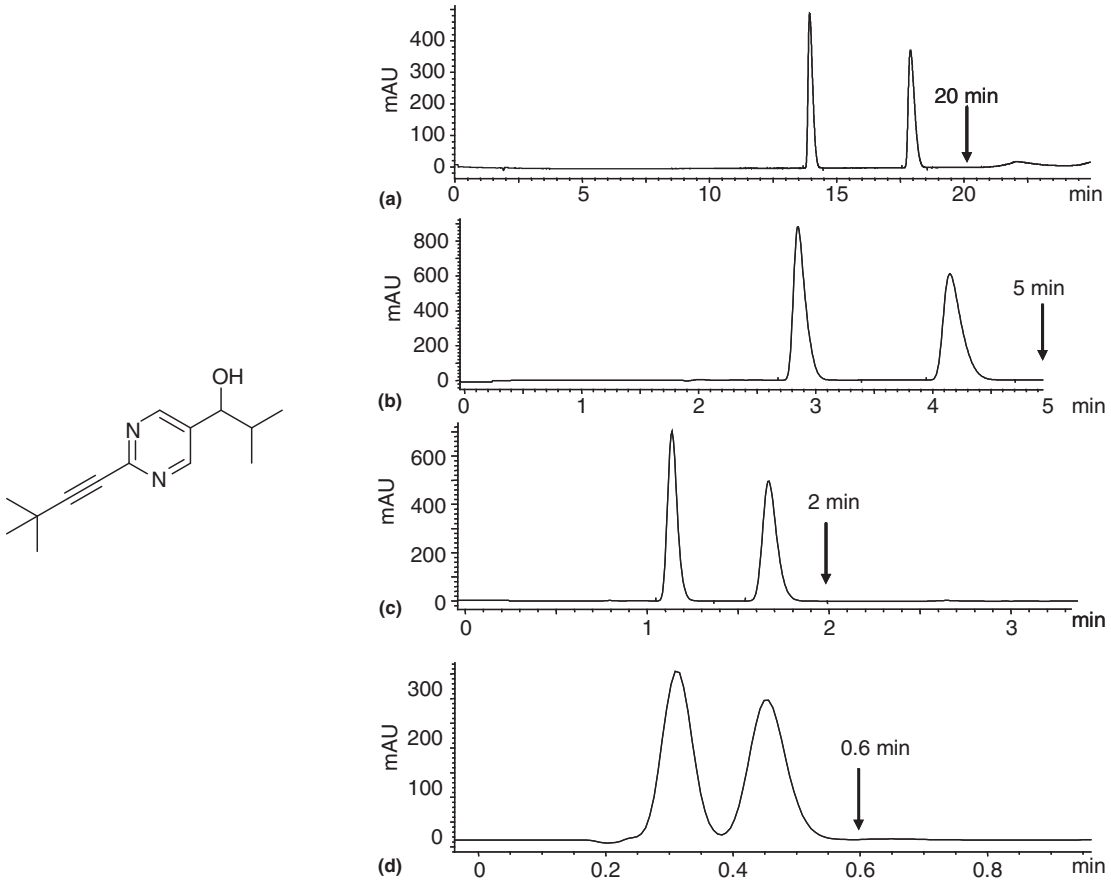


Figure 5 Conversion of an initial chiral SFC screening result into a HTA method for Soai alcohol. (a) Standard gradient method used in chiral SFC screening: Chiralcel OF column (250 × 4.6 mm); 4% MeOH/CO_2 for 4 min, then ramp to 40% MeOH/CO_2 @ 2%/min; 1.5 ml min^{-1}; UV 215 nm; 20 MPa (200 bar) outlet pressure, 35 °C. (b) Isocratic method using polar eluent: 40% MeOH/CO_2. (c) Isocratic method using polar eluent and faster flow rate: 40% MeOH/CO_2; 3.5 ml min^{-1}. (d) Optimized method using short column: Chiralcel OF column (50 × 4.6 mm); 30% MeOH/CO_2 @ 4.0 ml min^{-1}; all examples using 215 nm UV detection, 20 MPa (200 bar) outlet pressure and 35 °C column temperature.

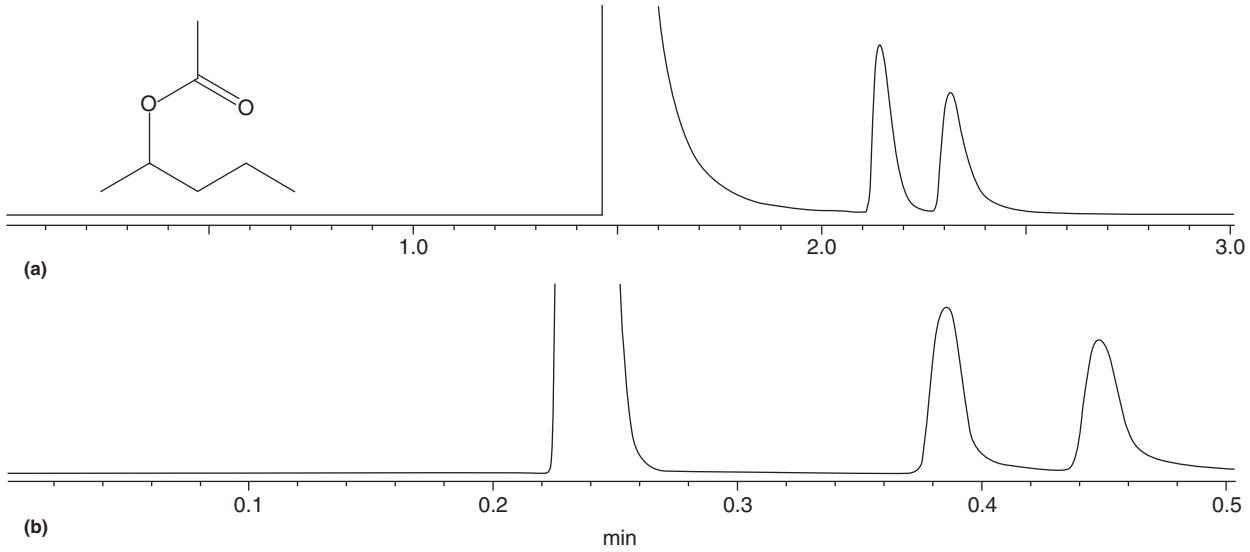


Figure 6 Fast analysis by GC on βDex-se chiral column. (a) Conversion of 20 min gradient temperature method to fast isothermal method, 30 m × 250 μm i.d. × 0.25 μm d_f column, 105 °C. (b) Column length shortened, temperature reduced to 90 °C to afford < 0.5 min separation time. Reproduced from Schafer, W.; Hamilton, S. E.; Pirzada, Z.; Welch, C. J. *Chirality* **2012**, *24*, 1–4, with permission from Wiley.

of 90 °C affords baseline separation in less than 0.5 min (Figure 6(b)). Indeed, surplus resolution in the separation suggests that even faster separations could be possible.

It should be noted that equation 1 is still generally applicable in open-tubular GC if the diameter of the column is substituted for the particle size and an additional multiplicative term (p_i/p_o) is added to account for the effect of the pressure drop across the column on the gaseous mobile phase. Thus for fast separations the smallest i.d. columns should be used (typically 100 or 180 μm for achiral phases). As shown in Figure 6, capillary silica columns are easily cut to the exact length required for a particular separation thereby facilitating fast GC method development. Additional speed is obtained when hydrogen is used as the carrier gas and when a vacuum is applied to the outlet as in GC/MS applications.[32]

For cases when thermal gradients are needed due to disparity in the volatility of the analytes of interest, several vendors have commercialized low thermal mass technology for fast GC applications. In these instruments, the column itself is wrapped in a resistive heating element to overcome the inherent slowness in heating and cooling the entire column oven. This allows extreme temperature ramps of greater than 600 °C min^{-1} and cooling times of a 1 min.[33]

Recently, Trapp and coworkers have developed an ultra HTA GC technique in which rapid injections leads to massively overlapping peaks, which are subsequently deconvoluted to obtain analysis cycle times of only a few seconds per sample. Although the technique is still evolving, and may not be suitable for all HTE scenarios, it certainly merits additional consideration.[34,35]

9.02.3.5 Monolithic Columns for HTA Chromatography

Monolithic columns are another approach that is frequently used for fast chromatography.[36–39] Rather than using small particles that are packed into a chromatographic column, monolith columns are generated *in situ* by polymerization of monomers in the presence of porogens and other templating molecules. The resulting polymer is continuous throughout the column, but contains pores through which the chromatographic eluent can flow. In addition to the smaller pores required for high performance chromatography, monolith columns are designed with larger flow through pores, which help to allow fast flow through the column with greatly reduced backpressure relative to what would be obtained with conventional particle-filled columns. Consequently, monolith columns are typically operated at significantly higher flow rates relative to conventional particle-filled columns. This leads to the generation of waste eluent, but this problem can be counteracted by using narrow diameter monolith columns. The use of monolithic columns in microfluidic channels is especially attractive, as these columns can be 'polymerized in place.'

9.02.3.6 Mass Spectrometry Detection for Fast Chromatographic Separations

The topic of HTA using mass spectrometry will be covered in a subsequent section, but the use of MS detection is so closely intertwined with modern analytical chromatographic methods that no discussion of HTA chromatography can be complete without it. LC–MS techniques are widely used in pharmaceutical analysis, where the ability to selectively monitor the mass of a particular product, intermediate or impurity is very convenient for reaction screening. The ability to selectively monitor a mass range is also very valuable. A commonly used approach for HTA analysis of coupling reactions is to set the beginning of the mass range window to be larger than either of the coupling partners, an approach which greatly simplifies 'needle in a haystack' experimental approaches.[7]

An important benefit of MS detection is the ability to deconvolute overlapping chromatographic peaks. Figure 7 illustrates a particular case where HTA analysis of the enzymatic reduction of a diaryl ketone was desired. Chromatographic separation of the enantiomers of the product alcohol was relatively straightforward; however peak overlap from the starting ketone was very severe, requiring analysis times of nearly an hour for complete resolution. In such cases, MS deconvolution can be used to separate the signal coming from species of different molecular weight, thereby enabling faster separations.[40] Care must be taken that sample overlap does not lead to either enhancement or suppression of the ion count of interest, but this is easily determined by spiking and coinjection experiments, and is generally not a significant problem for species showing significant chromatographic retention. However, coelution of the species of interest with baseline components such as solvents, base additives or other abundant species can severely impede accurate quantitation. Consequently, direct MS analysis without chromatographic separation is often unacceptable for HTA of complex mixtures containing interfering matrix components.

One of the disadvantages of using mass spectrometry for chromatographic detection is the very high cost of current mass spectrometers. There has been considerable recent progress in the development of smaller, less expensive mass spectrometers for routine analysis. Although such instruments are not well suited for challenging trace analysis and bioanalysis work, they often are adequate for routine HTA to support synthetic chemistry, where sample quantity is rarely limiting.[41] When more complex MS detection is necessary, the use of multiplexed chromatography can help to derive maximum value from this expensive investment.[42–44] This approach is frequently used in pharmaceutical bioanalysis, where expensive LC–MS/MS instrumentation is required for detection and quantitation of the compounds of interest in complex biological fluids to support drug metabolism and pharmacokinetic studies. Conventional LC–MS/MS analysis typically only utilizes the MS detector for a small portion of the total analysis cycle time, when the species of interest are eluting from the column. For much of the analysis cycle time (sample loading, early elution, washing, column equilibration) the expensive mass spectrometer is essentially sitting idle. Multiplexed LC–MS/MS systems utilize several parallel HPLC instruments plumbed into a single MS detector. Samples are introduced to the

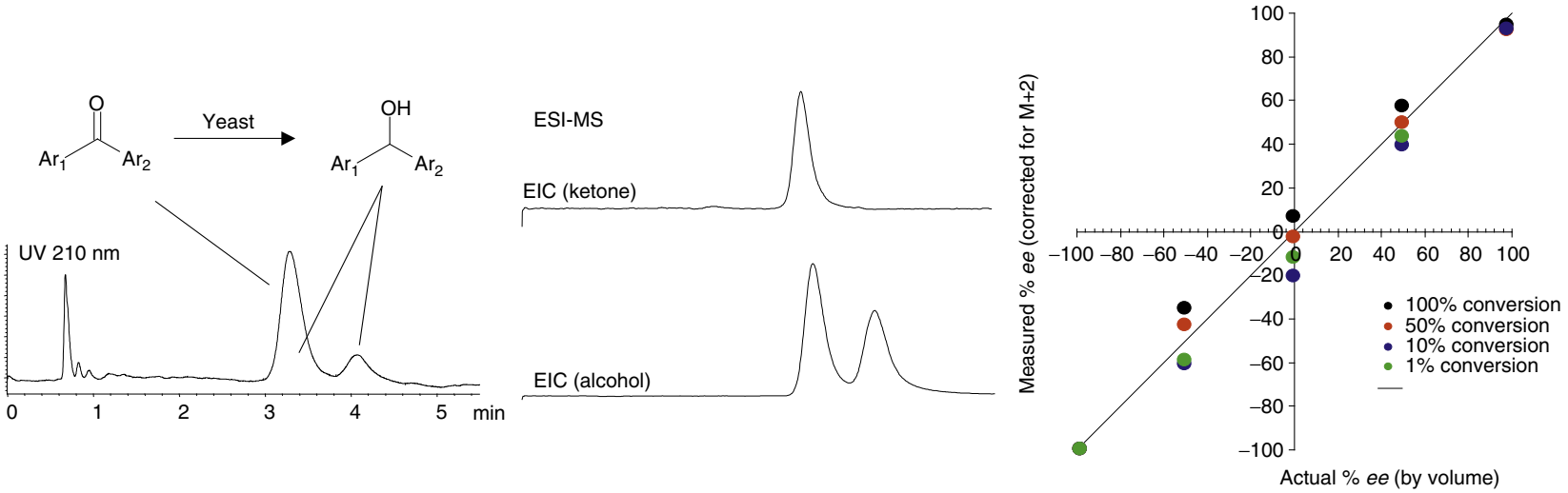


Figure 7 Use of mass spectrometry detection to deconvolute overlapping peaks.[42] EICs for species of different molecular weight (ketone and alcohol) allow deconvolution of overlapping peaks, enabling rapid quantitation acceptable for 'ballpark' reaction screening.

HPLC columns in a staggered fashion under software control, so the analytes of interest reach the mass spectrometer from each column sequentially without overlap.

9.02.3.7 Multiple Injections in a Single Experimental Run

Multiple injections in a single experimental run (MISER) chromatography is a useful tool for HTA that addresses significant problems associated with traditional LC–MS analysis.[45] The technique employs sequential injections of different samples into the same chromatographic run, with just enough chromatographic retention of the components of interest to allow separation from potentially interfering matrix components. MISER chromatography also affords a simplified chromatogram that records the relative amounts of the components of interest in each sample, which is helpful in quickly interpreting experimental results. This approach to HTA offers a number of advantages over conventional analytical chromatography approaches that employ a series of individual chromatographic runs to produce integrated peak area data, which are stored in individual data files, then transferred to a spreadsheet program and graphed to allow interpretation of experimental results. The simpler and more direct MISER chromatography approach produces a single chromatogram that also serves as a graph, summarizing the results of the entire HTE study – a significant advantage in simplification and time saving.

The MISER approach is best suited for optimization workflows with large groups of samples containing different levels of the same principal components. When all wells begin with the same amount of starting materials, the resulting MISERgram allows rapid and convenient comparison of the effectiveness of the various treatments. Several examples are illustrated in **Figure 8**.

High-throughput screening for impurity removal generates large number of samples, as many possible adsorbents and conditions are available. **Figure 8(a)** shows a MISERgram for a single row of wells from a HTE treatment of a solution of an impure pharmaceutical intermediate with a number of process adsorbents.[46] Comparison of the extracted ion chromatogram (EIC) at the m/z corresponding with product shows that none of the treatments significantly decrease product concentration, whereas comparison of the EIC at the m/z corresponding with the impurity shows that several of the treatment conditions have been very effective in reducing impurity levels.

Figure 8(b) shows a similar MISERgram from the HTE assessment of a number of enzymes for carrying out a lipase reaction, with EIC analysis highlighting signals from starting material and product. Since all wells begin with the same amount of substrate, the relative amounts of remaining substrate, the extent of product formation, and the extent of conversion can quickly be assessed by visual inspection, without the need for integration, data manipulation, or graphing. **Figure 8(c)** shows a similar use of MISER chromatography for analysis of samples coming from the HTE screening of liquid–liquid extraction conditions, whereas **Figure 8(d)** shows a MISERgram time course of product formation in a reaction carried out in an HPLC vial.

MISER chromatographic analysis was recently applied in an innovative HTE platform for general reaction improvement.[47] In this system, a wide variety of additives shown to be effective for improving various kinds of reactions were assembled into a screening kit consisting of four 96-well microplates. These additives range from Lewis acids, bases, halide ions, and alkali ions to transition metals, radical inhibitors, radical initiators, oxidants, antioxidants, etc. Although most of these additives have no effect or even decrease the yield of the reaction under study, occasional 'hits' identify additives that are effective for increasing reaction yield, sometimes turning up unexpected avenues for improvement. The example shown in **Figure 9** illustrates how a single chemist can set up and analyze $\sim$500 different reaction conditions in a single day using only 370 mg of substrate, leading to the discovery of additives that improve product yield while enabling the reaction temperature to be significantly lowered.

MISER chromatography can also be used for enantiopurity analysis. The example in **Figure 10(a)** shows a MISERgram for the injection of racemic binol with a period of 2 min.[47] Significant excess resolution is evident, allowing the injection period to be decreased to 0.7 min (**Figure 10(b)**), and enabling the analysis of 48 samples of differing enantiopurity in only 36 min (**Figure 10(c)**).

Figure 11 shows an example of achiral chromatography with circular dichroism (CD) detection, a convenient approach for ballpark estimation of enantiopurity.[32] The UV signal gives a sense of the amount of product present, whereas the CD signal gives a sense of the amount of optical activity. The ratio of the CD to UV signal can be used to afford a composite signal that is proportional to enantiomeric enrichment, although a quick visual inspection of the two raw signals can be used to identify wells with significant amounts of the product of interest, and with the correct absolute configuration. This approach is especially useful for quick assessment of the extent and sense of enantioenrichment provided by enzymes or catalysts.

9.02.3.8 Practical Considerations for HTA Chromatography

A variety of factors must be considered when developing a method for HTA chromatographic analysis:

- Although the fastest possible analysis methods are preferred, the amount of time and effort invested in further optimization of an already fast method must be weighed against the potential for significant time savings that the improved method will ultimately provide. If tens of thousands of samples will be analyzed with the method, significant efforts to optimize speed may be justified. However, if only a single 96-well plate will be analyzed, a less optimized 'fit for purpose' method may be more appropriate.
- In cases where the components of interest must be resolved from a variety of other species with vastly different retentions, gradient elution methods are typically preferred. Researchers typically begin with a generic fast gradient method with high peak

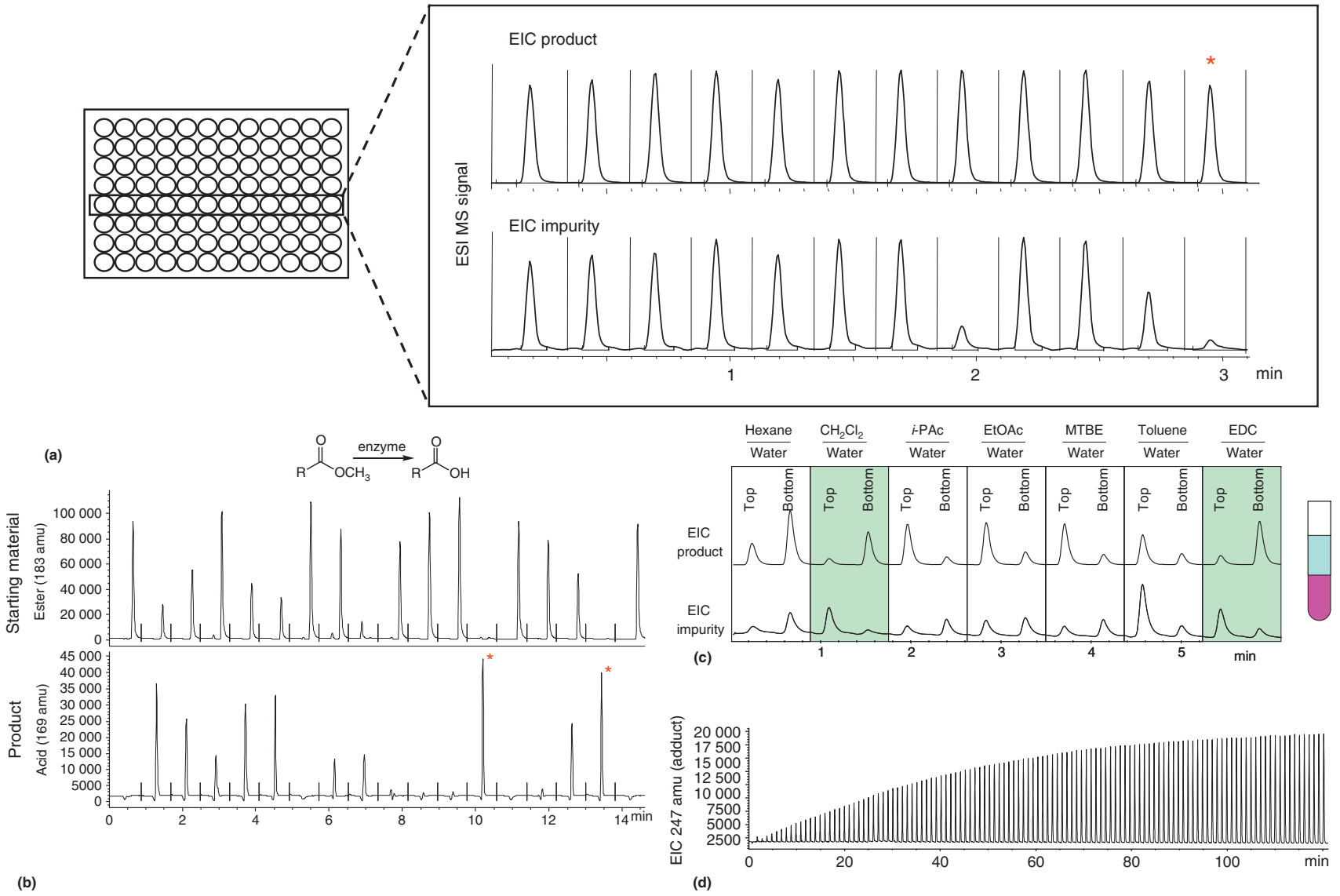


Figure 8 MISER chromatography for HTA in support of HTE process research investigations – 'the chromatogram is the graph.' (a) Identification of adsorbents for impurity removal, (b) screening enzymes for ester hydrolysis, (c) screening binary solvent extractions, and (d) reaction time course analysis.

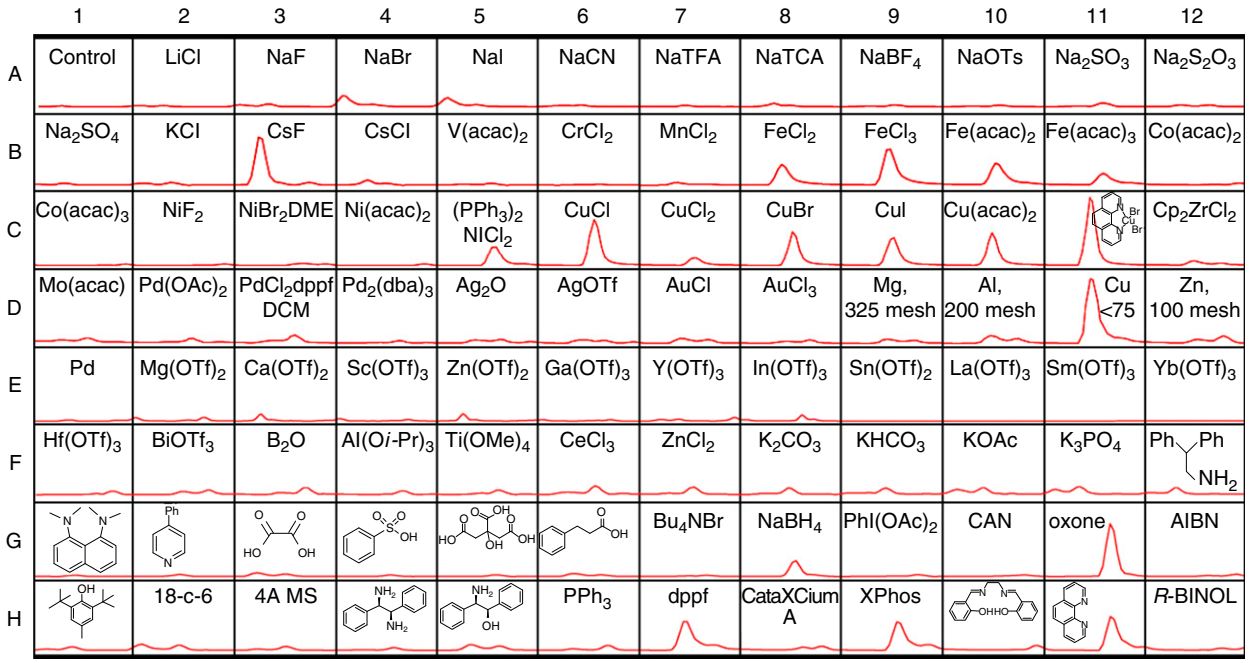


Figure 9 MISER chromatography enables microscale reaction improvement platform, designed for rapid improvement of difficult chemistry transformations.[49]

capacity and perform minimal fine-tuning on the gradient parameters to reduce the separation speed to an acceptable level. In cases where the components of interest are not contaminated with species with vastly different retentions, isocratic elution may be preferred, as this eliminates delays caused by the need for restoring the original eluent conditions at the beginning of each chromatographic run.

- Gradient dwell volume (or time) is a critical factor to consider in selecting optimal equipment or conditions for HTA chromatographic separations. The gradient dwell volume is the volume of eluent that must flow through the system before a change in composition at the pumps reaches the head of the column. Changes in eluent composition at the pumps show a delayed arrival at the column owing to the need for the eluent with the new composition to traverse the solvent mixer and connecting tubing before reaching the column. This delay time can be a minute or more for some conventional chromatographic systems, which places an unacceptable lower limit on the fast gradient separation speed that can be achieved with such systems. Gradient dwell volume can be drastically reduced by careful instrument design, minimizing the volume devoted to mixing, and reducing volume of connecting tubing. Most modern HPLC instrumentation incorporates such design changes, with significantly reduced gradient dwell volumes relative to the previous generation of instruments. Interestingly, the proportional volume devoted to mixing is much smaller for microfluidic chromatography, where rapid flow through a narrow capillary can effectively mix solvents. This inherent advantage of microcapillary chromatography helps to explain the continued growth of this new field, and suggests that microflow chromatography will ultimately displace the 4.6×250 mm column standard that has been in use for many years.
- Minimizing extracolumn volume is another consideration that is very important for obtaining optimal chromatographic results. The extracolumn volume refers to the volume between the sample injector and the head of the column, and the volume between the end of the column and the detector. The amount of time the peaks of interest spend traversing this volume should be kept to an absolute minimum, otherwise diffusion, mixing, and band broadening can occur, leading to degradation of chromatographic peakshape. In practice, the diameters for all connecting tubing should be minimized, ensuring that all fitting connections are snug and contain no voids. The width of a chromatographic peak is the sum of dispersion in the column plus any dispersion that occurs outside the column:

$$\sigma^2_{\text{total}} = \sigma^2_{\text{column}} + \sigma^2_{\text{injector}} + \sigma^2_{\text{tubing}} + \sigma^2_{\text{detector-cell}} + \sigma^2_{\text{detector-electronics}}$$

To prevent losses in column efficiency, the extracolumn volume contributions of the injection, tubing, and detector should be limited to 10% of the column volume. This becomes challenging with new column technologies that typically use shorter column lengths and smaller inner diameters. A typical 4.6×50 mm sub-2 μm column or 4.6×100 mm fused core column used in HPLC have column volumes of approximately 0.5 and 1 ml, respectively. Special care must be taken when using these new low band dispersion column technologies especially when legacy HPLC equipment is used.[48–50]

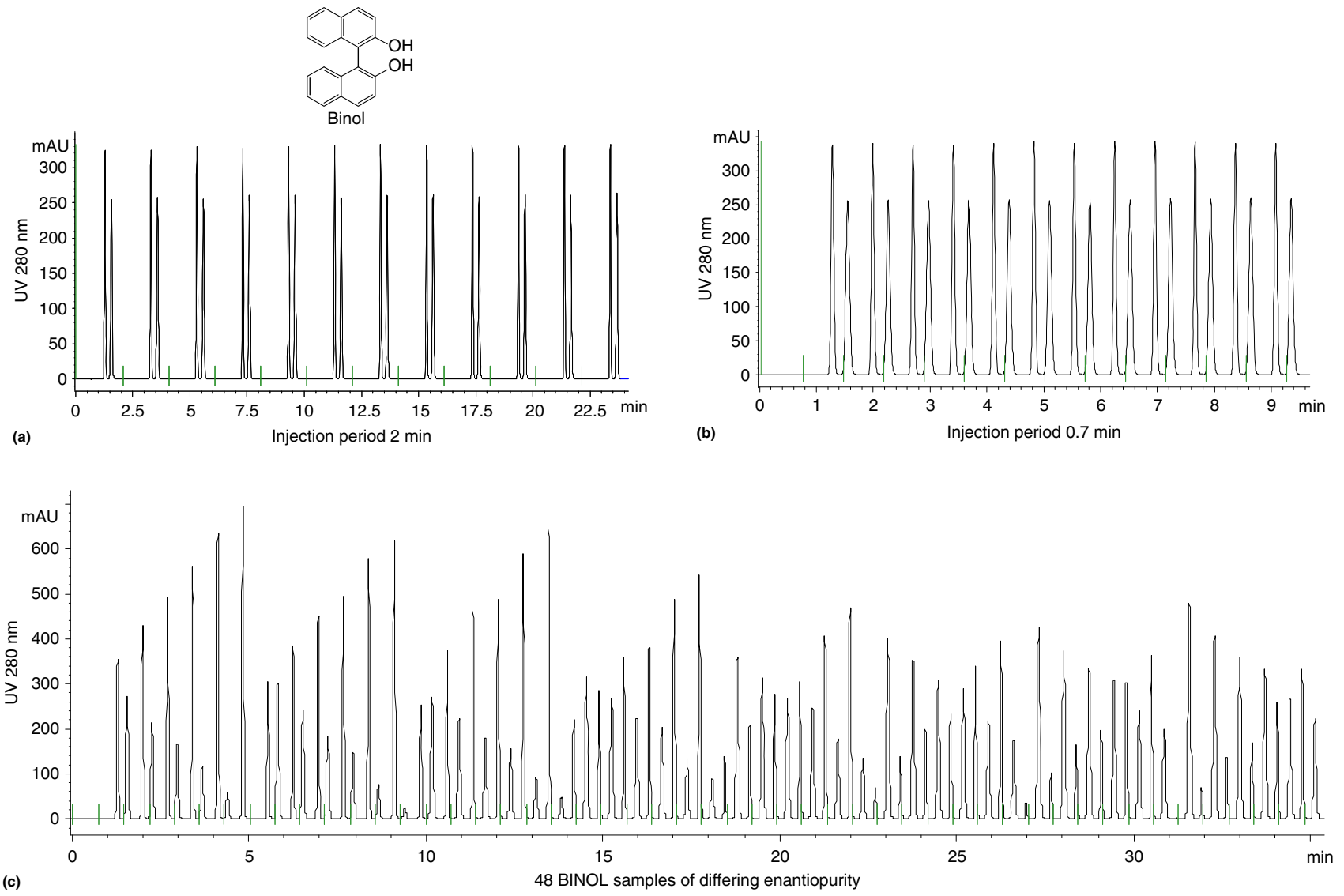


Figure 10 MISER chromatography using chiral chromatography. Decreasing injection period allows analysis of 48 samples of enantioenriched binol in only 36 min.

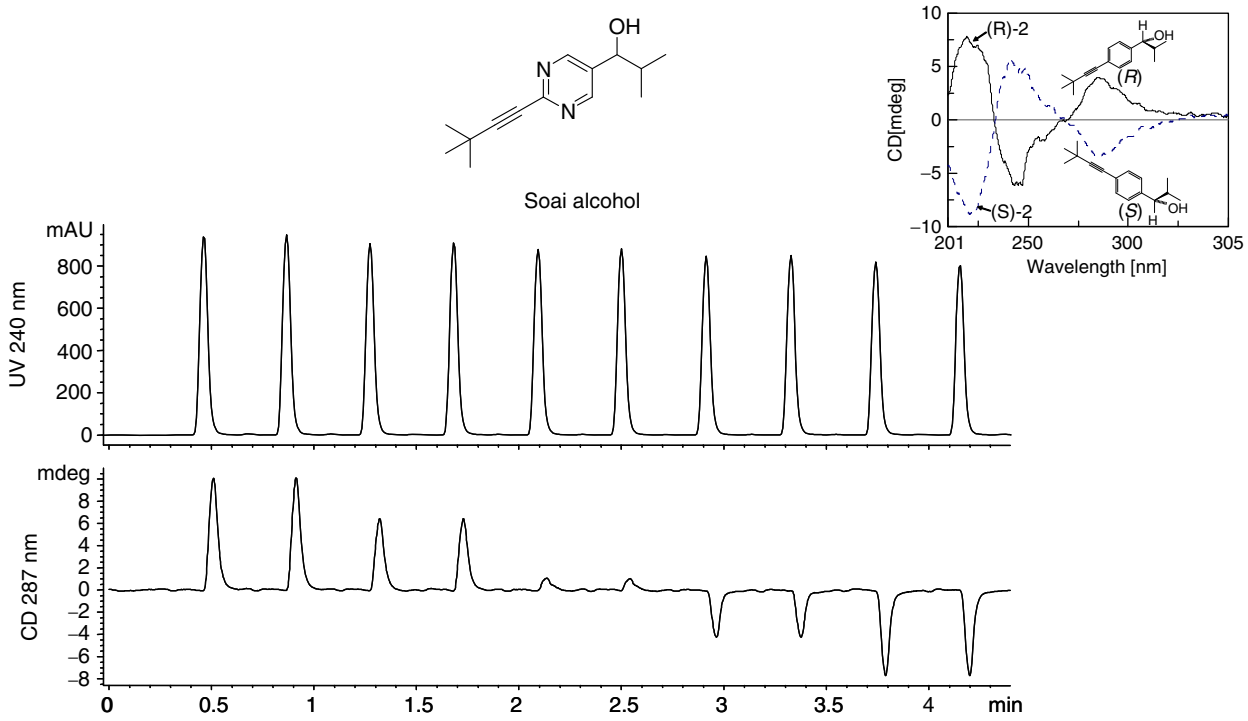


Figure 11 Achiral MISER chromatography with UV and CD detection allows rapid estimation of the extent (and direction) of enantioenrichment. Extend C18; 3.5 m; 4.6 × 50 mm; 1.5 ml min^{-1}; 40% ACN in 0.1% H_3PO_4; UV 240 nm; CD detection at 287 nm. Injection period 0.5 min.

- As the chromatographic peaks in HTA are typically much narrower than those in conventional chromatography, it is important to ensure that the detector response time allows for appropriate sampling of the signal across the peak of interest. Typical detector response settings are often too slow for HTA chromatography, leading to distorted peaks or inaccurate integration. In addition, many older detectors do not have appropriate signal sampling rates for effectively supporting HTA studies.
- Injector cycle time is another important factor to consider in developing HTA chromatographic separations. Historically, there has been little need to optimize injector autosampler cycle time less than 20–30 s that is typical for today's instruments. However, as the ability to perform fast chromatography continues to develop, HTA researchers often encounter a situation where the autosampler injection cycle time becomes rate limiting. Consequently, current instrumentation must evolve to allow HTA chromatographers the ability to take full advantage of sub-20 s separations.
- Investment in state of the art-expensive analytical equipment is not always required for HTA chromatography. Although modern UPLC equipment is clearly preferred, a properly configured and optimized conventional HPLC instrument can perform nearly as well in some applications and can approach half the speed of UPLC equipment in demanding high efficiency separations.[19]

9.02.4 Parallel Chromatography Approaches for HTA

Despite these recent advances in speeding chromatographic analyses, some separations remain very difficult, and can only be accomplished with longer analysis times. In such instances, the use of parallel analysis offers another important avenue for HTA support of HTE organic synthesis investigations. Parallel chromatography is in some ways very familiar to synthetic chemists, who have long used multiparallel thin-layer chromatography (TLC) analysis for rapid analysis of parallel reactions or quick assessment of flash chromatography fractions. HPLC is generally better suited than TLC for accurate quantitation and enantiopurity analysis, however continuing improvements and the introduction of higher performance versions of TLC increase the potential of this technique as an HTA tool[51–53] (see **Figure 12**).

Recently, there has been growing interest in the use of parallel high performance chromatography (UPLC, SFC, CE, etc.) for HTA applications. Several different instrument setups for parallel chromatography are illustrated in **Figure 13**. Perhaps the most straightforward and most commonly used approach for parallel HPLC is the simultaneous use of multiple instruments. Disadvantages of this approach include the need to split samples from a single experiment among multiple instruments, then merge the data afterwards to allow for interpretation of experimental outcome. The Eksigent Express 800 parallel microflow HPLC

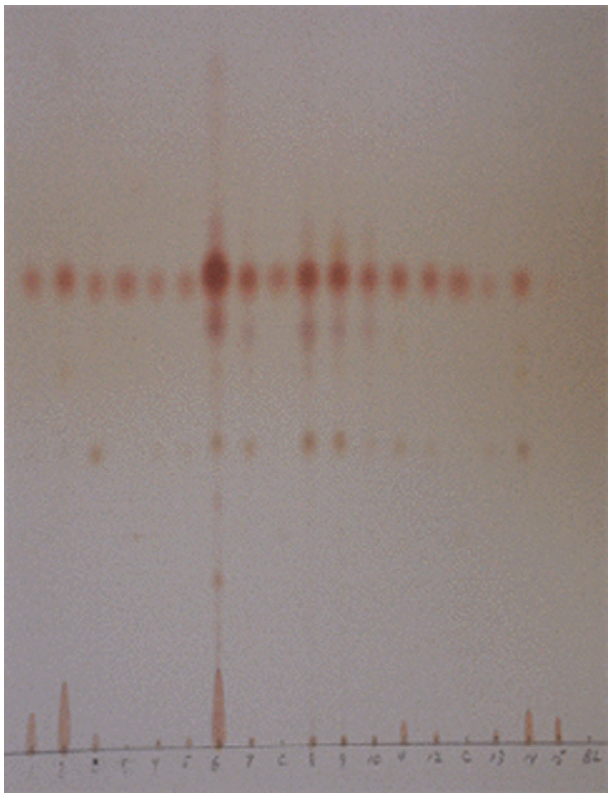


Figure 12 The familiar high-throughput analytical technique of parallel TLC has been used by synthetic chemists for decades, and has received renewed interest for HTA support of HTE.

instrument is specifically designed for carrying out HTA studies, and is essentially a single instrument containing the elements of eight individual miniaturized HPLC instruments (Figure 13(a)).[54] This system has tremendous flexibility, allowing the use of different columns, eluents, gradients, and run times on each of the eight channels.[55,56] Overall, this instrument is a powerful, general tool for HTA studies, although with 16 individual pumps and injection and flow control for eight columns, the system is significantly complex and expensive.

A simplified instrument design incorporates independent injection with shared flow across a number of columns (Figure 13(b)). A disadvantage of this approach is the fact that the same solvent composition and gradient must be used across all channels. In addition, flow among the different channels is determined by the relative backpressure on the different columns, which offers significant complications for the use of columns with different dimensions or stationary phases. In addition, increased backpressure on a single column owing to clogging will result in decreased flow through that particular column. Nevertheless, the significant simplification of using a single pumping system for a number of columns makes this general approach attractive as a potentially low cost solution to the HTA chromatography problem.

The Nanostream Veloce instrument is an example of an independent injection, shared flow HTA chromatography system.[56–58] This system utilizes a single binary gradient pump module, 24 UV or fluorescence detector channels, a multihead autosampler for injections from 96- or 384-well microplates, and a prefabricated plastic cartridge containing 24 square profile columns with microfluidic 'pits' for sample injection. Chromatographic performance on this system is considerably worse than with conventional chromatographic systems, owing to the use of large particle irregular chromatographic stationary phase, the need to operate at low pressure, and the large injection size relative to column dimensions. Consequently the system is poorly suited to the HTA of mixtures, and better suited for analyses in which quantitation of a single component was required. Despite these shortcomings, the design of a low cost, high performance HTA chromatography instrument based on the independent injection/shared flow principle remains a viable possibility.

Figure 13(c) illustrates a shared injection/shared flow for HTA chromatography. This approach is limited to use in the particular HTA task of chromatographic column screening and method development, where rapid assessment of the separation of a single analyte mixture on a number of columns is desired.[59] As with the independent injection/shared flow approach, the difference in flow through columns with different dimensions or different backpressures is a significant drawback. In addition, the requirement that all channels use the same mobile phase and gradient makes the system much less versatile than the independent injection/independent flow HTA systems. This limitation is especially important for the chromatographic stationary phases, where preferred solvents for one stationary phase may irreversibly damage another.

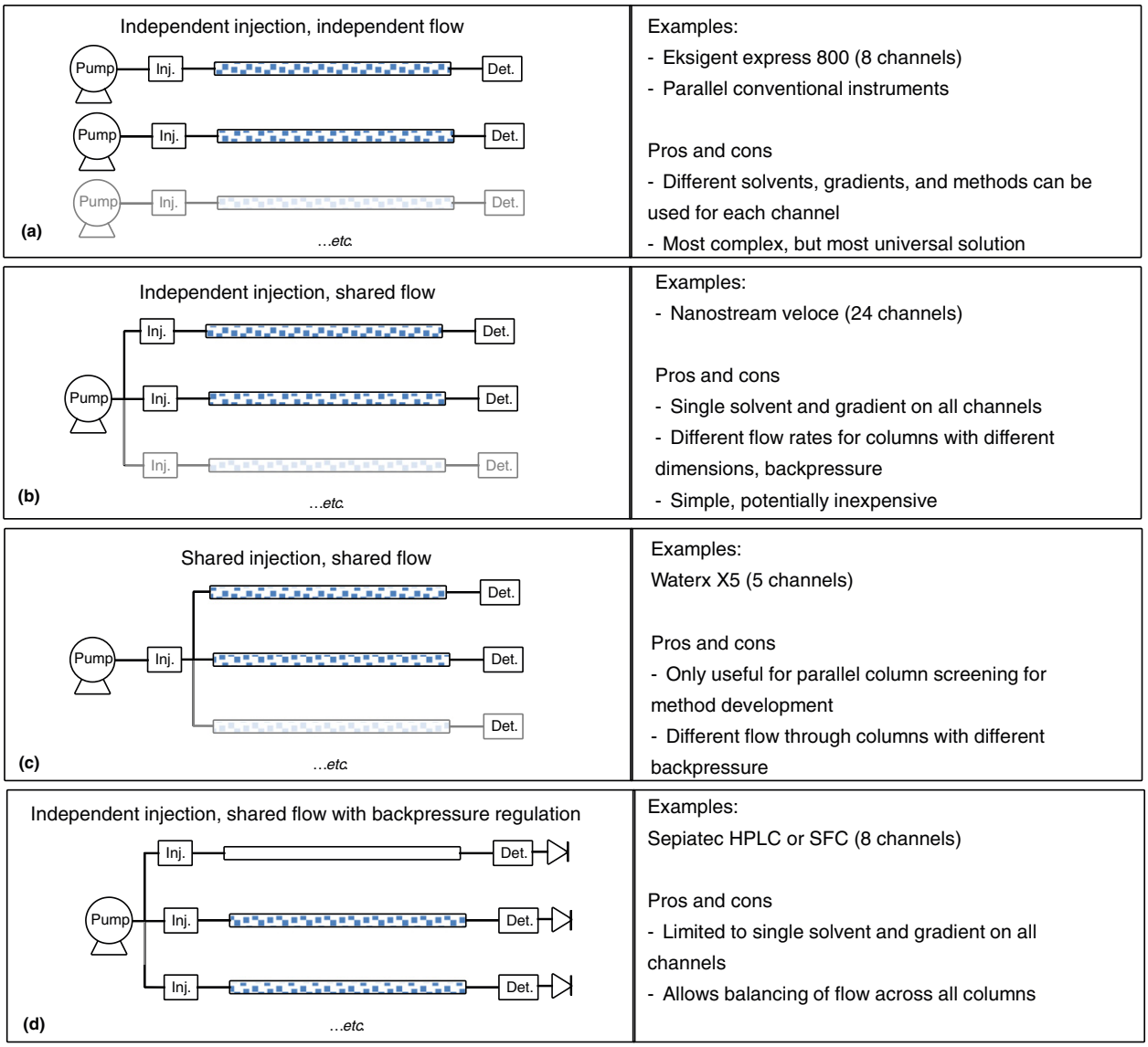


Figure 13 Different options for HTA chromatography.

The problem of differential flow through individual columns with different backpressures has been addressed by Sepiatec, through the clever use of a postdetector pressure regulator on each channel, which allows balancing of the backpressure on each channel, thereby allowing an even distribution of flow among the different channels.[60] The system illustrated in Figure 13(d) measures flow through each channel, then uses a software-controlled feedback algorithm to continuously adjust the backpressure regulators. A shared flow eight-channel HPLC instrument has been available for a number of years and an eight-channel SFC instrument was recently introduced.[61]

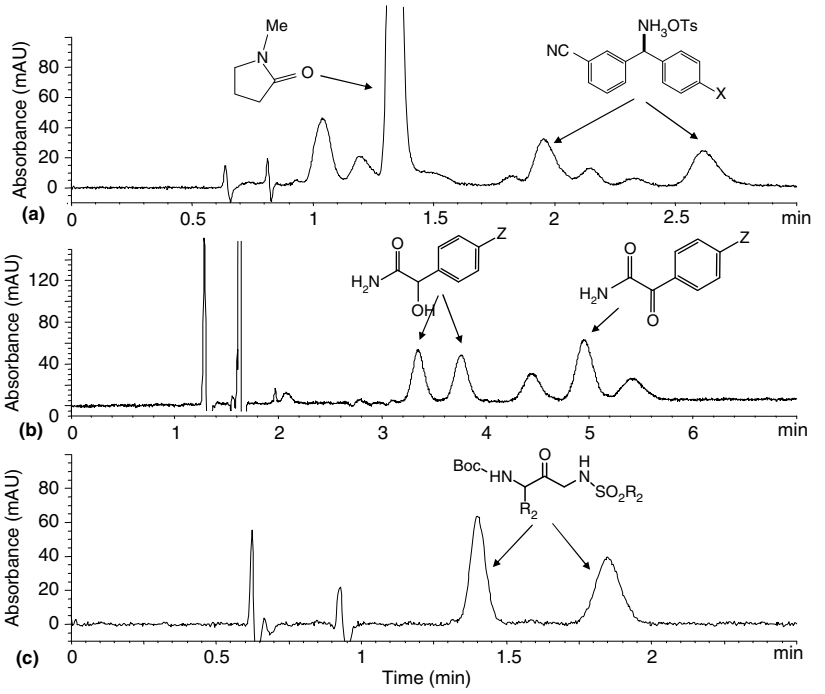
Figure 14 summarizes some of the advantages of the Eksigent Express 800 multiparallel HPLC system, currently state of the art for HTA chromatography. This instrument has extremely low dwell volume and extracolumn volume, and is well suited for high performance chromatographic separations. Plate time (time required to analyze a 96-well microplate) is typically between 30 min and 2 h, affording the rapid analysis turnaround time for supporting HTE studies.[56] The system is well suited for fast gradient chromatography, affording subminute run times for many sample mixtures.

Figure 15 shows an example of the use of the eight-channel Eksigent system for parallel chiral method development. Four different stationary phases and two different eluent systems can be simultaneously evaluated in less than 30 min, as opposed to ~6 h using conventional HPLC with a sequential column switching strategy. This approach results allows 'same day' problem solving, as opposed to the conventional 'next day' approach currently used today.

Figure 16 highlights some fast chiral separations developed using the multiparallel screening approach.[58] These analytes are routinely used as standards in chiral chromatography research, and dozens or even hundreds of methods have been reported for



- Designed for high-throughput analysis
- 8 Columns (0.3 mm i.d.) 16 pumps
- Low dwell volume, ultrafast gradients
- ~0.5–2 h for analysis of 96 well plate



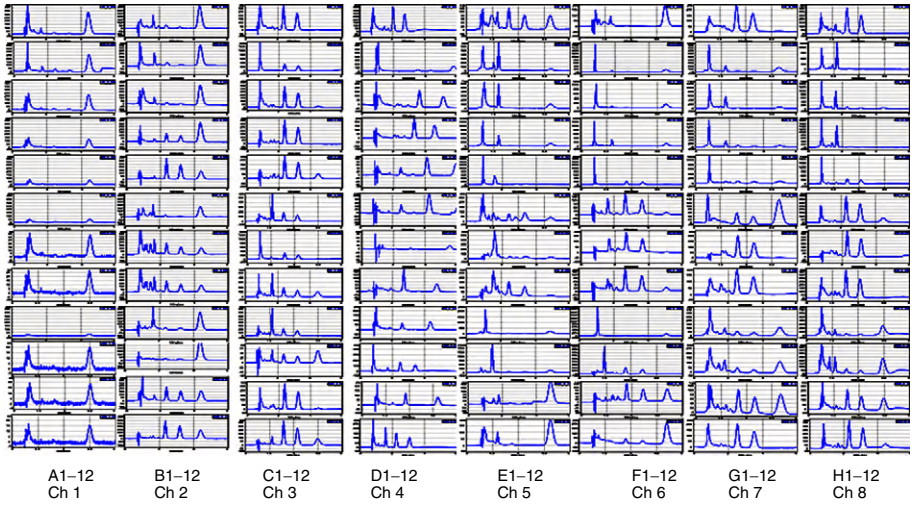


Figure 14 Eksigent Express 800 system, current state of the art for high-throughput HPLC.

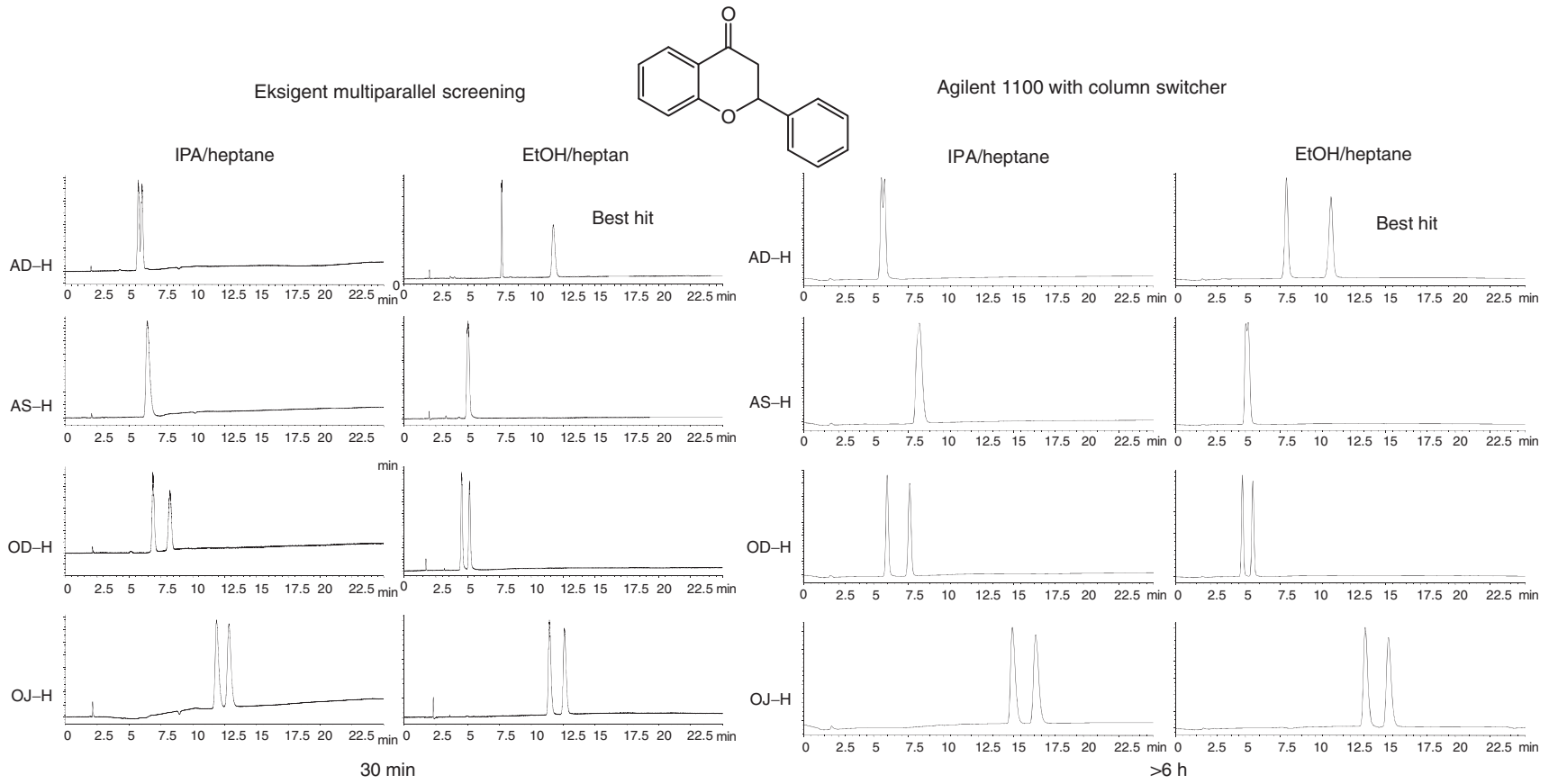


Figure 15 Multiparallel chiral HPLC method development affords significantly faster solutions than conventional HPLC approaches employing sequential column switching.

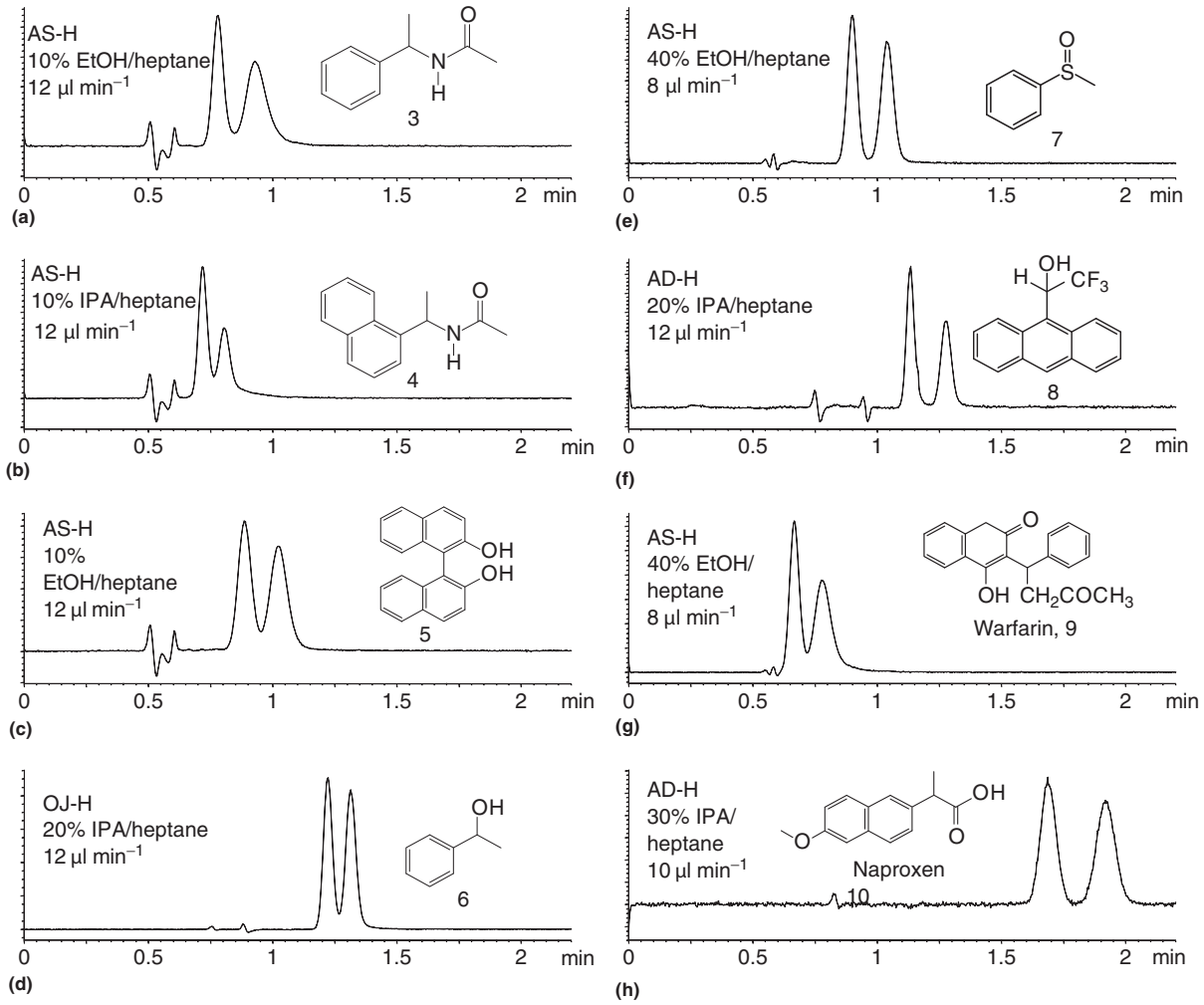


Figure 16 Fast chiral HPLC methods developed for commonly studied racemates using multiparallel chiral HPLC method development.

each one. Interestingly, multiparallel screening led to the development of very fast methods for each of these compounds, in all cases equivalent to or surpassing the fastest analysis method reported to date.

9.02.5 Parallel Electrophoresis Approaches for HTA

Like TLC in organic chemistry, slab gel electrophoresis has been used for parallel analysis of biomolecule for decades. In recent years multiplexed capillary electrophoresis has emerged as an important tool for HTA studies, especially in the biotechnology area.[62] Several 96-channel capillary gel electrophoresis instruments are currently available, and these instruments are typically equipped with multiplexed fluorescence detectors that are designed for the detection of DNA and protein molecules labeled with fluorescence tags. Needless to say, few molecules of interest in organic chemistry HTE studies contain sufficient fluorescence to be detected with these systems. A 96-channel capillary electrophoresis system with UV detection developed by Gong and Yeung[63] has been used for a variety of small molecule analysis applications such as combinatorial screening of homogeneous catalysts and reaction optimization,[64] enantiomeric separation,[65] p*K*a determination,[66,67] and log *P* measurement.[68] Continuing innovation in the area of parallel CE, combined with the inherent cost advantage of replacing precision fluidic pumps with voltage-driven flow of eluent, suggests a promising future for the use of CE in HTA.[69]

9.02.6 Nonchromatographic Approaches to HTA: Mass Spectrometry

Mass spectrometry continues to be one of the fastest growing areas in analytical instrumentation. The use of mass spectrometry in support of synthetic chemistry is becoming very well established, especially the technique of electrospray ionization (ESI) MS,

which is often used as a detection technique for liquid chromatography. The exquisite sensitivity and resolving power of MS offers strong advantages for HTA. However, one of the major drawbacks of the use of MS techniques for HTA of complex mixtures is the problem of ion suppression or ion enhancement that arises from the influence of one sample component on the ionization of another. For example, the presence of a small amount of an organic base in a sample can dramatically suppress the formation of a desired ion. This problem is easily eliminated by carrying out chromatographic separations upstream of the MS detection, or by carrying out offline sample preparation in which potentially interfering substances are removed from the compounds of interest. For some applications where the components of interest do not interfere with each other and where the sample matrix is constant from sample to sample, direct MS analysis can afford very fast HTA.

Matrix-assisted laser desorption/ionization (MALDI) is a soft ionization technique with extremely high throughput.[70,71] The technique is routinely used for the analysis of biomolecules (biopolymers such as DNA, proteins, peptides, and sugars) and large organic molecules that tend to fragment when ionized by more conventional ionization methods.[72,73] Samples are applied to a target plate containing a UV-absorbing matrix, then quickly irradiated by a UV laser. A hot plume produced during the ablation contains many species: neutral and ionized matrix molecules, protonated and deprotonated matrix molecules, matrix clusters, and nanodroplets. The compounds of interest are ionized in this plume, then analyzed by MS, often using time of flight (ToF) as a means of detection. Due to its ability to ionize spatially separated samples on solid surfaces, MALDI is especially well suited for HTA. Common examples include quality control of synthetic oligonucleotides and peptide mass fingerprinting.[74,75] Although MALDI is typically used for large molecule HTA, in some cases the technique works well for low molecular weight substances, with an overall propensity to form ions similar to that of thermal desorption atmospheric pressure chemical ionization (APCI).[76]

Several new atmospheric pressure MS ionization techniques have emerged recently and show considerable promise for HTA. Beginning with desorption electrospray ionization (DESI) and direct analysis in real time (DART), a number of additional techniques with promise for HTA have emerged in recent years, including MALDESI,[77] LAESI,[78] PADI,[79] ASAP,[80] DBDI,[81] and ELDI.[82]

DART is an atmospheric pressure ionization method that instantaneously ionizes gases, liquids, and solids in open air under ambient conditions. DART can be considered as a variation of APCI. It was developed in 2005 by Laramee and Cody[83] and is now marketed commercially by several vendors. DART was among the first ambient ionization techniques not requiring sample preparation, so solid and liquid materials can be analyzed by mass spectrometry in their native state. Initial ions are created with a discharge in a flowing stream of a hot noble gas such as argon or helium, forming metastable excited state atoms by Penning ionization which transfer charge to the background gas in an API source through a chemical ionization processes. The displaced analyte ions are carried by the heated gas stream into the aligned sampling orifice of the mass spectrometer atmospheric pressure interface.

Figures 17 and 18 show the value of DART MS for carrying out high-throughput analysis of microplates in support of HTE screening of an enzyme-mediated oxidation.[84] In this example the plate time (time required to analyze a 96-well microplate) is only 65 min, which compares favorably with fast LC–MS approaches. It should be noted that the sample matrix from this HTE enzyme screen was fairly simple and homogeneous, whereas a typical sample matrix from a screening of conventional catalysts would contain residual ligands, solvents and additives in the different wells, precluding the use of DART analysis without prior sample cleanup.

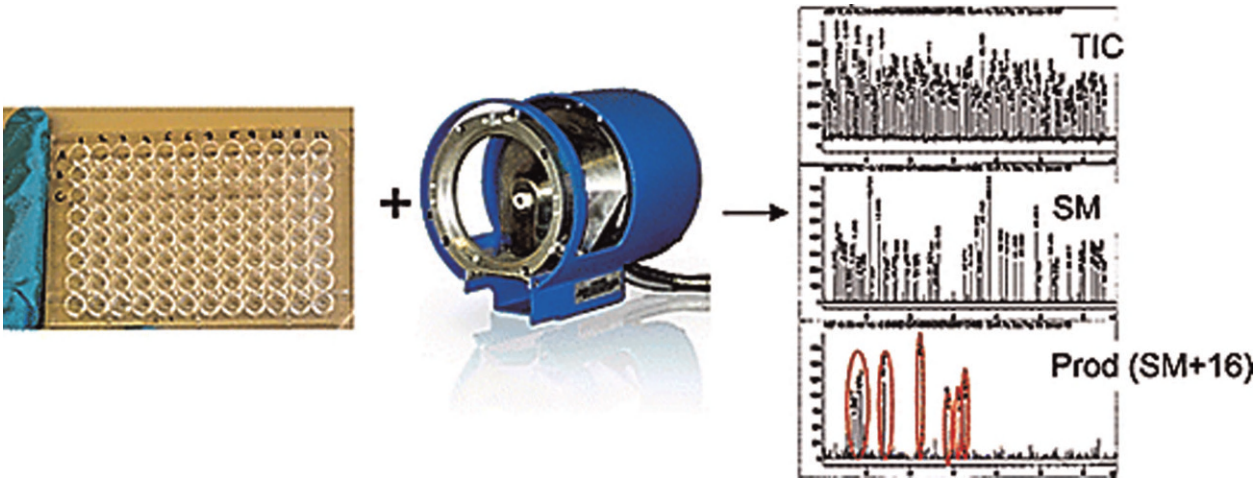


Figure 17 DART allows rapid MS analysis, and can be a useful tool for HTA in support of HTE organic chemistry studies.

DESI is another surface ionization technique with significant potential for HTA.[85–87] DESI operates by impacting high-velocity charged droplets from a pneumatically assisted electrospray with the surface to be analyzed, extracting the surface chemicals by the liquid that makes momentary contact. Ions of chemical species present on the surface are produced through the interaction of the

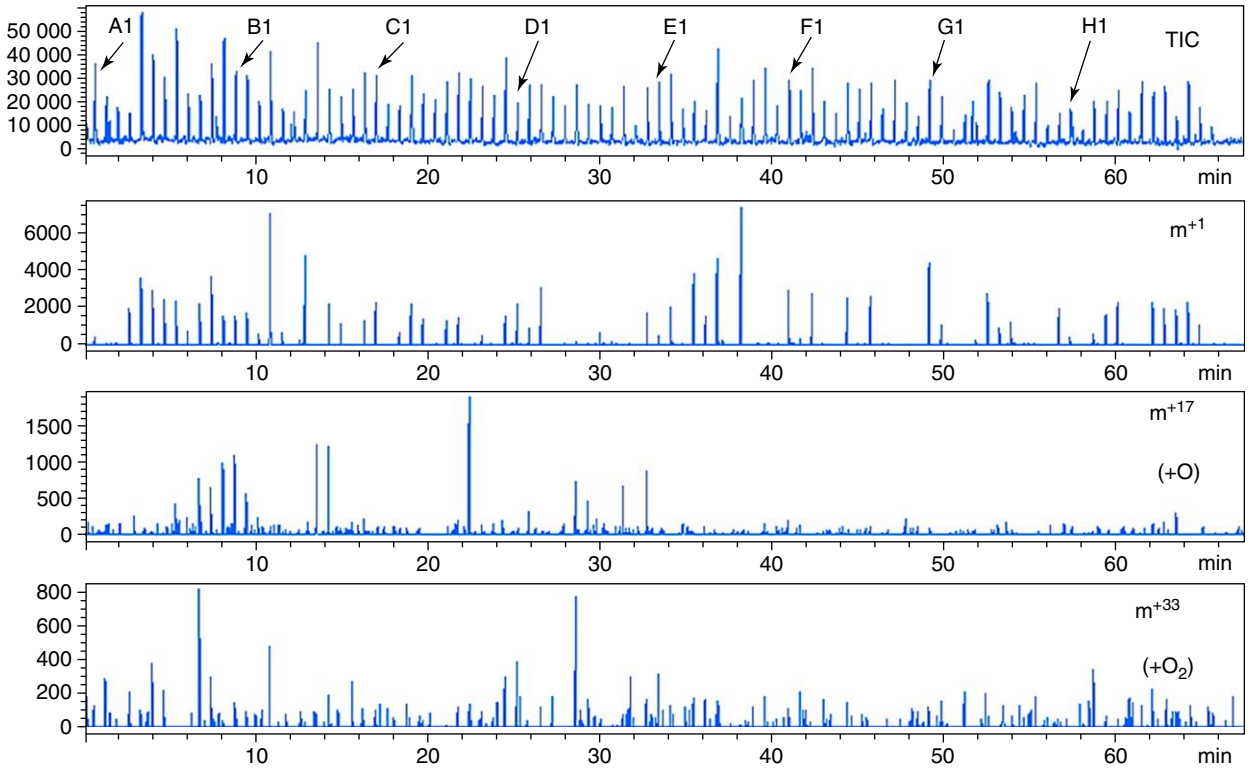


Figure 18 DART HTA of a 96-well microplate from an enzymatic oxidation HTE study, with plate time (time required for analysis of 96-well microplate) of <70 min. Reproduced from Helmy, R.; Schafer, W.; Buhler, L.; *et al. Org. Process Res. Dev.* **2010**, 386–392, with permission from American Chemical Society.

charged droplets and the sample. The sensitivity of DESI depends on the extraction efficiency that occurs during the impact event. The resulting mass spectra are similar to ESI mass spectra. The composition of the spray solvent, the gas flow rate, the magnitude of the applied voltage, the impact angle, as well as various distances in aligning the spray with respect to the surface and inlet of the mass spectrometer are variables that can be studied to achieve optimal performance. A similar approach, referred to as DeSSI, utilizes a sonic spray nozzle without the high voltage.[88]

DESI is especially suitable for high-throughput analysis by allowing mass spectrometry to be used for online high-throughput monitoring of pharmaceutical samples in the ambient environment, without prior sample preparation. Nicholas et al.[89] demonstrated that a 2D DESI–MS stage system with 96-sample array, containing pharmaceuticals in various matrices, was analyzed in a single run with a total analysis time of only 3 min. An emerging capability of DESI is automated high-throughput monitoring and molecular imaging of biological tissues. This technique has the ability to record molecular information and spatial distribution simultaneously, especially when limited preparation of the surface is required and the sample is under ambient conditions.[90,91] Another interesting application of DESI is for probing chemical reactions.[92] In an experiment referred to as reactive DESI, specific reagents are added to the spray solvent to react selectively with particular functional groups present in the mixture within the DESI analysis time (milliseconds). Girod et al.[93] explored these reactions in microdroplets and observed a rate acceleration phenomenon compared with bulk solution.

Ion mobility spectrometry is a gas-phase analytical technique that separates ions based on both size and shape.[94] In IMS, ions are created and then subjected to an electric field, causing the ions to travel through the ion mobility drift tube while colliding with neutral drift gas molecules. As the ions travel through the drift tube, they undergo random collisions and accelerations until reaching the end of the drift region, where they are either detected by a Faraday cup or transmitted through an interface to a mass spectrometer. IMS can be comparable to liquid-phase separations in resolution, but greatly superior in speed. Unlike an HPLC run lasting a minute or more, most ion mobility-based separations are achieved in tens to hundreds of milliseconds.[95–97] Thus, IMS may provide the basis for increasing the throughput of HTA.

A particular strength of the IMS method is the ability to separate stereoisomers. Dwivedi et al.[98] demonstrate that by modifying the drift gas with chiral molecules, IMS can provide a novel and rapid separation technique for chiral compounds. This unique system can not only separate chiral molecules in milliseconds, but also reduces method development time to a fraction of that normally required for HPLC. Additionally, coupling IMS with a MS detector provides a separation capability before entering the MS detector, so it can be useful in counteracting the problem of interfering substances in MS noted earlier.

Inductively coupled plasma–mass spectrometry (ICP–MS) is one kind of spectroscopy that is virtually free of sample interference issues, making it well suited for HTA. Analytes are completely combusted in a very hot plasma torch, allowing the specific

determination of noncombustible elements present in the samples. The technique is especially useful for metal analysis and can be interfaced with either MISER chromatography or simple flow-injection analysis (FIA, Figure 19).[99,100]

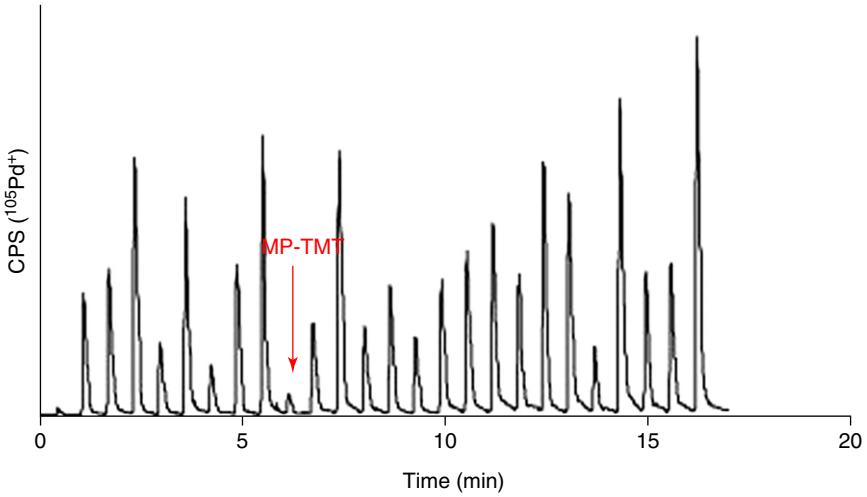


Figure 19 FIAgram obtained with the FI–ICP–MS system for Pd analysis in an adsorbent screening test. Reproduced from Tu, Q.; Wang, T.; Welch, C. J. *J. Pharm. Biomed. Anal.* **2010**, *51*, 90–95.

9.02.7 Sensor Technologies for HTA

The development of chemical sensors – systems that interact specifically with an analyte of interest and provide information on compound identity and amount – has been a growing area of research for more than a decade.[101–103] Sensor technologies are rapidly reaching a stage of development where they can begin to be useful tools for HTA studies. As with spectroscopic approaches, the presence of interfering substances can cause serious problems for many sensor-based approaches, although appropriate sample pretreatments can reduce this problem.

Prof. Koide at University of Pittsburgh has developed a chemosensor-based approach for the detection of palladium, a commonly used metal in pharmaceutical synthesis.[104] In this approach, Pd-catalyzed deallylation of a nonfluorescent substrate produces a highly fluorescent product (Figure 20). The rate of appearance of fluorescence can be used to accurately measure the Pd content of unknown samples, a useful tool for HTA support of Pd impurity removal studies, where parallel analysis of a variety of adsorbents and conditions can generate many samples for analysis.[101] Recent studies show the technique to be quite robust for correctly estimating Pd levels in a number of pharmaceutical intermediates, allowing rapid and accurate estimation using inexpensive plate reader technology, where an entire 96-well plate can be scanned in a few seconds.[105] In addition, naked-eye estimation of the intensity of the visible green color produced in the reaction can allow a direct ballpark estimation.

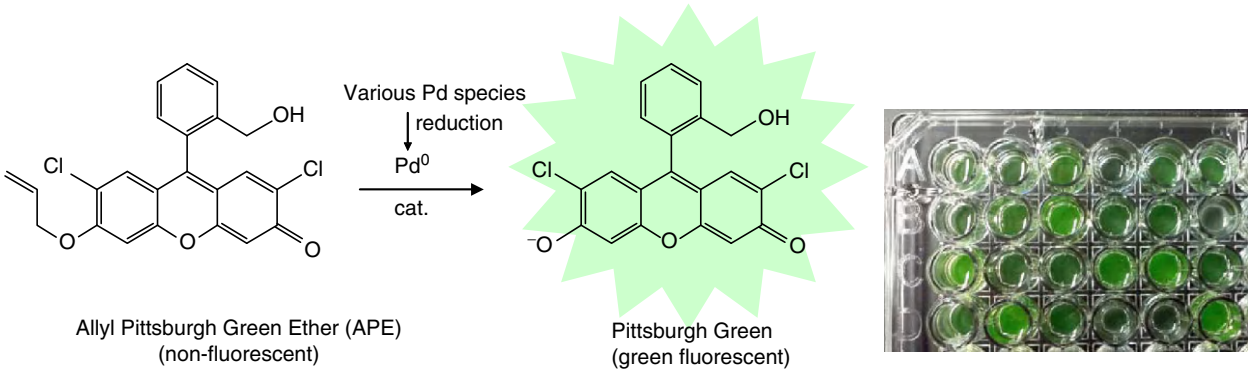


Figure 20 Method developed by the Koide group for fluorometric palladium determination based on the Pd^0-catalyzed deallylation of Allyl Pittsburgh Green Ether (APE).[107] The Pd-dependent appearance of fluorescence and color can be measured using plate reader technology, and can even be estimated with the naked eye. Reproduced from Bu, X.; Koide, K.; Carder, E. J.; Welch, C. *J. Org. Process Res. Dev.* **2013**, *17*, 108–113, with permission from American Chemical Society.

Considerable recent effort has gone into the development of sensor technologies for enantiopurity determination.[106,107] These receptors typically contain an enantioselective receptor where the analyte can bind and an indicator that communicates some

details of the binding event. Chiral solvating agents for NMR determination of enantiomeric purity are a very familiar form of sensor of this type,[108,109] although at present the throughput of NMR analysis is not well suited for HTE. In a similar approach, MS has seen utility as a tool to assess enantiomeric purity.[110,111] In an approach often termed the Sawada method, isotopically differentiated 'pseudoenantiomers' are used to complex the target analyte, giving rise to two diastereomeric complexes with differing molecular weight. Analysis of the resulting mass spectrum can allow deconvolution of the enantiomeric purity of the sample.

Sensor technologies relying on optical spectroscopy have a number of advantages, as a routine inexpensive plate reader can allow very fast analysis of microplates. One of the most widely applied means of optical detection is ultraviolet visible spectroscopy. For chromophores that absorb in the visible portion of the spectrum, this detection method can be amenable to 'naked-eye' detection. One of the first contributions to enantioselective colorimetric sensing was made by Kubo and coworkers,[112] who used a macrocyclic calixarene host containing a pendant (*S*)-BINOL moiety. Addition of (*R*)-phenylglycinol to the red calixarene solution led to the formation of a dark blue color, whereas minimal color change was observed when (*S*)-phenylglycinol was added. Thus, the chromophore of this synthetic receptor changes its color as a function of analyte binding to the complex. In addition to amino alcohols, Kubo has shown this method to be general to a variety of amine-containing species, such as amino acids, and chiral amines.[113] In this same way, Fuji and Tsubaki have reported chiral phenolphthalein-conjugated crown ethers that were first applied as chiral amine sensors,[114] and then further expanded to amino alcohols.[115] In this case, the colorless receptor solution became a pink color with the addition of the analyte.

Another approach introduced by Anslyn utilizes indicator displacement assays (IDAs). In an IDA, the indicator is reversibly associated with the receptor rather than synthetically appended.[116] Addition of the analyte causes a competitive binding event to occur, and the indicator is displaced from the receptor to the bulk solution. The indicators that are used are typically pH dyes, and their spectral properties change as a function of microenvironment. Hence, they have different optical signals when bound to the receptor than when free in solution. One example of this approach applied specifically for HTA was in the sensing of amino acids.[117] A chiral receptor was constructed in this manner by complexing an indicator to a copper center that contained a chiral diamine ligand. The blue complex formed between the indicator and receptor became brown/yellow on introduction of an amino acid guest as shown in **Figure 21**. 'Naked-eye' detection was possible in a few cases, but most-required spectroscopic measurements. This approach was optimized for HTA by transitioning to multiwell plates.[118] The plates were constructed by liquid dispensing robots, and consisted of known samples for calibration curves as well as samples of unknown enantiomeric composition. This optimization allowed 96 wells to be read in less than 1 min. The error associated with this approach is higher than an HPLC measurement, and the samples still require cleanup to avoid unwanted interactions and competitive absorption. Nevertheless, sample throughput can be greatly increased.

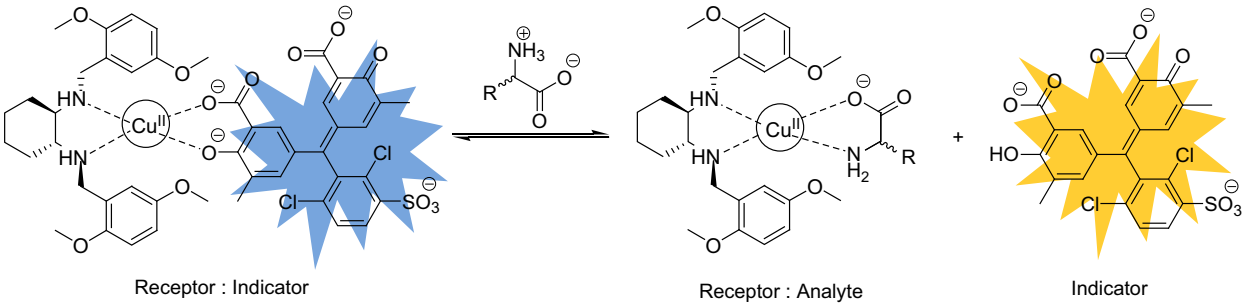


Figure 21 Schematic representation of the eIDA used to sense amino acids. Reprinted with permission from Leung, D.; Folmer-Andersen, J. F.; Lynch, V. M.; Anslyn, E. V. *J. Am. Chem. Soc.* **2008**, *130*, 12318–12327.

Lin Pu is one of the pioneers of enantioselective fluorescence sensing. Of the sensors Pu has reported, the vast majority of them are macrocycles containing enantiopure BINOL functionalities and additional chiral appendages.[119,120] These macrocycles are decorated with several hydrogen bond donors, such as amines and alcohols, which serve as binding sites for α-hydroxycarboxylates such as mandelic acid (**Figure 22**). Addition of (*R*)-mandelic acid to the receptor built around (*S*)-BINOL led to minute changes in fluorescence intensity, whereas dramatic enhancement was achieved on the addition of (*S*)-mandelic acid. A nonlinear calibration curve shows the change in fluorescence as a function of sample *ee*. Similar approaches have been pursued by Wolf, who used a 1,8-diacridylnaphthalene-based sensor for chiral carboxylic acids,[121] and Chan, who used an anthracene-containing cholic acid species to sense amino acids that are otherwise difficult to assess.[122]

Corradini and coworkers expanded the application of fluorescence assays to a platform that was complimentary for HTA in their report of sensing unmodified amino acids.[123,124] This approach was based on a dansyl fluorophore synthetically attached to a cyclodextrin core by chiral L-amino acid linkers. The receptor by itself had a large fluorescence signal, and this signal was quenched on addition of the combination of a copper metal ion and an amino acid guest. Interaction between each enantiomer of the amino acid analyte and the chiral linkers gives rise to differential fluorescence quenching. All D-amino acid analytes led to a greater extent of quenching than the corresponding L-enantiomers. Analyses were then carried out in multiwell plates to prove that this process is

amenable to HTA. The analysis plate is fitted with duplicate samples of known *ee* values and used to create a calibration curve. Six samples of unknown *ee* value were next added to the plate in triplicate to ensure accuracy, and all analyzed in 2 min.

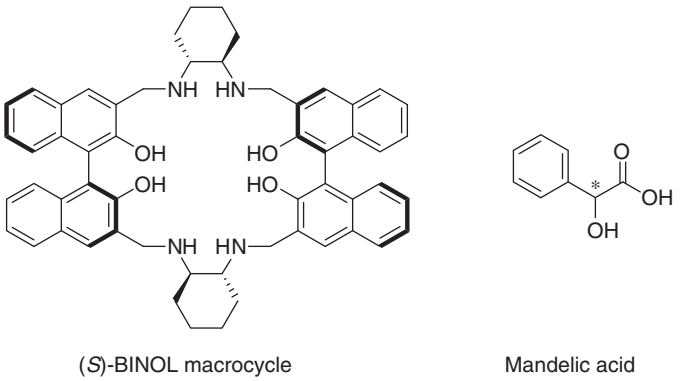


Figure 22 Chemical structures of the receptor and analyte Pu used for fluorescence sensing. Reproduced from Leung, D.; Folmer-Andersen, J. F.; Lynch, V. M.; Anslyn, E. V. *J. Am. Chem. Soc.* **2008**, *130*, 12318–12327, with permission from American Chemical Society.

Canary and coworkers utilized exciton-coupled CD (ECCD) to enantioselectively sense chiral amino acid guests.[125] This technique relies on the coupling of excited states of two or more chromophores held in close proximity, leading to degenerate excited states, and manifesting as a bisignate curve in the CD spectrum. The sign of the signal indicates the orientation of the chromphores in space. To this end, Canary derivatized the amino acid of interest with 2 equivalents of a quinoline chromophore. This tetradentate ligand is then complexed to copper, bringing the chomophores close to each other and creating an ECCD active molecule as shown in Figure 23. The observed sign of the CD signal was enantiospecific for the chiral amino acid, allowing the absolute configuration to be readily ascertained. Linear calibration curves were found for varying *ee* values, and subsequent efforts expanded the analyte tolerance to amino alcohols and amino acids.[126,127] Although derivatization is not optimal for HTA, this approach was simplified to minimize reaction time and allow for *in situ* complex formation on a microgram scale.

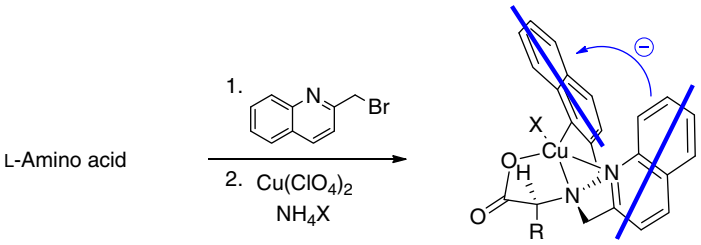


Figure 23 Schematic for the *in situ* formation of CD active metal complexes giving enantiomerically defined CD spectra. Reprinted with permission from Zahn, S.; Canary, J. W. *Org. Lett.* **1999**, *1*, 861–864.

In another approach aimed at increasing the throughput of CD detection, Anslyn and coworkers utilized metal-to-ligand charge transfer (MLCT) bands to enantioselectively sense chiral diamines.[128,129] The receptors for this task were constructed from enantiomerically pure chiral substituted BINAP structures, and a copper metal center to bind the diamine. On binding, the MLCT signal of the BINAP chromophore was enantiospecifically modulated. To determine the concentration as well as the *ee* of the analyte, the data were analyzed using a chemometric technique known as artificial neural network (ANN).[130] A CD reader capable of reading 96-well plates was applied. A plate was made with 33 wells of known value dedicated to train the ANN, and the remaining 63 wells were comprised of unknowns. The 63 unknown samples were analyzed at a rate of 2 min per sample, showing moderate errors in both concentration and *ee*.

The enantioselective assays described above helped prove the principle that optical sensors could be applied to the rapid determination of enantiomeric composition. Their broad applicability, however, remains largely limited by sample preparation. In most cases, the sample must be sufficiently pure such that no interfering signals are present in solution. Despite the activation barrier inherent to this process, several synthetic labs have created real-world examples using the optical sensing platform. Matt Shair reported a reaction microassay approach that was similar to DNA microarray technology.[131] In this approach, two fluorescent probes attached to proline molecules were used to derivatize amino acids that had been attached to a glass slide. The ratio of the fluorescent response was used to quantify *ee*, and this approach was used to analyze 15 552 samples. Scott Miller developed a fluorescent method to monitor catalyst activity for an acetylation reaction.[132] The ester formation also liberates an acetic acid molecule, which increased the fluorescent response of a peptide sensor. This approach was used to screen 1000 catalysts in as little as 60 min. This system sensed catalyst activity without consideration of enantioselectivity, however this reaction was proven

to be enantioselective. Finally, Ben Feringa and coworkers developed a colorimetric method to sense enantioselectivity of phosphoramidite-catalyzed addition of diethylzinc to a chalcone reactant.[133] The twisting of the product as a result of supramolecular interactions gave rise to a colored species, with the color directly related to the *ee* of the addition product. Each of these examples shows application of this methodology to synthetic examples; however each suffers from lack of substrate generality.

9.02.8 Conclusion and Future Prospects

Methods for carrying out HTA to support HTE in organic synthesis are evolving rapidly. The ability to obtain fast analytical results for HTE studies is now possible in many cases, and this 'same day' analysis time for microplates can be expected to become quite routine in the next few years. The rapid emergence of sensor and spectroscopy-based HTA approaches suggest that the dominance of analytical chromatography for HTA may be challenged by these inherently faster techniques. However, the vulnerability of these sensor and spectrosocopy methods to matrix interference in complex samples suggests that the some hybrid of chromatography and sensor or spectroscopy approaches may emerge as a preferred method HTA support of organic chemistry. In any case, an understanding and appreciation of high-throughput analytical chemistry is likely to continue to grow in importance for researchers in synthetic organic chemistry.

References

1. Beeler, A. B.; Schaus, S. E.; Porco, J. A. *Curr. Opin. Chem. Biol.* **2005**, *9*, 277–284.
2. Pfaltz, A. *Chimia* **2010**, *64*, 860–862.
3. Monfette, S.; Blacquiere, J. M.; Fogg, D. E. *Organometallics* **2011**, *30*, 36–42.
4. Reetz, M. T. *Tetrahedron* **2012**, *68*, 7530–7548.
5. Fenster, E.; Hill, D.; Reiser, O.; Aube, J. *Beil. J. Org. Chem.* **2012**, *8*, 1804–1813.
6. Bellomo, A.; Celebi-Olcum, N.; Bu, X.; *et al. Angew. Chem. Int. Ed.* **2012**, *51*, 1–5.
7. McNally, A.; Prier, C. K.; MacMillan, D. W. C. *Science* **2011**, *334*, 1114–1117.
8. Lefort, L.; Boogers, J. A. F.; de Vries, A. H. M.; de Vries, J. G. *Top. Catal.* **2006**, *40*(1–4), 185–191.
9. Webster, D. C. *Macromol. Chem. Phys.* **2008**, *209*, 237–246.
10. Rajan, K. *Ann. Rev. Mat. Res.* **2008**, *38*, 299–322.
11. Zhong, L. High-Throughput Analysis in Support of Process Chemistry and Formulation Research and Development in the Pharmaceutical Industry. In *High-Throughput Analysis in the Pharmaceutical Industry*; Wang, P. G. Ed.; CRC Press: Boca Raton, FL, **2009**, Chapter 9; pp 247–278.
12. Giddings, J. C. *Anal. Chem.* **1981**, *53*(8), 945A–952A.
13. Guichon, G. *Anal. Chem.* **1980**, *52*, 2002–2008.
14. Katz, E.; Scott, R. P. W. *J. Chromatogr.* **1982**, *253*, 159–178.
15. Welch, C. J.; Brkovic, T.; Schafer, W.; Gong, X. *Green Chem.* **2009**, *11*(8), 1232–1238.
16. Wu, N.; Welch, C. J.; Natishan, T. K.; *et al.* Practical Aspect of Ultrahigh Performance Liquid Chromatography. In *Ultra-High Pressure Liquid Chromatography*; Alan Xu, Q. Ed.; John Wiley & Sons, Inc.: Hoboken, NJ, **2013**, Vol. 1, Chapter 3; pp 55–94.
17. Duan, A.; Xie, S.; Yuan, L. *Trends Anal. Chem.* **2011**, *30*(3), 484–491.
18. Carr, P. W.; Wang, X. *Anal. Chem.* **2009**, *81*(13), 5342–5353.
19. Wu, Naijun; Clausen, A. M. *J. Sep. Sci.* **2007**, *30*, 1167–1182.
20. DeStefano, J. J.; Langlois, T. J.; Kirkland, J. J. *J. Chromatogr. Sci.* **2008**, *46*(3), 254–260.
21. Abrahim, A.; Al-Sayah, M.; Skrdla, P.; *et al. J. Pharm. Biomed. Anal.* **2010**, *51*, 131–137.
22. Vanhoenacker, G.; Sandra, P. *J. Sep. Sci.* **2006**, *29*, 1822–1835.
23. Cole, L. A.; John, D. *Anal. Chem.* **1992**, *64*, 1317–1323.
24. Teutenberg, T. *Anal. Chim. Acta.* **2009**, *643*, 1–12.
25. Yan, B.; Zhao, J.; Brown, J. S.; Blackwell, J.; Carr, P. *Anal. Chem.* **2000**, *72*(6), 1253–1262.
26. Stoll, D.; Cohen, J.; Carr, P. *J. Chromatogr. A* **2006**, *1122*, 123–137.
27. Guillareme, D.; Heinisch, S.; Rocca, J. L. *J. Chromatogr. A* **2004**, *1052*, 39–51.
28. Berger, T. A. *Packed Column SFC*; Royal Society of Chemistry: Cambridge, UK, **1995**; pp 43–71.
29. Welch, C. J. *LC-GC* **2005**, *23*(1), 16–29.
30. Welch, C. J.; Biba, M.; Sajonz, P. *Chirality* **2007**, *19*, 34–43.
31. Schafer, W.; Hamilton, S. E.; Pirzada, Z.; Welch, C. J. *Chirality* **2012**, *24*, 1–4.
32. Korytár, P.; Janssen, H-G.; Matisová, E.; Brinkman, U. A. Th. *Trends Anal. Chem.* **2002**, *21*(9–10), 558–572.
33. David, F.; Szűcs, R.; Makwana, J.; Sandra, P. *J. Sep. Sci.* **2006**, *29*, 695–698.
34. Trapp, O. *Angew. Chem. Int. Ed.* **2007**, *46*, 5609–5613.
35. Trapp, O. *J. Chromatogr. A* **2008**, *1184*, 160–190.
36. Cabrera, K.; Lubda, D.; Eggenweiler, H. M.; Minakuchi, H.; Nakanishi, K. *J. High Res. Chromatogr.* **2000**, *23*, 93–99.
37. Svec, F. *Sepu.* **2005**, *23*(6), 585–594.
38. Arrua, R. D.; Causon, T. J.; Hilder, E. F. *Analyst*, **2012**, *137*(22), 5179–5189.
39. Gritt, F.; Tanaka, N.; Guichon, G. *J. Chromatogr. A* **2012**, *1236*, 28–41.
40. Welch, C. J.; Grau, B.; Moore, J.; Mathre, D. J. *J. Org. Chem.* **2001**, *66*, 6836–6837.
41. Malcolm, A.; Wright, S.; Syms, R. A.; *et al. Rapid Commun. Mass Spectrom.* **2011**, *25*(21), 3281–3288.
42. Yang, L.; Mann, T.; Little, D.; *et al. Anal. Chem.* **2001**, *73*(8), 1740–1747.
43. Wei, R.; Li, G.; Seymour, A. B. *Anal. Chem.* **2010**, *82*(13), 5527–5533.
44. King, R. C.; Miller-Stein, C; Magiera, D. J.; Brann, J. *Rapid Commun. Mass Spectrom.* **2002**, *16*(1), 43–52.
45. Welch, C. J.; Gong, X.; Schafer, W.; *et al. Tetrahedron Asymmetry.* **2010**, *21*(13–14), 1674–1681.
46. Welch, C. J.; Shaimi, M.; Biba, M.; *et al. J. Sep. Sci.* **2002**, *25*, 847–850.

47. Bellomo, A.; Celebi-Olcum, N.; Bu, X.; *et al. Angew. Chem. Int. Ed.* **2012**, *51*, 1–5.
48. Alexander, A. J.; Waeghe, T. J.; Himes, K. W.; Tomasella, F. P.; Hooker, T. F. *J. Chromatogr. A.* **2011**, *1218*, 5456–5469.
49. Gritti, F.; Sanchez, C. A.; Farkas, T.; Guichon, G. *J. Chromatogr. A.* **2010**, *1217*, 3000–3012.
50. McCalley, D. V. *J. Chromatogr. A.* **2010**, *1217*, 4561–4567.
51. Morlock, G.; Schwack, W. *J. Chromatogr. A* **2010**, *1217*(43), 6600–6609.
52. Nyiredy, S. *J. Chromatogr. A* **2003**, *1000*(1–2), 985–999.
53. Kowalska, T., Sherma, J., Eds. *Thin Layer Chromatography in Chiral Separations*; CRC Press: Boca Raton, FL, **2007**, pp 1–10.
54. Welch, C. J.; Sajonz, P.; Biba, M.; Gouker, M.; Fairchild, J. *J. Liq. Chromatogr.* **2006**, *29*, 2185–2220.
55. Sajonz, P.; Schafer, W.; Gong, X.; *et al. J. Chromatogr.* **2007**, *1147*, 149–154.
56. Sajonz, P; Leonard, WR.; Biba, M.; Welch, C. J. *Chirality* **2006**, *18*, 803–813.
57. Guazzotti, S. A.; Bilbao, S. *LC GC North America* **2009**, *24*, 54–58.
58. Wu, J.; Barbero, R.; Vajjhala, S.; O'Connor, S. D. *Assay Drug Dev. Technol.* **2006**, *4*(6), 653–660.
59. Subbarao, L.; Cole, J; Chen, R. *LC GC North America* **2009**, *22*(12), 24–25.
60. God, R.; Gumm, H. *Parallel HPLC in High-Throughput Analysis and Purification, Analysis and Purification Methods in Combinatorial Chemistry*; Wiley: Hoboken, NJ, **2004**; pp 307–320.
61. Nelander, H.; Andersson, S.; Oehlen, K. *J. Chromatogr. A* **2011**, *1218*(52), 9397–9405.
62. Pang, H.; Kenseth, J.; Coldiron, S. *Drug Disc. Today* **2004**, *9*(24), 1072–1080.
63. Gong, X.; Yeung, E. S. *Anal. Chem.* **1999**, *71*, 4989–4996.
64. Zhang, Y.; Gong, X.; Zhang, H.; Larock, R. C.; Yeung, E. S. *J. Comb. Chem.* **2000**, *2*, 450–452.
65. Zhong, W.; Yeung, E. S. *Electrophoresis* **2002**, *23*, 2996–3005.
66. Gong, X.; Figus, M.; Plewa, J.; *et al. Chromatographia* **2008**, *68*, 219–225.
67. Shalaeva, M.; Kenseth, J.; Lombardo, F.; Bastin, A. *J. Pharm. Sci.* **2008**, *97*(7), 2581–2606.
68. Wong, K.; Kenseth, J.; Strasburg, R. *J. Pharm. Sci.* **2004**, *93*, 916–931.
69. Pei, J.; Nie, J.; Kennedy, R. T. *Anal. Chem.* **2010**, *82*(22), 9261–9267.
70. Yukihira, D.; Daisuke Miura, D; Saito, K.; Takahashi, K.; Hiroyuki Wariishi, H. *Anal. Chem.* **2010**, *82*, 4278–4282.
71. Sun, G.; Yang, K.; Zhao, Z.; *et al. Anal. Chem.* **2007**, *79*, 6629–6640.
72. Lewis, K. J.; Wei, J.; Siuzdak, G. Encyclopedia of Analytical Chemistry; Meyers, R. A. Ed.; John Wiley & Sons Ltd: Chichester, **2000**; pp 5880–5894.
73. Crecelius, A. C.; Baumgaertel, A.; Ulrich, U. S. *J. Mass. Spectrom.* **2009**, *44*, 1277–1286.
74. Shevchenko, A.; Sunyaev, H.; Loboda, A.; *et al. Anal. Chem.* **2001**, *73*(9), 1917–1926.
75. Tholey, A.; Heinzle, E. *Anal. Bioanal. Chem.* **2006**, *386*, 24–37.
76. Covey, T. R.; Thomson, B.; Schneider, B. B. *Mass Spectrometry Reviews*; John Wiley & Sons Ltd: Chichester, **2009**; Vol. 28, Issue 6, pp 870–897.
77. Sampson, J. S.; Hawkridge, A. M.; Muddiman, D. C. *J. Am. Soc. Mass Spectrom.* **2006**, *17*(12), 1712–1716.
78. Nemes, P.; Vertes, A. *Anal. Chem.* **2007**, *79*(21), 8098–8106.
79. Ratcliffe, L. V.; Rutten, F.; Barrett, D. A.; *et al. Anal. Chem.* **2007**, *79*, 6094–6101.
80. Bruns, E. A.; Perraud, V.; Greaves, J.; Finlayson-Pitts, B. J. *Anal. Chem.* **2010**, *82*(14), 5922–5927.
81. Hayen, H.; Michels, A.; Franzke, J. *Anal. Chem.* **2009**, *81*(24), 10239–10245.
82. Peng, I.; Ogorzalek, L. R.; Margalith, E.; Little, M. W.; Loo, J. A. *Analyst.* **2010**, *135*(4), 767–772.
83. Cody, R. B.; Laramée, J. A.; Durst, H. D. *Anal. Chem.* **2005**, *77*(8), 2297–2302.
84. Helmy, R.; Schafer, W.; Buhler, L.; *et al. Org. Process Res. Dev.* **2010**, 386–392.
85. Chen, H.; Talaty, N. N.; Takáts, Z.; Cooks, R. G. *Anal. Chem.* **2005**, *77*(21), 6915–6927.
86. Williams, J. P.; Scrivens, J. H. *Rapid Commun. Mass Spectrom.* **2005**, *19*(24), 3643–3650.
87. Kauppila, T. J.; Wiseman, J. M.; Ketola, R. A.; *et al. Rapid Commun. Mass Spectrom.* **2006**, *20*, 387–392.
88. Haddad, R.; Sparrapan, R.; Eberlin, M. N. *Rapid Commun. Mass Spectrom.* **2006**, *20*(19), 2901–2905.
89. Manicke, N. E.; Kistler, T.; Ifa, D. R.; Cooks, R. G.; Zheng, O. *J. Am. Soc. Mass Spectrom.* **2009**, *20*, 321–325.
90. Kertesz, V.; Van Berkel, G. J.; Vavrek, M.; *et al. Anal. Chem.* **2008**, *80*, 5168–5177.
91. Kertesz, V.; Berkel, G. J. *Rapid Commun. Mass Spectrom.* **2008**, *22*, 2639–2644.
92. Chen, H.; Cotte-Rodriguez, I.; Cooks, R. G. *Chem. Commun.* **2006**, *6*, 597–599.
93. Girod, M.; Moyano, E.; Dahlia, I.; Campbell, D. I.; Cooks, R. G. *Chem. Sci.* **2011**, *2*, 501–510.
94. Kanu, A. B.; Dwivedi, P.; Tam, M.; Matz, L.; Hill, H. H. *J. Mass Spectrom.* **2008**, *43*, 1–22.
95. Kurulugamaa, R. T.; Valentineb, S. J.; Sowella, R. A.; Clemmera, D. E. *J. Proteom.* **2008**, *71*, 318–331.
96. Tang, K.; Shvartsburg, A. A.; Lee, H.; Prior, D. C.; *et al. Anal. Chem.* **2005**, *77*, 3330–3339.
97. Merenbloom, S. I.; Bohrer, B. C.; Koeniger, S. L.; Clemmer, D. E. *Anal. Chem.* **2007**, *79*, 515–522.
98. Dwivedi, P.; Wu, C.; Matz, L. M.; *et al. Anal. Chem.* **2006**, *78*(24), 8200–8206.
99. Tu, Q.; Wang, T.; Welch, C. J. *J. Pharm. Biomed. Anal.* **2010**, *51*, 90–95.
100. Welch, C. J.; Albaneze-Walker, J.; Leonard, W. R.; *et al. Org. Process Res. Dev.* **2005**, *9*, 198–205.
101. Lehn, J. M. *Perspect. Supramol. Chem.* **1994**, *1*, 307–317.
102. Yatsimirsky, A. K. *Encycl. Supramol. Chem.* **2004**, *1*, 809–815.
103. McDonagh, C.; Burke, C. S.; MacCrain, B. D. *Chem. Rev.* **2008**, *108*, 400–422.
104. Song, F. L.; Carder, E. J.; Kohler, C. C.; Kohler, K. K. *Chem. Eur. J.* **2010**, *16*, 13500–13508.
105. Bu, X.; Koide, K.; Carder, E. J.; Welch, C. *J. Org. Process Res. Dev.* **2013**, *17*, 108–113.
106. Pu, L. *Chem. Rev.* **2004**, *104*, 1687–1716.
107. Leung, D.; Kang, S. O.; Anslyn, E. V. *Chem. Soc. Rev.* **2012**, *41*, 448–479.
108. Parker, D. *Chem. Rev.* **1991**, *91*, 1441–1457.
109. Wenzel, T. J.; Chisholm, C. D. *Chirality* **2011**, *23*, 190–214.
110. Sawada, M.; Takai, Y.; Yamada, H.; Hiriyama, S.; Kandea, T. *J. Am. Chem. Soc.* **1995**, *117*, 7726–7736.
111. Schug, K.; Frycak, P.; Maier, N. M.; Lindner, W. *Anal. Chem.* **2005**, *77*, 3660–3670.
112. Kubo, Y.; Maeda, S. Y.; Tokita, S.; Kubo, M. *Nature* **1996**, *382*, 522–524.
113. Kubo, Y.; Hirota, N.; Maeda, S.; Tokita, S. *Anal. Sci.* **1998**, *14*, 183–189.
114. Tsubaki, K.; Nuruzzaman, M.; Kusumoto, T.; *et al. Org. Lett.* **2001**, *3*, 4071–4073.
115. Tsubaki, K.; Tanima, D.; Nuruzzaman, M.; *et al. J. Org. Chem.* **2005**, *70*, 4609–4616.
116. Wiskur, S. L.; Ait-Haddou, A.; Levigne, J. J.; Anslyn, E. V. *Acc. Chem. Res.* **2001**, *34*, 963–972.
117. Leung, D.; Folmer-Andersen, J. F.; Lynch, V. M.; Anslyn, E. V. *J. Am. Chem. Soc.* **2008**, *130*, 12318–12327.
118. Leung, D.; Anslyn, E. V. *J. Am. Chem. Soc.* **2008**, *130*, 12328–12333.

119. Li, Z.-B.; Lin, J.; Pu, L. *Angew. Chem. Int. Ed.* **2005**, *44*, 1690–1693.
120. Li, Z.-B.; Lin, J.; Sabat, M. H.; Hyacinth, M.; Pu, L. *J. Org. Chem.* **2007**, *72*, 4905–4916.
121. Mei, X.; Wolf, C. *Chem. Commun.* **2004**, *18*, 2078–2079.
122. Wang, H.; Chan, W.-H.; Lee, A. M. W. *Org. Biomol. Chem.* **2008**, *6*, 929–934.
123. Corradini, R.; Paganuzzi, C.; Marchelli, R.; *et al. J. Mater. Chem.* **2007**, *57*, 625–630.
124. Corradini, R.; Paganuzzi, C.; Marchelli, R.; *et al. Inclus. Phenom. Macrocyc. Chem.* **2008**, *62*, 476–480.
125. Zahn, S.; Canary, J. W. *Org. Lett.* **1999**, *1*, 861–864.
126. Holmes, A. E.; Zahn, S.; Canary, J. W. *Chirality* **2002**, *14*, 471–477.
127. Zhang, J.; Holmes, A. E.; Sharma, A.; *et al. Chirality* **2003**, *15*, 180–189.
128. Nieto, S.; Lynch, V. M.; Anslyn, E. V.; Kim, H.; Chin, J. *J. Am. Chem. Soc.* **2008**, *130*, 9232–9233.
129. Nieto, S.; Lynch, V. M.; Anslyn, E. V.; Kim, H.; Chin, J. *Org. Lett.* **2008**, *10*, 5167–5170.
130. Burns, J. A.; Whitesides, G. M. *Chem. Rev.* **1993**, *93*, 2583–2601.
131. Korbel, G. A.; Lalic, G.; Shair, M. D. *J. Am. Chem. Soc.* **2001**, *123*, 361–362.
132. Copeland, G. T.; Miller, S. J. *J. Am. Chem. Soc.* **2001**, *123*, 6496–6502.
133. Eelkema, R.; van Delden, R. A.; Feringa, B. L. *Angew. Chem. Int. Ed.* **2004**, *43*, 5013–5016.

9.03 Organic Synthesis in Small Scale Continuous Flow: Flow Chemistry

S Born, E O'Neal, and KF Jensen, Massachusetts Institute of Technology, Cambridge, MA, USA

© 2014 Elsevier Ltd. All rights reserved.

9.03.1	**Introduction**	54
9.03.2	**Microreaction Technology**	55
9.03.3	**Fundamentals of Flow Chemistry**	57
9.03.3.1	Chemical Kinetics in Flow Systems	57
9.03.3.2	Dispersion	57
9.03.3.3	Mixing in Flow Systems	59
9.03.3.4	Mass Transfer	60
9.03.3.5	Heat Transfer	60
9.03.4	**Flow Chemistry**	61
9.03.4.1	Homogeneous Reactions	61
9.03.4.1.1	Lithiation	61
9.03.4.1.2	DIBALH reduction	61
9.03.4.1.3	Reactive and high temperature/pressure chemistry	62
9.03.4.2	Liquid–Liquid Systems	64
9.03.4.3	Gas–Liquid System	69
9.03.4.4	Heterogeneous Systems	72
9.03.5	**Photochemical Systems**	76
9.03.5.1	Homogeneous Photochemical Reactions	77
9.03.5.2	Multiphase and Heterogeneous Photochemical Reactions	78
9.03.6	**Multistep Synthesis**	80
9.03.7	**Automation of Microfluidics**	84
9.03.7.1	Analytical Tools	84
9.03.7.2	Reaction Screening and Optimization	85
9.03.8	**Scaling Up**	87
9.03.9	**Conclusions**	91
Acknowledgments		91
References		91

Glossary

Continuous-flow/Continuous It is used to describe reactions, separations, or other fluid manipulations being performed on fluids which are flowing through a device. The word continuous is meant to refer to the fact that fluid never stops flowing into/out of the device during operation.

Continuously stirred-tank reactor (CSTR) A continuous-flow reactor in which inlets are assumed to immediately mix fully with other contents of the reactor, with outlet material representing this uniform concentration in the reactor.

Flow chemistry Chemical transformations performed in small scale flow systems.

Gradient A gradual change in a value (temperature, concentration) occurring over space or time. For example, a concentration gradient across a microreactor channel refers to concentration increasing or decreasing from one side of the channel to the other.

Micromixer Any device which continuously mixes a fluid on a small scale (channel diameters less than a few millimeters).

Microreactor Tubing or channels serve as reactors for the flow chemistry. The channel widths or tube diameters should be less than a few millimeters to be considered as microreactors.

Pressure drop In a continuous-flow system, frictional forces arising from fluid motion along a channel causes the pressure of that fluid to fall along the channel length. For a system at a defined set of operating conditions (flow rate, channel width/length), the experimental difference in pressure at any two points (such as the inlet and the outlet) is called a pressure drop.

Residence time The average time spent by fluid in a reactor (batch or flow) under a specific set of conditions.

9.03.1 Introduction

Continuous-flow chemical synthesis in millimeter or submillimeter systems has developed rapidly in the past decade with applications in nanomaterials, fine chemicals, and pharmaceuticals.[1–9] This evolution has been driven by the potential advantages of continuous synthesis, specifically increased safety allowing an expanded toolbox of reactions. The small scales enhance heat

 doi:10.1016/B978-0-08-097742-3.00912-5

and mass transfer enabling highly exothermic reactions to be conducted safely. Moreover, the continuous operation eliminates headspace issues and avoids accumulation of reactive or toxic intermediates. Synthesis applications are further enhanced by automated optimization as well as mechanistic and kinetic information gained from integrating reaction components with sensors, actuators, and automated fluid handling. Additionally, flow systems allow experiments on well-defined samples at conditions not easily accessed by conventional means, such as reaction at high pressure and temperatures.[10]

Continuous operation implies steady-state operation imparting robustness, stability, and scalability. In continuous flow, time in the reactor (residence time, τ) becomes equivalent to batch volume and production can be scaled by increasing time without changing mixing efficiency as in batch, which would otherwise impact yields. In general, flow systems tend to be easier to scale than the mixing challenges and reduced heat transfer area to volume constraints faced when scaling batch processes.[3] The more reactive systems and aggressive reaction conditions facilitated by flow systems typically lead to increases in throughput, with a dramatically reduced equipment footprint.

Continuous-flow chemical synthesis in small-scale systems has been given different names, including microreactor technology, flow chemistry, and microfluidic synthesis. In this chapter, the authors use the microreactors to refer to the flow reactor units and flow chemistry to describe organic transformations occurring in microreactors. With the already large number of reviews[1–9] and recent books[11,12] covering fundamental and detailed aspects of flow chemistry, the aim is not another exhaustive review, but rather to provide selected examples that illustrate important elements of synthesis in small-scale flow systems. The authors apologize to the readers and other authors that reference limitations meant that many outstanding reviews and primary studies of this large and rapidly growing field could not be included.

9.03.2 Microreaction Technology

Microreaction technology has advanced significantly over the past decade from individual laboratories producing their own devices to the worldwide infrastructure of vendors of individual devices and complete systems in metals, polymers, and ceramics (*see* Chapter 9.01).[2] Flow chemistry systems consist of the components illustrated in **Figure 1**.

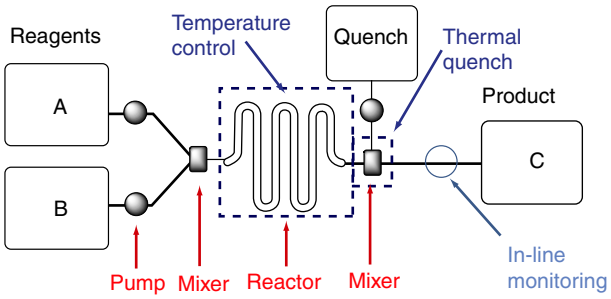


Figure 1 Components of a flow chemistry system.

Reagents are typically delivered in the $\mu l\,min^{-1}$ to $ml\,min^{-1}$ range by syringe and high precision liquid chromatography (HPLC) pumps. It is important to select chemically compatible syringes, seals, and pump heads. Most flow chemistry systems contain a mixing component to ensure rapid mixing of reagents before entering the reactor. In some designs, the mixing unit is part of the microreactor. There are two types of micromixers, active and passive.[13,14] The different mixing units and methods for determining the degree of mixing needed for a particular application are discussed in Section 9.03.3.3.

Microreactors are either microstructured devices made of glass, silicon–glass, ceramic, or stainless steel by microfabrication techniques (**Figure 2**) or they are tubes of fluorinated polymers or stainless steel (**Figure 3**). Microstructured devices can include mixing units, flow distributors, multiple channels, and means for immobilizing catalyst particles,[17] whereas the tube-based systems are often simpler to operate and maintain. Tube-based systems can be created from standard tubing, connectors, and HPLC components. Several commercial systems have been developed to enable scale-up of flow chemistry procedures to production levels (**Figure 4**). Production systems retain the heat and mass advantages of microreactors by introducing heat transfer layers between each reactor plate and employing static mixers on each plate.

A quench is needed at the exit of the microreactor to ensure that the reaction does not continue in the tube connecting the reactor to online concentration measurements. If the reaction is thermally activated, it may be sufficient to cool the reactor effluent. Otherwise, a quench stream has to be introduced in the outlet. Online measurements include the reactor temperature and the outlet concentrations by UV-visible, infrared, and Raman spectroscopies as well as HPLC.[18,19]

Work-up techniques are needed to implement continuous multistep synthesis. Continuous distillation and extraction systems known from commodity chemical production can be used at production scale. There has been considerable recent progress in developing miniaturized extraction[20] and distillation[21,22] units for laboratory scale, but most of these systems are still under development. In the following Section 9.03.3, the authors briefly review important fundamentals underlying the operation of flow chemistry systems.

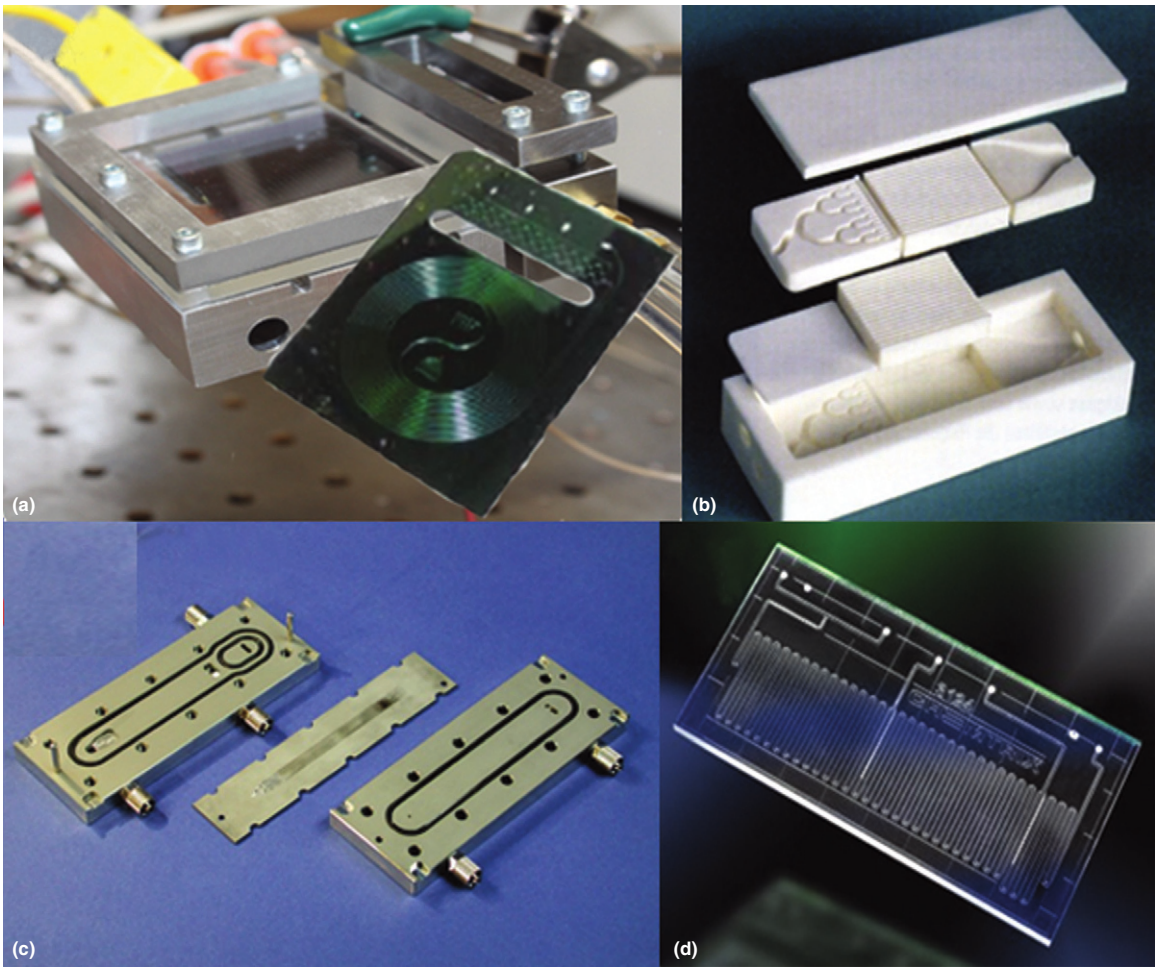


Figure 2 Examples of microstructured reactors in (a) silicon-Pyrex,[15] Reproduced from Bedore, M. W.; Zaborenko, N.; Jensen, K. F.; Jamison, T. F. *Org. Process Res. Dev.* **2010**, *14*, 432, with permission from American Chemical Society. (b) ceramics,[16] Reproduced from Knitter, R.; Liauw, M. A. *Lab Chip* **2004**, *4*, 378, with permission from Royal Society of Chemistry. (c) stainless steel (IMM). Reproduced from Hessel, V. R. A., Schouten, J. C., Yoshida, J. I., Eds. *Handbook of Micro Process Technology, Vol. 1–3*; Wiley-VCH: Weinheim, Germany, **2009**, and (d) glass (Chemtrix). Reproduced from Wiles, C.; Watts, P. *Micro Reaction Technology in Organic Synthesis*; CRC Press: Boca Raton, FL, USA, **2011**.

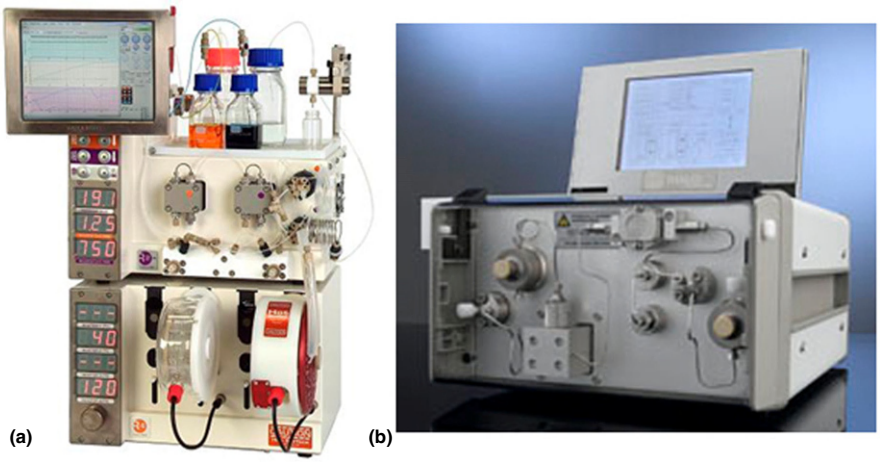


Figure 3 Examples of commercial systems using reactor tubes: (a) Vapourtec for general purpose flow chemistry and (b) ThalesNano H-Cube for catalytic hydrogenation.

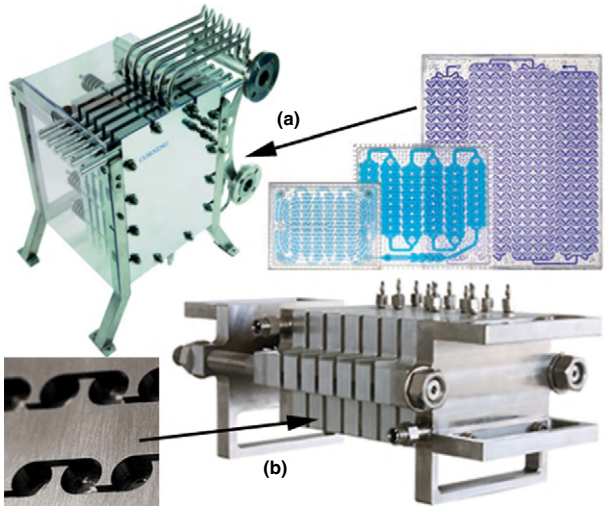


Figure 4 Examples of commercial flow reactor systems for production. (a) Corning Advanced Flow Reactors (AFR); the images on the left-hand side shows a silicon carbide Gen 4 reactor, the images on the right-hand side show glass reactor plates for Gen 1, 2, and 3. Note the size of the static mixer structures remain similar with scaling of the plates (Corning). (b) Lonza flow plate technology in stainless steel. The insert shows an example of a static mixing unit (Ehrfeld Mikrotechnik–BST).

9.03.3 Fundamentals of Flow Chemistry

9.03.3.1 Chemical Kinetics in Flow Systems

The simplest way to conceptualize a reaction occurring in a microfluidic system is to consider the reactor to be a steady-state, plug-flow reactor.[23] This means that there is no diffusion along the length of the reactor and concentration is uniform across the channel width. Moreover, the velocity in the reactor is the same for every fluid element in the reactor. At steady state, every point in a plug-flow reactor should have an unchanging concentration. Batch reactors and plug-flow reactors obey the same kinetic equation with the difference being that experimental time in a batch reactor corresponds to residence time in a plug-flow reactor. Consider the kinetic expression for a batch reaction, n^{th} order in reagent A:

$$\frac{dC_A}{dt} = -kC_A^n \tag{1}$$

where C_A is the concentration of reactant A, k is the rate constant, and t is experimental time. At steady state in a plug-flow reactor, it is also true that

$$\frac{dC_A}{d\tau} = -kC_A^n, \text{ where } \tau = V\dot{v} \tag{2}$$

where V is the reactor volume and $\dot{v}$ is the flow rate, and τ is the residence time in the reactor rather than the experimental time, t. In order to vary residence time in a microsystem, flow rates are normally changed, and three to five residence times are waited to ensure the system is at steady state (i.e., equation 2). This process can be time consuming; short residence times are measured much more accurately in flow experiments.

9.03.3.2 Dispersion

Treating a microreactor as a plug-flow reactor is a useful concept, but as flow rates increase and the width of the channel becomes larger, this approximation eventually fails. In laminar flow, which governs small-scale flow systems, the fluid in the center of the tube is moving twice as fast as the average fluid velocity, resulting in axial dispersion. This presence of dispersion in a reactor leads to a distribution of residence times rather than a single residence time (Figure 5). Many fluid elements spend substantially more or less time in the reactor than the 'average' residence time set by the flow rate and reactor volume, often reducing yield. Furthermore, there can be significant interaction between fluid packets of different residence times in the reactor, potentially affecting selectivity. It should be noted that the average residence time does not change as dispersion increases.

A continuously stirred tank reactor (CSTR) represents the extreme form of total dispersion, where fluids packets of all residence times are mixed together. As a plug-flow reactor approaches the behavior of a CSTR via increasing dispersion, yield and selectivity will suffer in most systems and can be predicted.[23] Thus, it is important to design microfluidic systems to avoid dispersion and to

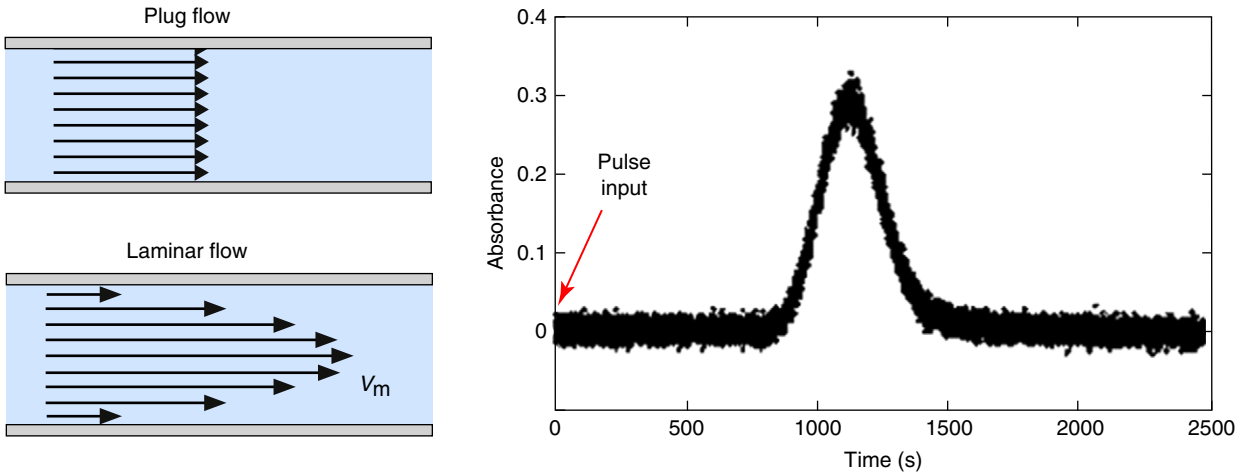


Figure 5 Fluid velocity profile in a plug flow vs. laminar flow (left). Residence time distribution of a microreactor (right).[24] When a tracer is pulsed into the reactor, the effluent concentration can be measured in terms of absorbance. Although the average residence time is 1143 s, the tracer also exits the reactor at substantially earlier and later residence times.

know when dispersion exists so as to appropriately interpret data. The magnitude of the Bodenstein number (Bo) indicates whether large deviations from plug flow exist. Bo is defined as

$$\mathrm{Bo} = \frac{uL}{D} \tag{3}$$

where u is the velocity of the fluid, L is the length of the reactor, and D is the dispersion number. The dispersion number represents the 'effective diffusivity' of a species along the length of a microreactor when including the hydrodynamic effects from laminar flow. It can be predicted depending on the flow conditions.[23] For Bo < 10 000, the Taylor–Aris dispersion model applies:

$$D = D + \frac{u^2 {d_t}^2}{4\beta D} \tag{4}$$

where D is the diffusion coefficient, d_t is the tube diameter or channel width, and the parameter β is 48 for tubes and 30 for square channels. Nagy et al.[25] give Bo as a function of channel width and the residence time (Figure 6). For Bo > 1000, plug flow is a good assumption. For 100 < Bo < 1000, small deviations from plug flow occur and for 1000 < Bo < 10 000, larger deviations occur. These cases can be modeled using the classical Taylor–Aris approach to dispersion (equation 4).[23] When Bo > 10 000, full simulations of the laminar flow becomes necessary for accurately predicting reactor performance.[23]

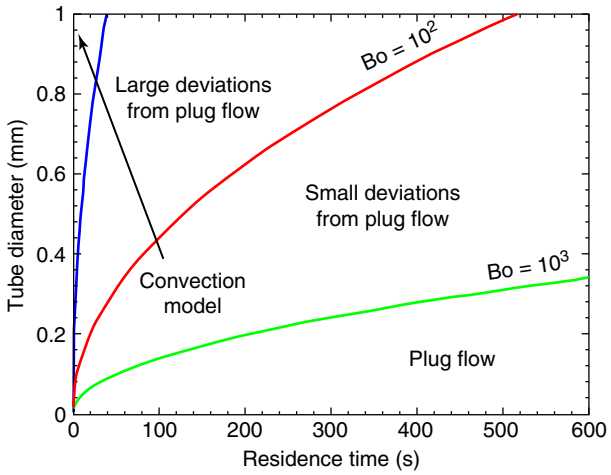


Figure 6 Given a certain tube diameter and the residence time, deviations from plug flow can be predicted. Reproduced from Nagy, K. D.; Shen, B.; Jamison, T. F.; Jensen, K. F. *Org. Process Res. Dev.* **2012**, *16*, 976, with permission from American Chemical Society.

As an example, consider a reaction that reaches 95% conversion at a 300 s residence time in a 400 μm diameter tubing. According to Figure 6, there will be small deviations from plug flow, which implies a <1% decrease in conversion for first- and

second-order reactions. When large deviations from plug flow are present, <3% decrease in conversion will generally result at 95% conversion. Effects will generally be larger for substantially lower conversions. For example, a <5% decrease in conversion is expected in the 'large deviations' regime when running a reaction at 50% conversion. Reaction engineering textbooks[23] provide details on how to calculate dispersion numbers and their effects for conditions not considered here (larger tubes, higher flow rates, and operation at different conversions). As mentioned in the introduction to this section, systems with high-dispersion approach the behavior of a CSTR in the limit of infinite dispersion. Reduced dispersion is one reason small-scale reactive flow systems often outperform larger scale flow systems. Special considerations have to be included when extending the above discussion for homogeneous laminar flow to reactors loaded with static mixers or solid spheres.

9.03.3.3 Mixing in Flow Systems

The rate at which two fluids are mixed can have a large effect on selectivity and yield for fast reactions.[13,26,27] When two miscible laminar streams are mixed in a T-junction, mixing occurs via diffusion only between the two streams (unless very high flow rates are used[28]), and a homogeneous mixture will result after some mixing time, τ_{Diff} the diffusion timescale:

$$\tau_{Diff} = \frac{{d_t}^2}{4D} \tag{5}$$

where d_t is the diameter or channel width and D is the diffusion coefficient. For a reactive process, comparing the reactive timescale with the diffusion timescale will allow us to estimate whether a reaction rate is limited by diffusive mixing. The Damköhler number represents the ratio of reaction to mixing rates:

$$\mathrm{Da} = \frac{Rate\ of\ reaction}{Rate\ of\ mixing} = \frac{\tau_{Diff}}{\tau_{Rxn}} = \frac{kC_0{}^{n-1}{d_t}^2}{4D} \tag{6}$$

Here, C_0 is the initial concentration of reacting species and k is the reaction rate constant. For Da < 1, improved mixing is expected to have a small impact, whereas for Da > 1 improved mixing is necessary for optimal yield and selectivity. The Damköhler number can be estimated even if the exact rate form is unknown as long as an approximate rate form can be assumed. Consider an example of a first-order reaction. The relationship between the rate constant and conversion follows the form:

$$k = -\frac{\ln(1-X)}{\tau} \tag{7}$$

where X is the conversion after some residence time, τ. For 95% conversion, $k\tau = 3$. Solving for the rate constant, k, and inserting into the expression for the Damköhler number (equation 6), the following is obtained:

$$\mathrm{Da} = = \frac{3{d_t}^2}{4\tau D} \tag{8}$$

This can be evaluated from known physical parameters for the system. For reactions of higher order and various initial concentrations, Nagy et al.[25] provide convenient tables and charts for estimating whether improved mixing is important for a reaction. A plot of various Damköhler numbers for an example of a first-order reaction is shown in Figure 7.

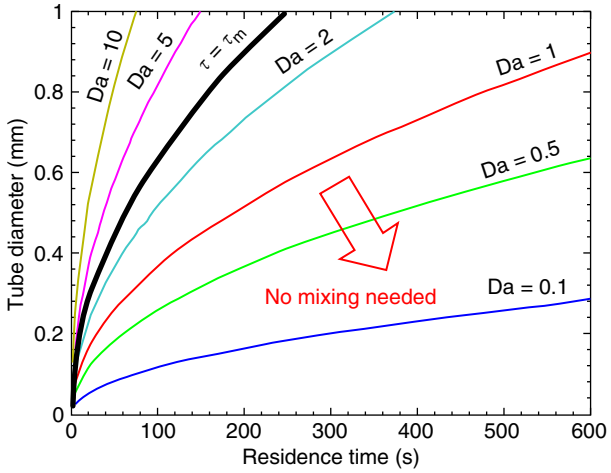


Figure 7 Plot of Da as a function of tube diameter and residence time, assuming a T- or Y-junction is used for mixing the streams. For Da < 1, the diffusion rates exceeds the reaction rate and so no additional mixing scheme is necessary. Reproduced from Nagy, K. D.; Shen, B.; Jamison, T. F.; Jensen, K. F. *Org. Process Res. Dev.* **2012**, *16*, 976, with permission from American Chemical Society.

For cases where Da > 1, improvements in mixing can be obtained using passive or active micromixers.[13,14] In passive systems, mixing is achieved by diffusion and chaotic advection created by specially designed internal flow geometries. Mixing is realized in active devices by applying external force fields such as thermal actuation, electrokinetics, mechanical motion, and dynamic pressure fluctuations and acoustics. The low maintenance of passive micromixers make them favored choices for chemical synthesis at laboratory, pilot, and plant scales, whereas active micromixers are generally useful for very low volume applications, such as diagnostic systems. The choice of a suitable micromixer for a reaction largely depends on the reaction time, physical properties of the fluids (relative difference in the viscosity and density), volumes of fluids to be mixed in a given time to match the time cycle with other unit operations, and materials of construction. In addition to mixing time, it is important to consider pressure drops. A pressure drop is the difference in pressure required to push a solution through a device, which arises due to frictional forces. The use of fluid lamination and focusing to increase contact area usually leads to significant pressure drops. Another effective method is introducing an inert second phase into the channel, causing segmented flow and internal mixing.[29] If the reaction does not proceed at low temperatures, a cooled mixing zone can be included in the system, to ensure that the reaction begins only after mixing is complete. The diffusive timescale (equation 5) can be used to estimate the required mixing time for this approach.

9.03.3.4 Mass Transfer

One outstanding property of microreactors is the ability to obtain high mass transfer rates between different phases. In Sections 9.03.4.2 and 9.03.4.3, the effects of this high mass transfer on yield and selectivity will become clear. This property will be cited a number of times in this chapter and often values for the relevant overall mass transfer coefficient between two phases, k_{La}, will be given.

Consider a gas–liquid reaction, where the gas phase (g) has some concentration of species A ($C_{A,g}$), which is transported to the liquid phase (l) where a fast reaction occurs with B. The reaction occurs fast enough so that the rate of transport of A from the gas to the bulk of the liquid phase limits the reaction rate. If it is assumed that the gas phase is well mixed and that equilibrium exists at the interface of the phases, the concentration of A at the gas–liquid interface on the liquid side becomes

$$C_{A,l,\text{interface}} = H_A C_{A,g} \tag{9}$$

where H_A is Henry's law constant for A in the gas and liquid phase. The rate of depletion of A from the gas phase depends on how fast this interfacial concentration of A is transported to the bulk liquid in which it reacts instantaneously:

$$\frac{dC_{A,g}}{dt} = -k_{La} C_{A,l,\text{interface}} = -k_{La} H_A C_{A,g} \tag{10}$$

Here, k_{La} is the mass transfer coefficient. This mass transfer coefficient has units of time^{-1}. When equation 10 is integrated, the form obtained is

$$C_{A,g} = C_{A0,g} e^{-H_A k_{La} t} \tag{11}$$

where $C_{A0,g}$ is the initial concentration of reactant in the gas phase. As this species partitions into the liquid phase where it reacts, the concentration of A in the gas phase, $C_{A,g}$, declines. Stating the mass transfer coefficient in this way illustrates its similarity with a typical kinetic expression for a first-order reaction:

$$C_A = C_{A0} e^{-k_{Rxn} t} \tag{12}$$

Thus, the k_{La} as defined and referenced throughout this chapter is a measure of the rate of mass transfer from one phase to the other. When a system is fully mass transfer limited, the k_{La} multiplied by the Henry's law constant (solubility constant) of the species of interest is analogous to the rate constant for a first-order reaction. For this simple case, mass transfer limitations are expected when $H_A k_{La} \ll k_{Rxn}$, since this implies that the intrinsic rate of transport of species to the reaction medium/site is much slower than the intrinsic rate of reaction. Not only does this substantially increase the residence time (and capital cost) of a reactor, it often leads to selectivity concerns. Chemical examples of this phenomenon are covered in Sections 9.03.4.2–9.03.4.4.

9.03.3.5 Heat Transfer

Microreactors typically have very good heat transfer properties, in part owing to the high surface-to-volume ratio of microfluidic systems. This means that the temperatures of highly exothermic reactions can be controlled, which reduces side reactions and allows for process intensification.[26] There are two resistances to heat transfer to be considered – heat transfer in the reactor wall and within the reacting fluid. The reactor material is normally contacted with a heating jacket at constant temperature and little heat transfer resistance at the point of contact is assumed. Making the reactor wall of thin layers of highly conductive materials keeps the jacket temperature representative of the temperature experienced by the outermost fluid in the reactor (i.e., they reduce the heat transfer resistance of the reactor wall). The Biot number, defined below, gives an estimate of whether this is the case:

$$\text{Bi} = \frac{\kappa_F t_W}{\kappa_W t_F} \tag{13}$$

Here, κ_F and κ_W is the thermal conductivity of the fluid in the reactor or the reactor wall material, respectively. The value of t_W is the thickness of the wall and t_F is either the radius or half-width of the fluidic channel. If the $Bi \ll 1$, then the wall of the reactor is providing a small amount of heat transfer resistance compared with the resistance of the fluid itself. Hence for a small Bi number, the temperature at the wall contacting the fluid is almost the same as that measured by a temperature probe outside of the tube. For a 500 μm inner diameter tubing (1/16" outer diameter) with water as a fluid, the Bi numbers for Teflon, stainless steel, and silicon would be 13, 0.13, and 0.01, respectively.

Next, let us consider gradients in temperature within the reaction medium that might arise when high heats of reaction are present. An upper bound on the temperature gradient along a tubular reactor is called the adiabatic temperature rise, which is simply the change in temperature of the reacting fluid if the reactor is perfectly insulated:

$$\Delta T_{Ad} = \frac{XC_0\Delta H_{rxn}}{\rho C_p} \tag{14}$$

Here, ΔH_{rxn} is the heat of reaction (J mol^{-1}), C_0 is limiting reagent feed concentration (mol l^{-1}), X is the reaction conversion, C_p is the specific heat capacity (J $(kg\ K)^{-1}$) of the reaction fluid, and ρ is the density of the fluid (kg l^{-1}). One can consider the ΔT_{Ad} as a worst-case scenario temperature gradient in a tubular reactor. The rate of heat generated in a channel can be compared with the rate of removal using the following equation[26]

$$\beta = \frac{\text{heat generated}}{\text{heat removed}} = \frac{-r\Delta H_{rxn} d_F^2}{4\Delta T_{Ad}\kappa_F} \tag{15}$$

where r is the reaction rate (mol $(l\ s)^{-1}$). Here, to avoid temperature gradients in the reaction mixture (assuming a small Bi number), $\beta 1$ is desired. Note that the performance improves dramatically as d_F, the tube diameter, is reduced. Calculations for silicon microreactors demonstrate small Biot numbers and small temperature gradients (even for fast exothermic reactions), enhancing chemical selectivity. These properties are both in stark contrast to typical glass batch reactors. Hartman et al.[26] provide examples of heat transfer scaling parameters for a few microreactor cases.

9.03.4 Flow Chemistry

9.03.4.1 Homogeneous Reactions

9.03.4.1.1 Lithiation

Lithiations and metal–halogen exchange reactions are known to be fast and highly exothermic. Slow addition at cryogenic temperatures is essential in order to avoid rapid temperature increases when the reaction is carried out in a conventional flask reactor. The excellent thermal conductivity and high surface-to-volume ratio of microreactors are especially useful in studying extremely fast and exothermic reactions, and for the control of highly reactive, short-lived reactive intermediates.[30]

Yoshida et al.[31] have demonstrated such control by performing the enantioselective carbolithiations of conjugated enynes **2** with a chiral organolithium species **1**, followed by the addition of the unstable intermediates **3** to various electrophiles, obtaining enantioenriched chiral allenes **4**. Their microfluidic system consisted of three T-shaped micromixers (M1, M2, and M3) and three microtube reactors (R1, R2, and R3) (**Figure 8**). Two significant trends were observed by varying the residence time in R2 (τ_{res}) across a range of temperatures. The first was that the yield increased with increasing τ_r and temperature. The second, in contrast, was that the enantiomeric ratio (*er*) decreased with increasing τ_r and temperature, presumably because of epimerization of the intermediate **3a**. This result implies that the decrease of *er* resulted from epimerization of the lithiated species rather than from its initial formation. The contrast between continuous and batch regimes ($\tau_r = 25$ s, $T = -78$ °C) was significant. Continuous production of **4a** in 91% yield and 91% selectivity (*er*) was superior to the batch production resulting in 99% yield and 61% selectivity.

9.03.4.1.2 DIBALH reduction

Aldehydes play a prominent role in synthetic organic chemistry, and reliable methods to prepare this versatile functional group are consequently of great importance. The partial reduction of esters using diisobutyl aluminum hydride (DIBALH) at low temperatures is particularly appealing conceptually; it converts widely available and inexpensive esters directly to the corresponding aldehyde, often proceeding in high yield. However, due to the greater reactivity of aldehydes, selectivity is strongly dependent on the reaction temperature, with overreduction to the alcohol observed, even at −78 °C. The requirement for cryogenic temperatures and a slow addition rate of DIBALH has deterred the use of this method on a large scale.

Webb and Jamison[32] have recently demonstrated the selective DIBALH reduction of esters to aldehydes (**Table 1**) by using a system composed of three precooling loops (ester, DIBALH, and MeOH feeds) and two reactors (R1 and R2), each constructed from standard perfluoroalkoxy (PFA) (0.75 mm ID) tubing T-shaped mixers (Tefzel, 0.50 mm ID) were used to combine the streams that were introduced by syringe pump devices, and the entire assembly was submerged in a cooling bath held at −78 °C.

A variety of esters were examined, including the more sterically encumbered cyclohexanecarboxaldehyde, which is prone to overreduction, and the epimerizable lactate and propanoate derivatives (**Table 2**). With the incorporation of an in-line quench (MeOH), these transformations were generally complete in less than 60 s. Mixing of the DIBALH and ester solutions was observed to be an exceptionally critical parameter for optimum results.

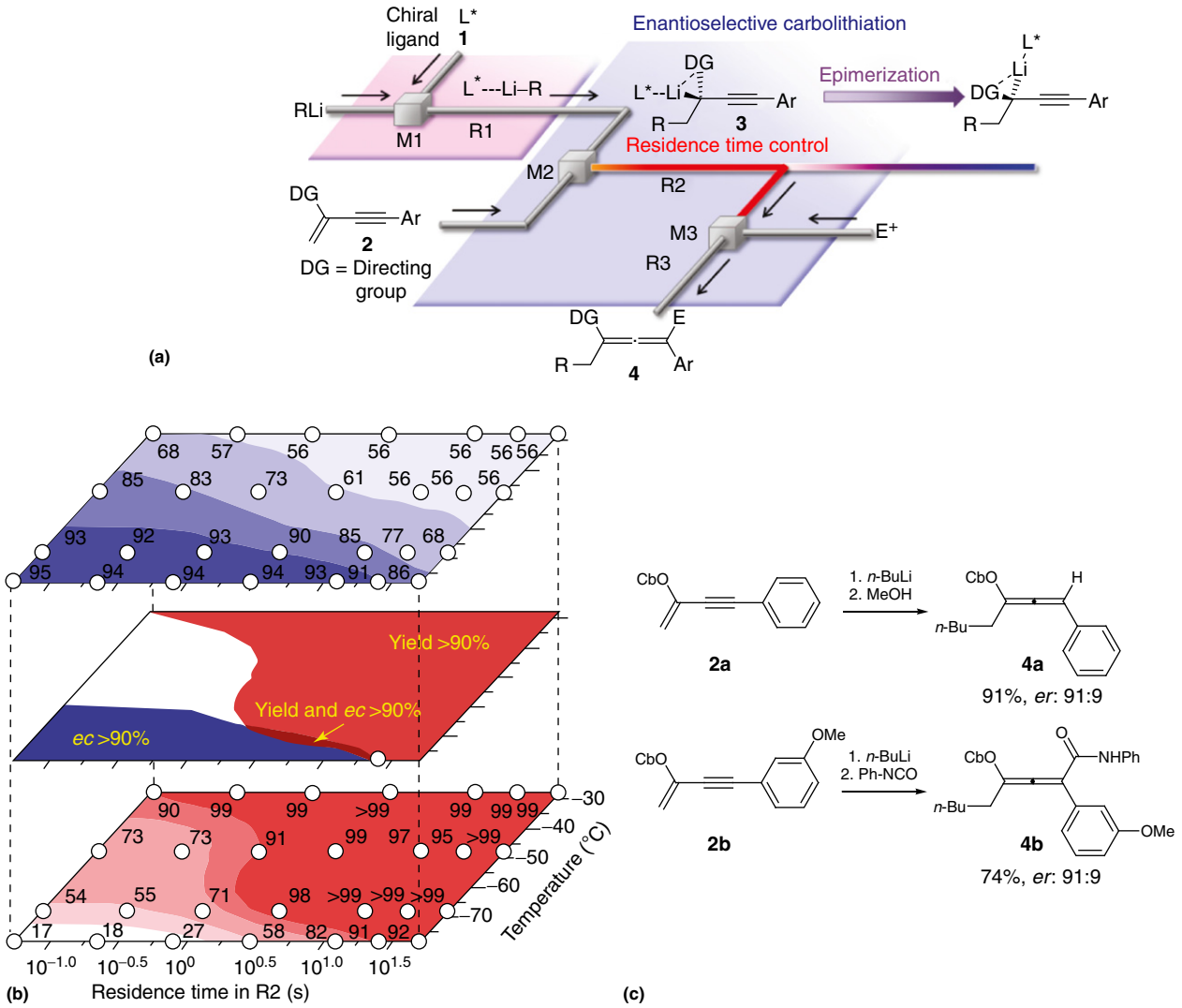


Figure 8 (a) A flow microreactor system for enantioselective carbolithiation and electrophile trapping. (b) Temperature–residence time (in R2) map for the reaction of **2a** in the presence of **1a**. Contour plot with scatter overlay of enantiomeric composition/ratio (*ec* or *er*) of **4a** (upper), contour plot with scatter overlay of the yield of **4a** (lower), and the domain that gave the highest yield (>90%) and highest *ec* (>90%) (middle). (c) Carbolithiation and electrophile trapping. Reproduced from Tomida, Y.; Nagaki, A.; Yoshida, J.-I. *J. Am. Chem. Soc.* **2011**, *133*, 3744, with permission from American Chemical Society.

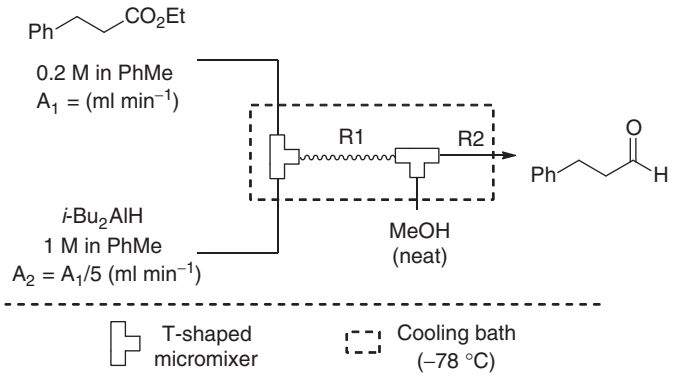
9.03.4.1.3 Reactive and high temperature/pressure chemistry

The use of hydrazoic acid as an azide source, based on reactivity, atom economy, waste generation, and economic considerations, is conceptually the most straightforward approach to a wide range of amines and heterocycles.[33] Unfortunately, HN_3 is extremely toxic (comparable to HCN) and owing to the explosive nature and low boiling point (37 °C) of this high-energy material,[34–36] procedures involving free HN_3 have not found many practical applications.

Interest in tetrazole chemistry over the past few years has been increasing rapidly, mainly as a result of the role played by this heterocyclic functionality in medicinal chemistry as a metabolically stable surrogate for carboxylic acid functionalities. Gutmann et al.[37] have safely demonstrated general and scalable methods for the continuous flow synthesis of 5-substituted 1H-tetrazole derivatives via hydrazoic acid addition to organic nitrile.[38,39] The key to this process is the *in situ* generation of HN_3 from NaN_3 and acetic acid in a microreactor coupled to an intensified high-temperature/high-pressure flow addition step to the nitrile. Owing to a lack of a reactor headspace, the risk of a HN_3 explosion is significantly reduced. Furthermore, the available concentration of HN_3 should in fact be significantly higher than that in a sealed microwave vessel, where a large amount of this volatile reagent can be expected to be in the gas phase.[40]

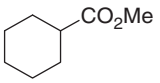
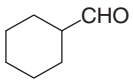
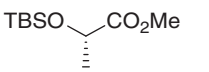
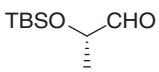
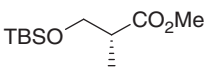
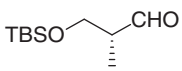
For flow processing (Figure 9), the nitrile solution was pumped into the mixer (M, T-piece), joining the azide solution at a differential flow rate providing approximately 2.5 mol l^{-1} excess of azide. The resulting stream was passed through the Sulfinert reactor coil (approximately 10 ml heated volume) at 220 °C at a system pressure of 3.6 MPa. The overall flow rate of 1.0 ml min^{-1} produced a residence time of 10 min in the reactor coil. After passing through a heat exchanger (providing a rapid thermal

Table 1 Evaluation of the effect of residence time on the continuous DIBALH reduction



A_1 (ml min^{-1})	R_1 (μl)	τ_R (s)	Yield (%)
5	23	0.23	36
10	23	0.11	50
30	23	0.04	96
5	228	2.28	43
10	228	1.14	61
30	228	0.38	97
5	684	6.84	57
10	684	3.42	85
30	684	1.14	96

Table 2 Representative conditions for the selective reduction of various commonly used esters

Substrate	Product	A_1 (ml min^{-1})	DIBALH (# Equivalents)	R_1 (μl)	τ_R (s)	Yield (%)
		10	1.1	1.62	8.0	>95
		5	1.6	1.62	15.0	>95
		5	1.5	1.62	15.0	>95

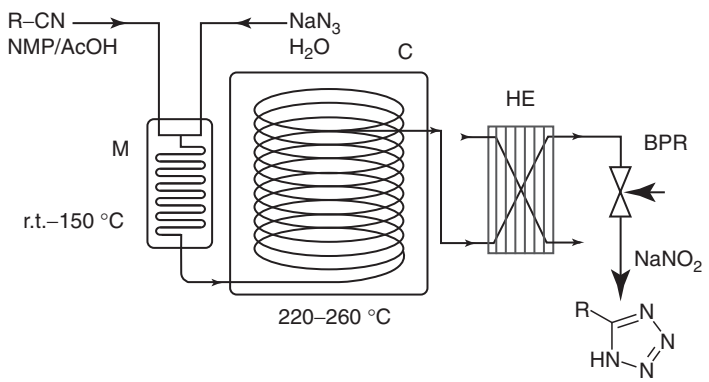
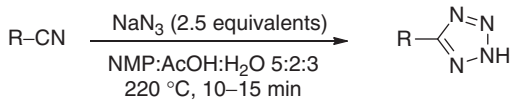
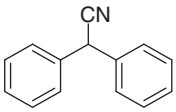
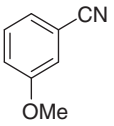
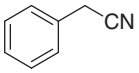
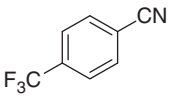
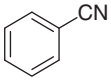
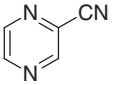


Figure 9 Schematic diagram for the continuous-flow tetrazole synthesis performed in a FlowSyn reactor from Uniqsis; C: coil reactor; HE: heat exchanger; BPR: back pressure regulator (3.4 MPa). Copyright © 2012 John Wiley and Sons.

quench) and back pressure regulator, the reaction mixture was flowed directly into a reservoir of aqueous $NaNO_2$ to decompose any unreacted HN_3. Under optimized conditions, tetrazoles are formed with quantitative conversion in residence times of a few minutes, providing excellent purities and yields of isolated product (Table 3).

Table 3 Synthesis of 5-substituted-1*H*-tetrazoles in a continuous-flow reactor under homogeneous conditions



Substrate	*Δ*	τ_R *(min)*	*Yield (%)*	*Substrate*	*Δ*	*Time (min)*	*Yield (%)*
	MW	15	81		MW	10	90
	Flow	15	82		Flow	10	90
	MW	10	94		MW	10	93
	Flow	10			Flow	10	97
	MW	10	86		MW	10	62
	Flow	10	95		Flow	10	68

Note: (i) Conditions MW: 1.0 mmol of nitrile, 2.0 mmol of NaN_3, 1.0 ml of solvent (NMP/AcOH/H_2O =7:2:1). Single-mode microwave heating at 220 °C (Biotage Initiator) and (ii) Flow conditions: nitrile solution (1 mol l^{-1}, NMP/AcOH=5:2) at a flow rate of 0.69 ml min^{-1}, and the azide solution (5.2 mol l^{-1}, H_2O) at 0.31 ml min^{-1}, through the reactor at 220 °C (FlowSyn, Uniqsis).

Source: Reproduced from Palde, P. B.; Jamison, T. F. *Angew. Chem. Int. Ed. Engl.* **2011**, *50*, 3525.

9.03.4.2 Liquid–Liquid Systems

The application of biphasic liquid–liquid reactions to microfluidic systems is particularly interesting because of the opportunities to manipulate flow patterns between the two immiscible phases (*see* Chapter 9.12). High rates of mass transfer between the two phases can be achieved, often leading to significant enhancements in reaction rates and selectivity. The flow of two immiscible liquids in a microreactor displays different hydrodynamics depending on both the absolute and relative velocities of the two liquids in Figure 10.[42,43] Segmented flow is the most common liquid–liquid flow regime used for chemical synthesis in microfluidic devices.

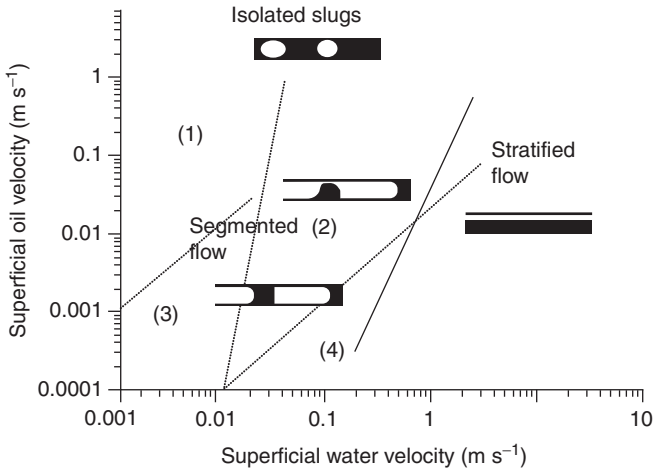


Figure 10 Different flow regimes for liquid–liquid flow in microchannels.[41] The continuous phase is defined as the phase wetting the walls of the channel. Copyright © 2006 Royal Society of Chemistry.

During segmented flow, the individual packets of fluid undergo internal recirculation, which improves mass transfer between the two phases. However, the mixing in segmented flow is not always sufficient. Further improvements in mixing can be achieved by using a tube packed with inert spheres (a 'packed bed'). As an example, Bogdon and McQuade[44] demonstrated that segmented flow into a packed bed created fine emulsions, significantly enhancing mass transfer between the two phases in alcohol oxidation experiments.

As one might expect, mixing two miscible liquids along with an inert immiscible liquid to form segmented flow will provide enhanced mixing exceeding that from just diffusion between the miscible liquids (Figure 11).[45] Mixing times between 100 ms and 10 s can be obtained in 400 μm channels depending on the flow conditions,[43] with mixing times less than 100 ms having been obtained for smaller channels.[45] This represents a significant improvement compared with mixing two miscible fluids without an added inert phase, which takes on the order of a minute for a 400 μm channel.

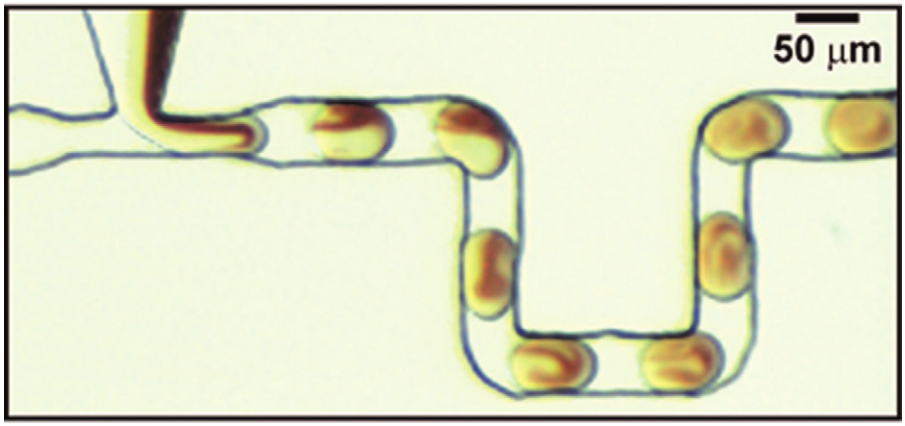
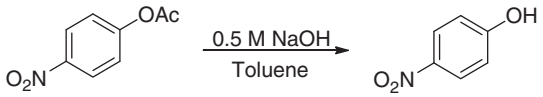


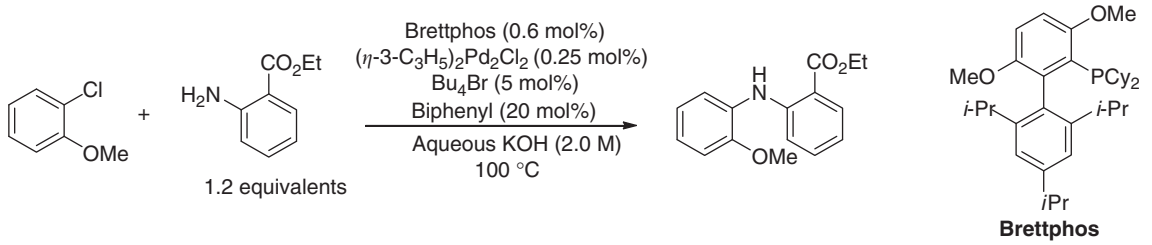
Figure 11 Mixing via segmented flow. Reproduced from Song, H.; Bringer, M. R.; Tice, J. D.; Gerdts, C. J.; Ismagilov, R. F. *Appl. Phys. Lett.* **2003**, *83*, 4664, with permission from American Institute of Physics.

The effect of recirculation on a two-phase chemical reaction can be exemplified by acetate hydrolysis (Scheme 1) in a biphasic water–toluene system.[46] Since the rate of transport of the relatively nonpolar reagent to the water containing the base is much slower than the intrinsic rate of reaction in this case, the transformation is mass transfer limited. Therefore, increasing the mass transfer rate (faster stirring in a flask or recirculation inside of a liquid slug in a microreactor) will increase the rate. Specifically, when the reaction was performed in a stirred flask and compared with the results using segmented flow in a microreactor, the continuous segmented flow considerably outperformed the batch experiment for equal reaction times.



Scheme 1 Hydrolysis of *p*-nitrophenyl acetate.

The improved rates of mass transfer in segmented liquid–liquid flow are not always sufficient to provide high conversions at low-enough residence times. This situation arises if the reaction is very fast or reactants of interest are both highly insoluble in the phase containing the other reactant (i.e., small Henry's constant in equation 9). For example, Naber and Buchwald[47] recently examined a palladium-catalyzed C–N cross-coupling reaction in water–toluene (Scheme 2). This two-phase approach was taken to avoid precipitation of salt byproducts in the microchannel but introduced a mass transfer limitation to the reaction rate. At 80 °C in batch with a fast stir rate (~900 rpm), 94% yield was obtained in 6 h. Using a small diameter PFA tube with segmented flow under similar conditions produced a yield of ~20% obtained in 10 min (Figure 12). When inert stainless steel beads were packed into the tube, the mass transfer was greatly enhanced and full yield was obtained in 6 min under equivalent conditions.



Scheme 2 Example of palladium-catalyzed C–N cross-coupling reaction run in two-phase (toluene–water) flow.

Mass transfer limitation can have significant impact on selectivity as exemplified by investigations of phase-transfer-catalyzed alkylations (Scheme 3).[48] In this case, both a side reaction and a consecutive reaction influence the yield of the desired monoalkylation product. In a biphasic environment, mass transfer limitations reduce the ideal kinetic selectivity of

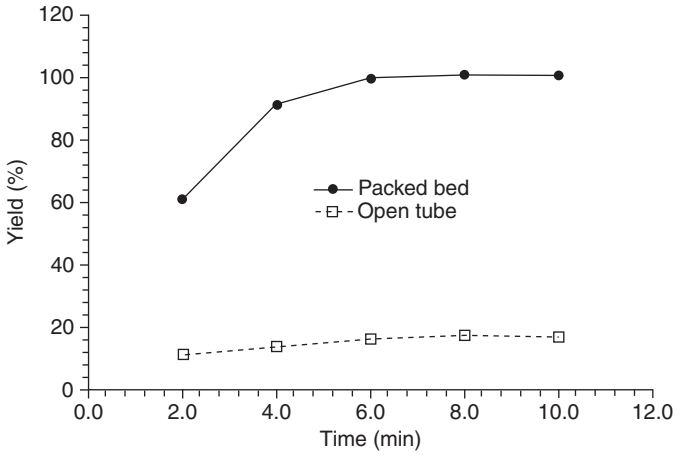
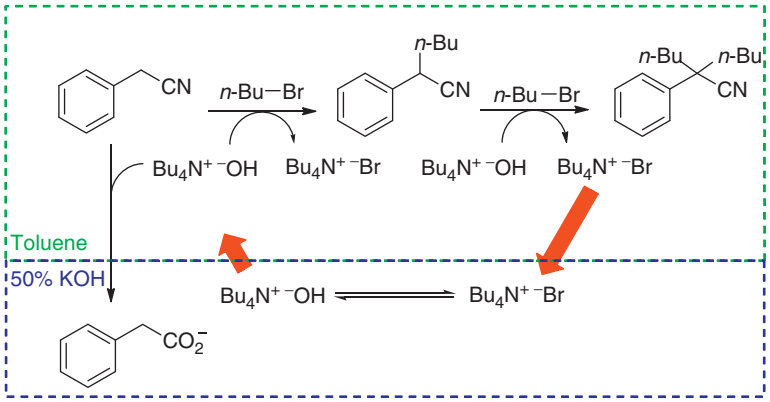


Figure 12 Coupling reaction using *n*-Bu_4Br as a phase transfer catalyst (optimized to 1 mol%). Segmented flow results vs. two-phase flow through an inert packed bed. Reproduced from Naber, J. R.; Buchwald, S. L. *Angew. Chem. Int. Ed.* **2010**, *49*, 9469, with permission from John Wiley and Sons.

monoalkylated product over dialkylated product. The sluggish removal of monoalkylated product from the liquid–liquid interface (slow mass transfer) after initial formation could result in higher concentrations of monoalkylated product being exposed to hydroxide at the interface. Increasing the mass transfer rate reduces the overalkylation. The amount of the carboxylic acid product relative to alkylated products will be unaffected by the mass transfer rate since it is formed in a parallel reaction to the first alkylation. When the segmented flow system was compared with batch, higher conversions and selectivities were obtained due to an increase in mass transfer rate (Figure 13).



Scheme 3 Example of phase-transfer-catalyzed alkylation run in a microreactor.[48]

The authors estimated an enhancement in the mass transfer coefficient (k_{La}) from 0.24 to 0.47 s^{-1} by increasing the aqueous-to-organic flow rate from 1 to 6. Higher ratios led to a flow regime change to an undesired parallel flow (Figure 10). An optimum ratio of 2:3 was found with respect to the production rate of product because varying the aqueous-to-organic ratio increases the mass transfer rate at the expense of throughput. The selectivity decrease at higher flow ratios was attributed to excess of KOH in the organic but increasing the concentration of hydroxide in the organic phase would be expected to speed up both the desired and undesired reaction equally. Instead, operation at a higher conversion is likely to cause selectivity issues as the higher concentration of monoalkylated product will lead to an increased rate of dialkylation.

A microreactor study of a phase-transfer-catalyzed Wittig reaction (Scheme 4) further illustrates the importance of mass transfer.[49] Increasing the ratio of aqueous flow rate to organic flow rate was 0.25–2, enlarged the active interfacial area fivefold (Figure 14). In fact, the mass transport became so fast that the high hydroxide concentrations in the organic phase lead to an increased decomposition of the phosphonium salt. As a result, there is an optimal mass transfer rate for selectivity.

Liquid–liquid biphasic systems can also be utilized to generate and separate reactive species, such as diazomethane. Despite being an extremely toxic, carcinogenic, odorless, and explosive yellow gas, diazaomethane is one of the most versatile reagents available for the preparation of carbon–carbon and carbon–heteroatom bonds. Maurya et al.[50] recently demonstrated a microfluidic reactor design fabricated in polydimethylsiloxane (PDMS) that not only safely and efficiently generates diazomethane, but also facilitates its separation and subsequent utilization (Figure 15). Key to this design was a dual-channel system that enabled diazomethane (generated from the union of aqueous KOH and Diazald/dimethylformamide (DMF) feeds) to be selectively transported across a 45 μm PDMS

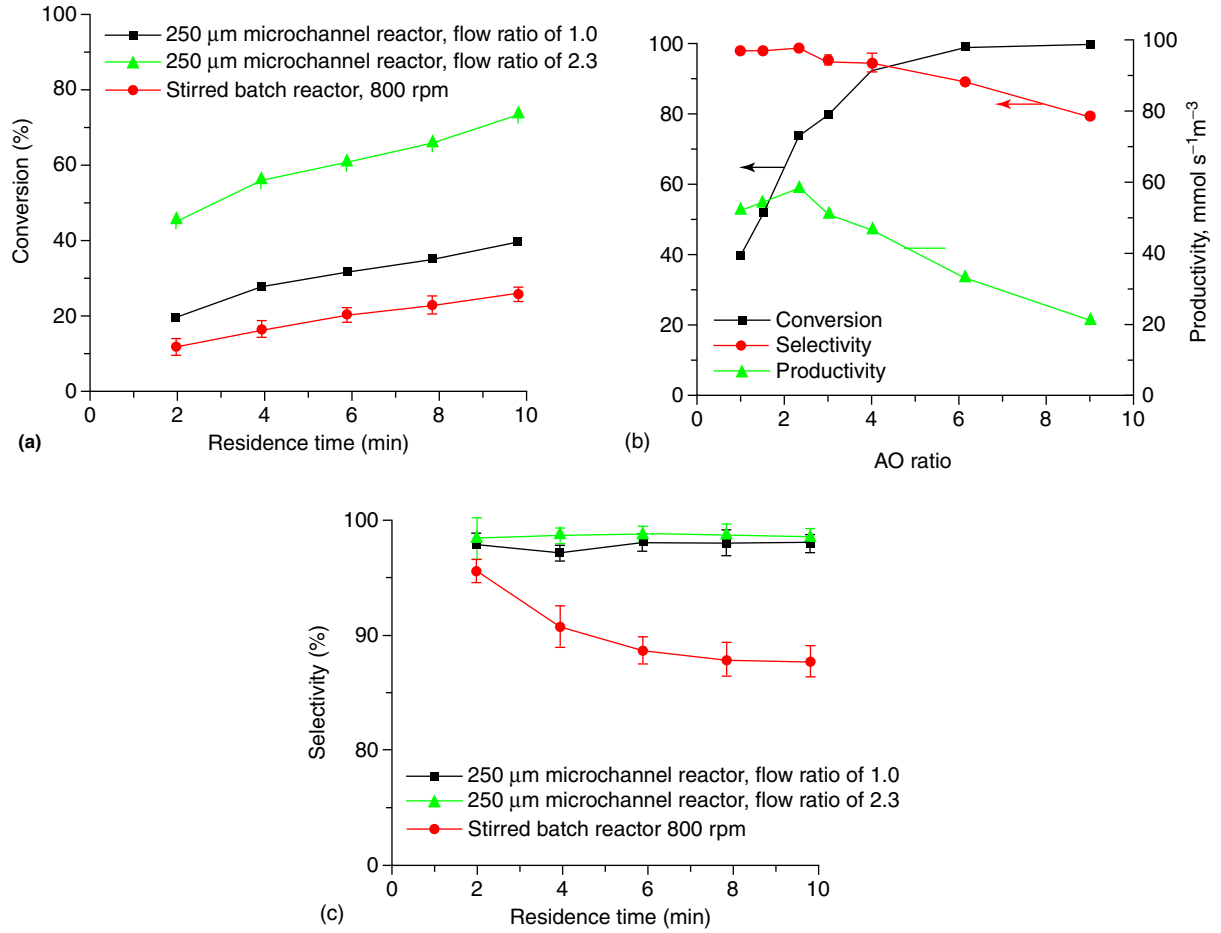
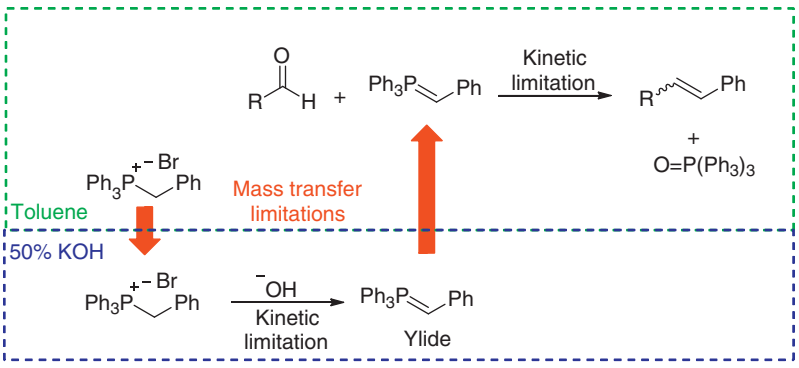


Figure 13 (a) Conversion as a function of residence time. (b) Optimization of aqueous-to-organic flow ratio at a constant residence time of 9.8 min at 80 °C. (c) Selectivity as a function of residence time. Reproduced from Jovanović, J.; Rebrov, E. V.; Nijhuis, T. A.; Hessel, V.; Schouten, J. C. *Ind. Eng. Chem. Res.* **2010**, *49*, 2681, with permission from American Chemical Society.

membrane to the other channel, eliminating the need to purify it via distillation. The separated diazomethane was subsequently reacted with the incoming substrate feed (Table 4). On reaction completion, no trace of diazomethane remains in microreactor system. Additionally, the outlet of the bottom channel is immersed in acetic acid, instantly quenching any trace diazomethane.



Scheme 4 Phase-transfer-catalyzed Wittig reaction.[49]

PDMS are widely used polymers for microfluidic devices for biological studies[51] because of the flexible and low-cost soft lithography process. The material has, however, significant limitations in organic chemistry, including a propensity to swell in the majority of organic solvents and a lack of integrity under pressurized conditions. Although the solvents used in this particular example are compatible with PDMS, the products, and more importantly, diazomethane, can readily diffuse into and through the reactor itself, which poses a serious safety concern. To address this, the researchers coated the PDMS channels with poly

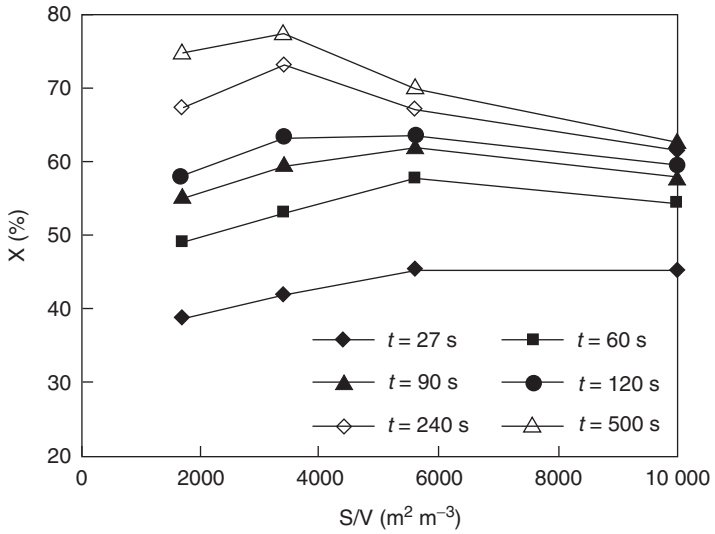


Figure 14 At a residence time of 500 s, increasing the mass transfer rate as reflected by the S/V (surface-to-volume ratio) beyond 3000 caused excessive decomposition of the phosphonium salt and consequently lower conversions of aldehyde. Reproduced from Šinkovec, E.; Krajnc, M. *Org. Process Res. Dev.* **2011**, *15*, 817, with permission from American Chemical Society.

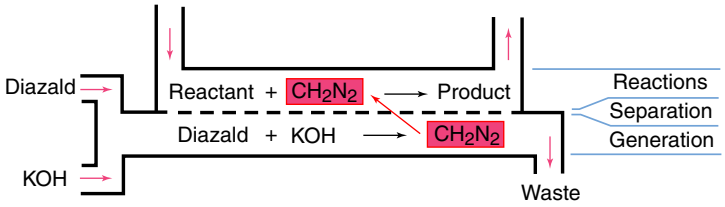
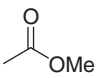
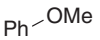
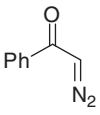


Figure 15 Illustration of the microreactor system for the *in situ* generation, separation, and utilization of diazomethane. Copyright © 2011 John Wiley and Sons.

Table 4 *In situ* generation, separation, and reactions of diazomethane in a PVSZ-coated dual-channel microreactor at room temperature

Substrate	*Flow rate (μl min^{-1})*[a]	*KOH + Diazald flow rate (μl min^{-1})*	*Product*	*Yield (%)*[b]	*Daily output (mmol)*
	4	10		>99	2.88
	1	4		>99	0.72
	1	4		81	0.58
	1	4		90	0.65

[a]Diazomethane was generated in the bottom channel by flowing solutions of diazald (1.0 mol l^{-1} in DMF) and KOH (2.0 mol l^{-1} in water and 0.01% Aliquat 336) with the same flow rate. Substrates were introduced to the top channel in DMF (0.5 mol l^{-1} solution).
[b]Yields were determined by GC/MS analysis using an internal standard.
Source: Reproduced from Maurya, R. A.; Park, C. P.; Kim, D.-P. *Beilstein J. Org. Chem.* **2011**, *7*, 1158.

(vinylsilazane) in a selective manner to prevent organics and diazomethane from diffusing into the channel walls. Although such treatments can alleviate technical challenges in prototype design, they are rarely a safe approach to reactor designs. A safer glass reactor approach is described in the section on scale-up (Section 9.03.8).

9.03.4.3 Gas–Liquid System

Analogous to the liquid–liquid flows in Section 9.03.4.2, gas–liquid flows in microreactors have different flow regimes depending on the flow velocities of the different phases (Figure 16). For a fixed liquid flow rate, adding gas first creates a bubbly flow, which at higher gas flow rates transitions to slug flow.[52] Slug flow is the analog of segmented flow for the liquid–liquid flows. Further increases in gas flow leads to annular flow in which a thin liquid flow wets the wall and the central core is solely gas flow. The different regimes have very different mass transport and residence time distribution properties.[43]

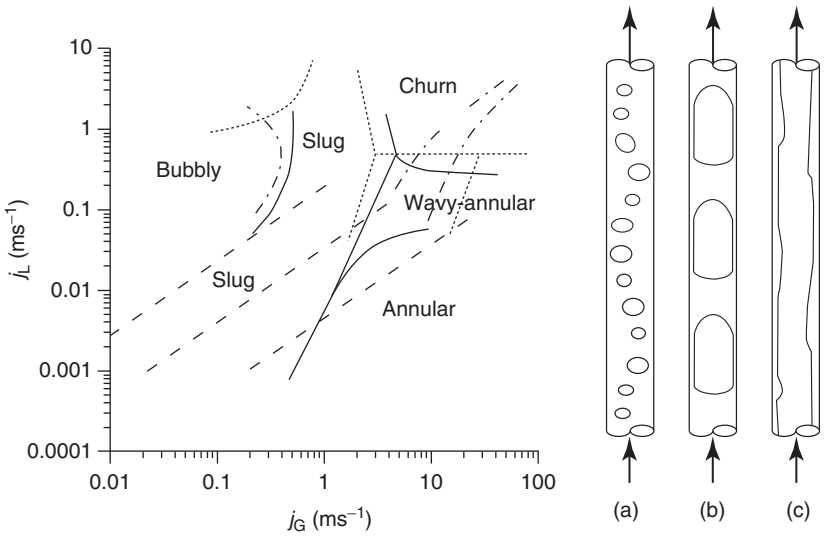


Figure 16 Gas–liquid flow regime diagram for microreactors (left). Reproduced from Gunther, A.; Jensen, K. F. *Lab Chip* **2006**, *6*, 1487. Picture of common gas–liquid flow conditions (left to right: bubbly, slug, and annular) (right). Reproduced from Kreutzer, M. T.; Kapteijn, F.; Moulijn, J. A.; Heiszwolf, J. J. *Chem. Eng. Sci.* **2005**, *60*, 5895.

Similar to liquid–liquid segmented flows, slug flow (Taylor flow) for gas–liquid flows occurs with strong internal recirculation, which provides increased mass transfer. The rate of mass transfer has been shown to depend on a number of variables including the length of the slugs/bubbles, channel diameter, and flow rates of the respective phases. These dependencies have been examined experimentally, as well as with computational fluid dynamic models.[53,54] Typical volumetric mass transfer coefficients quantifying the rate of mass transfer from the gas to the liquid are on the order of 0.01–0.1 s^{-1} are typical for gas–liquid Taylor flow.[55] If mass transfer from the liquid to the wall of the tube is of interest, coefficients of a similar order of magnitude have been observed[55] and calculated for variations in parameters such as slug length, gas holdup, and tube diameter.[54] If these mass transfer coefficients are insufficient, either an inert solid phase can be introduced or operation in the annular flow regime can be considered (Figure 16). This latter regime is particularly useful for highly exothermic reactions with low gas solubility such as the direct fluorination.[56]

Synthetic chemical transformations using toxic and/or corrosive gases are, in general, challenging to perform due to their hazardous and strongly reactive nature. Specially designed liquid–gas microreactors[57] allow the careful control of gas flow and pressure and ensure the uniform distribution and contact between the gas and liquid phases. Gas–liquid separators can also be integrated to separate the gaseous phase after completion of the reaction (additional detail appears in Section 9.03.6).[29] Gas–liquid reactions that have been successfully adapted to flow include hydrogenation,[58] aminocarbonylation,[59] fluorination,[56] and ozonolysis.[60] The use of high pressures allows a higher concentration of gas phase species in the liquid phase than is the case conventionally, leading to the common observation of faster reaction rates. Moreover, given the comparatively small amounts of gas used in these systems, many of the special precautions normally required for handling dangerous gases are significantly reduced.

The ozonolysis of alkenes to give aldehydes is a gas–liquid reaction, which is amenable to microreactors due to the efficient heat removal for this very exothermic (-472 kJ mol^{-1}) reaction,[61] as well as mitigation of explosion concerns due to the small active volume of the reactor. Furthermore, fast reaction quenching can be realized using microchannels, increasing selectivity toward partially oxidized products.[60] Normally, carboxylic acids are easily obtained through complete oxidation of the starting olefin. However, quenching the first ozonide intermediate with a reductant will yield the aldehyde. A microreactor study by Wada et al.[60] included this transformation and illustrated the importance of controlling gas and liquid pressure drop. Moreover, they demonstrated that microstructuring the flow channel by adding posts increased the mass transfer without adding significance to the pressure drop across the reactor. Roydhouse et al. followed this study by finding that a temperature of -10 °C was required for a microreactor and -78 °C for 50 ml batch reactor to obtain a similar throughput and yield of nonanal.[62] Ozonolysis to produce a vitamin D precursor has been applied with five different microreactor mixing configurations in an optimization effort.[63]

Fluorination of compounds using elemental fluorine[64] is another example of an atom-efficient transformation with synthetic value difficult to perform in batch. The high heat of reaction (~ -450 kJ mol^{-1}) combined with the relative ease of formation of fluorine radials means that batch reactions have to be conducted at cryogenic temperatures. The low solubility of fluorine gas in most solvents makes mass transfer an important consideration when obtaining high conversion and yield for a given residence time. A dedicated fluorination reactor was built using a nickel-plated, KOH-etched silicon microreactor and was found to provide efficient heat removal for the process (Figure 17).[65] As an illustration of the high mass transfer obtained in annular flow for a highly exothermic low solubility gas–liquid reaction, the throughput was increased with faster gas and liquid flow rates.[56]

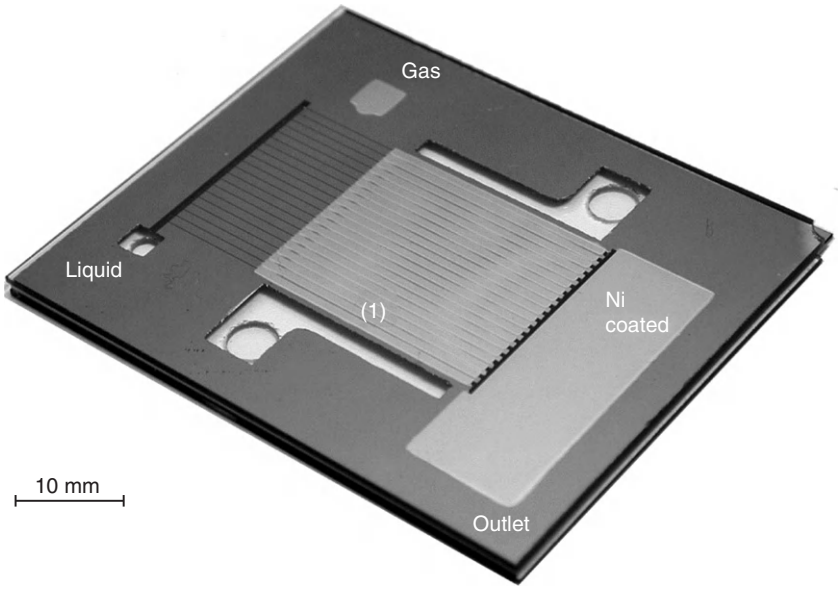
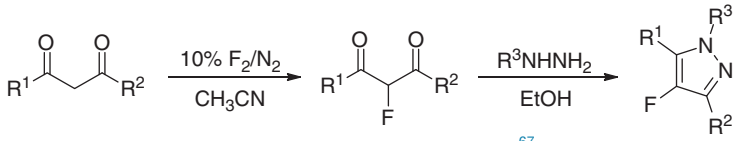


Figure 17 Photograph of the front side of the 20-channel reactor used for direct fluorination experiments. Its channels are formed in a silicon substrate and capped by Pyrex. The areas of the reactor wetted by fluorine or the reaction mixture, including the gas-inlet port, gas-inlet slit (on the back side), reaction channels (1), and outlet slit, are coated with silicon oxide and nickel. The uncoated downstream end of the reaction channels permits qualitative visualization of the gas–liquid flow. Reproduced from de Mas, N.; Günther, A.; Schmidt, M. A.; Jensen, K. F. *Ind. Eng. Chem. Res.* **2008**, *48*, 1428, with permission from American Chemical Society.

Fluorination of 1,3 ketones and ketoesters have been studied by Chambers et al.[66] In a subsequent study, this fluorination step was used in conjunction with hydrazine to synthesize fluorinated pyrazoles.[67] The 4-fluoropyrazole derivatives were synthesized in a continuous, microfluidic process (Scheme 5) with yields of 70–80%, demonstrating a relatively safe way to handle fluorine gas, hydrogen fluoride, and hydrazine.



Scheme 5 Fluorinated pyrazole synthesis using a simple two-step microfluidic procedure.[67]

One effective powerful oxidizing agent is HOF · CH_3CN,[68] which is formed by passing dilute fluorine gas into a solution of wet acetonitrile (20 v% water). The substrate is then typically added to this solution for oxidation. Although many previously unachievable oxidations have been possible using the HOF · CH_3CN complex, its relative instability at room temperature, short half-life (several hours), and material requirements for handling F_2 and HF prevent its wider application.

Chambers et al. designed a nickel–teflon microreactor to generate the HOF · CH_3CN complex quantitatively *in situ* (Figure 18), including its application to the epoxidation of alkenes (Scheme 6).[69] A 10% F_2/N_2 stream (flow rate set via mass flow controller) mixed with wet acetonitrile added via a second inlet (flow rate set by syringe pump). Complete conversion of F_2 was necessary to avoid alkenes preferentially reacting with F_2 in the presence of HOF · CH_3CN. On exiting the HOF · CH_3CN, stream is mixed with the alkene stream (1:1 v:v CH_3CN:CH_2Cl_2, flow rate set by syringe pump) using a T-piece, with an additional 30 cm length to ensure complete alkene oxidation. The reaction mixture was collected in a vessel containing an aqueous $NaHCO_3$ solution to immediately quench excess HOF and HF. Cooling the microreactor and collection vessel was found to be unnecessary as the reactions proceeded with high control under ambient conditions with no reduction in yield. Extraction of the aqueous solution

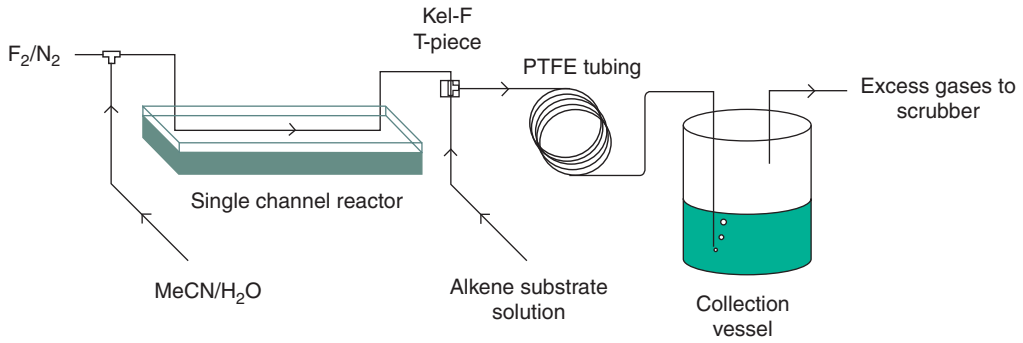
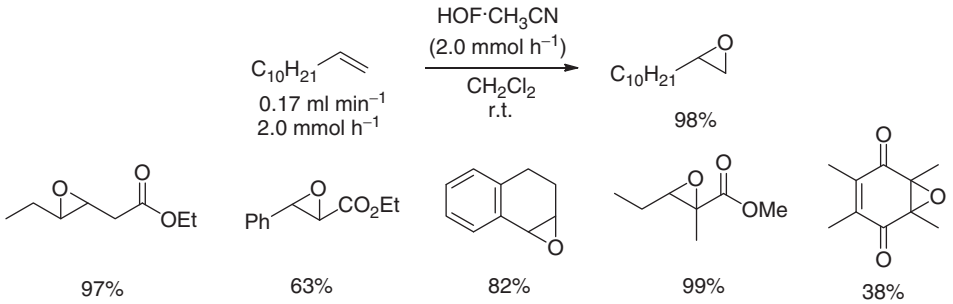


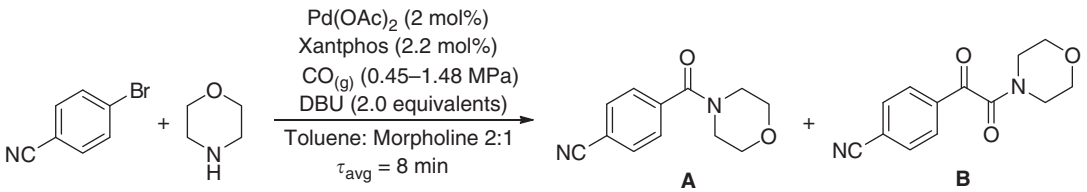
Figure 18 Flow reactor system for the sequential generation of HOF · MeCN, its use, and quench. Reproduced from Chambers, R. D.; Holling, D.; Rees, A. J.; Sandford, G. *J. Fluorine Chem.* **2003**, *119*, 81.

with CH_2Cl_2, drying, and evaporation gave the desired epoxide, typically in greater than 80% yield without the need for any further purification. A substrate scope of variously substituted alkenes was examined (Scheme 6), including known unreactive alkenes to demonstrate the potential of this technique. This reactor has also been applied to fluorinations,[64] alcohol, and Baeyer–Villiger oxidations of aldehydes and ketones,[69] as well as the oxidation of amines to nitro compounds.[70]



Scheme 6 Products from the flow epoxidation of alkenes using HOF · CH_3CN.

The increased transfer rate in gas–liquid flows has been observed to affect selectivity. In the case of aminocarbonylation (Scheme 7), Murphy et al.[59] found significant amounts of α-ketoamide that are not normally found in batch experiments (Figure 19). They attributed this to the increased mass transfer rate allowing more carbon monoxide to be present in the liquid phase during operation, as well as the higher pressures of the toxic gas that could be safely handled in a microreactor. Temperatures above the boiling point of toluene and high pressures of CO were easily probed using the system. Furthermore, an injection loop was used to rapidly screen various reagents in their system without stopping the flow through their system.



Scheme 7 Palladium-catalyzed aminocarbonylation.

Gas–liquid contact can also be achieved using tube-in-tube reactors, with the gas and liquid separated by a gas-permeable membrane. As shown in Figure 20, the liquid phase flows though gas-permeable Teflon AF-2400 tubing. The gas phase flows outside of the tubing and permeates through the Teflon AF into the liquid phase where it reacts.

Kockmann et al. used tube-in-tube reactors to both introduce carbon monoxide for the methoxycarbonylation of aryl and vinyl iodides.[71] The tube-in-tube reactor was used to presaturate the solvent with carbon monoxide and the reaction was carried out downstream in separate heated coils of tubing (Figure 21). The palladium was scavenged with a polymer-supported thiourea, yielding the desired aryl ester product.

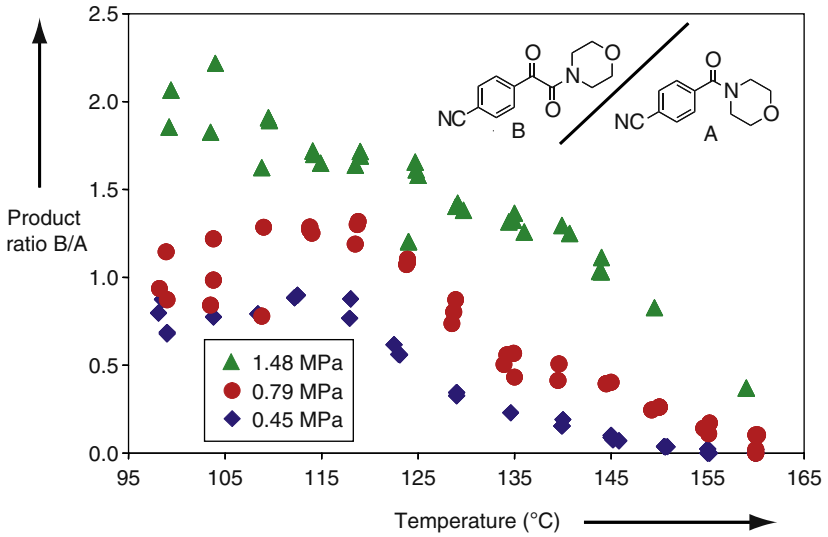


Figure 19 Temperature and pressure screening affecting selectivity of (B) over (A). (Defined in **Scheme 7**). Reproduced from Murphy, E. R.; Martinelli, J. R.; Zaborenko, N.; Buchwald, S. L.; Jensen, K. F. *Angew. Chem. Int. Ed.* **2007**, *46*, 1734, with permission from John Wiley and Sons.

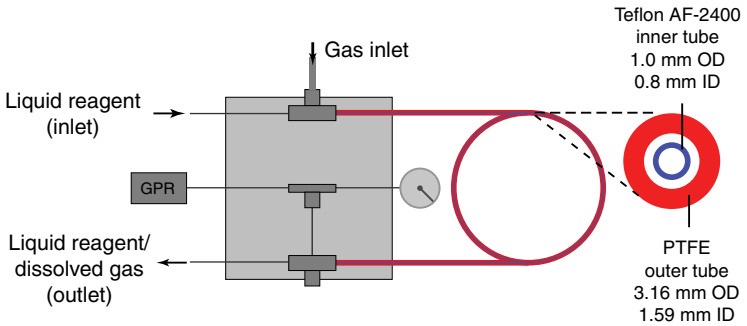


Figure 20 Tube-in-tube reactor used to both introduce and remove gas in a small-scale flow system. Reproduced from Kockmann, N.; Gottsponer, M.; Roberge, D. M. *Chem. Eng. J.* **2011**, *167*, 718, with permission from Royal Society of Chemistry.

The tube-in-tube design can be used as a reactor volume as well, provided the reaction conditions are mild enough. In terms of mass transfer, these reactors have the advantage of obtaining a reliable mass transfer rate into the reaction medium without relying on maintaining a particular two-phase flow regime such as Taylor flow. Experimental complexity is reduced with this setup since gas mass flow controllers are unnecessary. The rate of mass transfer is highly dependent on the nature of the gas molecule, however, as the permeability for different gases through Teflon AF spans many orders of magnitude. For example, hydrogenation reactions with Teflon AF[72] are much more efficient than ozonolysis reactions.[73]

9.03.4.4 Heterogeneous Systems

The most common reactor design for solid-supported catalysts is a packed bed, where the reaction solution or gas passes over retained catalyst particles. A packed-bed reactor can be created by packing an HPLC column with catalyst particles (particle size $< 1/10$ column inner diameter (ID)) or alternatively by microfabricating systems that include a weir to retain the catalyst particles (**Figure 22**). Solid–liquid catalytic systems hold potential advantages over homogeneous liquid phase and liquid–liquid biphasic systems. High catalyst loadings per unit volume may be achieved, which result in reduced residence times. Downstream purification steps to remove catalyst from the product are eliminated, and the production process is simplified. A recent detailed review by Frost and Mutton provides an overview of chemical transformations using supported catalysts.[76]

Some of the advantages of micropacked beds can be understood by considering the ratio of the packed particle surface area to reactor volume.[17] A 500 μm ID capillary tubing has 8000 $m^2\ m^{-3}$, whereas 1 mm ID tubing only has 4000 $m^2\ m^{-3}$. Conversely, the surface area to volume ratio in packed beds is determined as the product of the particle bulk density and surface area per mass. Commercially available silica gel has a bulk density of $\sim 700\ kg\ m^{-3}$ and surface area ranging from 450 to 600 $m^2\ g^{-1}$, giving a

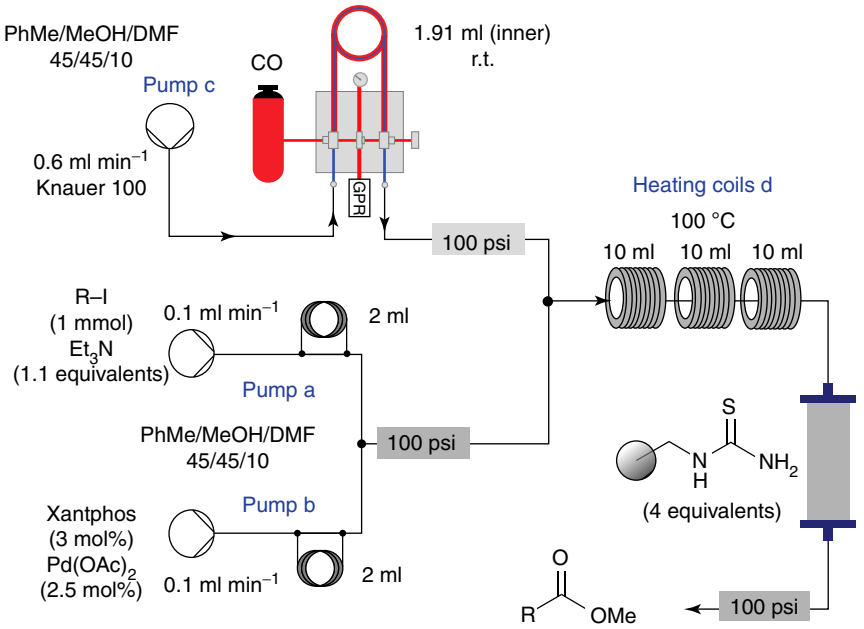


Figure 21 Use of a tube-in-tube reactor to introduce carbon monoxide into a solvent stream for use in palladium-catalyzed methoxycarbonylation of aryl and vinyl iodides. Reproduced from Kockmann, N.; Gottsponer, M.; Roberge, D. M. *Chem. Eng. J.* **2011**, *167*, 718, with permission from Royal Society of Chemistry.

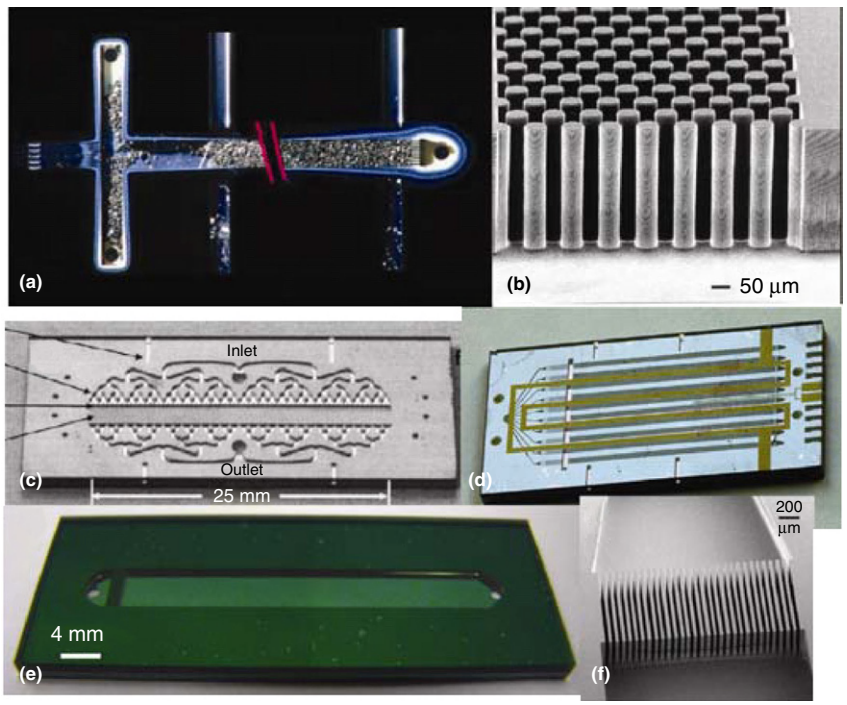


Figure 22 Examples of microreactors for studying heterogeneous reactions. (a) Gas–liquid packed bed reactor.[58] Reproduced from Losey, M. W.; Jackman, R. J.; Firebaugh, S. L.; Schmidt, M. A.; Jensen, K. F. *Microelectromech. Sys. J.* **2002**, *11*, 709. (b) structured bed of silicon posts for catalysts immobilization.[58] Reproduced from Losey, M. W.; Jackman, R. J.; Firebaugh, S. L.; Schmidt, M. A.; Jensen, K. F. *Microelectromech. Sys. J.* **2002**, *11*, 709. (c) cross flow packed bed.[74] Reproduced from Ajmera, S. K.; Delattre, C.; Schmidt, M. A.; Jensen, K. F. *Sensors Actuat. B Chem.* **2002**, *82*, 297. (d) parallel packed bed with integrated temperature sensors.[75] Reproduced from Inoue, T.; Schmidt, M. A.; Jensen, K. F. *Ind. Eng. Chem. Res.* **2007**, *46*, 1153, with permission from American Chemical Society. (e) packed bed and SEM detail, and (f) of weir for retaining solid catalyst particles.[17] Reproduced from Nagy, K. D.; Jensen, K. F. *Chem. Today* **2011**, *29*, 29.

surface area to volume ratio of $3.1–4.2 \times 10^8$ m^2 m^{-3}, a factor of 40 000–200 000 larger than capillary surface coatings. This provides a motivation to support catalysts in the form of packed beds rather than capillary coatings.

The mass transfer rate between two fluid phases is typically enhanced by flowing over an inert packed bed. The overall mass transfer coefficient between a solid catalyst and a fluid flowing through a packed-bed microreactor is typically on the order of 1–15 s^{-1}.[58,75,77] Losey et al. have found that these mass transfer coefficients are about two orders of magnitude greater than typical trick-bed reactors.[77,78] Furthermore, Losey found that the increased mass transfer in these packed beds does not come at the cost of efficiency on a power-per-reactor-volume basis.

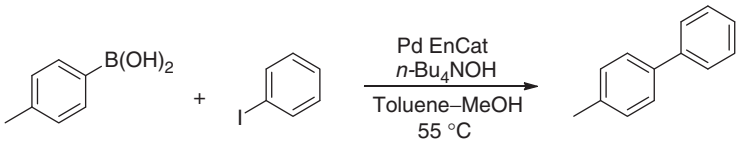
With respect to safety, working with micropacked beds on a small scale for catalytic processes is also advantageous. For example, palladium-mediated hydrogen peroxide synthesis from an explosive mixture of hydrogen/oxygen at 2–3 MPa.[75]

Heterogeneous catalytic systems also suffer from challenges at the microscale. Common polymeric supports, such as Merrifeld resins, can swell in organic solvents. Swelling can potentially reduce access to catalytic sites, whereas increasing pressure drop can even cause brittle reactors, such as those made from glass or silicon, to fail. Furthermore, the smaller interstitial path lengths in packed beds prohibit reactions that produce solids, as sonication and other techniques to control particle growth and deposition are ineffective.[79] Lastly, solid-supported catalysts that operate through so-called boomerang mechanisms, where the active species desorbs from the support under reaction conditions and readsorbs on completion of the reaction, are poorly suited to flow conditions.

Packed-bed microreactors are the smallest scale method of testing immobilized organometallic materials in a flow system, and so naturally they have found application in a number of catalytic processes including cross couplings, olefin metathesis, hydrogenation, hydroformylation, epoxidation, cyclopropanation, and benzannulation.[76] These immobilization tests are often contributions toward solving the industrial problem of downstream catalyst separation and recycling of the corresponding homogeneous catalyst. Some representative examples from this field are discussed in this section.

The reduced activity of a catalyst on immobilization is an issue in this field. Since one of the purposes of these immobilization techniques is to obtain a high turnover number (TON), and since a reduction in activity may require higher catalyst loadings (and therefore lower TON), maintaining an active catalyst is of paramount importance. The other purpose of the immobilization is to keep palladium metal concentrations in the effluent of the reactor low – typically less than 5 ppm for pharmaceutical applications.[80] Another economic advantage of packed beds is process intensification. Under typical conditions in a packed-bed microreactor, a large amount of catalyst is present compared with the amount of substrate in the reactor in given time (at steady-state operation). The high catalyst loadings relative to the substrate holdup in a packed bed reduces residence times, which implies smaller reactor volumes to meet a required throughput.

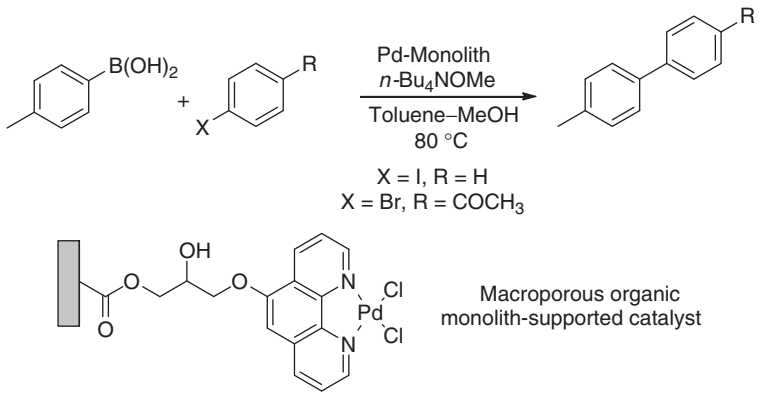
Palladium-based coupling reactions have been studied extensively in these microsystems. Despite the anchoring of palladium to a solid support, there is much evidence to suggest that 'leached' homogeneous palladium is often the active species, which may or may not return to the support.[81] One such example of palladium immobilization is the Pd EnCat system developed by Ley et al., which relies on a polyurea-encapsulated $Pd(OAc)_2$ precatalyst. In an application of this catalyst to a Suzuki coupling reaction (Scheme 8), full conversions were obtained at a residence time of 4 min (TOF 3 h^{-1}). The relatively high catalyst loading resulted in a TON of around 5 for this system, with 1–13 ppm palladium found in the product. There was effectively 480 mol% palladium at steady state in the reactor corresponding to 19 mol% Pd relative to the total reagent throughput. Microwave-assisted reactions with this immobilized catalyst were able to give TON of 500.[83] To put these results in perspective, one can consider the fact that adding approximately 1 ppm $Pd(OAc)_2$ to a more difficult substrate can go to full conversion in 4 h (TON: 5000, TOF 1250 h^{-1}).[84] Furthermore, TONs in the millions have been reported for 90 s reactions under microwave conditions for similar substrates.[85] This highlights the challenge in maintaining activity when immobilizing a palladium coupling catalyst.



Scheme 8 Simple Suzuki coupling over Pd EnCat.[82]

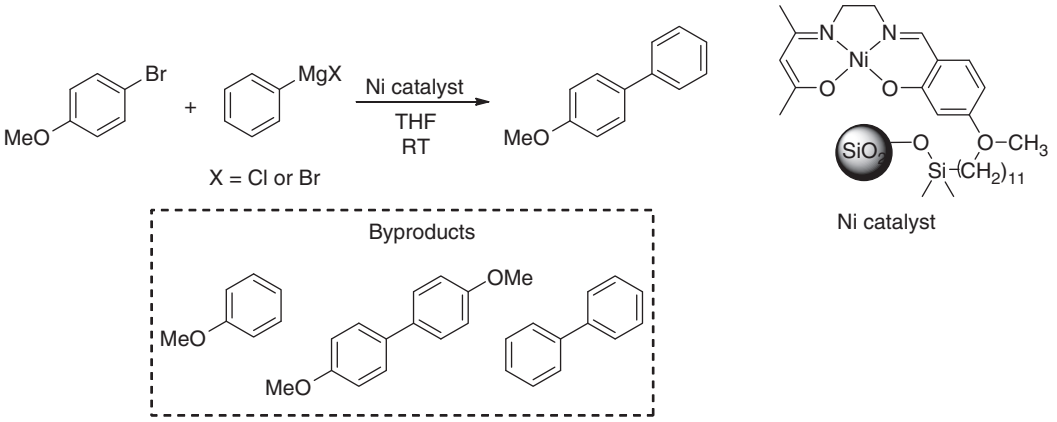
Monoliths are another microfluidic platform for heterogeneous catalysis. The inner walls of 0.5–5 mm diameter tubes may be coated with a catalyst or filled with a functionalized polymer. A monolith packed with functionalized GMA-*co*-EDMA [poly (glycidylmethacrylate-*co*-ethylene dimethacrylate)] was also used to enact a simple Suzuki coupling (Scheme 9). A TON of slightly greater than 200 was obtained for the palladium, with a TOF of 1.8 h^{-1} (and a yield of 59%) over a 96 h period where reportedly little change yield occurred.[86] Approximately 15–20% of the Pd had leached during this period. Since low catalyst loadings (1 ppm or less) can transform these relatively active substrates, heterogenized palladium catalysts enacting difficult coupling transformations would be more useful. Functionalized polymers have been loaded into monoliths to carry out a number of other transformations, including catalytic transfer hydrogenation, Heck reactions, and dynamic kinetic resolutions of epoxides.[87]

When a Merrifield resin-immobilized, nickel-based Kumada coupling catalyst was packed into a microchannel,[88] difficulties with swelling of the Merrifield resin (causing clogging of the microchannel) led the same group to consider a silica-supported version of the catalyst with a covalent ether linkage (Scheme 10). The authors reported that despite the differences in reaction rates between batch and flow, their calculated TOFs for the two cases are equivalent (this is due to the higher catalyst loading in a typical



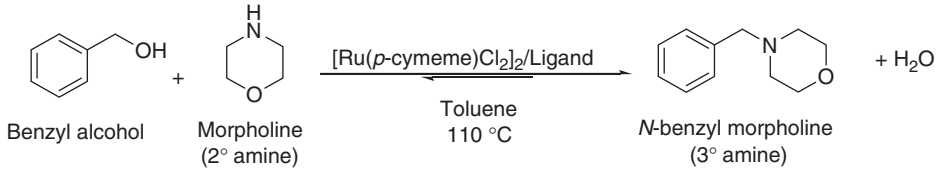
Scheme 9 Suzuki coupling with polymer-anchored catalyst packed in a microchannel.[86]

micropacked bed reactor). Their catalyst activity was under half that of a homogeneous catalyst, and they were able to achieve low catalyst leaching, although rapid deactivation of their catalyst did occur.[89]



Scheme 10 Salen-nickel Kumada catalyst immobilized on silica.[89]

As an example of solid-supported ruthenium catalysts, Lamb et al. successfully coupled amines and alcohols via a metal-catalyzed hydrogen transfer reaction utilizing ruthenium complexed to an immobilized, polymer-bound phosphine ligand (Scheme 11).[90] Initially running at 150 °C in toluene at 0.5 MPa backpressure, they observed a decrease in yield in conjunction with the reactor outlet's product stream turning from clear to dark red. This was attributed to ruthenium leaching. Running the reactor at 150 °C at 0.1 ml min^{-1} under atmospheric pressure with the higher boiling *p*-xylene led to high conversions (98%) and reduced ruthenium leaching. In order to test catalyst stability, the reactor was run continuously at these conditions, using a feed solution of 16 vol% reactants in *p*-xylene for 72 h, processing approximately 500 ml of feed. The calculated TON was 438, which compared favorably to typical homogeneous systems operating at 1 mol% of catalyst (TON = 100).



Scheme 11 Ruthenium-catalyzed hydrogen-transfer reaction.[90]

Lim et al.[91] attached a copper-based cyclopropanation to siliceous mesocellular foam (MCF) microparticles and capped residual silanol groups with hexamethyldisilazane (HMDS). The authors found the nitrogen byproduct to be detrimental to their conversions and enantioselectivity, so a recirculating flow setup was built to continuously remove the nitrogen from the system (Figure 23). The effluent was then fed back into the reactor until full conversion was obtained. They found their catalyst to retain its enantioselectivity, and good catalyst activity was obtained as well (75 min total recirculation time per run). Furthermore, only 8% of their copper leached from the bed after 20 reuses of the catalyst, giving a total TON of approximately 3500. These results

were the product of in-depth optimization of the catalyst support system. The linker length and rigidity, ligand loading on the MCF, and pre/postsilanol capping procedures were optimized to give good catalyst stability, activity, and enantioselectivity.[91] Lim et al.[92] also applied their recirculation flow reactor to a metathesis catalyst supported on MCF, this time to remove the ethylene byproduct with a TON of greater than 700 achieved (with high conversions). It should be noted that these recirculating flow reactors need to be run batchwise.

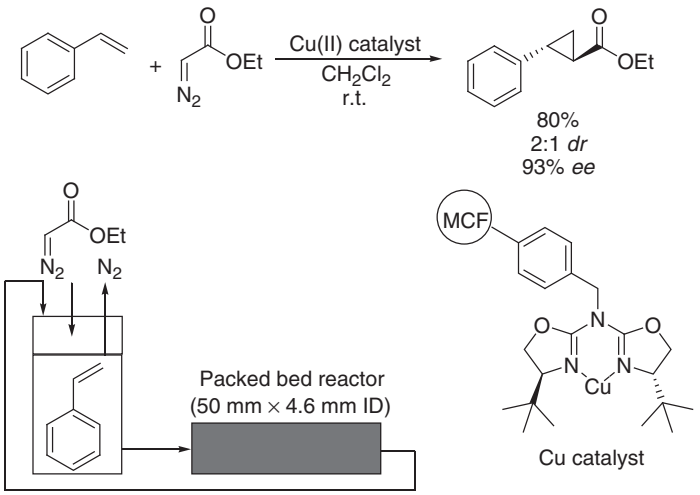
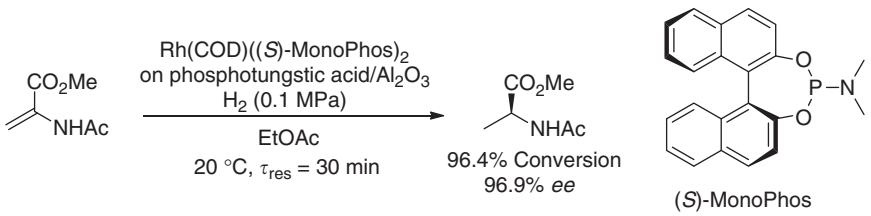


Figure 23 Enantioselective copper-catalyzed cyclopropanation supported on siliceous MCF microparticles. Recirculating flow reactor must be run in a batch-wise fashion. Reproduced from Lim, J.; Riduan, S. N.; Lee, S. S.; Ying, J. Y. *Adv. Synth. Catal.* **2008**, *350*, 1295.

Following explorations by Simons et al.[93], Madarász et al. heterogenized a cationic rhodium complex electrostatically to phosphotungstic acid/alumina and tested it in an H-Cube reactor.[94] The asymmetric hydrogenation of the common test substrate methyl-2-acetamidoacrylate (MAA) with the immobilized Rh(COD)((*S*)-MonoPhos)$_2$ (Scheme 12) was optimized over temperature, concentration, pressure, and residence time. After optimization, a packed bed was subjected to a continuous substrate feed for 700 min before conversions and *ee*'s dropped significantly. The authors estimate their TON to be at least 1400 with an average TOF of approximately 120 h^{-1} for residence times on the order of 1 s. This compares favorably to one-pass homogeneous tests for this substrate giving a TOF of approximately 1200 h^{-1} at 0.5 MPa.[95] Leaching was low ppm or less based on batch tests. One limitation of this technique is that polar protic solvents increase leaching substantially due to the noncovalent nature of the immobilization.



Scheme 12 Hydrogenation of MAA using an immobilized rhodium catalyst at a few bar of pressure.[94]

9.03.5 Photochemical Systems

Synthetic photochemistry is a powerful tool, enabling the construction of complex molecules such as natural products, as well as several impressive large-scale industrial applications (e.g., caprolactam synthesis for nylon production, vitamin D synthesis) (*see* Chapter 9.13). Light is also considered a clean and traceless reagent that makes photochemistry a green and sustainable discipline. Despite these successes, there is still some reluctance to use synthetic organic photochemistry due to the perception that it is difficult to scale. Given that typical organic photochemical reactions are usually performed in solution using immersion well reactors, and that the majority of photochemistry occurs within a short radius of the lamp, it is easy to see how mass and energy transfer limitations prohibit widespread application in traditional batch reactors.

The main advantages of continuous-flow microreactors over traditional batch systems are the greater spatial illumination homogeneity and light penetration achieved through the entire reactor depth, as well as conferring precise control over reaction

(residence) time, temperature, and the ability to separate the reaction products from the irradiated area. These advantages typically result in higher yields, better selectivities, and serve as a better platform to elucidate reaction space, all of which greatly enables the ability to scale-up a desired transformation.

9.03.5.1 Homogeneous Photochemical Reactions

Hook et al. pioneered a simple, general means of applying continuous flow to existing immersion lamps (Figure 24).[96] By wrapping transparent fluorinated ethylene propylene (FEP) tubing around a traditional water-cooled photochemistry lamp and pumping the reaction solution around the reactor via a common HPLC pump, they were able to perform and scale [5 + 2] (intermolecular) and [2 + 2] (intermolecular) cycloadditions with outputs of greater than 100 g of product in 24 h (Figure 24). Greater yields and selectivity could be achieved not only from a better utilization of light, but also through the ability to control the irradiation time through flow rate manipulation.

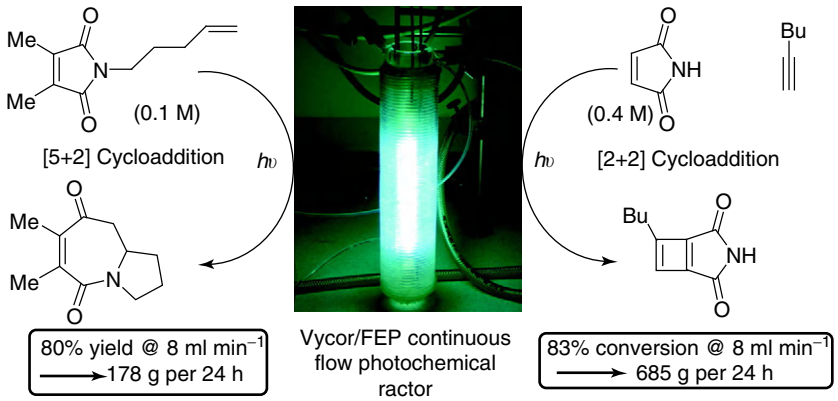


Figure 24 [5 + 2] and [2 + 2] Photocycloadditions performed in a Vycor-FEP continuous flow photochemical reactor. Reproduced from Hook, B. D. A.; Dohle, W.; Hirst, P. R.; *et al. J. Org. Chem.* **2005**, *70*, 7558, with permission from American Chemical Society.

Researchers at Abbott Laboratories introduced an alternative flow-based chemical reactor that effectively decouples the reactor temperature from the lamp's jacketed cooling line (Figure 25).[97] This provides several benefits, the foremost of which is greater temperature control of the reactor, enabling a wider range of temperatures while maintaining safe lamp-operating conditions. Fabricated from stainless steel, the machined reactor channels were effectively sealed with a 250 μm thick FEP film held in place by nitrogen pressure (0.10 MPa). An added advantage of this design over FEP tubing is that the system can be easily cleaned in the event of clogging. Additionally, selective light filtering could be provided without disassembling the system, enabling the prevention of possible unwanted side reactions from occurring.

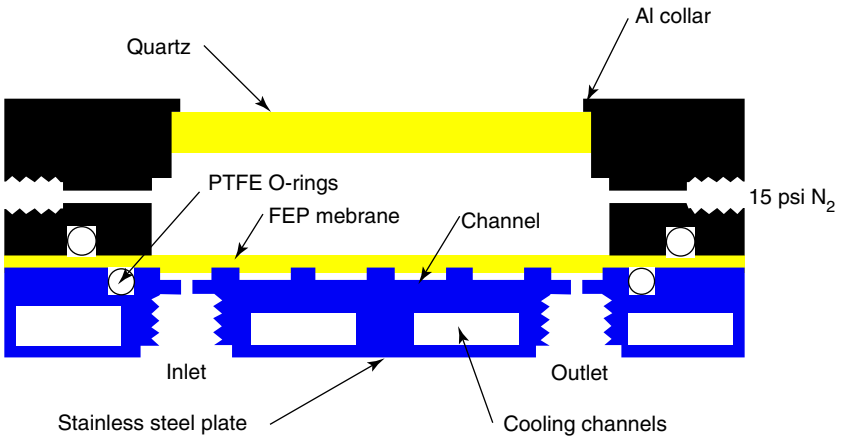
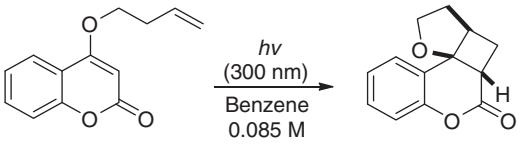


Figure 25 Cross-sectional view of a microreactor. Pressurized nitrogen pushes produces a robust seal between the FEP and the channels formed in stainless steel. Reproduced from Vasudevan, A.; Villamil, C.; Trumbull, J.; *et al. Tetrahedron Lett.* **2010**, *51*, 4007.

The reactor's performance was evaluated against a known intramolecular [2 + 2] enone cycloaddition. For comparison purposes, the same transformation was attempted in batch using a medium-pressure mercury lamp source (Table 5). In flow, the

intramolecular cycloaddition produced a 98% yield over a 2 h residence time. In comparison, the conventional batch reactor only produced a 30% yield after 24 h. The ease of setup and convenience of controlling the residence time via flow rate enabled the incorporation of an auto sampler, allowing a programmed set of conditions to be executed without human intervention. Using this platform, the reaction was scaled-up through a series of increased substrate concentrations. No reduction in yield was observed over the entire set of concentrations, (0.075–0.45 mol l^{-1}), thus providing a convenient means of scaling up to hundreds of milligram of material, which is ideally suited for early drug discovery.

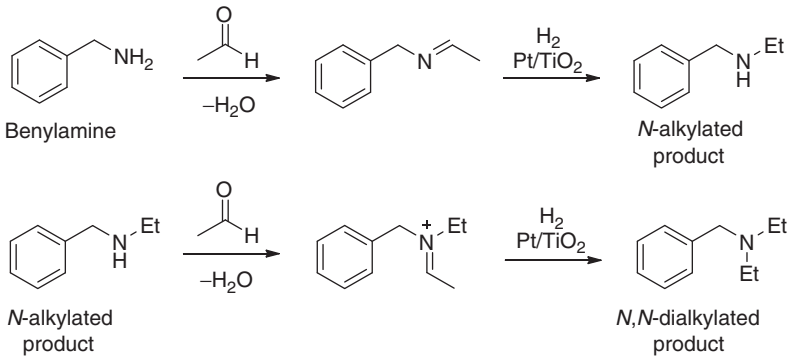
Table 5 Intramolecular [2 + 2] cycloaddition using batch and flow conditions[97]



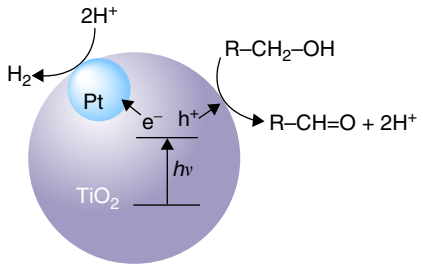
Format	*Duration (h)*	*Yield (%)*
Batch	24	30
Continuous	0.5	43
Continuous	1	67
Continuous	2	98

9.03.5.2 Multiphase and Heterogeneous Photochemical Reactions

A unique advantage of microreactor systems is the ability to successfully combine the increased mass transfer characteristics of packed-bed systems with photochemical heterogeneous catalysis. The *N*-alkylation of amines can also proceed by UV irradiation of Pt-loaded TiO_2 suspended in alcoholic solvents (Scheme 13) through a mechanism similar to the previously described hydrogen transfer system (Scheme 11), as reported by Ohtani et al.[98] The mechanism begins with alcohol dehydrogenation at the surface of the catalyst, forming H_2 and a carbonyl compound. The carbonyl then undergoes condensation with the amine, and the resulting imine is reduced by H_2 (generated by Pt) to afford the target *N*-alkyl derivative; dialkylation was observed to occur readily with secondary amines. Under batch conditions, the *N*-alkylation of benzylamine in EtOH occurred at 84% over a 4 h irradiation with a 400 W high-pressure Hg lamp. Pt-loaded TiO_2 was required, as no reaction was observed in its absence.



Scheme 13 Benzylamine alkylation on a photocatalytic surface.[98,99]



Using Pt/TiO_2 wall-coated microchannels fabricated from two Tempax plates (Schott) and a thin film of self-welding fluorinated polymer, Matsushita et al. evaluated the photocatalytic *N*-alkylation of a series of amines under continuous-flow conditions (Figure 26).[99] Microchannel coating was achieved by a process of flowing $Ti(Oi\text{-}Pr)_4$ through the channel network and calcination (497 °C). The platinum catalyst was uniformly deposited by flowing an aqueous solution of chloroplatinic acid and MeOH through the channels, and controlling catalyst loading through variation of the irradiation time.

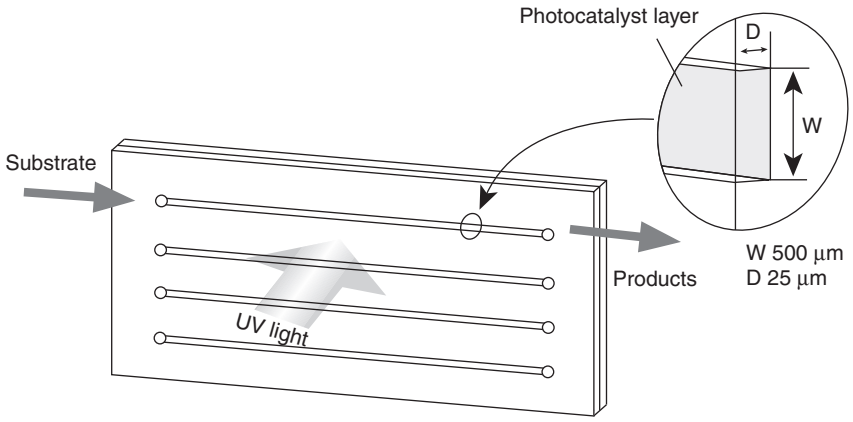


Figure 26 A photochemical microchannel reactor for *N*-alkylation. Reproduced from Matsushita, Y.; Ohba, N.; Suzuki, T.; Ichimura, T. *Catal. Today* **2008**, *132*, 153.

Comparing the product selectivity between flow and batch conditions revealed that not only was there greater selectivity under flow, but also a dramatic increase in rate of reaction, resulting in a reduction of reaction time from 5–20 h down to 6–150 s. The authors attribute this reduction to an increased surface-to-volume ratio and a more uniform irradiation depth when compared with batch vessels. Also in contrast to the batch results, they discovered that the *N*-alkylation of benzylamine could be performed with immobilized Pt-free TiO_2 as well as Pt/TiO_2. Both the decrease in reaction times and Pt-free catalysis were attributed to the microreactor's significantly larger surface-to-volume ratio. Moreover, they were able to observe reactions not permissible under batch conditions due to low reaction efficiency.

Singlet oxygen ($^1O_2$) is a clean and atom-efficient reagent used for the introduction of oxygen into hydrocarbon skeletons; as such, it has found wide-ranging application in organic synthesis, with examples even reported in natural product synthesis. Singlet oxygen is commonly prepared by the photoexcitation of molecular oxygen in the presence of a photosensitizer or thermally on treatment with H_2O_2 or sodium hypochlorite. In addition to the short-lived nature of the oxidant, the safety implications associated with the generation and handling of $^1O_2$ on a large scale has thus far precluded its common use. To address this, several authors have investigated not only the generation, but also the use of $^1O_2$ under continuous-flow conditions.[100,50]

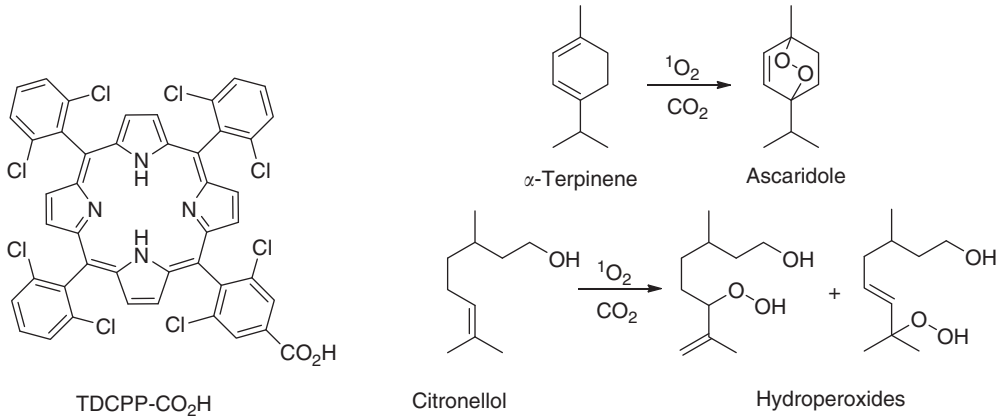
Bourne et al. have pioneered the use of supercritical carbon dioxide ($scCO_2$) as the reaction solvent for continuous-flow applications.[101] Unlike alcoholic solvents, the use of $scCO_2$ is advantageous as it has a low viscosity, has a high diffusivity, and is nonflammable. More recently, its ability to solubilize high quantities of O_2 has been useful in the photochemical generation of singlet oxygen, $^1O_2$.

The majority of advances in microreactor design as applied to the generation and use of $^1O_2$ have been dependent on the use of homogenous photosensitizers, which in practical use ultimately requires separation from the product stream. Han et al.[102] neatly circumvented the problem through immobilization of the photosensitizer, removing the need for its separation from the downstream solution. Their system based on a covalently coupled analog of tetra(2,6-dichlorophenyl)porphyrin (TDCPP) on polyvinyl chloride (PVC) showed high activity and an acceptable lifetime for the photooxidation of α-terpinene and of citronellol in continuous reactors over a 5 h period (Scheme 14).

In a typical flow experiment, the reactor was loaded with the immobilized photosensitizer and pressurized with a mixture of CO_2 and O_2 (2:1 mol l^{-1} ratio of O_2:substrate, 18 MPa). Irradiation was initiated using two arrays with four light emitting diodes (LEDs) apiece, along with starting the organic substrate feed (0.1 ml min^{-1}) simultaneously (Figure 27).

Lévesque and Seeberger have recently reported a continuous-flow conversion of dihydroartemisinic acid into artemisinin, which is the most effective treatment against multidrug-resistant malaria.[103] As artemisinic acid can be produced by engineered yeast, the continuous production of artemisinin would be a significant development, ensuring the drugs steady supply at greatly reduced cost. The key technological hurdle lies in developing a continuous photochemical singlet oxygen-induced ene reaction that is flexible enough to allow the acidic conditions necessary for subsequent Hock cleavage, while retaining the capacity to add triplet oxygen. The addition of triplet oxygen triggers the reaction cascade that incorporates the essential endoperoxide group of artemisinin (Scheme 15).

The photooxidation of dihydroartemisinic acid to the tertiary allylic hydroperoxide was explored in flow system (Figure 28). The 20-ml volume device consisted of FEP tubing wrapped around a Schenk photochemical reactor containing a 450 W medium-pressure lamp. The best results were obtained when a 42-ml reactor was used with the solution of the starting material and



Scheme 14 Oxidation-resistant photosensitizer and benchmark photooxidations.[102]

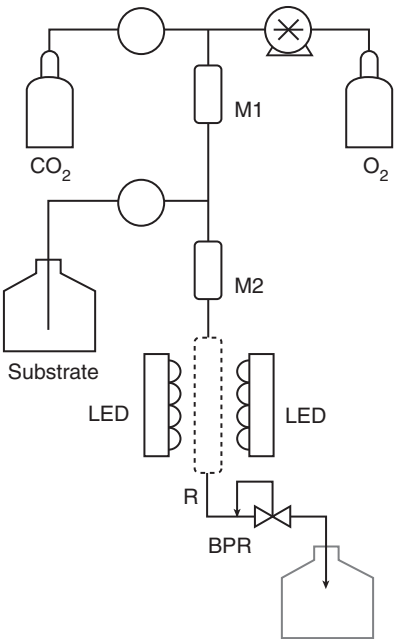
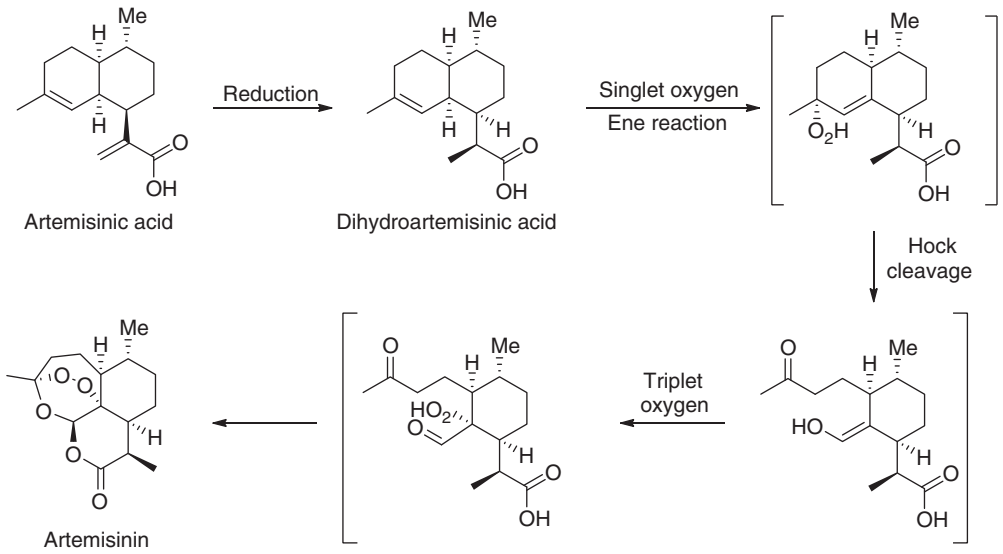


Figure 27 Flow equipment for continuous reactions. BPR – back-pressure regulator; R – photocatalyst-packed sapphire tube reactor. Reproduced from Han, X.; Bourne, R. A.; Poliakoff, M.; George, M. W. *Chem. Sci.* **2011**, *2*, 1059, with permission from Royal Society of Chemistry.

tetraphenylporphyrin (TPP) in dichloromethane added at optimized continuous rates of oxygen and trifluoroacetic acid (TFA)/dichloromethane. The first portion of the reactor (32 ml) was maintained at room temperature, whereas the last portion (10 ml) was heated to 60 °C to push the reaction to completion. Subsequent chromatographic purification yielded 46% of artemisinin from dihydroartemisinic acid in this sequential flow reaction.

9.03.6 Multistep Synthesis

Performing multistep chemical synthesis on the microscale requires development of reaction and separation techniques in microfluidic devices. Common separation processes, such as liquid–liquid extraction, are complicated by the need to continuously perform phase separation after mixing and contacting the phases. Traditional continuous phase separation is achieved using a settling tank, in which differences in the density of the two fluid phases drive the separation. But, at the small scales, gravitational forces are small compared with surface forces, so it is difficult to achieve complete phase separation using differences in density. Thus, alternative forces for driving phase separation must be considered. Surface tension effects are particularly



Scheme 15 Reaction sequence for the synthesis of artemisinin from artemisinic acid.[103]

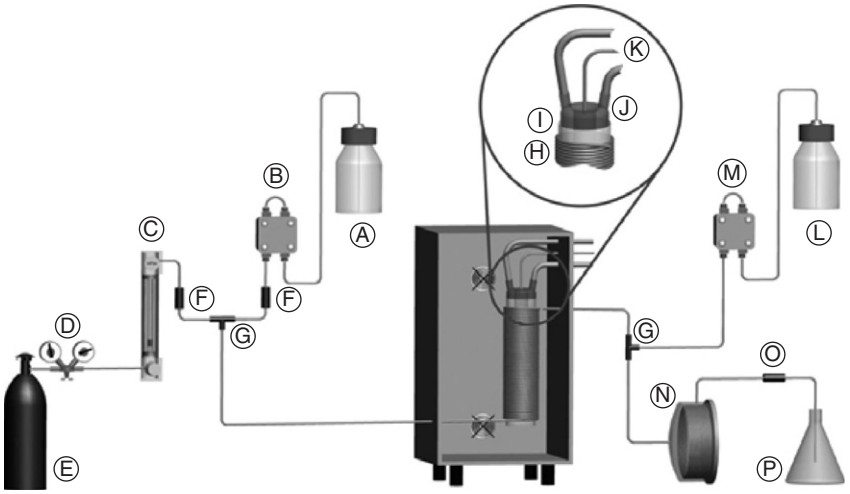
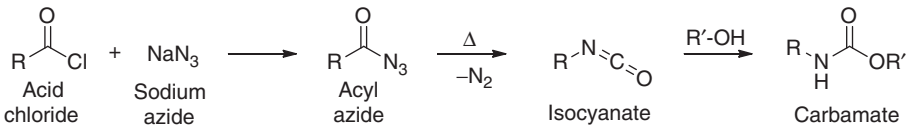


Figure 28 Continuous-flow process for the conversion of dihydroartesiminic acid into artemisinin. The reactor is composed of (A) reservoir for the solution of dihydroartemisinic acid and TPP in CH_2Cl_2, (B) HPLC pump, (C) O_2 mass-flow controller, (D) manometer, (E) oxygen tank, (F) check valve, (G) ETFE T-mixer, (H) FEP tubing, (I) quartz immersion well connected to a cooling system, (J) Pyrex filter, (K) connection to the medium-pressure Hg lamp (450 W), (L) reservoir for the TFA solution, (M) acid-resistant HPLC pump, (N) polytetrafluoroethylene (PTFE) thermal reactor, (O) back-pressure regulator, and (P) collection flask. In this reactor, a solution of dihydroartemisinic acid and the photosensitizer TPP in CH_2Cl_2 were mixed at a flow rate of 2.5 ml min^{-1} with a stream of oxygen gas (7.5 ml min^{-1}), and passed through the photoreactor. The residence time in the reactor is approximately 2.0 min. Reproduced from Lévesque, F.; Seeberger, P. H. *Angew. Chem. Int. Ed.* **2012**, *51*, 1706, with permission from John Wiley and Sons.

attractive as they dominate gravity and viscous forces at the microscale.[43] Liquid–liquid and gas–liquid membrane microextractors operate via such surface tension driving forces.[20]

As an example, Sahoo et al. reported a multistep synthesis of carbamates via the Curtius rearrangement of isocyanates (Scheme 16).[104] The authors selected carbamates as a synthetic target, not only because they serve as useful building blocks, but also require the use of hazardous azides as reactive intermediates, as well as the engineering challenge posed by the generation and separation of products, byproducts, and the N_2 evolved during acyl azide decomposition.

Using a silicon–glass microreactor, they employed biphasic conditions for the conversion of an acyl chloride (in toluene) to an acyl azide using aqueous sodium azide (Figure 29). Coupling the reactor outlet to a membrane separator, the authors readily removed water from the reaction mixture, before thermal rearrangement of the acyl azide (in the presence of a solid acid catalyst) to afford the respective isocyanate. The nitrogen evolved during this process was then removed from the reaction stream using a gas–liquid separator and the resulting liquid stream reacted with a series of alcohols to afford their respective carbamates. Using



Scheme 16 The Curtius rearrangement of isocyanates.[104]

this approach, the authors were able to efficiently synthesize phenyl isocyanate at a reactor temperature of 105 °C with a residence time of 60 min, affording the target compounds at a throughput of 80–120 mg day^{-1}.

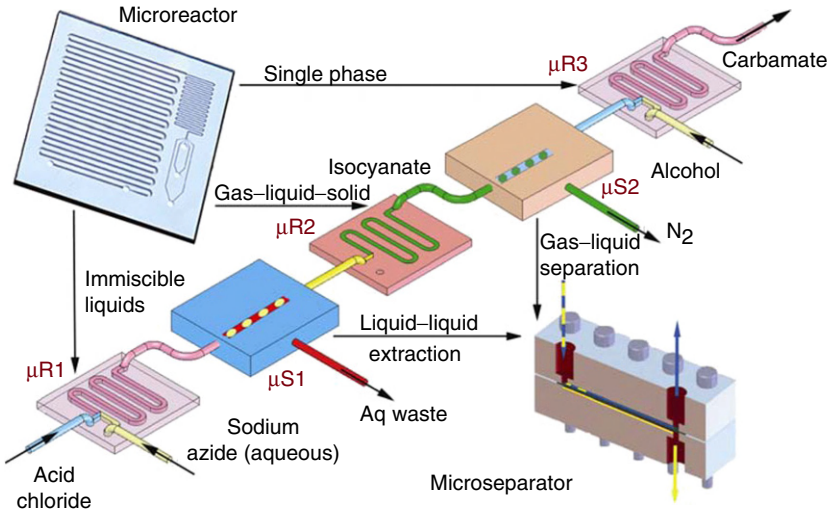
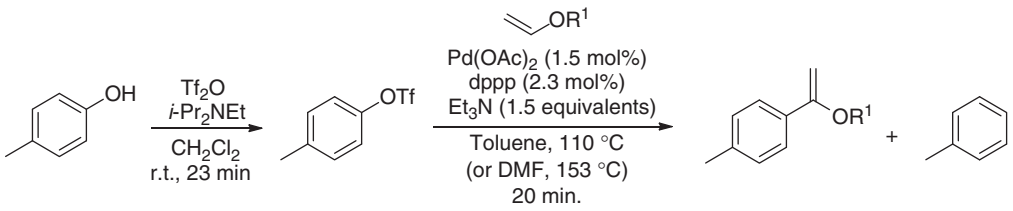


Figure 29 The experimental setup for carbamate synthesis. μR_1, microreactor for the conversion of an acid chloride to an acyl azide; μS_1, quantitative separation of organic and aqueous streams; μR_2, microreactor loaded with solid acid catalyst for the conversion of an acyl azide to isocyanate; μS_2, quantitative separation of gaseous N_2 from the liquid stream; μR_3, microreactor for the reaction of the isocyanate and an alcohol to a carbamate. Reproduced from Sahoo, H. R.; Kralj, J. G.; Jensen, K. F. *Angew. Chem. Int. Ed.* **2007**, *46*, 5704, with permission from John Wiley and Sons.

Work by Hartman et al. demonstrated the use of gas–liquid slug flow as a simple means to emulate larger scale distillation processes.[21] This process was used in a solvent switch from CH_2Cl_2 to toluene in protection reaction followed by a Heck reaction (Figure 30).[105] This process first required an acidic washing step, with the aqueous phase being removed via a teflon membrane liquid–liquid separation step, followed by a distillation step to exchange the low boiling dichloromethane for the higher boiling toluene.



Bogdan et al.[106] developed a continuous-flow multistep synthesis of ibuprofen (Figure 31) by telescoping the reactions so that no intermediate workup would be needed. The constraint of telescoping likely decreased the optimum yield that could have been obtained. For example, an $AlCl_3$ Friedel–Crafts catalyst was found to provide higher yields for the first step but was incompatible with the second step without an intermediate work-up stage. Note that mixing at 0 °C was necessary for the second step of this reaction. This is due to the mixing being important for the yield of this fast reaction (Section 9.03.3.3). Thus, the reaction is mixed at inhibitory temperatures in a T-junction packed with glass beads before being brought to the reaction temperature. The final exothermic reaction could be run under aggressive conditions without difficulties in controlling the temperature.

Carter et al. studied Roush crotylation in a Vapourtec R2 + /R4 flow chemistry platform (Figure 32).[107] The authors claimed that the lack of readily available aldehydes were responsible for this reaction being relatively unused for production purposes. Typically, esters need to be reduced to an alcohol and then oxidized back to an aldehyde. As discussed in Section 9.03.4.1.2, the partial reduction of an ester (or carboxylic acid) to an aldehyde is possible (in high yields) in microreactors due to the excellent

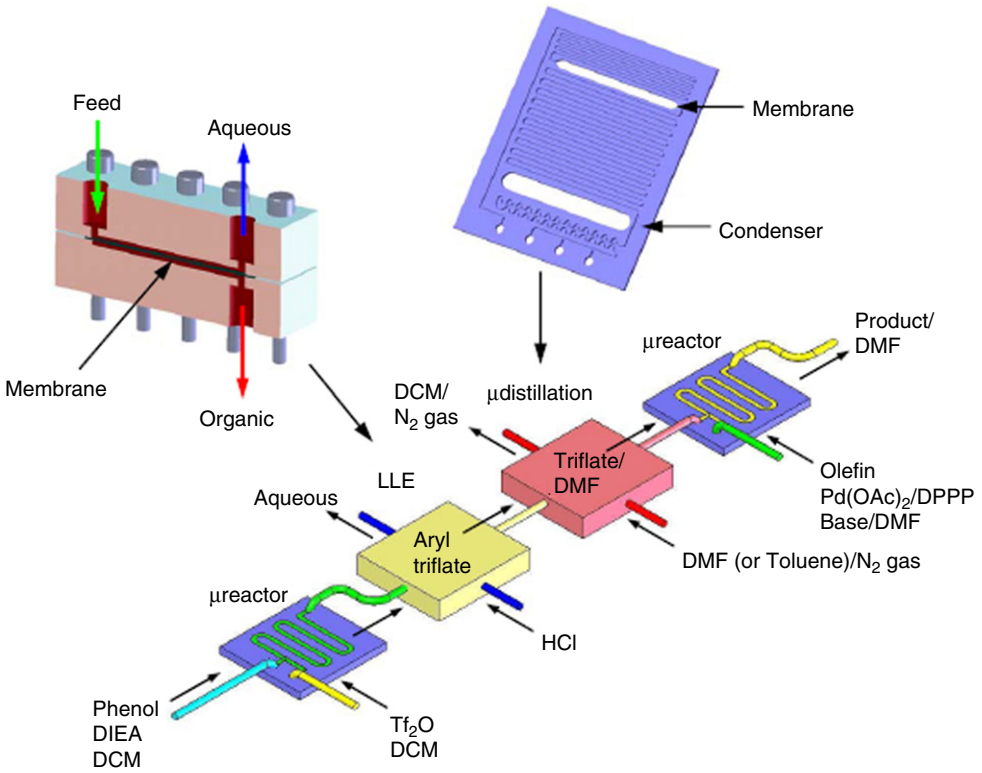


Figure 30 Multistep synthesis featuring microfluidic distillation to enact a solvent switch. Reproduced from Hartman, R. L.; Naber, J. R.; Buchwald, S. L.; Jensen, K. F. *Angew. Chem. Int. Ed.* **2010**, *49*, 899, with permission from John Wiley and Sons.

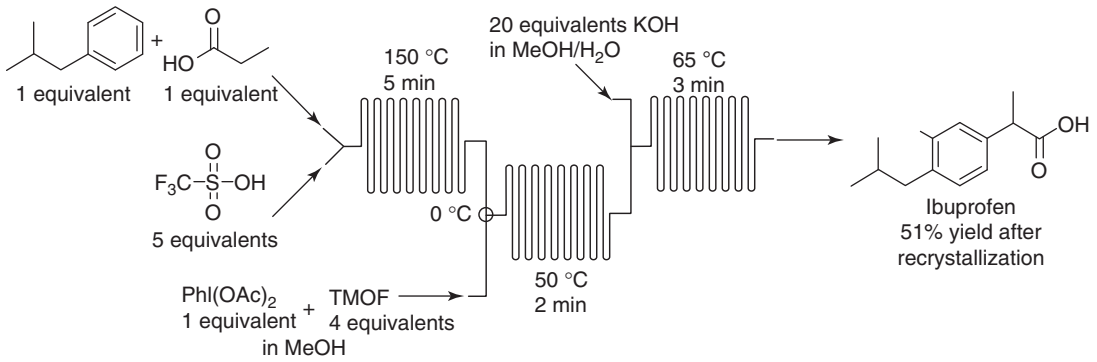


Figure 31 Continuous-flow synthesis of ibuprofen using short residence time transformations. Reproduced from Bogdan, A. R.; Poe, S. L.; Kubis, D. C.; Broadwater, S. J.; McQuade, D. T. *Angew. Chem. Int. Ed.* **2009**, *48*, 8547, with permission from John Wiley and Sons.

mixing and heat transfer. In this case, preparation of the aldehyde from an ester before diastereoselective crotylation was achieved in flow. Again, scavenger columns were used to remove aluminum and boron residues, and pulses of reagents were put through the system. An IR flow cell served to synchronize the borate addition to the aldehyde intermediate.

Following up their earlier investigation of selective reduction using DIBALH (see Section 9.03.4.1.2), Webb and Jamison successfully telescoped this reaction into a Horner–Wadsworth–Emmons olefination (Scheme 17).[108] The preparation of the deprotonated phosphonate (via *n*-BuLi) could be run at an 8 s residence time during the production process, exhibiting the excellent residence time control of these flow systems. Again, telescoping the reactions required less optimal conditions per reaction block (i.e., no excess of DIBALH), but lead to the reduction of process complexity (i.e., no work-up stage after the reduction step) and significantly reduced waste generation. High yields and E/Z ratios were obtained (>19:1) for a number of substrates, including the silyl ether of ethyl lactate, which is prone to racemization during purification after reduction.

The control over multiple steps of fast, exothermic reactions with short residence times has been demonstrated extensively by the Yoshida group.[30] One such example is the Li–Br exchange reaction of *p*-dibromobenzene with *n*-BuLi. By carefully controlling residence times of each step using micromixers, sequential addition of lithiation and electrophiles was achieved (Figure 33).

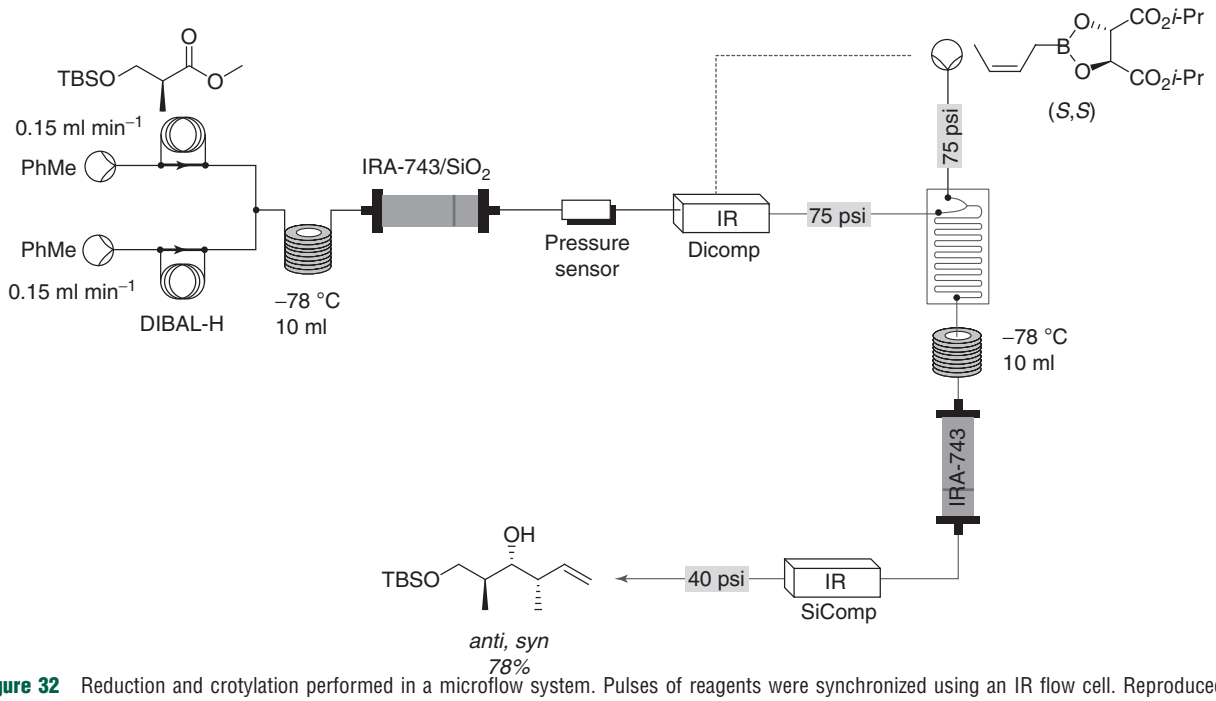
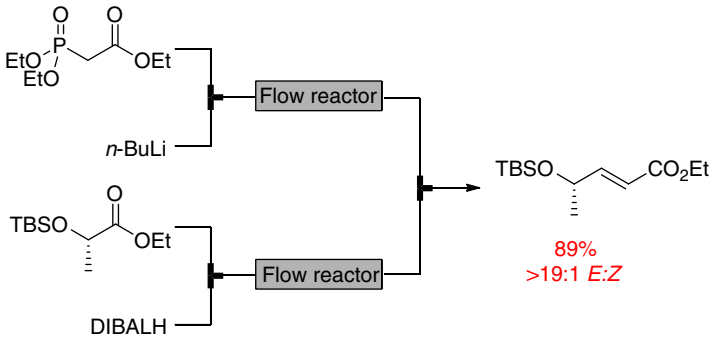


Figure 32 Reduction and crotylation performed in a microflow system. Pulses of reagents were synchronized using an IR flow cell. Reproduced from Carter, C. F.; Lange, H.; Sakai, D.; Baxendale, I. R.; Ley, S. V. *Chem. Eur. J.* **2011**, *17*, 3398, with permission from John Wiley and Sons.



Scheme 17 Selective ester reduction to an aldehyde, coupled to a Horner–Wadsworth–Emmons olefination.[108]

Residence times less than 100 ms to 1 s were screened for the lithiation step, and it was found that at −78 °C and 0.8 s residence time, side products arising from a benzyne intermediate were minimized.[109]

The application of heterogenized reagents, acids, and bases has seen considerable application at the microscale.[110] These heterogenized substrates can be applied to reduce process complexity.[111] For example, the acid wash used by Hartman et al.[105] (Figure 30) requires careful tuning of pressure drops in the system to achieve proper separation and an additional synchronized pump for the aqueous phase. A heterogenized sulfuric acid, however, simply serves as an in-line scavenger for basic byproducts. The disadvantage of heterogenized reagents is that their quick saturation requires injections of reagents into continuously flowing solvent rather than the typical continuous flow of reagents. This complicates data interpretation due to dispersion in these systems, creating very large concentration gradients that are not realized in scaled systems. One such use of heterogenized supports was utilized by Hopkin et al. in the multistep synthesis of Gleevec (Figure 34).[112] Immobilized acids and bases were used as scavengers since telescoping the reactions was not possible. An overall yield of 32% for Gleevec synthesis in flow was achieved.

9.03.7 Automation of Microfluidics

9.03.7.1 Analytical Tools

Researchers have investigated the coupling of microreactors with online analytical techniques such as UV-vis, Fourier transform infrared (FTIR), Raman, nuclear magnetic resonance, and mass spectroscopy in order to increase sample throughput (*see* Chapter 9.04).[18,19] In

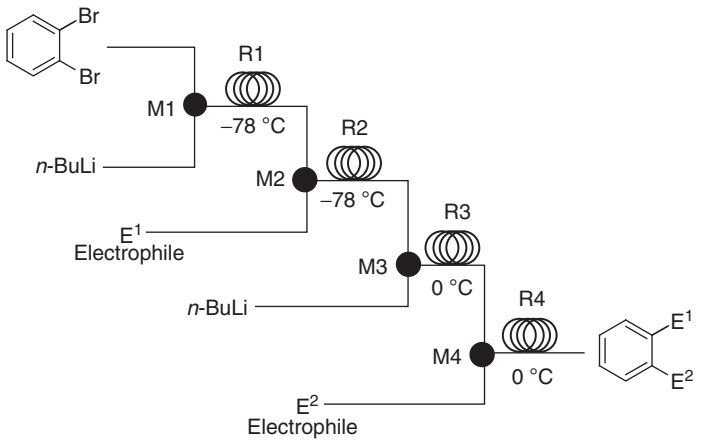


Figure 33 Lithiation and electrophilic addition steps in flow. Reproduced from Usutani, H.; Tomida, Y.; Nagaki, A.; *et al. J. Am. Chem. Soc.* **2007**, *129*, 3046, with permission from American Chemical Society.

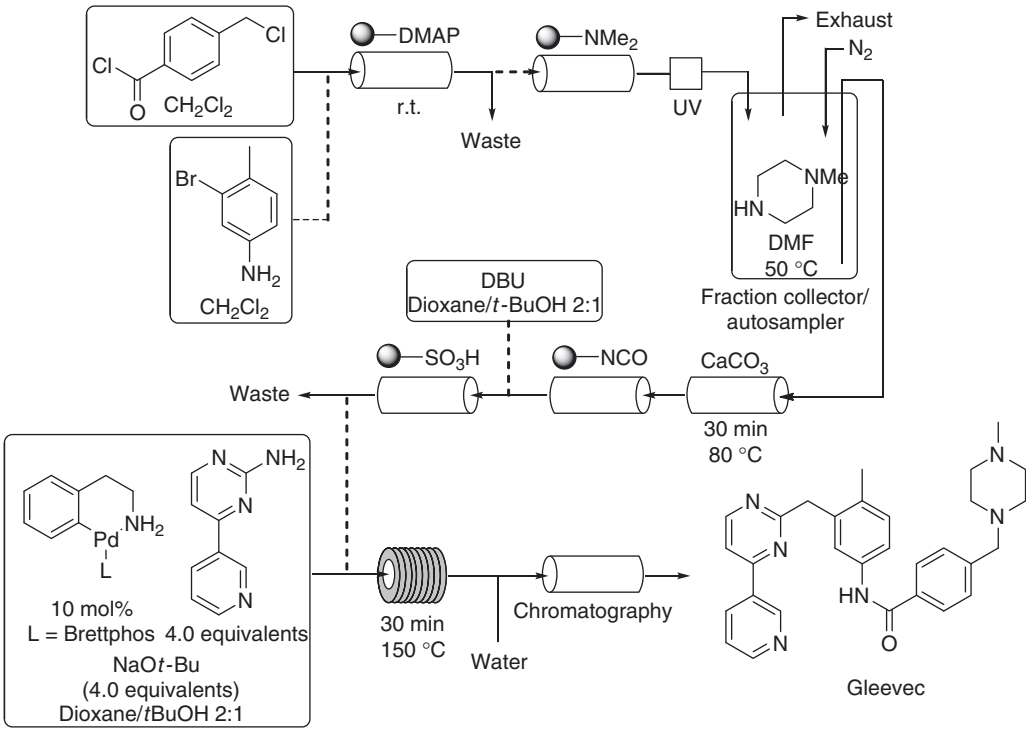


Figure 34 Synthesis of Gleevec in a microfluidic multistep system. Reproduced from Hopkin, M. D.; Baxendale, I. R.; Ley, S. V. *Chem. Commun.* **2010**, *46*, 2450, with permission from Royal Society of Chemistry.

particular, FTIR online microfluidic sensors (Figure 35) have lately found application in a number of microreactor systems where it has been used to study not just steady-state conditions, but also system dispersion, chromatographic effects, reaction screening, and monitoring reactor failures.[113]

9.03.7.2 Reaction Screening and Optimization

Integration of computer-controlled pumps, heaters, valves, and fraction collectors with microreactors enable screening of reagents for a target synthetic step, profiling the design space of a known reaction, or optimizing a known reaction (*see* Chapter 9.02).[18] Griffiths-Jones et al. have demonstrated a catch-and-release strategy for generating a sulfonamide library. Using an immobilized base to deprotonate and 'capture' a Boc-protected sulfamide, a series of alkyl bromide streams were then added, with the sulfamide being 'released' on *N*-alkylation (Figure 36).



Figure 35 ReactIR™ 45m with IR microfluidic flow cell attached. (a) Flow cell in line, connected with ¼–28 fittings; (b) flow cell with fittings removed, with direction of flow stream through the cell indicated; (c) head unscrewed, free view on diamond window (arrow). Reproduced from Carter, C. F.; Lange, H.; Ley, S. V.; *et al. Org. Process Res. Dev.* **2010**, *14*, 393, with permission from American Chemical Society.

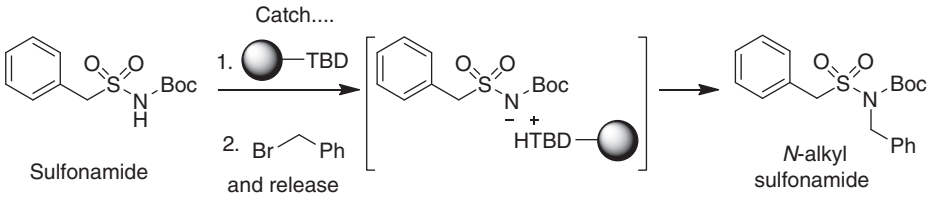


Figure 36 A 'catch-and-release' strategy for sulfonamide *N*-alkylation.

The resulting product stream underwent Boc cleavage on passing through a packed bed of immobilized sulfuric acid. The researchers were able to screen 48 combinations of sulfonamides (common medicinal functionalities) using the system outlined in Figure 37.[114] In many cases, the products were pure enough for direct biological application without further purification. Purity was determined by offline ultra performance liquid chromatography. At the end of each cycle, the spent column was regenerated by first eluting with an excess of allyl bromide to remove any remaining unreacted sulfonamide, followed by elution with a solution of the P_4-phosphazene base 2-*tert*-butylimino-2-diethylamino-1,3-dimethylperhydro-1,3,2-diazaphosphorine (BEMP) and a solvent wash.

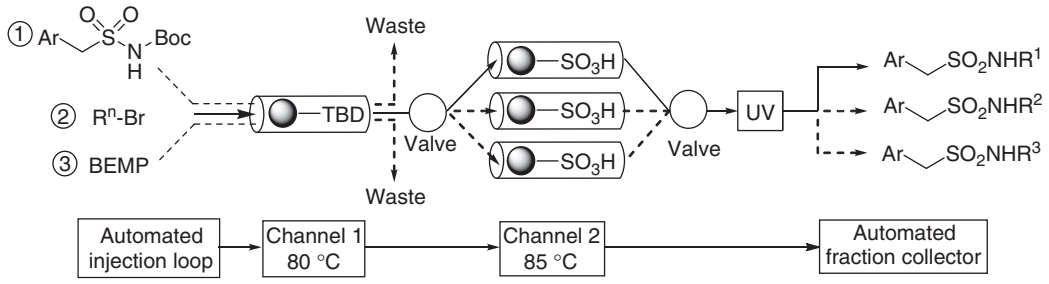


Figure 37 Automated screening system. Reproduced from Griffiths-Jones, C. M.; Hopkin, M. D.; Jönsson, D.; *et al. J. Comb. Chem.* **2007**, *9*, 422.

A related application of automated microreactor systems is systematically probing the design space of reactions of known interest. Sugimoto et al. recently built a system that automatically screened residence time and temperatures of a Sonogashira cross-coupling (Figure 38).[115] After intermediate offline HPLC analysis, new conditions were implemented using the information gained on an intuitive basis.

This organized method for probing a reaction's design space was significantly improved through the development of a truly automated optimization approach that continually updates the planned experiments using newly generated data. McMullen et al. demonstrated such an automated optimization by examining the oxidation of an alcohol to an aldehyde using CrO_3 (Figure 39).[18] Through the variation of temperature, residence time, and both reagent feeds, they were able to use online HPLC detection to have these results feed back to the computer and automatically update planned experiments using an optimization algorithm. This allowed the more efficient probing of design space and more optimal use of acquired data. The technology demonstrated to this point has the clear potential to expand on the standard batch optimization approaches.

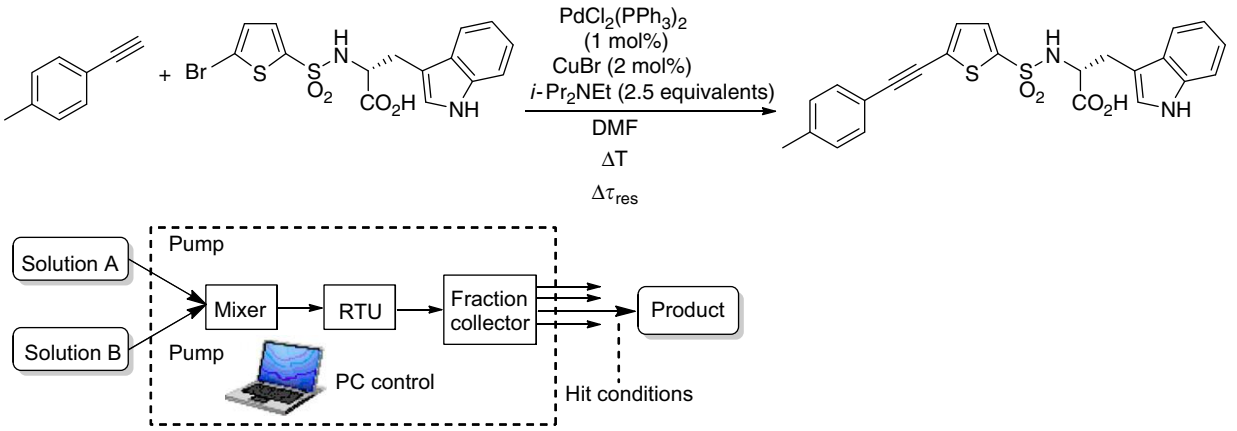
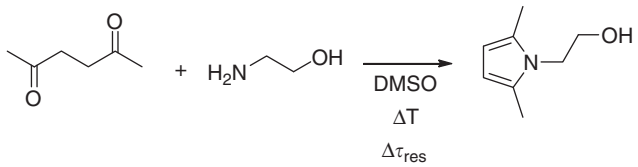


Figure 38 Optimization of a Sonogashira cross-coupling reaction. Reproduced from Sugimoto, A.; Fukuyama, T.; Rahman, M. T.; Ryu, I. *Tetrahedron Lett.* **2009**, *50*, 6364.

Optimization of a Paal–Knorr reaction by variation of temperature and residence time using an in-line FTIR measurement device was recently carried out using a similar setup. Moore and Jensen evaluated different optimization algorithms and found substantial differences in the number of required experiments to obtain an optimum value of productivity (Figure 40), illustrating the importance in selecting the proper optimization algorithm.[116] Additionally, the use of in-line FTIR enabled the algorithm to identify when steady-state conditions were reached, which greatly reduced the turnaround time between experiments and accelerated the optimization process.



9.03.8 Scaling Up

Scaling of small-scale flow chemistry processes can be achieved by the following two main approaches: (1) scaling out, i.e., using multiple microreactors or (2) scaling the size of the microreactor while maintaining heat and mass transfer advantages and then multiplying units (Figure 41). Scaling out of microreactors is feasible for a small number (typically <10), but the flow distribution becomes unwieldy for a large number of microreactors. The scale-up approach reduces the number of multiple reaction units and the large size of the units facilitates the integration of multiple units. Thus, this is the approach used in current production units such as the Corning AFR and the Ehrfeldt Mikrotechnik – BTS Lonza system (Figure 4). McMullen and Jensen[117] describe the use of Corning AFR system in developing and piloting a new process to perform a selective nitration under current good manufacturing process (cGMP) conditions. Weibel et al.[51] provide overview scale-up strategies for the Lonza plate technologies with examples selected from pharmaceutical applications. McMullen and Jensen[117] demonstrate how knowledge of the chemical kinetics acquired with an automated system can be combined with process models to scale predictably flow chemistry system to a size 500 times larger. In the following paragraphs, the authors present a few examples of scale-up for systems that would have been difficult to implement in batch operation.

Availability of a diverse array of aldehydes, as synthetic precursors/raw materials, is central to many drug discovery and production processes. With this in mind, Ducry and Roberge[118] investigated the DIBALH-promoted reduction of methyl butyrate to butyraldehyde, evaluating whether the use of continuous-flow processing could afford a selective route to the aldehyde without concomitant overreduction to the alcohol frequently observed in batch processes. Using operating temperature as the variable, the authors investigated its effect on yield and selectivity, for the model reaction illustrated in Scheme 18, conducting the reaction in a Corning AFR system, developed by Corning Reactor Technologies and an ER-25 from Ehrfeld Mikrotechnik.

In order to obtain the desired selectivity in batch, reductions had to be performed under cryogenic conditions, -65 to $-78\ ^{\circ}C$, but using a multi-injection flow concept made it possible to conduct the reactions at $-20\ ^{\circ}C$. Moreover, the authors obtained 89% yield of butyraldehyde in flow compared with only 63% in batch. In addition to the obvious advantages associated with obtaining products in higher yield and purity, the ability to perform reactions at higher temperatures is advantageous from a processing perspective as it reduces the capital costs associated with performing such reactions on a production scale.

Diazomethane is a valuable methylating agent but very difficult to handle for large-scale chemical transformations.[119] Rossi et al. reported the base-induced decomposition of *N*-methyl-*N*-nitrosourea under continuous-flow conditions using the Corning

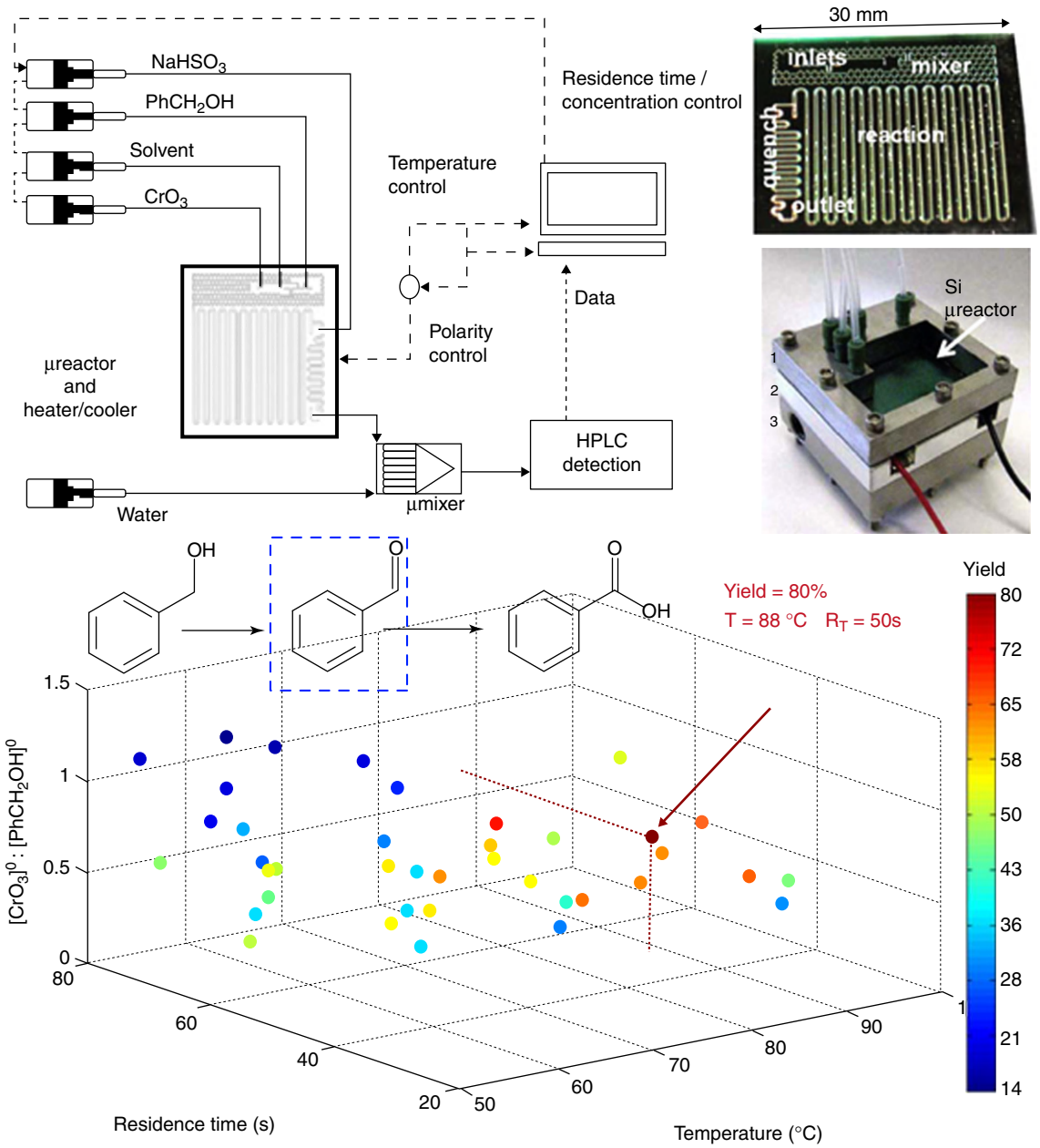


Figure 39 (Top, left) Schematic of automated microfluidic system consisting of syringe pumps, microreactor, micromixer, HPLC, and computer with associated LabVIEW interface hardware. (Top, right) Microreactor used in optimization study with mixing, reaction, and quench zones. Packaging scheme for the microreactor included fluidic connections in the top plate (1), a recessed plate (2) to house the microreactor and thermoelectric device, and baffled heat exchanger (3) for sufficient heat removal and additional temperature control. (Bottom) Benzaldehyde yield measured during four-dimensional optimization by a Simplex algorithm. Copyright © 2010 Annual Reviews.

AFR LowFlow reactor system, enabling the production of diazomethane up to 19 mol day^{-1} at a total flow rate of 53 ml min^{-1} (Figure 42).[120]

Boronic acids and esters are valuable synthetic building blocks. The synthesis of boronic esters, in particular, typically involves the addition of a Grignard reagent to a trialkoxyborate, forming a boronate intermediate (Scheme 19). Formation of this intermediate prevents polyalkylation, ensuring reasonable to high yields of the expected boronate product. Although this method is effective at smaller scales, scaling up poses significant hazards. In the case of propargylic boronates, the propargylic bromide Grignard precursor is shock sensitive, and the exothermic dissolving-metal Grignard formation presents safety and engineering issues.

A scalable process for the preparation of such an organoboron propargylation reagent from trimethylsilylpropyne, isopropyl pinacol borate, and *n*-butyllithium was examined by researchers at Boehringer Ingelheim (Scheme 20).[121] Problems associated

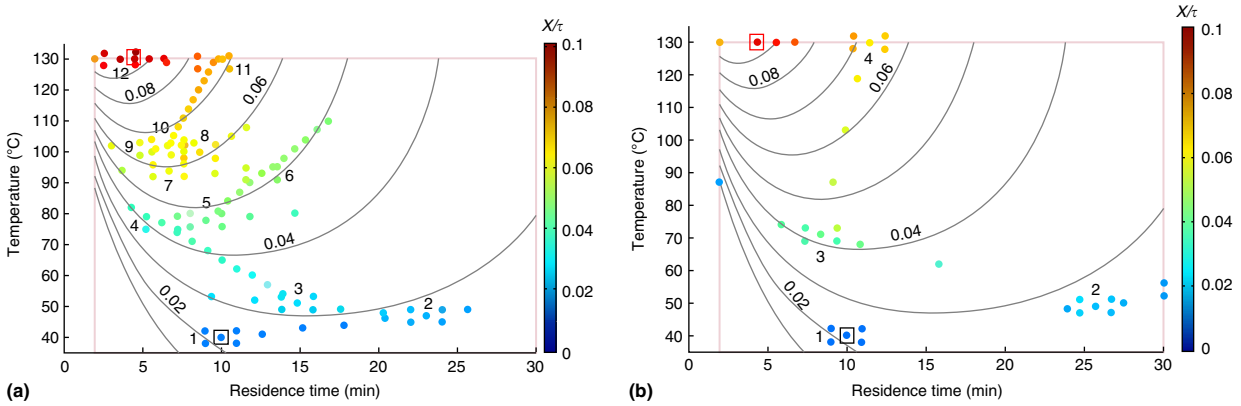


Figure 40 Optimization of the productivity of a Paal–Knorr reaction (X/t) showing the importance of selecting the appropriate optimization strategy. The number of experiments is greatly reduced by going from (a) steepest decent to (b) a conjugate gradient (with step-size regulation) algorithm. Reproduced from Moore, J. S.; Jensen, K. F. *Org. Process Res. Dev.* **2012**, *16*, 1409, with permission from American Chemical Society.

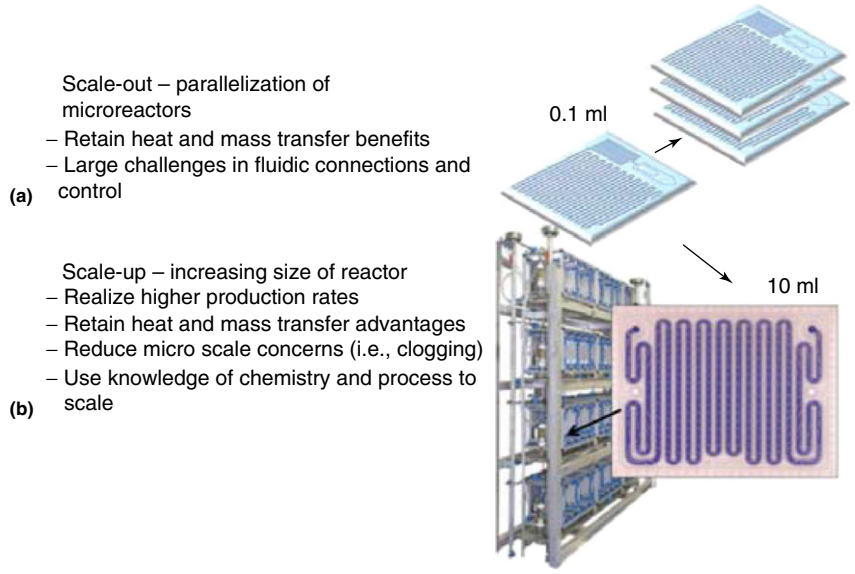
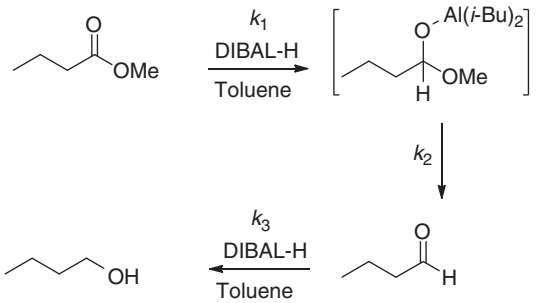


Figure 41 Approaches to scale-up of microreactor processes: (a) scale-out and (b) scale-up, illustrated with glass–silicon microreactors and Corning Gen 1 AFR units as examples.



Scheme 18 Mechanism of the DIBALH-mediated reduction of methyl butrate.[118]

with implementing a typical aqueous workup and batch process into production due to boronate equilibration and protonolysis were addressed through implementing a continuous flow and distillation process that efficiently produced 297 kg of the key

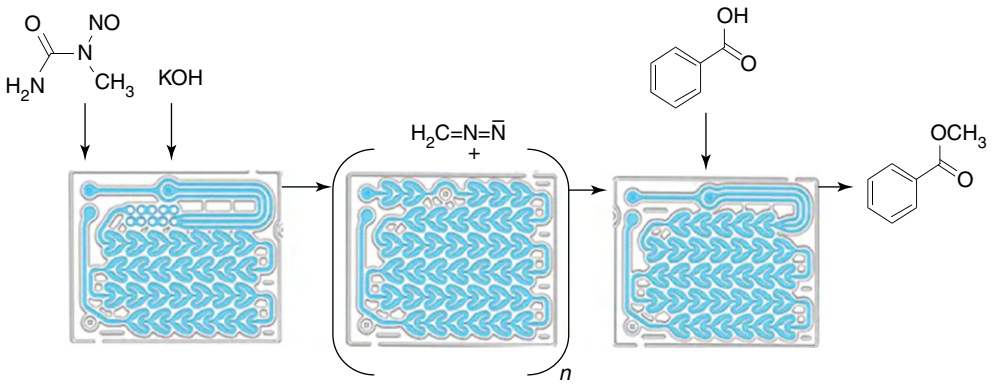
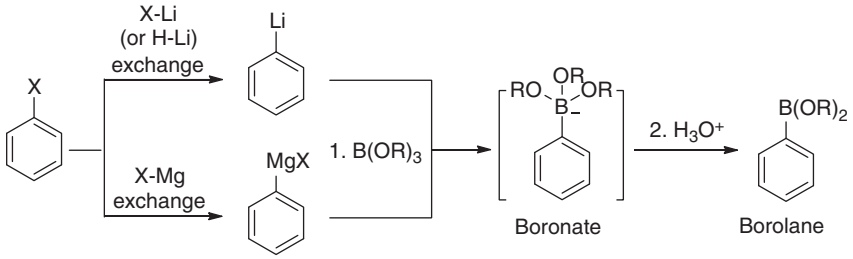
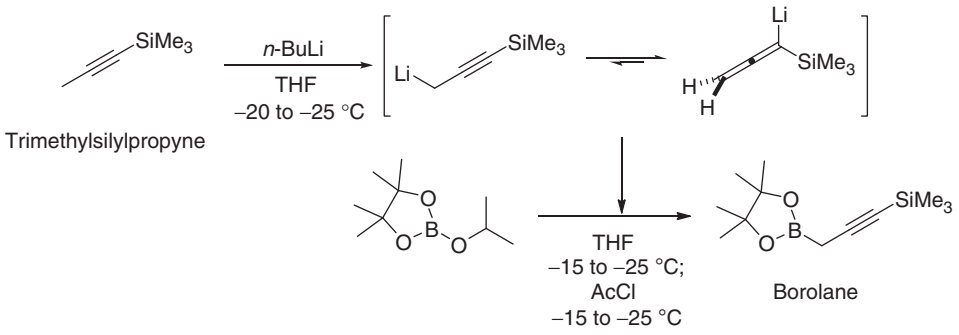


Figure 42 Corning Advanced-Flow LowFlow reactor used for production of diazomethane on demand. Reproduced from Rossi, E.; Woehl, P.; Maggini, M. *Org. Process Res. Dev.* **2011**, *16*, 1146.



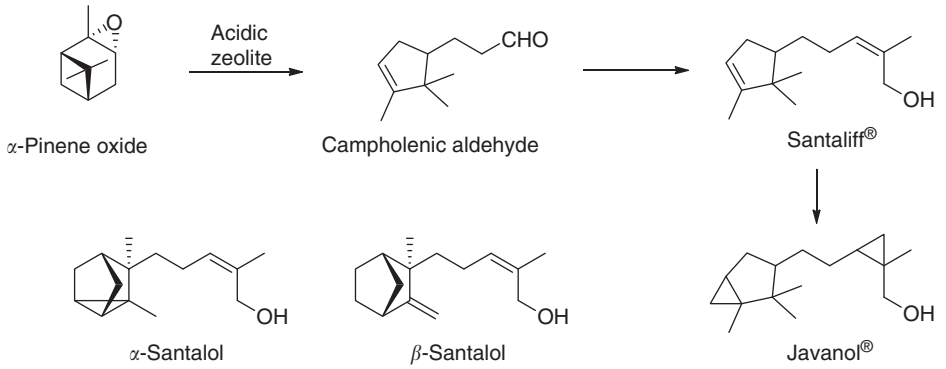
Scheme 19 Prevalent manufacturing methods for organoboron compounds, illustrated for a phenyl boronic ester.



Scheme 20 Direct approach to boronate via lithiated trimethylsilylpropyne.[121]

propargylation reagent. The process was designed in three phases. The first phase involved the generation of the lithium propargylide with *n*-BuLi, and a delay loop was installed to allow for the lithiation to run to completion. The second phase consists of the addition of the lithium propargylide with the isopropyl borate, again including a delay loop to ensure completion of the addition. The third phase consisted of quenching the isopropoxide with acetyl chloride, with the resulting reaction mixture being fed into a collection vessel.

Beyond pharmaceuticals, the fragrance industry has also benefited from continuous-flow processes as exemplified by synthesis of sandalwood oil substitutes derived from α-campholenic aldehyde. This aldehyde is prepared from the oxidation product of α-pinene, most of which is a byproduct of the paper industry (Scheme 21).[122] α-Pinene oxide is a very reactive substrate that rearranges under acidic conditions to α-campholenic aldehyde.[123] As a continuous-flow fixed-bed reactor implementation, the reaction was catalyzed by Ti-*β* zeolite with initial yields up to 93% at 90 °C when cofeeding a gaseous stream of α-pinene oxide and an inert organic carrier (e.g., *n*-heptane).[124] Complete regeneration of the catalytic activity (up to 100 times) could be achieved by an air burn-off at 480 °C.



Scheme 21 Synthesis of sandalwood mimics.

9.03.9 Conclusions

The authors have reviewed fundamentals of microreactor technology and chemistry in continuous flow with case studies selected to illustrate fundamental concepts and advantages of the approach. Flow chemistry in microchemical systems continues to evolve and is increasingly contributing to chemical discovery and development. Overcoming a number of scientific engineering challenges will be important to sustaining and expanding the impact of flow chemistry. Chemical and engineering strategies for handling solids before, during, and after synthesis both as reagents and products would be particularly enabling.[125] Further advances are also needed in multistage separations, in-line analysis, and online control and optimization. Innovation in the required infrastructure to operate microchemical systems, specifically pumps and valves, would also enhance the applications and impact of flow chemistry in chemical discovery, process development, and production.

Acknowledgments

The authors thank NIH (NIGMS P50 GM067041) and Novartis for support underlying this review.

References

1. Marre, S.; Jensen, K. F. *Chem Soc. Rev.* **2010**, *39*, 1183.
2. Hessel, V. R. A., Schouten, J. C., Yoshida, J. I., Eds. *Handbook of Micro Process Technology, Vol. 1–3*; Wiley-VCH: Weinheim, Germany, **2009**.
3. Hartman, R. L.; McMullen, J. P.; Jensen, K. F. *Angew. Chem. Int. Ed.* **2011**, *50*, 7502.
4. Hessel, V.; Gursel, I. V.; Wang, Q.; Noel, T.; Lang, J. *Chem. Eng. Technol.* **2012**, *35*, 1184.
5. Ley, S. V. *Chem. Rec.* **2012**, *12*, 378.
6. Malet-Sanz, L.; Susanne, F. *J. Med. Chem.* **2012**, *55*, 4062.
7. Webb, D.; Jamison, T. F. *Chem. Sci.* **2010**, *1*, 675.
8. Wegner, J.; Ceylan, S.; Kirschning, A. *Adv. Synth. Catal.* **2012**, *354*, 17.
9. Wiles, C.; Watts, P. *Chem. Commun.* **2011**, *47*, 6512.
10. Marre, S.; Adamo, A.; Basak, S.; Aymonier, C.; Jensen, K. F. *Ind. Eng. Chem. Res.* **2010**, *49*, 11310.
11. Yoshida, J.-I. *Flash Chemistry: Fast Organic Synthesis in Microsystems*; John Wiley & Sons Ltd: Chichester, West Sussex, UK, **2008**.
12. Wiles, C.; Watts, P. *Micro Reaction Technology in Organic Synthesis*; CRC Press: Boca Raton, FL, USA, **2011**.
13. Nguyen, N.-T.; Wu, Z. *J. Micromech. Microeng.* **2005**, *15*, R1.
14. Hessel, V.; Lowe, H.; Schonfeld, F. *Chem. Eng. Sci.* **2005**, *60*, 2479.
15. Bedore, M. W.; Zaborenko, N.; Jensen, K. F.; Jamison, T. F. *Org. Process Res. Dev.* **2010**, *14*, 432.
16. Knitter, R.; Liauw, M. A. *Lab Chip* **2004**, *4*, 378.
17. Nagy, K. D.; Jensen, K. F. *Chem. Today* **2011**, *29*, 29.
18. McMullen, J. P.; Jensen, K. F. *Ann. Rev. Anal. Chem.* **2010**, *3*, 19.
19. deMello, A. J. *Nature* **2006**, *442*, 394.
20. Kralj, J. G.; Sahoo, H. R.; Jensen, K. F. *Lab Chip* **2007**, *7*, 256.
21. Hartman, R. L.; Sahoo, H. R.; Yen, B. C.; Jensen, K. F. *Lab Chip* **2009**, *9*, 1843.
22. Lam, K. F.; Cao, E.; Sorensen, E.; Gavriilidis, A. *Lab Chip* **2011**, *11*, 1311.
23. Levenspiel, O. *Chemical Reaction Engineering*. 3rd ed.; Wiley: New York, **1999**.
24. Nagy, K. Ph.D. Thesis, MIT, Cambridge, MA, 2011.
25. Nagy, K. D.; Shen, B.; Jamison, T. F.; Jensen, K. F. *Org. Process Res. Dev.* **2012**, *16*, 976.
26. Hartman, R. L.; McMullen, J. P.; Jensen, K. F. *Angew. Chem. Int. Ed.* **2011**, *50*, 7502.
27. Yoshida, J.; Nagaki, A.; Iwasaki, T.; Suga, S. *Chem. Eng. Technol.* **2005**, *28*, 259.
28. Soleymani, A.; Yousefi, H.; Turunen, I. *Chem. Eng. Sci.* **2008**, *63*, 5291.
29. Gunther, A.; Jhunjhunwala, M.; Thalmann, M.; Schmidt, M. A.; Jensen, K. F. *Langmuir* **2005**, *21*, 1547.
30. Yoshida, J.-I.; Kim, H.; Nagaki, A. *ChemSusChem* **2011**, *4*, 331.
31. Tomida, Y.; Nagaki, A.; Yoshida, J.-I. *J. Am. Chem. Soc.* **2011**, *133*, 3744.

32. Webb, D.; Jamison, T. F. *Org. Lett.* **2011**, *14*, 568.
33. von Braun, J.; Keller, W. *Ber. Dtsch. Chem. Ges. (A and B Ser.)* **1932**, *65*, 1677.
34. Kopach, M. E.; Murray, M. M.; Braden, T. M.; Kobierski, M. E.; Williams, O. L. *Org. Process Res. Dev.* **2009**, *13*, 152.
35. King, B. R., Ed. *Encyclopedia of Inorganic Chemistry,* 2nd ed.; Wiley-VCH: Weinhiem, **2005**.
36. Hagenbuch, J. P. *Chimia* **2003**, *57*, 773.
37. Gutmann, B.; Roduit, J. P.; Roberge, D.; Kappe, C. O. *Angew. Chem. Int. Ed. Engl.* **2010**, *49*, 7101.
38. Kappe, C. O.; Roberge, D. M.; Roduit, J.-P.; Obermayer, D.; Gutmann, B. *J. Flow Chem.* **2012**, *2*, 8.
39. Palde, P. B.; Jamison, T. F. *Angew. Chem. Int. Ed. Engl.* **2011**, *50*, 3525.
40. Gonzalez-Bobes, F.; Kopp, N.; Li, L.; *et al. Org. Process Res. Dev.* **2012**, *16*.
41. Gunther, A.; Jensen, K. F. *Lab Chip* **2006**, *6*, 1487.
42. Dreyfus, R.; Tabeling, P.; Willaime, H. *Phys. Rev. Lett.* **2003**, *90*, 144505.
43. Gunther, A.; Jensen, K. F. *Lab Chip* **2006**, *6*, 1487.
44. Bogdan, A.; McQuade, D. T. *Beilstein J. Org. Chem.* **2009**, *5*, 17.
45. Song, H.; Bringer, M. R.; Tice, J. D.; Gerdts, C. J.; Ismagilov, R. F. *Appl. Phys. Lett.* **2003**, *83*, 4664.
46. Ahmed-Omer, B.; Barrow, D.; Wirth, T. *Chem. Eng. J.* **2008**, *135*(Suppl. 1), S280.
47. Naber, J. R.; Buchwald, S. L. *Angew. Chem. Int. Ed.*, **2010**, *49*, 9469.
48. Jovanović, J.; Rebrov, E. V.; Nijhuis, T. A.; Hessel, V.; Schouten, J. C. *Ind. Eng. Chem. Res.* **2010**, *49*, 2681.
49. Šinkovec, E.; Krajnc, M. *Org. Process Res. Dev.* **2011**, *15*, 817.
50. Maurya, R. A.; Park, C. P.; Kim, D.-P. *Beilstein J. Org. Chem.* **2011**, *7*, 1158.
51. Weibel, D. B.; DiLuzio, W. R.; Whitesides, G. M. *Nat. Rev. Microbiol.* **2007**, *5*, 209.
52. Kreutzer, M. T.; Kapteijn, F.; Moulijn, J. A.; Heiszwolf, J. J. *Chem. Eng. Sci.* **2005**, *60*, 5895.
53. van Baten, J. M.; Krishna, R. *Chem. Eng. Sci.* **2004**, *59*, 2535.
54. van Baten, J. M.; Krishna, R. *Chem. Eng. Sci.* **2005**, *60*, 1117.
55. Bercic, G.; Pintar, A. *Chem. Eng. Sci.* **1997**, *52*, 3709.
56. de Mas, N.; Günther, A.; Schmidt, M. A.; Jensen, K. F. *Ind. Eng. Chem. Res.* **2008**, *48*, 1428.
57. Doku, G. N.; Verboom, W.; Reinhoudt, D. N.; van den Berg, A. *Tetrahedron* **2005**, *61*, 2733.
58. Losey, M. W.; Jackman, R. J.; Firebaugh, S. L.; Schmidt, M. A.; Jensen, K. F. *Microelectromech. Sys. J.* **2002**, *11*, 709.
59. Murphy, E. R.; Martinelli, J. R.; Zaborenko, N.; Buchwald, S. L.; Jensen, K. F. *Angew. Chem. Int. Ed.* **2007**, *46*, 1734.
60. Wada, Y.; Schmidt, M. A.; Jensen, K. F. *Ind. Eng. Chem. Res.* **2006**, *45*, 8036.
61. Roberge, D. M.; Nobis, M. *Chim. Oggi/Chem. Today* **2011**, *29*.
62. Roydhouse, M. D.; Ghaini, A.; Constantinou, A.; *et al. Org. Process Res. Dev.* **2011**, *15*, 989.
63. Huübner, S.; Bentrup, U.; Budde, U.; *et al. Org. Process Res. Dev.* **2009**, *13*, 952.
64. Chambers, R. D.; Holling, D.; Spink, R. C. H.; Sandford, G. *Lab Chip* **2001**, *1*, 132.
65. de Mas, N.; Günther, A.; Schmidt, M. A.; Jensen, K. F. *Ind. Eng. Chem. Res.* **2003**, *42*, 698.
66. Chambers, R. D.; Fox, M. A.; Sandford, G. *Lab Chip* **2005**, *5*, 1132.
67. Breen, J. R.; Sandford, G.; Yufit, D. S.; *et al. Beilstein J. Org. Chem.* **2011**, *7*, 1048.
68. Rozen, S. *Eur. J. Org. Chem.* **2005**, *2005*, 2433.
69. Chambers, R. D.; Holling, D.; Rees, A. J.; Sandford, G. *J. Fluorine Chem.* **2003**, *119*, 81.
70. McPake, C. B.; Murray, C. B.; Graham, S. *Chim. Oggi* **2010**, *28*, 6.
71. Kockmann, N.; Gottsponer, M.; Roberge, D. M. *Chem. Eng. J.* **2011**, *167*, 718.
72. O'Brien, M.; Taylor, N.; Polyzos, A.; Baxendale, I. R.; Ley, S. V. *Chem. Sci.* **2011**, *2*, 1250.
73. O'Brien, M.; Baxendale, I. R.; Ley, S. V. *Org. Lett.* **2010**, *12*, 1596.
74. Ajmera, S. K.; Delattre, C.; Schmidt, M. A.; Jensen, K. F. *Sensors Actuat. B Chem.* **2002**, *82*, 297.
75. Inoue, T.; Schmidt, M. A.; Jensen, K. F. *Ind. Eng. Chem. Res.* **2007**, *46*, 1153.
76. Frost, C. G.; Mutton, L. *Green Chem.* **2010**, *12*, 1687.
77. Losey, M. W.; Schmidt, M. A.; Jensen, K. F. *Ind. Eng. Chem. Res.* **2001**, *40*, 2555.
78. Al-Dahhan, M. H.; Larachi, F.; Dudukovic, M. P.; Laurent, A. *Ind. Eng. Chem. Res.* **1997**, *36*, 3292.
79. Horie, T.; Sumino, M.; Tanaka, T.; *et al. Org. Process Res. Dev.* **2010**, *14*, 405.
80. Garrett, C. E.; Prasad, K. *Adv. Synth. Catal.* **2004**, *346*, 889.
81. Weck, M.; Jones, C. W. *Inorg. Chem.* **2007**, *46*, 1865.
82. Lee, C. K. Y.; Holmes, A. B.; Ley, S. V.; *et al. Chem. Commun.* **2005**, 2175.
83. Baxendale, I. R.; Griffiths-Jones, C. M.; Ley, S. V.; Tranmer, G. K. *Chem.–Eur. J.* **2006**, *12*, 4407.
84. Alimardanov, A.; Schmieder-van de Vondervoort, L.; de Vries, A. H. M.; de Vries, J. G. *Adv. Synth. Catal.* **2004**, *346*, 1812.
85. Leadbeater, N. E. *Chem. Commun.* **2005**, 2881.
86. Bolton, K. F.; Canty, A. J.; Deverell, J. A.; *et al. Tetrahedron Lett.* **2006**, *47*, 9321.
87. Kunz, U.; Kirschning, A.; Wen, H. L.; *et al. Catal. Today* **2005**, *105*, 318.
88. Haswell, S. J.; O'Sullivan, B.; Styring, P. *Lab Chip* **2001**, *1*, 164.
89. Phan, N. T. S.; Brown, D. H.; Styring, P. *Green Chem.* **2004**, *6*, 526.
90. Lamb, G. W.; Al Badran, F. A.; Williams, J. M. J.; Kolaczkowski, S. T. *Chem. Eng. Res. Des.* **2010**, *88*, 1533.
91. Lim, J.; Riduan, S. N.; Lee, S. S.; Ying, J. Y. *Adv. Synth. Catal.* **2008**, *350*, 1295.
92. Lim, J.; Seong Lee, S.; Ying, J. Y. *Chem. Commun.* **2010**, *46*, 806.
93. Simons, C.; Hanefeld, U.; Arends, I. W. C. E.; *et al. Chem. Commun.* **2004**, 2830.
94. Madarász, J.; Farkas, G.; Balogh, S.; *et al. J. Flow Chem.* **2011**, *1*, 62.
95. van den Berg, M.; Minnaard, A. J.; Schudde, E. P.; *et al. J. Am. Chem. Soc.* **2000**, *122*, 11539.
96. Hook, B. D. A.; Dohle, W.; Hirst, P. R.; *et al. J. Org. Chem.* **2005**, *70*, 7558.
97. Vasudevan, A.; Villamil, C.; Trumbull, J.; *et al. Tetrahedron Lett.* **2010**, *51*, 4007.
98. Ohtani, B.; Osaki, H.; Nishimoto, S.; Kagiya, T. *J. Am. Chem. Soc.* **1986**, *108*, 308.
99. Matsushita, Y.; Ohba, N.; Suzuki, T.; Ichimura, T. *Catal. Today* **2008**, *132*, 153.
100. Wootton, R. C. R.; Fortt, R.; de Mello, A. J. *Org. Process Res. Dev.* **2002**, *6*, 187.
101. Bourne, R. A.; Han, X.; Poliakoff, M.; George, M. W. *Angew. Chem. Int. Ed.* **2009**, *48*, 5322.
102. Han, X.; Bourne, R. A.; Poliakoff, M.; George, M. W. *Chem. Sci.* **2011**, *2*, 1059.
103. Lévesque, F.; Seeberger, P. H. *Angew. Chem. Int. Ed.* **2012**, *51*, 1706.
104. Sahoo, H. R.; Kralj, J. G.; Jensen, K. F. *Angew. Chem. Int. Ed.* **2007**, *46*, 5704.

105. Hartman, R. L.; Naber, J. R.; Buchwald, S. L.; Jensen, K. F. *Angew. Chem. Int. Ed.* **2010**, *49*, 899.
106. Bogdan, A. R.; Poe, S. L.; Kubis, D. C.; Broadwater, S. J.; McQuade, D. T. *Angew. Chem. Int. Ed.* **2009**, *48*, 8547.
107. Carter, C. F.; Lange, H.; Sakai, D.; Baxendale, I. R.; Ley, S. V. *Chem.–Eur. J.* **2011**, *17*, 3398.
108. Webb, D.; Jamison, T. F. *Org. Lett.* **2012**, *14*, 2465.
109. Usutani, H.; Tomida, Y.; Nagaki, A.; *et al. J. Am. Chem. Soc.* **2007**, *129*, 3046.
110. Myers, R. M.; Roper, K. A.; Baxendale, I. R.; Ley, S. V. In *Modern Tools for the Synthesis of Complex Bioactive Molecules*; Cossy, J.; Arseniyadis., S. Eds.; John Wiley: New York, **2012**; p 359.
111. Baxendale, I. R.; Deeley, J.; Griffiths-Jones, C. M.; *et al. Chem. Commun.* **2006**, 2566.
112. Hopkin, M. D.; Baxendale, I. R.; Ley, S. V. *Chem. Commun.* **2010**, *46*, 2450.
113. Carter, C. F.; Lange, H.; Ley, S. V.; *et al. Org. Process Res. Dev.* **2010**, *14*, 393.
114. Griffiths-Jones, C. M.; Hopkin, M. D.; Jönsson, D.; *et al. J. Comb. Chem.* **2007**, *9*, 422.
115. Sugimoto, A.; Fukuyama, T.; Rahman, M. T.; Ryu, I. *Tetrahedron Lett.* **2009**, *50*, 6364.
116. Moore, J. S.; Jensen, K. F. *Org. Process Res. Dev.* **2012**, *16*, 1409.
117. McMullen, J. P.; Jensen, K. F. *Org. Process Res. Dev.* **2011**, *15*, 398.
118. Ducry, L.; Roberge, D. M. *Org. Process Res. Dev.* **2008**, *12*, 163.
119. Struempel, M.; Ondruschka, B.; Daute, R.; Stark, A. *Green Chem.* **2008**, *10*, 41.
120. Rossi, E.; Woehl, P.; Maggini, M. *Org. Process Res. Dev.* **2011**, *16*, 1146.
121. Fandrick, D. R.; Roschangar, F.; Kim, C.; *et al. Org. Process Res. Dev.* **2011**, *16*, 1131.
122. Clerici, M. Topics in Catalysis. Springer: The Netherlands, **2000**, Vol. 13; p 373.
123. Muller, B.; Pamingle, H.; Schulte-Elte, K.-H. EP 0155591, 1988.
124. Kunkeler, P.; van der Waal, J.; Bremmer, J.; *et al. Catal. Lett.* **1998**, *53*, 135.
125. Hartman, R. L.; Naber, J. R.; Zaborenko, N.; Buchwald, S. L.; Jensen, K. F. *Org. Process Res. Dev.* **2010**, *14*, 1347.

9.04 Microcapillary Catalysis

O Trapp, Universität Heidelberg, Heidelberg, Germany

© 2014 Elsevier Ltd. All rights reserved.

9.04.1	**Introduction**	94
9.04.2	**Experimental Realization of On-Column Reaction Chromatography**	96
9.04.2.1	Setups of On-Column Reaction Chromatography	96
9.04.2.2	Preparation of Capillary Reactors	97
9.04.2.3	High-Throughput Approach	98
9.04.3	**Determination of Kinetic Data**	98
9.04.3.1	Classical Reaction Kinetics for On-Column Reaction Chromatographic Experiments with Reaction and Consecutive Separation	98
9.04.3.2	Evaluation of Conversion Profiles Obtained by On-Column Reaction Chromatography	98
9.04.3.2.1	Theoretical plate model	98
9.04.3.2.2	The unified equation of chromatography	100
9.04.3.3	Determination of Activation Parameters	101
9.04.4	**Catalytic Reactions Investigated by On-Column Reaction Chromatography**	102
9.04.4.1	Hydrogenations over Noble Metal Nanoparticles	102
9.04.4.2	Ring-Closing Metathesis	104
9.04.4.3	Gosteli–Claisen Rearrangement	105
9.04.4.4	Combinatorial High-Throughput Screening: Catalyst by the Meter	107
9.04.5	**Outlook**	109
References		110

Glossary

Dynamic chromatography A technique to investigate the stereodynamics of molecules during the separation process. Elution profiles are characterized by a distinct plateau formation.

Flow-through chemistry In flow-through chemistry reactions are typically carried out in a (micro) reactor, where the reactants are continuously pumped through. There are many advantages, for example, exact temperature control, short contact times, and high surface to volume ratios.

High-throughput reaction screening It aims at finding new catalysts, new reactions, and new materials by parallel screening under same reaction conditions. In a primary screening, for example, conversions under certain conditions are detected, whereas in a secondary screening more detailed information is obtained by kinetic analysis and variation of reaction conditions.

On-column reaction chromatography (ocRC) Integration of chromatographic analysis and chemical reaction in a single setup. The chemical transformation is directly performed on the separation column.

Unified equation of chromatography The unified equation allows the direct calculation of reaction rate constants k_1 and k_{-1} for all types of first-order reactions taking place during a chromatographic separation, regardless of the initial concentrations of the interconverting substances A and B, e.g., interconverting stereoisomers, or reacting reactants A to B and the equilibrium constant $K_{A/B}$ and vice versa. Catalyzed reaction can be studied by on-column reaction chromatography using the unified equation to evaluate the conversion profiles.

9.04.1 Introduction

Discovering new catalysts is of great importance to sustainable chemical processes for industrial applications as well as for widening the spectrum of synthetic methodologies and techniques in chemistry. The investigation of reaction kinetics, in particular of catalyzed reactions, is of fundamental interest in chemistry, biochemistry, and related research areas. Understanding how to control the transition state of a reaction allows for a directed design of new catalysts and benign processes. The expansion of synthetic techniques and methods in chemistry creates new opportunities for the discovery of highly productive and selective catalysts in both science and industry. Therefore, the development of techniques to comprehensively investigate the reaction kinetics of a variety of substrates is of great interest. In particular, the investigation of individual pathways in stereoselective transformations requires techniques to directly access enantioselectivities.

Despite these advantages, the majority of researchers still uses batch reactors to investigate novel reactions and catalytic processes. A major drawback of commonly used batch reactors is the limitation of studying only one reaction per run, because competing reactions lead to indefinable reaction kinetics. Furthermore, large quantities of substrates and catalysts are required.

 doi:10.1016/B978-0-08-097742-3.00919-8

The reaction, separation, and quantification of the reactants and products to determine conversions have to be performed consecutively. Therefore the integration of reaction and separation is not only a desired goal to determine reaction rate constants but, especially in chemical engineering, because pure products are obtained in a single step.[1,2]

Flow-through microreactors[3–7] represent an interesting alternative for carrying out chemical reactions in continuous flow and they are more and more used in the synthetic organic chemistry.[8–11] For example, highly exothermal reactions, i.e., fluorinations, can be safely performed. The striking advantage is the large surface-to-volume ratio that can be achieved in such miniaturized systems.

Inspired by micrototal analysis systems (μTAS), where sequential analytical operations can be automatically performed by computer control allowing the very efficient analysis of biomolecules, microfluidic devices are also employed in synthetic organic chemistry as lab-on-a-chip.[12–16] Even sequential reactions can be performed and high-throughput screening of reactions is feasible.[17–19]

Other advantages are the precise temperature control in such devices, in particular for quartz chips and fused-silica capillaries with high thermal conductivity, which allows performing precise kinetic measurements even for highly exergonic reactions. Furthermore, such devices are highly attractive to study multiphase catalytic systems,[20] which play a predominant role in industrial processes. Typically, such processes are difficult to investigate because the interaction of the reactant with the catalyst is controlled by the mass transfer between the different phases and therefore the directly measured apparent reaction rate is composed of the inherent reaction rate and diffusion rates. To reduce this effect the interfacial area has to be increased. Microstructured reaction systems intrinsically have a high specific interfacial area per volume ($a_{inter}=2/r$), only dependent on the radius for circular reaction channels, i.e., for capillaries with inner diameters between 250 and 100 μm the specific interfacial area per volume ranges from 16 000 to 40 000 $m^2\,m^{-3}$. It can be expected that microfluidic systems are revolutionizing chemical synthesis, because chemical processes can be easily controlled. However, there are still many experimental challenges that need to be addressed, among these are the efficient control of mixing, interfacing with standard analytical instruments for advanced analysis.

A major issue is also the uniform modification of reaction channels with immobilized catalysts and the use of these devices for performing kinetic measurements. Conventional microfluidic devices typically use square or rectangular-shaped reaction channels and the system is often closed by a cover glass glued on top of the chip. Uniform coating of open channels with polymeric materials is difficult, deviations in the thickness lead to nonlinear behavior, which makes kinetic analysis difficult. In contrast, microcapillaries are easier to uniformly modify by established coating procedures[21] allowing the creation of defined polymeric films with embedded catalysts. Microcapillaries are commonly used for performing separations in gas chromatography (GC), open-tubular liquid chromatography (OTLC), and capillary electrophoresis (CE). Therefore it is obvious to directly use catalytically active capillaries as separation capillaries at the same time and perform reactions and analysis in the same analytical device with all the advantages offered by modern analytical instrumentation. Over the past 10 years the investigation of degenerated interconversion processes such as the interconversion of stereoisomers, which is important to study the stereointegrity of drugs,[22] by dynamic chromatography[23–25] has attracted a lot of attention and stimulated the development of advanced reaction chromatographic techniques.

Despite the use of chromatographic separation methods as tools to investigate the course of reactions in detail, chromatographic data and reactions in the course of a chromatographic separation can be used to perform physicochemical measurements, i.e., the application of van Deemter's equation makes the determination of diffusion coefficients of analytes accessible.[26,27] It has to be noted that the original derivation of van Deemter's equation described heat and mass transport in a fixed catalyst bed during regeneration.[28]

Integrating a catalytic activity and separation selectivity into a single separation column offers many advantages. Reactants and products can be separated, and, in case of reversible reactions there is the possibility to shift the chemical equilibrium to the side of the reaction products. Reactions can be studied in great detail, because data collected in the experiments reflect reaction kinetics, chromatographic adsorption as well as parameters of diffusion.[29] According to the theoretical plate model of chromatography, each theoretical plate can be considered as a chemical reactor. If the reaction proceeds only in the catalytically active stationary phase conversions in the gas phase can be neglected (cf. Figure 1). The equilibria in the stationary phase can be distinguished between

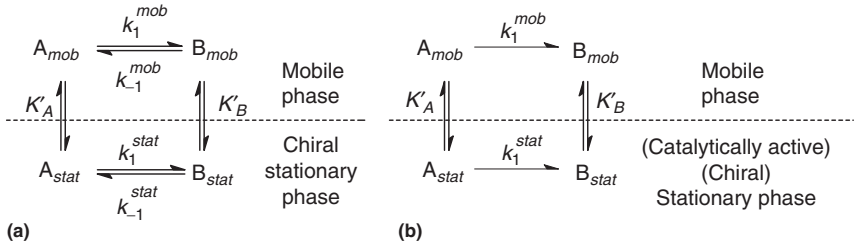


Figure 1 Equilibria in a chromatographic theoretical plate considering (a) reversible reactions (dynamic chromatography) and (b) irreversible reactions taking place in the mobile phase (*mob*) and stationary phase (*stat*). If the reaction proceeds only in presence of a catalyst, the reaction in the mobile phase can be neglected in scheme (b). k_1 and k_{-1} represent the forward and backward reaction rate constants in the mobile phase (*mob*) and stationary phase (*stat*), and *K* denotes the distribution constant.

physisorption (distribution between the gas and stationary phase) and chemisorption (in the stationary liquid phase the distribution of the reactants and products between the dissolved state and the state where the reactant and product form a complex).

The first report on integrating catalysis and chromatographic separation was published by Tamaru in 1959.[30] Palladium was deposited on Celite 545 and used as packing material in GC to study the decomposition of formic acid. Adsorption was investigated by using different carrier gases. It was found that the decomposition of formic acid on Pd^0 is of first-order with respect to formic acid in agreement with the Langmuir–Hinshelwood mechanism.

In 1960, Bassett and Habgood[31] investigated the isomerization of cyclopropane to propylene catalyzed by Linde molecular sieve 13X exchanged with Ni^{2+} ions on a packed column. Cyclopropane was injected as a pulse onto the column and the formation of the product was observed as an extremely broadened peak. Gil-Av and Herzberg-Minzly[32] investigated Diels–Alder reactions by impregnating the stationary phase of the GC column with chloromaleic anhydride and injecting various dienes to form the Diels–Alder product. However, in this approach they were not able to analyze the reaction product to study selectivities, because the product remained on the column. By variation of the contact time and the change of peak area reaction rate constants were determined. Langer et al.[33] extended the concept of chromatographic reactors as well experimentally as theoretically. They investigated very carefully the kinetics of the dissociation of endo-dicyclopentadiene (retro Diels–Alder reaction). Later Marriott et al.[34] investigated the same reaction and compared packed and capillary columns. They found that packed columns with larger diameters were more efficient than using coated capillary columns. In contrast to this, for catalyzed reactions high surface areas are desirable. Therefore using microcapillaries might be contra intuitive, however, the high specific interfacial area per volume is dramatically improved compared with packed columns, and detection sensitivity is improved.

Matsen et al.[35] focused on the investigation of reactions of the type $A \rightleftharpoons B + C$ (decompositions) on a chromatographic column. As example reaction the dehydrogenation of cyclohexane to benzene catalyzed by 0.6% Pt on an alumina support was chosen. The authors reported that under ideal conditions the conversion was 30% higher in the chromatographic reactor than under equilibrium conditions, attributing this difference to a shifting of the chemical equilibrium by the separation of hydrogen from the reaction product. Matsen et al. reported an attempt to modify or replace the stationary phase for the separation to improve the overall efficiency and resolution. They found that the isotherm for benzene adsorbed on fresh alumina was very nonlinear, causing the benzene peak to tail off slowly. Under such conditions the reactor could be pulsed only infrequently, and conversions were no better than for a continuous reactor operating at the same average dilution of cyclohexane by carrier gas. To overcome these problems an alumina was used which had been treated with a solution of 10% KOH in methanol. The treatment neutralized the very strongly acidic sites that were attributed to the nonlinear isotherm. Skrdla[36] investigated the thermal decomposition of *tert*-butyl peroxide in the injector of a GC and on the separation column. Measurements were performed at different temperatures and activation energies were calculated and compared with different kinetic models. It was found that the on-column column reactor approach utilizing peak area measurements (PACR, peak area, column reactor) is far superior in terms of its speed, robustness, and accuracy.

In this chapter, the author focuses on recent breakthroughs combining separation selectivity and catalytic activity in the same stationary phase of a chromatographic separation capillary, which allows tuning selectivities and reaction contact times of the reactants with the catalyst. This strategy overcomes the limitation to investigate only a single reaction in such a setup, because in typical batch reactors and also microreactors competing reactions lead to indefinable reaction kinetics.

9.04.2 Experimental Realization of On-Column Reaction Chromatography

9.04.2.1 Setups of On-Column Reaction Chromatography

Depending on the speed of a chemical transformation, two different approaches can be applied to perform kinetic investigations. The contact time is defined by the migration time of a reactant through the catalytically active column. Therefore, in case of fast reactions or highly active catalysts the catalytically active separation column should be short, otherwise complete conversion is achieved, which is desired in a preparative capillary reactor. The experimental setup consists of a preseparation column of approximately 5 m, a catalytically active separation capillary of a length between 2 and 1000 cm, and a separation column of 25–50 m coated with a suitable (chiral) stationary phase for complete and quantitative analysis (cf. **Figure 2(a)**). The preseparation column has three functions: (1) Thermal equilibration of the reactants, when they are injected into a hot injector, i.e., in GC; (2) separation of reactant libraries, so that no competing reactions occur during the migration through the reactive column; and (3) removal of impurities in the reactants, which is essential to study reactions without interference of impurities that enhance or decrease catalytic activity.

Depending on the properties of the reactant and product and the desired reaction conditions GC, HPLC, or CE can be used and the here described columns installed in these instruments. It is very important to note that the use of internal standards is highly recommended for quantitative analysis of reactants, products and byproducts, and as an analytical tool to recognize, for example on-column polymerizations of reactants, which would lead to a shift in the mass balance.

In such a setup, first-order reactions can be performed, i.e., intramolecular rearrangements, degradation reactions, etc., or pseudo-first-order reactions using a reactive carrier gas in GC, i.e., hydrogenations, or an additive in HPLC or CE. Higher-order reactions can be also performed by first injecting the slower migration reactant, followed by the faster migrating reactant, which will 'overtake' the first injected reactant at a certain point in the capillary. Such experiments have to be very carefully designed to match contact with the catalyst by precise control of the injection sequence.

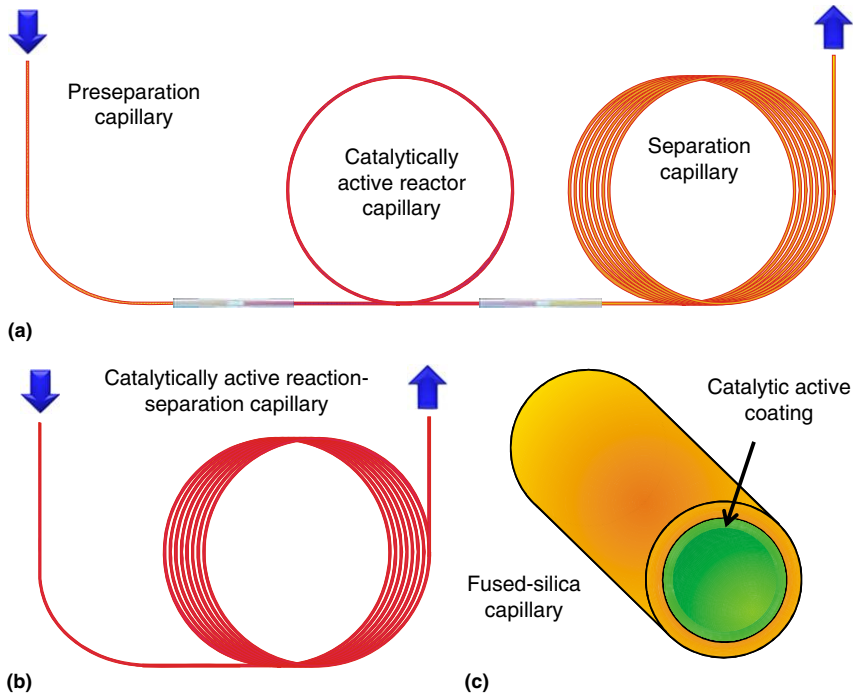


Figure 2 (a) On-column reaction chromatographic setup to investigate fast reactions, where catalytic transformation and separation are sequentially performed. (b) Complete integration of catalytic activity and separation selectivity by dissolving a catalyst in the stationary phase. (c) Schematic cross-section of a fused silica capillary with a homogeneous wall coating of a catalyst in a polymeric stationary phase.

Temperature and flow-dependent measurements are first performed without the catalytically active separation column to determine the migration times of the reactants without any interactions with the catalyst and the stationary phase employed to dissolve or to immobilize the catalyst. In a next step the same dataset is measured using the catalytically active capillary between the preseparation column and the separation column. The difference between the measurements without this capillary and the dataset employing the catalyst capillary gives the contact time Δt of the individual reactant with the catalyst. By integrating the reactant and product the reaction rate constants are directly accessible.

The second approach integrates both, catalytic activity and separation efficiency, by dissolving the catalyst in the stationary phase or immobilizing the catalyst to the stationary phase and using columns that are uniformly coated with the catalytically active stationary phase over the complete capillary length (cf. **Figure 2(b)**). In this case elution profiles are obtained, that are characterized by plateau formation or a more complex convolution of reactant and product. Reaction rate constants can be nowadays very easily determined by application of the unified equation of chromatography (*vide infra*).[37,38]

Both experimental approaches can be coupled with further detectors, i.e., mass spectrometry, to obtain also structural information about formed products and byproducts.

9.04.2.2 Preparation of Capillary Reactors

Catalytically active capillaries can be prepared by static coating,[21] which is an established method to prepare gas chromatographic separation columns. Here, the catalyst and a suitable polysiloxane are dissolved in a volatile solvent, i.e., diethyl ether or dichloromethane, and the capillary is filled, closed and the solvent slowly removed by application of a vacuum to one end of the capillary. The film thickness is defined by the concentration of the polymer and catalyst and the inner diameter of the capillary (cf. **Figure 2(c)**). After solvent removal the capillaries are flushed with N_2 or any other inert gas for several hours. Depending on the stability of the catalyst or activation protocol, the capillaries might be heated over several hours.

Catalysts immobilized to polysiloxanes can be prepared in a similar way. The use of immobilized ligands opens the opportunity to create catalyst libraries, because short pieces of capillaries modified with immobilized ligands can be flushed with suitable metal precursors to produce catalysts inside the capillary. This approach offers the advantage, as with solid-phase chemistry, of using excess of reagents to achieve high conversions, whereas allowing easy removal of unreacted reagents by flushing with solvents. This approach was introduced as 'catalyst by the meter.'[39]

It is recommended that one choose a stationary phase that is compatible with the reaction and catalysts. Typically polysiloxanes allow continuous tuning of solvent properties. In this context it is important to note that all reactions take place in the

liquid stationary phase and therefore reaction rate constants are absolutely comparable to reaction constant determined by reaction progress analysis, where samples are periodically taken from a reactor or vial.

9.04.2.3 High-Throughput Approach

On-column reaction chromatography using catalytically active capillaries enables high-throughput screening by simultaneous injection of a library of reactants to be performed (cf. Figure 3). Because of the chromatographic separation, competing reactions are prevented, making the kinetic analysis of several reactions possible under exactly the same reaction conditions. The synchronous combination of catalysis and separation was demonstrated for hydrogenations over highly active Pd nanoparticles and the ring-closure metathesis over Grubbs second generation catalyst.[40,41] In these studies up to 147 reactions h^{-1} could be performed and analyzed.

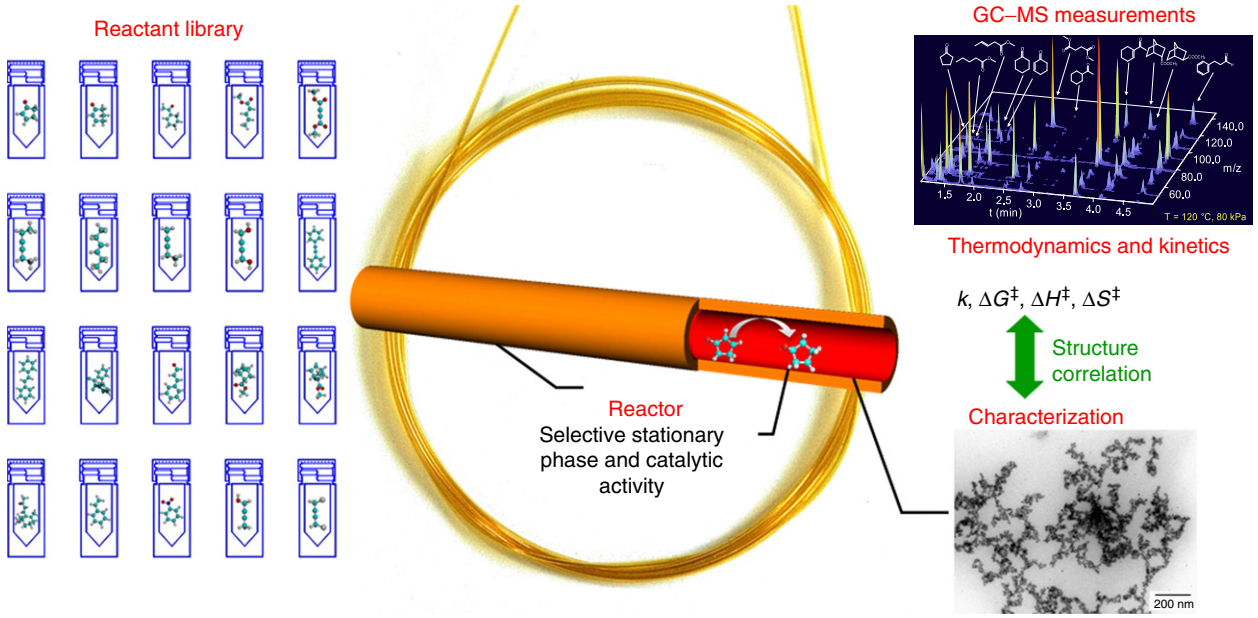


Figure 3 Schematic overview of on-column reaction chromatography. A reactant library is simultaneously injected onto a catalytically active separation column. From the conversions reaction kinetics can be determined.

9.04.3 Determination of Kinetic Data

9.04.3.1 Classical Reaction Kinetics for On-Column Reaction Chromatographic Experiments with Reaction and Consecutive Separation

For experiments where the catalyzed reaction and separation are consecutively performed, evaluation is quite straightforward, because classical approaches can be applied. The conversions are calculated from the integrated peak areas of the chromatograms, considering response factors of the compounds, which can be determined from calibration data. The reaction time is the contact time Δt determined by differential measurements with and without the catalytic capillary.

In the case of a first-order reaction, where the reactant E is converted into the product P, the following equation can be applied to determine the reaction rate constant:

$$[E] = ([P] + [E])e^{-k\Delta t} \tag{1}$$

Any other reaction rate law can be considered in such experiments, which gives the greatest flexibility to investigate catalytic reactions.

9.04.3.2 Evaluation of Conversion Profiles Obtained by On-Column Reaction Chromatography

9.04.3.2.1 Theoretical plate model

The theoretical plate model, which was originally developed to describe a separation process based on partitioning, is the most illustrative model. Here the separation is described by a discontinuous process, assuming that all steps proceed repeatedly in

separate uniform sections of a multicompartmentalized column consisting of N theoretical plates.[42] To integrate a reaction in this model, every theoretical plate is considered as a distinct chemical reactor (cf. Figure 1),[43,44] and three steps are performed in each plate (cf. Figure 4): (1) distribution of the stereoisomers A and B between mobile phase (*mob*) and the stationary liquid phase (*stat*), (2) reversible interconversion the stereoisomers during the residence time $\Delta t = t_M/N$ (hold-up time t_M), and (3) shifting the content of the mobile phase to the subsequent theoretical plate, whereas the content of the stationary phase is retained. In the case of irreversible reactions, i.e., irreversible rearrangements, the reaction scheme is simplified (cf. Figure 1(b)) and for catalyzed reactions the contribution of the reaction in the mobile phase can be neglected.

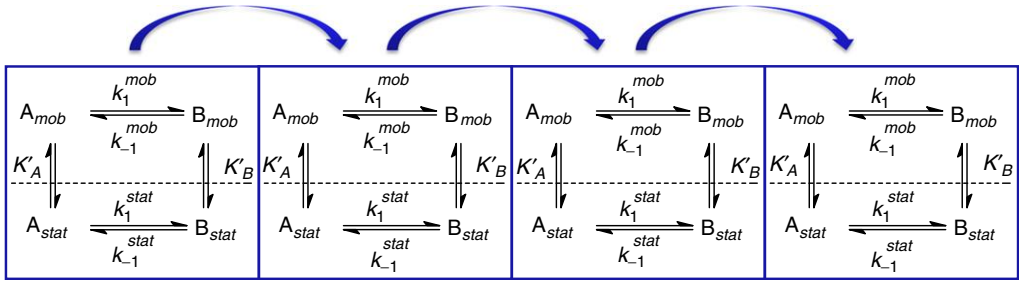


Figure 4 Application of the theoretical plate model of chromatography to evaluate on-column reactions in a chromatographic setup. Every theoretical plate is considered as chemical reactor.

The distribution of the reactant A and product B between mobile phase (*mob*) and the selective stationary phase (*stat*) is determined according to equations 2a and 2b, respectively.

$$A_{mob} = \frac{1}{1 + k'_A}\left(A^{\circ}{}_{mob} + A^{\circ}{}_{stat}\right)$$

$$B_{mob} = \frac{1}{1 + k'_B}\left(B^{\circ}{}_{mob} + B^{\circ}{}_{stat}\right) \tag{2a}$$

$$A_{stat} = \frac{k'_A}{1 + k'_A}\left(A^{\circ}{}_{mob} + A^{\circ}{}_{stat}\right)$$

$$B_{stat} = \frac{k'_B}{1 + k'_B}\left(B^{\circ}{}_{mob} + B^{\circ}{}_{stat}\right) \tag{2b}$$

where A_{mob}, B_{mob}, A_{stat}, B_{stat} are the amounts of the reactant A and product B at the equilibrium, $A^{\circ}{}_{mob}$, $B^{\circ}{}_{mob}$, $A^{\circ}{}_{stat}$, $B^{\circ}{}_{stat}$ are the amounts of A and B before the equilibrium (in the very general case), and k'_A and k'_B are the retention factors of A and B, calculated from the retention time t_R and the hold-up time t_0, determined by methane or regression of the retention times of n-alkanes, according to $k' = (t_R - t_0)/t_0$.

The converted part of the reactant during the residence time $\Delta t = t_0/N$ in the stationary phase and in the mobile phase in a theoretical plate is determined by the respective rate constants. For reversible processes the forward and backward rate constants ${k_1}^{mob}$ and k_{-1}^{mob} in the mobile phase are equal, the equilibrium constant K^{mob} is unity, whereas the equilibrium constant in the chiral stationary phase depends on the two-phase distribution constants (i.e., partition coefficients) K_A and K_B according to the principle of microscopic reversibility:[45]

$$K^{stat} = \frac{k_1^{stat}}{k_{-1}^{stat}} = \frac{K_B}{K_A} = \frac{k'_B}{k'_A} \tag{3}$$

This equation implies that the backward rate constant k_{-1}^{stat} is already determined for given values of k_1^{stat}, k'_A and k'_B and that k_1^{stat} differs from k_{-1}^{stat} when $K_B \neq K_A$. For the conversion of reactants the principle of microscopic reversibility has to be neglected. Typically only apparent rate constants k_1^{app} and k_{-1}^{app}, which represent a weighted mean of the reaction rate constants in the mobile and stationary phase, are experimentally accessible (cf. equation 4). By performing complementary experiments these reaction rate constants can be accessed.

$$k_1^{app} = \frac{1}{1+k'_A}k^{mob} + \frac{k'_A}{1+k'_A}k_1^{stat}$$

$$k_{-1}^{app} = \frac{1}{1+k'_B}k^{mob} + \frac{k'_B}{1+k'_B}k_{-1}^{stat} \tag{4}$$

The reversible first-order kinetics is described by

$$\frac{dx}{dt} = k_1^{app}([A_0] - [X]) - k_{-1}^{app}([B_0] + [X]) \tag{5}$$

where the amount $[X]$ is the change of A and B. Equation 5 is solved by integration, using the initial conditions:

$$[A] = \frac{k_{-1}^{app}}{k_1^{app} + k_{-1}^{app}}([A_0] + [B_0]) + \frac{k_1^{app}[A_0] - k_{-1}^{app}[B_0]}{k_1^{app} + k_{-1}^{app}} e^{-(k_1^{app} + k_{-1}^{app})\Delta t} \tag{6}$$

The amount of $[B]$ is calculated from the mass balance due to $[A_0] + [B_0] = [\mathrm{A}] + [\mathrm{B}]$. After these two steps (partitioning of the present species between mobile phase and stationary phase and undergoing (inter-)conversion) the content of the mobile phase is shifted to the subsequent theoretical plate, whereas the stationary phase is retained. Although the given amount of the enantiomers is initially introduced in the first theoretical plate, the content of the mobile phase of the last theoretical plate is finally recorded as a chromatogram featuring an interconversion profile over the time t.

It should be noted that in the past determination of reaction rate constants from such experiments was extremely time consuming and computationally expensive. However, the theoretical plate model can be easily modified to any type of reaction and allows quick adaption to experimental requirements.

The statistical description of the theoretical plate model leads to the stochastic model,[46] which is based on Gaussian distribution functions of the noninterconverted stereoisomers $\Phi(t)$ and uses a time-dependent probability density function $\Psi(t)$ to describe the conversion profile. Based on the stochastic model a unified equation was derived to access reaction rate constants directly.

9.04.3.2.2 The unified equation of chromatography

Applying the unified equation of chromatography allows reaction rate constants of any first-order reaction to be obtained directly from chromatographic elution profiles without the need of performing reaction progress analysis. This dramatically accelerates the evaluation of temperature-dependent kinetic, as the analysis time no longer limits the rate of measurements. Detailed kinetic data and activation parameters are of great importance to model and predict activities and selectivities by computational methods.

The unified equation of chromatography (equations 7a and 7b) allows the direct calculation of reaction rate constants k_1 and k_{-1} and Gibbs activation energies $\Delta G^{\ddagger}$ for all types of first-order reactions taking place in chromatographic or electrophoretic systems, regardless of the initial concentrations of the reactants A and B and the equilibrium constant $K_{\mathrm{A/B}}$.

A detailed description of the derivation is given in reference 37. Input parameters of the unified equation are the chromatographic parameters obtained from the experiment (cf. Figure 5). If the first eluted peak of the reaction profile is higher than the second eluted peak, equation 7a has to be applied, and in the case that the second peak is higher, equation 7b has to be applied.

$$k_1^{ue} = -\frac{1}{t_R^A}\left(\ln\left(B_0 e^{-\frac{A_\infty}{B_\infty}k_1^{ue}t_R^i}\left(\frac{100e^{-\frac{(t_R^B - t_R^A)^2}{8\sigma_B^2}} - h_p e^{-\frac{(t_R^B - t_R^A)^2}{2\sigma_B^2}}}{\sigma_B\sqrt{2\pi}} - \frac{100}{t_R^B - t_R^A}\right)\right) + \frac{100B_0 + A_0\left(100 - h_p\left(1 + \sqrt{\frac{2}{\pi N}}\right)\right)}{t_R^B - t_R^A}\right) - \ln\left(A_0\left(\frac{h_p - 100e^{-\frac{(t_R^A - t_R^B)^2}{8\sigma_A^2}}}{\sigma_A\sqrt{2\pi}} + \frac{100 - h_p\left(1 + \sqrt{\frac{2}{\pi N}}\right)}{t_R^B - t_R^A}\right)\right)\right) \tag{7a}$$

$$k_1^{ue} = -\frac{1}{t_R^A}\left(\ln\left(\begin{array}{l} B_0 e^{-\frac{A_\infty}{B_\infty}k_1^{ue}t_R^i}\left(\dfrac{100e^{-\frac{(t_R^A-t_R^B)^2}{8\sigma_B^2}}-h_p}{\sigma_B\sqrt{2\pi}}+\dfrac{h_p\left(1-\sqrt{\dfrac{2}{\pi N}}\right)-100}{t_R^B-t_R^A}\right) \\ +\dfrac{100A_0+B_0\left(100-h_p\left(1-\sqrt{\dfrac{2}{\pi N}}\right)\right)}{t_R^B-t_R^A} \end{array}\right) - \ln\left(A_0\left(\frac{h_p e^{-\frac{(t_R^B-t_R^A)^2}{2\sigma_A^2}}-100e^{-\frac{(t_R^B-t_R^A)^2}{8\sigma_A^2}}}{\sigma_A\sqrt{2\pi}}+\frac{100}{t_R^B-t_R^A}\right)\right)\right) \tag{7b}$$

with $\sigma_i = \frac{w_i}{\sqrt{8\ln 2}}$ and $i = \{A, B\}$.

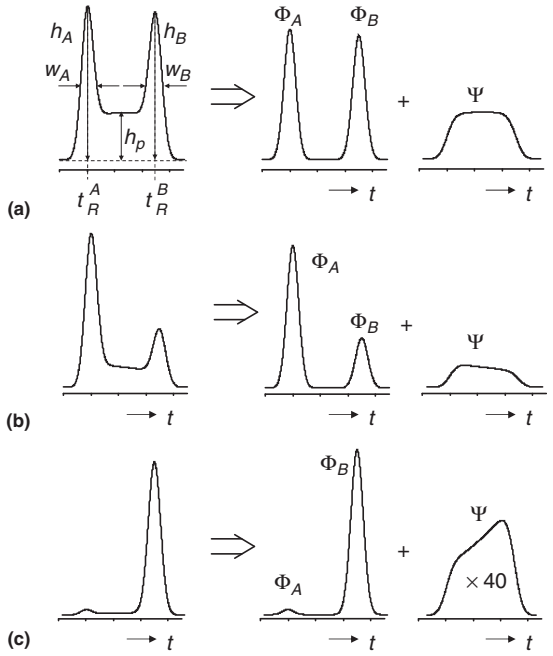


Figure 5 Mathematical separation of dynamic and on-column reaction chromatographic elution profiles into noninterconverted peaks, represented by time-dependent Gaussian distribution functions ΦA(*t*) and ΦB(*t*), and the interconverted part, represented by the stochastic distribution functions Ψ(*t*). (a) Degenerated reversible (pseudo-) first-order reaction with an equilibrium constant $K_{A/B}=1$, (b) reversible (pseudo-) first-order reaction with $K_{A/B}>1$, and (c) reversible (pseudo-) first-order reaction with $K_{A/B}<1$. Reproduced from Trapp, O. *Anal. Chem.* **2006**, *78*, 189–198, with permission from American Chemical Society.

k is the reaction rate constant, h_p is the height of the plateau between the individual peaks at the mean retention time, A_0 and B_0 represent the concentrations of the reactant and product, t_R denotes the retention time of the individual peaks, N is the theoretical plate number and w is the peak width (calculated from the outer parts of the individual peaks if the plateau height is greater than 50%).

9.04.3.3 Determination of Activation Parameters

The Gibbs free activation energy $\Delta G^{\ddagger}(T)$ can be calculated according to the Eyring equation (equation 8) with k_B as the Boltzmann constant ($k_B = 1.380662 \times 10^{-23}\,\mathrm{J \cdot K^{-1}}$), T as the reaction temperature [K], h as Planck's constant ($h = 6.62617 \cdot 10^{-34}\,\mathrm{J \cdot s}$), R as the gas constant ($R = 8.31441\,\mathrm{J\,(Kmol)^{-1}}$). The statistical factor κ is normally unknown and set to 1.0.

$$\Delta G^{+}(T) = -RT\ln\left(\frac{k_1 h}{\kappa k_B T}\right) \tag{8}$$

The activation enthalpy $\Delta H^{\ddagger}$ is then obtained from the slope and the activation entropy $\Delta S^{\ddagger}$ from the intercept of the Eyring plot ($\ln(k_1/T)$ as a function of T^{-1}).

9.04.4 Catalytic Reactions Investigated by On-Column Reaction Chromatography

9.04.4.1 Hydrogenations over Noble Metal Nanoparticles

Catalysts based on nonstabilized noble metal nanoparticles are very difficult to investigate, because agglomeration and change of the catalytic activity can occur during reaction, when these nanoparticles are dissolved in an organic solvent. On-column reaction gas chromatography (ocRGC) can be employed, where the catalysis is performed in a fused silica capillary. To realize this strategy, a catalytically active stationary phase has to be designed, compatible with the chromatographic requirements. Therefore, Pd nanoparticles embedded in an inert polydimethylsiloxane matrix without any interfering protecting shell, i.e., tetraalkylammonium salts as surfactant, were prepared and used in hydrogenations.[40,41] Methylvinylsiloxanedimethylsiloxane copolymer (4.5% Si(O)(CH_3) ($CH{=}CH_2$) groups) is used to coordinate Pd ions to the vinyl groups in diethyl ether. To this mixture hydridomethyldimethylpolysiloxane copolymer (25.7% Si(O)(CH_3)H groups) is added for (1) the reduction of Pd^{2+} to Pd^0 and (2) to crosslink with the methylvinylsiloxanedimethylsiloxane copolymer in a hydrosilylation reaction, catalyzed by Pd, to form a stabilizing matrix (cf. Figure 6).

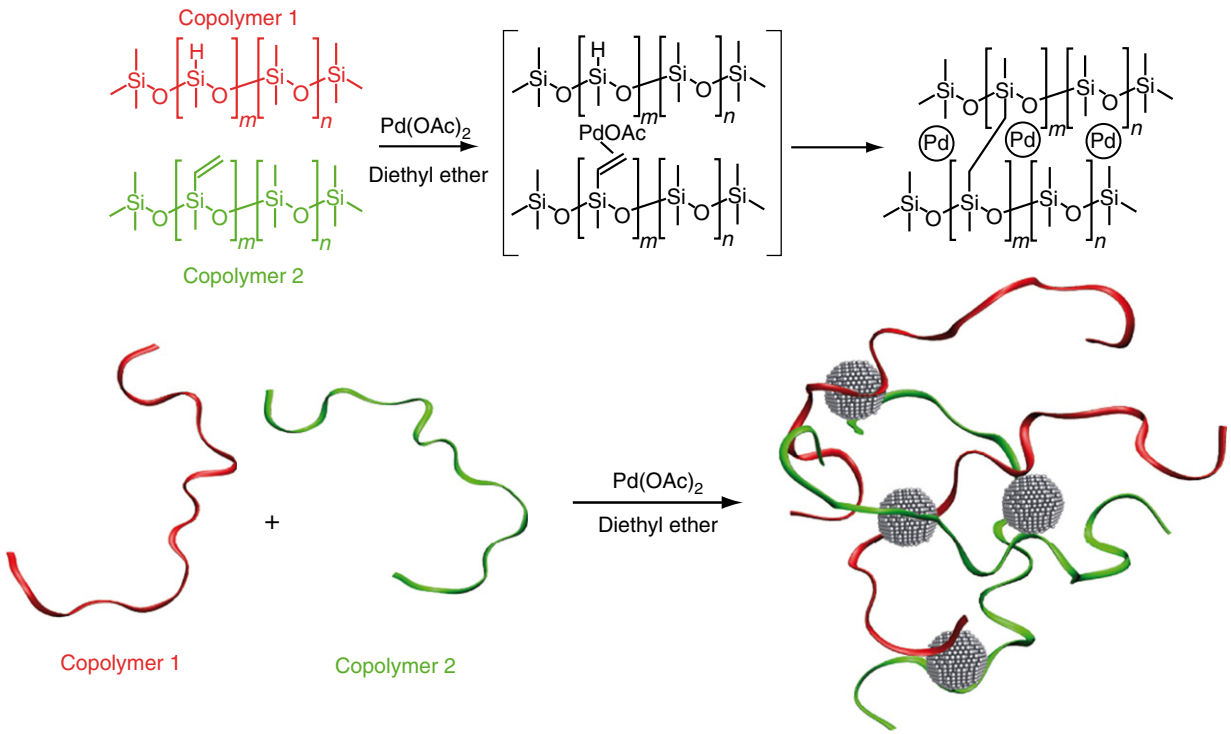


Figure 6 Preparation of highly active Pd nanoparticles embedded in a polysiloxane matrix. Reproduced from Trapp, O.; Weber, S. K.; Bauch, S.; Hofstadt, W. *Angew Chem. Int. Ed.* **2007**, *46*, 7307–7310.

The Pd nanoparticles are spherical and crystalline with a narrow size distribution, determined by transmission electron microscopy (TEM), of 3.2 ± 0.7 nm. The viscous brownish-grey polymers are then coated as a thin film of 0.25 μm onto the inner surface of fused-silica capillaries (i.d. 250 μm) and heated to 180 °C at a temperature rate of 0.5 K min^{-1} under hydrogen flow resulting in a permanently bonded polymer.

In Figure 7, a scanning electron microscopy (SEM) image of the capillary is depicted. SEM and energy dispersive X-ray (EDX) patterning of Si and Pd (16 h measurement) show the fused-silica microcapillary with the Pd/polysiloxane surface coating. The Pd loading is extremely low, only 0.73 ± 10^{-12} mol cm^{-1} capillary.

On-column catalysis is performed by coupling this Pd nanoparticle capillary between a preseparation capillary (1 m) and a separation column (25 m). H_2 is used as reactive carrier gas. Reactants and products are quantified by flame ionization detection

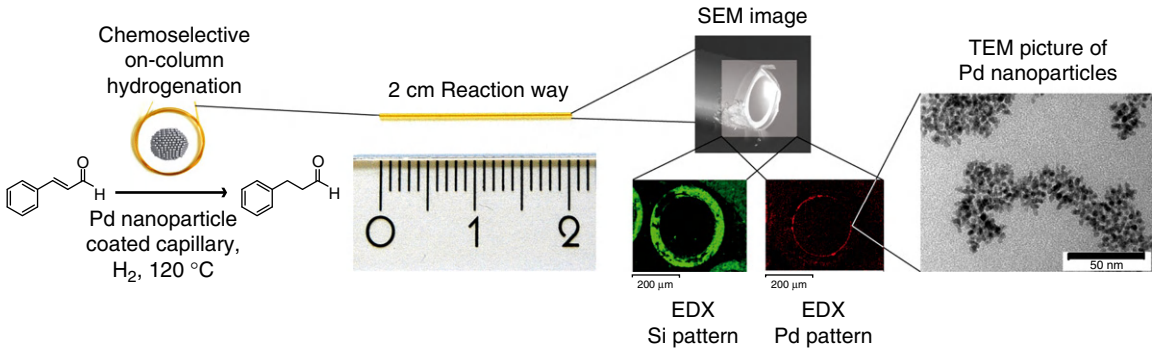
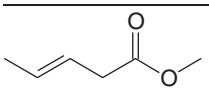
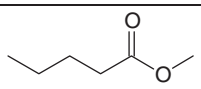
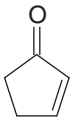
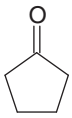
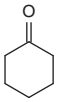
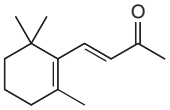
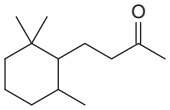
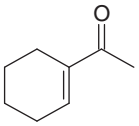
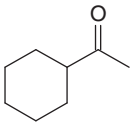
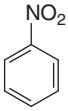
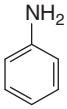


Figure 7 On-column hydrogenation over highly active Pd nanoparticles. Capillaries of only 2 cm coated with Pd nanoparticles stabilized in a polysiloxane matrix are used as reactor. SEM and Si/Pd EDX measurements show the coating of the fused silica microcapillaries (i.d. 250 µm, 0.25 µm film thickness). Reproduced from Trapp, O.; Weber, S. K.; Bauch, S.; Hofstadt, W. *Angew Chem. Int. Ed.* **2007**, *46*, 7307–7310.

(FID) and identified by MS. Reactant libraries consisting of 22 unsaturated compounds (alkenes, alkynes, aromatic hydrocarbons) and functionalized compounds (nitro compounds, aldehydes, ketones) to investigate the chemoselectivity could be simultaneously injected onto this column configuration at different temperatures and gas flows to vary the reaction time and to obtain temperature-dependent kinetic data. These Pd nanoparticles are extraordinarily active and fast hydrogenations lead to complete conversions even for capillaries of only 5 cm length and low temperatures of 60 °C. Therefore, to achieve incomplete conversions for the kinetic measurements all experiments have to be performed with a 2 cm capillary and reaction times in the range of 20 ms to 1 s. Still, for some compounds, i.e., *trans*-cinnamaldehyde, methylbicyclo[2.2.1]hept-5-en-2-carboxylate, dimethylacetylenedicarboxylate, and styrene, 100% conversion for Pd nanoparticles with the highest activity can be observed. Selected experimental data are summarized in Table 1.

Table 1 Selected results of the on-column hydrogenations over highly active Pd nanoparticles

Substrate	*Product*	k[a] (s^{-1})	$\Delta G^{\ddagger}$[b] (kJ mol^{-1})	$\Delta H^{\ddagger}$	$\Delta S^{\ddagger}$ (J $(Kmol)^{-1}$)	r[c] (s.d.)
		194	67.8	30.1 ± 0.5	− 126 ± 3	0.997 (0.057)
		42	70.4	25.2 ± 0.5	− 152 ± 4	0.996 (0.052)
		36	71.4	27.2 ± 0.7	− 148 ± 6	0.996 (0.046)
		4	82.3	56.0 ± 1.0	− 94 ± 2	0.998 (0.020)
		44	73.4	37.5 ± 0.6	− 121 ± 3	0.999 (0.025)
		23	75.3	38.3 ± 1.5	− 124 ± 7	0.985 (0.116)

[a]Reaction rate constant at 120 °C.
[b]Gibbs activation energy $\Delta G^{\ddagger}$ at 25 °C.
[c]Correlation factor *r* and residual standard deviation (*s.d*). of the linear regression of the Eyring plot.

From temperature and flow (contact time) dependent conversion measurements for each compound data sets are obtained which can be put into kinetic models based on a Langmuir–Hinshelwood mechanism to determine reaction rate constants *k* and activation

parameters (Gibbs activation energy $\Delta G^{\ddagger}$, activation enthalpy $\Delta H^{\ddagger}$, and activation entropy $\Delta S^{\ddagger}$). By continuous injection of single educts, i.e., cyclohex-2-enone, onto these columns also preparative hydrogenations in amounts of $\sim 20\ \mathrm{mg\ h^{-1}}$ can be performed.

9.04.4.2 Ring-Closing Metathesis

To prepare catalytically active microcolumns to perform ring-closing metathesis,[40] Grubbs second generation catalyst is dissolved in a dimethylpolysiloxane (GE-SE-30) and a capillary (10 m) with a film thickness of 1 μm under strict exclusion of oxygen is coated. It is very important that the catalyst loading is very low to avoid overly rapid reactions. Here only 1.6 μg catalyst per m ($1.9 \cdot 10^{-9}$ mol $\mathrm{m^{-1}}$) capillary is used. The on-column catalysis is performed by coupling this column with a preseparation column of 1 m. Eluted compounds can be quantified and identified by FID and MS detection. Simultaneous injection of a reactant library consisting of 12 different compounds for ring-closure metathesis onto the catalytically active separation column allowed performing high-throughput kinetic screening of the catalyst. The obtained elution profiles are characterized by a plateau formation between the reactant and the product. The obtained elution profiles can be analyzed by the unified equation to calculate reaction rate constants. The dissociation and chromatographic removal of the tricyclohexylphosphine ligand [$P(Cy)_3$] could not be detected in these experiments which can be explained by the fact that the phosphine ligand is dissolved in the polysiloxane and can stabilize the complex after the reaction. It is remarkable that the catalyst was stable over a wide temperature range up to 150 °C without any detectable degradation of the catalytic activity or leaching. From temperature-dependent measurements activation parameters can be obtained (cf. Figure 8), i.e., for *N*,*N*-diallyltrifluoroacetamide $\Delta G^{\ddagger}(298\ \mathrm{K}) = 84.1\ \mathrm{kJ\ mol^{-1}}$, $\Delta H^{\ddagger} = 15.5 \pm 0.9\ \mathrm{kJ\ mol^{-1}}$, $\Delta S^{\ddagger} = -230 \pm 8\ \mathrm{J/(Kmol)^{-1}}$. By simultaneous injection of the reactant library an extraordinary high throughput in the determination of reaction rate constants of 36 reaction rate constants per hour can be achieved.

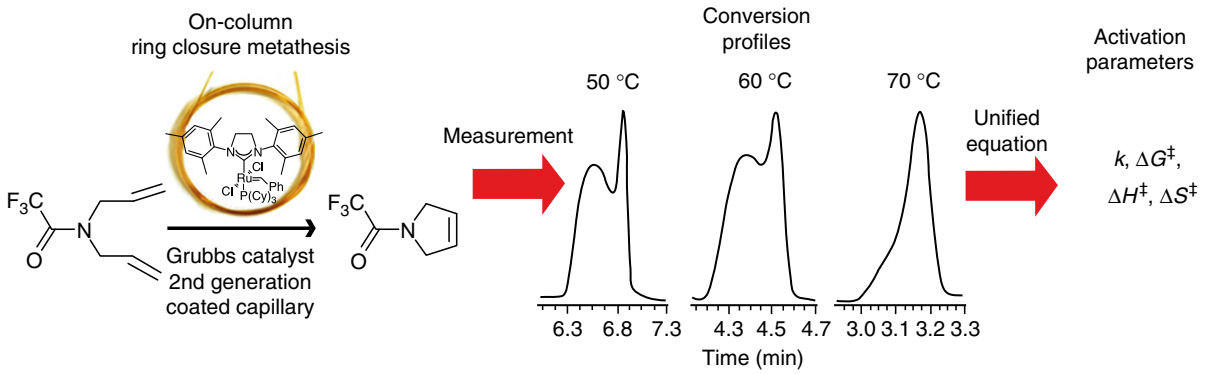


Figure 8 On-column metathesis over Grubbs second generation catalyst. In these experiments catalytic activity and separation selectivity is united in a single 10 m capillary by dissolving the catalyst in the stationary separation phase. Elution profiles are obtained characterized by a pronounced conversion profile from the reactant to the product. Kinetic analysis is directly performed with the unified equation. Reproduced from Trapp, O.; Weber, S. K.; Bauch, S.; Hofstadt, W. *Angew Chem. Int. Ed.* **2007**, *46*, 7307–7310.

Because these catalytically active separation capillaries are easy to handle and to prepare they can be used in a modular design for two-step cascade reactions. Coupling a 80 cm column, coated with the dissolved Grubbs second generation catalyst, and a 10 cm Pd nanoparticle column, followed by a separation column for product analysis a two-step synthesis can be realized. H_2 is used as reactive carrier gas. Ring-closing metathesis of *N*,*N*-diallyltrifluoroacetamide followed by on-column hydrogenation can be achieved in less than 6 min with an overall yield of 49% (cf. Figure 9).

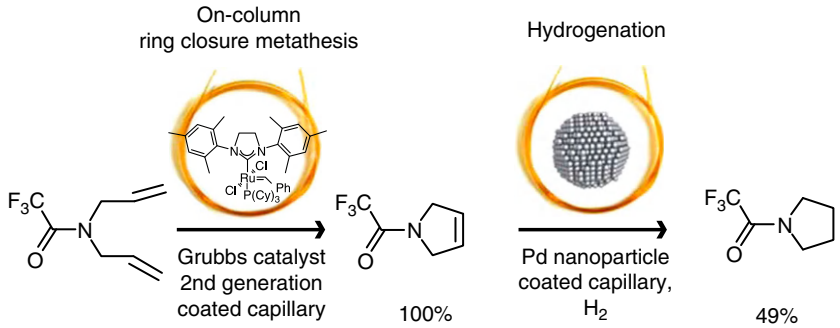
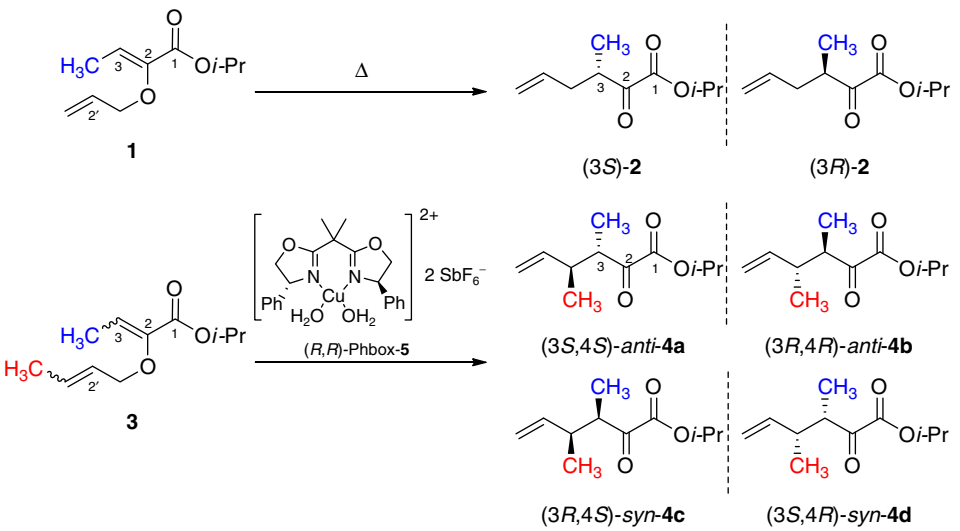


Figure 9 Modular design for a two-step on-column cascade reaction. *N*-Trifluoroacetylpyrrolidine was synthesized within 6 min via coupling an 80 cm metathesis column and a 10 cm Pd nanoparticle hydrogenation column. H_2 was used as reactive carrier gas.

9.04.4.3 Gosteli–Claisen Rearrangement

The feasibility of enantioselective catalysis in on-column reaction chromatography can be exemplified by the Gosteli–Claisen rearrangement of allyl vinyl ethers (cf. Scheme 1).[47]



Scheme 1 Catalytic asymmetric Gosteli–Claisen rearrangement studied by enantioselective on-column reaction GC (ocRGC).

The enantiomers of the α-keto ester **2** (cf. Scheme 1) can be separated with excellent resolution and selectivity by enantioselective GC in presence of the chiral stationary phase (CSP) Chirasil-β-Dex. It was observed that the allyl vinyl ether **1** already undergoes the uncatalyzed Gosteli–Claisen rearrangement during enantioselective GC analysis at moderate temperatures, which is visible by a distinct plateau formation between the peaks of the enantiomers **2** and the starting substrate **1**. The identity of the peaks has been proved by coinjection of substrate **1**, racemic **2**, and by GC–MS analysis, comparing fragmentation patterns of reference spectra. The presence of substrate **1** complicates determination of enantiomeric excesses (*ee*'s) in conventional reaction progress analysis, because of the competing thermal background rearrangement during analysis, which diminishes the true *ee* value, and furthermore influences the enantiomer separation by decreasing the resolution *R*. With increasing separation temperature between 70 °C and 120 °C the plateau formation clearly increases, whereas the time scale of separation and enantioselectivity of the separation decreases (cf. Figure 10).

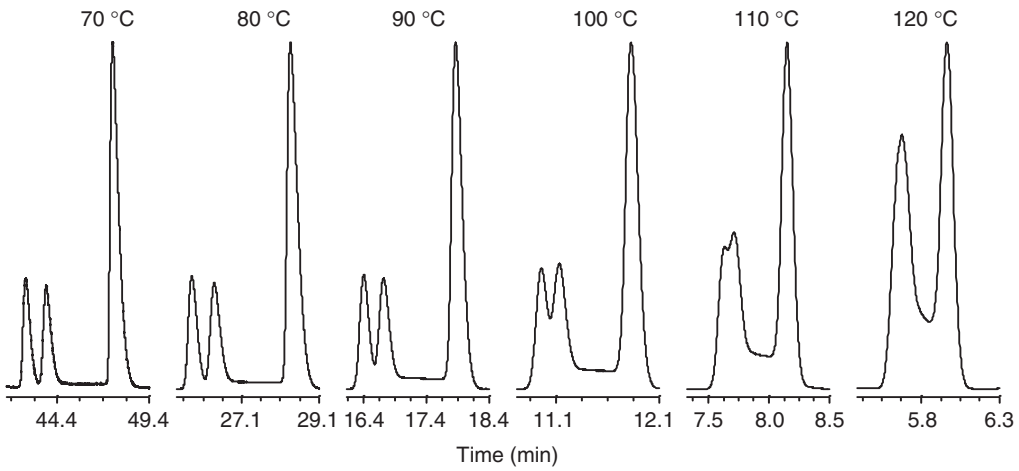


Figure 10 Elution profiles between 70 °C and 120 °C of enantioselective ocRGC of the uncatalyzed Gosteli–Claisen rearrangement of (Z)-**1** (last eluted peak) to (±)-**2** (first two eluted peaks) in the presence of the CSP Chirasil-β-Dex (length 25 m; i.d. 250 μm; film thickness 500 nm). Helium was used as inert carrier gas at 120 kPa inlet pressure. The elution profiles are characterized by a distinct plateau formation indication the conversion of **1** to **2**. Reproduced from Troendlin, J.; Rehbein, J.; Hiersemann, M.; Trapp, O. *J. Am. Chem. Soc.* **2011**, *133*, 16444–16450.

The experiments depicted here can be evaluated using the unified equation (cf. Table 2). An irreversible first-order reaction was considered, because the area under the plateau consists only of racemic compound **2**, which is corroborated by analysis of the GC–MS trace.

Table 2 Summarized results of the uncatalyzed Gosteli–Claisen rearrangement of (*Z*)-1 to (±)-2 obtained by enantioselective ocRGC in presence of the CSP Chirasil-*β*-Dex

Temperature (°C)	h_p *(%)*	*(Z)-**1** (%)*	*(±)-**2** (%)*	N_1	N_2	k_1 *(10^{-4} s^{-1})*	$\Delta G^{\neq}(T)$ *(kJ mol^{-1})*
70.0	1.1	65.7	34.3	1 01 500	24 700	0.14	116.2
80.0	2.0	64.2	35.8	84 100	28 400	0.46	116.3
90.0	3.1	62.7	37.3	58 500	29 300	1.12	117.0
100.0	5.5	60.3	39.7	39 200	27 700	2.85	117.4
110.0	10.3	57.1	43.0	19 200	22 200	6.84	117.9
120.0	21.8	51.8	48.2	6 800	12 500	15.56	118.3

Activation parameters were calculated from temperature-dependent measurements between 70 °C and 120 °C. The activation enthalpy $\Delta H^{\ddagger}$ of the reaction was obtained from the slope and the activation entropy $\Delta S^{\ddagger}$ from the intercept of the Eyring plot ($\ln(k_1/T)$ as a function of T^{-1}) (cf. Figure 11).

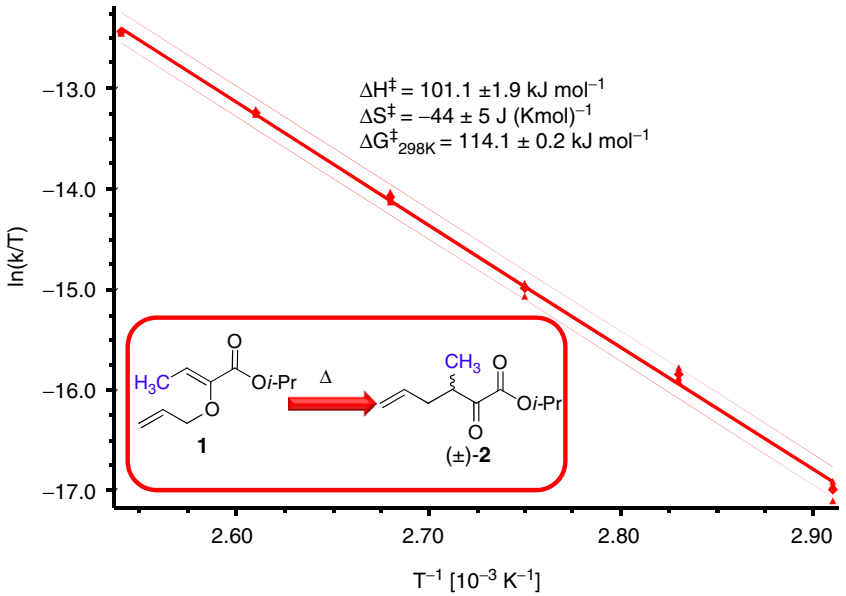


Figure 11 Eyring plot to determine activation parameters of the uncatalyzed Gosteli–Claisen rearrangement of (Z)-**1** to (±)-**2** obtained by temperature-dependent measurements using stereoselective ocRGC between 70 °C and 120 °C.

To extend ocRGC to the catalytic asymmetric Gosteli–Claisen rearrangement, the following experimental setup can be employed. Here, catalytically active separation columns are used as microcapillary reactor and are subsequently coupled with enantioselective separation columns to perform analysis of the reaction products. The inner surface of fused-silica capillaries (i.d. 250 µm) was coated with [Cu{(*R*,*R*)-Ph-box}]$(SbF_6)_2$ (*R*,*R*)-**5** dissolved in an inert polysiloxane matrix and using these capillaries as on-column microreactor in a GC, which allows control of reaction temperatures with high precision. It has to be pointed out that the catalyst [Cu{(*R*,*R*)-Ph-box}]$(SbF_6)_2$ (*R*,*R*)-**5** is completely dissolved in the viscous polysiloxane, representing fully homogeneous reaction conditions. The experimental setup (cf. Figure 12) consists of the catalytically active capillary coupled between a preseparation capillary (GE-SE-30; length 5 m; i.d. 250 µm; film thickness 500 nm) and an enantioselective separation capillary (CSP Chirasil-*β*-Dex; length 25 m; i.d. 250 µm; film thickness 500 nm). The enantioselective separation column separates stereoisomeric reactants and products to determine conversions and selectivities. The suitable temperature range to perform the Gosteli–Claisen rearrangement investigated here and achieving an excellent stereoisomer separation of the reaction products was determined to be between 65 °C and 85 °C.

In order to study the catalytic asymmetric Gosteli–Claisen of (*E*,*Z*)- and (*Z*,*E*)-**3** by ocRGC, these allyl vinyl ethers are injected onto the described capillary arrangement with or without the catalytically active capillary column (cf. Figure 12). *A priori*, the uncatalyzed Gosteli–Claisen rearrangement of either (*E*,*Z*)- or (*Z*,*E*)-**3** may provide a mixture of the four stereoisomers (±)-*anti*- and (±)-*syn*-**4**. Formation of (±)-anti-**4** from (*E*,*Z*)- or (*Z*,*E*)-**3** is energetically favored. In contrast to substrate **1** uncatalyzed formation of the rearrangement product from (*E*,*Z*)- or (*Z*,*E*)-**3** during the time scale of separation is not detectable by highly sensitive MS measurements and no characteristic plateau formation is observable in the applied temperature range.

The reactor capillary with the embedded catalyst (*R*,*R*)-**5** is coupled between the preseparation and enantioselective separation capillary. Using this experimental setup, the diastereo- and enantioselective formation of **4a** from (*E*,*Z*)-**3** and **4b** from (*Z*,*E*)-**3** can

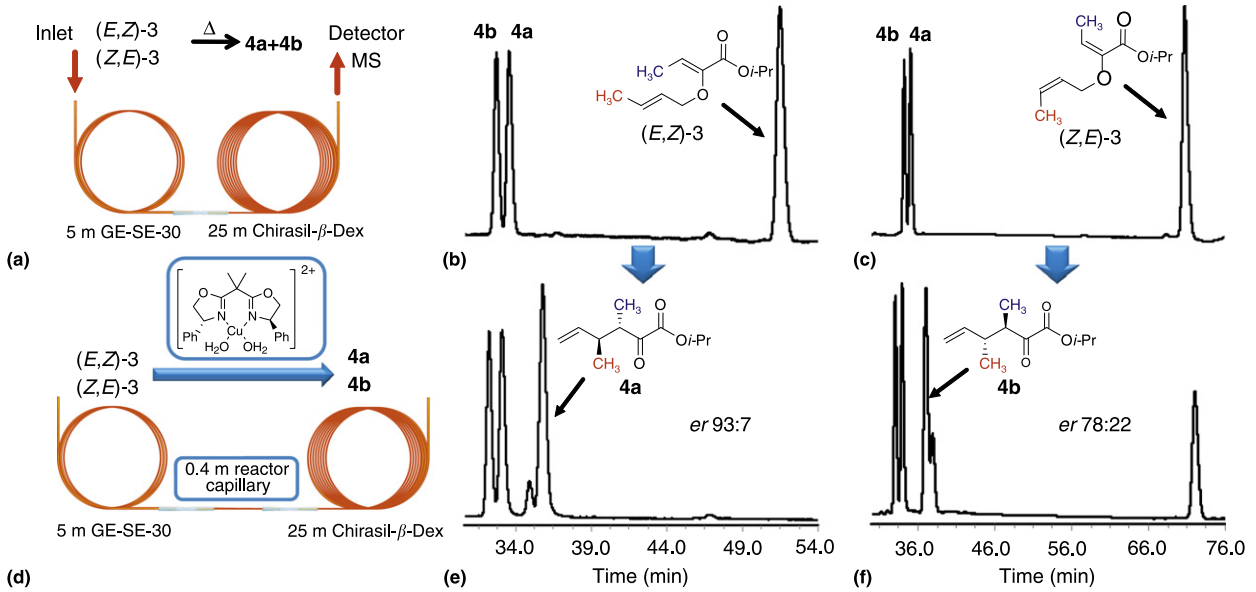


Figure 12 Experimental setup of the stereoselective on-column gas chromatographic experiment to investigate the catalytic asymmetric Gosteli–Claisen rearrangement of (*E*,*Z*)- and (*Z*,*E*)-3 in the presence of the Lewis acid catalyst (*R*,*R*)-5 dissolved in an inert polysiloxane matrix to form the corresponding α-keto isopropyl esters **4a** and **4b**, respectively. (b), (c), (e), and (f) show representative chromatograms of the on-column experiment. Reproduced from Troendlin, J.; Rehbein, J.; Hiersemann, M.; Trapp, O. *J. Am. Chem. Soc.* **2011**, *133*, 16444–16450.

be detected. The advantage of this approach is that the enantiomeric rearrangement products **4a** and **4b**, formed by the uncatalyzed rearrangement in the injector, can be used as internal standard to determine contact times Δt of the reactants and the catalytically active capillary. The enantiomeric products from the catalyzed rearrangement are eluted with a time delay compared with the racemate formed by the uncatalyzed background reaction, because of the separation of the reactants (*E*,*Z*)-**3** and (*Z*,*E*)-**3** from the noncatalytically formed product by the achiral preseparation column. Reaction products **4** show less retention compared with the reactant in presence of the achiral stationary-phase GE-SE-30 and Chirasil-β-Dex.

From these chromatographic data conversions of the individual stereoisomers, *er* values and, consequently, the catalytic activity can be precisely determined.

The embedded catalyst (*R*,*R*)-**5** provides excellent conversions and *er* values for the catalytic asymmetric Gosteli–Claisen rearrangement of (*E*,*Z*)-**3** to **4a** and, notably, the catalyst maintains its activity and selectivity within the investigated temperature range between 65 °C and 85 °C.

To obtain experimental activation parameters $\Delta H^{\ddagger}$ and $\Delta S^{\ddagger}$ of the catalytic asymmetric Gosteli–Claisen rearrangement catalyzed by (*R*,*R*)-**5**, the incomplete conversion of (*Z*,*E*)-**3** to **4a** and **4b** can be investigated by temperature-dependent measurements between 65 °C and 85 °C. Best agreement in the calculation of reaction rate constants can be achieved by application of a pseudo-first-order reaction rate law for parallel reactions, where both pathways yield the enantiomeric reaction products **4a** and **4b**. The Gibbs free activation energies $\Delta G^{\ddagger}(T)$ are calculated according to the Eyring equation. $\Delta G^{\ddagger}$ at 80 °C is 100.2 ± 0.3 kJ mol^{-1} for the rearrangement of (*Z*,*E*)-**3** to the major enantiomer **4b** and 104.2 ± 0.3 kJ mol^{-1} for the rearrangement of (*Z*,*E*)-**3** to the minor enantiomer **4a**. The activation enthalpy $\Delta H^{\ddagger}$ of the reaction is obtained from the slope and the activation entropy $\Delta S^{\ddagger}$ from the intercept of the Eyring plot ($\ln(k/T)$ as a function of T^{-1}) (cf. Figure 13). Rearrangement of (*Z*,*E*)-**3** to **4b** in presence of (*R*,*R*)-**5** gives $\Delta H^{\ddagger} = 106.1 \pm 6.6$ kJ mol^{-1}, $\Delta S^{\ddagger} = 17 \pm 19$ J (Kmol)$^{-1}$, and (*Z*,*E*)-**3** to **4a** gives $\Delta H^{\ddagger} = 106.9 \pm 12.3$ kJ mol^{-1} and $\Delta S^{\ddagger} = 8 \pm 35$ J (Kmol)$^{-1}$. It shoud be pointed out that this approach makes the investigation of single isomeric reactants possible, because even traces of isomers or isomerized reactants are removed by the first separation dimension, which would not make kinetic analysis at high precision feasible.

9.04.4.4 Combinatorial High-Throughput Screening: Catalyst by the Meter

N-Heterocyclic carbenes (NHCs) are highly versatile ligands and are of major focus in the development of highly active catalysts in a broad range of reactions with superior properties in regard to stability and use in various reaction media and conditions. Here a strategy is presented where permanent immobilization of NHC preligands on the inner surface of fused-silica capillaries (i.d. 250 μm) with a defined film thickness (between 50 and 1000 nm) of the polymeric matrix can be used to prepare rapidly NHC-based metal catalysts for high-throughput screening of reactions.

These NHC preligand modified fused-silica capillaries[39] can be converted to NHC ligands and with suitable organometallic precursors to precatalysts utilizing all advantages of solid-phase organic chemistry, i.e., high reagent concentrations, simple removal of nonreacted reagents.

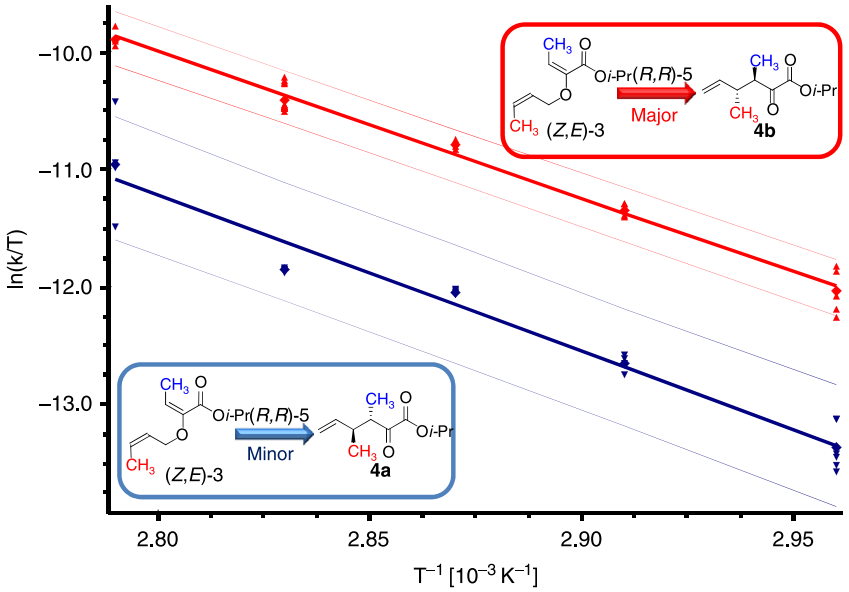
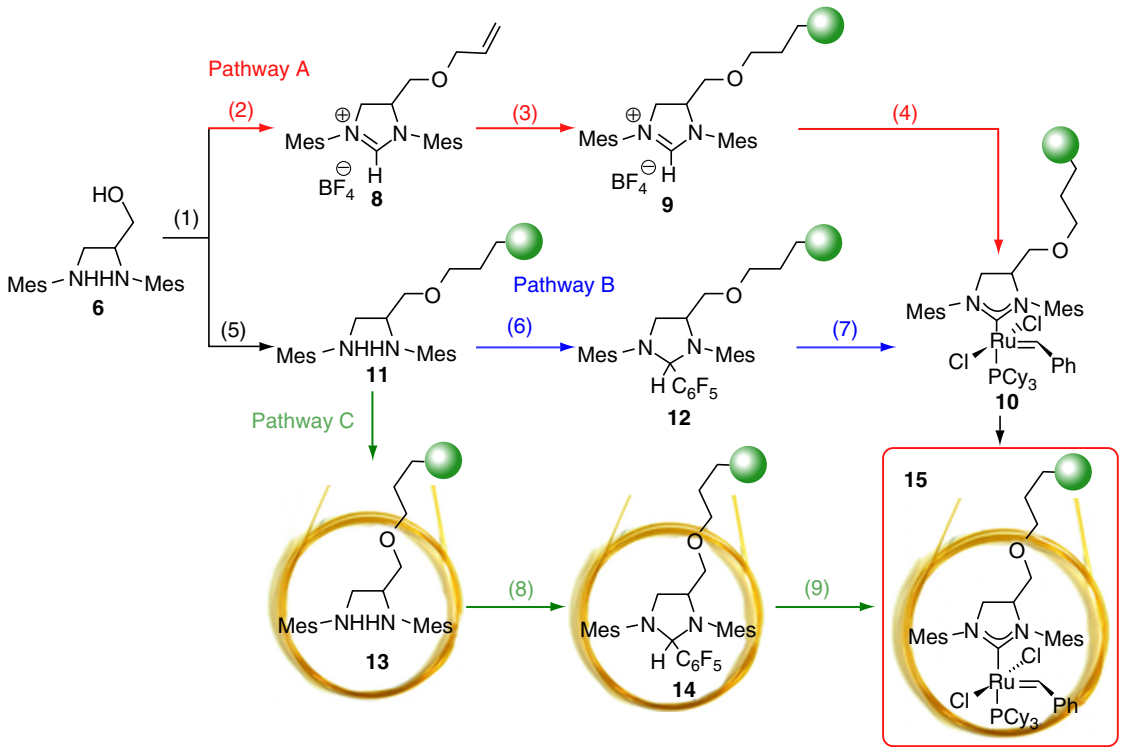


Figure 13 Eyring plot to determine activation parameters of the catalytic asymmetric Gosteli–Claisen rearrangement of (*Z,E*)-3 to **4a** and **4b** obtained by temperature-dependent measurements using stereoselective ocRGC between 65 °C and 85 °C. Reproduced from Troendlin, J.; Rehbein, J.; Hiersemann, M.; Trapp, O. *J. Am. Chem. Soc.* **2011**, *133*, 16444–16450.

To immobilize a 1,3-bismesityl-2-imidazolidinylidene ligand, a similar strategy used by Blechert et al.[48] was used in this study to modify the backbone of the 2-imidazolidinylidene moiety via an ether function, which allows to introduce terminal alkene chains, which can react under benign conditions in a hydrosilylation with hydridopolysiloxanes (cf. Scheme 2).



Scheme 2 (1) 3-Bromo-prop-1-ene, NaH, THF, 24 h, 64 °C. (2) NH_4BF_4, $HC(OEt)_3$. (3) Hydridomethyldimethylpolysiloxane, Karstedt catalyst, THF, ultrasonication for 3 h. (4) KOtBu, THF, rt, 1 h, $(Cy_3P)_2Cl_2Ru(=CHPh)$, toluene, 80 °C, 4 h. (5) Hydridomethyldimethylpolysiloxane, Karstedt catalyst, THF ultrasonication for 3 h. (6) Pentafluorobenzaldehyde, AcOH, 24 h. (7) $(Cy_3P)_2RuCl_2CHPh$, toluene, 80 °C, 4 h. (8) Pentafluorobenzaldehyd AcOH, *n*-pentane, 60 °C. (9) $(Cy_3P)_2RuCl_2CHPh$, *n*-pentane, 60 °C. Reproduced from Lang, C.; Gärtner, U.; Trapp, O. *Chem. Commun.* **2011**, *47*, 391–393, with permission from Royal Society of Chemistry.

Various reaction pathways were studied to prepare capillaries with immobilized NHC ligands. The base-free routes in pathways B and C (cf. Scheme 2) are superior to route A. In pathway B the diamine **7** is first immobilized via hydrosilylation to hydridomethyldimethylpolysiloxane to form polymer **11**. The bonded diamine **11** is then cyclized with pentafluorobenzaldehyde to the immobilized 2-(pentafluorophenyl)imidazolidine **12**. The advantage is that the bonded carbene can be thermally generated, which can be immediately converted to form the bonded Grubbs second generation catalyst **10** by ligand exchange against the tricyclohexylphosphine ligand. Polymeric diamine **11** can be coated onto the inner surface of a fused-silica capillary (i.d. 250 μm) with a film thickness of 250 nm. The polymer film is then immobilized onto the glass surface by heating the capillary to 180 °C. This polymer is highly reactive and is permanently bonded to the glass surface via Si–O–Si bonds. The polymeric diamine **13** is then converted with pentafluorobenzaldehyde to the permanently bonded polymeric 2-(pentafluorophenyl)imidazolidine **14**. Surface modified capillaries **14** are characterized by excellent long-term stability and easy activation to the carbene, to form together with organometallic precursors, NHC ligand-based catalysts by the meter. Heating modified capillaries **14** in a water bath to 60 °C results in the formation of the immobilized free carbene which reacts with Grubbs first generation catalyst by ligand exchange to give permanently bonded polymeric Grubbs second generation catalyst capillary **15**. Permanently bonded polymeric Grubbs second generation catalyst capillaries **15** show some remarkable properties in comparison to Grubbs second generation catalyst dissolved in poly(dimethylsiloxane) and coated onto the inner surface of fused-silica capillaries. These capillaries are moisture and air insensitive, can be installed several times over weeks without any loss of activity or leaching and are stable even at elevated temperatures of 105 °C for several hours.

Figure 14 shows an on-column reaction chromatographic experiments using a 10 cm permanently bonded polymeric Grubbs second generation catalyst capillary to achieve on-column ring-closing metathesis of *N*,*N*-diallyltrifluoroacetamide to *N*-trifluoroacetamide-3-pyrroline at 50 °C and 10 cm permanently bonded polymeric 1,3-bis(2,4,6-trimethylphenyl)imidazol-2-ylidene gold(I) chloride to hydrogenate nitrobenzene to aniline at 95 °C.

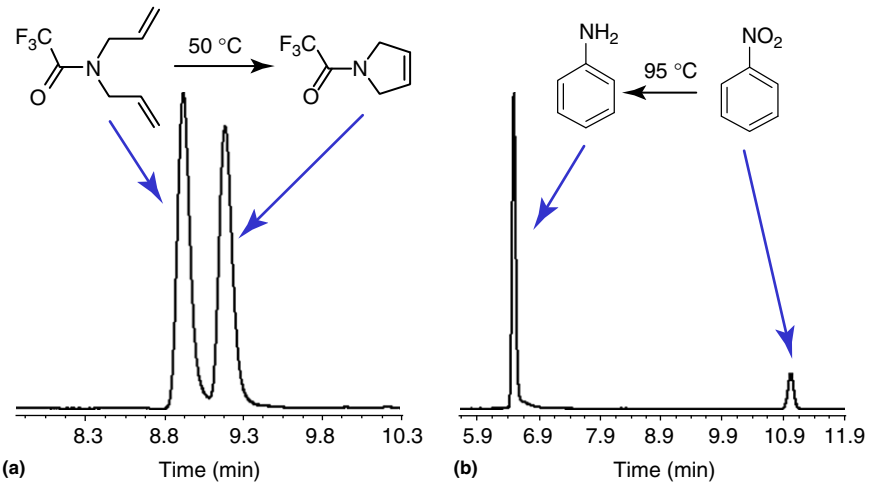


Figure 14 On-column reaction gas chromatographic experiments using (a) a 10 cm permanently bonded polymeric Grubbs second generation catalyst capillary 15 to achieve on-column ring-closing metathesis of *N*,*N*-diallyltrifluoroacetamide to *N*-trifluoroacetamide-3-pyrroline at 50 °C, and (b) a 10 cm permanently bonded polymeric 1,3-bis(2,4,6-trimethylphenyl)imidazol-2-ylidene gold(I) chloride to hydrogenate nitrobenzene to aniline at 95 °C. Reproduced from Lang, C.; Gärtner, U.; Trapp, O. *Chem. Commun.* **2011**, *47*, 391–393, with permission from Royal Society of Chemistry.

9.04.5 Outlook

These strategies for performing catalytic reactions in capillaries can be generally applied, and can be utilized in the comprehensive kinetic characterization of catalysts and materials. Furthermore, it can be envisioned that catalytic capillaries may also be useful for selective transformations in analytical applications for structure elucidation. Moreover, for a preparative scale-up, only a stack of reactor capillaries is necessary to increase the productivity.

These approaches impressively illustrate the (r)evolution of chemist's toolkits from flasks and beakers to miniaturized reactors with highly efficient and selective catalysts inherently combined with separation techniques. These reactors mimic biological systems where reactions efficiently take place at miniaturized interfaces and continuous-flow reactors. Therefore, the development of chemical microplants for the production of fine chemicals can be envisioned as a natural step in terms of energy efficiency and environmental impact.

For related chapters in this Comprehensive, you can refer to – Chapters 9.02, 9.03 and 9.10.

References

1. Falk, T.; Seidel-Morgenstern, A. *Chem. Eng. Sci.* **1999**, *54*, 1479–1485.
2. Vu, T. D.; Seidel-Morgenstern, A.; Grüner, S.; Kienle, A. *Ind. Eng. Chem. Res.* **2005**, *44*, 9565–9574.
3. Haswell, S. J.; Watts, P. *Green Chem.* **2003**, *5*, 240–249.
4. Haswell, S. J.; Skelton, V. *Trends Anal. Chem.* **2000**, *19*, 389–395.
5. Jas, G.; Kirschning, A. *Chem. Eur. J.* **2003**, *9*, 5708–5723.
6. Watts, P.; Haswell, S. J. *Chem. Soc. Rev.* **2005**, *34*, 235–246.
7. Valera, F. E.; Quaranta, M.; Moran, A.; *et al. Angew Chem. Int. Ed.* **2010**, *49*, 2478–2485.
8. Jähnisch, K.; Hessel, V.; Löwe, H.; Baerns, M. *Angew Chem. Int. Ed.* **2004**, *43*, 406–446.
9. Flögel, O.; Codée, J. D. C.; Seebach, D.; Seeberger, P. H. *Angew Chem. Int. Ed.* **2006**, *45*, 7000–7003.
10. Nikbin, N.; Ladlow, M.; Ley, S. V. *Org. Proc. Res. Dev.* **2007**, *11*, 458–462.
11. Bourne, S. L.; Koos, P.; O'Brien, M.; *et al. Synlett* **2011**, *18*, 2643–2647.
12. Knight, J. Honey *Nature* **2002**, *418*, 474–475.
13. Janasek, D.; Franzke, J.; Manz, A. *Nature* **2006**, *442*, 374–380.
14. Haswell, S. J. *Nature* **2006**, *441*, 705.
15. Belder, D. *Anal. Bioanal. Chem.* **2006**, *385*, 416–418.
16. Fritzsche, S.; Ohla, S.; Glaser, P.; *et al. Angew Chem.* **2011**, *123*, 9639–9642.
17. deBellefon, C.; Tanchoux, N.; Caravieilhes, S.; Grenouillet, P.; Hessel, V. *Angew Chem. Int. Ed.* **2000**, *39*, 3442–3445.
18. Sahoo, H. R.; Kralj, J. G.; Jensen, K. F. *Angew Chem. Int. Ed.* **2007**, *46*, 5704–5708.
19. Noel, T.; Kuhn, S.; Musacchio, A. J.; Jensen, K. F.; Buchwald, S. L. *Angew Chem.* **2011**, *123*, 6065–6068.
20. Kobayashi, J.; Mori, Y.; Okamoto, K.; *et al. Science* **2004**, *304*, 1305–1308.
21. Grob, K. *Making and Manipulating Capillary Columns for Gas Chromatography*; Huethig: Heidelberg, **1986**; pp 1–232.
22. Schoetz, G.; Trapp, O.; Schurig, V. *Electrophoresis* **2001**, *22*, 3185–3190.
23. Trapp, O.; Schoetz, G.; Schurig, V. *Chirality* **2001**; 13403–414.
24. Wolf, C. *Dynamic Stereochemistry of Chiral Compounds – Principles and Applications*; RSC Publishing: Cambridge, **2008**.
25. Trapp, O. *Electrophoresis* **2010**, *31*, 786–813.
26. Purnell, J. H. *Nature* **1955**, *175*, 2009.
27. Van Deemter, J. J.; Zuiderweg, F. J.; Klinkenberg, A. *Chem. Eng. Sci.* **1956**, *5*, 271–289.
28. Van Deemter, J. J. *J. Ind. Eng. Chem.* **1953**, *45*, 1227–1233.
29. Katsanos, N. A.; Thede, R.; Roubani-Kalantzopoulou, F. *J. Chromatogr. A* **1998**, *795*, 133–184.
30. Tamaru, K. *Nature* **1959**, *183*, 319–320.
31. Bassett, D. W.; Habgood, H. W. *J. Phys. Chem.* **1960**, *64*, 769–773.
32. Gil-Av, E.; Herzberg-Minzly, Y. *Proc. Chem. Soc.* **1961**, 316.
33. Pratt, G. L.; Langer, S. H. *J. Phys. Chem.* **1969**, *73*, 2095–2097.
34. Marriott, P. J.; Lai, Y. H. *Inorg. Chem.* **1986**, *25*, 3680–3683.
35. Matsen, J. M.; Harding, J. W.; Magee, E. M. *J. Phys. Chem.* **1965**, *69*, 522–527.
36. Skrdla, P. J. *Int. J. Chem. Kinet.* **2004**, *36*, 386–393.
37. Trapp, O. *Anal. Chem.* **2006**, *78*, 189–198.
38. Trapp, O. *Electrophoresis* **2006**, *27*, 534–541.
39. Lang, C.; Gärtner, U.; Trapp, O. *Chem. Commun.* **2011**, *47*, 391–393.
40. Trapp, O.; Weber, S. K.; Bauch, S.; Hofstadt, W. *Angew Chem. Int. Ed.* **2007**, *46*, 7307–7310.
41. Trapp, O.; Weber, S. K.; Bauch, S.; *et al. Chem. Eur. J.* **2008**, *14*, 4657–4666.
42. Craig, L. C. *J. Biol. Chem.* **1944**, *155*, 519–534.
43. Martin, A. J. P.; Synge, R. L. M. *Biochem. J.* **1941**, *35*, 1358–1368.
44. Kallen, J.; Heilbronner, E. *Helv. Chim. Acta* **1960**, *43*, 489–500.
45. Bürkle, W.; Karfunkel, H.; Schurig, V. *J. Chromatogr.* **1984**, *288*, 1–14.
46. Trapp, O.; Schurig, V. *Comput. Chem.* **2001**, *25*, 187–195.
47. Troendlin, J.; Rehbein, J.; Hiersemann, M.; Trapp, O. *J. Am. Chem. Soc.* **2011**, *133*, 16444–16450.
48. Schürer, S. C.; Gessler, S.; Buschmann, N.; Blechert, S. *Angew Chem. Int. Ed.* **2000**, *39*, 3898–3901.

9.05 Technology-Enabled Synthesis of Carbohydrates

NL Snyder, Davidson College, Davidson, NC, USA
PH Seeberger, Max Planck Institute for Colloids and Interfaces, Berlin, DE, Germany
GT Mukosera and EMK Held, Davidson College, Davidson, NC, USA

© 2014 Elsevier Ltd. All rights reserved.

9.05.1	**Introduction**	112
9.05.2	**Principles of Automated Oligosaccharide Synthesis**	113
9.05.3	**Automation Platforms**	113
9.05.3.1	First-Generation Automated Solid-Phase Oligosaccharide Synthesizer: Modified ABI 433 Peptide Synthesizer for Automated Oligosaccharide Synthesis	113
9.05.3.2	Second-Generation Automated Solid-Phase Oligosaccharide Synthesizer: The First Fully Automated Oligosaccharide Synthesizer	115
9.05.3.3	HPLC-Based Automated Oligosaccharide Synthesizer Platform	115
9.05.4	**Solid Support**	115
9.05.4.1	Merrifield Resin	116
9.05.4.2	TentaGel	116
9.05.5	**Linker**	116
9.05.5.1	Alkene–Diol Linkers	117
9.05.5.2	Bifunctional Linker	117
9.05.5.3	Succinamic Linker	117
9.05.6	**Building Blocks**	117
9.05.6.1	Anomeric Leaving Group	118
9.05.6.2	The C2 Position	123
9.05.6.3	Temporary Protecting Groups	123
9.05.6.4	Permanent Protecting Groups	124
9.05.6.5	Monosaccharide Reactivity	125
9.05.7	**Automated Synthesis of Oligosaccharides**	125
9.05.7.1	α-Mannans and a Phytoalexin β-Glucan	126
9.05.7.2	Leishmania Cap Tetrasaccharide	128
9.05.7.3	Malaria Vaccine Tetrasaccharide	128
9.05.7.4	Oligoglucosamines	128
9.05.7.5	Core *N*-linked Glycan	131
9.05.7.6	Gb-3 and Globo-H	132
9.05.7.7	Blood Group Antigens	135
9.05.7.8	Oligoglucose	135
9.05.7.9	Hyaluronan Oligosaccharides	139
9.05.7.10	β-Mannuronic Acids Alginates	139
9.05.7.10.1	Oligoarabinofuranosides	139
9.05.8	**Conclusion**	141
References		141

Glossary

Anchimeric effect The interaction of a reaction center with a lone pair of electrons from another atom or the electrons of a sigma or pi bond; the anchimeric effect is also known as neighboring group participation.

Anomeric effect A stereoelectronic effect that describes the tendency of heteroatomic substituents adjacent to a heteroatom within a cyclohexane ring to prefer the axial orientation instead of the less hindered equatorial orientation.

Glycoconjugate Mono-, di-, or oligosaccharide that is covalently bound to a molecule, often a peptide, protein, or lipid.

Glycosidic bond Covalent bond formed between the hemiacetal group of a mono-, di-, or oligosaccharide and the hydroxyl group of another molecule.

Glycosyl acceptor Mono-, di-, or oligosaccharide that serves as a nucleophile in a glycosylation reaction.

Glycosyl donor Mono-, di-, or oligosaccharide that serves as an electrophile in a glycosylation reaction; the glycosyl donor generally determines the nature of the glycosidic linkage.

Glycosylation reaction Reaction between glycosyl donor and a glycosyl acceptor that results in a glycosidic bond.

Monosaccharide A single sugar residue.

Oligosaccharide Multiple sugar residues connected via glycosidic bonds.

9.05.1 Introduction

Nucleic acids, proteins, and glycoconjugates play critical roles in a number of important signal transduction pathways. The development of rapid and efficient automated platforms for the synthesis of nucleic acids and peptides from their monomeric building blocks (Figure 1 (a) and (b)) has led to a better understanding of the fundamental interactions these biomolecules play in important biological processes. As a result, the fields of genomics and proteomics have grown exponentially with the development of new therapeutic strategies for disease prevention and treatment. Until recently, the lack of a general and accessible approach for the construction of oligosaccharides meant that only specialized research laboratories were capable of accessing defined glycoconjugates. This has slowed the pace of research in this area and in turn, our understanding of the diverse roles of these compounds in nature.

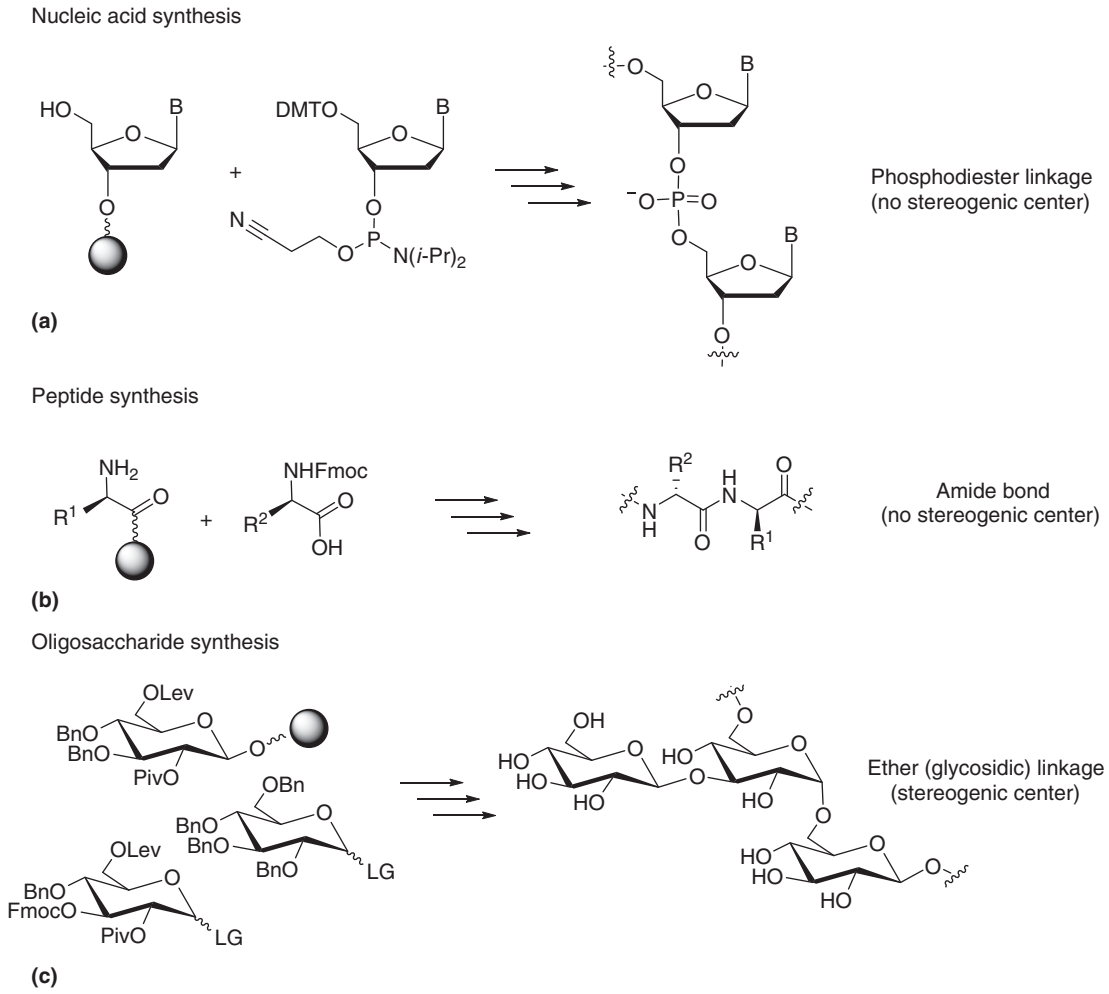


Figure 1 Oligonucleotide (a), peptide (b) and glycoconjugate (c) synthesis.

The major challenge with developing a general and accessible approach for the synthesis of oligosaccharides is inherent in the reaction products. The linear phosphodiester and amide bond linkages required for nucleic acid and peptide synthesis are easier to generate because the individual building blocks lack significant steric hindrance and the newly formed bonds are nonstereogenic. In contrast, the synthesis of oligosaccharides, which can be linear or branched, often involves more sterically encumbered building blocks and the newly formed bond is part of a stereogenic center. In order to be useful the reaction must generate the desired linkage with high selectivity.

The development of a first-generation automated solid-phase oligosaccharide synthesizer by Seeberger and coworkers[1] led to the first reported automated synthesis of three linear 1,2-α-linked mannan oligosaccharides and a branched phytoalexin elicitor β-glucan (Figure 2). The synthesis of these glycoconjugates, which play important roles in the immune response to pathogenic fungi such as *Candida albicans*,[2] began what would become a new chapter in the preparation of glycoconjugates for biological evaluation. Since then, automation has proven to be vastly beneficial. Additional bacterial antigens, cancer antigens, vaccine

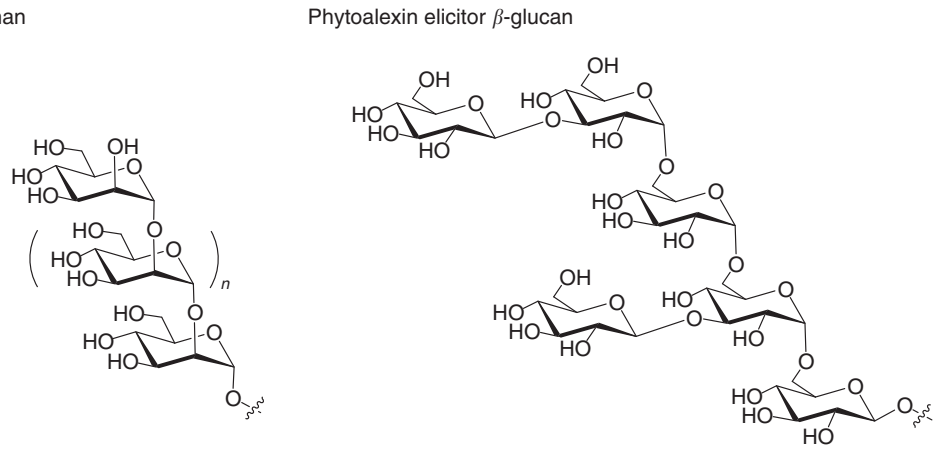


Figure 2 First oligosaccharides synthesized via automated solid-phase oligosaccharide synthesis.

candidates, and *N*-linked core oligosaccharides are just a few of the glycoconjugates that have been rapidly synthesized using automation. Moreover, these glycoconjugates have been synthesized on scales that would have been impossible using standard solution-phase synthetic techniques.

The goal of this chapter is to review the historical aspects of solid-phase oligosaccharide synthesis as well as recent developments including engineering advancements that have recently led to the design of a fully automated platform, and new and improved chemistries that have broadened the scope of the reactions that can be used in automation. The automated solid-phase synthesis of several carbohydrate constructs including bacterial and viral antigens, cancer antigens, vaccine candidates, and *N*-linked core oligosaccharides is also presented.

9.05.2 Principles of Automated Oligosaccharide Synthesis

Automated solid-phase oligosaccharide synthesis uses an automated synthesizer to make glycosidic linkages in an analogous process to the way DNA synthesizers generate phosphodiester linkages and peptide synthesizers generate peptide linkages. The general process is illustrated in **Figure 3**. Selectively functionalized monosaccharide building blocks containing temporary and permanent protecting groups (commonly referred to as donors) serve as electrophiles and are added sequentially to a growing oligosaccharide chain, which serves as a nucleophile (or acceptor). The acceptor is connected via an inert linker to a solid support that is generally insoluble in organic solvents. Each glycosidic linkage is made by activating the appropriately functionalized monosaccharide building block (donor) in the presence of the growing nucleophilic oligosaccharide (acceptor) to couple to the two molecules. After each glycosylation reaction, the growing oligosaccharide is washed, the appropriate temporary protecting groups are removed to expose the next functional group for coupling, and the process is repeated until the desired oligosaccharide has been synthesized. The oligosaccharide is then removed from the solid support, purified if necessary, and the remaining temporary and permanent protecting groups are removed. The oligosaccharide can then be functionalized for further study.

The key features of the automated process, shown in **Figure 4**, include the automation platform, an insoluble solid support, an inert linker, and selectively functionalized carbohydrate building blocks containing temporary and permanent protecting groups. Developments in each of these areas have had a significant impact on the evolution of automated solid-phase oligosaccharide synthesis.

9.05.3 Automation Platforms

9.05.3.1 First-Generation Automated Solid-Phase Oligosaccharide Synthesizer: Modified ABI 433 Peptide Synthesizer for Automated Oligosaccharide Synthesis

The first automated synthetic platform for automated solid-phase oligosaccharide synthesis was developed by Seeberger and coworkers[1] and based on a modified Applied Biosystems peptide synthesizer, the ABI 433. This system was chosen as a prototype because it was affordable and commercially available, it could accommodate up to nine different reagents/building blocks at one time, and required minimal modifications, namely a custom made jacketed reaction vessel connected to a variable cryostat to allow for controlled cooling of the reaction mixture.

As a prototype, the ABI synthesizer played a critical role in the development of automated oligosaccharide synthesis. The synthesizer was reliable, and solvent delivery and waste removal were relatively efficient. In addition, reaction mixing, which was

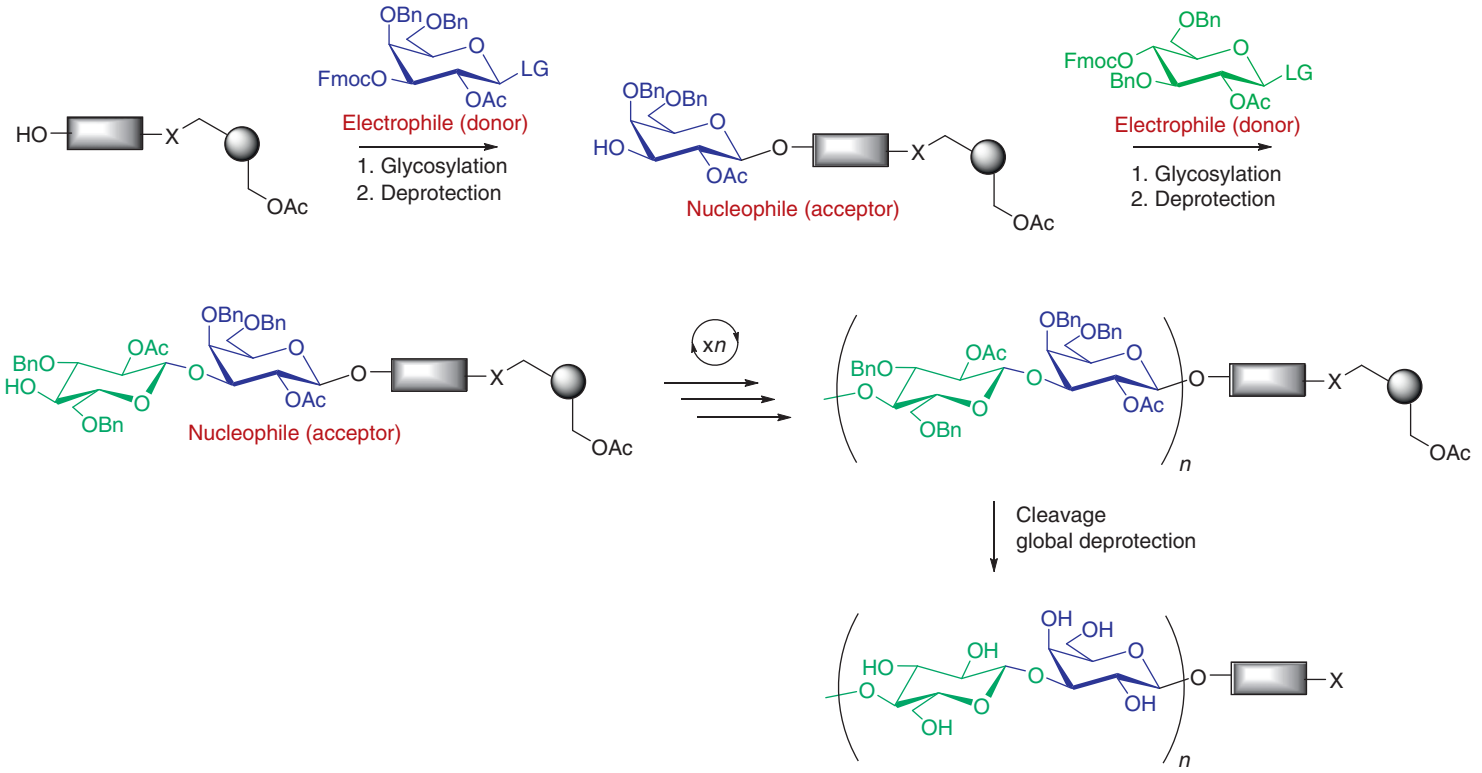


Figure 3 Automated solid-phase oligosaccharide synthesis.

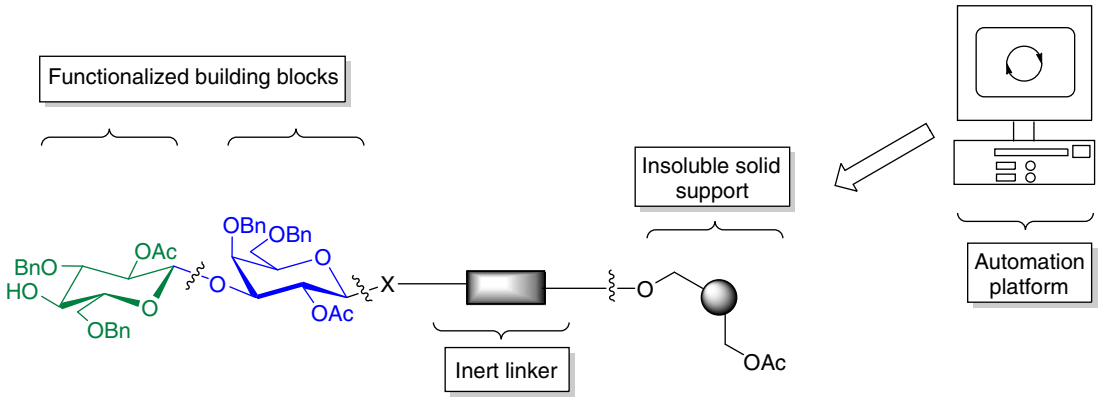


Figure 4 Key features of automated solid-phase oligosaccharide synthesis.

achieved by agitation of the reaction vessel, was effective in producing a uniform heterogeneous solution. However, the instrument, which was designed for peptide synthesis, had several shortcomings. Reagent delivery, which was achieved via solenoid valves, was imprecise. Therefore, the delivery of small reagent volumes or the delivery of reagents at a controlled delivery rate was difficult to achieve. In addition, the system could not be modified to accommodate additional reagents limiting the number of different glycosylation reactions that could be performed in a single run. Finally, temperature control required manual adjustment of the cryostat therefore, necessitating the continuous presence of an operator. For these reasons, the Seeberger group focused their efforts on the development of a new fully automated solid-phase oligosaccharide synthesizer.

9.05.3.2 Second-Generation Automated Solid-Phase Oligosaccharide Synthesizer: The First Fully Automated Oligosaccharide Synthesizer

In order to provide a more efficient platform for automated solid-phase oligosaccharide synthesis, Seeberger and coworkers collaborated with Ancora Pharmaceuticals to develop the first fully automated solid-phase oligosaccharide synthesizer.[3] The new design, introduced in 2012, addressed the shortcomings of the modified ABI 433 peptide synthesizer. Syringe pump technology for precise reagent delivery was combined with solenoid valves for rapid pressure-driven washing steps. The system also included 16 vessels capable of delivering up to 16 reagents building blocks at one time. In addition, a mechanical controller was designed to serve as an interface between the instrument and a personal computer, which provided full control of the system including temperature modulation. The instrument is capable of reaching temperatures as low as $-50\ ^{\circ}C$ via adjustable cryostat and as high as $90\ ^{\circ}C$ via heating block.

9.05.3.3 HPLC-Based Automated Oligosaccharide Synthesizer Platform

Demchenko and co-workers recently reported on the first modified HPLC for automated solid-phase oligosaccharide synthesis.[4] Their experimental setup, which includes an unmodified three-headed pump HPLC system and an onboard variable range UV detector, uses a standard chromatography column packed with preswelled polymer resin. The benefit of this system is that it employs a commercially available HPLC found in almost any synthetic or analytical laboratory, and the programming can be accomplished using standard HPLC operating software.

Demchenko's HPLC-based solid-phase oligosaccharide synthesizer is the first automated system that uses real-time UV-Vis reaction monitoring and shows significant promise as an emerging technology. However, one significant disadvantage is the limited number of reagents/building blocks the system can accommodate without significant modification or the continuous presence of an operator.

9.05.4 Solid Support

Commercially available nonsoluble polystyrene solid supports such as Merrifield resin and TentaGel (Figure 5) are most commonly employed in automated solid-phase oligosaccharide synthesis. These resins generally exhibit high loading, are chemically inert to most of the reaction conditions required for glycosylation, and can be easily filtered from the reaction solution. The only disadvantage is that they require swelling to expose the reactive sites of the resin. Incomplete swelling can lead to incomplete reactions and deletion sequences. Controlled pore glass (CPG), which is a rigid, mechanically robust material that does not shrink or swell in the presence of solvents, has been used with high success for the synthesis of oligonucleotides; however, it has not attracted much attention for automated oligosaccharides synthesis for two major reasons. First, CPG loading, which is

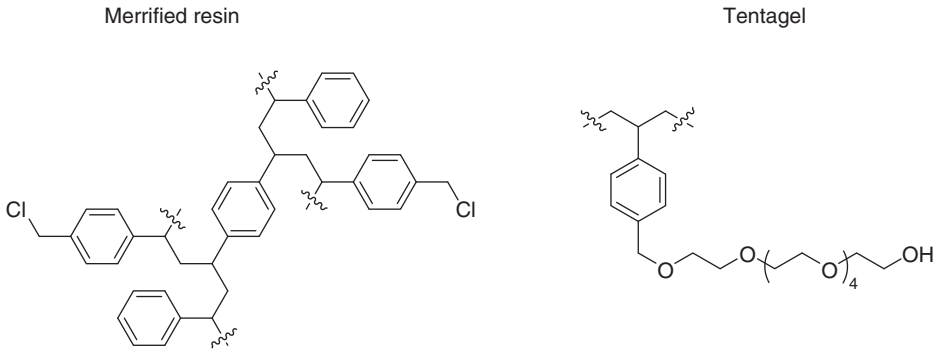


Figure 5 Nonsoluble solid supports used in automated solid-phase oligosaccharide synthesis.

approximately 0.02–0.03 mmol g^{-1}, is generally lower than Merrifield and Tentagel (0.30–0.40 mmol g^{-1}). Second, the growing oligosaccharide has been shown to eventually block the glass pores reducing diffusion of the reagents to the reactive sites. CPG with larger pore sizes has been used with some success, although the resin tends to be significantly more fragile.

9.05.4.1 Merrifield Resin

The majority of the automated solid-phase oligosaccharide syntheses reported to date have made use of Merrifield resin,[5] a chloromethylated polystyrene resin that has been widely employed in peptide synthesis. In addition to high loading, Merrifield resin is relatively inert under the acidic and basic conditions used in the automation process. One significant disadvantage in comparison to the CPG used in DNA synthesis is the number of washing steps required to completely remove excess reagents and byproducts from the porous polystyrene matrix. In addition, the reactive sites of the resin are only exposed in the presence of a swelling solvents such as dichloromethane, tetrahydrofuran, and toluene, prohibiting the use of nonswelling solvents such as hexane and methanol.

9.05.4.2 TentaGel

TentaGel[6] has also been used in the automated solid-phase synthesis of oligosaccharides. TentaGel consists of polyethylene glycol cross-linked to polystyrene via an ether linkage. Tentagel combines the benefits of a soluble polyethylene glycol support with the insolubility and handling characteristics of a polystyrene bead. TentaGel also displays relatively uniform swelling in a variety of solvents from medium to high polarity ranging from toluene to water. One significant disadvantage in comparison to Merrifield resin is that the hydrophilic nature of the resin can make the removal of residual water difficult, leading to reduced yields during glycosylation.

9.05.5 Linker

The linker connects the first unit of the growing oligosaccharide chain to the solid support. To be effective the linker must remain intact during synthesis, and be selectively cleavable under relatively mild conditions at the end of the synthesis. Optimally, the cleaved linker should have a functional handle for attachment to a protein carrier, chip, or other surface. To date, four linkers have been commonly employed in automated oligosaccharide synthesis (Figure 6): alkene–diol (octenediol or butenediol) linkers, a bifunctional linker, and a succinamic linker.

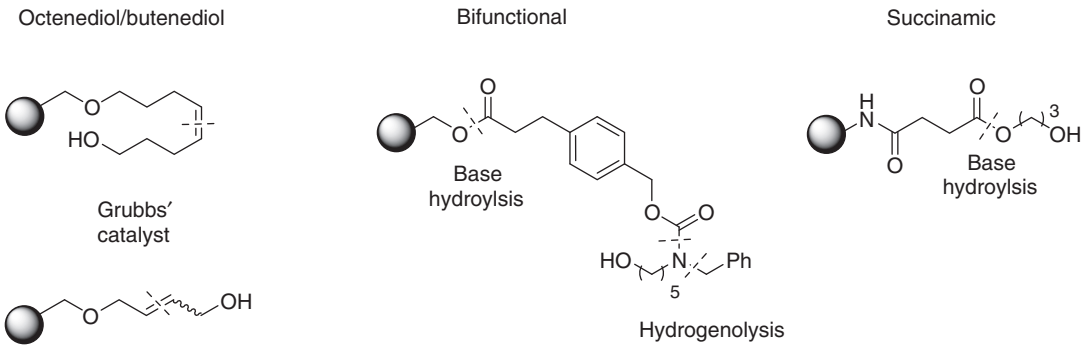


Figure 6 Linkers used in automated solid-phase oligosaccharide synthesis.

9.05.5.1 Alkene–Diol Linkers

Octenediol[1] and butenediol[7] linkers, which contain a single double bond, fit the requirements for a suitable linker for automated solid-phase oligosaccharide synthesis. These linkers are generally connected to the solid support via an ether or ester linkage. After synthesis, the linker is cleaved by cross-metathesis (or base hydrolysis then cross-metathesis) using Grubbs' first-generation catalyst (Grubbs' I) in the presence of ethylene. The resulting fully protected *n*-pentenyl glycoside (octenediol) or allyl glycoside (butenediol) can be hydrolyzed to the free reducing sugar or activated and then glycosylated. The carbon–carbon double bond can also be modified to produce a handle with a nucleophile suitable for conjugation.

There are three major disadvantages to the use of the octenediol and butenediol linkers. The first is that the alkene prohibits the use of electrophiles, such as those required for the activation of thioglycosides, during the automated process. The second is that the Grubbs' catalyst required for cleavage from the resin is expensive and often difficult to remove from the final reaction products. Finally, the alkene handle requires further functionalization to be useful for conjugation and biological evaluation; such transformations can reduce the overall yield of the final oligosaccharide product.

9.05.5.2 Bifunctional Linker

The bifunctional linker[8] was prepared to address the issues associated with the octenediol and butenediol linkers. The bifunctional linker, which is connected to the solid support via an ester linkage, is fully compatible with most common glycosylation conditions, including the electrophilic conditions required for the activation of thioglycosides. Cleavage of the ester using base-catalyzed hydrolysis is inexpensive and accomplished under mild conditions. After purification, hydrogenolysis of the remaining carbamate reveals a C5 linker with a terminal amine suitable for conjugation. The main disadvantage with the bifunctional linker is that it's use limits the types of temporary protecting groups that can be used; acetate groups can no longer serve as temporary protecting groups since the reaction conditions required to remove them would also result in the cleavage of the oligosaccharide from the resin.

9.05.5.3 Succinamic Linker

A succinamic linker[4] was recently reported for use in automated solid-phase oligosaccharide synthesis. This linker, which is connected to the solid support (TentaGel) via an amide linkage, can also be cleaved using base-catalyzed hydrolysis. The succinamic linker offers similar advantages to the bifunctional linker, and in principle could support the electrophilic conditions required for thioglycoside activation. The main disadvantage with the succinamic linker is that the alcohol handle produced on hydrolysis from the resin must be further functionalized for conjugation.

9.05.6 Building Blocks

The identification and synthesis of the building blocks required to construct the oligosaccharides is the most laborious and time-consuming task of the automated process. Protecting group patterns must be designed to achieve the desired connectivity and stereoselectivity in high yield. In addition, the nature of the protecting group can directly influence the reactivity of the building block, affecting reaction times and yield.

The basic features of a building block are highlighted in Figure 7 and include the anomeric leaving group (LG), a participating group (for 1,2-*trans* linkages) or nonparticipating group (for 1,2-*cis* linkages) at the C2 position (R_1), temporary protecting groups that are stable under glycosylation conditions but readily removed for the next glycosylation reaction (R_2) and permanent protecting groups that remain intact until the final global deprotection step (R_3).

Mammalian carbohydrates are commonly comprised of ten monosaccharides: glucose, galactose, mannose, sialic acid, *N*-acetylglucosamine, *N*-acetylgalactosamine, fucose, glucuronic acid, iduronic acid, and xylose (Figure 8). In principle, each carbohydrate residue can be linked through any of its different functional groups and each linkage generates a new stereocenter. The potential diversity is significant. For example, the number of theoretical structures possible for a hexasaccharide comprised from any one of the ten mammalian monosaccharides is approximately 190 billion!

It has been estimated that 224 building blocks would be required to assemble any given mammalian oligosaccharide.[9] However, recent studies have suggested that only 36 building blocks would be required to access approximately 75% of all known mammalian oligosaccharides due to significant overlaps in common connectivities.[10] Thirty of these building blocks are shown in Figure 9 and are ranked by relative abundance in mammalian oligosaccharides.

The type II Lewis blood group oligosaccharide Le^y–Le^x (nonasaccharide) provides a good example of the number and types of carbohydrate linkages that can be made. As illustrated in Figure 10, the Le^y–Le^x molecule is comprised of four β-linked sugar residues: glucose, galactose, *N*-acetylglucosamine, and fucose. Individual differences in the connectivities of these four sugars require that five differentially functionalized building blocks from Figure 10 would be required to synthesize Le^y–Le^x molecule.

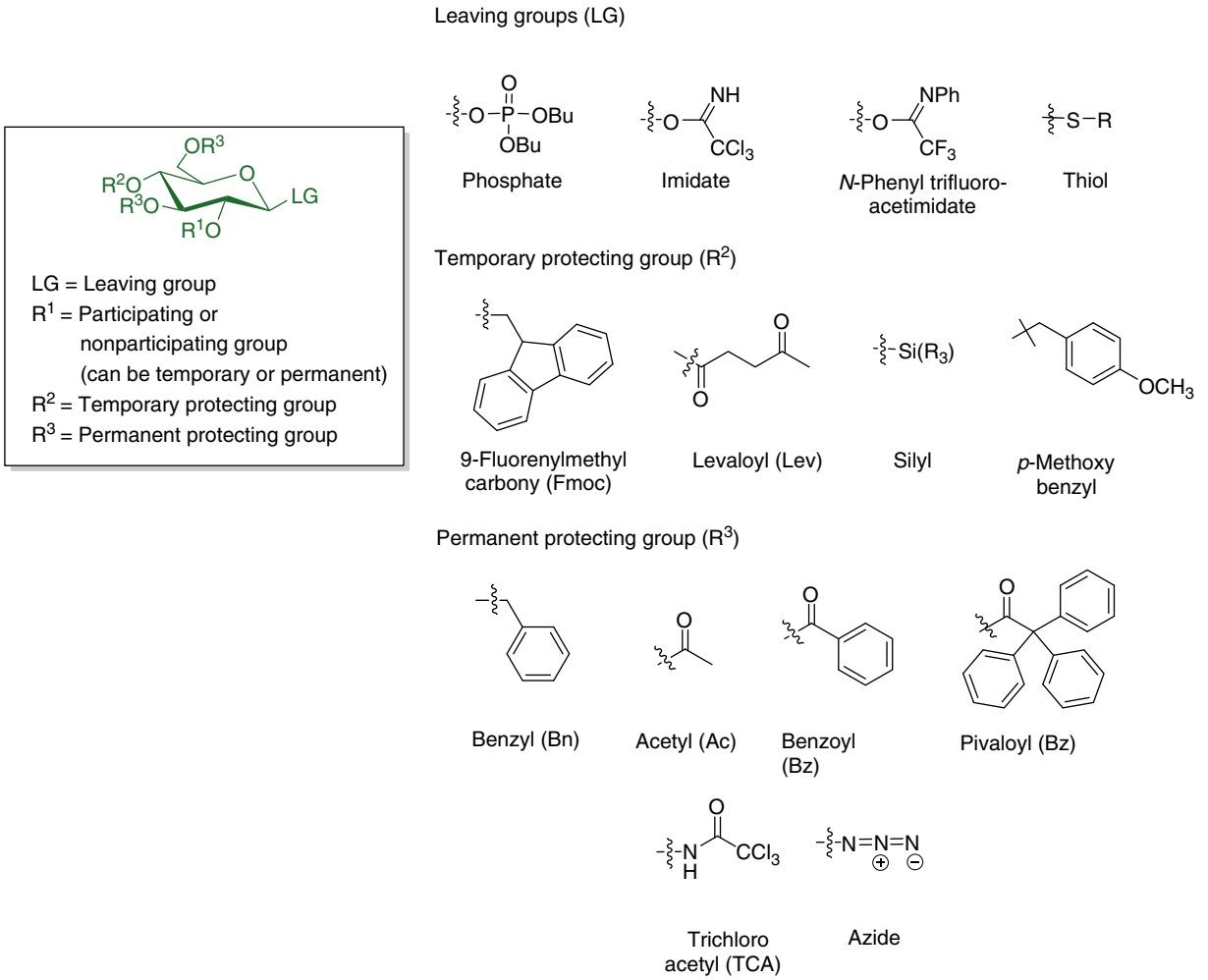


Figure 7 Basic features of building blocks used in automated solid-phase oligosaccharide synthesis.

9.05.6.1 Anomeric Leaving Group

In automated solid-phase oligosaccharide synthesis, the mono- or disaccharide with the LG, which serves as a glycosyl donor or electrophile, is activated in the presence of a nucleophile. There are three common LGs employed in automated solid-phase oligosaccharide synthesis (Figure 8): phosphates, imidates, and thiols. Historically, glycosyl phosphates and imidates have played the most important roles in automated solid-phase oligosaccharide synthesis. However, a number of automated solid-phase oligosaccharide syntheses employing thioglycosides have been reported recently in the literature.

The accepted mechanism for glycosidic bond formation using glycosyl phosphates, imidiates, and thiols under standard glycosylation conditions is illustrated in Scheme 1. Nucleophilic displacement (S_N1) results in a glycosidic bond with the C2 position playing a role in the resulting stereochemistry of the products. For this reason, the stereochemistry of the LG generally has little impact on the stereochemical outcome of the reaction. However, it has been demonstrated that in some cases anomers may have different chemical properties resulting in enhanced or reduced reactivity.

Glycosyl phosphates can be synthesized from lactols, glycosyl bromides, acetates, trichloracetimidates, nitrates, thioglycosides, 4-pentenyl and 2-buten-2-yl glycosides, glycals, 1,2-orthoesters, and oxazolines.[11] Dibutylphosphate is most commonly employed in automated solid-phase oligosaccharide synthesis, and it is generally activated with a stoichiometric amount of a Lewis acid, most often trimethylsilyl trifluoromethanesulfonate (TMSOTf), at temperatures approximately $-15\,^{\circ}C$ in the presence of a nucleophile (Scheme 2).

Glycosyl imidates are generally prepared from their corresponding lactols.[12] In general, glycosyl imidates are advantageous in comparison to glycosyl phosphates because the conditions required to activate them (catalytic TMSOTf or trifluoromethanesulfonic acid (TfOH)) are generally milder. Glycosyl trichloroacetimidates and *N*-phenyl trifluoroacetimidates are generally activated at temperatures between $-40\,^{\circ}C$ and $-15\,^{\circ}C$ (Scheme 2). Glycosyl phosphates and imidates have been shown to be reasonably stable for over a year at $-20\,^{\circ}C$.

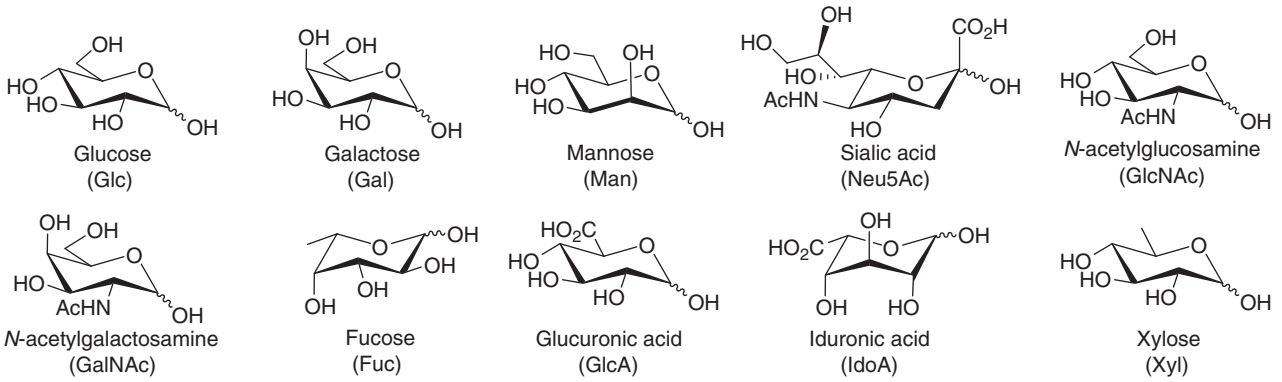


Figure 8 Ten common monosaccharides.

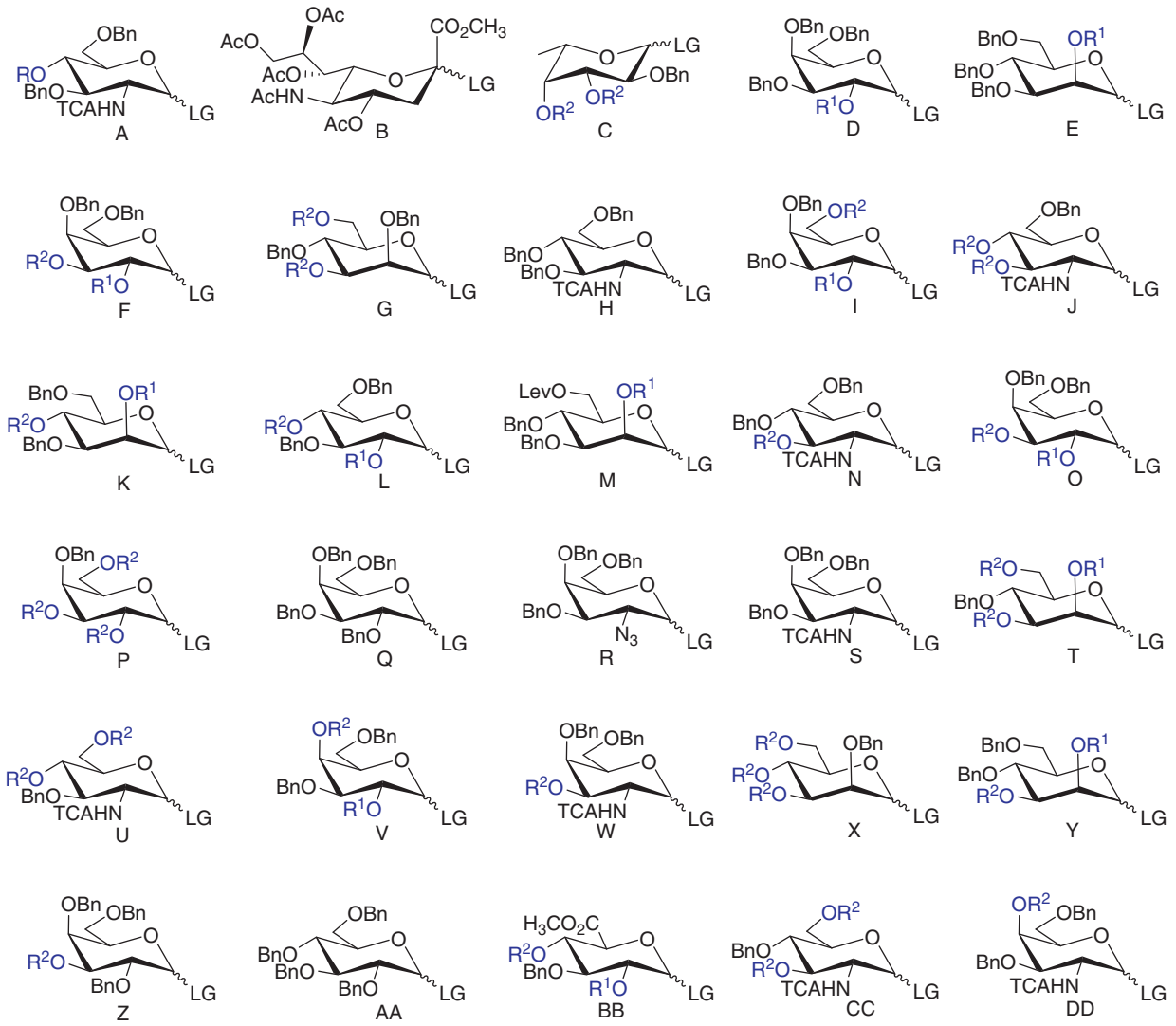


Figure 9 Building blocks required for the synthesis of approximately 75% of all known mammalian oligosaccharides.

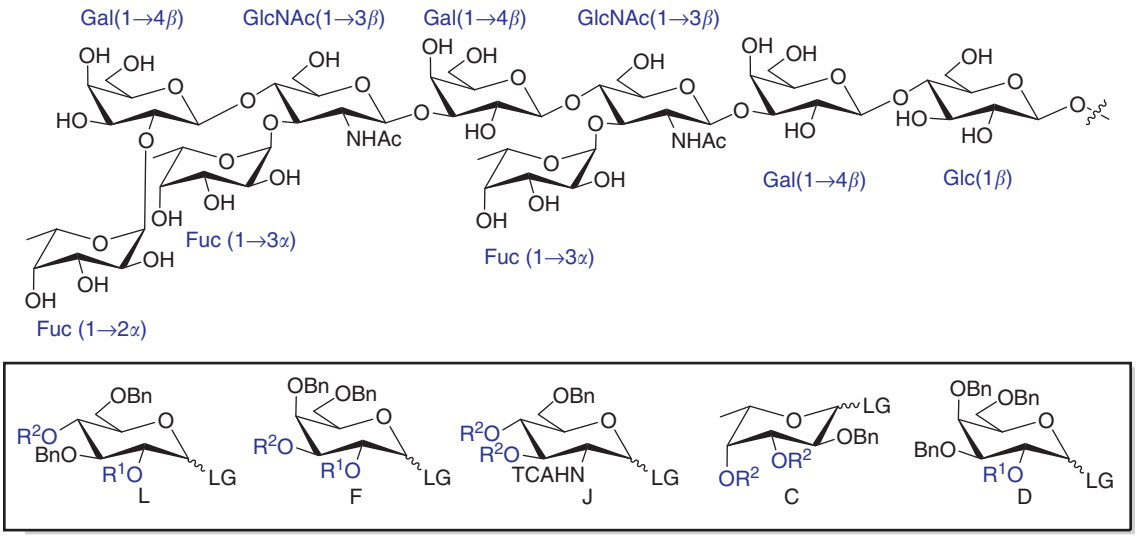
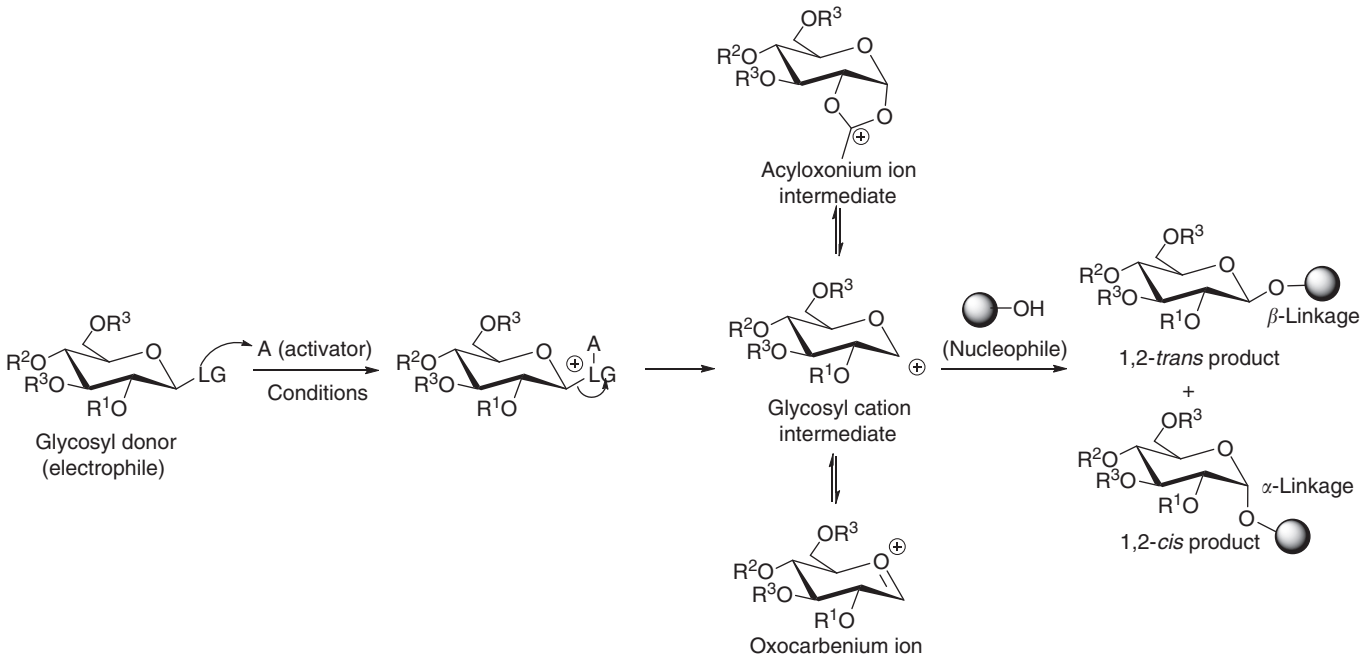
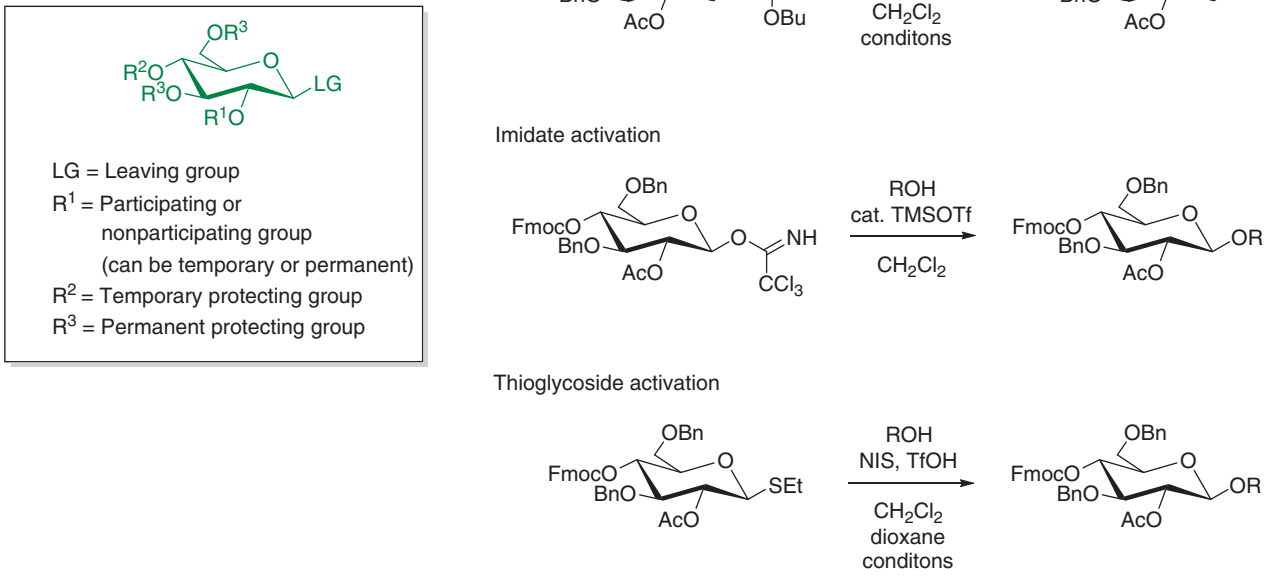


Figure 10 Le^y–Le^x (nonasaccharide) monosaccharide diversity.



Scheme 1 General glycosylation strategy.

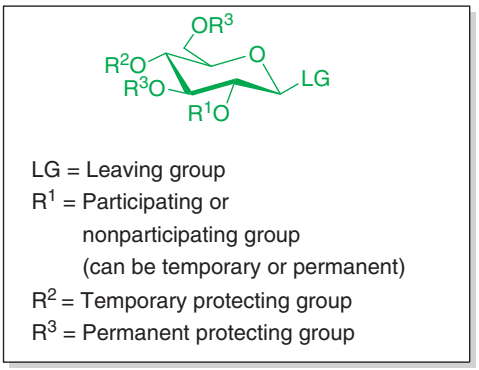


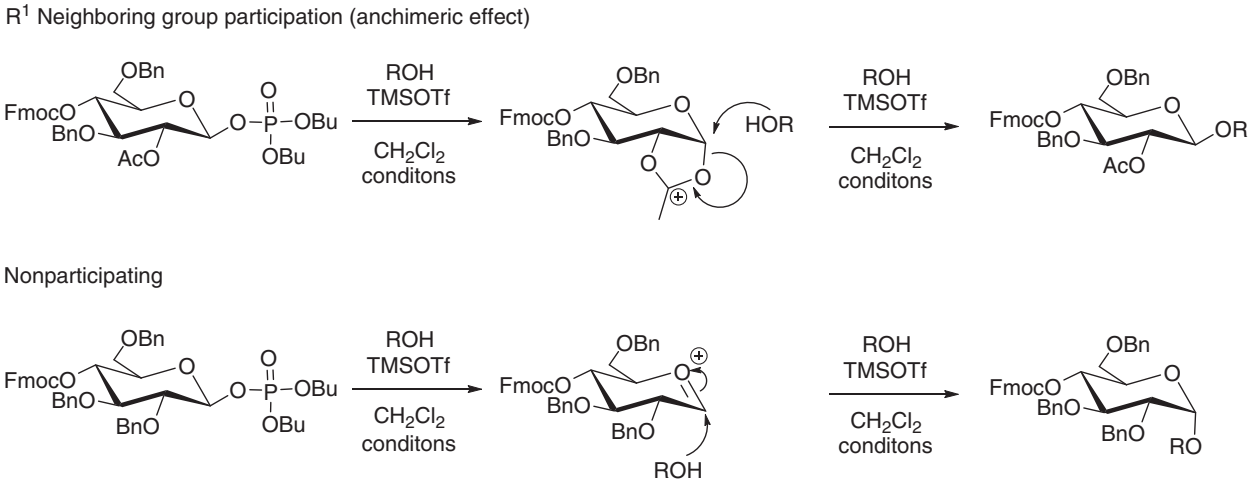
Scheme 2 Activation conditions for glycosyl phosphates, imidates and thioglycosides.

More recently, thioglycosides have been shown to be effective LGs in automated oligosaccharide synthesis. Thioglycosides can be prepared from a number of sources.[13] The most common include lactols, glycosyl halides, and peracetylated or 1-acylated sugars. In automated solid-phase oligosaccharide synthesis, thioglycosides are activated using either an *N*-iodosuccinimide (NIS)/TMSOTf or NIS/TfOH promoter system (Scheme 2) at temperatures approximately −40 °C. The major advantage to using thioglycosides in automated solid-phase oligosaccharide synthesis is their shelf stability. They generally remain stable, even at room temperature, for extended periods. In addition, thioglycosides can be used to access the other donors; phosphates can be accessed directly from thioglycosides, or the thioglycoside can be hydrolyzed to the lactol and then converted to the imidate in two steps.

9.05.6.2 The C2 Position

The C2 position plays an important role in directing the glycosidic linkage (Scheme 3). Participating groups such as esters, which form an intermediate acyloxonium ion intermediate, create steric hindrance on one face of the donor permitting attack at the opposite face favoring 1,2-*trans* linkages. Nonparticipating groups, such as ethers, are unable to participate and therefore, the intermediate oxocarbenium ion can be attacked from either side of the carbohydrate residue. However, formation of the 1,2-*cis* linkage is often favored due to the anomeric affect.



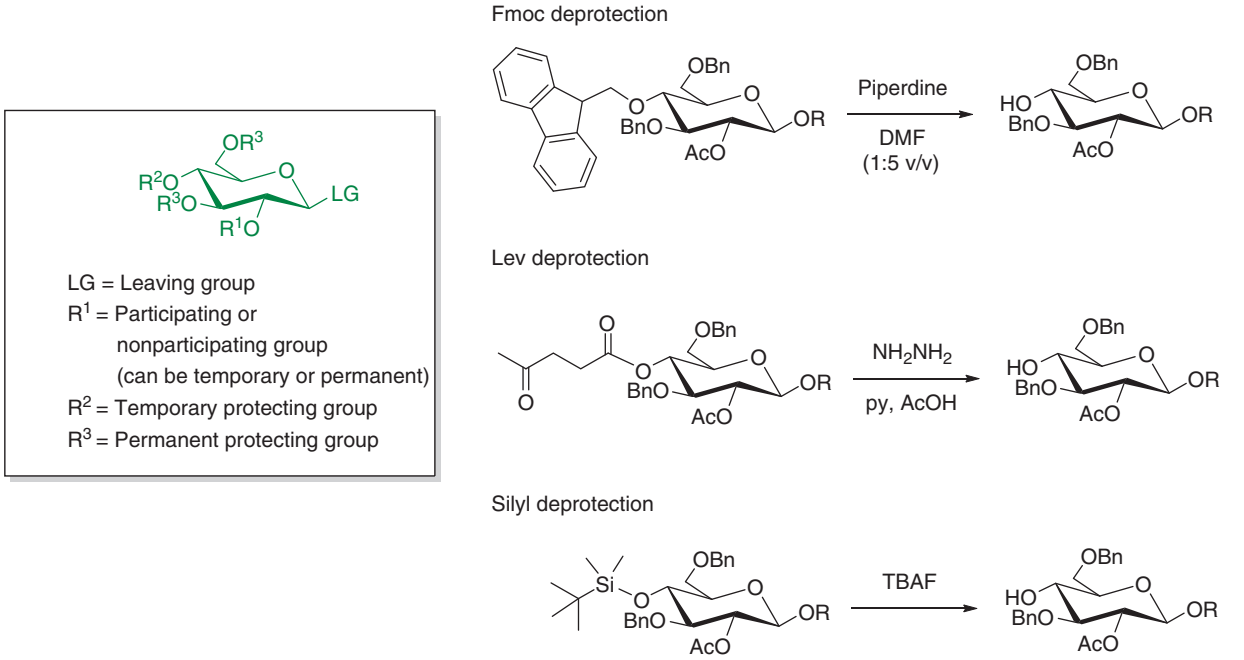


Scheme 3 Effects of the C2 position on glycosylation.

9.05.6.3 Temporary Protecting Groups

9-Fluorenyl carboxymethyl (Fmoc), levulinoyl (Lev) and silyl-protecting groups (Scheme 4) have proven to be effective temporary protecting groups in automation. The 9-fluorenylcarboxyl group is generally installed using FmocCl in the presence of a pyridine in high yield.[14] In automated solid-phase oligosaccharide synthesis, the Fmoc group is readily removed by treatment with a solution of piperidine in dimethyl formamide (DMF) to give a fulvene byproduct (which can be used to monitor the progression of the reaction) and the free alcohol, which serves as a nucleophile in the next glycosylation reaction (Scheme 4).

The levulinoyl (Lev) ester group is generally installed using levulinic acid, *N*′*N*′-dicyclohexylcarbodiimide (DCC), and dimethylaminopyridine (DMAP) at room temperature.[15] The Lev group is generally removed in automated solid-phase oligosaccharide synthesis using a 0.5 mol l^{-1} solution of hydrazine in a mixture of pyridine and acetic acid to give the desired alcohol (Scheme 4). These conditions do not affect normal esters such as acetates, benzoates, or pivaloates.



Scheme 4 Temporary protecting group deprotection strategies.

Although less common, silyl-protecting groups are gaining importance in automated solid-phase oligosaccharide synthesis. The most commonly employed silyl-protecting group, tert-butyldimethylsilyl ether (TBS or TBDMS) is commonly installed using TBDMSCl and imidazole in DMF.[16] Removal of the TBDMS group in automation is accomplished using tetrabutyl ammonium fluoride to give the free alcohol (Scheme 4).

9.05.6.4 Permanent Protecting Groups

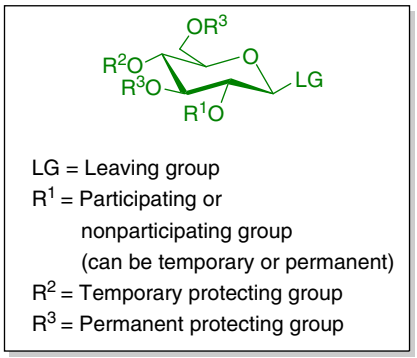
Permanent protecting groups used in automated solid-phase oligosaccharide synthesis include benzyl groups (Bn), pivaloyl (Piv) and benzoyl (Bz) esters, azides (N_3), and *N*-trichloroacetyl (TCA) groups (Scheme 5). These groups are generally removed after the newly oligosaccharide has been cleaved from the resin and purified.

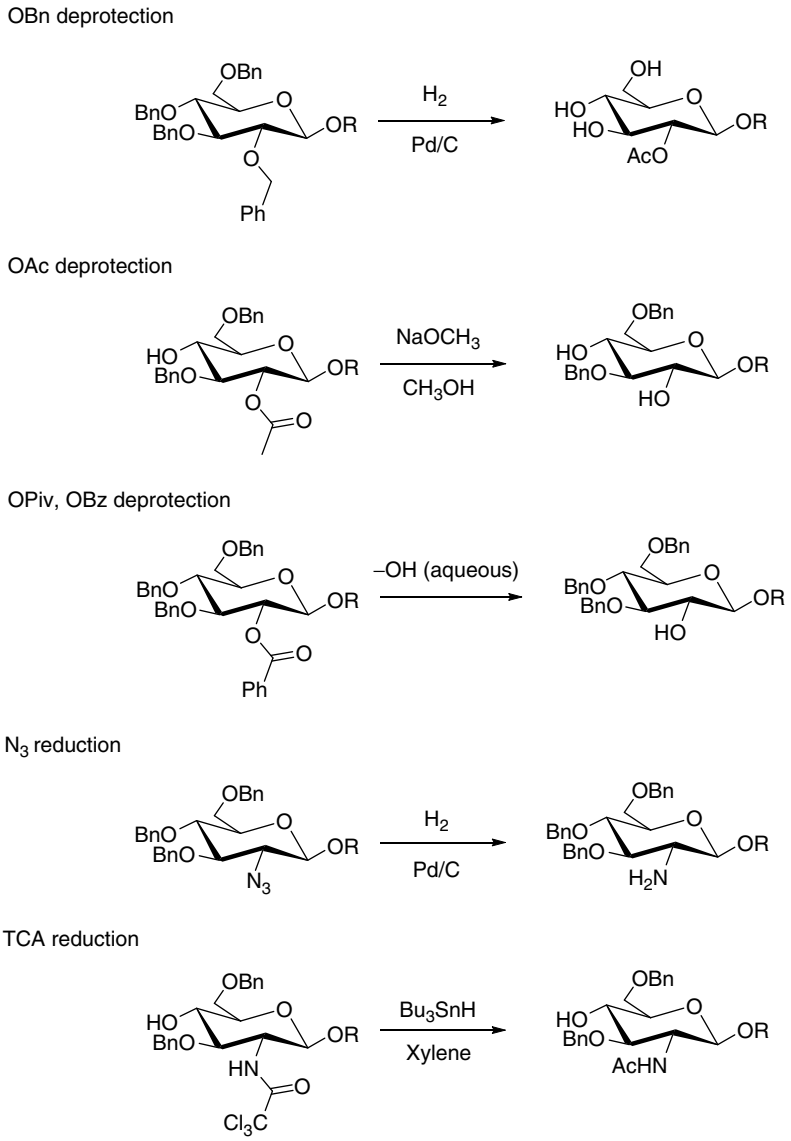
Benzyl groups (Bn) are the most common permanent protecting groups used in automation due to their stability under relatively acidic and basic conditions. They are generally installed via treatment of the corresponding alcohol with benzyl bromide and sodium hydride in DMF[17] and are removed using standard hydrogenolysis (Scheme 5).[18]

Azides (N_3) are generally employed as nonparticipating protecting groups for the synthesis of 2-amino sugars. Azides are commonly introduced by nucleophilic substitution of sugar derived tosylates,[19,20,21] mesylates,[22] and epoxides.[23] Azides can also be installed by treating the corresponding amino sugar with sodium azide and triflic anhydride[24] or triflate azide in copper sulfate.[25,26] Azides are most commonly reduced by hydrogenolyisis to the corresponding amine (Scheme 5).

Pivaloyl (Piv), benzoyl (Bz) esters, and *N*-trichloroacetamides (TCA) are more stable than acetates and do not hydrolyze readily under the standard reaction conditions used for automated solid-phase oligosaccharide synthesis. These groups are generally prepared by treating the free alcohol (Piv[27] or Bz[28]) or amine (TCA[29]) with the corresponding acyl chloride in the presence of a base. Piv and Bz groups are readily hydrolyzed by treatment with strong base. *N*-Trichloroacetyl (TCA) groups are generally reduced to the corresponding *N*-acetyl groups using tributyltin hydride in refluxing xylene.

Acetyl esters (Ac) can serve as temporary or permanent protecting groups depending on the linker chosen for automation. Acetates are most commonly prepared by treatment of the free alcohol with acetic anhydride in pyridine,[30,31] and they are hydrolyzed using a solution of sodium methoxide in methanol (Zemplén conditions).[32] Octenediol and butenediol inkers are unaffected by these conditions, but the bifunctional and succinamic linkers are readily cleaved. When these linkers are employed, acetate serves as a permanent protecting group.





Scheme 5 Permanent protecting group deprotection strategies.

9.05.6.5 Monosaccharide Reactivity

The nature of the protecting groups can also affect the general reactivity profile of an individual monosaccharide. With regards to glycosyl donors, electron-donating groups stabilize acyloxonium/oxocarbenium ion intermediates by donating electron density to this intermediate via induction. These groups tend to enhance the rate of the glycosylation reaction. In contrast, electron-withdrawing groups destabilize acyloxonium/oxocarbenium ion intermediates by withdrawing electron density from the reactive site. This can have the affect of decreasing the reaction rate, and in extreme cases can impede reactivity altogether. This stabilizing/destabilizing based on electron donation or withdraw is known as the 'armed-disarmed' concept, where electron-donating groups 'arm' the donor, whereas electron-withdrawing groups 'disarm' the donor.[33,34,35]

When considering the electronics of glycosyl acceptors, electron-donating groups near the nucleophilic hydroxyl group may enhance nucleophilicity. This can lead to faster reaction rates. Electron-withdrawing groups near the nucleophilic hydroxyl group, which remove electron density through induction, can diminish the overall rate of the reaction.

9.05.7 Automated Synthesis of Oligosaccharides

The first automated solid-phase oligosaccharide syntheses reported by Seeberger and co-workers[1] began a revolution in the preparation of glycoconjugates for biological evaluation. Since their initial report, automation has been used by scientists around

the world to synthesize more than 30 complex oligosaccharides including bacterial antigens, cancer antigens, vaccine candidates, and *N*-linked core oligosaccharides. The syntheses of several of these oligosaccharides are presented in Sections 9.05.7.1–9.05.7.10. Examples were chosen for historical purposes as well as to highlight the challenges and complexities of the oligosaccharides prepared using the automation solid-phase oligosaccharide process.

The majority of the oligosaccharides synthesized via automated oligosaccharide syntheses were synthesized using either the first- or second-generation automated solid-phase oligosaccharide synthesizer. In most cases Merrified resin was used as the solid-support. Glycosylation reactions typically employ a 'double-coupling' (Figure 11) or 'triple coupling' strategy which involves activating 3 to 5 equivalents of glycosyl donor two or three times with a washing step (to remove unreacted donor and reaction byproducts) in between. This process is employed to ensure complete reaction thereby minimizing deletion sequences which can have a negative impact on the purification of the desired oligosaccharide.

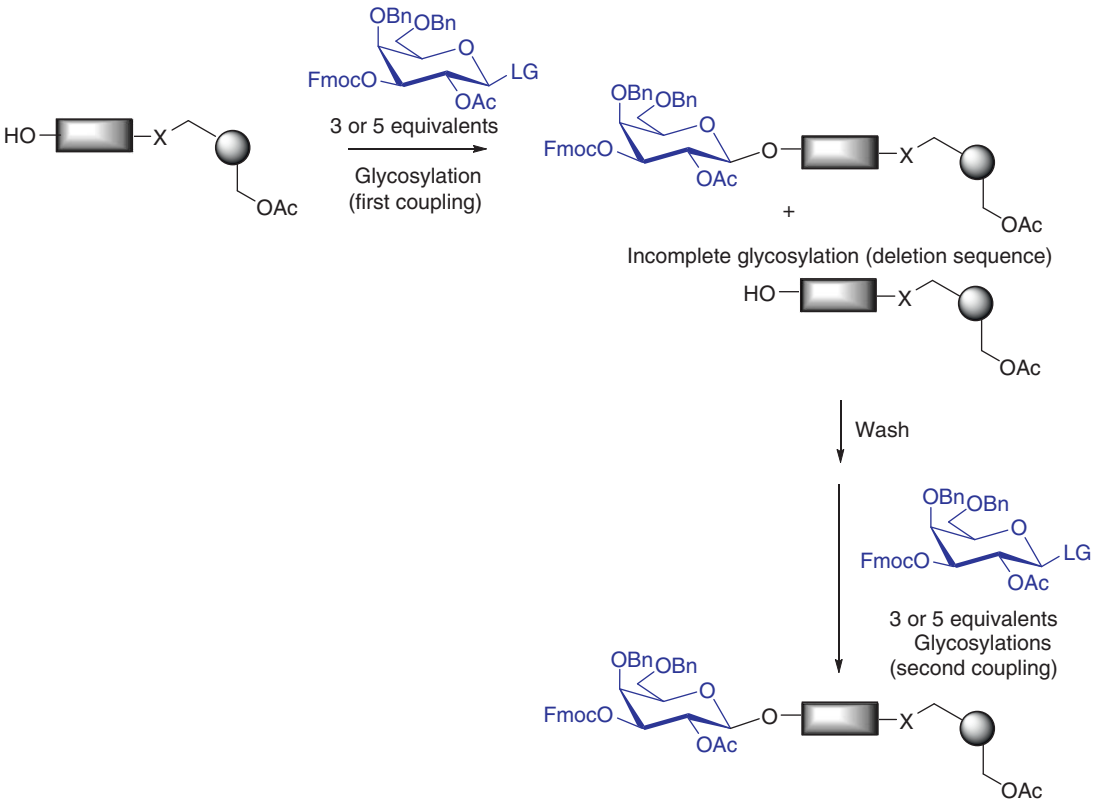


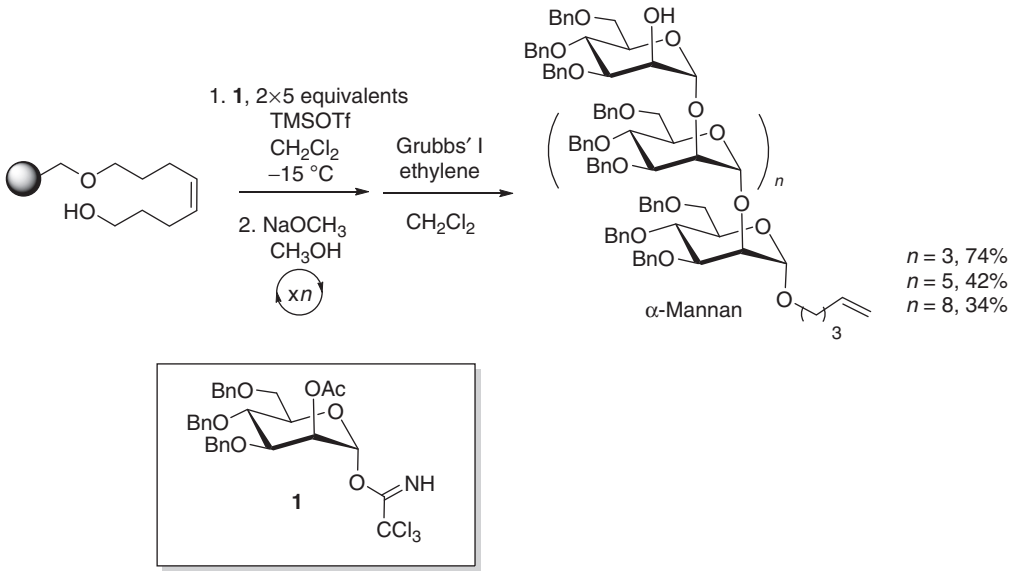
Figure 11 'Double coupling' strategy.

9.05.7.1 α-Mannans and a Phytoalexin β-Glucan

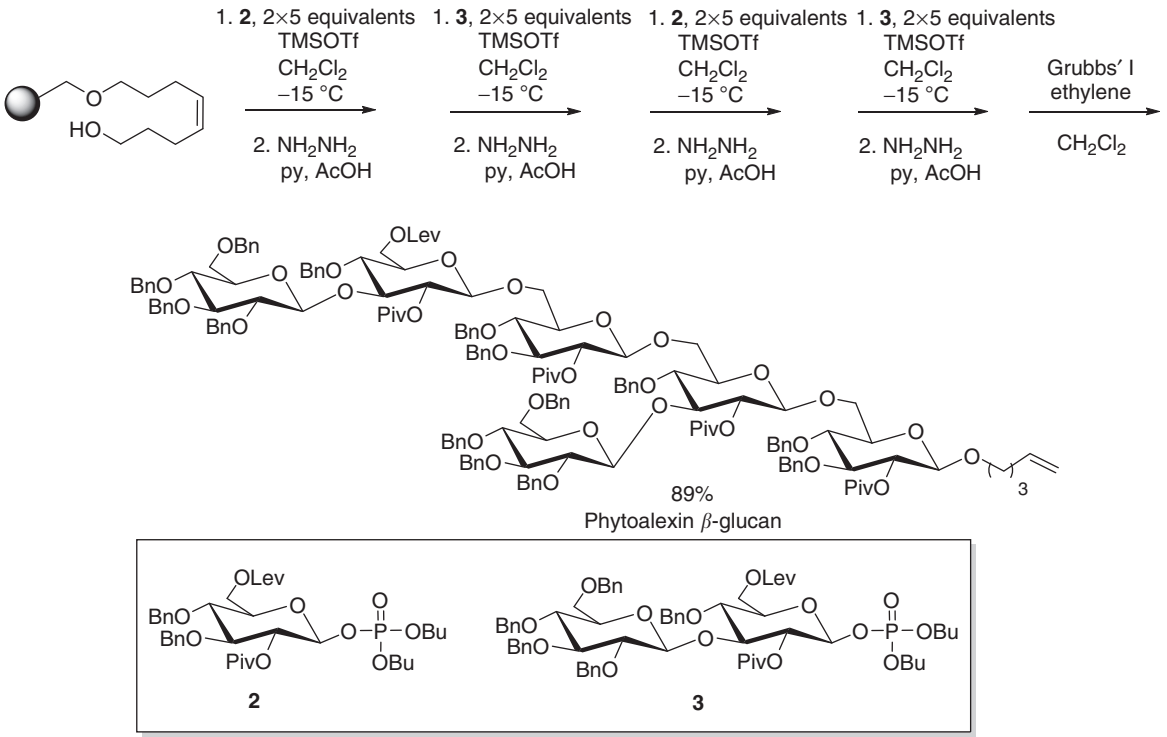
α-Mannan and β-glucans are known to play important roles in the pathogenesis of certain fungi.[2] The first automated solid-phase oligosaccharide syntheses of α-mannan and β-glucan oligosaccharides were reported in 2001 by Seeberger and co-workers using the first-generation automated solid-phase oligosaccharide synthesizer.[1] The syntheses of these compounds provided proof of principle that linear and branched oligosaccharides could be made in automation in high yield using standard LGs such as glycosyl imidates and phosphates.

The synthesis of α-1,2 linked penta-, hepta-, and deca-α-mannans was accomplished using the first-generation solid-phase oligosaccharide synthesizer.[1] Octenediol-functionalized Merrifield resin was repeatedly glycosylated with mannosyl imidate **1** using a double coupling approach (5 equivalents) per cycle in the presence of a catalytic amount of TMSOTf (Scheme 6). The C2 Ac served as both a directing group (for anchimeric assistance) and a temporary protecting group, which could be hydrolyzed under Zemplén conditions. The pentasaccharide ($n=3$) was generated in 74% yield demonstrating approximately 95% coupling efficiency at each step. The heptasaccharide ($n=5$) and decasaccharide ($n=8$) were produced 42% and 34% yields, respectively, demonstrating approximately 90% coupling efficiency at each step.

Two selectively functionalized glucose building blocks were used to generate a phytoalexin elicitor β-glucan (Scheme 7) as the first example of a branching glycan synthesized by automated solid-phase oligosaccharide synthesis. Octenediol-functionalized



Scheme 6 α-Mannan.

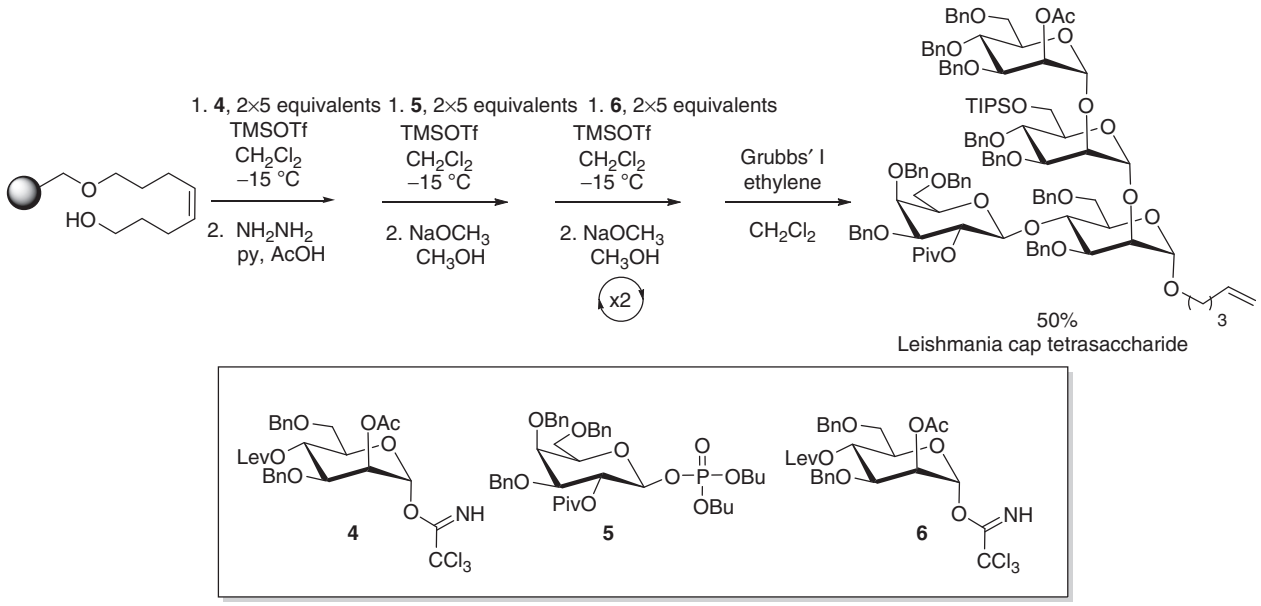


Scheme 7 Phytoalexin β-glucan.

Merrifield resin was coupled with two glycosyl phosphate building blocks, monosaccharide **2**, and 1,3-linked disaccharide **3**, containing C2 Piv participating groups. Each iterative 'double coupling' required 5 equivalents of the desired phosphate building block (**2** or **3**) and a stoichiometric amount of TMSOTf. After each glycosylation, the Lev ester of the growing oligosaccharide chain was removed using hydrazine/pyridine/acetic acid solution to furnish a nucleophile for the next glycosylation reaction. After four glycosylation reactions, the oligosaccharide was cleaved from the resin using Grubbs' catalyst under an ethylene atmosphere to produce the final protected phytoalexin elicitor β-glucan in 89% yield over five steps.

9.05.7.2 Leishmania Cap Tetrasaccharide

Leishmania, which is transmitted to humans via the sand fly, affects millions of people worldwide. Automated solid-phase oligosaccharide synthesis was used to synthesize the tetrasaccharide cap of the antigenic glycosylphosphatidylinositol (GPI) found on the surface of the Leishmania parasite,[36] providing the first example of the automated solid-phase synthesis of a branching glycan using functionalized monosaccharide building blocks with different LGs. Octenediol-functionalized Merrifield resin and three building blocks (**4**, **5**, and **6**, Scheme 8) containing C2 participating groups were employed in the synthesis of the tetrasaccharide cap. Mannosyl imidate **4** was glycosylated on to the linker using a catalytic amount of TMSOTf. Removal of the Lev group using hydrazine, followed by glycosylation with galactosyl phosphate **5** using a stoichiometric amount of TMSOTf gave the desired disaccharide. Hydrolysis of the C2 Ac under Zemplén conditions, followed by glycosylation with mannosyl imidate **6** gave the desired trisaccharide. A second hydrolysis and glycosylation with **6**, followed by cleavage with Grubbs' catalyst under an ethylene atmosphere gave the desired tetrasaccharide in 50% yield with approximately 85% coupling efficiency at each step.



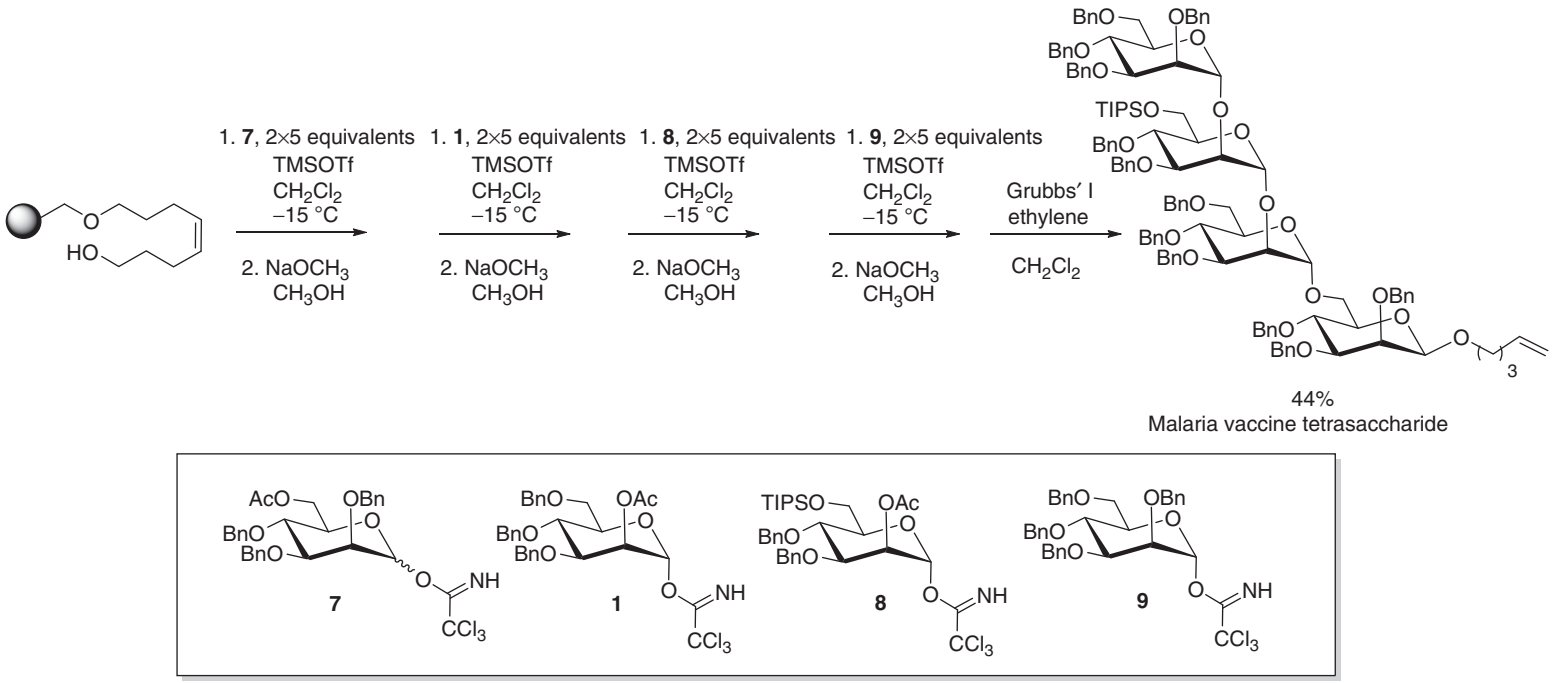
Scheme 8 *Leishmania* cap tetrasaccharide.

9.05.7.3 Malaria Vaccine Tetrasaccharide

Malaria is caused by the parasite *Plasmodium*, which is transmitted by the mosquito. In 2010, approximately 216 million cases of malaria were recorded worldwide with more than 655 000 deaths reported (Data obtained from the World Health Organization). In 2002, a GPI toxin responsible for the pathogenesis of the parasite was identified and targeted for vaccine development.[37] Shortly thereafter, the first automated solid-phase synthesis was reported.[38] Four selectively functionalized imidate building blocks, **7**, **1**, **8**, and **9**, were required for this synthesis (Scheme 9). The use of acetates as temporary protecting groups and the need to install a second mannose residue at the C6 position of the reducing sugar required that imidate **7**, with a nonparticipating group at C2, be employed for this synthesis. Glycosylation of mannosyl imidate **7** on to the octenediol-functionalized Merrifield resin using the 'double coupling' strategy and stoichiometric amount of TMSOTf led to a mixture of α and β anomers. This mixture was inconsequential since later steps in the synthesis of the vaccine candidate required hydrolysis of the pentenyl tether and refunctionalization of the reducing sugar. Methanolysis of the C6 Ac to the corresponding hydroxyl group using Zemplén conditions provided the corresponding nucleophile required for extension. Subsequent glycosylation/hydrolysis cycles with imidates **1**, **8**, and **9** gave the final tetrasaccharide in 44% yield after cleavage from the resin (approximately 82% coupling efficiency at each step). It is worth noting that the employment of building block **8** represented the first use of a silyl-protecting group in automated oligosaccharide synthesis.

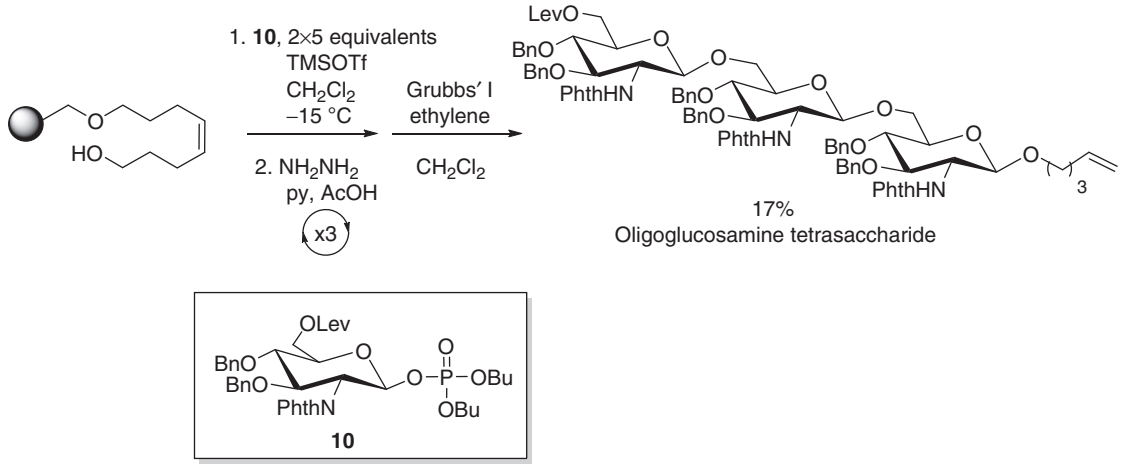
9.05.7.4 Oligoglucosamines

β-(1→6) and β-(1→4) linked oligoglucosamines are expressed on the surface of pathogenic *Staphylococcus aureus*[39] and are involved in a number of critical biological processes including cellular communication and adhesion. They are also antigenic. Therefore, interest in these compounds as potential vaccine candidates[40] has prompted the development of rapid synthetic strategies to access them. The first automated solid-phase synthesis developed for the synthesis of a β-(1→6) glucosamine was



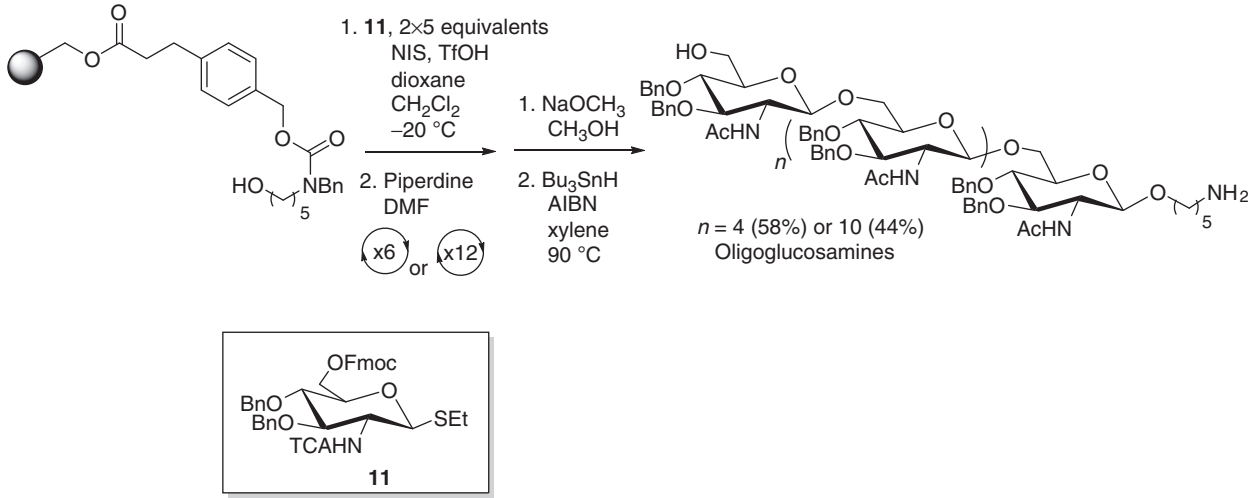
Scheme 9 Malaria vaccine tetrasaccharide.

reported in 2002.[41] An initial solution-phase screening led to the use of glucosylamine phosphate building block **10** functionalized with a participating phthalimido group (NPhth) at C2 and a temporary Lev group at C6. A 'double coupling' strategy was employed on the first-generation automated solid-phase oligosaccharide synthesizer. Glycosylation of the first building block with octenediol-functionalized Merrifield resin followed by removal of the Lev protecting group using a hydrazine/pyridine/acetic acid solution gave the free C6 hydroxy methyl group for extension. Two additional glycosylation/deprotection steps were required to access the final trisaccharide in 17% yield (55% coupling efficiency) after cleavage from the resin using Grubbs' I catalyst in the presence of ethylene (**Scheme 10**). The lower yield is likely due to the steric hindrance and conformational constraints of the participating phthalimido group.



Scheme 10 Oligoglucosamine tetrasaccharide.

Development of the bifunctional linker and the second-generation automated solid-phase oligosaccharide synthesizer permitted the use of thioglycosides in the automated synthesis of β-(1→6) oligoglucosamines[8] (**Scheme 11**). For this synthesis a 'double coupling' strategy was employed. Activation of glucosylamine thioglycoside **11** functionalized with a trichloroacetamide (TCA) participating group at the C2 amine and Fmoc group at C6 with a promoter system consisting of *N*-iodosuccinimide (NIS) and triflic acid (TfOH) in the presence of the bifunctional linker led to the initial monosaccharide bifunctional linker-functionalized resin. Hydrolysis of the Fmoc group using a solution of piperdine in DMF provided a free alcohol for extension. Subsequent glycosylation/deprotection cycles followed by base-mediated hydrolysis from the resin and reduction of the TCA groups led to the production of the hexasaccharide (five additional cycles) or the dodecasaccharide (11 additional cycles) in 58% yield with 92% coupling efficiency and 44% yield with close to 93% coupling efficiency, respectively. This synthesis indicated a marked improvement over the initial trisaccharide synthesis (**Scheme 10**). A similar strategy employing thioglycoside building block with a participating TCA group at C2 and an Fmoc group at C4 was used to synthesize a β-(1→4) hexasaccharide in 31%



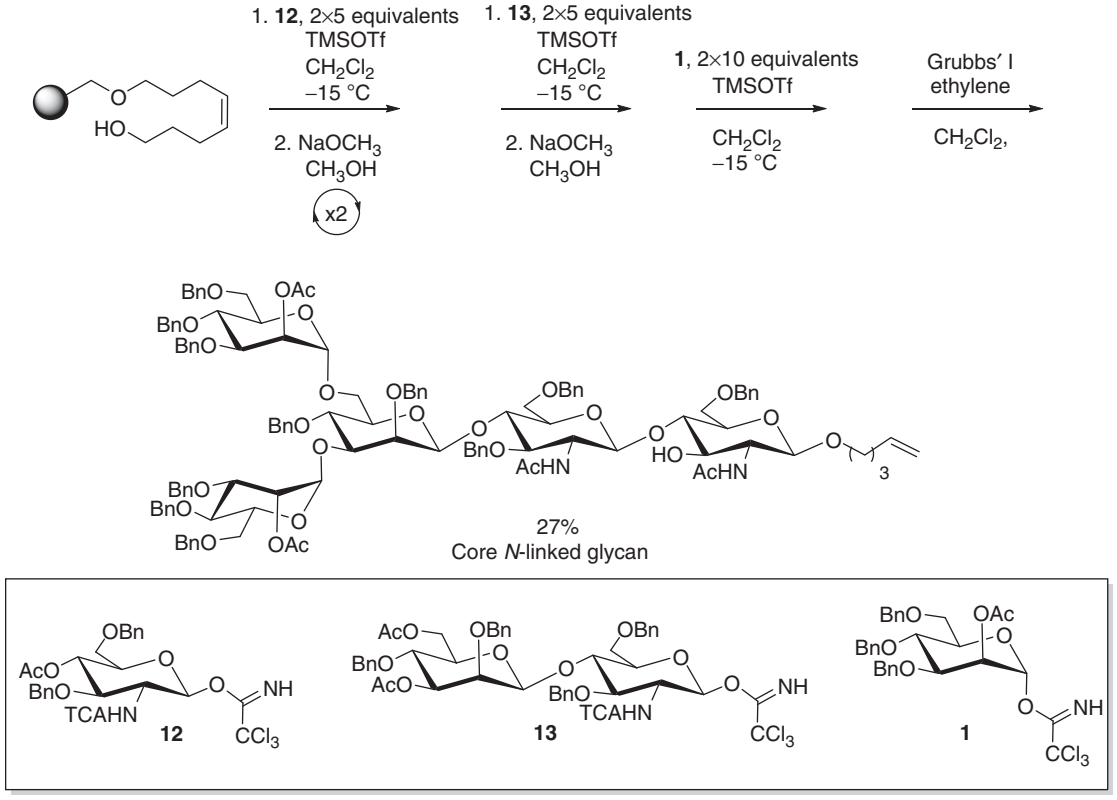
Scheme 11 Oligoglucosamine hexamer and dodecamer.

yield (not shown). The reduced yield for the β-(1→4) hexasaccharide is presumably due to the increased steric encumbrance of the nucleophile.

9.05.7.5 Core *N*-linked Glycan

N-Linked glycans play critical roles in cell–cell recognition and communication in mammals. *N*-Linked glycans have also been implicated in tumor progression and metastasis, and the pathogenesis of viruses such as HIV,[42] Ebola,[43] and some coronaviruses.[44] The pentasaccharide core of *N*-linked glycans, which consists of chitobiose (two β-(1→4) linked glucosamine residues) followed by a C3/C6 branching β-(1→4) linked mannose residue, presents a significant challenge due to the β-(1→4)-mannosidic linkage to the chitobiose disaccharide.

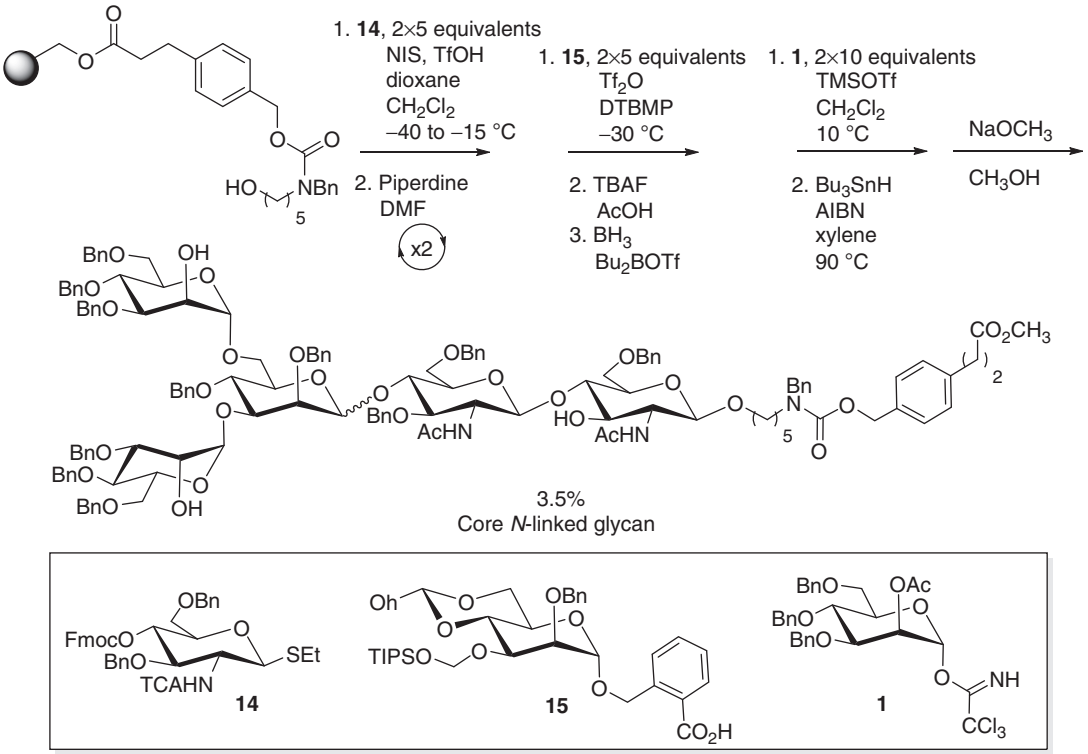
The first automated solid-phase synthesis of the core *N*-linked glycan by Seeberger and co-workers in 2003 employed the first-generation automated solid-phase oligosaccharide synthesizer, octenediol-functionalized Merrifield resin and a 'double coupling' strategy using three selectively functionalized imidates (Scheme 12).[45] The reducing glucosamine residue of the core chitobiose disaccharide was installed using imidate donor **12** functionalized with a participating TCA group at the C2 amine and a temporary Ac protecting group at C4 under standard conditions. Hydrolysis of the C4 Ac using Zemplén conditions provided a nucleophile for subsequent glycosylation. In this synthesis, installation of the difficult β-mannosidic linkage was avoided by using disaccharide building block **13** with a participating TCA group at the C2 position and temporary acetate groups at the C3 and C6 positions. Hydrolysis of the acetates at C3 and C6 followed by double glycosylation with mannosyl imidate **1** gave the core pentasaccharide in 27% yield with approximately 73% coupling efficiency after cleavage from the resin using Grubbs' catalyst.



Scheme 12 Core *N*-linked glycan.

The development of the second-generation solid-phase oligosaccharide synthesizer, the bifunctional linker and advances in the synthesis of β-mannosidic linkages encouraged Seeberger and co-workers to revisit the synthesis of the *N*-linked glycan in 2012. Their new approach is illustrated in Scheme 13.[8] The chitobiose core was installed using a 'double coupling' strategy with glucosylamine thioglyoside building block **14** functionalized with a TCA participating group at the C2 amine and a temporary Fmoc group on C4. Two glycosylation cycles were performed using an NIS/TfOH promoter system. Removal of the Fmoc group was accomplished between each cycle using piperidine to expose the next acceptor. The β-mannosidic linkage was then formed using mannosyl OCB building block **15** consisting of a nonparticipating benzylate at the C2 position, a temporary benzylidene acetal installed at the C4 and C6 positions, and a temporary silyl-protecting group at the C3 position, marking the first use of a

benzylidene acetal and an OCB donor in automation. Glycosylation of the chitobiose disaccharide with **15** using triflic anhydride (Tf_2O) and di-tert-butyl-4-methylpyridine (DTBMP), followed by removal of the silyl ether at C3 with TBAF and selective ring opening of the benzylidiene acetal using diborane and dibutylboron triflate (Bu_2BOTf), gave the core *N*-linked trisaccharide which underwent subsequent glycosylation with mannosyl imidate **1**. The final assembly of the core *N*-linked glycan was completed in 3.5% yield after cleavage from the resin under Zemplén conditions; the β-mannosidic linkage was installed with an α/β ratio of 1:3. Although the yields were far lower than the original synthesis of the core *N*-linked glycan, this work represents the first example of the direct generation of a beta-mannosidic linkage using an automated solid-phase platform.

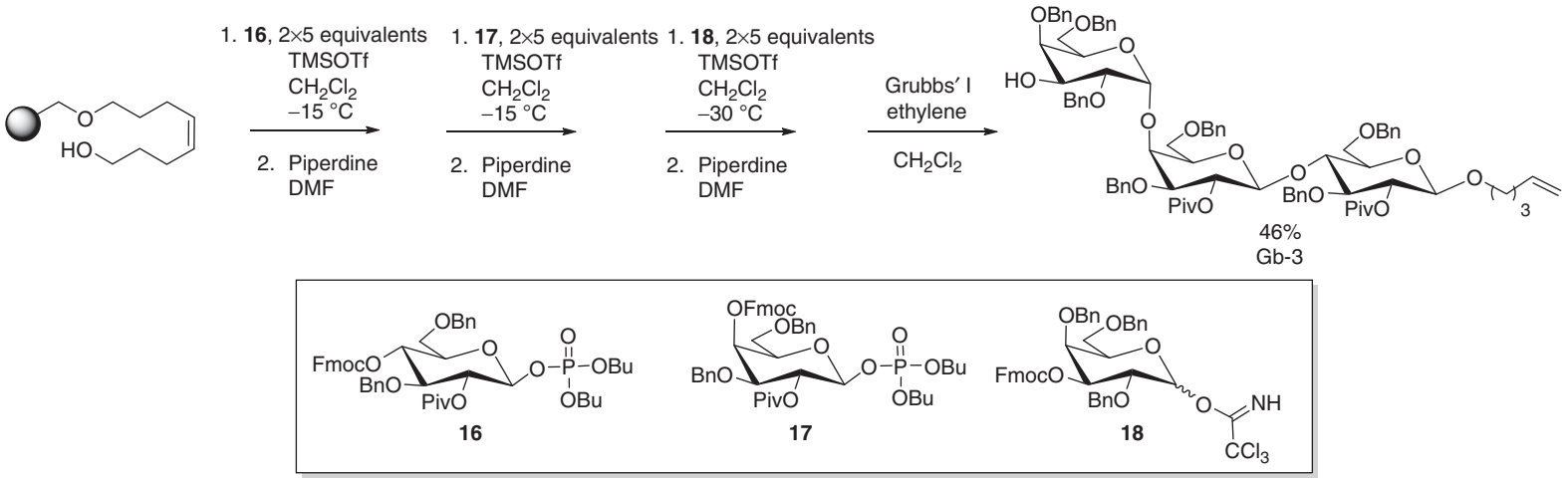


Scheme 13 Core *N*-linked glycan with bifunctional linker.

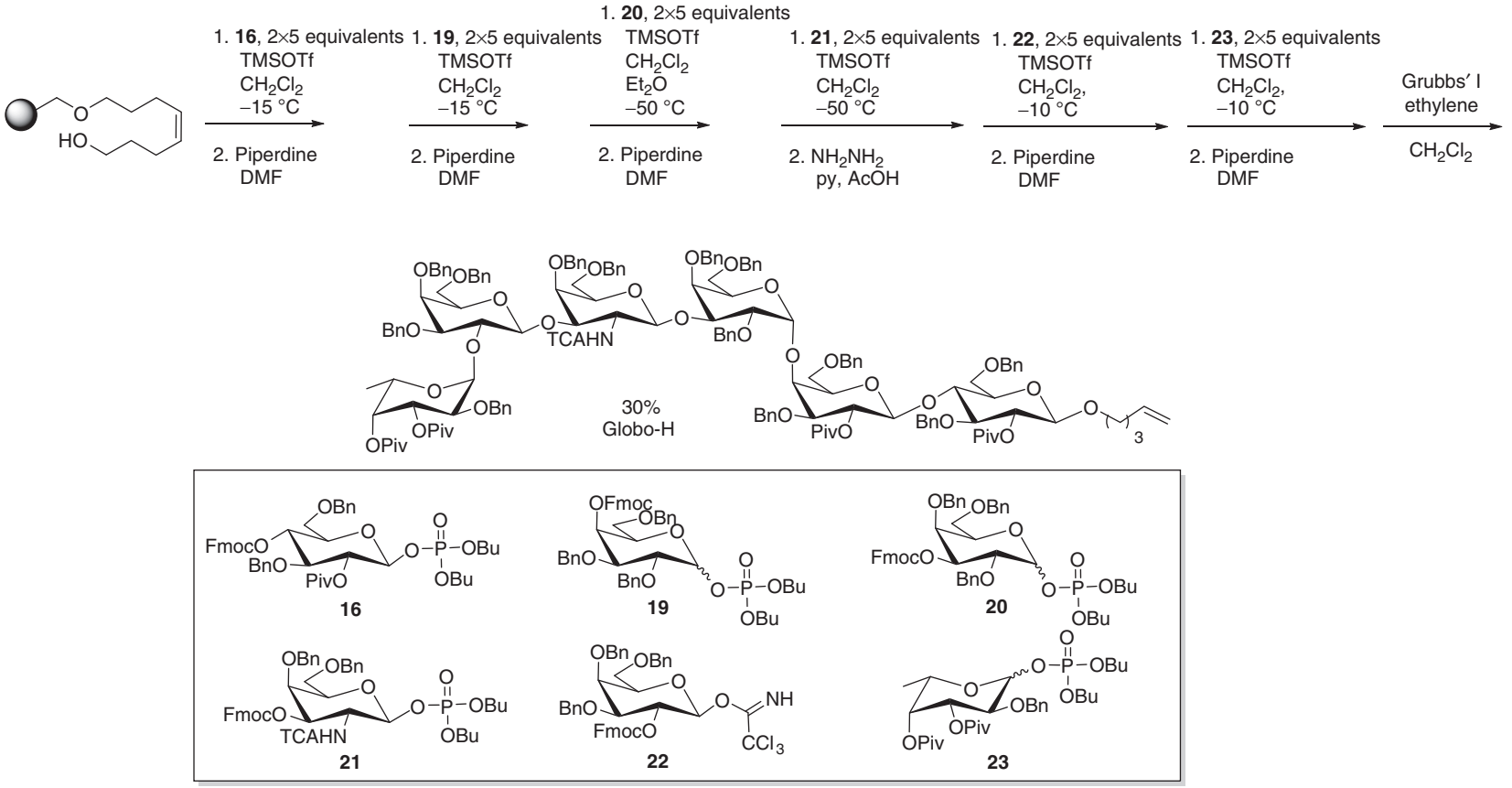
9.05.7.6 Gb-3 and Globo-H

The cancer antigen glycosphingolipids Gb-3 (Scheme 14) and Globo-H (Scheme 15) are of interests for vaccine development.[46] In addition, Gb-3 has recently been shown to play a role in HIV infectivity.[47] Gb-3 and Globo-H were synthesized in record time using an automated solid-phase approach employing the first-generation automated oligosaccharide synthesizer.[48] A *cis* α-galactosidic linkage linked to the axial C4 hydroxyl group of a second galactose residue is common motif to both glycans and presents a significant challenge in solution and in automation. After careful screening, it was determined that galactosyl imidate **18** (Gb-3) or galactosyl phosphate **19** (Globo-H), both containing a nonparticipating benzyl group at C2, could be used to selectively install this linkage efficiently. The protected oligosaccharides were subsequently assembled using octenediol-functionalized Merrifield resin under standard glycosylation conditions. Functionalized monosaccharides **16** through **18** were used to synthesize the Gb-3 trisaccharide (Scheme 14) in 46% yield with 77% coupling efficiency. Globo-H hexasaccharide was synthesized from building block **16**, and building blocks **19** through **23** in 25 h (Scheme 15) and 30% yield with a coupling efficiency of 82% per step.

The development of the second-generation automated solid-phase oligosaccharide synthesizer and the bifunctional linker led to the first automated synthesis of iso Gb-3 (Scheme 16), a glycan of biological interest due to its homology with Gb-3.[8] The synthesis of iso Gb-3 marked the first automated solid-phase oligosaccharide synthesis using a 'double coupling' strategy employing only differentially functionalized thioglycoside building blocks. The first glucose residue was installed by glycosylation of glucosyl thioglycoside building block **24**, functionalized with a permanent participating C2 Piv group and a temporary Fmoc group at C4 with bifunctional linker-functionalized Merrifield resin using an NIS/TfOH promoter system. After hydrolysis of the Fmoc group using piperdine, subsequent glycosylation/deprotection cycles, first with galactosyl thioglycoside building block **25** with a participating pivaloate C2 protecting group and a temporary Fmoc group at C3, followed by glycosylation with galactosyl thioglycoside building block **26** with a nonparticipating C2 Bn group provided the desired glycan in 80% yield (93% yield

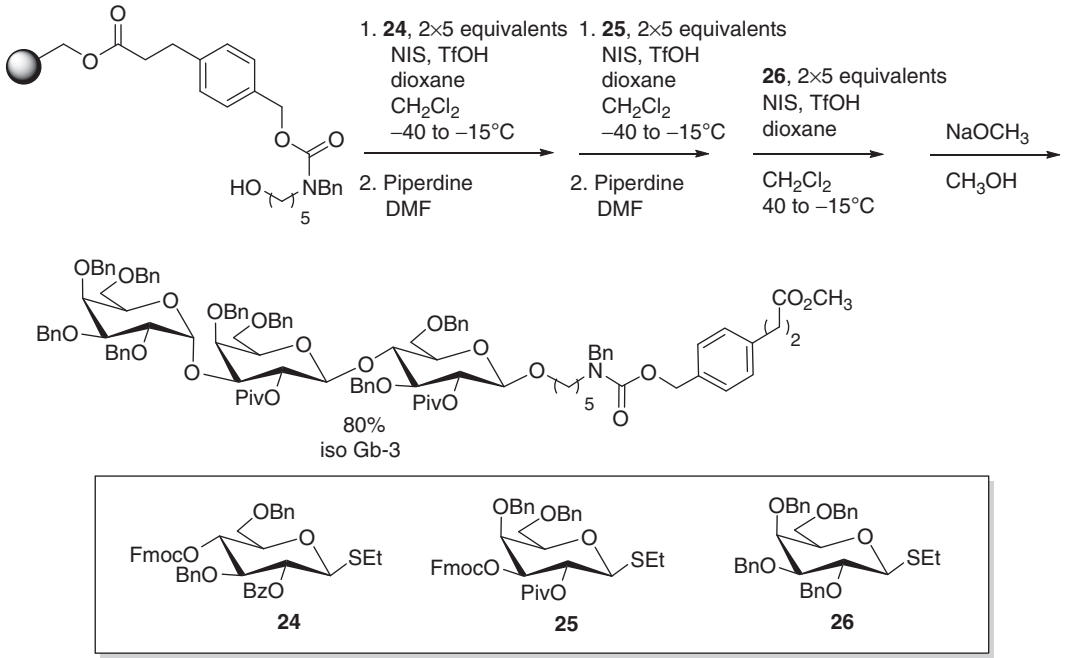


Scheme 14 Gb-3.



Scheme 15 Globo-H.

coupling efficiency) after cleavage from the resin using Zemplén conditions. The installation of the nonreducing terminal galactose building block **26** represented the greatest challenge.



Scheme 16 Iso Gb-3.

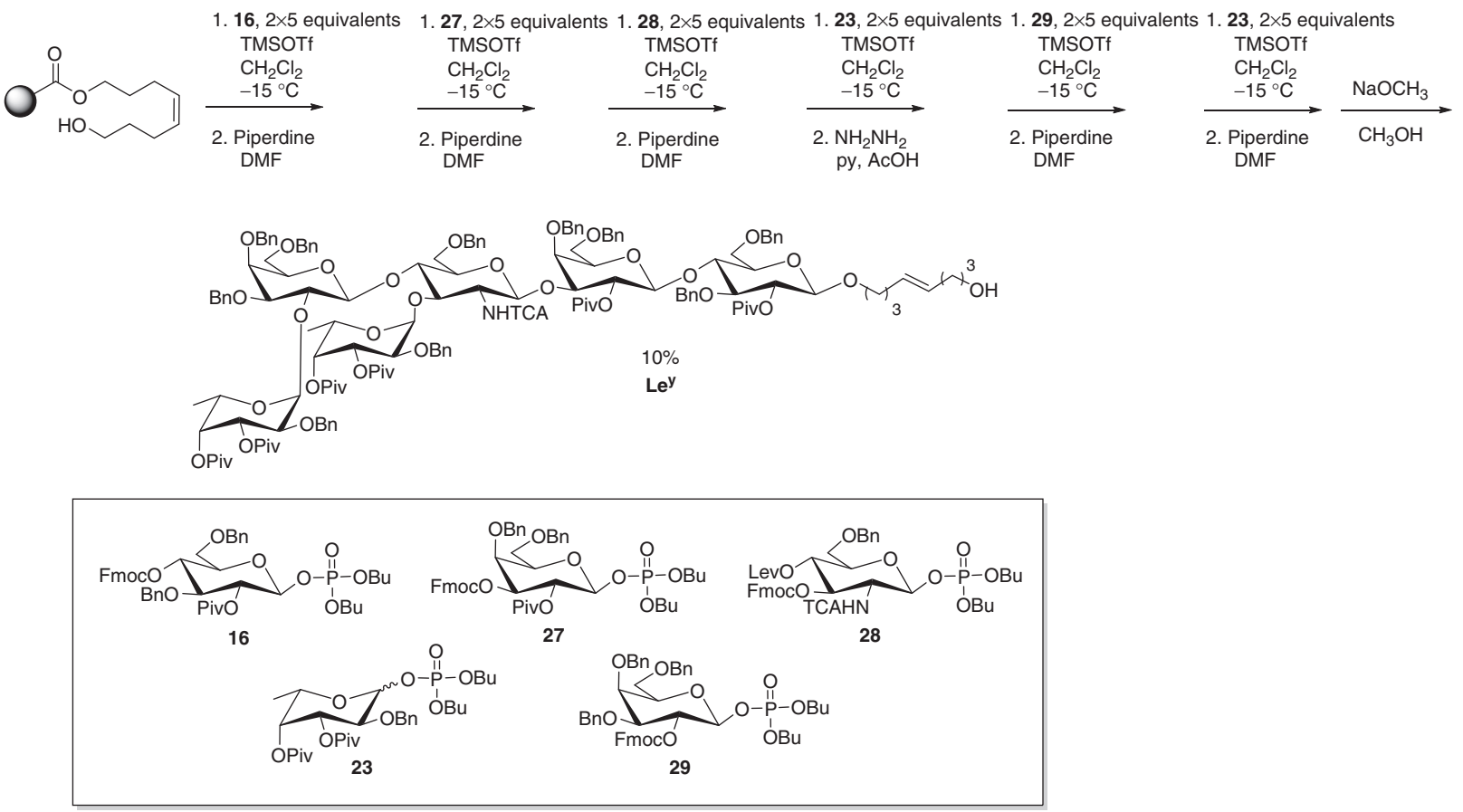
9.05.7.7 Blood Group Antigens

The type II Lewis blood group oligosaccharides Le^y (hexasaccharide) and Le^y–Le^x (nonasaccharide) are of interest as potential cancer vaccines.[49] Their complexity, including the number and different types of carbohydrate residues and challenging linkages, render them significant challenges for automated solid-phase oligosaccharide synthesis. The first automated synthesis of Le^y and Le^y–Le^x employed the first-generation automated oligosaccharide synthesizer, an ester-linked octenediol-functionalized linker, and five differentially functionalized phosphate building blocks: **16**, **27**, **28**, **23**, and **29**, under standard glycosylation conditions.[50] Fmoc and Lev groups were used as temporary protecting groups whereas Piv and TCA groups were used as C2 directing groups with the exceptions of galactose building block **29**, which used a C2 Fmoc group as both a temporary protecting and directing group, and fucose building block **23,** which required a nonparticipating group to install the desired *cis* linkage. The synthesis of Le^y is shown in Scheme 17. Successive 'double coupling' of building blocks **16**, **27**, **28**, **23**, **29**, and **29** gave the desired hexasaccharide in 10% yield after cleavage from the resin using Zemplén conditions. After each double coupling, the Fmoc or Lev protecting group was removed using piperdine or hydrazine, respectively. The Le^y–Le^x nonasaccharide was synthesized using a similar protocol (Scheme 18) to produce the desired product in 6.5% yield after cleavage from the resin.

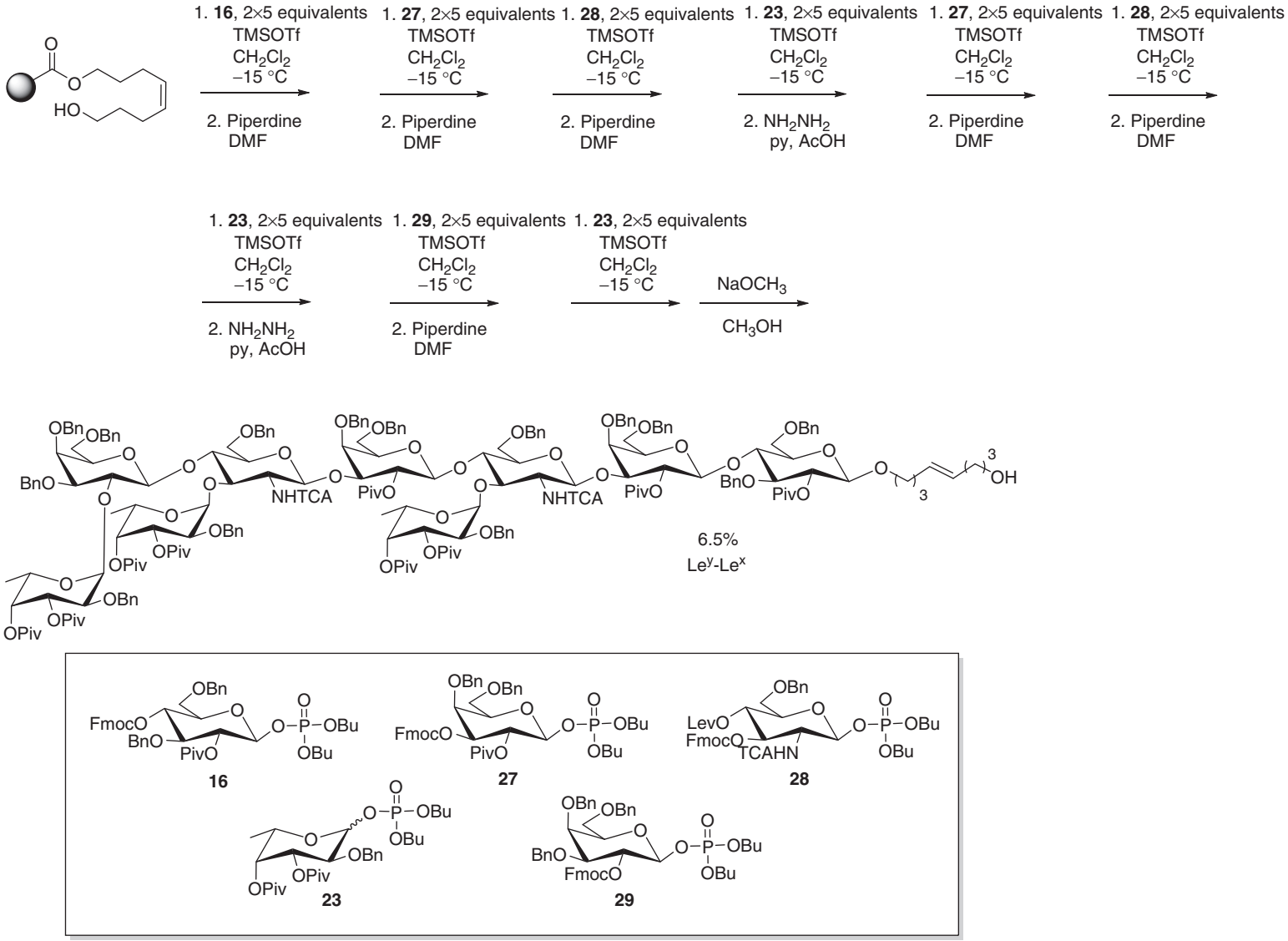
Sialic acid containing glycans mediate pathogen invasion and modulate important roles in cellular communication.[51] Despite their significance, the chemical synthesis of these glycans has been limited by the challenging installation of the sialic acid residue, which is often accomplished in low yield and limited selectivity. The automated solid-phase oligosaccharide synthesis of Sialyl $Lewis^x$ (SLe^x), a tetrasaccharide involved in inflammation and metastasis, demonstrated that sialic acid residues could be installed in automation.[8] The second-generation automated oligosaccharide synthesizer, bifunctional linker-functionalized Merrifield Resin and a 'double coupling' strategy employing three building blocks: glucosylamine thioglyoside **30** with a TCA participating group at C2 and temporary Fmoc and Lev protecting groups at C3 and C4; disaccharide imidate **31** containing an acetate participating group at C2; and fucosyl imidate **32** with a nonparticipating Bn group at C2 were required to complete the synthesis of SLe^x in just over 50% yield (80% coupling efficiency). The key to the success of this synthesis was the preparation of the disaccharide building block **31** incorporating the sialic acid residue. This method was applied to several sialyl lactose and sialyl lactosamine derivatives in excellent yields (Scheme 19).[52]

9.05.7.8 Oligoglucose

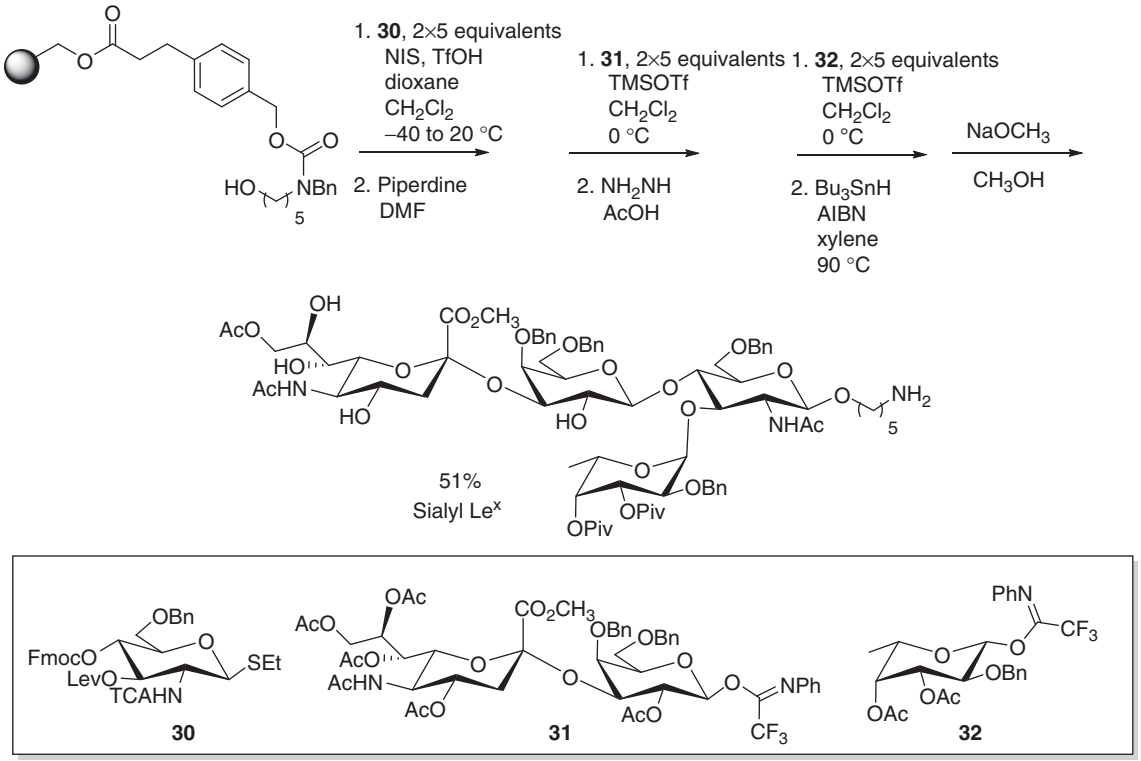
An HPLC-based automated oligosaccharide synthesizer was recently employed by Demchenko and co-workers in the generation of several β-(1→6) linked oligosaccharides.[4] The initial glucose residue containing a participating Bz group at C2 and a temporary trityl group at C6 was coupled to TentaGel resin using EDC and DMAP on column and then detritylated with wet TFA to expose



Scheme 17 Le^y.

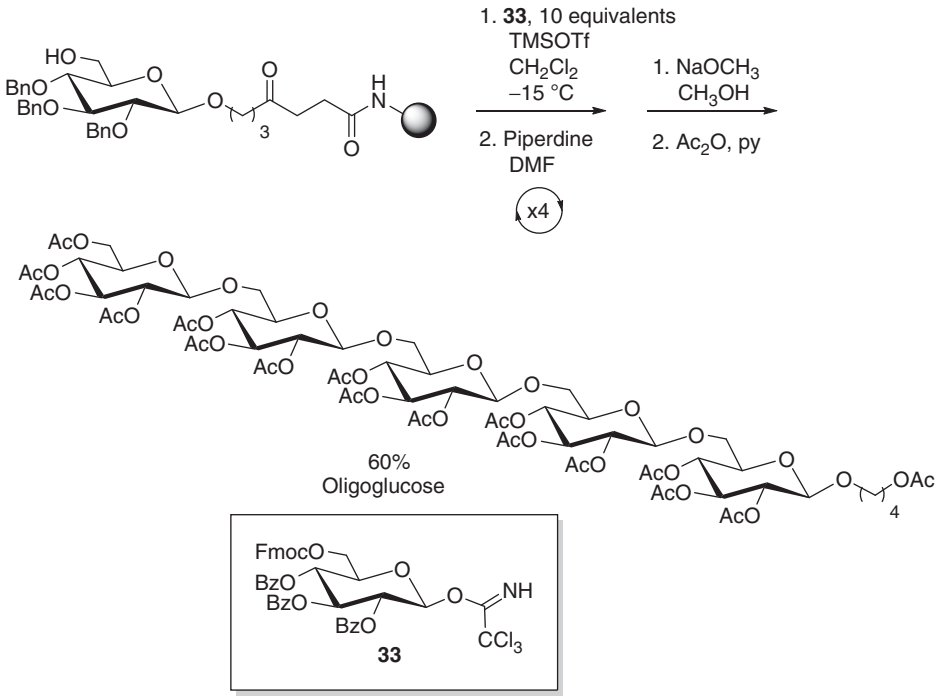


Scheme 18 Le^y–Le^x.



Scheme 19 Sialyl Le^x.

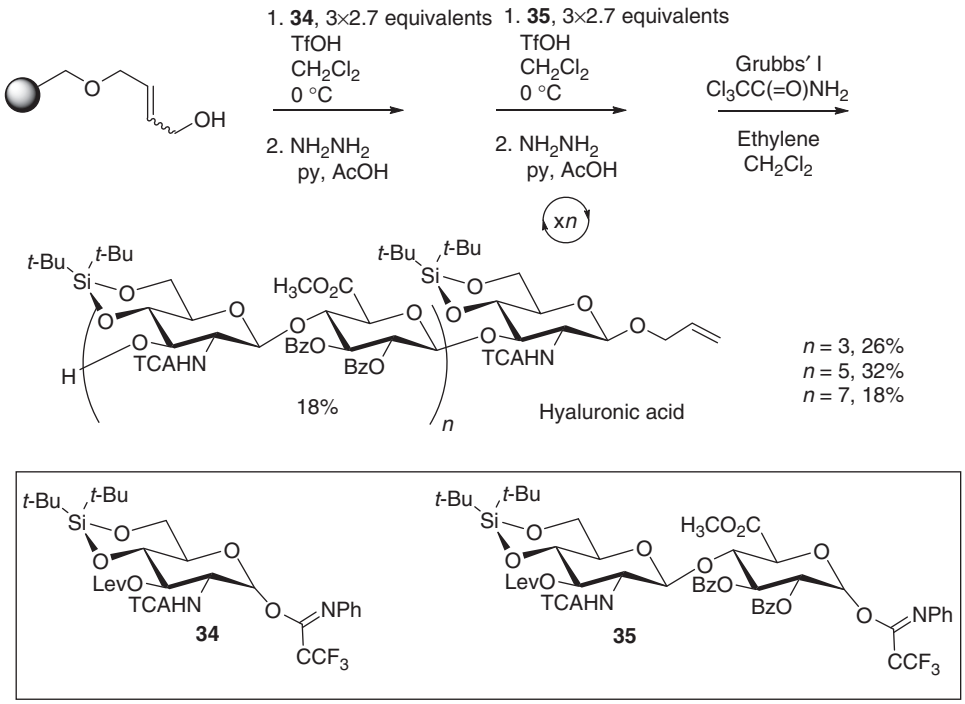
the C6 hydroxymethyl group for subsequent glycosylation (not shown). Four additional glycosylation/deprotection sequences using glucose building block **33**, with a participating Bz at C2 and a temporary Fmoc group at C6 gave the desired pentasaccharide in 60% yield and a coupling efficiency of approximately 90% after cleavage from the resin using Zemplén conditions (Scheme 20). The fully deprotected pentasaccharide was reacetylated to simplify purification.



Scheme 20 Oligoglucose.

9.05.7.9 Hyaluronan Oligosaccharides

Hyaluronic acids are glycosylaminoglycans composed of repeating units of glucuronic acid and *N*-acetylglucosamine monosaccharides. Hyaluronic acids function as molecular lubricants and have also been shown to play important roles in the inflammatory response, cell proliferation, recognition, migration, and adhesion.[53] The first automated solid-phase synthesis of well-defined hyaluronic acids employed the second-generation automated synthesizer. Butenediol-functionalized Merrifield resin and a 'triple coupling' strategy using 3 equivalents of two di-tert-butylsilylidene-protected imidate building blocks **34** and **35** (Scheme 21) incorporating C2 participating groups (TCA for building block **34** and Bz for building block **35**) and Lev groups as temporary protecting groups.[7] Activation of glucosylamine imidate **34** using TfOH, which was demonstrated to be more efficient than TMSOTf, followed by hydrolysis of the Lev protecting group with hydrazine and iterative glycosylation reactions with disaccharide **35** gave the desired glycans in 18–26% yield ($n=3$, 5, or 7) after cross-metathesis from the resin. Interestingly, the authors demonstrated that direct glycosylation of disaccharide **35** to the linker was unsuccessful, necessitating the synthesis of building block **34**. In addition, removal of the glycan from the resin using cross-metathesis using Grubbs' catalyst proved challenging due to the partial dechlorination of the TCA group. The use of a decoy substrate, trichloracetamide, was used to circumvent this unwanted reaction.



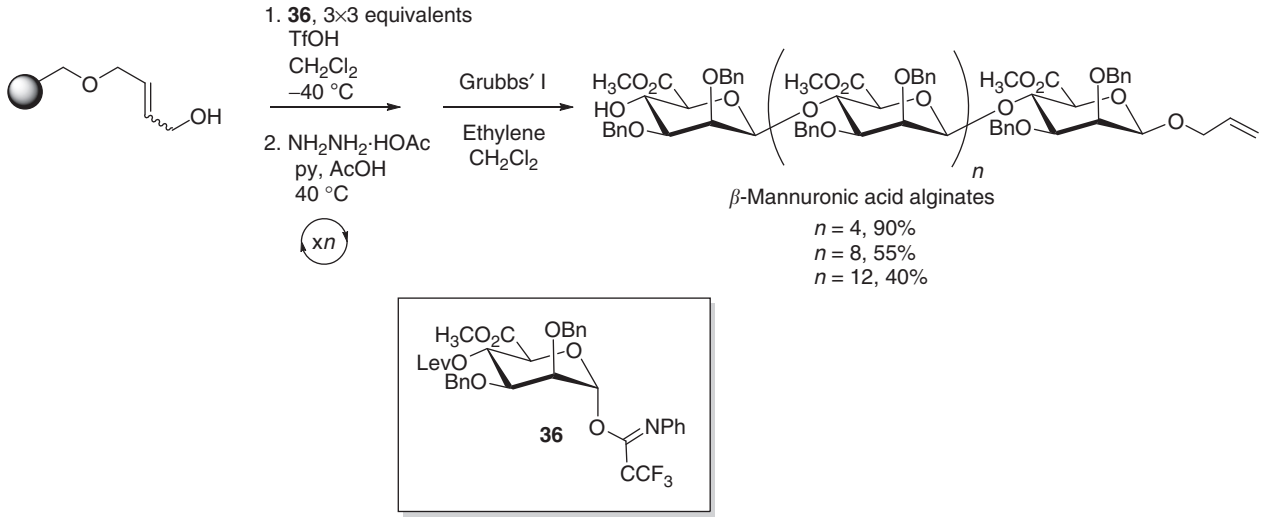
Scheme 21 Hyaluronic acid.

9.05.7.10 β-Mannuronic Acids Alginates

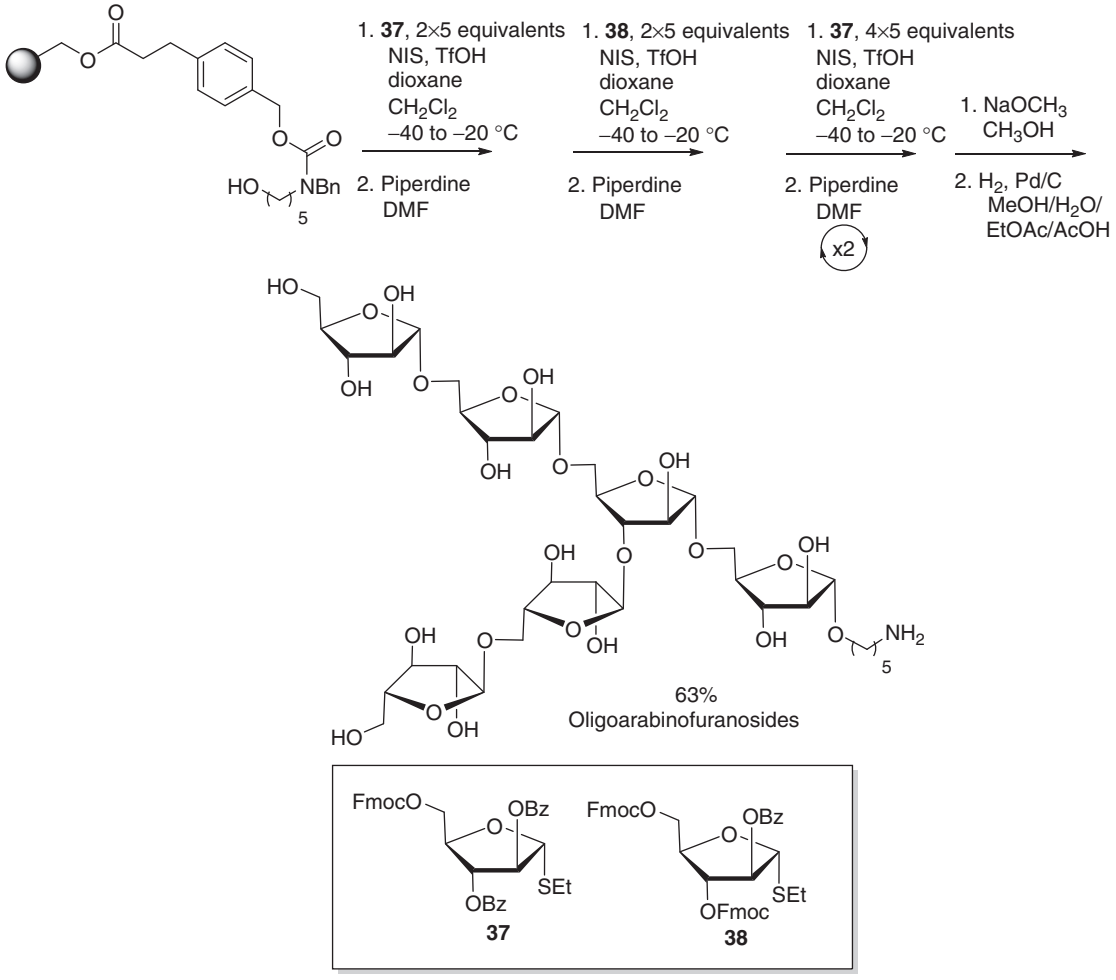
β-Mannuronic acid alginates are major components of the cell wall of algae. They are also major constituents of the *exo*-polysaccharides of *Pseudomonas aerigunosa*,[54] an opportunistic, nonsocomial gram-negative bacterium. The automated synthesis of tetra-, octa-, and dodeca-β-mannuronic acid alginates via automated solid-phase oligosaccharide synthesis was recently reported using the second-generation automated oligosaccharide synthesizer, butenediol-functionalized Merrifield resin, and a mannuronic imidate building block **36** functionalized with a nonparticipating Bn at C2 and a temporary Lev protecting group at C4 (Scheme 22).[55] The major challenge with this synthesis was the selective installation of each β-mannosidic residue. TfOH was found to be the most effective promoter and the reaction was found to be completely selective at temperatures near the decomposition of the donor ($-40\ ^{\circ}C$). Each glycosylation cycle required hydrolysis of the Lev group using hydrazine. The first oligosaccharide synthesized, a tetrasaccharide, was prepared using four glycosylation/deprotection cycles in 90% yield with approximately 98% coupling efficiency. The octasaccharide and dodecasaccharides were synthesized with 90% coupling efficiency at each step providing the final products in 55% and 40%, respectively.

9.05.7.10.1 Oligoarabinofuranosides

The first automated solid-phase oligosaccharide synthesis of oligoarabinofuranosides was recently reported.[56] Oligoarabinofuranosides and their analogs are the major components of mycobacterial cell envelopes and play important roles in a number of



Scheme 22 β-Mannuronic acid alginates.



Scheme 23 Oligoarabinofuranosides.

critical aspects of the life cycle of the mycobacterium.[57–59] The versatility of the second-generation synthesizer combined with the use of the bifunctional linker provided for the synthesis of a series of linear and branched oliogarabinofuranosides from the sequential 'double coupling' of two thiofuranosides **37** and **38**, both of which contained a Bz participating group at C2 and

temporary F-moc protecting groups at C5 (**37**) or C4 and C5 (**38**). The use of NIS/TfOH as a promoter system was shown to provide the best yields and selectivites. Piperdine was used to remove the Fmoc protecting groups in between coupling cycles. Overall, this process was shown to be efficient and rapid – the hexasaccharide in **Scheme 23** was prepared with 63% yield and 92% coupling efficiency in 14 h.

9.05.8 Conclusion

Fully automated solid-phase synthetic oligosaccharide platforms and new linker strategies have streamlined access to a host of carbohydrate constructs including bacterial and viral antigens, cancer antigens, vaccine candidates, and *N*-linked oligosaccharides. This has led to an increase in the general understating of the fundamental roles of these oligosaccharides in a number of biological processes. Current research is directed at identifying monosaccharide building blocks that can be used to access the major glycoconjugate classes including *N*-linked, *O*-linked, glycolipids, and glycosylaminoglycans. These oligosaccharides will be used to study important carbohydrate–protein, carbohydrate–nucleic acid, and carbohydrate–carbohydrate interactions involved in normal and abnormal cellular processes. The development of rapid and efficient synthetic protocols for commercialization of these building blocks is the next critical step for expanding the automated solid-phase platform for oligosaccharide synthesis.

References

1. Plante, O. J.; Palmacci, E. R.; Seeberger, P. H. *Science* **2001**, *291*, 1523–1527.
2. Castro, M.; Ralston, N. V.; Morgenthaler, T. I.; Rohrback, M. S.; Limper, A. H. *Infect. Immun.* **1994**, *62*, 3138–3145.
3. Werz, D. B.; Castagner, B.; Seeberger, P. H. *J. Am. Chem. Soc.* **2007**, *129*, 2770–2771.
4. Ganesh, N. V.; Fujikawa, K.; Tan, Y. H.; Stine, K. J.; Demchenko, A. V. *Org. Lett.* **2012**, *14*, 3036–3039.
5. Frechet, J. M. J.; Schuerch, C. *J. Am. Chem. Soc.* **1971**, *93*, 492–496.
6. Bayer, E. *Angew. Chem. Int. Ed. Engl.* **1991**, *30*, 113–126.
7. Walvoort, M. T. C.; Volbeda, A. G.; Reintjens, N. R. M.; *et al. Org. Lett.* **2012**, *14*, 3776–3779.
8. Kröck, L.; Esposito, D.; Castagner, B.; *et al. Chem. Sci.* **2012**, *3*, 1617–1622.
9. Laine, R. A. *Glycobiology* **1994**, *4*, 759–767.
10. Wertz, D. B.; Ranzinger, R.; Herget, S.; *et al. ACS Chem. Biol.* **2007**, *2*, 685–691.
11. Nakamura, S.; Nambu, H.; Hashimoto, S. Phosphates, Phosphites and Other O–P Derivatives. In *Handbook of Chemical Glycosylation*; Demchenko, A. V., Ed.; Wiley-VCH: New York, **2008**, pp 223–250.
12. Zhu, X.; Schmidt, R. R. Glycoside Synthesis from 1-Oxygen-Substituted Glycosyl Imidates. In *Handbook of Chemical Glycosylation*; Demchenko, A. V., Ed.; Wiley-VCH: New York, **2008**, pp 143–185.
13. Zhong, W.; Boons, G.-J. Glycoside Synthesis from 1-Sulfur/Selenium-Substituted Derivatives. In *Handbook of Chemical Glycosylation*; Demchenko, A. V., Ed.; Wiley-VCH: New York, **2008**, pp 261–361.
14. Gioeli, C.; Chattopadhyay, J. B. *J. Chem. Soc. Chem. Commun.* **1982**, 672–673.
15. Hassner, A.; Strand, G.; Rubinstein, M.; Patchornik, A. *J. Am. Chem. Soc.* **1975**, *97*, 1614–1615.
16. Corey, E. J.; Venkateswarlu, A. *J. Am. Chem. Soc.* **1972**, *94*, 6190–6191.
17. Fukuzawa, A.; Sato, H.; Masamune, T. *Tetrahedron Lett.* **1987**, *28*, 4303–4306.
18. Heathcock, C. H.; Ratcliffe, R. *J. Am. Chem. Soc.* **1971**, *93*, 1746–1757.
19. Meyer, W. *Chem. Ber.* **1968**, *101*, 3802.
20. Brimacombe, J. S.; Bryan, J. G. H.; Husain, A.; Stacey, M.; Tolley, M. S. *Carbohydr. Res.* **1967**, *3*, 318–324.
21. Williams, D. T.; Jones, J. K. N. *Can. J. Chem.* **1967**, *45*, 7–9.
22. Hill, S.; Hough, L.; Richardson, A. C. *Carbohydr. Res.* **1968**, *8*, 7–18.
23. Guthrie, R. D.; Liebmann, J. A. *Carbohydr. Res.* **1974**, *33*, 355–358.
24. Seeberger, P. H.; Bauman, M.; Zhang, G.; *et al. Synlett* **2003**, *9*, 1323–1326.
25. Luo, S.-Y.; Thopate, S. R.; Hsu, C.-Y.; Hung, S.-C. *Tetrahedron Lett.* **2002**, *43*, 4889–4892.
26. Liu, J.; Numa, M. M. D.; Liu, H.; *et al. J. Org. Chem.* **2004**, *69*, 6273–6283.
27. Robins, M. J.; Hawrelak, S. D.; Kanai, T.; Siefert, J.-M.; Mengel, R. *J. Org. Chem.* **1979**, *44*, 1317–1324.
28. Haines, A. H. *Adv. Carbohydr. Chem. Biochem.* **1976**, *33*, 11–109.
29. Love, K. R.; Seeberger, P. H. *J. Org. Chem.* **2005**, *70*, 3168–3177.
30. Weber, H.; Khorana, H. G. *J. Mol. Biol.* **1972**, *72*, 219–249.
31. Zhdanov, R. I.; Zhenodarvoa, S. M. *Synthesis* **1975**, *4*, 222–245.
32. Plattner, J. J.; Gless, R. D.; Rapoport, H. *J. Am. Chem. Soc.* **1972**, *94*, 8613–8615.
33. Mootoo, D. R.; Konradsson, P.; Udodong, U.; Fraser-Reid, B. *J. Am. Chem. Soc.* **1998**, *110*, 5583–5584.
34. Konradsson, P.; Mootoo, D. R.; McDevitt, R. E.; Fraser; Reid, B. *J. Chem. Soc. Chem. Commun.* **1990**, 270–272.
35. Konradsson, P.; Udodong, U. E.; Fraser- Reid, B. *Tetrahedron Lett.* **1990**, *31*, 4313–4316.
36. Hewitt, M. C.; Seeberger, P. H. *Org. Lett.* **2001**, *3*, 3699–3702.
37. Schofield, L.; Hewitt, M. C.; Evans, K.; Siomos, M. A.; Seeberger, P. H. *Nature* **2002**, *418*, 785–789.
38. Hewitt, M. C.; Snyder, D. A.; Seeberger, P. H. *J. Am. Chem. Soc.* **2002**, *124*, 13434–13436.
39. McKenney, D.; Pouliot, K. L.; Wang, Y.; *et al. Science* **1999**, *284*, 1523–1527.
40. McKenney, D.; Pouliot, K. L.; Wang, Y.; *et al. J. Biotechnol.* **2000**, *83*, 37–44.
41. Melean, L. G.; Love, K. R.; Seeberger, P. H. *Carbohydr. Res.* **2002**, *337*, 1893–1916.
42. Feizi, T. Glycobiology of AIDS. In *Carbohydrates in Chemistry and Biology*; Ernest, B., Hart, G. W., Sinaÿ, P., Eds.; Wiley-VCH: New York, **2000**, pp 851–863.
43. Lin, G.; Simmons, G.; Pohlmann, S.; *et al. J. Virol.* **2003**, *77*, 1337–1346.
44. Delmas, B; Laude, H. *Virus Res.* **1991**, *20*, 107–120.
45. Ratner, D. M.; Swanson, E. R.; Seeberger, P. H. *Org. Lett.* **2003**, *5*, 4717–4720.

46. Slovin, S. F.; Ragapathi, G.; Adluri, S.; *et al. Proc. Natl. Acad. Sci. USA* **1999**, *96*, 5710–5715.
47. Puri, A.; Hug, P.; Jernigan, K.; *et al. Proc. Natl. Acad. Sci. USA* **1998**, *95*, 14435–14440.
48. Wertz, D. B.; Castagner, B.; Seeberger, P. H. *J. Am. Chem. Soc.* **2007**, *129*, 2770–2771.
49. Ragupathi, G.; Deshpande, P. P.; Coltart, D. M.; *et al. Int. J. Cancer* **2002**, *99*, 207–212.
50. Love, K. R.; Seeberger, P. H. *Angew. Chem. Int. Ed.* **2004**, *43*, 602–605.
51. Angata, T.; Varki, A. *Chem. Rev.* **2002**, *102*, 439–469.
52. Esposito, D.; Hurevich, M.; Castagner, B.; Wang, C.-C.; Seeberger, P. H. *Beilstein J. Org. Chem.* **2012**, *8*, 1601–1609.
53. Esko, J. D.; Kimata, K.; Lindahl, U. Proteoglycans and Sulfated Glycosaminoglycans. In *Essentials of Glycobiology*; Varki, A., Cummings, R. D., Esko, J. D., *et al.*, Eds.; Cold Spring Harbor Laboratory Press: New York, **2009**, pp 7462–7468.
54. Campodónico, V. L.; Llosa, N. J.; Bentancor, L. V.; Maira-Litran, T.; Pier, G. B. *Infect. Immun.* **2011**, *79*, 3455–3464.
55. Walvoort, M. T. C.; van den Elst, H.; Plante, O. J.; *et al. Angew. Chem. Int. Ed. Engl.* **2012**, *51*, 4393–4396.
56. Kandasamy, J.; Hurevich, M.; Seeberger, P. H. *Chem. Comm.* **2013**, *49*, 44453–44455.
57. Zhang, J.; Angala, S. K.; Pramanik, P. K.; *et al. ACS Chem Biol.* **2011**, *6*, 819–828.
58. Zhang, J. A.; Amin, A. G.; Holemann, A.; Seeberger, P. H.; Chatterjee, D. *Bioorg. Med. Chem.* **2010**, *18*, 7121–7131.
59. Khasnobis, S.; Zhang, J.; Angala, S. K.; *et al. Chem. Biol.* **2006**, *13*, 787–795.

9.06 The Use of Preparative Chiral Chromatography for Accessing Enantiopurity in Pharmaceutical Discovery and Development

CJ Welch, Merck Research Laboratories, Rahway, NJ, USA

© 2014 Elsevier Ltd. All rights reserved.

9.06.1	**Introduction**	143
9.06.2	**Fundamentals of Stereochemistry**	143
9.06.3	**Fundamentals of Chromatography and the Chromatographic Separation of Enantiomers**	144
9.06.3.1	Preparative Chiral Chromatography: One of Many Choices for Accessing Enantiopurity	145
9.06.3.2	Preparative Chiral Chromatography: A Platform Approach with a Head-Start Advantage	146
9.06.3.3	The Stationary Phase in Preparative Chiral Chromatography	146
9.06.4	**Preparative Chromatography Instrumentation, Supercritical Fluid Chromatography, and Green Chromatography**	150
9.06.5	**Chromatographic Productivity**	150
9.06.6	**Method Development**	151
9.06.7	**The Role of Preparative Chromatography in Organic Synthesis**	152
9.06.8	**Examples and Case Histories**	152
9.06.9	**Conclusion**	158
References		158

Glossary

Chromatographic selectivity (α) A measure of the degree of the chromatographic separation – equal to the ratio of the adsorption equilibrium constants for the two species.

KKD Kilograms purified product per kilogram of stationary phase per 24 h day. A unit of chromatographic productivity.

Retention factor (k') A measure of the degree of retention of a chromatographic peak – equal to the ratio of time spent adsorbed versus free in solution.

9.06.1 Introduction

In the past few years, chiral chromatography has emerged as a preferred method for rapidly accessing enantiopure materials on small-to-medium scale in pharmaceutical discovery and development.[1–7] Owing to the relatively recent widespread adoption of the technique, many practicing synthetic chemists today have received only cursory formal introduction to the practice of preparative chromatographic enantioseparation or the incorporation of this technique into organic syntheses. Most practicing preparative chromatographers have instead learned these skills on the job. In the hopes of providing a clear introduction to this important and useful technique, the authors present here an overview of the key concepts relating to preparative chromatographic separation of enantiomers, and the strategic use of the technique within organic syntheses.

9.06.2 Fundamentals of Stereochemistry

Most readers will already be familiar with stereochemistry fundamentals, some highlights of which are recapped here:

- Most molecules are 'chiral', i.e., they cannot be superimposed on their mirror images.
- Only those simple and symmetrical structures that show a plane, center, or alternating axis of symmetry are 'achiral'.
- The two mirror image forms of a chiral molecule are called 'enantiomers', and a mixture comprised of equal amounts of the two enantiomers is called a 'racemic mixture' or 'racemate'.
- A mixture containing an excess of one enantiomer is said to be 'enantioenriched', whereas a mixture containing exclusively one enantiomer is said to be 'enantiopure'.
- Enantioenrichment is typically reported in terms of % *ee* or 'enantiomeric excess' using the relationship $ee = (\text{major} - \text{minor})/(\text{major} + \text{minor})$, where major and minor refer to the relative amounts of the more and less prevalent enantiomers. Alternatively, enantioenrichment is sometimes reported in terms of *er* or 'enantiomeric ratio', a more straightforward term that simply describes the ratio of the major to minor enantiomer.[8]
- A process wherein a racemic mixture is separated into its two component enantiomers is termed a 'resolution', and a process wherein enantioenriched mixture is converted to a racemate is termed a 'racemization'.
- As all living systems are enantioenriched, the two enantiomers of a chiral drug can have different physiological effects, leading to the development of most new chiral drugs as single enantiomers, and making the topic of chirality especially important in the pharmaceutical industry today.[9,10]

The interested reader should consult a standard reference[11,12] for a more comprehensive treatment of organic stereochemistry concepts.

9.06.3 Fundamentals of Chromatography and the Chromatographic Separation of Enantiomers

Chromatographic separation depends on the differential adsorption of compounds by a chromatographic stationary phase that is packed into a column through which a mobile phase flows (Figure 1). Compounds in solution, when brought into contact with an adsorbent stationary phase, can have differing adsorption equilibria. In the example presented in Figure 1(b), adsorption of blue squares is favored (three adsorbed, one free) relative to adsorption of yellow circles (two adsorbed, two free). When applied to a column containing the same stationary phase and eluted with mobile phase, compounds with differing adsorption equilibria

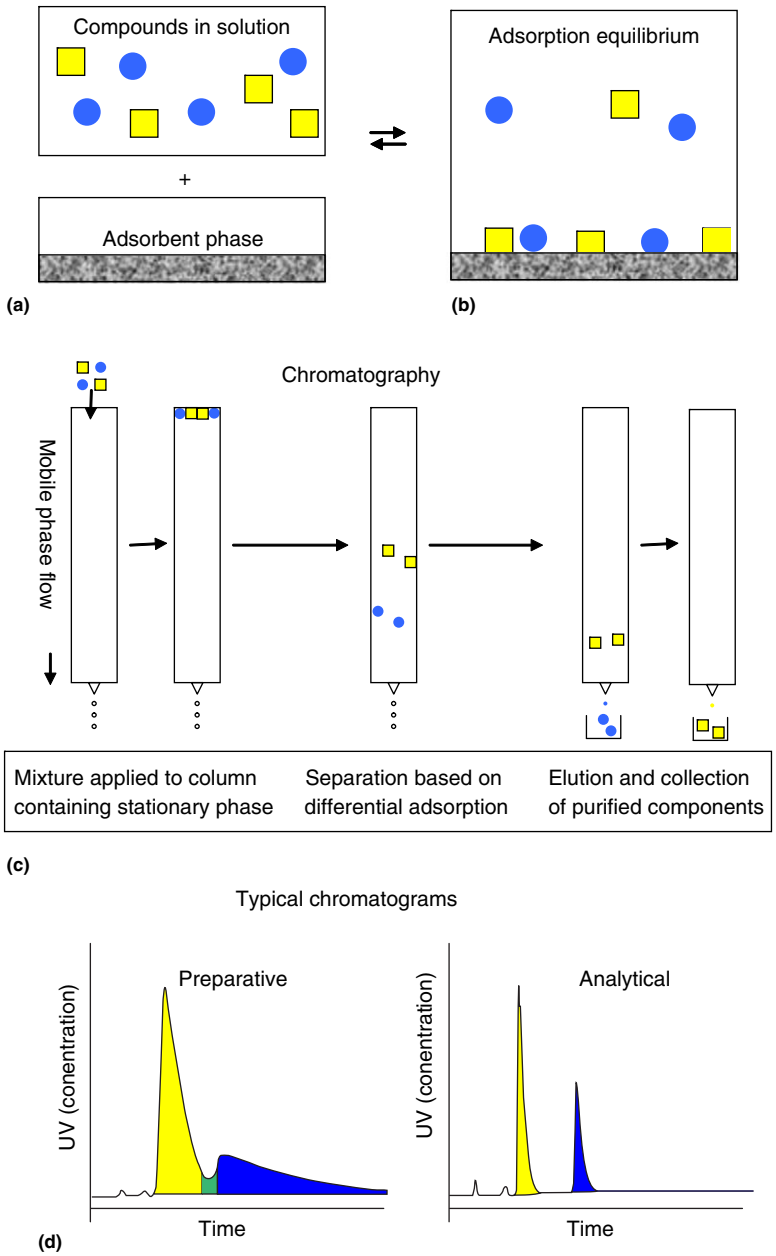


Figure 1 Principles of chromatographic separation. Compounds in solution (a) when brought in contact with an adsorbent stationary phase (b) may have differing adsorption equilibria – in this example, adsorption of yellow squares is favored (three adsorbed, one free) relative to adsorption of blue circles (two adsorbed, two free). When applied to a column containing the same stationary phase and eluted with mobile phase, compounds with differing adsorption equilibria are chromatographically resolved (c). Detection of compounds eluting from a chromatography column affords a chromatogram, a record of the separation (d).

can be chromatographically resolved (Figure 1(c)). Detection of compounds eluting from a chromatography column affords a chromatogram, a record of the separation (Figure 1(d)). Collection of the individual compounds eluting from a chromatography column can be used as a means of compound purification.

The chromatographic separation of enantiomers requires that the experiment depicted in Figure 1 be conducted in an enantioenriched environment. Usually this involves the use of an enantioenriched chiral stationary phase (CSP), depicted in Figure 2. Chromatographic separation of enantiomers using enantioenriched mobile phase additives in the presence of an achiral column is also possible, although this approach is seldom used in practice. When a mixture of enantiomers is injected at the head of the column, selective adsorption of one of the enantiomers leads to an increased residence time for that enantiomer in the column. The degree of adsorption of each enantiomer is described by the retention factor $k' = (t - t_0)/t_0$, where t is the retention time of the peak in question and t_0 is the retention time of an unretained void marker.[13] The retention factor k' is proportional to the equilibrium constant for adsorption, and describes the ratio of the time that the analyte spends adsorbed on the CSP relative to the time spent in the mobile phase.

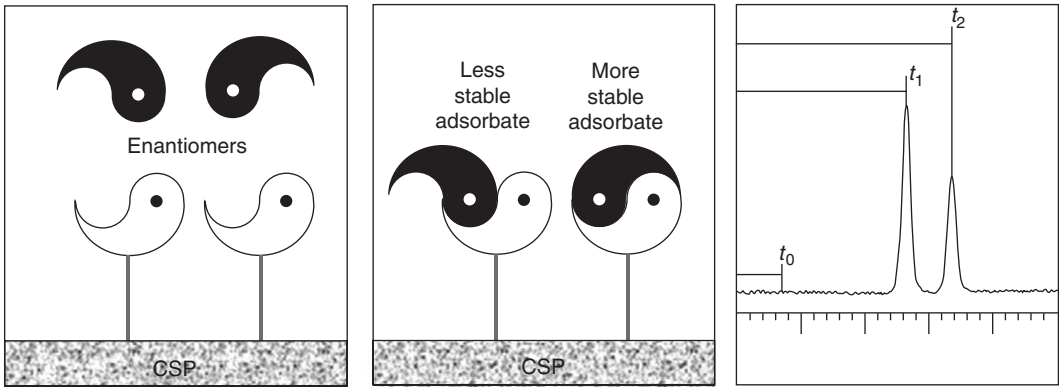


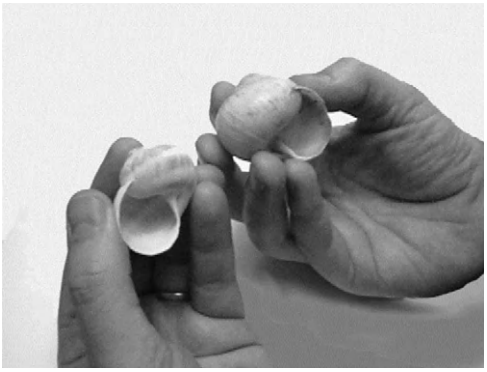
Figure 2 Chromatographic resolution of enantiomers (a). Differential adsorption of enantiomers by an enantioenriched CSP (b) leads to the formation of diastereomeric adsorbates of differing free energy (c) which are retained on the CSP to varying degrees. The retention factor (k') of a given peak is defined as $(t_n - t_0)/t_0$. The chromatographic selectivity, α, is defined as the ratio of the k' more retained enantiomer/k' less retained enantiomer.

The separation factor α characterizes the degree of chromatographic selectivity, and is given by the ratio of retention factors for the two enantiomers (k'_2/k'_1). Absence of separation for the two enantiomers corresponds to an α of 1.0. Typically, an α of at least 1.2 is required for convenient preparative chromatographic resolution, with larger separation factors being preferred and smaller separation factors being possible, although difficult. Separation factors as high as 10 are occasionally observed for pharmaceutical intermediates, and separation factors in excess of 100 are occasionally observed, although these are typically the product of some sort of structure – enantioselectivity design optimization.[14] In general, bigger separation factors are advantageous for preparative resolution of enantiomers, although other criteria are also important, as will be discussed later. Because the separation factor is the ratio of two numbers that are each proportional to adsorption equilibrium constants, α can be related directly to $\Delta\Delta G$, the difference in free energy of adsorption for the two enantiomer-stationary phase complexes, using the equation $\Delta\Delta G = -RT \ln \alpha$, where R is the universal gas constant and T is absolute temperature in Kelvin. Variable temperature chromatographic studies are sometimes used to further extract the enthalpic ($\Delta\Delta H$) and entropic ($\Delta\Delta S$) contributions to this free energy term, and are sometimes of value in studies of the mechanism of enantioselective adsorption.[15]

The chromatographic 'efficiency' is a measure of the ability of the column to elute a narrow chromatographic peak, characterized by the parameter N, with units given in 'theoretical plates'. Chromatographic efficiency increases as the size of the particles within the column is reduced. However, smaller particles also lead to an increase in system backpressure. Consequently, preparative chromatography separations often utilize larger particles than those traditionally used for analytical separations.[16]

9.06.3.1 Preparative Chiral Chromatography: One of Many Choices for Accessing Enantiopurity

It is worthwhile at the outset to show the technique of preparative chiral chromatography within the context of other competing approaches for accessing enantiopurity. There are two fundamentally different routes to obtaining enantiopure materials: synthesis and resolution. Synthetic approaches include 'chiral pool' strategies in which readily available starting materials are used as synthetic precursors, diastereoselective or 'chiral auxiliary' strategies in which a removable enantioenriched auxiliary is used to influence the stereochemistry at a newly forming stereocenter; and enantioselective synthesis strategies, in which the presence of some enantioenriched catalyst, reagent, additive, or force is used to influence the stereochemistry at a newly forming stereocenter. The interested reader is directed to any of a number of recent resources for additional information (Figure 3).[11,17–19]



Resolution
- Chromatography
- Diastereomeric salts
- Conglomerates
- Kinetic resolution

Enantioselective synthesis
- Chiral pool – 'chiron' approach
- Diastereoselective auxiliaries
- Catalysis
- Enzymatic methods

Figure 3 Many routes to enantiopurity. A variety of different routes are available for accessing pure enantiomers, and as there are currently not 'universal' techniques, process chemists must consider all approaches.

Resolution approaches for accessing enantiopurity involve some form of separation of the two enantiomers constituting a racemic mixture. The principal resolution approaches include classical resolution via diastereomeric salt formation, resolution of conglomerate crystals, kinetic resolution, and chromatographic resolution. Consideration of first principles of synthetic strategy suggests that all resolution approaches suffer from an inherent drawback, a maximum theoretical yield of only 50%, with the 50% corresponding to the undesired enantiomer being 'waste'. In some instances this drawback can be overcome with recycling of the undesired enantiomer enabling a higher yield (Figure 4).[20,21]

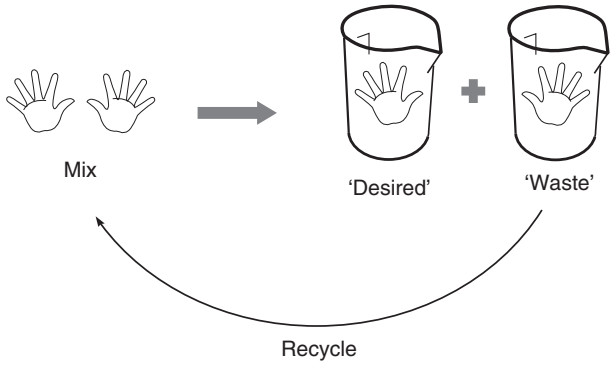


Figure 4 Overcoming the 'maximum 50% yield' problem. Recycling of undesired enantiomer via racemization is often key to the economic viability of large-scale resolution processes.

9.06.3.2 Preparative Chiral Chromatography: A Platform Approach with a Head-Start Advantage

Preparative chiral chromatography has a considerable head-start advantage relative to other synthetic or resolution strategies for accessing small amounts of the pure enantiomers of a novel compound. This advantage stems from the fact that in order to investigate the production of pure enantiomers via any of the techniques described above, one first needs an analytical method that will enable the measurement of enantiopurity. Because chiral chromatography has evolved to become the method of choice for stereochemical analysis, the first step in any investigation in enantioselective synthesis or resolution is typically the development of a chiral chromatographic assay, often carried out by automated method development screening of a number of column and mobile phase combinations.[22,23] Analytical chromatography conditions affording adequate resolution of enantiomers can normally be scaled up quickly to afford small amounts of purified enantiomers in the time that it takes to set up initial screening reactions for other techniques. This speed advantage has led to widespread adoption of preparative chiral chromatography for accessing small amounts of enantiopure material for the early stages of drug discovery and development, where material requirements are small. As material demand increases, other resolution or enantioselective synthesis strategies often supplant chiral chromatography (Figure 5).

9.06.3.3 The Stationary Phase in Preparative Chiral Chromatography

Many CSPs are available for use in analytical columns. Several of these are routinely used in gram scale preparative separations, but only a few materials are widely used for kilogram scale preparative separations. The most commonly used preparative CSPs at

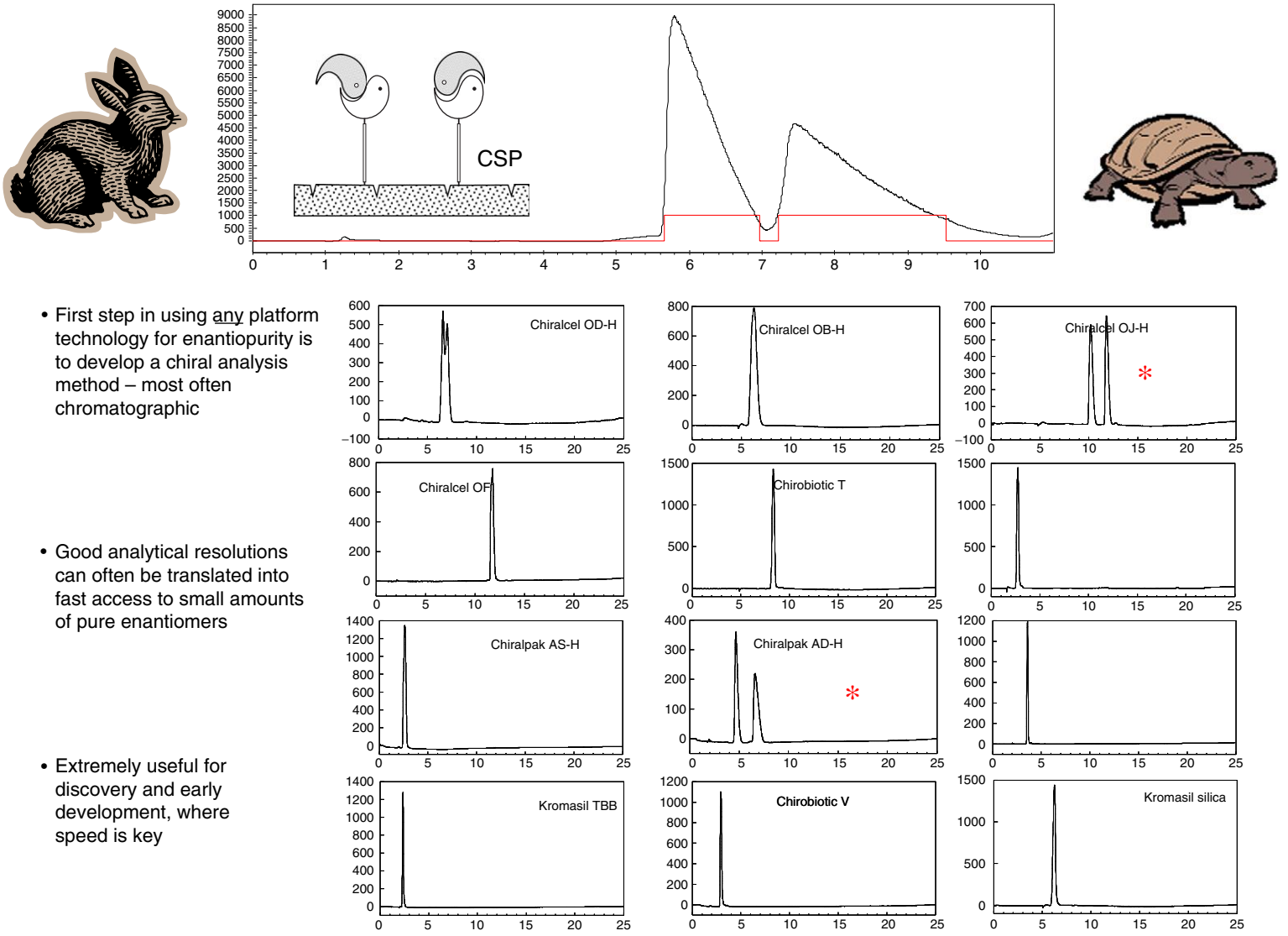


Figure 5 Preparative chiral chromatography – A platform technology with a head-start advantage. Because most methods for accessing enantiopurity require the development of a chiral chromatographic assay for measuring enantiopurity, chiral chromatography is often the fastest option for obtaining small amounts of enantiopure material (milligrams–grams).

this time are the modified cellulose and amylose CSPs invented by Okamoto and commercialized by Chiral Technologies,[24] with Chiralpak AD, based on the 3,5-dimethylphenylcarbamate derivative of amylose, being the most versatile and widely used preparative CSP on the market at the present time. Recent patent expiry on some of the Okamoto CSPs has led to the commercialization of generic versions of these columns.[25]

Several other CSPs are routinely used for preparative chiral chromatography, and new commercial CSPs are introduced each year. In addition, there are ongoing advances in the technology of CSP design and development.[26–33] The structures of several of the more commonly used preparative CSPs are illustrated in Figure 6.

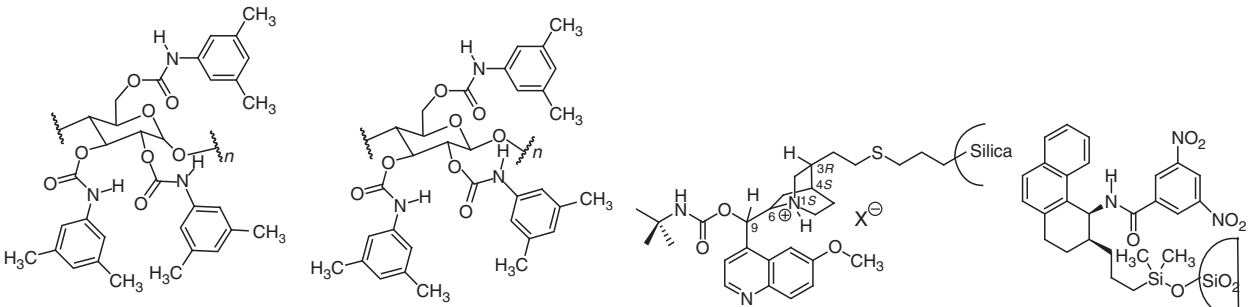


Figure 6 Chemical structures of several commonly used preparative CSPs.

Commercial CSPs are successful because they demonstrate some general ability to separate the enantiomers of a broad assortment of compounds. However, the chemist contemplating an industrial scale resolution may be more interested in the ability of a CSP to separate the enantiomers of one particular compound. In recent years there has been considerable interest in the preparation and evaluation of tailor made CSPs for carrying out given separation tasks. Several examples are shown in Figure 7.

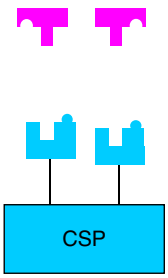
Custom CSPs capable of resolving the enantiomers of a particular compound ….  …. Can be produced by a variety of methods	Antibody CSPs Single enantiomer of the compound of interest conjugated to a 'hapten carrier', which is then injected into a mouse to elicit an immune response. Hybridoma antibody production, enantioselective Ab clones identified, then immobilized on a column to produce antibody CSP Drawbacks: 'Handle' for immobilization needed, potential for tether effect issues, Ab CSPs tend to have poor capacity and lower stability and robustness
	Immobilized guest method Single enantiomer of the compound of interest immobilized to create an 'immobilized guest CSP', which is used to screen a library of racemates. Compounds with highest enantioselectivity identified – single enantiomer used to prepare 'reciprocal CSP' Drawbacks: 'Handle' for immobilization needed, potential for 'tether effect' issues
	Imprinted polymer CSPs Single enantiomer of compound of interest added to mixture of monomers, polymerization. Resulting polymer is ground into particles, extracted to remove template molecule, then used as a chromatographic CSP Drawbacks: Tendency toward poor chromatographic performance, swelling and 'relaxation' of polymer upon solvent exposure
	High throughput screening of CSP libraries Small scale libraries of CSPs prepared by parallel solid phase synthesis. Enantioselective binding of target evaluated using high throughput assay, often LC-MS. CSPs identified, prepared at scale Drawbacks: Can only detect gross differences in CSP performance, not useful for detecting CSPs with very low enantioselectivity, requires analyte that can be detected at low levels (strong chromophore or good MS isonization)

Figure 7 Strategies for the preparation of CSPs that are 'tailor made' for a specific compound.

Antibody technology can be used for preparing highly specific stationary phases, including CSPs for the separation of enantiomers.[34,35] A single enantiomer of the compound of interest is immobilized onto a 'hapten carrier' such as bovine serum albumen (BSA) or keyhole limpet hemocyanin (KLH) to produce an immunogen, which is then injected into a mouse to elicit an immune response. Mouse spleen cells are then isolated and fused with an immortal mouse tumor cell line to produce so-called hybridomas, each of which produces a unique antibody. Assessment of the enantioselectivity of the antibodies produced by different hybridoma clones, as well as an assessment of the amount of antibody produced by each clone, allows the selection of an antibody-producing clone with the desired properties. Antibody production can then be scaled up, ultimately producing sufficient quantities of the desired antibody for immobilization onto a chromatographic support to create a CSP. In practice, the antibody CSP approach is only rarely used, and then primarily for analytical, rather than preparative purposes. Antibody stationary phases tend to have poor capacity relative to other choices, a limitation that stems from the fact that they contain only two binding sites in a molecule with a mass of $\sim$150 KD. Antibody CSPs can also suffer from limited long-term stability and robustness issues. In addition, preparation of antibody CSPs for a specific target compound requires the presence of a chemical 'handle' on the compound of interest that can be used in preparation of the immunogen. Some compounds are fundamentally lacking in such groups and are very difficult to immobilize onto a hapten carrier. In addition, care must be taken in the immobilization so that antibodies are produced which recognize and bind to the compound of interest, and not just to an immobilized version of it. In many cases, antibodies can be produced that recognize the compound of interest only when it contains the immobilization tether. Although weeding out such artifacts is possible during clone selection, this phenomenon can present a significant problem. Despite these shortcomings, continuing progress in antibody production technologies and protein engineering, combined with the outstanding selectivity possible with this approach, suggest a possible future of antibody derived CSPs.

The immobilized guest method shares some similarities – and liabilities – with the antibody approach. In this technique, a single enantiomer of the compound of interest is immobilized on a chromatographic support to create an 'immobilized guest CSP', which is then used to screen a library of racemates.[36,37] A significant advantage of this approach is that only tiny amounts of the racemic test compounds are required, and they need not be completely pure. Compounds showing high enantioselectivity on the immobilized guest CSP are identified, and for the most promising, a single enantiomer is used to prepare a reciprocal CSP which can then be used for resolving the enantiomers of the original compound of interest. As with the antibody CSP approach, a significant drawback of the immobilized guest method is the requirement of a handle for immobilization of the target compound as well as the potential for tether effect issues, where the CSP ultimately produced works well for analogs of the target containing the immobilization tether, but poorly for the underivatized target molecule.

The imprinted polymer approach for CSP preparation uses a single enantiomer of the molecule of interest as a template for the polymerization of a number of monomer units containing different functional groups capable of interaction with the target molecule.[38–40] The resulting polymer is milled and sieved, then extracted to remove the template molecule or other residual monomers. The CSP thus produced contains cavities that are complementary to the template molecule, which enable enantioselective adsorption of the target molecule. Owing to the irregular shape of the polymeric material and the presumed heterogeneity of binding sites, the chromatographic efficiency for these stationary phases can be considerably less than that obtained with conventional CSPs, with broad and distorted peaks often being observed. Nevertheless, some impressive enantioselectivities and chromatographic separations have been obtained with this approach. An additional liability of the imprinted polymer approach is a tendency for the resulting polymers to swell on exposure to solvent – an undesirable property in a high performance chromatographic support. In addition, there is some tendency for the enantioselective binding sites in the imprinted polymer to gradually relax, leading to a decrease in enantioselectivity of the CSP over time.

An additional approach to the preparation of tailor-made CSP involves the preparation of libraries of different CSPs on very small scale, using parallel solid-phase synthesis technologies.[41–44] Loose samples of the resulting stationary phase particles are then evaluated for their ability to adsorb the compound of interest enantioselectively in a high throughput screening assay. CSPs with desirable properties identified in the screens are then scaled up and packed into a column for more detailed evaluation. Drawbacks of this approach include the fact that the high throughput screening assay can typically only detect gross differences in CSP performance. Consequently, the approach is not useful for detecting CSPs with very low enantioselectivity. In addition, the high throughput performance assay requires that the analyte of interest be detected at low levels, which typically requires either a strong chromophore or good MS ionization.[45]

Finally, economics is an important additional consideration in the choice and availability of preparative CSPs. Current retail costs for preparative CSPs are approximately \$15 000–\$25 000 kg^{-1}, which represents a considerable barrier to entry for setting up a laboratory for large-scale separations, where a single 30 cm inner diameter (i.d.) column can use 10 kg or more of CSP, and where a number of different types of CSP are typically used. However, CSPs are reusable and tend to last for many years, even with continual use, so there are opportunities to recoup CSP investments over time. Despite this apparent high price for CSPs, overall sales volumes can be relatively small, largely owing to a somewhat limited customer base as well as the abovementioned durability and longevity. Consequently, to be economically viable, the manufacturing processes for new CSPs are often rather straightforward, typically employing affordable starting materials and only a few synthetic steps.[46] In addition, the underlying chromatographic support material, typically spherical, porous silica, can be a significant contributor to the overall costs of a CSP. At present, 20 μm diameter particles are the standard for multikilogram scale separations, with more expensive 5 μm particles being preferred in the smaller columns ($<$5 cm i.d.) used for gram scale separations. A recent trend toward the use of smaller diameter particles continues in the analytical realm, with an increasing use of more expensive sub 2 μm particles being seen in recent years.

A continued trend toward the use of smaller, more uniform particle in preparative chromatography is likely, although the pace of this change is uncertain at present.

9.06.4 Preparative Chromatography Instrumentation, Supercritical Fluid Chromatography, and Green Chromatography

The fundamental instrumentation used in modern preparative chromatography, i.e., computer-controlled automated injection, elution, fraction collection, and continuous distillation of eluate, was demonstrated more than three decades ago[47]; however, ongoing innovations in the past decade have helped to make the technique much more accessible and user-friendly than in the past. Most analytical high pressure liquid chromatography (HPLC) instrumentation manufacturers now carry products for use in preparative separations, and the robustness and ease of use of this equipment has improved considerably in recent years. Automation is becoming increasingly important in preparative chromatography, with an emphasis in recent years on fully automated injections of smaller amounts of sample, with shorter individual runtimes.

Most preparative chromatographic enantioseparations required for pharmaceutical development can be achieved with traditional elution chromatography utilizing 'touching band' separations (i.e., separations in which the two enantiomer peaks are still baseline or nearly baseline resolved). As sample load is increased, the touching band chromatogram gives rise to a more complex chromatogram with partially overlapping peaks. Chromatographic productivity using such an approach can be superior to the touching band method, provided one understands the appropriate place for fraction cutting within the complex peak. In addition, the solvent requirements for such separations can be reduced, although a considerable disadvantage is the need to collect and reprocess a middle fraction consisting of a mixture of the two peaks. The technique of simulated moving bed chromatography (SMB) uses multiple columns for continuous chromatography with continuous reprocessing of the mixed fraction (*see* Chapter 9.08). SMB has gained attention as a useful tool for industrial scale chromatographic separations,[3–5,48–51] and can often lead to gains in productivity, reduced solvent usage, and improved separation economy. A single column innovation has been developed that utilizes recycling of the mixed fraction with augmentation with fresh feed solution so that a 'steady state recycling' situation can be reached.[52]

Solvent use is a very important parameter for larger scale chromatographic separations. A low productivity resolution might require the use of more than 10 tons of solvent to afford a single kilogram of purified material, whereas an outstanding resolution might require only a few hundred liters. Not surprisingly, solvent distillation and recycling is an important factor contributing to the overall economics of industrial scale preparative chromatographic resolutions.[53] The use of supercritical fluid chromatography (SFC) for preparative enantioseparation has enjoyed considerable recent attention,[54–56] and is the method of first choice in our own laboratories. In this approach, supercritical or subcritical carbon dioxide replaces petrochemical-derived hydrocarbons, resulting in reduction in solvent utilization by as much as 95%. Preparative SFC is not a net generator of carbon dioxide, a known greenhouse gas. Instead, it utilizes carbon dioxide that is condensed from the atmosphere, then later returned to the atmosphere. Furthermore, with prep SFC the product is recovered in a more concentrated form relative to HPLC, greatly reducing the amount of solvent for evaporation, and resulting in considerable savings in labor. Finally, because of the low viscosity of the supercritical fluid eluent, separations may be conducted at flow rates that would be impossible with liquid solvents, an advantage that can contribute to the oftentimes higher productivity of preparative SFC enantioseparations relative to HPLC methods. Cumulatively, these advantages make preparative SFC enantioseparation an attractive and 'greener' alternative to conventional HPLC approaches, and a technique with a promising future.

9.06.5 Chromatographic Productivity

In addition to the familiar parameters (retention, selectivity, and efficiency) that are useful for describing any chromatographic separation, preparative chromatography is most concerned with the additional parameter, productivity. The chromatographic productivity is a measure of how much purified material can be prepared with a given mass of stationary phase per unit time. Owing to the predictable scalability of chromatographic processes, a measurement of productivity developed using a small column can accurately predict the requirements for separation on much larger scale. Chromatographic productivity can be estimated by carrying out loading studies, where injection of progressively larger amounts of material onto an analytical HPLC column packed with the adsorbent of interest are analyzed. Small columns are often used to model chromatographic enantioseparation.[57] However, care must be taken in such experiments to ensure that both columns contain the same stationary phase particles (**Figure 8**).

Because of the ready scalability of chromatography, loading studies carried out on a small column can be used to predict separation conditions accurately at larger scale. An extreme example of this phenomenon can be seen in **Figure 9**, where results from a loading study using a 0.3 mm i.d. column were scaled up by a factor of one million to accurately predict performance on a 30 cm i.d. column. Chromatographic productivity is expressed with units of kkd (kilograms of purified enantiomer per kilogram of stationary phase per day), with a poor separation having a productivity of 0.1 kkd or lower, and a good separation having a productivity in the range of 1 kkd. A truly remarkable separation might have productivity greater than 10 kkd.

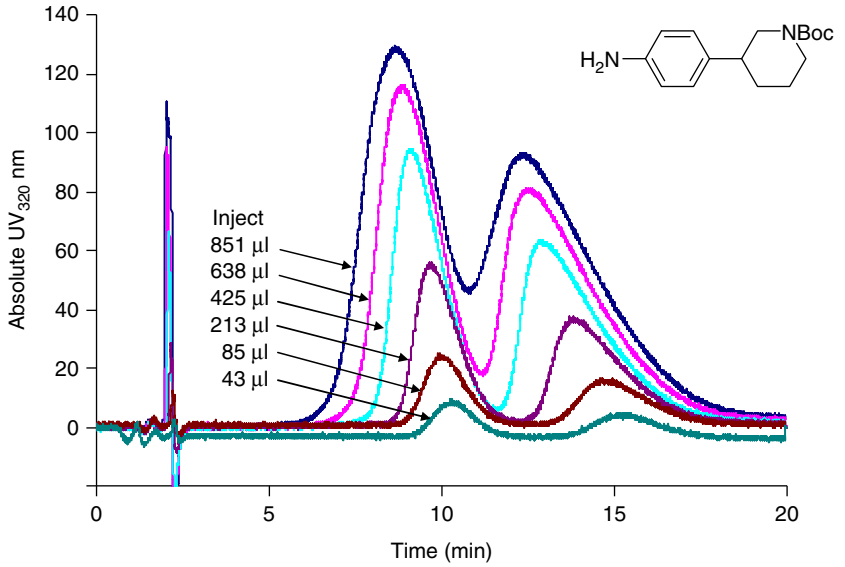


Figure 8 Chromatographic loading study using microcolumn format allows estimate of productivity with minimal material requirement. Conditions: Chiralpak AD, 300 µm i.d. × 25 cm length, 20 µm particle size; 6.0 µl min^{-1} 5% ethanol in heptane; injection volume as indicated; feed concentration = 90 mg ml^{-1} in ethanol; UV_{320} nm; ambient temperature.

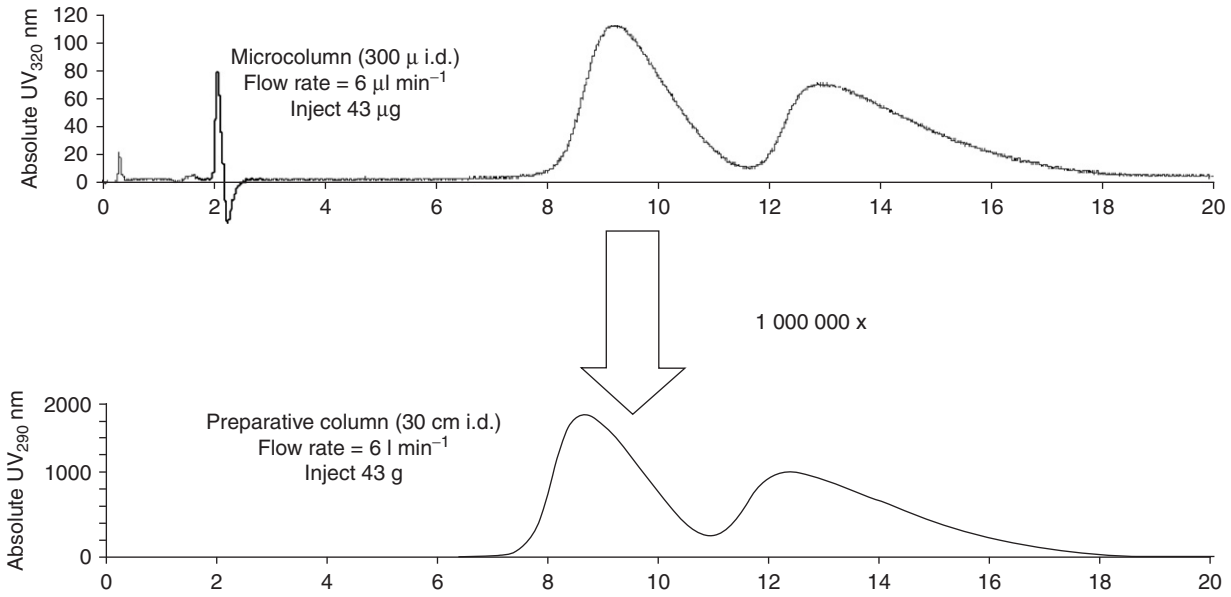


Figure 9 Loading studies carried out using microcapillary columns can be used to predict preparative chromatographic performance accurately at large scale.

9.06.6 Method Development

Method development for preparative chiral chromatography typically begins with automated column screening in which a variety of column and mobile phase combinations are evaluated via automated screening, typically using gradient elution.[22,23,58] Promising separations are next translated to isocratic separations, and the separation factor (α) as well as the resolution (Rs) are compared. Typically, methods with large separation factors are preferred for preparative separations, although other factors are also important. Estimation of α from gradient chromatograms may be possible in some instances.[59] In general, retention is kept to a minimum, with retention factors typically less than 3, and sometimes considerably less. Longer retention is sometimes required for marginally resolved compounds, although in this situation, overlapping or staggered

injections are often used to maximize column productivity. Maximizing solubility of the racemic feed in the chromatographic eluent is critically important for optimizing chromatographic productivity, and the method with the greatest productivity can sometimes have a lower separation factor, but increased solubility of the feed in the eluent. Consequently, the ultimate selection of a method following analytical column screening should be based on estimations of chromatographic productivity provided by preparative loading studies.

9.06.7 The Role of Preparative Chromatography in Organic Synthesis

The incorporation of preparative HPLC into organic synthesis is by no means a new phenomenon. R. B. Woodward, perhaps the most famous synthetic chemist of the twentieth century, was an early advocate of preparative HPLC, using some of the first commercial HPLC equipment to separate complex mixtures of closely related isomeric intermediates required for the vitamin B-12 synthesis. Woodward's experience with preparative HPLC led him to predict in 1973 that "The power of these high pressure liquid chromatographic methods hardly can be imaged by the chemist who has not had experience with them; they represent relatively simple instrumentation and I am certain that they will be indispensable in the laboratory of every organic chemist in the near future".[60] Despite the accuracy of Woodward's prediction, it is worth noting that several decades elapsed before the Woodward vision began to be widely realized. In recent years there has been a growing appreciation of the value that preparative chromatography can bring to enable organic synthesis in a powerful manner. Although most industrial scale processes are still generally chromatography-free, there have been a growing number of examples in recent years where large-scale chromatography has proven to be the preferred approach on a production cost basis.

Furthermore, the vast majority of the syntheses developed in academia and industry are performed on relatively small scale, and destined to be repeated infrequently, if ever. This includes early preclinical drug candidates, the large majority of which are unsuccessful. In such cases, there is little practical advantage to developing a chromatography-free process, particularly when one considers the developmental labor required to do so. Understandably, the use of the enabling technology of preparative chiral chromatography is becoming increasingly accepted in pharmaceutical development. Given the fact that only a small fraction of all lead compounds in early pharmaceutical development survive the increased scrutiny of later stage preclinical investigation, a high value is placed on methods that can provide the compound needed for preclinical investigation quickly and with minimum labor and materials costs. A downside to this chromatographic shortcut is that should the candidate survive preclinical evaluation, a route with potential for larger scale manufacturing will be needed quickly. Thus, a balance between synthetic quality and speed often characterizes modern pharmaceutical process research, where demands for rapid production of necessary material are weighed against the need to develop a process that is suitable for industrial scale.

Although the paradigm for developing and carrying out an enantioselective synthesis is now quite well established, strategies for the efficient use of preparative chiral chromatography within a synthesis are still evolving. As with the planning of any resolution, a certain degree of flexibility should be maintained regarding placement within the overall synthetic scheme. Even more so than with enantioselective synthesis or nonchromatographic resolution approaches, seemingly minor changes in compound structure, for instance a change in protecting group, can dramatically influence chromatographic resolution and productivity. Consequently, a development strategy that examines a variety of intermediates and structural variants is more likely to afford a convenient and highly productive enantioseparation than a strategy that demands the resolution of one particular compound.

9.06.8 Examples and Case Histories

Several examples will be used to illustrate the various ways that preparative chiral chromatography is routinely used for accessing enantiopure compounds. The example shown in **Figure 10** illustrates the value of the preparative chromatography approach for speeding medicinal chemistry investigations. In this study, more than 65 racemates were resolved to support early lead optimization for a γ secretase program.[61] The compounds of interest are subtly chiral, with stereochemistry at the quaternary center being dependent on the placement of a substituent five bonds removed. Not surprisingly, compounds in this class are not easily accessible by conventional enantioselective synthesis. Nevertheless, the compounds are readily resolved using chiral chromatography, which allowed rapid prosecution of lead optimization of this series.

In the study illustrated in **Figure 11**, the enantiomers of an arylthiazolinedione were resolved by preparative chiral chromatography on the Whelko CSP, providing individual enantiomers that were used to study the rate of racemization under a variety of conditions.[62] Such studies are often performed to gain an appreciation of potential vulnerabilities of drug candidates. In this particular case, the propensity for racemization was so great that special care had to be taken to avoid racemization in the chromatographic resolution and subsequent evaporation of isolated fractions.

Small-scale chromatographic resolutions are routinely carried out to obtain small amounts of material for characterization of physical properties or biological performance of the individual enantiomers. In the study shown in **Figure 12**, researchers at AstraZeneca studied the preparative chromatographic separation of omeprazole and a number of structurally related proton pump inhibitors, carrying out chiroptical spectroscopy investigations on the isolated enantiomers.[63] Optimization of the resolution for omeprazole led to a productivity of greater than 1 kkd.

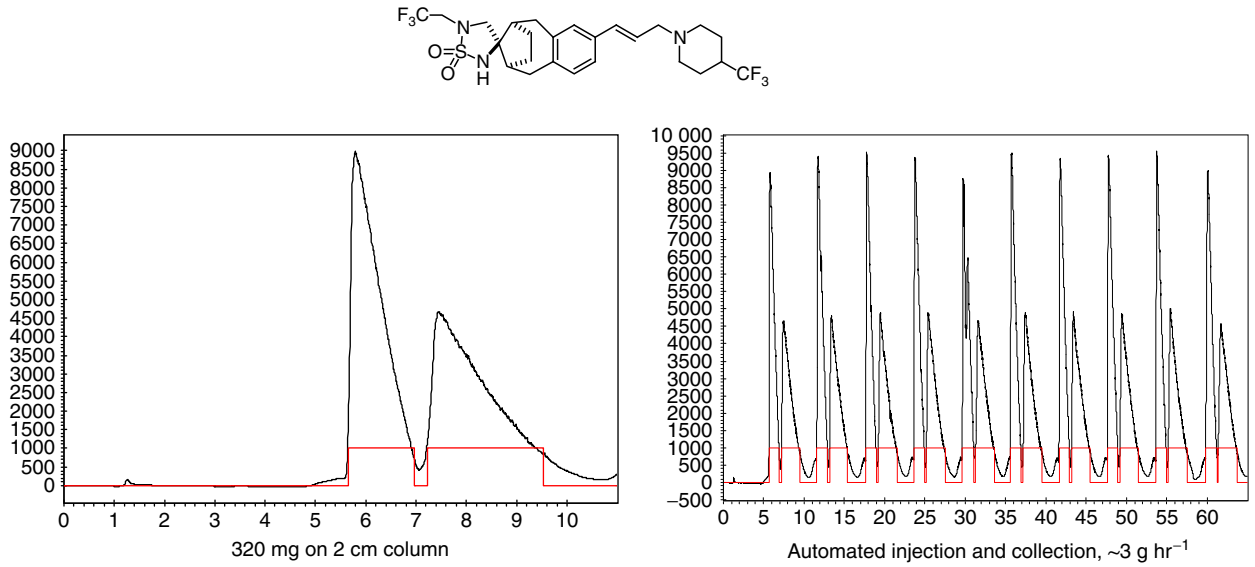


Figure 10 Preparative chiral SFC in support of pharmaceutical drug discovery – more than 65 different racemates were resolved to support early lead optimization for a γ-secretase program involving 'cryptochiral' structures not easily accessed via enantioselective synthesis.

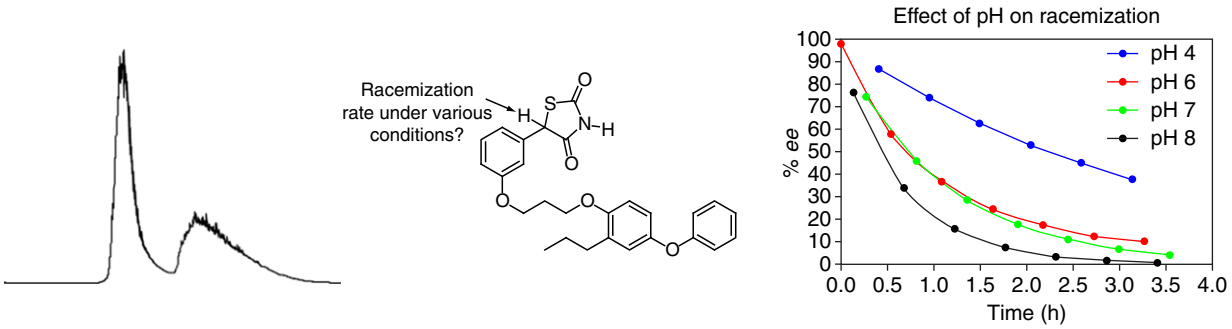


Figure 11 Preparative chromatographic isolation of a single enantiomer of arylthiazolinedione allows the rate of racemization in a variety of media to be studied.

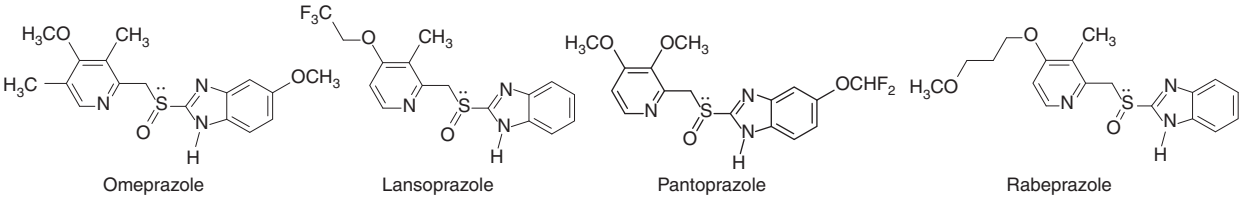


Figure 12 Preparative resolution of enantiomers of omeprazole and related analogs allow measurement of chiroptical properties of individual enantiomers.

Another common use of small-scale preparative chiral chromatographic resolution in pharmaceutical research involves studies of atropisomeric species. Compounds such as those shown in Figure 13 are chiral owing to restricted rotation about sterically-congested bonds. When the barrier to rotation is sufficiently high, enantiomers can be resolved on the 'HPLC time scale'.[64] In the example presented in Figure 13, rapid application of preparative chiral chromatography and a variety of other analytical techniques allowed fine tuning of the rate of atropisomerization of a family of selective benzodiazepine sulfonamide bombesin receptor subtype 3 (BRS-3) agonists during lead optimization, simply by adjusting a single 'R' group substituent.[65,66] Understanding gained during these studies allowed medicinal chemists to design molecules at will that would be locked into a single atropisomeric form or that would be rapidly interconverting during the course of treatment.

In recent years small-scale preparative chiral chromatography has become routinely used in many areas of chemical research. Several interesting examples include the separation of the enantiomers of fullerene adducts,[67] trefoil knot molecules,[68] and chiral

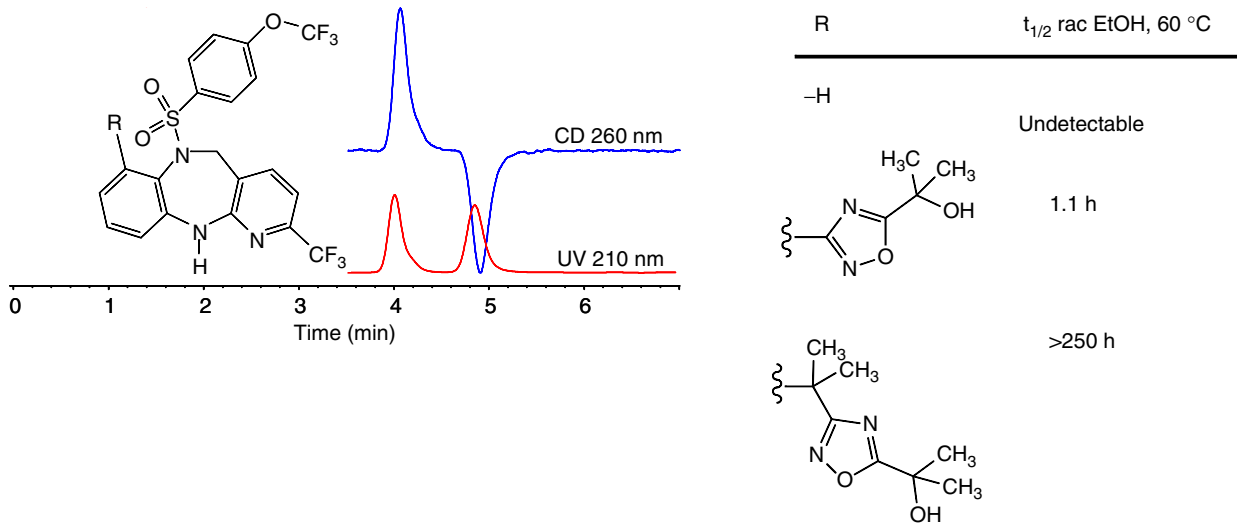


Figure 13 Preparative resolution of atropisomers allows fine tuning of rate of atropisomerization of a family of selective benzodiazepine sulfonamide bombesin receptor subtype 3 (BRS-3) agonists.

molecular switch elements.[69] Recently, preparative chromatography has also begun to be used in the investigation into new ligands and catalysts for use in enantioselective synthesis. Prof. Gregory Fu has been an early adopter of this technology, using rapid chromatographic enantioseparation to enable rapid prototyping of new catalyst families. Two examples of enantioselective catalysts from the Fu group that were initially resolved via preparative chiral chromatography are shown in Figure 14.[70,71]

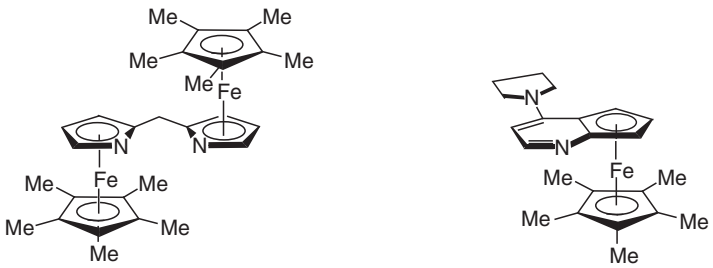


Figure 14 Preparative chiral chromatography provides rapid access to enantiopure catalysts, speeding new catalyst discovery – examples from laboratory of Gregory C. Fu, MIT.

Figure 15 shows another recent example from Prof. Robert Gawley that illustrates the value of using preparative chiral chromatographic resolution to enable the search for new ligands and catalysts. In this example, a complex mixture of stereoisomers of an otherwise easy to synthesize molecule was chromatographically resolved, with a single isomer carried forward to make a new imidazolium ligand, which shows great promise for enantioselective catalysis.[72] An important element of this strategy

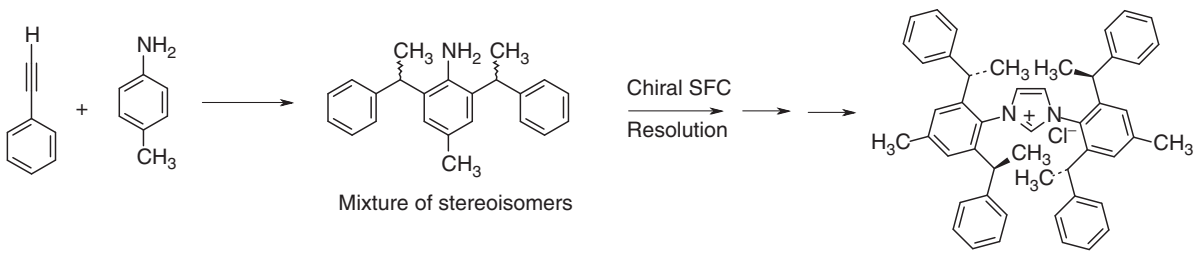


Figure 15 Preparative chiral SFC resolution of key intermediate provides rapid access to new ligand for enantioselective catalysis.

is that although chromatography can enable rapid discovery of new catalysts, long-term catalyst production can utilize whatever synthetic or separation approach is most cost effective.

Preparative chiral chromatography is increasingly used to access the tens of grams to kilograms of enantiopure material required for studying the safety and efficacy of new pharmaceutical candidates.[73,74] Fast and labor efficient racemic synthesis combined with preparative chiral chromatography can in many cases offer a strategic advantage over enantioselective synthesis approaches, especially in early development where compound attrition is very high. Figure 16 shows a typical example of the use of preparative chiral chromatography to resolve the enantiomers of an intermediate for the synthesis of a preclinical drug candidate.[75] In this example, attempts at carrying out enantioselective synthesis had been partially successful, resulting in product with 70% *ee*. Preparative chiral chromatography was used to prepare sufficient enantiopure material rapidly for early safety studies. This example highlights the utility of the preparative chromatographic approach as a 'safety net' that can be used to upgrade unsatisfactory enantiopurity or to remove unanticipated byproducts and impurities.

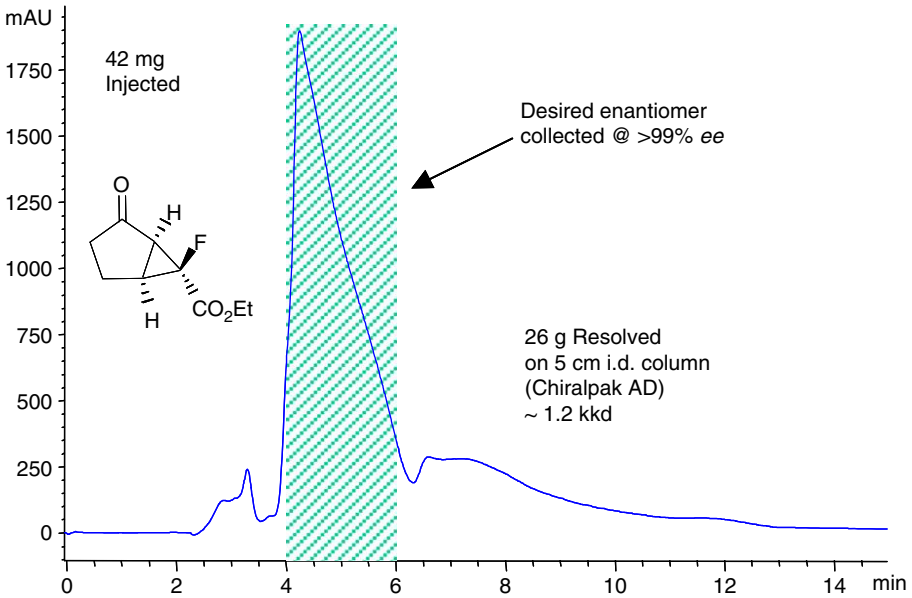


Figure 16 Rapid 'polishing' to upgrade enantiopurity of intermediate from 70% to >99% *ee*. Chiralpak AD (4.6 × 250 mm); 20 m particles; 15% IPA in heptane, 1.2 ml min; injection of 210 mg ml^{-1} of 70% *ee* feed. Desired enantiomer collected with >99% *ee*, >90% recovery. Estimated productivity = 1.2 kkd.

The example shown in Figure 17 highlights the speed and ease with which kilogram amounts of enantiopure material can be prepared. In this example, preparation of a kilogram of an enantiopure epoxide via enantioselective synthesis was not straightforward, making chromatography the best alternative. Although the ability to access a kilogram of enantiopure material in less than a week is impressive, the fact that 2000 l of solvent was required for this separation highlights a current drawback of the chromatographic approach and illustrates the reason why preparative chromatographers are increasingly interested in the use of solvent-sparing technologies such as SFC and continuous solvent recycling.

As the use of preparative chiral chromatography within organic synthesis becomes more widespread, strategies for positioning the resolution step within an organic synthesis continue to evolve. Is it better to resolve greater amounts of a smaller, lower cost starting material, or lesser amounts of a more expensive end product? Which potential synthetic intermediates show the greatest chromatographic productivity, and how can this be quickly and easily determined? Is it better to simply prepare a racemate and chromatographically resolve, or should an enantioselective synthesis that affords incomplete selectivity be used? The study illustrated in Figure 18 highlights how flexibility in the choice of synthetic route and protecting groups can enable the choice of intermediates for resolution with optimal productivity, thereby speeding and simplifying the overall synthesis.[76]

As strategies for incorporating preparative chromatographic resolutions into organic synthesis continue to evolve, global optimization of the entire synthetic route is becoming more common. The example illustrated in Figure 19 highlights the different criteria for route optimization in early versus late development of a pharmaceutical candidate.[77] The synthetic route for initial preparation of the candidate on kilogram scale involved a reasonably productive (0.34 kkd) chromatographic resolution of a doubly protected BOC/CBZ intermediate followed by a four-step transformation to the desired product. Although this route was suitable for early development, a more cost-effective synthesis was required for late development and commercialization. In an effort to optimize the synthetic route globally, a number of potential chromatographically resolvable intermediates were investigated, and an optimized synthesis utilizing a much more productive (2.5 kkd) chromatographic resolution of a monoprotected trfluoroacetamide derivative followed by a two-step conversion to the desired product was ultimately selected. In addition to an

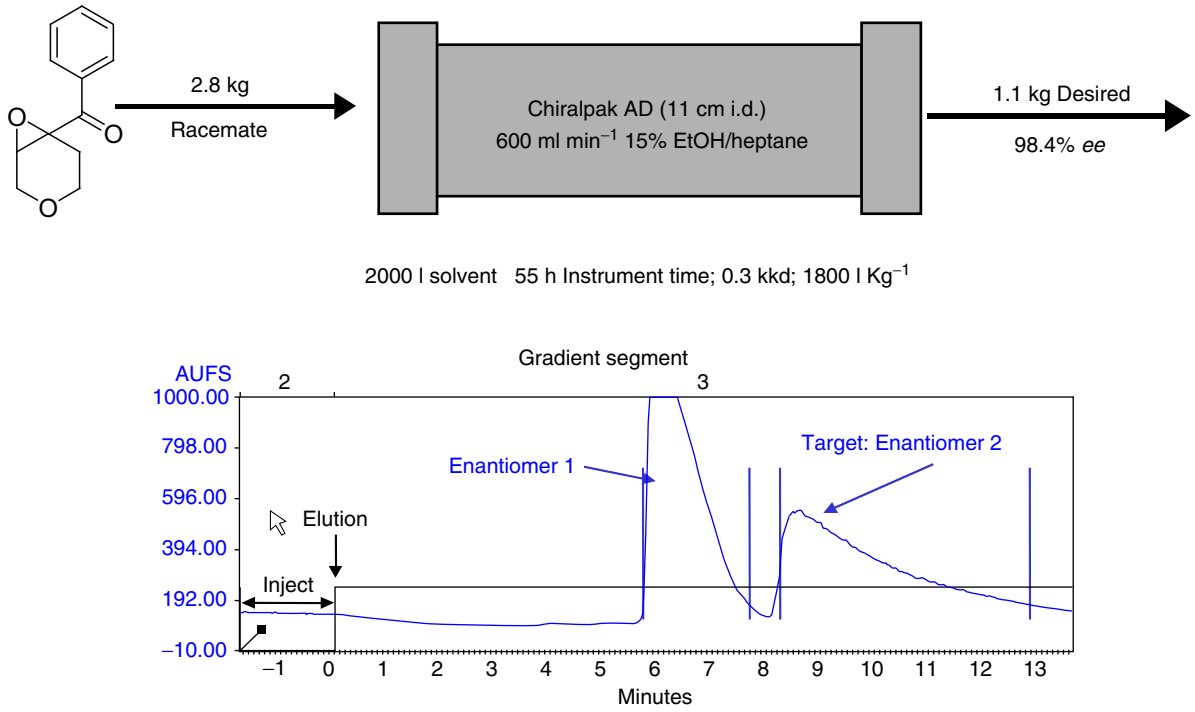


Figure 17 Preparative chiral chromatography provides rapid access to kilogram quantities of enantiopure materials.

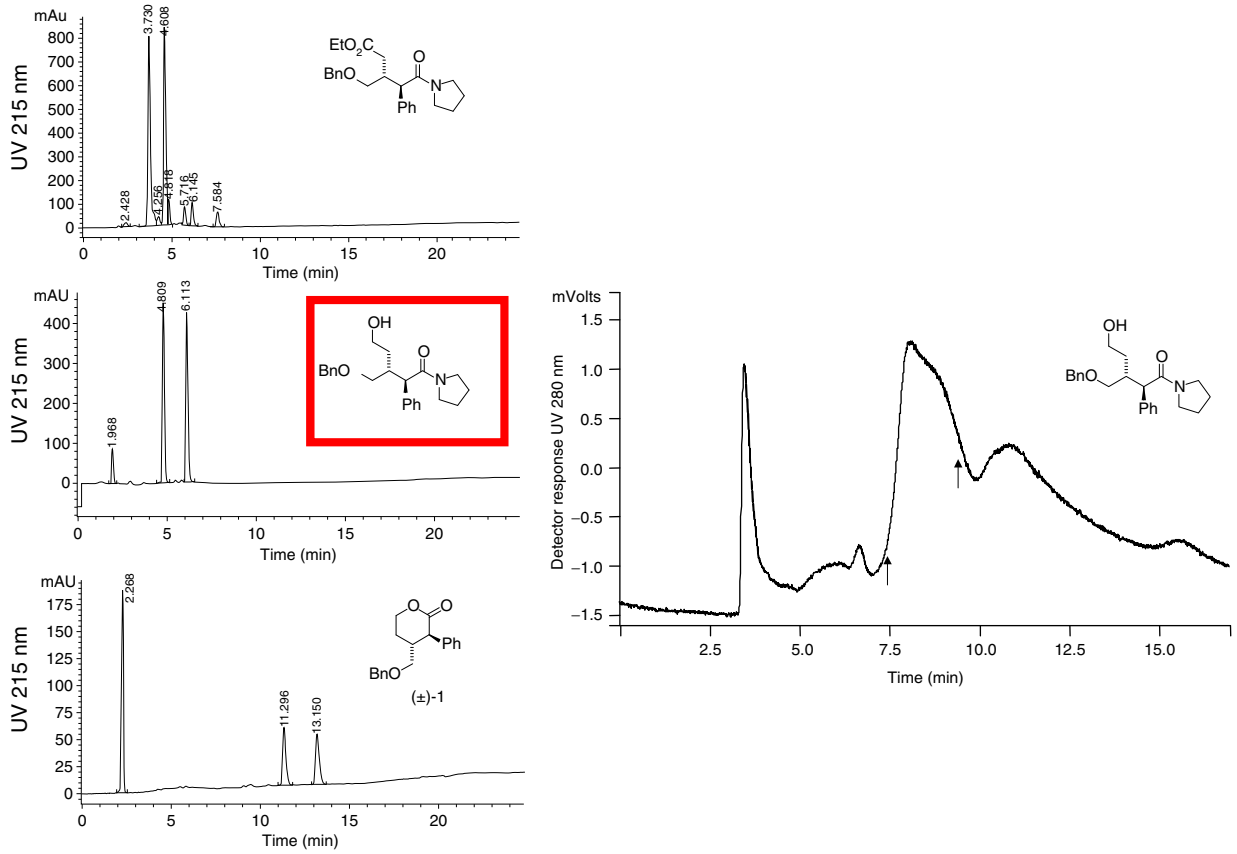


Figure 18 Flexibility in choice of synthetic route and intermediate structure can allow selection of the best candidates for chromatographic resolution.

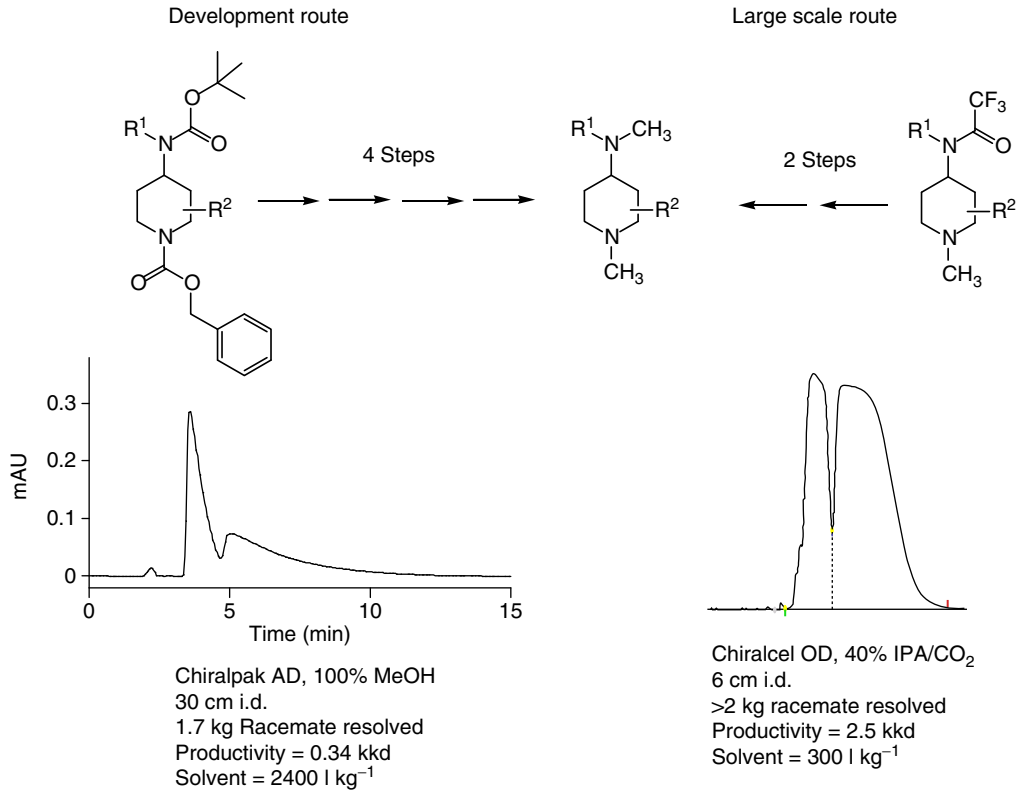


Figure 19 Different criteria for early development and larger scale manufacturing lead to optimization of both synthetic route and chromatographic resolution.

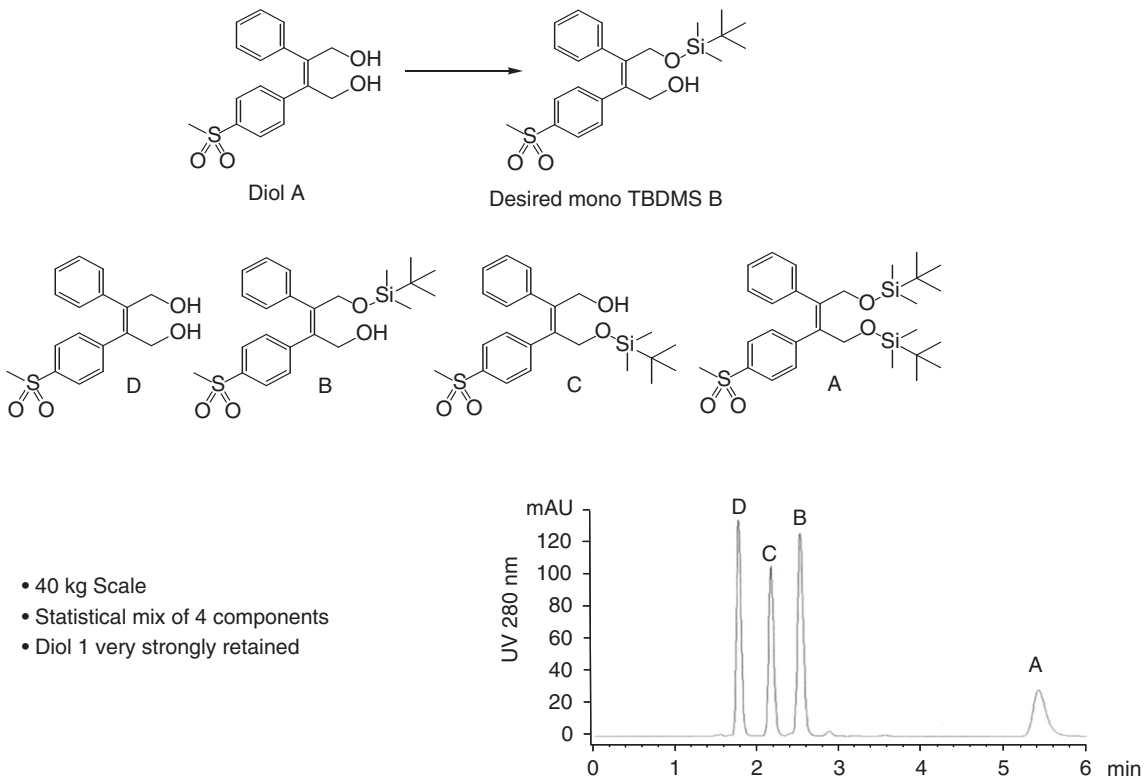


Figure 20 Achiral preparative chromatography can rapidly solve complex chemo- and regioselectivity problems.

elimination of two synthetic steps and a sevenfold increase in chromatographic productivity, the new resolution is also eightfold better in terms of specific solvent consumption, an important cost and green chemistry consideration.

Finally, it is worth pointing out that achiral chromatography can be very valuable to solve complex chemo and regiochemical selectivity problems quickly.[78–80] In this example, alkylation of an unsymmetrical diol with a single equivalent of *t*-butyldimethylsilyl chloride afforded a statistical mixture of starting material, bisalkylated product, and the two monoalkylated products, affording the desired mono TBS isomer in only ~25 yield. When faced with such daunting challenges, the chromatographic option can usually be relied on to provide a fast approach to the desired material. In this example, 40 kg of crude product were rapidly resolved on a highly productive achiral chromatographic separation to provide ~10 kg of the desired intermediate (**Figure 20**).

9.06.9 Conclusion

Preparative chiral chromatography has become a preferred method for rapidly obtaining enantiopure compounds in the pharmaceutical industry, largely owing to the speed with which a chromatographic method can be developed and executed as well as the comparatively small labor requirements of the chromatographic approach, relative to other methods. As Woodward predicted, the use of preparative chromatography within the field of organic synthesis can be expected to increase as the technique becomes more familiar to synthetic chemists. As this occurs, it can be expected that there will be an increasing prevalence of syntheses that are designed from the outset with a view toward utilization of best advantages that preparative enantioseparation has to offer.

References

1. Welch, C. J. Chiral Chromatography in Support of Pharmaceutical Process Research. In *Preparative Enantioselective Chromatography*; Cox, G. B., Ed.; Blackwell: London, **2005**, pp 1–18.
2. Francotte, E., Lindner, W. W., Eds. *Chirality in Drug Research: Methods and Principles in Medicinal Chemistry*; Wiley: Weinheim, **2006**.
3. Andersson, S.; Allenmark, S. G. *J. Biochem. Biophys. Methods* **2002**, *54*, 11–23.
4. Blehaut, J.; Ludemann-Hombourger, O.; Perrin, S. R. *Chim. Oggi* **2001**, *19*, 24–28.
5. Alves, G. G.; Fortuna, A. A.; Falcao, A. A. *Trends Chromatogr.* **2008**, *4*, 1–10.
6. Freund, Ernst; Abel, Stefanie; Huthmann, Elke; Lill, J. *Chim. Oggi* **2009**, *27*, 62–64.
7. Schmidt-Traub, H., Ed. *Preparative Chromatography: Of Fine Chemicals and Pharmaceutical Agents*; Wiley: Weinheim, **2005**.
8. Gawley, R. E. *J. Org. Chem.* **2006**, *71*, 2411–2416.
9. Thayer, A. M. *C&E News* **2007**, *85*, 11–19.
10. O'Brien, M. K.; Vanasse, B. B. *Curr. Opin. Drug Disc. Devel.* **2000**, *3*, 793–806.
11. Eliel, E. L.; Wilen, S. H.; Maunder, L. N. *Stereochemistry of Organic Compounds*; Wiley: New York, **1994**.
12. Jacques, J.; Collet, A.; Wilen, S. H. *Enantiomers, Racemates and Resolutions*; Wiley: New York, **1981**.
13. Pirkle, W. H.; Welch, C. J. *J. Liq. Chromatogr.* **1991**, *14*, 1–8.
14. Pirkle, W. H.; Bowen, W. E. *J. High Res. Chromatogr.* **1994**, *17*, 629–633.
15. Pirkle, W. H.; Welch, C. J. *J. Liq. Chromatogr.* **1991**, *14*, 2027–2042.
16. Bidlingmeyer, B. A., Ed. *Preparative Liquid Chromatography*; Elsevier: New York, **1987**. *Journal of Chromatography Library*, Vol. 38.
17. Corey, E. J.; Kurti, L. *Enantioslelective Chemical Synthesis: Methods, Logic and Practice*; Direct Book Publishing: Dallas, **2010**.
18. Carriera, E. M.; Kroerno, L. *Classics in Stereoselective Synthesis*; Wiley: Weinheim, **2009**.
19. Jacobsen, E. N.; Pfaltz, A.; Yamamoto, H. *Comprehensive Asymmetric Catalysis*; Springer-Verlag: Berlin, **2004**.
20. Quallich, G. J. *Chirality*; Wiley: New York, **2005**, Vol. 17; pp S120–S126.
21. Hauck, W.; Adam, P.; Bobier, C.; Landmesser, N. *Chirality*; Wiley: New York, **2008**, Vol. 20; pp 896–899.
22. Sajonz, P.; Gong, X.; Leonard, W. R.; Biba, M.; Welch, C. J. *Chirality*; Wiley: New York, **2006**, Vol. 18; pp 803–813.
23. Sajonz, P.; Schafer, W.; Gong, X.; *et al. J. Chromatogr.* **2007**, *1147*, 149–154.
24. Yashima, E. *J. Chromatogr. A* **2001**, *906*, 105–125.
25. Pirzada, Z. Z; Personick, M. M.; Biba, M. M.; *et al. J. Chromatogr. A* **2010**, *1217*, 1134–1138.
26. Welch, C. J. *J. Chromatogr.* **1994**, *666*, 3–26.
27. Armstrong, D. W.; Zhang, B. *Anal. Chem.* **2001**, *73*, 557A–561A.
28. Lammerhofer, M. M.; Maier, N. M.; Lindner, W. W. *Amer. Lab.* **1998**, *30*, 71–78.
29. Davankov, V. A. *J. Chromatogr. A* **2003**, *1000*, 891–915.
30. Allenmark, S.; Schurig, V. V. *J. Mater. Chem.* **1997**, *7*, 1955–1963.
31. Francotte, E.; Huynh, D. D. *J. Pharm. Biomed. Anal.* **2001**, *27*, 421–429.
32. Gasparrini, F.; D'Acquarica, I. I.; Misiti, D. D.; Pierini, M. M.; Villani, C. C. *Pure Appl. Chem.* **2003**, *75*, 407–412.
33. Kontrec, D. D.; Vinkovic, V. V.; Sunjic, V. V.; *et al. Chirality*; Wiley: New York, **2003**, Vol. 15; pp 550–557.
34. Franco, E. J.; Hofstetter, H. H.; Hofstetter, O. O. *J. Pharm. Biomed. Anal.* **2008**, *46*, 907–913.
35. Hofstetter, H.; Hofstetter, O. O. *Trends Analyt. Chem.* **2005**, *24*, 869–879.
36. Pirkle, W. H.; Welch, C. J.; Lamm, B. *J. Org. Chem.* **1992**, *57*, 3854–3860.
37. Pirkle, W. H.; Welch, C. J. *J. Liq. Chromatogr.* **1992**, *15*, 1947–1955.
38. Sellergren, B.; Ekberg, B.; Mosbach, K. *J. Chromatogr. A* **1985**, *347*, 1–10.
39. Baggiani, C.; Anfossi, L.; Giovannoli, C. *Curr. Pharm. Anal.* **2006**, *2*, 219–247.
40. Maier, N. M.; Lindner, W. *Anal. Bioanal. Chem.* **2007**, *389*, 377–397.
41. Welch, C. J.; Bhat, G.; Protopopova, M. N. *J. Comb. Chem.* **1999**, *1*, 364–367.
42. Blodgett, J.; Wang, Y.; Li, T.; *et al. Anal. Chem.* **2002**, *74*, 5212–5216.
43. Brahmachary, E.; Ling, F. H.; Svec, F.; Frechet, J. M. J. *J. Comb. Chem.* **2003**, *5*, 441–450.

44. Welch, C. J.; Protopopova, M. N.; Bhat, G. A. Microscale Synthesis and Screening of Combinatorial Libraries of New Chromatographic Stationary Phases. In *Fundamental and Applied Aspects of Chemically Modified Surfaces*; Blitz, J. P., Little, C. B., Eds.; Royal Society of Chemistry: Cambridge, **1999**, pp 129–138.
45. Welch, C. J.; Pollard, S. D.; Mathre, D. J.; Reider, P. J. *Org. Lett.* **2001**, *3*, 95–98.
46. Welch, C. J.; Hyun, M. H.; Kubota, T.; *et al. Chirality*; Wiley: New York, **2008**, Vol. 20; pp 815–819.
47. Pirkle, W. H.; Anderson, R. W. *J. Org. Chem.* **1974**, *39*, 3901–3903.
48. Colin, H.; Ludemann-Hombourger, O.; Nicoud, R. M. *Chromatogr. Sep. Tech.* **2003**, *28*, 8–12.
49. Ludemann-Hombourger, O.; Pigorini, G.; Nicoud, R. M.; Ross, D. S.; Terfloth, G. *J. Chromatogr. A* **2002**, *947*, 59–68.
50. da Silva, A. C.; Salles, A. G.; Perna1, R. F.; Correia, C. R. D.; Santana, C. C. *Chem. Eng.Technol.* **2012**, *35*, 83–90.
51. Rajendran, A.; Paredes, G.; Mazzotti, M. *J. Chromatogr. A* **2009**, *1216*, 709–738.
52. Grill, C. M.; Miller, L. *J. Chromatogr. A* **1998**, *827*, 359–371.
53. DeSimone, J. M. *Science* **2002**, *297*, 799–803.
54. Welch, C. J. *LC-GC* **2005**, *23*, 16–29.
55. Welch, C. J *Drug Disc. World* **2007**, *8,* 71–77, Fall.
56. Berger, T. A.; Smith, J.; Fogelman, K.; Kruluts, K. *Amer. Lab.* **2002**, *34*, 14–20.
57. Welch, C. J.; Sajonz, P.; Spencer, G. A.; *et al. Org. Proc. R&D* **2008**, *12*, 674–677.
58. Webster, G. K.; Kott, L. *Sep. Sci. & Tech.* **2011**, *10*, 251–282.
59. Gong, X.; Craven, T.; Schafer, W.; *et al. Chirality*; Wiley: New York, **2011**, Vol. 23; pp 128–132.
60. Woodward, R. B. *Pure Appl. Chem.* **1973**, *33*, 145–177.
61. Keown, L. E.; Collins, I.; Cooper, T.; *et al. J. Med. Chem.* **2009**, *52*, 3441–3444.
62. Welch, C. J.; Kress, M. H.; Beconi, M.; Mathre, D. J. *Chirality*; Wiley: New York, **2003**, Vol. 15; pp 143–147.
63. Andersson, S.; Nelander, H.; Ohlen, K. *Chirality*; Wiley: New York, **2007**, Vol. 19; pp 706–715.
64. Pirkle, W. H.; Welch, C. J.; Zych, A. J. *J. Chromatogr. A* **1993**, *648*, 101–109.
65. Welch, C. J.; Gong, X.; Schafer, W.; *et al. Chirality*; Wiley: New York, **2009**, Vol. 21; pp S105–S109.
66. Chobanian, H. R.; Guo, Y.; Liu, P.; *et al. Bioorg. Med. Chem.* **2012**, *20*, 2845–2849.
67. Wilson, S. R.; Wu, Y.; Kaprindis, N.; Schuster, D. I.; Welch, C. J. *J. Org. Chem.* **1993**, *58*, 6548–6549.
68. Vogtle, F.; Hunten, A.; Vogel, E.; *et al. Angew. Chem. Int. Ed.* **2001**, *40*, 2468–2471.
69. Welch, C. J.; Biba, M.; Pye, P.; Angelaud, R.; Egbertson, M. *J. Liq. Chromatogr. B* **2008**, *875*, 118–121.
70. Ruble, J. C.; Fu, G. C. *J. Am. Chem. Soc.* **1998**, *120*(44), 11532–11533.
71. Lo, M. C. C.; Fu, G. C. *J. Am. Chem. Soc.* **1998**, *120*, 10270–10271.
72. Albright, A.; Eddings, D.; Black, R.; *et al. J. Org. Chem.* **2011**, *76*, 7341–7351.
73. Miller, L.; Potter, M. *J. Chromatogr. B* **2008**, *875*, 230–236.
74. Freund, E.; Abel, S.; Huthmann, E.; Lill, J. *Chim. Oggi* **2009**, *27*(5), 62–64.
75. Wong, A.; Welch, C. J.; Kuethe, J. T.; *et al. Org. Biomol. Chem.* **2004**, *2*, 168–174.
76. Nelson, T. D.; Welch, C. J.; Rosen, J. D.; *et al. Chirality*; Wiley: New York, **2004**, Vol. 16; pp 609–613.
77. Leonard, W. R.; Henderson, D. W.; Miller, R. A.; *et al. Chirality*; Wiley: New York, **2007**, Vol. 19; pp 693–700.
78. Welch, C. J.; Fleitz, F. .; Antia, F. .; *et al. Org. Proc. R&D* **2004**, *8*, 186–191.
79. Welch, C. J.; Henderson, D. W.; Pipik, B.; *et al. Org. Proc. R&D* **2010**, *14*, 905–907.
80. Kaiser, P.; Ottolina, G.; Carrera, G.; Wohlgemuth, R. *N. Biotechnol.* **2009**, *25*, 220–225.

9.07 High-Throughput Purification in Support of Pharmaceutical Discovery

R McClain, Merck Research Laboratories, PA, USA
E Streckfuss, Merck Research Laboratories, NJ, USA

© 2014 Elsevier Ltd. All rights reserved.

9.07.1	Introduction	160
9.07.2	High-Throughput Chromatography	163
9.07.2.1	RP-UV–HPLC in HTP	164
9.07.2.2	MS-Directed RP-HPLC	164
9.07.2.3	Parallel Mass-Directed HPLC	164
9.07.3	Parallel Channel, MUX Mass-Directed Purification	165
9.07.4	Chromatographic Hardware/Software Optimization	165
9.07.5	Passive and Active Splitting	166
9.07.6	Boolean Logic Fraction Triggers	166
9.07.7	Sample Loading Techniques for HTP	168
9.07.8	High pH Chromatography	168
9.07.9	Focused Gradients	169
9.07.10	Autopurify – Automated Analytical to Preparative	170
9.07.11	Normal Phase Mass-Directed HPLC	172
9.07.12	General SFC Characteristics	172
9.07.13	Use of Cyclones for Handling Expansion of Supercritical CO_2	173
9.07.14	UV-Based SFC for HTP	173
9.07.15	Mass-Directed SFC for HTP	173
9.07.16	HTP Workflows	175
9.07.17	Prepurification Workflow	175
9.07.17.1	Submission/Request/Initiation	175
9.07.18	Analytical Screening	176
9.07.19	Visualization/Interpretation of Screening Data, Choice of Purification Conditions	176
9.07.20	Postpurification Workflow	177
9.07.21	Processing of Fractions from Purification	177
9.07.22	Current Needs and Future Outlook	178
9.07.23	Conclusion	179
References		179

Glossary

Boolean logic fraction trigger The use of and/or statements to satisfy fraction triggering criteria in preparative chromatography. Triggering criteria can include mass and UV thresholds and slopes as well as time windows.

High-throughput purification The treatment of either singleton or libraries of compounds by established procedures and dedicated instrumentation to enable rapid isolation of desired product from mixtures.

Mass-directed purification The separation technique utilizing a mass spectrometer interfaced to a preparative chromatograph to trigger isolation of a desired species with a defined monoisotopic exact mass.

Supercritical fluid A substance that is above its critical temperature and pressure that takes on unique properties that are not experienced in single phase states such as the liquid or gaseous form. CO_2 is the most commonly used supercritical fluid for chromatographic purposes.

Supercritical fluid chromatography Utilization of a supercritical fluid in a chromatographic system.

9.07.1 Introduction

High-throughput purification (HTP) has become an integral component of the modern drug discovery process. Currently, as high-throughput organic synthesis is becoming more widely embraced in both academia and other industries, the process of HTP has attracted increasing interest. The drug discovery process comprises a number of component parts – from compound design to synthesis, purification, and ultimately activity screening – not to mention the data handling and information storage involved in tracking all of these activities. Any slow step in the process can create a bottleneck that limits the overall pace of new drug candidate synthesis and evaluation. In the transition of conventional organic synthesis to the high-throughput experimentation

 doi:10.1016/B978-0-08-097742-3.00918-6

mode, compound purification can easily become a bottleneck. In this chapter, the authors describe the adoption and utilization of HTP tools in the pharmaceutical industry, along with its fundamental principles, associated equipment, strategies, best practices, as well as current unmet needs and areas for future growth.

The discovery of novel and safe, effective therapies for disease management is an increasingly difficult undertaking, and pharmaceutical corporations are under increasing pressures to evolve new mechanisms to find continued success in this endeavor. Surveys of drug discovery research throughout the past 10 years have estimated a 93–96% attrition rate of drug candidates in clinical trials.[1–3] The overall process comprises a vast array of scientific disciplines, all of which must be efficient to enable the advancement of a developmental compound to the clinic and hopefully to the marketplace. As with any multicomponent process, drug discovery moves only as fast as its slowest contributor, which inherently drives efficiency enhancements within each area on a continual basis. Thus, there is a constant push toward identifying operating models that increase productivity and therefore reduce the duration of the discovery timeline.

The drug discovery process typically begins with lead identification and validation of a biological target. Possible lead molecules are most often identified via high-throughput screening, competitive analysis, and through literature searches. At this point, the focus shifts toward the optimization of the preferred chemotype(s) from lead identification. The resulting lead compounds are modified and subjected to further *in vitro* and/or *in vivo* biological testing to characterize Structure–Activity Relationships (SAR) (**Figure 1**). The medicinal chemists performing the synthesis follow the SAR and tune each subsequent iteration of molecules to deliver the desired properties.

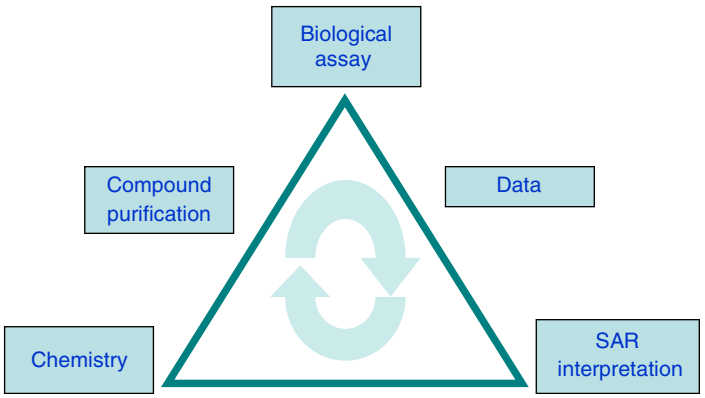


Figure 1 SAR triangle diagram, highlighting the cyclic nature of fine tuning molecules through an iterative process.

The highly iterative nature of the lead optimization stage of drug discovery highlights the need to keep data cycles as short as possible.[4,5] Attending to this critical need will facilitate timely advancement from lead identification through lead optimization, and eventually discovery of candidates for development and clinical testing.

Drug discovery companies have continuously driven down SAR cycle times lower in an effort to shorten the overall timelines of the lead optimization process. There has been a corresponding drive to increase probability of success by synthesizing and evaluating more compounds per cycle, in order to more effectively evaluate hypothesis and guide strategies for the next rounds of synthesis. It became critical to provide technological tools to realize these strategies without a corresponding increase in the work force.

In response to the above need, specialized automated synthesis groups were created with the goal to leverage expertise with parallel synthesis and automation to create many analogous compounds quickly.[5–7] These groups' efforts are strategically aligned with the overall goals of a particular discovery project and they work in collaboration with project chemists. These goals may include introducing new chemical diversity, identification of a new SAR direction, improvement of pharmacokinetic properties, reducing lypophilicity (logP), and introduction of novel structural classes for patent purposes.

Through the utilization of enabling technologies, such as solid-phase-supported reagents, microwave synthesizers, flow cell chemistry systems, and liquid handlers modified to perform rapid reaction set up, automated synthesis groups strive to leverage reaction schemes that are amenable to automated synthesis in order to have the most impact.[8] Often, difficult chemistries are required to access compound libraries that feature activity and appropriate drug-like properties. Recent surveys of reaction types used in the creation of new molecular entities have found that medicinal chemists have historically used only a small portion of the possible synthetic routes available to them.[9–11] Therefore, medicinal chemists are under increased pressure to utilize more complex chemical transformations in their work. As more of the chemical space is explored, there has been a corresponding increase in the resulting complexity of the mixtures from these syntheses. The result of all these pressures is a dramatic increase in the number, and complexity, of compounds that will require purification before *in-vitro* testing.

Many researchers have endeavored to validate that SAR results are most reliable when purified compounds are tested.[12,13] Purity is generally expressed as relative purity, as determined by a simple calculation of area percentage from a high-performance liquid chromatography (HPLC)–ultraviolet (UV) chromatogram or from interpretation of proton nuclear magnetic resonance

(NMR) spectra. However, it has been shown that these techniques cannot, in fact, account for all of the material present within a final reaction mixture. Comparisons of initial relative purity with absolute purity, as determined by quantitative techniques such as quantitative NMR and LC with chemiluminescent nitrogen detection (CLND) have shown large discrepancies (20–40%) in the amount of desired product actually present.[14,15] Even compounds that may have appeared to be relatively pure before a defined purification protocol can yield vastly different results in a biological assay than the same compounds that were subjected to purification. This discrepancy is attributed to the presence of 'invisible' impurities that remain after organic synthesis; for example: trifluoroacetic acid (TFA), residual solvents, dimethyl sulfoxide (DMSO), water, inorganic salts, leached plastics, and resins. The presence of these impurities may cause errors in weight determination and can also interfere with the mechanism of some biological assays leading to false positive and false negative results. Thus, it has become widely accepted that all compounds should be subjected to some type of purification before biological assay. Screening of highly pure compounds is critical to the reliability of the composite structural activity data generated by biological assays; the application of a consistent purification process to all compounds to be assayed leads to higher quality results.

Between 20% and 50% of a medicinal chemist's time is spent with nonsynthetic chemistry tasks such as purification, evaporation, reformatting of material, and documentation.[16,17] In a high-throughput chemistry environment, these nonsynthetic tasks can quickly balloon to fill an impracticable amount of time. Cleanup procedures utilizing techniques such as crystallization, liquid–liquid extraction, scavenger resins, fluorous cleanup, thinlayer chromatography (TLC), or low pressure normal phase (Flash) chromatography are valuable tools that are heavily utilized by medicinal chemists.[18–24] However, the demands of short timelines and high throughput present a challenge for the above-mentioned cleanup procedures to keep pace.

To realize fully the potential benefits of high-throughput chemistry, there needed to be a corresponding development of supporting centralized HTP technology and workflows. The operational efficiency of these centralized functions can provide very high levels of productivity through increased asset utilization and employment of subject matter experts. This also allows continuous refinement of the equipment, process, and surrounding infrastructure. Through the effective implementation of HTP workflows, consisting of dedicated purification and automation specialists, the purification bottleneck can be eliminated.

Throughout the past 15 years, the development of HTP faced many rigorous demands. A successful workflow must simultaneously be capable of returning large numbers of compounds of very high purity, despite dramatically decreased project timelines and increasingly complex mixtures. Although the synthetic routes chosen to deliver desired compounds are highly variable, a common purification platform could be employed to handle the vast majority of molecules originating from automated synthesis laboratories, if the proper attributes are present.

The early development efforts of HTP quickly highlighted key elements that were critical for effective implementation. The resulting purification platforms evolved to provide purification support capable of handling the demands of automated synthetic chemistry. There was an immediate demand for a purification technique that could allow a single chemist to purify at least 5–10 compounds per hour. As the authors shall discuss in greater detail, reversed-phase (RP)-HPLC quickly became the preferred tool for addressing this need. RP chromatography systems were readily amenable to application-specific automation. Additionally, RP chromatography column stationary phases (C-18) provided nearly 'universal' applicability and selectivity for most drug-like molecules and their corresponding crude reaction mixtures. Similarly, analytical HPLC–mass spectrometry (LC–MS) was adopted as the primary analytical tool for both the initial screening process and for QC analysis after purification. The predictive scalability of HPLC from analytical to preparative was also a major driver toward adopting this platform as the primary tool for HTP. Other analytical techniques such as NMR and accurate mass determination by high resolution mass spectrometer (MS) were widely adopted for subsequent absolute identification of purified compounds.

In conjunction with the rapid development and adaptation of HPLC–MS equipment for HTP, there was a parallel development of tools to support the remainder of this complex workflow. This supplemental instrumentation proved to be just as critical to the successful incorporation of HTP in drug discovery efforts. Large capacity and highly efficient evaporators were required to evaporate many fractions simultaneously in a rapid manner. Robotic weighing instruments that could perform hundreds of accurate gravimetric analyses a day were also required; as were liquid handler instruments for other highly precise, repetitive tasks such as dilution, liquid transfers, reformatting, and cherry picking of vials.

The early pioneers of HTP also quickly realized that intensive development of software applications that could manage the entire process was crucial to realizing a truly optimized workflow. None of the hardware discussed in the preceding paragraph was specifically designed to work in concert with one another to complete the complex task of delivering pure compounds in suitable form. The chromatographic instrument vendors have incorporated many software features that are specific to the task of MS-directed purification. However, other custom software tools were developed within pharmaceutical companies to generate work lists and accept data from the many disparate types and brands of equipment being utilized. Additional custom software tools for compound submission, sample tracking, data interpretation, and reporting were also developed. As the authors shall discuss in further detail, the development of software tools continues to be one of the primary focal points of HTP work-flow refinement.

The steps shown in **Figure 2** constitute a complete HTP workflow from submission of impure samples to submission of purified compounds to biological assay. It is important to realize that incorporation of every single step is not required, and the exact inputs and outputs of HTP may differ for each particular platform. The highlighted steps represent the core capabilities of a typical HTP group in drug discovery. The more of these steps that are included in an optimized workflow, the larger the overall gains in efficiency can be.

The rapid evolution of HTP as an integral part of the modern drug discovery process was due to the efforts of many exceptional scientists. The authors present here a brief historical survey of progress in this field. This will be told initially from the perspective

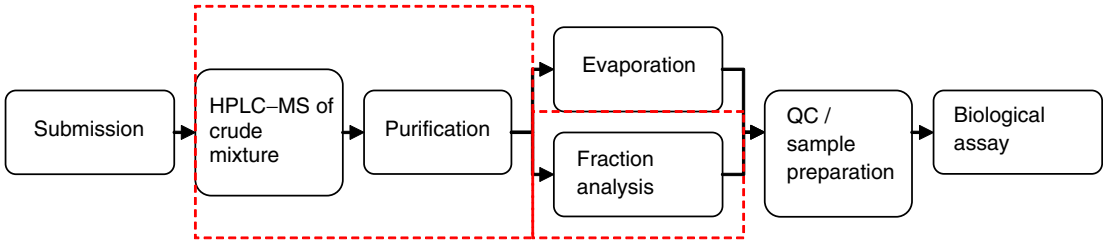


Figure 2 Flow chart of the basic steps in a typical HTP process. The steps surrounded in red are core capabilities.

of chromatographic system development. The authors will then shift to a review of the other core components of the HTP workflow in greater detail and end with a discussion of critical unmet needs and areas for future growth potential for HTP.

9.07.2 High-Throughput Chromatography

The challenge of adopting a purification platform that was widely applicable, selective, and fast has been noted in section 9.07.1. RP preparative chromatography became the focus of interest due to its high efficiency and powerful and predictable selectivity. Another positive attribute of RP chromatography resides in its scalability, which is critical to allow the advancement of successful compounds through the drug discovery process; as each successive biological assay requires increased amounts of compound.

RP preparative chromatography has the ability to be used in either a centralized, service-based mode of operation or in an open access, walk-up mode. The centralized purification approach employs a limited number of specialized preparative chromatographers to process compounds on a service basis for the medicinal chemist. This approach allows the medicinal chemist to focus on synthesizing additional compounds and following SAR data, whereas the purification specialists purify and characterize the resulting molecules. An alternative approach is to share common purification platforms among a number of users, with systems strategically located and administered by a specialized chromatographer to ensure maximum efficiency and reliability. As the chromatographer is not conducting the actual separation and performing all the associated wet steps of the process, a single chromatographer can support more purification systems than would be possible if they were performing the actual separations. A benefit of this open access approach is that the synthetic chemist may possess intimate knowledge of their reaction products and the associated physical characteristics that would allow for more informed decisions to be made about separation conditions used to process the compound.

Regardless of the style of operation, either centralized purification service or walk-up/open access systems, the chromatographic system used for the purification comprises the same key components. A binary pumping system capable of executing a linear gradient at flow rates between 5 and 100 ml min^{-1} is required to successfully utilize 1–3 cm inner diameter semipreparative columns. Columns of this size are appropriate for the crude reaction scales of 5–100 mg, which are frequently encountered in high-throughput synthesis laboratories. Other key components are an injector, a detector, and a fraction collector. The injector needs to be capable of injecting between 100 and 2000 µl of sample dissolved in organic solvent into the system's mobile phase path. The detector needs to be capable of monitoring the semipreparative column eluent to serve as a fraction triggering device, whereas the fraction collector needs to be able to route system eluent either to waste or fraction vessel through use of a diverter valve. An example of the above described preparative chromatography system can be viewed in Figure 3.

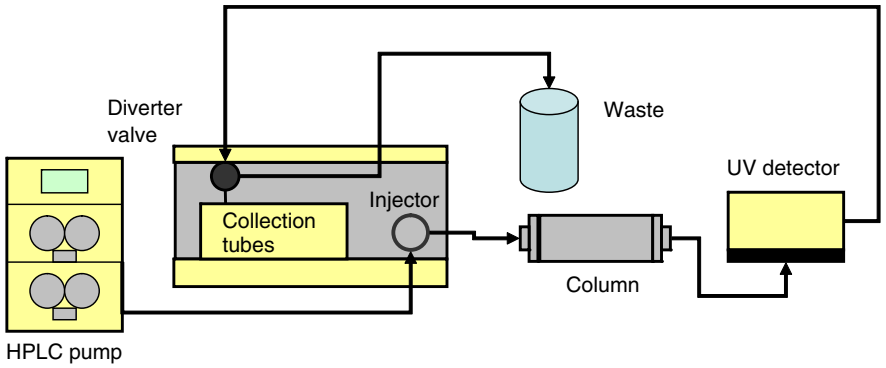


Figure 3 Illustration of preparative HPLC system configured with a preparative flow cell and a combined autosampler/fraction collector. The mobile phase sweeps the injector en route to the column. The UV detector triggers collection of desired compound.

9.07.2.1 RP-UV–HPLC in HTP

One of the first HTP systems was set up as an open access system and was capable of purifying 80 compounds a day in an automated fashion.[25] The use of rapid gradients and high linear velocities of mobile phase were used to achieve run times of 7 min per reaction product. Linear gradients were run on the system and samples were added to the running sample queue by the medicinal chemist. Six columns were contained on the preparative system and the user could specify which stationary phase to employ through previously performed analytical screening. An UV detector was used as the fraction triggering device. Six fraction collectors were plumbed into the system as the UV detector lacked the ability to differentiate which peaks to collect if multiple peaks satisfied the fraction triggering criteria. The propensity of UV-triggered purification systems to collect multiple fractions per crude reaction product presents a potential throughput bottleneck since each fraction must be analyzed by either flow injection analysis (FIA) or analytical LC–MS to locate fractions containing the desired compound. A detector with more specificity than the UV detector currently employed and that could selectively trigger fraction collection of only the desired compound would be much more efficient. The number of fractions to be analyzed would be minimized as would be the necessary capacity of the fraction collector(s).

9.07.2.2 MS-Directed RP-HPLC

An alternative approach to the totally UV-based purification platform is the incorporation of a MS into the analytical screening system used to analyze the crude reaction products. The crude products are analyzed via analytical LC–MS to confirm the synthesis was successful through detection of the desired mass by the MS. The analytical LC–MS data also confirm that the chromatographic conditions being used are compatible with the physical properties of the reaction products and are capable of producing pure product. Another pioneer of HTP utilized the specificity of an analytical LC–MS to identify the peak of interest, and then used a software package to predict the time window the compound would elute within on an UV-based semipreparative chromatography system.[26] The software package also set the UV threshold to serve as the fraction trigger. This approach limited the number of fractions collected except in cases where extremely close eluting impurities still coeluted within the time window selected by the software application.

The utilization of MS data to predict elution time of the desired compound selectively on the preparative scale was found to be a substantial productivity enhancement. The minimization of the number of fractions captured by the UV-based preparative system led the scientific community to desire a yet higher level of specificity for fraction triggering. If only fractions containing the desired mass of interest were collected, the laborious task of analyzing fractions to locate the material of interest would be greatly reduced as would the requirement for large fraction collector capacity. A major technological breakthrough in HTP occurred when a MS was introduced into a semipreparative purification system and used as the fraction triggering device.[27] System eluent was routed to a fraction vessel only when the user-defined threshold of the reconstructed ion chromatogram for the mass of interest was exceeded. The ability of the MS to monitor the semipreparative column eluent in real time and actively detect the mass of interest proved successful at limiting the number of fractions collected for each sample processed. The sensitivity of the MS combined with its destructive nature require that only a small portion of the preparative chromatograph's eluent stream be introduced to the detector. Otherwise excessive loss of compound and contamination of MS occurs. This is accomplished through the use of a passive splitter.

In addition to using m/z values observed by a MS, early mass-directed HPLC systems incorporate a UV detector to share in the fraction triggering criteria.[28] **Figure 4** represents a purification system capable of fraction triggering by UV and/or MS detector signals. The ability to store both wide range UV data from the photodiode array (PDA) detector and full-range total ion current scans from the MS allowed for more conclusive decisions to be made regarding purity of isolated fractions.

9.07.2.3 Parallel Mass-Directed HPLC

The large expense incurred with purchasing a MS coupled with the need to increase the purification throughput steadily led to innovative approaches for maximizing the productivity of this detector. One of the first mass-directed purification systems was optimized to have 10 min cycle times, allowing the purification of approximately 100 compounds a day.[27] This mass-directed platform was later optimized to deliver parallel channel mass-directed purification capable of processing 200 compounds a day, as well as an additional 200 compounds per night.[29]

The parallel system encompassed two semipreparative columns run simultaneously, a shared autosampler, a single set of gradient pumps, and a single MS. An additional fraction collector was introduced into the system to provide a dedicated fraction collector for each of the two columns. To minimize the possibility of intermingling samples from independent libraries, each of the parallel columns were dedicated for a unique library. The shared MS monitored both targeted masses of interest and differentiated which fraction collector to initiate collection based on the targeted masses specified in the user input sample queue. A modified dual spray electrospray source ensured both column eluent streams were delivered to the MS in equal proportions.[29] Simultaneous fraction tracking of two libraries required an error proof mechanism to track the resulting fractions accurately. Limiting isolation of one fraction, per sample, per column in combination with the destination fraction location being the same well id in the fraction plate from which it was injected proved to be a good solution. The reduced number of fractions collected and the ability to use the sample queue to summarize the sample parameters associated with isolated fractions allowed this

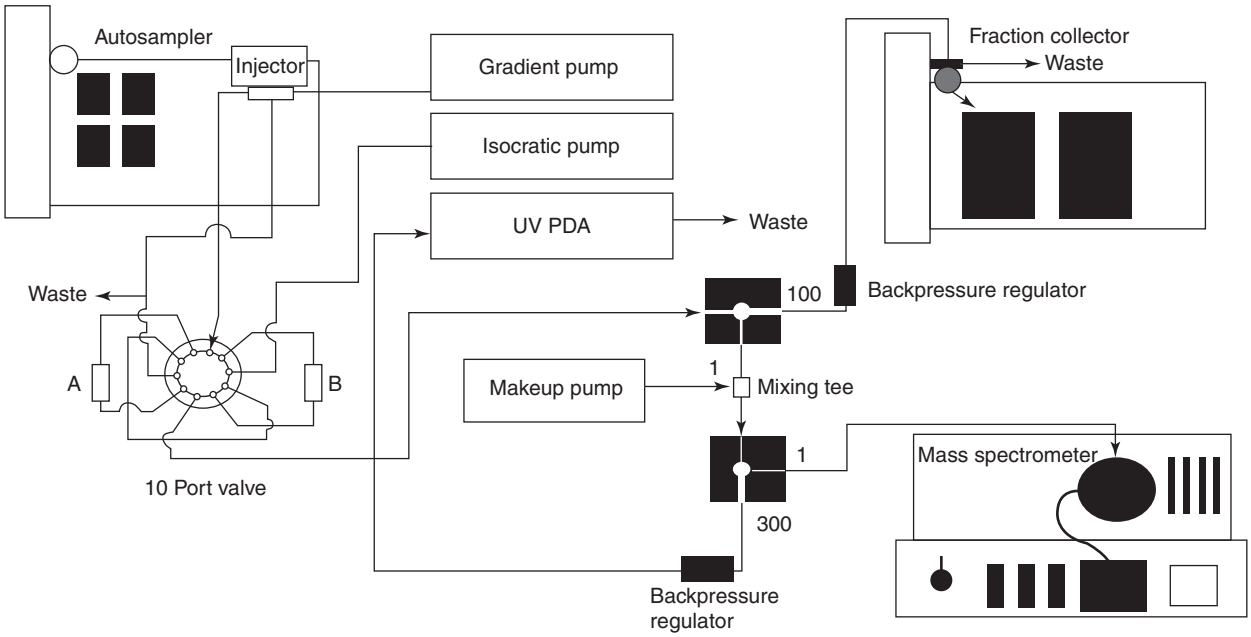


Figure 4 Schematic showing the incorporation of an UV detector as an additional fraction triggering device into a mass-directed HPLC system. Comparison of **Figures 3** and **4** highlight the complexities arising from incorporation of mass triggering capabilities into an HPLC system. Reprinted with permission from Kiplinger, J. P.; Cole, R. O.; Robinson, S.; *et al. Rapid Commun. Mass Spectrom.* **1998**, *12*, 658–664.

parallel system to double the throughput without presenting a postpurification bottleneck. This concept established that parallel purification leveraged a HTP lab to keep pace with the parallel synthesis laboratories they support.

The success experienced by parallel channel mass-directed purification systems in isolating a single fraction per reaction encouraged some UV-based purification groups to adopt this collection principle. One HTP group combined the use of a maximum-seeking computer algorithm with a six-port valve configured with a collection buffer coil to ensure the correct fraction was dispensed into the fraction vessel at the completion of the run.[30] Once a fraction was routed to this valve-controlled collection coil, subsequent peaks were monitored in real time to determine whether another peak could produce a larger peak height detector response. If so, the valve would rotate to route the previously captured fraction out of the coil to be replaced with the newly selected peak. At the conclusion of the run, the peak representing the compound producing the most intense detector response was routed to the fraction vessel. A follow-up FIA and HPLC analysis then confirmed that the proper compound was isolated in sufficient purity. The follow-up analysis of several preparative HPLC systems could be performed on a shared MS.

9.07.3 Parallel Channel, MUX Mass-Directed Purification

The ever-present need to maximize MS productivity led to the incorporation of MUX technology into a four-channel parallel mass-directed purification system.[31] The flow from a single set of preparative pumps was split in fourths through a Valco manifold Tee to feed all four chromatography columns simultaneously. An autosampler was configured with four independent valves to load four individual samples from unique sample sets onto their respective semipreparative columns. Each column's eluent was passed through a shared UV detector before being split to the MUX interface of the single MS interfaced to the preparative system. MUX is an abbreviation for multiplexed ion source, which consists of a disk of four needles that rotate to align with the inlet leading to the high vacuum region of the MS. Through rotation of the independent needles, a split amount of the eluent from individual columns can be introduced to the MS to monitor a specific mass of interest. The MUX interface was favored over previous versions of shared interfaces such as the dual ion interface because MUX can successfully detect compounds possessing the same mass on multiple channels in the same purification run. In addition, the ability of the MUX to introduce the eluent stream independently from a column into the MS prevented any type of suppression effects encountered with simultaneous ionization sources.[31] The commonly utilized fraction tracking scheme of one fraction, per sample, per column was utilized on this platform to deliver four plates containing purified product, each mirroring the injection plate used at the outset of the purification process.

9.07.4 Chromatographic Hardware/Software Optimization

The productivity enhancements experienced by HTP groups utilizing mass-directed HPLC were quickly realized, and the technique was readily adopted throughput the HTP community within several years. Once these powerful systems were optimized for

throughput, the administrators of the systems began to implement enhancements to improve the quality of separations being performed. One of the main areas of focus was the mechanism of splitting the semipreparative column eluent to enable both detection and fraction collection of the compound of interest. Particular emphasis was placed on ensuring accurate timing calibration between the two fluidic streams resulting from splitting. Another closely related area of focus was the improvement of peak efficiency to ensure accurate fraction triggering and delivery of the highest recovery of compound while satisfying the desired purity requirements of 85–90%.[32] The authors will now review these developments that refined the technique of HTP as it emerged.

9.07.5 Passive and Active Splitting

The extreme sensitivity of mass spectrometry in conjunction with the destructive nature of the detector mandates that only a small portion of the semipreparative column's eluent stream be introduced to the detector. Splitting of the column eluent allows a small amount of sample to be routed to the detector whereas greater than 99% of the sample is routed to the fraction collector. The synchronization of the timing between the MS detecting the mass of interest and the arrival of the main flow to the fraction collector's diverter valve is extremely important for both compound purity and recovery. A delay coil of adequate volume must be introduced between the splitter and fraction collector to provide the detector time to observe the mass of interest and trigger collection before the sample in the mobile phase stream passes the diverter valve of the fraction collector. Failure to align the two independent fluidic paths originating from the splitter degrades sample purity and diminishes sample recovery. The original splitter design incorporated nothing more than a fluidic tee connected to a length of capillary tubing being directed to the inlet of the MS. The split ratio of compound routed to the MS and compound routed to the fraction collector was determined by path of least resistance principles and allowed only a small amount of sample flow to enter the MS.[27] This method of splitting would later become known as passive splitting; subsequently, commercial versions of passive splitters that contain preconfigured capillaries and delay coils were made available. More recent examples include braided delay coils that are engineered to minimize turbulence, and therefore, undesirable chromatographic band broadening.

The importance of controlling the mass of sample introduced to the MS resulted in incorporation of a make-up pump into a second fluid path through the splitter to the MS.[28] The electrospray atmospheric pressure ionization sources used on typical mass-directed purification systems are optimized to accommodate 0.5–1.0 ml min^{-1} of flow. The make-up pump provided a controlled mechanism of introducing small aliquots of sample into the ionization source of the MS at an appropriate flow rate and scale to prevent severely tailing peaks and very long delay times. The tailing MS peaks caused by decay from overloading the MS could result in the ion of interest remaining above the triggering threshold and result in cocollection of close eluting impurities that were actually fully resolved by the chromatography column. A make-up pump incorporated into a purification platform is visible in the schematic contained in Figure 4.

One limitation of passive splitters is that they are configured to work at a fixed split ratio and within a fixed flow rate range. Applications requiring a different split ratio or flow rate range will require the use of different splitter assemblies. The scale of chromatography and the required sensitivity will dictate which passive splitter will be optimal. The split ratio is inversely proportional to the resistance to flow through the internal capillary. Delay is a function of flow rate and the volume of the delay coil. Figure 5 depicts a passive splitter, highlighting the split flow traveling to the make-up pump's fluidic path as well as the presence of the delay coil or loop.

One strategy for addressing the limitations of passive splitting is the incorporation of a device known as an active splitter into the mass-directed purification system. These devices allow automated control of variable split ratios and flow rates.[33] The active splitter consists of a Rheodyne valve with a modified rotor seal containing three small orifices with the following volumes: 20, 100, and 300 nl. The four-port stator accepts the preparative system flow through one port and allows its exit through another for delivery to the fraction collector. An isocratic make-up pump is attached to the third port of the valve to sweep material split through these fixed volume channels on to the MS at a constant rate. The final port of the splitter is connected to the ionization source of the MS and delivers the flow stream from the isocratic make-up pump combined with the split aliquots of sample to the source. A schematic of the stator of the active splitter can be viewed in Figure 6.

Through a software interface, the actuator is set to a user-defined frequency which routes the 20, 100, or 300 nl aliquots into the make-up stream and consequently delivers to the MS at a fixed rate. The ability to change the spilt ratio actively allows the mass of material being delivered to the MS to be optimized for each sample without requiring any plumbing changes or timing calibrations. This optimization prevents oversaturation of the MS and allows accurate fraction collection.

Both active and passive splitting techniques are widely utilized as a core component of MS-directed purification systems. The understanding and proper utilization of these splitting technologies have enabled chromatographers using MS-directed purification to consistently collect pure compounds with high recovery.

9.07.6 Boolean Logic Fraction Triggers

The acceptance of active splitter technology highlights the importance of the peak shape of the MS signal on the purity of the isolated fractions. Even with the MS signal on scale, the broad tailing nature of MS decay can sometimes result in close eluting

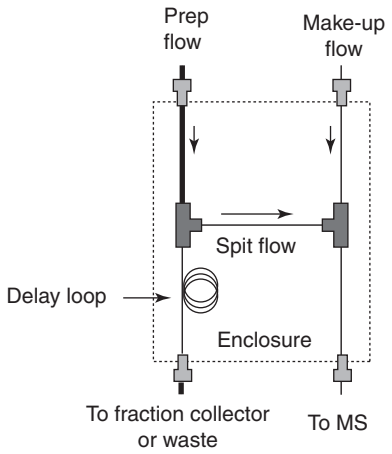


Figure 5 Illustration of a passive splitter. The make-up flow delivers the small amount of column eluent from the split flow to the ionization source of the MS. The delay coil is visible and is adjusted to ensure proper timing between the fraction collector's diverter valve and the MS detector. Reprinted with permission from Cai, H.; Kiplinger, J. P.; Goetzinger, W.; *et al. Rapid Commun. Mass Spectrom.* **2002**, *16*, 544–554.

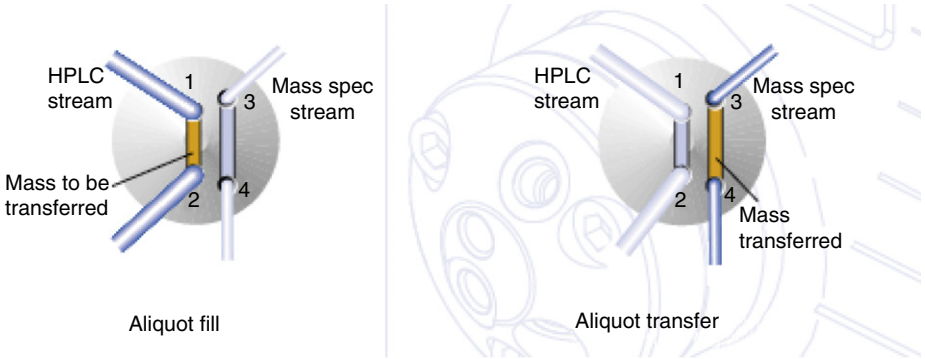


Figure 6 Illustration of a Rheodyne mass rate attenuator (MRA). The yellow 'plug' of sample is moved from the column eluent stream to the make-up fluidic path through actuation of the valve. Image reproduced with permission of IDEX Health and Science LLC.

impurities being collected in the same fraction vessel as the desired compound. The use of Boolean logic to combine fraction triggering criteria from several detectors increases the probability of successfully cutting fractions to prevent cocollection of desired/undesired compounds.[34] Frequently, a UV fraction trigger will be combined with a mass fraction trigger through an AND statement. This instructs the purification system on seeing the UV criterion satisfied, to confirm the proper mass is being simultaneously observed in the MS. If the answer is no, the eluent is allowed to pass the diverter valve into waste. If the mass of interest is simultaneously detected, both UV and mass criteria are met, and the eluent will be collected as a fraction. The preparative UV flow cell is located directly after the column and displays the more accurate representation of peak integrity when comparing UV and mass detector signals. The fraction ending criterion of the UV detector terminates the fraction collection before the end of the tailing MS peak, resulting in less fraction volume and minimizes the possible cocollection of close eluting impurities. The slope of the UV signal can be used to advance the fraction collector to the next fraction vessel if the slope of the signal changes direction. In this case, a portion of the sample could be collected in its pure state, whereas the remainder would be collected and could be repurified to separate the coeluting peak that caused the change in UV slope.

Preparative RP chromatography has proven to be an excellent platform for processing large numbers of compounds rapidly due to its efficiency and high degree of selectivity. The partition mechanism employed in RP chromatography delivers efficient peaks that are capable of being baseline resolved from structurally similar compounds, thus allowing the isolation of pure compound. Preparative chromatography run times are proportional to column length and to ensure maximum productivity in terms of separations per unit time, short columns are often desired.[25] Many high-throughput separations groups rely on short preparative columns with bed lengths of 5–10 cm. As widely understood from the concept of geometric scaling, the sample size dictates the inner diameter of the column selected for the separation.[35] It was common in the earlier days of high-throughput preparative chromatography to find groups utilizing 1 cm inner diameter prep columns, although most groups currently rely on 2 or 3 cm inner diameter columns. Emphasis has been put on optimizing throughput by maximizing column volumes through use of exceptionally high linear velocities.[25]

9.07.7 Sample Loading Techniques for HTP

Sample loading techniques have a profound impact on peak efficiency and, if done incorrectly, can add complexities to the chromatographic process before the separation process even begins. It is well understood that the most suitable diluent for a sample being purified is the initial mobile phase composition used in the separation.[36] For RP chromatography this would typically be mostly water. However, it is typical for organic synthesis products on the order of tens of milligrams to be insoluble in 1–2 ml of water, which is the range of injection volumes commonly used in HTP. This has led to DMSO and *N*,*N*-dimethylformamide being selected as preferred diluents because of their strong solvating properties. The use of these solvents allows dilution of reaction mixtures in the lowest possible volume and also facilitates formatting of compound libraries in 2 ml, 96-well microtiter plates.

This highlights two related issues with sample loading that must be addressed by HTP groups. First is the issue of poor solubility of the reaction mixtures in RP mobile phases, which can lead to precipitation or 'crashing' of compounds on injection into the chromatographic system. Second is the probability of poor chromatographic effects such as fronting or band broadening caused by the use of these strong sample diluents. As the sample is being loaded on the head of the column in a plug of strong solvent such as DMSO, some of the material present may streak forward or break through. With respect to both of these issues, it is important to realize that they do not just apply to the compound of interest, but also all of the other components present in the mixture.

An early strategy that was employed in an attempt to minimize these effects was using autosampler routines to bracket the sample plug en route to the column with alternating 50 µl 'slugs' of air and DMSO. This serves to postpone contact of the sample with water until it reaches the head of the chromatographic column.[6] The DSMO slugs mix with the aqueous-based mobile phase whereas the air slugs isolate this DMSO/mobile phase mixture from the sample. This DMSO slug approach can be viewed in Figure 7. A similar approach was used in an UV-based purification system bracketing the sample with acetonitrile and experienced comparable success.[30]



Figure 7 Illustration of the DMSO slug approach injection technique. The sample is isolated from contact with aqueous-based mobile phase until it safely arrives at the head of the chromatographic column. Reprinted with permission from Leister, W.; Strauss, K.; Wisnoski, D.; Zhao, Z.; Lindsley, C. *J. Comb. Chem.* **2003**, *5*, 322–329.

Generally, material that precipitates at the column is recoverable by rinsing with organic solvent. In contrast, it is much more problematic to recover material that precipitates in the autosampler or tubing. By prolonging contact of concentrated sample with the aqueous mobile phase, this sandwiching technique can alleviate undesirable precipitation of compounds. However, it does not address the potential for poor chromatographic effects due to DMSO breakthrough described above.

In response to these demands, a novel approach of sample loading called at-column-dilution (ACD) was developed as a method of efficiently loading samples, regardless of diluent strength or volume.[37–40] ACD uses an organic solvent, usually the stronger chromatographic elution solvent, to sweep the autosampler and deliver the sample in the organic stream to a mixing tee located directly before the head of the semipreparative column. The aqueous portion of the mobile phase is delivered simultaneously to this mixing tee. This serves to dilute the organic stream containing the sample in an effective manner. The diluting out of the sample diluent and organic modifier of the mobile phase results in the sample partitioning into the stationary phase in a tight plug. The enhanced sample loading delivered by ACD delivers increased chromatographic efficiency, and 10-fold loading increases are routinely experienced when compared with the traditional method of sweeping the autosampler with mixed mobile phase.[38] One common implementation of ACD utilizes an additional analytical pump that delivers organic solvent at a constant rate through the autosampler loop and then to the mixing tee.[38] Comparable performance was later demonstrated through a simpler alternative of sweeping the autosampler with the organic solvent being delivered by the preparative gradient pump.[39,40] In addition to the loading enhancement that ACD delivers, rates of sample precipitation in the autosampler are reduced as the sample, which is frequently hydrophobic, never encounters water until the mixing Tee which is located outside the actual instrument modules (Figure 8).

9.07.8 High pH Chromatography

TFA is often used in HTP laboratories to control peak shape of basic compounds by ensuring residual silanols ubiquitous in the silica-based C18 columns are in their neutral charge state. If the pH of the mobile phase is greater than the p*K*a of these silanols, the negatively charged silanols can participate in ion exchange interactions with positively charged molecules, leading to significant peak tailing. Although TFA helps minimize peak tailing and thus minimizes fraction volumes, long-term stability of TFA salt forms of basic compounds as well as biases against the presence of TFA in the biological assays make it an undesired mobile phase additive.[41] Chromatography performed at pH 9 or 10 on C18 columns with a silica support capable of handling the

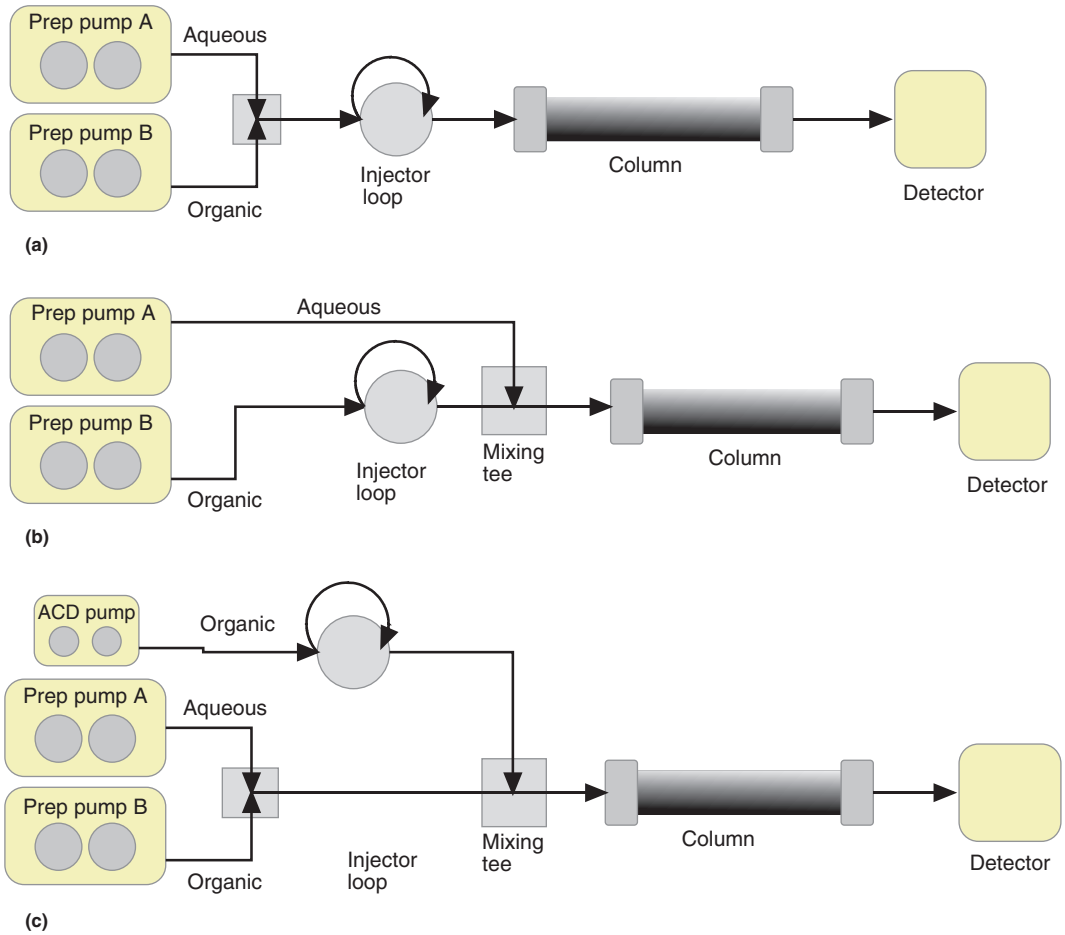


Figure 8 Diagram showing system layout for (a) Traditional (linear) loading, (b) ACD with two pumps, and (c) ACD with three pumps (stand-alone loading pump).

high pH environment is a viable alternative to the use of TFA. RP-HPLC separations performed on C18 columns predominately rely on the mechanism of hydrophobic partitioning to separate molecules. Neutrally charged molecules are more hydrophobic than their ionized forms and will thus be retained longer in RP-HPLC. The specific p*K*a of each molecule encountered in a chromatographic system will determine its charge state in a specific pH environment, but in general, basic molecules will be in their neutral charge state in a pH range of 9–10. Consequently, neutral compounds will typically be retained longer and eluted in a higher organic composition mobile phase, leading to easier solvent removal for purified compounds. The strong partitioning of the neutral molecules into the stationary phase on injection dramatically increases loading capacity of basic compounds.[38] Mass loading of neutral compounds can be as much as 14 times greater than loading of the ionized form of the molecule.[42] Figure 9 serves as an example of the optimized loading of a basic compound at a pH above the p*K*a of the molecule. The benefits experienced through utilization of high pH chromatography for purification of basic compounds have led to the technique becoming an important alternative to low pH chromatography.

9.07.9 Focused Gradients

The successful loading of a mixture on a semipreparative column is only the beginning of the separation process. The chromatographic parameters controlling peak efficiency and resolution, such as gradient range and slope, are of utmost importance in delivering pure compound at a high rate of recovery. A universal full-range gradient of fixed gradient range and slope, 5–10% initial organic modifier to a final composition of 90–100% organic over the course of 5–8 min, was employed as the method of choice on mass-directed purification systems.[27,29,31] The desire for increased resolution on the mass-directed purification systems led to decreasing the gradient slope through the use of 20% focused gradients.[40] A 5 min analytical LC–MS analysis was performed on short, 5 cm length column. The observed retention time for the compound of interest was extracted from this analytical LC–MS data and used to assign a focused gradient for the semipreparative analysis. A threefold average increase in

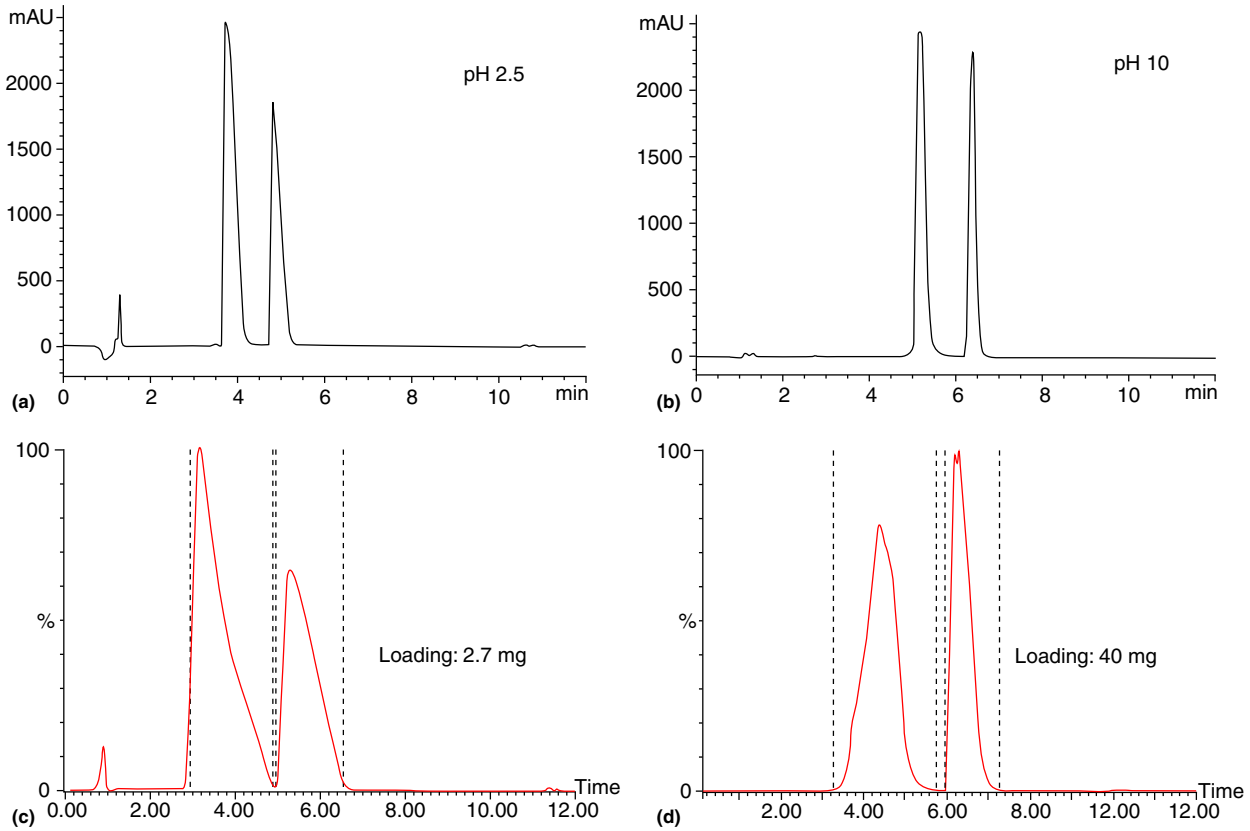


Figure 9 Comparison of mass loading under acidic (a and c) and basic (b and d) conditions. Gradient elution (left chromatograms): mobile phase, aqueous buffer (A)–MeCN (B), from 30% to 60% B in 10 min, stay at 60% B for 2 min, and then 2 min to initial conditions. Gradient elution (right chromatograms): mobile phase, aqueous buffer (A)–MeCN (B), from 40% to 65% B in 10 min, stay at 65% B for 2 min, and then 2 min to initial conditions. Flow rate: (a and b) 1 ml min^{-1}; (c and d) 20 ml min^{-1}. Buffers: (a and c) 0.05% TFA, pH 2.5; (b and d) 10 mM NH_4HCO_3, pH 10. Time scales in min. Figure and caption reproduced with permission of Espada, A.; Marin, A.; Anta, C. *J. Chromatogr. A* **2004**, *1030*, 43–51.

resolution was experienced with using focused gradients when compared with full-range gradients executed over the same time frame.[40] Figure 10 highlights the resolution enhancement provided by utilization of focused gradients.

These shallow gradients elute the more polar undesired components together at the beginning of the separation, maximize resolution of the desired component from close eluting impurities, and elute the nonpolar undesired components at the organic blow off at the conclusion of the run. The real-time monitoring of the mass of interest protects from loss of compound if the gradient is set incorrectly, as the material will be collected even if it elutes with the polar or nonpolar clusters. The same software package that selected the focused gradient method also allows selection of the appropriate fraction triggering method containing the proper mass threshold. The ability to set a mass fraction triggering threshold intelligently on a sample by sample basis from observed analytical values provides a method of isolating compounds that do not ionize well with the same accuracy as compounds that ionize extremely well.

The success experienced through the use of focused gradients in HTP groups resulted in their widespread use.[8,43,44] Such widespread acceptance of focused gradients resulted in chromatographic data acquisition software packages being modified to deliver a commercially available method of automatically assigning focused gradients.[45,46] The typical sequence of events performed by such software begins with an extremely fast gradient performed on an analytical LC–MS. The M + 1 adduct of the monoisotopic exact mass of the desired compound is extracted from the total ion chromatogram recorded by the MS. This retention time is cross referenced to an empirically derived table that associates semipreparative methods to retention time windows broken down from the analytical method. The semipreparative method that is matched to the observed analytical retention time is written to a sample queue to be executed on the mass-directed system.

9.07.10 Autopurify – Automated Analytical to Preparative

Totally automated purification systems were developed that enabled users to log in a library of compounds, set up a queue to handle the entire analysis, purification, and reanalysis of the fractions. Figure 11 displays a totally automated analytical-to-preparative system. An autosampler capable of routing flow through an analytical flow path as well as a preparative flow path was

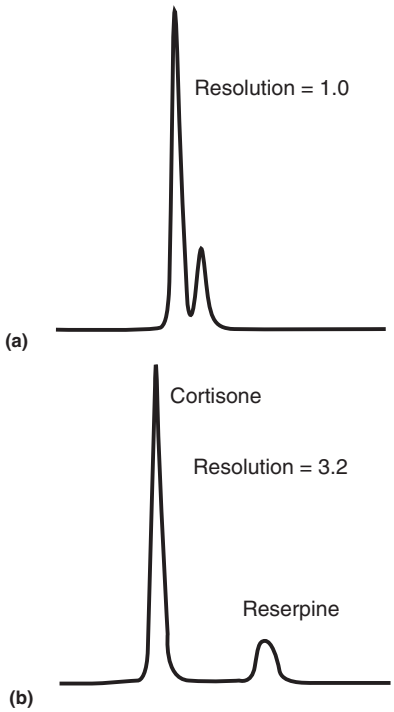


Figure 10 (a) Prep LC–MS separation of cortisone and reserpine using a 10–100% full-range acetonitrile gradient performed over 5 min. (b) Prep LC–MS separation of cortisone and reserpine using a 30–50% focused acetonitrile gradient performed over 5 min. Resolution is increased by a factor of 3. Reprinted with permission from Blom, K. F.; Sparks, R.; Doughty, J.; *et al. J. Comb. Chem.* **2003**, *5*, 670–683.

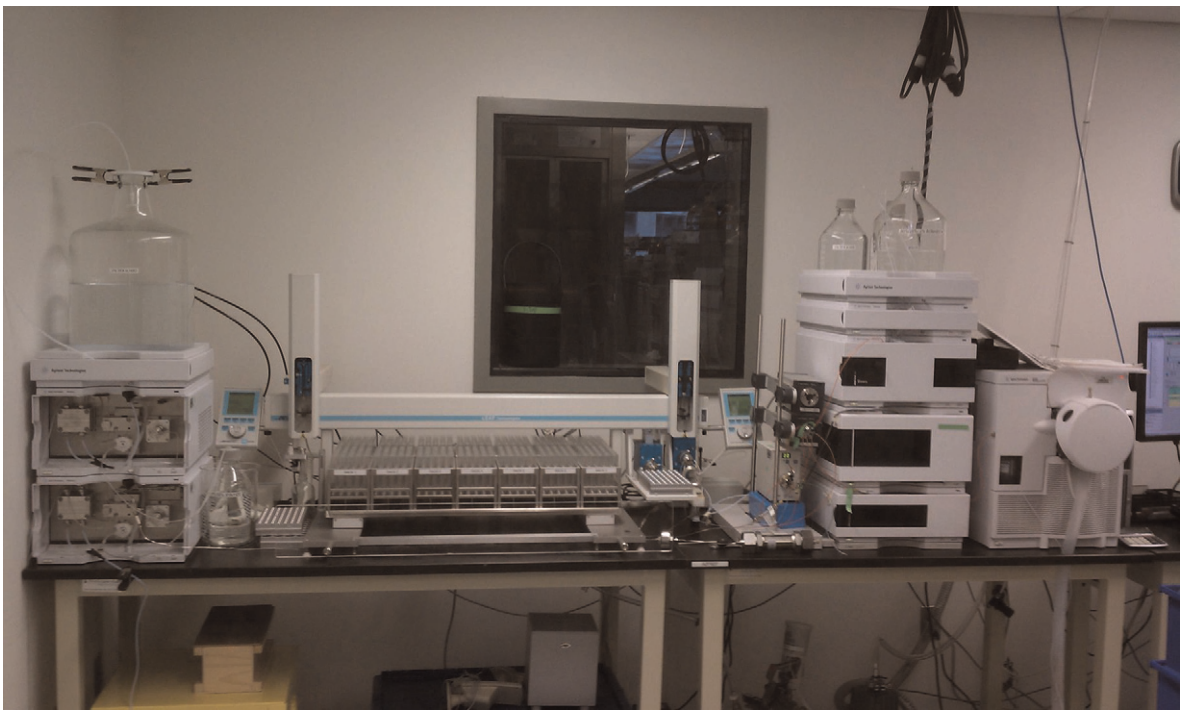


Figure 11 Photo of an automated analytical-to-preparative, mass-directed purification system. The dual head, CTC Pal system in the middle of the platform serves as an autosampler for injection of both analytical and preparative aliquots of crude reaction products. Reanalysis of isolated fractions is also performed by the CTC Pal autosampler. In addition to the automation afforded by this platform, it is also an affordable solution for smaller laboratories as the user obtains analytical and preparative capabilities through use of shared diode array detector and MS detectors. Photo courtesy of David Smith, Merck Research Laboratories, Boston, MA.

a key component of the system. The first step of the process involved the analytical LC–MS analysis of the reaction products via a fast gradient on an analytical column. At the conclusion of the analytical LC–MS analysis of the library, focused gradients would be assigned through the use of the empirically derived retention time window table. The resulting semipreparative queue would be executed using the preparative injection loop/valve and the narrow, focused gradient selected by the previous step. At the conclusion of the preparative queue, the fractions obtained would be injected by the fraction collector cannula for analytical LC –MS analysis by the same method used to assess the state of the original crude products. The chemist who initiated the run only had to set up an original sample queue, and on arriving at the completion of that queue would possess an analytical LC–MS trace for each crude product, a semipreparative LC–MS chromatogram of the focused gradient separation, and an analytical LC–MS analysis of each isolated fraction.

9.07.11 Normal Phase Mass-Directed HPLC

One of the most time-consuming stages of the entire purification process, which is inherent to RP preparative chromatography, is the removal of water in isolated fractions. It often takes an overnight cycle of 12–15 h in a centrifugal solvent evaporation system to remove water from the isolated fractions without excessive heating. Lyophilization typically takes even longer and is occasionally done in two steps. The first step eliminates the organic component of the chromatographic system eluent, whereas the second step freezes the aqueous component and allows sublimation to deliver dry compound. Two modes of high-throughput chromatography have been examined to eliminate water from the entire purification process: normal phase liquid chromatography and supercritical fluid chromatography (SFC).

Medicinal Chemists for many years have utilized normal phase separation techniques such as TLC and flash chromatography. Indeed, some of the first fully automated preparative chromatography systems were developed for normal phase separations.[47] Flash chromatography utilizes a polar stationary phase such as bare silica and a binary mobile phase system to purify reaction products.[24] The binary mobile phase typically comprises a nonpolar component such as hexane and a more polar component such as ethyl acetate to control the retention and elution of compounds. TLC is used as an analytical tool to gauge compound polarity and thus provides the chromatographer an estimate of the proper starting conditions to be used on the preparative scale.[48] An UV detector has frequently been used as the fraction triggering device on the earlier automated normal phase systems. The advantages experienced through incorporating a MS as the fraction triggering device into RP purification platforms, resulted in this trend extending into the normal phase mode of operation. Mass-directed normal phase purification systems can be implemented with the same hardware and software platforms used in RP mode. Cyano-based stationary phases were found to be an appropriate column of choice for use on mass-directed normal phase systems. They possessed similar selectivity to silica but were less retentive, resulting in elimination of sample pretreatment that was required with silica columns.[49] There are several limitations of normal phase chromatography that prevent its widespread use. The technique generally requires utilization of large volumes of flammable, environmentally harmful solvents. In addition, residual amounts of water found in normal phase solvents leads to inconsistent chromatographic performance.

9.07.12 General SFC Characteristics

SFC using carbon doxide (CO_2)-based eluents is often viewed as a viable option to replace normal phase liquid chromatography and minimize the consumption of these harmful solvents.[50] SFC is a normal phase- like separation technique that utilizes a supercritical fluid in the mobile phase system in conjunction with a polar stationary phase. A supercritical fluid is a substance that is pressurized above its critical pressure and heated above its critical temperature that simultaneously possesses the combined properties of a liquid and a gas. The supercritical fluid possesses the solvating properties of a liquid while having the diffusivity of a gas. Although various substances such as water and ammonia can be placed in the supercritical state, CO_2 is the most widely used supercritical fluid for chromatographic purposes. This is because of the low cost to purchase CO_2 and its 'green' nature. Supercritical CO_2 displays similar chromatographic properties as hexane, which allows it to be substituted into a chromatographic system in place of the flammable, hazardous alkane. A polar modifier, referred to as a cosolvent in SFC, is added to the binary mobile phase to control the elution strength of the mobile phase. Methanol is the most widely used cosolvent being the most polar, totally miscible solvent with supercritical CO_2.[51]

The high diffusion coefficients experienced in SFC allow flow rates typically 3–5 times greater than those experienced in HPLC. At these higher SFC flow rates, there is little loss of efficiency caused by resistance to mass transfer between the mobile and stationary phases. The low viscosity of the supercritical CO_2 prevents an excessive pressure drop from forming, which would occur in HPLC due to the higher viscosities of the traditional liquid mobile phase systems. In general, retention is halved in SFC for every doubling of cosolvent resulting in a full-range gradient in SFC utilizing a maximum mobile phase composition of 50% cosolvent.[51] If higher percentages of cosolvent are used, column back pressure will increase and the benefits associated with SFC, such as high diffusion coefficients and low viscosities, will disappear. The mobile phase takes on the characteristics of the tradition liquids used in HPLC.

CO_2 is inexpensive to purchase when compared with the harmful solvents it replaces in a typical normal phase chromatographic system. Another benefit experienced in preparative SFC is the lesser requirement in energy and the rapid recovery of

purified product from the column eluent when compared with HPLC. In HPLC, the entire volume of column eluent routed to independent fraction vessels must be evaporated to reclaim chromatographically resolved products. In SFC, the natural conversion of CO_2 to its gaseous state at atmospheric condition postcolumn leaves the isolated compound in the remaining cosolvent. The desired compound is reclaimed through evaporation of the small volume of cosolvent leading to fast recovery and minimal waste as the CO_2 is either released to the atmosphere or reclaimed through a recycler.

9.07.13 Use of Cyclones for Handling Expansion of Supercritical CO_2

There are a few conceptual differences between preparative HPLC and SFC systems. One of the most important differences is incorporation of a back pressure regulator into the preparative SFC system downstream of the column and UV detector. This allows the fluidic path where the separation is performed to be maintained above the critical pressure of the mobile phase system being utilized. Another major difference in SFC is the method of handling the expansion of the supercritical CO_2 during the fraction collection process as it occurs after the back pressure regulator. Immediately on exiting the back pressure regulator, the CO_2 begins to expand to its natural gaseous state. This leads to a 500-fold volume expansion that must be handled safely as it occurs at approximately the speed of sound. A common practice is to route the back pressure regulator eluent to a conical bottom cyclone to allow safe separation of the gaseous CO_2 and the cosolvent containing the solute. The flow of expanding fluid leaving the back-pressure regulator is directed at an angle toward the wall of the cyclone. The centrifugal force created by the expansion of the CO_2 drives the fluid stream around the inside the cyclone. The rapid motion draws the cosolvent containing the solutes to the outer edge of the cyclone while allowing the gaseous CO_2 to migrate toward the middle and escape out a vent line on top of the cyclone. The pressure of the gaseous CO_2 inside the cyclone assists in pushing the cosolvent containing the solute out the conical bottom into a bottle serving as the collection vessel. Final removal of residual pressure happens inside the bottle, which contains a vent line to carry the final gaseous CO_2 away.

The use of pressurized cyclones in combination with stacked injections has elevated SFC as the preferred purification method for chiral molecules.[52–54] As each cyclone is dedicated for an individual isomer, repetitive injections essentially wash residual pure compound from the previous injection into the collection vessel. On completion of a sample, the cyclones must be cleaned through repetitive rinsing and draining to ensure maximum recovery of the completed sample and prevent contamination of the next sample to be purified. Although cyclones are effective and efficient at processing chiral and other bulk samples using isocratic separation conditions and stacked injections, they will not support a high-throughput work-flow samples requiring unique gradient separation conditions. Most preparative SFC systems have a maximum of six to eight cyclones, which could rapidly be consumed in a single gradient separation of a complex parallel synthesis product. An alternative approach to fraction collection would be necessary to enable high-throughput SFC purification.

9.07.14 UV-Based SFC for HTP

Development of semipreparative SFC systems capable of processing arrays of compounds in a high-throughput environment followed the same technological advances as the comparable RP HTP systems. A semipreparative SFC system using a UV fraction trigger and a novel gas–liquid separator that prevented aerosol formation pioneered the way for high-throughput semipreparative SFC.[51] The self-cleaning nature of the gas–liquid separator allowed four, 50 ml fraction tubes to be quickly exchanged through opening of a sealed, pressurized cassette. The ability of the system to execute a 5–55% methanol in supercritical CO_2 gradient in less than 10 min to process samples up to 50 mg combined with not having to stop the system to clean cyclones between samples was a major advancement in incorporating SFC into HTP environments. Successful utilization of UV-based semipreparative SFC systems for HTP fueled the development of mass-directed purification systems. The same benefit of reducing the amount of analytical method development before purification and reducing the number of fractions requiring analysis postpurification experienced in HPLC would be possible in SFC.

9.07.15 Mass-Directed SFC for HTP

Handling the rapid depressurization of supercritical CO_2 to enable successful fraction collection and splitter performance are the inherent problems associated with mass-directed SFC. Open bed SFC fraction collection at atmospheric pressure was desired but would have to be performed with extreme caution. The risk and complexity involved with open bed collection revolved around the fact that if the CO_2 was allowed to depressurize and aerosolize too quickly, it could carry compound away and thus sacrifice recovery, cross contaminate other samples, and/or create a safety hazard for laboratory occupants. The first mass-directed semipreparative SFC system utilized a 10–60% methanol in CO_2 gradient over 5 min on 1 cm i.d. by 10 cm length columns.[55] The flow rate used was 15 ml min^{-1} and open bed fraction collection was enabled by switching the three-way switching low pressure valve on the Gilson 215 fraction collector to a high pressure valve. Original recoveries averaged 45–50% and were improved on by incorporating the use of foil to cover the top of the fraction tubes, boosting recovery to an average of 77%. Another early developed mass-directed SFC system utilized a 3.2 mm i.d. Teflon tube in place of the smaller ID stainless steel needle

traditionally used on the fraction collector to minimize aerosol formation and delivered recoveries of up to 85% for flows up to 30 ml min^{-1}.[56] The tip of the fraction collector was set 1.5 mm beneath the top of the fraction vessel to capture small droplets that were formed and could potentially splash out if collected above the tube. Both of these early mass-directed SFC systems used small inner diameter capillaries as passive splitters to route a small portion of the chromatographic fluid stream to the MS serving as the fraction triggering detector. The split ratio of these passive splitters is determined by the restriction created by the length and inner diameter of the capillary as well as the viscosity of the mobile phase. The viscosity of the mobile phase increases as the percentage of cosolvent increases during execution of the chromatographic gradient, decreasing the volume of mobile phase that enters the capillary and is introduced to the MS. The split ratio consequently decreases during the purification resulting in decreased MS signal for later eluting compounds. A 0.3% formic acid in methanol make-up solution was found to aid in the ionization efficiency and help maximize the MS signal for later eluting compounds.[56] It was also determined that maintaining an elevated pressure on the passive splitter capillary through use of a back pressure regulator helped prevent saturation of the MS signal resulting in severe tailing.[56]

Early adopters of UV-based semipreparative systems in high-throughput environments demonstrated the technique's power and confirmed the benefits that led to its implementation.[57,58] The pioneers who developed the original customized mass-directed semipreparative SFC systems confirmed the possibility of merging the power of mass-directed fraction collection and SFC.[55,56] The commercialization of mass-directed SFC took place in 2008 with the delivery of the Thar Technology, (now Waters Corporation), commercially available MS30. The MS30 was an off the shelf 30 g min^{-1} mass-directed SFC system with open bed fraction collection performed at atmospheric pressure. The system ran off a single computer running MassLynx 4.1 as the user interface for data acquisition and data processing. The system was capable of being incorporated into a drug discovery group with automated assignment of narrow gradient semipreparative methods through the AutoPurify feature of FractionLynx.[59] The semipreparative separations were performed on 1 cm i.d. by 10 cm length, 5 µm, 2-ethylpyridine columns. Five percent gradient ranges were assigned based on empirical retention correlation with an established analytical SFC–MS method. Standard mixes purified on the MS30 revealed recoveries of 82–84% for purified masses of 10–20 mg.

The success of the 30 g min^{-1}, commercially available mass-directed SFC led to the delivery of a larger capacity mass-directed SFC system capable of delivering 100 g min^{-1} of flow. The increased flow capacity of the Waters MS100 was more appropriately matched to the 2–3 cm inner diameter semipreparative columns frequently used in high-throughput environments. A unique fraction collection mechanism was required for the MS 100 to handle the larger volume of CO_2. The MS30 handled the CO_2 expansion during fraction collection in a similar fashion to the first two customized systems: though use of larger tubing on the fraction collector cannula in addition to the tip being midway inside the tube and aimed at the side of the vessel. The 100 g min^{-1} system utilized a proprietary gas–liquid separator as illustrated in Figure 12.[60]

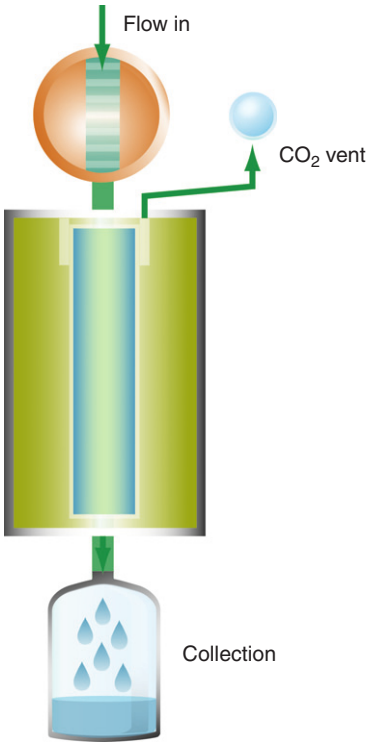


Figure 12 Gas–liquid separator (GLS) from the Waters 100 g min^{-1} mass-directed SFC system. Reprinted with permission from Subbarao, L.; Rolle, D.; Chen, R. http://www.ChromatographyOnline.com 2010 (accessed on 15 December 2012).

The main system eluent is directed toward the inner wall of a conical device. The internal pressure of the gas–liquid separator pushes the liquid flow through the bottom tubing and on to the diverter valve of the fraction collector. The CO_2 is allowed to vent through the top of the gas–liquid separator. A make-up pump is used to ensure the liquid portion of the main eluent routed to the fraction collector through the gas–liquid separator is a constant 30 ml min^{-1}. The 40 psi of pressure inside the separator in conjunction with this 30 ml min^{-1} of flow ensure full transfer and flushing of liquid containing the separated solutes to the fraction vessels. This process maximizes recovery and eliminates cross contamination of neighboring fractions. Normal recoveries of standards analyzed on the MS100 at 100 ml min^{-1} of flow have been found to be 90–95% though use of this gas–liquid separator technology and make-up flow scheme.[61] In addition to delivering open bed atmospheric pressure fraction collection at 100 ml min^{-1} of flow, the MS100 also provides various split ratios through a proprietary tunable splitter. The tunable splitter maintains a consistent split ratio despite the column eluents density changes associated with the changing composition of super/subcritical CO_2. The splitter is also important in maintaining proper system timing through precise delivery of analyte to the MS.

SFC and RP chromatography using C18 columns are considered to be orthogonal separation techniques. Polar compounds that are difficult to retain on C18 columns in RP chromatography are strongly retained in SFC using silica-, 2-ethylpyridine-, cyano-, and amino-based columns. Nonpolar compounds that are difficult to elute from C18 columns in RP systems are weakly retained in achiral SFC and are thus easily eluted. Compounds that coelute on a C18 column in RP chromatography frequently are easily resolved on an achiral SFC column such as silica, 2-ethylpyridine, cyano, or amino columns with little or no method development required. The reverse is true as well where coelution on an achiral SFC column is remedied by successful separation on a C18 column on a RP system. The orthogonal nature of SFC has led to mass-directed separations being utilized to purify compounds that could not be successfully chromatographed by RP chromatography using C18 columns.[62] Many comparison studies have been performed on achiral SFC and RP-HPLC.[63–66] The results overwhelmingly show a large overlap between the two techniques in terms of successful chromatography. The successful hit rate of observing a peak with the desired mass from a 2153 compound study was found to be within 4.4% for HPLC–MS and SFC–MS. On the semipreparative scale, average yield of purified product isolated libraries of 16–48 members was found to be within 1% for the two techniques.[64]

9.07.16 HTP Workflows

As the authors have shown, there has been dramatic advancement in MS-directed chromatography techniques to address the need for a suitable HTP platform. It is important to realize that the majority of time and effort is still spent on the remainder of the HTP workflow: Sample preparation, screening, evaporation, fraction tracking, data interpretation, reformatting of material, registration, QC, reporting, and data archiving. Without corresponding development of all the remaining parts of the process, there can be no full realization of the promise to reduce cycle times.

Many of the early HTP visionaries quickly found that that once the preparative chromatography bottleneck was removed, the postpurification sample handling was found to be the rate-limiting step in the workflow. Increasing purification channels (more instruments) did not increase potential throughput proportionally. In fact, doubling the number of purification systems only increased potential throughput by 30%.[67] Thus, it is critical not to underestimate the complexities in the remainder of the workflow and to dedicate adequate resources to address them. The ongoing development and optimization of software tools and automation instruments to manage the entire HTP process has been critical to the successful implementation of HTP work-flow platforms into the drug discovery process.

9.07.17 Prepurification Workflow

9.07.17.1 Submission/Request/Initiation

The first stage of any library purification workflow is the creation of an electronic request for purification. This will certainly include the transfer of a spreadsheet or database file that includes the pertinent information for each compound in the library. This process will serve to initiate the workflow and create an electronic record for tracking the library through each step in the process. The creation of this request may be an extension of the software that is used to actually plan, enumerate, and direct automated synthesis. The file that is created by the request process will typically contain the following fields for each compound in the library:

- A unique reference number, sample ID, or job code for each compound;
- Electronic drawing file of compound;
- Exact mass of target(s) in mixture;
- Well plate position;
- Crude scale of reaction (mg);
- Desired concentration of final dissolved product;
- Disposition of purified product; and
- Project/assay name.

9.07.18 Analytical Screening

The process of selecting conditions for purification is very complex and can be approached with many different strategies. There is an almost universal reliance on some level of analytical LC–MS screening to select appropriate purification conditions. Pre-existing chromatographic data can be utilized; typically this is generated by the chemists who synthesized the compound. The ability to interpret this data accurately and reliably is crucial for the selection of appropriate purification conditions, therefore for this approach to work, it is imperative that the conditions used for analysis is consistent across all instruments used for this task.

Alternatively, the purification group can perform the LC–MS analysis themselves, using their own instrumentation and routines to find conditions that fully resolve the target compound. This approach can enable the incorporation of more extensive analytical screening methods.[68] The advent of fast HPLC and UPLC systems has allowed more complex initial analyses to take place, without sacrificing time. One needs to consider the incremental time required to screen each additional condition. Ideally, the screening process should be designed to reveal conditions that will increase the probability of success for the entire process without the sacrifice of excess time and resources. In a true high-throughput environment, this screening should be performed on the same day that the compounds were submitted to the HTP group.

These analyses can include investigation of any or all of the following parameters:

- Aqueous modifiers (acids, bases, and buffers);
- Organic solvent choice (MeOH or MeCN);
- Column stationary phase (column packing material); and
- Chromatography type: RP/NP/SFC.

It is advantageous to utilize two screening conditions that can provide the most chromatographic orthogonality; in other words, conditions that give the most different results. Examples of this strategy are screening with both high and low pH RP chromatography, or with RP and SFC.[66,68,69]

This process can take place in parallel on different analytical instruments to save time, but this approach requires automation to create secondary plates for analysis. Obviously, any parallel screening or division of a library will require more automation to work efficiently. Alternatively, this process can be serial on the same instrument, which requires more time. It is also feasible to institute an escalation process that relies on a simple, first-pass, screen that will work for the majority of mixtures. Those samples that do not show sufficient chromatographic resolution of the target peak using the initial conditions can be subjected to further screening.

Some groups have attempted to augment or even partially bypass this process, by relying on predictive modeling of chromatographic behavior based on physiochemical properties (LogD, p*K*A, surface polarity, etc.) of the target molecules. The simplest implementation of this strategy can utilize commercially available products that predict these values (ACD/Laboratories) and/or products that predict chromatography based on these values (Dry-Lab). Others have incorporated more sophisticated decision engines that model chromatographic retention of a molecule based on validated correlation with many predicted physiochemical properties.[70]

9.07.19 Visualization/Interpretation of Screening Data, Choice of Purification Conditions

Primarily, the goal of any screening process is to choose appropriate preparative chromatographic conditions based on these results. Review and interpretation of the data created by this analysis can be a time-consuming task. This part of the process can benefit from software tools for automatic interpretation and visualization of this data. Generally, there is still some level of human intervention in this stage, and the minimization of software level manipulation of data (mouse clicks) can speed the process. Software tools are required to make correct decisions most of time and flag compounds that may present a problem. The software can then create a run list for the purification instrument to process. Most of the functions described in the following workflow are generally part of the chromatographic data acquisition and processing software. The following sequential steps of analytical LC–MS data interpretation are employed for this stage of the overall process:

a. Chromatogram extraction: Chromatogram(s) that will be used is this process will need to be extracted from three-dimensional data. For LC–MS data, this will include the extracted ion trace of the target compound(s). For PDA UV data, this may be one or more single UV wavelength chromatograms.
b. Integration: Chromatographic peaks in the relevant chromatograms will then be integrated.
c. MS spectral averaging (normalization): The MS spectra throughout each chromatographic peak are combined and normalized.
d. Target ID: For each chromatographic peak, the software can search through the composite spectra for the presence of the target m/z value. With the target peak identified, the software can flag this peak.
e. Spectral matching: Because many compounds can share the same nominal mass, it is imperative to exclude target peaks that do not have the correct isotopic spectral pattern. In some data packages, processed MS spectrum of the target peak can be compared with a predicted spectral pattern based on the molecular formula of the target. Software can overlay and score these spectra to flag peaks, which may not be the correct compound.
f. Area %/initial purity: With the target peak identified, a calculation is made of the percentage area this peak contributes to the total peak area (relative purity). This initial purity is crucial in determining the best path forward.

g. To purify or not to purify? Any software used to process and interpret this data should have the ability to locate target peaks based on exact mass. The relative size (%) of this target peak can be used to determine whether or not to proceed with the purification. In general, there is a minimum area % in an UV and/or evaporative light scattering detector (ELSD) trace that will be chosen as an acceptable threshold for continuing with the process. There may also be a consideration of the crude scale, and the predicted yield of the reaction that generated each product.
h. Chromatographic variables of target peak(s) are established: The retention time in the analytical run is assigned, and other chromatographic factors such as peak symmetry, peak width, and resolution may also be considered.
i. Purification method choice: As the authors have discussed in Section 9.07.9, the retention time and the target peak is then used to establish chromatographic conditions for the purification process. This may be the basis for the selection of a particular focused gradient that positions the target peak exactly in the solvent percentage range that will allow for maximum resolution.

9.07.20 Postpurification Workflow

Following purification, the collected fractions will be further processed before returning to the chemist or sending for biological assay. The extent of this processing can significantly increase the complexity and time required to process the material fully. In fact, the downstream postpurification process can easily become the rate-limiting step in the overall HTP process. These post-purification sample steps must be executed with comparable efficiency to the preparative chromatography process to avoid becoming the bottleneck in the cyclic process of high-throughput synthesis and purification.

The postpurification workflow can contain all or some of the following steps: evaporation, gravimetric analysis, LC–MS analysis and interpretation, NMR analysis, dissolution to a desired concentration, plating, registration, reporting, and archival of excess material. HTP of compound libraries by a centralized group is highly reliant on work-flow software tools and automation instrumentation to complete this complex process efficiently.

9.07.21 Processing of Fractions from Purification

There are many different strategies being employed for the handling and processing of fractions. Earlier chapters discussed plate-mapping routines that limited fraction collection for each compound to a single vessel or a fixed set of vessels to simplify downstream processing.[29,31,71] As the HTP workflow developed and evolved, it became more common not to limit fraction collection to a set number of vessels but rather allow for flexible mapping. This will allow collection of multiple tubes due to the presence of isomers or to tailing chromatographic peaks.

The net weight of the material in the collected fractions will be determined after drying. One automation strategy that facilitates this is collection directly into pretared vials or tubes. Alternatively, it is also common to collect into vials or tubes, and then transfer into separate, tared vessels before evaporation. The latter option allows pooling of multiple tubes from a single chromatographic peak. Either approach requires an inventory of bar coded and tared vessels. Many suppliers can provide the tare weights of the vials as a service. However, since the net weight of the material present after drying could be as little as a few milligrams, the accuracy and repeatability of the weighing process is critical. Therefore, the vessels are often tare weighed on site using the same automation instruments that will perform the gross weighing later in the process.

An aliquot of each fraction is taken at this stage for analysis of purity by analytical HPLC. Liquid handlers may be utilized to transfer a small volume (<100 μl) of the fraction to vials or well plates for analysis. This analysis takes place in parallel with the evaporation process. Work-flow software can be utilized to create a work list for the HPLC instrument that associates each fraction with the corresponding submission request.

Evaporation of RP chromatographic fractions can be accomplished using several methods. It is feasible when working with relatively low numbers of fractions to utilize more traditional evaporation instruments such as Rotovaps or lyophilization. However, in a high-throughput environment there is the requirement of determining gross weight for a very high number of fractions. For a typical workflow, this could be hundreds of fractions per day; obviously traditional evaporation techniques are not practical. Centrifugal evaporation instruments have become the preferred method for automated processing of large batches in parallel. These instruments can be configured to accommodate hundreds of fraction vessels in a single chamber; therefore, there is no requirement for reformatting to a separate vessel before evaporation. This approach utilizes high-capacity vacuum pumps and heat lamps for efficient removal of solvents and water. Centrifugation during evaporation eliminates loss of material and cross contamination by preventing solvent bumping under vacuum. With these instruments, complete evaporation of fractions from RP chromatography fractions (acetonitrile and water) can be completed in approximately 16 h. As noted in the section that discusses SFC purification above, evaporation of fractions that contain only organic solvent can be completed in 2 h or less using centrifugal evaporators. Following complete evaporation of the solvent, the vessels are transferred to robotic weighing instruments to obtain a gross weight for each. The net weight for each vessel is calculated and can be stored in a database for subsequent retrieval by work-flow software.

The quality of each fraction is determined both by review of data from the postpurification HPLC–MS analysis and parallel correlation with the net weights. The goal of the quality assessment process is to choose fraction(s) that meet established criteria for quality and therefore will be submitted to a biological assay. The net weight of the fraction may be the first assessment, as fractions of very low net weight may not be useful. Another important quality indicator is the verification of the presence of the target molecule in the fraction. This may be accomplished by checking that the predicted m/z is present in the target peak. Additionally, it is feasible to apply algorithms to evaluate matching of actual spectra to predicted spectra of the given target formulae.

Fraction purity is expressed as area percentage of the targeted peak in a particular single UV wavelength chromatogram or by that of an ELSD. Evaluation of purity by ELSD has been purported to give a more accurate result due to better universality of response. Any fractions that do not meet the minimum purity cut off will be excluded from further processing and may be rediluted and subjected to a second purification to achieve the desired purity level. The minimum purity requirements reported in the literature generally ranges from 85% to 95%.

All fractions of a sufficient quality will be redissolved to a fixed concentration in solvent that is compatible with the downstream biological assay. Typically, this solvent is DMSO, which has the benefits of being of providing high solubility for most compounds and of having a very low evaporation rate. The amount of solvent required to dissolve the dry material to the given concentration is calculated, taking the molecular weight of the target into account. Establishing the actual salt form of the molecule is also critical for calculating the amount of solvent to be added. The p*K*a value(s) of the target molecule and the mobile phase modifiers used during purification will dictate which salt form is used for this calculation. The salt form can be predicted using physicochemical property prediction software (ACD/Laboratories).

The calculated dissolution volumes for each compound can be combined in a work list for a robotic liquid handler instrument. This work list will be imported into the liquid handler software and the instrument will process the library of compounds in a batch-wise manner. Any required reformatting can also take place at this stage. The desired final sample format will be dictated by the downstream assay process. Typically, an aliquot of each resultant solution will be transferred from the vessel that the dry material was dissolved in, into smaller vials, or into a well plate.

At this point in the process the molecule can be registered as a new chemical entity in a centralized database, providing an electronic date stamp for the synthesis of the compound. The registration process captures the chemical structure, salt form, destination assay, biological target, and stereochemistry of the target molecule. A unique identification number will be assigned that will link all subsequent data for this molecule.

Before distribution of the compounds for downstream assay, additional aliquots of the final solution may be taken at this stage for further quality assessment. An additional HPLC–MS analysis may be conducted to establish purity of the compound following the evaporation and dissolution process. Pure fractions that were chosen based on data obtained before evaporation may have undergone degradation and therefore should not be submitted for assay. NMR analysis of the final solution should be conducted to verify the structure of the compound. NMR instruments that incorporate a capillary flow probe and an automated flow injection interface are being utilized to facilitate acquisition of these data. These instruments allow for the unattended processing of large numbers of compounds in a batch-wise fashion. A flow NMR instrument can acquire high-quality NMR spectra with a 10-min cycle time. In conjunction with the distribution of purified material, there is a corresponding distribution of accompanying electronic data that occurs at the end of the HTP workflow. The final data package can include final HPLC–MS and NMR data, as well as a description of the conditions used for the purification.

9.07.22 Current Needs and Future Outlook

HTP has benefited from the commercialization of sub-2 μm particle analytical columns, enabling much faster decision making on both the method development and purity assessment stages of the process. Efficiency gains have also been experienced on the preparative chromatography portion of the workflow with narrower particle size distribution, more rugged stationary phase bonding techniques, and more rugged column hardware such as the axial compression housings. However, more development is needed for the preparative columns to deliver higher loading while minimizing run times. Preparative run times continue to be considerably longer than their associated analytical runs, and the column is a key contributor to this fact.

Removal of water from RP column eluent stemming from mass-directed platforms continues to be a time-consuming step. An easy to use, rugged method of isolating chromatographically pure material from aqueous-based eluent streams is needed. Automated methods of solid phase extraction on various chromatographic platforms would help with this need and are being optimized.

Mass-directed SFC is continually developing through hardware advances and development of new column chemistries. Continued advancement of hardware ruggedness and ease of use and development of stationary phases possessing selectivity to resolve a wide range of molecules will increase the presence of this technique in HTP laboratories.

Work-flow management software capable of processing sample submission through delivery of purified, characterized material is frequently custom built, requiring employment of specialized computer programmers. Development of commercially available packages that are easy to customize to individual groups needs without intervention from internal programmers are highly desirable. Continued evolution of such packages to track barcodes of samples in various completion states and populate databases should enable more purification groups to embrace centralized HTP.

9.07.23 Conclusion

HTP has been a rapidly evolving tool with many technological breakthroughs over the past 15 years. Development of more efficient and automated hardware and software platforms and higher performance consumables continue to deliver advances in the field. The need to conduct science at a higher standard of quality while minimizing cost and human intervention ensures that the field of HTP will continue to evolve.

References

1. Kubiyi, H. *Nat. Rev. Drug Discov.* **2003**, *2*, 665–668.
2. Kola, I.; Landis, J. *Nat. Rev. Drug Discov.* **2004**, *3*, 711–715.
3. Paul, S. T.; Mytelka, D. S.; Dunwiddie, C. T.; *et al. Nat. Rev. Drug Discov.* **2010**, *9*, 203–214.
4. Kennedy, J. P.; Williams, L.; Bridges, T. M.; *et al. J. Comb. Chem.* **2008**, *10*, 345–354.
5. Weller, H. N.; Nirschl, D. S.; Petrillo, E. W.; *et al. J. Comb. Chem.* **2006**, *8*, 664–669.
6. Leister, W.; Strauss, K.; Wisnoski, D.; Zhao, Z.; Lindsley, C. *J. Comb. Chem.* **2003**, *5*, 322–329.
7. Koppitz, M.; Brailsford, A.; Wenz, M. *J. Comb. Chem.* **2005**, *7*, 714–720.
8. Koppitz, M.; Eis, K. *Drug Discov. Today* **2006**, *11*(11/12), 561–568.
9. Carey, J. S.; Laffan, D.; Thompson, C.; Williams, M. T. *Org. Biomol. Chem.* **2006**, *4*(12), 2337–2347.
10. Cooper, T. W. J.; Campbell, I. B.; Macdonald, S. J. F. *Angew Chem. Int. Ed.* **2010**, *49*, 8082–8091.
11. Roughley, S. D.; Jordan, A. M. *J. Med. Chem.* **2011**, *54*(10), 3451–3479.
12. Lorthioir, O.; Carr, O.; Congreve, M.; *et al. Anal. Chem.* **2001**, *73*, 963–970.
13. Guintu, C.; Kwok, M.; Hanlon, J. J.; *et al. J. Biomol. Screen.* **2006**, *11*(8), 933–939.
14. Yan, B.; Fang, L.; Irving, M.; *et al. J. Comb. Chem.* **2003**, *5*, 547–559.
15. Letot, E.; Koch, G.; Falchetto, R.; *et al. J. Comb. Chem.* **2005**, *7*, 364–371.
16. Schaffrath, M.; Roedern, E.; Hamley, P.; Stilz, H. *J. Comb. Chem.* **2005**, *7*, 546–553.
17. Espada, A.; Molina-Martin, M.; Dage, J.; Kuo, M. *Drug Discov. Today* **2008**, *13*, 417–423.
18. Peng, S. X.; Henson, C.; Strojnowski, M. J.; Golebiowski, A.; Klopfenstein, S. R. *Anal. Chem.* **2000**, *72*, 261–266.
19. Breitenbucher, J. G.; Arienti, K. L.; McClure, K. J. *J. Comb. Chem.* **2001**, *3*, 528–533.
20. Boger, D. L.; Goldberg, J.; Andersson, C. M. *J. Org. Chem.* **1999**, *64*, 2422–2427.
21. Studer, A.; Hadida, S.; Ferritto, R.; *et al. Science* **1997**, *275*, 823–826.
22. Lindsley, C. W.; Zhao, Z.; Leister, W. H. *Tetrahedron Lett.* **2002**, *43*, 4225–4228.
23. Lindsley, C. W.; Zhao, Z.; Newton, R. C.; Leister, W. H.; Strauss, K. A. *Tetrahedron Lett.* **2002**, *43*, 4467–4470.
24. Still, W. C.; Kahn, M.; Mitra, A. *J. Org. Chem.* **1978**, *43*, 2923–2925.
25. Weller, H. N.; Young, M. G.; Michalczyk, S. J.; *et al. Mol. Diversity* **1997**, *3*, 61–70.
26. Kibbey, C. E. *Lab. Robotics Automat.* **1997**, *9*, 309–321.
27. Zeng, L.; Burton, L.; Yung, K.; Shushan, B.; Kassel, D. B. *J. Chromatogr. A* **1998**, *794*, 3–13.
28. Kiplinger, J. P.; Cole, R. O.; Robinson, S.; *et al. Rapid Commun. Mass Spectrom.* **1998**, *12*, 658–664.
29. Zeng, L.; Kassel, D. B. *Anal. Chem.* **1998**, *70*, 4380–4388.
30. Karancsi, T.; Godorhazy, L.; Szalay, D.; Darvas, F. *J. Comb. Chem.* **2005**, *7*, 58–62.
31. Xu, R.; Wang, T.; Isabell, J.; *et al. Anal. Chem.* **2002**, *74*, 3055–3062.
32. Zhang, X.; Picariello, W.; Hosein, N.; Towle, M.; Goetzinger, W. *J. Chromatogr. A* **2006**, *1119*, 147–155.
33. Cai, H; Kiplinger, J. P.; Goetzinger, W.; *et al. Rapid Commun. Mass Spectrom.* **2002**, *16*, 544–554.
34. Rosentreter, U.; Huber, U. *J. Comb. Chem.* **2004**, *6*, 159–164.
35. Snyder, L. R.; Kirkland, J. J.; Glajch, J. L. *Preparative HPLC Separations, Practical HPLC Method Development*, 2nd ed.; John Wiley & Sons, Inc.: Hoboken, NJ, **1997**; pp 616–641.
36. Snyder, L. R.; Kirkland, J. J.; Glajch, J. L. *Basics of Separation, Practical HPLC Method Development*, 2nd ed.; John Wiley & Sons, Inc.: Hoboken, NJ, **1997**; pp 21–57.
37. Neue, U. D.; Carmody, J.; Cheng, Y. F.; *et al.* Design of Rapid Gradient Methods for the Analysis of Combinatorial Chemistry Libraries and the Preparation of Pure Compounds. In *Advances in Chromatography*; Grushka, E., Brown, P., Eds.; Marcel Dekker: New York, Basel, **2001**, Vol. 41, Chapter 3; pp 93–136.
38. Neue, U. D.; Mazza, C. B.; Cavanaugh, J. Y.; Lu, Z.; Wheat, T. E. *Chromatographia Suppl.* **2003**, *57*, 121–127.
39. Blom, K. F. *J. Comb. Chem.* **2002**, *4*, 295–301.
40. Blom, K. F.; Sparks, R.; Doughty, J.; *et al. J. Comb. Chem.* **2003**, *5*, 670–683.
41. Isbell, J. *J. Comb. Chem.* **2008**, *10*, 150–157.
42. Espada, A; Marin, A.; Anta, C. *J. Chromatogr. A* **2004**, *1030*, 43–51.
43. Yan, B.; Collins, N.; Wheatley, J.; *et al. J. Comb. Chem.* **2004**, *6*, 255–261.
44. Blom, K. F.; Glass, B.; Sparks, R.; Combs, A. *J. Comb. Chem.* **2004**, *6*, 874–883.
45. A2PREP software, http://leapwiki.com/mediawiki/images/archive/c/ce/20090403003213!IFC-LEAP_Manual_Rev1-7.pdf (accessed on 15 December 2012).
46. Waters MassLynx software, http://www.waters.com/waters/nav.htmcid=513164 (accessed on 15 December 2012).
47. Pirkle, W. H.; Anderson, R. W. *J. Org. Chem.* **1974**, *39*, 3901–3903.
48. Renold, P.; Madero, E.; Maetzke, T. *J. Chromatogr. A* **2001**, *908*, 143–148.
49. Kagan, M.; Chlenov, M.; Bach, A.; McConnell, O. *J. Liq. Chromatogr. Relat. Technol.* **2004**, *27*, 1817–1834.
50. Farrell, W. P.; Aurigemma, C. M.; Masters-Moore, D. F. *J. Liq. Chromatogr. Relat. Technol.* **2009**, *32*, 1689–1710.
51. Berger, T. A.; Fogleman, K; Staats, T.; *et al. J. Biochem. Biophys. Meth.* **2000**, *43*, 87–111.
52. Welch, C. J.; Leonard, W. R.; DaSilva, J. O.; *et al. LC GC N. Am.* **2005**, *23*, 16–29.
53. White, C. *J. Chromatogr. A* **2005**, *1074*, 163–173.
54. Miller, L.; Potter, M. *J. Chromatogr. B* **2008**, *875*, 230–236.
55. Wang, T.; Barber, M.; Hardt, I.; Kassel, D. B. *Rapid Commun. Mass Spectrom.* **2001**, *15*, 2067–2075.
56. Zhang, X.; Towle, M. H.; Felice, C. E.; Flament, J. H.; Goetzinger, W. K. *J. Comb. Chem.* **2006**, *8*, 705–714.
57. Ventura, M.; Farrell, W.; Aurigemma, C.; Tivel, K.; Greig, M. *J. Chromatogr. A* **2004**, *1036*, 7–13.
58. White, C.; Burnett, J. *J. Chromatogr. A* **2005**, *1074*, 175–185.

59. McClain, R. T.; Dudkina, A.; Barrow, J.; Hartman, G.; Welch, C. J. *J. Liq. Chromatogr. Relat. Technol.* **2009**, *32*, 483–499.
60. Subbarao, L.; Rolle, D.; Chen, R. http://www.ChromatographyOnline.com 2010 (accessed on 15 December 2012).
61. Ebinger, K.; Weller, H. N.; Kiplinger, J.; Lefebvre, P. *JALA* **2011**, *16*, 241–249.
62. Lazarescu, V., Mulvihill, M. J.; Ma, L. http://www.ChromatographyOnline.com 2011 (accessed on 15 December 2012).
63. Pinkston, J. D.; Wen, D.; Morand, K. L.; Tirey, D. A.; Stanton, D. T. *Anal. Chem.* **2006**, *78*, 7467–7472.
64. Searle, P. A.; Glass, K. A.; Hochlowski, J. E. *J. Comb. Chem.* **2004**, *6*, 175–180.
65. Mich, A.; Matthes, B.; Chen, R.; Buehler, S. http://www.ChromatographyOnline.com 2011 (accessed on 15 December 2012).
66. Weller, H. N.; Ebinger, K.; Bullock, W.; *et al. J. Comb. Chem.* **2010**, *12*, 877–882.
67. Isbell, J. J.; Zhou, Y.; Guintu, C.; *et al. J. Comb. Chem.* **2005**, *7*, 210–217.
68. Font, L.; Fontana, A.; Galceran, M.; Iturrino, L.; Perez, V. *J. Chromatogr. A* **2011**, *1218*, 74–82.
69. Liu, M.; Chen, K.; Christian, D.; *et al. ACS Comb. Sci.* **2012**, *14*, 51–59.
70. Schefzick, S.; Kibbey, C.; Bradley, M. P. *J. Comb. Chem.* **2004**, *6*, 916–927.
71. Goetzinger, W.; Zhang, X.; Bi, G.; *et al. Int. J. Mass Spectrom.* **2004**, *238*, 153–162.

9.08 Use of Industrial Scale Chromatography in Pharmaceutical Manufacturing

O Dapremont, AMPAC Fine Chemicals LLC, Rancho Cordova, CA, USA

© 2014 Elsevier Ltd. All rights reserved.

9.08.1	**Introduction**	182
9.08.2	**Generalities on Prep**	183
9.08.2.1	A Brief History	183
9.08.2.2	Modes of Chromatography	184
9.08.2.2.1	Batch chromatography	184
9.08.2.2.1.1	Small-molecule purification	185
9.08.2.2.1.2	Bio chromatography	185
9.08.2.2.2	SFC	185
9.08.2.2.3	Continuous chromatography	186
9.08.2.2.3.1	Process overview	186
9.08.2.2.3.2	A binary separator well suited for chiral separations	186
9.08.2.2.3.3	Other types of purifications suitable for SMB	187
9.08.2.2.3.4	Reactor SMB	187
9.08.3	**Process Development**	187
9.08.3.1	Strategies	187
9.08.3.1.1	Early discovery	188
9.08.3.1.2	Clinical phases	188
9.08.3.1.3	Commercial scale	188
9.08.3.1.4	Coupling reaction and purification steps	188
9.08.3.1.5	Adapting the chemistry for a better chiral separation	188
9.08.3.2	Development of a Separation for Commercial Scale	189
9.08.3.2.1	Stationary-phase considerations	189
9.08.3.2.2	Screening separation conditions	189
9.08.3.2.3	Selection of the mobile phase	190
9.08.3.2.3.1	Quality	190
9.08.3.2.3.2	Composition	190
9.08.3.2.3.3	Thermal properties	190
9.08.3.2.3.4	Compatibility	191
9.08.3.2.3.5	Toxicity	191
9.08.3.2.3.6	Viscosity and solubility	191
9.08.3.2.3.7	Modifier	191
9.08.3.2.4	Batch separations	192
9.08.3.2.5	Continuous separations	192
9.08.3.2.6	Optimization and scale-up considerations	193
9.08.4	**Equipment and Technique for Large-Scale Manufacturing**	194
9.08.4.1	Column Technology	194
9.08.4.1.1	Low pressure	194
9.08.4.1.2	Prepacked columns	194
9.08.4.1.3	Axial compression advantages	194
9.08.4.1.4	Column inlet/outlet design	195
9.08.4.1.5	Effect of temperature	196
9.08.4.2	Downstream Processing Technology	196
9.08.4.2.1	Concentration	196
9.08.4.2.1.1	Lab-scale rotary evaporators	197
9.08.4.2.1.2	Large-scale evaporation devices	197
9.08.4.2.2	Product isolation	197
9.08.4.3	Brief Review of Continuous Chromatography Process	197
9.08.4.3.1	SMB versus varicol	197
9.08.4.3.2	Turbo® SMB	198
9.08.4.3.3	Other variations	198
9.08.5	**Implementation for Commercial-Scale Manufacturing**	199
9.08.5.1	Quality/Regulatory Requirements	199
9.08.5.1.1	Basic requirements	199

9.08.5.1.2	Definition of a batch	199
9.08.5.1.3	Quality by design (QbD)	199
9.08.5.1.3.1	Process development	200
9.08.5.1.3.2	Production monitoring (PAT)	200
9.08.5.1.3.3	Transient mode versus steady state	200
9.08.5.1.3.4	Unexpected parameter variations	201
9.08.5.2	Manufacturing Point of View	202
9.08.5.2.1	Manpower	202
9.08.5.2.2	Maintenance	202
9.08.5.2.3	Recycling strategies	203
9.08.5.2.3.1	Solvent recycling	203
9.08.5.2.3.2	Unwanted enantiomer	203
9.08.5.2.3.3	Packing material care and usage	203
9.08.5.3	Price Considerations	203
9.08.5.3.1	Productivity and production rate	203
9.08.5.3.2	Equipment cost and amortization	204
9.08.5.3.3	Cost of recycling	204
9.08.5.3.4	Manpower	204
9.08.5.4	Environmental	204
9.08.6	**Conclusion**	204
References		205

Glossary

Bioseparation Chromatographic separation of biopharmaceutical molecules, such as proteins, peptides, nucleic acids, and carbohydrates.

Chiral separation Separation of chiral entities using either chromatography or other techniques.

Chirality Discovered by Pasteur in 1848, chirality is a physical property of molecules with an asymmetric carbon resulting in two possible geometrical forms called enantiomers. The two enantiomers are mirror images of each other. A 50:50 mixture of both enantiomers is called a racemic mixture. Both enantiomers have very similar physical properties and hence are very difficult to separate.

Preparative chromatography Chromatography technique used as a manufacturing unit operation for the purification of chemical entities.

Purification Unit operation consisting of the removal of one or several impurities from a product of interest.

Simulated moving bed Continuous separation technique first developed for the petroleum industry using the chromatographic principle. By using multiple short columns the batch process is converted into a more efficient continuous separation process. The process is similar to continuous distillation.

Supercritical fluid Physical state of a liquid when above its critical temperature and pressure. The supercritical fluid combines the properties of a liquid (good solvent) and a gas (low viscosity, high diffusion coefficient). These properties can be adjusted by modulating the pressure and the temperature.

9.08.1 Introduction

Chromatography is a very well known, powerful analytical technique used by chemists to analyze the product of their reaction. However, the formidable separation power of chromatography can also be used to purify large quantities of product with high yield while achieving high purity. This is the domain of preparative chromatography (Prep). It is a unit operation used as a separation technique for the purification of a product resulting from chemical reactions or natural product extraction. It is a unit operation in the chemical engineering sense of the term, which means that it is a well-defined process that can be represented by mathematical models of various levels of complexity[1] and thus can be efficiently optimized. More specifically, it is a chemical operation based on the equilibrium of a mixture of solutes between two phases, in this case a solid and a liquid or a gas. Each solute in the mixture has a different 'affinity' with the solid phase, and this affinity is exploited to achieve a separation. Based on this definition, there is a large variety of processes that are part of the chromatography family. The differentiation between each process is based on the nature of the equilibrium achieved; it could be based on size, polarity, or complex interactions, for example. For each case there are several options available depending on the nature of the mobile phase (liquid, gas, or supercritical fluid) and the operating mode (simple batch, stacked injections, flip-flop,[2] shave recycling, cyclo-jet,[3] simulated moving bed (SMB), etc.).[4–13] An extensive description of Prep can be found in many published materials and it is not the objective of this chapter to repeat this work. It will also be assumed that basic chromatographic notions such as selectivity, plate count, efficiency, and retention times are known to the reader; descriptions of these can also be found elsewhere.[4,6,14,15,16]

After a brief introduction to Prep through generalities and a quick review of the history of the technique and different modes available, the author has discussed the implementation of Prep for the purification of Active Pharmaceutical Ingredients (APIs) and intermediates for mainly small molecules. More specifically, he has presented possible strategies for the implementation of a Prep step in the life cycle of an API. He also has discussed several aspects of the equipment required, including the equipment needed for downstream processing. Finally, he has commented on the implementation of the production of an API at commercial scale in a highly regulated environment (current good manufacturing practice; cGMP). He further has discussed the development of the separation process from milligram quantities to the multiton commercial production scale and has addressed some of the related process development issues such as process robustness, quality, and pricing.

9.08.2 Generalities on Prep

Prep is a fairly old technique that is unfortunately often misunderstood by process development chemists and hence is underused for the manufacturing of small-molecule APIs and intermediates. In part because of the cost of the high-pressure high performance liquid chromatography (HPLC) equipment required for Prep, low-pressure glass column chromatography known as 'column' chromatography is still predominantly taught in chemistry classes. It is a very labor- and solvent-intensive process, and as a result it is often considered impractical and expensive to use this type of chromatography to achieve large-scale purification for commercial scale. Instead, the effort will be put into developing and optimizing a purification procedure using crystallization or extraction instead of chromatography. This perception is slowly changing and more API manufacturing processes including chromatography are being developed and are reaching commercial scale.[17] However, other industries such as the oil and food industries adopted chromatography early on as a powerful production tool. For example, water treatment is conducted on large beds of resins for softening or demineralization. The food industry uses ion exchange chromatography for multiple applications such as fructose purification from molasses, demineralization of citric acid, and the production of sorbitol and gelatin. The fructose purification process more specifically uses continuous chromatography units equipped with very large multi-ion exchange columns in a process called ISMB (Improved or Intermittent SMB).[18] A similar process is applied at large scale for the production of L-ascorbic acid[19] and for the purification of lactic acid.[20] Adsorption processes are also used in the oil refinery industry, which originated the conversion of the batch chromatographic process into a continuous, more efficient, more economical process in the early 1960s, the SMB process.[21] These processes are very efficient and are used at very large scale, resulting in a very low price per kilogram of product produced.

9.08.2.1 A Brief History

It was toward the end of the last century that the pharmaceutical industry started to use Prep as a production tool. It took almost a century for the technique to move from its discovery to large-scale applications for API manufacturing. It is commonly admitted that Russian botanist Mikhail Twsett (interestingly enough, the name Twsett (*цвет*) in Russian means color) is the father of column chromatography as he was the first to report, in 1905, the separation of bands of color in a glass tube filled with calcium carbonate.[22] He named this process 'chromatography,' in 1906, from the combination of ancient Greek *Khrôma* and *Graphein* meaning literally 'writing in colors.' From there, the development of the technique and the technology was rather slow, with mostly applications for gas chromatography (GC) for the oil industry, thin layer chromatography (TLC), and size exclusion chromatography (SEC) for polymer purification. In the late 1960s, the improvement of the technology to manufacture consistently small particles allowed the development of 'modern liquid chromatography,' and in 1974 the basic principles of chromatography were laid down by L. R. Snyder and J. J. Kirkland in their seminal book 'Introduction to Modern Liquid Chromatography.'[14] In the mid-1970s the development of dynamic axial compression columns (DAC) allowed for easy, reproducible, consistent column packing with an extended lifetime.[23,24] This also facilitated the scale-up process as wall effects became less important and very large-diameter columns could be packed with similar packing densities and performance to small narrower columns. With these technological improvements, more complex separations became possible, and in the early 1990s the first chiral stationary phases (CSPs) based on silica beads coated with a functionalized amylose or cellulose polymers developed by Professor Okamoto were commercialized by Daicel (Japan). It was at about this time that a continuous adsorption process originally developed in the 1960s for the petroleum industry was adapted to the purification of pharmaceutical compounds: the SMB process. SMB is the conversion of a batch process into a continuous process with better performance and lower manufacturing cost at larger scale. This technology rapidly found a niche in the pharmaceutical industry with chiral separations as SMB is a binary separation technique. Today several pharmaceutical compounds, such as Pfizer's Zoloft (Sertraline Tetralone[25,26]), Lundbeck's Lexapro (Escitalopram), and UCB's Keppra (leviteracetam), have one SMB step in their manufacturing process using units equipped with several columns of large diameter.[17] In 1990, another chromatographic technique was brought to large scale, i.e., supercritical fluid chromatography (SFC) using CO_2 for mobile phase. This technique is still underutilized for large-scale manufacturing, but it has found its place in process development laboratories where milligram to gram quantities are easily and rapidly separated, resulting in a lower solvent consumption and a lower operating cost.

9.08.2.2 Modes of Chromatography

In this section, the author differentiates between *mode* and *type* of chromatography. For example, he considers adsorption chromatography to be a type of chromatography whereas he considers batch and continuous to be different modes of chromatography.

9.08.2.2.1 Batch chromatography

The intrinsic nature of chromatography is batch as the process relies on the different elution velocity of each species in the mixture to be separated as they come out of a column flushed by a mobile phase (liquid, gas, or supercritical fluid). As a result, the process is based on an injection/elution/collection sequence, which is repeated until the entire product has been processed. This sequence can be optimized quite efficiently.[1,5,27] The set-up for a batch chromatography process is usually composed of the following elements (Figure 1): a column, one or more eluent pumps (for complex eluent compositions and gradients), a mixing device for the eluent (static or dynamic mixer), a mean of injection of the product (syringe or feed pump), a flow meter, a detection device (e.g., a UV detector), a set of valves to control the flow distribution and the product collection, and an automation system (computer or PLC). Based on the responses from the flow meter and the detector, the automation unit controls the valves and the pumps to perform the separation as intended. Once the separation conditions are established, the controller takes charge and the operator ensures supply of product and eluent, as well as recovery of the collected product fractions. The proper design of every part of the equipment is important to minimize back mixing and reduction of efficiency.[4,14]

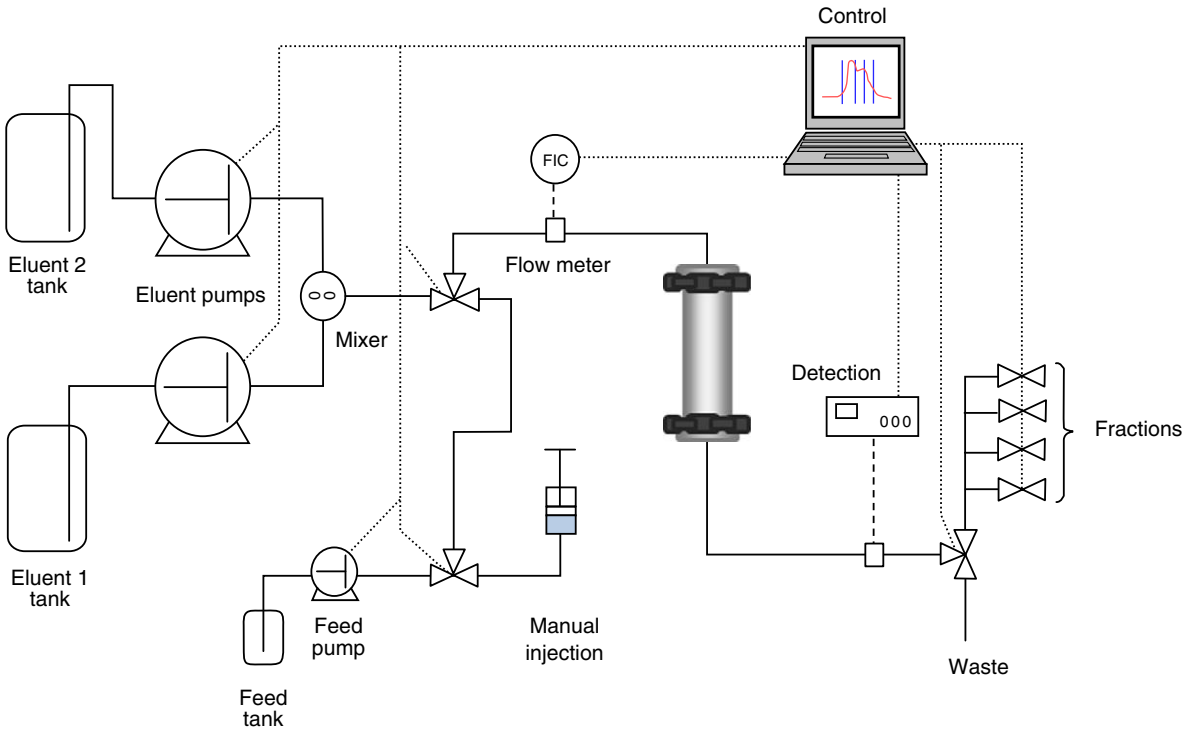


Figure 1 Basic design of a batch chromatography unit: continuous lines are for process flow, dashed lines are for measured signal, and dotted lines are for process control.

Typically, a column is packed with small porous particles (chromatographic media) of a given particle size and shape and a mixture of solutes is pushed through the column with a fluid (gas, liquid, or supercritical) of appropriate composition to provide elution with a range of retention for the various solutes. Because of the difference in interactions of the solutes with the solid media, they migrate down the column at different velocities, and if the process parameters (i.e., column length, particle size, mobile-phase flow rate, temperature, quantity injected) are well selected a complete separation can be achieved (Figure 2). As shown in Figure 2, a certain length of column is required to allow for the difference in velocities between the solutes to produce a separation. In addition, Figure 2 shows that the part of the column that is active is the part where the mixture is present. This 'active zone' is diminishing as the separation progresses down the column. Material already separated (in front or in back) only gets more diluted before exiting the column. As a result, a large amount of packing material in a column is necessary to separate a small amount of product. Thus, the efficiency of the packing material is limited by the nature of the process.

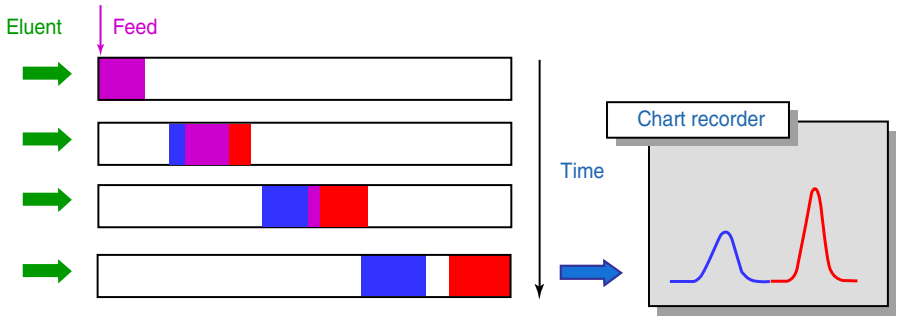


Figure 2 Batch chromatography process illustration.

9.08.2.2.1.1 Small-molecule purification

Small molecules are usually the product of chemical synthesis and are thus usually relatively clean compared to biomolecules, which are often produced by living organisms. At completion of the chemical reaction, the products from side reactions need to be eliminated to achieve the desired purity typically required for APIs. Prep competes with other purification techniques such as crystallization or extraction to achieve this goal. It is very common for chromatography to be used as a last resort when other unit operations have failed at delivering the desired purity with a decent yield. It is also very common to see crystallization yields of 85% or lower per step with more than one step to be able to achieve the desired purity. Some impurities can be very closely related to the desired product and hence will exhibit very similar solubility and polarity profiles, making the separation by crystallization difficult to achieve. For example, dimers or mono-substituted molecules are very difficult to separate by crystallization from the desired monomer or bis-substituted product. Chromatography can bring a significant advantage as these species are likely to be separated using a reverse phase or a normal phase or a CSP even if the separation is not chiral. Chiral separations are also very efficiently performed using chromatography, and multiple batch and continuous applications are currently being developed and are making their way to commercial scale.

9.08.2.2.1.2 Bio chromatography

The purification of biomolecules typically uses several types of chromatography, because it is often impossible to crystallize the product of a bio reaction efficiently, as multiple species (e.g., proteins) are often present along with the product of interest. Therefore, in contrast to traditional pharmaceutical small-molecule manufacturing, bio-pharmaceuticals are typically produced with several chromatography steps.[10,15,28] Each step is a different type of chromatography using a variety of solvents and buffer solutions. Chromatography for biomolecules is typically done in batch mode using low-pressure columns, as the chromatographic medium is usually a soft gel. The purification process is quite intensive and the cost of these purification methods is usually high. The chromatographic medium has to be replaced frequently as it can become permanently contaminated by impurities from the bio reaction and thus loses performance and efficiency over time. Additionally, large volumes of aqueous solvent and buffer solutions are used in a gradient mode and thus solvent recycling is not always possible. In the past few years, there has been growing interest in using continuous chromatography for bio separations as a potential way to improve process economics.

9.08.2.2.2 SFC

SFC using CO_2 as a mobile phase is a very efficient alternative to batch liquid chromatography. In the past few years this technology has seen a growing interest and has been intensively promoted as a 'green' separation technique. Today many laboratories use it for small-scale Prep separations. The technology was developed in the early 1990s for Prep but took some time to reach the market.[29] The use of CO_2 as the main component of the mobile phase is very attractive as it is an inexpensive raw material and is easy to discard. Because the CO_2 is the side product of other industries and is not generated by the separation, the SFC process is considered green as it uses less organic solvent than conventional batch chromatography. However, most SFC separations require the addition of a modifier, example, methanol, to achieve a separation. In certain cases, the amount of modifier is such (30% or more) that the supercritical state of the mobile phase is questionable. By tuning the pressure, temperature, and modifier ratio, separation can be adjusted and very short separation times, sometimes less than a minute, can be achieved.[30] Additionally, because the viscosity of the mobile phase is very low (close to the viscosity of a gas), very high flow rates can be achieved and small chromatographic media can be used, resulting in columns with very high plate count (efficiency). Because the solute diffusivity is increased with SFC, the efficiency of the separation is typically better than HPLC as reported by Jusforgues and Shaimi.[30] The combination of these advantages allows for very rapid injection/elution/collection sequences. Hence, very high productivities can be achieved with batch SFC, and especially for chiral separations, that are sometimes superior to productivities achieved by SMB.[31] The major challenges with this type of chromatography, other than the very high pressures (200 bars), are the recovery of the product and the recycling of the mobile phase. By simple depressurization, the CO_2 returns to its gaseous state leaving behind the product neat or in the modifier. This operation is conducted in cyclones that allow the CO_2 gas to exit at the top while leaving the droplets of product-modifier mixture to coalesce and collect at the bottom of the device. However, the design of a cyclone can be very specific for each separation. The flow rate and the size of the product droplet are critical to

ensure the highest recovery of product. It is necessary to avoid entrapment in the CO_2 outlet, and hence oversized cyclones may be required to cover many applications. Regardless of this technical issue, the ability to recover the product neat or highly concentrated straight out of the column is very attractive as energy-hungry solvent evaporation systems are not required. Note that CO_2 is not subjected to ICH Q3C for residual solvent and thus has no restrictions for use in pharmaceutical manufacturing.[32]

Although analytical SFC units are becoming more available in laboratories, Prep units up to several 100 g product per day are slowly making their way into laboratories. Units with full recycling of the eluent are now available, significantly reducing CO_2 consumption. Today this technology is still confined to the early discovery laboratories, as large SFC units are not available. It is, however, expected that multi kilo commercial-scale units will be installed for routine production of API in the next few years.

9.08.2.2.3 Continuous chromatography

The basis for this process was developed in 1961 by the petroleum industry for the purification of xylenes.[21,33] The process is very similar to a continuous distillation column; the liquid/vapor equilibrium involved in a distillation column is simply replaced by the liquid/solid equilibrium that occurs in chromatography.

9.08.2.2.3.1 Process overview

Because very detailed descriptions of the process can be found in many publications[4,6,8,12,13,17,34–39] the author will not discuss here the principle of continuous chromatography, but rather discuss some of the specificities, benefits, and drawbacks.

The SMB process is presented in **Figure 3**: a counter-current of solid and liquid is created to allow the migration of the fast species (red in the figure) with the eluent and the slow species (blue) with the solids. Because a true continuous flow of solid is not possible without major problems (attrition, low efficiency, etc.) the solid is packed in several short columns of equal characteristics (8–12 typically). The periodic displacement of the columns by one position to the left is equivalent to a solid-phase velocity. Because the periodicity has to be constant (switch time) all the columns must be of equal length. Moreover, because each column will be rotating through all the positions, they all must be identical as the SMB performance is strongly linked to the performance of the worst column.[40,41] The 'train' of columns defines four zones that are delimited by the inlet/outlet streams (eluent and feed inlet, extract and raffinate outlet). The two middle zones (II and III) are the separation zones. This is where most of the product is found. The flow rates must be carefully selected so that the fast-eluting compounds move with the eluent (i.e., exit the column before the column is moved to the left) and the slow-eluting compounds remain on the column and are entrained to the left. Zones I and IV are the 'cleaning' zones. The flow rate in zone IV is significantly reduced because of the raffinate flow rate. The flow in zone IV is selected so that the retention time of the fast-eluting product increases so much because of the low flow rate that the compound is now entrained by the column toward zone III when the column switch occurs. For similar reasons, the zone I flow rate is increased to the point that the retention time of the strongly retained compound becomes shorter than the switch time and hence the product can exit the column toward zone II before the column is moved to the left when the column switch occurs. The selection of the flow rates is strongly linked to the retention times of the species in each zone. Thus, the equilibrium isotherms must be measured carefully if accurate modeling of the process is required. In the case of the 'simple' Langmuir type isotherm, it is quite intuitive to understand how the system dynamic works, and with a bit of hands-on experience a separation can quickly be manually optimized. When the isotherms are more complex (S-Shape or anti-Langmuir), the manual optimization is not trivial and proper modeling of the separation provides a better understanding of the interaction of the parameters.[1,4,6,8,14,16,17,34–39,42,43] However, the modeling of such isotherms is rather challenging, and compromises must be made to gain the necessary information in a timely manner when developing a separation.

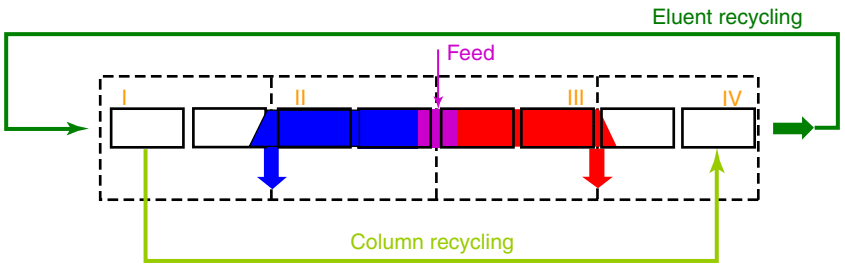


Figure 3 Continuous chromatography process illustration.

9.08.2.2.3.2 A binary separator well suited for chiral separations

As mentioned above, continuous chromatography is a binary separation tool and hence it is well suited for the separation of enantiomers. The need for enantiomerically pure entities has been growing for more than 20 years. In 1992, the FDA acknowledged the existence of technologies that allow the isolation of a pure single enantiomer.[44] Thus, the regulatory agencies have pushed the pharmaceutical industry to provide pure single enantiomer drugs.[6] Pharmaceutical companies must demonstrate the activity of both enantiomers (this also applies to stereoisomers, regioisomers, and diastereoisomers). If one of the enantiomers presents a risk of side effects, or shows no activity, then the regulatory agencies will require its removal from the final API, as it is

considered an impurity. As a result, the technologies available to achieve enantiomeric purity have grown significantly. There are many ways to achieve enantiopurity. The chiral entity can be directly synthesized. This requires usually expensive metal catalysts and specialized capabilities. Sometimes it is a naturally occurring chiral starting material and will require extraction from biomass. The chiral entity can also be obtained by enzymes. This can be very effective, but finding the right enzyme followed by engineering the enzyme strains to increase yield, throughput, and selectivity can be time consuming. The resolution of the racemate to obtain the pure enantiomers can be done by converting the racemate to a diastereomeric mixture. This is achieved by combining the racemate with a chiral agent such as tartaric acid to form a salt. The separation of the desired diastereoisomer salt is then conducted by a simple crystallization followed by the removal of the chiral agent. This process requires a minimum of three steps but is relatively simple to implement. It is, however, quite solvent and manpower intensive. The overall yield is typically low because each step results in product loss; yields lower than 35% versus a theoretical yield of 50% are frequent. Another way to achieve chiral resolution is to separate the enantiomers by chiral chromatography. This technique is now possible thanks to the development of CSPs using a variety of principles since the 1980s.[45,46] The development of chiral phases by Professor Okamoto from Japan using functionalized amylose and cellulose polymer-based coatings on silica beads[6] significantly helped the development of chiral chromatography for manufacturing, as these CSPs allowed high-throughput separations to be achieved. However, in some cases, the productivity may have to be reduced significantly to achieve high purity and high yield. Nevertheless, because of the availability of new CSPs and the wider range of solvents that can be used, very high productivities have been identified in the laboratory. A decade ago a productivity of 1 kg Feed per day kg CSP^{-1} was considered satisfactory, whereas nowadays productivities greater than 3 and even as high as 15[47] have been reported. Note that productivity is commonly expressed as a quantity of feed processed per unit of time and quantity of stationary phase instead of quantity of product produced by unit of time and quantity of stationary phase.

9.08.2.2.3.3 Other types of purifications suitable for SMB

Continuous chromatography is not limited to the separation of chiral entities; more complex mixtures can be considered. During the process development phase, the separation can sometimes be developed to obtain a 'binary' separation; the objective is to bundle all the impurities on one side of the product peak. It is important to have a very thorough understanding of the downstream processing to know what impurities can be ignored or which one should be removed and to what level. For example, the SMB purification of paclitaxel, a high-potency natural product (HPAPI) used for cancer treatment, is reported by Metz et al.[48] The crude feed is the result of multiple extraction steps from the tree biomass. The purity is in the range 65–85% depending on the harvesting season. An SMB separation was developed to isolate the desired Paclitaxel from some key impurities (e.g., cephalomanine). The product recovered from the SMB is greater than 97% and the final crystallization brings the product to the final specification (no less than 98.5%). The authors report a reduction in labor by 78% and a reduction in solvent consumption by 68% compared to the batch purification process. They also note a yield increase of 15% and a fourfold increase in productivity, resulting in a significant saving of US$45 000 kg^{-1} of pure paclitaxel.[48]

Other types of separations can be conducted using SMB technologies, such as product recovery from waste stream (SMB Mining®[9,49]) or complete removal of a specific impurity (i.e., cytotoxic or genotoxic impurities[50]).

Continuous separations are very attractive because the overall operating cost can be significantly lower at large scale as the throughput and the solvent consumption are superior to batch. For this reason the biopharmaceutical industry is very interested in converting batch purification processes to continuous processes. However, owing to the complexity of these separations, multiple modifications to the process need to be implemented.

9.08.2.2.3.4 Reactor SMB

The continuous separation process can be combined with a continuous reaction to optimize the overall process. For example, the reaction can be conducted inside an SMB unit packed with a mixture of catalyst and stationary phase. As the reaction occurs, the product of the reaction is separated from the starting material. This can cause a displacement of the reaction equilibrium and allow for a better yield and faster conversion rate.[14,51] O'Brien et al. presented an alternative combination whereby a tubular continuous reactor directly feeds an SMB unit,[52] reducing the downtime and improving the throughput.

9.08.3 Process Development

The use of Prep is typically considered as a last resort, and often the necessary amount of time to properly develop a separation is not available. However, if the chromatography step is included early in the selection of the chemistry route, then it can be fully optimized. Manufacturing processes usually evolve as the synthetic scheme matures. The approach to the development of a chromatographic separation varies as a function of the development stage of the molecule, and the strategy must adapt accordingly.

9.08.3.1 Strategies

As pointed out by E. Francotte,[6] the importance of the scale-up feasibility, cost, amount, and time required varies considerably with the development stage. Regardless of the type of chromatography, it is necessary to define the problem properly so that the

process development is conducted efficiently. During the preclinical stage, the goal is to rapidly discard candidate drugs that will most likely fail before reaching the market. Cutting the loss early can save pharmaceutical companies millions of dollars. Therefore, accessing the purified product or the single enantiomer in a very short time is essential (the cost is almost irrelevant). When the product is getting close to commercial launch, the goal is to have a process that can be scaled up with minimum changes or tweaking, but this process should be economical, consistent, and robust.

9.08.3.1.1 Early discovery

For early discovery, the preparation of small quantities of product is usually time sensitive and thus a rapid screening of a few 'standard' conditions is conducted until a separation is achieved. These conditions are then used for batch chromatography (liquid or SFC) using the equipment and packing material available in the laboratory. This method is certainly not fully optimized and is typically not considered for scale-up without significant changes. The solvent recovery is typically not considered, as the solvent quantities required remain small.

Note that chiral chromatographic separations provide both enantiomers in good purity. The unwanted enantiomer is used for toxicology studies to satisfy regulatory agencies and to establish final product specification.

9.08.3.1.2 Clinical phases

During clinical phases the synthetic route still has some variability, but steps are becoming more defined as the product moves toward commercial launch and process validation. Typically, process development groups try to remove chromatography because equipment for large scale is less readily available. The separation is bound to evolve because the quality and impurity profile of the feed material will change significantly from the early discovery to the commercial scale as the synthetic route evolves and matures. Screening of separation conditions may be repeated as different impurities are introduced by modification of the upstream process. At this stage, it may be worth looking into the use of other chromatographic techniques such as SMB to obtain the necessary data to extrapolate the manufacturing cost. A significant amount of work is conducted during these phases to gain valuable knowledge on the separation and hence help define critical parameters.

9.08.3.1.3 Commercial scale

Assuming that the chromatography is maintained in the synthetic scheme, if the quantities to be produced are expected to be large (more than a few metric tons) then continuous chromatography, if applicable, should be considered as it is more efficient and less expensive than batch. The cost of production using SMB is higher for small scale than using batch simply because the cost of setting up and cleaning represents a large portion of the campaign cost and hence a single batch column will be more cost effective at small scale. However, as the quantity increases, the cost of SMB drops to a lower value because throughput and solvent consumption are usually in favor of SMB.[6]

9.08.3.1.4 Coupling reaction and purification steps

The location of the purification step comes necessarily after the reaction generating the impurities to be removed. Some pre-purification (extraction, crystallization) may be required to remove strongly adsorbed impurities that can limit the life of the column, and hence forces frequent unpacking/packing procedures, increasing the operating cost.[10] Chemists are trained to develop a chemical reaction with the objective of making the product but also pushing the conversion of the key reagent to the maximum. Sometimes this equates to a long reaction time, which causes an increase in the impurity level as either side reactions occur or the product degrades. Pushing the reaction to a certain conversion, i.e., 40–60%, and then isolating the product from the starting material may be a more efficient solution. This process could result in a shorter cycle time but also, and more importantly, in a cleaner reaction mixture to process. The unreacted starting material can be recycled with the next batch after minimum processing. Mihlbachler et al.[50] presented an example of a cyanation reaction with a long cycle time to reach a conversion rate in excess of 95%. At completion, the product is recovered from a reaction mixture containing a large amount of impurities resulting from the degradation of the product and side reactions. By collecting kinetic data and modeling both the reaction and the SMB separation of the starting material from the product, the authors could optimize the combined process resulting in a reduction of the cycle time by 75%, and a yield increase from 33.7% to 48.1% using 30% less raw material and generating less waste.

9.08.3.1.5 Adapting the chemistry for a better chiral separation

When considering a chiral purification, the chromatographic resolution step can be moved within the synthetic scheme to optimize the process. Preferably, the separation will be conducted as early as possible to avoid carrying the unwanted enantiomer through the downstream synthesis. It is, however, necessary to ensure that the subsequent chemistry steps will not cause racemization of the product. If the unwanted enantiomer can be racemized at one point of the synthetic scheme, then this may be a better location for the chiral separation, as the theoretical yield will increase from 50% to 100% (note that the SMB separation yield is typically 95%, but some losses are to be expected in the handling and work-up of the product post SMB).

It is recommended that the various synthesis options (i.e., using different protecting groups) be discussed as this may result in a significant increase in the chromatography performance. The change in molecular weight with different protecting groups should be taken into consideration when comparing (costing) the processes. Typical protecting groups for a chiral amine with corresponding molecular weight are presented in Figure 4. For example, if the productivity of the separation of an acetamide-protected molecule (330 g mol^{-1}) is 1.5 kg Feed per day per kg CSP, the corresponding molecular productivity is 4.29 mol d^{-1} (kg CSP)$^{-1}$.

The productivity of the same molecule protected with a CBz group (408.1 g mol^{-1}) must be greater than 1.75 kg Feed per day per kg CSP (4.29 mol day^{-1} (kg CSP)$^{-1}$ × 408.1 g mol^{-1} = 1750 g Feed per day per kg CSP) to show an improvement in throughput.

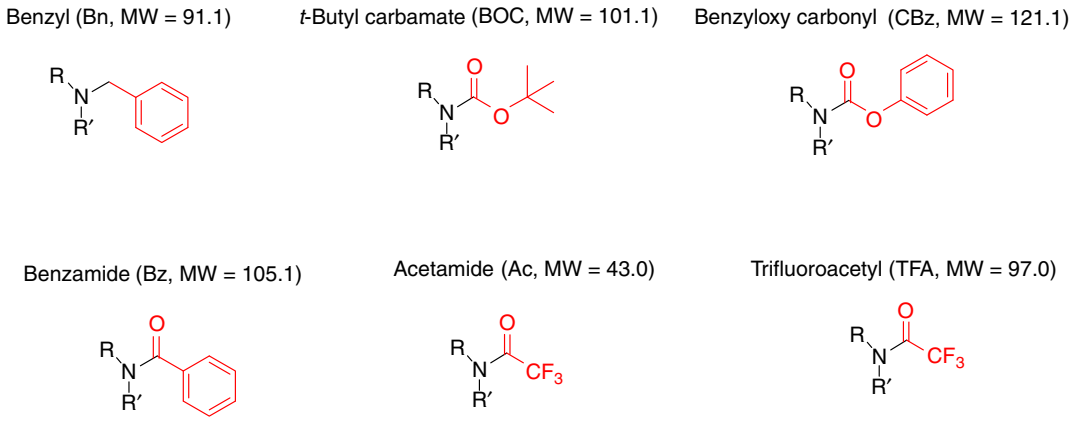


Figure 4 Example of protecting groups for an amine and their contribution to the molecular weight.

9.08.3.2 Development of a Separation for Commercial Scale

The development of a separation requires a good knowledge of the product chemistry. The separation conditions are driven by the separation achieved but also by the stability of the molecule in various solvent and pH conditions. A good understanding of the upstream and downstream process helps to make decisions on the development of the chromatographic conditions.

9.08.3.2.1 Stationary-phase considerations

There is a large variety of packing available for all sorts of separation types. Multiple suppliers provide a selection of particle sizes, surface chemistries, and pore sizes. These suppliers also provide the packing in prepacked columns (low or high pressure) for immediate use. Subtle variation of the surface chemistry from one supplier to the next makes the selection of the packing material for the separation quite difficult. Ideally, a sample of each phase available at commercial scale should be tested for the separation to provide the best possible solution. However, in practice, because of time constraints or simply availability, only a handful of phases are tested and the best one is selected for the scale-up. Therefore, the selection of the separation conditions often relies on the expertise and experience of the chromatographer. Regardless of the supplier, the solid media packed in the column can either be a randomly shaped solid, i.e., irregular media (it is typically a low-cost media), or spheroids, i.e., spherical media (more difficult to manufacture and thus more expensive). The solid medium can be made of soft polymer particles and is used in low-pressure chromatography as it is a compressible medium or made of silica with a stronger back bone, which can be used at pressures exceeding 200 bars (SFC). Other types of media can also be found but they remain less common for Prep. Typically, for small-molecule API and intermediate separations, it is preferable to use spherical beads with a silica backbone having a variety of surface chemistries depending on the separation considered. The irregular media have a tendency to fracture under stress caused by operating pressure, which generates fines that migrate down the column and eventually block the frits. This results in poor column performance, increase in pressure, and eventually column death. It is now common to find perfectly spherical beads with a very narrow particle size distribution, a well-defined surface chemistry and pore sizes, and an excellent reproducibility from batch to batch, which is a key parameter for commercial-scale use. For polymeric beads, the particle size is usually well controlled and monodispersed packing can be found readily. The particle size distribution is very important as this parameter controls the efficiency of the column and the operating pressure. The separation is typically optimized to operate at the maximum operating pressure allowed by the equipment, and thus a compromise between the column length (more plates for the separation) and the pressure drop should be found.

Assuming that the objective is to develop a viable large-scale purification method, any packing used for the screening should be available in bulk in large quantities and manufactured in large batches (10–50 kg) under cGMP. Otherwise, the method would have to be modified at a later stage to use a packing material that will satisfy cGMP requirements. Packing one's own columns using bulk packing material is preferable as additional knowledge on the packing handling is gained:

- Are there fines in the packing?
- Does the packing need to be decanted before packing?
- What is the best solvent to use?

9.08.3.2.2 Screening separation conditions

Pharmaceutical companies are investing a significant amount of resources, time, and money to develop screening tools to rapidly identify separation conditions, as well as to purify milligram quantities.[53,54] Regardless of the type and the mode of

chromatography (batch or continuous), the screening is conducted on a limited selection of stationary phases. For chiral separations, there is no predictive tool that can facilitate the selection of the conditions because the mechanism of chiral recognition is very complex. The number of chiral phases increases regularly, which in turn increases the chances of finding a good separation, as well as the complexity of the screening process.[46] It is unfortunately necessary, and expensive, to have a collection of a variety of packing material available in the laboratory, as well as automated HPLC units. However, Suteu from Chiral Technologies indicates that approximately 95% of the chiral compounds can be separated with only four chiral phases (Chiralpak AD, Chiralpak AS, Chiralcel OD, and Chiralcel OJ).[6] The recent development of the immobilization process for these coated CSPs has been a significant improvement in the choice of solvents for process development. Historically, the coated phases could only be used with a handful of solvents (mainly alcohol, alkanes, and sometimes acetonitrile). Thanks to the immobilization process, these new phases (e.g., Chiralpak IA, Chiralpak IC) can handle all sorts of solvents such as methyl *tert*-butyl ether (MTBE) or ethyl acetate.

The screening process consists of injecting the crude product on every column available with different mobile-phase compositions using automated methods. This is typically conducted on 'analytical'-size columns packed with the preparative chromatographic media (4.6 mm ID × 250 mm long), and the flow rate is typically 1 ml min^{-1}. The use of solvent gradients can help to speed up the identification of conditions that can potentially result in a productive separation. The chromatographer needs to sort out all the chromatograms generated and determine which condition has the potential to be used for Prep. Developing chiral separations is relatively simple as the result of the screening is two peaks, one peak, or no peak at all. From there, tweaking the conditions that gave two peaks gives a process that can be taken further. Note that the effect of modifier on CSPs should be considered. It is strongly recommended to keep track of the columns used with a modifier, as they will have different retention characteristics compared to new columns.[55]

The screening for a purification method is more complicated as several peaks can be coeluting with the product. The peaks integration may give some indications as to the performance of the conditions, as the lowest purity means that most of the impurities are eluting at a different retention time than the product. This can be considered as a first elimination criterion. Eventually, a fraction collection is conducted. This method consists in collecting fractions of a given length of time as the product leaves the column. Each collected fraction is analyzed using an analytical method to quantify the different species in the fraction. The results are then reported in a spreadsheet. The purity and the recovery of pooled fractions can be easily calculated using the spreadsheet. Once this work is performed the batch separation can be conducted to confirm the calculated results from the spreadsheet. The separation may be further optimized by considering variation of the solvent composition, column length, or injected quantity (load). This process is unfortunately time consuming.

9.08.3.2.3 Selection of the mobile phase

The selection of the mobile phase is important, as it is one of the largest cost contributors of the process. For Prep, isocratic separations are preferred to gradients as the mobile phase is easier to recycle.

9.08.3.2.3.1 Quality

Although the small-scale separation is usually performed using high-quality HPLC-grade solvents, large-scale separation is typically conducted with lower-quality solvents. Evaluation of the separation using these lower-grade solvents to ensure that no new impurity is added to the final product or that a small amount of other solvents (e.g., residual water) does not affect the separation is important. Because the solvent is most likely to be recycled, it is also essential to avoid an accumulation effect that could potentially hurt the product or the stationary phase. Trace level of water in the mobile phase can affect the retention times and peak shape. This effect should be evaluated to define a range of moisture that will not be detrimental to the separation performance.

9.08.3.2.3.2 Composition

It is preferable to favor single-solvent systems versus binary or ternary solvent systems as the preparation and the recycling of the mobile phase become critical at larger scale. If a binary solvent is used, it is necessary to evaluate the effect of a small change in the solvent composition on the retention times. Typically when the eluent is made of similar volumes of two different solvents such as a 60/40 ratio, a small change in composition has very little effect on the separation. However if the ratio is significantly different, such as 96/4 for example, a small variation will have a significant impact on the separation resulting in a possible loss of resolution. When considering a binary mixture, the existence of an azeotrope should be factored in as the recycling of the solvent is much easier if the azeotropic composition is used for the separation. Note that the azeotropic composition changes with pressure, and hence must be taken into consideration when developing the method.

9.08.3.2.3.3 Thermal properties

The ease of evaporation of the mobile phase should be taken into consideration as it influences the product recovery and the operating cost. Low-boiling point and high-vapor pressure solvents are preferred as they are easier to evaporate at low temperature, minimizing the potential degradation of the product. However, these solvents are difficult to pump as they tend to evaporate in the pump head during the suction phase, resulting in a lower volume of liquid displaced and causing variability of the flow rate. Some physical properties of solvents used for Prep are listed in **Table 1**.

The heat of vaporization indicates how much energy is required to distill the solvent. At commercial scale the solvent must be recovered and recycled to maintain a low operating cost. The contribution of the solvent to the operating cost is then reduced to

Table 1 Physical properties of organic solvents used for chromatography[4,12,47,56]

Solvent	*Viscosity (cPO at ambient)*	*Solubility*	*Boiling point (T_b in °C)*	*H_{Vap} (at T_b, in KJ mol^{-1})*
n-Hexane	0.31	Null-low	68.7	28.9
n-Heptane	0.39	Null-low	98.4	31.8
Acetonitrile	0.38	High	81.6	29.8
Methanol	0.55	Medium low	64.6	35.2
Ethanol	1.19	Medium	78.3	38.6
Isopropanol	2.40	Medium high	82.3	39.8
Methyl *tert*-butyl ether	0.35	Medium high	55.0	29.7
Ethyl acetate	0.43	Medium high	77.1	31.9
Toluene	0.59	Medium	110.6	33.2
Water	1.00	Low-high	100.0	40.7

the energy required for the evaporation and the condensation of the solvent. This information, in addition to the chromatographic performance, must be considered for the solvent selection to offer the best solution for the separation and a fair way of comparing process routes.

9.08.3.2.3.4 Compatibility

The choice of solvent must also be driven by the compatibility of the product with the mobile phase, i.e., the purification of an ester using an alcohol-based mobile phase can result in trans-esterification during the separation or during the solvent evaporation. An evaluation of the compatibility of the solvent with the product should be conducted in collaboration with the chemists and, if necessary, accelerated degradation experiments should be conducted. Typically, a small amount of product in solution is stored in the oven for a period of time and tested analytically to observe degradation.

Compatibility with construction material of the equipment should be evaluated (coupon testing). Most of the equipment for commercial-scale use is made of stainless steel 316L and Teflon. Equipment suppliers often offer alternate construction material for seals and gasket. However, some difference in mechanical strength or hardness should be expected, possibly resulting in leaks.

9.08.3.2.3.5 Toxicity

Certain solvents should be avoided if the product is the final API as they could be listed on the ICH topic Q3C.[32] Solvents pertaining to Class 1 are to be avoided (e.g., benzene). Class 2 contains the solvents to be limited below a certain value; for example, acetonitrile is limited to 410 ppm. There are 27 solvents listed in Class 2 with levels ranging from 50 to 3880 ppm. The third class contains 16 solvents such as acetone and heptane that are considered less toxic, and their level should be limited for reasons other than toxicity.

9.08.3.2.3.6 Viscosity and solubility

The mobile-phase viscosity and the product solubility in the mobile phase should be carefully evaluated. A more productive separation can be achieved with a mobile phase of lower viscosity as the flow in the column can be increased significantly to maximize the operating pressure even if the selectivity of the separation is not as good. For example, the best selectivity (~3) for a chiral separation is achieved using a mobile phase made of 70% ethanol and 30% *n*-heptane. The same separation using 100% acetonitrile leads to a selectivity of ~1.45. If the loading capacity and the solubility are the same for both systems (solubility is usually higher in acetonitrile but we are considering here a case where solubility is not a limiting factor), a productivity based on estimation of the flow rates in the various zones of the SMB can be calculated. The viscosity of the first system is estimated at 0.86 cPo whereas the viscosity of the acetonitrile is approximately 0.38 cPo at room temperature. As a result, the productivity of the acetonitrile system can potentially be approximately 2.3 times larger. Hence, even if the loading can potentially be lower with acetonitrile because of a lower selectivity, a better separation can be achieved in terms of throughput.

Whenever possible, it is preferable to dissolve the feed product in the mobile phase. This greatly simplifies the process as the injection will not create unnecessary perturbations on the column (e.g., viscous fingering,[54]) and it will also not add a different solvent to the eluent, simplifying the recovery process. Note that for SMB separations the feed solution must be of the same composition as the eluent to ensure stable operations of the SMB unit.

9.08.3.2.3.7 Modifier

The selection of a modifier such as an amine or an acid for chiral separation must be factored into the recycling of the modifier. Low-boiling point amines or acids should be considered so that they can be recycled with the mobile phase and not become concentrated with the product causing potential degradation issues, as the pH of the solution changes with the concentration process.

9.08.3.2.4 Batch separations

The objective of Prep is very different from the objective of analytical chromatography. The goal is economical: to process as much product as possible in the minimum amount of time. As a result, the process is conducted under strongly nonlinear conditions where a variety of effects are occurring.[1,4,6,14,27] Understanding these effects is very important as they can be leveraged to increase the throughput of the separation. After the screening is performed and one or several methods are identified, the chromatographer needs to select the best one. It is difficult to select the preparative method based on a single analytical injection, as this will not provide enough information on the loading capacity and the productivity of the method. If time permits, a full measurement of the isotherm of each species involved should be done so that an accurate mathematical modeling of the separation can be conducted.[1,6] In this way, each separation condition can be optimized and the best can be selected. Unfortunately, this approach requires time and a large amount of material, as well as a sophisticated modeling tool. Hence, this is saved for commercial-scale production when a more thorough understanding of the process is required (quality by design, QbD). For early development, the chromatographer will conduct a few overloaded injections and select from these the best separation conditions. For chiral separations where tag-along and displacement effects are limited, a touching band separation is most likely to be the best combination of throughput, yield, and purity. Additional techniques can be used to further optimize the throughput of the separation: stacked injections,[31] shave recycling, flip-flop,[2] cyclo-jet,[3] or continuous processes.[38,39]

9.08.3.2.5 Continuous separations

Continuous chromatography is superior to the batch process in terms of efficiency, but it is more complex to develop and operate. Because the process is more efficient, it is not necessary to have a large selectivity to achieve purity, yield, and productivity. As shown in Figure 5, the maximum loading to achieve high purity and high recovery in batch corresponds to touching band conditions (especially chiral separations). In SMB, because only a fraction of the peak is collected and high selectivity is not required, higher loading can be used while maintaining purity and yield. As a result, the productivity is significantly higher. It can actually be counterproductive to have high selectivity, as higher flow rates will be required to recover the extract stream affecting the average operating flow rate and hence the throughput. Thus, a separation with a lower selectivity and a low viscosity mobile phase can result in a very productive SMB separation process.

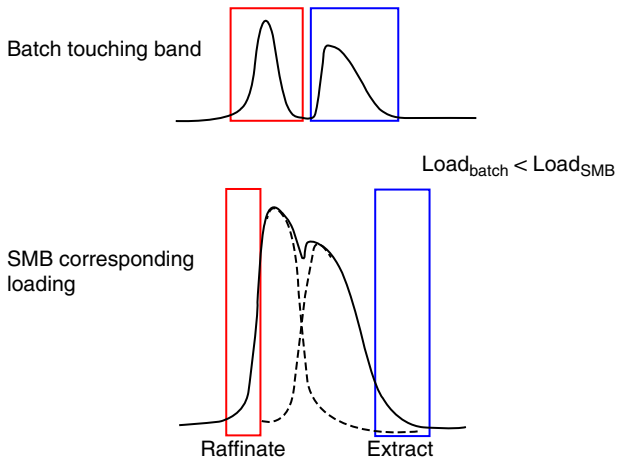


Figure 5 Comparison of the loading using an SMB or a batch process to achieve same yield and purity.

The gain in performance by going continuous comes at a cost: Only two 'fractions' or streams are collected from the unit and hence it is exclusively a binary separation unit. Similar to continuous distillation of complex mixtures, an intermediate fraction will contain a mixture of some of the constituents of the feed (similar to petroleum distillation and cuts such as a C_6–C_8 cut).[13] To achieve multi-component separations, several SMB in series need to be considered, and the increase in complexity and in equipment cost can be such that batch chromatography remains far more preferable. In the last few years, hybrid systems (semi-continuous) have been developed to try to accomplish multi-component separations.[39]

The development of a continuous separation requires a few more experiments compared to batch, as the process is more complex. As shown earlier, the separation does not need as much selectivity compared to batch, and hence more separation condition options may be available. However, because the loading achieved by SMB is usually higher than by batch, it is necessary to have an approximation of the equilibrium isotherm to calculate the productivity of the separation without having to actually run the separation on a small SMB unit. For chiral separations, the measurement of the isotherm is usually quite simple. A few overloaded injections (Figure 6) are performed and from these chromatograms data points can be collected to approximate the equilibrium isotherm.[1,6] The data can then be entered into a model and the SMB parameters (flow rates, switch time, feed concentration) and the productivity are calculated. When the isotherms are more complex, the optimization may require

additional data. The development of the triangle theory by Morbidelli's group at ETH in Zurich has made a significant impact on the understanding of the process.[8,34,35,37,38,46]

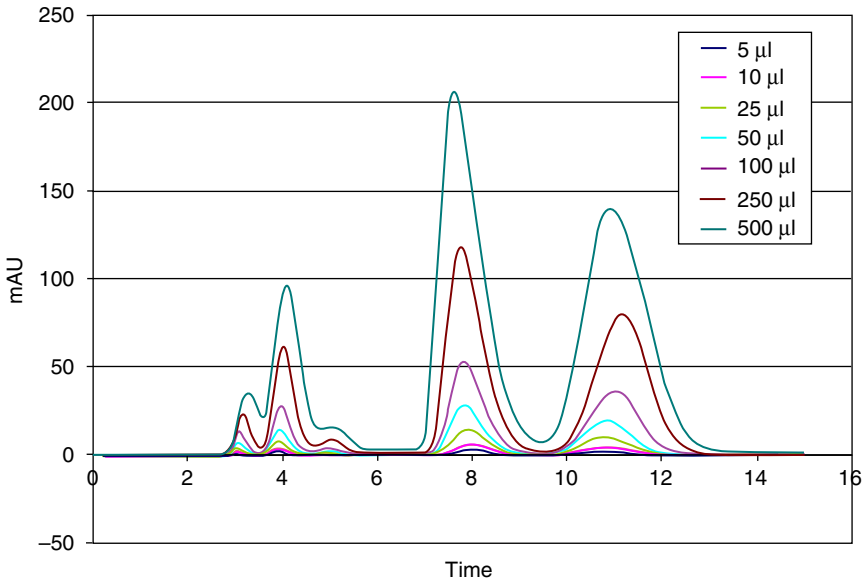


Figure 6 Example of a loading study for a chiral separation.

The screening of conditions is conducted in a similar fashion to the screening for a batch separation. However, because selectivity is not as critical, a separation that can be achieved with the maximum possible selectivity within 10 min is preferred (on a 4.6 × 250 mm analytical column at 1 ml min^{-1}). Larger selectivity can be detrimental to the separation, as a high zone I flow rate will be required to 'clean' the column before recycling.

9.08.3.2.6 Optimization and scale-up considerations

The optimization of a chromatographic process relies on several parameters[1,4,6,14] such as resolution, speed, and capacity. Ultimately the objective function to optimization is a compromise between three objectives: purity, production rate (throughput), and yield. The desired purity is the highest priority as large quantities of a product cannot be produced if specifications are not satisfied. In order of importance the yield comes next and finally the throughput (i.e., production rate). The combination of these three objectives leads directly to the cost of the manufacturing. This is ultimately the parameter to consider when selecting the synthetic route. Once the separation conditions are defined, several techniques are available to increase the throughput and the yield.[1,5,42] A solvent step gradient to speed up the end of the batch separation once the product is out of the column can be used, but it makes the solvent recycling more complicated and potentially more expensive. Whenever possible 'stacked' injections should be used to shorten the cycle time per injection and hence increase the throughput, but the presence of early or late eluting impurities may make this technique impossible to implement. Reprocessing intermediate fractions should be considered when the product is of very high value, but the gain in throughput by increasing the load versus the amount of product lost in the intermediate fractions should be evaluated. Evaluation of displacement and tag-along effects must be conducted to fully optimize the load on the column. The best method is usually case specific and a thorough understanding of the chromatography is essential to design the most efficient and economical route. Methods to develop these techniques can be found in the literature.[1,4,5,6,14,16]

As Guiochon et al. reported, the optimization of a separation is based on the optimization of the ratio $dp^2\ L^{-1}$.[1] For high-pressure batch chromatography, the column length is usually between 15 and 30 cm and the particle size is 10, 13, 15, or 20 µm depending on the number of plates required for the separation. For high-pressure continuous chromatography, the columns are shorter, 6–12 cm, with larger particles, 15, 20, and 30 µm, as fewer plates are required to achieve complete separation. To avoid high pressure using soft gel, the beads are usually of larger diameter (e.g., 300 µm) and thus the columns have to be longer to provide enough separation capacity. Once the parameters of the separation are defined the scale-up for both batch and continuous is performed by increasing the column diameter while maintaining the column length constant. The flow rate and the load on the column will be increased by a factor calculated from the ratio of the column cross-section. For example, for a separation optimized on a 4.6 mm ID column with a length of 25 cm using a 10 µm-particle size medium, a load of 5 mg per injection with a flow rate of 2 ml min^{-1} can be scaled up to a 300 mm diameter column using a ratio of $300^2/4.6^2 = 4253.3$. This results in a separation using a flow rate of 510.4 l h^{-1} and a load of 21.3 g $injection^{-1}$. Typically, as the scale increases, the performance improves as the extra column effects and the column internal thermal radial gradient become less important,[57] providing that the inlet and outlet column distributors are designed properly.

9.08.4 Equipment and Technique for Large-Scale Manufacturing

The objective of Prep is production and thus the equipment and the process are approached differently.

9.08.4.1 Column Technology

The core of the Prep process is the column. The column must be well packed to guarantee homogeneity of the bed, which in turn leads to high performance. There are several types of columns that can be used for preparative separations.

9.08.4.1.1 Low pressure

Low-pressure glass columns are used on a routine basis by organic chemists to purify the result of their synthesis. Typically, low-quality silica with a broad particle size distribution is used. The packing of the column is conducted by either pouring the dry silica inside the column or by using a thick slurry. Sand is added to the top of the column to act as a distributor and to 'absorb' the perturbation created by pouring the product and the solvent on the top of the column for each injection. After a few injections channeling can be observed and the performance of the column drops drastically.

This type of column is not very efficient as the bed is not homogeneous. Moreover, the elution relies on gravity to drive the solvent through the column and thus the cycle time for each injection is very long. A slight nitrogen pressure can be applied at the top of the column to help the elution, but this comes with the risk of breaking the column and losing the product. Finally, owing to the large particle size to minimize the pressure drop through the column, the number of theoretical plates is rather low and hence poor separation is achieved. It is often quite difficult to recover the product at a purity greater than 98% without sacrificing yield. The separation parameters are based on a few TLC experiments to approximate the load and the solvent ratio to use for the elution.[58] Because the outlet of the column is not connected to a detector the product is collected in several fractions, which need to be analyzed individually. Reproducibility of the process is questionable and scale-up is not straightforward. Hence, this process is usually not considered a viable option for large-scale manufacturing.

9.08.4.1.2 Prepacked columns

In the past decade, several suppliers have developed technology to use the packing material more efficiently and make the separation easier without increasing the cost of purification (and equipment) significantly. Prep packed columns were developed either in cartridges for Flash chromatography with a size as large as 150 mm in diameter and 60 cm-long beds or in high-pressure prepacked columns (5 cm ID × 250 mm long). The cartridges have the advantage of being more homogeneous than the glass column, and hence allow for better separation with longer lifetime and reproducibility. However, they are often limited to low pressure (100 PSI) and hence have limited throughput.

The high-pressure prepacked columns are made of stainless steel and contain smaller-particle size packing material (5, 10, 13, 15, 16, 20, 25 μm). These columns are typically a scale-up of an analytical column and can be used for high-pressure Prep. They work well but are limited to a certain maximum diameter (2 or 3 in.) as the difficulty of obtaining a stable chromatographic bed increases with the column diameter.

The length of these prepacked columns is predetermined and hence the separation has to be adapted to the column length. After a number of injections the column performance starts to degrade as the packing inside can collapse, generating gaps and eventually channels through the bed, destroying the column efficiency.

9.08.4.1.3 Axial compression advantages

To eliminate gaps and channels in a packed column, the DAC was developed as early as 1974 by Roussel Uclaf.[24] A piston located inside the column tube maintains a constant pressure, greater than the elution pressure, on the packing material. The other end of the column is closed with a bolted flange. If, during the life of the column, a gap is created in the bed, the piston compresses the bed and maintains the bed homogeneity. It is very common to see a column lose as much as 5 mm over a period of several months without significant reduction of the separation performance. Colin et al. presented the advantage of DAC versus a traditional packed column and demonstrated that the column retains efficiency for a significant amount of time.[23] The homogeneity of a column has been studied by Koh et al.,[59] who demonstrated that despite the dynamic compression, a radial and axial gradient of packing density exists, resulting in some variation of the performance of the column.

There are several designs to a DAC column but the most common design is the use of a hydraulic jack to maintain the piston under pressure. Regardless of the design, the sealing between the piston and the column wall is critical. A Teflon seal, reinforced or not with carbon, is used to maintain the packing and eluent in the column. The seal is also used to hold the frit in place and block particles to go behind the frit. Generally, a couple of chevron seals are added to strengthen the sealing system and eliminate leaks. When the column is unpacked and repacked frequently, the seal is replaced to guarantee a perfect seal each time.

The columns are packed using a slurry technique.[22,60] Viscous solvents, such as IPA, are preferred to maintain the slurry in suspension longer and favor a better homogeneity of the bed. A ratio of two volumes of solvent for one volume of packing material is typical. Some manufacturers recommend packing the column in stages, increasing the packing pressure slowly as the column is being eluted until the maximum packing pressure is reached. This is to leave time for the particles to migrate inside the column and hence obtain a better bed density. Other manufacturers recommend letting the slurry settle and then opening the

bottom of the column and letting the column drain until the top of the decanted solid becomes visible (vacuum can be applied to speed up the draining process). The piston is then lowered and the column is packed to the desired pressure. A simple way to pack the column in two steps is presented here. Once the slurry is in the column, the piston is moved slowly until the slurry solvent starts to come out of the top of the column so all the air located between the slurry and the piston is removed. That line is then closed and the line at the bottom of the column is opened. The column is then packed as fast as possible, letting the slurry solvent percolate through the bed down to the outlet of the column (Figure 7). If the column is with the piston at the bottom, the procedure is similar, except that the piston moves up, causing the whole bed to move up until the solvent comes through the top flange. It is preferable to use columns that have the flange at the bottom and the piston on top for the simple reason that the unpacking of the column is simplified. Once the flange is removed the piston pushes the bed into a receiver. Note that for small-diameter columns, the bed stays inside the column when the flange is removed. For larger-diameter (800 and 1000 mm) columns, the bed comes with the flange as the flange is separated from the column. The bed is then recovered by scooping the packing material into a container.

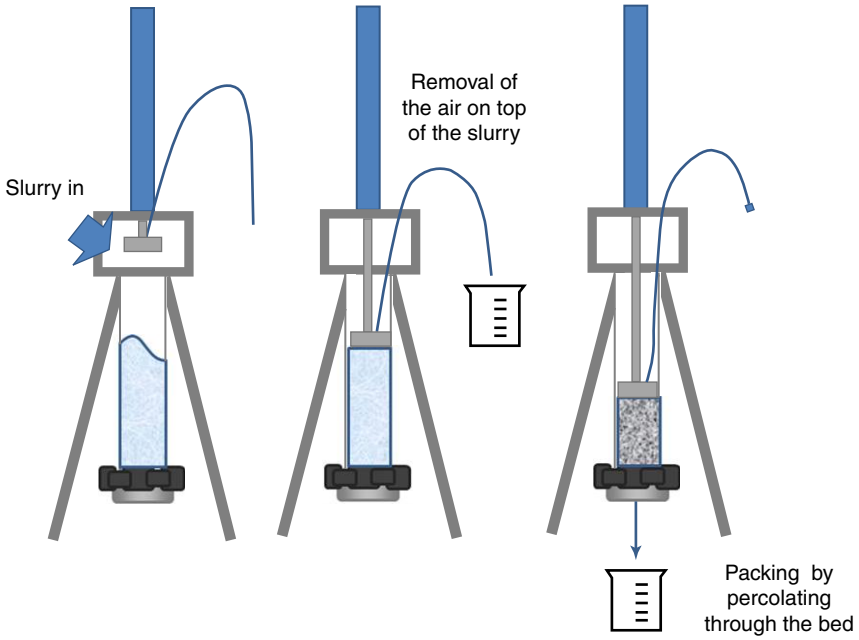


Figure 7 Example of a packing procedure for a DAC column showing a two-step process.

The DAC columns are typically very easy to use and can be scaled up with great success to columns as large as 1600 mm in diameter.[7,28] As the column becomes larger the design of the inlet and outlet of the column and the thermal performance need to be considered.

9.08.4.1.4 Column inlet/outlet design

The extremities of the columns are designed to allow the flow of liquid while retaining the packing material inside the column. They also contribute to the peak shape as they affect flow distribution. Two parameters are to be considered: the ratio of the column's internal diameter (ID) to the ID of the inlet tube and the ratio of the column length to the column's diameter. The first ratio provides an indication of the potential for heterogeneity of the profile distribution, which causes tailing, and the second provides an indication of the capacity of the column to absorb the heterogeneity from the inlet of the column. The first ratio should be as small as possible whereas the second one should be as large as possible. For analytical columns, the ratio of the column length to the column diameter (i.e., 250/4.6 = 54.3) is such that the influence of the inlet and outlet design is almost without consequence for the elution and the peak shape, as it is easily compensated by the intrinsic column band spreading. The analytical column inlet connection is usually a capillary tube with a narrow bore (0.13–3.05 mm ID). If the column ID is 4.6 mm then the resulting ratio is 18 to 36. For preparative columns this ratio can become critical as the ratio can change significantly. For example, an 11 cm ID column packed to 25 cm in length, i.e., a ratio of 2.3, is typically connected to a 1/4″ (6.35 mm) tube (3.05–4.6 mm ID), resulting in a ratio of 24 to 36. Hence, it is expected that the perturbation introduced by the inlet of the column is similar to both column sizes (4.6 and 110 mm), but the perturbation will be more visible on the larger diameter column as the relative column length is shorter. For SMB columns the bed length is typically significantly shorter (8–12 cm) and hence the influence of the inlet distribution is more significant. Column suppliers have studied this problem carefully, and with the development of powerful hydrodynamic modeling software such as ANSYS Fluent, the representation of the inlet and outlet of the column is possible.[62] In the past, sintered frits were used but were replaced in the mid-1990s by mesh frits. The mesh frits are

more difficult to cut but they provide a better flow distribution. The mesh is made of multiple layers of metal sheets of different porosity. The sheet providing the filtration is typically located close to the surface of the frit under a few layers of protective mesh. The frit is either welded to a support or held in place by a Teflon seal. The assembly is done by cooling the frit with dry ice or, better, liquid nitrogen, to shrink the metal and then letting it warm up to room temperature, and, once it is in place, ensuring a tight seal. The mesh design has the advantage of providing a better radial distribution of the sample entering the column, resulting in a more homogeneous distribution across the diameter of the column.[31] As the stream entering the column goes from a narrow tube to a wider tube, a semi parabolic distribution of the sample is achieved (Figure 8). This distribution is the cause of peak tailing. It is more desirable to achieve a flatter distribution.[31,61,62] The mesh design helps significantly compared to the sintered frit design, but for large columns a distributor plate is usually inserted under the frit, forcing the distribution more evenly across the entire diameter. As a result, a flatter elution band is achieved resulting in more efficient columns with much less tailing. Depending on the equipment supplier, the distribution plate can be a simple disk with holes distributed across the diameter or it can be a fractal design that ensures a perfect distribution of the sample at the inlet of the column.[63,64]

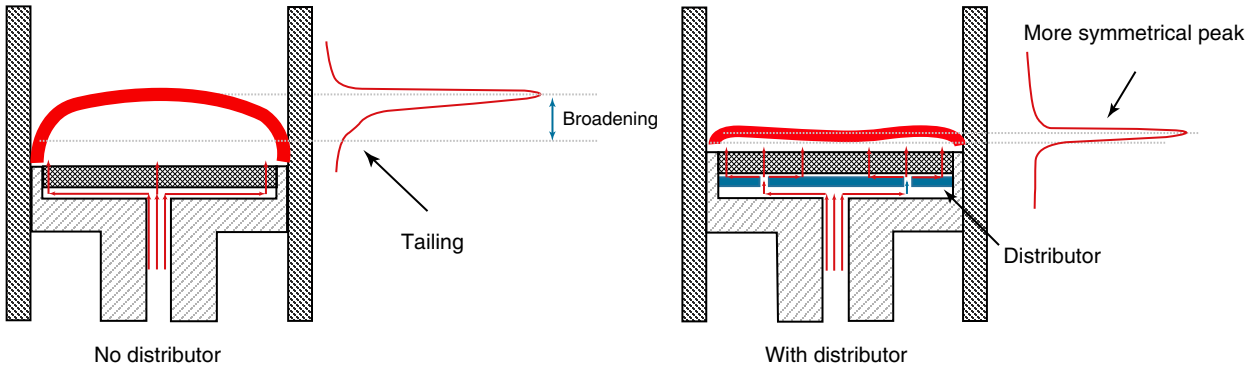


Figure 8 Column inlet – distribution of the sample at the entrance of the column with and without distribution plate. The resulting peak shape is indicated on the side of the figure. Left: no distributor, Right: with a distributor.

The outlet of the column is equally important to ensure a proper elution profile from the diameter of the column to the diameter of the outlet tube.

9.08.4.1.5 Effect of temperature

Pumping a liquid at high velocity through a porous medium generates heat owing to viscous heat dissipation.[57,65] Because porous silica beds are notoriously poor heat conductors, a gradient of temperature can be generated inside the column if the eluent and the column jackets are set at different temperatures. Because the retention of a molecule is strongly affected by temperature, a radial and axial gradient of temperature can result in a nonhomogeneous band distribution inside the column. Dapremont et al.[31,57] demonstrated that these effects are a function of the flow rate, the column size, the solvent, and the solute. For very small diameter columns (less than 1 cm) the flow entering the columns rapidly equilibrates to the column wall temperature and no significant effect of temperature gradient is observed. Thus, all analytical columns should be maintained in a temperature-controlled compartment to ensure the thermal stability of the separation. For very large columns (greater than 300 mm ID), the radial gradient is mostly located at the wall, and hence most of the column will be operating at the temperature of the eluent entering the column. For intermediate diameters (10–300 mm ID), the temperature of both the eluent and the columns should be controlled accurately. Dapremont pointed out that a small difference in temperature between the column wall and the eluent could be beneficial as this difference can compensate for an imperfect distribution of the sample at the inlet of the column. The optimum difference in temperature is, however, a function of the flow rate, the column dimension, and the solute retention.

9.08.4.2 Downstream Processing Technology

Once the separation is complete, it is necessary to recover the product from a large volume of solvent before the next step of chemistry or the final isolation of the API. Regardless of the type or mode of chromatography, the product recovered from the outlet stream is quite diluted in the mobile phase and thus several techniques can be used to recover the product.

9.08.4.2.1 Concentration

The recovery of the product should be conducted in a way that does not compromise the purity, i.e., the product does not react owing to the temperature or the pH of the solution. Additionally, it is important to recover the mobile phase and reuse it to minimize the raw material contribution to the cost of the process. It is essential to have a good estimation of the solubility of the product in the mobile phase as a function of temperature because this information will dictate the maximum concentration that

can be achieved during this step of the process. Depending on the scale of the separation process, several techniques can be used to recover the product.

9.08.4.2.1.1 Lab-scale rotary evaporators

For small-scale quantities, up to a few kilograms, rotary evaporators are used. These are common pieces of equipment in chemistry labs and they are very easy and quick to set up. The rotovap capacity ranges from 100 ml flasks to 50 l flasks with various levels of automation. Small-scale rotovaps require constant attention as their operation is mostly manual. Larger units come with sophisticated controls that automatically refill the flask and evacuate the distillate without breaking vacuum. Complete drying of the product, which can be recovered as a solid, is possible in rotary evaporators. However, the product remains inside the rotary evaporator flask the entire time, which can potentially result in thermal degradation. Finally, product carry over can occur resulting in a loss of product, but also in the inability to recycle the solvent.

9.08.4.2.1.2 Large-scale evaporation devices

For larger quantities and longer campaigns, it is necessary to use a continuous evaporation device to facilitate the product concentration and the solvent recycling. Technologies such as wipe film or falling film evaporators work well for most of the small molecules as they minimize the thermal exposure of the product to heat. It is critical to know the maximum solubility because there is a high risk of plugging the lines. It is time consuming to clear the lines to resume activity, and this activity can potentially result in significant product losses. These devices usually come with automation and hence require more knowledgeable manpower to operate, especially during start-up and shutdown to avoid carry over. For a continuous chromatography process, the two outlets of the separators can be directly connected to the evaporators or the dilute product can be temporarily stored in tanks, which then feed the evaporation devices. Because the distillate from each side is to be recycled as eluent, it is possible to have a common condenser to minimize the footprint of the equipment and optimize the energy consumption. The size of the unit is dependent on the solvents, and hence it is better to consult with the manufacturers to calculate the required surface area for the unit. However, because the vacuum and temperature can be adjusted, the unit should be able to accommodate most of the organic solvents typically used for chromatography. If the size is too small, it will affect the final concentration that can be achieved, as the evaporation cycle time should remain faster than the time required to purify the product to avoid accumulation.

9.08.4.2.2 Product isolation

Once the product is concentrated, it needs to be recovered as a solid or an oil. Concentrated product is typically stored in temporary tanks before being sent to the final isolation step. At this stage there are two options. The first option is to take the concentrate and send it to the downstream chemistry (assuming there are more steps). The second option is to isolate the product as a dry solid or oil. The first option eliminates an isolation step, which can result in product losses, but also removes an opportunity to recycle the leftover solvent in the concentrated material. The second option allows for the highest solvent recovery. Hamende[66] reports recovery in excess of 99.7% for the mobile phase, and Mihlbachler et al.[47] reports solvent recycling in excess of 99.9% for SMB separations using a combination of falling film evaporators and conical driers. This option also provides a more precise evaluation of the process yield as the product is recovered as an isolated solid or oil. Both options are viable but need to be evaluated carefully as they both can have a significant impact on the overall cost of the process.

9.08.4.3 Brief Review of Continuous Chromatography Process

Since its conception, several variations of the process have been developed to respond to certain applications.[38,39] The author presents below the main version of the process that is used for small-molecule purifications. He also introduces a modification of the process that can provide some benefits under certain conditions.

9.08.4.3.1 SMB versus varicol

SMB is the basic way of doing continuous chromatography. To simulate the movement of the solid phase, all the inlet and outlets are 'moved,' i.e., activated at the same time, in a synchronous shift. This approximates the velocity of the solid by dividing the length of the column by the period. The number of columns can vary from a classical configuration of two columns per zone (<2>, <2>, <2>, <2>) or a specific set-up to allow more separation plates in a desired section (<2>, <3>, <2>, <1>). Regardless of the configuration, the number of columns remains an integer value, and hence the optimum column length will be an average of the optimum column length for each zone. The VARICOL (TM) process developed by Novasep in 2000 is a variation of the standard SMB in which the valves are activated with a nonsynchronous sequence.[7] This allows for a more precise distribution of the column plates by artificially adjusting the length of each zone to a noninteger value regardless of the column's physical length. As a result, the average column length per zone of the separator is optimized and an increase in throughput is expected. This set-up allows for a reduction in the number of columns without loss of performance, and a Varicol unit can function with five columns and provide the same productivity as a six-column SMB unit.[43] It is common to see longer column lengths for a Varicol unit compared to an SMB unit. It is recommended to carefully evaluate both techniques as the definition of productivity does not take into consideration the column configuration and existing IP can increase the cost. It is strongly recommended to perform a full costing analysis of the process to calculate the final cost in dollars per kilograms as this should be the final decision criterion.

9.08.4.3.2 Turbo® SMB

This variation of the standard SMB is to address the specific cases where the separation selectivity is very large or the most retained compound follows an antiLangmuir isotherm (the retention time increases with the increased injected quantity).[67] In both cases, owing to the high retention of the most retained species, the flow rate in zone I of the SMB must be very high to completely elute the product out of the column. Because the maximum operating pressure is usually fixed and is the direct result of the flow rates in each zone of the SMB, a high flow rate in zone I means that the flow rates in the remaining sections of the SMB will be strongly limited. For example, assuming an SMB unit with 8 columns of 50 mm in diameter and 10 cm in length, using acetonitrile as mobile phase, the average flow rate in this unit with a 2 column per zone configuration is 258 ml min^{-1}. The separation is optimized and the flow rates reported in Table 2 are determined to achieve the highest allowable throughput of 1.15 kg Feed per day. The throughput is limited because the flow rates in the separation zones (II and III) are forced to be low by the high zone I flow rate. The Turbo SMB process decouples zone I from the rest of the SMB by introducing a zone 0 made of a single column (Figure 9). Because it is a single column, the maximum flow rate is set by the pressure drop of the single column. A calculated flow rate of 1032 ml min^{-1} will result in the maximum pressure drop for the column and ensure a complete rinse before recycling the column at the end of zone IV. The remaining flow rates of the SMB are calculated assuming a 'normal' Langmuir behavior with flow rates maximized for the pressure drop. In the example in Table 2, this leads to an increase in the overall throughput by ~41%. The design of a Turbo SMB requires the addition of two three-way valves per column. These valves are used to isolate the column in zone 0 from the rest of the unit. An additional pump is required to flush zone 0 independently of the regular eluent pump. The outlet of zone 0 and the extract flow can be combined or kept separated. This process requires a very large amount of solvents per unit of time, but solvent recycling is possible and hence the additional processing cost is mainly a result of the increase in energy consumption for the evaporation/condensation of the solvent. This additional cost should be easily outweighed by the increased daily throughput.

Table 2 Example of the Turbo SMB benefit. Feed concentration is 40 g/l

Process	*Zone 0 (ml min^{-1})*	*Zone I (ml min^{-1})*	*Zone II (ml min^{-1})*	*Feed rate (ml min^{-1})*	*Zone III (ml min^{-1})*	*Zone IV (ml min^{-1})*	*Production rate (kg Feed per day)*
SMB	NA	600	170	20	190	72	1.15
Turbo-SMB	1032	423	183	28.2	267.9	101.5	1.62

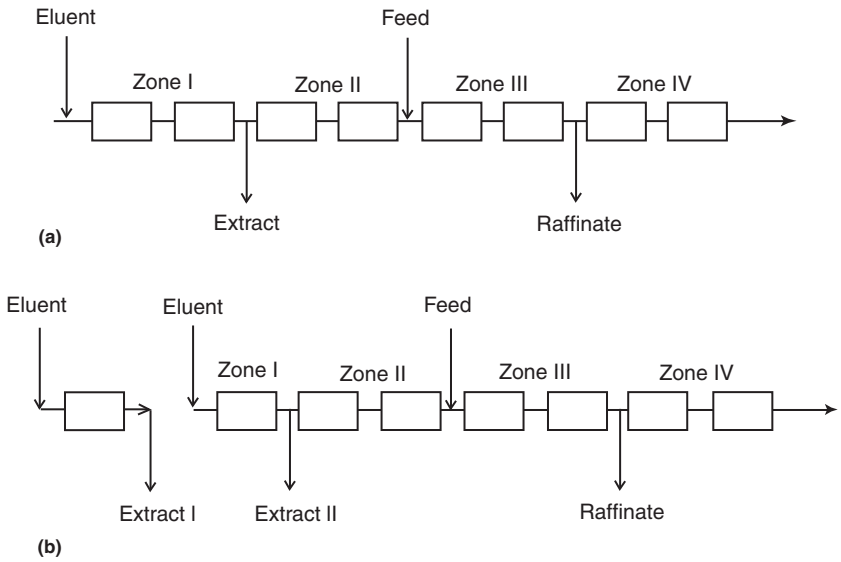


Figure 9 Standard SMB vs. Turbo® SMB.

9.08.4.3.3 Other variations

Many other variations of the SMB process have been developed in the past few years.[38,39,43] The objective of these variations is to increase the flexibility of the unit to allow for an increase in throughput for specific applications. The increased complexity of these systems results in an increase in the degree of freedom of the process. This permits a better optimization and potentially higher

throughput and lower cost. The variation of the flow rates throughout the cycle, and the increased number of zones, and even semicontinuous operations are some of the modifications to the standard SMB process that can be done to allow for ternary separations, higher throughput, and better recovery.[4,38,39,43] The equipment required for these variations of the process is more complex and hence the required capital investment is greater. In addition, these units are designed specifically for an application and are thus difficult to adapt to a different product once the original product is off the market.

9.08.5 Implementation for Commercial-Scale Manufacturing

In the past 15 years, several large-scale units have been installed either at pharmaceutical companies for internal use or at CMO for supporting various customers.[17] These processes are used for the manufacturing of APIs (either the final API or early intermediates) and hence are operated under cGMP.

9.08.5.1 Quality/Regulatory Requirements

Once the process has been demonstrated at small scale and the compound is moving closer to commercialization, the quality department gets more involved to ensure that the product is manufactured according to cGMP standard to provide consistent quality.

9.08.5.1.1 Basic requirements

As soon as the product enters clinical trials, the quality department requires an increased level of controls (cGMP). As a minimum all raw materials, the feed, the stationary phase, and the solvent, are tested against preestablished specifications with at a minimum a test for appearance and identity.

The equipment is cleaned and verified clean following appropriate procedures. For small-scale equipment, used for many different products and early in the lifecycle of a product, data on dosage and toxicity are not always available. Thus, the calculation of the Maximum Allowable Carry Over (MACO) is not always possible and a default value of 5 or 10 ppm is often used. The MACO calculation is a formula that allows the evaluation of the maximum amount of the previous product that can be allowed to be found in the current product based on both toxicity (LD50) and dosage.

At this stage cleaning solvents are identified based on a solubility study on the compound. Depending on the toxicity (known or expected) of the product, swab testing of the equipment surface may be required, and hence this work should be initiated early on.

The equipment used for the process should have a tracking history retained by the quality department, and all qualification documents (e.g., installation qualification, process diagrams, operation qualification) should be available and up to date.

Validation of the process or the analytical methods may not be required yet, but this will eventually be necessary when the product enters the later clinical phase and goes commercial.

9.08.5.1.2 Definition of a batch

Regulatory agencies define a batch as follows (ICHQ7A): "A specific quantity of material produced in a process or a series of processes so that it is expected to be homogeneous within specified limits. In the case of a continuous production, a batch may correspond to a defined fraction of the production. The batch size can be defined either by a fixed quantity or by the amount produced in a fixed time interval."

Based on this definition, the batch size of a small-scale production may be simply dictated by the amount of feed material available. In the case of batch chromatography, because there are multiple discrete injections, a batch could be the combination of several injections that can fit inside a vessel or the number of injections performed in one day. In the case of continuous chromatography, the batch size can be defined by the amount of product produced in a given period of time (e.g., 1 day or 1 week) or by the amount of product that can be isolated in one homogeneous 'batch' in the downstream process. In general, the continuous process is in between two batch processes. The feed is prepared in a batch-wise fashion and the product is recovered in a dryer as a single batch. Thus, the definition of the batch can be based on several choices. One important parameter is the monetary value of the batch. If the batch fails or if any of its quality attribute is compromised and needs to be either wasted or reprocessed (or reworked), the financial burden can be too high for a very large batch. Using small batches to minimize economic impact causes additional work as each batch requires testing, batch record review, etc. A risk-based analysis should be performed to properly define the batch size that works best for the process. As a final note, it is important to also consider the upstream and downstream chemistry to define the batch size as batch traceability is important. The tracking of a batch pedigree is simplified when partials and fractions of lots are avoided.

9.08.5.1.3 Quality by design (QbD)

The production of three consecutive batches without changing anything about the process for validation used to be the norm. This approach to validation is evolving. Emphasis is now placed on the process operating space. This approach is designed to develop a deeper understanding of all the variables and their interactions. Critical parameters that have an impact on the final product purity

are then derived from the parameter study. Other parameters will be considered process control parameters. A significant amount of R&D work is required to identify all parameters (Design of Experiments, DoE). This QbD approach is becoming more important and chromatography is very well suited to address all these issues. Eventually this approach should provide a more robust process with tools to anticipate problems and hence be proactive to maintain the product quality.

9.08.5.1.3.1 Process development

During the development of the separation process a large amount of data is generated. The goal of the work, summarized in the process development report, is to provide the basis for the critical process parameters definition.

For Prep processes the number of parameters is fairly limited. Because the SMB is a closed-loop system, most of the parameters are interconnected. An analysis of the degree of freedom of the process shows that five parameters are sufficient to define the SMB operation once the stationary phase, the eluent composition, and the column dimensions are selected.[31,36] The five parameters are typically the switch time and four flow rates: feed, eluent, zone I (i.e., recycle), and extract or raffinate. A modification of one or several of these parameters can affect the performance of the separation. In the process design space, several combinations of these parameters will result in the desired product purity (quality parameter) with variation of the recovery or the throughput (financial parameters). These parameters are optimized to provide the highest throughput based on the maximum operating pressure.

Uncontrolled variations of the feed concentration, the eluent composition, and the operating temperature can change the designed space and hence result in low product. These three parameters can be compensated by adjusting the other SMB parameters. For this reason, the feed (through the feed load), the eluent composition, and the separation temperature are often considered critical parameters. All other parameters of the process are considered controlled parameters.

During the process development, it is necessary to evaluate operating ranges for the various parameters (critical and controlled). Effect of mobile-phase composition, temperature, and concentration can be easily evaluated using an analytical column extrapolated to SMB. The modeling of the continuous process permits the evaluation of the flow rate ranges that provide the necessary separation robustness. Conducting a few experiments on a small-scale unit helps confirm the accuracy and the predictions of the model. As discussed earlier, the triangle theory developed by Morbidelli's group allows for a greater understanding of the expected response of an SMB unit to parameter changes.[8,34,35,37,46,68]

9.08.5.1.3.2 Production monitoring (PAT)

Regardless of the type of chromatography, the process can be easily monitored. For batch processes only a few variables have to be closely monitored compared to continuous processes. Both processes rely heavily on automation and thus events and parameters recording (such as temperature, pressure, and flow rates) allow for constant monitoring of the process. Considering batch chromatography, the collection of the product is typically based on either a time window or a threshold (or both). With the development of more powerful computers, the automation system can anticipate some variations of the column output and still collect the product within the desired purity and yield. The product collection on a continuous process relies exclusively on the consistency of the retention time and therefore it is essential that all parameters remain reasonably constant over time. The monitoring of the performance of the unit is typically conducted off-line by collecting and testing a sample of the collected fractions (batch chromatography) or the outlet streams (SMB). In the past 20 years the direct monitoring of the purity (more specifically the chiral purity) has been investigated. By coupling two detectors (UV+polarimeter for chiral separations) and using mathematical deconvolution of the two signals, the purity of the stream can be measured in real time and adjustment of the separation parameters or the collection can be done.[43,69] It is conceivable that, once the equipment is calibrated, a controller can take over the piloting of the process automatically. Such a controller has been developed at ETH, Zurich.[43,69] and shows great promise. However, certainly because of quality concerns (validation of the process, calibration, etc.) commercial scale units are not yet equipped and off-line monitoring remains the preferred way of monitoring a separation.

9.08.5.1.3.3 Transient mode versus steady state

For continuous processes it is necessary to differentiate between the transient mode occurring when the system starts or shuts down and the steady state when the concentration profile in the system is established. During the transient mode, the purity and the recovery may be outside their expected respective ranges. It is recommended at small scale to redirect the product collection to a temporary container during these periods until steady state is achieved. If the separation requires tuning to increase the purity, the yield, and the throughput (**Figure 10**) the material generated can be off specification. At larger scale, it is expected that the impact on the batch final purity of the material produced during transient mode has been evaluated and that appropriate procedures are in place to ensure that the batch quality is not compromised.

During the steady state, the purity of both extract and raffinate should be constant over time. By sampling at regular time intervals it is possible to confirm the steady state, i.e., the purity and the area under each peak should remain constant (with some acceptable variability).

The collection of an internal concentration profile provides useful information, especially during the tuning of the separation. The collection of a sample in between two columns gives a picture of separation once a full cycle is completed (a cycle is the number of switches required for one column to complete a full rotation, i.e., for an eight column SMB, a cycle is eight switches). Typically one or two samples per switch (at different times) are collected. The more samples are taken the smoother and more accurate the profile. The profile in **Figure 11** illustrates a steady-state separation, with a maximized throughput and high product purity on both extract and raffinate streams.

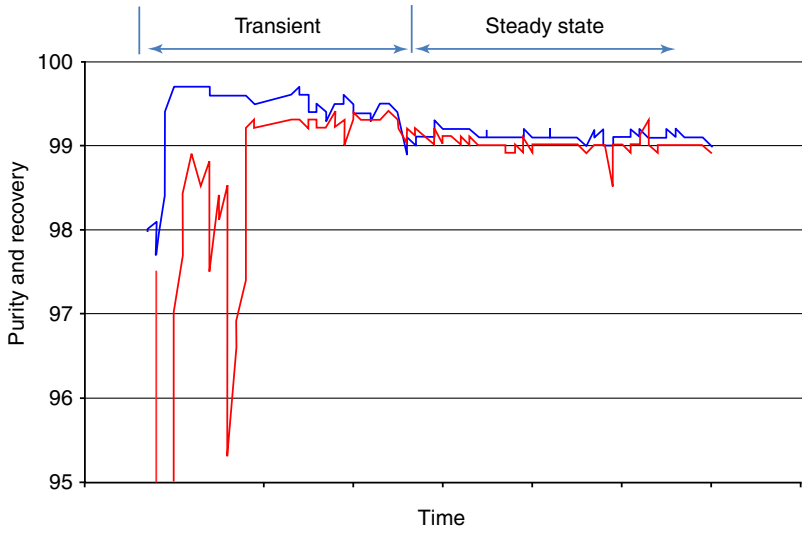


Figure 10 Example of a separation start-up; the separation is tuned to achieve the product target purity rapidly (blue line), then the yield is increased to approximately 99% (red line), and finally the feed rate (throughput) is maximized and then the steady state is established.

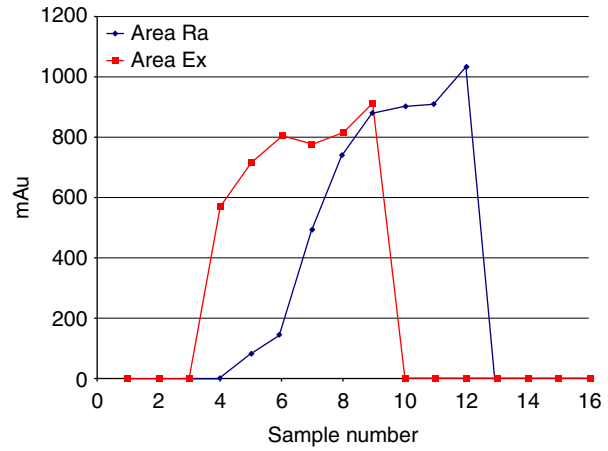


Figure 11 Example of a 16-point profile for a 8 × 50 SMB unit at steady state.

9.08.5.1.3.4 Unexpected parameter variations

Unless the stationary phase evolves over time, the process output should be of constant quality if all parameters are maintained constant. Particularly for SMB, a change in one parameter can significantly affect the quality of the product. Two types of changes can be considered: the gradual change and the quick change. The first one may not be immediately visible and diagnosed, and thus some out of specification material can be produced before the problem is detected and identified. However, if it is observed early enough the process engineer can make process modifications (within the confines of the regulatory filling) to ensure that the final purity remains within the target specification. Fast and abrupt changes that are temporary or permanent are more of a concern as they can quickly destroy the separation, for example, if the target purity is 98% and the production rate is 100 kg day^{-1} for an SMB separation and the batch size is 500 kg (i.e., 5 days). The SMB at steady state produces material at 99% (1% above specification). How long does it take to produce a batch out of specification if the product purity drops temporarily to 85%? Can the batch be recovered by operating the separation at the highest possible purity for the rest of the batch? The graph in Figure 12 shows the impact on the total purity when the material produced is out of specification for various lengths of time (1 h to 1 day). In most cases, if the separation purity recovers to the normal 99% then depending on the perturbation duration (less than 12 h in this example) the purity can be recovered within a few hours or days. If the perturbation is too long, the unit must be operated at a higher purity (which means a lower throughput) for the rest of the batch to recover the final batch purity. In this specific example, after 1 day at low purity, the batch will never recover even if the purity of the product is increased to 100% (black solid line). This example shows the importance of monitoring the separation parameters to ensure that the final batch meets the target specifications.

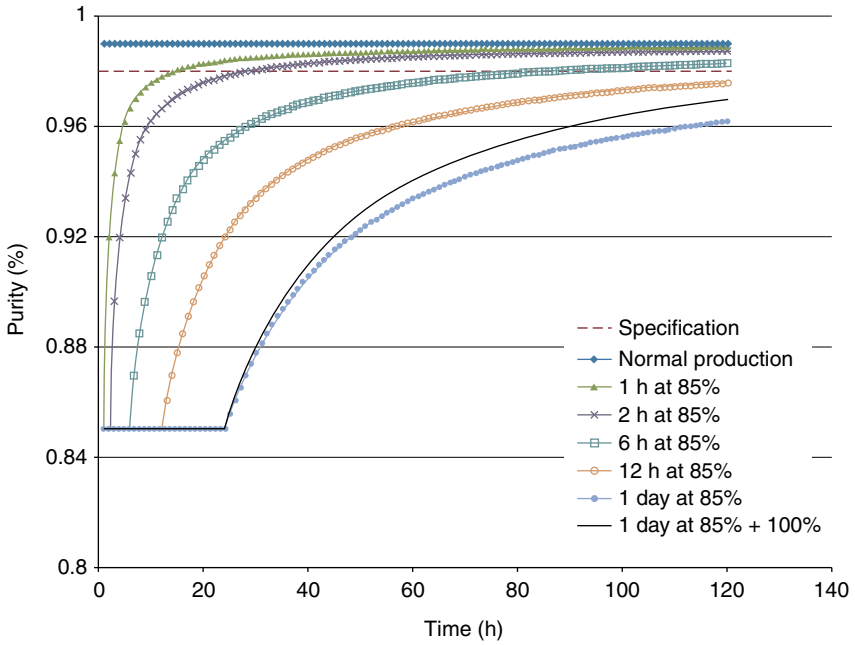


Figure 12 Example of the effect of a low-purity production for a period of time and the impact on the final batch purity. The dotted line is the specification. The other lines represent the cumulative purity of the batch as a function of time when part of the batch is producing low-purity product for a given period of time (here set at the beginning of the batch).

9.08.5.2 Manufacturing Point of View

The implementation of a large-scale continuous chromatographic process in a traditional batch manufacturing setting requires few adjustments. Continuous processes are efficient because they do not stop, and hence all the necessary activities should be planned carefully to minimize downtime.

9.08.5.2.1 Manpower

Continuous processes are labor intensive during the set-up and start-up as many activities are taking place. Packing the column is greatly facilitated by the use of DAC technology, which allows for reproducible and efficient columns. Each column is then tested with a preestablished protocol to ensure consistency from column to column. During the start-up phase, additional sampling is also conducted until the steady state is achieved. During the transient mode, the evaporators must be carefully monitored to avoid carry over or accumulation. Even if the equipment is highly automated, these activities still require a well-trained work force. In case of an unscheduled shutdown, the team operating the SMB should be able to restart the unit rapidly to minimize downtime. During normal production, few activities are done on a routine basis; the feed for the SMB is usually prepared in batch reactors in quantities corresponding to several hours of operation, and the purified material is charged to a dryer and recovered when necessary. On a regular basis samples of the SMB outlet but also of the eluent and the feed material are collected and submitted to the quality control department. During start-up, two operators per shift are recommended with additional engineering supervision. Once the separation is at steady state a full-time operator is required to monitor the process and collect samples. An additional operator is available to help during feed preparation and product recovery. Operator training is very important, and it can take several months for an operator to be fully operational. Regardless of the size of the equipment, the same number of operators and engineers is required. As a consequence, the cost contribution from manpower is greatly reduced as scale increases, resulting in significant savings.

9.08.5.2.2 Maintenance

The maintenance of a continuous process is very important as the process is designed to run continuously. Any shutdown is associated with a loss of production and a loss of revenue. Scheduling maintenance should be done very carefully to avoid additional delays. Any unscheduled shutdown should be used if possible to conduct maintenance and hence minimize the impact of the unscheduled downtime. A SMB unit has a variety of pieces of equipment that are susceptible to breakdown: pumps, valves, and temperature control unit. These parts should be on a preventive maintenance schedule and multiple spare parts should be kept ready at all times. This represents a significant inventory cost that needs to be factored in when evaluating the cost of manufacturing.

Column maintenance is a specialized activity, as this is not performed by the maintenance group. Column performance is monitored using an indirect method during production. The purity and the yield over time can slowly degrade owing to partial plugging of the frits. This is the result of fines generated by the slow breakdown of the weakest stationary-phase particles, which

migrate down the column and accumulate in the frit. By measuring the column's back-pressure, the plugging of the frit can be evaluated. The decision to unpack the column is the result of the balance between the gradual loss of yield and throughput and the time required to repack a column. Again to minimize the downtime, a set of frits and a full column's worth of packing should be available to repack as soon as possible. The cleaning of the used frit and the regeneration of the packing material are done off-line.

9.08.5.2.3 Recycling strategies

9.08.5.2.3.1 Solvent recycling

As mentioned earlier, chromatographic processes can be solvent intensive as the process is very dilute, and therefore recycling the solvent is important. However, this activity must be conducted with caution as impurity accumulation (trace water, other solvents, volatile impurities) can occur, which will affect the separation in the long run by slightly changing the mobile-phase composition over time. If the solvent recycling is possible, significant saving can be made on the process.[50,66,70] It should be noted that solvent recycling is dedicated for a single product and not for other processes to avoid any potential cross-contamination.

9.08.5.2.3.2 Unwanted enantiomer

The unwanted fraction that is generated during the separation will be wasted unless reused. This can represent 50% of the starting material and is hence a significant cost contributor. If the molecule can be easily racemized, the theoretical process yield increases from 50 to 100%. The feed product coming from the racemization should be evaluated and compared to fresh feed. It is very important to keep track of the impurities that may be eluting with the unwanted enantiomer as they can potentially be recycled during the racemization step and reach a level that can become problematic. In this case a purge should be implemented after several racemization steps.

9.08.5.2.3.3 Packing material care and usage

The stationary phase (more specifically chiral phases) can be an expensive component of the process. If the packing is poisoned by impurities or needs to be replaced frequently then the separation cost can be high. However, if the quality of the feed to be separated is well controlled and the unit is maintained properly, the packing material can be used for a long time. At AMPAC the same CSP has been used for the same separation since 1999. The columns have all been repacked several times but the packing has been recovered and regenerated. The packing regeneration process is a simple decantation to remove the fines that may have been accumulating over time. The packing is then dried and reused when required. Note that the packing is tested by the quality control department to ensure that the performance remains equivalent or better than fresh packing. Under these conditions the contribution of the packing for the product price is very low (a few dollars per kilogram of product). Finally, for large-scale manufacturing, the stationary phase is dedicated for a single product to again avoid potential cross-contamination.

9.08.5.3 Price Considerations

The chromatographic separation process is often considered expensive compared to other techniques because it is not well understood. If it is true that at small scale the use of chromatography may be an expensive solution, at larger scale the cost can drop drastically as the process is optimized, recycling solutions are implemented, and investment costs are amortized over larger volumes. The economic advantage of chiral separation over other techniques has been reported by Hamende,[66] who showed that the chiral SMB manufacturing cost was a quarter of the salt crystallization and approximately half the cost of the chiral synthesis. The calculation of the price for a separation step is not much different from the costing of other unit operations. Typically, the price for small- to pilot-scale separations will be based on the campaign time. For these campaigns the solvent contribution and the start-up and clean-up of the equipment can represent a significant portion of the final cost. Because of efficient solvent recycling strategies, the cost of solvent can remain low but regardless of the size of the campaign a minimum quantity of solvent is required to clean the equipment, set up the columns, and run the separation (Table 3). For large-scale commercial manufacturing the price is based on weight and may include other chemistry steps. The price is calculated based on a demonstrated throughput and an estimated on-stream factor. The on-stream factor is usually expected to be greater than 90%, i.e., 90 days of production for every 100 calendar days. On-stream factor greater than 95% is typically achieved in SMB production.

Table 3 Quantity of solvent to start and to clean an SMB unit as a function of the column size

SMB unit	*8 × 10*	*8 × 50*	*8 × 200*	*6 × 800*	*5 × 1000*
Solvent required to start (L)	20	200–300	2000–2500	25 000–30 000	40 000–60 000
Solvent required for cleaning (L)	5	300	4000	40 000–50 000	50 000–80 000

9.08.5.3.1 Productivity and production rate

Productivity is a metric used to compare two separation processes. It is conventionally reported as the amount of feed material produced per unit of time and per unit of weight of stationary phase, i.e., kilogram Feed per day per kilogram SP. This unit puts

emphasis on the stationary phase, as it is usually the most expensive item for chiral separations. This number can be misleading as it implies a certain column configuration. To compare two processes using this metric, both processes should have the same column number and configuration. When comparing two processes such as batch against SMB, the actual throughput, example: kg of F d^{-1}, should be considered as this measures the actual production rate that can be achieved on a given instrument. Further analysis on the cost of manufacturing should also be included as discussed below.

9.08.5.3.2 Equipment cost and amortization

Regardless of the size considered, the chromatographic equipment comes with a large quantity of vessels, and thus a relatively large footprint is required for the ancillary equipment. Fortunately, as the scale increases, the size of the ancillary equipment does not increase as fast as the throughput, and hence the portion of the cost associated with the equipment decreases as scale increases. Regardless of the size of the equipment, the equipment and installation costs are high because of the complexity of the process and the high level of automation. The cost of preparing the feed and recovering the product post separation are similar to the cost of running a batch reactor. The amortization can be done over different periods of time for different parts of the equipment.

9.08.5.3.3 Cost of recycling

There is a cost associated with the solvent recycling and the unwanted enantiomer racemization. The solvent recycling cost is associated with power consumption as solvent is distilled and condensed. This is a relatively low contributor as the cost of fresh solvent is usually several orders of magnitude higher than the cost of the energy used for the recycling.

The recycling of the unwanted enantiomer should obviously be considered if the starting racemic material is expensive, as this will eventually lower the final product price.

9.08.5.3.4 Manpower

The cost associated with manpower is relatively low compared to other unit operations because of the high throughput achieved and the high level of automation of the process. For costing purposes, 1.3 to 1.5 operators per shift is often used as a rule of thumb. This number increases to 2 to 2.5 for start-up and shut-down.

9.08.5.4 Environmental

With the exception of SFC, liquid chromatography is often regarded as a solvent-intensive process and hence is a long way from being accepted as a green technology. To evaluate the environmental impact of the process, many metrics can be used.[50,70] The environmental factor (E Factor) is the ratio of the waste generated (not including water) to the amount of product produced and it gives an idea of atom efficiency. For example, a chiral separation for which the unwanted enantiomer is not recycled will have a factor of at least 1. Another useful metric for the evaluation of the environmental impact of a chromatographic process is the SI factor, which is a measurement of the amount of solvent used per kilogram of product (Solvent Intensity). The dilution is often very high for batch chromatography (0.0001 g l^{-1}–0.01 g l^{-1}) and better for SMB (0.001 g l^{-1}–0.5 g l^{-1}), resulting in a very high SI factor, but as recycling strategies are implemented this number drops significantly. Regardless of the quantity to purify, a minimum of solvent is used to start the separation and this solvent will be discarded at the end of the campaign. An approximated quantity of solvent used per campaign as a function of the size of the equipment is provided in **Table 3**. Mihlbachler et al. report an SI factor of 321.5 for a large SMB production if the solvent is not recycled and 0.2 with recycling (99.93% recycled).[50] The corresponding E factor is 1.8 assuming the replacement of the solvent and the CSP every year. This process is compared to the tartaric resolution with an E factor of 28.3 and an SI factor of 30.2. Similar numbers can be calculated from the example provided by Hamende.[66] Grinter [70] compares the chromatographic resolution process to two synthetic routes and a dynamic kinetic resolution (DKR). The SMB route is reported with the lowest E factor (23). Based on the results of the analysis of the four routes, environmental, energy, safety, and efficiently criteria, the author concluded that the SMB route was clearly the most desirable.

9.08.6 Conclusion

Prep is a mature technology that is being slowly integrated into the manufacturing of intermediates and APIs. Recent advances in packing material technology and equipment have made this technology very efficient and cost effective at commercial scale. The process development requires know-how and specialized equipment, but once a method is developed at small scale the implementation at larger scale is straightforward as the scale-up is linear. Many options are available for the process optimization using either batch or continuous techniques that should be considered on a case-by-case basis. Chromatography is a process that can be relatively easy to model and hence it is very amenable to Quality by Design and Process Analytical Technologies. By implementing simple recycling strategies, chromatography is a truly green, environmentally friendly process. Finally, chromatography proves itself superior to many other purification processes in term of purity, yield, and throughput, resulting in lower manufacturing cost.

References

1. Guiochon, G.; Shirazi, S. G.; Katti, A. M. *Fundamental of Preparative and Nonlinear Chromatography*; Academic Press: New York, **1994**.
2. Colin, H.; Hilaireau, P.; Martin, M. *J. Chromatogr.* **1991**, *557*, 137–153.
3. Grill, C. M. *J. Chromatogr A* **1998**, *796*, 101–113.
4. Schmidt-Traub, H. *Preparative Chromatography*; Wiley-VCH: Weinheim, **2005**.
5. Nicoud, R. M.; Bailly, M. Choice and Optimization of Operating Mode. In *PREP 92: 6-7-8 April 1992, Nancy-France: Proceeding of the 9th International Symposium on Preparative and Industrial Chromatography*. Société Francaise de Chimie: Paris, **1992**.
6. Cox, G. *Preparative Enantioselective Chromatography*; Blackwell Publishing: Oxford, UK, **2005**.
7. Colin, H.; Ludemannn-Hombourger, O.; Nicoud, R. M. *CAST* **2003**, *28*, 8–12.
8. Storti, G.; Mazzotti, M.; Morbidelli, M.; Carra, S. *AIChE J.* **1993**, *39*, 471–492.
9. Dapremont, O. *Pharm. Technol.* **2010**, s22–s27, Supplement.
10. Fraud, N.; Gottschalk, U. *CEP* **2010**, 27–31.
11. Francotte, E. R.; Richert, P. *J. Chromatogr. A* **1997**, *767*, 101–107.
12. Nicoud, R. M. *LCGC* **1992**, *5*, 43–47.
13. Navarro, A.; Caruel, H.; Rigal, L.; Phemius, P. *J. Chromatogr. A* **1997**, *770*, 39–50.
14. Snyder, L. R.; Kirkland, J. J. *Introduction to Modern Liquid Chromatography*; Wiley Interscience: New York, **1974**.
15. Janson, J.-C. *Protein Purification: Principles, High Resolution Methods, and Applications*, 3rd ed.; J. Wiley & Sons: Hoboken, **2011**, Vol. 54.
16. Cazes, J.; Scott, R. P. W. *Chromatography Theory*; Marcel Dekker, Inc.: New York, **2002**.
17. Abel, S.; Juza, M. Less Common Applications of Enantioselective HPLC using the SMB Technology in the Pharmaceutical Industry. In *Chiral Separation Techniques – A Practical Approach*, 3rd ed.; Subramanian, G., Ed.; Wiley-VCH: Weinheim, **2007**, Chapter 7; pp 203–273.
18. Tanimura, M.; Ikemoto, M. (Nippon Rensui Co., Tokyo, Japan) Chromatographic Separation Process. US Patent 6,482,323, **2002**.
19. Makino, K.; Kawai, K.; Tanimura, M.; Tamura, M. (Nippon Rensui Co., Tokyo, Japan) Process for Producing Purified L-ascorbic acid. US Patent 5,817,238, **1998**.
20. Kulprathipanja, S.; Oroskar, A. (UOP, USA) Separation of Lactic Acid from Fermentation Broth with an Anionic Polymeric Absorbent. US Patent 5,068,418, **1991**.
21. Broughton, D.B.; Gerhold, C.G. (Universal Oil Product Co., USA) Continuous Sorption Process Employing Fixed Bed if Sorbent and Moving Inlet and Outlets. US Patent 2,985,589, **1961**.
22. Ettre, L. S. *LCGC N. Am.* **2003**, *2*(5), 458–467.
23. Colin, H.; Hilaireau, P.; De Tournemire, J. *LCGC* **1989**, *8*(4), 301–302.
24. Godebille, E.; Devaux, P. *J. Chromatogr. Sci.* **1974**, *12*(10), 564–569.
25. Berger, L.; Duval, R.; Taillasson, P.; Weber, I.; Wick, A. (Pfizer Inc., USA) Process for the Purification of Optically Pure or Enriched Racemic Tetralone. US Patent 6,683,220 B2, **2004**.
26. Quallich, G. J. *Chirality* **2005**, *17*, S120–S126.
27. Rouchon, P.; Schonauer, M.; Valentin, P.; Guiochon, G. *Separ. Sci. Tech.* **1987**, *22*(8–10), 1793–1833.
28. Ruland, Y.; Colin, H.; David, L. *Biopharm. J.* **2011**, *3*(1), 4–11.
29. Taylor, L. T. *Anal. Chem.* **2008**, *80*(12), 4285–4294.
30. Jusforgues, P.; Shaimi, M. Analusis Mag. **1998**, *26*(*7*), M55–M60.
31. Dapremont O., Ph. D. Thesis, University Pierre And Marie Curie, Paris VI, Paris, France, **1997**.
32. ICH topic Q3C (R4) European Medicines Agency. *Impurities: Guidelines for Residual Solvents*; European Medicines Agency, **2009**. Available at: http://www.ema.europa.eu/ema/index.jsp?curl=pages/regulation/general/general_content_000431.jsp (accessed on 19 August 2013).
33. Broughton, D. B.; Neuzil, R. W.; Pharis, J. M.; Brearley, C. S. *Chem. Eng. Prog.* **1970**, *6*(9),
34. Mazzotti, M.; Storti, G.; Morbidelli, M. *J. Chromatogr. A* **1997**, *769*, 3–24.
35. Storti, G.; Masi, M.; Carra, S.; Morbidelli, M. *Chem. Eng. Sci.* **1989**, *6/44*, 1329–1345.
36. Charton, F.; Nicoud, R. M. *J. Chromatogr. A* **1995**, *702*, 97–112.
37. Migliorini, C.; Mazzotti, M.; Morbidelli, M. *J. Chromatogr. A* **1998**, *827*, 161–173.
38. Rajendran, A.; Paredes, G.; Mazzotti, M. *J Chromatogr. A* **2009**, *1216*, 709–738.
39. Seidel-Morgenstern, A.; Keßler, L. C.; Kaspereit, M. *Chem. Eng. Technol.* **2008**, *31*(6), 826–837.
40. Mihlbachler, K.; Fricke, J.; Yun, T.; *et al. J. of Chromatogr. A* **2001**, *908*, 49–70.
41. Mihlbachler, K.; Fricke, J.; Yun, T.; *et al. J. Chromatogr. A* **2002**, *944*, 3–22.
42. Lode, F. G.; Rosenfeld, A.; Yuan, Q. S.; Root, T. W.; Lightfoot, E. N. *J. Chromatogr. A* **1998**, *796*, 3–14.
43. Rajendran, A.; Paredes, G.; Mazzotti, M. *J. Chromatogr. A* **2009**, *1216*, 709–738.
44. FDA'S Policy Statement for the Development of New Stereoisomeric Drugs, **1992**. Available at: http://www.fda.gov/drugs/GuidanceComplianceRegulatoryInformation/Guidances/ucm122883.htm (accessed on 19 August 2013).
45. Porter, W. H. *Pure Appl. Chem.* **1991**, *63*(8), 1119–1122.
46. Ward, T. J.; Ward, K. D. *LCGC N. Am.* **2012**, 43–45, Supplement.
47. Welch, C. J.; Henderson, D. W.; Tschaen, D. M.; Miller, R. A. *Org. Process Res. Dev.* **2009**, *13*(3), 621–624.
48. Metz, P.; Dapremont, O. *Pharma. Mfg.* **2004**, *3*(9), 27.
49. Dapremont, O.; Malik, A. (AMPAC Fine Chemicals, USA) Reaction Systems with Incorporated Chromatography Units for Enhanced Product Recovery. WO 2012/018737, 2012.
50. Mihlbachler, K.; Dapremont, O. Preparative Chromatography. In *Green Techniques for Organic Synthesis and Medicinal Chemistry*; Zhang, W., Cue, B., Eds.; Wiley: West Sussex, UK, **2012**, Chapter 22; pp 589–612.
51. Aida, T.; Silverston, P. L. *Cyclic Separation Reactors*; Blackwell Publishing: Boca Raton, FL, **2005**.
52. O'Brien, A. G.; Horvath, Z.; Levesque, F.; *et al. Angew. Chem. Int. Ed.* **2012**, *51*, 1–4.
53. Schafer, W. A.; Hobbs, S.; Rehm, J.; *et al. Org. Proc. Res. Dev.* **2007**, *11*, 870–876.
54. Sajonz, P.; Gong, X.; Leonard, W. R.; Biba, M.; Welch, C. J. *Chirality* **2006**, *18*, 803–813.
55. Ye, Y. K.; Lord, B.; Stringham, R. W. *J. Chromatogr. A* **2002**, *945*(1–2), 139–146.
56. Perry, R. H.; Green, D. W. *Perry's Chemical Engineers' Handbook*, 7th ed.; Mc Graw-Hill: New York, **1997**.
57. Dapremont, O.; Cox, G. B.; Martin, M.; Hilaireau, P.; Colin, H. *J. Chromatogr. A* **1998**, *796*, 81–99.
58. Still, W. C.; Kahn, M.; Mitra, A. *J. Org. Chem.* **1978**, *43*(14), 2923–2925.
59. Koh, J.; Guiochon, G. *J. Chromatogr. A* **1998**, *796*, 41–57.
60. Hofmann, H. *J. Chromatogr. A* **1998**, *796*, 75–80.
61. Broyles, B. S.; Shalliker, R. A.; Cherrak, D. E.; Guiochon, G. *J. Chromatogr. A* **1998**, *822*, 173–187.
62. Lang, E.; Valery, E.; Ludemann-Hombourger, O.; Majewski, W.; Blehaut, J. Preparative and Industrial Scale Chromatography: Green and Integrated Process. In *The Pharmaceutical Industry*; Dunn, P. J., Wells, A. S. S., Williams, M. T., Eds.; Wiley-VCH: Weinheim, **2010**, Chapter 12; pp 243–268.

63. Kearney, M. M.; Mumm, M. W.; Peterson, K. R. (Amalgamated Research, Inc. USA) ID Fractal Stack for Scaling and Distribution of Fluids. US Patent 6,616,327, **2003**.
64. McNeil, R. J. (The Perkin-Elmer Corporation, USA) Fluid Flow Control Device. US Patent 4,354,932, **1982**.
65. Gritti, F.; Guiochon, G. *J. Chromatogr. A* **2007**, *1166*, 47–60.
66. Hamende, M. Case study in Production-Scale Multicolumn Continuous Chromatography. In *Preparative Enantioselective Chromatography*; Cox, G., Ed.; Blackwell Publishing: Oxford, UK, **2005**, Chapter 10; pp 253–276.
67. Dapremont, O. (AMPAC Fine Chemicals, USA) Simulated Moving Bed Chromatography for Strongly Retained Compounds. US Patent 7,618,539 B2, **2009**.
68. C Grossmann, C.; Langel, C.; Mazzotti, M.; Morari, M.; Morbidelli, M. *J Chromatogr. A* **2010**, *1217*, 2013–2021.
69. Kiesswetter, R.; Brandl, F.; Kastner-Pustet, N.; Mannschreck, A. Chiroptical Detection During Liquid Chromatography: Deconvolution of Overlapping Peaks of Enantiomers and its Applications. Proceedings for 14th International Symposium on Chiral Discrimination, Hamburg, Germany, 2002. Chirality **2003**, 15, S40–S49.
70. Grinter, T. The Development of an Environmentally Sustainable Process for Radafaxine. In *Green Chemistry in the Pharmaceutical Industry*; Dunn, P. J., Wells, A. S. S., Williams, M. T., Eds.; Wiley-VCH: Weinheim, **2010**, Chapter 10; pp 197–220.

9.09 High-Throughput Screening to Enable Salt and Polymorph Screening, Chemical Purification, and Chiral Resolution

N Variankaval, M McNevin, S Shultz, and S Trzaska, Merck & Co., Summit, NJ, USA

© 2014 Elsevier Ltd. All rights reserved.

9.09.1	**Introduction**	207
9.09.2	**High-Throughput Experimentation**	209
9.09.3	**Salt and Polymorph Screening**	209
9.09.3.1	Salt and Cocrystal Screening	211
9.09.3.1.1	Case study in salt screening	214
9.09.3.2	Polymorph Screening	214
9.09.3.2.1	Slurry conversion	215
9.09.3.2.2	Antisolvent precipitation	216
9.09.3.2.3	Evaporation and cooling crystallization	216
9.09.3.2.4	Case study in polymorph screening	217
9.09.3.3	Analytical Considerations in Salt and Polymorph Screening	218
9.09.3.3.1	Polarized optical microscopy	218
9.09.3.3.2	X-ray powder diffraction	219
9.09.3.3.3	Raman spectroscopy	219
9.09.3.4	Other Considerations in Salt and Polymorph Screening	221
9.09.3.4.1	Solubility information	221
9.09.3.4.2	Optimizing screen design to meet the product profile	221
9.09.3.4.3	Purity of the source material	221
9.09.3.4.4	Inclusion of water as a solvent–antisolvent in salt screening	222
9.09.3.4.5	Temperature effects	224
9.09.3.5	Thermal Methods for Discovering New Phases	225
9.09.3.6	New Approaches in High-Throughput Crystal Form Screening	225
9.09.3.7	Prediction of Crystal Forms	226
9.09.3.8	Data Analysis in HTE	227
9.09.4	**Purification of Drug Molecules**	229
9.09.5	**Enantiomeric Purification**	230
9.09.6	**Perspectives**	231
References		232

Glossary

Diastereomer Stereoisomers that have different configurations at one or more of the stereocenters.
Enantiomer One of two stereoisomers that are mirror images of each other that are nonsuperimposable.
Nucleation The localized creation of a crystalline phase, usually the first step in a crystallization process.
Polymorph A unique crystalline phase of a molecule.
Supersaturation State of a solution with a concentration higher than the solubility of the crystalline or amorphous phase of interest. Supersaturation has to always be defined relative to a specific phase of the molecule.

9.09.1 Introduction

High-throughput experimentation (HTE) is a method that enables the conceptualization, design, execution, analysis, and reporting of hundreds to thousands (and in some cases millions) of individual experiments in a single overall workflow. This technique has found application in drug discovery, development, materials design, and various other fields. This chapter will focus on the application of high-throughput screening and experimentation applied to crystalline phase discovery, chemical purification, and chiral resolutions with specific emphasis on organic molecules.

The diverse chemical structures of drug molecules give rise to a variety of different physicochemical properties. One of the most important of such properties is solubility in bio-relevant aqueous media such as stomach and intestinal fluids, which along with permeability determines the *in vivo* bioavailability of a drug. Drugs with high aqueous solubility can often be developed in their neutral or unionized form; however, if molecules are poorly soluble, acid or base salts of drugs are often prepared to improve

solubility. Crystalline phases of drugs are in general preferred for pharmaceutical development since crystallinity confers various advantages during isolation, processing, and storage of the drug. Common advantages include better impurity rejection, improved handling characteristics such as sticking and flow, and, in the majority of cases, better physical and chemical stability than the amorphous phase.[1]

Molecules can crystallize or organize into various lattice structures referred to as polymorphs. These crystalline phases have identical chemical composition but differ in their physical properties such as melting point, heat of fusion and density. These molecules can also cocrystallize with other components such as water to form hydrates, with solvents to form solvates and with acids and bases to form crystalline salts. A comprehensive search and analysis of crystalline phases of drug molecules can greatly enable selection of the most suitable phase for pharmaceutical development. Typical criteria used for such phase selection include physical and chemical stability, solubility, and chemical and formulation processability.

Pharmaceutical companies currently employ a variety of tools to screen for crystalline phases of drugs. Historically, manual crystallization efforts have been used to isolate different crystalline phases of a molecule. The first recorded observations of polymorphism in organic small molecules are usually attributed to Wohler and Liebig for their discovery of benzamide polymorphs in 1832.[2] The propensity of molecules to crystallize into different lattice structures was nicely summed up by W. C. McCrone by his statement, 'every compound has different polymorphic forms, and in general, the number of forms known for a given compound is proportional to the time and money spent in research on that compound'.[3] Although exploration of different conditions for crystallization may lead molecules to crystallize into different unit cell packings, it is generally not possible to predict specific structures from the conditions that generate them. Hence, it may be advantageous to consider a high-throughput method to screen for crystalline phases of molecules.

High-throughput materials screening has taken a page from the combinatorial screening first employed in the synthesis of large numbers of diverse but structurally related molecules in chemistry. P. G. Schultz was a pioneer in applying the principles of combinatorial chemistry to the field of materials science – specifically, the preparation of ferroelectric materials.[4] Subsequently, companies like Symyx Technologies, Dow, and GE have used HTE methods in areas as diverse as catalysis, coatings, magnetic materials, and polymorph and salt screening. In addition to using such high-throughput platforms for crystal form discovery to aid pharmaceutical development, other applications that can be enabled include enantiomeric purification including mapping of phase diagrams by combining high-throughput experiments with solubility measurements[5] and screening for conditions that reject impurities from drugs through crystallization.[6] Both these activities are critical in the early stages of drug development.

Chemical syntheses often result in impurities. One of the most common methods to remove these impurities is through crystallization. In many cases the structure of these impurities is similar to the molecules being synthesized, and this poses significant problems for impurity removal. High-throughput crystallization followed by measurements of impurity content in various solvent compositions and at a range of different temperatures can be employed to screen for the best crystallization conditions for impurity rejection in chemical syntheses. Likewise, impurities in the form of undesired enantiomers, racemic compounds, or diastereomers can also be removed through crystallization. High-throughput methods are quite useful for rapidly measuring the solubility of the different crystalline phases during enantiomeric purification since it involves measurements in a number of different solvents at various temperatures before selecting an optimal solvent–temperature combination can be selected to increase the enantiopurity.

High-throughput methods are particularly important in cases where a number of possible options need to be explored simultaneously involving variables such as solvent composition, temperature, and supersaturation. Although these are not meant to replace traditional methods of crystallization, they should be viewed as a supporting tool to explore a wide design space.

An alternative way to discover crystalline forms of a drug molecule is through *ab initio* predictions. There have been scattered efforts over the past 10 years in the area of predicting polymorphs of drug molecules through computational simulations.[7–11] Success in this is highly dependent on a number of factors: (1) conformational flexibility, (2) atom type, (3) number of molecules in the asymmetric unit, and (4) the presence of permanent charges on molecules such as in salts or zwitterions. In spite of several efforts, the only example of a stable crystalline form that was predicted *in silico* and subsequently produced experimentally in the laboratory is the case of racemic progesterone.[12] No such example exists for a marketed drug molecule. This is a consequence of the tremendous complexity of determining the optimal packing arrangements of molecules in lattices, our inadequate understanding of subtle yet important nonbonded molecular interactions that can influence such packing and errors in energies associated with force-fields used for such calculations. In order to appreciate the challenges in predictions, it is worth noting that the free energy difference between polymorphs could be of the order of 1 kcal mol^{-1} (recall RT = 0.6 kcal mol^{-1}) or less thus limiting the application of conventional force-field based approach to the problem. In spite of these challenges, efforts are currently ongoing to develop better methods based on hybrid quantum mechanic and density-functional theory (DFT)-based methods to predict polymorphs or organic molecules. The state-of-the-art is represented by the program called GRACE developed by Neumann et al.[13] GRACE uses a combination of DFT calculations and custom-made force-fields for each molecule to predict polymorph. Of course, several limitations still exist – the method is currently limited to: (1) neutral molecules, (2) single component crystals, (3) one molecule in the asymmetric unit, and (4) molecules that contain on the average 50–60 atoms. Given the diversity of drug molecules and the variety of crystal structures into which they organize themselves, experimental screening still represents the best way to discover crystalline forms of drug molecules.

9.09.2 High-Throughput Experimentation

The core component of HTE is the microtiter plate or microwell plate and it is the location of the experiment that is conducted – be it crystallization, purification, or resolution. A typical plate contains anywhere from 6 to 1536 individual sample wells, each of which can be viewed as a reactor (Figure 1). These microtiter plates can be constructed of glass, metal, plastic, or any material that is chemically compatible with the reagents and chemicals being screened. Although the volume of each individual well can range from nanoliters to milliliters, typical screening wells for crystallization fall in the microliter–milliliter range. Staged HTE can also be carried out wherein the number of experiments is gradually reduced over time as hits are focused into promising leads and ultimately the desired material is isolated – a crystalline salt in the case of salt screening or a pure crystalline diastereomer in the case of a chiral resolution screen.

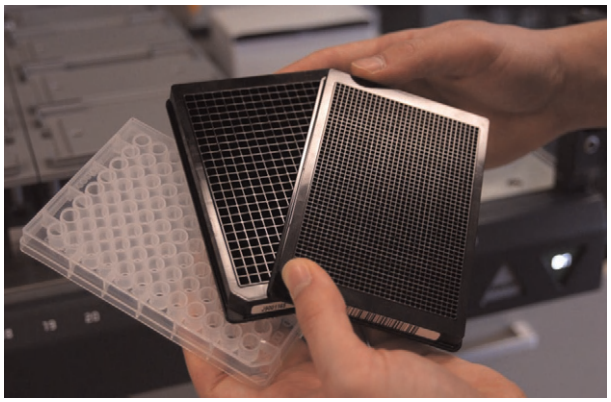


Figure 1 Example of a microplates used for high-throughput experimentation (HTE) studies. (http://www.labautopedia.org/mw/index.php/Image:Microplates.jpg).

The essential concept of HTE is the incorporation of all the elements of design, preparation, execution, analysis, and reporting into a single workflow. This includes any robotic systems for handling liquids and solids, dosing units, analytical instruments that are coupled to the screening platforms and data analysis and sorting programs.

On completion of experimentation and data generation, sorting of the data is required to be able to classify hits and narrow down the conditions generating 'useful' and 'identical' crystalline phases. Software programs such as Spectra Studio™ are available to compare, sort, and classify hits.[14] User-defined correlation factors for sorting into groups are available. This creates the ability to sort across multiple libraries in a project using multiple pattern recognition algorithms. There is also the capability to load data from entire libraries or individual experiments thus enabling the handling of large volumes of data for sorting. The human element in interpreting and classifying data, although minimized, cannot be completely divorced from HT-analysis as exemplified by the salt screening case study.

Manual design of experiments/statistical approaches are especially valuable for mapping continuous variables such as temperature and pressure. For discontinuous variables such as solvent type, choice of counter-ion, discrete stoichiometries, and resolving agent, HT-screening is much more effective in reducing the number of manual experiments.

9.09.3 Salt and Polymorph Screening

Selection of an optimal solid phase of the drug molecule is a critical element of the drug development process. Factors to consider in selecting the phase include solubility, physical and chemical stability, processability, and, in some cases, freedom to operate.[1] Pharmaceutical companies conduct their phase selection activities during various stages of development as shown schematically in Figure 2. Some complete the selection of the final phase for development before the first toxicology study, whereas others defer this activity until the program enters PhII clinical trials. It is of course highly desirable to lock in a suitable phase of the drug molecule before commercial-scale operations are launched.

There are typically three steps in the selection of a suitable solid phase for development:

1. Solid-phase generation;
2. Solid-phase identification and characterization; and
3. Phase evaluation for processing, stability and bioavailability.

The first step involves salt and polymorph screening. This is typically done in high-throughput mode and involves preliminary characterization of hits. Detailed physicochemical evaluations are then carried out followed by assessment of processability,

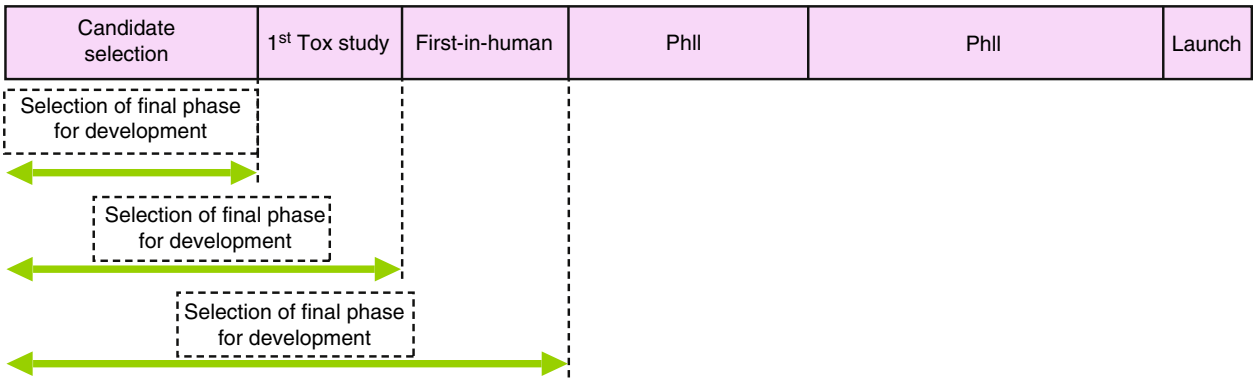


Figure 2 Schematic of timelines associated with the salt and polymorph selection process.

physical and chemical stability, and bioavailability in suitable formulations. At the end of this exercise an optimal solid phase is chosen to enter formulation development. This process is schematically shown in Figure 3.

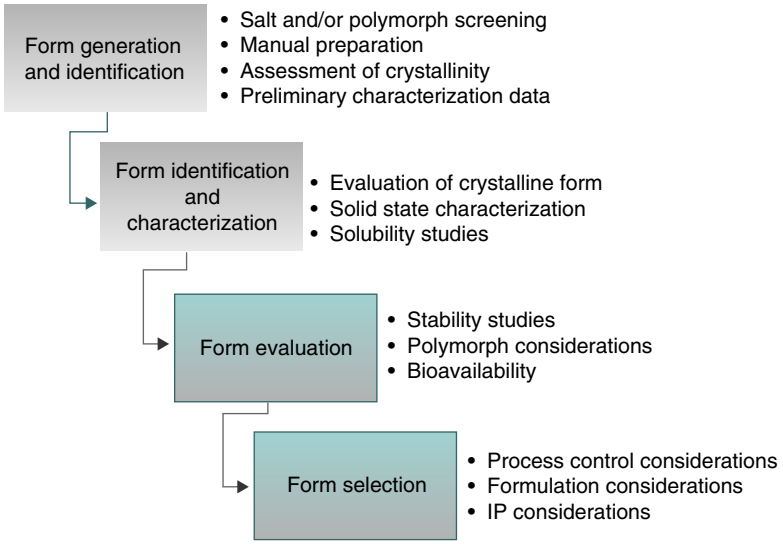


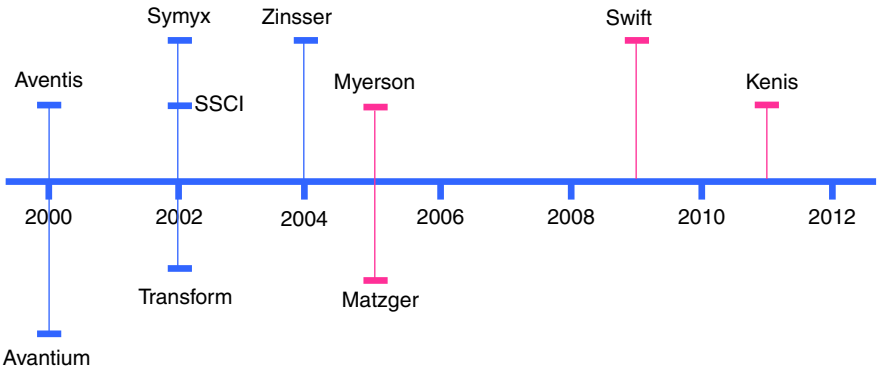
Figure 3 General schematic of phase selection workflow.

Small organic drug molecules possess great diversity in chemical structure, functionality, and hence intra- and intermolecular bonding. In addition, drug molecules are conformationally flexible to varying degrees. These very aspects that enable successful target engagement also contribute to a diverse landscape of crystalline forms – both salts as well as neutral phases. Many of these molecules have pKas that are relevant to salt formation – some form salts that are stable in the physiological pH range, whereas others tend to disproportionate into the free acid or base forms on dissolution. In addition, chemical and functional diversity leads to a plethora of solid phases with different free energies of which the most stable crystalline phase having the lowest free energy is highly desirable from a stability perspective. Conversely, the form with the highest stability will have the lowest solubility. It is very rare, however, for pharmaceutical companies to develop a metastable crystalline phase of a drug because of the risk of conversion to the most stable phase during development, storage, or use. This implies that it is critical to identify the most stable polymorph of a drug molecule early in development to avoid late-stage phase changes. The presence of a physiological pKa ($3 < pKa < 10$) and the desire to identify the most stable polymorph leads to a need to screen for salts and polymorphs.

Recognition of the need to screen for crystalline phases led to the development of automated platforms for performing high-throughput salt and polymorph screening. This concept of implementing a combinatorial approach to crystallization was borrowed from platforms that were developed for high-throughput protein crystallizations. Although HT-protein crystallization methods have had a focus on identifying conditions under which crystals could be grown to enable structure solution or to identify conditions under which proteins crystallize, the general idea of needing to do tens or hundreds of experiments in parallel to maximize the chances of identifying crystalline phases applies to both small and large molecules. Despite that, both types of crystallization screening for both proteins and small molecules involves HTE methods, the technical minutiae involved in the two screening approaches are vastly different. Protein screenings are primarily focused on aqueous media, with the addition of polymers and salts for precipitation. In contrast, the screens implemented for small organic molecules require organic solvents in

addition to aqueous media. Salts are typically not used as precipitants and there is a larger focus on various other methods of supersaturation generation that will be highlighted throughout this chapter.

A historical snapshot of the development of high-throughput screening is provided in Figure 4.



Source	Type of screen	Reference
Aventis	Microplate salt screening	14
Avantium/Crystallics	HT-screening platform	15
Symyx	Polymorph discovery tools	16
SSCI	Capillary based polymorph discovery system	17
Transform	Crystal Max polymorph system	18, 19
Zinsser	Crissy® platform for polymorph screening	20
Myerson	Self-assembled monolayer-based polymorph screen	21
Matzger	Polymer heteronuclei based polymorph screen	22
Swift	Siloxane monolayer templates for polymorph screening	23
Kenis	Microfluidic platform for salt screening	24

Figure 4 Timeline of HT crystallization technologies (▬ traditional solvent mediated platforms) (▬ nontraditional platforms/approaches). Source: Microplate salt screening.[14–24]

It is interesting to note a trend in the evolution of screening methods over the years. Establishing screening platforms seems to have been largely driven by industry in the early years as the need to find crystalline phases early in drug development became critical. Starting in the mid-2000s, academic groups have started becoming interested in developing new methods for screening crystalline phases. A detailed discussion of some of these newer techniques will be provided in Section 9.09.3.6.

The most common protocols employed by pharmaceutical companies to generate crystalline hits during screening are anti-solvent precipitation, cooling, and evaporation. These are typically passive or homogeneous nucleation-based methods and do not rely on additional modes of nucleation. In addition, slurries of the drug in various solvent combinations can also be set up and monitored over time. Before screens can be run, some fundamental information is required. These include:

- Solubility in solvents and identification of antisolvents;
- Temperature stability of the drug;
- Reactivity of the drug to specific solvents;
- Purity of the starting material; and
- Presence of rotamers or tautomers.

This information can enable the appropriate design of solvent/antisolvent combinations, water activities, and heat–cool protocols.

A typical experimental workflow could involve the steps outlined in Figure 5.

This basic workflow is usually adapted and modified according to user needs, an example of which is the Symyx workflow (Figure 6).

9.09.3.1 Salt and Cocrystal Screening

Frequently salts are required to impart adequate solubility and ideally, impart satisfactory bioavailability to the drug molecule. Since drugs can occur as free acids or bases, acidic and basic counter-ions are typically used in high-throughput screening for salts. A comprehensive listing of potential acids and bases is available in Stahl et al.[25] Although the typical rule of thumb for successful salt formation is the often quoted 2 pKa units difference between the acid and the base, any salt screen will usually involve

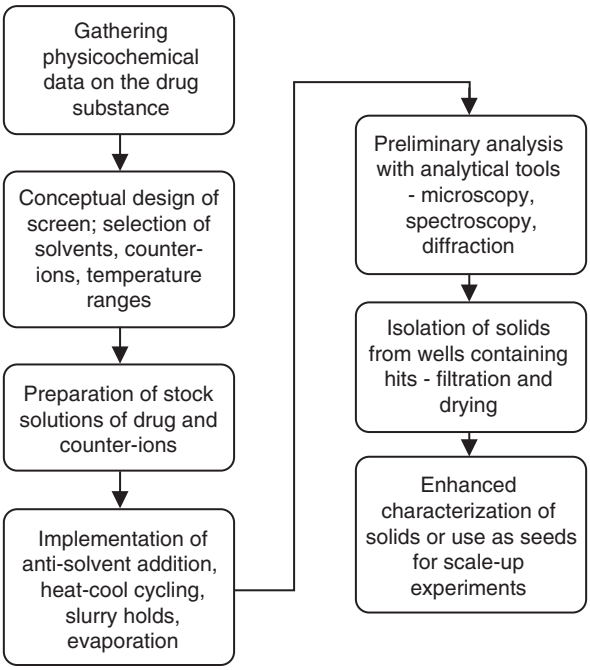


Figure 5 General steps in a crystallization screening experiment.

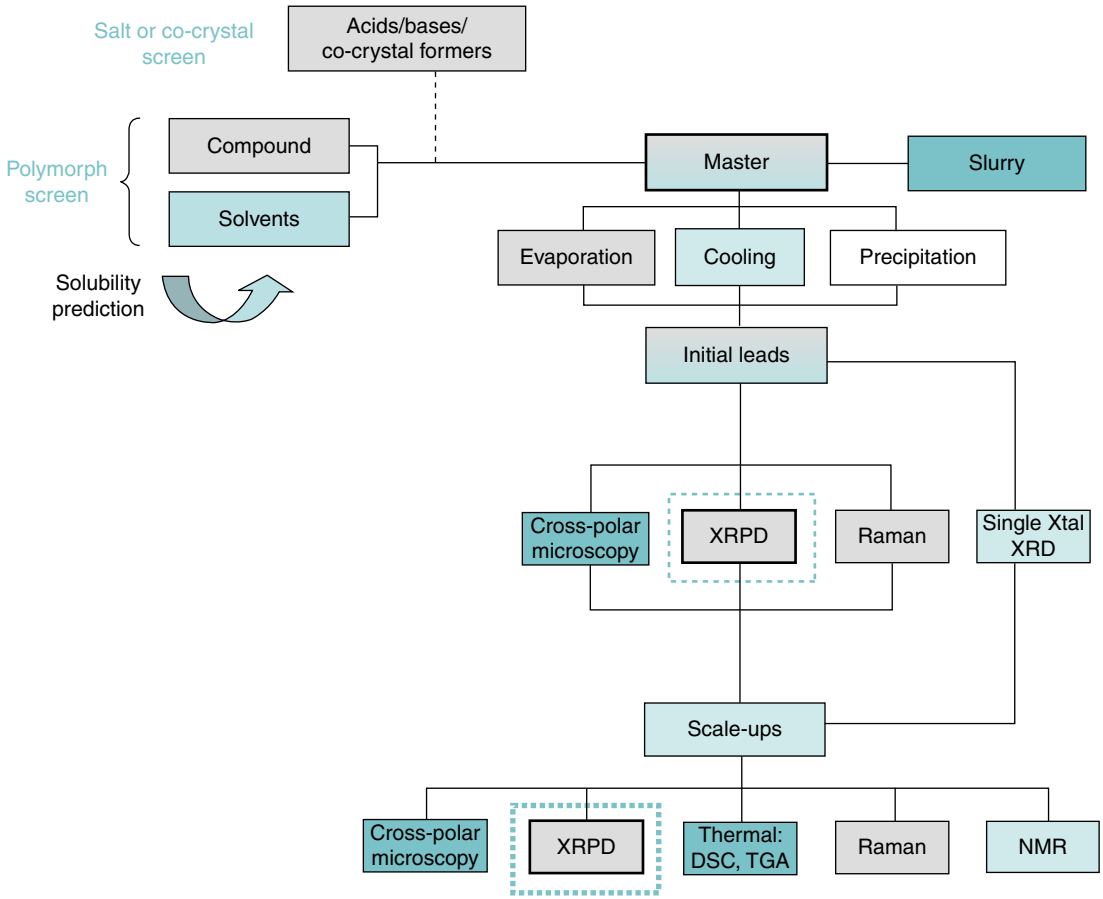


Figure 6 Symyx workflow for polymorph screening. Adapted from http://www.symyx.com/products/pdfs/2003_PharmaChem_2_10.pdf.

screening all possible acids and bases. One of the reasons for this is the likelihood that even if formation is not viable, the acid and the base could form a cocrystal through strong hydrogen-bonded interactions. It is possible to modulate the likelihood of salt formation by selecting either aqueous or nonaqueous solutions of counterions. The influence of water in salt formation is discussed in Section 9.09.3.4.4.

A typical HT-plate for salt screening is shown schematically in Figure 7.

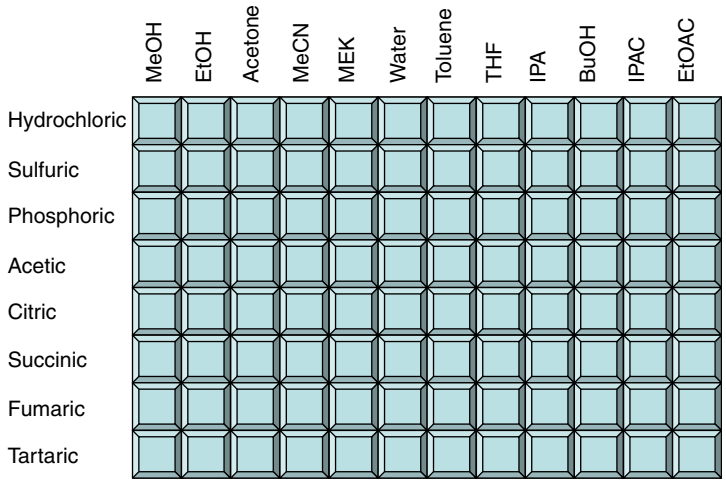


Figure 7 Schematic of a typical salt screening plate. Abbreviations: MeOH, methanol; EtOH, ethanol; MeCN, acetonitrile; MEK, methyl ethyl ketone; THF, tetrahydrofuran; IPA, isopropyl alcohol; BuOH, butanol; IPAc, isopropyl acetate; EtOAc, ethyl acetate.

Alternately, depending on the pKa of the molecule or the specific application intended – such as IV delivery, for example, certain coformers can be targeted and instead a range of stoichiometries can be explored as depicted in Figure 8.

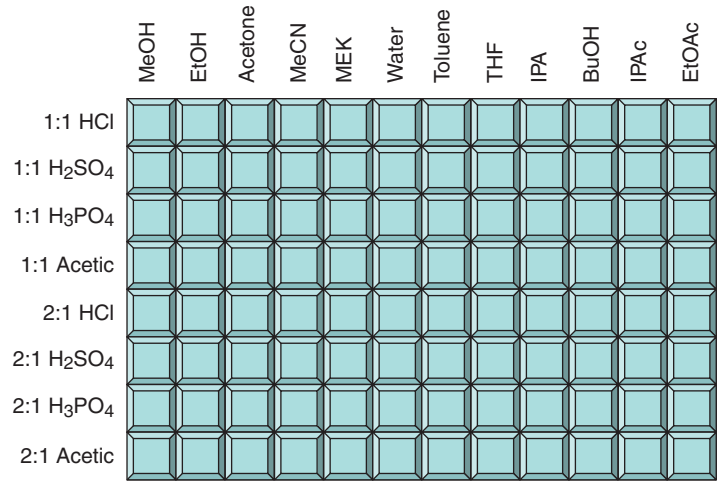


Figure 8 Modification to the HT-plate to explore multiple stoichiometries of coformers. This is an example of a plate using only strong acids. But the plate can be designed to have any combination of coformer type, stoichiometry and/or solvent type depending on the need.

These screens can also be staged depending on whether crystalline salt hits were obtained in the first round of screening with mono-stoichiometric amounts of coformers. An ideal screening protocol could be to include several stoichiometries (whole number ratios of acid:base) in the first round of screening and then, depending on the hits, to narrow down on more controlled experiments. Frequently it may be necessary to use nonaqueous sources of counter-ions (e.g., sodium *tert*-butoxide, HCl in isopropyl alcohol, etc.), depending on specific considerations such as reactivity, chemical stability, and solubility of the active ingredient in water. Again, it may be advantageous to incorporate both aqueous and nonaqueous sources of counter-ions in any screening protocol, irrespective of how it is staged.

In the following section, an example is provided of salt screening on a developmental compound, particularly highlighting the advantage of HTE.

9.09.3.1.1 Case study in salt screening

An active pharmaceutical ingredient (API) was received as an oil with a purity of $<80\%$. Oils are typically unacceptable for the development of a solid dosage form. The pKa of the molecule was 9. Sixteen different acids in six different crystallization solvents were screened. HT-slurry, evaporation, and cooling crystallizations were screened in an attempt to discover a crystalline salt phase. Only one very weakly crystalline hit was obtained from 288 individual experiments – an acetate salt with an X-ray powder diffraction (XRPD) pattern shown in Figure 9(a). Subsequently scale-up experiments using the conditions that produced the hit were attempted, which resulted in a crystalline monoacetate salt (Figure 9(b)).

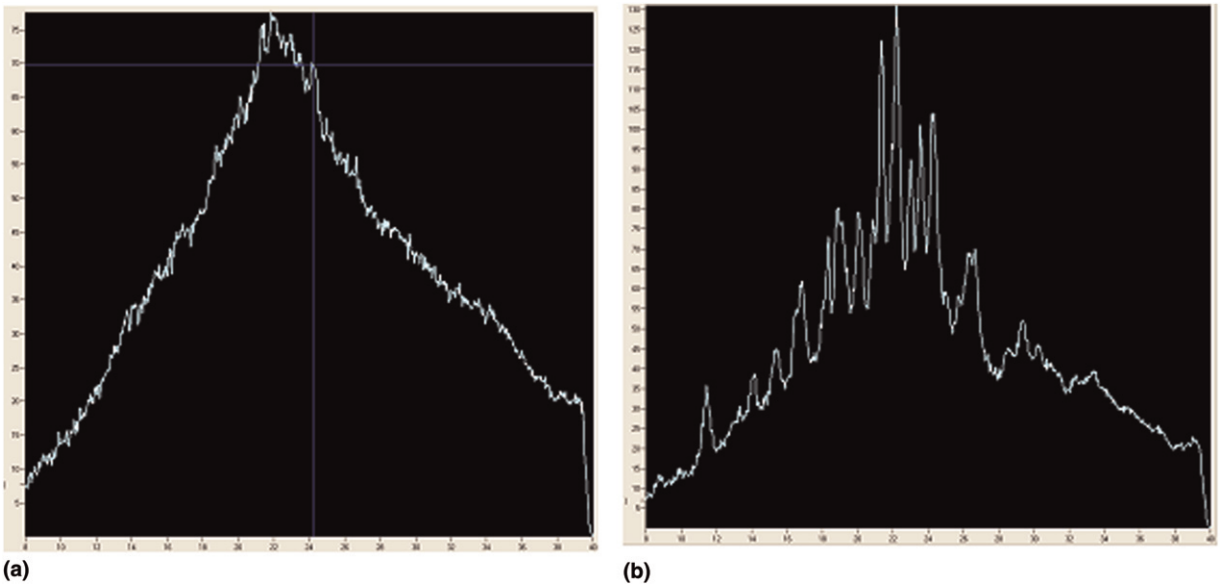


Figure 9 (a) Original hit from a HT-screen, (b) scaled-up crystalline monoacetate salt. Note: The sample is prepared on a glass slide which imparts an amorphous background halo to all sample scans.

Crystallization from isopropyl acetate afforded solids that were easily filterable enabling the program to advance to first-in-human clinical studies. This case highlights two crucial features of salt screening:

1. Multiple experiments (hundreds) may be needed until a single crystalline hit can be obtained and
2. Careful manual observation is absolutely critical to take advantage of HTE.

9.09.3.2 Polymorph Screening

The discussion in this section will be limited to the conventional methods of high-throughput polymorph screening – slurry, antisolvent, evaporation, and cooling crystallization. Newer platforms for polymorph screening will be discussed later in Section 9.09.3.6.

It is worthwhile reviewing some of the fundamentals of crystallization as it underscores much of the rationale behind the design of polymorph screens. Nucleation of crystalline phases occurs because of concentration fluctuations in supersaturated solutions leading to the formation of a solid phase. Depending on conditions of supersaturation release – rate of cooling, presence of templates, impurities, inherent nucleation rates of different phases, and interactions in solution, either amorphous or crystalline phases can be produced from supersaturated solutions. It can be safely said that the ultimate goal of high-throughput polymorph screening is to maximize the number of crystalline hits. Thus an intimate knowledge of crystallization, and more importantly nucleation, is necessary to design an effective polymorph screen.

Nucleation is a highly stochastic process because it can be influenced by a number of variables – some known and controllable, others known and uncontrollable, and still others that are unknown and hence, uncontrollable. Variables that influence nucleation include mixing dynamics, temperature fluctuations, impurity levels, and chemical specificity of the impurities, heterogeneous surfaces that may be present during the experiment and specific solvent–solute interactions. Nucleation can also be classified into homogeneous and heterogeneous. The former is driven purely by free energy considerations, whereas the latter is

additionally driven by the presence of seed (either of the same composition or a different material altogether). The classical nucleation picture is presented in Figure 10 which simply shows that a critical cluster or aggregate size of solute molecules is required before it becomes advantageous for the nucleation and growth to proceed by increasing the size of the cluster/aggregate. Also shown in the figure is the effect of supersaturation – increasing the supersaturation lowers the entropy of phase transformation, thereby lowering the free energy for formation of a crystalline solid.

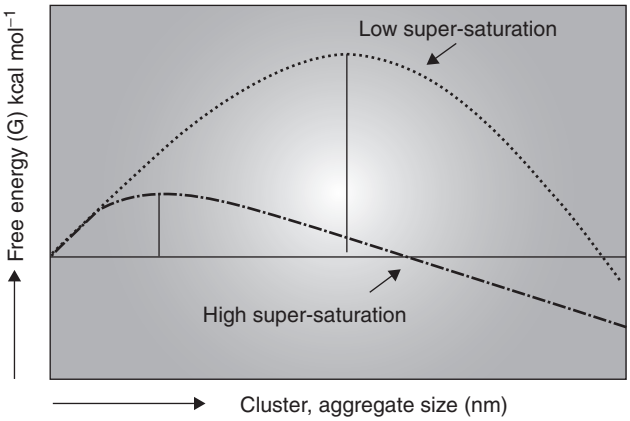


Figure 10 Plot of free energy vs. cluster or aggregation size. This is based on the classical theory of nucleation.

Several limitations to classical nucleation theory exist. Some of these are listed below:

- The nonspherical nature of organic molecules and resulting anisotropy of interactions that introduces complications beyond classical theory;
- Growth of nuclei can occur by addition of clusters or more than one molecule rather than molecule by molecule;
- Local concentration fluctuations; and
- Generally weak intermolecular interactions holding together 'soft crystals' such as those of organic molecules, resulting in higher rates of addition to the growing front compared with 'reorientation' of molecules to ensure lattice registry.

The last factor is particularly important for polymorph screening, since it can result in the formation of amorphous materials or at best, partially crystalline solids. Although these apply to homogeneous nucleation from solution, heterogeneous 'primary' and 'secondary' nucleation can also come into play in screening. Here, primary refers to growth onto foreign particles such as impurities or dust particles, and secondary refers to growth on preexisting seed particles. A nice example of primary heterogeneous nucleation – a potential impurity templating the nucleation of a new polymorph of ritonavir – is highlighted later in Section 9.09.3.4.3.[26] An example of heterogeneous secondary nucleation is the seeded crystallization of polymorphs in process development.[27]

We will now examine each of the main protocols used in high-throughput screening of polymorphs and attempt to relate them back to the fundamental principles of crystallization.

9.09.3.2.1 Slurry conversion

An oft-quoted empirical law in crystallization is the Ostwald's rule of stages which states that, in crystallization from solutions, the most stable phase crystallizes last – being most separated from the initial state in terms of free energy.[28] This principle led to the development of the slurry conversion protocol wherein solutions with excess of the available solid phase (in equilibrium with the saturated solution) are slurried over extended periods of time. During the progress of this experiment, the solubility difference between the metastable and the stable phases drives the dissolution of the former since the starting concentration of the compound in solution will be above the solubility of the stable phase, i.e., supersaturated relative to this phase (cf. Figure 11).

With time, as the more stable phase nucleates and grows, the concentration in the supernatant will fall below the solubility of the less stable phase, driving dissolution of this phase. Although it is impossible to know the end-point of such an experiment (i.e., has the most stable phase been found?), typical slurries are either held isothermally or cycled through a temperature range for weeks (or a length of time that is consistent with project timelines, for want of a better yardstick) and the conversion monitored as a function of time. A high-throughput approach is particularly valuable since it is impossible to predict the kinetics of conversion in various combinations of solvent systems other than a general trend of faster kinetics in those solvents where the compound has higher solubility.

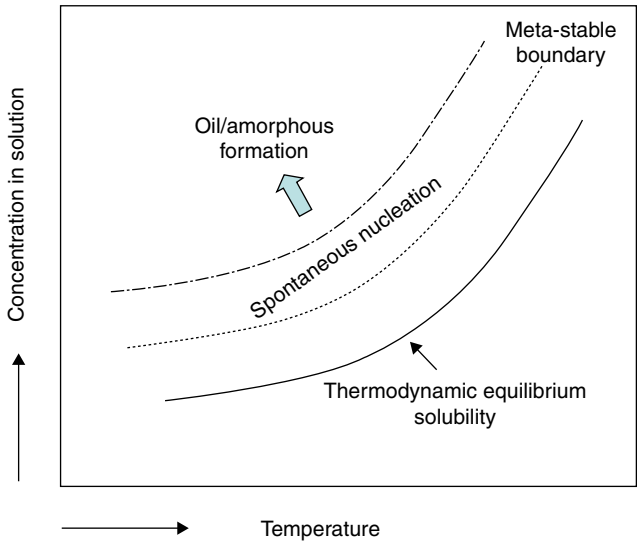


Figure 11 Solubility and metastable zone width. At high supersaturations, the probability of oiling out or amorphous formation increases. At lower supersaturations, spontaneous nucleation and growth can occur from solution. If a crystalline phase has already been identified, knowledge of the solubility of that phase vs. *T* can help in designing appropriate experiments using this data as a rough starting point.

9.09.3.2.2 Antisolvent precipitation

This method relies on the relief of supersaturation by introduction of a poor solvent for the compound, into a saturated solution of the compound in a good solvent. If we apply the same Ostwald's Rule of Stages, one would predict that antisolvent precipitation could result in the production of less stable forms at the expense of more stable ones because less stable forms are closer in energy to that of the molecule in solution compared with the more stable forms. This can be mitigated to some extent by: (1) controlling the rate of antisolvent addition, (2) modulating the temperature, or (3) introducing mechanical mixing into the sample wells. Any one or combination of these approaches could contribute to diversity in process space and may help to drive the system toward the more stable phases – but this cannot be guaranteed. Hence antisolvent precipitation is more useful in the discovery of metastable phases, solvates, and hydrates compared with slurry conversion. Since large-scale chemical processes need access to a large solvent-space, this type of screening is particularly useful in highlighting the risk of formation of undesirable phases in particular solvent–antisolvent combinations. Slow introduction of antisolvent can also be used to grow large crystals – to be used in structure elucidation, for example. A controlled version of this approach is vapor diffusion, wherein, a saturated solution of the compound is exposed to the vapors of the antisolvent. Again, this method is more useful in growing large crystals than in ferreting out more stable phases. The likelihood of oiling out can be reduced by slowing supersaturation release and by providing adequate mixing during addition of antisolvent so as to avoid local regions of high supersaturation.[29]

9.09.3.2.3 Evaporation and cooling crystallization

Both these protocols use temperature as a means to relieve supersaturation. Evaporation is usually carried out at room temperature (r.t.) or higher depending on the vapor pressure of the solvents used in the screens. Since the vapor pressure of solvents can vary over a wide range, the rate of supersaturation release can also vary widely in an evaporative crystallization experiment. Higher boiling solvents may require some amount of heating to ensure solvent removal and subsequent nucleation and crystallization. For cooling crystallizations, several cooling protocols are available to relieve supersaturation,[30] cubic cooling being one of the more common methods employed (cf. **Figure 12**).

Choosing between different types of cooling becomes easy in a high-throughput automated setting and may need to be considered depending on the ease of crystallization of the molecule. Typically, the type of cooling in crystallization processes depends on whether the objective is to nucleate a crystalline phase or grow on seeds that are already present in the system. For purposes of polymorph screening, since the objective is to nucleate a new phase, the rate of supersaturation release becomes particularly important. Shown in **Figure 13** is the relationship between nucleation rate and supersaturation.

At high supersaturation, an exponential increase in nucleation rate is observed.[31] This has three implications: (1) a large number of nuclei can be generated at high supersaturation, (2) the growth of crystals can be limited because of the increase in the number of nuclei formed, and (3) oiling out can occur similar to the case of rapid release of supersaturation with antisolvent. One or more of these consequences may be deleterious to the discovery of crystalline phases. Controlled cooling programs, such as cubic cooling, are often employed as a compromise between the desire to nucleate a new phase and the necessity to avoid aggregation and oiling out or formation of amorphous phases.

In Section 9.09.3.2.4, a case study is provided of an actual compound in development to illustrate the utility of polymorph screening.

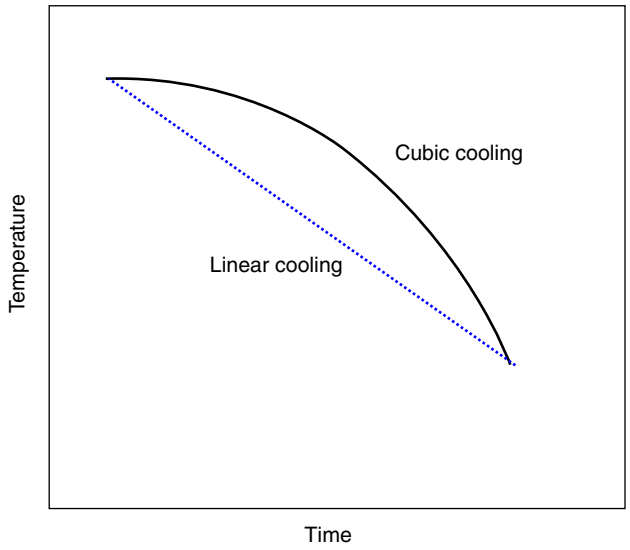


Figure 12 Cooling protocols. The dotted line represents linear cooling which is almost never used in polymorph screening, whereas the solid line represents cubic cooling, more often used in screens.

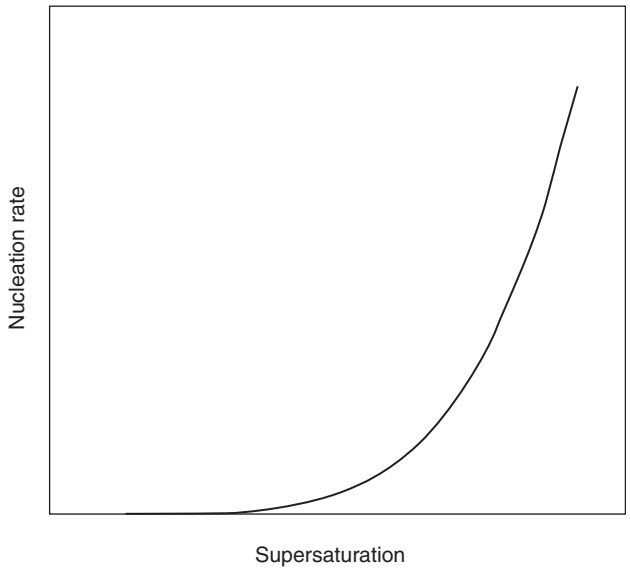


Figure 13 The relationship between nucleation rate and supersaturation, assuming classical nucleation theory.

9.09.3.2.4 Case study in polymorph screening

Two anhydrous crystalline forms of the compound were known – Form I and Form II, the latter being the more stable form at r.t. as determined by competition slurry experiments in certain specific solvent systems. A typical polymorph screen was conducted on a compound using multiple slurry experiments in various solvents and solvent combinations to ensure that no other polymorphs exist for this compound. The results of the screen were analyzed by XRPD analysis of the residual solids as shown in Figure 14.

Surprisingly, conversion from the more stable Form II to the less stable Form I was observed in a number of wells. Wet cakes from these slurries were analyzed again by XRPD and monitored as a function of drying in ambient conditions. A gradual change in XRPD patterns was noticed between wet and dry conditions in those cases where conversion to Form I was observed. Further analysis of some of these samples by solid-state nuclear magnetic resonance (NMR) indicated the presence of the respective solvent in the crystal lattice. These transient solvates were drying consistently to Form I in those wells where conversion was observed. This case study shows how manual follow-up experiments and additional analytical techniques may be needed to make sense of the results from polymorph screens. Another important outcome of the slurry polymorph screen was the elimination from process considerations of those solvents in which conversion to Form I was observed. Thus a polymorph screen can also provide valuable information for designing a robust process.

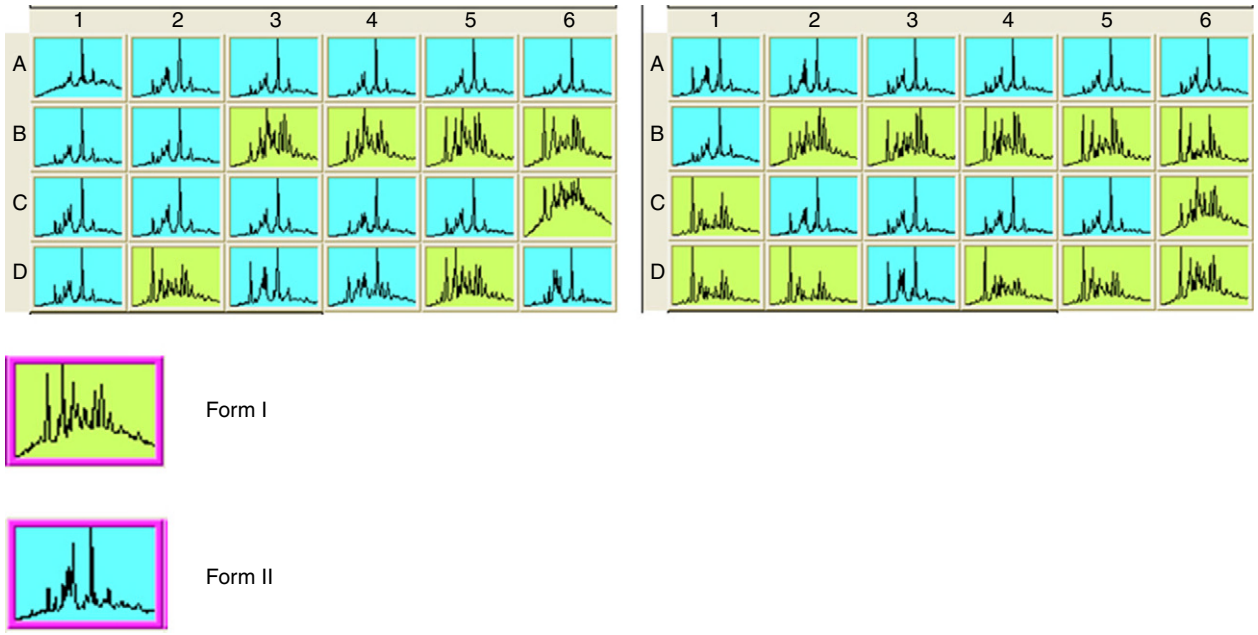


Figure 14 Results from a polymorph screen at two different timepoints. With time, a conversion to Form I was observed – as shown by the X-ray diffraction patterns of the wells B2, C1, D1, D4, and D6.

9.09.3.3 Analytical Considerations in Salt and Polymorph Screening

Analytics is a key component of any high-throughput screening. By its very nature HTE generates vast amounts of data. HT-screening for crystalline forms has to be intimately coupled with methods to reliably detect and characterize the physical properties of the hits. The most common analytical techniques used for characterization of the solids include polarized optical microscopy, XRPD, Raman spectroscopy, infrared (IR) spectroscopy, and melting point determination. In addition other methods such as Karl-Fisher titration for water content, gas chromatographic analysis for residual solvent, NMR/mass spectrometry for identity testing, and high performance liquid chromatography (HPLC) for solution concentration measurement are often employed in tandem at various stages of salt and polymorph screening. Any solid-state characterization technique that is used for analysis should be capable of being automated to allow operation in the HTE-mode. Certainly XRPD, Raman, and optical microscopy have been adapted and designed to analyze solids in microplates. For other analyses like differential scanning calorimetry (DSC), wells need to be sampled and transferred to DSC pans manually before they can be run on an instrument with an autosampler. At present, there is no easily available automated method for performing DSC experiments directly on the solids in the microplates.

In the next section, each of the techniques and their adaption to handle HTE are discussed in more detail.

9.09.3.3.1 Polarized optical microscopy

Crystalline solids display birefringence. Hence polarized optical microscopy can be a very quick first-pass technique to detect crystallinity, which is helpful in determining whether a screen has been successful in producing a hit. Most optical microscopes have stages to handle HTEs. In addition to indicating whether a particular well has birefringent solids, microscopy also provides a way to classify hits according to shape or habit of a crystal.[32] A typical example of a plate with crystalline hits showing birefringence is given in Figure 15.

The corresponding X-ray diffraction analysis on the same plate is shown in Figure 16. There is a clear correlation between the wells in which birefringent solids are obtained and crystalline peaks in the corresponding diffraction pattern.

In some instances, microscopy may be able to pick up small amounts of crystalline material in wells where insufficient crystallinity may result in very low intensity or lack of Bragg peaks in the corresponding X-ray diffraction pattern. Generally, a combination of orthogonal analytical techniques is always preferred in screening.

Microscopy data is particularly useful for process development since the shape of a crystal can affect unit operations like filtration and flow.[33] In fact one can imagine developing a morphology screen akin to a polymorph screen whereby different crystallization conditions can be screened with a goal of modifying the shapes of crystals. It is possible that the amount of solid material in a well may be too small to permit assessment by birefringence. So it is the best practice to analyze plates by diffraction and/or spectroscopic techniques in any case to avoid errors in identifying hits.[19] As will be seen in Section 9.09.3.3.3, a combination of microscopy with spectroscopy[34] may offer a nice alternative to any single technique for hit-analysis.

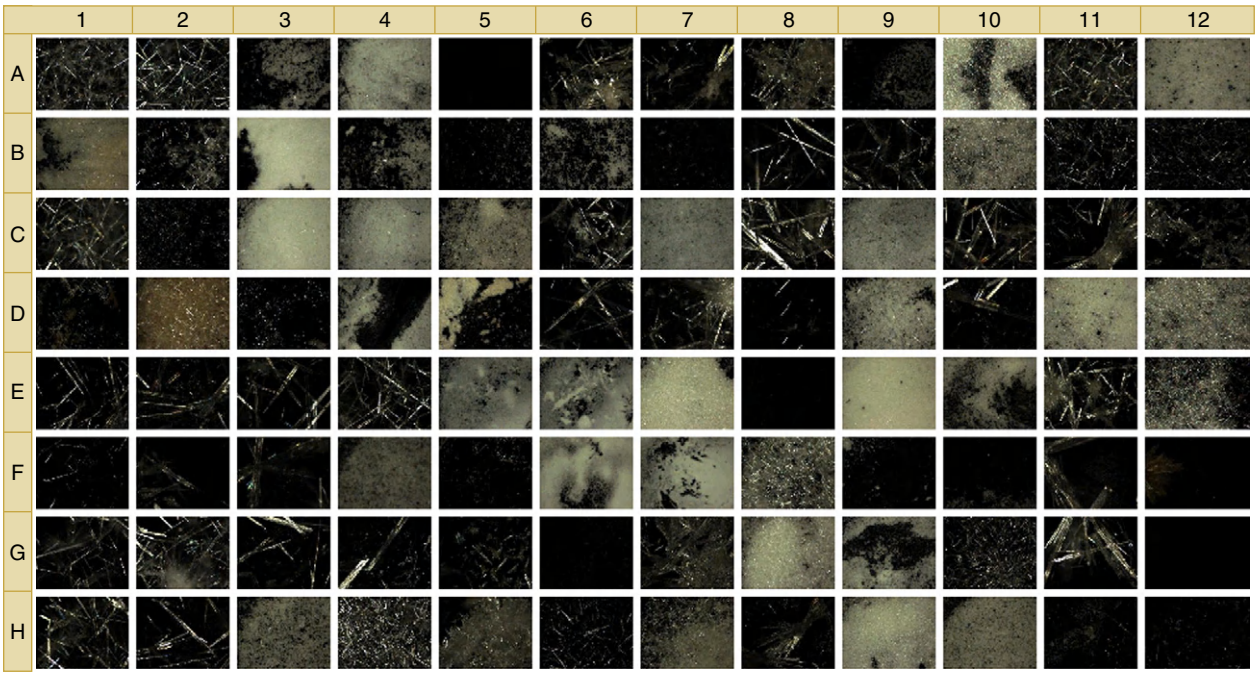


Figure 15 HT-polarized optical microscope images of a well plate after polymorph screening. Microscopy often serves as a first-pass method to detect crystallinity in a screen. It can also provide information on the morphology of particles produced with certain solvent combinations.

9.09.3.3.2 X-ray powder diffraction

Often, X-ray diffraction is the preferred method of characterization of the crystalline state of solids. Each crystal phase gives a characteristic diffraction pattern that enables its identification. However, there are numerous cases where different solvent molecules can be included in the lattice without significant changes in the diffraction pattern. Characterization of such isomorphous or isostructural crystalline solids may often require orthogonal techniques to enable unambiguous identification.

Because of the configuration of plates in a screening experiment two modes of XRPD are possible – reflection and transmission. In the reflection-mode the source and detector are positioned on the same side of the plate, whereas in the transmission mode they are on either side of the sample plate. The most commonly used substrate for transmission-mode geometry is a Kaptan surface. Although Kaptan by itself does not possess any diffraction peaks, a broad amorphous background is often observed in diffraction patterns obtained in transmission geometry; but this is not a significant limitation since only peak positions and not intensity are important in the initial stages of screening. However, when the scale of screening is reduced such that only small amounts of solids are available in each well in a plate, the scattering from the amorphous Kaptan film may make peak identification challenging. In such cases sample analysis in reflection-mode can be worthwhile. Table 1 lists two XRPD options available for handling HT-screening samples.

9.09.3.3.3 Raman spectroscopy

Raman spectroscopy has evolved in some instances as the first-pass technique for analysis of hits from HT-screening.[19] This has been motivated by the specificity of Raman scattering to polymorphs. It is especially useful in those cases where XRPD results are ambiguous, especially isomorphous solvates. Solvent molecules trapped in lattices typically give strong Raman scattering signals, especially when the sample resulting from a screening experiment has been dried thoroughly. More importantly, when screening involves salts and cocrystal formers, spectroscopic methods allow for detection of these additional components in the hits. Thus it may be possible to determine whether a crystalline hit contains the coformer or if it is just another crystalline form of the free acid or base. Crystalline phases that show isomorphous X-ray diffraction patterns may display differences in Raman spectra. An additional advantage of Raman spectroscopy is the acquisition time – in most cases, this time is much shorter than a typical X-ray diffraction run. The most common mode for HT-Raman spectroscopy is backscattering dispersive optics but, similar to XRPD, transmission-mode Raman is available as well.[35]

It may also be useful to consider a combination of microscopy and spectroscopy in those cases where mixtures are suspected and specific portions of the sample need to be analyzed. This can be accomplished with Raman microspectroscopy wherein an optical microscopy image of the sample well can be obtained and specific locations in the sample can be highlighted and picked for Raman analysis. Such microscopic capabilities also allow one to obtain multiple Raman spectra from each well for purposes of reproducibility and/or mixture analysis. The other advantage of Raman spectroscopy for analysis of hits from a screening experiment is that it is relatively insensitive to preferred orientation of crystals that can arise because of overexpression of the

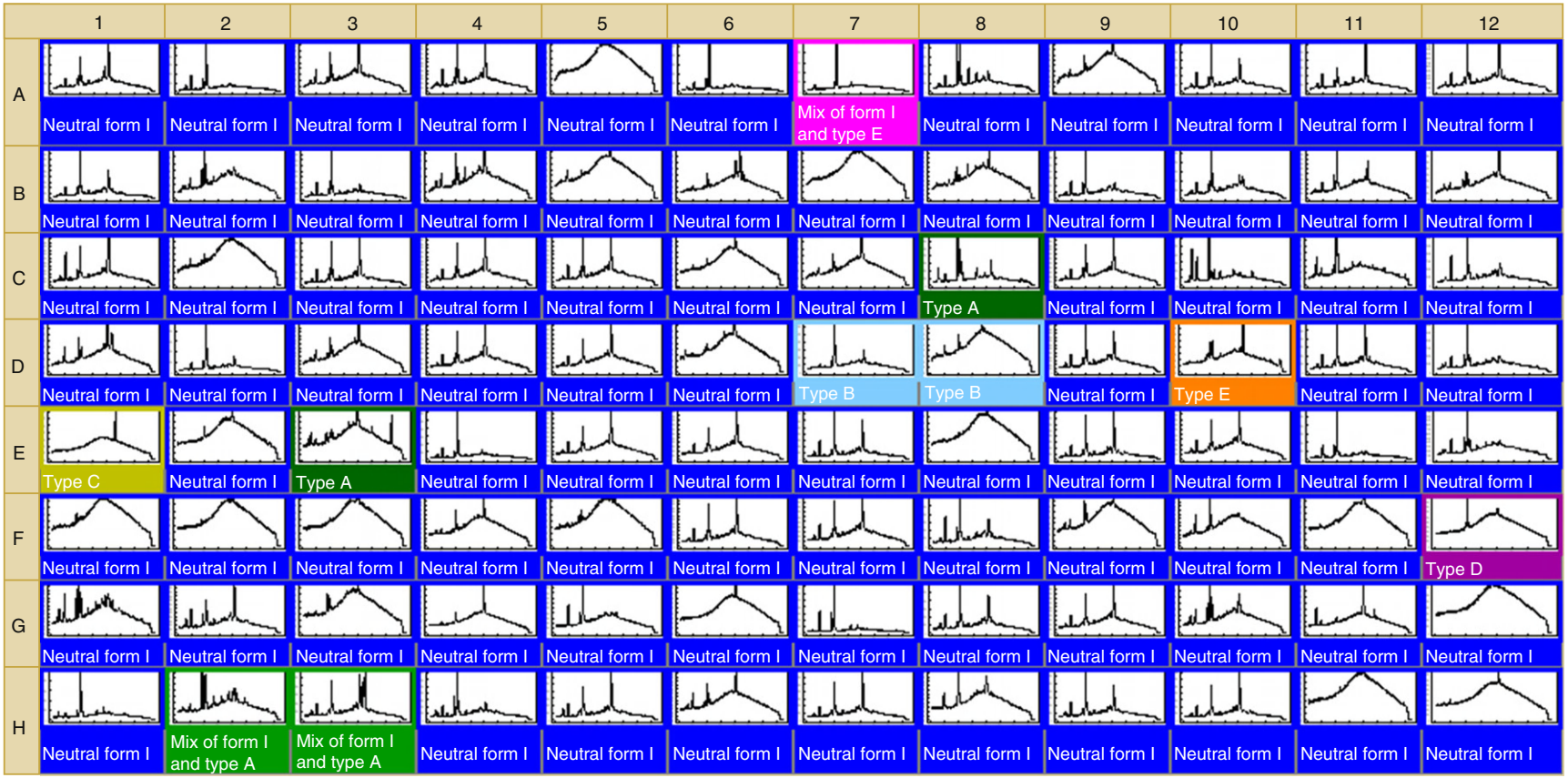


Figure 16 HT-X-ray diffraction data on the same well plate as shown in **Figure 15**. The text at the bottom of each image refers to nomenclature associated with each unique phase discovered in the screen.

Table 1 Examples of X-ray diffraction units with associated details

X-ray diffraction	*Model*	*Mode*	*Detector*	*HT-software platform*
Bruker	D8 Discover with GADDS	Transmission and reflection	Hi-Star	PolySNAP
Panalytical	Empyrean	Transmission and reflection	PIXcel^{3D}	HighScore Plus

scattering from certain crystal planes because of the high aspect ratios of crystals. Some examples of commercially available Raman instruments are listed in Table 2.

Table 2 Examples of commercial Raman scattering instrument platforms

Raman spectroscopy	*Model*	*Mode*	*HT-software platform*
Horiba	AccuRA	Transmission	LabSpec, KnowItAll®
Kaiser	Raman WorkStation	Transmission	Holo Map/HoloWell
ThermoFisher	DXR SmartRaman Spectrometer	Backscattering	OMNIC Array
Bruker	MultiRAM	Backscattering	OPUS

9.09.3.4 Other Considerations in Salt and Polymorph Screening

9.09.3.4.1 Solubility information

Any crystallization involves solubilizing the compound of interest in a suitable solvent at sufficient concentrations followed by precipitation using either antisolvent or temperature. It is often helpful to determine the solubility of the compound of interest in a wide solvent range to help with the design of suitable screens. Although the very nature of HT-screening implies the unrestricted use of tens of solvents, solubility measurements can help to focus the screen to a smaller subset of solvents to maximize the chances of getting a crystalline hit. Several methods exist for generating solubility data quickly for drug molecules – experimental, computational, or a combination of the two. Software platforms such as ASPEN[36] enable the prediction of the solubility of drugs in various solvents and solvent combinations using experimental data on less than five solvent systems. These predictions can be used as a guide to design screens.

One of the fundamental challenges facing HT-screening of crystal forms of drugs is the highly stochastic nature of nucleation. Despite several efforts it has not been possible to determine the reason why certain molecules crystallize relatively easily compared with others. In addition to any inherent crystallization propensity of molecules, several other environmental factors could affect nucleation such as surfaces of high energy, foreign particles, impurities, mechanical stress, and small temperature fluctuations. It is sometimes possible to take advantage of some of these aspects in modifying or broadening crystallization screens. However, given the chemical and conformational diversity of molecules it has been impossible to guarantee that a HT-screen will be able to identify all possible crystalline forms of a drug substance. Some recent examples where researchers have used a variety of templates to nucleate crystalline forms are discussed later in Section 9.09.3.6.

9.09.3.4.2 Optimizing screen design to meet the product profile

When designing screens to identify salt forms of a drug, it is important to have a perspective of the disease area and/or indication that the drug is being targeted for. Downstream formulation approaches can be developed to mitigate any potential drawbacks in the inherent properties of the solid phase of the drug. A classic example in this case is the need for a drug to remain solubilized across the physiological pH range (typically pH 3–7). This is often a requirement for HIV or oncology drugs wherein many patients on these drugs are also achlorhydric (higher stomach pH than normal). In such cases form screening could focus on discovering acid salts of drugs which when formulated appropriately may be able to overcome absorption issues at higher pH. In the case of indinavir salt screening focused on acid salts and ultimately a sulfate salt of indinavir was discovered and used in the product Crixivan.[1]

Another example of judicious screening and avoidance of particular counterions is in intravenous delivery of drugs. In such cases one should avoid screening for potassium salts. In the past several years, combination products involving multiple drugs in the same dosage unit are being developed. Counter-ion compatibility between the individual component drugs in the formulation should be a significant consideration in such cases. For example if one of the drugs in the product is already a basic salt, it may be advantageous to screen for basic salts of the other drug in the combination to mitigate any potential incompatibility and counter-ion exchange between the two drugs.

Finally a short list of counterions is provided in Tables 3–6. A more comprehensive listing is available in Stahl et al.[25]

9.09.3.4.3 Purity of the source material

Impurities can affect crystallization in numerous ways. The most obvious one is by affecting the solubility of the drug in the solvent. In general, the presence of impurities will increase the solubility of drugs in organic solvents. Impurities can occur on the

Table 3 List of Class 1 acid salt formers

Name	*Mw*	*pKa1*	*pKa2*	*pKa3*
Hydrochloric	36.46	−6		
Sulfuric	98.08	−3	1.92	
Phosphoric	98.00	1.96	7.12	12.32
*Glutamic(L)**	147.13	2.19	4.25	9.67
*Tartaric(+ L)**	150.09	3.02	4.36	
Citric	192.12	3.13	4.76	6.40
*Malic(− L)**	134.09	3.46	5.10	
Gluconic(D)	196.16	3.76		
*Lactic(L)**	90.08	3.86		
Ascorbic(L)	176.12	4.17	11.57	
Succinic	118.09	4.21	5.64	
Adipic	146.14	4.44	5.44	
Acetic	60.05	4.76		
Stearic	284.49	4.9		
Carbonic	62.02	6.46	10.3	
Thiocyanic	59.09	−1.33		
Glycerophosphoric	172.07	1.47	6.19	
*Aspartic(L)**	133.10	1.88	3.65	9.60 B
Maleic	116.07	1.92	6.23	
Pyruvic	88.06	2.39		
Glucaric(D)	210.14	3.01	3.94	
Fumaric	116.07	3.03	4.38	
Galactaric	210.14	3.08	3.63	
Glucuronic(D)	194.14	3.18		
Lactiobionic	358.29	3.2		
Glucoheptanoic(D)	226.18	3.3		
Hippuric	179.17	3.55		
Aceturic	117.10	3.82		
Glycolic	76.05	3.82		
Glutaric	132.11	4.34	5.27	
Sebacic	202.25	4.59	5.59	
Butyric	88.11	4.82		
Capric	172.27	4.9		
Palmitic	256.43	4.9		
Lauric	200.32	5.3		

Chiral salt formers are in italics.

Chiral salt formers with an asterisk (*) available as enantiomer.

Class 1: Physiologically ubiquitous ions.

Source: Reproduced from Stahl, P. H.; Wermuth, C. G. *Handbook of Pharmaceutical Salts: Properties, Selection, and Use*, 2nd ed.; Verlag Helvetica Chimica Acta: Zurich, **2011**; pp 265–344.

surfaces of crystals in which case they can sometimes be easily removed by several washing cycles. Impurities can also be incorporated into crystals in the forms of occlusions or as a solid compound with the main component. In the latter cases, given the tight binding of the impurity in the crystal, several heat–cool cycles may be necessary to purge the crystal of the impurity. Such impurities can affect hit-rates in screening especially when surface-adsorbed impurities impede dissolution in a dissolution-recrystallization experiment such as a slurry-screen. Detailed descriptions of the role of impurities in crystallization – kinetics, thermodynamics, and crystal shape are given in Tung et al. and Myerson.[29,31]

Conversely, the oft-cited case of ritonavir presents an interesting case study in the role played by impurities in nucleating new crystalline forms of a drug.[26] In this example it is purported that a cyclic-carbamate impurity adopts a conformation that can act as a nucleus to seed the more stable Form II of ritonavir that was discovered crystallizing out of marketed capsules. However, it should be noted that the speculative nature of this work and the difficulty in mechanistically studying such hypotheses poses complications in designing a rational screening strategy based on impurities. To minimize problems arising from impurities, compounds are generally purified before submission for a salt or a polymorph screen.

9.09.3.4.4 Inclusion of water as a solvent–antisolvent in salt screening

Choice of solvent can be crucial in designing a crystallization screen, especially in those cases where the drug has either very limited solubility or very high solubility in selected solvents. In cases where the solubility is very high in all organic solvents, it may be challenging to design a screen, especially if only limited amounts of material are available. Additionally, if the compound is difficult to crystallize, the high organic solvent solubility may result in gelation at high concentrations, resulting in difficulties in

Table 4 List of Class 2 acid salt formers

Name	*Mw*	*pKa1*	*pKa2*
Alginic	24 000	3.5	
Benzoic	122.12	4.19	
Nicotinic	123.11	4.84	2.07
Propionic	74.08	4.87	
Caprylic	144.21	4.91	
Naphthalene-1,5-disulfonic	288.30	−3.37	−2.64
Di(*t*-butyl)naphthalenedisulfonic	400.51	−3.05	−2.32
Di(*t*-butyl)naphthalenesulfonic	320.45	−2.48	
Ethane-1,2-disulfonic	190.20	−2.1	−1.5
Ethanesulfonic	110.13	−2.05	
Cyclamic	179.24	−2.01	
Ethanesulfonic,2-hydroxy-	126.13	−1.66	
Toluenesulfonic	172.20	−1.34	
Methanesulfonic	96.11	−1.2	
Dodeclsulfuric	266.40	−0.09	
Naphthalene-2-sulfonic	208.24	0.17	
Benzenesulfonic	158.18	0.7	
Oxalic	90.03	1.27	4.27
Pamoic	388.37	2.51	3.1
Glutaric, 2-oxo-	146.10	2.7	4.5
Naptholic, 1-hydroxy (2-)	188.18	2.7	13.5
Orotic	156.10	2.8	9.45
Malonic	104.06	2.83	5.70
Gentisic	154.12	2.93	
*Pyroglutamic (− L)**	129.11	3.32	
Benzoic 2-(4-hydroxybenzoyl)-	242.23	3.35	7.96
Oleic	282.47	4	
Camphoric (+)	200.23	4.72	5.83
Isobutyric	88.11	4.84	

Chiral salt formers are in italics.

Chiral salt formers with an asterisk (*) available as enantiomer.

Class 2: Lox toxicity and good tolerability.

Source: Reproduced from Stahl, P. H.; Wermuth, C. G. *Handbook of Pharmaceutical Salts: Properties, Selection, and Use*, 2nd ed.; Verlag Helvetica Chimica Acta: Zurich, **2011**; pp 265–344.

Table 5 List of Class 3 acid salt formers

Name	*Mw*	*pKa1*	*pKa2*	*pKa3*
Hydrobromic	80.91	−6		
Nitric	63.01	−1.32		
Trifluoroacetic	114.02	0.23		
Saccharin	183.19	1.31		
Acetic, 2,2-dichloro-	128.94	1.35		
Acesulfame	163.15	2		
Camphor-10-sulfonic (+)	232.29	2.17		
Salicylic	138.12	2.97	13.82	
Salicylc, 4-amino-	153.14	3.25	10	3.5
Mandelic (DL)	152.15	3.37		
Formic	46.02	3.75		
Benzoic, 4-acetamido-	179.17	4.3		
Cinnamic	148.16	4.40		
Caproic	116.16	4.8		
Undec-10-enoic	184.28	4.9		

Chiral salt formers are in italics.

Class 3: Less advisable for general use, but used in the past.

crystallization over short timescales. A judicious choice of antisolvent and temperature are important in this regard. Aqueous solubility of a drug molecule can be particularly important in salt screening. An interesting study by Tarsa et al.[37] showed that improved hit-rates could be obtained for water-insoluble drugs from solutions that included at least low levels of water in the solvent system. Conversely, organic solvents were found to improve the hit-rate for those compounds that were highly soluble in

Table 6 List of basic salt formers

Name	*Mw*	*pKa1*	*pKa2*	*pKa3*	*Class*
Potassium hydroxide	56.10	14			1
Sodium hydroxide	40.00	14			1
Magnesium hydroxide	58.32	14	11.4		1
Calcium hydroxide	74.10	12.6	11.57		1
Choline hydroxide	121.18	11			1
Ammonia volatile	17.03	9.27			1
*Arginine (L)**	174.20	13.2	9.09	2.18 A	1
*Lysine (L)**	146.19	10.79	9.18	2.16 A	1
t-Butylamine	73.14	10.68			1
Glucamine, N-methyl-	195.21	8.03			1
Hydrabamine low solubility, secondary amine	596.97	11.92	11.32		2
Diethylamine secondary amine	73.14	10.93			2
Benzathine low solubility, secondary amine	240.35	9.99	9.39		2
Ethanol, 2-(diethylamino)- Nitrosamines	117.19	9.58			2
Pyrrolidine, 1-(2-hydroxyethyl)-	115.18	9.44			2
Benethamine low solubility, secondary amine	211.30	9.41			2
Deanol	89.14	8.83			2
Tromethamine	121.14	8.02			2
Morpholine, 4-(2-hydroxyethyl)- prodrugs	131.17	7.39			2
Zinc hydroxide	99.40	14	9.64		3
Ethylenediamine	60.10	10.09	7.00		3
Piperazine	86.14	9.82	5.68		3
Ethanolamine (2-aminoethanol)	61.08	9.50			3
Dietanolamine (2,2′-iminobis(ethanol))	105.14	8.96			3
Triethanolamine (2,2′,2″-nitrilotris(ethanol))	149.19	7.82			3
Imidazole (1H-)	68.08	6.95			3

Chiral salt formers are in italics.

Chiral salt formers with an asterisk (*) available as enantiomer.

water. This is because of the changes in pKa of the compounds and counter-ions as a function of solvent or water content in mixed solvent systems.

9.09.3.4.5 Temperature effects

Although a systematic study of the influence of temperature on hit-rate in screening across multiple types of drug molecules has not been conducted, there are some logical considerations worth noting. Temperature cycling of slurries resulting in several cycles of dissolution and recrystallization may result in conversion of the starting crystal phase into other crystalline phases – typically more stable in nature. There are obvious caveats to this theory – two of the most common being (1) the rate of nucleation of the most stable phase may be much higher than that of the metastable phase and (2) ambiguities about interpreting this rule in situations where solvates crystallize from the cycling experiment. It is interesting here to note the analogy to simulated annealing. This *theoretical* concept is often used in molecular modeling to search for different packing arrangements of molecules in crystal lattices – the so called predictive methods for polymorph discovery. The concept originated in metallurgy where annealing involved the heating and cooling of crystals such that on heating atoms are coaxed to move from their original positions to occupy higher states of energy and the subsequent cooling induces them to localize into regions of lower free energy than the starting configuration. An illustration of this is shown in Figure 17.

The reaction coordinate can be any parameter that changes along a transformation pathway such as a torsion angle or a packing conformation (e.g., dimer). Phases A, B, and C represent viable crystalline phases that can be isolated in a screen. In the overwhelming majority of cases, Phase C will be preferred on account of it having the lowest free energy and hence highest stability. A polymorph screen may result in discovering any of these phases; an effective polymorph screen will be able to identify Phase C as one of the hits. The tricky – and hence interesting – aspect of this is that there is no deterministic way of knowing the *complete* energy landscape for a given molecule, hence the need to rely on a multitude of experiments. HT-screening goes a long way in satisfying this condition – but it is impossible to guarantee that the crystalline phase corresponding to the global minimum has been identified in each and every case.

The complexities and challenges inherent in polymorphism and screening in particular is amply demonstrated by the purported discovery of a second polymorph of aspirin – Form II, in 2005 by Zaworotko et al.[38] and later substantiated by Desiraju et al.[39] – that was hitherto unknown in the experimental domain but had hints in earlier theoretical work.[5] Given that aspirin was discovered sometime in the nineteenth century it is amazing that alternate crystalline packings are still being discovered for this molecule. Similarly, ritonavir was shown to have additional crystalline phases in 2003 by Morrisette et al.[40] However, in general more stable polymorphs are rarely discovered in later screens.

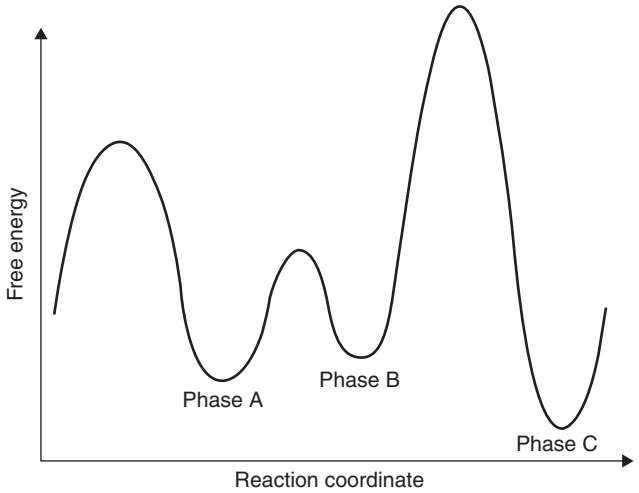


Figure 17 Energy landscape of crystalline phases for a hypothetical molecule. In reality, the reaction coordinate can be n-dimensional. It is restricted to 1-dimension in this schematic for ease of visualization. The minima in the curves correspond to basins where individual crystal forms can be found. For a given molecule, multiple minima can exist. The number of these minima are unpredictable.

9.09.3.5 Thermal Methods for Discovering New Phases

Thermal treatment such as storing materials isothermally or subjecting materials to varying heating and cooling rates is a method that is useful for discovering and isolating new crystalline phases. Two previously undiscovered polymorphs of highly polymorphic 5-methyl-2-[(2-nitrophenyl)amino]-3-thiophenecarbonitrile (ROY) evaded discovery from solution-based crystallization experiments and were discovered by direct crystallization from the melt and a direct solid-to-solid transition.[41] Hot-stage optical microscopy and DSC are often used to conduct these types of thermal treatment experiments. DSC is of particular usefulness in that it affords excellent control over temperature as well as heating and cooling rates, whereas monitoring heat flow in and out of the material being studied to determine if a phase transition occurred. New crystalline phases are discovered on occasion during initial characterization by DSC of materials isolated from solution crystallizations. Scale up of these newly discovered crystalline phases is often achieved on a gram scale using common laboratory vacuum ovens to provide sufficient amounts for additional characterization as well as seed material for solution based crystallization experiments.

There are a few mechanisms by which materials can be converted to new crystalline phases using thermal treatment including direct crystallization from the melt, solid-to-solid transitions, and desolvation of solvates. Direct crystallization from the melt by cooling is the most straightforward and offers one significant advantage over solution-based crystallizations in that the melt provides the highest degree of supersaturation possible when cooled below the melt temperature. The melt provides a system in which the material is dissolved in itself with the concentration being the density of the molten state. There is no solvent to dilute the material such that on cooling, crystallization can occur. Although direct crystallization from the melt is useful from a perspective of discovering new crystalline phases, there are a number of drawbacks such as high viscosity, scalability, and lack of impurity rejection when compared with solution crystallization that limits direct crystallization from the melt from being used to deliver large batches of a desired crystalline phase of a drug.

A solid-to-solid transition from one crystalline phase into another without going through the melt is another mechanism by which thermal treatment of a material results in a new crystalline phase. This mechanism involves a direct rearrangement on a molecular level of the molecules in the crystal lattice of the starting form to a new polymorph of the material. These solid-to-solid transitions can be reversible or irreversible depending on the thermodynamic relationships of the two polymorphs as well as the rate at which these two polymorphs can interconvert. These solid-to-solid transitions can be detected by DSC and in some cases materials that undergo these types of transitions have been used in DSC calibrations.[42]

Desolvation of a crystalline solvate is another route to new crystalline phases using thermal treatment. This applies to crystalline hydrates as well since crystalline hydrates are solvates where water is the solvent molecule incorporated into the crystal lattice instead of organic solvent. Desolvation on heating under a sweep of inert gas or dynamic vacuum to remove the solvent molecules from the system can be a direct pathway to a new crystalline phase. An alternate pathway to a new crystalline phase can be achieved through the collapse or melt of the desolvated structure into a melted state which can then directly crystallize from the melt into a new crystalline phase as previously described. Desolvated crystalline solvates, and especially dehydrated crystalline hydrates, can be hygroscopic and absorb water from ambient humidity to produce crystalline hydrates.

9.09.3.6 New Approaches in High-Throughput Crystal Form Screening

This section focuses on novel methods for high-throughput screening for crystalline phases that go beyond the usual slurry, heat–cool, evaporation, cooling, and antisolvent precipitation. Before delving into some of the newer literature in this area it is

instructive to consider the illuminating article by Bernstein, 'Cultivating crystal forms,' published in 2005. Bernstein highlights the case of ROY, a compound discovered at Eli Lilly that holds the current record for the maximum number of 'true' polymorphs, nine in total so far.[41] The interesting point here is that the ninth form of ROY is the second-most stable form of this compound and was the last discovered chronologically. Yu et al. also comment that they are not convinced all possible polymorphs of ROY have been discovered yet. This raises the possibility that increasing the diversity of screening and also the total number of experiments may result in the discovery of additional crystalline forms of molecules and may have been the motivation for a burst of activity in the past 10 years or so in new methods and platforms for high-throughput polymorph screening. Some general characteristics of such screening that complements earlier versions of HT-screening include: (1) chemical templating, (2) modulating mixing mechanisms, and (3) influencing nucleation through geometry and epitaxy. However, although it is attractive to think about a mechanistic basis for nucleation in HT-screening, it is not clear whether hits that are obtained in screens are driven explicitly by one of these mechanisms.

The use of polymers as nuclei for the crystallization of organic molecules was discussed by Lang et al. in their work on acetaminophen.[43] Various polymers with diverse chemistry were loaded onto 96-well plates and acetaminophen solutions added to these wells. Following heating and subsequent cooling, the solutions were allowed to slowly evaporate in the presence of the polymers. Different polymorphs of acetaminophen were observed in different wells including the orthorhombic polymorphs which could not be isolated without polymers in a control study carried out simultaneously. Subsequent work in 2005 by the same group showed that this method could be robustly adapted to an HT-screening format and was successful in discovering one new form of carbamazepine and two new forms of sulfamethoxazole.[22] Given the diversity of polymers used in these studies and relative promiscuity of hits in wells it has not been possible to ascribe a mechanistic basis for nucleation of one form versus the other.

Lee et al. describe a method using self-assembled monolayers to nucleate crystalline forms.[21] The fundamental basis for this seems to be restricting the domain size available for nucleation and crystallization. This was implemented in a HT fashion. Hydrophilic gold islands surrounded by hydrophobic regions are created whereby wetting can be modulated leading to the formation of droplets. It is not clear from this study that chemical specificity of the monolayers influenced the crystallization of different polymorphs of glycine. The emphasis instead was on confining crystallization to produce small crystals and also accessing high supersaturation regimes that drive nucleation and growth of metastable forms. Later that year, Hiremath et al.[23] published some work 1,3-bis(m-nitrophenyl) urea (MNPU) that underscores potential selectivity in polymorphism. MNPU suffered from concomitant polymorphism – crystallization of multiple polymorphs simultaneously from solution, specifically the α- and the β-forms. Using gold-thiol self-assembled monolayers of substituted 4′-X-mercaptobiphenyls (X=H, I, Br), selective nucleation and growth of α-, β-, and γ-forms of MNPU were observed. This selectivity has been ascribed to two effects: (1) long-range 2D lattice matching and (2) local complementary chemical interactions at the self-assembled monolayer/crystal interface. Several years later, Alvarez et al. in an article compared the 'productivity' of semiautomated screens versus HT-screens using self-assembled monolayers and concluded that increasing the number of experiments could indeed improve hit-rate in those cases where the molecules are highly polymorphic.[44]

In early drug development, supply of compound may be limited. To address this, further scale-down of HT-screening may be necessary. The first steps toward this was addressed by the work of Thorson et al.[24] in using a microfluidic platform based on polydimethylsiloxane with 48 individual wells for salt screening of some model compounds such as ephedrine and naproxen. Using microfluidics it may also be possible to control the range of supersaturation by modulating mixing conditions. Each well in this chip has a volume of 87.5 nl. Individual chambers and feedlines are isolated by valves that are opened by the application of pressure. Each well acts as a reactor into which salt-former and compound solutions are fed in and crystallization and salt formation occurs within these wells. Analysis of solids is accomplished by microscopy and Raman spectroscopy. Although solvent absorption by the substrate was minimized by reducing the thickness of the polydimethylsiloxane layer, the list of solvents that was used in the screening was limited to alcohols. It is anticipated that additional technical developments including alternate substrate materials may be required before wide application of microfluidics to expanded salt and polymorph screening including a wider range of solvents.

9.09.3.7 Prediction of Crystal Forms

Predicting polymorphs has remained a very challenging area owing to various reasons:

1. Complex chemical and conformational structure of organic molecules coupled with limitations of current calculations to relatively lower molecular weight species;
2. Complexities in the nature and extent of nonbonded interactions that exist amongst molecules in the crystal lattice;
3. Presence of ionized species and the associated long-range electrostatic interactions such as in salts;
4. Relatively small energy differences that can exist between polymorphs, especially when these are of the same order of magnitude as the accuracies of typical force-fields used in molecular modeling; and
5. Costly computational time associated with *ab initio* calculations utilizing quantum mechanics as opposed to force-field based molecular mechanics approaches.

In spite of these limitations, there are scattered efforts on improving polymorph predictions based on hybrid approaches using molecular mechanics, quantum mechanics, and DFT which will be discussed in this section.

Without considering the historical developments in the field of polymorph prediction, we will limit ourselves to the state-of-the-art. A number of different types of modeling approaches can be used for structure prediction. The most common ones are simulated annealing, genetic algorithm-based methods, and topological modeling methods. For molecular crystals, the most successful of these methods has been a hybrid approach using DFT supported by Van der Waals energies. It is not an exaggeration to state that if a force-field approach is to be used, then it has to be tailor-made for each and every molecule in the current state of modeling.

It is useful to ask the question – how would prediction of crystal forms be useful in drug development? If one assumes that such predictions are successful then there are two possible approaches that can be taken – one more practical than the other. If a high-throughput screening experiment has already been conducted then it should be possible to compare the most stable polymorph generated by the experimental approach with that tagged as the lowest lattice energy form from simulations. A match in these two structures implies that the most stable form has been found experimentally and hence the risk of a phase conversion over time or on processing and/or storage will be nonexistent. If, however, the energy of the predicted lowest energy form is very different from that of the experimentally determined form, additional screening work may be needed. The obvious complexity here is that it may be impossible to design a crystallization experiment(s) just from a knowledge of the predicted structure, since solvent, temperature, and kinetic aspects are very difficult to predict.

A classic example of experimental discovery of a crystal form of an organic molecule following the prediction of the same structure is 5-fluorouracil described by Woodley and Catlow.[45] Predictions using a combination of MOLPAK which generates hypothetical densely packed structures and another program called DMAREL that minimizes these structures, showed a previously unknown low energy polymorph of the compound. This particular form of 5-fluorouracil displays a doubly hydrogen-bonded synthon (cf. Figure 18).

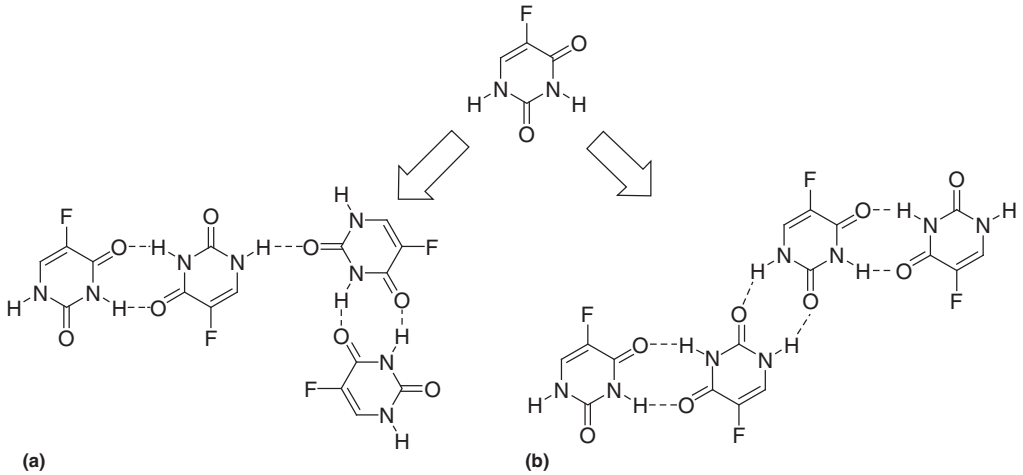


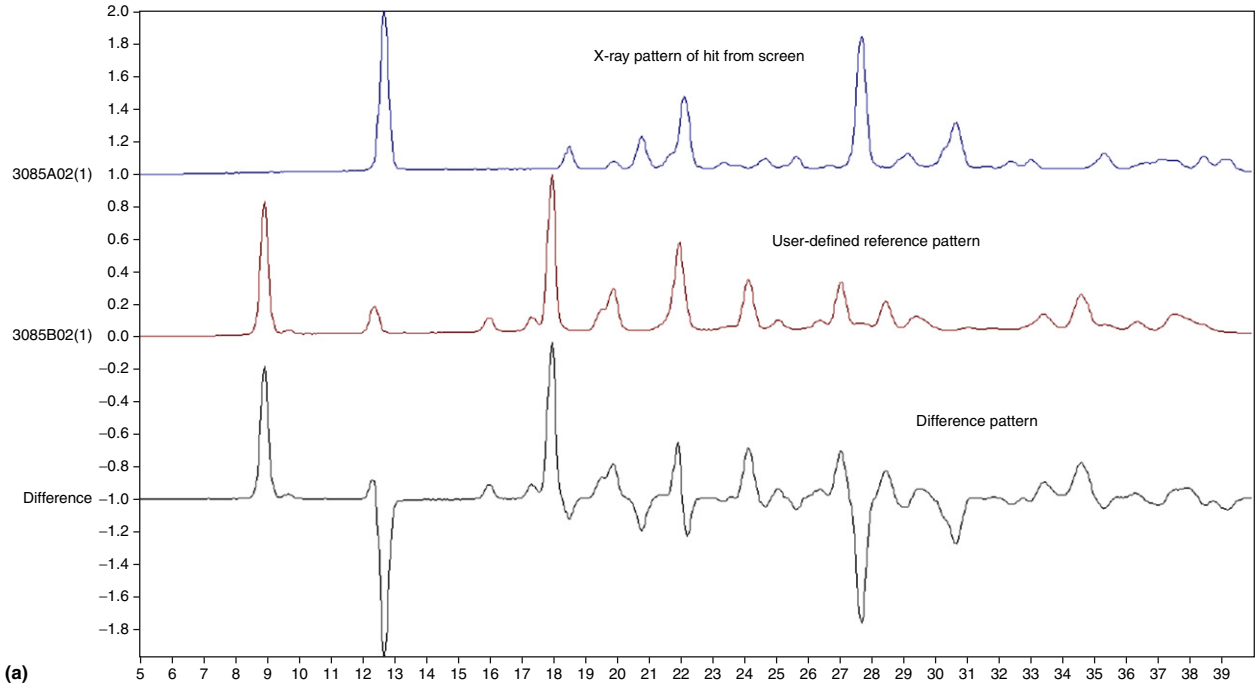
Figure 18 5-Fluorouracil and the polymorphs it crystallizes into with only hydrogen-bonding patterns: (a) Form I and (b) Form II.

Follow-up work by the same authors utilizing molecular dynamics simulations of the compound in various solvents showed that a similar hydrogen-bonded motif could be generated in a solution of nitromethane. Based on this information, crystallizations were attempted in dry nitromethane and the Form II of 5-fluorouracil was observed to nucleate and grow. Although this result is a wonderful example of how theoretical predictions can nicely supplement high-throughput approaches, it represents a rare case of simulations guiding experiments. 5-Fluorouracil is a relatively small and simple molecule with few conformational degrees of freedom. Because of the presence of hydrogen-bonding groups, it is possible to intuitively construct various synthons and use these to rationally explain and design experiments. However, in reality, interactions are often very subtle. Nonhydrogen-bonded packing interactions such as dispersive, CH–π, π–π, dipole–dipole, and dipole-induced dipole are often very important in determining low energy crystal packing configurations. When such interactions predominate in crystal structures, it is not only challenging to predict these structures, it may also be more difficult to design crystallization conditions that can actually reproduce the predicted structure if this were indeed achieved.

9.09.3.8 Data Analysis in HTE

HTE often results in immense amounts of raw data. Frequently, several rounds of screening may be needed for a particular molecule – a salt screen followed by a polymorph screen on promising salt hits and additional screens to ferret out stable forms or forms that are relevant to processing conditions. Raw data from such screens are usually collected from multiple instruments and could first be sorted into groups based on (1) user-defined correlations, (2) user-defined reference patterns, or (3) some predetermined similarity measure. There is the capability to load data from entire libraries or from individual experiments and this

program can handle very large volumes of data in the process. An example of such a comparison and sorting is shown in Figure 19(a) and (b). Such classification then allows the user to bucket the wells according to the crystal form and enable identification of unique crystalline phases. If needed, solids can be isolated from representative wells belonging to each group, for use in manual seeded growth experiments.



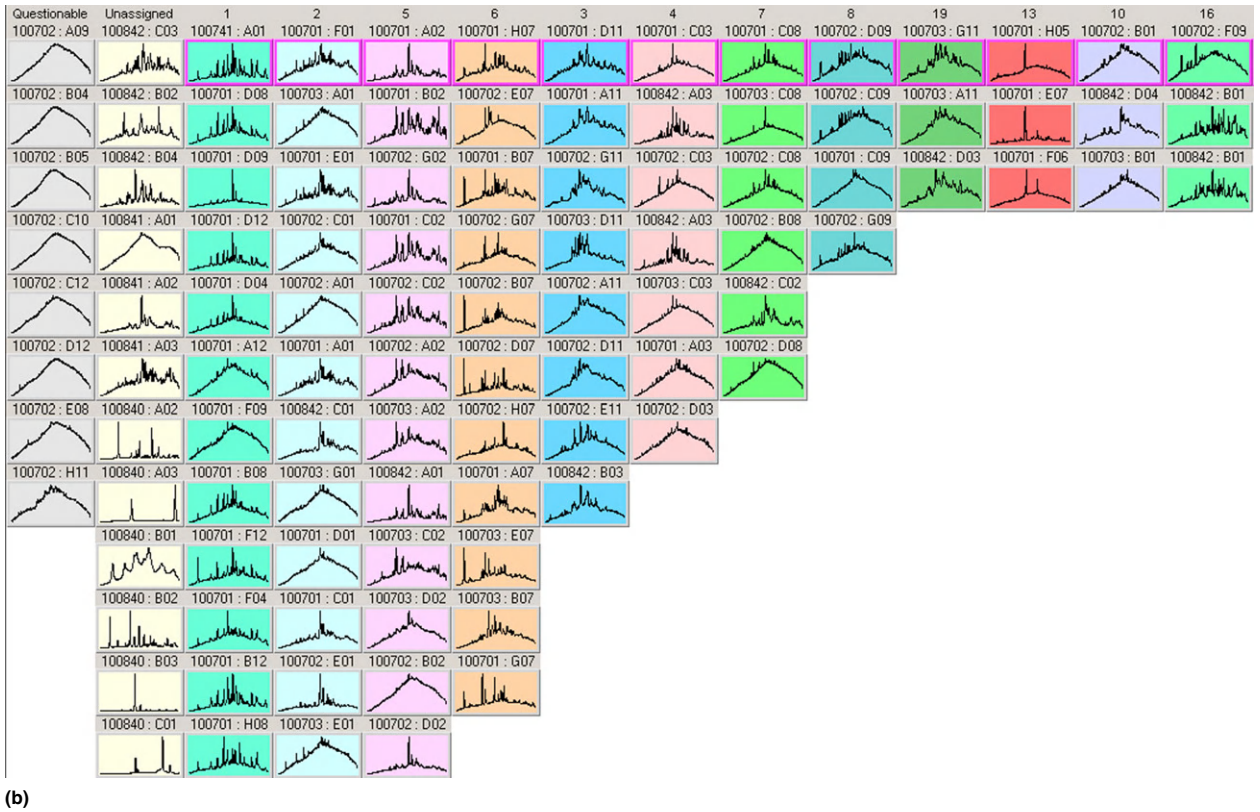


Figure 19 (a) Comparison of X-ray patterns from the screen with user-defined reference patterns. (b) Sorting of X-ray diffraction patterns in groups based on predefined criteria.

9.09.4 Purification of Drug Molecules

In the pharmaceutical industry, separation of the API from process impurities is generally achieved via solvent mediated crystallization or by use of a chromatographic purification step. Chromatographic methods are generally implemented more frequently on gram to low kilogram scale because of the increasing availability of laboratory scale preparative instruments as well as an increasing breadth of stationary phase resins. With chromatographic separation, theoretical recoveries of API can be 100%. In reality, practitioners may accept lower yields to gain time and/or throughput efficiency. Crystallization as a purification method, in contrast, requires no specialized hardware or resins but practical yields will be limited by a combination of the solubility difference between the API and the impurity being purged and the overall impurity reduction required to achieve target specification. An example of the power of purification by crystallization is seen with the commercial production of artemisinin, an antimalarial drug. Artemisinin is a naturally occurring compound in the Chinese medicinal herb *Artemisia annua* that is present at an estimated 0.8–1% in the dry plant.[46] Manufacturing facilities in China and Vietnam have traditionally isolated artemisinin from extraction streams via a series of multiple crystallizations.[47]

Isolation of APIs from synthetic process streams via crystallization is the most common method implemented across the pharmaceutical industry.[48–57] Synthetic intermediates may be crystallized directly or as a salt if the compound has an acidic or basic moiety and the strategy will depend on the complexity of the crystallization and the purification requirements of the processing step. In pharmaceutical processing, often the final API crystallization step is more focused on targeting a set of well-defined physical attributes of the solid API (crystal morphology and habit, particle size, surface area, etc.) rather than purification of the compound. Generally, the physical attributes are of critical importance in determining bulk properties such as dissolution characteristics, powder flow, etc. However, just before the final 'attribute setting' crystallization step, an initial crystallization of the crude API stream will often be performed to improve the purity of the batch and ultimate usage of the material for research or commercial purposes. If process impurities can be controlled either upstream in the API synthesis or by a suitably robust final isolation process then the crude and final steps may optimally be combined into a single crystallization step to set both the final compound purity and API physical attributes.

Developing a suitable crystallization to purify a synthetic intermediate or API is traditionally the laborious and iterative process of measuring the solubility of the compound and related impurities in a variety of solvents and solvent combinations as a function of temperature and solvent ratio. This manual 'screening' of conditions often can take weeks or even months to develop an efficient and robust set of conditions and can require tens of grams of compound or more to complete. Although the early implementation of automation in pharmaceutical process R&D can be traced to the early 1990s with Botteger's work at Bristol-Myers Squibb[58] on screening catalysts for a Pd-catalyzed coupling reaction, reports on the implementation of automation for crystallization process development did not start to show up in the literature until about a decade later.[19,59–67] Not surprisingly, though, these reports are almost exclusively focused on the discovery of crystalline phases of the API and the subsequent form selection process. The specific application of automated crystallization toward the goal of compound purification, however, was not reported until just a few years ago. In 2008, Tan and coworkers disclosed the development of a high-throughput screening workflow in a 96-well array format specifically designed to identify suitable conditions for the purification of process intermediates via crystallization or trituration.[5] The compound solubility and overall purity was then determined via HPLC analysis. This approach is particularly attractive as it enables rapid and parallel evaluation of a range of solvents and solvent mixtures. It is not uncommon to observe enhanced solubility in a binary solvent mixture versus either pure solvent and therefore, evaluating a broad range of solvent combinations and ratios can quickly enable the scientist to identify those unique conditions that enable the maximum separation efficiency while maintaining respectable yield. In Tan's report, whenever a binary solvent system was identified as a potential hit, a follow-up screen was executed to refine the lead condition and understand the gradient effect of each component.

Key to this success, however, is the utilization of representative process samples that contain the specific impurities in roughly the same amounts that they will be present during scale up. The reason for this is that the solubility of the compound of interest can be often enhanced by the very presence of the impurities needing to be purged. This phenomenon is illustrated quite nicely in the same report. The solubility of pure acetyl salicylic acid and in toluene at 25 °C is 2.1 mg ml^{-1}. However, the introduction of salicylic acid as a second component in the system results in a marked increase in the acetyl salicylic acid solubility by more than threefold to a maximum of 7.0 mg ml^{-1} when the system is saturated with salicylic acid at 10.5 mg ml^{-1}. Although this may seem an unlikely occurrence in a real processing scenario, the desire to minimize solvent usage and maximize crystallization yield generally will drive process design toward higher solute loadings thereby enhancing the potential impact of impurities on the solubility of the main component. Finally, the presence of even small amounts of certain impurities can have substantial effects on nucleation, morphology and growth kinetics which has been reviewed in detail by Meenan et al.[6]

Utilizing the salicylic acid/acetyl salicylic acid mixtures as a test case and a second test case with a proprietary Amgen compound containing several process impurities, Tan et al. demonstrated that a set of conditions suitable for further optimization could be identified with good reproducibility utilizing their screening methods.[5] To speed up the development of clinical drug candidates, identifying this design space must be achieved in days and weeks rather than months and also on a smaller scale than historically allowed. This type of work is typically followed up with more detailed experiments to map out the design space for isolation and purification to meet commercial-scale process needs.

An example of leveraging a suitably tuned crystallization process to enable purification of a synthetic intermediate was provided by Hansen et al. at Merck while working on Aprepitant, an NK-1 receptor antagonist used for the treatment of

chemotherapy-induced emesis.[68] In the synthetic sequence, (R)-alcohol **1** was prepared via a transfer hydrogenation step to provide the intermediate in 90% enantiomeric excess (*ee*) (cf. Figure 20). Removal of the undesired (S)-alcohol and upgrade of the *ee* was required before further processing to the API. Both the pure enantiomers and the racemate of alcohol **1** are crystalline; however, the solubility of the racemate is significantly lower (21 mg g^{-1} heptane at 21 °C) than the pure enantiomer (52 mg g^{-1} heptane) making it very difficult to achieve rejection of a large portion of the undesired (S)-alcohol without taking a large yield hit on the desired (R)-alcohol.

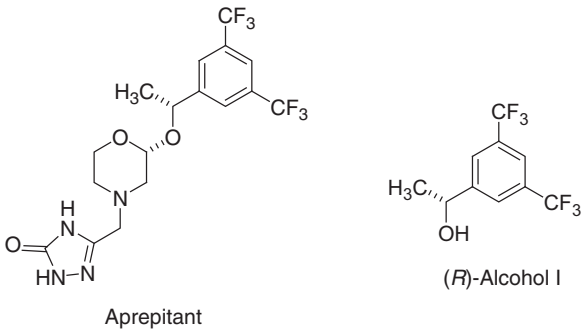


Figure 20 Molecular structures of Aprepitant and the (*R*)-Alcohol (**I**).

Based on literature precedent from Toda with structurally similar secondary alcohols,[69] the Merck team discovered that the enantiomerically pure alcohol forms a 2:1 cocrystal with 1,4-diazabicyclo[2.2.2]octane (DABCO). Encouraged by this, the team designed a crystallization process to isolate enantiomerically pure **1** in good yield. However, it was subsequently discovered that the racemic alcohol also forms a 2:1 cocrystal with DABCO with lower solubility (16 mg g^{-1} solvent vs. 20 mg g^{-1} solvent at 0 °C in the mother liquors). The crystallization process was subsequently modified to ensure that all of (S)-**1** present potentially as the racemic cocrystal would remain dissolved throughout the isolation. Ultimately, crystallization of the enantiopure DABCO complex allowed for isolation of the (R)-alcohol on multi-kg scale in >99% *ee* from the process stream (92% *ee*) after only a single crystallization in heptane. This example highlights the need for having a full working knowledge of all phases (polymorphs, solvates, hydrates) of the compound being crystallized in order to develop a truly robust process (Figure 21).

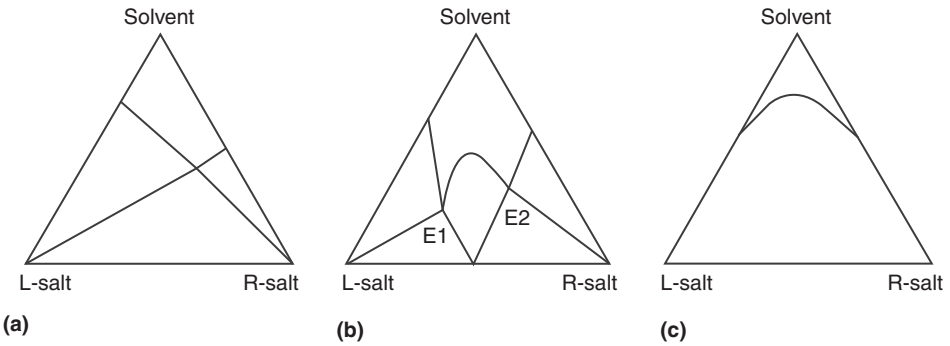


Figure 21 Types of phase diagrams for diastereomeric salts. From left to right – cases of a (a) conglomerate, (b) multiple eutectics, and (c) solid solution. Of these, direct separation of pure enantiomers by crystallization is possible only for conglomerates as they simply represent physical mixtures of the two.

9.09.5 Enantiomeric Purification

Enantiomeric purification is the separation of racemic compounds into optically pure enantiomers. Many drugs are chiral in nature and optical purity is often necessary for target engagement. There are many ways to enhance the optical purity of organic molecules – classical resolution through formation of diastereomeric salts, chiral chromatography, kinetic resolution, and enzymatic resolution. One of the most efficient ways to resolve racemic compounds is through the formation of a disatereomeric salt of one of the enantiomers of the racemic compound with the resolving chiral agent. A typical example is the formation of a salt between an amine of a specific enantiopurity and a chiral carboxylic acid. Often two diastereomeric salts with different physicochemical properties such as solubility are formed and can be separated by fractional crystallization. It is preferable to conduct this crystallization under equilibrium conditions rather than relying on kinetic control of crystallization. This is possible

because the solubility of the diastereomeric salts formed with opposite enantiomers is usually very different – as opposed to the solubility of the pure enantiomers which are identical.

Diastereomeric resolution hence becomes similar to salt screening with the restriction that the counterions be chiral and enantiopure. Also unlike conventional salt screening, successful resolution depends on the types of resolving agent, molar ratio of resolving agent to racemate, and racemate concentration, in addition to the typical variables of solvent type and temperature. It is sometimes difficult to predict whether an enantiomer will form a salt with a resolving agent because it is beset by the same challenges as salt formation especially if the pKa of the acid and base are close. In addition to this issue a critical problem is that it is impossible to predict *a priori* the solubility difference between the two diastereomeric salt pairs. This is important because the higher the solubility difference, the greater is the potential to perform the resolution under thermodynamic conditions. Thus resolution efficiency is directly related to this solubility difference and finding an optimal resolving agent requires screening of various chiral salt formers with the pure enantiomers, which may or may not be accessible.

Effective diastereomeric resolution depends not only on solubility differences between the salts but also on the nature of the phase diagram (two diastereomers and a solvent). The three types of phase behavior that can occur are: (1) formation of the diastereomeric salt, (2) solid solutions with varying compositions of the acid and base in a single crystalline lattice, and (3) a simple eutectic.

It is obvious that the formation of a diastereomeric salt represents the best scenario for effecting a separation of pure chiral isomers. In addition to the simple phase behavior shown here, complexities may arise if the molecules form solvates or hydrates. In such cases, the phase diagram has to be appropriately modified to take into account the solubilities of these species.

Despite many approaches such as analysis of crystal structure data of the diastereomeric salts, lattice energy differences and empirical correlations, classical resolution remains a highly empirical science. A completely rational approach to classical resolution would involve the construction of ternary phase diagrams (assuming the solvent is treated as a single component), and subsequent identification of optimal conditions for carrying out the resolution with maximum efficiency. However, given the diversity in acidic or basic resolving agents available, an initial screen of such agents in a high-throughput manner could provide a beneficial first step in developing an optimized resolution process. A combinatorial method affords the possibility of trying out tens of salt formers under multiple solvent conditions and, potentially, temperatures. Based on the result of this screen, a shorter list of resolving agents can then be targeted for carrying out larger scale resolutions. This approach, also referred to as Dutch resolution, was espoused in the work of Vries et al.[70] where the authors added a family of resolving agents at one time to the mixture to be separated. The rationale was that this could cut down the time required to try out one agent at a time and also the separation might be enabled by the crystallization of the least soluble diastereomeric salt. For more than 200 cases such an approach resulted in the production of a crystalline diastereomeric salt of high enantiopurity and yield. Additionally, the precipitate contained more than one component of the mixture of resolving agent as confirmed by ^{1}H NMR and chromatography. However, repeated crystallizations were necessary to obtain a stoichiometric salt with a single resolving agent. The yield of this method depends on the use of a 'family' of resolving agents and not just random mixtures. Some examples of such families include (1) dibenzoyl tartaric acid, di-*p*-toluoyltartaric acid and di-*p*-anisoyltartaric acid and (2) mandelic acid, *p*-methylmandelic acid and *p*-bromomandelic acid. Employing such an approach in industry can be greatly facilitated by the HT-screening approach wherein stock solutions of the families of resolving agents are made and then dosed into wells containing the mixture of enantiomers. Scientists at Amgen have developed an approach wherein racemates are dosed using solid-dispensing units to a 96-well plate and standard solutions of various resolving agents are added at the appropriate molar ratio to these wells.[71] Crystallization is carried out in these 96-well plates using temperature, stirring, and/or antisolvent addition followed by subsequent analysis of the solids in the wells by microscopy and X-ray powder diffraction. HPLC can be used to measure the enantiopurity of the solid isolated. This screening approach allows one to select and subsequently scale up the conditions that produce the highest enantiopurity.

It is also possible to couple a high-throughput DSC approach to either prescreen or add to the 96-well plate crystallization screen. Dyer et al.[72] describe an automated DSC procedure originally established by Collet et al.[73] wherein binary phase diagrams are obtained starting from the 1:1 diastereomeric salt mixture. The advantage with this approach is that it is restricted to the solid-state precluding the need for solvents. Additionally it also precludes the need for pure starting materials. A 'desired' DSC thermogram will show two endotherms – the first corresponding to the eutectic melt and a second endotherm corresponding to the melting of the remaining diastereomeric salt. Libraries of resolving acids and bases can be stored in microtiter plates and used as needed when a resolution needs to be performed. This highly automated process aided by thermal analysis could very efficiently drive the process of chiral resolution.

9.09.6 Perspectives

With the advent of high-throughput crystallization screening and analysis, it has been possible to conduct even more experiments in parallel than at any preceding time in the history of drug development. The resulting increase in productivity has allowed multiple crystalline forms to be discovered early in development, while enabling optimization of crystallization through impurity rejection and allowing for rapid access to pure enantiomers through high-throughput classical-resolution. Future possibilities include the development of diverse mechanisms for form discovery that can be automated as highlighted by the recent examples of microfluidics, self-assembled monolayer templates and functionalized polymer surfaces among other platforms. In the absence

of a robust, reliable computational method for predicting crystal forms, it is expected that high-throughput screening will continue to drive efficiencies in salt and form discovery in drug development. One of the biggest benefits of HT-screening for crystalline phases is the discovery and identification of solvates that could be crucial in informing process development risk. This outcome of crystallization screening is seldom highlighted in publications, but is apparent to chemists and engineers developing synthetic processes who find themselves isolating the API with solvent included in the lattice. As pointed out in the case study on polymorph screening, early identification of solvates can very effectively drive solvent selection in processing. HTE can also enable the design of focused crystallization conditions especially when these screens are expanded to incorporate specific heating and cooling protocols.

The application of HT-screening in crystal salt and form discovery is critically important to modern pharmaceutical development and manufacturing. Early discovery of developable forms lays the basis for much of formulation development. Physical properties of an API such as solubility, stability, hygroscopicity, melting point, and mechanical strength are a function of the solid-state phase in which an API is isolated. Performance of an API can be tuned and improved on by isolation of the API in different solid phases. Screening and identification of a suitable solid phase for development is critical to achieving acceptable bioperformance while minimizing difficulties with API and drug product manufacturing. Bioperformance is the most critical consideration for developing a new API. A drug development program cannot move forward if the API does not exhibit acceptable *in vivo* performance, even if all the other aspects of the program are exemplary. Solid phase, particle size, and formulation design are all elements which can be tuned to impact and improve bioperformance and all three of these elements should be considered when designing a new pharmaceutical product to achieve optimal performance. In an ideal case, the solid-state phase with the best combination of physical properties such as minimal phase complexity, manufacturing ease, and acceptable mechanical properties would exhibit the best bioperformance but this is often not the case. A compromise is often needed when selecting a solid phase to achieve the best overall combination of properties to achieve acceptable bioperformance with a phase that can be crystallized, isolated in the desired particle size, and formulated so that the selected phase can be manufactured on a commercial scale. The first step in this process is always the discovery of crystalline forms.

References

1. Variankaval, N.; Cote, A.; Doherty, M. F. *AIChE J.* **2008**, *54*(7), 1682–1688.
2. Thun, J.; Seyfarth, L.; Butterhof, C.; *et al. Cryst. Growth Des.* **2009**, *9*(5), 2435–2441.
3. McCrone, W. C. Polymorphism. In *Physics and Chemistry of the Organic Solid State*; Fox, D., Labes, M. M., Weissberger, A., Eds.; Wiley-Interscience: New York, **1965**, Vol. 1; pp 726–767.
4. Chang, H.; Gao, C.; Takeuchi, I.; *et al. Appl. Phys. Lett.* **1998**, *72*(17), 2185–2187.
5. Tan, H.; Reed, M.; Gahm, K. H.; *et al. Org. Process Res. Dev.* **2008**, *12*, 58–65.
6. Meenan, P. A.; Anderson, S. R.; Klug, D. The Influence of Impurities and Solvents on Crystallization. In *Handbook of Industrial Crystallization*, 2nd ed.; Myerson, A. S., Ed.; Butterworth-Heinemann: Boston, **2002**; pp 67–100.
7. Ouvrard, C.; Price, S. L. *Cryst. Growth Des.* **2004**, *4*, 1119–1127.
8. Neumann, M. A.; Perrin, M. A. *J. Phys. Chem. B* **2005**, *109*, 15531–15541.
9. Florence, A. J.; Johnston, A.; Price, S. L.; *et al. J. Pharm. Sci.* **2006**, *95*, 1918–1930.
10. Hulme, A. T.; Price, S. L. *J. Chem. Theory Comput.* **2007**, *3*, 1597–1608.
11. Price, S. L. *Int. Rev. Phys. Chem.* **2008**, *27*, 541–568.
12. Lancaster, R. W.; Karamertzanis, P. G.; Hulme, A. T.; *et al. Chem. Commun.* **2006**, 4921–4923.
13. Neumann, M. A.; Leusen, F. J. J.; Kendrick, J. *Angew. Chem. Int. Ed.* **2008**, *47*, 2427–2430.
14. www.accelrys.com
15. Bastin, R. J.; Bowker, M. J.; Slater, B. J. *Org. Proc. Res. Dev.* **2000**, *4*, 427–435.
16. Kuil, M. E.; Abrahams, J. P.; Hoedemaeker, P. J.; Maxwell, I. E. (Universitiet Leiden & Avantium) Screening Crystallization Conditions for Organic Compounds. *Eur Pat. EP 1* **2003**, *172*, 646.
17. Carlson E.D.; Cong P.; Chandler W.H., *et al.* Apparatuses and Methods for Creating and Testing Pre-formulations and Systems for the Same. *World Pat.* WO 03/014732 A1, **2003**.
18. Chyall, L. J.; Tower, J. M.; Coates, D. A.; Houston, T. L.; Childs, S. L. *Cryst. Growth Des.* **2002**, *2*(6), 505–510.
19. Peterson, M. L.; Morrissette, S. L.; McNulty, C.; *et al. J. Am. Chem. Soc. B* **2002**, *124*, 10958–10959.
20. http://www.zinsserna.com/crissy.htm
21. Lee, A. Y.; Lee, I. S.; Dette, S. S.; Boerner, J.; Myerson, A. S. *J. Am. Chem. Soc.* **2005**, *127*, 14982–14983.
22. Price, C. P.; Grzesiak, A. L.; Matzger, A. J. *J. Am. Chem. Soc.* **2005**, 5512–5517.
23. Hiremath, R.; Basile, J. A.; Varney, S. W.; Swift, J. A. *J. Am. Chem. Soc.* **2005**, 18321–18327.
24. Thorson, M. R.; Goyal, S.; Schudel, B. R.; *et al. Lab Chip.* **2011**, *11*, 3829–3837.
25. Stahl, P. H.; Wermuth, C. G. *Handbook of Pharmaceutical Salts: Properties, Selection, and Use,* 2nd ed.; Verlag Helvetica Chimica Acta: Zurich, **2011**; pp 265–344.
26. Bauer, J.; Spanton, S.; Henry, R.; *et al. Pharm. Res.* **2001**, *18*(6), 859–866.
27. Patience, D.; Dell'Orco, P.; Rawlings, J. *Org. Process Res. Dev.* **2004**, *8*(4), 609–615.
28. Nyvlt, J. *Crystal Res. Tech.* **1995**, *30*(4), 443–449.
29. Tung, H-H.; Paul, E. L.; Midler, M.; McCauley, J. A. *Crystallization of Organic Compounds: An Industrial Perspective. John Wiley & Sons: New York,* **2009**.
30. Mullin, J. W.; Nývlt, J. *Chem. Eng. Sci.* **1971**, *26*, 369–377.
31. Myerson, A. S. *Handbook of Industrial Crystallization.* 2nd ed.; Butterworth-Heinemann: Woburn, **2002**.
32. Nichols, G. *Microscope* **1998**, *46*(3), 117–122.
33. Gordon, R. E.; Amin, S. I. Crystallization of Ibuprofen. U.S. Patent Number 4,476,248, 1984.
34. Brittain, H. G. *J. Pharm. Sci.* **1997**, *86*(4), 405–412.
35. Matousek, P.; Parker, A. W. *Appl. Spectrosc.* **2006**, *60*(12), 1353–1357.
36. Tung, H. H.; Tabora, J.; Variankaval, N.; Bakken, D.; Chen, C-C. *J. Pharm. Sci.* **2008**, *97*(5), 1813–1820.

37. Tarsa, P. B.; Towler, C. S.; Woollam, G.; Berghausen, J. *Eur. J. Pharm. Sci.* **2010**, *41*, 1–23.
38. Vishweshwar, P.; MacMahon, J. A.; Oliveira, M.; Peterson, M. L.; Zaworotko, M. J. *J. Am. Chem. Soc.* **2005**, *127*(48), 16802–16803.
39. Bond, A. D.; Boese, R.; Desiraju, G. R. *Ang. Chem. Int. Ed.* **2007**, *46*, 618–622.
40. Morrisette, S. L.; Soukasene, S.; Levinson, D.; Cima, M. J.; Almarsson, O. *Proc. Natl. Acad. Sci.* **2003**, *100*, 2180–2184.
41. Chen, S.; Guzei, I. A.; Yu, L. *J. Am. Chem. Soc.* **2005**, *127*, 9881–9885.
42. Hakvoort, G.; Hol, C. M. *J. Therm. Anal. Calorim.* **1999**, *56*, 717–722.
43. Lang, M.; Grzesiak, A. L.; Matzger, A. J. *J. Am. Chem. Soc.* **2002**, *124*, 14834–14835.
44. Alvarez, A. J.; Singh, A.; Myerson, A. S. *Cryst. Growth Des.* **2009**, *9*(9), 4181–4188.
45. Woodley, S. M.; Catlow, R. *Nat. Mater.* **2008**, *7*, 937–946.
46. Grevsen, K.; Jensen, M.; Fretté, X. C.; Henriksen, J. J. Artemisia annua anti-malaria project in Vietnam. Report No. 1. Danish Institute of Agricultural Sciences, Development Center Aarslev: Aarslev, Denmark, **2006**; 42 pp.
47. Qu, H.; Christensen, K. B.; Fretté, X. C.; *et al. Org. Process Res. Dev.* **2010**, *14*, 585–591.
48. Byrn, S. R.; Pfeiffer, R. R.; Stowell, J. G. *Solid-State Chemistry of Drugs*. SSCI: West Lafayette, IN, **1999**.
49. Threlfall, T. *Org. Process Res. Dev.* **2000**, *4*, 384–390.
50. Bernstein, J. *J. Phys. D. Appl. Phys.* **1993**, *26*, B66–B76.
51. Bernstein, J. *Polymorphism in Molecular Crystals*. Clarendon Press: Oxford, **2002**.
52. Davey, R.; Garside, J. *From Molecules to Crystallizers*. Oxford University Press: New York, **2000**.
53. Guillory, J. Generation of Polymorphs, Hydrates, Solvates and Amorphous Solids. In *Polymorphism in Pharmaceutical Solids*; Brittain, H., Ed.; Marcel Dekker: New York, **1999**, Vol. 95; pp 183–226.
54. Lahav, M.; Leiserowitz, L. *Chem. Eng. Sci*. **2001**, *56*, 2245–2253.
55. Khoshkhoo, S.; Anwar, J. *J. Phys., D. Appl. Phys.* **1993**, *26*, B90–B93.
56. Blagden, N.; Davey, R. J.; Lieberman, H. F.; *et al. J. Chem. Soc. Faraday Trans.* **1998**, *94*, 1035–1044.
57. Davey, R. J.; Allen, K.; Blagden, N.; *et al. Cryst. Eng. Comm.* **2002**, *4*, 257–264.
58. Boettger, S. D. *Lab. Robotics Automat* **1992**, *4*, 169–181.
59. Rubin, A. E.; Tummala, S.; Both, D. A.; Wang, C.; Delaney, E. *J. Chem. Rev.* **2006**, *106*, 2794–2810.
60. Hu, Y.; Liang, J. K.; Myerson, A. S.; Taylor, L. *Ind. Eng. Chem. Res.* **2005**, *44*, 1233–1240.
61. Birch, M.; Fussell, S. J.; Higginson, P. D.; McDowall, N.; Marziano, I. *Org. Process Res. Dev.* **2005**, *9*, 360–364.
62. Storey, R. A.; Docherty, R.; Higginson, P. D. *Am. Pharm. Rev.* **2003**, *6*, 100–105.
63. Carlson, E. D.; Cong, P.; Chandler, W. H., Jr; *et al. PharmaChem* **2003**, *2*, 10–15.
64. Remenar, J. F.; MacPhee, J. M.; Larson, B. K.; *et al. Org. Process Res. Dev.* **2003**, *7*, 990–996.
65. Storey, R.; Docherty, R.; Higginson, P.; *et al. Crystallogr. Rev.* **2004**, *10*, 45–56.
66. Desrosiers, P. J. *Mod. Drug Discovery* **2004**, *7*, 40–43.
67. Pommier, C. J.; Rosso, V.; Song, A. *Am. Pharm. Rev.* **2005**, *8*, 19–24.
68. Hansen, K. B.; Chilenski, J. R.; Desmond, R.; *et al. Tetrahedron Asymmetry* **2003**, *14*, 3581–3587.
69. Toda, F.; Tanaka, K. *Chem. Lett.* **1986**, 1905–1908.
70. Vries, T.; Wynberg, H.; van Echten, E.; *et al. Angew. Chem. Int. Ed.* **1998**, *37*(17), 2349–2354.
71. Tan, H.; Cui, S.; Gahm, K.; Luu, V.; Walker, S. D. *Org. Process Res. Dev.* **2011**, *15*, 53–63.
72. Dyer, U. C.; Henderson, D. A.; Mitchell, M. B. *Org. Process Res. Dev.* **1999**, *3*, 161–165.
73. Jacques, J.; Collet, A.; Wilen, S. H. *Enantiomers, Racemates and Resolutions*. Wiley Interscience: New York, **1981**.

9.10 Organic Synthesis Using Microwave Heating

NE Leadbeater, University of Connecticut, Storrs, CT, USA

© 2014 Elsevier Ltd. All rights reserved.

9.10.1	**Introduction**	235
9.10.2	**Physical Chemistry Concepts**	236
9.10.2.1	Introduction	236
9.10.2.2	Microwave Effects	237
9.10.2.2.1	Introduction	237
9.10.2.2.2	Specific microwave effects	237
9.10.2.2.3	Nonthermal microwave effects	238
9.10.3	**Equipment**	238
9.10.4	**Safety**	239
9.10.5	**Application of Microwave Heating as a Tool in Organic Chemistry**	239
9.10.5.1	Introduction	239
9.10.5.2	Metal-Catalyzed Reactions	239
9.10.5.2.1	Introduction	239
9.10.5.2.2	Metal-catalyzed coupling reactions	240
9.10.5.2.3	Alkene metathesis	244
9.10.5.2.4	Functionalization of unactivated carbon–hydrogen bonds	245
9.10.5.2.5	Selected additional examples	246
9.10.5.3	Cycloaddition and Rearrangement Chemistry	247
9.10.5.3.1	Introduction	247
9.10.5.3.2	The Diels–Alder cycloaddition	247
9.10.5.3.3	[2 + 2 + 2] Cyclotrimerization reactions	249
9.10.5.3.4	The Claisen rearrangement	251
9.10.5.3.5	The Newman–Kwart rearrangement	252
9.10.5.3.6	The use of heating aids	253
9.10.5.4	Carbonyl Chemistry	254
9.10.5.4.1	Introduction	254
9.10.5.4.2	Condensation reactions	254
9.10.5.4.3	Multicomponent reactions	255
9.10.5.4.4	Solvent-free reactions	257
9.10.5.5	Organocatalysis	258
9.10.5.6	Reactions Involving Gaseous Reagents	259
9.10.5.6.1	Introduction	259
9.10.5.6.2	Use of precursors that liberate gas upon heating	259
9.10.5.6.3	Preloading reaction vessels with gas	261
9.10.5.6.4	Use of a gas-loading accessory	261
9.10.6	**Use of Microwave Heating in Combinatorial Chemistry**	264
9.10.6.1	Introduction	264
9.10.6.2	Parallel Processing	264
9.10.6.3	Solid-Phase Organic Synthesis	265
9.10.7	**Microwave-Assisted, Continuous-Flow Organic Synthesis**	268
9.10.7.1	Introduction	268
9.10.7.2	Microcapillary Reactors for Microwave-Assisted Continuous-Flow Synthesis	268
9.10.7.2.1	Construction of microcapillary reactors	268
9.10.7.2.2	Synthesis using microcapillary reactors	268
9.10.7.3	Other small-scale approaches to continuous-flow chemistry	269
9.10.8	**Additional Applications of Microwave Heating in Organic Synthesis**	270
9.10.9	***In situ* Monitoring of Reactions Performed using Microwave Heating**	271
9.10.9.1	Introduction	271
9.10.9.2	Watching Reactions in Real Time	271
9.10.9.2.1	Use of a digital camera	271
9.10.9.2.2	Use of thermal imaging	271
9.10.9.3	*In situ* Spectroscopy	272
9.10.9.3.1	Introduction	272
9.10.9.3.2	Infrared spectroscopy	272

 doi:10.1016/B978-0-08-097742-3.00920-4

9.10.9.3.3 UV–visible spectroscopy 272
9.10.9.3.4 Raman spectroscopy 272
9.10.9.3.4.1 Qualitative reaction monitoring 272
9.10.9.3.4.2 Quantitative reaction monitoring 273
9.10.9.3.4.3 Probing microwave effects 273
9.10.9.3.5 Nuclear magnetic resonance spectroscopy 274
9.10.10 Scale-Up of Reactions using Microwave Heating 274
9.10.10.1 Introduction 274
9.10.10.2 Open-Vessel Batch Processing 274
9.10.10.3 Sealed-Vessel Batch Processing 275
9.10.10.3.1 Multiple-vessel processing 275
9.10.10.3.2 Stop-flow processing 276
9.10.10.3.3 Use of one sealed vessel 276
9.10.10.4 Continuous-flow Processing 277
9.10.10.5 Energy Efficiency 277
9.10.11 Conclusion 278
Acknowledgment 278
References 278

Glossary

Heating aids (also known as passive heating elements) Microwave absorbing materials added to a reaction vessel to allow for effective heating of nonpolar reaction mixtures. Heating aids include some ionic liquids as well as solids such as graphite and silicon carbide (SiC).

Microwave-assisted continuous-flow organic synthesis (MACOS) Centered around the use of microcapillary reactors. By coating the inside of the capillaries with metal, it is possible not only to use them to perform heterogeneous catalysis but also simply to heat reaction mixtures very effectively.

Monomode microwave unit Apparatus for small-scale synthesis. The cavity of a monomode microwave system is the width of just one wave (mode) and it is possible to heat volumes as small as 0.2 ml effectively. The upper limit of monomode units is determined by the size of the microwave cavity and is usually in the region of 100 ml.

Multimode microwave unit Type of microwave apparatus including household microwave ovens. When microwaves come into the cavity (heating chamber), they move around and bounce off the walls. As they do so, they generate pockets (called modes) of high energy and low energy as the waves either reinforce or cancel each other out. As a result, the microwave field in the cavity is not uniform. There will instead be hot spots and cold spots, these corresponding to the pockets of high and low energy, respectively.

Nonthermal microwave effects Effects resulting from direct interaction of the electric component of the microwave irradiation with specific molecules in a reaction medium leading to orientation effects of dipolar molecules or intermediates and hence changing the pre-exponential factor (A) or the activation energy. Additionally, in the case of polar reaction mechanisms where the relative polarity of the reaction is enhanced from the ground state to the transition state, acceleration due to an increase in microwave absorbance of the intermediate could occur. When nonthermal microwave effects are discussed, they are generally invoked as a result of inaccurate comparison of the outcome of microwave and conventionally heated experiments.

Simultaneous cooling Cooling the walls of a reaction vessel with compressed air or a cryogenic fluid while irradiating the vessel contents with microwave irradiation. The objective is to keep the bulk reaction temperature relatively low while maximizing the applied microwave power. This technique has been found to open the door to the possibility of data misinterpretation, especially with regard to accurate temperature monitoring.

Specific microwave effects Macroscopic heating events that occur slightly differently under microwave irradiation than when using conventional (convection) heating methods. They are often difficult (but not impossible) to reproduce without the use of microwave irradiation.

9.10.1 Introduction

Microwave heating is proving to be a transformational technique in preparative chemistry. Using modern scientific microwave apparatus it is possible to access elevated temperatures in an easy, safe, and reproducible way.[1,2] In the primary literature, the origins of microwave heating as a tool for organic chemistry dates back to 1986 when two research papers were published, reporting that reactions can be performed rapidly in domestic microwave ovens.[3,4] A report in the patent literature pre-dates these.[5] Subsequent research articles, now numbering into the thousands, have shown that by using microwave heating, reaction times can be decreased, product yields increased, and purity enhanced as compared with conventional heating methods. The origins of the rate enhancements observed have been a topic of considerable debate over the years. It is now accepted that heating

is just that – heating. From a preparative chemistry standpoint, the use of microwave heating is not limited to organic synthesis.[2] Microwave heating has found application in materials[6] and polymer chemistry,[7] the preparation of inorganic and organometallic compounds[8] as well as in the biosciences.[9]

Given the vast array of reactions that have been performed using microwave heating, it is essentially impossible to provide a comprehensive overview of the field in one chapter. Instead, some of the key tenets of microwave-assisted organic chemistry are explored in the context of particular classes of reaction. The chapter discusses topics such as (1) nonthermal microwave effects (see Sections 9.10.5.3.2, 9.10.5.3.5, 9.10.9.3.4.3), (2) simultaneous cooling while irradiating reactions with microwave energy (see Sections 9.10.5.2.2, 9.10.5.5), (3) temperature gradients at vessel walls (see Section 9.10.5.3.3), (4) the use of heating aids (see Sections 9.10.5.3.6, 9.10.5.4.2, 9.10.6.2), (5) open-vessel processing (see Section 9.10.5.4.2.), (6) solvent-free reactions (see Section 9.10.5.4.4), (7) dealing with exothermic reactions (see Section 9.10.5.4.4), (8) monitoring reactions in real-time (see Section 9.10.9), and (9) scale-up of microwave-assisted synthesis (see Section 9.10.10).

9.10.2 Physical Chemistry Concepts

9.10.2.1 Introduction

The microwave region of the electromagnetic spectrum is classified as that between 0.3 and 300 GHz, corresponding to wavelengths of 1 m to 1 mm (Figure 1). Because applications such as wireless devices and air traffic control operate in this range, regulatory agencies allow equipment for industrial, scientific, and medical use to operate at only five specific frequencies. Household microwave ovens and scientific microwave apparatus typically operate at 2.45 GHz (12.25 cm wavelength), with few exceptions.[10]

Microwave heating is based on the ability of a particular substance to absorb microwave energy and convert the electromagnetic energy to heat. Molecules with a dipole moment attempt to align themselves with the oscillating electric field of the microwave irradiation, leading to rotation. One molecule excited rotationally by incident irradiation can strike a second, converting rotational energy into translational energy. Under microwave irradiation, a large number of molecules are being rotationally excited and, as they strike other molecules, rotational energy is converted into translational energy (i.e., kinetic energy) and as a consequence, heating is observed (Figure 1).

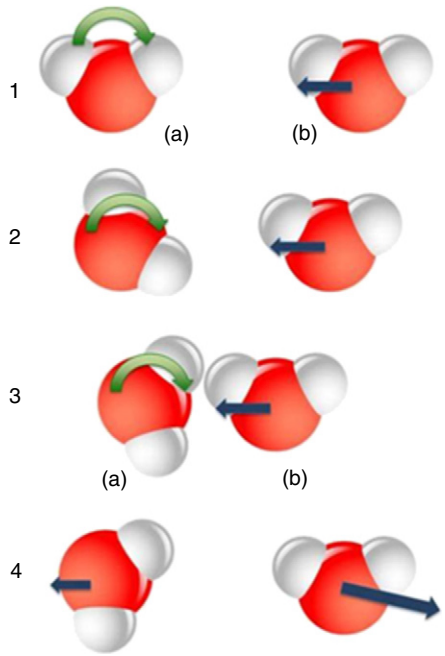


Figure 1 On the left, a molecule (a) that has been rotationally excited by microwave irradiation is approached by a second molecule (b), panels 1–3. Upon impact (panel 3), the rotational energy of (a) is converted to translational movement of (b). In panel 4, notice the increase in translational vector magnitude, the consequence of which is an increase in molecular collisions (kinetic energy).

Because microwave heating is dependent on the dipole moment of a molecule, it stands to reason that more polar solvents, such as dimethylsulfoxide (DMSO), dimethylformamide (DMF), ethanol, and water, better convert microwave irradiation into heat as compared with nonpolar ones, such as toluene or hexane. Efforts have been undertaken to quantify relative microwave absorptivities and correlate this with dielectric constant (ε'), dielectric loss (ε''), or a combination of both, termed loss tangent or

loss angle (tan $\delta = \varepsilon''/\varepsilon'$).[11] Although the tan δ value of a molecule can be used to assess microwave absorbance, the use of any single parameter drastically oversimplifies the issue of 'efficient' microwave heating. A number of other factors contribute to this. Attributes such as specific heat capacity and heat of vaporization of the substance, as well as the depth to which microwave irradiation can penetrate into the sample can sometimes have a larger impact on heating rate than its respective dielectric loss or loss tangent. In addition, dielectric loss and dielectric constant are functions of irradiation wavelength as well as temperature, specific heat changes as a function of temperature, and heat of vaporization changes as a function of pressure. These can all effect microwave absorptivity individually, and in combination. Room temperature water, for instance, is most microwave absorbent at approximately 18 GHz, but as temperature increases, so does the optimum frequency at which water converts microwave irradiation to heat. Generally, however, when synthetic chemists speak of 'good' or 'bad' microwave absorbers, implied is a 2.45 GHz irradiation source, a small depth of field (1–10 cm) and synthetically relevant temperatures (50–150 °C).

9.10.2.2 Microwave Effects

9.10.2.2.1 Introduction

Heating can enhance the rate of many reactions, regardless of whether it comes from a microwave or a conventional source. That said, microwave heating can be different than 'conventional,' solely convection-based heating. Numerous attempts have been made to evaluate differences between microwave versus conventional heating, either real or perceived. For the most part, these differences have been divided into two categories: 'specific' microwave effects and 'nonthermal' microwave effects.

9.10.2.2.2 Specific microwave effects

'Specific' microwave effects encompass macroscopic heating events that occur slightly differently under microwave irradiation than when using conventional (convection) heating methods. Additionally, specific microwave effects are often difficult (but not impossible) to reproduce without the use of microwave irradiation. The first specific microwave has already been addressed: substrates that better convert incident microwave irradiation into heat, heat the bulk faster. Heating 2 ml of water to 100 °C from room temperature will take considerably less time than heating 2 ml of toluene across the same temperature range and utilizing the same applied microwave power at 2.45 GHz. Although other attributes certainly impact the rate of heating, because the differences in dielectric loss factors (water: $\varepsilon'' = 9.89$; toluene: $\varepsilon'' = 0.096$) are so profound, any variations in heat capacities or heats of vaporization will have negligible impact on the rate of heating. Differences in microwave absorptivity are generally of little impact. Commercial scientific microwave units are able to heat effectively the majority of organic solvents. Also, since reaction mixtures generally contain multiple components such as acid, base, or metal catalysts, and one or more reactants, reactions will often heat much more efficiently than the solvent alone.

The next specific effect of microwave irradiation is that of inverted temperature gradients. Conventional heating must heat reactions from the outside in, and the walls of the reaction vessel are generally the hottest part of the reaction, especially during the initial ramp to the desired temperature. Microwave heating, however, can lead to inversion of this gradient as heat is generated across the entire reaction volume and a larger cross section of the reaction may reach the ideal reaction temperature sooner than it would have with conventional heating. However, efficient stirring and controlled heating can generally mitigate temperature gradients in both microwave and conventionally heated reactions.

A third example of specific microwave effects is the phenomenon of macroscopic superheating.[12,13] Solvents will only boil when they are in contact with their own vapor and, if this is not the case, they can be heated to above their normal (atmospheric) boiling point without the onset of boiling.[14] Without nucleation sites, solvents are only in contact with their own vapor at the top of the vessel, thus boiling (and hence release of heat) is limited to this relatively small interface. Using microwave irradiation, solvents have been held well above their boiling points for extended periods of time. For example, acetonitrile has been maintained at over 100 °C (normal b.p. 82 °C). The phenomenon has been exploited in reaction chemistry. The acid-catalyzed esterification of 1-hexanol with benzoic acid is an example.[15] Temperatures of some 38 °C above the normal boiling point of 1-hexanol can be obtained and rate enhancements observed at these higher temperatures when compared with conventionally heated reactions. The potential for superheating is virtually eliminated with effective stirring and there would be few synthetic chemists willing to give up stirring for a few degrees in reaction temperature. In addition, there are significant safety concerns, as anyone who has heated a cup of coffee or water in a microwave oven at home and then taken it out and stirred it may well have seen. The contents can boil very rapidly and, in some cases, with such vigor as to eject the hot contents from the container. In the case of a reaction mixture, this can have significant effects, including contamination of a considerable area and, at worst, significant personal injury.

The final example of a specific microwave effect is the ability to heat very microwave absorbant substrates and/or catalysts selectively under heterogeneous reaction conditions. Selective heating at the point of reaction seems to be the exception rather than the rule, existing in only very specific instances. An example is in the synthesis of cadmium selenide and cadmium telluride nanomaterials using the nonpolar hydrocarbons heptane, octane, and decane as solvents.[16] The precursor substrates are purported to absorb the microwave irradiation selectively, this leading to more uniform morphology in the resulting nanomaterials as compared with conventional heating methods.

9.10.2.2.3 Nonthermal microwave effects

Unlike specific microwave effects, entering the world of 'nonthermal microwave effects' puts the scientist on rather tenuous ground.[17] Numerous attempts have been made over the past 20 years to rationalize perceived enhancements in reaction rates that could not be explained according to typical models (e.g., the Arrhenius equation). Reactions were often performed side by side, one in a microwave unit and one in an oil bath, and these reactions were purportedly carried out at identical temperatures, with increased yields or decreased reaction times almost exclusively reported when using microwave as opposed to 'conventional' heating. However, when meticulous attention is paid to reaction set up and accurate temperature monitoring, the playing field again becomes level.[18] The topic of nonthermal microwave effects is discussed at various junctures in this chapter.

9.10.3 Equipment

There are two major types of microwave apparatus (Figures 2 and 3). The larger of these is termed a 'multimode' unit; household microwave ovens are an example of this category. When the microwaves come into the cavity (heating chamber), they will move around and bounce off the walls. As they do so, they will generate pockets (called modes) of high energy and low energy as the waves either reinforce or cancel each other out. As a result, the microwave field in the cavity is not uniform. There will instead be hot spots and cold spots, these corresponding to the pockets of high and low energy, respectively. This is why domestic microwave ovens (and their scientific cousins) often have turntables installed. The turntable allows for movement of food (or reaction vessels) around the cavity and equaling out the microwave energy that the sample is exposed to. It is possible to heat a number of reaction vessels at the same time by loading them onto a turntable and rotating them through the microwave field.

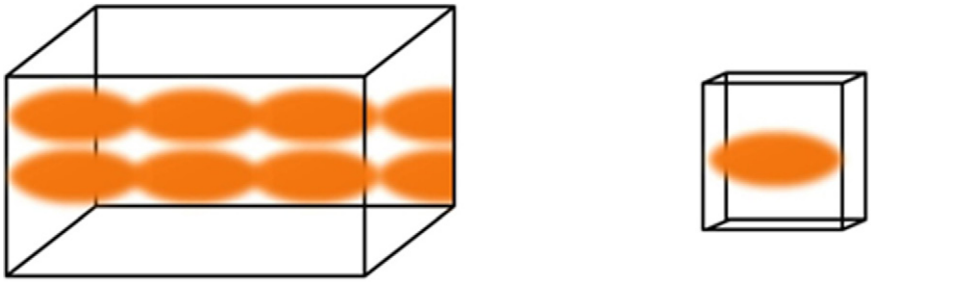


Figure 2 Differences between multimode and monomode microwave units.



Figure 3 A (larger) multimode and a (smaller) monomode scientific microwave unit. Reproduced with permission from CEM Corporation, Matthews NC.

When performing reactions on a small scale it is sometimes difficult to heat the mixture effectively in a multimode microwave unit. With the hot and cold spots that occur, it is hard to get constant microwave energy to heat a small sample. To overcome this, single-mode (also called monomode) units have been developed. The cavity of a monomode microwave system is the width of just one wave (mode) and it is possible to heat volumes as small as 0.2 ml effectively. The upper limit of monomode units is determined by the size of the microwave cavity and is usually approximately 100 ml.

One of the driving forces for the development of microwave-assisted synthesis has been the range of peripheral tools that have become available for interfacing with both monomode and multimode scientific microwave apparatus. They range from devices to increase throughput to those that allow for novel applications of microwave irradiation, thus opening new avenues for fundamental research. A number of them are discussed in pertinent sections of this chapter and include (1) simultaneously cooling while irradiating reactions with microwave energy (Section 9.10.5.2.2), (2) design of experiments (DoE) approaches (Section 9.10.5.4.3), (3) loading reaction vessels with gases (Section 9.10.5.6), (4) microwave heating and photochemistry combined (Section 9.10.5.6.4), (5) well plates for combinatorial chemistry (Section 9.10.6.2), and (6) *in situ* reaction monitoring (Section 9.10.9).

9.10.4 Safety

Household microwaves are not suitable for chemistry and should be relegated to where they belong – the kitchen. All scientific microwave apparatus is built with safety in mind and comes with temperature, pressure, and microwave power measurement devices. This said, attention to safety is still essential. Basic safety checks such as ensuring that reaction vessels are in good condition and that all other aspects of instrumentation are in good working order are important each time a microwave unit is used. Elevated pressure in sealed systems poses a significant hazard. If gases or other volatile components are produced stoichiometrically during the course of a reaction, this will add to the internal pressure. Efficient stirring is very important in any chemical reaction, be that performed conventionally or using microwave heating. An additional precaution related to magnetic stirrer bars when used in reaction vessels that are placed into a microwave field is that they should not be one quarter of the wavelength of the radiation in length (i.e., $\sim$3 cm), otherwise they can function as an antenna and may lead to destruction of the stirring bar and even rupture of the vessel.

When performing a reaction on a small scale using a monomode microwave unit, a temptation is to heat the reaction mixture with the full microwave power available. However, this can sometimes lead to uncontrollable temperature and pressure rises and, as a result, vessel failure. On a related note, although most reactions performed using microwave heating are endothermic in nature (which is why they are being heated in the first place), exothermic decomposition can occur in some cases. Although reactions performed using microwave heating can potentially be scaled directly in a linear manner, it is important to take a gradual approach; test reactions at intermediate scales being a wise precaution. This is particularly important when performing chemistry using concentrated or solvent-free protocols.

9.10.5 Application of Microwave Heating as a Tool in Organic Chemistry

9.10.5.1 Introduction

Given that many chemical reactions require heating in order for them to be completed within a reasonable time period, the fact that there is an ever-increasing range of examples of the use of microwave heating in organic chemistry comes as no surprise. Certainly the most useful attribute of the scientific microwave is its ability to aid the user when developing new chemistry. Due to the ease of which reactions can be performed under sealed-vessel (autoclave) conditions, microwave heating opens access to a process window that is otherwise difficult to access (though not impossible). For instance, a stubborn reaction may traditionally be carried out in refluxing xylenes (boiling point (b.p.) 137–140 °C), 1,2-dichlorobenzene (b.p. 178–180 °C), or possibly *N*-methyl pyrrolidinone (NMP, b.p. 202 °C). The very reason to choose these solvents (namely, high boiling point) is the same attribute that can make them difficult to remove upon workup, especially as scale increases. However, under sealed-vessel conditions, nearly any solvent the bench chemist selects becomes a viable option. Ethanol or acetonitrile can replace NMP, ethyl acetate or methyl ethyl ketone can serve as an alternative to xylenes, and even dichloromethane (b.p. 40 °C at 1 atm) can be heated to 160 °C within the typical pressure limitations of most commercially available scientific microwave units.

To review each individual reaction performed using microwave heating is both beyond the scope of this chapter and also not particularly useful. Instead, the aim here is to present some of the broad areas in which microwave heating has proved to be a valuable tool and to direct the reader to reviews of these topics for more detailed information. Attention is focused on classes of reaction used widely as part of the organic chemist's toolbox.

9.10.5.2 Metal-Catalyzed Reactions

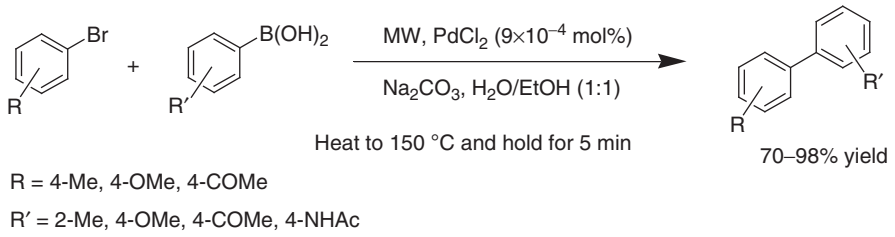
9.10.5.2.1 Introduction

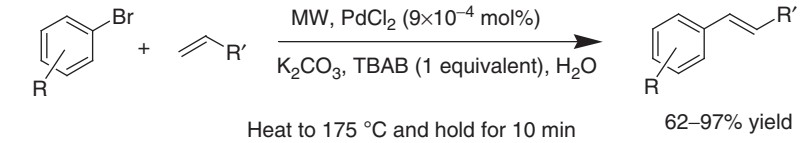
The application of metal catalysts has undoubtedly been one of the biggest steps forward in synthetic organic chemistry over the last 50 years and is a topic of ever-increasing interest. Because many metal-catalyzed reactions require heating, often for extended times, microwave heating has found significant application.[19,20] By working in sealed tubes and at high temperatures, reactions can be complete within minutes instead of hours at reflux. This said, one drawback to a 'hot and fast' approach to catalysis using microwave heating can be the formation of elemental metal during the course of the reaction. Deposition of this metal on the surface of a glass tube can lead to superheating. This in turn can result in localized melting of the reaction vessel wall and a

pinhole fracture of the tube. If the contents of the vessel are under pressure, a small fracture like this can lead to catastrophic destruction of the tube. For this reason, care needs to be taken, especially when performing a reaction for the first time. In this section, attention is focused predominantly on three broad classes of reaction that are of topical interest: metal-catalyzed couplings, alkene metathesis, and functionalization of unactivated carbon–hydrogen bonds. A selection of additional examples will be included to show the breadth of metal-catalyzed reactions for which microwave heating can be used.

9.10.5.2.2 Metal-catalyzed coupling reactions

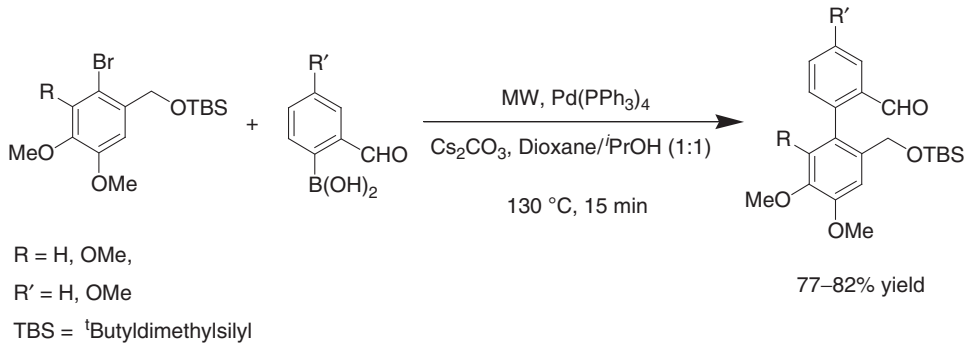
Palladium-catalyzed coupling and cross-coupling reactions have perhaps been the subject of most attention when using microwave heating in metal catalysis.[21–24] This is most probably due to their wide application in academic and industrial laboratories. In a number of cases, so-called ligandless catalysts have been used – these being simple palladium salts. Under the reaction conditions employed, highly catalytically active nanoparticulate palladium is formed and reactions such as the Suzuki[25] and Heck[26] couplings can be performed using catalyst loadings of as low as 50 ppb to 10 ppm (Scheme 1). Reactions can be complete after 5 min heating at 150 °C.





Scheme 1 Suzuki and Heck coupling reactions performed using ultralow catalyst loadings.

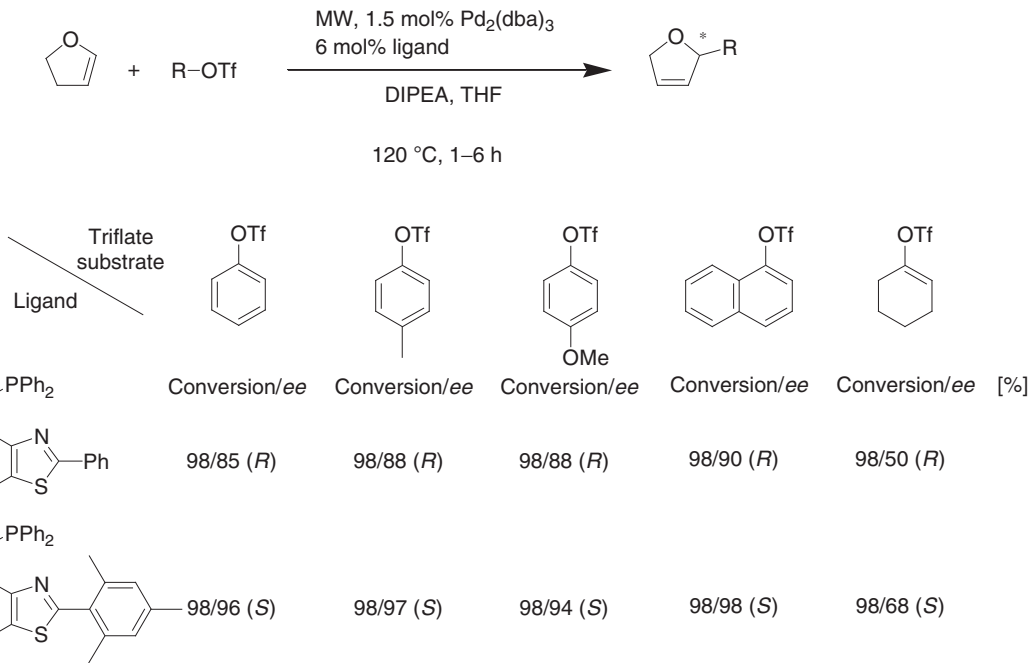
The boronic acid substrates used in Suzuki couplings can, on some occasions, undergo competitive protonolysis reactions under the conditions used. As a result, a stoichiometric excess of the boronic acid is often added to the reaction mixture to obtain an acceptable yield of the biaryl product. By performing the reaction at elevated temperatures using microwave heating, it can be possible to circumvent this problem. An example is in the case of coupling of electron-rich aryl bromides with substituted *o*-formylphenylboronic acids.[27] By performing the reactions at 130 °C for 15 min, the biaryl products can be obtained in yields of 77–82% as compared with 42–50% using the previous conventional approach (Scheme 2).



Scheme 2 Suzuki coupling of electron-rich aryl bromides with substituted *o*-formylphenylboronic acids.

Stereoselective coupling reactions can be performed using microwave heating, even though elevated temperatures are used. The asymmetric intramolecular Heck reaction is an example; sugar-based phosphite-oxazoline ligands being used and the reaction

being complete in 10 min at 70 °C in high yield and enantiomeric excess.[28] Working at higher temperatures, asymmetric intermolecular Heck reactions can be achieved.[29] Phosphine-thiazole ligands are used and the coupling of 2,3-dihydrofuran with a range of triflates performed at 120 °C for 1–6 h (Scheme 3).



Scheme 3 Asymmetric intermolecular Heck reactions of 2,3-dihydrofuran with a range of triflates.

Microwave heating has been used as an enabling technology for the preparation of natural products by way of metal-catalyzed coupling reactions as key steps. Examples include the synthesis of the 15-membered cyclophane biphenomycin B,[30,31] the lactone methysticin,[32] and the alkaloid minfiensine (Figure 4).[33,34]

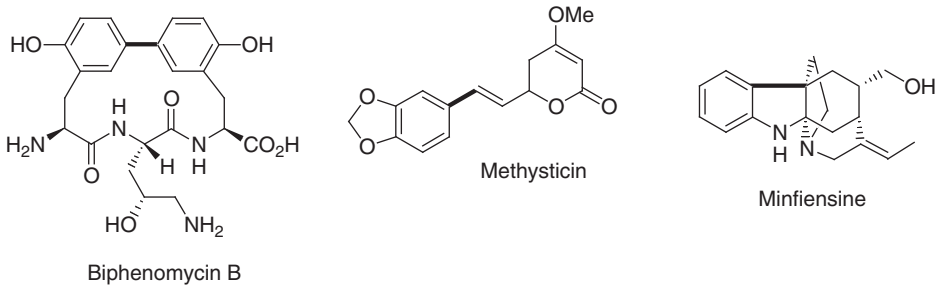
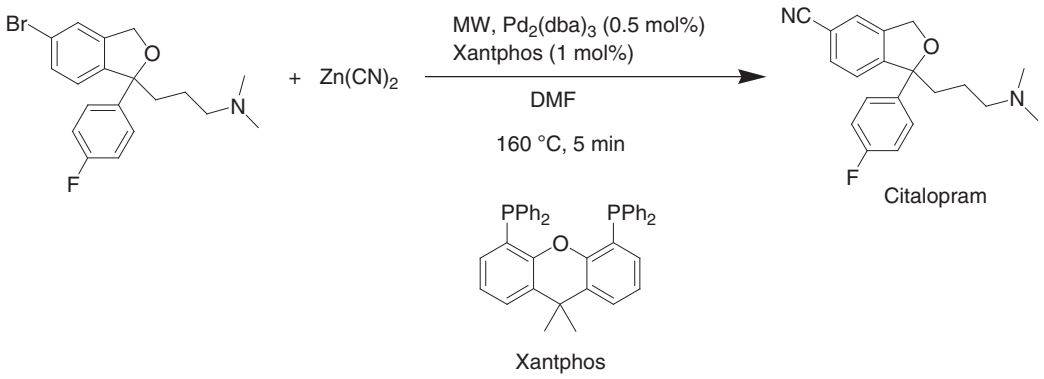


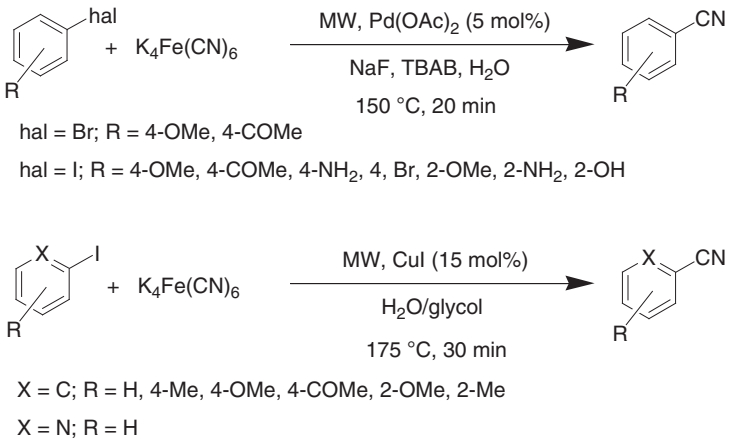
Figure 4 A range of natural products prepared using a microwave-assisted cross-coupling reaction as a key step (highlighted in bold).

The use of microwave heating for preparing aryl nitriles has received some considerable attention, most likely due to their application as dyes, herbicides, agrochemicals, and pharmaceuticals, as well as being intermediates for the formation of heterocycles.[35] One example is a palladium-catalyzed cyanation used as the final step in the synthesis of the antidepressant citalopram (Scheme 4).[36] Using $Zn(CN)_2$ as the source of cyanide, the reaction is effectively performed at 160 °C with an overall process time of 5 min. Moving away from toxic cyanide sources, such as metal cyanide salts, the use in potassium hexacyanoferrate (II), $K_4[Fe(CN)_6]$ is noteworthy. By employing either palladium acetate[37] or copper(I) iodide[38] as a catalyst, aryl halides can be effectively cyanated in water in short reaction times (Scheme 5).

Microwave-assisted coupling reactions have also found application in the preparation of organic materials. For example, polythiophenes can be synthesized by sequential borylation/Suzuki coupling protocols (Scheme 6).[39,40] Quinque- and sexithiophenes can be prepared this way. Longer oligomers can be synthesized by a similar method but by incorporating both microwave heating and ultrasound irradiation, another modern processing tool.[41,42] Suzuki coupling and borylation reactions are



Scheme 4 Preparation of citalopram using a microwave-assisted palladium-catalyzed cyanation.



Scheme 5 Palladium- and copper-catalyzed cyanation using $K_4Fe(CN)_6$ as the cyanide source.

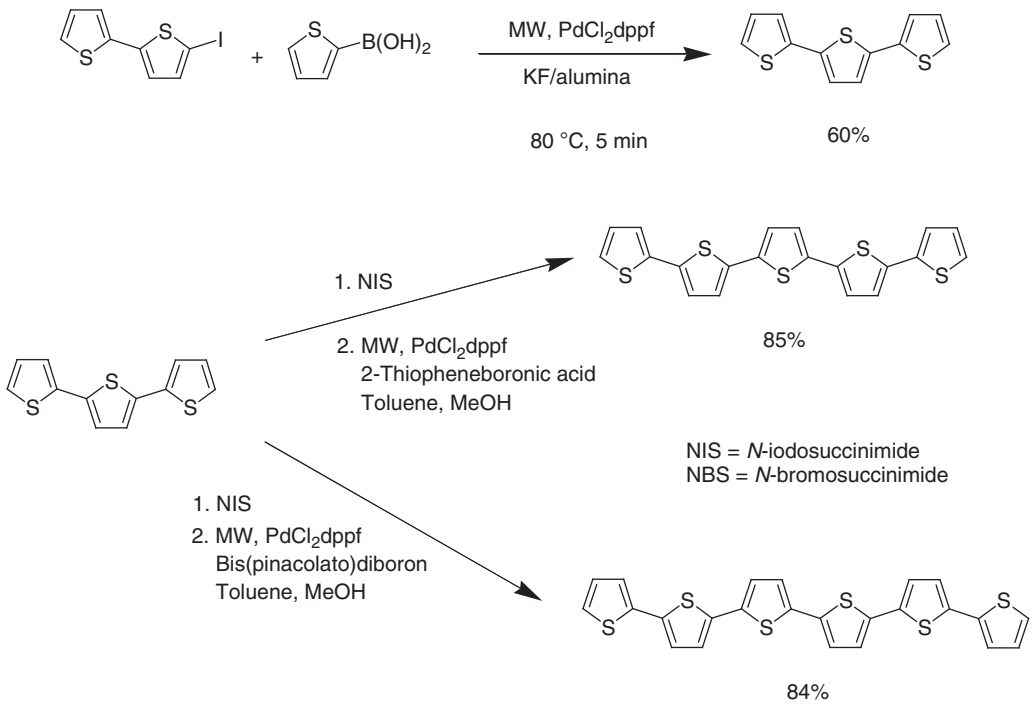
performed using microwave heating, with selective bromination of thiophene rings being achieved under ultrasound irradiation.[43]

In addition to homogeneous examples, a wide range of heterogeneous catalysts have been used for C–C coupling reactions employing microwave heating.[44] Although claims have been made that it is possible to superheat supported catalysts when using microwave heating, experimental evidence for this is lacking in all but a few extreme cases.[16] Although the supported catalyst may in some cases be the most microwave-absorbing component of the reaction mixture, the dissipation of heat is rapid, especially if the reaction mixture is stirred.[45] Therefore, any temperature gradient between the catalyst and bulk reaction medium is most likely small. That said, heterogeneous catalysis and microwave heating do form a valuable partnership.[46]

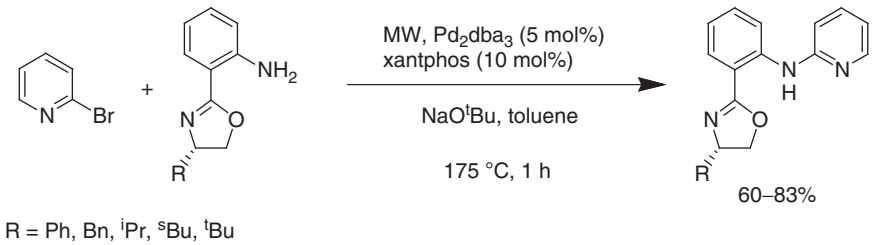
The application of microwave heating is by no means limited to carbon–carbon coupling reactions. It has been used for C–N, C–O, C–P, and C–S couplings with success.[24,43] In the case of C–N bond-forming reactions, although a wide range of common aryl halides generate high yields of amination products,[47] using conventional heating aryl halides bearing heteroatoms have been significantly less studied. Microwave heating has found application in this area, an example being the coupling of 2-bromopyridine with oxazoline-containing anilines (**Scheme 7**).[48] The reaction is complete in 1 h at 175 °C, without significant contamination due to the formation of palladium–pyridyl complexes.

For C–O bond-forming reactions, microwave heating has found use particularly in the synthesis of ethers[49] and phenols[50] from aryl halide precursors using copper catalysts. One compound that has been challenging to employ in C–O coupling reactions is tetrahydrofurfuryl alcohol, with degradation occurring above its atmospheric boiling point and the ring being particularly susceptible to cleavage. A solution to this problem involves the use of an organosoluble copper cluster as a reservoir of catalytically active Cu(I) (**Scheme 8**).[51] Using this catalyst, high yields of alkyl–aryl ethers are obtained after microwave heating at 125 °C for 1–3 h, an added advantage being that the reaction is run solvent-free. As well as homogeneous metal complexes, a range of heterogeneous catalysts have also been used. Copper-in-charcoal[52] and copper + nickel-in-charcoal[53] can both be used for the preparation of diaryl ethers from phenols and aryl bromides; in the case of the latter it is the copper component that is catalytically active.

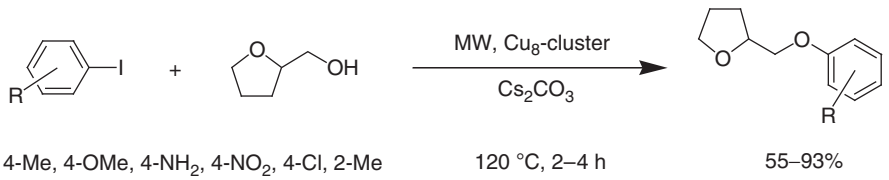
In the arena of metal-catalyzed C–S bond-forming reactions,[54] the Liebeskind–Srogl cross-coupling proves particularly effective and, although often run at room temperature, it has been performed in conjunction with microwave heating.[55]



Scheme 6 Microwave-assisted synthesis of polythiophenes.



Scheme 7 Palladium-catalyzed coupling of 2-bromopyridine with oxazoline-containing anilines.



Scheme 8 Copper-catalyzed C–O coupling reactions involving tetrahydrofurfuryl alcohol.

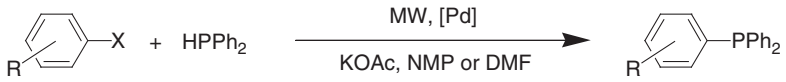
The coupling involves the coupling of a thioether with a boronic acid using common palladium catalysts such as $Pd(PPh_3)_4$ together with co-catalysts such as copper thiophene-2-carboxylate. The functionalization of resin-bound pyrazinones has been performed employing the coupling.[56] Using conventional heating, the reaction stopped at moderate conversion (63–80%) after 1 day at 65 °C. Analogous reactions using microwave irradiation in conjunction with simultaneous (cryogenic) cooling afforded the coupling products in yields as high as 90% in 1 h at 35 °C. In a related study, a copper-catalyzed C–N bond-forming reaction of pyrazinones with boronic acids has also been reported to benefit from simultaneous cooling when using microwave irradiation.[57]

The subject of simultaneously cooling while heating reactions with microwave energy deserves a little further discussion here because it may seem a bit counterintuitive, and indeed it has seen limited practical application in synthesis.[58] Although monomode units use compressed air to cool reaction vessels upon completion, this function also allows for simultaneous cooling during sample irradiation.[59] The role of simultaneous cooling is to keep the bulk reaction temperature relatively low while maximizing the applied microwave power. In addition to air cooling, it is also possible to pump microwave-transparent cryogenic

fluid around a specially designed microwave vessel while a reaction is being irradiated with microwave energy. The fluid can be cooled to temperatures as low as −60 °C, allowing maximum microwave irradiation while keeping the solution relatively cool. There have been only a handful of reports in the scientific literature of the use of this in synthetic chemistry.[60]

Cooling reactions while simultaneously heating with microwave irradiation have been found to open the door to the possibility of data misinterpretation, especially with regard to accurate temperature monitoring. A significant temperature gradient can be established across the reaction vessel. In addition, if using the built-in infrared sensor on the microwave unit for temperature measurement when applying simultaneous cooling, issues arise around accuracy, a topic discussed in Section 9.10.5.5. Using external temperature measurement it is possible to, in effect, 'trick' the temperature sensor by blowing air over it; the temperature reading being significantly lower than the actual bulk temperature in the reaction vessel. Therefore, a difference in reactivity could be attributed simply to a difference in reaction temperature. As a result, it is important to monitor the internal temperature of a reaction mixture and this involves the use of a temperature measurement device located inside the reaction vessel.

Metal-catalyzed C–P bond formation can be used to prepare tertiary phosphines when employing microwave heating,[61] among other reactions in this class.[62] A number of aryl bromides, iodides, and triflates can be coupled with diphenylphosphine, using palladium or nickel complexes as the catalyst (Scheme 9). Of note is that in the case of palladium acetate, the temperature must not exceed 200 °C or else a film of palladium black is formed on the reaction vessel walls. The deposited palladium on the inner glass surface can be used (albeit less efficiently) as a catalyst in subsequent runs. However, as mentioned in the introduction to this section, there is the proviso that metal deposits can superheat when irradiated with microwave energy, leading to possible vessel failure.



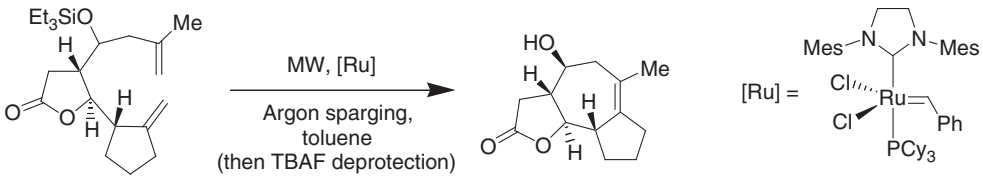
180–200 °C, 5–20 min 26–96%

X = I, R = H, [Pd] = 2.5 mol% $Pd(OAc)_2$ X = I, R = 2-Br, 3-OMe, 2-CO_2H, [Pd] = 1–2 mol% Pd/C

Scheme 9 Copper-catalyzed C–O coupling reactions involving tetrahydrofurfuryl alcohol.

9.10.5.2.3 Alkene metathesis

The scope of alkene metathesis in organic chemistry is considerable and microwave heating has been used as a tool on many occasions (*see* Chapter 5.26).[63] Among the numerous different classes of reaction, ring-closing metathesis using ruthenium-based catalysts has perhaps seen the most attention with reactions reported to be completed within minutes or even seconds at elevated temperatures, instead of hours at room temperature. Early reports suggested that the rate enhancements observed were as a result of the direct activation of the catalyst and/or the alkene[64] but performing the reaction using microwave and conventional heating under strictly isothermal conditions shows no evidence for such effects.[65] That said, microwave heating does still serve as a useful tool for metathesis reactions and additional benefit can be gained by careful control of reaction conditions, for example, by combining microwave irradiation with inert-gas sparging (Scheme 10).[66]

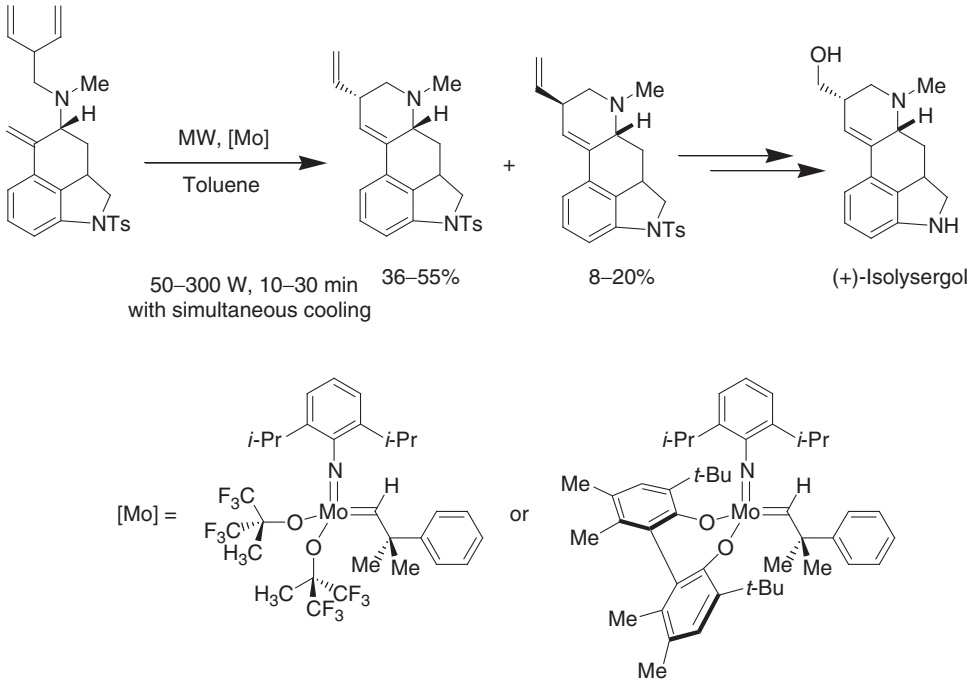


110 °C, 1–4 h 60–98%

Scheme 10 Ruthenium-catalyzed alkene metathesis.

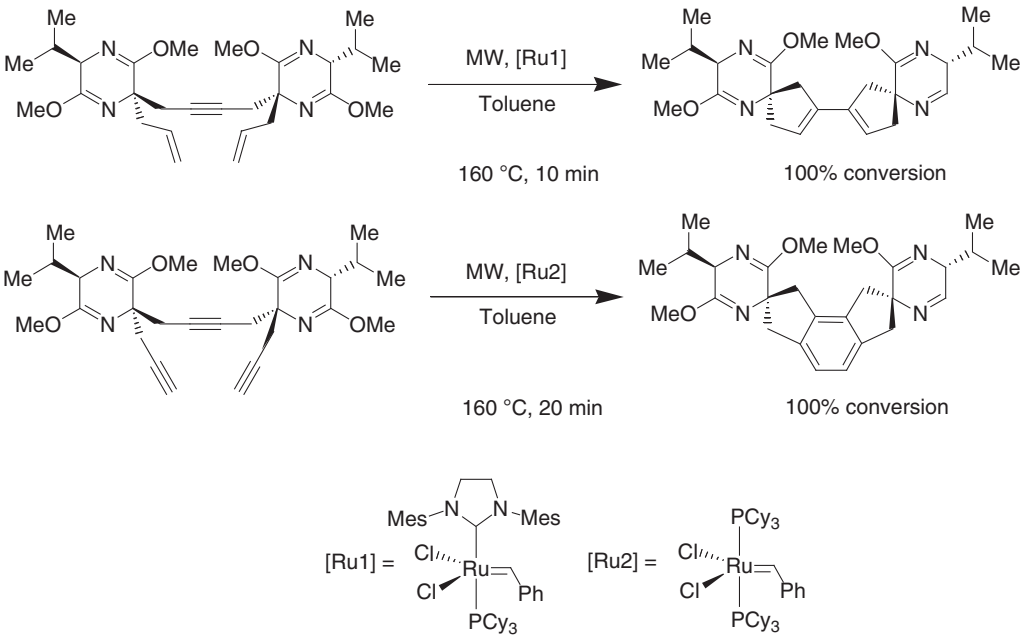
Microwave heating has been especially useful for the preparation of macrocycles.[67,68] One particular example is the enantioselective synthesis of (+) – isolysergol, which features a late-stage diastereomeric ring-closing metathesis reaction catalyzed by Schrock and Schrock–Hoveyda molybdenum catalysts (Scheme 11).[68] This represents the first example of the use of microwave heating with molybdenum-based metathesis catalysts. The reaction is performed using a constant microwave power input and simultaneous air-cooling and temperature data are not reported.

The use of microwave heating for metathesis is not limited to alkenes; alkyne and ene-yne metathesis have also benefited (*see* Chapters 5.27 and 5.28).[69] One particularly interesting case is the domino dienyne and triyne ring-closing metathesis of suitably functionalized substrates (Scheme 12).[70] Performing the reaction conventionally at 95 °C in toluene requires multiple additions of



Scheme 11 Molybdenum-catalyzed alkene metathesis.

fresh catalyst over the course of 9 h to obtain a good yield of the products. Using microwave heating, one dose of catalyst followed by 10 min at 160 °C is sufficient to obtain complete conversion.

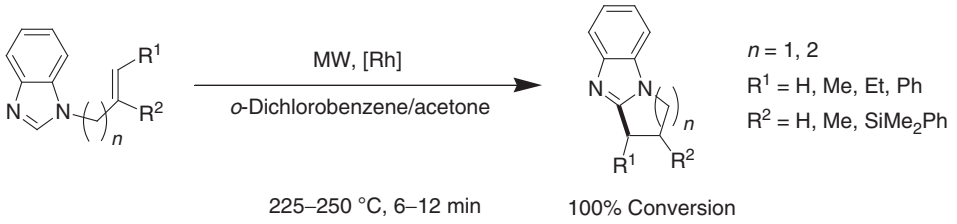


Scheme 12 Domino dienyne and triyne ring-closing metathesis.

9.10.5.2.4 Functionalization of unactivated carbon–hydrogen bonds

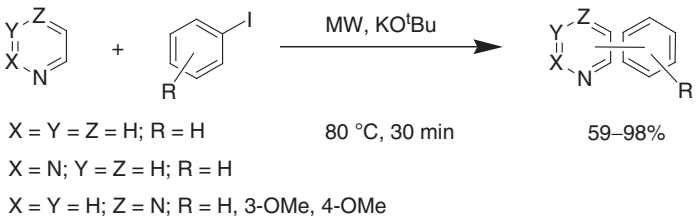
The selective functionalization of unactivated carbon–hydrogen bonds has proved to be one of the most challenging transformations for synthetic chemists to accomplish.[71] Metal catalysis has proved invaluable in this endeavor and applications extend from the transformation of simple alkanes to the synthesis of complex molecules.[72,73] As many reactions require elevated temperatures and lengthy reaction times, microwave heating has a role to play. One of the first examples pertained to a series of

inter- and intramolecular rhodium-catalyzed reactions leading to tricyclic heterocycle products (Scheme 13).[74] Heating olefin-tethered benzimidazole starting materials at 225–250 °C for 6–12 min in the presence of the catalyst leads to the formation of the products in good-to-excellent yield.



Scheme 13 Intramolecular rhodium-catalyzed C–H bond activation.

Rhodium catalysis has also been used for the direct coupling of heterocycles with aryl bromides and iodides.[75,76] In a similar vein, electron-deficient nitrogen heterocycles can be coupled with iodoarenes without the addition of a transition-metal catalyst, the reaction being promoted by KO^{t}Bu (Scheme 14).[77] There is evidence for a radical mechanism in this and subsequent similar couplings reported in the literature, the combination of a strong base and an amine ligand initiating a single electron transfer to an aryl–halide bond at high temperatures.[78] That said, following a number of previous transition-metal free couplings that have later been found to contain adventitious metal as contaminants in reagents that subsequently acts as a catalyst,[79] care needs to be taken when defining a reaction as truly 'transition-metal free.' This is especially the case when reactions are performed at elevated temperatures because very low loadings of metal can affect remarkably fast catalysis. As noted in a perspective on the topic, even when performing a barrage of tests before publishing any metal-free transformation and taking a gut check when assessing the viability of the chemistry based on the basic tenets of science, it is still difficult in some of these special cases to prove definitively what is going on.[80]



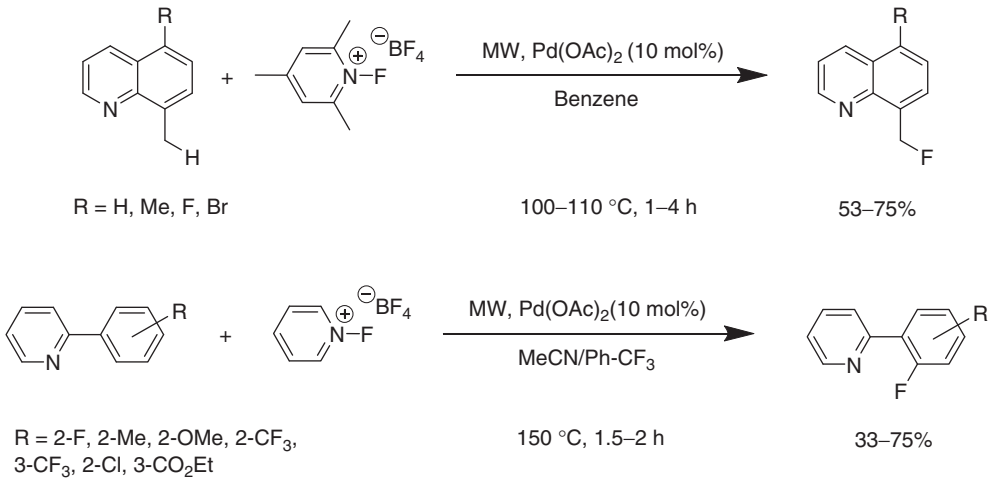
Scheme 14 Potassium tert-butoxide promoted coupling of electron-deficient nitrogen heterocycles and aryl iodides.

Microwave heating can also be used in conjunction with iridium,[81] palladium,[82] and copper[83] catalysis to form C–H bond-activated products. With the increasing interest in the incorporation of fluorine into molecules,[84] the Pd-catalyzed fluorination of C–H bonds is a noteworthy example.[85] The reaction involves the use of electrophilic *N*-fluoropyridinium reagents. Heating in the presence of catalytic palladium acetate allows for the fluorination of C–H bonds in a variety of substituted 2-arylpyridine and 8-methylquinoline derivatives (Scheme 15).

9.10.5.2.5 Selected additional examples

Beyond couplings, metathesis, and C–H bond activation, microwave heating has, of course, found application in a range of other metal-catalyzed processes that require heat. Hydrogenation and carbonylation reactions are discussed in Section 9.10.5.6. Gold catalysis, a topic of much current interest,[86] can benefit from microwave heating; hydroaminations,[87] hydroarylations,[88] and intramolecular [4 + 2] cycloadditions[89] being examples (Scheme 16).

Click reactions such as the Huisgen 1,3-dipolar cycloaddition of azides and alkynes,[90] along with its copper-catalyzed analog,[91] are widely used today in many areas of preparative chemistry.[92] Microwave heating is a valuable tool in this area.[93,94] The main advantages are increased rate of reaction and improved yields. In some cases, reactions reach completion only if microwave irradiation is used and, in a few instances, the click reaction is apparently not possible without it. A classic example of a copper-catalyzed click reaction using microwave heating is the three-component, one-pot procedure for preparing 1,4-disubstituted-1,2,3-triazoles from alkyl halides, alkynes, and sodium azide (Scheme 17).[95] The organic azide is formed *in situ*, avoiding the handling of these potentially explosive materials. Heating at 70 °C for 10–15 min is sufficient to generate the triazoles in excellent yield. In this case the active copper (I) catalyst is generated by the comproportionation of Cu(0) and Cu(II) precursors. Both copper-in-charcoal[96] and polymeric alkynylcopper(I) ladder complexes[97] can be used as effective heterogeneous catalysts in 'on water' click



Scheme 15 Palladium-catalyzed fluorination of C–H bonds.

reactions in conjunction with microwave heating. Microwave-assisted copper-catalyzed click chemistry is not limited to organic chemistry. Application has been found in supramolecular,[98] oligonucleotide,[99] carbohydrate,[100] and polymer chemistry,[101] to mention a few.

A common misconception is that microwave heating is not suitable for enantioselective reactions. This is definitely not the case. Metal-catalyzed asymmetric allylic alkylation reactions can be performed in high yield and enantioselectivity.[102] They are generally run at 145–220 °C for between 30 s and 20 min. The same reactions often take a day or more at room temperature. This chemistry has been used as a key step in the synthesis of tipranavir, an orally bioavailable HIV inhibitor (**Scheme 18**).[103]

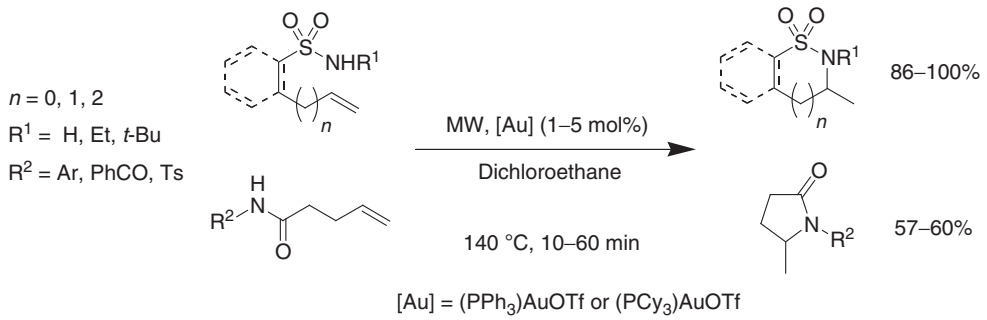
9.10.5.3 Cycloaddition and Rearrangement Chemistry

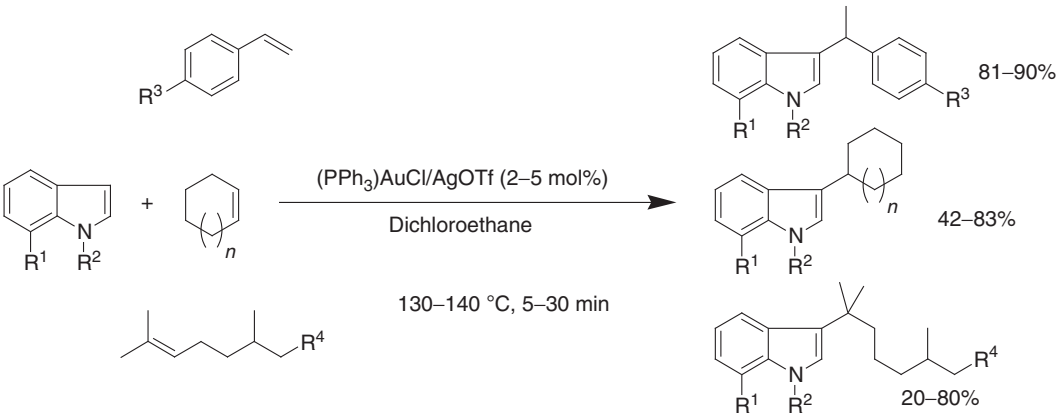
9.10.5.3.1 Introduction

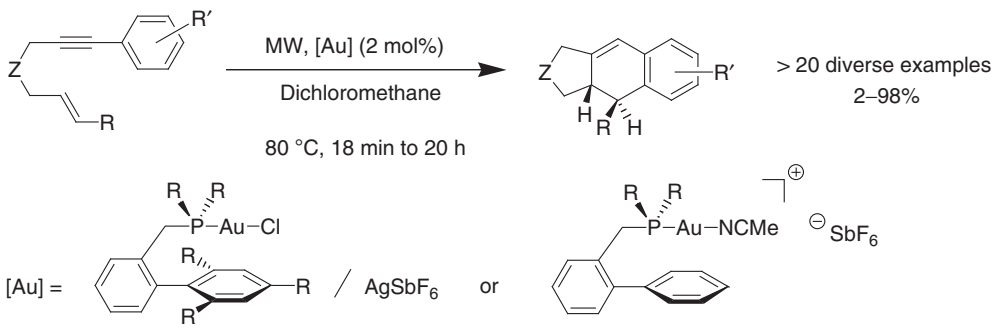
The origins of many cycloadditions and rearrangements used today dates back to the early days of organic chemistry. They were (and still are) often performed at high temperatures (see Volume 5 for more information on 'Combining C–C π-Bonds'). A glance at the literature shows that these reactions are now frequently carried out using microwave heating and thus they have been the subject of a wide array of research articles in the field.[104] Here, four specific classes of reaction are discussed, drawing out some key points as well as showing the range of reactions that have benefited from this improved heating method. This is followed by a discussion of the topic of the use of heating aids in microwave-assisted synthesis through the lens of cycloaddition and rearrangement chemistry.

9.10.5.3.2 The Diels–Alder cycloaddition

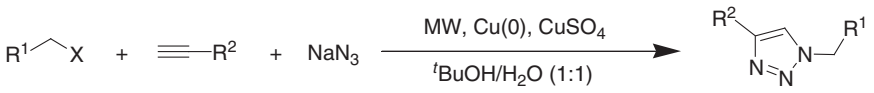
The application of microwave heating to the Diels–Alder [4 + 2] cycloaddition goes back to one of the two initial papers on microwave-assisted organic synthesis published in 1986.[4] There, and in a subsequent report,[105] five Diels–Alder reactions were performed in sealed tubes using a domestic microwave oven. In each case, the reaction time is decreased and the yield increased over the conventional approach. The microwave reactions were performed at higher temperatures than the conventional comparisons, as well as being run in sealed tubes rather than reflux, these factors explaining the rate acceleration seen. These early reports sparked other work in the area, and it was not long before the topic of nonthermal microwave effects raised its head. In one example, cyclic dienes were reacted with acetylenic dienophiles under solvent-free conditions.[106] Calculations were also performed, predicting asynchronicity in the reaction mechanism with a large enhancement in the dipole moments from the ground states to the transition state. Stabilization of polar transition states by the microwave field has been argued to reduce the required energy of activation and therefore to accelerate such transformations.[17] Comparing experimental results obtained with microwave and conventional heating, and taking into account the calculations the conclusion was drawn that nonthermal microwave effects were at play. However, a reassessment of the work shows that differences in yield and regiochemical outcome between conventional and microwave heating come down to inaccurate temperature measurement.[107,108] When microwave and oil-bath experiments were both performed using *in situ* temperature measurement by means of a fiber-optic probe identical results were obtained. A more egregious example of a purported nonthermal microwave effect is the case of the reaction of 6,6-dimethylfulvene with alkenes and alkynes (**Scheme 19**).[109] When using microwave heating, the reactions were performed at 120–150 °C in DMSO as the solvent. Conventionally heated examples were run at 80 °C in benzene and different products obtained. The conclusion drawn is that that microwave irradiation can alter the pathway of the reaction but this is clearly not a fair comparison of the two heating methods; different solvents and different temperatures and different reaction times being used. The reaction has more recently been assessed computationally and, not surprisingly, thermal effects alone deemed responsible for the differences in regioselectivity or product yield.[110]







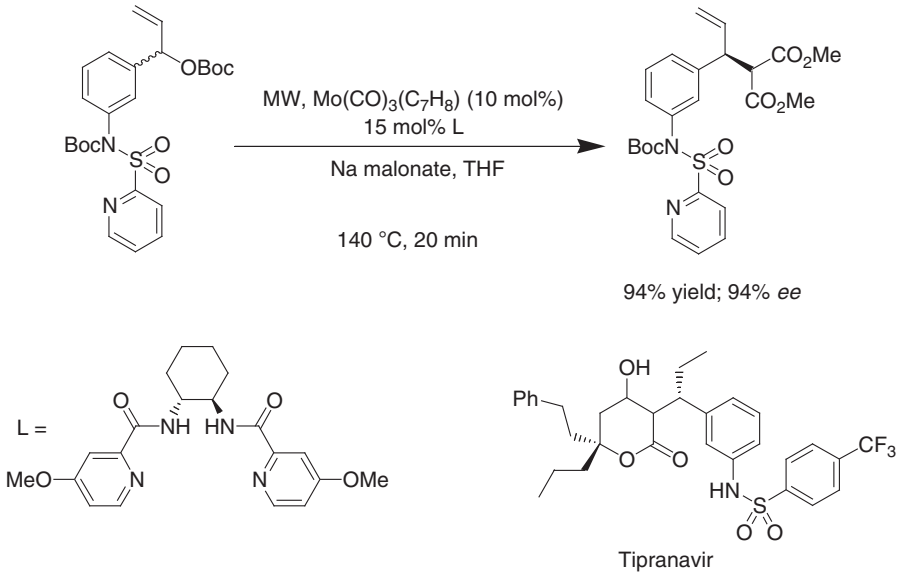
Scheme 16 Gold-catalyzed transformations.



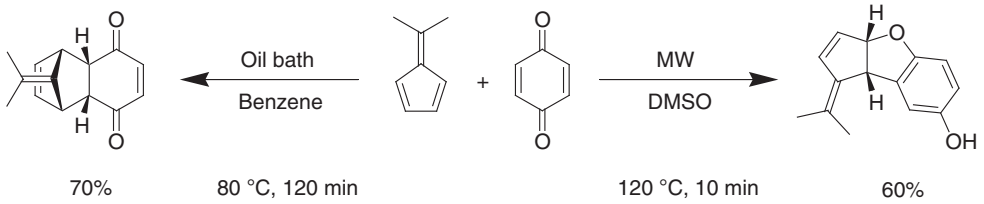
R^1 = Ph; X = Br; R^2 = CH_2CH_2OH, $C(Me)_2OH$, $C(OH)C_5H_{13}$, CO_2Et, $SiMe_3$

R^2 = Ph; X - Br, I; R^1 = Ph, 2 or 4-$NO_2C_6H_4$,4-$(CN)C_6H_4$, 3,4,5-$(OMe)_3C_6H_2$, 3-Cl-4-$OMeC_6H_3$, CH_2Ph, Me

Scheme 17 Copper-catalyzed click reaction.



Scheme 18 Molybdenum-catalyzed double dynamic kinetic asymmetric transformation in the synthesis of Tipranavir.



Scheme 19 Diels–Alder reaction of 6,6-dimethylfulvene with benzoquinone.

Intramolecular Diels–Alder reactions can also benefit from microwave heating.[111] One example involves the preparation of 4-substituted indoles from furan precursors (Scheme 20).[112] The Boc-protected homoallylic furanyl amine starting materials undergo an *in situ* cycloaddition and subsequent dehydrative aromatization with thermal Boc-deprotection to generate the indole products in one step. The resulting indole formed using a cyclohexenol-substituted starting material resembles the core heterocycle of many Ergot alkaloids.

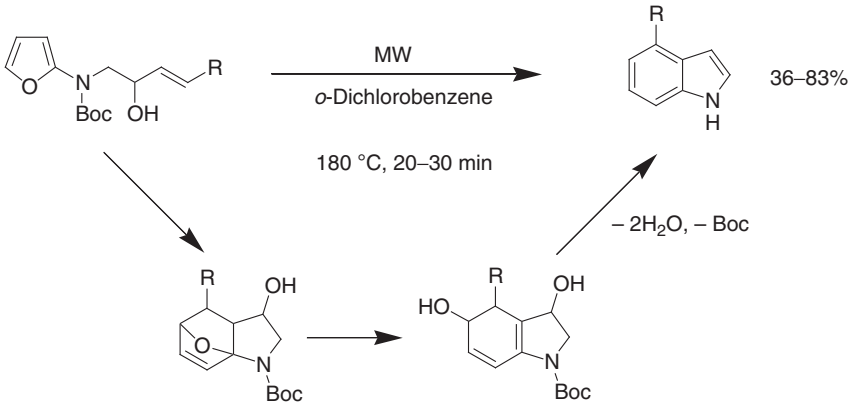
Hetero-Diels–Alder cycloadditions can also be performed using microwave heating[113] as can retro-Diels–Alder reactions.[114] In the case of the latter, the Lewis acid-catalyzed unmasking of cyclopentenone building blocks can be used to prepare precursors to arachidonic acid derivatives, maleic anhydride being used as a trap for the cyclopentadiene by-product (Scheme 21).[115]

Diels–Alder reactions can be performed in a highly stereoselective manner using microwave heating.[116] This often requires the use of a chiral catalyst. One interesting example pertains to rhodium-catalyzed intramolecular [4 + 2] cycloadditions using a chiral phosphine–phosphite ligand (Scheme 22).[117] Reactions were first performed by stirring a mixture of rhodium precursor, ligand, and substrate at room temperature. However, optimal results are obtained by first microwave heating the Rh salt and ligand, L, for 2 h at 80 °C before substrate addition and heating the entire reaction mixture at 50 °C for a further 20 h. The $[Rh\ (L_2)_2]^+$ species generated in the 'conditioning' step acts as a more selective catalyst.

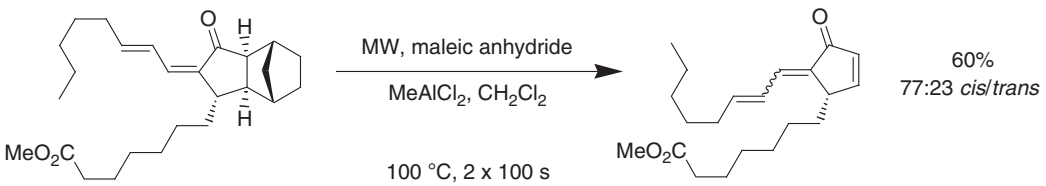
From a materials chemistry perspective, single-walled nanotubes and fullerenes, such as C_{60}, can be derivatized by means of Diels–Alder and hetero-Diels–Alder reactions.[118] The relatively low-lying LUMO of C_{60} makes it behave as an electron-deficient alkene and it reacts relatively rapidly under high temperature conditions. Nanotubes react similarly, albeit significantly slower.

9.10.5.3.3 [2 + 2 + 2] Cyclotrimerization reactions

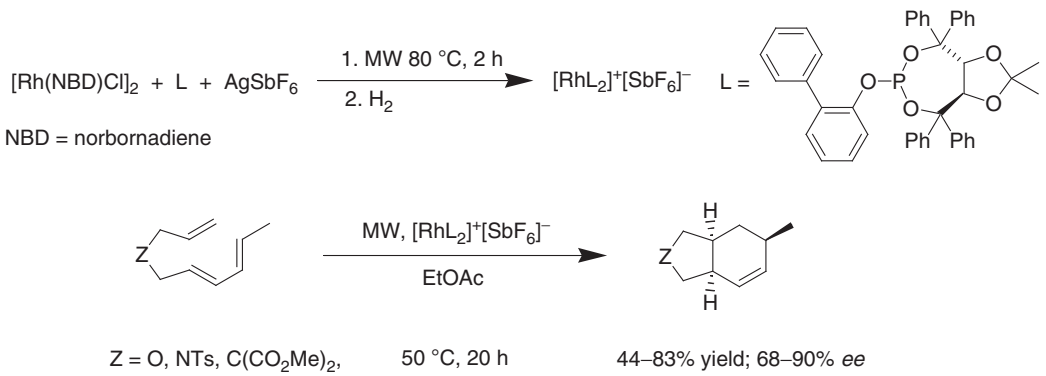
Transition-metal-catalyzed [2 + 2 + 2]-cyclotrimerization reactions of alkynes, nitriles, isocyanates, carbodiimides, and other coupling partners offer a valuable route into highly functionalized aromatic carbocyclic and heterocyclic structures, and microwave heating has been used on a number of occasions. Both solution-phase and solid-supported cyclotrimerizations can be carried out in short reaction times using cobalt,[119,120] nickel,[120,121] or ruthenium[122,123] catalysts (*see* Chapter 5.31). Rhodium[123,124] and iridium[125] complexes have also seen application as catalysts when using microwave heating. The use of an open-vessel approach and Co, Ni, or Ru catalysis can be used for the chemoselective preparation of benzenes, pyridines, pyridones, and iminopyridines, one of the reagents being added via a syringe pump during the course of the reaction (Scheme 23).[126]



Scheme 20 Intramolecular-furan-Diels–Alder approach to 4-substituted indoles.



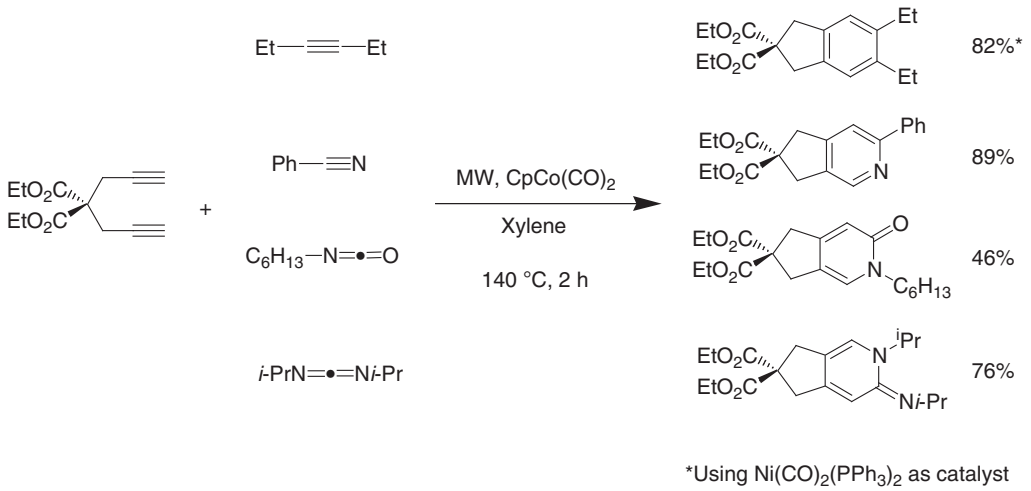
Scheme 21 Unmasking of a cyclopentenone building block by a Lewis acid-catalyzed retro-Diels–Alder reaction.



Scheme 22 Stereoselective Diels-Alder reactions.

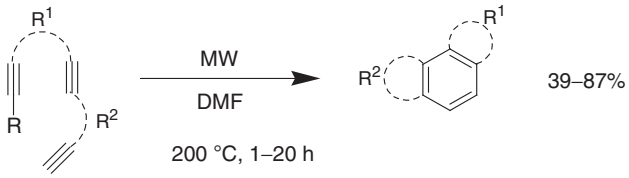
Comparison of conventional and microwave heating for some of these sealed- and open-vessel procedures at first suggests a difference in catalytic activity. When using microwave heating, the entire reaction mixture is heated directly rather than in an oil-bath where the vessel walls are heated and the vessel contents increase in temperature through conduction and convection. This generally results in the temperature of a conventionally heated reaction vessel being higher than that of the reaction mixture. Because metal catalysts can undergo decomposition on hot reactor surfaces, the elimination of such a hot surface by microwave

heating has been suggested to increase the lifetime of the catalyst and therefore may lead to better conversions as compared with a conductively-heated process. These so-called wall effects have been invoked to explain the differences in the results of cyclotrimerization reactions depending on the heating method. This has been probed in detail and again the differences are attributed to temperature; conventional and microwave heating experiments not being performed under isothermal conditions.[127] This reiterates the need for accurate internal temperature measurements when making comparisons.



Scheme 23 Preparation of benzenes, pyridines, pyridones, and iminopyridines by [2 + 2 + 2] cyclotrimerization reactions.

In certain cases, intramolecular [2 + 2 + 2] cyclotrimerization of alkynes is possible without the addition of a metal catalyst when using microwave heating (Scheme 24).[128] Reactions are performed at 200 °C for 1–20 h. The choice of DMF as solvent is interesting, given that it is prone to decompose to carbon monoxide (CO) and dimethylamine at temperatures in excess of 165 °C.[129] Because both the decomposition products are gases at these elevated temperatures and the reactions are run in sealed vessels, overpressurization and tube failure could be a potential issue.



R = H, $(CH_2)_3CCH$
R^1 = $(CH_2)_3$, CH_2OCH_2, CH_2SCH_2, $CH_2N(Ts)CH_2$
R^2 = $(CH_2)_3$, $(CH_2)_4$, $(CH_2)_3CH{=}CH_2$, CH_2OCH_2CCH

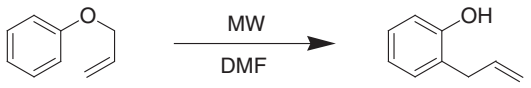
Scheme 24 Catalyst-free [2 + 2 + 2] cyclotrimerization reactions.

9.10.5.3.4 The Claisen rearrangement

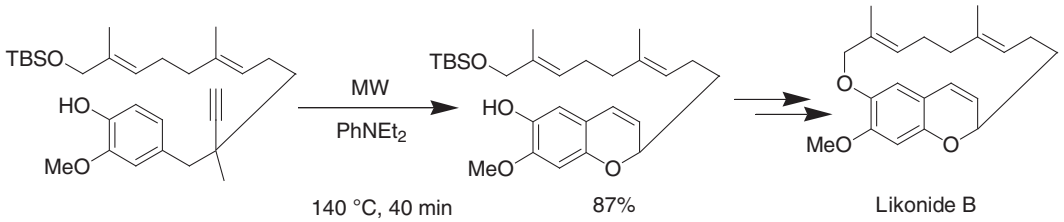
The Claisen rearrangement (the [3,3] sigmatropic rearrangement of allyl vinyl ethers to γ-δ-unsaturated carbonyl compounds) is a very useful synthetic transformation but often requires the use of high temperatures and long reaction times to obtain reasonable product yields. As with the Diels–Alder reaction, the application of microwave heating for the Claisen rearrangement dates back to the first reports in organic chemistry, allyl phenyl ether being converted to 2-allyl phenol in 80% yield after 5 h at approximately 200 °C (Scheme 25).[4,105,130] This same reaction has been studied using a range of different microwave equipments, serving as a good example of a high-temperature transformation.[131,132]

There have been numerous applications of the microwave-assisted Claisen rearrangement in the preparation of natural products, such as (±)-likonide B (Scheme 26)[133] A Claisen rearrangement is also a key step in the construction of the skeleton of the triterpenoid natural product azadirachtin. In this case, optimal results are obtained when 15 pulses of 1 min irradiation are used.[134]

Microwave heating has also seen significant application in the aza–Claisen rearrangement.[135,136] Again, natural products have been prepared this way, one example being the α-substituted α-amino acid sulfamisterin.[137] The polar part of the molecule is

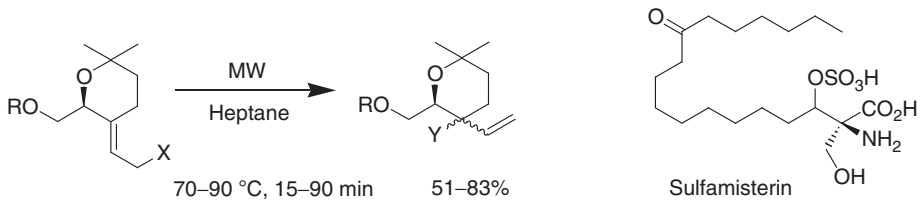


Scheme 25 The Claisen rearrangement of allyl phenyl ether to 2-allyl phenol.



Scheme 26 A Claisen rearrangement as a key step in the synthesis of (±)-likonide B.

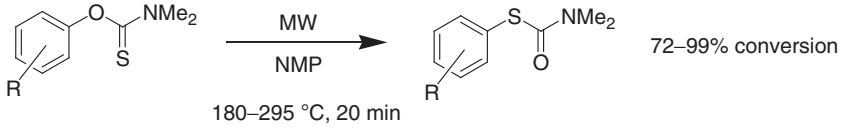
prepared by an aza-Claisen rearrangement of an allylic thiocyanate or trichloroacetimidate, generating a quaternary carbon bearing an amino group as one of the substituents (Scheme 27).



Scheme 27 Aza–Claisen rearrangements as a key step in the synthesis of the polar part of sulfamisterin.

9.10.5.3.5 The Newman–Kwart rearrangement

The Newman–Kwart rearrangement (NKR) offers a route to thiophenols from phenols, via their O- and S-thiocarbamates.[138] It is very useful synthetically and proceeds via an O- to S-aryl migration. Due to the high activation energy, the reaction typically requires heating at temperatures between 200 and 300 °C. As with the Claisen rearrangement, the NKR has been used as a probe for the effectiveness of different microwave apparatus.[139–141] From a synthetic chemistry standpoint, microwave heating for 20 min at 180–295 °C allows for the conversion of a range of O-thiocarbamates into their S-thiocarbamate analogs (Scheme 28).[142] Of the substrates which could be prepared, none of the examples tested are beyond the scope of available instruments.[143]



Scheme 28 The Newman–Kwart rearrangement of O-thiocarbamates into S-thiocarbamates.

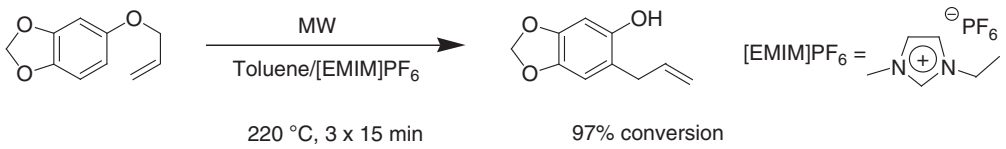
A microwave-facilitated kinetic study of the NKR has been undertaken. Microwave heating proved to be an ideal method for the rapid acquisition of data required for a kinetic investigation.[144] Reactions were performed either in sealed tubes or in an open

vessel and conversions were determined by high-performance liquid chromatography analysis of diluted samples. Data were gathered and analyzed to determine the effects of substituent, solvent, and concentration on the reaction order. Reaction rate constants, Arrhenius constants, and activation energies were also determined. Overall, the study allowed for some considerable insight into the mechanism of the NKR and the reaction rate order was found to be more complex than previously thought.[145] The general area of reaction monitoring of reactions involving microwave heating is addressed in more depth in Section 9.10.9.

The microwave-assisted NKR, along with a Diels–Alder reaction, has also been the subject of a computational study with the objective of assessing any potential microwave effects.[146] As expected, no nonthermal effects were predicted. Of note was that the study did show that it was possible to investigate the existence of nonthermal microwave effects on chemical reactions theoretically without having to undertake a real-time simulation of microwave–molecule interactions. This greatly reduces the amount of computational power (and time) required. Instead, transition state theory, which provides the rate constants for elementary reactions at a given temperature, was used to verify that experimentally determined results could be explained purely by reaction temperature.

9.10.5.3.6 The use of heating aids

Given that many cycloadditions and rearrangements require elevated temperatures, that the reagents are often nonpolar and that the transformations are traditionally performed in nonpolar solvents, heating the reaction mixture using microwave irradiation can sometimes be a challenge. To overcome this, highly microwave absorbing heating aids have been used. This indirect heating of the reaction mixture allows for the elevated temperatures to be reached quickly and effectively. Clearly, the heating aid must not react chemically with the reagents. One class of compounds that has been used is ionic liquids because many are immiscible with common organic solvents.[147] The majority of the attention has been focused on 1,3-dialkylimidazolium salts. In the Diels–Alder reaction between 2,3-dimethylbutadiene and methyl acrylate using toluene as the solvent, 20 mg of 1-isopropyl-2-methylimidazolium hexafluorophosphate, [*i*-PMIM]PF_6, is sufficient to heat the reaction mixture to 200 °C and an 80% yield of the cycloaddition product is formed in 5 min.[148] Likewise, Claisen rearrangement of allyl ethers can be performed in toluene doped with1-ethyl-3-methylimidazolium hexafluorophosphate, [EMIM]PF_6 (Scheme 29).[149]

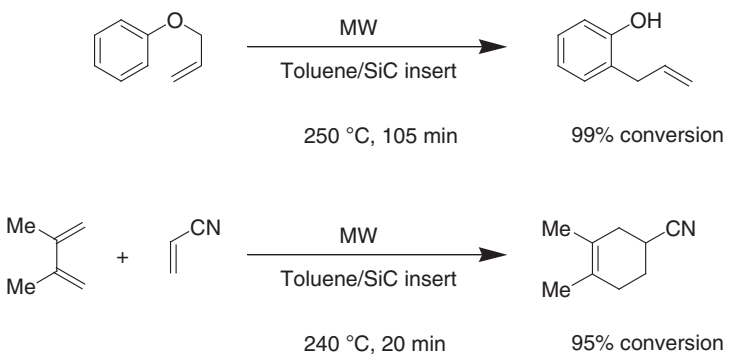


Scheme 29 A Claisen rearrangement performed in toluene doped with an ionic liquid.

The application of ionic liquids as heating aids is not limited to cycloaddition and rearrangement chemistry, other reactions can also benefit.[150] However, it is not possible to perform reactions that use or generate nucleophiles, such as halide ions. In these cases, the ionic liquid reacts to form unwanted by-products.[148] In addition, there can be issues associated with temperature measurement when using ionic liquids as dopants.[151] Most ionic liquids are more dense than the solvent used for the reaction and, even with effective stirring, they tend to sink to the bottom of the vessel. Microwave units measure temperature indirectly by means of an infrared sensor located on the side or the bottom of the microwave cavity. If the sensor is measuring from the bottom of the vessel, it can lead to a value significantly higher than that of the bulk reaction mixture because it is recording the temperature of the ionic liquid component. If the reading is taken from the side of the reaction vessel, it is more representative of the bulk reaction temperature. The most accurate way to perform reactions using dopants is to employ a fiber-optic temperature measurement device located in the reaction mixture itself.

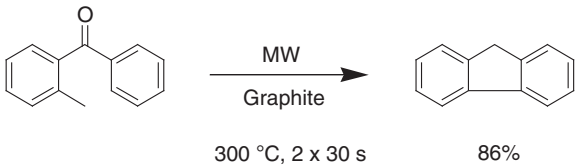
With these inherent disadvantages, other ways of indirectly heating a reaction mixture have been sought. SiC heating elements can be used effectively.[152] This material is highly microwave absorbing, chemically inert, and has a very high thermal conductivity and melting point. Small SiC cylinders can be added to reaction mixtures without compromising the ability to stir the vessel contents. The Claisen rearrangement of allyl phenyl ether, the Diels–Alder reaction of 1,3-dimethylbutadiene and acrylonitrile can both be performed effectively using this approach (Scheme 30).[153] Rather than use a cylinder of SiC as a heating aid, the entire microwave vessel can be made of SiC.[154] This option, albeit costly, does allow for interesting comparisons between microwave and conventional heating to be made.[155] SiC is so highly microwave absorbing that the contents of the vessel are essentially shielded from microwave irradiation. As a result, heating of the reaction mixture is purely 'conventional'; that is, by convection and conduction. SiC can additionally be used as a material for manufacturing well plates with application in combinatorial chemistry (see Section 9.10.6).[156]

At this point it is also worth mentioning the use of graphite as a microwave absorber. Rather than putting graphite into a reaction mixture containing solvent and using it as a heating element, a significant amount of attention has been focused on performing the reaction solvent-free on graphite.[157] As such, it has been dubbed 'graphite-supported microwave synthesis.' Graphite has a very high thermal conductivity and can reach highly elevated temperatures very rapidly. In a monomode microwave unit, temperatures in excess of 300 °C can be reached within a few seconds of irradiation at 300 W. For that reason, most chemistry is performed at lower power input levels. Diels–Alder cycloaddition reactions can be complete after a few 1-min pulses of 30 W of microwave power.[158] The sample is heated for 1 min and then allowed to cool for 2 min before repeating



Scheme 30 Silicon carbide heating aids in cycloaddition and rearrangement reactions

the process. This proves more successful than continuous microwave irradiation because as the temperature increases to above approximately 200 °C, retro-Diels–Alder reactions begin to predominate, thus compromising product yields. A dichotomy is that while high power is better for product conversion, lower powers often lead to sublimation rather than reaction. As well as cycloadditions, a range of other reactions have been performed using this approach. It can be used to carry out reactions more typically accomplished by flash vacuum pyrolysis and which usually require temperatures much higher than the limit of most commercially available scientific microwave units.[159] An example is the Elbs cyclization (pyrolysis of an *ortho*-methyl substituted benzophenone to generate a condensed polyaromatic). Reaction of 2-methylbenzophenone on graphite yields primarily fluorene (Scheme 31). Alongside the new chemistry developed, there are some safety concerns. With large graphite particles, such as flakes, electric discharges can occur. Also, if reactions are performed in glass tubes or flasks, the temperature has to be carefully moderated so as not to melt the vessel walls. The safest way to use graphite as a heating aid is to perform reactions in quartz vessels under a nitrogen atmosphere.



Scheme 31 The pyrolysis of an ortho-methyl substituted benzophenone on graphite.

9.10.5.4 Carbonyl Chemistry

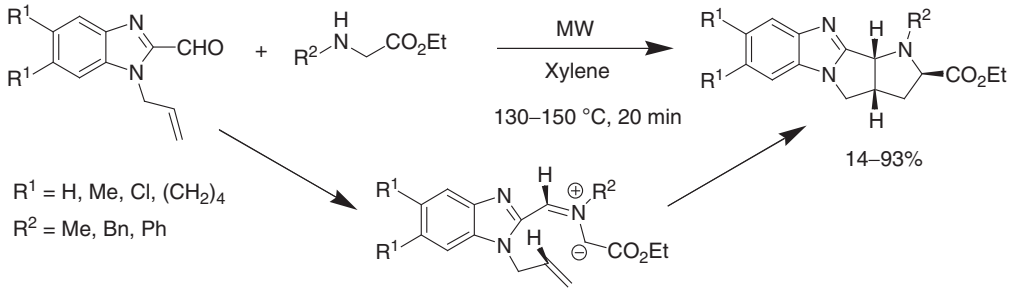
9.10.5.4.1 Introduction

Microwave heating has been used extensively for reactions involving carbonyl compounds. Many of these transformations lead to heterocyclic products, which are of great interest to medicinal chemists. A glance at the literature in this area shows a significant number of contributions from the pharmaceutical industry. This is not totally surprising given that in such a setting time is money and the application of microwave heating offers a rapid (and frequently automated) route to the preparation and decoration of heterocyclic scaffolds that can be submitted for biological screening. Since the number of reactions leading to heterocyclic products using microwave heating is vast, only a select number of examples are discussed here. For a broader overview, readers are directed to the many reviews of the field.[160–162]

9.10.5.4.2 Condensation reactions

Condensation reactions often require heat and have been performed extensively using microwave irradiation. Examples include Knovenagel,[163] aldol,[164] and Dieckmann[165] condensations. Often the condensation reaction is concatenated with another transformation. One example is the synthesis of fused pyrrolidine scaffolds by condensation of benzimidazolecarbaldehydes with secondary amino esters to form an ylide, which then undergoes an intramolecular 1,3-dipolar cycloaddition (Scheme 32).[166] The products are obtained with high regio- and stereoselectivity.

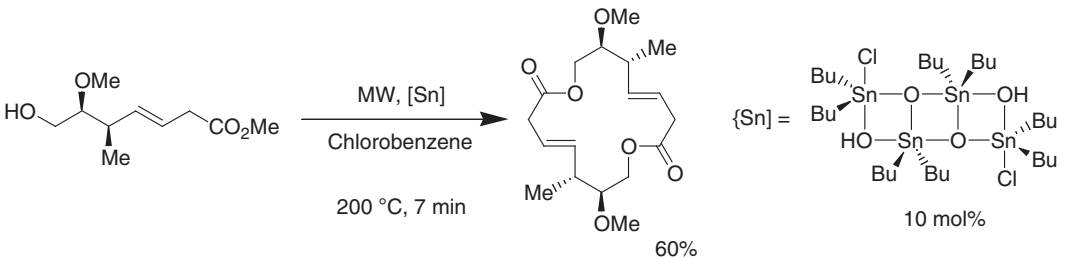
Broadening the topic somewhat, esterification and transesterification reactions have been performed extensively using microwave heating.[167] As well as being a tool for preparation of simple esters, the technology has been used for the acid-[168] or base-[169,170] catalyzed preparation of biodiesel, a biorenewable fuel formed as the product of the transesterification of vegetable oil and methanol. The base-catalyzed reaction is very rapid and, by working in continuous-flow mode, it is possible to produce up to 7 l of biodiesel per minute with a modestly-sized microwave unit.[171] When using butanol instead of methanol as a reagent, the



Scheme 32 Preparation of fused pyrrolidine scaffolds.

reaction can be performed in the absence of a catalyst by operating in a sealed vessel at 310 °C for 4 h.[172] To reach this temperature six SiC inserts are used as heating aids and the reaction has to be performed in a thick-walled quartz vessel capable of withstanding the 80-bar autogenic pressure involved. The same reaction can be performed more rapidly and at ambient pressure by using an acid catalyst.[173]

From a natural product standpoint, microwave-assisted transesterification can be used to prepare macrodiolides.[174] The reaction involves cyclodimerization of nonracemic chiral hydroxy esters using a distannoxane catalyst. Heating at 200 °C for 7 min in a sealed tube is sufficient for preparation of a 16-membered macrodiolide (Scheme 33).



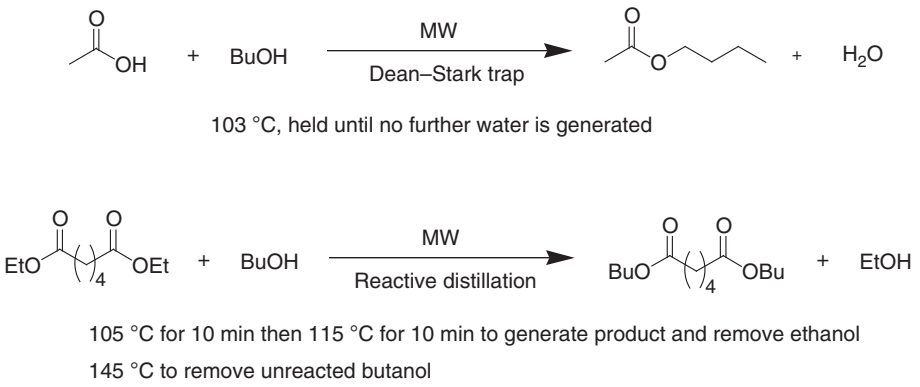
Scheme 33 Preparation of a macrodiolide by transesterification.

These condensation reactions involve loss of a small molecule, often water. In addition, many of the reactions are reversible in nature, an equilibrium being established in solution. This can pose a problem when using a sealed tube to perform the reaction. Although elevated temperatures can be achieved under these conditions, removal of water as it is formed is not possible unless a drying agent is added. The obvious choice may be molecular sieves. However, the literature suggests that they cannot be used efficiently as water scavengers under standard sealed-vessel microwave heating conditions.[175] The reasons for this are not so much associated with the fact that these zeolite materials are strong microwave absorbers but more because their ability to remove water is at its maximum at room temperature. The issues associated with operating in sealed-vessel mode can be overcome by using an open-flask approach in conjunction with a Dean–Stark trap[176] or reactive distillation.[177] Take, for example, the esterification of acetic acid with butanol.[178] Using a 1:1 M ratio of the reagents and sulfuric acid (1 wt%) as catalyst, the reaction mixture is heated until water starts to accumulate in the Dean–Stark trap and then held at this temperature (103 °C) until water stops being generated. Looking at the case of the acid-catalyzed reaction of diethyl adipate with butanol, the reaction could be driven toward completion by removing the ethanol by-product.[178] Working with a 2:1 M ratio of butanol to diethyl adipate, the reaction mixture is first heated to 105 °C, holding it at this temperature for 10 min. The temperature is then raised to 115 °C and held for another 10 min. By this time all the ethanol produced in the reaction is removed. The temperature is then raised one more time, to 145 °C, to strip off any butanol remaining in the reaction mixture, leaving the dibutyl adipate product in the reaction vessel (Scheme 34).

Clearly operating in open-vessel mode means that the maximum temperature reached is that of reflux, negating one of the main advantages of microwave heating; namely, accessing high temperatures and short reaction times. However, the examples shown here demonstrate that performing a distillation from a scientific microwave allows an exquisite level of control not easy to duplicate in an oil or sand bath.[179] As well as in preparative chemistry, this has been leveraged in the natural products, flavors, and fragrances fields, being used extensively as a tool for extraction of essential oils from plants and fruits.[180,181]

9.10.5.4.3 Multicomponent reactions

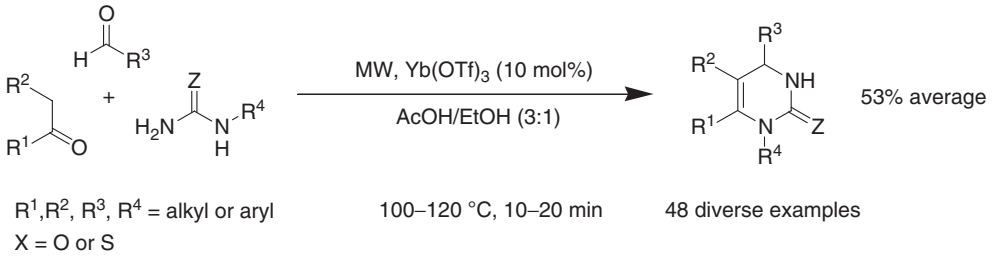
Multicomponent reactions (MCRs), defined as one-pot processes in which at least three easily accessible starting materials react to give a single reaction product, are of tremendous use for the introduction of many points of structural diversity into heterocyclic compounds in a single synthetic step. Combining these features with the short reaction times possible when using microwave heating provides a rapid and efficient route to heterocyclic libraries suitable for biological evaluation and structure–activity relationship (SAR) studies.[182] Microwave heating has found application in synthetic routes in a wide array of nitrogen-, oxygen-, and



Scheme 34 Application of a Dean–Stark trap or reactive distillation for reactions involving equilibria.

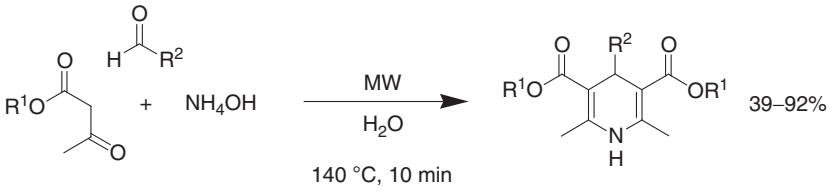
sulfur-containing, five- and six-membered, partially unsaturated or fully aromatic heterocyclic rings by means of MCRs involving carbonyl compounds.

The acid-catalyzed cyclocondensation of urea, β-ketoesters, and aromatic aldehydes to yield dihydropyrimidines (the Biginelli reaction) has received significant attention.[183,184] A number of lanthanide-based Lewis acid catalysts can be used, the reaction being complete in 10–20 min at 120–140 °C (Scheme 35).[185]



Scheme 35 Biginelli dihydropyrimidine synthesis.

The Hantzsch 1,4-dihydropyridine (DHP) synthesis is another multicomponent process that has proved popular when using microwave heating.[186] It involves the reaction of an aldehyde, β-ketoester, and ammonia and can be performed in water as the solvent, facilitating product isolation (Scheme 36).[187,188]



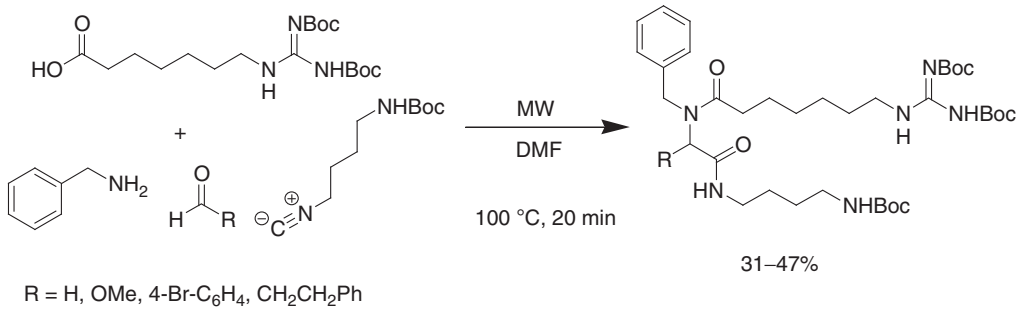
R^1 = Et; R^2 = Ph, 2-NO_2-C_6H_4, 2-OMe-C_6H_4, 2-Me-C_6H_4, 2-Br-C_6H_4, 3,4,5-$(OMe)_3$-C_6H_2

R^1 = Et, *t*-Bu, Bz or diketone = dimedone; R^2 = C_6H_{11}, *i*-Pr, 4-OMe-C_6H_4, 4-CN-C_6H_4, 2-thiophenyl, 2-pyridyl

Scheme 36 Hantzsch 1,4-dihydropyridine (DHP) synthesis.

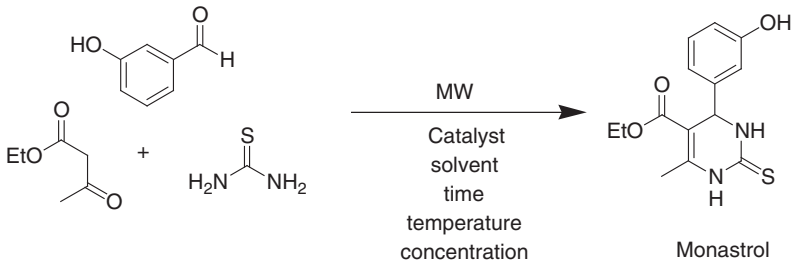
A final example where microwave heating has made a significant impact is in Ugi condensation.[189] This valuable four-component reaction involving a ketone or aldehyde, an amine, an isocyanide, and a carboxylic acid can be used as an expeditious route to 15-deoxyspergualin (15-DSG) analogs.[190] Spergualin is a natural product that exhibits immunosuppressive, antitumor and antibacterial activities. Its derivatives such as 15-DSG have been clinically approved for acute organ transplant rejection. The approach using microwave heating generates the peptoid core in a single step (Scheme 37).

Given the number of variables involved in multicomponent reactions (including reagent stoichiometry, catalyst, solvent, temperature, and time), optimization can be a labor-intensive process. A Design of experiments (DoE) approach can be used to accelerate this.[191] Simple experimental designs and statistical tools for data analysis can provide a great deal of information about a reaction after only a few experiments. Instead of having to optimize each parameter individually, a DoE approach involves



Scheme 37 Ugi reaction to prepare 15-deoxyspergualin analogs.

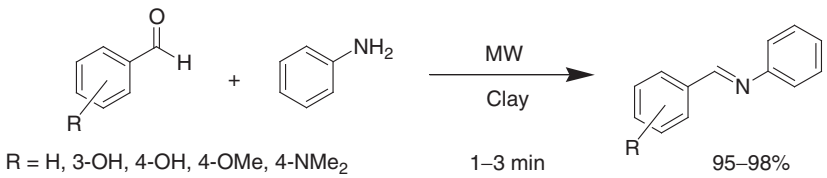
performing a set of key reactions, the statistical analysis of which can give a valuable insight into which parameters are most important. This is followed by an optimization component where the best settings for the important variables are determined, again by performing a discrete set of reactions and analyzing the data using statistical methods. As most synthetic chemists are not by their training statisticians, there is an array of commercially available software packages available to help. A DoE approach has been combined with microwave heating for optimizing both the Biginelli[192] and Ugi[193] reactions, among others.[194] In the synthesis of the mitotic kinesin Eg5 inhibitor monastrol by the Lewis-acid catalyzed Biginelli reaction of ethyl acetoacetate, 3-hydroxybenzaldehyde, and thiourea, a series of 29 experiments was all that was needed in order both to identify catalyst loading, temperature, and concentration as the key parameters and then to determine the optimal conditions for the reaction (Scheme 38).[192]



Scheme 38 A design-of-experiments approach to the Biginelli reaction.

9.10.5.4.4 Solvent-free reactions

With the increasing drive toward cleaner, greener processing, performing reactions in the absence of a solvent is receiving increasing attention (*see* Chapter 9.11).[195] A wide array of synthetic transformations has been performed solvent-free using microwave heating and those involving carbonyl compounds predominate.[196] In the early days when domestic microwave ovens were the only equipment available, performing reactions in the absence of an organic solvent was particularly attractive because it reduced the risk of an accident. One technique used extensively then, and even now, is to adsorb the starting materials onto a solid support and irradiate this with microwave energy.[197] The support can either be inert or an acidic or basic material, offering the capability to catalyze the reaction.[198] For example, the reaction of aromatic aldehydes with aniline to yield imines can be achieved in 1–3 min of microwave heating after adsorbing the reagents on a clay support (Scheme 39).[199] MCRs can also be performed using this approach, the Hantzsch[200] and Ugi[201] reactions being examples.



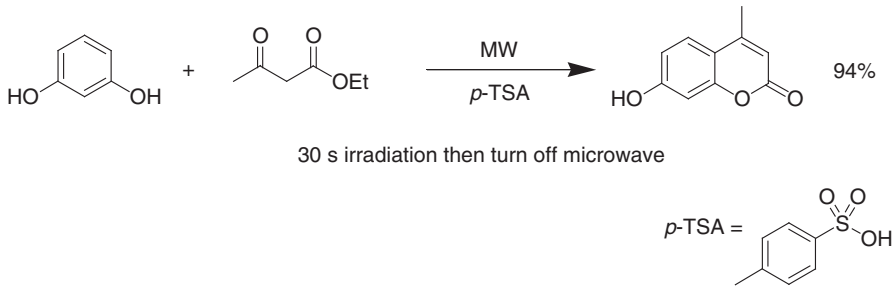
Scheme 39 Solid-supported solvent-free synthesis of imines.

An interesting way to perform and monitor these solid-supported solvent-free reactions is to use a thin-layer chromatography (TLC) plate.[202] Reagents are co-spotted onto the plate, it then being placed into the microwave cavity, irradiated, allowed to cool, and then eluted and visualized to assay the extent of reaction. Several TLC plates can be irradiated at the same time, each with a

different stoichiometry of reagents, or else different reagents. This process allows for more rapid optimization of reactions and also for the synthesis of a library of examples.[203]

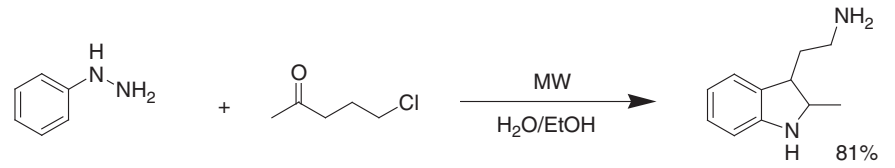
In some of the examples of solid-supported solvent-free reactions, the reaction times reported are very short; a matter of seconds or a minute of irradiation in a domestic microwave oven. Further examination shows that the reagents are evenly adsorbed onto the support by dissolving them in an organic solvent, adding the support material, and then removing the solvent on a rotary evaporator. A note of caution needs to be made in these cases. Many condensation reactions occur very readily upon heating, especially when in a concentrated form. It could well be that the reaction is actually taking place on the rotary evaporator as the solvent is being removed. A few seconds of microwave heating in a domestic microwave oven is often not enough to heat the support very significantly. When assessing reports of solid-supported solvent-free reactions, it is important to look at them through the lens of discerning whether they are truly microwave-assisted or are, instead, rotary-evaporator mediated.

Another method for performing solvent-free synthesis is simply to heat the reagents in a reaction vessel. This has been used on a number of occasions.[204] Because many reactions involving carbonyl compounds are actually exothermic, one approach has been to use a short burst of irradiation initially and then turn the microwave off for the remainder of the synthesis. This has been used for the Biginelli reaction, as well as the Pechmann synthesis of coumarins (**Scheme 40**).[205] The issue with this approach is that it is essentially uncontrollable and is certainly not scalable.



Scheme 40 Pechmann synthesis of coumarins using a short burst of microwave irradiation.

Exothermic reactions are better performed using a solvent to act as a heat sink and with very controlled microwave heating in staged heating ramps. An example is the Grandberg synthesis of 2-methyltryptamine from 5-chloropentan-2-one and phenylhydrazine; in essence, it is a modified Fisher indole synthesis (**Scheme 41**).[132] The reaction mixture is first heated to 75 °C and held at this temperature for 10 min before continuing to ramp slowly to 150 °C and holding for 15 min. Using this two-step protocol it is possible to heat the reaction mixture controllably, and upon workup an 81% isolated product yield is obtained.

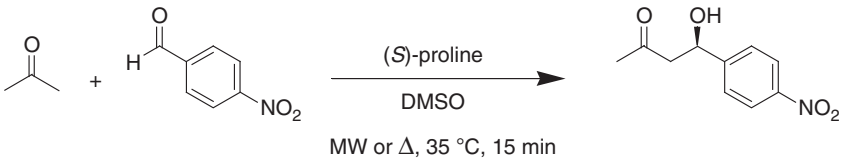


Scheme 41 Grandberg synthesis of 2-methyltryptamine using controlled two-stage heating.

9.10.5.5 Organocatalysis

Organocatalysis is one of the fastest growing areas in modern preparative chemistry (*see* Chapter 4.03).[206] Defined as an organic molecule that does not contain a metal which in substoichiometric amounts accelerates a reaction, organocatalysts are often natural products. Examples include L-proline and Cinchona alkaloids.[207] As well as yield, enantioselectivity is often a key metric in organocatalysis, with many secondary amine catalysts performing in an exemplary manner across a wide range of synthetic transformations. By virtue of the focus on selectivity, the majority of organocatalyzed reactions are performed at room temperature or lower. As a consequence, the kinetics are often slow, meaning that reactions can take a long time to reach completion. There is therefore a dichotomy when it comes to application of microwave heating to these transformations. Although it may reduce the reaction time, this may be at the cost of selectivity. As a result, there are not many examples in the literature.[208] Transformations that have been studied include the Mannich reaction,[209] aldol condensation,[210] Michael addition,[211] Diels–Alder cycloaddition,[210] Baylis–Hillman reaction,[212] and anomerization.[213] Unfortunately, of these examples, significant issues arise in many cases related to temperature measurement. They are performed using simultaneous cooling, either with compressed air or

cryogenic fluid. When reassessed using fiber-optic probes placed inside the reaction mixture, the purported rate accelerations observed when using microwave heating were found to be artifacts of inaccurate temperature measurement.[214] A case in point is the intermolecular, asymmetric aldol reaction of acetone with 4-nitrobenzaldehyde (Scheme 42). When performed at room temperature using DMSO as the solvent and 30 mol% of (S)-proline as the organocatalyst, the product is obtained in 68% isolated yield and 76% ee after 4 h.[215] Using microwave heating in conjunction with simultaneous air cooling at 35 °C (measured by an external infrared (IR) sensor), almost identical results (69% yield, 70% ee) are obtained after just 15 min, even with a reduced catalyst loading of only 20 mol%.[210] However, using conventional heating an identical result is obtained. The same is true when using microwave heating without any external cooling or with cryogenic cooling; the results in terms of both product yield and enantiomeric purity are identical. The same has been found to be true in a side-by-side comparison of conventional and microwave heating in the nitro-Michael addition of carbonyl compounds catalyzed by L-proline.[216]



Heating method	Average MW power input (W)	Yield/*ee* (%)
Oil-bath	–	63/68
MW	2	62/69
MW + cryogenic cooling	114	62/68

Scheme 42 The aldol reaction of acetone with 4-nitrobenzaldehyde performed under various conditions.

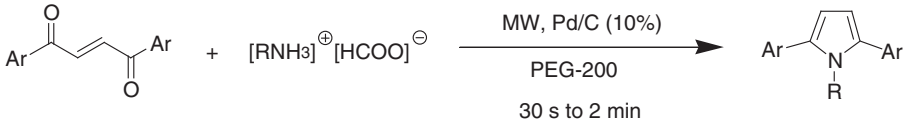
9.10.5.6 Reactions Involving Gaseous Reagents

9.10.5.6.1 Introduction

Scientific microwave units are, in essence, modern autoclaves. They are designed with safety in mind and reaction vessels can hold at least moderate pressures (generally up to 30 bar). They are therefore ideal to interface with gas-loading accessories capable of introducing an atmosphere of reactive gas into a vessel while in the microwave cavity.[217] However, the history of microwave-assisted reactions involving gases as reagents dates back to before these accessories were available. One approach was simply to bubble gas through the reaction mixture before sealing the vessel with a cap, but chemists were limited by the quantity of gas that could be predissolved in the reaction mixture. Gas can also be loaded into a sealed tube before placing it in the microwave cavity. This has seen limited application, most likely due to the safety concerns of handling and moving vessels under pressure. Alternatively, precursors could be used that, upon heating, liberate the gas. In this section, selected examples using these different approaches are discussed.

9.10.5.6.2 Use of precursors that liberate gas upon heating

Instead of using gaseous hydrogen for hydrogenation reactions, a range of formate salts can be used as reagents in conjunction with microwave heating.[218] One example is the application of ammonium formates in the preparation of pyrroles from 1,4-enediones (Scheme 43).[219] In this domino reaction, the formate salt serves both as a source of hydrogen for the reduction of the enedione to the dione and also as a source of ammonia or amine for the subsequent amination–cyclization step.



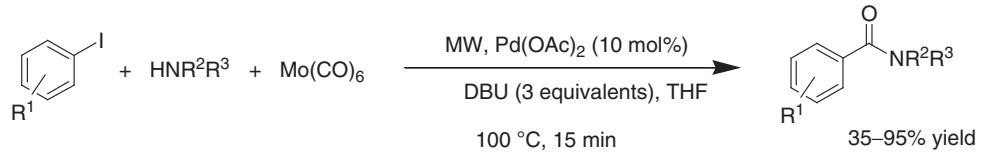
Ar = Ph, 4-Cl-C_6H_4, 4-Br-C_6H_4, 4-Me-C_6H_4, 4-OMe-C_6H_4,4-Cl-3-Me-C_6H_3, 56–92%

R = H, Ph, Bz, *n*-C_4H_9

Scheme 43 Preparation of pyrroles from 1,4-enediones using ammonium formate as a source of hydrogen and ammonia.

Molybdenum hexacarbonyl, $Mo(CO)_6$, can be used as a CO source, the organometallic complex starting to dissociate at temperatures approximately 150 °C. A range of palladium-catalyzed carbonylation reactions have been performed, the most

common of which are three-component couplings involving CO; an aryl-, benzyl-, or vinyl halide (or pseudohalide); and a suitable nucleophile.[220] This allows for the preparation of esters (alkoxycarbonylation) and amides (aminocarbonylation) when using alcohols or amines as the nucleophile coupling partner, respectively.[221,222] When performing aminocarbonylations using aryl iodides, the reactions can be performed at approximately 100 °C, this being well below the onset temperature of decomposition for $Mo(CO)_6$ (Scheme 44).[223] 1,8-Diazabicyclo [5.4.0] undec-7-ene used as a base in these reactions accelerates the release of CO via a ligand exchange process. Although not in this example, in some cases it is possible to use a substoichiometric quantity of molybdenum hexacarbonyl; more than one molecule of CO per $Mo(CO)_6$ molecule reacting productively. Carbonylative cross-coupling reactions are also possible, generating unsymmetrical ketones.[224]

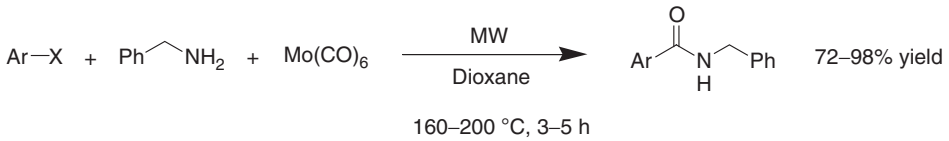


R^1 = H, 4-OMe, 2-Me, 4-CF_3

HNR^2R^3 = pip, $C_6H_5NH_2$, $PhCH_2NH_2$, *t*-$BuNH_2$, 2-aminothiazole, H-Gly-O^{t}Bu, H-Gly-OH, H-L-Leu-OH

Scheme 44 Palladium-catalyzed preparation of amides from aryl halides and amines using $Mo(CO)_6$ as a source of carbon monoxide.

It is possible to perform aminocarbonylations without the use of a palladium catalyst. $Mo(CO)_6$ serves both as a source of CO and also as a precursor to a molybdenum species that mediates the reaction.[225] An example is the preparation of amides from aryl halides and benzylamine, excellent yields of the products being obtained after 3 h at 160 °C for aryl iodides and 5 h at 200 °C for the less reactive bromides, a stoichiometric quantity of $Mo(CO)_6$ being used (Scheme 45).[226] Activation of the metal carbonyl with an additive is sometimes required to generate the active Mo species and the reaction can, in some cases, be performed using a substoichiometric quantity of the hexacarbonyl starting material. This approach is not limited to $Mo(CO)_6$, $Co_2(CO)_8$ being used as both a source of CO and also as the catalyst for the preparation of diaryl ketones[227] and ureas.[228]

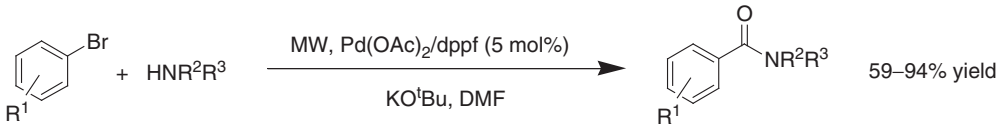


X = I or Br; Ar = Ph, 2-Me-C_6H_4, 3-Cl-C_6H_4, 4-OMe-C_6H_4, 4-$Et_2NC(O)$-C_6H_4, 3-thienyl, 3-pyridyl

X = Br; Ar = 2-naphthyl, β-styryl

Scheme 45 Preparation of amides from aryl halides and amines using $Mo(CO)_6$ as a source of carbon monoxide without a palladium catalyst.

DMF readily decarbonylates in the presence of base, and upon heating, yields CO and dimethylamine.[229] This can be leveraged in the palladium-catalyzed aminocarbonylation of aryl bromides to provide the dimethylamide product.[230] Addition of an excess of exogenous amines to the reaction mixture delivers the corresponding aryl amides in good yields (Scheme 46). In a similar vein, formamide can be used as a combined ammonia and CO source for generation of primary amides from aryl halides using palladium catalysis[231] and aqueous formalin as a H_2 and CO surrogate for rhodium-catalyzed hydroformylation reactions.[232]



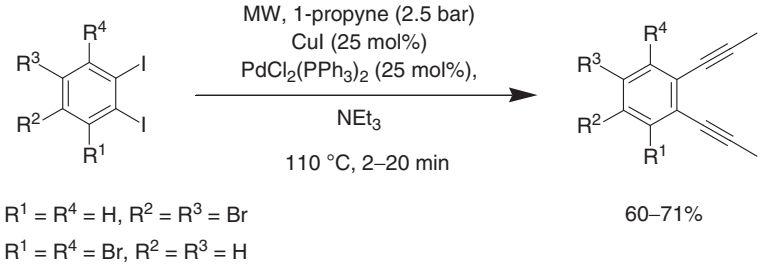
R^1 = H, 4-OMe, 4-Me

HNR^2R^3 = none, $C_6H_5NH_2$, $PhCH_2NH_2$, morpholine

Scheme 46 Palladium-catalyzed preparation of amides from aryl halides and amines using dimethylformamide (DMF) as a source of carbon monoxide.

9.10.5.6.3 Preloading reaction vessels with gas

In the earlier days of scientific microwave apparatus, glass tube reaction vessels were usually sealed by means of a stainless steel crimp top bearing a Teflon septum and then placed into the microwave cavity. This Teflon septum could be penetrated by a needle and loaded with gas. By charging with 2.5 bar of 1-propyne, Sonogashira reactions can be performed to generate diynes using different isomers of dibromo-diiodobenzene as the aryl halide coupling partners (Scheme 47).[233] By heating at 100–110 °C for 2–20 min, only the iodo functionalities react. A similar approach can be taken in the Sonogashira reaction between acetylene derivatives and polymer-supported aryl halides.[234] In another example, by bubbling ethene through a toluene solution of substrate and catalyst and then sealing the reaction vessel, it is possible to perform ene-yne metathesis reactions.[235] Reactions have to be performed at a concentration of 0.15 M because they are limited by the solubility of ethene in the solution.



Scheme 47 Preparation of diynes by Sonogashira coupling reactions using 1-propyne.

9.10.5.6.4 Use of a gas-loading accessory

A number of commercially available scientific microwave units have the capability to load gas into the reaction vessel, safely, controllably, and reproducibly, a general schematic representation being shown in Figure 5. Hydrogen gas has been one of the most widely used gaseous reagents in microwave-assisted reactions using this equipment, examples including hydrogenation of alkenes,[236] debenzylation,[237] and dearomatization of pyridine derivatives to form saturated piperidines.[238] Ethene can be used as a dienophile in Diels–Alder reactions using substituted 2(1H)-pyrazinones as dienes.[239] When working at the elevated temperatures needed, the overpressure of ethene helps prevent the competing retro-Diels–Alder reaction to regenerate starting materials. In another example, by careful optimization of the catalyst system it is possible to perform Heck reactions between ethene and aryl halides to generate styrenes (Scheme 48).[240] There are in fact very few reports of ethene as a reagent in the Heck reaction because its use is fraught with difficulties. The main problem is overreaction with the aryl halide coupling partner to give the symmetric stilbene product rather than the monosubstituted alkene. Another problem is that under the high temperature/long reaction time conditions often used, polymerization of the desired monosubstituted alkene product can occur. By leveraging the controlled heating that is possible when using microwave irradiation and by loading with a precise quantity of ethene, these problems can be overcome.

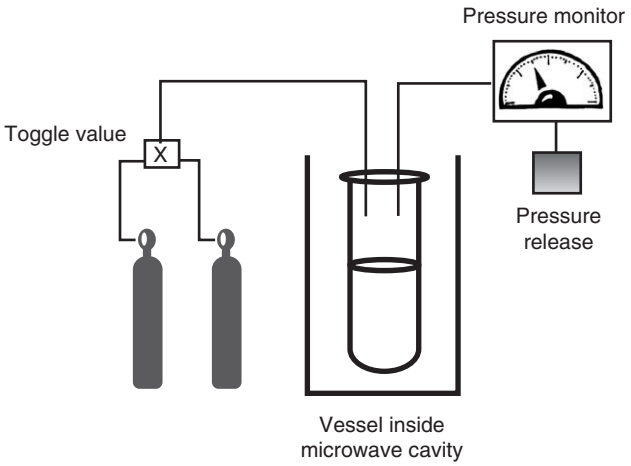
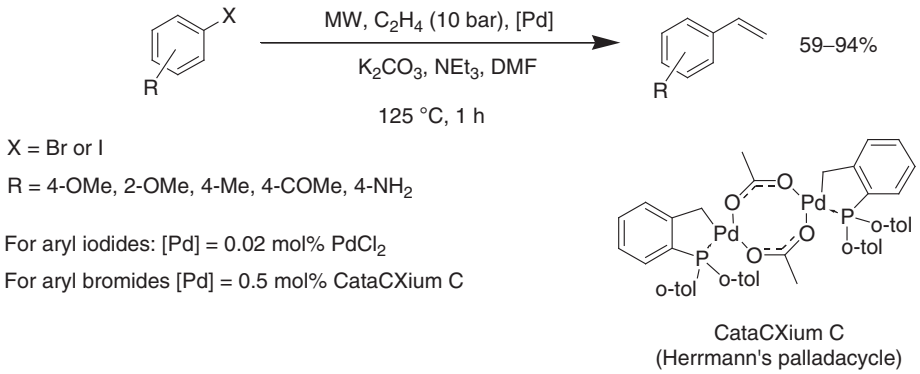


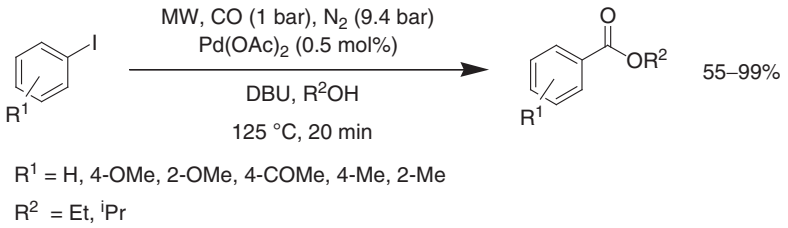
Figure 5 A schematic representation of a gas-loading accessory.

Although using $Mo(CO)_6$ as a CO surrogate does have some advantages, including the fact that it is a solid and is easily used on a small scale, its use results in metal waste; this being a particular problem if the reaction is to be scaled up. Using CO gas in



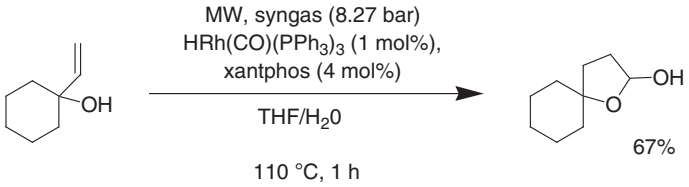
Scheme 48 Palladium-catalyzed preparation of styrenes using ethene as a coupling partner.

palladium-catalyzed hydroxy-,[241] alkoxy-,[242] and amino-carbonylation[243] reactions is an alternative, and this has been successfully achieved. That said, there are a number of disadvantages to using a significant excess of CO. From a practical standpoint, because it is highly toxic, extreme care must be taken when venting a vessel at the end of the reaction. In addition, efficient palladium catalysis in the presence of a large excess of CO can be difficult. The rate of oxidative addition is greatly reduced, this being a result of the strong π-acceptor character of CO as a ligand. Clustering of Pd atoms is also facile in the presence of CO, leading to the formation of catalytically inactive Pd species. By controlled loading of the reaction vessel, alkoxycarbonylation reactions can be performed effectively using a near-stoichiometric quantity of CO (Scheme 49).[244] Key to the success of the reaction is an additional load of nitrogen gas.



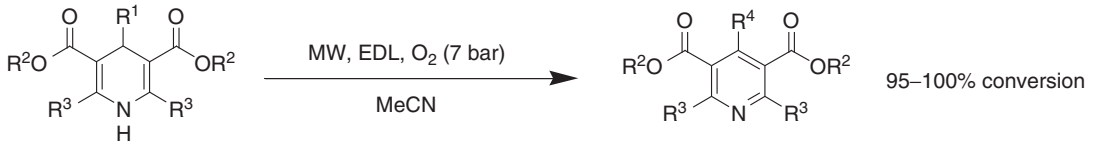
Scheme 49 Palladium-catalyzed alkoxycarbonylation reactions using a near-stoichiometric quantity of carbon monoxide.

Rhodium-catalyzed hydroformylation reactions can be performed using syngas (1:1 mix of CO and H_2). Loading with 40 psi of gas and using an ionic liquid as the solvent, a range of substrates can be hydroformylated in 4–6 min at 110 °C.[245] This method can be extended to domino hydroformylation–cyclization sequences when suitably functionalized substrates are used. For example, allyl and homoallyl alcohols can be converted to lactols (Scheme 50).[246] Hydroformylation followed by a Pictet–Spengler reaction[246] or an aza-Sakurai cyclization[247] opens up expedited routes to the synthesis of alkaloids.



Scheme 50 Domino hydroformylation–cyclization sequence.

Molecular oxygen can be employed in oxidative Heck reactions.[248] Another use of oxygen brings together a range of techniques. By performing simultaneous microwave heating and ultraviolet (UV) irradiation, 1,4-dihydropyridines (DHPs) can be converted to pyridines using singlet oxygen as the oxidant, offering a cleaner, greener alternative to stoichiometric metal oxidants (Scheme 51).[249] The electrodeless discharge lamps (EDLs) used in this method had their genesis in a series of experiments focused on the observation that a high-frequency electromagnetic field can trigger gas discharge, leading to the emission of electromagnetic radiation.[250] Using these EDLs, it is possible to place the lamp directly into a microwave vessel and run a reaction under simultaneous UV and microwave irradiation. Because a range of filling gases can be placed into EDLs, the emission wavelength can be varied.[251] In the field of environmental chemistry, increased efficiency is seen when using microwave irradiation in the photocatalytic degradation of various substrates.[252] The technique has seen some, but albeit limited, application in synthetic chemistry.[253,254]



150 °C, 30 min, simultaneous air cooling throughout

$R^1 = R^4$ =Ph, R^2 = Et, R^3 = Me

$R^1 = R^4$ =Ph, R^2 = NHPh, R^3 = Me

$R^1 = R^2 = R^3$ = Me, R^4 = Me (90%) or H (10%)

R^1 = pentyl, R^2 = Et, R^3 = Me, R^4 = pentyl (28%) or H (72%)

R^1 = cyclohexyl, R^2 = Et, R^3 = Me, R^4 = cyclohexyl (3%) or H (97%)

Scheme 51 Oxidation of 1,4-dihydropyridines with oxygen gas using microwave irradiation in conjunction with UV irradiation.

One of the challenges when performing a combination of microwave heating and photochemistry is finding conditions under which the EDL remains illuminated throughout the reaction. Solvents with high dielectric constants heated very well but, because they absorb much of the microwave irradiation, do not allow the EDL to illuminate. Low dielectric constant solvents such as hexane, while they heat slowly and the EDL can be illuminated, are incompatible with the oxidation chemistry because of poor substrate solubility. Acetonitrile, a moderately microwave absorbing solvent in which DHPs are soluble, turns out to be the best option. Because once a reaction mixture reaches temperature, the microwave power drops substantially just to hold the contents steady, therefore the EDL can be prone to stop emitting light. This can be overcome by using simultaneous cooling in conjunction with the microwave heating. By removing heat from the reaction vessel, it is possible to increase the microwave energy required to maintain the target temperature, which allows the EDL to continue emitting light. By using *in situ* fiber-optic temperature measurement, some of the pitfalls of using simultaneous cooling (namely, inaccurate temperature measurement) can be overcome. Overall, optimum conditions for the oxidation reaction require loading the reaction vessel with the EDL and 100 psi of oxygen and then heating to 150 °C with simultaneous air-cooling running throughout. The apparatus in use is shown in **Figure 6**. The outcome of the oxidation depends on the DHP substrate used. When the substituent at the 4-position of the DHP ring is an

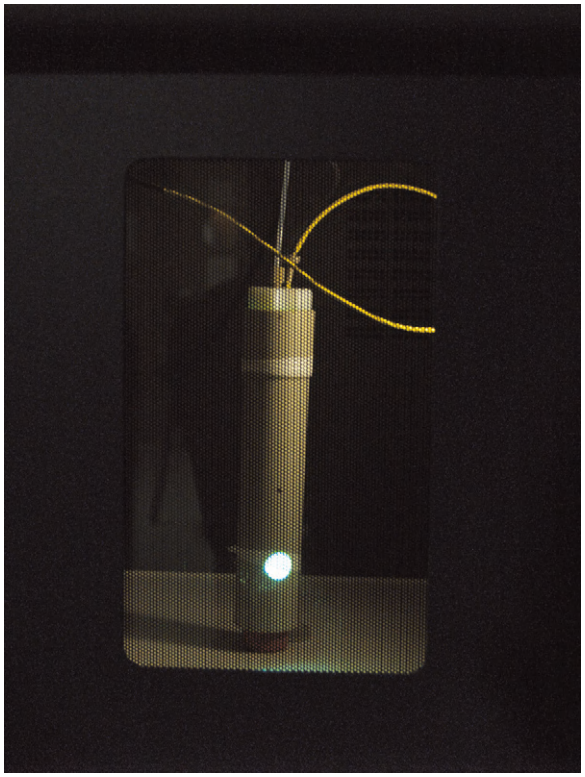


Figure 6 Vessel assembly in use for oxidation of 1,4-dihydropyridines with oxygen gas using microwave irradiation in conjunction with UV irradiation.

aromatic ring, the only product observed is the substituted pyridine. When an alkyl group is in the 4-position, formation of the corresponding pyridine product that has been de-alkylated at the 4-position is observed. The extent to which de-alkylation occurs depends on whether the substituent is primary or secondary.

9.10.6 Use of Microwave Heating in Combinatorial Chemistry

9.10.6.1 Introduction

The synthesis of a large number of different but often structurally related molecules or materials is the essence of combinatorial chemistry.[255] Key to success in this endeavor is the ability to access these compounds rapidly. As a result, microwave heating can play an important role.[256,257] Although automated sequential processing of reactions is an option, it is far more efficient to use parallel processing, running more than one reaction at a time. To do this, multimode microwave units are generally used, in conjunction with well plates or modules capable of holding multiple reaction vessels. Also intimately linked to combinatorial chemistry is the use of solid-phase synthesis techniques.[258] These topics have been the subject of considerable attention, often driven by the desire to prepare libraries of small molecules for biological screening with drug discovery in mind.[259] In this section, the key tenets of microwave-assisted combinatorial chemistry are discussed, with the objective of giving an overview of the field.

9.10.6.2 Parallel Processing

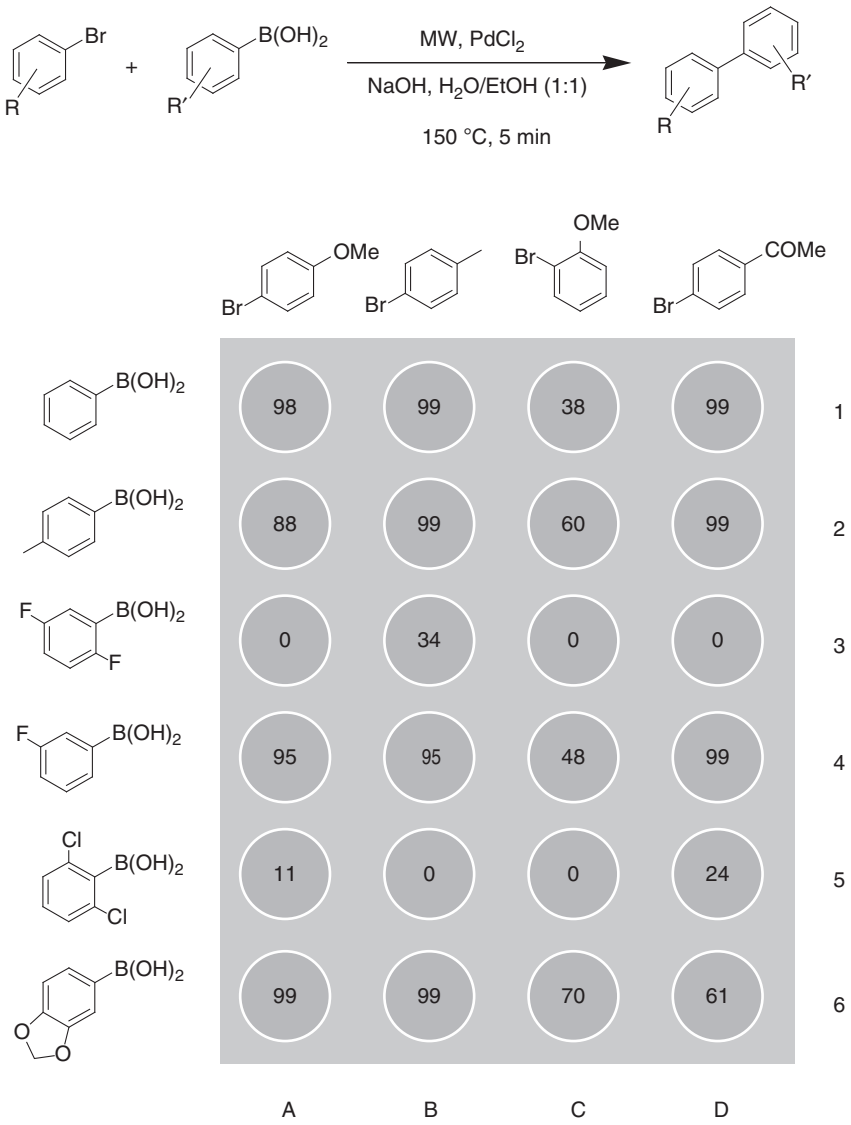
To perform multiple reactions concurrently using microwave heating, one of two approaches can be taken, both of which involve the use of multimode microwave apparatus. The first is to use a carousel into which reaction vessels can be loaded. Depending on the equipment used, it is possible to monitor the temperature of either one reaction vessel or a number of vessels simultaneously. However, one vessel is usually designated the 'control' and the microwave unit programmed to heat this to the requisite temperature. If all the reaction mixtures comprise of components that are of roughly the same microwave absorptivity, temperature variation between vessels is often not a significant issue. This is especially the case when all the reactions are performed in the same, strongly absorbing solvent. However, when there is a significant difference in microwave absorptivity across the reaction vessels, there can be considerable discrepancy in the temperature the contents of each tube reaches, this impacting the yield of the products.

Another approach is to use a well plate, each reaction being performed in an individual well. This can be advantageous because reactions can be performed on small scales and a large number can be performed in each run, using, for example, a 96-well plate (*see* Chapter 9.01). In addition, the well plates used can be interfaced with equipment for product purification and high-throughput screening. Early attempts at using these plates in conjunction with microwave heating were fraught with difficulties.[260] Standard polypropylene well plates are not compatible with the relatively high-temperature conditions employed when using microwave heating. In addition, significant temperature gradients occur between individual wells, leading to nonuniform heating across the plate. This affects both yield and purity of products. Although the issue of temperature stability can be resolved in part by employing materials such as Teflon, addressing the issues associated with nonuniform heating is a more challenging proposition. A range of plates have been developed that contain strongly microwave-absorbing components such as graphite. However, the best option is to use plates made from SiC.[261] As already discussed, SiC has a number of attractive features when it comes to microwave heating. In particular, it is highly microwave absorbing and also chemically inert. This means that reaction mixtures can be placed directly into wells in an SiC plate,[262] or alternatively in vials that themselves are placed into SiC blocks (**Figure 7**).[263] Using these accessories, it is possible to perform up to 192 reactions at one time in parallel. It is the SiC that is absorbing essentially all the microwave irradiation and the plates heat very uniformly.[264] The microwave absorptivity of the individual reaction mixtures is no longer a factor; the reaction mixtures being heated by the plate itself.



Figure 7 A 48-position silicon carbide plate and a 24-position silicon carbide plate capable of holding standard glass vials.

The SiC plates have been used for a range of synthetic chemistry, an example being the preparation of a library of 24 biaryls by Suzuki coupling reactions (Scheme 52).[265] Four aryl bromides and six arylboronic acids are used as substrates, performing each reaction on the 0.25 mmol scale in glass vials, which in turn are placed into a 24-position SiC plate. Good yields are obtained with the exception of the couplings with 2,5-difluorophenylboronic acid and 2,6-dichlorophenylboronic acid, presumably because these two substrates are electron-poor and sterically congested. SiC plates have also been used in analytical and biological chemistry for applications such as sample extraction,[266] forced degradation,[267] and protein hydrolysis.[268]



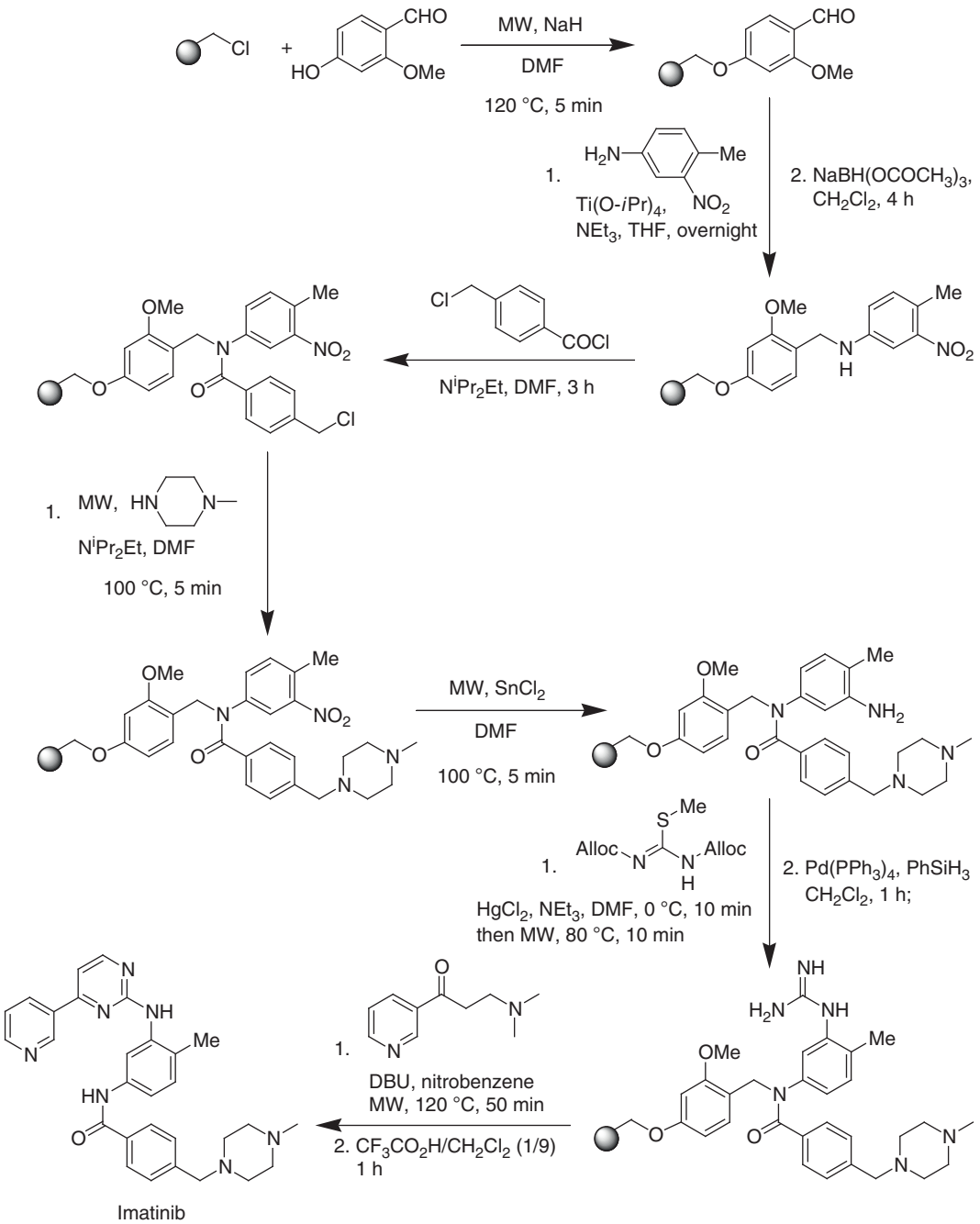
Scheme 52 Preparing a library of biaryls in a 24-position SiC plate. Values shown represent product conversions (%).

9.10.6.3 Solid-Phase Organic Synthesis

Since the first use of polystyrene resins for the preparation of peptides,[269] solid-phase organic synthesis has grown to be a branch of chemistry in its own right. Solid-supported synthesis offers operational advantages, such as ease of product isolation from reaction mixtures and applicability to automation. A drawback, however, is that reactions can be slow when using a solid-phase approach. For that reason, and others, microwave heating can be a beneficial tool.[270,271] A common misnomer is that the polystyrene resins used as support limit the user to reaction conditions below 130–140 °C. For 20–30 min, these resins can tolerate heating to temperatures up to 200 °C.[272] The support used need not be a polymer. Planar supports such as cellulose are a possibility.[273] The advantage of using an insoluble polymer support is the ease of extraction at the end of a reaction; a simple filtration being all that is needed. Another option is to use polymers that are soluble in the reaction medium or else from a

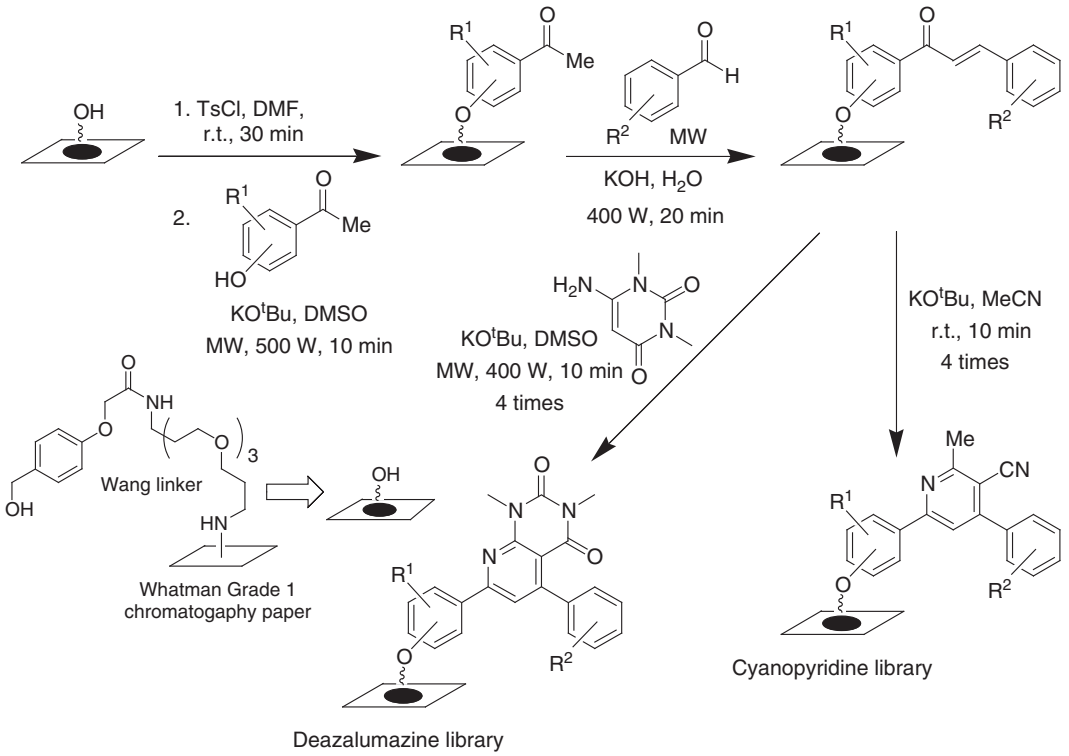
biphasic mixture.[274] Soluble supports feature homogeneous reaction conditions and enable the application of standard analytical techniques as well as the orthogonal use of insoluble reagents. Efficient removal of the supported material at the end of the reaction can be achieved using techniques such as ultrafiltration, dialysis, precipitation, or liquid-phase separation.

A wide range of synthetic transformations can be performed on a solid-support using microwave heating. Examples include metal-catalyzed couplings,[275] MCRs,[276] rearrangements,[277] and cycloadditions,[278] as well as peptide synthesis (see Section 9.10.8). A case in point is the solid-phase synthesis of the selective tyrosine kinase inhibitor imatinib (marketed as Gleevec or Glivec), where microwave heating is used in five of the steps (**Scheme 53**).[279] The key transformations benefitting from microwave heating are (a) preparation of the linker, (b) nucleophilic substitution, (c) reduction of a nitro group, (d) the formation of a guanidine moiety from a hindered aniline, and (e) the cyclization of the guanidine to generate a 4-substituted pyrimidine. All can be performed more easily than when using conventional approaches. An additional advantage is that, because reaction times are shortened using microwave heating, the polymer-support is not prone to degradation.



Scheme 53 Solid-phase synthesis of imatinib incorporating microwave heating in five steps.

Using cellulose as a support, a range of reactions can be performed by microwave heating.[280,281] One example is in the discovery of fluorescent cyanopyridine and aeazalumazine dyes (Scheme 54).[282] A standard chromatography paper derivatized with an acid-cleavable, Wang-type linker can be used as the solid-support system and spatially addressed synthesis of the heterocycles can be performed by means of condensation reactions. Practically speaking, the appropriate reagent(s) are applied to each spot on the paper and it is then placed into the microwave and irradiated for 10 min. The spot and heat process are then repeated a number of times.



Scheme 54 Spatially addressed synthesis of cyanopyridine and deazalumazines dye libraries.

Simple visual inspection of the arrays under irradiation from a handheld UV lamp (at 254 nm) provides a straightforward primary screen to determine if the compounds are fluorescent (Figure 8). In some cases, this visual assay also facilitates qualitative SAR to be derived across the entire macroarray. The individual compounds can also be cleaved off the paper support by punching out each spot from the macroarray with a desktop hole-punch and placing them in individual vials, followed by treatment with trifluoroacetic acid.

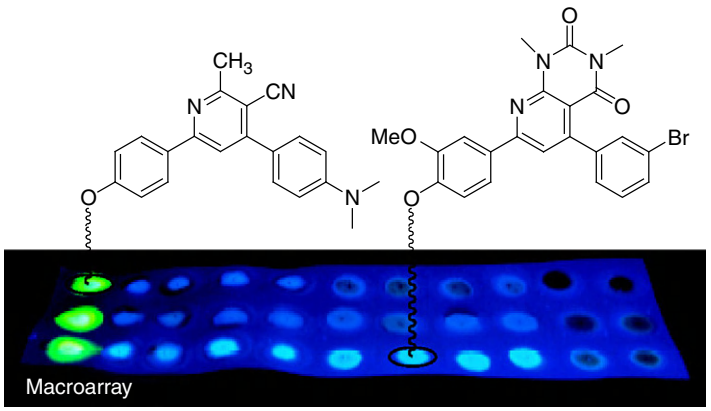


Figure 8 UV assay of small molecule macroarrays of cyanopyridines and deazalumazines prepared via spatially addressed synthesis on planar cellulose supports. Reproduced from Bowman, M. D.; Jacobson, M. M.; Blackwell, H. E. *Org. Lett.* **2006**, *8*, 1645–1648, with permission from American Chemical Society.

9.10.7 Microwave-Assisted, Continuous-Flow Organic Synthesis

9.10.7.1 Introduction

So far, this chapter has focused attention on performing reactions in batch mode. However, continuous-flow processing has a number of attractive features, including aspects of enhanced safety, ease of scale-up, and efficient mixing of reagents.[283,284] The application of continuous-flow processing in conjunction with microwave heating falls into two categories. Its use in the scale-up of reactions to the multigram level and beyond is addressed in Section 9.10.10. Here, attention is focused on continuous-flow processing as a tool for highly effective smaller scale synthesis and sequential parallel synthesis, a technique dubbed as MACOS.[285] Much of this is centered around the use of microcapillary reactors. By coating the inside of the capillaries with metal, it is possible not only to use them to perform heterogeneous catalysis but also simply to heat reaction mixtures very effectively (*see* Chapter 9.04). Selected examples are given here that illustrate some of the key features of the range of microcapillary reactors used in conjunction with microwave heating as well as other small-scale approaches to continuous-flow chemistry.

9.10.7.2 Microcapillary Reactors for Microwave-Assisted Continuous-Flow Synthesis

9.10.7.2.1 Construction of microcapillary reactors

There are two designs for the construction of microcapillary reactors (Figure 9). One has three inlet ports that merge into one outlet; this being used for small-scale synthesis and allowing separate reagent streams to be flowed into the capillary where they mix and react.[286] The other comprises of four pairs of two inlet ports that merge into four different outlets, this being used for sequential parallel synthesis.[287] Both capillary reactors fit into the cavity of a monomode microwave unit. The capillaries are generally of approximately 200–1200 μm diameter and flow rates vary from 10 to 60 μl min^{-1}. When depositing metal onto the inner walls of capillaries, a two-stage process is often used. For example, in the case of gold[288] a very fine layer of densely packed gold particles is first deposited directly on the capillary wall from a diethylene glycol/gold(III) chloride solution. This is then followed by a more random-appearing layer of gold nanoparticle clusters deposited on top of the first layer from an aqueous sodium citrate solution of $AuCl_3$.

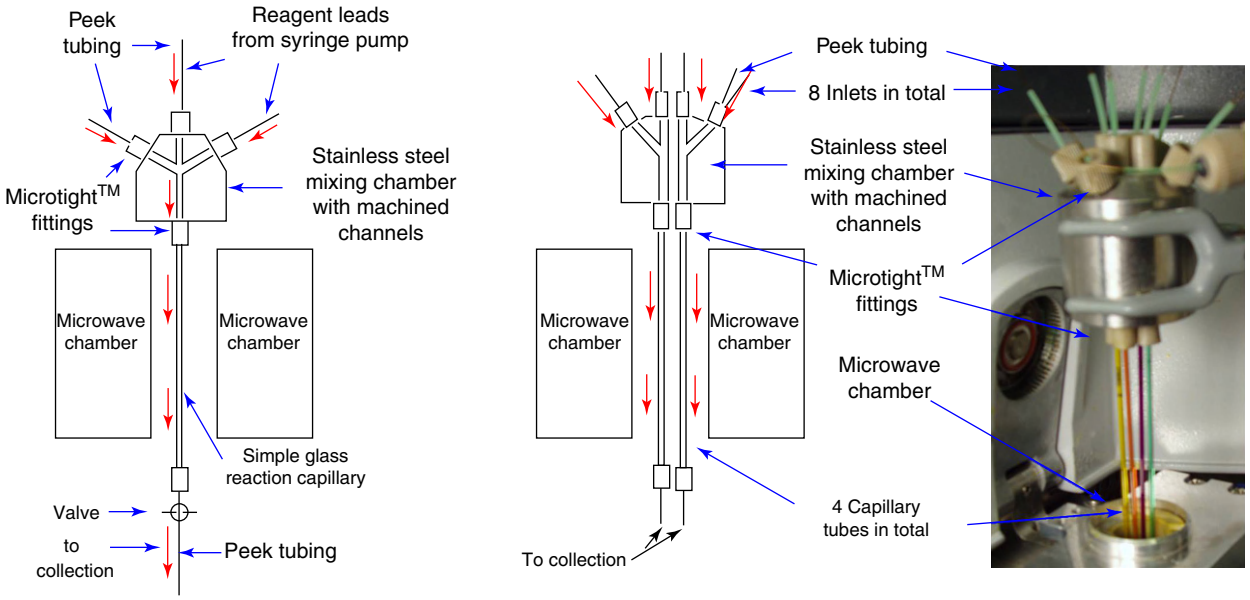
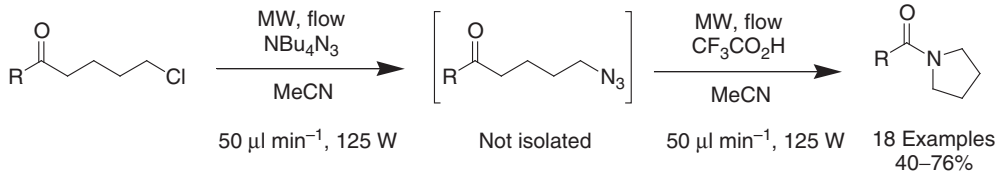


Figure 9 Microcapillary reactors used in conjunction with microwave heating. Reproduced with permission from Professor Michael Organ, York University, Canada.

9.10.7.2.2 Synthesis using microcapillary reactors

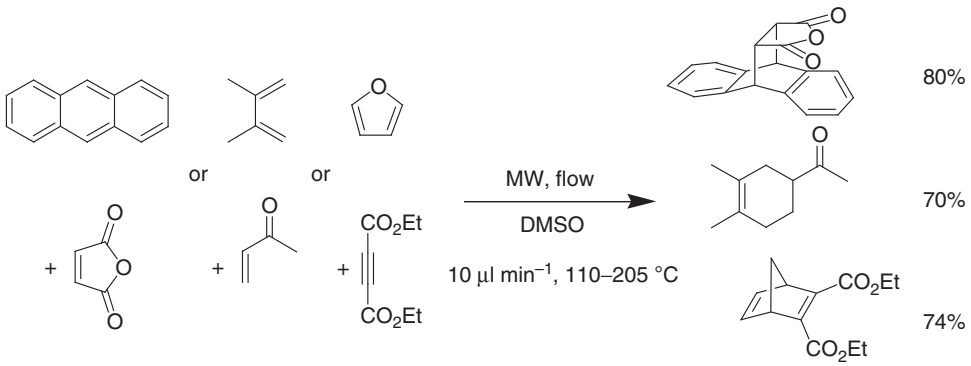
Numerous synthetic transformations have been performed using a microcapillary reactor. Examples range from nucleophilic aromatic substitutions to metal-catalyzed couplings and alkene metathesis.[286] In addition, a heterogeneous Wittig reaction has been successfully executed without clogging the narrow-bore capillary tube.[286] Click reactions can also be performed[289] as can the synthesis of lactams via *in situ* generation of organic azides (Scheme 55).[290] MCRs are also possible; three-component reactions being performed by introducing each of the reagents as a separate stream into the reactor at the same flow rate and same concentration.[291] Using the multiple-capillary reactor, compound libraries can be effectively generated. Suzuki couplings and S_NAr reactions lead to libraries of biaryls and anilines, respectively.[287] Also, rather than pass different reagents through each of the

capillaries to make a library of different compounds, the same reaction mixture could feasibly be passed through each capillary, offering a way to scale-up a reaction performed in the single-channel cousin.



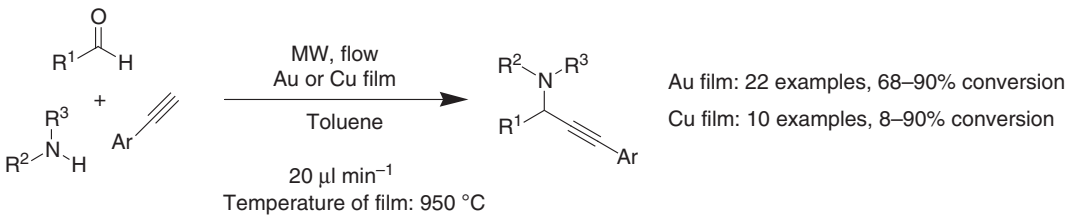
Scheme 55 Synthesis of lactams in flow via *in situ* generation of organic azides.

By coating the inside of a capillary with palladium, Suzuki and Heck couplings can be effectively performed.[292] Reactions are run at approximately 200 °C and are complete in a residence time on the order of seconds. Although palladium leaching is low (2–19 ppm), the fact that these coupling reactions can be performed using sub-ppm levels of Pd[25,26] means that it is hard to determine whether the reactions are catalyzed by heterogeneous palladium or by the low levels of metal leached into solution. These same palladium-coated capillaries can be used for performing Diels–Alder reactions (Scheme 56).[293] The metal film serves two roles. Owing to its high microwave absorbtivity, the metal film helps effectively heat the mixture but it also serves as a catalyst for the reaction, feasibly coordinating the dieneophile.



Scheme 56 Synthesis of lactams in flow via *in situ* generation of organic azides.

Turning to gold-coated capillaries, rapid benzannulation of aryl aldehydes with alkynes[294] and hydrosilylation of alkynes[288] is possible. Using either a gold- or copper-coated capillary, the three-component coupling of an aldehyde, amine, and alkyne can be performed, generating a propargylamine product (Scheme 57).[295] In another approach, the outside walls of a capillary can be coated with gold, this serving as an efficient way to heat the reaction mixture flowing through it.[296]



R^1 = Ph, 4-BrC_6H_4, 2-Br-C_6H_4, 4-CF_3-C_6H_4, CH_2CHMe_2

Amine = piperidine, morpholine, HNBzEt

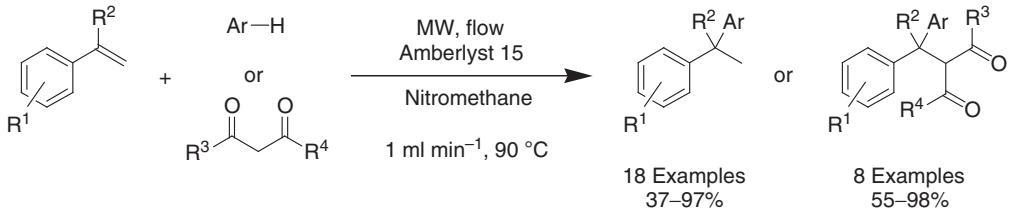
Ar = Ph, thienyl, *N*-methylimidazole

Scheme 57 Synthesis of lactams in flow via *in situ* generation of organic azides.

9.10.7.3 Other small-scale approaches to continuous-flow chemistry

A survey of the literature shows that palladium catalysis has served as a sharpening stone for the development of a number of small-scale approaches to continuous-flow synthesis incorporating microwave heating. A flow reactor that contains a porous

composite glass/polymer material doped with palladium nanoparticles performs well in transfer hydrogenation reactions.[297] By using microwave irradiation as opposed to conventional heating, catalytic activity is higher and the system is more effectively reused. A microencapsulated palladium catalyst packed into a U-shaped glass tube can be used for Suzuki coupling reactions.[298] However, to avoid the polymer matrix melting, pulsed microwave irradiation needs to be used. Immobilizing a chiral palladium complex bearing an oxazoline-based ligand allows for the enantioselective allylic amination to be performed.[299] Employing a 10 ml glass tube as a flow cell (identical to that used for batch synthesis), and packing it with sand or glass beads to increase residence time, a range of organic reactions can be performed in flow. These include the Bohlmann–Rahtz cyclodehydration[300] and the Biginelli reaction.[301] The acid-catalyzed hydroarylation and hydroalkylation of styrene can be performed by replacing the sand or glass as packing material with Amberlyst 15, a strongly acidic, sulfonic acid, macroreticular polymeric resin (Scheme 58).[302] Use of a coil instead of a tube is also an option when it comes to using microwave heating in small-scale continuous-flow synthesis.[128,303]



Scheme 58 Hydroarylation and hydroalkylation of styrene.

9.10.8 Additional Applications of Microwave Heating in Organic Synthesis

Beyond those covered in Sections 9.10.5–7, microwave heating has found use in a range of synthetic transformations and areas related to organic chemistry. Key examples are presented in Table 1.

Table 1 Examples of areas related to organic chemistry in which microwave heating has had a significant impact

Topic	*Leading references*	*Comments*
Carbohydrate chemistry	304,305	A range of reactions involving carbohydrate substrates can benefit from microwave heating, including protection, acylation, deprotection, O-, N- and C-glycosylation, as well as the preparation of di- and polysaccharides.
DNA-related applications	306	Microwave heating can be used for DNA amplification using the polymerase chain reaction as well as the preparation of oligonucleotides.
Drug discovery	307	As well as being useful for the preparation of potential lead compounds, the impact of microwave heating is further enhanced by the combination with other novel approaches such as combinatorial chemistry and solid-phase or solution-phase parallel synthesis. Integration of the synthesis platform with automated purification, evaporation, high-throughput screening, and cheminformatics modules further facilitates the drug discovery process.
Equipment	141,308,309	A wide array of scientific microwave apparatus is available, capable of processing from microliters to multiple liters of reaction mixture.
Peptide synthesis	310–312	Microwave heating can be used to prepare a wide array of peptides, including those that are traditionally very difficult to synthesize. The process can also be automated using a scientific microwave unit capable of performing deprotection, coupling, and cleavage steps.
Proteomics	311,313,314	Protein hydrolysis as well as enzymatic and chemical proteolysis can be performed using microwave heating.
Polymer chemistry	315–317	Preparation and postsynthesis modification of organic polymers benefits greatly from microwave heating. Radical as well as step-growth and ring-opening polymerizations have all been studied. In addition, the field has broadened to the fabrication of polymer/metal composites as well as bio-based materials.
Radiochemistry	318,319	As reaction times are often short when using microwave heating, the technology is ideally suited to preparing compounds that contain short half-life radioisotopes such as ^{11}C and ^{18}F.
Supported catalysts and reagents	320,321	By using solid-supported catalysts it is possible to perform a wide array of synthetic transformations in both batch and continuous-flow modes.
Undergraduate education	322–324	The short reaction times possible when using microwave heating open avenues for incorporation of a wider range of experiments into the organic chemistry laboratory curriculum. Students gain more time for activities involved in reaction planning, workup, purification, and product identification as well as designing their own projects in an advanced laboratory or undergraduate research setting.

9.10.9 *In situ* Monitoring of Reactions Performed using Microwave Heating

9.10.9.1 Introduction

One of the attractive features of using scientific microwave apparatus to perform chemical reactions is the ability to work at elevated temperatures and pressures in a safe, controllable, and reproducible way. In the event of a vessel failure, the microwave equipment is designed to cease irradiation immediately and to contain the vessel and its contents in the microwave cavity, thus protecting the user. An unavoidable consequence of this peace of mind, however, is the chemist's inability to monitor the progress of a reaction visually. For example, it is not possible to see if a reaction is stirring adequately, whether a precipitate is forming or if there is a color change. Another consequence of working at high temperatures is that reaction times can often be on the order of minutes instead of hours and there may be a narrow time window in which product yield is maximized and the onset of decomposition has not started. When optimizing a new synthetic protocol or monitoring the progress of reactions, the chemist generally is required to stop the heating, allow the reaction mixture to cool, and then use standard analysis techniques, such as nuclear magnetic resonance (NMR) spectroscopy or TLC. As a result, optimization of reaction conditions, such as time and temperature, is often a matter of trial and error: a process which can be costly with regard to the scientist's time in an otherwise highly efficient approach to the development of new reaction conditions.

To overcome these problems, chemists have become interested in developing tools for monitoring, in real-time, reactions performed using microwave heating.[325] An additional advantage that a scientific microwave apparatus brings is that reaction temperature can be very much controlled accurately and monitored on a second-by-second basis. As a result, the high fidelity of temperature control with microwave heating in conjunction with *in situ* spectroscopy lends itself as an ideal approach to quantitative kinetic analysis. It is possible to determine physical parameters such as activation energies and/or activation enthalpies, orders of reactions, and rate constants for reactions.

9.10.9.2 Watching Reactions in Real Time

9.10.9.2.1 Use of a digital camera

By interfacing a digital camera with a scientific microwave unit, it is possible to watch reactions in real time.[326] As discussed earlier in the chapter, an issue when using metal-containing compounds either as catalysts or reagents in conjunction with microwave heating is that deposition of metal on the surface of a glass tube can lead to arcing and superheating. A camera allows such reactions to be closely monitored and stopped before vessel failure. Examples include monitoring ligand substitution reactions of metal complexes[327] as well as the formation of Grignard reagents from magnesium turnings.[328]

9.10.9.2.2 Use of thermal imaging

Infrared thermography equipment, often known as thermal imaging, can sense temperatures ranging from -20 to 2000 °C. Using microwave irradiation it is sometimes possible to heat microwave absorbant substrates and/or catalysts selectively under heterogeneous reaction conditions. Infrared thermography can been used to monitor the temperature of these solids. For example, in an unstirred vessel the insoluble oxidant CrO_2 (Magtrieve™) can reach temperatures of approximately 140 °C in toluene.[329] Along the same lines, thermal imaging can be used to determine the temperature across a magnesium ribbon when immersed in tetrahydrofuran and irradiated with microwave energy as part of a study into the preparation of Grignard reagents.[330]

Infrared thermography can be used to probe the homogeneity of heating in SiC well plates under microwave irradiation (Figure 10).[262] Stopping the heating, opening the microwave cavity, and using a infrared imaging camera, the temperature of each individual well can be observed. *In situ* temperature measurement is also possible.[262] When heating an empty 24-well plate, a

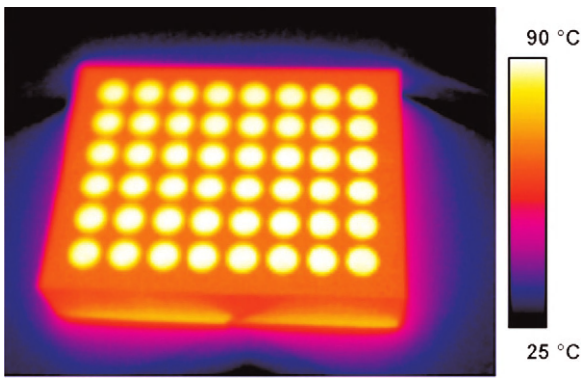


Figure 10 Infrared thermal image of a silicon carbide plate containing 300 μl of water in each of the 48 wells. The plate had been exposed to 300 W microwave irradiation for 1 min inside a multimode microwave cavity. Reproduced from Kremsner, J. M.; Stadler, A.; Kappe, C. O. *J. Comb. Chem.* **2007**, *9*, 285–291, with permission from American Chemical Society.

maximum temperature of ~260 °C is reached after 1 min of microwave heating using a modest input microwave power of 1000 W. Significant temperature inhomogeneities on the surface of the SiC plate are only evident during the first few seconds of irradiation. The temperature of the metal films in capillaries used in continuous-flow microwave synthesis measurement can be measured by use of a high-definition IR camera.[295] They seem to reach temperatures approximately 950 °C. This provides a very good rationale for the significant reaction rate enhancement seen in these metal-film catalyzed microwave-assisted continuous-flow reactions.

9.10.9.3 *In situ* Spectroscopy

9.10.9.3.1 Introduction

Although watching a reaction using a digital camera or probing temperature using thermal imaging technology is useful for observing macroscopic phenomena, in most cases it does not provide data that are detailed enough to be of use to the synthetic chemist whose objective is to determine if their reaction has reached completion or indeed is even proceeding as planned. To achieve this, *in situ* spectroscopy offers a better solution. The range of spectroscopic techniques available to the synthetic chemist is wide and a number of these have been interfaced with microwave apparatus, this proving a feat in itself. The data that has been obtained from *in situ* monitoring tools have proved valuable for the rapid optimization of reaction conditions and also deepened the understanding of the interaction of microwave energy with reaction mixtures.

9.10.9.3.2 Infrared spectroscopy

In situ tools based on IR spectroscopy have been developed and used successfully in conventional chemistry for many years, these including the ReactIR. This instrument comprises an attenuated total reflectance probe, which is inserted directly into the reaction mixture, and a detector. In addition, the concentration changes of all components of the reaction mixture are data logged and can be analyzed by proprietary software. This tool can be interfaced with a scientific microwave unit and used as a tool for monitoring organic transformations from a qualitative perspective using an open-vessel approach.[331] The insertion of the ReactIR probe, made of an alloy, directly into the reaction mixture poses two potential problems. It can feasibly act as an antenna, in essence drawing microwave radiation out of the cavity into the environment around the user. Linked to this, a build-up of charge on the probe could occur during a run. The latter issue is resolved by grounding the probe using a wire to link the probe to the attenuator of the microwave unit. When using high to moderate microwave-absorbing solvents (such as ethanol and water), microwave leakage is below the Food and Drug Administration (FDA)-mandated limit for household microwave ovens of 5 $mW \cdot cm^{-1}$ at 5 cm from the oven surface. In the case of poorer microwave absorbers such as tetrahydrofuran, at low to moderate microwave power levels leakage is below the FDA limit, but at higher powers the limit can be exceeded.

9.10.9.3.3 UV–visible spectroscopy

If starting materials and products exhibit a significant difference in absorbance, UV–visible (UV–vis) spectroscopy can potentially prove a useful tool for reaction monitoring. To obtain a UV–vis spectrum, analyte concentrations of approximately 10^{-4} M are most commonly used. However, chemical reactions are usually performed at significantly higher concentrations (0.1–1.0 M). This can make reaction monitoring a challenge. A UV–vis probe has been developed for performing *in situ* reaction monitoring of reactions performed in a microwave field.[332] It comprises two optical fibers, one bringing the incident light and one taking the transmitted signal to the detector, linked to a quartz glass sleeve. The very short path length used means that reaction monitoring is possible at synthetically-relevant concentrations. The method works with the proviso that the starting materials and products from the reactions selected do not absorb near the absorption maximum of the solvent.

9.10.9.3.4 Raman spectroscopy

9.10.9.3.4.1 Qualitative reaction monitoring

As borosilicate glass is essentially 'Raman transparent,' it is possible to monitor reactions without having to place any components of the spectrometer into the reaction vessel. Instead, the Raman probe can be placed close to the outside wall of the vessel. This means that both the standard sealed-vessel and open-vessel configurations can be used. There are also some significant drawbacks that need to be taken into account when considering Raman spectroscopy as a tool for reaction monitoring. First, a Raman scattering event is rare compared with an absorption event. This means that concentrated reaction mixtures or long acquisition times are often required to obtain satisfactory spectral data. Second, if molecules under observation show electronic excitation sympathetic with the excitation source (laser), fluorescence becomes a major issue. Indeed, because fluorescence is orders of magnitude more intense than Raman spectroscopy, even limited excitation of molecules to their excited electronic states quickly renders Raman spectroscopy worthless. Third, to use Raman spectroscopy in dynamic systems, like monitoring the progress of reactions, the solution must remain completely homogeneous throughout. Any precipitate or turbidity immediately alters the path length of the system and hence Raman signal strength. All this said, of all the *in situ* monitoring tools used in conjunction with microwave heating, Raman spectroscopy has seen the most application. Reactions that have been monitored in real-time include a Knovenagel condensation,[333] a series of Suzuki couplings,[334,335] and an esterification.[336]

When monitoring reactions, only functional groups that change are generally of importance. Therefore, when acquiring spectral data, if a background scan is taken at the start of the reaction and this then subtracted from all subsequent scans, Raman signals due to solvent and starting materials can be excluded. A case in point is the synthesis of coumarins. Salicylaldehyde and ethyl acetoacetate react in the presence of piperidine as a base catalyst to yield 3-acetylcoumarin.[337] Focusing attention on the strong Raman-active stretching modes at 1608 and 1563 cm^{-1} found in the coumarin product, the reaction can be monitored easily (Figure 11). From the data obtained, reaction conditions can be quickly optimized; in this case 8 min at 130 °C being sufficient for complete conversion of starting materials to the coumarin product. Not surprisingly, when replacing ethyl acetoacetate with diethyl malonate, the rate is slowed somewhat as the activated methylene moiety is less acidic. This difference in reaction rate can be identified during the course of the reaction when monitoring spectroscopically. As a result, an on-the-fly extension of reaction time is possible to maximize product yield.

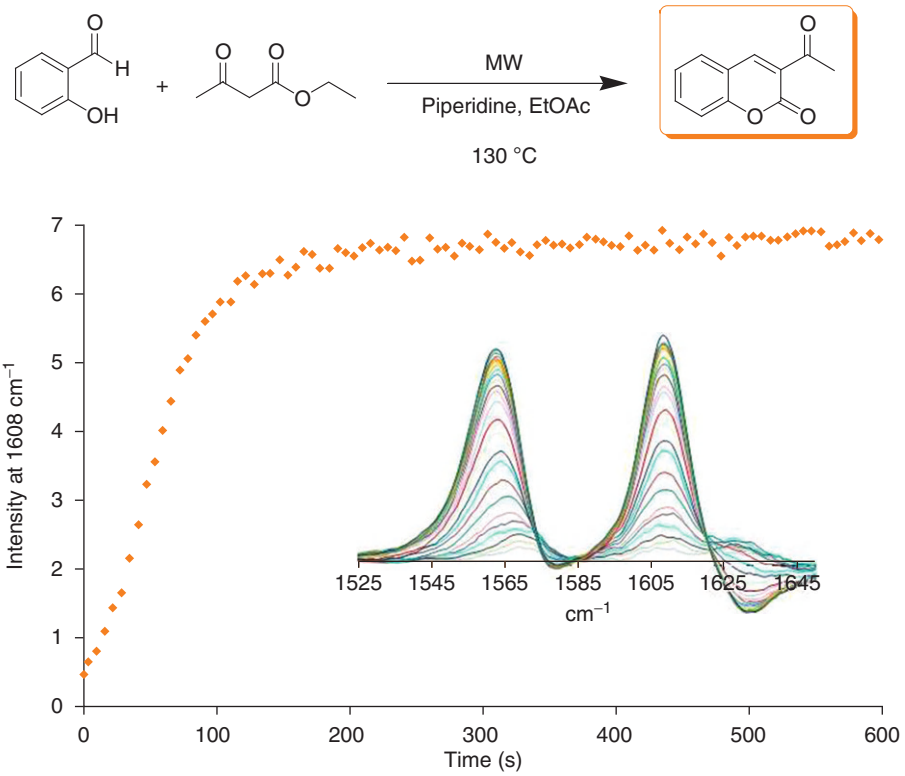


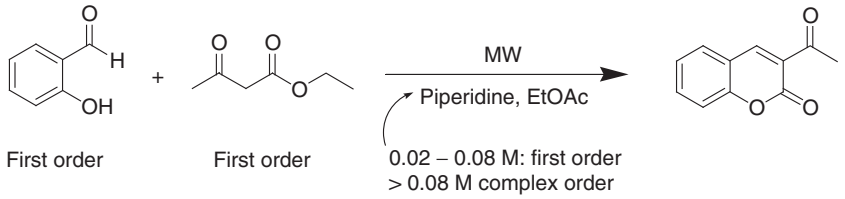
Figure 11 Monitoring the formation of 3-acetylcoumarin using Raman spectroscopy.

9.10.9.3.4.2 Quantitative reaction monitoring

In many aspects, Raman spectroscopy in conjunction with microwave heating is an ideal tool for performing kinetic studies. The microwave offers reproducible noncontact heating as well as precise temperature monitoring and data recording. The Raman spectrometer is able to acquire data at such a rate that quantitative information can be extracted for even the most rapid of reactions. Furthermore, Raman spectroscopy is in theory an effective means to measure concentration changes in a dynamic system. Returning to the synthesis of 3-acetylcoumarin as an example, it is possible to obtain orders of reaction with respect to each substrate as well as the activation energy (Scheme 59). In another case, the Claisen–Schmidt condensation has been studied with the objective of corroborating results obtained using Raman spectroscopy with those from laboratories that utilized other spectroscopic techniques.[338] The condensation between acetophenone and benzaldehyde to yield chalcone was calculated to have an activation enthalpy of 49.0 kJ mol^{-1}, which is in good agreement with the previously reported value of 48.5 kJ mol^{-1} (11.6 kcal mol^{-1}).

9.10.9.3.4.3 Probing microwave effects

In situ Raman spectroscopy can also be used to investigate the impact of microwave power input on spectroscopic signatures of molecules, and thus serve as a probe for the existence (or not) of microwave effects.[339] The intensity of observed signals in Raman spectroscopy is temperature dependent. If some molecules are being heated to temperatures exceeding the observed bulk temperature (specific microwave effects), the Raman spectrum should bear this out with a change in signal intensity that is a function of the applied power of the microwave field. In addition, because Raman spectroscopy has its origins in the polarizability of a



Scheme 59 Kinetic data obtained for the piperidine-catalyzed reaction of salicylaldehyde with ethyl acetoacetate to yield 3-acetylcoumarin.

molecule, if microwave irradiation can distort the electron cloud of a molecule or couple selectively to a more polar region of a molecule (nonthermal microwave effects), it is an ideal technique for investigating this phenomenon. No superheating events, nor any selective heating of parts of molecules, are observed.

9.10.9.3.5 Nuclear magnetic resonance spectroscopy

Of all the analytical techniques employed by organic chemists on a day-to-day basis, NMR spectroscopy is probably the most widely used. Traditionally, the compounds are dissolved in a deuterated solvent, placed into a sample tube, and the spectrum recorded. However, the combination of chromatography and NMR has also made its way into the analytical laboratory.[340] A liquid-chromatography (LC) system can be coupled directly to an NMR unit, the sample being transferred into the spectrometer 'as is.' That is, it arrives at the concentration and in the (nondeuterated) solvent supplied by the LC. The NMR spectra are then acquired either in on-flow mode (continuously, while the chromatography is running) or in stop-flow mode (while a selected peak is held in the NMR probe and chromatography is paused). In an extension of this technology, a microliter microwave flow reactor has been hyphenated with a custom-made nanoliter flow-NMR unit.[341] A reaction flow cell of 2 μl volume is used along with a microfluidic NMR chip with a detection volume of 6 nl. The rationale behind making the detection volume of the NMR chip much smaller than that of the microwave cell is to allow the outcome of a range of different reaction times to be assayed in one experiment. The reaction cell is filled with a plug of reagents and the flow rate set to 0.21 μl min^{-1}, with the solvent behind the plug pushing it through. The microwave irradiation is then turned on and spectroscopic data recorded every few seconds. Reagents that start off close to the top of the reaction cell are in the microwave field for much less time than those at the bottom of the cell. This means that as the mixture passes through the NMR spectrometer, data for different 'reaction times' can be acquired. As the volume of the microwave-heated zone is very small, the ramp time from ambient to the target temperature is very short, a matter of a few seconds. Although in its infancy, this technique does show significant promise. The Diels–Alder cycloaddition of 2,5-dimethylfuran and dimethylacetylene dicarboxylate has been used as a test case. Signals for the reagents (3.3 ppm for the dienophile and 5.8 ppm for the diene) are seen to decrease in intensity as reaction time increases. Performing the reaction first at 125 °C and then repeating at 135 and 150 °C, it is possible to start to obtain kinetic data.

9.10.10 Scale-Up of Reactions using Microwave Heating

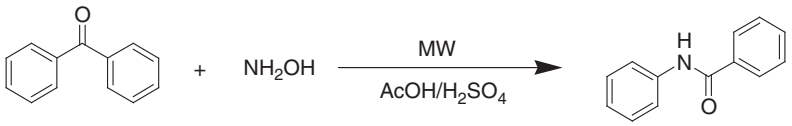
9.10.10.1 Introduction

'Microwave heating seems useful for preparation of the first gram or so of a compound, but is it scalable?' This is a question that is frequently asked and it certainly has some validity. For microwave heating to be a technology that continues to be useful from an industrial standpoint, the methods developed on a small scale need to be able to be scaled up to make more significant quantities of material. Although the use of microwave heating for performing reactions on the millimole scale in sealed vessels is straightforward, there are a number of potential issues associated with scale-up. These range from accessing suitable equipment through to safety considerations when working on a larger scale. Manufacturers of microwave equipment have, for the most part, developed equipment to meet scale-up needs using three main approaches: (1) open-vessel batch, (2) sealed-vessel batch, and (3) continuous-flow processing.[342] Here, selected examples will be highlighted with the objective of giving an overview of the scope of each.

9.10.10.2 Open-Vessel Batch Processing

When working on a larger scale, performing reactions in standard laboratory glassware at atmospheric pressure can offer operational advantages over a sealed-vessel approach. However, as discussed in Section 9.10.5.4.2 in the chapter, this eliminates one of the greatest attributes of microwave heating; namely, the ability to heat reactions to well above the normal boiling points of solvents in a safe and effective manner. As a result, open-vessel approaches to scale-up have seen somewhat limited application.[343–345] The Beckmann rearrangement (acid-catalyzed conversion of ketoximes to *N*-substituted amides) proves very amenable to translation from small-scale sealed-vessel processing to a larger open-vessel approach (Scheme 60).[178] In a sealed

tube, benzophenone can be converted to *N*-phenylbenzamide in 74% yield on the 5 mmol scale. The reaction mixture is heated to 140 °C and held at this temperature for 20 min. Moving to an open-vessel, the maximum temperature that can be reached is that of reflux (120 °C). On the 1 mol scale, a 90% yield of product can be obtained after 20 min.



Sealed vessel (10 mmol): heat to 140 °C and hold for 20 min – 74 % yield

Open vessel (1 mol): heat to reflux (120 °C) and hold for 20 min – 90 % yield

Scheme 60 Scale-up of the Beckmann rearrangement using an open-vessel approach.

9.10.10.3 Sealed-Vessel Batch Processing

A sealed-vessel batch approach represents an attractive choice in the scale-up of reactions performed using microwave heating. The primary advantage is that most small-scale reactions are developed under sealed-vessel conditions, thus scale-up is potentially straightforward with little or no re-optimization needed. Disadvantages to this approach are the limits of reaction volume that can be irradiated as well as the safety requirements when working with larger vessels under pressure. There are three options available for sealed-vessel processing (Figure 12); namely, (1) use of multiple smaller reaction vessels, (2) an automated stop-flow approach, and (3) using one larger vessel.

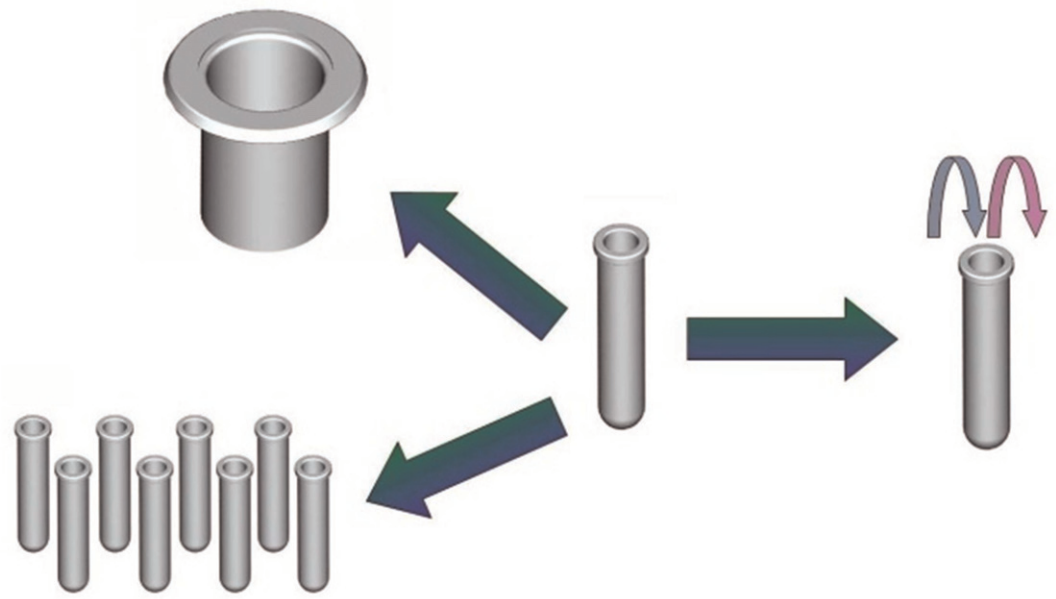
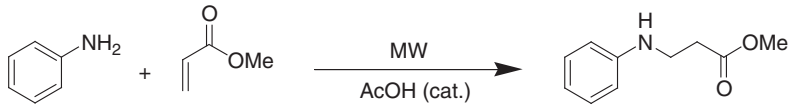


Figure 12 Approaches to scale-up using sealed-vessel processing.

9.10.10.3.1 Multiple-vessel processing

When using multiple vessels processed in a carousel, it is generally possible to scale reactions without re-optimization of conditions developed on small-scale equipment.[346] An example is the synthesis of *N*-aryl functionalized *β*-amino esters using a Michael addition protocol (Scheme 61).[347] The reaction was optimized on the 13 mmol scale, optimal conditions being heating at 200 °C for 20 min without using a solvent.[347] It can be scaled to 2.8 mol by placing 20 ml (0.14 mol) of reaction mixture into each of 20 vessels, thus processing a total substrate volume of 0.4 l. After the reaction, and before pooling into one collection vessel, the contents of representative vessels were assayed. An overall 78% yield was obtained for the reaction with very little variation from vessel to vessel.



Sealed vessel (13 mmol): heat to 200 °C and hold until a total time of 20 min has elapsed – 81 % yield

Sealed vessel (2.8 mol): irradiate for 20 min (maximum temperature reached is 198 °C) – 78 % yield

Scheme 61 Scale-up of the synthesis of an *N*-aryl functionalized *β*-amino ester using multiple sealed vessels.

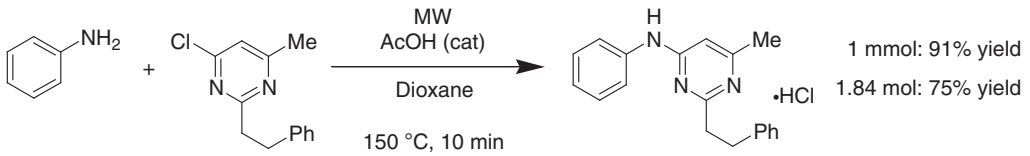
9.10.10.3.2 Stop-flow processing

A drawback to using multiple sealed reaction vessels is that the loading and sealing of the tubes before heating, and then the opening and emptying afterward, are all time-consuming processes. In an attempt to overcome this, a stop-flow route can be used for modest scale-up.[141,348] Having optimized reaction conditions on a small scale, it is possible in principle to move directly to a stop-flow using the same equipment, comprising a glass reaction vessel with a maximum operating volume of 50 ml. Reagents are loaded in and products pumped out by means of a number of polytetrafluoroethylene (PTFE) lines. Although allowing for automation, this also leads to issues if the mixtures going in or coming out of the reaction vessel are not homogeneous because the PTFE lines can be prone to blockage. A case in point is palladium-catalyzed coupling chemistry performed in water as a solvent. Both Suzuki and Heck coupling reactions require some re-optimization to overcome the clogging issue.[349] Problems are particularly apparent at the end of the reaction. Although liquids at elevated temperatures, the products solidify as they begin to exit the microwave cavity. They are often insoluble in the aqueous reaction medium and so block the exit lines, even at temperatures of up to 90 °C. To overcome this, it is necessary to add a small charge of organic solvent into the reaction vessel at the end of the reaction to solubilize the products and allow them to be pumped out. To give an idea of scale, 10 cycles of each reaction yield 15–20 g of product. A stop-flow approach has been used in a step of the synthesis of citalopram, a reaction discussed in Section 9.10.5.2.2 (Scheme 4).[36] The key palladium-catalyzed cyanation is performed on 12 g of starting material per batch. When addition and removal of material is factored in, the total cycle time is approximately 10 min per batch, allowing for the preparation of 150 g in less than 2 h.

9.10.10.3.3 Use of one sealed vessel

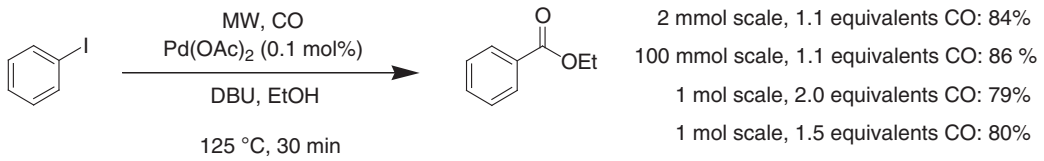
A single, larger, reaction vessel for scale-up avoids the issues encountered both with using multiple, smaller, vessels and stop-flow processing. However, a number of new potential problems arise. First, the equipment used must be designed with additional safety measures in mind if larger volumes are going to be heated to elevated temperatures and pressures. Second, significant changes in engineering are required to obtain heating profiles that in any way mirror those of smaller microwave units. Third, although it may be possible to heat a reaction mixture effectively using microwave irradiation, it is also important that the contents of the vessel be cooled back to ambient temperature in a timely manner. The increased safety measures needed to withhold a potential vessel failure at elevated temperature and pressure generally mean that thick-walled vessels and microwave cavities are used. As a result, cooling can be very slow. This can be overcome by use of adiabatic cooling, the contents of the reaction vessel being ejected into a holding tank. Using this, the temperature of the mixture can be reduced rapidly to the boiling point of the solvent used.

A number of reactions have been scaled up using a single sealed-vessel approach, most in the 0.1–1 l range.[132,140,350] Equipment is also available capable of processing from 2 to 12 l at a time.[351] This can feasibly help bridge the gap between a small-scale protocol and larger kilo- or pilot-plant scale. As an example, the synthesis of 3-acetylcoumarin from salicylaldehyde and ethyl acetoacetate can be performed on the 18 mol scale, yielding 1.8 kg of product. In another case, an acid-catalyzed nucleophilic aromatic substitution protocol can be performed on 1.84 mol of starting material with no changes made from a protocol originally developed on the 1 mmol level, this representing a greater than 18 000-fold increase in scale (Scheme 62).



Scheme 62 Scale-up of a nucleophilic aromatic substitution reaction using a single sealed vessel.

Reactions using gaseous reagents can also be scaled up in a single sealed-vessel approach. Returning to the near-stoichiometric palladium-catalyzed alkoxycarbonylation reaction discussed earlier in the chapter, ethyl benzoate can be prepared on the 0.1–1 mol scale in 80–86% isolated yield from iodobenzene (Scheme 63).[352]

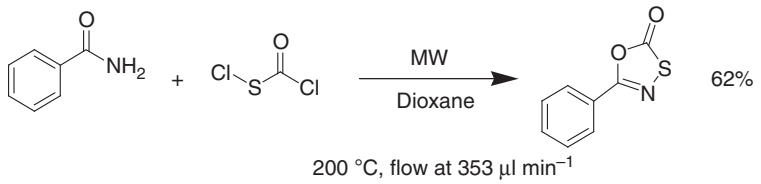


Scheme 63 Scale-up of the palladium-catalyzed ethoxycarbonylation of iodobenzene using a single sealed vessel.

9.10.10.4 Continuous-flow Processing

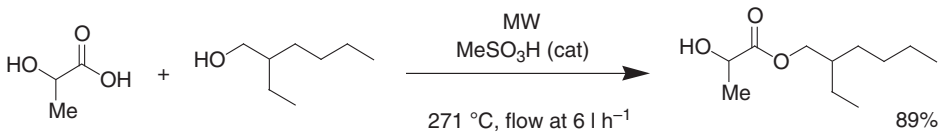
There are a number of reasons to adopt a continuous-flow approach for scale-up.[353] Reactions are actually 'scaled-out' rather than scaled-up. Maximum throughput is only a matter of run time and the total number of units operating in parallel. Furthermore, catastrophic loss of a large quantity of valuable substrate can be avoided, as only a small portion of the reaction is subjected to reaction conditions at any given time. Drawbacks to this approach are that reaction mixtures are generally required to be homogeneous before, during, and until out of the microwave apparatus. A consequence of this is that extensive re-optimization may need to be undertaken to develop appropriate homogeneous reaction conditions and suitable residence times. This in itself may require additional solvent and/or catalyst screening. Another option is to use additional solvent or a co-solvent, but this too can lead to a drop in product conversion depending on the nature of the reaction.

Despite these drawbacks, a number of synthetic transformations have been successfully scaled-up using continuous-flow processing.[141,178,354] At the smaller-sized end is a special microwave unit comprising a 3 mm inner diameter reactor.[355] The total length of the tubular reactor is 200 mm, although only 90 mm is within the microwave field. It has been used to perform a number of synthetic transformations, including the cyclization of benzamide and chlorocarbonyl sulfenyl chloride (Scheme 64). The 5-substituted 1,3,4-oxathiazol-2-one is a potent *Mycobacterium tuberculosis* proteasome inhibitor. Passing the reagents through the reactor at a flow rate of 353 µl min^{-1} and with a residence time of 1 min at 200 °C, the product can be isolated in 62% yield with a throughput of 3.3 mmol h^{-1} (0.58 g h^{-1}).



Scheme 64 Preparation of an oxathiazolone using continuous-flow processing.

At the higher throughput end, an example is the esterification of lactic acid.[356] Using methanesulfonic acid as a catalyst, the 2-ethylhexyl ester can be performed at a flow rate of 6 l min^{-1} with a residence time in the microwave cavity of 28 s (Scheme 65).



Scheme 65 Scale-up of an esterification reaction using continuous-flow processing.

There is a clear parallel between microwave irradiation and conventionally heated continuous-flow processing. Both technologies offer the ability to heat reaction mixtures rapidly, safely, and (in most cases) easily. It therefore comes as no surprise that synthetic methods developed on small scale in batch using microwave heating can be scaled-up using conventionally heated flow reactors.[357] When using micro- and meso-flow reactors, the rapid heat transfer that is possible means that comparable heating rates can often be obtained regardless of whether the thermal energy comes from a conventional or microwave source.

9.10.10.5 Energy Efficiency

When using microwave heating for scale-up of synthetic chemistry, the issue of energy efficiency has to be considered. Transitioning from conventional heating approaches to microwave heating often involves moving away from laboratory infrastructure that has been designed over the years to maximize efficiency. For example, many chemical production facilities generally have easy access to cheaply generated steam heating.[358] A number of energy assessments have been performed, comparing microwave and conventional heating across a range of scales.[359–361] Small monomode microwave units, the likes of which are used on a daily

basis in academia and industry for reaction optimization, are undoubtedly not energy efficient. In many cases, the microwave field is simply too dense in a monomode cavity to be completely absorbed by the reaction mixture.[362] Moving up in scale to multimode microwave systems, they appear to be more energy efficient than their monomode cousins and sometimes more so than conventional heating methods. On the basis of kilojoule energy used per mole of product made, an improvement in energy efficiency is noticed with increasing scale. Beyond scale, energy efficiency also depends on parameters such as the manufacturer of the equipment, the microwave absorptivity of the reagents and solvent, as well as the temperature at which the reaction is run and for how long. The biggest issue when it comes to energy efficiency is the conversion of electrical energy to microwave energy by the magnetron. That said, the most efficient microwave equipment operating under optimal conditions can be significantly more energy efficient than conventional pilot-scale reactors even up to 40 l.[361]

9.10.11 Conclusion

Just as microwave ovens have found wide acceptance in the home, so the same technology is making vast inroads into synthetic chemistry. This chapter has shown some of the many synthetic transformations that can be performed using microwave heating. Using scientific microwave apparatus it is possible to perform chemical reactions, quickly, easily, and safely. For many chemists, the microwave is the go-to appliance whenever they need to perform a reaction that requires heat and it has been dubbed 'the Bunsen burner of the twenty-first century.'[363] Microwave heating often offers significant timesaving over conventional approaches. This proves particularly valuable in an industrial R&D setting where time is money. In an interesting 'competition' at Boehringer Ingelheim Pharmaceuticals, two chemists were tasked with the same scaffold to synthesize.[364] One was told to use just conventional heating and the other just microwave heating. The conventional approach was unsuccessful, even after 37 days of effort. The microwave approach was complete in 2 days. As stressed several times in the chapter, microwave heating is just that – heating. There is nothing mythical to microwave irradiation when used as a tool by the synthetic chemist. It just gives them easy access to elevated temperature/pressure conditions. Accurate temperature measurement is essential when making comparisons with conventional methods. It is becoming more and more apparent that, when using identical conditions, the same reactions can be performed with the same outcome and the same product yield using either microwave or conventional heating.

But microwave heating goes beyond being a useful tool for routine laboratory work to affording the bench chemist an opportunity to carry out exciting new chemistry. Some of this has been shown here in the chapter and includes designer catalysis, C–H bond activation, reactions under an atmosphere of reactive gas, combinatorial chemistry, and using the microwave as a precise heating tool for kinetic study by means of *in situ* spectroscopy. The scale-up of microwave reactions from the milligram, through the multigram to the kilogram and beyond has also been a subject of this chapter. At the upper end of this scale, it is very a much 'work in progress' and it will be interesting to see the equipment capable of operating at larger throughput continue to evolve. Alongside this will be the need for careful evaluation of energy efficiency. As mentioned at various junctures along the way, microwave heating is not an 'organic chemistry' technique. Its application is far broader than that. Other disciplines are catching onto the benefits and the added convenience that a dedicated scientific microwave unit can add to the laboratory setting. Accordingly, as these tap into the potential of microwave irradiation, new applications will be found, more efficient syntheses will be realized, and the microwave will continue to demonstrate its worth in the laboratory.

Acknowledgment

Section 9.10.2 contributed by Jason R. Schmink, Bryn Mawr College, PA.

References

1. (a) de la Hoz, A., Loupy, A., Eds.; *Microwaves in Organic Synthesis*, 3rd ed.; Wiley-VCH: Weinheim, **2012**. (b) Kappe, C. O.; Stadler, A.; Dallinger, D. *Microwaves in Organic and Medicinal Chemistry*, 2nd ed.; Wiley-VCH: Weinheim, **2012**.
2. Leadbeater, N. E., Ed. *Microwave Heating as a Tool for Sustainable Chemistry*; CRC Press: Boca Raton, FL, **2010**.
3. Gedye, R.; Smith, K.; Westaway, H. *Tetrahedron Lett.* **1986**, *27*, 279–282.
4. Giguere, R. J.; Bray, T. L.; Duncan, S. M.; Majetich, G. *Tetrahedron Lett.* **1986**, *27*, 4945–4948.
5. Vanderhoff, J. W. (Dow Chemical Co.) Method for Carrying Out Chemical Reactions Using Microwave Energy. US 3,432,413, **1969**, *Chem. Abstr.* 1970, 97422.
6. Bilecka, I.; Niederberger, M. *Nanoscale* **2010**, *2*, 1358.
7. Ebner, C.; Bodner, T.; Stelzer, F.; Wiesbrock, F. *Macromol. Rapid Commun.* **2011**, *32*, 254.
8. (a) Abe, T.; Miyazawa, A.; Kawanishi, Y.; Konno, H. *Mini-Rev. Org. Chem.* **2011**, *8*, 315. (b) Navarro, O. *Chemistry Today* **2010**, *28*, 15.
9. (a) Sandoval, W. N.; Pham, V. C.; Lill, J. R. *Drug Discov. Today* **2008**, *13*, 1075. (b) Sabatino, G.; Papini, A. M. *Curr. Opin. Drug Discov. Dev.* **2008**, *11*, 762. (c) Collins, J. M.; Leadbeater, N. E. *Org. Biomol. Chem.* **2007**, *5*, 1141.
10. (a) Horikoshi, S.; Iida, S.; Kajitani, M.; Sato, S.; Serpone, N. *Org. Proc. Res. Dev.* **2008**, *12*, 257–263. (b) Gedye, R. N.; Wei, J. B. *Can. J. Chem.* **1998**, *76*, 525–532. (c) Möller, M.; Linn, H. *Key Eng. Mater.* **2004**, *264–268*, 735–739. (d) Takizawa, H.; Uheda, K.; Endo, T. *J. Am. Ceram. Soc.* **2000**, *83*, 2321–2323. (e) Malinger, A. K.; Ding, Y.-S.; Sithambaram, S.; *et al. J. Catal.* **2006**, *239*, 290–298.
11. Hayes, B. L. *Microwave Synthesis: Chemistry at the Speed of Light*; CEM Publishing: Matthews, NC, **2002**.
12. Saillard, R.; Poux, M.; Berlan, J. *Tetrahedron* **1995**, *51*, 4033–4042.

13. Baghurst, D. R.; Mingos, D. M. P. *J. Chem. Soc. Chem. Commun.* **1992**, 674–677.
14. Lienhard, J. H. I. V.; Lienhard, J. H. V. *A Heat Transfer Textbook*, 3rd ed.; Phlogiston Press: Cambridge, MA, **2008**; 457–463.
15. Chemat, F.; Esveld, E. *Chem. Eng. Technol.* **2001**, *24*, 735–744.
16. (a) Washington, A. L.; Strouse, G. F. *Chem. Mat.* **2009**, *21*, 2770–2776. (b) Washington, A. L.; Strouse, G. F. *J. Am. Chem. Soc.* **2008**, *130*, 8916–8922.
17. (a) Perreux, L.; Loupy, A. Nonthermal Effects of Microwaves in Organic Synthesis. In *Microwaves in Organic Synthesis*, 2nd ed.; Loupy, A., Ed.; Wiley-VCH: Weinheim, **2006**, Chapter 4; pp 134–218. (b) De La Hoz, A.; Diaz-Ortiz, A.; Moreno, A. *Chem. Soc. Rev.* **2005**, *34*, 164–178.
18. Nüchter, M.; Ondruschka, B.; Weiss, D.; *et al. Chem. Eng. Technol.* **2005**, *28*, 871–881.
19. Larhed, M.; Moberg, C.; Hallberg, A. *Acc. Chem. Res.* **2002**, *35*, 717–727.
20. Hájek, M. Microwave Catalysis in Organic Synthesis. In *Microwaves in Organic Synthesis*, 2nd ed.; Loupy, A., Ed.; Wiley-VCH: Weinheim, **2006**, Vol. 2, Chapter 13; pp 615–652.
21. Mehta, V. P.; Van der Eycken, E. *Chem. Soc. Rev.* **2011**, *40*, 4925–4936.
22. Nilsson, P.; Olofsson, K.; Larhed, M. *Top. Curr. Chem.* **2006**, *266*, 103–144.
23. Singh, B. K.; Kaval, N.; Tomar, S.; Van der Eycken, E.; Parmar, V. S. *Org. Proc. Res. Dev.* **2008**, *12*, 468–474.
24. Olofsson, K.; Nilsson, P.; Larhed, M. Microwave-Assisted Transition Metal-Catalyzed Coupling Reactions. In *Microwaves in Organic Synthesis*, 2nd ed.; Loupy, A., Ed.; Wiley-VCH: Weinheim, **2006**, Vol. 2, Chapter 13; pp 68–725.
25. Arvela, R. K.; Leadbeater, N. E.; Sangi, M. S.; *et al. J. Org. Chem.* **2005**, *70*, 161–168.
26. Arvela, R. K.; Leadbeater, N. E. *J. Org. Chem.* **2005**, *70*, 1786–1790.
27. Beryozkina, T.; Appukkuttan, P.; Mont, N.; Van der Eycken, E. *Org. Lett.* **2006**, *8*, 487–490.
28. Mata, Y.; Diéguez, M.; Pàmies, O. *Chem. Eur. J.* **2007**, *13*, 3296–3304.
29. Kaukoranta, P.; Källström, K.; Andersson, P. G. *Adv. Synth. Catal.* **2007**, *349*, 2595–2602.
30. Waldmann, H.; He, Y.-P.; Tan, H.; Arve, L.; Arndt, H.-D. *Chem. Commun.* **2008**, 5562–5564.
31. Lépine, R.; Zhu, J. *Org. Lett.* **2005**, *7*, 2981–2984.
32. Moro, A. V.; Cardoso, F. S. P.; Correia, C. R. D. *Org. Lett.* **2009**, *11*, 3642–3645.
33. Shen, L.; Zhang, M.; Wu, Y.; Qin, Y. *Angew. Chem. Int. Ed.* **2008**, *47*, 3618–3621.
34. Dounay, A. B.; Humphreys, P. G.; Overman, L. E.; Wrobleski, A. D. *J. Am. Chem. Soc.* **2008**, *130*, 5368–5377.
35. Leadbeater, N. E.; Rudzinski, D. M. *Chemistry Today* **2011**, *29*, 22–25.
36. Pitts, M. R.; McCormack, P.; Whittall, J. *Tetrahedron* **2006**, *62*, 4705–4708.
37. Velmathi, S.; Leadbeater, N. E. *Tetrahedron Lett.* **2008**, *49*, 4693–4694.
38. DeBlase, C.; Leadbeater, N. E. *Tetrahedron* **2010**, *66*, 1098–1101.
39. Melucci, M.; Barbarella, G.; Sotgiu, G. *J. Org. Chem.* **2002**, *67*, 8877–8884.
40. Melucci, M.; Barbarella, G.; Zambianchi, M.; Di Pietro, P.; Bongini, A. *J. Org. Chem.* **2004**, *69*, 4821–4828.
41. (a) Mason, T. J.; Peters, D. *Practical Sonochemistry: Power Ultrasound Uses and Applications*, 2nd Ed.; Woodhead Publishing: Cambridge, UK, **2002**. (b) Nowak, F. M., Ed.*Sonochemistry: Theory, Reactions and Syntheses, and Applications*; Nova Science Publishers Inc.: New York, **2011**.
42. (a) Mason, T. J. *Chem. Soc. Rev.* **1997**, *26*, 443–451. (b) Sillanpää, M.; Pham, T.-D.; Shrestha, R. A. *Ultrasound Technology in Green Chemistry*; Springer: Berlin, **2011**.
43. Di Maria, F.; Olivelli, P.; Gazzano, M.; *et al. J. Am. Chem. Soc.* **2011**, *133*, 8654–8661.
44. (a) Estrada, G. O. D.; Blanco, A. L. P.; da Silva, J. F. M.; *et al. Tetrahedron Lett.* **2012**, *53*, 1089–1093. (b) Leonhardt, S. E. S.; Stolle, A.; Ondruschka, B.; *et al. Appl. Catal. A* **2010**, *379*, 30–37. (c) Sedelmeier, J.; Ley, S. V.; Lange, H.; Baxendale, I. R. *Eur. J. Org. Chem.* **2009**, 4412–4420. (d) Glasnov, T. N.; Findenig, S.; Kappe, C. O. *Chem. Eur. J.* **2009**, *15*, 1001–1010. (e) Butler, T. A.; Swift, E. C.; Lipshutz, B. H. *Org. Biomol. Chem.* **2008**, *6*, 19–25. (f) Sharma, A. K.; Gowdahalli, J. K.; Amin, S. *J. Org. Chem.* **2007**, *72*, 8987–8989. (g) Arvela, R. K.; Leadbeater, N. E. *Org. Lett.* **2005**, *7*, 2101–2104.
45. Irfan, M.; Fuchs, M.; Glasnov, T. N.; *et al. Chem. Eur. J.* **2009**, *15*, 11608–11618.
46. (a) Bag, S.; Dasgupta, S.; Török, B. *Curr. Org. Synth.* **2011**, *8*, 237–261. (b) Desai, B.; Kappe, C. O. *Top. Curr. Chem.* **2004**, *242*, 177–208.
47. (a) Wan, Y.; Alterman, A.; Hallberg, A. *Synthesis* **2002**, 1597–1600. (b) Antane, S. *Synth. Commun.* **2003**, *33*, 2147–2149.
48. Coeffard, V.; Muller-Bunz, H.; Guiry, P. J. *Org. Biomol. Chem.* **2009**, *7*, 1723–1734.
49. (a) Mehmood, A.; Devine, W. G.; Leadbeater, N. E. *Top. Catal.* **2010**, *53*, 15–18. (b) Benaskar, F.; Engels, V.; Patil, N.; *et al. Tetrahedron Lett.* **2010**, *51*, 248–251. (c) D'Angelo, N. D.; Peterson, J. J.; Booker, S. K.; *et al. Tetrahedron Lett.* **2006**, *47*, 5045–5048. (d) Rudolph, J.; Esler, W. P.; O'Connor, S.; *et al. J. Med. Chem.* **2007**, *50*, 5202–5216.
50. (a) Yu, C.-W.; Chen, G. S.; Huang, C.-W.; *et al. Org. Lett.* **2012**, *14*, 3688–3691. (b) Mehmood, A.; Leadbeater, N. E. *Catalysis Comm.* **2010**, *12*, 64–66. (c) Kormos, C. M.; Leadbeater, N. E. *Tetrahedron* **2006**, *62*, 4728–4732.
51. Manbeck, G. F.; Lipman, A. J.; Stockland, R. A.; *et al. J. Org. Chem.* **2005**, *70*, 244–250.
52. Lipshutz, B. H.; Unger, J. B.; Taft, B. R. *Org. Lett.* **2007**, *9*, 1089–1092.
53. Lipshutz, B. H.; Nihan, D. M.; Vinogradova, E.; *et al. Org. Lett.* **2008**, *10*, 4279–4282.
54. (a) Kelly, C. B.; Lee, C.; Leadbeater, N. E. *Tetrahedron Lett.* **2011**, *52*, 4587–4589. (b) Yuan, Y.-Q.; Guo, S.-R. *Synlett* **2011**, 2750–2756. (c) Lengar, A.; Kappe, C. O. *Org. Lett.* **2004**, *6*, 771–774. (d) Macmillan, D.; Anderson, D. W. *Org. Lett.* **2004**, *6*, 4659–4662.
55. Prokopcová, H.; Kappe, C. O. *J. Org. Chem.* **2007**, *72*, 4440–4448.
56. Singh, B. K.; Appukkuttan, P.; Parmar, V. S.; *et al. Org. Biomol. Chem.* **2006**, *5*, 2962–2965.
57. Singh, B. K.; Appukkuttan, P.; Claerhout, S.; *et al. Org. Lett.* **2006**, *8*, 1863–1866.
58. (a) Humphrey, C. E.; Easson, M. A. M.; Tierney, J. P.; *et al. Org. Lett.* **2003**, *5*, 849–852. (b) Chen, J. J.; Deshpande, S. V. *Tetrahedron Lett.* **2003**, *44*, 8873–8876. (c) Mathew, F.; Jayaprakash, K. N.; Fraser-Reid, B.; *et al. Tetrahedron Lett.* **2003**, *44*, 9051–9054. (d) Jachuck, R. J. J.; Selvaraj, D. K.; Varma, R. S. *Green Chem.* **2006**, *8*, 29–33.
59. Hayes, B. L.; Collins, M. J. Jr., World Pat. WO04002617, **2004**.
60. (a) Lange, S. M.; Torok, B. *Catal. Lett.* **2009**, *131*, 432–439. (b) Horikoshi, S.; Tsuzuki, J.; Kajitani, M.; *et al. New J. Chem.* **2008**, *32*, 2257–2262. Horikoshi, S.; Ohmori, N.; Kajitani, M.; *et al. J. Photochem. Photobiol. A* **2007**, *189*, 374–379.
61. Stadler, A.; Kappe, C. O. *Org. Lett.* **2002**, *4*, 3541–3544.
62. (a) Rummelt, S. M.; Ranocchiari, M.; van Bokhoven, J. A. *Org. Lett.* **2012**, *14*, 2188–2190. (b) Karlstedt, N. B.; Beletskaya, I. P. *Russ. J. Org. Chem.* **2011**, *47*, 1011–1014. (c) Yang, G. Q.; Shen, C. R.; Zhang, L.; *et al. Tetrahedron Lett.* **2011**, *52*, 5032–5035. (d) Damian, K.; Clarke, M. L.; Cobley, C. J. *Appl. Organomet. Chem.* **2009**, *23*, 272–276. (e) Kalek, M.; Ziadi, A.; Stawinski, J. *Org. Lett.* **2008**, *10*, 4637. (f) Beletskaya, I. P.; Karlstedt, N. B.; Nifant'ev, E. E.; *et al. Russ. J. Org. Chem.* **2006**, *42*, 1780–1785. (g) Stockland, R. A.; Lipman, A. J.; Bawiec, J. A.; *et al. J. Organomet. Chem.* **2006**, *691*, 4042–4053. (h) Stone, J. J.; Stockland, R. A.; Reyes, J. M.; *et al. J. Mol. Cat. A. Chem.* **2005**, *226*, 11–21. (i) Villemin, D.; Elbilali, A.; Siméon, F.; *et al. J. Chem. Res.* **2003**, 436–437.
63. (a) Coquerel, Y.; Rodriguez, J. *Eur. J. Org. Chem.* **2008**, 1125–1132. (b) Aitken, S. G.; Abell, A. D. *Aust. J. Chem.* **2005**, *58*, 3–13.
64. (a) Grigg, R.; Martin, W.; Morris, J.; *et al. Tetrahedron Lett.* **2003**, *44*, 4899–4901. (b) Thanh, G. V.; Loupy, A. *Tetrahedron Lett.* **2003**, *44*, 9091–9094. (c) Mayo, K. G.; Nearhoof, E. H.; Kiddle, J. J. *Org. Lett.* **2002**, *4*, 1567–1570.
65. Garbacia, S.; Desai, B.; Lavastre, O.; *et al. J. Org. Chem.* **2003**, *68*, 9136–9139.

66. Nosse, B.; Schall, A.; Jeong, W. B.; *et al. Adv. Synth. Catal.* **2005**, *347*, 1869–1874.
67. Sharma, A.; Appukkuttan, P.; van der Eycken, E. *Chem. Commun.* **2012**, *48*, 1623–1637.
68. (a) Yadav, D. B.; Morgans, G. L.; Aderibigbe, B. A.; *et al. Tetrahedron Lett.* **2011**, *67*, 2991–2997. (b) Baron, A.; Verdie, P.; Martinez, J.; *et al. J. Org. Chem.* **2011**, *76*, 766–772. (c) Vu, N. Q.; Chai, C. L. L.; Lim, K. P.; *et al. Tetrahedron* **2007**, *63*, 7053–7058. (d) Appukkuttan, P.; Dehaen, W.; van der Eycken, E. *Org. Lett.* **2005**, *7*, 2723–2726.
69. (a) Debleds, O.; Campagne, J. M. *J. Am. Chem. Soc.* **2008**, *130*, 1562–1563. (b) Comer, E.; Rohan, E.; Deng, L.; *et al. Org. Lett.* **2007**, *9*, 2123–2126. (c) Salim, S. S.; Bellingham, R. K.; Brown, R. C. D. *Eur. J. Org. Chem.* **2004**, 800–806. Fürstner, A.; Stelzer, F.; Rumbo, A.; Krause, H. *Chem. Eur. J.* **2002**, *8*, 1856–1871.
70. Efskind, J.; Undheim, K. *Tetrahedron Lett.* **2003**, *44*, 2837–2839.
71. (a) Yu, J.-Q., Shi, Z., Eds.*C–H Activation, Topics in Current Chemistry Series 292*; Springer: Berlin, **2010**. Gütekunst, W. R.; Baran, P. S. *Chem. Soc. Rev.* **2011**, *40*, 1976–1991. (c) Collet, F.; Lescot, C.; Dauban, P. *Chem. Soc. Rev.* **2011**, *40*, 1926–1936.
72. Pérez, P. J., Ed. *Alkane C–H Activation by Single-Site Metal Catalysis*; Springer: Berlin, **2012**.
73. (a) Gaillard, S.; Cazin, C. S. J.; Nolan, S. P. *Acc. Chem. Res.* **2011**, *45*, 778–787. (b) Vedernikov, A. N. *Acc. Chem. Res.* **2011**, *45*, 803–813. (c) Colby, D. A.; Tsai, A. S.; Bergman, R. G.; Ellman, J. A. *Acc. Chem. Res.* **2011**, *45*, 814–825. (d) Powers, D. C.; Ritter, T. *Acc. Chem. Res.* **2011**, *45*, 840–850.
74. Tan, K. L.; Vasudevan, A.; Bergman, R. G.; Ellman, J. A.; Souers, A. J. *Org. Lett.* **2003**, *5*, 2131–2134.
75. (a) Lewis, J. C.; Berman, A. M.; Bergman, R. G.; Ellman, J. A. *J. Am. Chem. Soc.* **2008**, *130*, 2493–2500. (b) Lewis, J. C.; Wu, J. Y.; Bergman, R. G.; Ellman, J. A. *Angew. Chem. Int. Ed.* **2006**, *45*, 1589–1591.
76. Yanagisawa, S.; Sudo, T.; Noyori, R.; Itami, K. *J. Am. Chem. Soc.* **2006**, *128*, 11748–11749.
77. Yanagisawa, S.; Ueda, K.; Taniguchi, T.; Itami, K. *Org. Lett.* **2008**, *10*, 4673–4676.
78. (a) Liu, W.; Cao, H.; Zhang, H.; *et al. J. Am. Chem. Soc.* **2010**, *132*, 16737–16740. (b) Sun, C.-L.; Li, H.; Yu, D.-G.; *et al. Nature Chem.* **2010**, *2*, 1044–1049. (c) Deng, G.; Ueda, K.; Yanagisawa, S.; Itami, K.; Li, C.-J. *Chem. Eur. J.* **2009**, *15*, 333–337.
79. (a) Leadbeater, N. E.; Marco, M. *Angew. Chem. Int. Ed.* **2003**, *42*, 1407–1409. (b) Buchwald, S. L.; Bolm, C. *Angew. Chem. Int. Ed.* **2009**, *48*, 5586–5587. (c) Lauterbach, T.; Livendahl, M.; Rosellón, A.; Espinet, P.; Echavarren, A. M. *Org. Lett.* **2010**, *12*, 3006–3009.
80. Leadbeater, N. E. *Nature Chem.* **2010**, *2*, 1007–1009.
81. (a) Tajuddin, H.; Shukla, L.; Maxwell, A. C.; Marder, T. B.; Steel, P. G. *Org. Lett.* **2010**, *12*, 5700–5703. (b) Harrisson, P.; Morris, J.; Marder, T. B.; Steel, P. G. *Org. Lett.* **2009**, *11*, 3586–3589.
82. (a) Baghbanzadeh, M.; Pilger, C.; Kappe, C. O. *J. Org. Chem.* **2011**, *76*, 8138–8142. (b) Campeau, L. C.; Schipper, D. J.; Fagnou, K. *J. Am. Chem. Soc.* **2008**, *130*, 3266–3267. (c) Sahnoun, S.; Messaoudi, S.; Peyrat, J.-F.; Brion, J.-D.; Alami, M. *Tetrahedron Lett.* **2008**, *49*, 7279–7283. (d) Besselièvre, F.; Mahuteau-Betzer, F.; Grierson, D. S.; Piguel, S. *J. Org. Chem.* **2008**, *73*, 3278–3280. (e) Bedford, R. B.; Betham, M. *J. Org. Chem.* **2006**, *71*, 9403–9410.
83. Yotphan, S.; Bergman, R. G.; Ellman, J. A. *Org. Lett.* **2009**, *11*, 1511–1514. (b) Johansen, M. B.; Kerr, M. A. *Org. Lett.* **2010**, *12*, 4956–4959.
84. (a) Müller, K.; Faeh, C.; Diederich, F. *Science* **2007**, *317*, 1881–1886. (b) Purser, S.; Moore, P. R.; Swallow, S.; Gouverneur, V. *Chem. Soc. Rev.* **2008**, *37*, 320–330.
85. Hull, K. L.; Anani, W. Q.; Sanford, M. S. *J. Am. Chem. Soc.* **2006**, *128*, 7134–7135.
86. Hashmi, A. S., Toste, F. D., Eds. *Modern Gold Catalyzed Synthesis*; Wiley-VCH: Weinheim, **2012**.
87. Liu, X. Y.; Li, C. H.; Che, C. M. *Org. Lett.* **2006**, *8*, 2707–2710.
88. Wang, M. Z.; Wong, M. K.; Che, C. M. *Chem. Eur. J.* **2008**, *14*, 8353–8364.
89. Nieto-Oberhuber, C.; Pérez-Galán, P.; Herrero-Gómez, E.; *et al. J. Am. Chem. Soc.* **2008**, *130*, 269–279.
90. Huisgen, R. *Angew. Chem. Int. Ed.* **1963**, *2*, 565–598.
91. Liang, L.; Astruc, D. *Coord. Chem. Rev.* **2011**, *255*, 2933–2945.
92. Hein, J. E.; Fokin, V. V. *Chem. Soc. Rev.* **2010**, *39*, 1302–1315.
93. (a) Barge, A.; Tagliapietra, S.; Binello, A.; *et al. Curr. Org. Chem.* **2011**, *15*, 189–203. (b) Kappe, C. O.; Van der Eycken, E. *Chem. Soc. Rev.* **2010**, *39*, 1280–1290.
94. (a) Khanetskyy, B.; Dallinger, D.; Kappe, C. O. *J. Comb. Chem.* **2004**, *6*, 884–892. (b) Beckmann, H. S. G.; Wittmann, V. *Org. Lett.* **2007**, *9*, 1–4. (c) Moorhouse, A.; Moses, J. E. *Synlett* **2008**, 2089–2092.
95. Appukkuttan, P.; Dehaen, W.; Fokin, V. V.; Van der Eycken, E. *Org. Lett.* **2004**, *6*, 4223–4225.
96. Lipshutz, B. H.; Taft, B. R. *Angew. Chem. Int. Ed.* **2006**, *45*, 8235–8238.
97. Buckley, B. B.; Dann, S. E.; Heaney, H.; Stubbs, E. C. *Eur. J. Org. Chem.* **2011**, 770–776.
98. (a) Munteanu, M.; Choi, S.; Ritter, H. *Macromolecules* **2008**, *41*, 9619–9623. (b) Hoogenboom, R.; Moore, B. C.; Schubert, U. S. *Chem. Commun.* **2006**, 4010–4012. (c) Song, Y.; Kohlmeir, E. K.; Meade, T. J. *J. Am. Chem. Soc.* **2008**, *130*, 6662–6663. (d) Fazio, M. A.; Lee, O. P.; Schuster, D. I. *Org. Lett.* **2008**, *10*, 4979–4982. (e) Ortega-Muñoz, M.; Morales-Sanfrutos, J.; Perez-Balderas, F.; *et al. Org. Biomol. Chem.* **2007**, *5*, 2291–2301.
99. (a) Bouillon, C.; Meyer, A.; Vidal, S.; *et al. J. Org. Chem.* **2006**, *71*, 4700–4702. (b) Géci, V.; Filichev, V.; Pedersen, E. B. *Chem. Eur. J.* **2007**, *13*, 6379–6386. (c) Lucas, R.; Zerrouki, R.; Granet, R.; *et al. Tetrahedron* **2008**, *64*, 5467–5471.
100. (a) Pietrzik, N.; Schips, C.; Ziegler, T. *Synthesis* **2008**, 519–526. (b) Broggi, J.; Díez-González, S.; Petersen, J.; *et al. Synthesis* **2008**, 141–148. (c) Pradere, U.; Roy, V.; McBrayer, T. R.; *et al. Tetrahedron* **2008**, *64*, 9044–9051. (d) Cheshev, P.; Marra, A.; Dondoni, A. *Org. Biomol. Chem.* **2006**, *4*, 3225–3227. (e) Joosten, J. A. F.; Tholen, N. T. H.; Maate, F. A. E.; *et al. Eur. J. Org. Chem.* **2005**, 3182–3185.
101. (a) Poon, C. K.; Chapman, R.; Jolliffe, K. A.; Perrier, S. *Polymer Chem.* **2012**, *3*, 1820–1826. (b) Yan, L. S.; Ding, J. X.; Qi, R. G.; *et al. J. Control. Release* **2011**, *152*, E249–E250. (c) van Dijk, M.; Nollet, M. L.; Weijers, P.; *et al. Biomacromol.* **2008**, *9*, 2834–2843.
102. (a) Braga, A. L.; Vargas, L. F.; Sehnem, J. A.; *et al. Eur. J. Org. Chem.* **2006**, 4993–4997. (b) Yeager, A. R.; Min, G. K.; Porco, J. A.; *et al. Org. Lett.* **2006**, *8*, 5065–5068. (c) Kaiser, N.-F. K.; Bremberg, U.; Larhed, M.; *et al. J. Organomet. Chem.* **2000**, *603*, 2–5. (d) Bremberg, U.; Lutsenko, S.; Kaiser, N.-F. K.; *et al. Synthesis* **2000**, 1004–1008. (e) Kaiser, N.-F. K.; Bremberg, U.; *et al. Angew. Chem. Int. Ed.* **2000**, *39*, 3596–3598. (f) Belda, O.; Kaiser, N.-F. K.; Bremberg, U. *J. Org. Chem.* **2000**, 5868–5870. (g) Belda, O.; Moberg, C. *Synthesis* **2002**, 1601–1606.
103. Trost, B. M.; Andersen, N. G. *J. Am. Chem. Soc.* **2002**, *124*, 14320–14321.
104. (a) Appukkuttan, P.; Mehta, V. P.; Van der Eycken, E. V. *Chem. Soc. Rev.* **2010**, *39*, 1467–1477. (b) Bougrin, K.; Soufiaoui, M.; Bashiardes, G. Microwaves in cycloadditions. In *Microwaves in Organic Synthesis*, 2nd ed.; Loupy, A., Ed.; Wiley-VCH: Weinheim, **2006**, pp 524–578. (c) de la Hoz, A.; Díaz-Ortiz, A.; Moreno, A.; *et al. Eur. J. Chem.* **2000**, 3659–3673.
105. Majetich, G.; Hicks, R. *J. Microw. Power Electromagn. Energy* **1995**, *30*, 27–45.
106. Loupy, A.; Maurel, F.; Sabatie-Gogova, A. *Tetrahedron* **2004**, *60*, 1683–1691.
107. Herrero, M. A.; Kremsner, J. M.; Kappe, C. O. *J. Org. Chem.* **2008**, *73*, 36–47.
108. Leadbeater, N. E.; Pillsbury, S. J.; Shanahan, E.; Williams, V. A. *Tetrahedron* **2005**, *61*, 3565–3585.
109. Hong, B. C.; Shr, Y. J.; Liao, J. H. *Org. Lett.* **2002**, *4*, 663–666.
110. de Cózar, A.; Millán, M. C.; Cebrián, C.; *et al. Org. Biomol. Chem.* **2010**, *8*, 1000–1009.
111. (a) Juranovic, A.; Kranjc, K.; Polanc, S.; *et al. Monatsh. Chem.* **2012**, *143*, 771–777. (b) Almeida, A. I. S.; Silva, V. L. M.; Silva, A. M. S.; *et al. Synlett* **2012**, 889–892. (c) Fusi, S.; Ferrini, S.; Ponticelli, F. *Tetrahedron Lett.* **2011**, *52*, 6911–6915. (d) Dejmek, M.; Hrebabecky, H.; Sala, M.; *et al. Synthesis* **2011**, 4077–4083. (e) Dong, S.; Cahill, K. J.; Kang, M.-I.; *et al. J. Org. Chem.* **2011**, *76*, 8944–8954. (f) Sarotti, A. M.; Pisano, P. L.; Pellegrinet, S. C. *Org. Biomol. Chem.* **2010**, *8*, 5069–5073. (g) Kissane, M.; Lynch, D.; Chopra, J.; *et al. Org. Biomol. Chem.* **2010**, *8*, 5602–5613.
112. Petronijevic, F.; Timmons, C.; Cuzzupe, A.; *et al. Chem. Commun.* **2009**, 104–106.

113. (a) Ghoshal, A.; Sarkar, A. R.; Kumaran, R. S.; *et al. Tetrahedron Lett.* **2012**, *53*, 1748–1752. (b) Long, S.; Monari, M.; Panunzio, M.; *et al. Eur. J. Org. Chem.* **2011**, 6218–6225. (c) Jha, M.; Guy, S.; Chou, T.-Y. *Tetrahedron Lett.* **2011**, *52*, 4337–4341. (d) Lee, Y. A.; Kim, S.-C. *J. Ind. Eng. Chem.* **2011**, *17*, 401–403.
114. (a) Fordyce, E. A. F.; Morrison, A. J.; Sharp, R. D.; *et al. Tetrahedron* **2010**, *66*, 7192–7197. (b) Kranjc, K.; Kocevar, M. *Synlett* **2008**, 2613–2616. (c) Miklos, F.; Stajer, G.; Fulöp, F. *Lett. Org. Chem.* **2006**, *3*, 915–916. (d) Garrigues, P.; Garrigues, B. *CR Acad. Sci. II C* **1998**, *1*, 545–550. (e) Bortolussi, M.; Bloch, R.; Loupy, A. *J. Chem. Res. S* **1998**, 34–35.
115. (a) Iqbal, M.; Li, Y.; Evans, P. *Tetrahedron* **2004**, *60*, 2531–2538. (b) Eddolls, J. P.; Iqbal, M.; Robert, S. M.; *et al. Tetrahedron* **2004**, *60*, 2539–2550.
116. Adams, H.; Jones, S.; Meijer, A. J. H. M.; *et al. Tetrahedron Asymm.* **2011**, *22*, 1620–1625.
117. Falk, A.; Fiebig, L.; Neudörfl, J.-M.; *et al. Adv. Synth. Catal.* **2011**, *353*, 3357–3362.
118. Langa, F.; de la Cruz, P. Application of Microwave Irradiation in Fullerene and Carbon Nanotube Chemistry. In *Microwaves in Organic Synthesis*, 2nd ed.; Loupy, A., Ed.; Wiley-VCH: Weinheim, **2006**, Vol. 2, Chapter 21; pp 931–958,
119. (a) Young, D. D.; Deiters, A. *Angew. Chem. Int. Ed.* **2007**, *46*, 5187–5190. (b) Zhou, Y.; Porco, J. A.; Snyder, J. K. *Org. Lett.* **2007**, *9*, 393–396. (c) Park, K. H.; Choi, S. Y.; Kim, S. Y.; Chung, Y. K. *Synlett* **2006**, 527–532. (d) Hrdina, R.; Kadlcíková, A.; Valterová, I.; Hodacová, J.; Kotora, M. *Tetrahedron Assym.* **2006**, *17*, 3185–3191.
120. McIver, A.; Young, D. D.; Deiters, A. *Chem. Commun.* **2008**, 4750–4752.
121. Zou, Y.; Young, D. D.; Cruz-Montanez, A.; Deiters, A. *Org. Lett.* **2008**, *10*, 4661.
122. Sripada, L.; Teske, J. A.; Deiters, A. *Org. Biomol. Chem.* **2008**, *6*, 263–265.
123. Young, D. D.; Sripada, L.; Deiters, A. *J Comb. Chem.* **2007**, *9*, 735–738.
124. (a) Garcia, L.; Pla-Quintana, A.; Roglans, A.; *et al. Eur. J. Org. Chem.* **2010**, 3407–3415. (b) Novák, P.; Cíhalová, S.; Otmar, M.; *et al. Tetrahedron* **2008**, *64*, 5200–5207.
125. Shanmugasundaram, M.; Aguirre, A. L.; Leyva, M.; Quan, B.; Martinez, L. E. *Tetrahedron Lett.* **2007**, *48*, 7698–7701.
126. Young, D. D.; Teske, J. A.; Deiters, A. *Synthesis* **2009**, 3785–3790.
127. Dallinger, D.; Irfan, M.; Suljanovic, A.; Kappe, C. O. *J. Org. Chem.* **2010**, *75*, 5278–5288.
128. Saaby, S.; Baxendale, I. R.; Ley, S. V. *Org. Biomol. Chem.* **2005**, *3*, 3365–3368.
129. Muzart, J. *Tetrahedron* **2009**, *65*, 8313–8323.
130. Tymoshenko, D. O. *Mini Rev. Org. Chem.* **2008**, *5*, 85–95.
131. Raner, K. D.; Strauss, C. R.; Trainor, R. W. *J. Org. Chem.* **1995**, *60*, 2456–2460.
132. Bowman, M. D.; Schmink, J. R.; McGowan, C. M.; *et al. Org. Proc. Res. Dev.* **2008**, *12*, 1078–1088.
133. (a) Bruder, M.; Smith, S. J.; Blake, A. J. *Org. Biomol. Chem.* **2009**, *7*, 2127–2134. (b) Bruder, M.; Moody, C. J. *Synlett* **2008**, 575–577.
134. Durand-Reville, T.; Gobbi, L. B.; Gray, B. L.; *et al. Org. Lett.* **2002**, *4*, 3847–3850.
135. Majumdar, K. C.; Bhattacharyya, T.; Chattopadhyay, B.; *et al. Synthesis* **2009**, 2117–2142.
136. (a) Symeonidis, T. S.; Kallitsakis, M. G.; Litinas, K. E. *Tetrahedron Lett.* **2011**, *52*, 5452–5455. (b) El Ashry, E. S. H.; El Tamany, E. S. H.; El Fattah, M. E. D. A.; *et al. Lett. Org. Chem.* **2009**, *6*, 462–469. (c) Gonda, J.; Martinkova, M.; Zadrosova, A.; *et al. Tetrahedron Lett.* **2007**, *48*, 6912–6915.
137. Martinkova, M.; Gonda, J.; Uhrikova, A.; *et al. Carbohydrate Res.* **2012**, *352*, 23–36.
138. Lloyd-Jones, G. C.; Moseley, J. D.; Renny, J. S. *Synthesis* **2008**, 661–689.
139. Dallinger, D.; Lehmann, H.; Moseley, J. D.; *et al. Org. Proc. Res. Dev.* **2011**, *15*, 841–854.
140. Lehmann, H.; LaVecchia, L. *Org. Proc. Res. Dev.* **2010**, *14*, 650–656.
141. Moseley, J. D.; Lenden, P.; Lockwood, M.; *et al. Org. Proc. Res. Dev.* **2008**, *12*, 30–40.
142. Moseley, J. D.; Sankey, R. F.; Tang, O. N.; *et al. Tetrahedron* **2006**, *62*, 4685–4689.
143. Moseley, J. D.; Lenden, P. *Tetrahedron* **2007**, *63*, 4120–4125.
144. Gilday, J. P.; Lenden, P.; Moseley, J. D.; *et al. J. Org. Chem.* **2008**, *73*, 3130–3134.
145. Burns, M.; Lloyd-Jones, G. C.; Moseley, J. D.; *et al. J. Org. Chem.* **2010**, *75*, 6347–6353.
146. Kanno, M.; Nakamura, K.; Kanai, E.; *et al. J. Phys. Chem. A* **2012**, *116*, 2177–2183.
147. (a) Martinez-Palou, R. *Mol. Divers.* **2010**, *14*, 3–35. (b) Leadbeater, N. E.; Torenius, H. M. Microwaves and Ionic Liquids. In *Microwaves in Organic Synthesis*, 2nd ed.; Loupy, A., Ed.; Wiley-VCH: Weinheim, **2006**, Vol. 1, Chapter 7; pp 327–361. (c) Leadbeater, N. E.; Torenius, H. M.; Tye, H. *Comb. Chem. High T. Scr.* **2004**, *7*, 511–528.
148. Leadbeater, N. E.; Torenius, H. M. *J. Org. Chem.* **2002**, *67*, 3145–3148.
149. Baxendale, I. R.; Lee, A.-l.; Ley, S. V. *J. Chem. Soc. Perkin Trans. 1* **2002**, 1850–1857.
150. (a) Brummond, K. M.; Chen, D. *Org. Lett.* **2005**, *7*, 3473–3475. (b) Hoffman, J.; Nüchter, M.; Ondruschka, B.; Wasserscheid, P. *Green Chem.* **2003**, *5*, 296–299. (c) Van der Eycken, E.; Appukkuttan, P.; De Borggraeve, W.; *et al. J. Org Chem.* **2002**, *67*, 7904–7907.
151. Obermayer, D.; Kappe, C. O. *Org. Biomol. Chem.* **2010**, *8*, 114–121.
152. Kremsner, J. M.; Kappe, C. O. Silicon Carbide. In *Encyclopedia of Reagents for Organic Synthesis II*; Paquette, L. A., Ed.; John Wiley & Sons: Chicester, UK, **2009**, Vol. 11, pp 8659–8661.
153. Kremsner, J. M.; Kappe, C. O. *J. Org. Chem.* **2006**, *71*, 4651–4658.
154. Gutmann, B.; Obermayer, D.; Reichart, B.; *et al. Chem. Eur. J.* **2010**, *40*, 12182–12194.
155. Obermayer, D.; Gutmann, B.; Kappe, C. O. *Angew. Chem. Int. Ed.* **2009**, *48*, 8321–8324.
156. Kappe, C. O.; Damm, M. *Mol. Divers.* **2012**, *16*, 5–25.
157. Besson, T.; Thiéry, V.; Dubac, J. Microwave-assisted Reactions on Graphite. In *Microwaves in Organic Synthesis*, 2nd ed.; Loupy, A., Ed.; Wiley-VCH: Weinheim, **2006**, Vol. 1, Chapter 9; pp 455–476,
158. (a) Laporte, C.; Oussaid, A.; Garrigues, B. C. *CR Acad. Sci. II C* **2000**, *3*, 321–325. (b) Garrigues, P.; Garrigues, B. *CR Acad. Sci. II C* **1998**, *1*, 545–550. (b) Garrigues, B.; Laporte, C.; Laurent, R.; *et al. Liebigs Ann.* **1996**, 739–741.
159. Cho, H. Y.; Ajaz, A.; Himali, D.; *et al. J. Org. Chem.* **2009**, *74*, 4137–4142.
160. Bazureau, J. P.; Hamelin, J.; Mongin, F.; Texier-Boullet, F. Microwaves in Heterocyclic Chemistry. In *Microwaves in Organic Synthesis*, 2nd ed.; Loupy, A., Ed.; Wiley-VCH: Weinheim, **2006**, Vol. 1, Chapter 9; pp 456–523,
161. van der Eycken, E., Kappe, C. O., Eds. *Microwave-Assisted Synthesis of Heterocycles Topics in Heterocyclic Chemistry*; Springer: Berlin, **2006**, Vol. 1.
162. (a) Srinivasan, K. V.; Chaskar, P. K.; Dighe, S. N.; *et al. Heterocycles* **2011**, *83*, 2451–2488. (b) Mehta, V. P.; Appukkuttan, P.; Van der Eycken, E. *Curr. Org. Chem.* **2011**, *15*, 265–283. (c) Kranjc, K.; Kocevar, M. *Curr. Org. Chem.* **2010**, *14*, 1050–1074. (d) Polshettiwar, V.; Varma, R. S. *Curr. Opin. Drug Discovery Dev.* **2007**, *10*, 723–737.
163. (a) Deshpande, S. J.; Leger, P. R.; Sieck, S. R. *Tetrahedron Lett.* **2012**, *53*, 1772–1775. (b) Ghosh, S.; Das, J.; Chattopadhyay, S. *Tetrahedron Lett.* **2011**, *52*, 2869–2872. (c) Crecente-Campo, J.; Pilar Vazquez-Tato, M.; Seijas, J. A. *Eur. J. Org. Chem.* **2010**, 4130–4135. (d) Peng, Y. Q.; Song, G. H. *Green Chem.* **2003**, *5*, 704–706.
164. (a) Staderini, M.; Cabezas, N.; Bolognesi, M. L.; *et al. Synlett* **2012**, 2577–2579. (b) Sharma, L. K.; Kim, K. B.; Elliott, G. I. *Green Chem.* **2011**, *13*, 1546–1549. (c) Schramm, O. G.; Müller, T. J. J. *Synlett* **2006**, 1841–1846. (d) Jung, M. E.; Maderna, A. *Tetrahedron Lett.* **2005**, *46*, 5057–5061.

165. (a) Zhou, Z.-Z.; Deng, Y.-H.; Jiang, Z.-H.; *et al. Adv. Synth. Catal.* **2010**, *352*, 1909–1913. (b) Yougnia, R.; Rochais, C.; de Oliveira Santos, J. S.; *et al. Tetrahedron* **2010**, *66*, 2803–2808. (c) Rochais, C.; Yougnia, R.; Dallemagne, P.; *et al. Tetrahedron Lett.* **2009**, *50*, 5704–5708. (d) Fustero, S.; Sanchez-Rosello, M.; Luis Acena, J.; *et al. J. Org. Chem.* **2009**, *74*, 3414–3423.
166. Meng, L.; Fettinger, J. C.; Kurth, M. J. *Org. Lett.* **2007**, *9*, 5055–5058.
167. (a) Altman, E.; Stefanidis, G. D.; van Gerven, T.; *et al. Ind. Eng. Chem. Res.* **2012**, *51*, 1612–1619. (b) Keglevich, G.; Kiss, N. Z.; Mucsi, Z.; *et al. Org. Biomol. Chem.* **2012**, *10*, 2011–2018. (c) Devine, W. G.; Leadbeater, N. E.; Jacob, L. A. *Future Med. Chem.* **2008**, *2*, 225–230.
168. (a) Melo Junior, C. A. R.; Albuquerque, C. E. R.; Carneiro, J. S. A.; *et al. Ind. Eng. Chem. Res.* **2010**, *49*, 12135–12139. (b) Zhang, S.; Zu, Y.-G.; Fu, Y.-J.; *et al. Bioresource Technol.* **2010**, *101*, 931–936.
169. Leadbeater, N. E.; Stencel, L. M. *Energy Fuels* **2006**, *20*, 2281–2283.
170. (a) Chen, K.-S.; Lin, Y.-C.; Hsu, K.-H.; *et al. Energy* **2012**, *38*, 151–156. (b) Koberg, M.; Abu-Much, R.; Gedanken, A. *Bioresource Technol.* **2011**, *102*, 1073–1078.
171. Barnard, T. M.; Leadbeater, N. E.; Boucher, M. B.; *et al. Energy Fuels* **2007**, *21*, 1777–1781.
172. Geuens, J.; Kremsner, J. M.; Nebel, B. A.; *et al. Energy Fuels* **2008**, *22*, 643–645.
173. Leadbeater, N. E.; Barnard, T. M.; Stencel, L. M. *Energy Fuels* **2008**, *22*, 2005–2008.
174. Su, Q.; Beeler, A. B.; Lobkovsky, E.; *et al. Org. Lett.* **2003**, *5*, 2149–2152.
175. Baghbanzadeh, M.; Kappe, C. O. *Aust. J. Chem.* **2009**, *62*, 244–249.
176. (a) Veillet, S.; Tomao, V.; Visinoni, F.; *et al. Anal. Chim. Acta* **2009**, *632*, 203–207. (b) Filippi, J.-J.; Dunach, E.; Fernandez, X.; *et al. Tetrahedron* **2008**, *64*, 9999–10003. (c) Lukacs, G.; Porcs-Makkay, M.; Komaromi, A.; *et al. Arkivoc* **2008**, (iii), 17–24. (d) Vo-Tanh, G.; Lahrache, H.; Loupy, A.; *et al. Tetrahedron* **2004**, *60*, 5539–5543.
177. (a) Altman, E.; Stefanidis, G. D.; van Gerven, T.; *et al. Ind. Eng. Chem. Res.* **2010**, *49*, 10287–10296. (b) Razzaq, T.; Kappe, C. O. *Tetrahedron Lett.* **2007**, *48*, 2513–2517.
178. Bowman, M. D.; Holcomb, J. L.; Kormos, C. M.; *et al. Org. Proc. Res. Dev.* **2008**, *12*, 41–57.
179. Guerrero-Sanchez, C.; Lobert, M.; Hoogenboom, R.; Schubert, U. S. *Macromol. Rapid Commun.* **2007**, *28*, 456–464.
180. (a) Chemat, F.; Lucchesi, M.-E. Microwave-assisted Extraction of Essential Oils. In *Microwaves in Organic Synthesis*, 2nd ed.; Loupy, A., Ed.; Wiley-VCH: Weinheim, **2006**, Vol. 2, Chapter 22; pp 959–985. (b) Raynie, D. E. *Anal. Chem.* **2010**, *82*, 4911–4916.
181. (a) Kahriman, N.; Tosun, G.; Iskender, N.; Yilmaz; *et al. Nat. Prod. Res.* **2012**, *26*, 703–712. (b) Gunes, M.; Alma, M. H. *IEEE T Instrum. Meas.* **2010**, *59*, 2243–2245. (c) Sahraoui, N.; Vian, M. A.; Bornard, I.; *et al. J. Chromatogr. A* **2008**, *1210*, 229–233. (d) Virot, M.; Tomao, V.; Ginies, C.; *et al. J. Chromatogr. A* **2008**, *1196*, 147–152.
182. (a) Chebanov, V. A.; Desenko, S. M. *Chem. Heterocycl. Compd.* **2012**, *48*, 566–583. (b) Eckert, H. *Molecules* **2012**, *17*, 1074–1102. (c) Kruithof, A.; Ruijter, E.; Orru, R. V. A. *Curr. Org. Chem.* **2011**, *15*, 204–236. (d) Jiang, B.; Shi, F.; Tu, S.-J. *Curr. Org. Chem.* **2010**, *14*, 357–378. (e) Hugel, H. M. *Molecules* **2009**, *14*, 4936–4972. (f) Bagley, M. C.; Lubinu, M. C. *Top. Heterocycl. Chem.* **2006**, *1*, 31–58. (g) de Boer, T.; Amore, A.; Orru, R. V. A. Multicomponent Reactions Under Microwave Irradiation Conditions. In *Microwaves in Organic Synthesis*, 2nd ed.; Loupy, A., Ed.; Wiley-VCH: Weinheim, **2006**, Vol. 2, Chapter 17; pp 788–819,
183. (a) Singh, K.; Singh, K. *Adv. Heterocycl. Chem.* **2012**, *105*, 223–308. (b) Panda, S. S.; Khanna, P.; Khanna, L. *Curr. Org. Chem.* **2012**, *16*, 507–520. (c) Kappe, C. O. *QSAR Comb. Sci.* **2003**, *22*, 630–645.
184. (a) Mukhopadhyay, C.; Datta, A.; Banik, B. K. *J. Heterocycl. Chem.* **2011**, *44*, 979–981. (b) Fang, Z.; Lam, Y. *Tetrahedron* **2011**, *67*, 1294–1297. (c) Dallinger, D.; Kappe, C. O. *Nat. Protoc.* **2007**, *2*, 317–321.
185. Stadler, A.; Kappe, C. O. *J. Comb. Chem.* **2001**, *3*, 624–630.
186. (a) Saini, A.; Kumar, S.; Sandhu, J. S. *J. Sci. Ind. Res.* **2008**, *67*, 95–111. (b) Eynde, J. J. V.; Mayence, A. *Molecules* **2003**, *8*, 381–391.
187. Kormos, C. M.; Hull, R. M.; Leadbeater, N. E. *Aust. J. Chem.* **2009**, *62*, 51–57.
188. Ohberg, L.; Westman, J. *Synlett* **2001**, 1296–1298.
189. Dai, W.-M.; Shi *J. Comb. Chem. High Throughput Screen.* **2007**, *10*, 837–856.
190. Evans, C. G.; Smith, M. C.; Carolan, J. P.; *et al. Bioorg. Med. Chem. Lett.* **2011**, *21*, 2587–2590.
191. (a) Moore, K. W.; Pechen, A.; Feng, X.-J.; *et al. Phys. Chem. Chem. Phys.* **2011**, *13*, 10048–10070. (b) O'Brien, M.; Denton, R.; Ley, S. V. *Synthesis* **2011**, 1157–1192. (c) Tye, H. *Drug Discov. Today* **2004**, *9*, 485–491.
192. Glasnov, T. N.; Tye, H.; Kappe, C. O. *Tetrahedron* **2008**, *64*, 2035–2041.
193. Tye, H.; Whittaker, M. *Org. Biomol. Chem.* **2004**, *2*, 813–815.
194. (a) Gopalsamy, A.; Shi, M.; Nilakantan, R. *Org. Proc. Res. Dev.* **2007**, *11*, 450–453. (b) Sarotti, A. M.; Spanevello, R. A.; Suárez, A. G. *Green Chem.* **2007**, *9*, 1137–1140. (c) McLean, N. J.; Tye, H.; Whittaker, M. *Tetrahedron Lett.* **2004**, *45*, 993–995. (d) Evans, M. D.; Ring, J.; Schoen, A.; *et al. Tetrahedron Lett.* **2003**, *44*, 9337–9341.
195. Tanaka, K.; Kaupp, G. *Solvent-free Organic Synthesis*; Wiley-VCH: Weinheim, **2009**.
196. (a) Baig, R. B. N.; Varma, R. S. *Chem. Soc. Rev.* **2012**, *41*, 1559–1584. (b) Polshettiwar, V.; Varma, R. S. Environmentally Benign Chemical Synthesis via Mechanochemical Mixing and Microwave Irradiation. In *Eco-Friendly Synthesis of Fine Chemicals*; Ballini, R., Ed.; Royal Society of Chemistry: Cambridge, **2009**, Chapter 8; pp 275–292.
197. Polshettiwar, V.; Varma, R. S. *Acc. Chem. Res.* **2008**, *41*, 629–639.
198. (a) Varma, R. S.; Ju, Y. Organic Synthesis using Microwaves and Supported Reagents. In *Microwaves in Organic Synthesis*, 2nd ed.; Loupy, A., Ed.; Wiley-VCH: Weinheim, **2006**, Vol. 1, Chapter 8; pp 362–415. (b) Varma, R. S. *Green Chem.* **1999**, *1*, 43–55. (c) Loupy, A.; Petit, A.; Hamelin, J.; *et al. Synthesis* **1998**, 1213–1234.
199. Varma, R. S.; Dahiya, R.; Kumar, S. *Tetrahedron Lett.* **1997**, *38*, 2039–2042.
200. Cotterill, I. C.; Usyatinsky, A. Y.; Arnold, J. M.; *et al. Tetrahedron Lett.* **1998**, *39*, 1117–1120.
201. Varma, R. S.; Kumar, D. *Tetrahedron Lett.* **1999**, *40*, 7665–7669.
202. Williams, L. *Chem. Commun.* **2000**, 435–436.
203. (a) Kidwai, M.; Saxena, S.; Mohan, R. *J. Heterocycl. Chem.* **2005**, *42*, 703–705. (b) Williams, L.; Sjovik, R.; Falck-Pedersen, M. L. *J. Planar Chromatogr.-Mod. TLC* **2004**, *17*, 244–249. (c) Williams, L.; Bergersen, O. *J. Planar Chromatogr.-Mod. TLC* **2001**, *14*, 318–321.
204. (a) Caceres-Castillo, D.; Carballo, R. M.; Tzec-Interian, J. A.; *et al. Tetrahedron Lett.* **2012**, *53*, 3934–3936. (b) Collados, J. F.; Toledano, E.; Guijarro, D.; *et al. J. Org. Chem.* **2012**, *77*, 5744–5750. (c) Yin, G.; Liu, Q.; Maa, J.; *et al. Green Chem.* **2012**, *14*, 1796–1798. (d) Dejmek, M.; Hrebabecky, H.; Sala, M.; *et al. Synthesis* **2011**, 4077–4083. (e) Matteo, C.; Nieves, B.; Maria, L.; *et al. Synlett* **2011**, 2577–2579.
205. Manhas, M. S.; Ganguly, S. N.; Mukherjee, S.; Jain, A. K.; Bose, A. K. *Tetrahedron Lett.* **2006**, *47*, 2423–2425.
206. (a) List, B., Ed.*Asymmetric Organocatalysis Topics in Current Chemistry Series*; Springer: Berlin, **2012**. (b) Berkessel, A.; Gröger, H. *Asymmetric Organocatalysis: From Biomimetic Concepts to Applications in Asymmetric Synthesis*; Wiley-VCH: Weinheim, **2005**.
207. Song, C. E., Ed. *Cinchona Alkaloids in Synthesis and Catalysis*; Wiley-VCH: Weinheim, **2009**.
208. Bruckmann, A.; Krebs, A.; Bolm, C. *Green Chem.* **2008**, *10*, 1131–1141.
209. (a) Westermann, B.; Neuhaus, C. *Angew. Chem. Int. Ed.* **2005**, *44*, 4077–4079. (b) Rodríguez, B.; Bolm, C. *J. Org. Chem.* **2006**, *71*, 2888–2891.
210. Mossé, S.; Alexakis, A. *Org. Lett.* **2006**, *16*, 3577–3580.
211. Hagiwara, H.; Inotsume, S.; Fukushima, M.; *et al. Chem. Lett.* **2006**, *35*, 926–927.
212. Octavio, R.; de Souza, M. A.; Vasconcellos, M. L. A. A. *Synth. Commun.* **2003**, *33*, 1383–1389.
213. (a) Massi, A.; Dondoni, A. *Angew. Chem. Int. Ed.* **2008**, *47*, 4638–4660. (b) Massi, A.; Nuzzi, A.; Dondoni, A. *J. Org. Chem.* **2007**, *72*, 10279–10282.
214. Hosseini, M.; Stiasni, N.; Barbieri, V.; *et al. J. Org. Chem.* **2007**, *72*, 1417–1424.

215. List, B.; Lerner, R.; Barbas, C. F. *J. Am. Chem. Soc.* **2000**, *112*, 2395–2396.
216. Russo, A.; Leadbeater, N. E.; Lattanzi, A. *Lett. Org. Chem.* **2010**, *7*, 98–102.
217. Petricci, E.; Taddei, M. *Chemistry Today* **2008**, *26*, 18–22.
218. (a) Nandy, S. K.; Liu, J.; Padmapriya, A. A. *Tetrahedron Lett.* **2008**, *49*, 2469–2471. (b) Srinivasa, G. R.; Babu, S. N. N.; Lakshmi, C.; *et al. Synth. Commun.* **2004**, *34*, 1831–1837. (c) Danks, T. N.; Desai, B. *Green Chem.* **2002**, *4*, 179–180.
219. (a) Rao, H. S. P.; Jothilingam, S.; Scheeren, H. W. *Tetrahedron* **2004**, *60*, 1625–1630. (b) Rao, H. S. P.; Jothilingam, S. *Tetrahedron Lett.* **2001**, *42*, 6595–6597.
220. (a) Odell, R.; Russo, F.; Larhed, M. *Synlett* **2012**, 685–698. (b) Wannberg, J.; Ersmark, K.; Larhed, M. *Top. Curr. Chem.* **2006**, *266*, 103–144.
221. Georgsson, J.; Hallberg, A.; Larhed, M. *J. Comb. Chem.* **2003**, *5*, 350–352.
222. (a) Wieckowska, A.; Fransson, R.; Odell, L. R.; Larhed, M. *J. Org. Chem.* **2011**, *76*, 978–981. (b) Lagerlund, O.; Mantel, M. L. H.; Larhed, M. *Tetrahedron* **2009**, *65*, 7646–7652. (c) Begouin, A.; Queiroz, M.-J. R. P. *Eur. J. Org. Chem.* **2009**, 2820–2827. (d) Odell, L. R.; Sävmarker, J.; Larhed, M. *Tetrahedron Lett.* **2008**, *49*, 6115–6118. (e) Letavic, M. A.; Ly, K. S. *Tetrahedron Lett.* **2007**, *48*, 2339–2343. (f) Wu, X.; Wannberg, J.; Larhed, M. *Tetrahedron* **2006**, *62*, 4665–4670. (g) Wu, X.; Larhed, M. *Org. Lett.* **2005**, *7*, 3327–3329. (h) Kaiser, N. F. K.; Hallberg, A.; Larhed, M. *J. Comb. Chem.* **2002**, *4*, 109–111.
223. Wannberg, J.; Larhed, M. *J. Org. Chem.* **2003**, *68*, 5750–5753.
224. (a) Jafarpour, F.; Rashidi-Ranjbar, P.; Kashani, A. O. *Eur. J. Org. Chem.* **2011**, 2128–2132. (b) Lindh, J.; Fardost, A.; Almeida, M.; *et al. Tetrahedron Lett.* **2010**, *51*, 2470–2472. (c) Sävmarker, J.; Lindh, J.; Nilsson, P. *Tetrahedron Lett.* **2010**, *51*, 6886–6889. (d) Stonehouse, J. P.; Chekmarev, D. S.; Ivanova, N. V.; *et al. Synlett* **2008**, 100–104. (e) Karpov, A. S.; Merkul, E.; Rominger, F.; Müller, T. J. J. *Angew. Chem. Int. Ed.* **2005**, *44*, 6951–6956.
225. (a) Roberts, B.; Liptrot, D.; Luker, T.; *et al. Tetrahedron Lett.* **2011**, *52*, 3793–3796. (b) Ren, W.; Emi, A.; Yamane, M. *Synthesis* **2011**, 2303–2309. (c) Ren, W.; Yamane, M. *J. Org. Chem.* **2010**, *75*, 3017–3020. (d) Ren, W.; Yamane, M. *J. Org. Chem.* **2010**, *75*, 8410–8415.
226. Roberts, B.; Liptrot, D.; Alcaraz, L.; *et al. Org. Lett.* **2010**, *12*, 4280–4283.
227. Enquist, P. A.; Nilsson, P.; Larhed, M. *Org. Lett.* **2003**, *5*, 4875–4878.
228. Enquist, P. A.; Nilsson, P.; Edin, J.; *et al. Tetrahedron Lett.* **2005**, *46*, 3335–3339.
229. Farhi, M.; Morel, M.; Cavigneaux, A. *Cahier de notes documentaires* **1968**, *50*, 91–93.
230. Wan, Y. Q.; Alterman, M.; Larhed, M.; *et al. J. Org. Chem.* **2002**, *67*, 6232–6235.
231. Wan, Y. Q.; Alterman, M.; Larhed, M.; *et al. J. Comb. Chem.* **2003**, *5*, 82–84.
232. Cini, E.; Airiau, E.; Girard, N.; *et al. Synlett* **2011**, 199–202.
233. Milijanić, O. Š.; Vollhardt, P. C.; Whitener, G. D. *Synlett* **2003**, 29–34.
234. Erdélyi, M.; Gogoll, A. *J. Org. Chem.* **2003**, *68*, 6431–6434.
235. Castagnolo, D.; Renzulli, M. L.; Galletti, E.; *et al. Tetrahedron Asym.* **2005**, *16*, 2893–2896.
236. (a) Schmöger, C.; Gallert, T.; Stolle, A.; *et al. Chem. Eng. Technol.* **2011**, *34*, 445–451. (b) Vanier, G. S. *Synlett* **2007**, 131–135. (c) Heller, E.; Lautenschläger, W.; Holzgrabe, U. *Tetrahedron Lett.* **2005**, *46*, 1247–1249.
237. Kennedy, D. P.; Kormos, C. M.; Burdette, S. C. *J. Am. Chem. Soc.* **2009**, *131*, 8578–8586.
238. Piras, L.; Genesio, E.; Ghiron, C.; *et al. Synlett* **2008**, *8*, 1125–1128.
239. Kaval, N.; Dehaen, W.; Kappe, C. O.; *et al. Org. Biomol. Chem.* **2004**, *2*, 154–156.
240. Kormos, C. M.; Leadbeater, N. E. *J. Org. Chem.* **2008**, *73*, 3854–3858.
241. Kormos, C. M.; Leadbeater, N. E. *Synlett* **2006**, 1663–1666.
242. Kormos, C. M.; Leadbeater, N. E. *Org. Biomol. Chem.* **2007**, 65–68.
243. (a) Pizzetti, M.; Russo, A.; Petricci, E. *Chem. Eur. J.* **2011**, *17*, 4523–4528. (b) Salvadori, J.; Balducci, E.; Zaza, S.; *et al. J. Org. Chem.* **2010**, *75*, 1841–1847. (c) Cardullo, F.; Donati, D.; Merlo, G.; *et al. Synlett* **2009**, 47–50.
244. Kormos, C. M.; Leadbeater, N. E. *Synlett* **2007**, 2006–2010.
245. Petricci, E.; Mann, A.; Schoenfelder, A.; *et al. Org. Lett.* **2006**, *8*, 3725–3727.
246. Airiau, E.; Chemin, C.; Girard, N.; *et al. Synthesis* **2010**, 2901–2914.
247. Airiau, E.; Spangenberg, T.; Girard, N.; *et al. Chem. Eur. J.* **2008**, *14*, 10938–10948.
248. Andappan, M. M. S.; Nilsson, P.; von Schenck, H.; Larhed, M. *J. Org. Chem.* **2004**, *69*, 5212.
249. Kormos, C. M.; Hull, R. M.; Leadbeater, N. E. *Aust. J. Chem.* **2009**, *62*, 51–57.
250. (a) Hruda, R.M.; De Haven, H.E. US Pat. US 3,826,950, **1974**. (b) Wilkinson, P. G.; Tanaka, Y. *J. Opt. Soc. Am.* **1955**, *45*, 344–349.
251. (a) Horikoshi, S.; Miura, T.; Kajitani, M.; *et al. Photochem. Photobiol. Sci.* **2008**, *7*, 303–310. (b) Církva, V.; Vlková, L.; Relich, S.; *et al. J. Photochem. Photobiol. A* **2006**, *179*, 229–233. (c) Müller, P.; Klán, P.; Církva, V. *J. Photochem. Photobiol. A* **2005**, *171*, 51–60.
252. (a) Serpone, N.; Horikoshi, S.; Emeline, A. V. *J. Photochem. Photobiol. C* **2010**, *11*, 114–131. (b) Horikoshi, S.; Serpone, N. *J. Photochem. Photobiol. C* **2009**, *10*, 96–110.
253. (a) Církva, V.; Relich, S. *Mini Rev. Org. Chem.* **2011**, *8*, 282–293. (b) Klán, P. Microwaves in Photochemistry. In *Microwaves in Organic Synthesis*, 2nd ed.; Loupy, A., Ed.; Wiley-VCH: Weinheim, **2006**, Vol. 2, Chapter 19; pp 860–897,
254. (a) Müller, P.; Loupy, A.; Klán, P. *J. Photochem. Photobiol. A* **2005**, *172*, 146–150. (b) Müller, P.; Klán, P.; Církva, V. *J. Photochem. Photobiol. A* **2005**, *171*, 51–57. (c) Klán, P.; Ruzicka, R.; Heger, D.; *et al. Photochem. Photobiol. Sci.* **2002**, *1*, 101–110. Nüchter, M.; Ondruschka, B.; Jungnickel, A.; *et al. J. Phys. Org. Chem.* **2000**, *13*, 579–586.
255. Terrett, N. K. *Combinatorial Chemistry*; Oxford University Press: Oxford, **1998**.
256. (a) Matloobi, M.; Kappe, C. O. *Chemistry Today* **2007**, *25*, 26–31. (b) Stadler, A.; Kappe, C. O. Microwave-assisted Combinatorial and High-Throughput Synthesis. In *Microwaves in Organic Synthesis*, 2nd ed.; Loupy, A., Ed.; Wiley-VCH: Weinheim, **2006**, Vol. 2, Chapter 16; pp 726–787. (c) Martínez-Palou, R. *Mol. Divers.* **2006**, *10*, 435–462.
257. Blackwell, H. E. *Org. Biomol. Chem.* **2003**, *1*, 1251–1255.
258. Dörwald, F. Z. *Organic Synthesis on Solid Phase: Supports, Linkers, Reactions*; Wiley-VCH: Weinheim, **2002**.
259. Kappe, C. O.; Dallinger, D. *Nat. Rev. Drug Discov.* **2006**, *5*, 51–63.
260. Kappe, C. O.; Matloobi, M. *Comb. Chem. High T. Scr.* **2007**, *10*, 735–750.
261. Kappe, C. O.; Damm, M. *Mol Divers.* **2012**, *16*, 5–25.
262. Kremsner, J. M.; Stadler, A.; Kappe, C. O. *J. Comb. Chem.* **2007**, *9*, 285–291.
263. (a) Damm, M.; Kappe, C. O. *J. Comb. Chem.* **2009**, *11*, 460–468. (b) Treu, M.; Karner, T.; Kousek, R.; *et al. J. Comb. Chem.* **2008**, *10*, 863–868.
264. Damm, M.; Kappe, C. O. *Mol. Divers.* **2009**, *13*, 529–543.
265. Stencel, L. M.; Kormos, C. M.; Avery, K. B.; *et al. Org. Biomol. Chem.* **2009**, *7*, 2452–2457.
266. Damm, M.; Kappe, C. O. *Anal. Chim. Acta.* **2011**, *707*, 76–83.
267. Prekodravac, B.; Damm, M.; Kappe, C. O. *J. Pharm. Biomed. Anal.* **2011**, *56*, 867–873.
268. Damm, M.; Holzer, M.; Radspieler, G.; *et al. J. Chromatogr. A* **2010**, *1217*, 7826–7832.
269. Merrifield, R. B. *J. Am. Chem. Soc.* **1963**, *85*, 2149–2154.
270. (a) O'Neill, J. C.; Blackwell, H. E. *Comb. Chem. High T. Scr.* **2007**, *10*, 857–876. (b) Dai, W. M.; Shi, J. *Comb. Chem. High T. Scr.* **2007**, *10*, 837–856.
271. Lew, A.; Krutzik, P. O.; Hart, M. E.; *et al. J. Comb. Chem.* **2002**, *4*, 95–105.

272. Pérez, R.; Beryozkina, T.; Zbruyev, O. I.; *et al. J. Comb. Chem.* **2002**, *4*, 501–510.
273. (a) Frei, R.; Breitbach, A. S.; Blackwell, H. E. *Chem. Sci.* **2012**, *3*, 1555–1561. (b) Frei, R.; Blackwell, H. E. *Chem. Eur. J.* **2010**, *16*, 2692–2695. (c) Volkmer, R. *ChemBioChem* **2009**, *10*, 1431–1442.
274. (a) Obermeier, B.; Wurm, F.; Mangold, C.; *et al. Angew. Chem. Int. Ed.* **2011**, *50*, 7988–7997. (b) Bergbreiter, D. E.; Tian, J.; Hongfa, C. *Chem. Rev.* **2009**, *109*, 530–582. (c) Dickerson, T. J.; Reed, N. N.; Janda, K. D. *Chem. Rev.* **2002**, *102*, 3325–3344.
275. (a) Cerezo, V.; Amblard, M.; Martinez, J.; *et al. Tetrahedron* **2008**, *64*, 10538–10545. (b) Tsukamoto, H.; Suzuki, R.; Kondo, Y. *J. Comb. Chem.* **2006**, *8*, 289–292. (c) Kaval, N.; Dehaen, W.; Van der Eycken, E. *J. Comb. Chem.* **2005**, *7*, 90–95.
276. Tullberg, M.; Luthman, K.; Grøtli, M. *J. Comb. Chem.* **2006**, *8*, 915–922. (b) Henkel, B. *Tetrahedron Lett.* **2004**, *45*, 2219–2221. (c) Frutos Hoener, A. P.; Henkel, B.; Gauvin, J.-C. *Synlett* **2003**, 63–66. Cotterill, I. C.; Usyatinsky, A. Y.; Arnold, J. M.; *et al. Tetrahedron Lett.* **1998**, *39*, 1117–1120.
277. (a) Schobert, R.; Jagusch, C. *Tetrahedron Lett.* **2003**, *44*, 6449–6451. (b) Kumar, H. M. S.; Anjaneyulu, S.; Reddy, B. V. S. *Synlett* **2000**, 1129–1130.
278. Feliu, L.; Vera-Luque, P.; Albericio, F.; *et al. J. Comb. Chem.* **2007**, *9*, 521–565.
279. Leonetti, F.; Capaldi, C.; Carotti, A. *Tetrahedron Lett.* **2007**, *47*, 3455–3458.
280. Blackwell, H. E. *Curr. Opin. Chem. Biol.* **2006**, *10*, 203–212.
281. (a) Bowman, M. D.; Jacobson, M. M.; Pujanauski, B. G.; *et al. Tetrahedron* **2006**, *62*, 4715–4727. (b) Bowman, M. D.; Jeske, R. C.; Blackwell, H. E. *Org. Lett.* **2004**, *6*, 2019–2022.
282. Bowman, M. D.; Jacobson, M. M.; Blackwell, H. E. *Org. Lett.* **2006**, *8*, 1645–1648.
283. (a) Wiles, C.; Watts, P. *Micro Reaction Technology in Organic Synthesis*; CRC Press: Boca Raton, **2011**. (b) Luis, S. V., Garcia-Verdugo, E., Eds. *Chemical Reactions and Processes Under Flow Conditions*; Royal Society of Chemistry: Cambridge, **2010**.
284. (a) Wiles, C.; Watts, P. *Chem. Comm.* **2011**, *47*, 6512–6535. (b) Wegner, J.; Ceylan, S.; Kirschning, A. *Chem. Comm.* **2011**, *47*, 4583–4592. (c) Mark, D.; Haeberle, S.; Roth, G.; von Stetten, F.; Zengerle, R. *Chem. Soc. Rev.* **2010**, *39*, 1153–1182.
285. Wegner, J.; Ceylan, S.; Kirschning, A. *Adv. Synth. Catal. 354*, 17–57.
286. Comer, E.; Organ, M. G. *J. Am. Chem. Soc.* **2005**, *127*, 8160–8167.
287. Comer, E.; Organ, M. G. *Chem. Eur. J.* **2005**, *11*, 7223–7227.
288. Shore, G.; Organ, M. G. *Chem. Eur. J.* **2008**, *14*, 9641–9646.
289. Zang, Q.; Javed, S.; Ullah, F.; *et al. Synthesis* **2011**, 2743–2750.
290. Painter, T. O.; Thornton, P. D.; Orestano, M.; *et al. Chem. Eur. J.* **2011**, *17*, 9595–9598.
291. Bremner, W. S.; Organ, M. G. *J. Comb. Chem.* **2007**, *9*, 14–16.
292. Shore, G.; Morin, S.; Organ, M. G. *Angew. Chem. Int. Ed.* **2006**, *45*, 2761–2766.
293. Shore, G.; Organ, M. G. *Chem. Commun.* **2008**, 838–840.
294. Shore, G.; Tsimerman, M.; Organ, M. G. *Beilstein J. Org. Chem.* **2009**, *5*. No. 35.
295. Shore, G.; Yoo, W.-J.; Li, C.-J.; *et al. Chem. Eur. J.* **2010**, *16*, 126–133.
296. He, P.; Haswell, S. J.; Fletcher, P. D. I. *Appl. Catal. A* **2004**, *274*, 111–114.
297. Mennecke, K.; Cecilia, R.; Glasnov, T. N.; *et al. Adv. Synth. Catal.* **2008**, *350*, 717–730.
298. (a) Yu, J.-Q.; Wu, H.-C.; Ramarao, C.; *et al. Chem. Commun.* **2003**, 678–679. (b) Baxendale, I. R.; Griffiths-Jones, C. M.; Ley, S. V. *Chem. Eur. J.* **2006**, *12*, 4407–4416.
299. Popa, D.; Marcos, R.; Sayalero, S. *Adv. Synth. Catal.* **2009**, *351*, 1539–1556.
300. Bagley, M. C.; Jenkins, R. L.; Lubinu, M. C.; *et al. J. Org. Chem.* **2005**, *70*, 7003–7006.
301. Glasnov, T. N.; Vugts, D. J.; Koningstein, M. M.; *et al. QSAR Comb. Sci.* **2006**, *25*, 509–518.
302. Rueping, M.; Bootwicha, T.; Sugiono, G. *Adv. Synth. Catal.* **2010**, *352*, 2961–2965.
303. (a) Wilson, N. S.; Sarko, C. R.; Roth, G. P. *Org. Proc. Res. Dev.* **2004**, *8*, 535–538. (b) Shieh, W.-C.; Dell, S.; Repic, O. *Org. Lett.* **2001**, *3*, 4279–4281.
304. (a) Cioffi, E. A. *Curr. Top. Med. Chem.* **2008**, *8*, 152–158. (b) Corsaro, A.; Chiacchio, U.; Pistara, V.; *et al. Curr. Org. Chem.* **2004**, *8*, 511–538.
305. (a) Bieg, T.; Kral, K.; Paszkowska, J.; *et al. J. Carbohydr. Chem.* **2012**, *31*, 593–601. (b) Garcia-Martin, F.; Hinou, H.; Matsushita, T.; *et al. Org. Biomol. Chem.* **2012**, *10*, 1612–1617. (c) Wadouachi, A.; Kovensky, J. *Molecules* **2011**, *16*, 3933–3968. (d) Maza, S.; de Paz, J. L.; Nieto, P. M. *Tetrahedron Lett.* **2011**, *52*, 441–443.
306. (a) Grunefeld, P.; Richert, C. *Nucleos. Nucleot. Nucl.* **2006**, *25*, 815–821. (b) Orrling, K.; Nilsson, P.; Gullbergh, M.; *et al. Chem. Commun.* **2004**, 790–791.
307. (a) Nascimento-Junior, N. M.; Kuemmerle, A. E.; Barreiro, E. J.; *et al. Molecules* **2011**, *16*, 9274–9297. (b) Cao, P.; Leadbeater, N. E. Microwave Heating as a Tool for Drug Discovery. In *Microwave Heating as a Tool for Sustainable Chemistry*; Leadbeater, N. E., Ed.; CRC Press: Boca Raton FL, **2010**, Chapter 4; pp 73–103. (c) Dolle, R. E.; Le Bourdonnec, B.; Worm, K.; *et al. J. Comb. Chem.* **2010**, *12*, 765–806. (d) Alcazar, J.; Oehlrich, D. *Future Med. Chem.* **2010**, *2*, 169–176. (e) Santagada, V.; Frecentese, F.; Perissutti, E.; *et al. Mini-Rev. Med. Chem.* **2009**, *9*, 340–358.
308. (a) Kappe, C. O.; Stadler, A.; Dallinger, D. *Microwaves in Organic and Medicinal Chemistry*, 2nd ed.; Wiley-VCH: Weinheim, **2012**, Chapter 3; pp 41–81. (b) Ondruschka, B.; Bonrath, W.; Stuerga, D. Development and Design of Laboratory and Pilot Scale Reactors for Microwave-assisted Chemistry. In *Microwaves in Organic Synthesis*, 2nd ed.; Loupy, A., Ed.; Wiley-VCH: Weinheim, **2006**, Vol. 1, Chapter 2; pp 62–107.
309. (a) Anton Paar: http://www.anton-paar.com. (b) Biotage: http://www.biotage.com. (c) CEM Corp. http://www.cem.com. (d) Milestone Srl: http://www.milestonesrl.com. (e) Püschner: http://www.pueschner.com. (f) Sairem: http://www.sairem.com. (g) UpScale Microwave: Available at: http://www.upscalemicrowave.com (accessed on 23 July 2013).
310. (a) Collins, J. M.; Singh, S. K.; Vanier, G. S. *Chem. Today* **2012**, *30*, 26–29. (b) Pedersen, S. L.; Tofteng, A. P.; Malik, L.; *et al. Chem. Soc. Rev.* **2012**, *41*, 1826–1844. (c) Sandoval, W. N.; Pharn, V. C.; Lill, J. R. *Drug Discov. Today* **2008**, *13*, 23–24. (d) Collins, J. M.; Collins, M. J. Microwave-enhanced Solid-phase Peptide Synthesis. In *Microwaves in Organic Synthesis*, 2nd ed.; Loupy, A., Ed.; Wiley-VCH: Weinheim, **2006**, Vol. 2, Chapter 20; pp 898–930,
311. Collins, J. M.; Leadbeater, N. E. *Org. Biomol. Chem.* **2007**, *5*, 1141–1150.
312. (a) Yamada, K.; Nagashima, I.; Hachisu, M.; *et al. Tetrahedron Lett.* **2012**, *53*, 1066–1070. (b) Rizzolo, F.; Testa, C.; Lambardi, D.; *et al. J. Peptide Sci.* **2011**, *17*, 708–714. (c) Freeman, N. S.; Tal-Gan, Y.; Klein, S.; *et al. J. Org. Chem.* **2011**, *76*, 3078–3085. (d) Friligou, I.; Papadimitriou, E.; Gatos, D.; *et al. Amino Acids* **2011**, *40*, 1431–1440. (e) Bacsa, B.; Bosze, S.; Kappe, C. O. *J. Org. Chem.* **2010**, *75*, 2103–2106. (f) Muthusamy, K.; Albericio, F.; Arvidsson, P. I.; *et al. Biopolymers* **2010**, *94*, 323–330. (g) Banerjee, J.; Hanson, A. J.; Muhonen, W. W.; *et al. Nat. Protoc.* **2010**, *5*, 39–50. (h) Pedersen, S. L.; Sorensen, K. K.; Jensen, K. J. *Biopolymers* **2010**, *94*, 206–212. (i) Palasek, S. A.; Cox, Z. J.; Collins, J. M. *J. Peptide Sci.* **2007**, *13*, 143–148. (j) Rizzolo, F.; Sabatino, G.; Chelli, M.; *et al. Int. J. Pept. Res. Ther.* **2007**, *13*, 203–208. (k) Santagada, V.; Fiorino, F.; Perissutti, E.; *et al. Tetrahedron Lett.* **2001**, *42*, 5171–5173.
313. Lill, J. R. *Microwave-Assisted Proteomics*; The Royal Society of Chemistry: Cambridge UK, **2009**.
314. (a) Damm, M.; Nusshold, C.; Cantillo, D. *J. Proteomics* **2012**, *75*, 5533–5543. (b) Na, Y.; Kim, S. H.; Lee, T. G.; *et al. Langmuir* **2011**, *27*, 10098–10105. (c) Pritchard, C.; Torma, F. A.; Hopley, C.; *et al. Anal. Biochem.* **2011**, *412*, 40–46. (e) Liu, X.; Chan, K.; Chu, I. K.; *et al. Carbohydr. Res.* **2008**, *343*, 2870–2877. (f) Lill, J. R.; Ingle, E. S.; Liu, P. S.; *et al. Mass. Spectrom. Rev.* **2006**, *26*, 657–671.
315. Bogdal, D.; Prociak, A. *Microwave-Enhanced Polymer Chemistry and Technology*; Blackwell: Oxford, **2007**.
316. (a) Ebner, C.; Bodner, T.; Stelzer, F.; *et al. Macromol. Rapid Commun.* **2011**, *32*, 254–288. (b) Iannelli, M. Microwave Heating as a Tool for Sustainable Polymer Chemistry. In *Microwave Heating as a Tool for Sustainable Chemistry*; Leadbeater, N. E., Ed.; CRC Press: Boca Raton, FL, **2010**, Chapter 3; pp 53–71. (c) Sosnik, A.; Gotelli, G.; Abraham, G. A. *Prog. Polym. Sci.* **2010**, *36*, 1050–1078. (d) Hoogenboom, R.; Schubert, U. S. *Macromol. Rapid Comm.* **2007**, *28*, 368–386.

317. (a) Guo, W.; Hensarling, R. M.; LeBlanc, A. L.; *et al. Macromol. Rapid Comm.* **2012**, *33*, 863–868. (b) Cook, J. P.; Goodall, G. W.; Khutoryanskaya, O. V.; *et al. Macromol. Rapid Comm.* **2012**, *33*, 332–336. (c) Bloksma, M. M.; Paulus, R. M.; van Kuringen, H. P. C.; *et al. Macromol. Rapid Comm.* **2012**, *33*, 92–96. (d) Lambermont-Thijs, H. M. L.; Fijten, M. W. M.; van der Linden, A. J.; *et al. Macromolecules* **2011**, *44*, 4320–4325. (e) Gotelli, G. A.; Bonelli, P.; Abraham, G. A.; *et al. J. Appl. Polym. Sci.* **2011**, *121*, 1321–1329. (f) Lambermont-Thijs, H. M. L.; Jochems, M. J. H. C.; Hoogenboom, R.; *et al. J. Polym. Sci. A* **2009**, *47*, 6433–6440.
318. (a) Jones, J. R.; Lu, S. Y. Microwave-Enhanced Radiochemistry. In *Microwaves in Organic Synthesis*, 2nd ed.; Loupy, A., Ed.; Wiley-VCH: Weinheim, **2006**, Vol. 2, Chapter 18; pp 820–859. (b) Elander, N.; Jones, J. R.; Lu, S. Y.; *et al. Chem. Soc. Rev.* **2000**, *29*, 239–249.
319. (a) Olafsen, T.; Sirk, S. J.; Olma, S.; *et al. Tumor Biol.* **2012**, *33*, 669–677. (b) Belanger, A. P.; Pandey, M. K.; DeGrado, T. R. *Nucl. Med. Biol.* **2011**, *38*, 435–441. (c) Kallmerten, A. E.; Jones, G. B. *Curr. Alzheimer Res.* **2010**, *7*, 251–254. (d) LaBeaume, P.; Placzek, M.; Daniels, M.; *et al. Tetrahedron Lett.* **2010**, *51*, 1906–1909.
320. (a) Richel, A.; Laurent, P.; Wathelet, B.; *et al. Catal. Today* **2011**, *167*, 141–147. (b) Durka, T.; Van Gerven, T.; Stankiewicz, A. *Chem. Eng. Technol.* **2009**, *32*, 1301–1312. (c) Baxendale, I. R.; Lee, A.-L.; Ley, S. V. Integrating Microwave-Assisted Synthesis and Solid-Supported Reagents. In *Microwave Assisted Organic Synthesis*; Tierney, J. P., Lidström, P., Eds.; Blackwell, Oxford, **2005**, Chapter 6; pp 133–176. (d) Crosignani, S.; Linclau, B. *Top. Heterocycl. Chem.* **2006**, *1*, 129–154. (e) Bhattacharyya, S. *Mol. Div.* **2005**, *9*, 253–257. (f) Desai, B.; Kappe, C. O. *Top. Curr. Chem.* **2004**, *242*, 177–208.
321. (a) Lagiakos, H. R.; Walker, A.; Aguilar, M.-I.; *et al. Tetrahedron Lett.* **2011**, *52*, 5131–5132. (b) Radi, M.; Saletti, S.; Botta, M. *Tetrahedron Lett.* **2008**, *49*, 4464–4466. (c) Alesi, S.; DiMaria, F.; Melucci, M.; *et al. Green Chem.* **2008**, *10*, 517–523. (d) Bai, L.; Wang, J. X. *Adv. Synth. Catal.* **2008**, *350*, 315–320. (e) Humphries, P. S.; Finefield, J. M. *Tetrahedron Lett.* **2006**, *47*, 2443–2446. (f) Wang, Y.; Miller, R. L.; Sauer, D. R.; Djuric, S. W. *Org. Lett.* **2005**, *7*, 925–928. (g) Lei, X.; Porco, J. A. *Org. Lett.* **2004**, *6*, 795–798. (h) Vasudevan, A.; Ji, Z.; Frey, R. R.; *et al. Bioorg. Med. Chem. Lett.* **2003**, *13*, 3909–3913.
322. (a) McGowan, C. B.; Leadbeater, N. E. Microwave Heating as a Tool for the Undergraduate Organic Chemistry Laboratory. In *Microwave Heating as a Tool for Sustainable Chemistry*; Leadbeater, N. E., Ed.; CRC Press: Boca Raton, FL, **2010**, Chapter 6; pp 149–174. (b) Baar, M. R. Greener Organic Reactions Under Microwave Heating. In *Green Organic Chemistry in Lecture and Laboratory*; Dicks, A. P., Ed.; CRC Press: Boca Raton, FL, **2011**, Chapter 8; pp 225–256,
323. McGowan, C. B.; Leadbeater, N. E. *Laboratory Experiments Using Microwave Heating*; CRC Press: Boca Raton, Fl, **2013**.
324. (a) Shell, T. A.; Shell, J. R.; Poole, K. A.; *et al. J. Chem. Ed.* **2011**, *88*, 1439–1441. (b) Pohl, N. L. B.; Kirshenbaum, K.; Yoo, B.; *et al. J. Chem. Ed.* **2011**, *88*, 999–1001. (c) Baar, M. R.; Falcone, D.; Gordon, C. *J. Chem. Ed.* **2010**, *87*, 84–86. (d) Murphree, S. S.; Kappe, C. O. *J. Chem. Ed.* **2009**, *86*, 227–229. (e) Katritzky, A. R.; Cai, C. M.; Collins, M. D.; *et al. J. Chem. Ed.* **2006**, *83*, 634–636.
325. Leadbeater, N. E.; Schmink, J. R.; Hamlin, T. A. Tools for Monitoring Reactions Performed Using Microwave Heating. In *Microwaves in Organic Synthesis*, 3rd ed.; de la Hoz, A., Loupy, A., Eds.; Wiley-VCH: Weinheim, **2012**.
326. Bowman, M. D.; Leadbeater, N. E.; Barnard, T. M. *Tetrahedron Lett.* **2008**, *49*, 195–198.
327. Leadbeater, N. E.; Shoemaker, K. M. *Organometallics* **2008**, *27*, 1254–1258.
328. Gutmann, B.; Schwan, A. M.; Reichart, B.; *et al. Angew. Chem. Int. Ed.* **2011**, *50*, 7636–7640.
329. Bogdal, D.; Lukasiewicz, M.; Pielichowski, J.; Miciak, A.; Bedaarz, S. Z. *Tetrahedron* **2003**, *59*, 649–653. (b) Lukasiewicz, M.; Bogdal, D.; Pielichowski, J. *Adv. Synth. Catal.* **2003**, *345*, 1269–1272.
330. van de Kruijs, B. H. P.; Dressen, M. H. C. L.; Meuldijk, J.; Vekemansa, J. A. J. M.; Hulshof, L. A. *Org. Biomol. Chem.* **2010**, *8*, 1688–1694.
331. Leadbeater, N. E. *Chem. Commun.* **2010**, *46*, 6693–6695.
332. Heller, E.; Klöckner, J.; Lautenschläger, W.; Holzgrabe, U. *Eur. J. Org. Chem.* **2010**, *5*, 3569–3573.
333. Pivonka, D. E.; Empfield, J. R. *Appl. Spectrosc.* **2004**, *58*, 41–46.
334. Leadbeater, N. E.; Smith, R. J. *Org. Lett.* **2006**, *8*, 4589–4591.
335. Leadbeater, N. E.; Smith, R. J. *Org. Biomol. Chem.* **2007**, *5*, 2770–2774.
336. Leadbeater, N. E.; Smith, R. J.; Barnard, T. M. *Org. Biomol. Chem.* **2007**, *5*, 822–825.
337. Leadbeater, N. E.; Schmink, J. R. *Nature Protoc.* **2008**, *3*, 1–7.
338. Schmink, J. R.; Holcomb, J. L.; Leadbeater, N. E. *Org. Lett.* **2009**, *11*, 365–368.
339. Schmink, J. R.; Leadbeater, N. E. *Org. Biomol. Chem.* **2009**, *7*, 3842–3846.
340. (a) Dalitz, F.; Cudaj, M.; Maiwald, M.; *et al. Prog. Nucl. Mag. Res. Sp.* **2012**, *60*, 52–70. (b) Goekay, O.; Albert, K. *Anal. Bioanal. Chem.* **2012**, *402*, 647–669.
341. Gomez, M. V.; Verputten, H. H. J.; Diaz-Ortiz, A.; *et al. Chem. Commun.* **2010**, *46*, 4514–4516.
342. (a) Moseley, J. D. Microwave Heating as a Tool for Process Chemistry. In *Microwave Heating as a Tool for Sustainable Chemistry*; Leadbeater, N. E., Ed.; CRC Press: Boca Raton, FL, **2010**, Chapter 5; pp 105–148. (b) Leonelli, C.; Mason, T. J. *Chem. Eng. Process.* **2010**, *49*, 885–900. (c) Strauss, C. R. *Org. Proc. Res. Dev.* **2009**, *13*, 915–923. (d) Kremsner, J. M.; Stadler, A.; Kappe, C. O. *Top. Curr. Chem.* **2006**, *266*, 233–278.
343. Barnard, T. M.; Vanier, G. S.; Collins, M. J. *Org. Proc. Res. Dev.* **2006**, *10*, 1223–1237.
344. Leadbeater, N. E.; Williams, V. A.; Barnard, T. M.; *et al. Org. Proc. Res. Dev.* **2006**, *10*, 833–837.
345. Leadbeater, N. E.; Williams, V. A.; Barnard, T. M.; *et al. Synlett* **2006**, 2953–2958.
346. (a) Alcázar, J.; Diels, G.; Schoentjes, B. *QSAR Comb. Sci.* **2004**, *23*, 906–910. (b) Stadler, A.; Yousefi, B. H.; Dallinger, D.; Walla, P.; Van der Eycken, E.; Kaval, N.; Kappe, C. O. *Org. Proc. Res. Dev.* **2003**, *7*, 707–716. (c) Nüchter, M.; Ondruschka, B. *Mol. Div.* **2003**, *7*, 253–264.
347. Amore, K. M.; Leadbeater, N. E.; Miller, T. A.; Schmink, J. R. *Tetrahedron Lett.* **2006**, *47*, 8583.
348. (a) Marafie, J. A.; Moseley, J. D. *Org. Biomol. Chem.* **2010**, *8*, 2219–2227. (b) Loones, K. T. J.; Maes, B. U. W.; Rombouts, G.; Hostyn, S.; Diels, G. *Tetrahedron* **2005**, *61*, 10338–10348.
349. Arvela, R. K.; Leadbeater, N. E.; Collins, M. J. *Tetrahedron* **2005**, *61*, 9349.
350. Raner, K. D.; Strauss, C. R.; Trainor, R. W.; *et al. J. Org. Chem.* **1995**, *60*, 2456–2460.
351. Schmink, J. R.; Kormos, C. M.; Devine, W. G.; Leadbeater, N. E. *Org. Proc. Res. Dev.* **2010**, *14*, 205–214.
352. Iannelli, M.; Bergamelli, F.; Kormos, C. M.; Paravisi, S.; Leadbeater, N. E. *Org. Proc. Res. Dev.* **2009**, *13*, 634–637.
353. Moseley, J. D. *Chemistry Today* **2009**, *27*, 6–10.
354. (a) Ali, A. A.; Gaikar, V. G. *Ind. Eng. Chem. Res.* **2011**, *50*, 6543–6555. (b) Bergamelli, F.; Iannelli, M.; Marafie, J. A.; *et al. Org. Proc. Res. Dev.* **2010**, *14*, 926–930. (c) Nakamura, T.; Nagahata, R.; Kunii, K.; *et al. Org. Proc. Res. Dev.* **2010**, *14*, 781–786. (e) Bagley, M. C.; Fusillo, V.; Jenkins, R. L.; *et al. Org. Biomol. Chem.* **2010**, *8*, 2245–2251. (f) Moseley, J. D.; Lawton, S. J. *Chemistry Today* **2007**, *25*, 16–19. (g) Cablewski, T.; Faux, A. F.; Strauss, C. R. *J. Org. Chem.* **1994**, *59*, 3408–3412.
355. Ohrngren, P.; Fardost, A.; Russo, F.; *et al. Org. Proc.. Res. Dev.* **2012**, *16*, 1053–1063.
356. Morschhäuser, R.; Krull, M.; Kayser, C.; *et al. Green Process Synth.* **2012**, *1*, 281–290.
357. (a) Wilson, N. S.; Osuma, A. T.; Van Camp, J. A.; *et al. Tetrahedron Lett.* **2012**, *53*, 4498–4501. (b) Glasnov, T. N.; Kappe, C. O. *Chem. Eur. J.* **2011**, *17*, 11956–11968.
358. Dressen, M. H. C. L.; van de Kruijs, B. H. P.; Meuldijk, J.; *et al. Org. Proc. Res. Dev.* **2010**, *14*, 351–361.
359. Moseley, J. D.; Kappe, C. O. *Green Chem.* **2011**, *13*, 794–806.
360. (a) Devine, W. G.; Leadbeater, N. E. *ARKIVOC* **2011**, *part 5*, 127–143. (b) Moseley, J. D.; Woodman, E. K. *Energy Fuels* **2009**, *23*, 5438–5447. (c) Hoogenboom, R.; Wilms, T. F. A.; Erdmenger, T.; *et al. Aust. J. Chem.* **2009**, *62*, 236–243. (d) Komorowska, M.; Stefanidis, G. D.; Van Gerven, T.; *et al. Chem. Eng. J.* **2009**, *155*, 859–866. (e) Razzaq, M.; Kappe, C. O. *ChemSusChem* **2008**, *1*, 123–132. (f) Godwin, D. R.; Lawton, S. J.; Moseley, J. D.; *et al. Org. Proc. Res. Dev.* **2005**, *9*, 516–518, corrigendum: Gronnow, M.J.; White, R.J. Clark, J.H.; *et al. Org. Proc. Res. Dev.* **2007**, *11*, 293–293.
361. Godwin, D. R.; Lawton, S. J.; Moseley, J. D.; *et al. Energy Fuels* **2010**, *24*, 5446–5453.

362. (a) Robinson, J.; Kingman, S.; Irvine, D.; *et al. Phys. Chem. Chem. Phys.* **2010**, *12*, 4750–4758. (b) Robinson, j.; Kingman, S.; Irvine, D.; *et al. Phys. Chem. Chem. Phys.* **2010**, *12*, 10793–10800.
363. Bose, A. K.; Banik, B. K.; Lavlinskia, N.; *et al. Chemtech* **1997**, *27*, 18–24.
364. Sarko, C. R. Timesavings Associated with Microwave-Assisted Synthesis: A Quantitative Approach. In *Microwave-Assisted Organic Synthesis*; Lidström, P., Tierney, J. P., Eds.; Blackwell Publishing: Oxford, **2005**, Chapter 8; pp 22–236.

9.11 Useful Chemical Activation Alternatives in Solvent-Free Organic Reactions

JG Hernández, CG Avila-Ortiz, and E Juaristi, Centro de Investigación y de Estudios Avanzados del I. P. N., México, D.F. Mexico

© 2014 Elsevier Ltd. All rights reserved.

9.11.1	**Introduction**	287
9.11.2	**Mechanochemistry**	287
9.11.2.1	Grinding Technique	288
9.11.2.2	Ball-Milling Technique	292
9.11.2.3	Organocatalyzed Reactions in Solvent-Free Ball-Milling Conditions	299
9.11.3	**Microwave Irradiation Under Solvent-Free Conditions**	301
9.11.4	**Miscellaneous Solvent-Free Strategies**	309
9.11.5	**Solvent-Free Philosophy in the Chemical Industry**	311
Acknowledgments		312
References		312

Glossary

Asymmetric organocatalysis A stereoselective reaction catalyzed exclusively by a small organic molecule in the absence of metals.

High-speed ball milling A sustainable mechanochemical technique used commonly for milling materials into fine particles and more recently used to carry out chemical reactions under solvent-free conditions.

Mechanochemical reaction A chemical transformation induced by the direct absorption of mechanical energy.

Microwave irradiation Electromagnetic energy that falls in the frequency range of 0.3–300 GHz. It is a low-energy, nonionizing radiation that transfers energy by its interaction with polar substances.

Ultrasonic activation High-energy input that leads to the formation of reactive chemical species via the formation, growth, and implosive collapse of bubbles in a liquid (acoustic cavitation).

9.11.1 Introduction

During the past two decades, a significant number of chemical reports describe the use of alternative reaction media such as water, ionic liquids, cyclic carbonates, fluorinated solvents, and the use of supercritical fluids among others, aiming to transform organic synthesis into a more sustainable chemical process. Despite the potential advantages specific to each of these strategies, all the aforementioned reaction media have particular drawbacks. In particular, some of the main concerns refer to high-energy requirements, potential human and environmental toxicity, poor biodegradability, difficult purification methods, and the non-existence of a general procedure for proper after-treatment work up. In keeping with Sheldon's statement that 'the best solvent is no solvent,'[1] a powerful alternative to render synthetic organic protocols greener, consists in 'avoiding the use of reaction solvents altogether.' In some cases, this has been achieved by using an excess of one of the liquid reagents; nevertheless, in some cases it has been possible to employ approximately equimolar amounts of reactants, making the synthetic process truly solventless.

In recent years the considerable increase in the number of literature reports describing solventless reactions, has resulted in the publication of excellent books[2,3] and reviews[4–7] on the subject. In these monographs, solventless reactions have been usually classified according to the type of bonds being formed in the chemical process involved; nevertheless, some reviews have focused in the classification of the particular system being synthetized or in a characteristic application, for example, in asymmetric catalysis. However, several outstanding reviews have recently discussed the use of nonconventional energy sources such as mechanochemistry (ball milling), microwave, and ultrasound activation, which have been employed to promote traditional organic reactions and organocatalytic processes.[8–12] The abovementioned techniques present the essential properties to being carried out in the absence of solvent, however not all discussed examples in these reviews were performed under truly solvent-free conditions. As a consequence, herein the authors want to review some recent examples of solventless organic reactions performed principally through mechanical activation and microwave irradiation.

9.11.2 Mechanochemistry

According to IUPAC, a mechanochemical reaction is defined as a chemical reaction that is induced by the direct absorption of mechanical energy.[13] Interestingly, the first mechanochemical reactions were performed by simple grinding procedures using

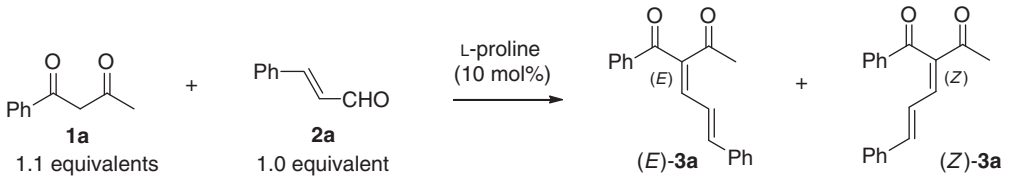
traditional mortars and pestles – now emblematic of the chemical profession! Nevertheless, practical applications have generally been restricted to reactions which take place in few minutes, that is processes for which manual grinding provides sufficient activation energy for the desired reaction to take place within a reasonable time. An interesting and more convenient alternative has been the use of high velocity ball mills, which permit the development of challenging reactions minimizing the problems associated with long reaction times or high-frequency milling.

9.11.2.1 Grinding Technique

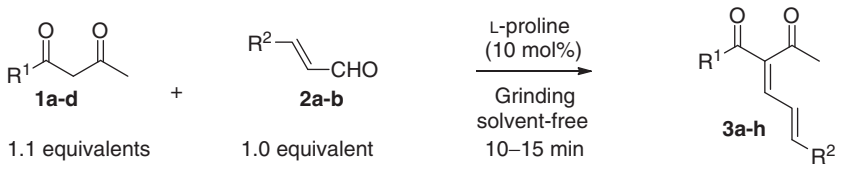
Since the first-documented mechanochemical reaction in the fourth century BC (native mineral cinnabar (mercuric sulfide, HgS) was rubbed with vinegar in a copper mortar with a copper pestle yielding the liquid metal)[14] to the present day, it has been clear that the use of mortar and pestle is probably the easiest way to perform a mechanochemical process by simply grinding diverse substrates. In recent years, grinding techniques in the absence of solvent have been applied in the preparation of several types of organic compounds such as various heterocycles with relevance in synthetic and pharmaceutical chemistry because of their biological activity, as well as several derivatives used as versatile building blocks in the synthesis of natural products. In the majority of cases the reactions carried out under solvent-free conditions showed shorter reaction times, and higher chemical yields and selectivity, when compared with the same processes under traditional solution chemistry. An additional bonus in these developments consists in the fact that solventless grinding procedures avoid the serious environmental concerns associated with previous methods.

In a particular example, α,β-enones are an important kind of substrate used extensively in Diels–Alder reactions[15] and in 1,4-additions;[16] however, their preparation through traditional methods in solution presented the problem of poor stereoselectivity owing to the possibility of obtaining either the *E*- or *Z*-isomer of the desired unsaturated product. In this context, in 2009 Goswami and Das reported the selective synthesis of the *E* isomer of the conjugated dienones and enones via Knoevenagel condensation of 1,3-diketones using as catalyst a variety of amines as well as amino acids under solvent-free reaction conditions.[17] In particular, in the presence of a catalytic amount of L-proline (10 mol%) the reaction between benzoyl acetone **1a** and cinnamaldehyde **2a**, performed by grinding in a mortar under solvent-free conditions afforded the expected α,β-enone **3a** in good to high yield and complete stereoselectivity, giving exclusively the (*E*)-**3a** isomer (entry 5 in Table 1). In contrast, the reaction in solution afforded a mixture of both *E*- and *Z*-isomers (entries 1–4 in Table 1). The selectivity observed in the solventless process suggests that the solvent is involved in undesirable *cis–trans* isomerization of the product. This simple and efficient environmentally benign method was also applied in the reaction between 1,3-dicarbonyl compounds **1a–d** and unsaturated aldehydes **2a–b**. In all cases the *E*-isomers were selectively obtained in high yield using essentially stoichiometric amounts of reagents (equation 1).

Table 1 Screening of solvents in the Knoevenagel condensation of 1,3-diketones using as catalyst a variety of amines as well as amino acids[17]



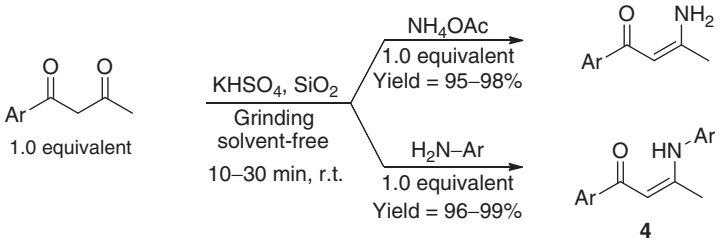
Entry	*Solvent (3 ml)*	*Time (min)*	*E:Z*	*Yield (%)*
1	CH_2Cl_2	35	65:35	90
2	$CHCl_3$	40	60:40	88
3	MeCN	30	71:29	75
4	EtOH	40	80:20	88
5	—	10	100:0	87



(1)

R^1 = Ph, OMe, OEt, OBu^t; R^2 = Ph, Me
Yield = 72–91%

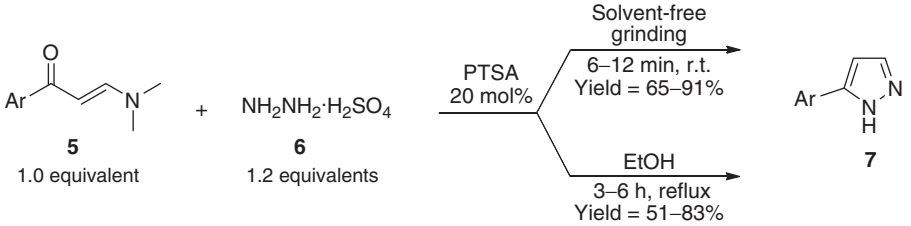
High stereo- and regioselectivity was also observed in the preparation of β-enamino ketones under solvent-free conditions reported by Li et al.[18] In this study, the condensation reaction activated by mechanochemical grinding between 1,3-dicarbonyl compounds and ammonium salts or amines was described. The process was catalyzed by $KHSO_4/SiO_2$ and led to the exclusive formation of the *Z*-isomers in excellent yields with short grinding times. Furthermore, in the case of unsymmetrical β-diketones the reaction also exhibited high regioselectivity (equation 2).



(2)

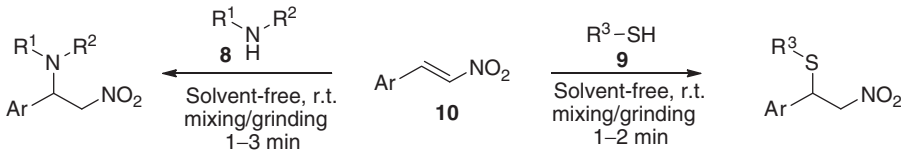
In comparison, when this catalytic system was evaluated using dichloromethane as reaction medium, both the reaction rate and yields were lower. The development of solvent-free methods in the preparation of β-enamino ketones is particularly significant because traditional routes involve heating to reflux in toxic solvents such as benzene or toluene.

β-Enamino ketones are privileged intermediates used in pharmaceutical and synthetic chemistry in the preparation of several relevant drugs and heterocyclic systems.[19] For example, Martins et al.[20] demonstrated the value of β-enaminones during the synthesis of pyrazoles **7** by the cyclization reaction of β-dimethylaminovinylketones **5** and hydrazine sulfate **6** in the presence of *p*-toluenesulfonic acid (PTSA). The reaction was evaluated both in solution and under solvent-free conditions affording the respective pyrazoles. In particular, using the grinding technique at room temperature and in the absence of solvent, reaction times, and yields were superior relative to the same reaction in solution at reflux temperature (equation 3). These independent works are an example of complementary research that shows how solvent-free methods can be assembled to perform an ecologically friendly solventless synthesis of valuable heterocyclic compounds presenting a wide diversity of biological activities.[21]



(3)

For most organic chemists, an ideal chemical reaction can be conceived as a waste-free, atom-economic process where inert conditions are not required to generate the desired product in quantitative yield, without the need of catalysts, and proceeding in short reaction times. Although the above requirements may seem difficult to fulfill, recently Peddinti and Choudhary reported the catalyst-free and solvent-free Michael addition of amines **8** and thiols **9** to nitroolefins **10** (equation 4).[22]



(4)

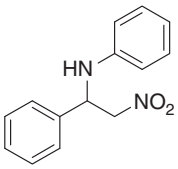
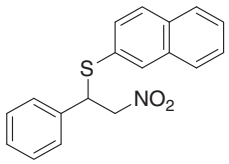
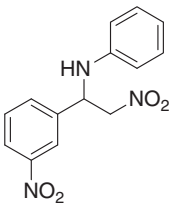
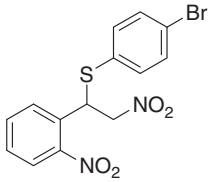
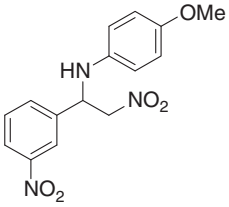
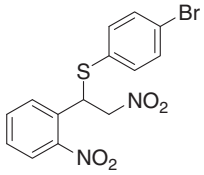
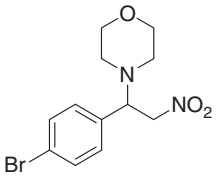
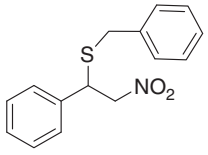
10:**8**, **10**:**9** 1 equivalent:1 equivalent

The reactions were carried out by simple mixing or grinding the substrates at room temperature, obtaining the corresponding addition products in very short reaction times (Table 2). Most importantly, the products were obtained in quantitative yields, without the need of chromatographic purification steps. Finally, the entire process was totally solvent free. The resulting nitroamines and nitrosulfides are interesting products because of their value as building blocks for the preparation of various natural products.[23] The synthetic importance of nitroamines is further supported by the fact that these compounds can be transformed into useful diamines or aminoacids, by well-established reductive or oxidative protocols, respectively.[24]

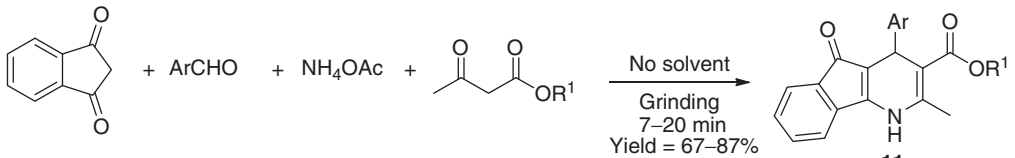
Multicomponent reactions (MCRs) are one of the most effective strategies for the synthesis of complex molecular structures via sequential multiple chemical steps taking place in a single reaction vessel. This strategy avoids the time-consuming and costly steps of protection and deprotection, as well as the corresponding work-up procedures.

An improvement associated with MCRs has been the development of solvent-free protocols that have further increased the synthetic utility of MCR synthetic methods. Indeed, recent examples of solvent-free MCRs were reported by Singh[25] and Kumar.[26] Both research groups studied the preparation of dihydropyridines by simple and highly efficient one-pot procedures in the

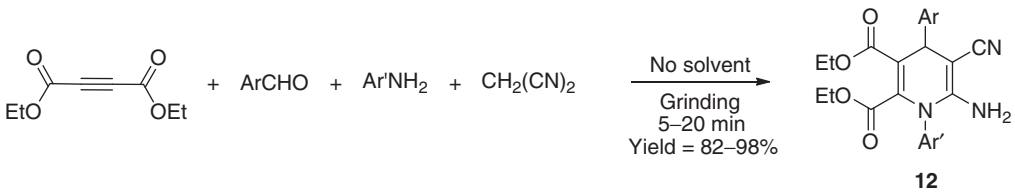
Table 2 Scope of solvent-free Michael reaction

Entry	*Product*	*Yield (%)*	*Entry*	*Product*	*Yield (%)*
1		99	5		99
2		100	6		100
3		100	7		100
4		100	8		100

absence of solvent and catalyst. The MCRs took place under mild conditions by simple grinding, affording unsymmetrical dihydropyridine derivatives **11**[25] and **12**[26] in good to excellent yield, avoiding the use of traditional solvents such as toluene, xylene, and dioxane (equations 5–6).



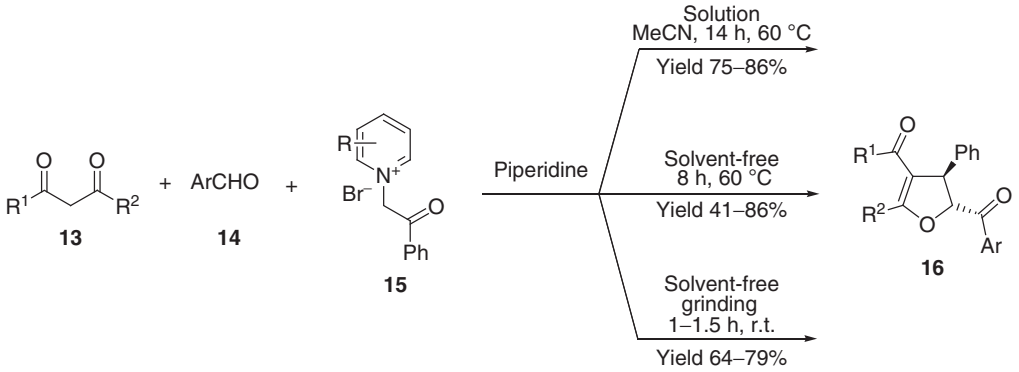
(5)



(6)

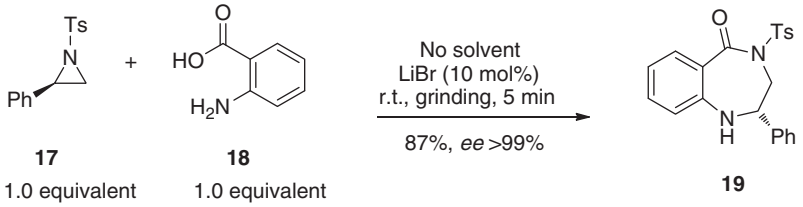
In recent work, Chuang and Chen reported the diastereoselective synthesis of 2,3-dihydrofurans using a one-pot three-component strategy.[27] Dihydrofurans are a well-known kind of heterocycles commonly found in natural products, and frequently exhibit relevant biological activities.[28] The tandem one-pot reaction of 1,3-dicarbonyl compounds **13**, aromatic aldehydes **14**, and *N*-phenacylpyridinium bromide **15a** was initially evaluated in solution using acetonitrile as solvent. The reaction afforded the corresponding 2,3-dihydrofurans **16** in moderate to good yields after 14 h of stirring at 60 °C (equation 7). When the same reaction was studied under solvent-free conditions (at 60 °C) using *N*-phenacyl-3,5-lutidinium bromide **15b** as the precursor of pyridinium ylide, the yields were generally lower although the required reaction times were shorter (equation 7). Finally, when the

reactions were carried out by grinding the substrates in a mortar and pestle in the absence of solvent for only 1 h at room temperature the desired dihydrofurans were formed in moderate to good yields (equation 7).



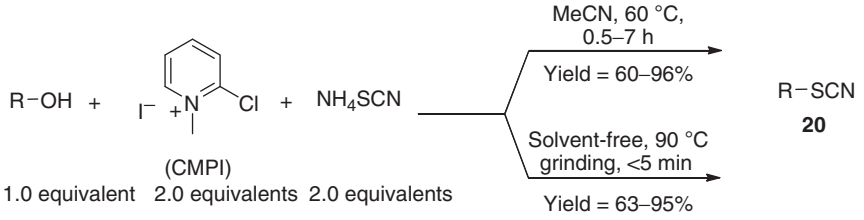
(7)

Recently, Yadav and Singh reported the solventless synthesis of benzo-1,4-diazepin-5-ones, via a grinding-induced, one-pot protocol employing *N*-tosylaziridines, anthranilic acid derivatives, and LiBr as Lewis acid catalyst. The reaction mixture was ground during 5 min at room temperature using only a mortar and pestle. The reaction proved rather efficient, affording the expected benzodiazepinones in excellent yields (72–91%) and high regioselectivity.[29] It is worth to mention that during initial screening the reaction was evaluated in solution, by stirring in various solvents (THF, dioxane, CH_2Cl_2, EtOH, toluene, and $CHCl_3$); however, even after long reaction times (13–19 h) the benzodiazepinones were obtained in lower yield. Of course, the preparation of benzodiazepinone derivatives, which are well-recognized drugs for the treatment of central nervous diseases, via such sustainable and simple protocol is of great interest to the pharmaceutical industry.[30] As an illustrative example, equation 8 shows the reaction between chiral aziridine **17** and anthranilic acid **18** to produce the (*S*)-benzo-1,4-diazepin-5-one **19** in good yield and excellent stereospecificity.



(8)

Additionally, in the past years several reports describe solvent-free grinding methods for the preparation of interesting substrates such as homoallylic alcohols (from aldehydes),[31] aryl halides (from aryl amines),[32] aldehydes (from diols),[33] oximes,[34] and alkyl thiocyanates. In particular, this last group of organosulfur compounds is used extensively in the synthesis of various pharmaceuticals, insecticides, and biocides.[35] In all cases, the grinding strategy presented advantages relative to similar procedures performed under traditional solution conditions. For example, Mokhtari et al. reported the preparation of thiocyanates from alcohols, avoiding the use of phosphine-based reagents, by using 2-chloro-1-methylpyridinium iodide (CMPI). The thiocyanation reaction of alcohols using NH_4SCN and CMPI was initially evaluated in acetonitrile as solvent. After 0.5–7 h of stirring the corresponding products were obtained in good yield and with high selectivity (RSCN vs. RNCS).[35] Nevertheless, the same reaction carried out by grinding in the absence of solvent generated the alkyl thiocyanates **20** in short reaction times (<5 min), also in high yield and selectivity (equation 9).



(9)

In general, grinding protocols are at least as efficient as their counterparts in solution, affording the respective products in high yield, short reaction times, and good selectivity. Nevertheless, although grinding techniques have demonstrated to be an alternative to solution-based chemistry, its application in large scale using traditional mortar and pestle is of course inconvenient. For instance, there are issues such as the risk associated with the open grinding of hazardous reagents, high human energy requirements, and lack of reproducibility of the processes. To solve the aforementioned weaknesses of grinding procedures, the

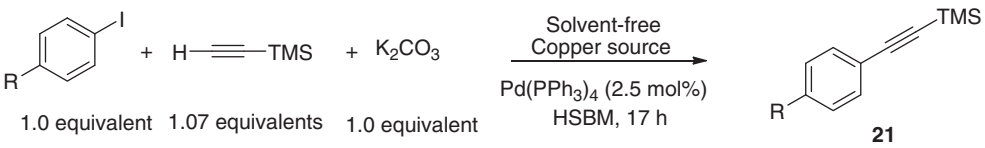
use of laboratory-size ball mills is becoming more popular, specially to carry out reactions where higher energy is required, and when milling times are prolonged (hours or days). Modern ball mills offer the opportunity to achieve high reproducibility of the process, and to reduce risks avoiding manual milling. Furthermore, solvent-free reactions can be scaled-up by using an appropriately sized ball mill.

9.11.2.2 Ball-Milling Technique

High-Speed Ball Milling (HSBM) is a sustainable mechanochemical technique that is being increasingly used in synthetic organic chemistry to promote several synthetically useful reactions, under solvent-free conditions. However, it is important to clarify that mechanochemical activation by ball milling does not necessarily imply a solvent-free process, because the milling can occasionally be performed in the presence of solvents or additives that facilitate and accelerate the milling processes (liquid-assisted grinding, LAG, also known as solvent-drop grinding). The solvent-free ball-milling reactions described in the present review are mainly procedures that use mixtures of liquids and solid substrates under near stoichiometric amounts, or reactions involving the use of only a small excess of one of the reagents.

The abovementioned HSBM technique is being increasingly used in synthetic organic chemistry to promote several solvent-free reactions. Salient reported applications include cross-coupling procedures such as Mizoroki–Heck, Suzuki–Miyaura, and Sonogashira reactions among others, which are very valuable tools in the construction of new carbon–carbon bonds. In this sense, in 2009 Mack et al. studied the Sonogashira reaction between several substituted aryl halides and trimethylsilylacetylene or phenylacetylene under solvent-free conditions.[36] Initially the coupling reaction was examined under HSBM conditions using potassium carbonate, tetrakis(triphenylphosphine) palladium(0), and a catalytic amount of copper(I) iodide. After 17 h of milling using a stainless steel vial with a tungsten carbide ball, iodo, and bromo aryl halides coupled to both trimethylsilylacetylene and phenylacetylene in moderate to high yields. The same reaction was then evaluated under copper-free conditions observing that even when the process proceeded in the absence of CuI, the yields were generally lower than when copper(I) iodide was used as cocatalyst. In a clever approach, the reaction was then carried out using a ball made of copper that indeed acted simultaneously as catalyst. Under these conditions the milling afforded the corresponding coupling products **21** in moderate yield, although still lower relative to the same process using copper(I) iodide. Finally, the reaction was repeated employing both vial and ball made of copper; now the yields were increased considerably presumably as consequence of the more extensive catalytic surface of copper available (**Table 3**).[36]

Table 3 Sonogashira reaction under HSBM conditions

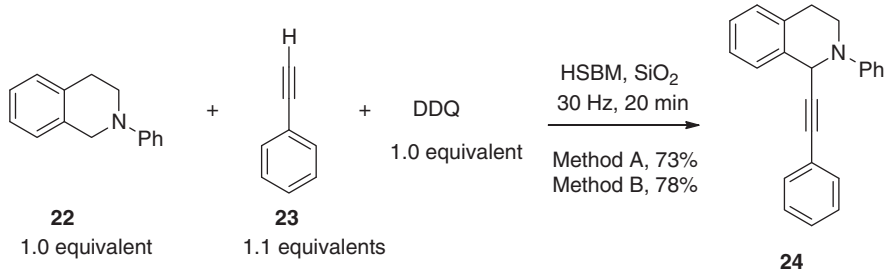


Entry	*R*	*Yield (%) CuI (1 mol%)*	*Yield (%) Cu-free*	*Yield (%) Copper Ball*	*Yield (%) Copper (Vial + Ball)*
1	H	95	39	87	88
2	Me	84	17	46	83
3	Br	88	43	31	89
4	Cl	87	37	52	86
5	OMe	84	58	40	42

A related approach has been recently applied by Su and coworkers for the cross-dehydrogenative coupling reaction between 2-phenyltetrahydroisoquinoline **22** and ethynylbenzene **23** in the absence of solvent.[37] Initially, the reaction was carried out in a high-energy vibrational micromill, using traditional stainless steel balls, with 2,3-dichloro-5,6-dicyanoquinone (DDQ) and in the presence of 5 mol% of different copper catalysts (CuBr, $Cu(OAC)_2 \cdot H_2O$, $Cu(OTf)_2$, and copper powder). The coupling process afforded the corresponding product **24** in good yields (55–79%). Nevertheless, when the reaction was examined using two copper balls in the absence of additional catalysts, the coupling reaction provided the desired product **24** with slightly higher yield (equation 10). Additionally, the solvent-free procedure was also applied in the functionalization of tetrahydroisoquinolines with several alkynes and indoles. In these cases short milling times were sufficient to obtain the coupling products in moderate to good yield. This is another interesting example where copper balls used to mill are also activating catalysts, which can be easily removed from the reaction medium.

In pharmaceutical and cosmetic industries the presence of heavy metals in their products is a constant concern, because of the danger that metal impurities can cause to human health. For this reason there exist severe regulations that set limits for the presence of trace metals in the commercialized product. Ball-milling techniques, in addition to being an attractive option to

perform organic reactions in the absence of solvent, can also be used as a convenient approach to avoid the use of metal catalysts in the synthetic chemical processes, turning solvent-free HSBM into an attractive option for the industrial sector.



22 1.0 equivalent

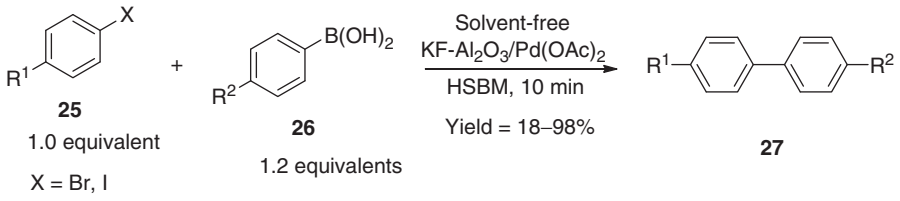
23 1.1 equivalents

24

(10)

Method A: two stainless steel balls were used and 5 mol% of copper powder
Method B: two copper balls were used without additional catalyst

The Suzuki protocol is another very important cross-coupling reaction for the selective formation of carbon–carbon bonds. This strategy has been applied extensively in natural product synthesis and pharmaceutical chemistry.[38] Traditionally, the Suzuki reaction is carried out in solution, employing organic solvents such as benzene, toluene, or ethanol. Nevertheless, solvent-free alternatives, in particular under HSBM conditions, have been documented in recent years.[39–42] In this sense, Ondruschka and Schneider reported an efficient solvent-free Suzuki reaction under HSBM conditions using $Pd(OAc)_2$ as catalyst, and an inorganic solid support ($KF–Al_2O_3$) as base.[40] In particular, the coupling reaction between aryl bromides and iodides **25** with phenylboronic acid afforded the corresponding products **27** in moderate to high yields after 10 min of milling at 800 rpm. This method was also examined in the Suzuki reaction of 4-bromoacetophenone with different boron-containing derivatives **26**. In this case, the coupling products were obtained in high yield only when *p*-substituted boronic acid were used (equation 11). More recently, Ondruschka et al. studied the effect of milling frequency, milling time, the material of the milling balls, and reaction containers, as well as the size and number of milling balls on the yield of solvent-free Suzuki reactions.[41]



25 1.0 equivalent

X = Br, I

26 1.2 equivalents

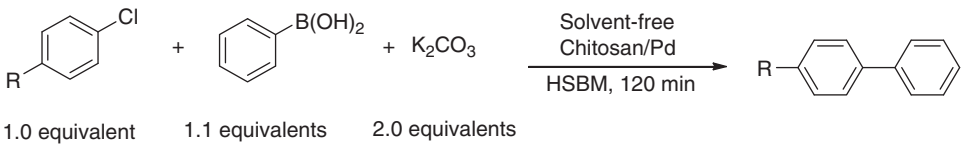
27

(11)

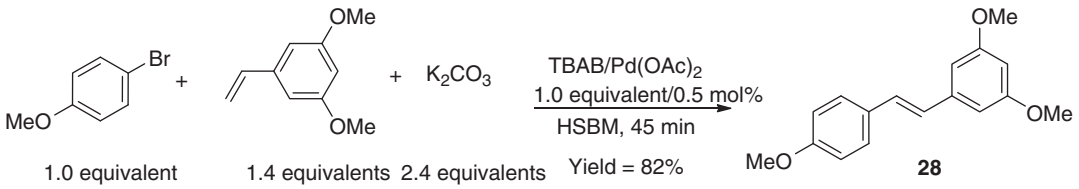
Usually, Suzuki cross-coupling reactions are performed using aryl bromides and iodides instead of aryl chlorides, even when chloride derivatives are more readily available, inexpensive, and environmentally safer reagents. The principal reason for this situation is that aryl chlorides are much more difficult to activate than their bromide and iodide analogs. However, from a very recent study Cravotto and coworkers reported the solvent-free Suzuki reaction of aryl halides (including aryl chlorides) with phenylboronic acid catalyzed by a cross-linked chitosan/Pd(II) catalytic material under HSBM conditions.[42] The reactions were carried out at 600 rpm and afforded the coupling products in moderate to excellent yield after 90–120 min of milling. In particular, this method worked better with the less active aryl chlorides, and it is worth to mention that it was possible to recover and reuse up to three times the catalytic material by simple filtration, showing only minor diminution in yield (**Table 4**). In addition, the coupling reaction of heterocyclic 2-chloropyridine and 4-chlorobenzoxazole with phenylboronic acid was also successful (**Table 4**).

Stilbenes are low-molecular weight compounds that are found in a wide range of natural sources and that exhibit a broad spectrum of biological activities, as well as application in molecular photonics and optoelectronics. Probably the most-recognized natural stilbene is *trans*-resveratrol (*trans*-3,5,4′-trihydroxystilbene), which has received significant attention because of its anti-inflammatory, antitumorigenic, and antioxidant properties.[43] Furthermore, trimethyl *trans*-resveratrol derivative **28** has also demonstrated to be a selective human cytochrome P450 1B1 inhibitor.[44] In this context, very recently Su et al. developed a solvent-free method for the synthesis of (*E*)-stilbene derivatives by means of HSBM via a palladium-catalyzed Heck cross-coupling reaction.[45] The reaction of aryl halides with styrene derivatives in the presence of $Pd(AcO)_2$ generated a series of substituted (*E*)-stilbenes in high yield after 45–90 min of milling at 1290 rpm. Of particular interest, the synthesis of the relevant resveratrol derivative **28** was achieved with 82% yield (equation 12). In the same work, traditional solution reaction conditions, conventional heating, and mechanical grinding were compared with the HSBM method, showing the advantages provided by ball-milling procedures: shorter reaction times and higher yields.

Table 4 Suzuki reaction under HSBM conditions



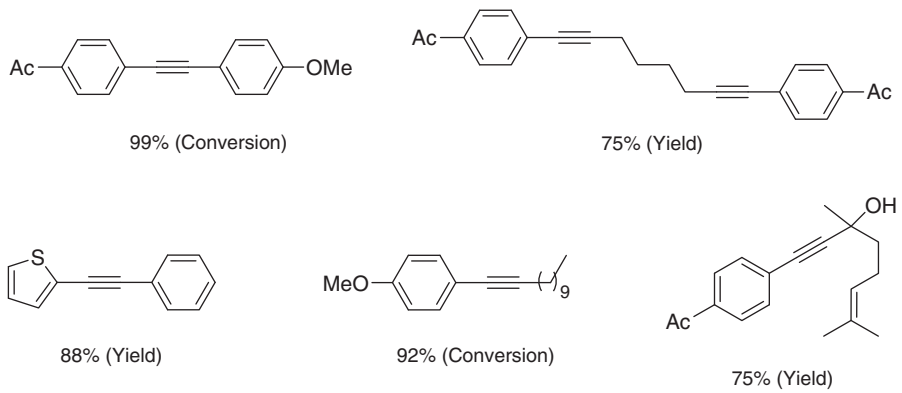
Entry	*R*	*Yield (%)*
1	H	99
2	*p*-Ac	29
3	*m*-Ac	36
4	*o*-Ac	39
5	*p*-NO_2	84
6	2nd run	75
7	3rd run	64
8	4th run	50



(12)

TBAB = tetra-*n*-butylammonium bromide

As already mentioned above, the Sonogashira reaction is an important cross-coupling strategy that is used frequently in the formation of new carbon–carbon bonds through the alkynylation of aryl or alkenyl halides. The relevance of Sonogashira couplings is well recognized in total synthesis of natural products, and in the preparation of precursors of pharmaceutical molecules and molecular materials.[38,46] In 2010, Stolle and coworkers presented an elegant and efficient version of solvent-free Sonogashira coupling in the absence of ligand and copper metal, under HSBM conditions in a planetary ball mill.[47] For example, the reaction of aryl iodides with several aryl and alkyl-substituted acetylenes catalyzed by $Pd(OAc)_2$ and 1,4-diazabicyclo[2.2.2]-octane (DABCO) afforded the corresponding cross-coupling products in good to high yield, after a short milling process (20 min at 800 rpm). Figure 1 shows the diversity of products obtained with this solvent-free method.

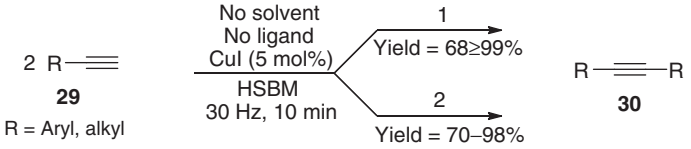


Aryl iodide (1.0 equivalent), acetylene (1.0–1.25 equivalents), DABCO (1.25 equivalents), $Pd(OAc)_2$ (5 mol%), SiO_2.

Figure 1 Some Sonogashira coupling products obtained under HSBM conditions.

Cross-coupling strategies are often plagued by the challenge of competitive homo-coupling reactions; thus, in the case of Sonogashira reactions there is the possibility that terminal alkynes react together generating dimeric coupling products. This side-reaction is known as the Glaser reaction and is quite important in the synthesis of materials, supramolecular chemistry, and

synthesis of natural products.[48] The solvent-free Glaser reaction was recently evaluated using the HSBM technique by Stolle et al. who after a meticulous study of the reaction conditions (milling auxiliary, base, air exposure (O_2), catalyst, etc.) applied it to the coupling of terminal alkynes **29** in the presence of CuI (5 mol%) using (1) KF–Al_2O_3 (γ-Al_2O_3, neutral, 60 wt% KF) or (2) DABCO and KF–Al_2O_3 with a lower KF loading, and subsequent oxidative regeneration of the Cu catalyst by exposure to air. The corresponding coupling products **30** were obtained with good to excellent yields in short reaction times through both protocols (equation 13).

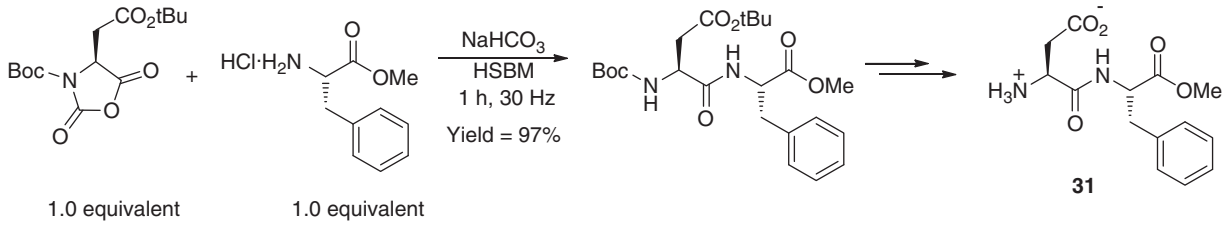


(13)

1. KF-Al_2O_3 (γ-Al_2O_3, neutral, 60 w% KF), 30 min air exposure
2. KF-Al_2O_3 (32 w%, commercial), DABCO

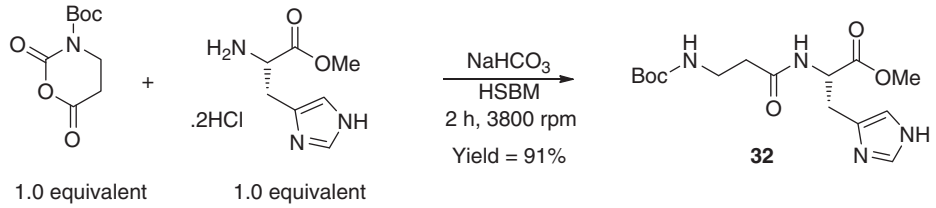
The very high mixing efficiency and energy content present in HSBM procedures make it as competitive as other alternatives (e.g., microwave activation) in solvent-free Sonogashira and Glaser reactions, affording the coupling products with high yields and selectivities under comparable reaction conditions. Additionally, the HSBM technique frequently reduced the required reaction times when compared with stirring protocols and offers the advantage of avoiding the pretreatment often present in microwave irradiation processess.[48,49]

The applicability of HSBM procedures has also been highlighted by Lamaty and coworkers in the first reported synthesis of α,α-dipeptides under solvent-free conditions.[50] The synthesis of peptides is an important and active field in the search of therapeutic agents; nevertheless the preparation of peptides is always associated with the use of large amounts of organic solvents. In the Lamaty's strategy, peptide bond formation is achieved by the coupling of urethane-protected α-amino acid *N*-carboxyanhydride (α-UNCA) derivatives with amino esters in the absence of any solvent. After 1 h of milling at 30 Hz the reaction afforded the desired dipeptides in high yield and with no epimerization. The method was also effective in the formation of tripeptide (Boc–Val–Ala–Gly–OMe), and its versatility was evident by the preparation of the commercially important dipeptide aspartame[51] (α-L-aspartyl-L-phenylalanine methyl ester) **31** (**Scheme 1**).



Scheme 1 Solvent-free synthesis of dipeptide aspartame.

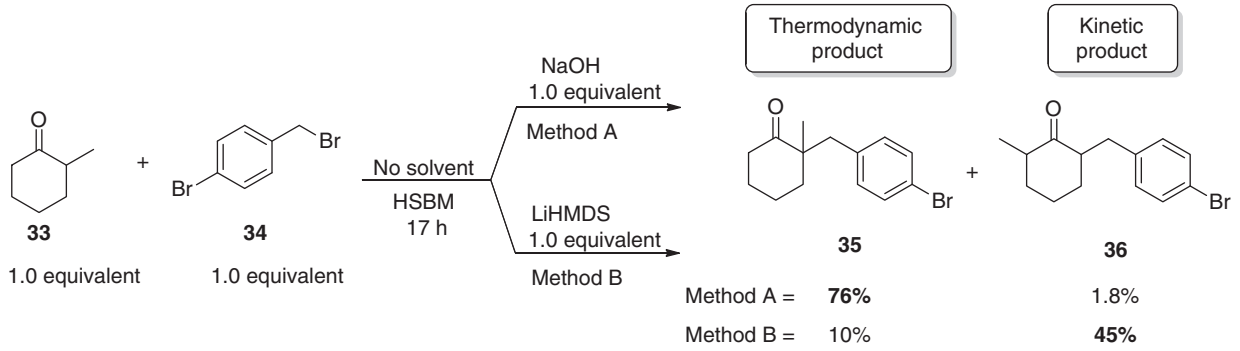
More recently, Hernández and Juaristi applied Lamaty's strategy for the high-yield synthesis of α,β-dipeptides and several novel β,β-dipeptides under solvent-free conditions, starting with urethane-protected β-amino acid *N*-carboxyanhydrides and α- or β-aminoesters.[52] An illustrative application of this strategy was the synthesis in high yield of *N*-Boc-L-carnosine-OMe **32**, a protected derivative of natural α,β-dipeptide L-carnosine (equation 14). L-Carnosine is an interesting compound which has proved to be an effective antiglycating agent, antioxidant, and hydroxyl radical scavenger.[53]



(14)

Ball-milled reactions are classified as high-energy procedures and their application under solvent-free conditions could be associated with processes that take place without chemical control and with low selectivity in comparison with solution chemistry. However, in some cases HSBM protocols show pronounced selectivity depending on reaction conditions. For example, it has been reported that under conventional reaction conditions in solution, bulky strong bases lead to the formation of kinetic enolates, whereas weaker bases generate the thermodynamic enolates. In contrast, in 2010 Mack et al. studied the relative formation of

kinetic versus thermodynamic enolates under solvent-free conditions using a ball mill,[54] finding that the reaction of 2-methylcyclohexanone **33** with *p*-bromobenzyl bromide **34** when catalyzed by NaOH (method A) afforded a mixture where thermodynamic alkylated product **35** was predominant. When the same process was carried out with lithium hexamethyldisilazide (LiHMDS, a strong bulky base, method B) the kinetic product **36** formed predominantly. This result shows that despite the fact that HSBM is an extremely high-energy technique it is possible to control the formation of a particular enolate by selection of the appropriated base, as long as similar reaction conditions (time, frequency, temperature) are maintained (equation 15).



(15)

Other examples of high selectivity in reactions activated with ball mills have been recently reported by Lamaty et al.[55] and Stolle and Thorwirth[56] during the preparation of unsaturated amino esters and enamines, respectively. Thus, Lamaty and coworkers reported a solvent-free synthesis of Boc-protected unsaturated amino esters in a ball mill starting from aminophosphoryl acetate **37** and diverse solid and liquid aldehydes **38**.[55] The reaction was catalyzed by Cs_2CO_3 or K_2CO_3 and after 7 h of milling at 550 rpm the corresponding amino esters **39** were obtained in good to high yield (61–95%) with high (*Z*)-selectivity (**Figure 2(a)**). However, Stolle and Thorwirth reported the fast ball-milled addition of amines **40** to dialkylacetylendicarboxylates or alkylpropiolates **41** in the absence of solvent.[56] After 5 min of milling at 13.3 Hz the addition products **42** were formed in high yield (81–96%) and the *E*/*Z* ratio depended of the substrates; (*E*)-isomers were always obtained in the reaction of dialkyl acetylenedicarboxylates and also in the addition of secondary alkyl amines to propiolates, whereas anilines and propiolates afforded the (*Z*)-isomers (**Figure 2(b)**). The formation of enamine was also evaluated by simple stirring in the absence of solvent; in that case the yield and *E*/*Z* selectivity were lower.

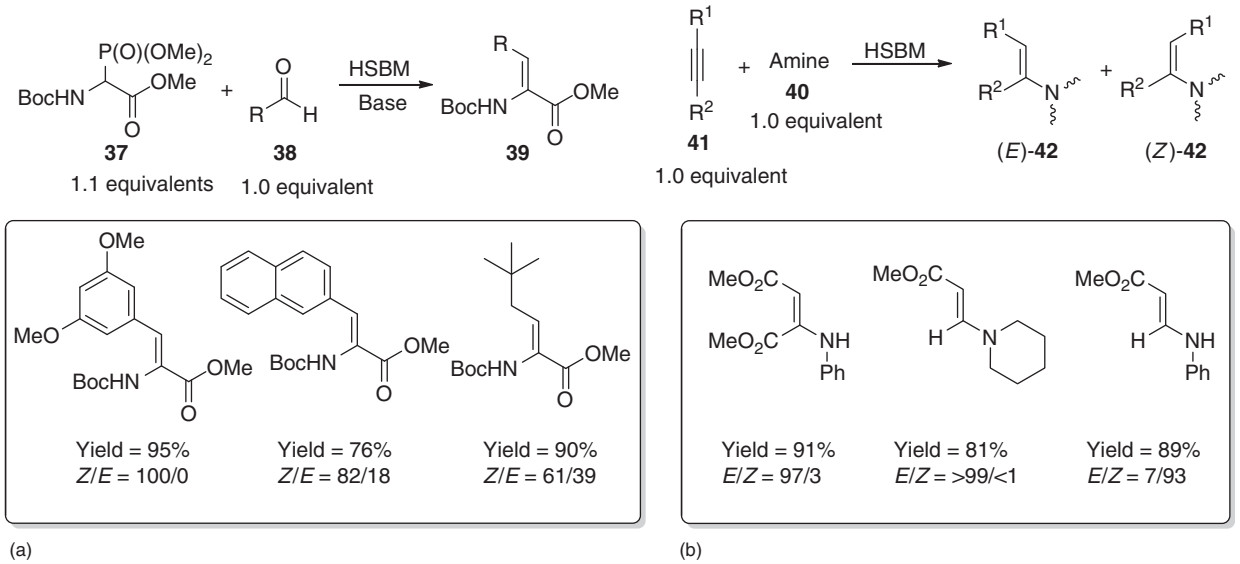
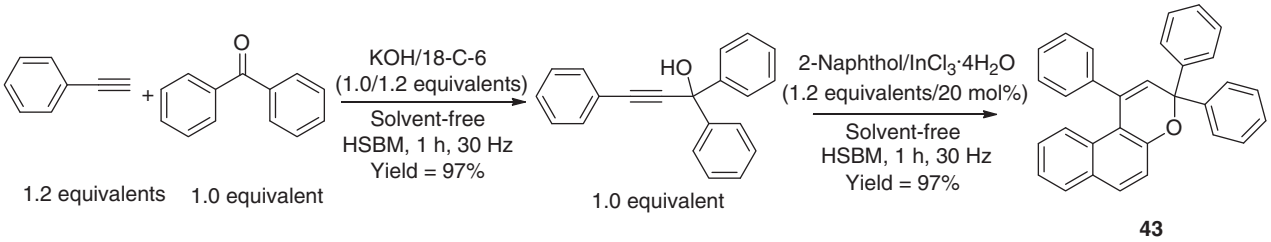


Figure 2 Amino esters **39** and enamines **42** obtained under solvent-free HSBM conditions.

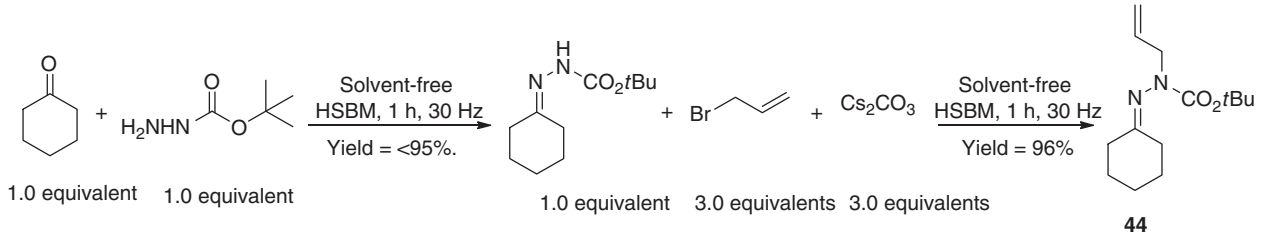
Individual solvent-free ball-milled protocols can also be combined to create an efficient mechanochemical sequential reaction, making it possible to reduce the traditional amount of solvent required in those procedures. In this regard, Wang and coworkers reported the preparation of naphthopyrans through a nucleophilic addition reaction of terminal alkynes to carbonyl compounds and the subsequent cyclization of propargylic alcohols with 2-naphthol.[57] In this work, both steps were efficiently carried out under ball-milling conditions. In the first step the reaction starting with alkynes, diverse ketones, and KOH in the presence of

18-crown-6 was performed in a ball mill and afforded the corresponding alcohols in short reaction times and with moderate to high yields (54–97%). Following a column chromatography separation, the resulting alcohols were subjected to a ball-milled cyclization reaction with 2-naphthol using a catalytic amount of $InCl_3 \cdot 4H_2O$ to give the naphthopyran derivatives in good to excellent yields (76–97%) (Scheme 2).



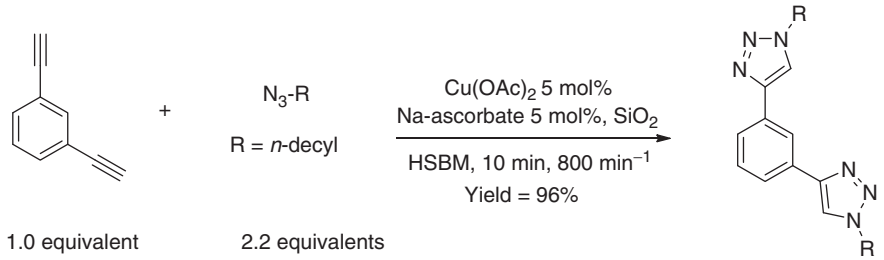
Scheme 2 Two-step ball-milled synthesis of naphthopyran **43** under solvent-free conditions.

In a more recent article, Lamaty et al. described the preparation of protected hydrazones and their subsequent *N*-alkylation, both solvent-free processes under ball-milling conditions.[58] The synthesis of hydrazones was achieved by milling several aldehydes or ketones and hydrazine derivatives obtaining the desired products in quantitative yield. Subsequently, without the need of any purification process the hydrazones were subjected to an alkylation procedure using allyl or phenyl bromide and Cs_2CO_3. After 1 h at 30 Hz the reaction afforded the expected *N*-alkylated products in high yields (85–96%) (Scheme 3). In summary, the aforementioned works[57–58] demonstrated how ball-milled protocols may be combined to obtain the products of several transformations, avoiding the use of large amounts of volatile (contaminating) solvents during the purification steps.



Scheme 3 Synthesis of *N*-alkylated hydrazone **44** under solvent-free HSBM conditions.

One of the most popular 'click' reactions is the so-called Huisgen cycloaddition, a 1,3-dipolar cycloaddition between an azide and a terminal or internal alkyne to give a 1,2,3-triazole. This reaction has demonstrated its potential in diverse fields such as drug discovery, material science, supramolecular chemistry, and modification of biomolecules among others.[59] In 2011 Stolle and coworkers reported the solvent-free Huisgen 1,3-dipolar cycloaddition between alkynes and azides catalyzed by $Cu(OAc)_2$ under HSBM conditions. After 10 min at 800 rpm the reaction afforded the corresponding triazoles with high conversion and selectivity.[60] The method was also successful using electron-poor alkynes, propargyl-functionalized polystyrene, or bis-ethynyl benzenes (equation 16). Additionally, it is worth mentioning that despite the fact that low-molecular weight azides tend to be unstable and are classified as highly explosive by shock, the cycloaddition reaction under HSBM conditions ('high-energy procedure') was totally safe when using decyl-, mesityl-, benzyl-, and adamantly azide derivatives.



(16)

In addition to triazoles, other heterocyclic systems have been successfully prepared by ball-milling procedures; in particular, solvent-free one-pot reactions are some of the most effective strategies for the synthesis of complex molecular structures. By carrying out multiple chemical steps sequentially in a single reaction vessel, these protocols avoid the time and cost-consuming steps of protection and deprotection, as well as the corresponding work-up procedures. Furthermore, solvent-free one-pot methods minimize or avoid the generation of waste associated with the purification of intermediates. In this sense, in 2009

Naimi-Jamal and Mashkouri described the solvent-free synthesis of pyrano[2,3-d]pyrimidine-2,4(1*H*,3*H*)-diones without any catalyst in a ball mill. The one-pot reaction was performed by milling a stoichiometric mixture of several aldehydes, malononitrile, and barbituric acid, generating the corresponding products in quantitative yield after 15–90 min of milling at 96 °C, and using a double-walled ball mill beaker equipped with fittings for circulating hot water.[61] However, Wang and Gao recently reported a one-pot and solvent-free reaction between dimedone and various aldehydes to selectively create spiro dihydrofurans. These reactions employed DMAP as activating agent and were further catalyzed by iodine in a ball mill, affording the furan derivatives after 1 h of milling in high yield (77–92%).[62] Finally, very recently Khaligh developed a highly efficient multicomponent reaction between 2-hydroxynaphthalene-1,4-dione, aromatic aldehydes, and 2*H*-indene-1,3-dione.[63] The one-pot condensation in the presence of poly(4-vinylpyridinium) hydrogen sulfate as a solid acid catalyst was carried out in a ball mill during 90 min at 100 °C. The solvent-free protocol was able to afford the indeno-fused naphthopyranones in high to excellent yield (84–92%). Furthermore, this HSBM method allowed the recovery and recycling of catalyst by simple filtration, and subsequent runs showed no decrease in activity (**Figure 3**).

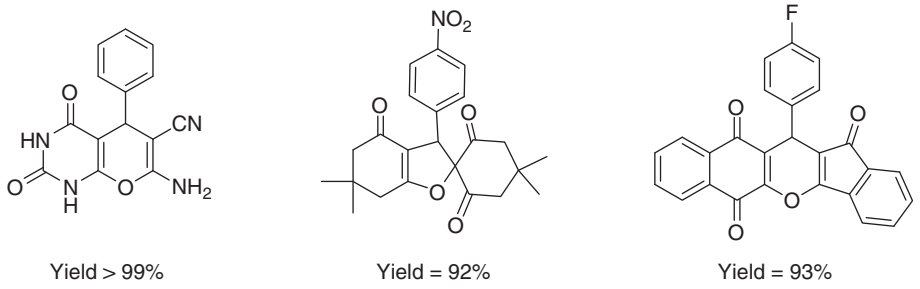
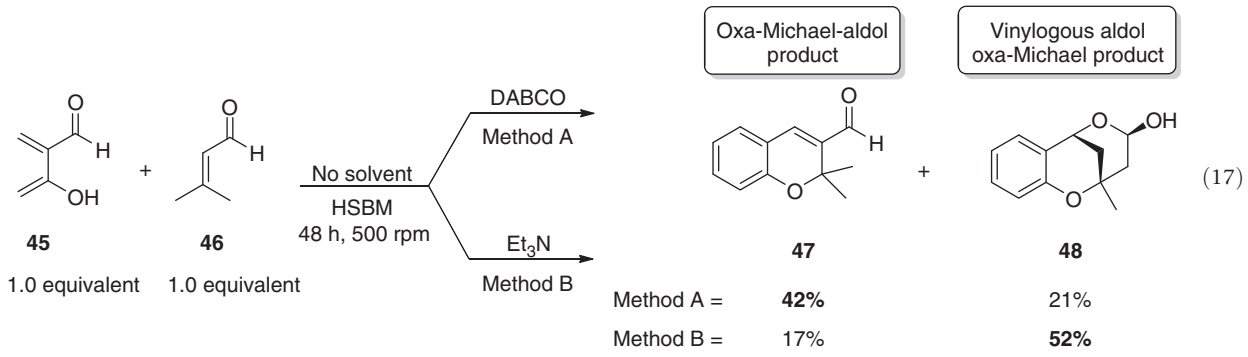


Figure 3 Examples of heterocycles synthesized by solvent-free ball-milled one-pot reactions.

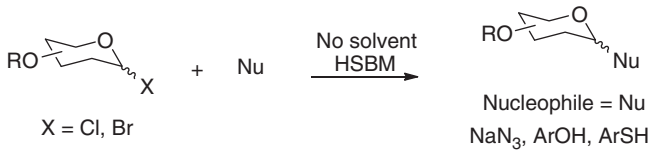
Recently, other interesting heterocyclic compounds have been obtained under solvent-free ball-milled protocols. Salient examples include benzofuranone derivatives, substituted pyrazolines, and dibenzophenazines, which were obtained by cycloaddition, cyclization, and condensation reactions, respectively.[64–66]

Solvent-free domino reactions have also been carried out under HSBM. For example, Bräse et al. optimized the reaction parameters (ratio of the reactants, the frequency of the mill, the number of balls, and milling time) in the oxa-Michael-aldol process between salicylaldehyde **45** and cyclohexenone. Additionally, the chemioselectivity of the domino reaction was examined using prenal **46** instead cyclohexenone. Under these conditions, it was possible to obtain two different products: xanthone **47** (through an oxa-Michael-aldol reaction) or dihydrobenzopyran **48** (via vinylogous aldol reaction followed by oxa-Michael addition).[67] Choosing the appropriate base, the solvent-free ball-milled procedure could produce mainly one of the products. Interestingly, the same chemoselectivity was observed when using H_2O–dioxane as reaction medium. Nevertheless, under HSBM and using triethylamine as base, product **48** was obtained in higher yield (equation 17).



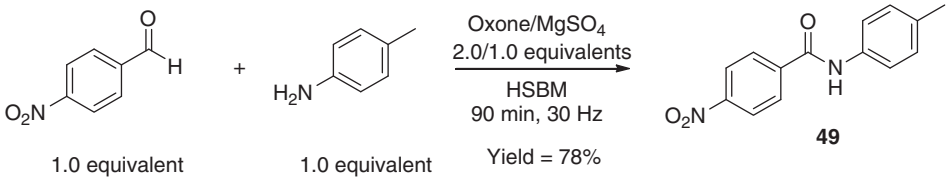
(17)

Nucleophilic substitution is one of the basic processes in classical synthetic organic chemistry. Traditionally, substitution reactions are performed in solution; however, highly efficient solvent-free procedures under HSBM conditions have recently been reported. For example, Mack and coworkers developed a method for conducting the substitution reaction between *p*-bromobenzyl bromide and nucleophilic ionic reagents using HSBM 'in the absence of a phase-transfer catalyst.'[68] Furthermore, the solvent-free substitution strategy has been applied in the synthesis of glycosyl azides, aryl glycosides, and thioglycosides, which are valuable compounds used in oligosaccharide synthesis, through the reaction of glycosyl halide and the respective nucleophile in a ball mill (equation 18).[69–71]



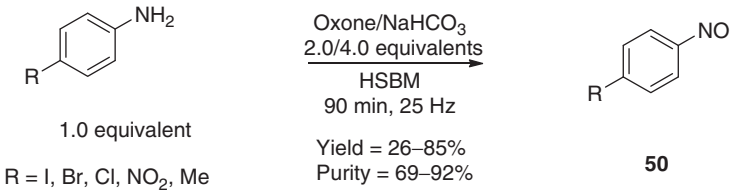
(18)

By the same token, other interesting ball-milled transformations in the absence of solvent have been reported in the past 5 years. Representative examples include Tishchenko[72] and dehydrogenation reactions,[73] Diels–Alder cycloadditions,[74] bromination protocols,[75] oxidation reactions,[76] as well as the synthesis of supramolecular assemblies,[77] and transesterification procedures.[78] Particularly remarkable is the synthesis of amides recently reported by Wang and Gao through oxidative amidation of aryl aldehydes with anilines under HSBM conditions.[79] This solvent-free procedure was catalyzed by Oxone (potassium hydrogen peroxosulphate), an efficient oxidant. After 90 min of milling at 30 Hz the one-pot oxidation protocol afforded the corresponding amides in moderate to good yields (38–78%). This method works especially well when using electron-rich anilines and aromatic aldehydes containing electron-withdrawing groups (equation 19).



(19)

To finalize this section, it is important to mention that all the abovementioned solvent-free reactions are not necessarily processes that take place in the total absence of solvent. In the great majority of examples, with the exception of solvent-free, stoichiometric, quantitative, catalyst-free cases,[22] a purification step is always required (e.g., chromatography, crystallization, filtration, or extraction) in which organic solvents are usually employed. Nevertheless, it should be mentioned that very recently Halasz and coworkers described the solvent-free oxidation of anilines into nitrosobenzenes in a ball mill, and the subsequent solvent-free product isolation by sublimation, taking advantage of the high vapor pressures of nitrosobenzenes.[80a] The oxidation procedure was carried out using Oxone as oxidizing agent in the presence of $NaHCO_3$. Thus, after 20–30 min of milling the reaction mixture was sublimed under reduced pressure to afford nitrosobenzenes **50** in moderate to good yields, and with good purity after sublimation (equation 20). This purification strategy is a very valuable approach because it converts a single solvent-free reaction into an overall solvent-free process. In the same way, recently Mack et al. reported a ball-milled Horner–Wadsworth–Emmons reaction in the absence of solvent; in that case the corresponding products were successfully isolated using a chromatography-free method.[80b]



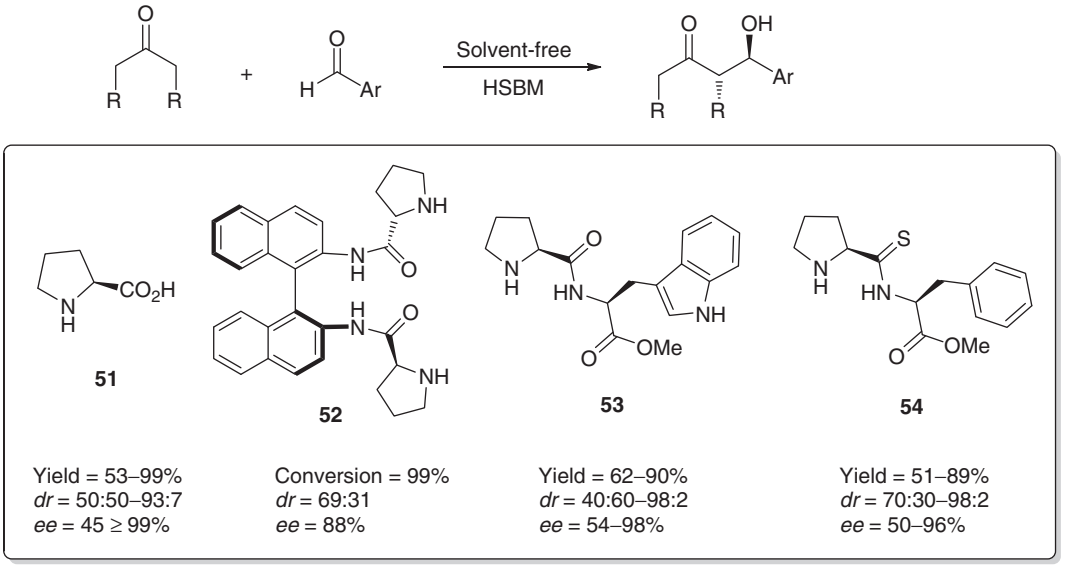
(20)

9.11.2.3 Organocatalyzed Reactions in Solvent-Free Ball-Milling Conditions

Organocatalytic reactions are chemical transformations catalyzed essentially by a nonmetal-containing, relatively small organic molecule. In the past years, nonasymmetric[81] and asymmetric[82] organocatalyzed reactions have demonstrated to be one very valuable alternative for the preparation of commercially important substances such as natural products, drugs, and fragrances, among others.

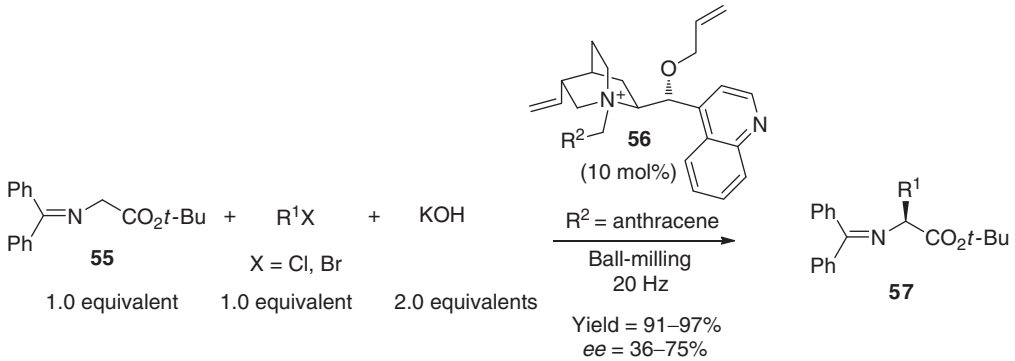
In particular, the fact that organocatalysis avoids the use of a metal means that organocatalytic processes are sustainable alternatives to accelerate and render more efficient chemical reactions. Furthermore, during the past decade diverse experimental protocols have turned organocatalysis even safer and 'greener,' in particular by the use of unconventional reaction media[10] or by the application of solvent-free procedures.[83] In this context, the HSBM technique has contributed to the growth of this area, starting with the pioneering work of Bolm et al., who reported the asymmetric aldol reaction catalyzed by (*S*)-proline **51** (10 mol%) under solvent-free conditions.[84] The reaction proceeded efficiently to give the *anti*-aldol products in high yields and with up to 99% enantiomeric excess (*ee*). In addition, the reaction took place in shorter reaction times and with higher chemical yields and stereoselectivity, in comparison with the same reaction carried out under traditional magnetic or mechanic stirring.[84] In this regard, Nájera and coworkers evaluated the activity of (S_a)-binam-L-prolinamide **52** as organocatalyst in solvent-free ball-milled aldol reactions.[85] More recently, Hernández and Juaristi reported the solvent-free asymmetric aldol reaction

between representative ketones and various aromatic aldehydes catalyzed by (*S*,*S*)-dipeptide **53** and (*S*,*S*)-thiodipeptide **54**.[86–88] In general, the ball-milled reaction proceeds efficiently, affording the *anti*-aldol products with good diastereo- and enantioselectivity (equation 21).



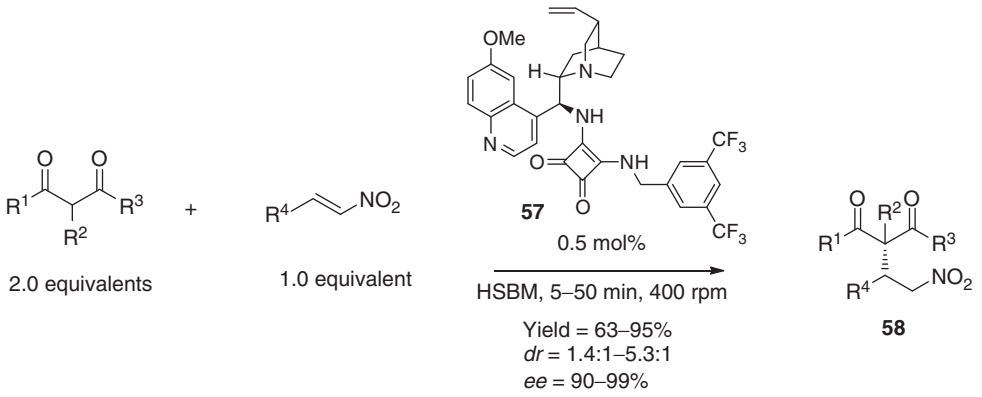
(21)

Other organocatalyzed asymmetric processes have also been reported under solvent-free condition using HSBM. In 2012, Lamaty and coworkers reported the enantioselective reaction of the Schiff base of glycine *tert*-butyl ester **55** with several electrophiles under basic conditions, using a chiral ammonium salt derived from cinchonidine **56** (10 mol%).[89] The solvent-free asymmetric phase-transfer process under ball-milling conditions afforded the desired alkylated products **57** (precursors of enantioenriched α-amino acids), in excellent yields and with moderate to good enantioselectivities (equation 22).



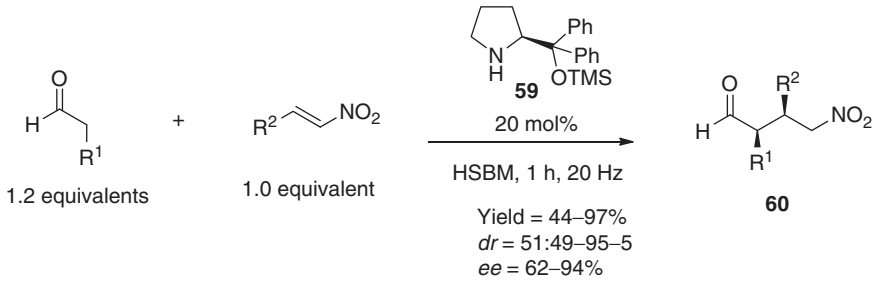
(22)

Very recently, Xu et al.[90] and Šebesta et al.[91] independently reported the solvent-free asymmetric organocatalyzed Michael addition in a ball mill. Xu et al. examined the conjugated addition reaction of 1,3-dicarbonyl compounds to nitroolefins under solvent-free conditions.[90] In the event, the reaction catalyzed by the bifunctional cinchona-based squaramide derivative **57** (0.5 mol%) afforded the corresponding adducts **58** in very short milling times and with high yields and stereoselectivities (equation 23).



(23)

However, Šebesta and coworkers studied the Michael addition of aldehydes to nitroalkenes under HSBM conditions.[91] After screening diverse pyrrolidine-derived organocatalysts, and comparing traditional versus the ball-milling technique, it became evident that HSBM afforded the desired products in higher yield and with better stereoselectivity in shorter reaction times. In particular, the most efficient organocatalyst turned out to be the Hayashi–Jorgensen catalyst **59** (20 mol%), which allowed the formation of the corresponding addition products in good yields using essentially stoichiometric amounts of reactants. Under solvent-free conditions the reaction proceeded efficiently to give mainly the *syn*-products **60** with high *ee* (equation 24).



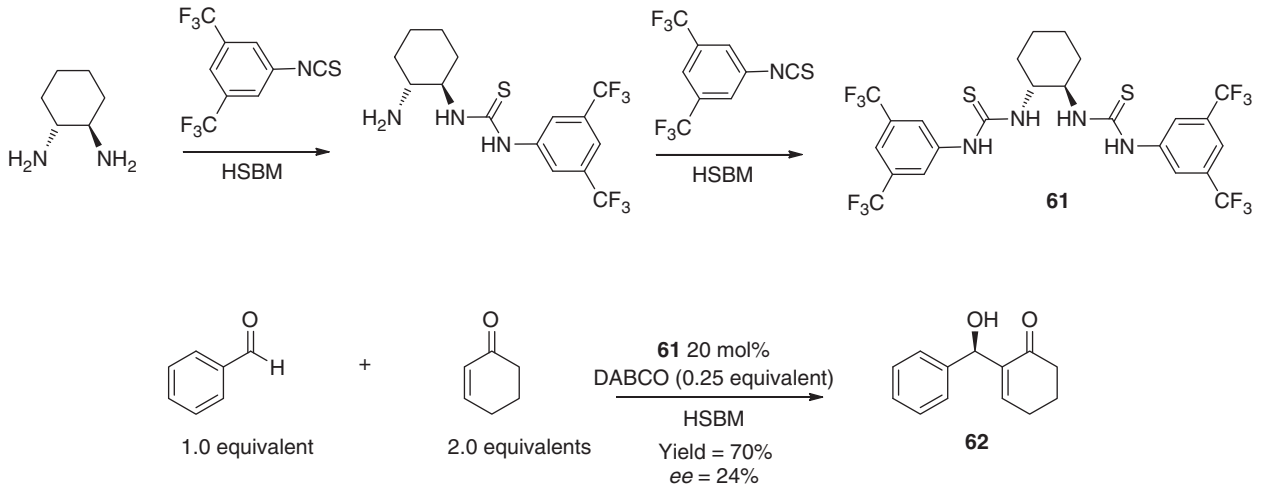
(24)

Finally, in 2012 Friščić et al.[92] reported the quantitative preparation of mono- and bis-thioureas by the reaction of aromatic and aliphatic diamines with aromatic isothiocyanates using the HSBM technique. Particularly interesting is that the method could be applied in the efficient synthesis of chiral bis-thiourea **61**, which was subsequently evaluated as organocatalyst in the Morita–Baylis–Hillman reaction affording product **62** (Scheme 4). Although stereoinduction using thiourea **61** was low, the ability to create a totally mechanochemical procedure to synthesize the catalyst and perform the organocatalytic reaction under solvent-free conditions is a real advancement in the quest for making organocatalysis a truly sustainable synthetic tool.

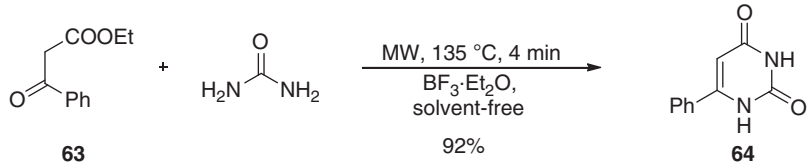
9.11.3 Microwave Irradiation Under Solvent-Free Conditions

The use of microwave irradiation in organic synthesis has increased significantly in recent years not only because of the large variety of processes that can be carried out with microwave activation, but also because of the advantages it offers: (1) high yields and purities of the obtained products, (2) short reaction times, and (3) substantial energy savings (*see* Chapter 9.10).[93] This chemistry is characterized by an incredibly accelerated heating of the reaction mixture that cannot be achieved by classical heating techniques, allowing the reduction of reaction times under mild conditions. If the reaction is run in a closed vessel it will generate an increment in the pressure of the system which might be beneficial, especially in condensation reactions. Microwave irradiation is electromagnetic irradiation operating in the range of 0.3 to 300 GHz. This energy input is too low to break bonds, so there is no way for microwaves to induce chemical reactions that would be different to the ones proceeding under thermal activation. The phenomenon depends on the ability of certain materials to absorb this type of energy and transform it into heat.[94]

Microwave chemistry has resulted in multiple applications such as solventless reactions, peptide synthesis, polymer chemistry, cycloaddition reactions, catalysis, and combinatorial chemistry, just to enlist some of them.[94] One example showing how a solventless process can be improved by the use of microwave activation was reported in 2012 by Kundu et al.[95] This work consists in the synthesis of uracil and cytosine derivatives from β-ketoesters and urea in the presence of a Lewis acid. Salient results were obtained with substrate **63** and urea with $BF_3 \bullet Et_2O$ acid catalysis to give product **64** in good yields, in very short reaction times (equation 25).

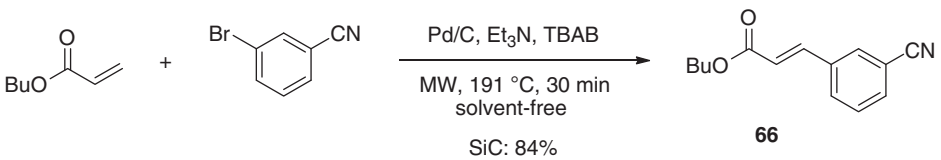


Scheme 4 Synthesis and application of thiourea organocatalyst **61** under HSBM conditions.



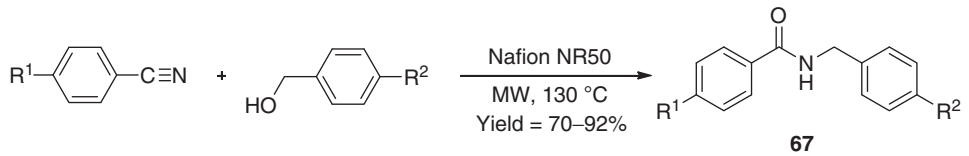
(25)

In recent years there has been some controversy regarding the way by which microwave irradiation enhances chemical reactivity. Microwaves act as electromagnetic fields that heat a specific material containing mobile charges (polar substances) – this is called the nonthermal effect. Nevertheless, Kappe and coworkers[96] demonstrated that for some chemical processes, the electromagnetic effect (nonthermal effect) is not the determining factor for the reaction to proceed; instead, the thermal effect would be the only one responsible. A particular development involves the use of silicon carbide (SiC) vessels to eliminate the nonthermal effect from the reaction system. SiC has the ability to completely absorb microwave irradiation and transform it into heat in a very effective way, so that an autoclave effect can be achieved. Kappe and coworkers applied this strategy to a particular group of reactions: Mizoroki–Heck couplings, triphenylphosphine alkylation, the Newman–Kwart rearrangement, and Claisen's rearrangement. Equation 26 illustrates a particular example of the Mizoroki–Heck coupling reaction that was carried out under solvent-free conditions and purely thermal activation.[96]



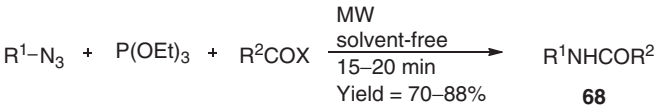
(26)

Amides are the most essential segments in natural products such as peptides and proteins, and can also be found in a variety of synthetic materials.[97] There are various coupling agents that facilitate the coupling condensation reaction between a carboxylic acid and an amine.[98,99] In 1948, Ritter reported an efficient protocol for the synthesis of amides through the reaction of alkenes and nitriles.[100] Later, the groups of Jaouen[101] and Iqbal,[102] reported the use of alcohols instead of alkenes for this reaction. Recently, Polshettiwar and Varma reported a Nafion® NF50-catalyzed Ritter reaction assisted by microwave irradiation[103] (equation 27). This solid catalytic support may be reused up to six times without change of its activity, its toxicity is very low, and it is also inexpensive. The yields of amides **67** obtained by this method varied from good to excellent after 30 min under microwave irradiation. An extra bonus of the use of Nafion® NF50 consists in the fact that it is easily removed from the reaction mixture and only requires a washing with acetone to be reused in the next cycle.



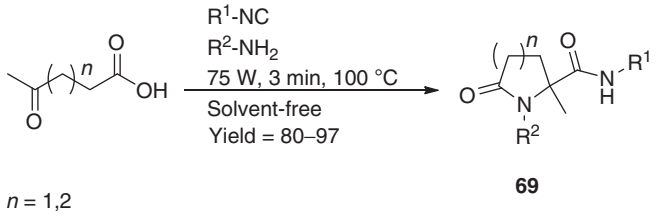
(27)

Another very recent example of the application of microwave irradiation for the synthesis of amides is the protocol reported by Ponnuswamy and coworkers.[104] In this work, these researchers performed a microwave-assisted aza-Wittig coupling reaction between azides and carboxylic acids under solvent-free conditions to obtain a large variety of amides **68**. The main advantage of this method is that the reactions come to completion in very short reaction times (15–30 min) in comparison with traditional heating (up to 3 days under reflux). When triphenylphosphine was changed to triethyl phosphite, the isolation of the desired products was even easier[105] (equation 28). The reactions were performed at 100–150 °C.



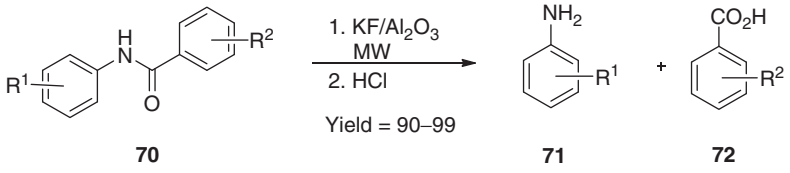
(28)

The synthesis of heterocyclic molecules has received increased attention in recent years. In this sense, there are various reports of the synthesis of this kind of compounds which combine microwave irradiation and solventless conditions.[106,107] In this sense, the Ugi reaction is a good example of a multicomponent reaction with industrial application.[108,109] In 2010, Deprez and coworkers[110] reported the synthesis of five- and six-membered lactam heterocycles via the Ugi reaction employing microwaves (equation 29). The best results were obtained with 75 W at 100 °C to obtain the desired lactam **69** with good to excellent yields within 3 min.



(29)

Another important reaction type in organic synthesis is amide hydrolysis, since amides are usual protecting groups for amines. These reactions often involve aggressive reaction conditions that often give the desired product in moderate yield. There are numerous reports of the use of KF–Alumina in various hydrolysis protocols. This versatile reagent allowed for amide hydrolysis to proceed in solvent-free media under microwave irradiation, as shown in Lei and coworkers' protocol (equation 30).[111] The reaction can be performed with conventional heating although reaction times turn out to be too long. The microwave procedure is very simple; the amide is mixed with the doped alumina and stirred for a while at room temperature. Then, the flask with the mixture is placed in a 900 W microwave oven and irradiated for 4 min at 100% power. Standard acid/base extraction work-up procedures for the isolation of the amine **71** and the carboxylic acid **72**, afforded both products in excellent yields. This method was performed with a variety of aromatic amides **70**.

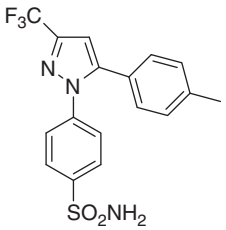


(30)

Pyrazoles are present in many important molecules with pharmaceutical and agrochemical relevance. Some remarkable examples of this kind of compounds are Celecoxib (Celebrex), a nonsteroidal antiinflammatory and analgesic,[112] as well as Fenpyroxymate, and Cyenopyrafen, which have pesticide activity as acaricides (**Figure 4**).[113]

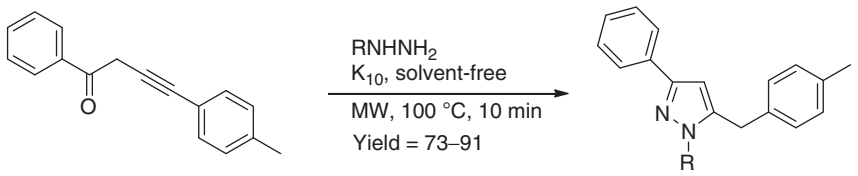
There are several methods for the synthesis of pyrazoles. One of the most common involves an intermolecular cycloaddition reaction between hydrazines and 1,3-dicarbonyl compounds. However, the use of dissymmetric diketones gives a mixture of regioisomers. In this sense, Török and Dembinski's research groups recently developed a regioselective procedure for the synthesis of 5-benzyl substituted pyrazoles.[114] This procedure consists in a cycloaddition reaction between phenyl or *p*-tolyl substituted butynones and several hydrazines under solvent-free conditions and microwave irradiation. Several catalysts were probed, such as Ambelyst-15 and Nafion-H; however, best results were observed with the use of montmorillonite K-10. A group of different 5-aryl substituted pyrazoles **73** were obtained by this method, with good to excellent yields and regioselectivity (equation 31).





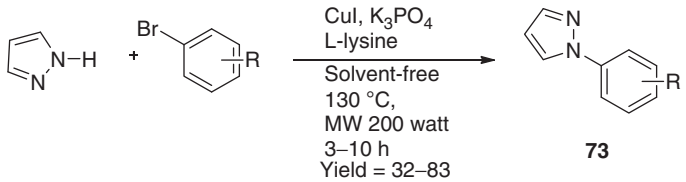
Celecoxib
(Celebrex)

Figure 4 Examples of pyrazoles with biological activity.



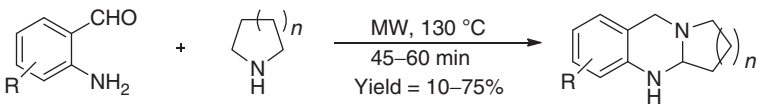
73 (31)

In 2009, Chan and Chow reported the *N*-arylation of imidazole and pyrazole with aryl bromides under solvent-free conditions and microwave irradiation.[115] The catalysts employed were L-amino acids and copper(I) iodide. The reactions were performed with one equivalent of the aryl bromide, 1.2 equivalents of imidazole or pyrazole, 10 mol% of CuI, 20 mol% of the L-amino acid (best results were obtained with L-lysine) and 2 equivalents of K_3PO_4 in a sealed vessel at 130 °C under microwave irradiation for 3–10 h (equation 32). The presence of the amino acid is necessary; otherwise the yield was rather poor.



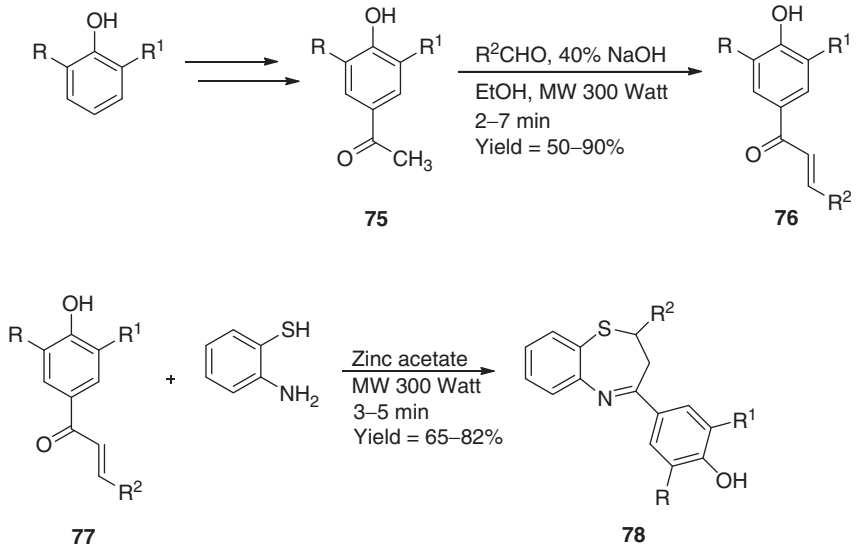
73 (32)

Other group of relevant heterocyclic compounds present in several natural products are ring-fused aminals,[116] which present potential biological activity.[117] Polshettiwar and Varma reported in 2008 the use of microwaves in the synthesis of ring-fused aminals without the need of any catalyst.[118] The method consists of the α-amination of pyrrolidine with 2-amino benzaldehydes (equation 33). The reactions were performed with many aldehyde substrates and cyclic amines at 130 °C. When ethanol was used as solvent the reaction proceeded with 30% conversion after 30 min; nevertheless, in the absence of solvent the reactions afforded the desired products **74** in higher yields.



74 (33)

Benzodiazepines are well known for their relevant activity at the central nervous system (CNS); indeed, several widely used anticonvulsants and antidepressant agents present this structure. Related to this family of compounds are benzothiazepines, which have similar activity in the CNS. Recently, Nikalje and Vyawahare reported a green synthesis of 2,4-substituted-2,3-dihydro-1,5-benzothiazepine derivatives (Scheme 5).[119] First of all, dichloroacetophenones **75** were prepared to serve as substrates in the preparation of chalcones **76**, by a solvent-phase protocol. The final cyclo-condensation step with the appropriate amino thiophenol was carried out with zinc acetate as catalyst, under solvent-free conditions. Both reactions were performed under microwave irradiation with very short reaction times.

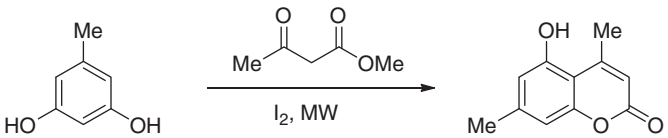


Scheme 5 Synthetic route to benzothiazepines **78**.

A salient example of how microwave irradiation may shorten reaction times is the coumarin synthesis reported by Prajapati and Gohain in 2007.[120] In this work is presented a comparison between experimental protocols at room temperature, either under conventional heating or with microwave irradiation. The reaction chosen in study was a von Pechmann condensation of different phenols and ethyl acetoacetate in the presence of elemental iodine as catalyst. Although this reaction proceeds at room temperature, when it is performed with conventional heating (in acetonitrile as solvent at 80 °C), reaction times became shorter – within few minutes – and yields higher when carried out using microwave irradiation (at 110 °C). Table 5 summarizes the results for the condensation reaction between resorcinol and ethyl acetoacetate leading to the formation of coumarin **79**.

Table 5 Synthesis of coumarin **79** via von Perchmann condensation[120]

MW		*Thermal heating*		*Room temperature*	
Reaction time (min)	*Yield (%)*	*Reaction time (h)*	*Yield (%)*	*Reaction time (h)*	*Yield (%)*
2.5	96	1.5	91	5.0	70



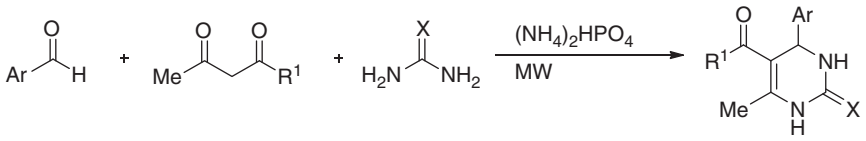
79

Very recently, Bhuiyan[121] reported a convenient, solvent-free multicomponent Biginelli reaction to obtain commercially-valuable dihydropyrimidinones **80**. The three-component condensation [aldehyde, 1,3-dicarbonyl compound and (thio)urea] was promoted by the readily accessible and nonexpensive diammonium hydrogen phosphate acid under microwave irradiation and under solvent-free conditions. This reaction had been previously catalyzed by strong Brönsted or Lewis acids, which in both cases

can lead to functional group incompatibility. The present strategy was useful for the preparation of a variety of aromatic aldehydes (Table 6).

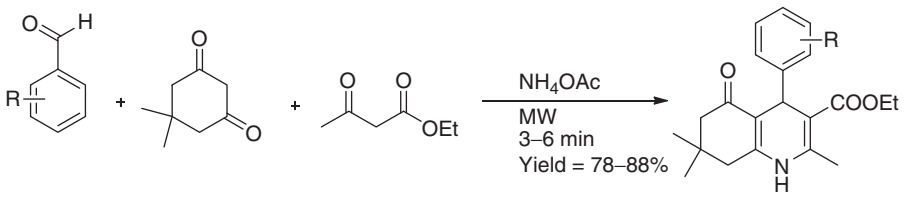
Table 6 Solvent-free synthesis of dihydropyrimidinones using $(NH_4)_2HPO_4$ as catalyst, and under microwave irradiation

R^1	X	Reaction time (min)	Yield (%)
EtO	O	2	96
EtO	S	1.5	85
EtO	S	1.5	95
Me	S	1.5	90
Me	S	2	84



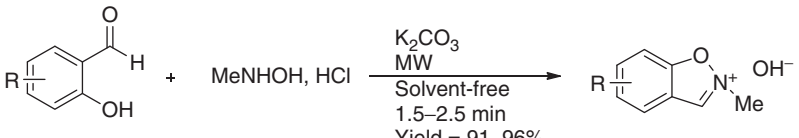
80

Another useful multicomponent reaction was reported by Hajra et al.[122] for the synthesis of polyhydroquinolines **81** under solvent-free conditions. Thus, the condensation of aromatic aldehydes with dimedone, ethyl acetoacetate and ammonium acetate was performed in a microwave reactor at 90 °C with reaction times lesser than 6 min. This protocol also avoids the use of a catalyst, and chromatographic separation. The simplicity of the method makes it amenable for industrial scale up (equation 34).



81 (34)

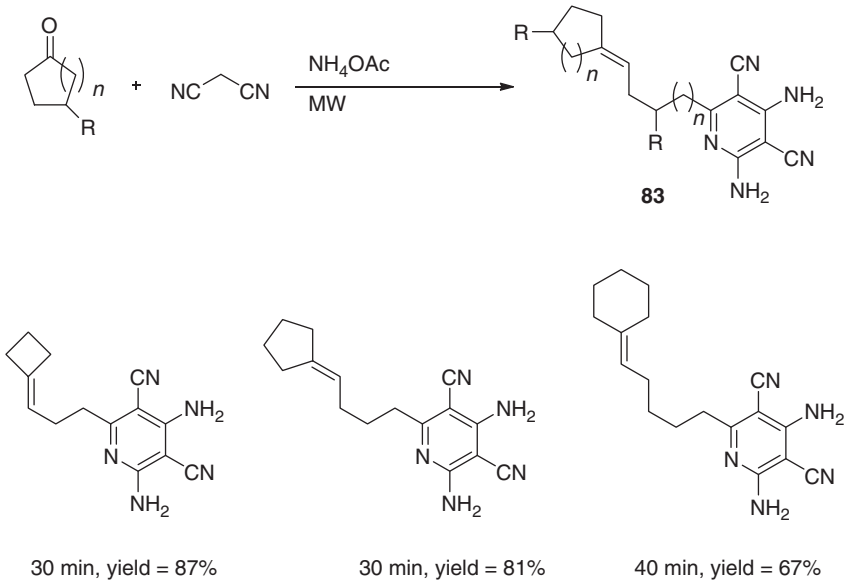
It is clear that microwave irradiation has gained popularity in the organic synthesis field because of its increased efficacy in a great number of reactions. Indeed, by the use of microwaves, a particular synthetic procedure may afford the desired product with high yield and purity, in short reaction times. These advantages make microwave synthesis highly attractive for industrial applications, especially in combination with solvent-free protocols. In this regard, recently Valizaeh et al.[123] reported a microwave irradiated synthesis of methylbenzo(d)isoxazolium hydroxides in the absence of solvent within excellent yields (equation 35). The reaction consists in a condensation reaction of monosubstituted hydroxylamines with salicylaldehydes catalyzed by potassium carbonate. This method is fast and products **82** are obtained with high purity, so further purification is not required.



82 (35)

R = H, 5-Br, 3-OH, 4-OH

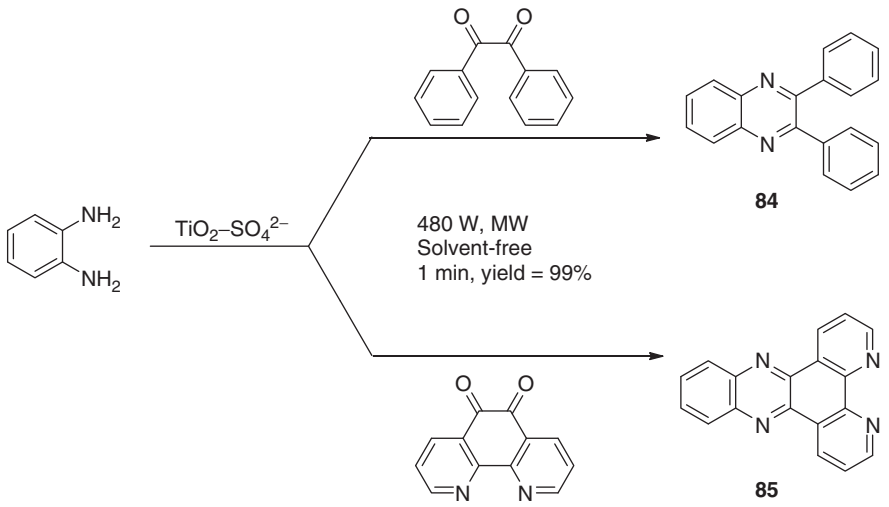
Also very recently, Tu and coworkers reported an efficient method for the synthesis of functionalized pyridines.[124] This method involves a domino reaction in which five σ bonds are formed under microwave irradiation and solvent-free conditions. As illustrative example, the four-component domino reaction between malononitrile, various cyclic ketones and ammonium acetate is depicted in equation 36. Several pyridine derivatives **83** were synthetized by this protocol, observing that when small cycloketones were used (cyclobutanone and cyclopentanone) the reaction times were shorter and yields higher relative to cyclohexanone as substrate (Figure 5). This procedure presents additional advantages: the only significant byproduct is water, and the work-up procedure only requires filtration.



(36)

Figure 5 Examples of the pyridine derivatives obtained via solvent-free domino synthesis.[124]

A further example of solvent-free, microwave-assisted synthesis of commercially important nitrogen-containing heterocyclic compounds was reported by Krishnakumar and Swaminathan in 2011.[125] This work uses a solid TiO_2–SO_4^{2-} catalyst for the synthesis of quinoxalines and dipyridophenazines. Compounds of the quinoxaline family are of synthetic interest because of their biological activity as antimycotics, antibacterials, antihelmintics, antidepressants, and antitumor agents, whereas dipyridophenazines have been used for the formations of ligand complexes of value in synthesis. The reaction has been performed with other catalysts and in solvent media, but the Krishnakumar and Swaminathan protocol has the advantage that the catalyst can be recovered by simple filtration and the products are formed within few minutes at 480 W of microwave irradiation. This reaction was tested with different substrates, observing excellent yields and very short reaction times of 1–8 min. As an illustrative example, equation 37 shows the reaction of *o*-phenylenediamine with benzyldiketone to obtain quinoxaline **84**, as well as the reaction of the same diamine with 1,10-phenanthroline-5,6-dione affording dipyridophenazine **85**. In both cases the desired product was obtained in almost quantitative yield in just one minute.



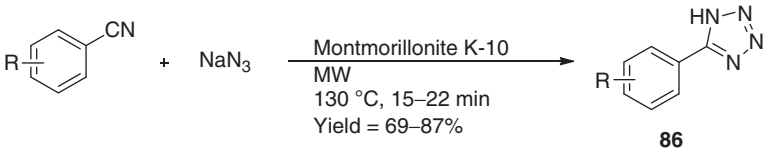
(37)

Zare and coworkers reported a similar method for the synthesis of quinolines. These molecules are of biological interest because of their antimalarial, antiasthmatic, antihypertensive, and antibacterial properties. This reaction is catalyzed by silica nanoparticles under microwave irradiation and solvent-free conditions obtaining the desired quinolines in excellent yields and short reaction times.[126] However, Hamidian and coworkers[127] used nanosilica sulfuric acid obtained from nano-SiO_2 as catalyst for a one-pot synthesis of triazolo[1,2-a]indazole-triones. In this case, the reaction products were obtained within 10 min, affording the products of interest in excellent yields.

In this context, the use of heterogeneous catalysts is attractive because of their easy removal and recovery. A salient example of the use of heterogeneous solid catalysts was reported by Phukan and Devi[128] in 2011 in the synthesis of 2-nitroimidazoles with biological activity. For instance, the reaction of 2-aminoimidazoles with $NaNO_2$ in the absence of solvent and catalyzed by natural clay was performed using microwave irradiation to give the expected 2-nitroimidazoles in moderate to good yields after 10–25 min. The 2-aminoimidazoles used as starting materials were previously obtained via the reaction of *O*-methyl-*iso*-urea with acetals or ketals, employing the same natural clay and 5–10 min irradiation with microwaves.[129]

Montmorillonite K-10 is also widely used as solid catalyst in heterogeneous, solvent-free reactions activated by microwave irradiation. For example, Törökand and coworkers[130] reported in 2008 a one-pot solvent-free, microwave-assisted synthesis of isobenzofuran-1(3*H*)-ones. More recently, in 2011, Marvi and coworkers[131] used this same heterogeneous catalyst for the synthesis of 5-substituted 1*H*-tetrazoles in a solvent-free procedure under microwave irradiation.

Although tetrazoles are nonnatural products, they are of industrial relevance because of their applications in pharmaceuticals, photography, explosives, and materials science. In this context, the reaction of different benzonitriles with sodium azide was catalyzed by Montmorillonite K-10 in a solvent-free medium when irradiated with microwaves at 130 °C. The reactions were completed after 15–22 min affording the tetrazoles **86** in good yield (equation 38).

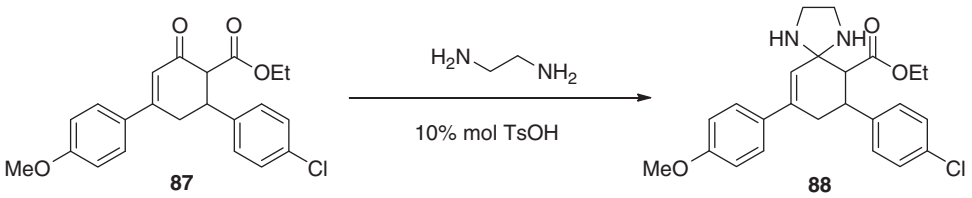


86 (38)

Imidazolidines are a family of compounds with multiple pharmacological activities as drugs or drug-intermediates. In 2012 Gopalakrishnan et al.[132] reported a green synthesis of ethyl 7,9-diazaspiro[4,5]-deca-9-ene-6-carboxylate **88** from enone **87**, under solvent-free conditions and microwave irradiation. With conventional heating *N*,*N*-acetal formation with ethylenediamine proceeded with very low yield (entry 1 in Table 7). Low conversion was also observed when the reaction was run in DMF solution (entry 2 in Table 7). Optimal results were observed when the reaction was carried out in the absence of solvent, under microwave irradiation, at 400 kPa pressure (entry 4 in Table 7). The lower yield found at 200 kPa pressure (entry 3 in Table 7) shows the additional influence of pressure in this reaction.

Table 7 Synthesis of 1,4-diazaspiro[4.5]-deca-9-ene-6-ethylcarboxylate 88

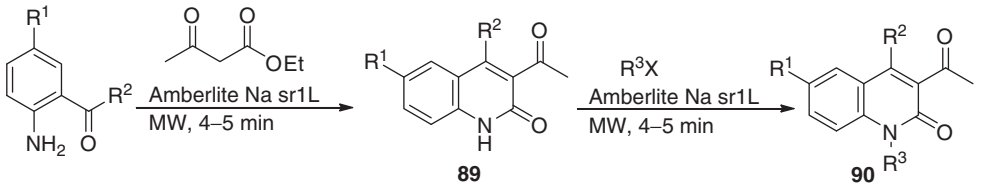
Entry	*Heating*	*Temperature (°C)*	*Pressure (bar)*	*Time (min)*	*Conversion (%)*
1	Thermal	90	1	45	20
2	MW (DMF)	120	4	5	20
3	MW	120	2	5	70
4	MW	120	4	5	95



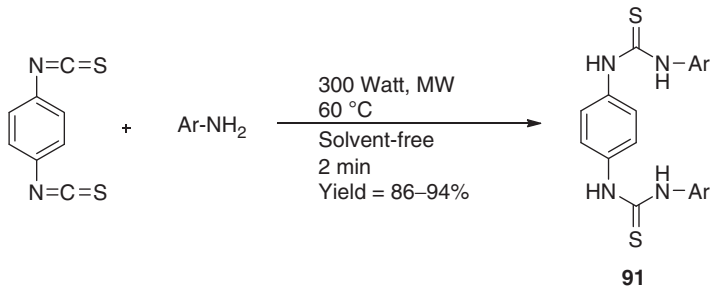
87 **88**

Quinolinones have been found as constituents of several naturally occurring alkaloids; thus, functionalized quinolinones are attractive in the pharmaceutical industry. Subashini and Khan[133] reported the two-step synthesis, solvent-free, and microwave enhanced synthesis of this kind of aromatic heterocycles. The first step consisted in the condensation of ethyl acetylacetate with 2-aminoaryl alkyl ketones catalyzed with Amberlite Na sr1L. Although conventional heating during 8 h afforded approximately 70% yield of the desired product **90**, microwave irradiation led to 90% yield within 5 min of reaction time (Scheme 6).

A very recent report by Zhang et al.[134] describes an efficient method for the synthesis of 1,4-phenylenedithioureas under solvent- and catalyst-free conditions, and with microwave irradiation. The reaction was examined at a range of temperatures between 25 °C and 80 °C, finding that the reaction proceeds best (in only 2 min) at 60 °C. In contrast, with conventional heating in different solvents the reaction required at least 30 min to take place (equation 39).



Scheme 6 Solvent-free, microwave-assisted synthesis of quinolinones **90**.[133]



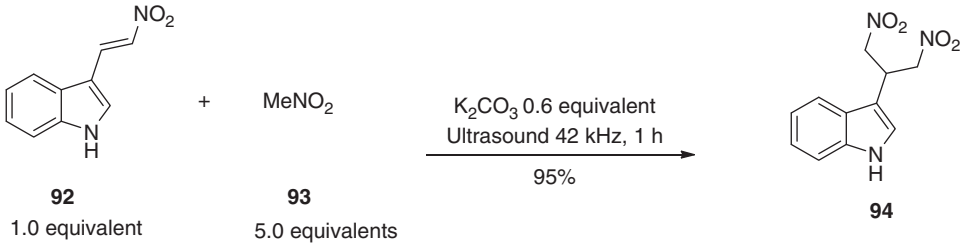
(39)

In this context, Mane et al.[135] reported the solventless *N*-arylation of phenylurea with aryl halides catalyzed by copper(I) oxide and potassium phosphate as a base. The coupling reaction took place with moderate to good yields within 50 min at 120 °C.

9.11.4 Miscellaneous Solvent-Free Strategies

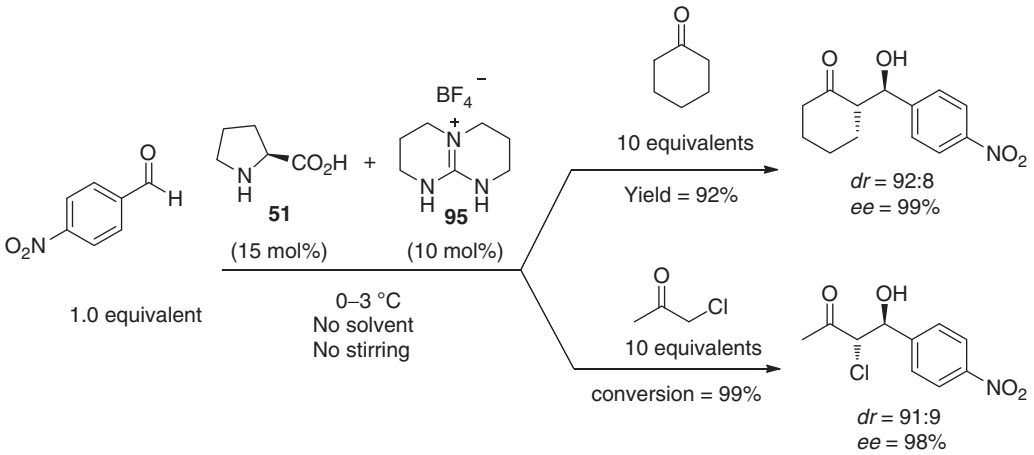
In addition to grinding, ball-milling activation, and microwave irradiation other alternative solvent-free procedures have been developed. Salient examples include the application of sonochemical protocols, photochemical activation, and traditional stirring employing an excess of one of the reagents. In this regard, the application of ultrasound irradiation in organic reactions has proved to be most beneficial, because it avoids energy-intensive traditional heating to reach high reaction temperatures, while simultaneously leading to an enhancement in reaction rates even at ambient temperature. Typically, ultrasound-assisted reactions are performed using organic solvents such as MeCN, EtOH, MeOH, CH_2Cl_2, and THF. Nevertheless, ultrasound-promoted reactions have also been reported in the absence of solvent, which allows for the advantageous acoustic cavitation process associated with ultrasound activation.

Recently, Popowycz et al.[136] described the solvent-free Michael addition reaction of nitromethane **93** to conjugated indole **92**. The process was activated by ultrasound irradiation and afforded the expected product **94** in excellent yield (equation 40). It is worth mentioning that this reaction was also performed in solution using MeOH and toluene as reaction media, both under traditional thermal conditions and with sonochemical activation. Nevertheless, the most successful method was observed in the total absence of solvent under sonochemical activation. Other ultrasound-promoted reactions that have been developed under solvent-free conditions include various cyclization reactions,[137] protection/deprotection protocols,[138] Michael additions,[139] and one-pot reactions,[140] among others.



(40)

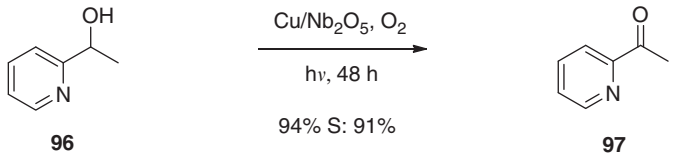
Particularly interesting are the solvent-free organocatalyzed aldol reactions reported by Nájera and coworkers,[141] and del Amo et al.[142,143] that take place with no stirring. For example, the reaction between aldehydes and ketones catalyzed by (*S*)-proline **51** using TBD (triazabicyclo[4.4.0]dec-5-ene)-derived guanidinium salt **95** as cocatalysts afforded the desired aldol adducts in good to excellent yields, and with very high diastereo- and enantioselectivities (equation 41).



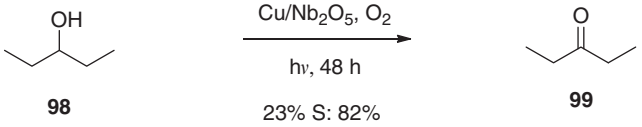
(41)

UV–vis irradiation is also capable of promoting chemical reactions in the absence of solvent when applied to suitable substrates. The two more relevant processes activated by UV–vis activation are photooxidation and photoreduction. Photolytic and photocatalytic reactions induced by UV–vis light have distinct applications because they are environmentally friendly, safe, and inexpensive. In recent years there has been an effort to develop new photochemical processes avoiding the use of commonly used toxic metal complexes [Ru(II), Ir (III), Cr (VI), and (Hg (II)].[144,145]

Tanaka and coworkers reported in 2011 an example of a solvent-free, UV-catalyzed oxidation process.[146] Tanaka's work consisted in the photooxidation of alcohols by O_2 in the absence of solvent. The process was performed at room temperature and atmospheric pressure. The selectivities (S, which refers to oxidation of the carbinol to the corresponding ketone vis-à-vis *N*-oxidation) were in the range of 80–99% and the Cu/Nb_2O_5 catalyst was easily removed from the reaction mixture for its reuse. Equations 42 and 43 show representative results with aromatic and aliphatic alcohols **96** and **98** as substrates.

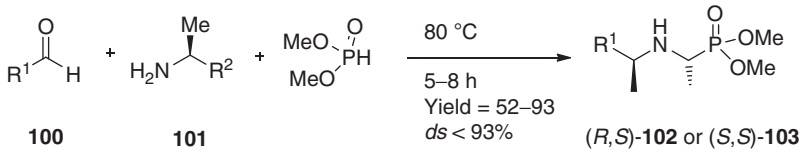


(42)



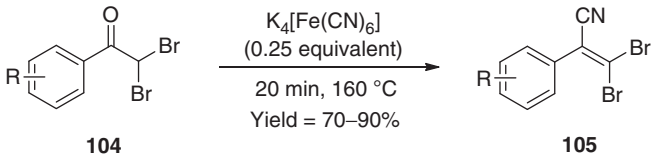
(43)

A representative example of solvent-free reactions activated by conventional heating is the report by Ordoñez et al.[147] of the uncatalyzed one-pot diastereoselective synthesis of α-amino phosphonates. The reaction was carried out at 80 °C with the three neat components: chiral amines **101**, aldehydes **100**, and dimethyl phosphite affording diastereomeric products (*R*,*S*)-**102** and (*S*,*S*)-**103** with up to 93% of diastereoselectivity (equation 44).



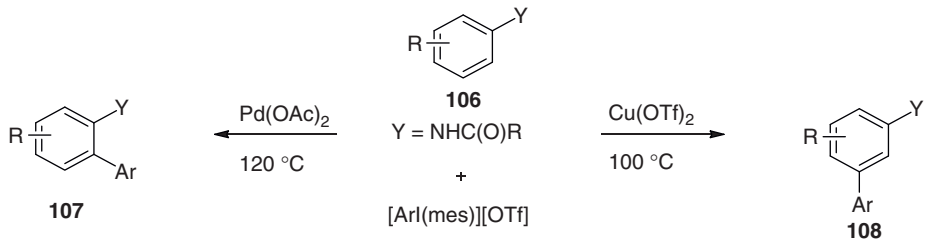
(44)

In this context, a chemoselective cyanation of α,α-dibromoacetophenones promoted by traditional heating under solvent-free conditions was reported by Zhao and Li,[148] with potassium hexacyanoferrate(II) as an 'eco-friendly' cyanide source. Another merit of this procedure consists in avoiding the use of highly toxic cyanide. Cyanide addition to the carbonyl afforded a cyanohydrin intermediate that dehydrates to give conjugated cyanide **105** (equation 45).



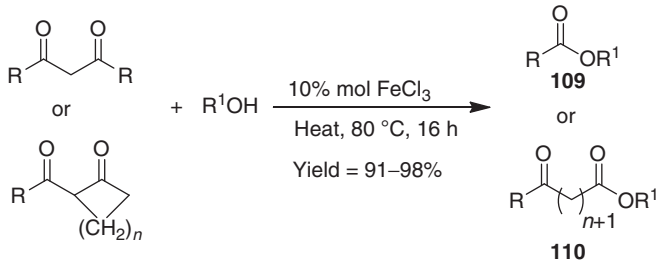
(45)

However, C–H activation is one hot topic in current synthetic chemistry. One example of this kind of chemistry under solvent-free conditions was recently reported by Bedford et al.[149] In this communication, aryl carbamates and aryl amides undergo a palladium acetate-catalyzed *ortho*-arylation with excellent selectivity (**Scheme 7**).



Scheme 7 Solvent-free *ortho*- and *meta*-functionalization of aryl carbamates and aryl amides.

In another interesting development, a solvent-free retro-Claisen condensation between an alcohol and a 1,3-diketone with iron(III) chloride as catalyst afforded the esterification product in good yields (equation 46). It was notable the regioselectivity found in the formation of the product. The method described could be used with open structures to afford esters **109** or with cyclic diketones to afford the linear derivatives **110**.[150]



(46)

9.11.5 Solvent-Free Philosophy in the Chemical Industry

In the past decade, interest in Green Chemistry has expanded and it now encompasses wide areas of the chemical enterprise. Of particular interest are developments with potential impact in industry and laboratory research as a means to continue chemical development in a more sustainable manner. Indeed, Noyori[151] has stated that the future of chemists and actually the survival of humankind depends on the ability to manufacture useful compounds in an economical, energy-efficient, resource-preserving, and environmentally benign way. In this context, HSBM is a sustainable mechanochemical technique, which has commonly been used for milling minerals into fine particles, as well as in the synthesis and modification of inorganic solids and organometallic materials. Furthermore, in the area of synthetic organic chemistry, this technique has been successfully used to promote several solvent-free reactions.

According with the Sheldon's statement 'the best solvent is no solvent,' a powerful alternative to make synthetic organic protocols greener, consists of avoiding the use of solvents as a reaction media.

By the same token, microwave chemistry has an edge over conventional heating techniques for conducting chemical reactions, and it is becoming the preferred method for performing chemical synthesis in pharmaceutical companies, especially since scaling up from milligrams to kilograms is now feasible. Indeed, microwave technology enables chemists to achieve cleaner chemical reactions, with higher yields and shorter reaction times, which is lower energy consumption.

Of course, to be competitive, chemical industries strive to develop and implement more economical processes that will result in lower prices, more attractive and accessible to the potential customers. In this regard, there is frequently a happy coincidence where 'greener,' more sustainable strategies tend also to be more energy and cost efficient. More to the point, solvent-free processes avoid expending resources in the acquisition of solvents, simultaneously avoiding the cost of solvent recovery and purification, or eventually safe disposal.

Acknowledgments

The authors are indebted to Conacyt, México for financial support via grant No. 130826. J.G.H. thanks Conacyt, México for a doctoral fellowship (No. 22211).

References

1. Sheldon, R. A. *Green Chem.* **2005**, *7*, 267–278.
2. Varma, R. S.; Ju, Y. Solventless Reactions. In *Green Separation Processes: Fundamentals and Applications*; Afonso, C. A. M., Crespo, J. P. S. G., Eds.; Wiley-VCH: Weinheim, **2005**, Chapter 2.2; pp 53–87.
3. Tanaka, K. *Solvent-free Organic Synthesis*, 2nd ed.; Wiley-VCH: Weinheim, **2009**.
4. Toda, F.; Tanaka, K. *Chem. Rev.* **2000**, *100*, 1025–1074.
5. Parkin, I. P. *Transition Met. Chem.* **2002**, *27*, 569–573.
6. Walsh, P. J.; Li, H.; Parrodi, C. A. *Chem. Rev.* **2007**, *107*, 2503–2545.
7. Martins, M. A. P.; Frizzo, C. P.; Moreira, D. N.; Buriol, L.; Machado, P. *Chem. Rev.* **2009**, *109*, 4140–4182.
8. Bruckmann, A.; Krebs, A.; Bolm, C. *Green Chem.* **2008**, *10*, 1131–1141.
9. Stolle, A.; Szuppa, T.; Leonhardt, S. E. S.; Ondruschka, B. *Chem. Soc. Rev.* **2011**, *40*, 2317–2329.
10. Toma, Š.; Šebesta, R.; Mečiarová, M. *Curr. Org. Chem.* **2011**, *15*, 2257–2281.
11. James, S. L.; Adams, C. J.; Bolm, C.; *et al. Chem. Soc. Rev.* **2012**, *41*, 413–447.
12. Nasir-Baig, R. B.; Varma, R. S. *Chem. Soc. Rev.* **2012**, *41*, 1559–1584.
13. McNaught, A. D., Wilkinson, A., Eds. *IUPAC Compendium of Chemical Technology (the "Gold Book"),* 2nd ed.; Blackwell Scientific Publications: Oxford, **1997**.
14. Takacs, L. *J. Mineral Met. Mater. Soc.* **2000**, *52*, 12–13.
15. Takao, K.; Munakata, R.; Tadano, K. *Chem. Rev.* **2005**, *105*, 4779–4807.
16. Guo, H-C.; Ma, J-A. *Angew. Chem. Int. Ed.* **2006**, *45*, 354–366.
17. Goswami, P.; Das, B. *Tetrahedron Lett.* **2009**, *50*, 897–900.
18. Xu, S.-L.; Li, C.-P.; Li, J.-H. *Synlett* **2009**, 818–822.
19. (a) Eddington, N. D.; Cox, D. S.; Khurana, M.; *et al. Eur. J. Med. Chem.* **2003**, *38*, 49–64. (b) Al-Omran, F.; El-Khair, A. A. *J. Heterocycl. Chem.* **2005**, *42*, 307–312.
20. Longhi, K.; Moreira, D. N.; Marzari, M. R. B.; *et al. Tetrahedron Lett.* **2010**, *51*, 3193–3196.
21. (a) Bekhit, A. A.; Abdel-Aziem, T. *Bioorg. Med. Chem.* **2004**, *12*, 1935–1945. (b) Selvam, C.; Jachak, S. N.; Thilagavathi, R.; Chakraborti, A. K. *Bioorg. Med. Chem. Lett.* **2005**, *15*, 1793–1797.
22. Choudhary, G.; Peddinti, R. K. *Green Chem.* **2011**, *13*, 276–282.
23. (a) Enders, D.; Reinhold, U. *Tetrahedron Asymmetry* **1997**, *8*, 1895–1946. (b) Mizuno, H.; Domon, K.; Masuya, K.; Tanino, K.; Kuwajima, I. *J. Org. Chem.* **1999**, *64*, 2648–2656.
24. Ballini, R.; Petrini, M. *Tetrahedron* **2004**, *60*, 1017–1047.
25. Samai, S.; Nandi, G. C.; Kumar, R.; Singh, M. S. *Tetrahedron Lett.* **2009**, *50*, 7096–7098.
26. Kumar, A.; Sharma, S. *Green Chem.* **2011**, *13*, 2017–2020.
27. Chuang, C.-P; Chen, K.-P. *Tetrahedron* **2012**, *68*, 1401–1406.
28. Lipshutz, B. *Chem. Rev.* **1986**, *86*, 795–819.
29. Singh, A. K.; Yadav, L. D. S. *Synthesis* **2012**, *44*, 591–599.
30. (a) Breslin, H. J.; Kukla, M. J.; Ludovici, D. W.; *et al. J. Med. Chem.* **1995**, *38*, 771–793. (b) Clark, R. L.; Carter, K. C.; Mullen, A. B.; *et al. Bioorg. Med. Chem. Lett.* **2007**, *17*, 624–627.
31. Bora, P. P.; Sema, A. A.; Wahlang, B.; Bez, G. *Can. J. Chem.* **2011**, *90*, 167–172.
32. Moon, M. E.; Choi, Y.; Lee, Y. M.; *et al. Tetrahedron Lett.* **2010**, *51*, 6769–6771.
33. Dakdouki, S. C.; Villemin, D.; Bar, N. *Eur. J. Org. Chem.* **2012**, 780–784.
34. Saikia, L.; Baruah, J. M.; Thakur, A. J. *Org. Med. Chem. Lett.* **2011**, *1*, 12–17.
35. Mokhtari, B.; Azadi, R.; Mardani, E. *Tetrahedron Lett.* **2012**, *53*, 491–493.
36. Fulmer, D. A.; Shearouse, W. C.; Mendoza, S. T.; Mack, J. *Green Chem.* **2009**, *11*, 1821–1825.
37. Su, W.; Yu, J.; Li, Z.; Jiang, Z. *J. Org. Chem.* **2011**, *76*, 9144–9150.
38. (a) Nicolaou, K. C.; Bulger, G. P.; Sarlah, D. *Angew. Chem. Int. Ed.* **2005**, *44*, 4442–4489. (b) Tucker, C. E.; de Vries, J. G. *Top. Catal.* **2002**, *19*, 111–118.
39. Nielsen, S. F.; Peters, D.; Axelsson, O. *Synth. Commun.* **2000**, *30*, 3501–3509.
40. Schneider, F.; Ondruschka, B. *ChemSusChem* **2008**, *1*, 622–625.
41. Schneider, F.; Stolle, A.; Ondruschka, B.; Hopf, H. *Org. Process Res. Dev.* **2009**, *13*, 44–48.
42. Cravotto, G.; Garella, D.; Tagliapietra, S.; *et al. New. J. Chem.* **2012**, *36*, 1304–1307.
43. Smoliga, J. M.; Baur, J. A.; Hausenblas, H. A. *Mol. Nutr. Food Res.* **2011**, *55*, 1129–1141.
44. Kim, S.; Ko, H.; Park, J. E.; *et al. J. Med. Chem.* **2002**, *45*, 160–164.
45. Zhu, X.; Liu, J.; Chen, T.; Su, W. *Appl. Organometal. Chem.* **2012**, *26*, 145–147.
46. Bunz, U. H. F. *Chem. Rev.* **2000**, *100*, 1605–1644.
47. Thorwirth, R.; Stolle, A.; Ondruschka, B. *Green Chem.* **2010**, *12*, 985–991.
48. (a) Siemsen, P.; Livingston, R. C.; Diederich, F. *Angew. Chem. Int. Ed.* **2000**, *39*, 2632–2657. (b) Liu, J.; Lam, J. W. Y.; Tang, B. Z. *Chem. Rev.* **2009**, *109*, 5799–5867. (c) Gleiter, R.; Werz, D. B. *Chem. Rev.* **2010**, *110*, 4447–4488.
49. Stolle, A.; Ondruschka, B. *Pure Appl. Chem.* **2011**, *83*, 1343–1349.
50. Declerck, V.; Nun, P.; Martinez, J.; Lamaty, F. *Angew. Chem. Int. Ed.* **2009**, *48*, 9318–9321.
51. Mazur, R. H.; Schlatter, J. M.; Goldkamp, A. H. *J. Am. Chem. Soc.* **1969**, *91*, 2684–2691.
52. Hernández, J. G.; Juaristi, E. *J. Org. Chem.* **2010**, *75*, 7107–7111.
53. (a) Hipkiss, R. A.; Brownson, C.; Carrier, J. M. *Mech. Ageing Dev.* **2001**, *122*, 1431–1445. (b) Guiotto, A.; Calderan, A; Ruzza, P.; Borin, G. *Curr. Med. Chem.* **2005**, *12*, 2293–2315. (c) Bauer, K. *Neurochem. Res.* **2005**, *30*, 1339–1345. (d) Chan, W. K. M.; Decker, E. A.; Lee, J. B.; Butterfield, D. A. *J. Agric. Food Chem.* **1994**, *42*, 1407–1410. (e) Heck, T.; Makam, V. S.; Lutz, J.; *et al. Adv. Synth. Catal.* **2010**, *352*, 407–415. (f) Heyland, J.; Antweiler, N.; Lutz, J.; *et al. Microb. Biotechnol.* **2010**, *3*, 74–83.
54. Waddell, D. C.; Thiel, I.; Clark, T. D.; Marcum, T.; Mack, J. *Green Chem.* **2010**, *12*, 209–211.
55. Baron, A.; Martinez, J.; Lamaty, F. *Tetrahedron Lett.* **2010**, *51*, 6246–6249.

56. Thorwirth, R.; Stolle, A. *Synlett* **2011**, 2200–2202.
57. Dong, Y.-W.; Wang, G.-W.; Wang, L. *Tetrahedron* **2008**, *64*, 10148–10154.
58. Nun, P.; Martin, C.; Martinez, J.; Lamaty, F. *Tetrahedron* **2011**, *67*, 8187–8194.
59. Gil, M. V.; Arévalo, M. J.; López, O. *Synthesis* **2007**, 1589–1620.
60. Thorwirth, R.; Stolle, A.; Ondruschka, B.; Wild, A.; Schubert, U. S. *Chem. Commun.* **2011**, *47*, 4370–4372.
61. Mashkouri, S.; Naimi-Jamal, M. R. *Molecules* **2009**, *14*, 474–479.
62. Wang, G.-W.; Gao, J. *Org. Lett.* **2009**, *11*, 2385–2388.
63. Khaligh, N. G. *Tetrahedron Lett.* **2012**, *53*, 1637–1640.
64. Wang, G.-W.; Dong, Y.-W.; Wu, P.; Yuan, T.-T.; Shen, Y.-B. *J. Org. Chem.* **2008**, *73*, 7088–7095.
65. Zhu, X.; Li, Z.; Jin, C.; *et al. Green Chem.* **2009**, *11*, 163–165.
66. Carlier, L.; Baron, M.; Chamayou, A.; Couarraze, G. *Tetrahedron Lett.* **2011**, *52*, 4686–4689.
67. Gérard, E. M. C.; Sahin, H.; Encinas, A.; Bräse, S. *Synlett* **2008**, 2702–2704.
68. Vogel, P.; Figueira, S.; Muthukrishnan, S.; Mack, J. *Tetrahedron Lett.* **2009**, *50*, 55–56.
69. Mugunthan, G.; Kartha, K. P. R. *J. Carbohydr. Chem.* **2008**, *27*, 294–299.
70. Patil, P. R.; Kartha, K. P. R. *J. Carbohydr. Chem.* **2008**, *27*, 411–419.
71. Patil, P. R.; Kartha, K. P. R. *Green Chem.* **2009**, *11*, 953–956.
72. Waddell, D. C.; Mack, J. *Green Chem.* **2009**, *11*, 79–82.
73. Szuppa, T.; Stolle, A.; Ondruschka, B.; Hopfe, W. *Green Chem.* **2010**, *12*, 1288–1294.
74. Zhang, Z.; Peng, Z.-W.; Hao, M.-F.; Gao, J.-G. *Synlett* **2010**, 2895–2898.
75. Wang, G.-W.; Gao, J. *Green Chem.* **2012**, *14*, 1125–1131.
76. Thorwirth, R.; Bernhardt, F.; Stolle, A.; Ondruschka, B.; Asghari, J. *Chem. Eur. J.* **2010**, *16*, 13236–13242.
77. Chen, P.-N.; Lai, C.-C.; Chiu, S.-H. *Org. Lett.* **2011**, *13*, 4660–4663.
78. Chatterjee, T.; Saha, D.; Ranu, B. C. *Tetrahedron Lett.* **2012**, *53*, 4142–4144.
79. Gao, J.; Wang, G.-W. *J. Org. Chem.* **2008**, *73*, 2955–2958.
80. (a) Huskić, I.; Halasz, I.; Friščić, T.; Vančik, H. *Green Chem.* **2012**, *14*, 1597–1600. (b) Shearouse, W. C.; Korte, C. M.; Mack, J. *Green Chem.* **2011**, *13*, 598–601.
81. Renzi, P.; Bella, M. *Chem. Commun.* **2012**, *48*, 6881–6896.
82. Busacca, C. A.; Fandrick, D. R.; Song, J. J.; Senanayake, C. H. *Adv. Synth. Catal.* **2011**, *353*, 1825–1864.
83. Hernández, J. G.; Juaristi, E. *Chem. Commun.* **2012**, *48*, 5396–5409.
84. (a) Rodríguez, B.; Rantanen, T.; Bolm, C. *Angew. Chem. Int. Ed.* **2006**, *45*, 6924–6926. (b) Rodríguez, B.; Bruckmann, A.; Bolm, C. *Chem. Eur. J.* **2007**, *13*, 4710–4722.
85. (a) Guillena, G.; Hita, M. C.; Nájera, C.; Viózquez, S. F. *Tetrahedron Asymmetry* **2007**, *18*, 2300–2304. (b) Guillena, G.; Hita, M. C.; Nájera, C.; Viózquez, S. F. *J. Org. Chem.* **2008**, *73*, 5933–5943.
86. Hernández, J. G.; Juaristi, E. *J. Org. Chem.* **2011**, *76*, 1464–1467.
87. Hernández, J. G.; Juaristi, E. *Tetrahedron* **2011**, *67*, 6953–6959.
88. Hernández, J. G.; García-López, V.; Juaristi, E. *Tetrahedron* **2012**, *68*, 92–97.
89. Nun, P.; Pérez, V.; Calmès, M.; Martinez, J.; Lamaty, F. *Chem. Eur. J.* **2012**, *18*, 3773–3779.
90. Wang, Y.-F.; Chen, R.-X.; Wang, K.; *et al. Green Chem.* **2012**, *14*, 893–895.
91. Veverková, E.; Poláčková, V.; Liptáková, L.; *et al. ChemCatChem* **2012**, *4*, 1013–1018.
92. Štrukil, V.; Igrc, M. D.; Eckert-Maksić, M.; Friščić, T. *Chem. Eur. J.* **2012**, *18*, 8464–8473.
93. Kappe, C. O. *Angew. Chem. Int. Ed.* **2004**, *43*, 6250–6284.
94. De la Hoz, A; Díaz-Ortiz, A.; Moreno, A. *Chem. Soc. Rev.* **2005**, *34*, 164–178.
95. Burgula, L. N.; Radhakrishnan, K.; Kundu, L. M. *Tetrahedron Lett.* 10.1016/j.tetlet.2012.03.056
96. Obermayer, D.; Gutmann, B.; Kappe, C. O. *Angew. Chem. Int. Ed.* **2009**, *48*, 8321–8324.
97. Singh, G. S. *Tetrahedron* **2003**, *59*, 7631–7649.
98. Gelens, E.; Smeets, L.; Sliedregt, L. A. J. M.; *et al. Tetrahedron Lett.* **2005**, *46*, 3751–3754.
99. El-Faham, A.; Albericio, F. *Chem. Rev.* **2011**, *111*, 6557–6602.
100. Ritter, J. J.; Minieri, P. P. *J. Am. Chem. Soc.* **1948**, *70*, 4045–4048.
101. Top, S.; Jaouen, G. *J. Org. Chem.* **1981**, *46*, 78–82.
102. Mukhopadhyay, M.; Iqbal, J. *J. Org. Chem.* **1997**, *62*, 1843–1845.
103. Polshettiwar, V.; Varma, R. S. *Tetrahedron Lett.* **2008**, *49*, 261–2664.
104. Sathishkumar, M.; Shanmugavelan, P.; Nagarajan, S.; *et al. Tetrahedron Lett.* **2011**, *52*, 2830–2833.
105. Sathishkumar, M.; Nagarajan, S.; Velan, P. S.; Dinesh, M.; Ponnuswamy, A. *J. Braz. Chem. Soc.* **2011**, *22*, 2065–2069.
106. Dandepally, S. R.; Williams, A. L. *Tetrahedron Lett.* **2009**, *50*, 1071–1074.
107. Seijas, J. A.; Vázquez-Tato, M. P.; Crecente-Campo, J. *Tetrahedron* **2008**, *64*, 9280–9285.
108. Dömling, A. *Chem. Rev.* **2006**, *106*, 17–89.
109. Marcaccini, S.; Torroba, T. *Nat. Protoc.* **2007**, *2*, 632–639.
110. Jida, M.; Malaquin, S.; Deprez-Pouain, R.; Laconde, G.; Deprez, B. *Tetrahedron Lett.* **2010**, *51*, 5109–5111.
111. Xiuli, Z.; Kai, L.; Wei, C.; Lei, W. *Chin. J. Chem.* **2011**, *29*, 2209–2212.
112. Oh, L. M. *Tetrahedron Lett.* **2006**, *47*, 7943–7946.
113. Yu, H.; Xu, M.; Cheng, Y.; *et al. Arkivoc* **2012**, 26–34.
114. Borkin, D. A.; Puscau, M.; Carlson, A.; *et al. Org. Biomol. Chem.* **2012**, *10*, 4505–4508.
115. Chow, W. S.; Chan, T. H. *Tetrahedron Lett.* **2009**, *50*, 1286–1289.
116. Crich, D.; Banerjee, A. *Acc. Chem. Res.* **2007**, *40*, 151–161.
117. Zhou, Q.; Xiang, J.; Tang, Y.; *et al. Colloid Surf. B: Biointerface* **2008**, *61*, 75.
118. Polshettiwar, V.; Varma, R. S. *Tetrahedron Lett.* **2008**, *49*, 7165–7167.
119. Nikalje, A. P.; Vyawahare, D. *Afr. J. Pure Appl. Chem.* **2011**, *5*, 422–428.
120. Prajapati, D.; Gohain, M. *Catal. Lett.* **2007**, *119*, 59–63.
121. Bhuiyan, M. M. H.; Nessa, H.; Mahmud, M. M. *J. Sci. Res.* **2012**, *4*, 143–153.
122. Das, S.; Santra, S.; Roy, A.; *et al. Green Chem. Lett. Rev.* **2012**, *5*, 97–100.
123. Valizadeh, H.; Heravi, M. M.; Amiri, M. *Mol. Divers.* **2010**, *14*, 575–579.
124. Jiang, B.; Wang, X.; Shi, F.; Tu, S-H.; Li, G. *Org. Biomol. Chem.* **2011**, *9*, 4025–4028.
125. Krishnakumar, B.; Swaminathan, M. *Bull. Chem. Soc. Jpn.* **2011**, *84*, 1261–1266.
126. Hasaninejad, A.; Shekouhy, M.; Zare, A. *Catal. Sci. Technol.* **2012**, *2*, 201–214.

127. Hamidinan, H.; Fozooni, S.; Hassankhani, A.; Mohammadi, S. Z. *Molecules* **2011**, *16*, 9041–9048.
128. Phukan, K.; Devi, N. *J. Chem. Pharm. Res.* **2011**, *3*, 1037–1044.
129. Phukan, K.; Devi, N. *Der Chemica Sinica* **2011**, *2*, 32–41.
130. Landge, S. M.; Berryman, M.; Török, B. *Tetrahedron Lett.* **2008**, *49*, 4505–4508.
131. Marvi, O.; Alizadeh, A.; Zerrabi, S. *Bull. Korean Chem. Soc.* **2011**, *32*, 4001–4003.
132. Thanusu, J.; Kanagarajan, V.; Gopalakrishnan, M. *Green Chem. Lett. Rev.* **2012**, *5*, 65–72.
133. Subashini, R.; Khan, F-R. N. *Monatsh. Chem.* **2012**, *143*, 485–489.
134. Zhang, L.-P.; Shang, X.-B.; Wu, Q.-F.; Zhang, Y.; Li, J.-P. *Synth. Commun.* **2012**, *42*, 1045–1052.
135. Gadave, S.; Shingare, M.; Mane, D. *Bull. Korean Chem. Soc.* **2011**, *32*, 4167–4170.
136. Baron, M.; Métay, E.; Lemaire, M.; Popowycz, F. *J. Org. Chem.* **2012**, *77*, 3598–3603.
137. (a) Gutiérrez-Sánchez, C.; Calvino-Casilda, V.; Pérez-Mayoral, E.; *et al. Catal. Lett.* **2009**, *128*, 318–322. (b) Jiang, Y.-J.; Cai, J.-J.; Zou, J.-P.; Zhang, W. *Tetrahedron Lett.* **2010**, *51*, 471–474. (c) Shukla, G.; Verma, R. K.; Verma, G. K.; Singh, M. S. *Tetrahedron Lett.* **2011**, *52*, 7195–7198.
138. Procopio, A.; Cravotto, G.; Oliverio, M.; *et al. Green Chem.* **2011**, *13*, 436–443.
139. (a) Fu, Z.; Shao, H. *Ultrason. Sonochem.* **2011**, *18*, 520–526. (b) Amara, Z.; Drège, E.; Troufflard, C.; Retailleau, P.; Joseph, D. *Org. Biomol. Chem.* **2012**, doi: 10.1039/C2OB25963J.
140. Kaboudin, B.; Fallahi, M. *Tetrahedron Lett.* **2011**, *52*, 4346–4348.
141. Almaşi, D.; Alonso, D. A.; Nájera, C. *Adv. Synth. Catal.* **2008**, *350*, 2467–2472.
142. Martínez-Castañeda, A.; Poladura, B.; Rodríguez-Solla, H.; Concellón, C.; Del Amo, V. *Org. Lett.* **2011**, *13*, 3032–3035.
143. Martínez-Castañeda, A.; Poladura, B.; Rodríguez-Solla, H.; Concellón, C.; Del Amo, V. *Chem. Eur. J.* **2012**, *18*, 5188–5190.
144. Bendicho, C.; Pena, F.; Costas, M.; Gil, S.; Lavilla, I. *Trends Anal. Chem.* **2010**, *29*, 681–691.
145. Ho, X.; Kang, M.; Kim, S.; Park, E. D.; Jang, H. *Catal. Sci. Technol.* **2011**, *1*, 923–926.
146. Furukawa, S.; Tamura, A.; Shishido, T.; Teramura, K.; Tanaka, T. *Appl. Catal. B: Environ.* **2011**, *110*, 216–220.
147. Tibhe, G. D.; Lagunas-Rivera, S.; Vargas-Díaz, E.; García-Barradas, O.; Ordoñez, M. *Eur. J. Org. Chem.* **2010**, 6573–6581.
148. Zhao, Z.; Li, Z. *Eur. J. Org. Chem.* **2010**, 5460–5463.
149. Bedford, R. B.; Mitchell, C. J.; Webster, R. L. *Chem. Commun.* **2010**, *46*, 3095–3097.
150. Rao, C. B.; Rao, D. C.; Babu, D. C.; Venkateswarlu, Y. *Eur. J. Org. Chem.* **2010**, 2855–2859.
151. Noyori, R. *Tetrahedron* **2010**, *66*, 1028.

9.12 Fluorous Linker-Enabled Organic Synthesis

W Zhang, University of Massachusetts Boston, Boston, MA, USA

© 2014 Elsevier Ltd. All rights reserved.

9.12.1	Introduction	315
9.12.2	Fluorous Linkers and Separation Techniques	315
9.12.3	Fluorous Parallel Synthesis	317
9.12.4	Fluorous DOS	318
9.12.5	Fluorous Mixture Synthesis	321
9.12.6	Conclusion	329
References		329

Glossary

Chemical library A collection of stored chemicals with information such as the chemical structure, purity, quantity, and physiochemical characteristics. Compounds from the chemical libraries are commonly used in high-throughput screening.

Diversity-oriented synthesis Synthesis of a collection of compounds with their structures having substitution, functional group, skeleton, and stereochemistry variations.

Fluorous Highly fluorinated molecules or materials with low lipophilicity and hydrophilicity.

Linker Chemical moiety attaching a compound to a solid, fluorous or other support that can be cleaved to release compounds from the support.

Parallel synthesis Synthesis of discrete compounds simultaneously in arrays of physically separate reaction vessels without interchange of intermediates during the reaction process.

9.12.1 Introduction

Separation of reaction mixtures is a time-consuming process and a bottleneck in the synthesis of chemical libraries. Phase tagging strategies such as solid-phase synthesis of peptides have been developed to address the separation issue. Application of solid-supports for the synthesis of small molecules and other biomolecules has achieved a certain level of success.[1] Different from the synthesis of peptides, which is a repeating process of making amide bonds, the scope for the synthesis of small molecules are much broader and reaction conditions are more complicated. Heterogenous solid-phase synthesis is good for product purification, but it decreases the reaction efficiency because of unfavorable reaction kinetics. In addition, it is difficult to monitor a solid-phase reaction with conventional analytical tools such as TLC and LC-MS. Fluorous technology integrates the advantages of homogenous solution-phase reactions and phase tag separations. It is a more feasible and compatible method for the synthesis of small molecules.

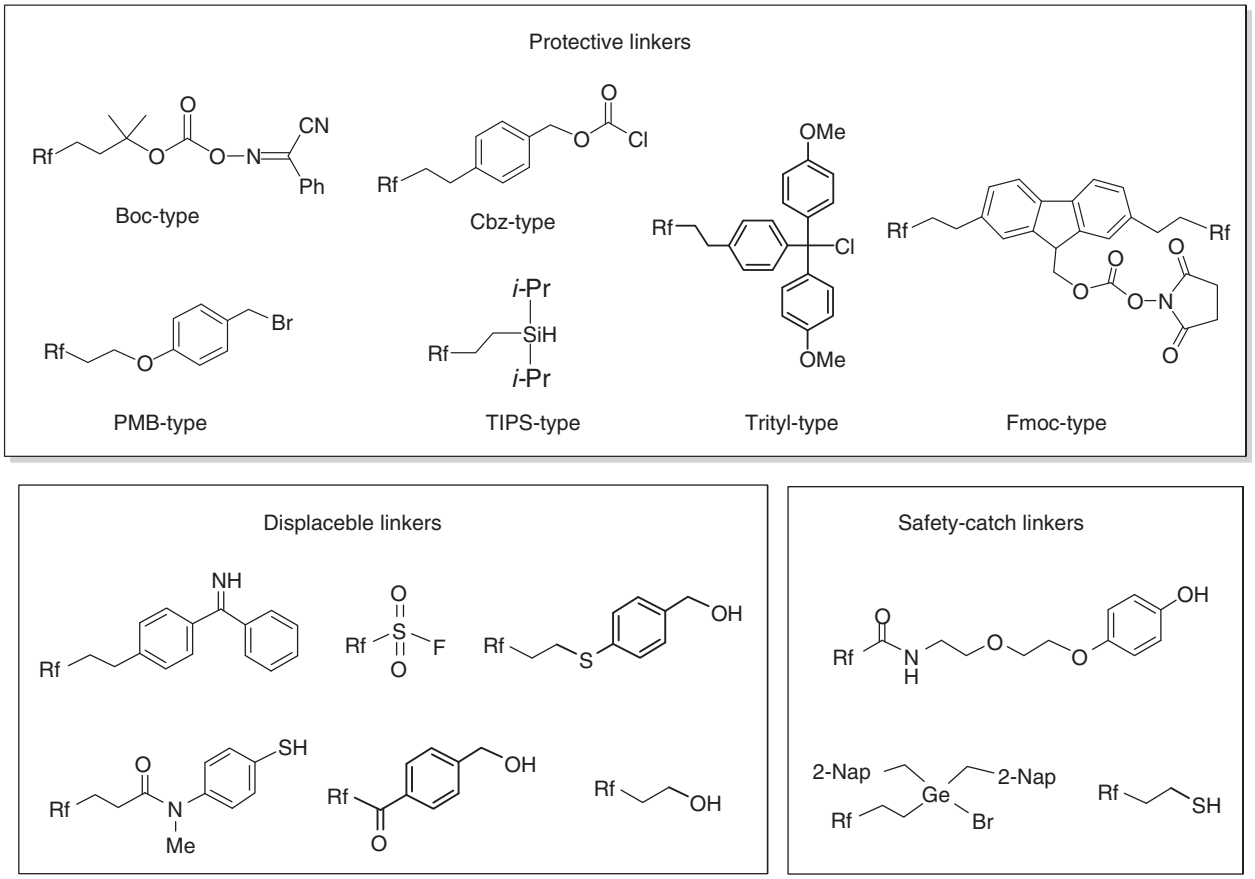
Organic compounds can be rendered fluorous by attaching a perfluoronated alkyl tag (Rf). Attached fluorous compounds are more solvophobic with aqueous and common organic solvents, but are fluorophilic with fluorous media including fluorous solvents and fluorous silica gel. This special property has been utilized in the development of novel separation and immobilization techniques for applications in organic, bioorganic, biomedical, analytical, separation, material, and surface sciences.[2,3]

Fluorous technology was first introduced for biphasic catalysis in the mid-1990s.[4] The utility of fluorous tagging and associated separations have been quickly applied to the synthesis of small molecules,[5–7] natural product analogs,[8,9] and biomolecules.[10,11] The combination of fluorous solid-phase extraction (F-SPE) with light fluorous phase tags has dramatically increased the potential of fluorous technology.[12] A light fluorous tag usually has <8 perfluorocarbons. Molecules attached with a light fluorous tag still have a reasonable solubility in organic solvents, which is good for chemical and biological transformations. It is worth mentioning that light fluorous tag-based synthesis does not require perfluorocarbon solvents for reactions or separations. It significantly reduces cost and environmental impact of persistent perfluorocarbon chemicals.[13] In addition, cleaved fluorous tags can be easily recovered for reuse or centralized for disposal. Over the years, fluorous tags have been used to attach with catalysts, reagents, scavengers, and linkers.[2,12] This chapter only presents examples of fluorous linker-facilitated synthesis of drug-like molecules and natural product analogs.[14,15] Fluorous synthesis of biomolecules such as peptides, oligosaccharides, glycopeptides, and oligonucleotides are not covered in this chapter. Interested readers are encouraged to read reviews and book chapters on these topics.[2,3,10,11,16]

At different stages of the drug discovery program, the requirements for structure diversity, size of the library, and compound amounts are different. Parallel synthesis, high-throughput synthesis, and diversity-oriented synthesis (DOS) have been developed to fulfill these needs. As an enabling technology, fluorous chemistry has been well-integrated with parallel synthesis and DOS. In addition, fluorous mixture synthesis (FMS) has been developed as a stand-alone technique for the synthesis of analogs and stereoisomers of complex molecules.

9.12.2 Fluorous Linkers and Separation Techniques

Fluorous linker-facilitated synthesis makes a fluorous Rf tag (usually C_6F_{13} or C_8F_{17}) attach to a selected functional group of the reaction substrate. The linker is used to facilitate the purification of intermediates. It is cleaved from the final product at the end of multistep synthesis. Protective linkers, displaceable linkers, and safety-catch linkers are three kinds of fluorous linkers classified based on the method of linker cleavage (Scheme 1).[14] Protective linkers regenerate the original functional group after cleavage. Their structures resemble the protecting groups such as *t*-butyloxycarbonyl (Boc), 9-fluorenylmethoxycarbonyl (Fmoc), *p*-methoxybenzyl (PMB), triisopropylsilyl (TIPS), and benzyloxycarbonyl (Cbz) and are used to protect common functional groups such as amino, hydroxyl, and carboxyl groups. Displaceable linkers have the efficiency of 'killing two birds with one stone', combining the introduction of a new functional group and the cleavage of the linker in a single operation. The linker can be cleaved by an intermolecular displacement reaction to introduce a new functionality or by an intramolecular (cyclization) reaction to generate a new ring. Displaceable linkers have a good utility in DOS for substitution and skeleton variations. Safety-catch linkers are stable under common reaction conditions. They are cleaved after activation by oxidation, photolysis, or other selective reactions. Safety-catch linkers have relatively narrow but special utilities.



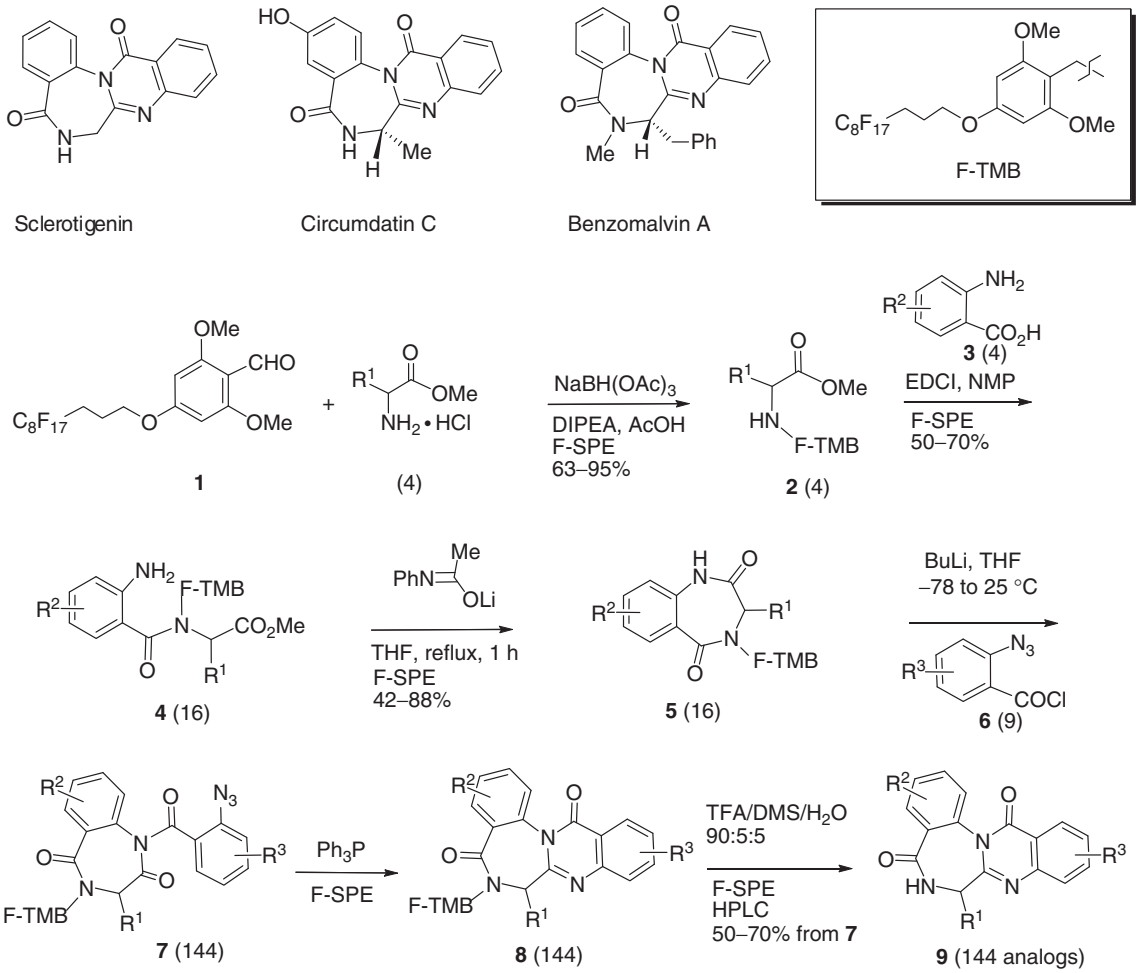
Scheme 1 Three types of fluorous linkers.

Application of fluorous linkers is not only limited to attaching to reaction substrates. In the synthesis of bioconjugates, fluorous linkers can be used to cap the deletion sequences, while the desired substrates are untagged.[10] In the synthesis of small molecules and the separation of natural products, fluorous linkers can be used as catch-and-release agents to isolate a desired component from the mixture.[14] In fluorous microarray, the linker has dual functions: (1) as a phase tag to facilitate separation and (2) as an affinity tag to immobilize products on a fluorous surface for screening.

A light fluorous Rf tag usually contains <8 perfluorinated carbons. The solubility and reactivity of attached molecules can be similar to the nonattached molecules and only mild effort is required to modify the reaction conditions. The Rf tags have excellent thermal and chemical stability. They are expected to be inactive during the reaction steps and play the phase tag role during separation. Fluorous intermediates and products can be isolated by a simple and quick F-SPE. Depending on the scale and the throughput of the synthesis, F-SPE can be carried out with a single cartridge, or with 24- and 48-well plates. In FMS,[17] demixing of the fluorous mixture has to be conducted by LC with fluorous stationary phase.[18] LC has the power to separate tagged-substrates with only a difference of CF_2.

9.12.3 Fluorous Parallel Synthesis

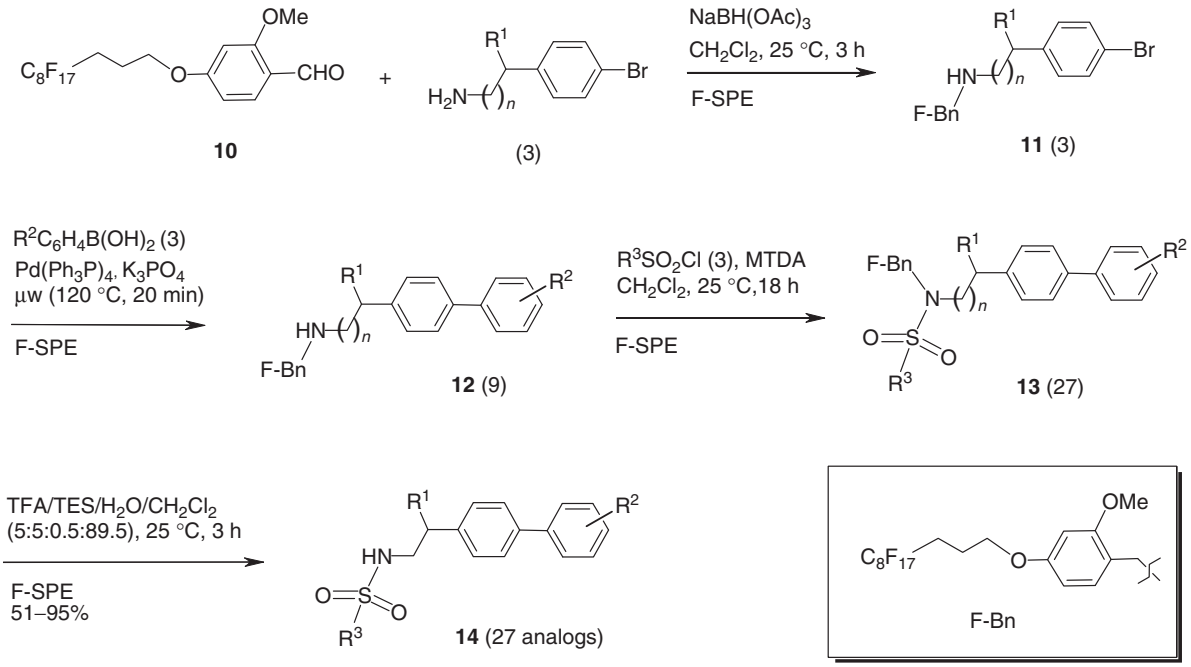
Most chemical libraries only contain compounds with substitution and functional group variations. Parallel synthesis is a general approach to make this kind of library. An example of using fluorous trimethoxybenzyl (TMB)-type protective linker for parallel synthesis of sclerotigenin analogs is shown in Scheme 2.[19] The scaffold has three substitution diversity points (R^1–R^3). Sclerotigenin has a unique ring skeleton that can be found in several other natural products, such as circumdatin C and benzomalvin A. The fluorous TMB-type linker **1** was attached to four different amino esters by reductive amination. Amide coupling of amines **2** with four anthranilic acids **3** afforded 16 amides **4**. Base-promoted cyclization of **4** gave 1,4-benzodiazepine-2,5-diones **5** that were then reacted with nine azidobenzoyl chlorides **6** to afford 144 *N*-acylated products **7**. The azido group of **7** was reduced with triphenylphosphine (TPP) followed by the spontaneous cyclization to form **8**. Fluorous linker cleavage afforded 144 final products **9**. Only the final products were purified by prep-HPLC, whereas the reaction intermediates were purified by F-SPE.



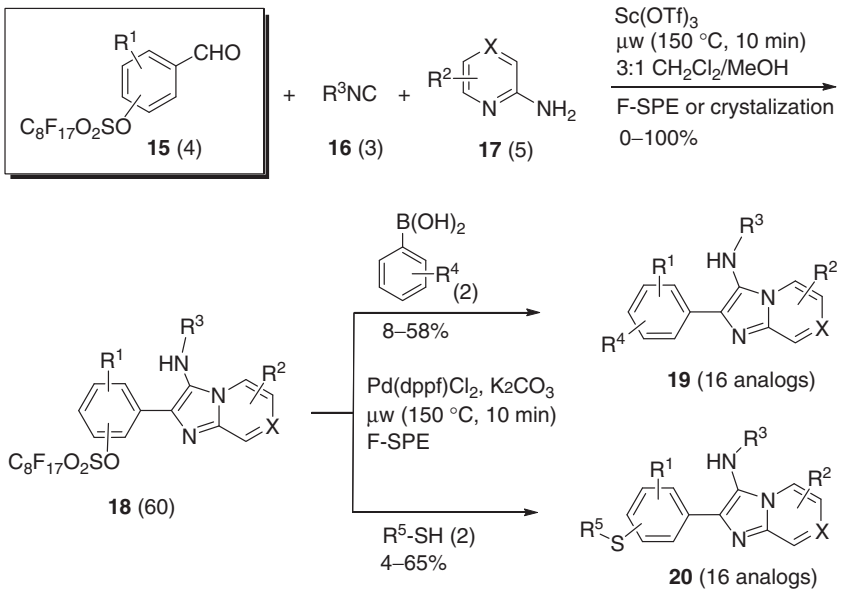
Scheme 2 F-TMB-assisted synthesis of sclerotigenin library.

A protective linker-assisted parallel synthesis of a biaryl-substituted sulfonamide library is shown in Scheme 3.[20] The acid-labile fluorous benzaldehyde linker **10** was attached to three aryl bromides by reductive amination to form **11** and then the Suzuki coupling with three boronic acids afforded nine analogs of **12**. Sulfonamidation of **12** with three sulfonyl chlorides **13** followed by the linker cleavage yielded biaryl sulfonamides **14**. The library scaffold has three points of diversity (R^1–R^3) and contains a total of 27 analogs. Intermediates as well as the products were purified by F-SPE.

Highlighted in Scheme 4 is a displaceable linker-assisted parallel synthesis of heterocyclic libraries **19** and **20**.[21] Four perfluorooctylsulfonyl-attached benzaldehydes **15** were used as a limiting agent for multicomponent reactions with three isonitriles **16** and five 2-aminopyrimidines/2-aminopyrazines **17** under $Sc(OTf)_3$-catalyzed microwave heating to afford 60 condensation products **18**. Parts of compounds **18** were removed by two different coupling reactions to afford 16 Suzuki coupling products **19** and **16** alkythio-substituted products **20.** This library only has two synthetic steps, but it generated the heterocyclic scaffolds with five substitution diversities (R^1–R^5).



Scheme 3 F-Bn-facilitated synthesis of sulfonamides.



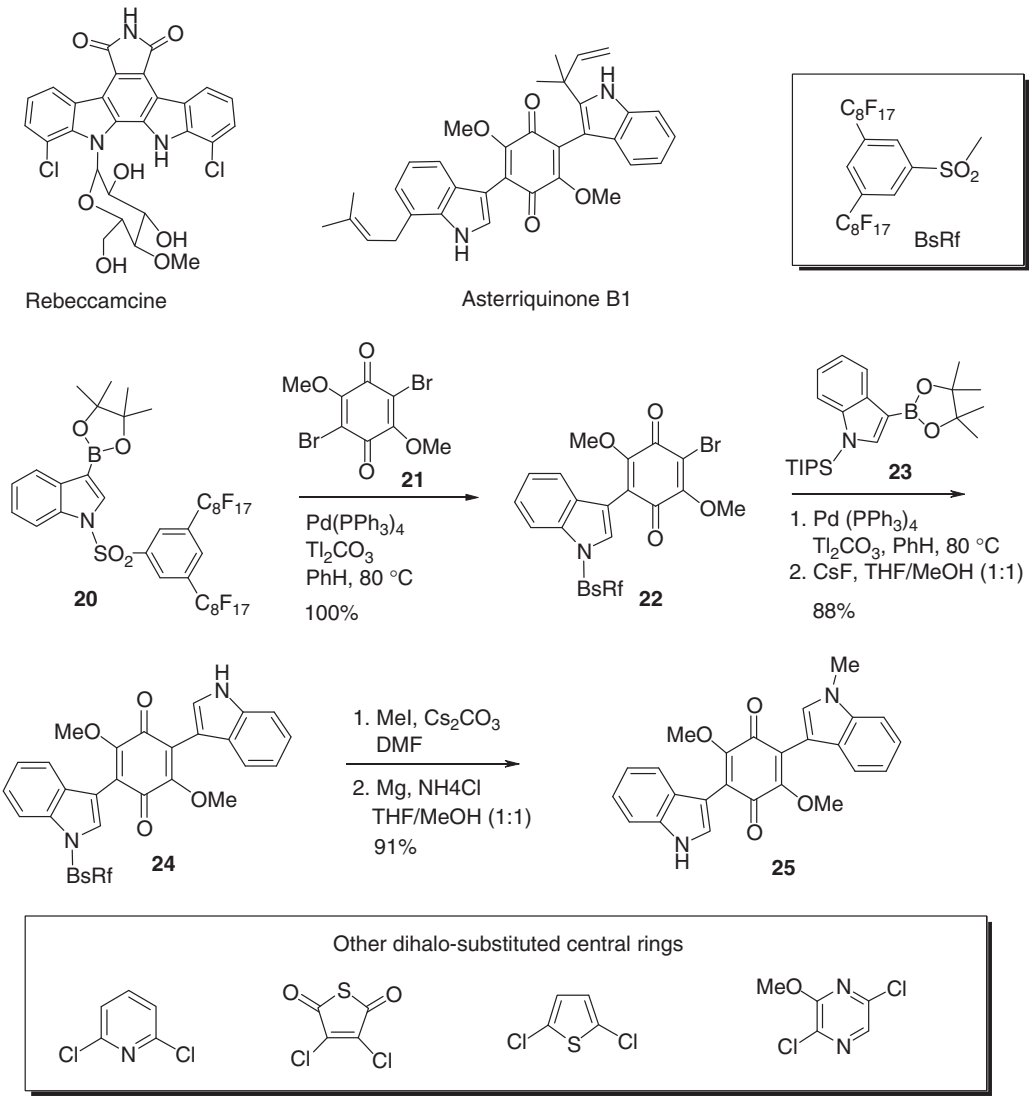
Scheme 4 Displaceable sulfonate linker-assisted parallel synthesis.

9.12.4 Fluorous DOS

Discovery libraries are not designed for particular biological targets. The structural novelty and diversity are critical for the libraries to be screened against new targets for lead generation and target validation purposes. There are three different kinds of diversities for the discovery libraries: (1) substitution/functional group diversity; (2) skeletal diversity; and (3) stereochemistry diversity.[22,23] The substitution/functional group diversity is usually achieved by parallel synthesis (see Section 9.12.3). The stereochemistry diversity has been well established by FMS (see Section 9.12.5). This section mainly focuses on the libraries with skeletal diversity.

Rebeccamycin and asteeriquinone B1 have antitumor activity and are insulin receptor activators. They belong to the bisindole natural alkaloid family. Two indoles of bisindoles are linked through a central five- or six-membered heterocyclic ring. A series of

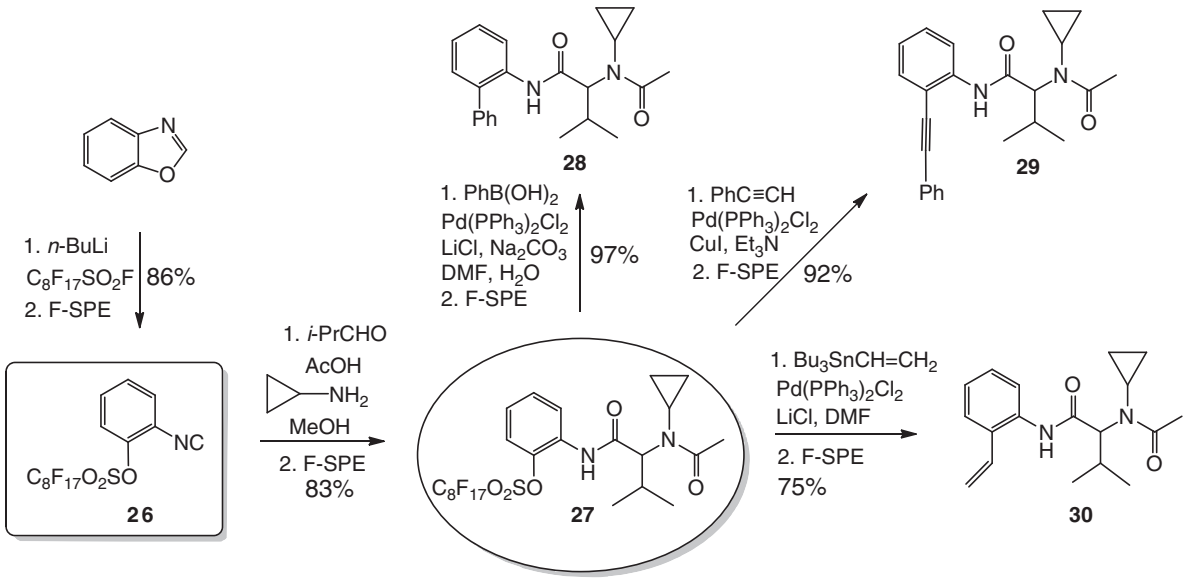
nonnatural bisindole compounds have been synthesized for biological tests (Scheme 5).[24] A fluorous sulfonyl linker-attached indolylboron **20** was subjected to two consecutive cross-coupling reactions, first with a dibromo-substituted central ring **21** to form compound **22**, and then with TIPS-protected indolylboron **23** followed by the cleavage of TIPS to give **24**. Methylation followed by Mg-promoted fluorous tag cleavage afforded bisindole **25**. The skeletal diversity was achieved by using a set of different dihalo-substituted central rings for double coupling and derivatization reactions.



Scheme 5 Synthesis of bisindoles bearing different central rings.

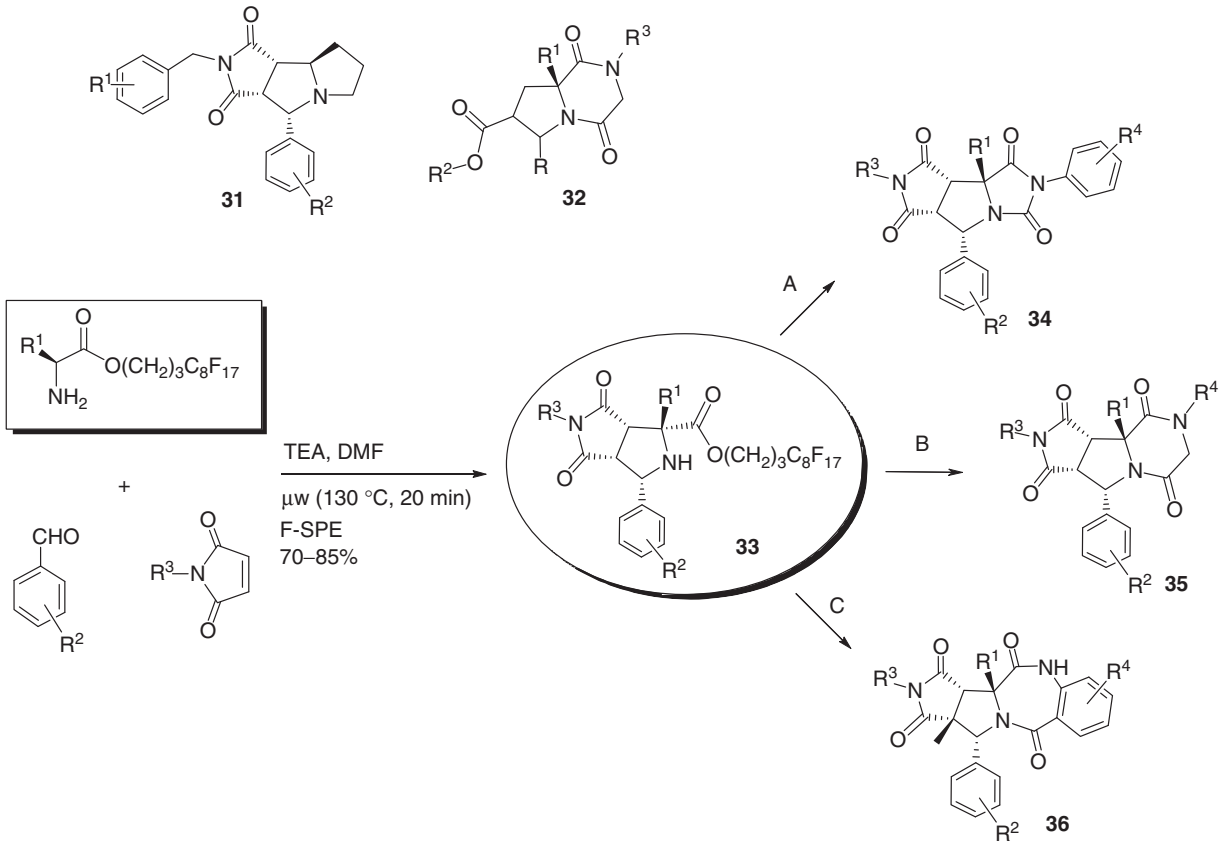
Isonitriles are versatile reagents for organic transformations including the Ugi four-component reaction. However, the synthetic advantages of isonitriles are offset by the notorious odor of this class of chemicals. Fluorous sulfonyl-attached arylisonitriles no longer have the unpleasant odor and can be used as a displaceable linker. Its application for the Ugi reaction followed by a metal-catalyzed linker cleavage reaction to make diverse compounds is shown in Scheme 6.[25] The freshly prepared isonitrile **26** was used as a limiting agent for the Ugi reaction to form **27**. This intermediate was then subject to different coupling reactions to remove the fluorous linker and also to introduce a new functional group to the Ugi condensation product. Different reactions such as Suzuki coupling, Sonogashira reaction, and Stille coupling were employed for linker cleavage to form benzyl-, alkynyl-, and vinyl-substituted compounds **28**, **29**, and **30**, respectively. In this case, displacement reactions at the last step were used to establish the substitution/functional group diversity. It is different from the library shown in Scheme 4, which has central ring diversity introduced by using different starting materials.

Displacement reactions are good for the generation of substitution diversity, whereas cyclization and cycloaddition reactions are powerful for the generation of skeletal diversity. Three libraries shown in Scheme 7 are produced from the same [3 + 2]



Scheme 6 Displaceable sulfonate linker for DOS.

cycloaddition intermediates **33**, but with different derivatization and cyclizations to afford hydantoin-, piperazinedione-, and benzodiazepine-fused scaffolds **34–36**.[26] The structure of **34** is similar to tricyclic thrombin inhibitor **31**, the structure of **35** is similar to diketopiperazine-based inhibitors of human hormone-sensitive lipase **32**, and the structure of **36** features a privileged benzodiazepine moiety.



Scheme 7 Libraries with skeletal diversity.

The synthesis of hydantoin-fused tricyclic compounds **34** was accomplished by a two-step reaction sequence shown in Scheme 8 (path A).[27] The reaction of **33** with phenylisocyanate and a catalytic amount of *N*,*N*-4-dimethylaminopyridine (DMAP) in toluene gave urea **37**. F-SPE purified **37** were heated with microwaves at 100 °C for 5 min in the presence of K_2CO_3 to cleave the fluorous linker and form the hydantoin-fused products **34**. The synthesis of piperazinedione-fused tricyclic compounds **35** is shown in Scheme 8 (path B).[28] The [3 + 2] cycloaddition products **33** were treated with chloroacetyl chloride to afford *N*-acylated products, which were then converted into **38** by the displacement of the chloride with amines. The microwave-promoted cyclization of **38** cleaved the fluorous linker and generated the piperazinediones **35**. In the synthesis of benzodiazepine-fused tetracyclic compounds **36**, the [3 + 2] cycloaddition compounds **33** were used for *N*-acylation followed by nitro group reduction with zinc dust to give **39** (Scheme 8, path C).[27] Cyclative linker cleavage with 1,8-diazabicyclo[4.3.0]non-5-ene (DBU) produced the corresponding benzodiazepine-fused tetracyclic compounds **36**.

A DOS based on fluorous TIPS-attached benzopyrans is shown in Scheme 9. Four fluorous benzopyrans **40** underwent five different paths of derivatizations to form libraries **41–45** (Scheme 10).[29] The synthetic pathways for these libraries are illustrated in Scheme 8. The synthesis of library **41** was carried out by the Suzuki coupling of **40** with vinylboronate. The resulting dienes **46** were subjected to a Diels–Alder reaction with twelve 1,2,4-triazoline-3,5-diones as azadienophiles to afford library **41** with **48** analogs. Diels–Alder reactions of **46** with 12 *N*-substituted maleimides yielded **48** analogs of compounds **47.** Half of these compounds were used for linker cleavage to afford library **42**, whereas the other half of **47** was oxidized with 2,3-dichloro-5,6-dicyano-1,4-benzoquinone (DDQ) followed by linker cleavage to give library **43**. Libraries **44** and **45** were produced by Click cycloaddition reactions of **48** with azides. The terminal alkynyl group was introduced to **40** by Pd-catalyzed Stille coupling. The resulting compounds **48** were reacted with 16 alkyl- and aryl azides using $BrCu(PPh_3)_3$ as a catalyst to give 1,4-disubstituted-1,2,3-triazoles **44**. Under the different cycloaddition conditions of using ruthenium(II) as a catalyst, the reaction of **48** with the azides gave 1,5-disubstituted-1,2,3-triazoles **45** regioselectively. In this project, F-SPE is the primary tool to separate the fluorous reaction intermediates. The overall yields for the multistep synthesis of different libraries were in the range of 50–80% and the purities for most compounds were >85% without further purification.

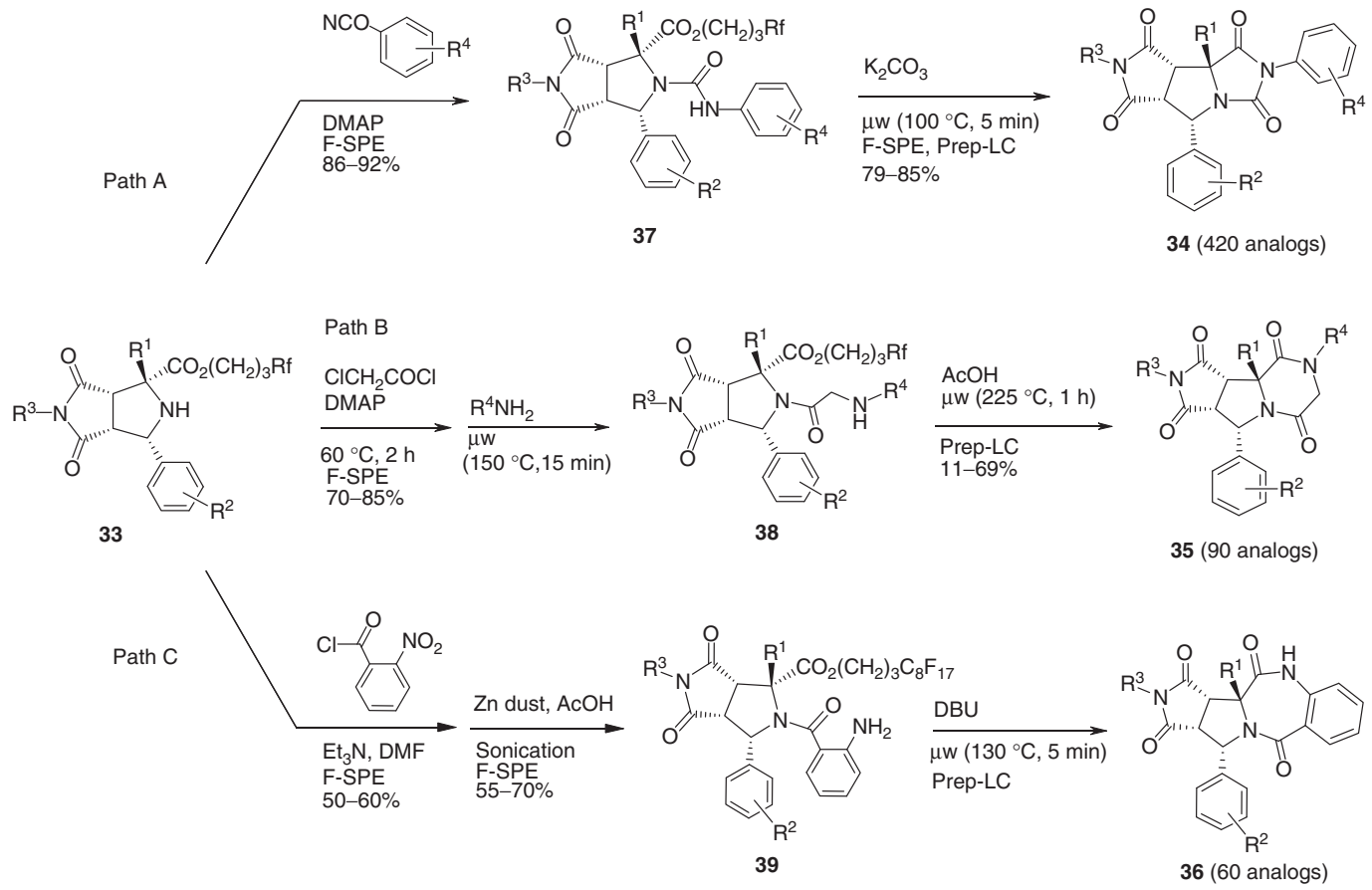
Use fluorous thiol linker-captured Pummerer cyclative products **49** for DOS is shown in Scheme 11. A series of post-Pummerer reactions has been developed to generate numbers of indolinone-based scaffolds **50–59**. Michael addition of **49** followed by SmI_2-promoted removal of the thiol linker afforded scaffold **50**.[30] Oxidative linker cleavage of **49** with ceric(IV) ammonium nitrate (CAN) could lead to the formation of **51** in quantitative yield. Oxidative linker cleavage of **49** followed by a reaction with 2-thienyllithium or DAST led to the formation of **52** or **53**.[31] Bucherer–Bergs reaction of **49** converted the linker cleavage product into spirohydantoins **54**. The reaction of oxidative linker cleavage product of **49** with 1,2-diaminobenzene led to the formation of tetracyclic compounds **55**. Sequential reactions of linker oxidation of **49** with *m*CPBA, alkylation with α,α'-dibromo-*o*-xylene, and SmI_2-promoted linker cleavage afforded spirocycle **56.** Another sequential reaction of linker oxidation of **49** involves oxidation with *m*CPBA, alkylation with 2-nitrobenzyl bromide, SmI_2-promoted linker cleavage and cyclization to yield tetracyclic compounds **57**. Alkylation of **49** with divinyl sulfone followed by SmI_2-triggered linker cleavage and cyclization afforded spirocyclic sulfones **58**.[32] Lastly, allylation of **49** followed by SmI_2-triggered reaction with imines produced pyrrolidinyl-spirooxindoles **59**.[33] Thus, the feasibility of the fluorous thiol linker-captured Pummerer cyclative products **49** for DOS is well-demonstrated.

9.12.5 Fluorous Mixture Synthesis

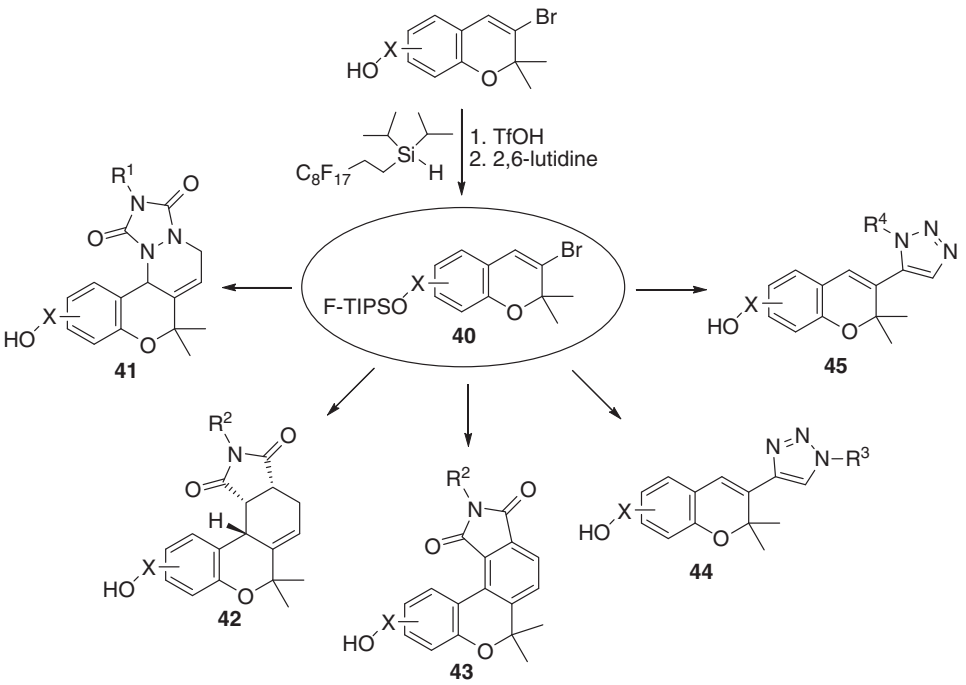
Mixture synthesis is highly efficient in producing chemical libraries. However, mixture compound-based biological screening is no longer a preferred practice in the pharmaceutical industry, because it is difficult to do compound management and the effort to deconvolute the active compound from a mixture is hard to justify. FMS is able to produce individual pure compounds with high efficiency.[8,34] In FMS, a set of fluorous linkers with different fluorine contents is paired with a set of reactants. The reactants can be analogs, diastereomers, or enantiomers. The paired fluorous starting materials are mixed together for multistep synthesis. Fluorous-attached final products are separated by a prep-HPLC with fluorous stationary phase followed by linker cleavage to give products in individual and pure forms.[18] FMS has been well-demonstrated in the synthesis of libraries containing nature product analogs, diastereomers, and enantiomers.

Natural product (*S*)-mappicine is active against the herpes viruses (HSV). Its ketone analog, nothapodytine B, is active against human cytomegalovirus (HCMV). A seven-component mixture synthesis of the 560-member mappicine library is a good example for demonstrating the power of FMS (Scheme 12).[35] Seven fluorous TIPS-type linkers were used to attach and encode seven analogous substrates with different R^1. Seven-component mixture *M*-**60** was split into eight portions for *N*-propargylation with eight different bromides to afford eight mixtures of *M*-**61**. Each of the eight mixtures of *M*-**62** was further split into 10 portions for radical annulation reaction with different isonitriles. The resulting 80 mixtures of *M*-**62** were demixed by F-HPLC and then treated with HF-pyridine for linker cleavage to give a 560-member mappicine library **63**. If this library were made by parallel synthesis, each of the three reaction steps shown in Scheme 12 would need to have 560 reactions. FMS of the same library only needs one reaction for the first step, eight reactions for the second, and 80 reactions for the last step. The numbers for reaction and intermediate separation were significantly reduced.

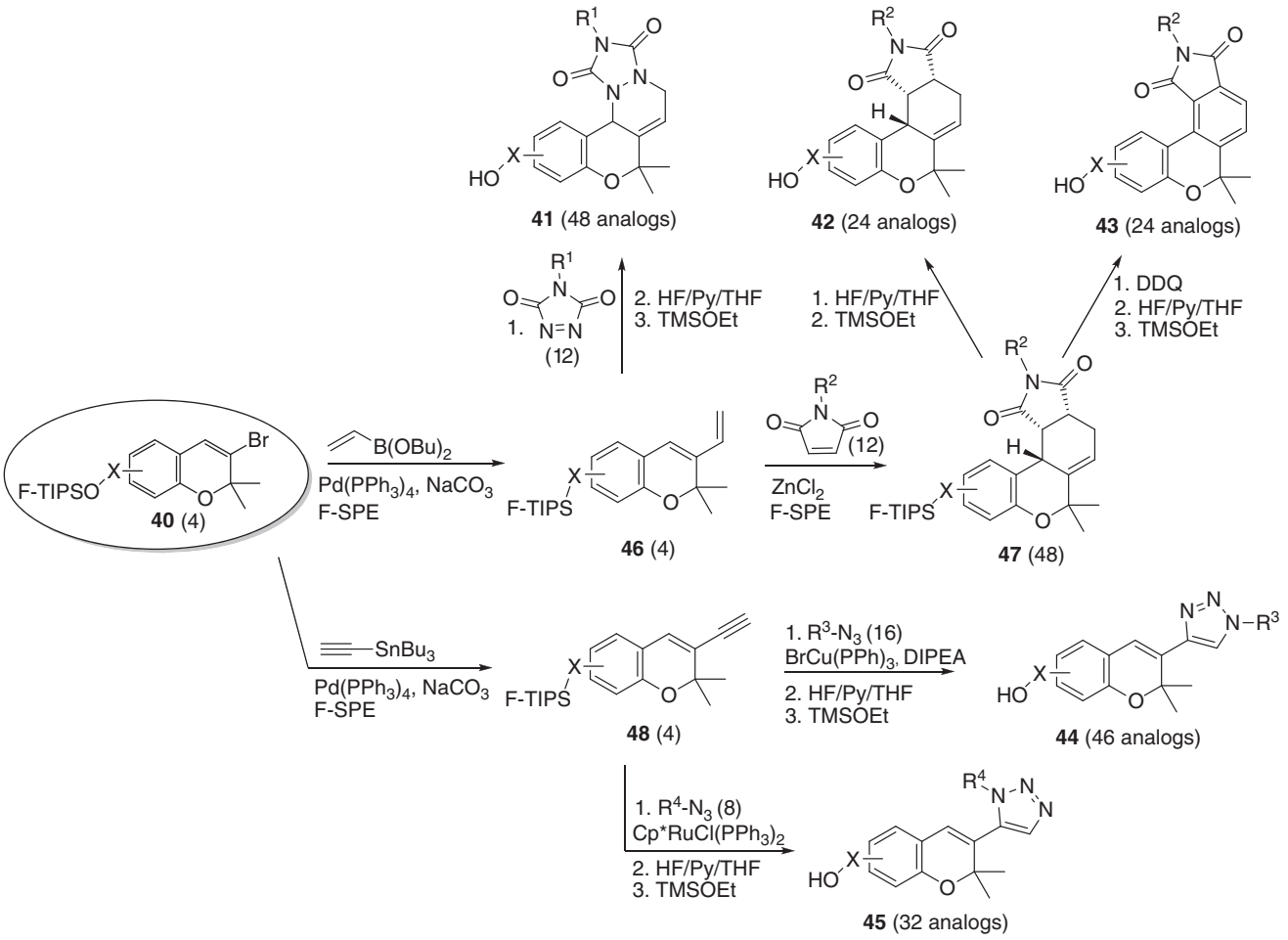
A fluorous linker usually has a fluorous tag with <10 perfluorocarbons ($C_{10}F_{21}$). Longer tags will reduce the solubility of the attached molecule in common organic solvents. In addition, the even number fluorous tags (C_4F_9, C_6F_{13}, C_8F_{17}, and $C_{10}F_{21}$) are



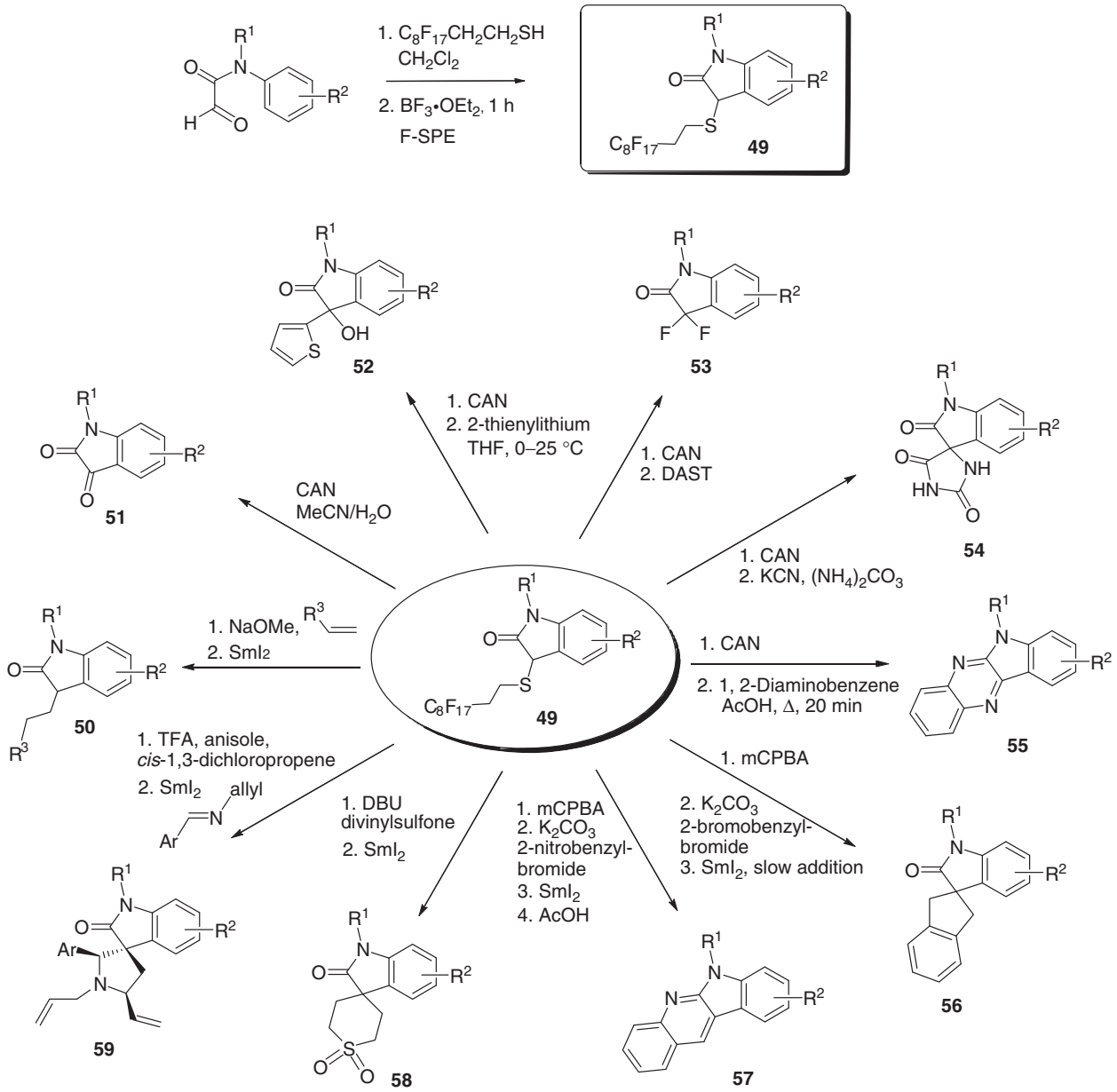
Scheme 8 Synthesis pathways for libraries with different skeletons.



Scheme 9 DOS libraries derivatized from fluorous benzopyrans **40**.



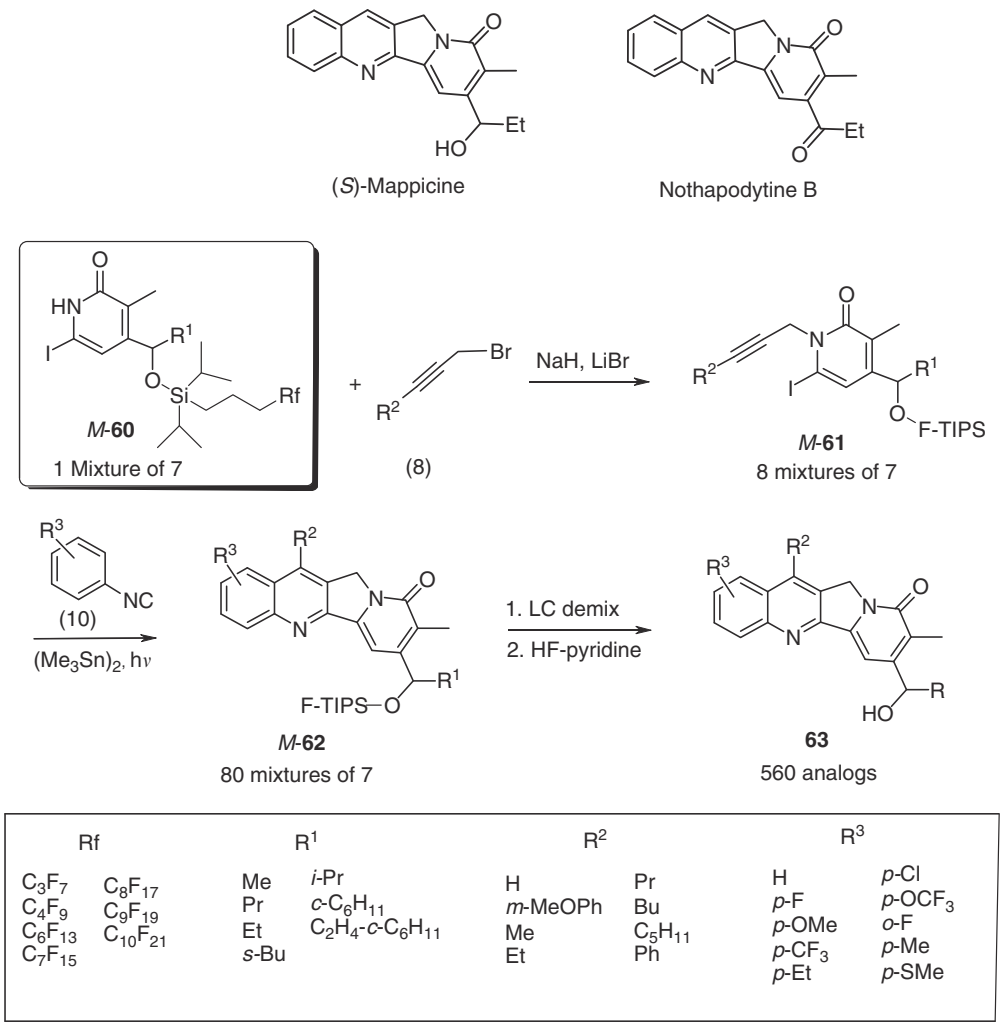
Scheme 10 Synthetic pathways for benzopyrans-based DOS.



Scheme 11 Fluorous thiol as a catch-and-release linker for DOS.

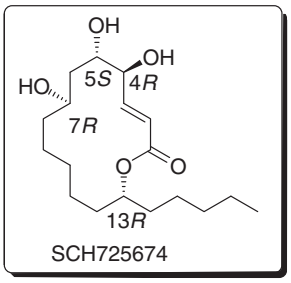
much cheaper than odd number fluorous tags (C_3F_7, C_5F_{11}, C_7F_{14}, and C_9F_{19}), so the selection of fluorous tags could be limited. Binary tagging is a new strategy to encode two or more stereocenters with only few fluorous tags.

A good example of binary tagging is the synthesis of the complete stereoisomer library of SCH725674 macrolactones (Scheme 13).[36] SCH725674 has antifungal activity against *Saccharomyces cerevisiae* and *Candida albicans*. It has four stereocenters at C4, C5, C7, and C13 positions and 16 stereoisomers. The synthesis of 16 stereoisomers of SCH725674 is shown in Scheme 11. Two TIPS-type linkers were employed to attach to the hydroxyl groups at C4, C5, and C7. Since one of the tags is nonfluorous, the only fluorous tag is C_2F_5. These two tags were introduced to 4,5-*trans* and 4,5-*cis* series to form two sets of mixtures, *M*-**64a-d** and *M*-**64e-h**, each containing four components with fluorine content of 0, 5, 10, and 15. Each mixture was first treated with potassium trimethylsilanolate (TMSOK) to remove the methyl group and then the acid was divided in half and each portion was coupled with either (*R*)-**65** or (*S*)-**65** under Yamaguchi conditions to give esters *M*-**66** as four mixtures of four. Ring-closing metathesis with the second-generation Grubbs catalyst followed by hydrogenation with a poisoned Pd catalyst gave the final tagged mixtures *M*-**67** as four mixtures of four. Each *M*-**67** was demixed by LC followed by the cleavage of TIPS with tetra-*n*-butylammonium fluoride (TBAF) to give a total of 16 stereoisomers of SCH725674. This is the first time that a complete stereoisomer library has been made by FMS to assign a natural product of completely unknown configuration.

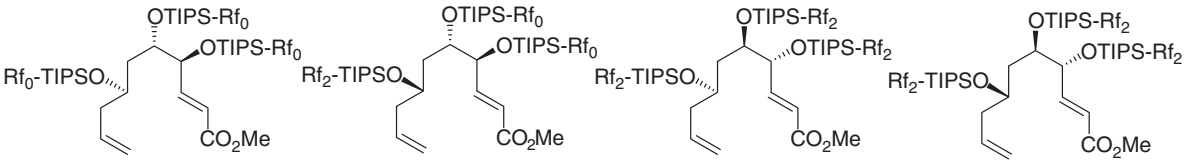


Scheme 12 FMS of mappicine library.

The use of two different kinds of linkers for binary tagging has been introduced recently. This new FMS strategy has been well-illustrated in the synthesis of stereoisomers of macrosphelides. Natural products macrosphelides have high anticancer activity (Scheme 14).[37] A library of 16 stereoisomers with the *S*-configuration fixed at C3 and all possible configurations at the other four stereocentres (C8, C9, C14, and C15) was synthesized by FMS. Fluorous TIPS-type and PMB-type linkers were used to attach to the hydroxyl groups at C8 and C1 positions, respectively. Each of the linkers has four different tags (C_2F_5, C_4F_9, C_6F_{13}, and C_8F_{17}). A set of four stereoisomers was paired with TIPS-type linkers bearing different fluorous tags to form **68a-d**. Another set of four stereoisomers was paired with PMB-type linkers also bearing different fluorous tags to form **69a-d**. A four-component mixture of *M*-**68a-d** was coupled with the *tert*-butyldimethylsilyl (TBS) ether of (*S*)-3-hydroxybutanoic acid to give *M*-**70a-d**. After removal of the TBS group with HCl, the resulting mixture was coupled with a four-component mixture of *M*-**69a-d** to give *M*-**71a-d/a-d** as single mixture containing 16 quasiisomers. The TES group was removed, and the 2,2,2-trichloroethyl ester was cleaved with zinc dust. The resulting hydroxy acid mixture was subjected to Yamaguchi lactonization to give macrolactone *M*-**72a-d/a-d** still as a single mixture containing 16 quasiisomers. This 16-quasiisomer was purified by flash chromatography in a single fraction to provide the sample for demixings. The combination of two sets of fluorous tags generated some quasiisomers containing same numbers of fluorine. The LC demixing of *M*-**72a-d/a-d** gave seven fractions. Only fractions 1, 6a, 6b, and 7 contained single isomers (**72aa**, **72dc**, **72cd**, and **72dd**). They were detagged directly to give first four macrosphelide isomers **73aa, 73dc, 73cd, 73dd**. Fractions 2–5 are mixtures of quasiisomers because of fluoroine redundancy. Fraction 2 contains two components (**7ab** and **72ba**), each with 14 fluorines. Fraction 3 contains three components (**72ac, 72bb**, and **72ca**), each with 18 fluorines. Fraction 4 contains four components (**72ad, 72bc**, **72cb**, and **72da**), each with 22 fluorines. Fraction 5 contains three components (**72bd**, **72cc**, and **72db**), each with 26 fluorines. The fluorous TIPS group was removed from fractions 2–5 with TBAF. The resulting four mixtures only have single fluorous PMB linkers and without fluorine redundancy. They were subject to second LC demixing followed by removal of PMB linker to give 12 macrosphelide stereoisomers. Thus, the synthesis of total 16 stereoisomers with the *S*-configuration fixed at C3 was accomplished. Despite the structural similarities, each of the 16 macrosphelide stereoisomers

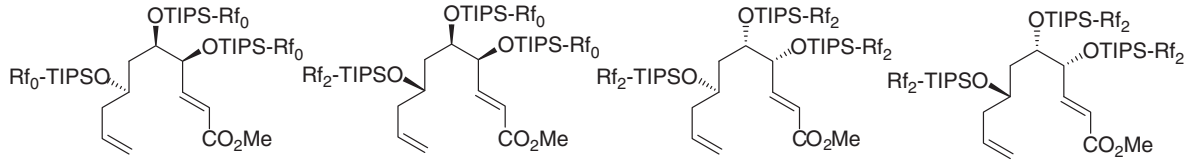


Mixture 1, *M*-**64a**–**d**



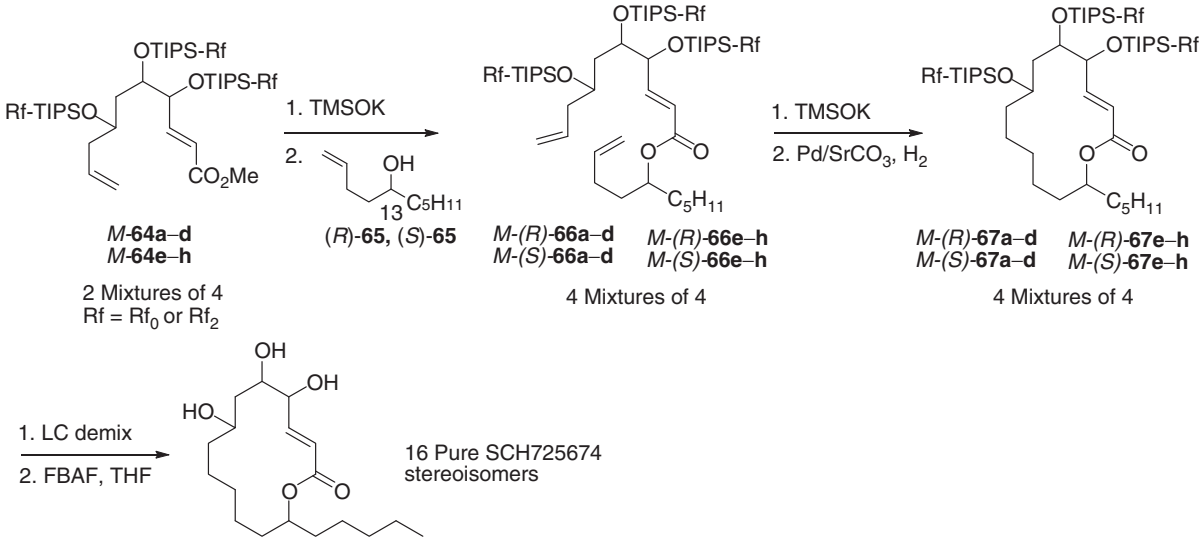
(*S,S,R*)-**64a** (0 F) (*S,S,S*)-**64b** (5 Fs) (*R,R,R*)-**64c** (10 Fs) (*R,R,S*)-**65d** (10 Fs)

Mixture 2, *M*-**64e**–**h**



(*S,S,R*)-**64e** (0 F) (*S,S,S*)-**64f** (5 Fs) (*R,R,R*)-**64g** (10 Fs) (*R,R,S*)-**64f** (10 Fs)

Rf_0-TIPS= –Si(*i*-Pr)$_3$ Rf_2-TIPS= –Si(*i*-Pr)$_2$$CH_2CH_2C_2F_5$



M-**64a**–**d**
M-**64e**–**h**

2 Mixtures of 4
Rf = Rf_0 or Rf_2

(*R*)-**65,** (*S*)-**65**

M-(*R*)-**66a**–**d** *M*-(*R*)-**66e**–**h**
M-(*S*)-**66a**–**d** *M*-(*S*)-**66e**–**h**

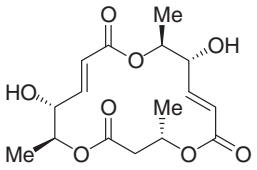
4 Mixtures of 4

M-(*R*)-**67a**–**d** *M*-(*R*)-**67e**–**h**
M-(*S*)-**67a**–**d** *M*-(*S*)-**67e**–**h**

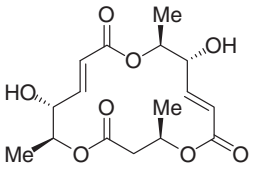
4 Mixtures of 4

16 Pure SCH725674 stereoisomers

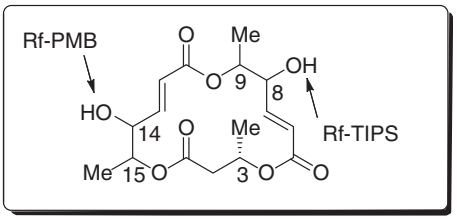
Scheme 13 Binary tagging for synthesis of stereoisomers of SCH725674.

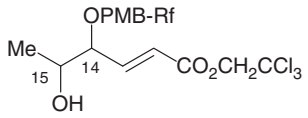


Macrosphelide A
(3*S*,8*R*,9*S*,14*R*,15*S*)

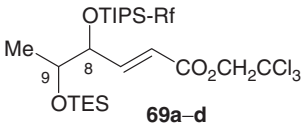


Macrosphelide E
(3*R*,8*R*,9*S*,14*R*,15*S*)





68a–d
1 mixture of 4

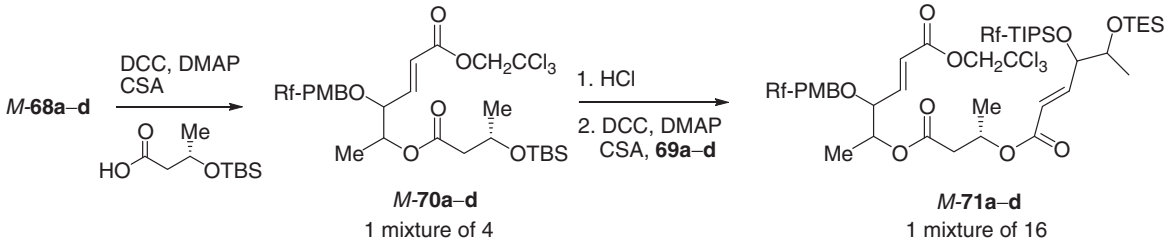


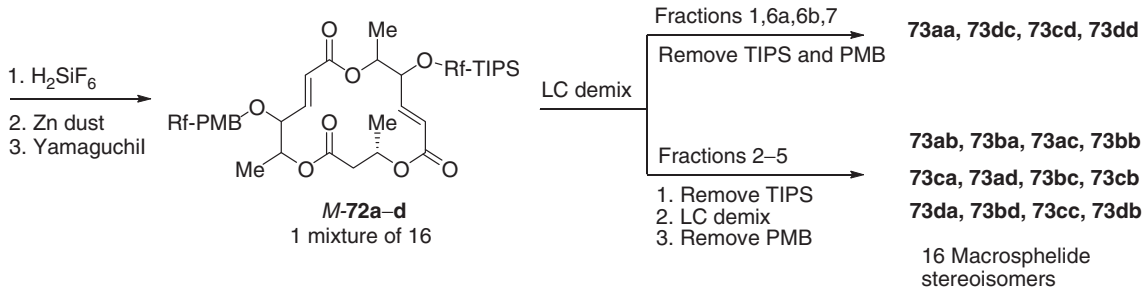
69a–d
1 mixture of 4

Encoding stereocenters with Rf-PMB and Rf-TIPS

Letter	Configuration	Rf
a	(*R*,*R*)	C_2F_5
b	(*S*,*S*)	C_4F_9
c	(*S*,*R*)	C_6F_{13}
d	(*R*,*S*)	C_8F_{17}

Rf-PMB = $Rf(CH_2)_3O$-*p*-$C_6H_4CH_2$
Rf-TIPS = $Rf(CH_2)_2(i\text{-}Pr)_2Si$





Scheme 14 One-pot FMS of 16 stereoisomers of macrosphelides.

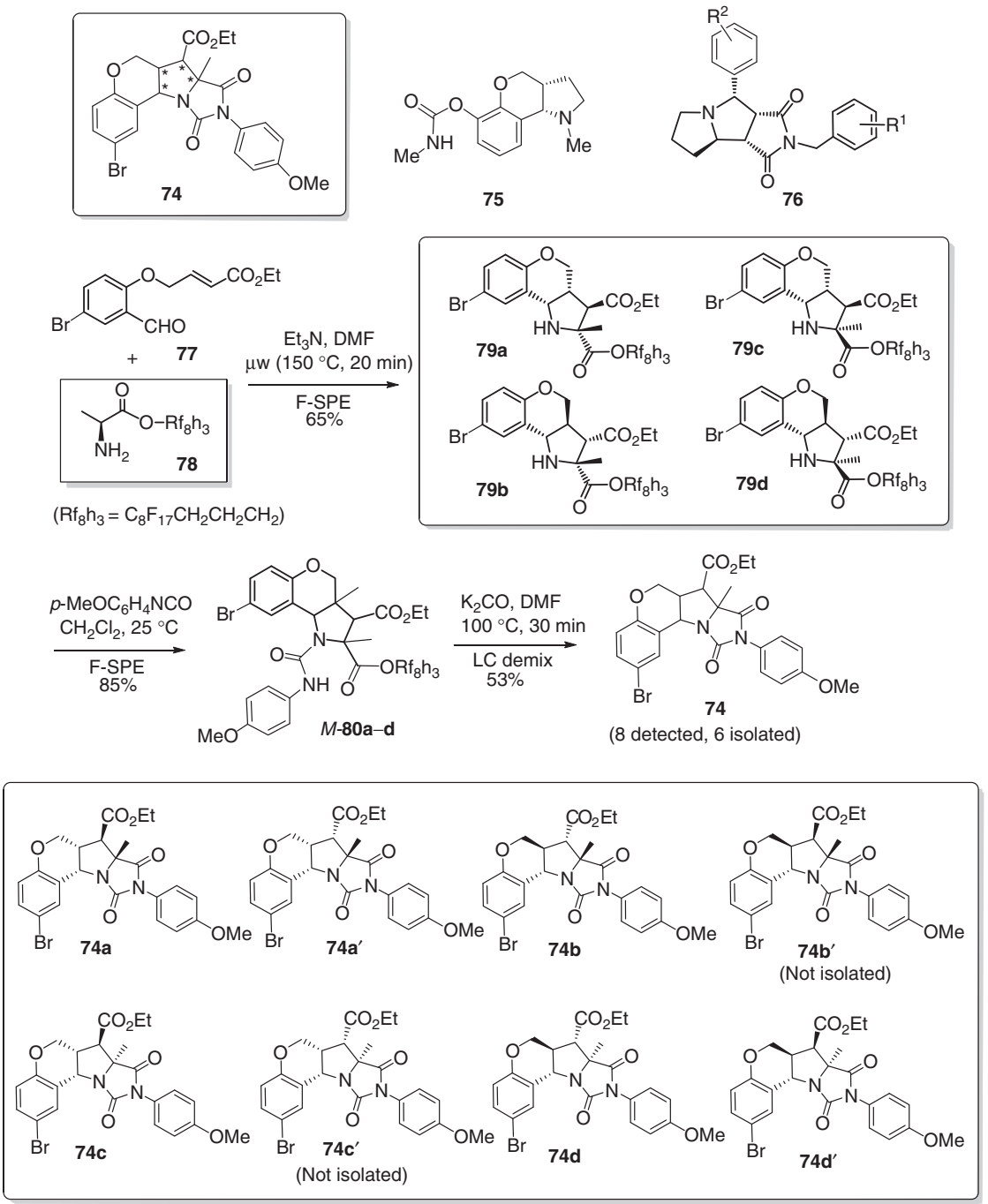
exhibited unique ^1H and ^{13}C NMR spectra. The configuration of macrosphelide A was confirmed to be **73dd** (3*S*,8*R*,9*S*,14*R*,15*S*), and macrosphelide E was confirmed to be the enantiomer of **73cc** (3*S*,8*S*,9*R*,14*S*,15*R*).

In the previously mentioned FMS, multiple fluorous linkers are used to encode different stereocenters for making stereoisomers. A new strategy to use only one fluorous linker to make diastereomers has been introduced recently. A reaction that is able to generate multiple stereocenters could result in a set of diastereomers. If a fluorous component is involved in the reaction, all the diastereomers will bear the same fluorous tag. F-SPE is able to separate diastereomers as a family from the reaction mixture without demixing. The fluorous diastereomeric mixture can be treated as a single component for reaction and separation. At the end of synthesis, the fluorous linker is cleaved and the final products as diastereomers are separated by prep-LC to provide individual isomers. This so-called fluorous diastereomeric mixture synthesis (FDMS) is different from previously mentioned FMS. In FDMS, the fluorous tag is only used to hold the intermediate diastereomers together during F-SPE separation, not for encoding

the stereocenters. The second difference is that the fluorous linker is cleaved first, and then the mixture is separated by LC with C_{18} stationary phase.

FDMS has been demonstrated in the synthesis of hydantoin-fused hexahydrochromeno[4,3-*b*]pyrrole **74** (Scheme 15).[38] There are four stereocenters on the central pyrrolidine ring, which could generate many diastereomers. A tricyclic fragment of **74** is related to hexahydrochromeno[4,3-*b*]pyrrole **75**, which is a potent compound against human acetylcholinesterase and butyryl-cholinesterase for the potential treatment of Alzheimer diseases. Compound **74** also has a structural similarity with tricyclic thrombin inhibitors **76**. Diastereomers of **74** could be interesting compounds to screen against known and new biological targets.

The synthesis of diastereomers of **74** is highlighted in Scheme 15. Intramolecular [3 + 2] cycloaddition of **77** with fluorous L-alanine ester **78** under microwave heating generated four diastereomers *M*-**79a-d**. Since all the diastereomers bear the same fluorous linker, they could be isolated by F-SPE in the same fraction. The purified mixture was reacted with an isocyanate to form



Scheme 15 One-pot synthesis of diastereomers of **74**.

ureas *M*-**80a-d,** which is also a mixture of four diastereomers. Base-promoted linker cleavage and cyclization under microwave heating of *M*-**80a-d** yielded eight diastereomers *M*-**80**, because the acidic proton next to the ester group was epimerized. Six of the diastereomers were isolated by prep-LC with a C_{18} stationary phase. Their structures were determined by 2D NMR analysis and X-ray crystal structure of **80a**. Described in Scheme 15 is only a single set of diastereomers. By using analogs of **77**, **78**, and isocyanate, many more sets of diastereomers with substitution and stereochemistry diversities can be prepared by FDMS.

9.12.6 Conclusion

Fluorous linker-facilitated synthesis is a nice combination of solution-phase reaction and easily phase-tag-based separation, which has favorable homogenous reaction kinetics, broad synthetic scope, and good compatibility with other analytical, synthetic, and separation technologies. Fluorous silica gel-based solid-phase extraction and prep-LC enhances the utility of fluorous separation techniques in parallel synthesis, DOS, and FMS. The cost and environmental impact of perfluorinated chemicals have been minimized by the development of light fluorous technologies.

References

1. Nicolaou, K. C., Hanko, R., Hartwig, W., Eds. *Handbook of Combinatorial Chemistry*; Wiley: Weinheim, **2002**.
2. Gladysz, J. A., Curran, D. P., Horvath, I. T., Eds. *Handbook of Fluorous Chemistry*; Wiley-VCH: Weinheim, **2004**.
3. Horvath, I., Ed. *Fluorous Chemistry, Top. Curr. Chem*; Springer-Verlag: Berlin, **2012**.
4. Horvath, I. T.; Rabai, J. *Science* **1994**, *266*, 72–75.
5. Studer, A.; Hadida, S.; Ferritto, S. Y.; *et al. Science* **1997**, *275*, 823–826.
6. Curran, D. P. *Angew. Chem. Int. Ed. Engl.* **1998**, *37*, 1174–1196.
7. Zhang, W. *Tetrahedron* **2003**, *59*, 4475–4489.
8. Zhang, W. Fluorous Mixture Synthesis (FMS) of Drug-Like Molecules and Enantiomers, Stereoisomers, and Analogs of Natural Products. In *Fluorine in Medicinal Chemistry and Chemical Biology*; Ojima, I., Ed.; Wiley-Blackwell: Chichester, **2009**, pp 335–359.
9. Zhang, W. Fluorous Linker-facilitated Synthesis of Biologically Interesting Molecules. In *Modern Chemoselective Tools for the Synthesis of Complex Bioactive Molecules*; Cossy, J., Arseniyadis, S., Eds.; Wiley: Chichester, **2012**, pp 349–373.
10. Zhang, W. *Curr. Opin. Drug Discovery Dev.* **2004**, *7*, 784–797.
11. Yoder, N. C.; Yuksel, D.; Dafik, L.; Kumar, K. *Curr. Opin. Chem. Biol.* **2006**, *10*, 1–8.
12. Zhang, W.; Curran, D. P. *Tetrahedron* **2006**, *62*, 11837–11865.
13. Zhang, W. *Green Chem.* **2009**, *11*, 911–920.
14. Zhang, W. *Chem. Rev.* **2004**, *104*, 2531–2556.
15. Zhang, W. Fluorous Linker Units. In *Linker Strategies in Solid-Phase Organic Synthesis, Solid-phase Palladium Chemistry*; Scott, P., Ed.; Wiley: Chichester, **2009**, Vol. 2, pp 553–576.
16. Song, E.-H.; Pohl, N. L. B. *Future Med. Chem.* **2009**, *1*, 889–896.
17. Zhang, W.; Lu, Y.; Nagashima, T. *J. Comb. Chem.* **2005**, *7*, 893–897.
18. Zhang, W. *J. Fluorine Chem.* **2008**, *129*, 910–919.
19. Lu, Y.; Nagashima, T.; Miriyala, B.; Conde, J.; Zhang, W. *J. Comb. Chem.* **2010**, *12*, 125–128.
20. Villard, A.-L.; Warrington, B. H.; Ladlow, M. *J. Comb. Chem.* **2004**, *6*, 611–622.
21. Lu, Y.; Zhang, W. *QSAR Comb. Sci.* **2004**, *23*, 827–835.
22. Burke, M. D.; Berger, E. M.; Schreiber, S. T. *Science* **2003**, *302*, 613–618.
23. Tan, D. *Nat. Chem. Biol.* **2005**, *1*, 74–84.
24. Kasahara, T.; Kondo, Y. *Chem. Commun.* **2006**, 891–893.
25. Pirrung, M. C.; Ghorai, S.; Ibarra-Rivera, T. R. *J. Org. Chem.* **2009**, *74*, 4110.
26. Zhang, W.; Lu, Y.; Chen, C. H.-T.; Curran, D. P.; Geib, S. *Eur. J. Org. Chem.* **2006**, 2055–2059.
27. Zhang, W.; Lu, Y.; Chen, C. H.-T.; Zeng, L.; Kassel, D. B. *J. Comb. Chem.* **2006**, *8*, 687–695.
28. Werner, S.; Nielsen, S. D.; Wipf, P.; *et al. J. Comb. Chem.* **2009**, *11*, 452–459.
29. Zhu, M.; Lim, B. J.; Koh, M.; Park, S. B. *ACS Comb. Sci.* **2012**, *14*, 124.
30. McAllister, L. A.; McCormick, R. A.; Brand, S.; Procter, D. J. *Angew. Chem. Int. Ed. Engl.* **2005**, *44*, 452–455.
31. McAllister, L. A.; McCormick, R. A.; James, K. M.; *et al. Chem. Eur. J.* **2007**, *13*, 1032–1046.
32. James, K. M.; Willetts, N.; Procter, D. *J. Org. Lett.* **2008**, *10*, 1203–1206.
33. Coote, S. C.; Quenum, S.; Procter, D. *Org. Biomol. Chem.* **2011**, *9*, 5104–5108.
34. Zhang, W. *ARKIVOC* **2004**, *i*, 101–109.
35. Zhang, W.; Luo, Z.; Chen, H.-T.; Curran, D. P. *J. Am. Chem. Soc.* **2002**, *124*, 10443–10450.
36. Moretti, J. D.; Wang, X.; Curran, D. P. *J. Am. Chem. Soc.* **2012**, *134*, 7963–7970.
37. Curran, D. P.; Sinha, M. K.; Zhang, K.; Sabatini, J. J.; Cho, D.-H. *Nat. Chem.* **2012**, *4*, 124–129.
38. Lu, Y.; Steven, J.; Geib, S. J.; *et al. Chem. Commun.* **2010**, *46*, 7578–7580.

9.13 Organic Photochemistry

CG Bochet, University of Fribourg, Fribourg, Switzerland

© 2014 Elsevier Ltd. All rights reserved.

9.13.1	**Introduction**	331
9.13.2	**Fundamentals**	331
9.13.2.1	Excitation of Molecules	331
9.13.2.2	Quantum Yield	331
9.13.3	**Experimental Aspects**	332
9.13.3.1	Mercury Lamps	332
9.13.3.2	Fluorescent Tubes	332
9.13.3.3	LEDs	332
9.13.4	**Photochemistry of Alkenes**	333
9.13.4.1	Isomerizations	333
9.13.4.2	Pericyclic Rearrangements	333
9.13.4.3	Cycloadditions	334
9.13.4.4	The Di-π-Methane Rearrangement	337
9.13.4.5	Additions	337
9.13.4.6	Reactions with Aromatic Compounds	338
9.13.5	**Photochemistry of Carbonyl Compounds**	339
9.13.5.1	Norrish-Type I	339
9.13.5.2	Norrish-Type II	340
9.13.5.3	Photoenolization	341
9.13.5.4	Paternò–Büchi Reaction	342
9.13.6	**Singlet Oxygen**	343
9.13.7	**Photolabile Protecting Groups**	343
9.13.8	**Photoredox Catalysis**	345
9.13.9	**Miscellaneous Reactions**	346
9.13.9.1	The Barton Reaction	346
9.13.9.2	Hoffmann–Löffler–Freytag reaction	347
9.13.9.3	Azo-Compounds	347
9.13.9.4	Asymmetric Photochemistry	347
9.13.10	**Conclusion**	348
References		349

Glossary

Actinometer Device or chemical reaction capable of measuring a photon flux in a given configuration.

Beer–Lambert law Linear equation relating absorbance to concentration of a solution and optical path.

Bleaching Loss of color (absorbance).

Circularly polarized light Chiral form of light.

De Mayo reaction [2 + 2] Photocycloaddition of an alkene with the enolic form of a 1,3-dicarbonyl compound.

Di-π-methane rearrangement Formation of a vinylcyclopropane by irradiation of a 1,4-diene.

Excited state Unstable electronic state of a molecule, usually with an electronic distribution different from the ground state.

Frank–Condon principle Principle stating that the nuclei do not move during an electronic excitation.

Ground state Most stable electronic state of a molecule.

***Meta*-cycloaddition** Cycloaddition of an alkene with a benzene derivative, leading to a tricyclic core.

Norrish-type-I reaction Photochemical fragmentation of a bond located in the alpha position of a carbonyl group.

Norrish-type-II reaction Photochemical fragmentation of a bond located in the beta position of a carbonyl group.

***Ortho*-cycloaddition** Cycloaddition of an alkene with a benzene derivative, leading to a bicyclo[4.2.0]octadiene core.

***Para*-cycloaddition** Cycloaddition of an alkene with a benzene derivative, leading to a bicyclo[2.2.2]octadiene core.

Paternò–Büchi reaction [2 + 2] Photocycloaddition of an alkene with a carbonyl group.

Photostationary state Chemical equilibrium under continuous irradiation.

Quantum yield Ratio of the number of molecules undergoing a photochemical/photophysical event over the number of absorbed photons.

Rayonet Popular type of cylindric irradiation device.

Rose Bengal Pink sensitizer, absorbing visible light.

 doi:10.1016/B978-0-08-097742-3.00939-3

Sensitizer Substance capable of absorbing light and transferring its energy to another molecule.
Singlet Electronic state in which the number of electrons of different spin is the same. It is always the case for closed shell species.
Triplet Electronic state in which two unpaired electrons have the same spin.

9.13.1 Introduction

Photochemical reactions arise from electronically excited states, where the electron distribution can significantly differ from that in the more stable ground state. As a consequence, unusual reactivity is frequently observed, and this is precisely what makes such reactions a useful complement to the more classical ground state reactions (also called 'thermal' reactions, although this term also encompasses reactions carried out at low temperature). This unusual reactivity allows one to connect atoms that would normally not form bonds, or it allows a normally unfeasible process to proceed at reasonable temperatures. Of course, high-energy metastable electronic states also have their drawbacks, such as uncontrolled decomposition of the substrate ('black tar' at the bottom of the reaction flask), short lifetime of the excited state (often rendering bimolecular reactions impossible), or technical difficulties (in particular with respect to scale-up).

This chapter aims at illustrating what can be achieved by photochemical reactions with a series of selected examples for each of the most important classes of reactions, taken from syntheses of interesting molecules (natural or not). In recent years, several excellent reviews have been published,[1,2] together with textbooks,[3] overviews,[4,5] and reference handbooks.[6,7] Whenever possible, examples taken from more recent literature, other than those already presented in these publications, are presented.

9.13.2 Fundamentals

9.13.2.1 Excitation of Molecules

In order to be excited, a molecule needs to absorb a photon. For this event to be possible, an essential condition must be met:

$$\Delta E = h\nu,\ \nu = \frac{hc}{\lambda} \tag{1}$$

where ΔE is the energy difference between the ground and excited states, h is the Planck's constant (6.62×10^{-34} J s), and ν is the frequency (or λ the wavelength) of an electromagnetic wave. Practically, it means that this energy difference should match exactly (give or take some vibrational energy) the energy of the incident light. Thus, it is not possible to provide the system with high energy, hoping that it will absorb what it needs and leave the rest. This adds to the difficulty of photochemistry, because one should know this energy in order to choose the right light source. However, a simple UV–vis absorption spectrum gives this information. A second condition is:

$$\Delta S = 0 \tag{2}$$

The electronic configuration of the ground state of the molecule corresponds to a spin state (usually a singlet, $S=0$). Excitation by light should preserve this spin state. An important consequence of this is that it is not possible to generate a triplet excited state by irradiation of a singlet ground state species. This is unfortunate, as triplets are frequently involved in useful organic reactions. An indirect approach is nevertheless possible, i.e., by using a sensitizer (*vide infra*). It is worth mentioning that this rule can be violated through spin–orbit coupling, which increases with the atomic number, and can be significant with atoms as heavy as bromine.

As the time scale of electronic excitation is much shorter than that of nuclear motions ($\sim$fs), the nuclei do not move during the excitation. This is known as the Frank–Condon principle, and has the consequence that excited states are formed at non-equilibrated geometries; in some cases, a state can be reached at a geometry where it is dissociative. In cases where the potential energy surface of the excited state is significantly shifted with respect to the ground state, the energy difference between the two states increases, i.e., a higher excitation energy is necessary.

9.13.2.2 Quantum Yield

It can be useful to consider light as a particle (a photon). In this perspective, one can consider light as a reagent. In fact, there is even a unit for 1 mol of photons: the Einstein. In classical reactions, the yield is defined as the fraction of the reactant ending up as a product. Likewise, the fraction of photons ending up converting a molecule of substrate into a product defines the 'quantum yield.' Its experimental determination can be cumbersome, as it is necessary to know with precision the amount of light that was absorbed by the solution. This is typically done by using a 'chemical actinometer,' which is a chemical reaction for which the

quantum yield is known. Potassium ferrioxalate is one of the most popular actinometers (but there are many others, such as valerophenone and phenylglyoxylic acid), and its photoreaction should be carried out under the exact same conditions (meaning also the same reaction vessel) as the reaction to be studied. In addition, in order to avoid bleaching of the solution due to the substrate photoconversion, the irradiation should be stopped at very low conversion (typically less than 10%). When determined with precision, the quantum yield can provide useful insights into the reaction mechanism, as it is an indication of the ratio of the rate of the desired process over those for all competing nonproductive processes. In some cases, quantum yields higher than unity are observed; this is a symptom of a radical-chain reaction.

9.13.3 Experimental Aspects

As mentioned in Section 9.13.2.1, the light source should be chosen so that its emission spectrum matches the desired absorption as closely as possible. In practice, this is not always possible in a precise fashion, as tunable light sources are not common. There are essentially three types of sources that are commonly used in organic photochemistry (lasers are not included, as they are not, so far, used in a preparative sense. However, the reactions listed in this chapter can of course be triggered by laser light, for example on a silica surface or within living cells.).

9.13.3.1 Mercury Lamps

Low-pressure mercury vapor lamps emit 254 nm radiation as a quite sharp monochromatic line, with a good intensity and a low thermal output. They are frequently used as immersion lamps, meaning that the lamp is placed at the center of a triple-walled vessel. In an intermediate compartment, cold water is circulated to keep the outer compartment, where the reacting solution is stirred, at a low temperature. As glass is opaque at 254 nm, the inner part of the apparatus has to be made of quartz.

Medium-pressure mercury vapor lamps operate with the same principle as the low-pressure ones, but approximately a dozen emission lines appear, of which those at 314 and 366 nm are particularly strong. The generation of heat becomes an issue with these lamps, and cooling becomes mandatory, but a Pyrex apparatus can be used.

High-pressure mercury vapor lamps are polychromatic, with some spikes at defined wavelength; addition of xenon makes the emission much more continuous. Again, cooling of the reaction mixture is essential.

If irradiation must be carried out at a specific wavelength, the use of a monochromator is possible, but the resulting intensity is rather low, making it quite impractical for preparative purpose. However, the use of cutoff filters is usually a good compromise, in particular if used in conjunction with a high-pressure mercury lamp. These filters are transparent to light of longer wavelength than the cutoff. For example, Pyrex filters light below approximately 300 nm; in such a case, simple use of Pyrex glassware is sufficient. It is worth noting that glasses have variable quality, and a prior check of transmittance is recommended. Aqueous solutions of transition metal ions are also efficient filters, which can be used in combinations. A very detailed description of filters is available from glass manufacturers or from reference handbooks.[8]

9.13.3.2 Fluorescent Tubes

Tubes containing mercury with an inner coating acting either as a filter or a fluorescent emitter are available as very convenient and cost-effective 'monochromatic' sources (within approximately 50 nm). They are currently available for 254, 300, 350, 360, and 419 nm, and can be mounted on the inside walls of a metallic cylinder, at the center of which the reaction vessel can be placed (Rayonet® reactor). For irradiation times of less than an hour, cooling is not strictly necessary. A typical setup involves 16 tubes, making a wavelength change quite cumbersome; the tubes have a limited lifetime, typically approximately 1000 h of operation.

9.13.3.3 LEDs

The most recent development in light sources is light emitting diodes (LEDs) capable of providing UV light with reasonable intensities (less than 500 mW per unit) down to 360 nm. Shorter wavelengths can be attained, down to 250 nm, but the intensity drops to less than 10 mW, while raising the cost to thousands of dollars apiece. However, it is still an emerging technology, and further reduction of cost and increase in intensity are expected. Already at the present time, preparative reactions up to 100 mg are possible (and flow techniques can increase this amount) (*see* Chapter 9.03). The advantages of LEDs are narrower spectral bands, stable intensities and virtually no heating time, and longer lifetimes.

An important parameter to consider in photochemical reactions is the reactor geometry. Using the Beer–Lambert law, it is easy to calculate the thickness of the solution layer still receiving some radiation. At a typical concentration for organic reactions (1 mM to 0.1 M), this layer may range from a few millimeters to one centimeter, meaning that no radiation penetrates the center of a large reaction vessel. Thus, efficient stirring is important to ensure homogeneous exposure of the whole solution.

Solvents should not absorb light (unless they are used as sensitizers, such as benzene or acetone) at the operating wavelength. Cyclohexane is a good candidate, but solubility of the reactants might be an issue; acetonitrile is one of the most commonly used solvents, with a good balance of absorbance, polarity, and nonparticipation. The presence of air may cause interferences in the

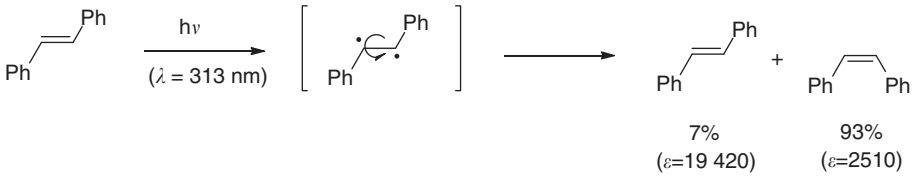
reaction (triplet oxygen is an efficient triplet quencher), and it is a good work practice to systematically deaerate the solution before irradiation, and to keep an inert atmosphere throughout the reaction.

9.13.4 Photochemistry of Alkenes

Whereas simple alkanes are normally inert to photochemical reactions (there are no electronic transitions available for the energy range typically used in organic photochemistry), alkenes can undergo $\pi - \pi^*$ transitions. In the absence of conjugation, this excitation is rather high in energy (approximately 200 nm), but proximity to an aromatic or a carbonyl group shifts the absorbance into the range of mercury lamps. Alkenes typically undergo *cis–trans* isomerization, pericyclic rearrangements (electrocyclic and sigmatropic) (*see* Chapter 5.16), cycloadditions (*see* Chapter 5.04), additions, and other reactions such as the di-π-methane rearrangement (*see* Chapter 5.06).

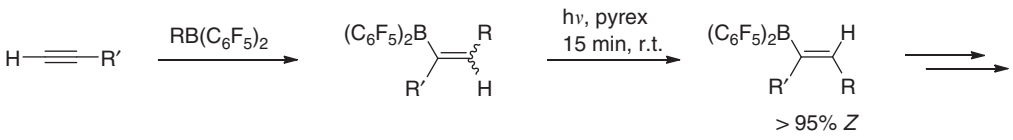
9.13.4.1 Isomerizations

Electronic excitation of an alkene corresponds to the promotion of an electron from the highest occupied molecular orbital to the lowest unoccupied molecular orbital, provoking formally the rupture of the double bond; free rotation around the remaining σ-bond becomes possible and a subsequent re-pairing can provide both geometric isomers of the initial alkene, in a ratio that depends on the ability of the substrates to absorb a photon (ε_{cis} and ε_{trans}) at the working wavelength, and the probability of the excited state to give one or the other isomer ($\phi_{cis-trans}$ and $\phi_{trans-cis}$). If the irradiation is maintained long enough, a 'photostationary state' is reached. The ratio of both products thus depends on the wavelength (Scheme 1).



Scheme 1

As this reaction mode is quite efficient, it can significantly compete with, if not completely overshadow, other reactions of unsaturated molecules, thus reducing their quantum yields. This can be a major issue in acyclic alkenes. An application of this reaction is the correction of faulty stereochemistry or nonselective reaction (*see* Chapter 1.15); for example, Erker and coworkers converted a stereorandom vinylborane completely into the *Z*-isomer by irradiation (Scheme 2).[9]



Scheme 2

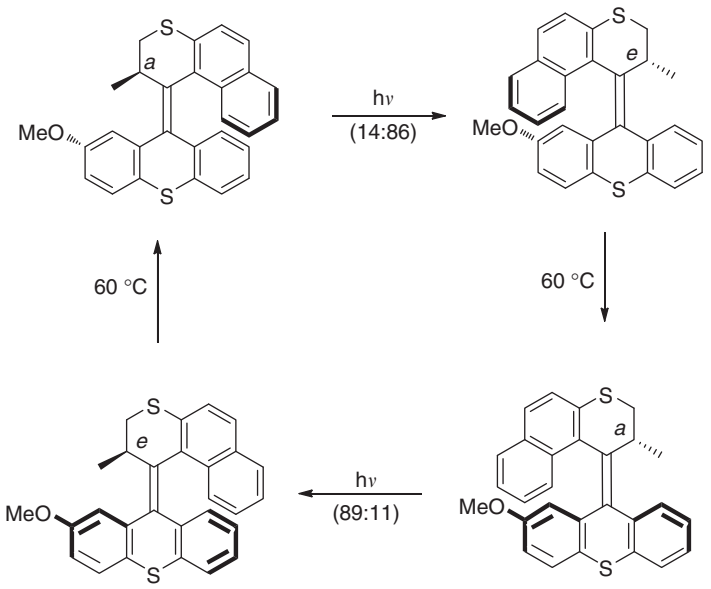
The reaction has also been applied in molecular devices, such as molecular motors, where a full turn can be promoted by a succession of photochemical and thermal steps (Scheme 3, a and e stand for axial and equatorial).[10]

Extending the π conjugation shifts the absorbance toward visible light, and the mechanism of vision is actually based on *E–Z* isomerization of polyenes. However, when the polyene is located inside a protein pocket, the simple rotational mechanism (one-bond flip) operating in alkenes is spatially too demanding. Alternative mechanisms involving a series of rotations have been proposed, such as the Hula-Twist or the Bicycle-Pedal mode illustrated in Scheme 4.[11]

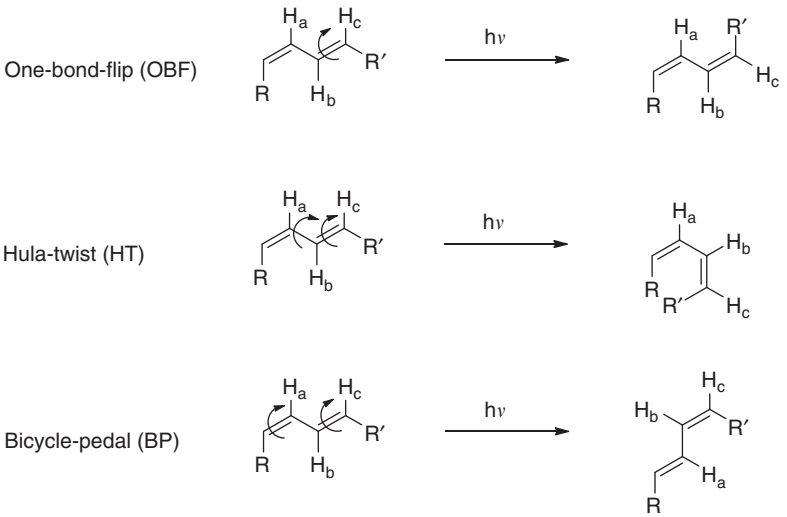
9.13.4.2 Pericyclic Rearrangements

Electrocyclic ring-closure or ring-opening can be photoinduced to occur with opposite rotatory movements to their thermal counterparts. For example, the biosynthesis of vitamin D involves the photochemical conrotatory electrocyclic opening of pro-vitamin D (Scheme 5), followed by a [1,7] sigmatropic shift (thermal, but in an antarafacial mode).

In addition, [1,3]-sigmatropic rearrangements, which are forbidden by the Woodward–Hoffmann rules in the ground state, can proceed photochemically. A remarkable example of such a reaction was used in the first steps of Wender's total synthesis of Taxol (Scheme 6).[12] In this case, as it was at the beginning of a very long synthesis, the reaction was carried out at a multigram



Scheme 3



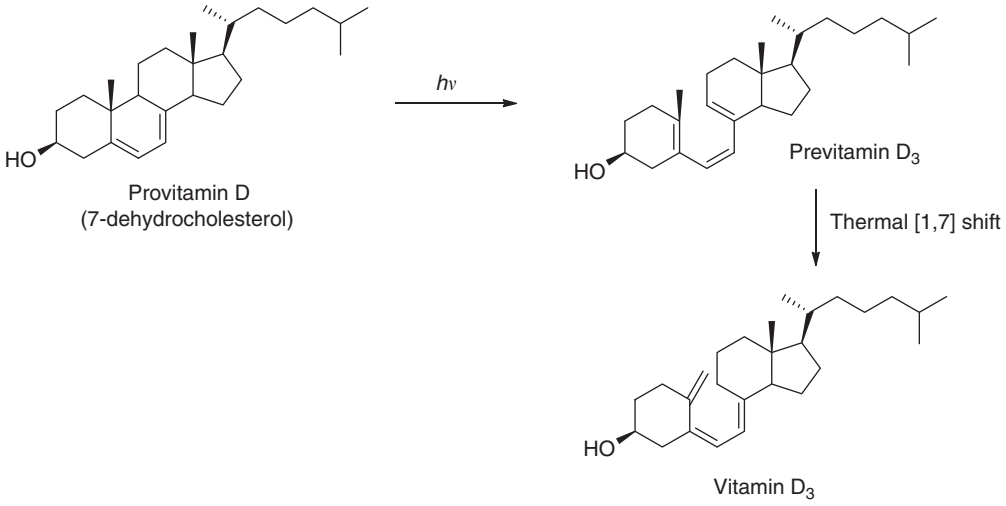
Scheme 4

scale. It is also worth noting that the rearrangement was compatible with otherwise sensitive functional groups (a ketone, a terminal double bond, and an aryl bromide).

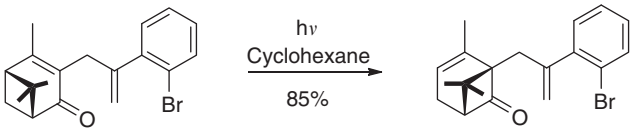
9.13.4.3 Cycloadditions

[2 + 2] Cycloadditions are photochemically allowed by the Woodward–Hoffmann rules, and indeed, these reactions constitute a good way of accessing cyclobutanes. The usefulness of 'intermolecular' [2 + 2] cycloadditions is, however, limited by the short lifetime of alkene singlet excited states, which precludes efficient bimolecular processes. Workarounds were designed, for example, by temporarily associating both reaction partners by covalent tethering,[13] coordination with transition metal cations,[14] or supramolecular interactions.[15] Despite these drawbacks, a number of well-functioning cycloadditions have been reported, sometimes by using an excess of one of the olefinic partners. Thus, even ethylene can react with α,β-unsaturated lactames[16] or lactones[17] in good yields (Scheme 7).

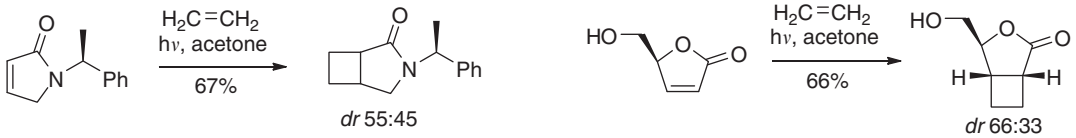
Another interesting example shows the formation of an enoate by a base-induced elimination, followed by the [2 + 2]-cycloaddition with 1,2-dichloroethylene. In this particular case, the *trans* relationship of the two chlorine atoms is evidence for a nonconcerted radical pathway (Scheme 8).[18]



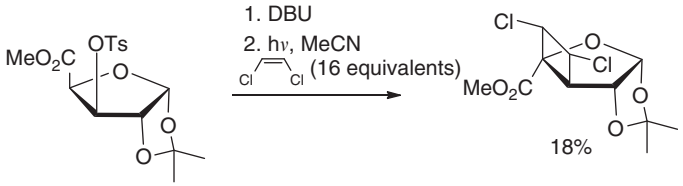
Scheme 5



Scheme 6

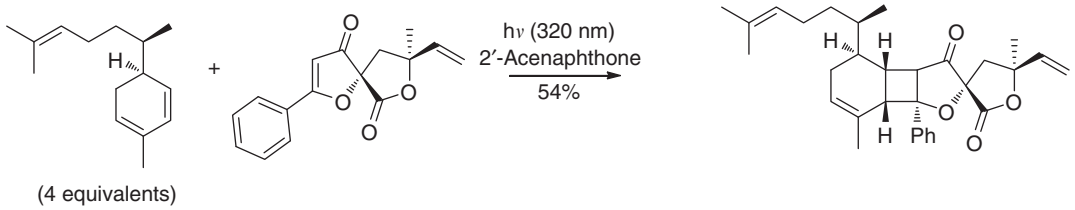


Scheme 7



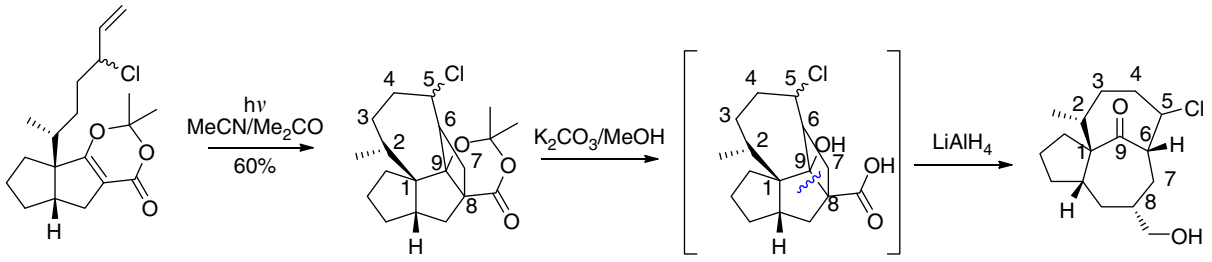
Scheme 8

In a spectacular example of what can be achieved without requiring particular tricks, Nicolaou et al. coupled two potentially problematic partners by a [2 + 2] cycloaddition (Scheme 9).[19] Interestingly, it is clearly the phenyl-substituted enoyl moiety that is excited (using a triplet sensitizer), subsequently reacting with the only disubstituted double bond on the other reaction partner. The latter is nevertheless used in excess (4 equivalents).



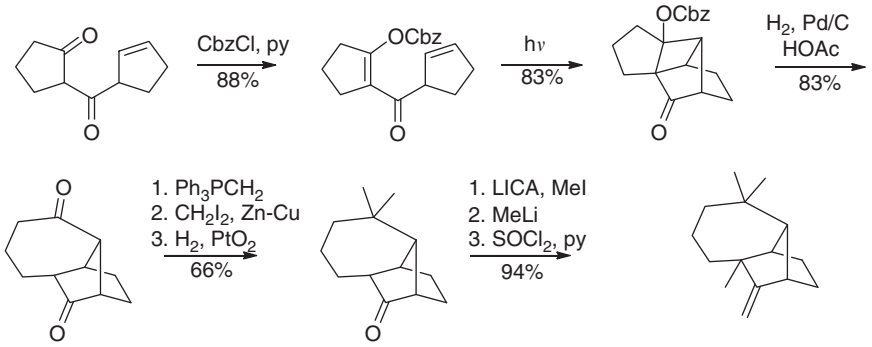
Scheme 9

The problem of having to use an excess of one of the reaction partners in order to avoid self-dimerization vanishes in the *intra*molecular case, and there are numerous examples of such reactions. For example, the skeleton of an ingenol precursor was assembled by an acetone-sensitized intramolecular cycloaddition (Scheme 10).[20]



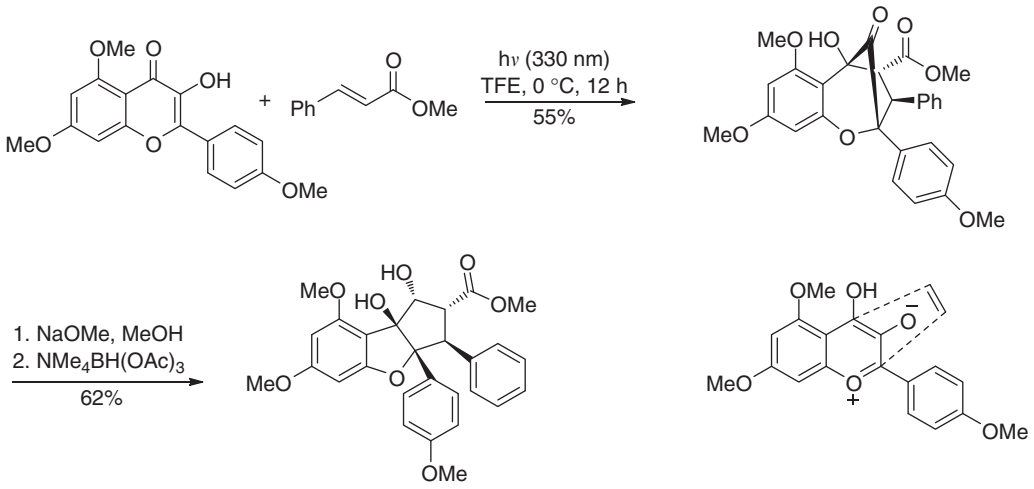
Scheme 10

The hydrolysis of the acetonide-protecting group uncovers a free alcohol, which is part of an aldol-type arrangement, prone to a retro-aldol reaction, for which the driving force is the opening of the strained cyclobutane ring. In fact, [2 + 2] cycloadditions of enolic forms of 1,3-diketones are also known as the de Mayo reaction, which was exploited in many syntheses of natural products.[21] Noteworthy is Oppolzer's synthesis of longifolene by such a cycloaddition (Scheme 11). Hydrogenolytic restoration of the free hydroxyl group provoked the ring-opening and established the bridged tricyclic cycloheptanone scaffold.[22]



Scheme 11

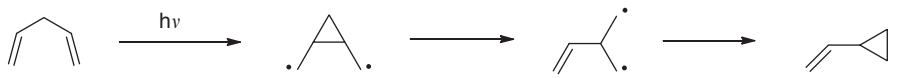
Photoinduced [3 + 2] cycloadditions take advantage of the *in situ* formation of an oxidopyrilium cation by irradiation of a 3-hydroxyflavone precursor in the presence of a hydrogen-bonding solvent (Scheme 12). Similar to the two previous examples, fragmentation of an aldol-type intermediate is this time followed by a new aldol condensation.[23]



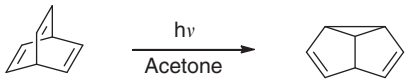
Scheme 12

9.13.4.4 The Di-π-Methane Rearrangement

The di-π-methane rearrangement was first reported by Zimmermann in 1967.[24,25] It consists of a photoinduced rearrangement of two olefin fragments separated by a single sp^3 carbon atom (Scheme 13). It stemmed from the observation of an unusual reaction of barrelene (Scheme 14).

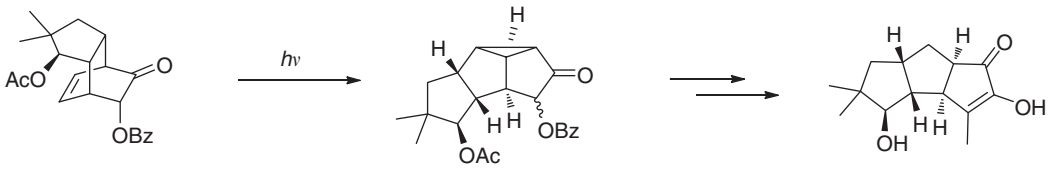


Scheme 13



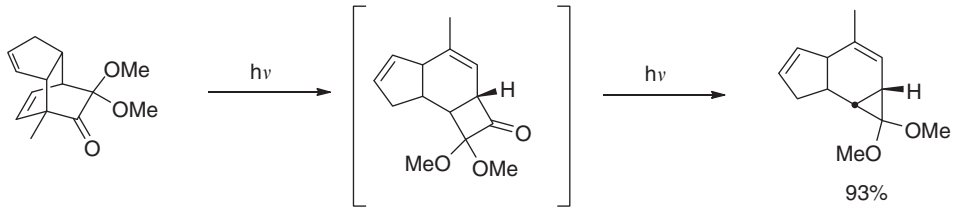
Scheme 14

The mechanism formally involves the excitation of one of the alkene moieties into some kind of biradical, which adds to the other alkene in a 3-*exo*-trig fashion, leading to a nonconjugated biradical, which undergoes a ring-cleavage and final recombination to the vinylcyclopropane product. In a variant of this reaction, the oxa-di-π-methane, one of the olefins is replaced by a ketone.[26,27] It has been used on several occasions in natural product synthesis, such as that of (–)-connotusin A by Banwell et al. (Scheme 15).



Scheme 15

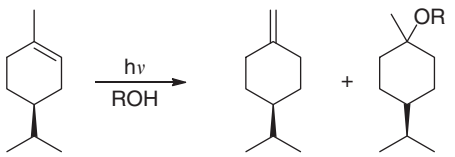
Small changes on the substrate's structure can, however, lead to a completely different reaction pathway, as seen in the following example (Scheme 16), where a Norrish-type I (*vide infra*) process takes over.[28] This illustrates very well one of the main criticisms of photochemistry in terms of difficulty in predicting what class of reaction will result from the irradiation.



Scheme 16

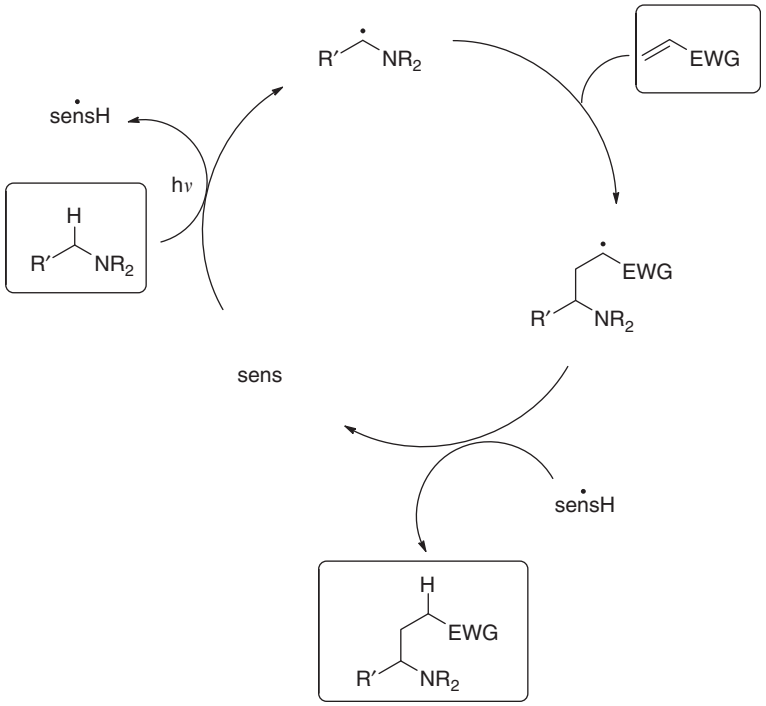
9.13.4.5 Additions

Alkenes can undergo photochemical addition by nucleophiles (alcohols), but the reaction is not very general (Scheme 17). Mechanistic studies suggest that photolysis might form a highly strained *trans* alkene, which then undergoes a classical electrophilic reaction, by prior protonation and trapping of the carbocation by the nucleophile (*see* Chapter 4.05).[29]



Scheme 17

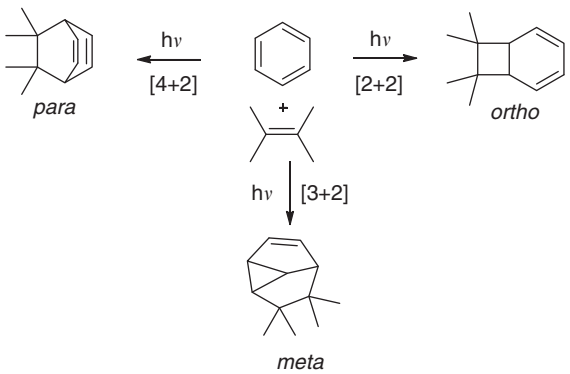
In contrast, electron-deficient alkenes undergo additions by photochemically generated radicals (Scheme 18). A photoexcited sensitizer abstracts a hydrogen atom adjacent to a stabilizing group (typically a nitrogen or oxygen atom), generating a nucleophilic radical capable of adding to a radical acceptor (typically an enone or an enoate) (*see* Chapter 4.12). The newly formed radical then recovers the initially lost hydrogen atom from the sensitizer, thus completing the cycle.[30]



Scheme 18

9.13.4.6 Reactions with Aromatic Compounds

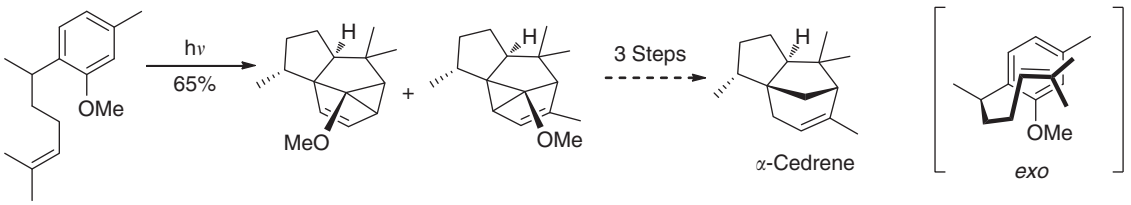
Excitation of benzene rings allows the normally aromatic double bonds to react either as an individual alkene or as a diene with another olefinic partner (*see* Chapter 5.15). This property is a valuable tool for synthesis because one can take advantage of the remarkable stability of such rings and the wealth of chemical transformations associated with them, and then further manipulate the ring by a cycloaddition. Three main reaction modes are possible (Scheme 19).[31]



Scheme 19

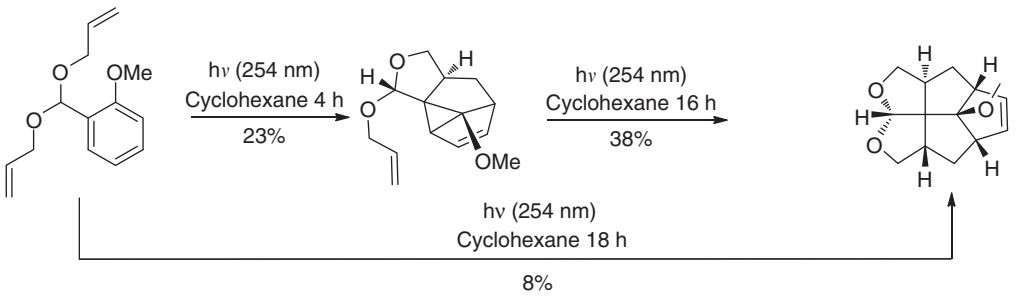
The 1,2-addition, also called *ortho-cycloaddition*, is in fact a regular [2 + 2] photocycloaddition. This mode of reaction is rarely encountered, but there are a few examples, some of them exploited in natural product synthesis. Much more frequent, but less intuitive in the connectivity of the resulting product, is the 1,3-addition, also called [3 + 2] or *meta-cycloaddition*. It provides

bridged tricyclic ring systems, bearing a cycloheptyl and a cyclopropyl part. One can take advantage of the strain of the cyclopropyl ring to further manipulate the scaffold. One of the early spectacular examples of the power of this reaction is Wender's total synthesis of cedrene in a total of only four steps, the first being the *meta*-cycloaddition (Scheme 20).[32]



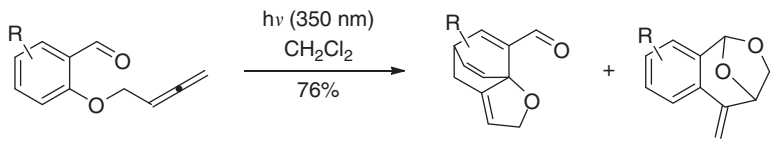
Scheme 20

A more recent but no less spectacular example is a cascade of two consecutive cycloadditions leading to a fenestrane-type core in high yield, considering the complexity of the product and the readily available starting material (Scheme 21).[33,34]



Scheme 21

The third reaction mode, called 1,4- or *para-cycloaddition*, is in fact a [4 + 2] Diels–Alder-like reaction. This mode is very rare, and only unusual substrates show this orientation. One of these substrates is allenyl-salicylaldehydes (Scheme 22), where bicyclo[2.2.2]octane cores can be accessed in one step, together with a tricyclic benzoxepine side product.[35] The ratio of these products varies with the substituents on the aromatic rings, but the side product can be totally suppressed with sterically demanding R groups.



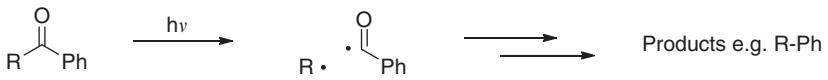
Scheme 22

9.13.5 Photochemistry of Carbonyl Compounds

Carbonyl compounds exhibit a rich photochemistry. In addition to the intense $\pi - \pi^*$ transition (symmetry allowed, usually large ε), they also show a weak $n - \pi^*$ transition of much lower energy. Typical reactions of ketones are rupture of the α-bond (type-I fragmentation) or the β-bond (type-II fragmentation), radical cyclizations, and [2 + 2]-cycloadditions (Paternò–Büchi reaction).

9.13.5.1 Norrish-Type I

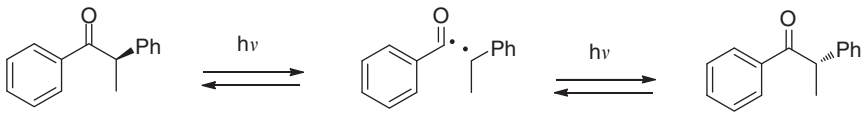
One of the early examples of photofragmentation of ketones reported in 1935 by Bamford and Norrish was the homolytic scission of the C–C bond adjacent to a carbonyl group (Scheme 23).[36,37] This process is particularly efficient if the resulting alkyl radical $R^{\bullet}$ is stabilized by suitable substituents, such as a benzylic or tertiary alkyl group. However, a simple methyl or phenyl group does not mediate such a reaction, i.e., benzophenone and acetophenone are photostable (they are in fact so stable that they are used as sensitizers). Each radical of the pair then follows its own reaction pathway, that of the acyl radical frequently being



Scheme 23

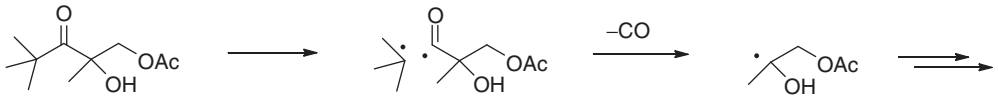
decarbonylation (*see* Chapter 3.22). If this happens at a time when the other radical is still in the proximity (for example, in a viscous solvent where diffusion is slow, or in a crystal, or in an intramolecular process), recombination can be observed.

This recombination is the cause of the racemization of α-chiral ketones (Scheme 24).[38]



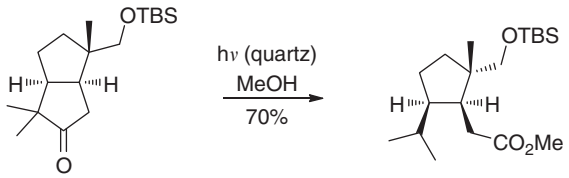
Scheme 24

The Norrish-type I reaction has been exploited by Giese and coworkers for the photorelease of carboxylic acids (Scheme 25, the terminal acetoxy group is eventually released as acetic acid, together with acetone).[39–42]



Scheme 25

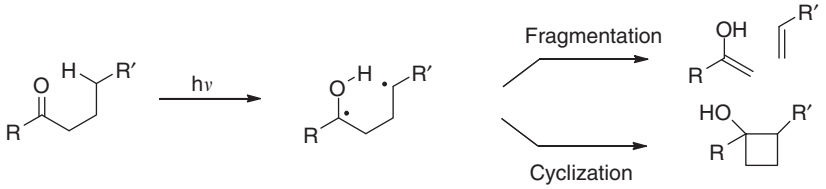
This reaction was also exploited many times in natural product synthesis, for example in Dake's approach to Nitiol (Scheme 26), where a bicyclo[3.3.0]octane core (typically obtained by a Pauson–Khand reaction) is fragmented by a Norrish-type I reaction (at high dilution).[43] In this case, it is interesting to note that the intermediate biradical undergoes an intramolecular hydrogen transfer, leading on one hand to the isopropyl group, and to a ketene on the other. Trapping of the latter by the solvent (methanol) leads to the methyl ester.



Scheme 26

9.13.5.2 Norrish-Type II

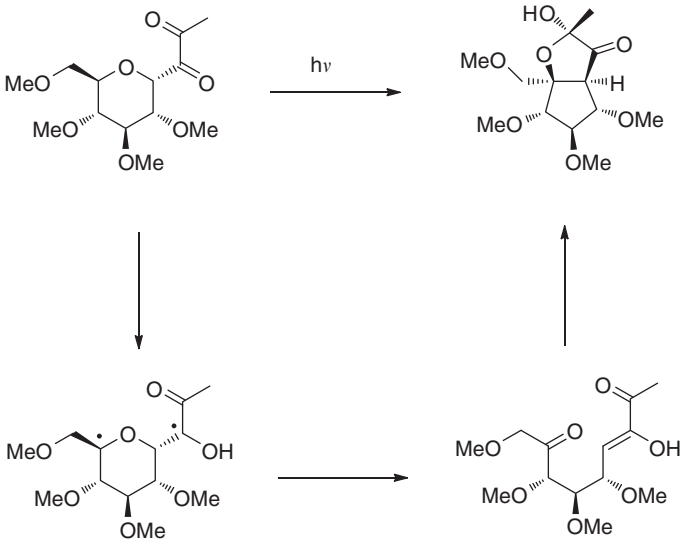
The Norrish-type-II reaction also begins by the excitation of a carbonyl group, which then abstracts a hydrogen atom from the γ-position, leading to a biradical intermediate (in some cases, when no hydrogen is present at this position, the ε or even δ-position then reacts).[36,37] Depending on the exact structure of this intermediate, two reaction pathways are now possible: either a fragmentation, leading to an enol (eventually tautomerizing back into a ketone) and an olefinic residue (Scheme 27). Globally, it corresponds to the rupture of the β-C–C bond. Alternatively, the biradical can recombine, leading to a hydroxycyclobutyl system



Scheme 27

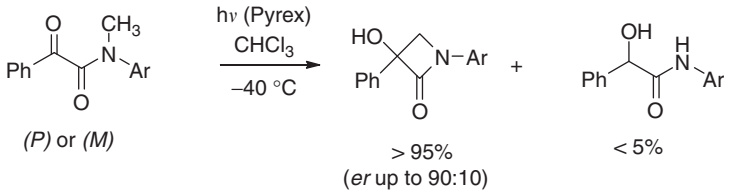
(or cyclopentyl/cyclopropyl, depending on the initial H-abstraction site). The latter reaction is also known as the Norrish–Yang cyclization.

The fragmentation was used for the release of fragrances,[44] or in the synthesis of complex molecules. In the following example, an α-diketone is used as the chromophore, and the Norrish-type-II fragmentation releases an enol, which recyclizes in an aldol condensation (Scheme 28).[45]



Scheme 28

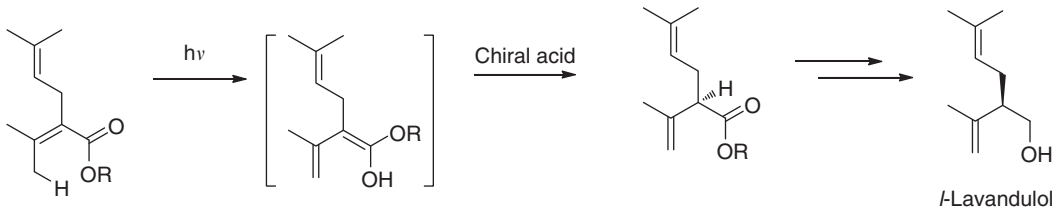
There is a multitude of examples of Norrish-type-II cyclizations, but in a recent example, Sivaguru and coworkers took advantage of the atropisomerism of α-oxoamides. The frozen chirality of the starting material is transferred with a high enantiospecificity onto the product (Scheme 29).[46]



Scheme 29

9.13.5.3 Photoenolization

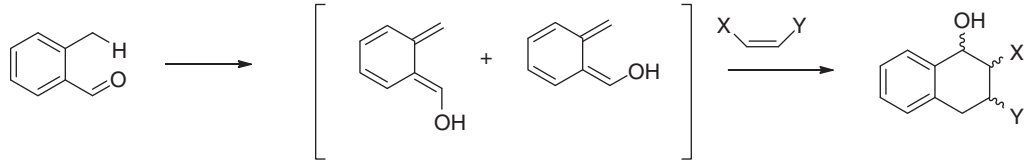
Reminiscent of a Norrish-type-II reaction, enones and enoates can abstract a hydrogen atom, but the conjugated biradical can be considered as a resonance structure of a dienol, which can restore the carbonyl function by protonation. Piva has exploited this process by an enantioselective protonation of the enol, leaving a chiral unconjugated product (Scheme 30).[47]



Scheme 30

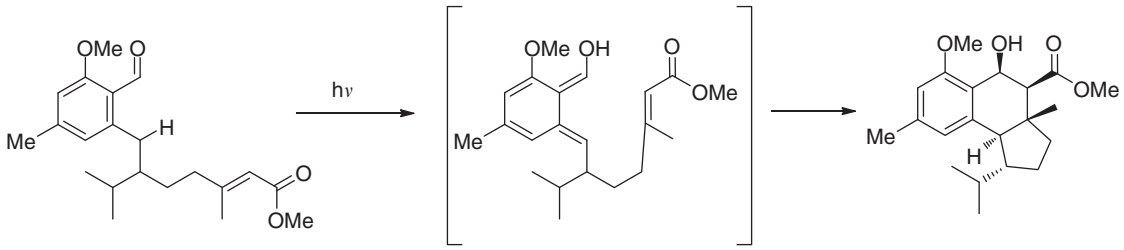
This reaction also applies to aromatic carbonyl compounds, and the photoenolization leads to two diastereomeric dearomatized highly reactive quinodimethanes, of which the *E*-isomer reacts readily with alkenes in a Diels–Alder reaction (Scheme 31); the

Z-isomer returns to the benzaldehyde faster than any bimolecular reaction. Only the deconjugation step is actually photochemical, and thus the expected reaction should be stereospecific. Unfortunately, this is not the case, as the alkene is also exposed to the incident light and undergoes a *cis–trans* isomerization. A workaround was devised by Charlton and Durst, by trapping the quinodimethane with sulfur dioxide.[48] A subsequent thermolysis (in the absence of light, but in the presence of the alkene) restored the quinodimethane, which then could react stereospecifically in the cycloaddition. Work in the laboratory suggests that the use of a triplet quencher can, to a certain extent, preserve the stereospecificity, as the isomerization arises from the triplet state, and the singlet also leads to the reaction.



Scheme 31

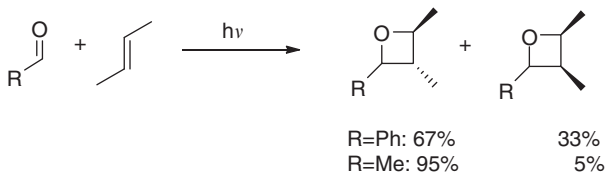
In the intramolecular mode, this reaction can be stereospecific, and it was used in the construction of complex natural products, such as the hamigerans, by Nicolaou et al. (Scheme 32).[49]



Scheme 32

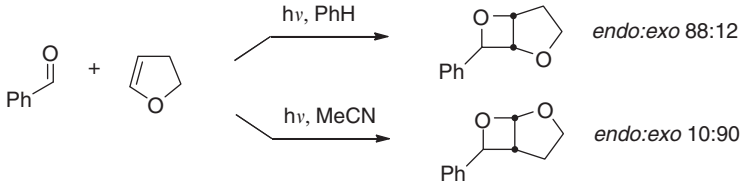
9.13.5.4 Paternò–Büchi Reaction

Aldehydes also undergo [2 + 2]-cycloadditions with alkenes, and this reaction is also known as the Paternò–Büchi reaction (*see* Chapter 5.05). The reaction proceeds via a biradical, and the stereoselectivity is influenced by the spin state. In the following example (Scheme 33), the different ratios reflect different spin states; the phenyl-substituted substrate favors the triplet pathway, whereas the methyl-substituted substrate retains mostly the singlet pathway.



Scheme 33

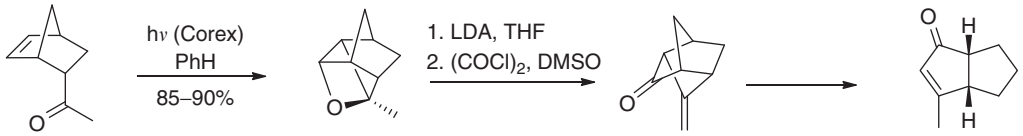
The solvent is also an important parameter, and switching from apolar to polar solvents changes the regioselectivity (Scheme 34). In polar solvents, electron transfer generates ion pairs, with an accumulation of negative charge on the



Scheme 34

benzaldehyde oxygen atom, while accumulation of positive charge in the vicinity of the electron pairs-bearing oxygen atom of the dihydrofuran. In apolar medium, the 'most stabilized radical pair' rule applies.[50]

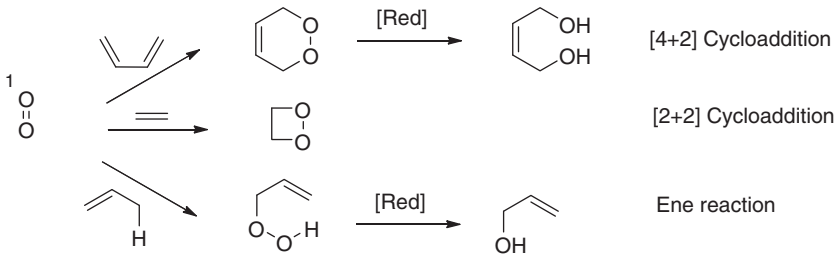
This reaction was applied very frequently in natural product synthesis, for example in an intramolecular fashion by Rawal and Dufour (Scheme 35).[51]



Scheme 35

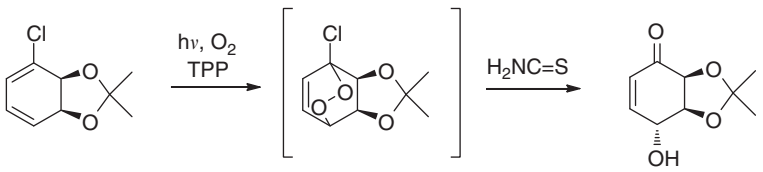
9.13.6 Singlet Oxygen

Atmospheric oxygen exists as a stable triplet, which is quite fortunate, because its 'spin isomer,' 'singlet oxygen,' is extremely reactive. Its lifetime is very short, and therefore it has to be generated *in situ*, mainly by sensitized excitation with visible light. Typical sensitizers are Rose Bengal (a pink dye), tetraphenylporphyrin (TPP), and methylene blue (MB). Singlet oxygen behaves in a mode reminiscent of a very reactive alkene (Scheme 36), meaning that it undergoes Diels–Alder reactions with dienes, leading to endoperoxides. The latter can be explosive, and are thus quite dangerous to store, and they are usually immediately reduced into the corresponding diol with a mild reductant, typically thiourea, dimethyl sulfide, or a phosphine. In the presence of isolated alkenes, a [2 + 2]-cycloaddition can sometimes occur, leading to an unstable dioxetane, but the reaction typically proceeds via an ene-reaction to give a hydroperoxide, which can also be reduced like the endoperoxides.



Scheme 36

The reaction with dienes is highly diastereoselective, and the following sequence is a frequent starting point of asymmetric syntheses (Scheme 37).[52–54]

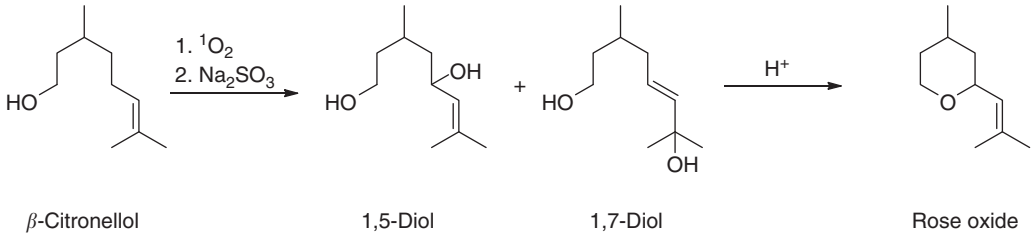


Scheme 37

The ene-type reaction is also very common, and is at the heart of one of the rare industrial photochemical processes, the preparation of Rose oxide, a component of fragrances, from β-citronellol (Scheme 38). Interestingly, the same process can also proceed using singlet oxygen formed chemically, in the absence of light, by transition metal-catalyzed decomposition of hydrogen peroxide.[55]

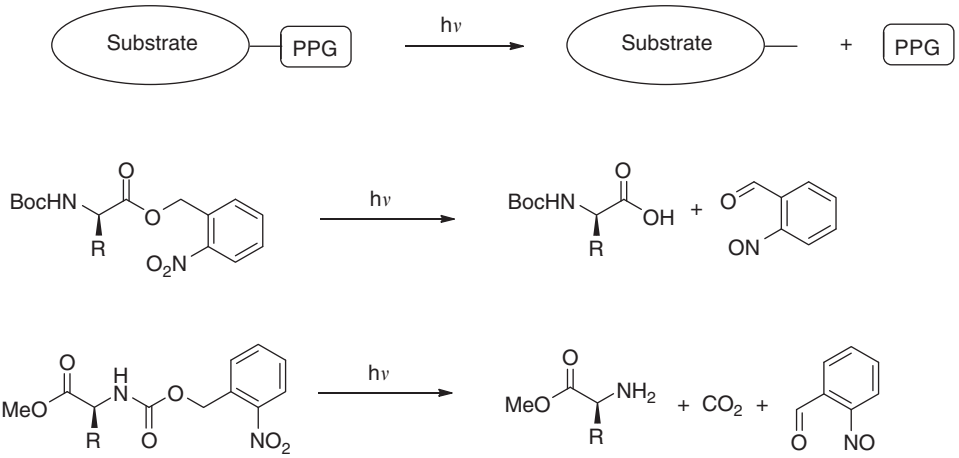
9.13.7 Photolabile Protecting Groups

The possibility of making a molecule react without the addition of a reagent is particularly appealing for the removal of protecting groups, because it adds an additional dimension to the orthogonal space (which is composed of sets of conditions that do not



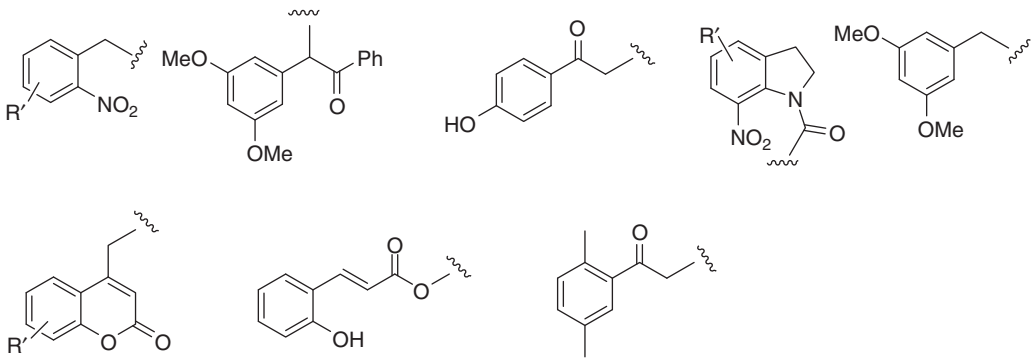
Scheme 38

interfere with each other). Since their initial discovery in the 1960s, photolabile protecting groups (PPGs) have been developed to protect virtually every type of functional group (e.g. carboxylic acids, alcohols, amines, ketone, and thiols), and the field has been abundantly reviewed in the past decades (Scheme 39).[6,7,56–62] Historically, the *N*- and *C*-termini of amino acids have been among the most frequently protected functions, and the *ortho*-nitrobenzylic derivatives have been among the most popular PPGs.



Scheme 39

The photolysis mechanism of the previous examples involves an intramolecular hydrogen shift from the benzylic methylene group to the excited nitro group, followed by a fragmentation cascade, eventually leading to the release of the carboxylic acid (or amine) and a nitrosoaldehyde byproduct. This process is reminiscent of the Norrish-type-II reaction. There are currently hundreds of different PPGs, and Scheme 40 summarizes some of the most frequently used groups.

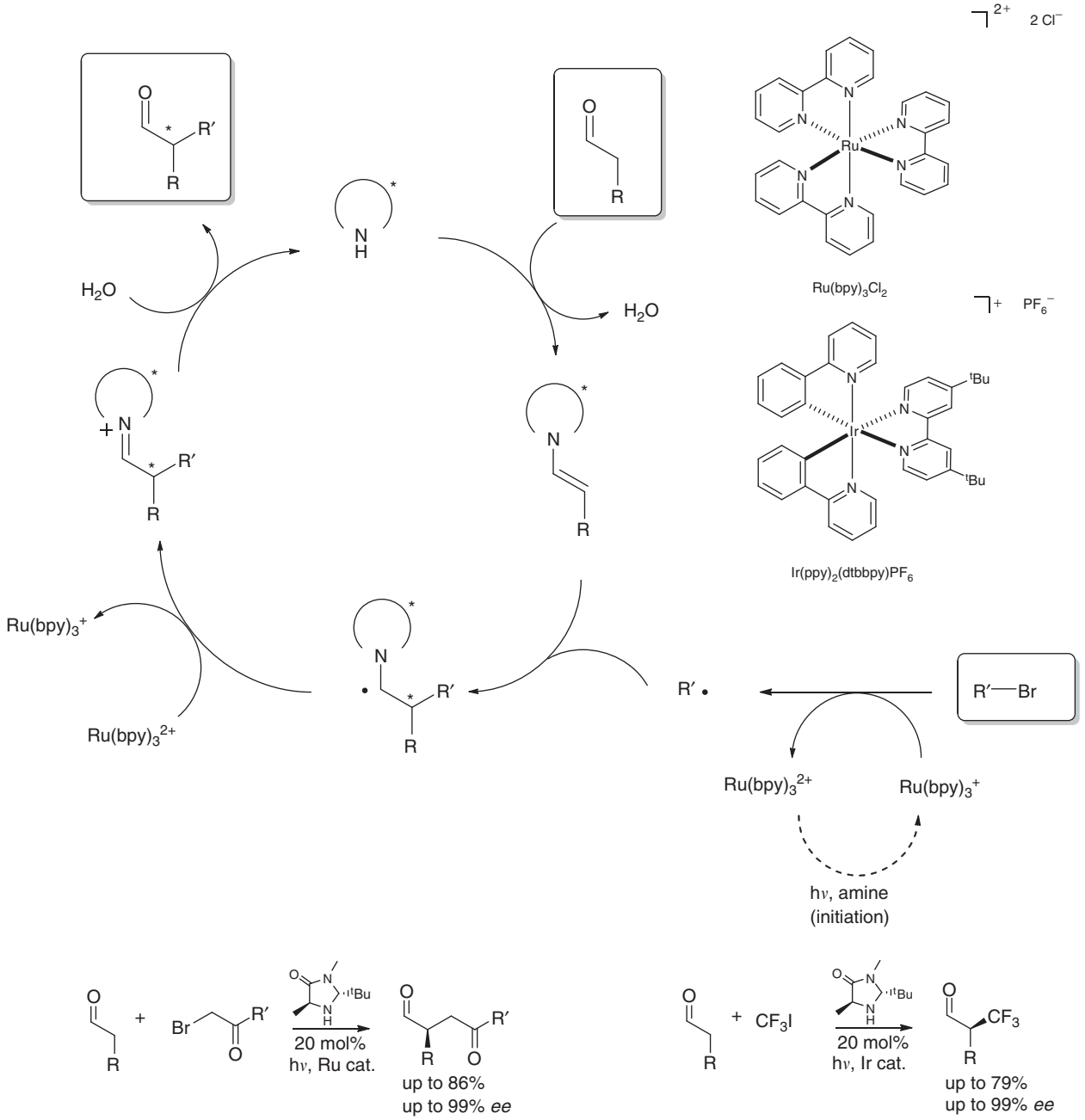


Scheme 40

The photolysis of most of these PPGs can be carried out using standard UV light sources, and their wavelength requirements are not extremely strict. However, if one uses monochromatic light sources, discrimination between PPGs on the same molecule can be achieved. This property is called chromatic orthogonality.[61,63–67]

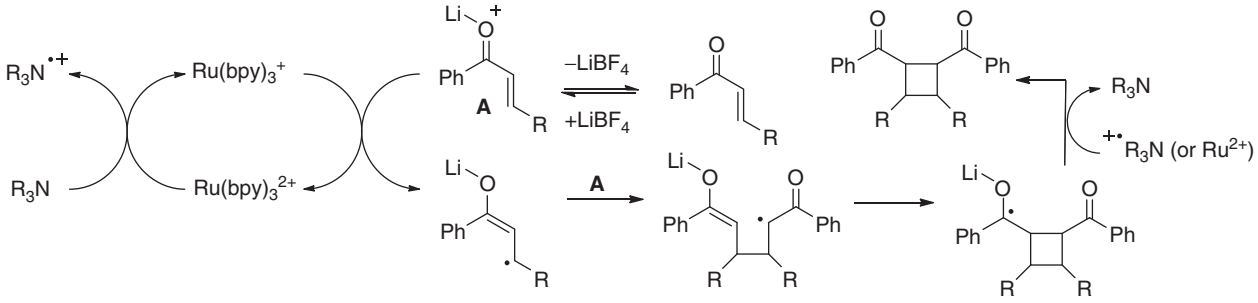
9.13.8 Photoredox Catalysis

A new emerging field relies on the rich photoredox chemistry of ruthenium(II) complexes. Such complexes, when excited with visible light, become both better oxidants and better reductants than they are in their ground states, thus allowing the initiation of otherwise impossible radical reactions. Seminal work by the groups of MacMillan,[68–70] Stephenson,[71,72] Yoon,[73,74] and König[75,76] laid the ground for a reliable and promising synthetic method for preparing complex molecules. An example is shown in Scheme 41, where an organocatalyst, such as MacMillan's imidazolidinone, forms an enamine with a suitable aldehyde. At the same time, an α-bromoketone is reduced by a $Ru(bpy)_3^{+}$ complex (itself formed by the reaction of an excited $Ru(bpy)_3^{2+}$ with a sacrificial reductant, most probably the enamine itself. This reduction is not a problem since the ruthenium is only present in low quantities) to an electrophilic α-keto radical. This radical reacts with the nucleophilic enamine, leading to an α-amino radical, which is now oxidized by an excited $Ru(bpy)_3^{2+}$, leading in turn to an iminium immediately hydrolyzed into the final product, and restoring the amine catalyst and a $Ru(bpy)_3^{+}$ complex ready to enter a new cycle. Another spectacular application of such a reaction is the asymmetric α-trifluoromethylation of carbonyl compounds, using a more reductive iridium complex.

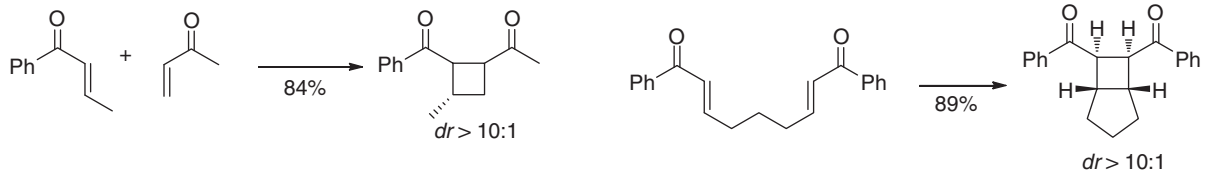


Scheme 41

Yoon et al. employed the reductive quenching cycle of $Ru(bpy)_3^{2+}$ to initiate formal [2 + 2] cycloadditions of α,β-unsaturated ketones (Scheme 42). Intramolecular [2 + 2] cyclizations are *cis* selective, whereas crossed intermolecular cycloadditions are *trans* selective (Scheme 43). The intermolecular cycloadditions can be achieved by careful choosing of the reaction partners; phenylenones are more easily reduced, whereas methyl vinyl ketones are more reactive toward radical addition.



Scheme 42



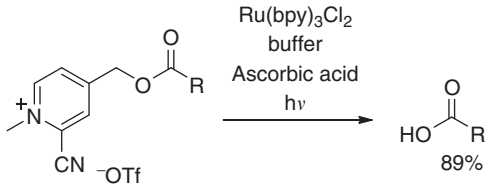
Scheme 43

Stephenson and coworkers, however, developed a clean dehalogenation reaction using a photoredox catalyst and formic acid or Hantsch ester as the stoichiometric reductant.[77] The intermediate radical can be trapped by a suitable nucleophile, and the formation of C–C bonds could thus be achieved (Scheme 44). [78]



Scheme 44

Falvey and coworkers used this strategy for the visible light-induced deprotection of carboxylic acids (Scheme 45).[79,80]



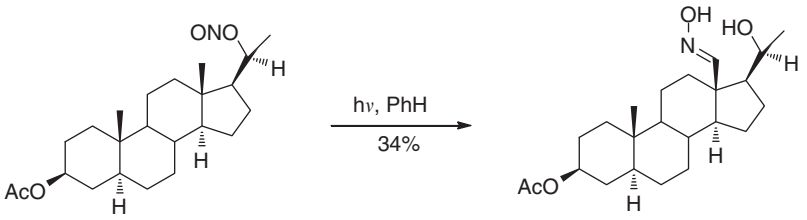
Scheme 45

9.13.9 Miscellaneous Reactions

9.13.9.1 The Barton Reaction

An early example of remote C–H activation reaction was designed in the 1960s by Barton, exploiting the facile homolytic photochemical dissociation of the O–N bond of nitrites (*see* Chapter 6.03), and generating a highly reactive hydroxyl radical.[81] The latter

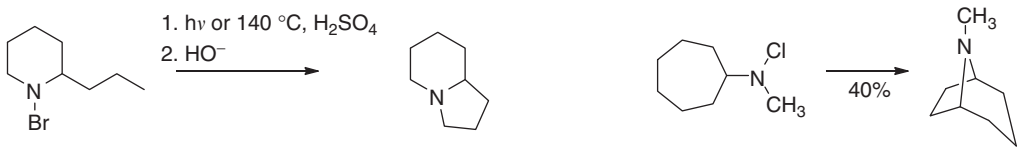
abstracts a hydrogen atom in its vicinity, usually favoring a six-membered cyclic transition state. In steroids, a nitrite on the D-ring substituent reacts with the angular methyl group at the C–D ring junction (Scheme 46). The newly formed radical reacts with the nitrosyl radical, eventually ending up as an oxime, which can then be further converted by classical means, into a nitrile, aldehyde, or amine.



Scheme 46

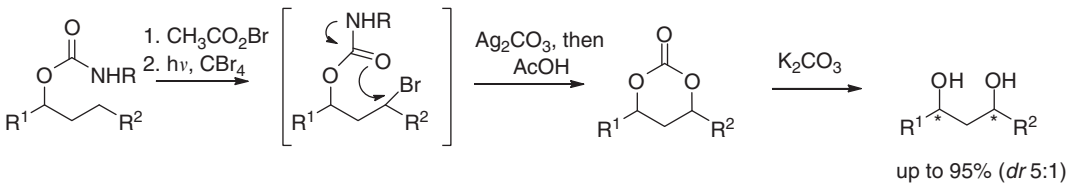
9.13.9.2 Hoffmann–Löffler–Freytag reaction

Similar to the Barton reaction, but requiring harsher conditions, the Hoffmann–Löffler–Freytag (HLF) reaction is based on the thermal (at high temperature) or photochemical dissociation of N-halogen bonds in acidic medium, which places the halogen at the γ-position with respect to the nitrogen. Basic treatment induced an intramolecular alkylation forming a new ring. This reaction has been used to prepare alkaloids, such as δ-coniceine or tropanes (Scheme 47).[82]



Scheme 47

More recently, this reaction was used by Baran and coworkers for the stereoselective preparation of 1,3-diols, with a carbamate spacer (Scheme 48).[83]



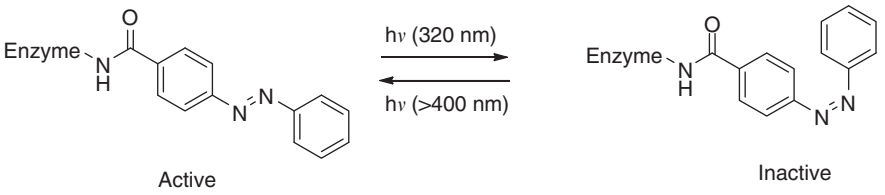
Scheme 48

9.13.9.3 Azo-Compounds

Similar to alkenes, azo-compounds (bearing an N═N double bond) undergo a reversible *cis–trans* isomerization, which has been exploited abundantly in the synthesis of optical switches and other molecular devices. A representative example is the inactivation of an enzyme by photolysis at a certain wavelength, caused by a change of conformation. Irradiation at a different wavelength restores the initial geometry, and thus the activity (Scheme 49).[84]

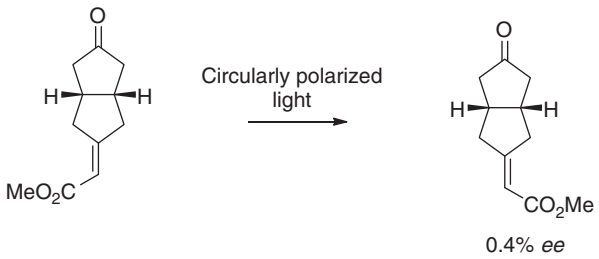
9.13.9.4 Asymmetric Photochemistry

Light can be rendered chiral by making it 'circularly polarized,' i.e., by passing it through a series of optical filters (successively a monochromator, a linear polarizer, and a quarter-wave plate; note that with a laser, the first two elements can be omitted). In theory, such light can induce asymmetric reactions.[85] Proof of principles has been established, for example with a photostationary



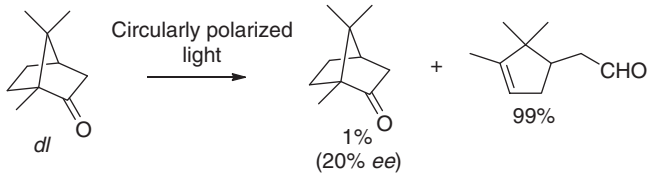
Scheme 49

equilibrium of alkene-containing bicyclic ketones (Scheme 50).[86] So far, the enantiomeric excesses remain too low for an application in natural product synthesis.



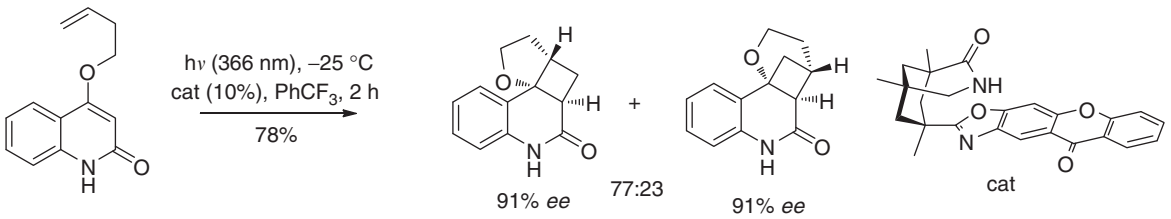
Scheme 50

However, amplification systems have been used, such as a kinetic resolution at extremely high conversion (Scheme 51). Thus, Kagan and coworkers were able to enrich racemic camphor to 20% *ee*, at the expense of yield (1%).[87] Autocatalysis and other techniques have also been used.[88]



Scheme 51

A more efficient induction was obtained by Bach and coworkers, who pioneered the design and use of chiral templates, bearing a chiral molecular recognition unit tethered to a sensitizing unit. Thus, a substrate can dock onto the template with hydrogen bonds, and be excited as a triplet by the sensitizer. Intramolecular [2 + 2]-cycloadditions were carried out in high chemical and optical yields (Scheme 52).[89]



Scheme 52

9.13.10 Conclusion

This catalog of reaction classes shows the breadth of synthetic methods that photochemistry can provide. The sometimes cumbersome experimental constraints that hampered photochemistry in the past century are now gradually being removed by new concepts (such as photoredox catalysis, exploiting more easily handled visible light), new experimental setups (such as flow

reactors), and new light sources (such as LEDs). There is no doubt that photochemical steps will increasingly become part of complex synthetic schemes. Better knowledge of their mechanisms and the underlying fundamental phenomena will also help in the design of new reactions or the improvement of existing ones. We hope that with time, photochemical reactions will become a natural extension, if not replacement, of the traditional chemist's toolbox. Ciamician's dream might, after all, come true.

> "On arid lands there will spring up industrial colonies without smoke and without smokestacks, forests of glass tubes will extend over the plains and glass buildings will rise everywhere; inside of these will take place the photochemical processes that hitherto have been the guarded secret of the plants, but that will have been mastered by human industry which will know how to make them bear even more abundant fruit then nature, for nature is not in a hurry and mankind is."[90]

References

1. Hoffmann, N. *Chem. Rev.* **2008**, *108*, 1052–1103.
2. Bach, T.; Hehn, J. P. *Angew. Chem. Int. Ed. Engl.* **2011**, *50*, 1000–1045.
3. Klán, P.; Wirz, J. *Photochemistry of Organic Compounds: From Concepts to Practice*; Wiley: Chichester, **2009**.
4. Bochet, C. G. *Adv. Org. Synth.* **2005**, *1*, 3–23.
5. Ciana, C. L.; Bochet, C. G. *CHIMIA* **2007**, *61*, 650–654.
6. Albini, A. *Handbook of Synthetic Photochemistry*; Wiley-VCH: Weinheim, **2010**.
7. Griesbeck, A.; Oelgemoeller, M.; Ghetti, F. *CRC Handbook of Organic Photochemistry*, 3rd ed.; CRC Press: Boca Raton, London, New York, **2012**.
8. Scaiano, J. *CRC Handbook of Organic Photochemistry*; CRC Press Inc.: Boca Raton, FL, **1989**.
9. Chen, C.; Voss, T.; Fröhlich, R.; Kehr, G.; Erker, G. *Org. Lett.* **2011**, *13*, 62–65.
10. van Delden, R. A.; Hurenkamp, J. H.; Feringa, B. L. *Chem. Eur. J.* **2003**, *9*, 2845–2853.
11. Dugave, C.; Demange, L. *Chem. Rev.* **2003**, *103*, 2475–2532.
12. Wender, P. A.; Mucciaro, T. P. *J. Am. Chem. Soc.* **1992**, *114*, 5878–5879.
13. Fleming, S. A.; Parent, A. A.; Parent, E. E.; Pincock, J. A.; Renault, L. *J. Org. Chem.* **2007**, *72*, 9464–9470.
14. Ghosh, S. Copper(I)-catalyzed Inter- and Intramolecular [2 + 2] Photocycloaddition Reactions of Alkenes. In *CRC Handbook of Organic Photochemistry and Photobiology*, 2nd ed.; Horspool, W. M.; Lenci, F. Eds.; CRC Press: Boca Raton, FL, **2004**, Chapter 18; pp 1–24.
15. Bassani, D. M.; Darcos, V.; Mahony, S.; Desvergne, J.-P. *J. Am. Chem. Soc.* **2000**, *122*, 8795–8796.
16. André, V.; Vidal, A.; Ollivier, J.; Robin, S.; Aitken, D. J. *Tetrahedron Lett.* **2011**, *52*, 1253–1255.
17. Flores, R.; Rustullet, A.; Alibés, R.; *et al. J. Org. Chem.* **2011**, *76*, 5369–5383.
18. Nicolaou, K. C.; Ellery, S. P.; Rivas, F.; *et al. Bioorg. Med. Chem.* **2011**, *19*, 5648–5669.
19. Nicolaou, K. C.; Wu, T. R.; Sarlah, D.; *et al. J. Am. Chem. Soc.* **2008**, *130*, 11114–11121.
20. Winkler, J. D.; Rouse, M. B.; Greaney, M. F.; Harrison, S. J.; Jeon, Y. T. *J. Am. Chem. Soc.* **2002**, *124*, 9726–9728.
21. Oppolzer, W. *Acc. Chem. Res.* **1982**, *15*, 135–141.
22. Oppolzer, W.; Godel, T. *J. Am. Chem. Soc.* **1978**, *100*, 2583–2584.
23. Roche, S. P.; Cencic, R.; Pelletier, J.; Porco, J. A., Jr. *Angew. Chem. Int. Ed.* **2010**, *49*, 6533–6538.
24. Zimmerman, H. *Pure Appl. Chem.* **2006**, *78*, 2193–2203.
25. Zimmerman, H. E.; Armesto, D. *Chem. Rev.* **1996**, *96*, 3065–3112.
26. Armesto, D.; Ortiz, M. J.; Agarrabeitia, A. R.; El-Boulifi, N. *Tetrahedron* **2010**, *66*, 8690–8697.
27. Armesto, D.; Ortiz, M. J.; Agarrabeitia, A. R.; Martín-Fontecha, M. *Org. Lett.* **2005**, *7*, 2687–2690.
28. Hsu, D.-S.; Chou, Y.-Y.; Tung, Y.-S.; Liao, C.-C. *Chem. Eur. J.* **2010**, *16*, 3121–3131.
29. Marshall, J. A. *Acc. Chem. Res.* **1969**, *2*, 33–40.
30. Griesbeck, A. G.; Hoffmann, N.; Warzecha, K.-D. *Acc. Chem. Res.* **2007**, *40*, 128–140.
31. Streit, U.; Bochet, C. G. *Beilstein J. Org. Chem.* **2011**, *7*, 525–542.
32. Wender, P. A.; Howbert, J. J. *J. Am. Chem. Soc.* **1981**, *103*, 688–690.
33. Penkett, C. S.; Woolford, J. A.; Read, T. W.; Kahan, R. J. *J. Org. Chem.* **2011**, *76*, 1295–1304.
34. Penkett, C. S.; Woolford, J. A.; Day, I. J.; Coles, M. P. *J. Am. Chem. Soc.* **2010**, *132*, 4–5.
35. (a) Birbaum, F.; Neels, A.; Bochet, C. G. *Org. Lett.* **2008**, *10*, 3175–3178. (b) Streit, U.; Birbaum, F.; Quattropani, A.; Bochet, C. G. *J. Org. Chem.* **2013**, *78*, 6890–6910.
36. Norrish, R. G. W.; Bamford, C. H. *Nature* **1937**, *140*, 195–196.
37. Norrish, R. G. W.; Bamford, C. H. *Nature* **1936**, *138*, 1016.
38. Lewis, F. D.; Magyar, J. G. *J. Am. Chem. Soc.* **1973**, *95*, 5973–5976.
39. Kessler, M.; Glatthar, R.; Giese, B.; Bochet, C. G. *Org. Lett.* **2003**, *5*, 1179–1181.
40. Glatthar, R.; Giese, B. *Org. Lett.* **2000**, *2*, 2315–2317.
41. Schoenleber, R. O.; Giese, B. *Synlett* **2003**, *14*, 501–504.
42. Peukert, S.; Giese, B. *J. Org. Chem.* **1998**, *63*, 9045–9051.
43. Wilson, M. S.; Woo, J. C. S.; Dake, G. R. *J. Org. Chem.* **2006**, *71*, 4237–4245.
44. Levrand, B.; Herrmann, A. *Photochem. Photobiol. Sci.* **2002**, *1*, 907–919.
45. Alvarez-Dorta, D.; León, E. I.; Kennedy, A. R.; Riesco-Fagundo, C.; Suárez, E. *Angew. Chem. Int. Ed. Engl.* **2008**, *47*, 8917–8919.
46. Ayitou, A. J.-L.; Jesuraj, J. L.; Barooah, N.; Ugrinov, A.; Sivaguru, J. *J. Am. Chem. Soc.* **2009**, *131*, 11314–11315.
47. Faure, S.; Connolly, J. D.; Fakunle, C. O.; Piva, O. *Tetrahedron* **2000**, *56*, 9647–9653.
48. Charlton, J. L.; Durst, T. *Tetrahedron Lett.* **1984**, *25*, 5287–5290.
49. Nicolaou, K. C.; Gray, D. L. F.; Tae, J. *J. Am. Chem. Soc.* **2004**, *126*, 613–627.
50. Griesbeck, A. G.; Abe, M.; Bondock, S. *Acc. Chem. Res.* **2004**, *37*, 919–928.
51. Rawal, V. H.; Dufour, C. *J. Am. Chem. Soc.* **1994**, *116*, 2613–2614.
52. Oppolzer, W.; Spivey, A. C.; Bochet, C. G. *J. Am. Chem. Soc.* **1994**, *116*, 3139–3140.
53. Giró Mañas, C.; Paddock, V. L.; Bochet, C. G.; *et al. J. Am. Chem. Soc.* **2010**, *132*, 5176–5178.
54. Hudlicky, T.; Luna, H.; Olivo, H. F.; *et al. J. Chem. Soc. Perkin Trans. 1* **1991**, 2907–2917.

55. Alsters, P. L.; Jary, W.; Nardello-Rataj, V.; Aubry, J.-M. *Org. Process Res. Dev.* **2010**, *14*, 259–262.
56. Bochet, C. G. *J. Chem. Soc. Perkin Trans. 1* **2002**, 125–142.
57. Pelliccioli, A. P.; Wirz, J. *Photochem. Photobiol. Sci.* **2002**, *1*, 441–458.
58. Yu, H.; Li, J.; Wu, D.; Qiu, Z.; Zhang, Y. *Chem. Soc. Rev.* **2010**, *39*, 464–473.
59. Bochet, C.G.; Blanc, A. *Handbook of Synthetic Photochemistry*; Wiley-VCH: Weinheim, **2010**, 417–447.
60. Bochet, C.; Mercier, S. *Linker Strategies in Solid-Phase Organic Synthesis*; Wiley: Chichester, **2009**; pp 151–193.
61. Bochet, C. G. *Synlett* **2004**, 2268–2274.
62. Klán, P.; Šolomek, T.; Bochet, C. G.; *et al. Chem. Rev.* **2013**, *113*, 119–191.
63. Bochet, C. G. *Angew. Chem. Int. Ed.* **2001**, *40*, 2071–2073.
64. San Miguel, V.; Bochet, C. G.; del Campo, A. *J. Am. Chem. Soc.* **2011**, *133*, 5380–5388.
65. Blanc, A.; Bochet, C. G. *J. Org. Chem.* **2002**, *67*, 5567–5577.
66. Blanc, A.; Bochet, C. G. *Org. Lett.* **2007**, *9*, 2649–2651.
67. Bochet, C. G. *Tetrahedron Lett.* **2000**, *41*, 6341–6346.
68. Nagib, D. A.; Scott, M. E.; MacMillan, D. W. C. *J. Am. Chem. Soc.* **2009**, *131*, 10875–10877.
69. Nagib, D. A.; MacMillan, D. W. C. *Nature* **2011**, *480*, 224–228.
70. Pham, P. V.; Nagib, D. A.; MacMillan, D. W. C. *Angew. Chem. Int. Ed. Engl.* **2011**, *50*, 6119–6122.
71. Narayanam, J. M. R.; Stephenson, C. R. J. *Chem. Soc. Rev.* **2010**, *40*, 102–113.
72. Tucker, J. W.; Stephenson, C. R. J. *J. Org. Chem.* **2012**, *77*, 1617–1622.
73. Du, J.; Yoon, T. P. *J. Am. Chem. Soc.* **2009**, *131*, 14604–14605.
74. Ischay, M.A.; Ament, M.S.; Yoon, T. *Chem. Sci.* **2012**, *3*, 2807–2811.
75. Neumann, M.; Füldner, S.; König, B.; Zeitler, K. *Angew. Chem. Int. Ed.* **2010**, *50*, 951–954.
76. Lechner, R.; Kümmel, S.; König, B. *Photochem. Photobiol. Sci.* **2010**, *9*, 1367–1377.
77. Narayanam, J. M. R.; Tucker, J. W.; Stephenson, C. R. J. *J. Am. Chem. Soc.* **2009**, *131*, 8756–8757.
78. Tucker, J. W.; Narayanam, J. M. R.; Krabbe, S. W.; Stephenson, C. R. J. *Org. Lett.* **2010**, *12*, 368–371.
79. Borak, J. B.; Falvey, D. E. *J. Org. Chem.* **2009**, *74*, 3894–3899.
80. Borak, J. B.; Lee, H.-Y.; Raghavan, S. R.; Falvey, D. E. *Chem. Commun.* **2010**, *46*, 8983–8985.
81. Barton, D.; Beaton, J.; Geller, L.; Pechet, M. *J. Am. Chem. Soc.* **1961**, *83*, 4076–4083.
82. Corey, E.; Hertler, W. R. *J. Am. Chem. Soc.* **1960**, *82*, 1657–1668.
83. Chen, K.; Richter, J. M.; Baran, P. S. *J. Am. Chem. Soc.* **2008**, *130*, 7247–7249.
84. Willner, I.; Rubin, S.; Riklin, A. *J. Am. Chem. Soc.* **1991**, *113*, 3321–3325.
85. Inoue, Y. *Chem. Rev.* **1992**, *92*, 741–770.
86. Burnham, K. S.; Schuster, G. B. *J. Am. Chem. Soc.* **1999**, *121*, 10245–10246.
87. Balavoine, G.; Moradpour, A.; Kagan, H. B. *J. Am. Chem. Soc.* **1974**, *96*, 5152–5158.
88. Sato, I.; Sugie, R.; Matsueda, Y.; Furumura, Y.; Soai, K. *Angew. Chem. Int. Ed.* **2004**, *43*, 4490–4492.
89. Bauer, A.; Westkämper, F.; Grimme, S.; Bach, T. *Nature* **2005**, *436*, 1139–1140.
90. Ciamician, G. *Science* **1912**, *36*, 385–394.

9.14 Preparative Electrochemistry for Organic Synthesis

GG Botte, DA Daramola, and M Muthuvel, Ohio University, Athens, OH, USA

© 2014 Elsevier Ltd. All rights reserved.

9.14.1	**Introduction**	351
9.14.2	**Fundamental Electrochemistry**	353
9.14.2.1	Electrochemical Principles	354
9.14.2.1.1	Cathodic reactions	356
9.14.2.1.1.1	Adiponitrile	357
9.14.2.1.1.2	Carbon dioxide	358
9.14.2.1.2	Anodic reactions	360
9.14.2.1.2.1	Methanol	360
9.14.2.2	Multiscale Modeling	362
9.14.2.2.1	Computational hydrogen electrode	363
9.14.2.2.2	Double reference method	364
9.14.3	**Laboratory Research**	367
9.14.3.1	Combinatorial Chemistry	367
9.14.3.1.1	Combinatorial electrochemistry for methanol oxidation	369
9.14.3.1.2	Combinatorial electrochemistry for carbon dioxide reduction	369
9.14.3.2	Nanotechnology	370
9.14.3.2.1	Nanotechnology in methanol oxidation	372
9.14.3.2.2	Nanotechnology in carbon dioxide reduction	373
9.14.3.3	*In situ* Characterization	374
9.14.3.3.1	*In situ* characterization of methanol oxidation	374
9.14.3.3.2	*In situ* characterization of carbon dioxide reduction	375
9.14.4	**Electrochemical Technology**	377
9.14.4.1	Microfuel Cells for Methanol Oxidation	381
9.14.4.2	Microfuel Cells for Carbon Dioxide Reduction	383
9.14.5	**Pilot Plant Trials**	384
9.14.6	**Industrial Production**	385
9.14.7	**Summary**	386
References		386

Glossary

Current density The kinetics of an electrochemical reaction. The term density is used to normalize the current with respect to a dimension (area or volume).

Hydrodynamics The study of the motion of gases and liquids. This motion could be due to a difference in momentum, energy, and/or mass.

Multiscale modeling The use of mathematical equations to predict and describe phenomena occurring in chemical reactions based on different time and length dimensions.

Potential A measure of the energy required to move a charge through space.

Reference electrode This is an electrode that is used as the zero potential and the other potentials in the chemical system are measured with respect to it.

9.14.1 Introduction

Organic compounds are ubiquitous in the average person's daily activity. From plastic containers for liquids to sweeteners in food products, from buttons to electrical insulation, organic compounds cover a broad spectrum of industries, including pharmaceutical, fashion, food, paper, and construction. Consequently, the synthesis of organic compounds is an essential and necessary field of study and it is imperative that this field is continually improved and developed.

Traditionally, the synthesis of organic compounds has been accomplished via chemical routes through the reaction of one or more compounds or heterogeneous catalysis to produce the desired organic compound. Alternatively, over the last century, the use of electrochemical methods for organic synthesis has been investigated at both the laboratory and industrial scale. Some of the benefits of electrochemical organic synthesis are (1) higher product selectivity and purity, (2) lower number of reaction steps, (3) inexpensive starting materials, (4) less polluting chemicals or byproducts, (5) less hazardous routes, and (6) lower consumption of energy.[1,2] However, these advantages for electrochemical routes for organic synthesis have not translated to a

widespread use as only a few processes have been commercialized from the laboratory scale. A list of organic compounds produced using the electrochemical route and their proximity to industrial application is indicative of the current status of this method (Table 1).

Table 1 Examples of industrial organic electrosynthetic processes at commercial and pilot plant stages of operation

Product	*Starting material*	*Company*
	Commercial process	
Acetoin	Butanone	BASF
Acetylenedicarboxylic acid	1,4-Butynediol	BASF
Adipoin dimethyl acetal	Cyclohexanone	BASF
Adiponitrile	Acrylonitrile	Monsanto (Solutia), BASF, Asahi Chemical
4-Aminomethylpyridine	4-Cyanopyridine	Reilly Tar
Anthraquinone	Anthracene	L. B. Holliday, ECRC
Azobenzene	Nitrobenzene	Johnson Matthey Company
p-t-Butylbenzaldehyde	*p*-t-Butyltoluene	BASF, Givaudan
L-cysteine	L-cystine	Wacker Chemie AG
1,4-Dihydronaphthalene	Naphthalene	Clariant
2,5-Dimethoxy-2,5-dihydrofuran	Furan	BASF
Hexafluoropropyleneoxide	Hexafluoropropylene	Clariant
m-Hydroxybenzyl alcohol	m-Hydroxybenzoic acid	Otsuka
p-Methoxybenzaldehyde	*p*-Methoxytoluene	BASF
Perfluorinated hydrocarbons	Alkyl substrates	3M, Bayer, Clariant
Salicylic aldehyde	*o*-Hydroxybenzoic acid	India
Succinic acid	Maleic acid	CERCI, India
3,4,5-Trimethoxytolyl alcohol	3,4,5-Trimethoxytoluene	Otsuka Chemical
	Pilot process	
1-Acetoxynaphthalene	Naphthalene	BASF
2-Aminobenzyl alcohol	Anthranilic acid	BASF
Anthraquinone	Naphthalene, butadiene	Hydro Quebec
Arabinose	Gluconate	Electrosynthesis Co.
1,2,3,4-Butanetetracarboxylic acid	Dimethyl maleate	Monsanto
3,6-Dichloropicolinic acid	3,4,5,6-Tetrachloro-picolinic acid	Dow
Ethylene glycol	Formaldehyde	Electrosynthesis Co.
Glyoxylic acid	Oxalic acid	Rhone Poulenc, Steetley
Hydroxymethylbenzoic acid	Dimethyl terephthalate	Clariant
Monochloroacetic acid	Tri- and di-chloroacetic acid	Clariant
Nitrobenzene	*p*-Aminophenol	India, Monsanto
5-Nitronaphthoquinone	1-Nitronaphthalene	Hydro Quebec
Partially fluorinated hydrocarbons	Alkanes and alkenes	Phillips Petroleum
Propiolic acid	Propargyl alcohol	BASF
Propylene oxide	Propylene	Kellog, Shell
Substituted benzaldehydes	Substituted toluenes	Hydro Quebec, W.R. Grace

Source: Adapted from Sequeira, C. A. C.; Santos, D. M. F. *J. Braz. Chem. Soc.* **2009**, *20*, 387–406, with permission from S.B.Q., Sociedade Brasileira de Quimica (Brazilian Chemical Society).

The reasons for this lack of increased commercialization were previously attributed to a lag in the education of organic chemists in electrochemistry, a lack of suitable resources for cell construction, and most importantly the prohibitive costs involved in the electrochemical synthesis.[3] Other reasons provided have been related to the absence of a market for the organic compound produced and the development of improved chemical process for organic synthesis.[2]

However, in the last 40 years, there have been significant developments in electrochemical synthesis and methods as a result of the advances in materials science and nanotechnology,[4] the development of *in situ* spectroscopy techniques,[5–7] and the progress in multiscale modeling.[8–10] Within this context, it would prove useful and relevant to revisit some of the methods and approaches to electrochemical organic synthesis by implementing and incorporating these aforementioned advances in science and technology.

Therefore, the focus of this chapter is to provide an outlook on the optimum steps in bringing an electrochemical organic synthetic process to commercialization using approaches that incorporate improved research methods as depicted in Figure 1. This template has been previously provided by Herman Pütter[3] and it has been enhanced to include modern approaches in science and technology and strategies that could be incorporated into organic electrochemistry research and development.

First, in initiating an electrochemical process, some knowledge of Fundamental Electrochemistry is required, including the thermodynamics and kinetics of the process, the amount, phase, and type of materials needed for production as well as the environment in which these materials will be combined. These principles can subsequently be implemented in models that have

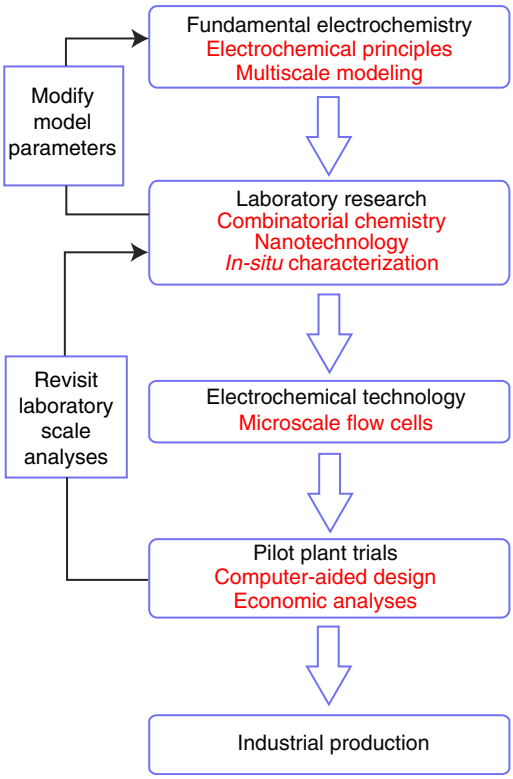


Figure 1 Electrochemical organic synthesis from calculated predictions to large-scale processing. Adapted from Pütter, H. Industrial Electroorganic Chemistry. In *Organic Electrochemistry*, 4th ed.; Lund, H., Hammerich, O., Eds.; Marcel Dekker, Inc.: New York, **2001**, pp 1259–1308.

become ubiquitous in the study of chemical reactions and can aid in fine-tuning experimental plans and negating steps that would normally be implemented in experimental tests. Consequently, the hypotheses constructed from the fundamental principles and models can be translated into actual investigation at the bench-scale by performing Laboratory Research. In this phase, tests are performed with the materials identified and are tested in varying combinations for optimal production. These tests can serve a dual purpose in providing progress in the research process while providing insights that enhance, eliminate, or refine the hypotheses previously formed. The latter purpose would thus result in parameters modification. Although these bench scale studies are experimental, the engineering of these tests will be required to ensure that small scale tests can be effective when transport phenomena are included. In this phase, different principles involved in implementing the Electrochemical Technology can be explored by investigating momentum, heat, and mass transfer profiles within the electrochemical cell. The engineering improvements can then be effected at a medium scale where Pilot Plant Trials are implemented. At this stage, a percentage of the product is generated and the bench scale results are used as a basis to ensure that results obtained do not diverge. In this phase, issues related to safety can also be investigated through the use of engineering simulations, similar to the computational science models from the first phase. Often times, the results from the pilot plant trials may show that the bench scale tests need to be revisited because of certain inefficiencies observed, including, for example, the type of catalysts used and volume of the electrolyte tested. The success of the pilot scale is then used to bring the final product to the consumer through Industrial Production.

To further crystallize the approach presented in Figure 1, two reactions are used as examples: methanol oxidation for hydrogen production and CO_2 reduction for fuel syntheses.

9.14.2 Fundamental Electrochemistry

An organic synthesis reaction can be initiated from the most fundamental principles of chemistry and physics (Figure 1). These principles serve as the building block for a proposed reaction and therefore form the first phase in the research and development of a chemical process. This section introduces some basic electrochemical principles, including nomenclature and the components of an electrochemical system. In addition, the use and application of multiscale modeling is discussed. Multiscale models have proved to be valuable aids in fine-tuning ensuing experimental research. Specifically, the use of models and simulation has been calculated to yield US$3–$9 for every US$1 invested.[11] These returns were based on efficacy related to cost reduction associated with exploratory experimental techniques and safety analyses as well as revenue generation from improvement of

previously stalled products and projects, including the aforementioned disabled projects (Table 1). Two methods in the literature for describing electrochemical reactions at the quantum mechanical scale are discussed.

9.14.2.1 Electrochemical Principles

The syntheses of organic compounds have been accomplished by chemical reactions in beakers and reactors. However, the organic compounds can also be synthesized using electrochemical methods in a reactor known as cell. The electrochemical cell comprises electrodes, substrates, electrolytes, solvent, and various additives. An electrochemical cell is differentiated into two- and three-electrode systems based on the number of electrodes present in the cell. A two-electrode system of the electrochemical cell consists of an anode and a cathode electrode, whereas the usage of a reference electrode along with the anode and the cathode electrodes forms the three-electrode configuration of the electrochemical cell.

In the electrochemical route, the reaction takes place on the surface of the electrode and it involves transfer of electrons between the electrode and the electroactive species. The electrode where the oxidation reaction, or loss of electrons from a molecule or ion, takes place is known as the anode electrode. The cathode electrode is the one where reduction of the electroactive species is observed. The reaction pathway and the yield of the final product can be controlled with the electrode potential, and the choice of the electrode material and electrolyte. Therefore, the choice of electrode material is key to avoid secondary and undesired reactions. Predominantly insoluble electrodes are used in organic synthesis processes, but in some occasion sacrificial anodes or cathodes have also been used.[12] The most commonly used electrode materials are platinum (Pt), lead, copper, carbon, titanium, titanium composite or commonly known as dimensionally stable anodes, stainless steel, magnesium, reticulated vitreous carbon, mercury, and nickel.[12–14]

The electrochemical reactions taking place on the surface of the electrode are controlled by the potential of the electrode, which is the unique advantage of the electrosynthesis method over the chemical method of synthesizing organic compounds. However, the potential of any electrode cannot be determined as absolute value, only be referred with respect to a reference electrode. The reference electrode, used in the three-electrode cell configuration, helps to monitor and control the electrochemical reactions on an electrode, which is known as working electrode. The standard hydrogen electrode (SHE) is the primary reference electrode, but it is not commonly used in the experiments owing to practical difficulty. Other reference electrodes such as silver/silver chloride (Ag/AgCl), mercury/mercury oxide (Hg/HgO), and saturated calomel electrode (SCE) are used in the experiments depending on the pH of the solution.[15]

The electrodes are externally connected to a potentiostat/galvanostat instrument, which controls the voltage/current and monitors current/voltage of the electrochemical cell. At the same time, the electrodes are immersed in the solution of electrolyte, solvent, and if any additives to form the electrochemical cell. Electrons from the potentiostat/galvanostat instrument travel through the external wires to the electrode surface. These electrons on the electrode surface are transferred to molecules or ions to signify the electrochemical reaction. The mobility of the ions in the solution constitutes the conductivity in liquid. The movement of electrons in the external wires and also in the form of ions in the solution is sufficient to complete the electrical circuit for the electrochemical cell.

The solvent used for the organic synthesis should possess good ionic conductivity, ability to dissolve the electrolytes, tolerance to operate in acceptable temperature and potential range, and composed of economically feasible chemical compounds.[12] Examples of the solvents used in the organic electrosynthesis experiments are methanol, acetonitrile, ammonia, dichloromethane, dimethylformamide, dimethyl sulfoxide, tetrahydrofuran, and propylene carbonate (PC).[12–14] The electrolytes are salts, which dissolve into ions, therefore good electrolytes should have high solubility and high ionic conductivity. Examples of electrolytes used in the synthesis of organic compounds are lithium perchlorate, tetrabutylammonium tetrafluoroborate, tetrabutylammonium acetate, and any other tetraalkyl ammonium salt.[12,14]

The electrochemical cells can also be categorized into divided and undivided cells based on compartmentalization of the electrodes. The schematic diagram of an undivided electrochemical cell is shown in Figure 2. Both the anode and the cathode electrodes, connected to the potentiostat, are immersed in the same solution without any physical separation. In an undivided

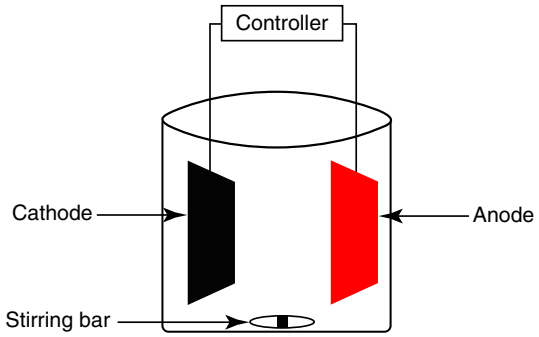


Figure 2 Schematic diagram of a typical undivided electrochemical cell. The controller used could be either a potentiostat or a galvanostat, which control either the voltage or the current, respectively.

cell, the intermediates and/or the products formed at one electrode, say anode electrode, can undergo chemical or electrochemical reaction on the cathode electrode. Therefore, the chemicals formed at one electrode can interfere with the electrode where the primary electrochemical reaction is supposed to take place. The products formed using the undivided electrochemical cell need to be purified or separated from other chemicals so as to increase their yield percentage. In some instances where secondary electrochemical reactions are not observed, stirring (Figure 2, employs a stir bar for mixing) is used in an undivided cell to uniformly mix the solution. Mixing the solution brings the reactant species to the electrode surface, where the electrochemical reaction takes place; this in turn speeds up the rate of that electrochemical reaction when compared with a static system.

A divided cell is shown in Figure 3, where the electrochemical reaction on the electrode is controlled by applied potential. In this divided cell, the working electrode is separated from the auxiliary electrode with the help of a porous disk or frit. The porous disk or frit is known as separator, which physically isolates the chemical constituents present in the working electrode side from the auxiliary electrode side. To maintain the ionic conductivity in the divided cell and also to complete the electrical circuit for the electrochemical cell, the separators are known to provide access to certain ions to travel or migrate across them. But the intermediates and/or products formed on the side of one electrode will not be mixed with the contents of other side. This separation of the chemicals is beneficial to prevent secondary reactions and also improve the yield for the product.

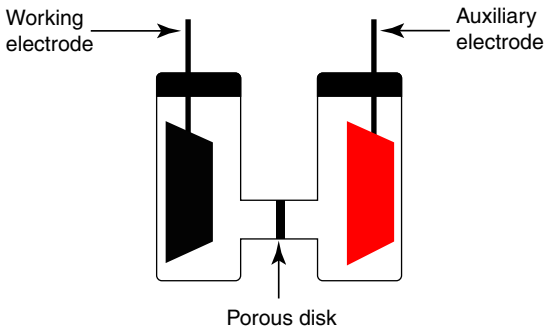
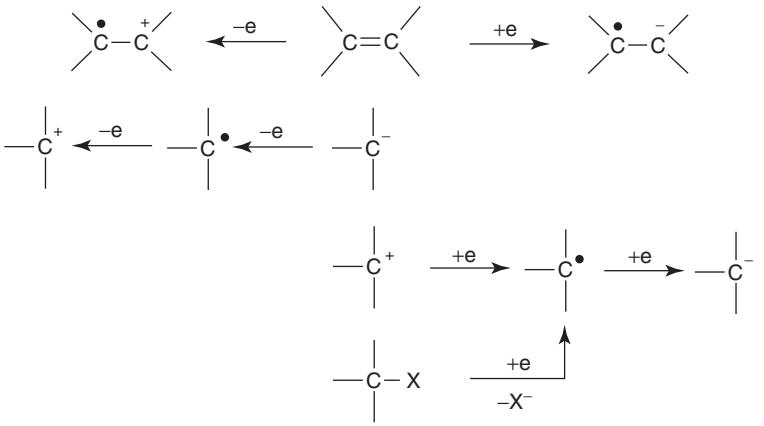


Figure 3 Schematic diagram of a divided cell, also known as a H-cell.[14] The porous disk is a membrane that separates the components of either electrode. A reference electrode can also be included in this cell if needed.

There are several publications describing the electrochemistry principles related to synthesis of organic compounds and reaction mechanisms encountered using electrochemical cells.[12,15–17] All the electrochemical reactions involve the transfer of electron to or from electroactive species to form an anion, a cation, or a radical. The electron transfer reactions are shown in Scheme 1.[18]

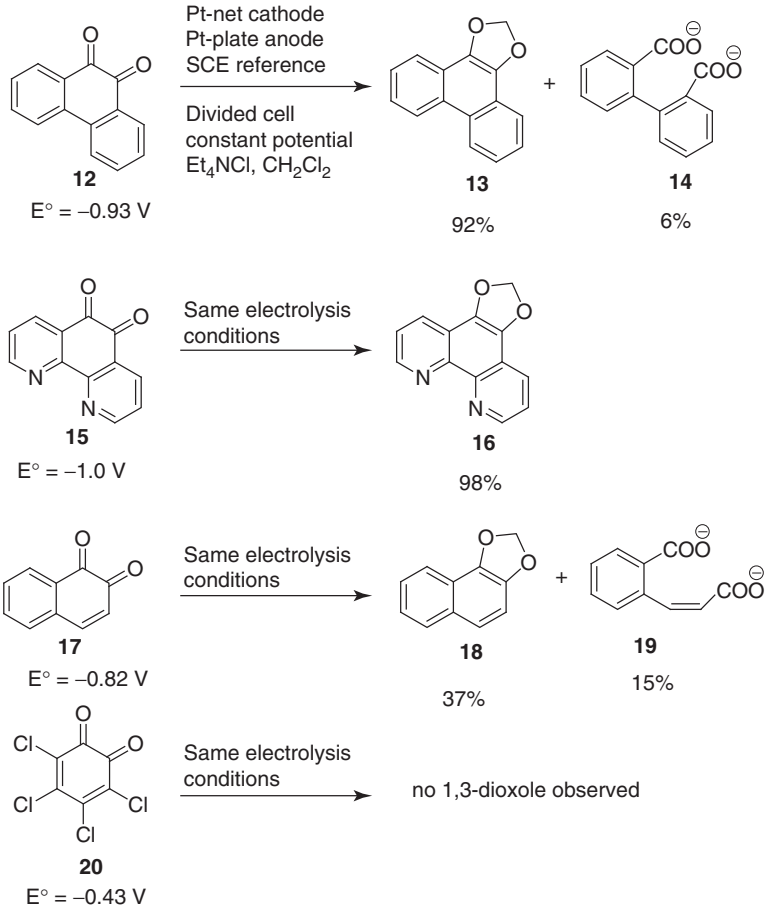


Scheme 1 Formation of carbanions, carbocations, and radicals from electron transfer reactions. Reproduced from Schäfer, H. J. Comparison Between Electrochemical Reactions and Chemical Oxidations and Reductions. In *Organic Electrochemistry*, 4th ed.; Lund, H., Hammerich, O., Eds.; Marcel Dekker, Inc.: New York, **2001**, pp 207–221.

A compound containing C–C double bond will be converted to carbanion during the electrochemical reduction reaction at the cathode electrode by the addition of a single electron. The same compound, C–C double bond, can be transformed into carbocation by withdrawing a single electron using the anode electrode via oxidation reaction. Scheme 1 also illustrates the transition of a carbanion to radical species to carbocation using the subsequent oxidation reaction involving withdrawal of single electron in each step. The carbon radical form of the compound can also be formed by dehalogenation reaction combined with addition of electron. These reactions display the potential of the electrochemical method to synthesize compounds with high specificity.

The electrochemical synthesis of the organic compounds can be controlled with the applied cell voltage or even the electrode potential. The control on the electrochemical reaction with electrode potential is the unique advantage the electrochemical synthesis has over the traditional chemical methods. The electrochemical reductions of some quinones to produce 1,3-dioxolanes illustrates the effect of electrode potential and the importance of divided cells (Scheme 2).[14] The reactions shown in Scheme 2 take place in an electrochemical system where the cathode is made of Pt net, and it is separated from the Pt plate anode and the reference electrode (SCE) by glass frit, and the electrolyte consists of tetraethylammonium chloride (Et_4NCl) and dichloromethane (CH_2Cl_2). In this cell configuration, the electrochemical synthesis of 1,3-dioxolanes was achieved by choosing the appropriate formal potential ($E^{\circ\prime}$). High yield percentage of more than 90% for the 1,3-dioxolanes was achieved when the formal potential was more negative than -0.9 V versus SCE. For example, the quinones **12** and **15** were electrochemically reduced to **13** (92% yield) and **16** (98% yield), respectively, at -0.93 and -1.0 V versus SCE. However, the electrochemical reduction of **17** at -0.82 V versus SCE resulted in only 37% yield of **18**, and when tetrachloro-*o*-quinone **20** was subjected to electrochemical reduction at -0.43 V versus SCE, there were no 1,3-dioxole observed or formed. These cathodic reduction reactions illustrate the importance of the potential for electrochemical synthesis.

A few important and commercially successful chemical processes utilizing the electrochemical technology are briefly described in the following Sections 9.14.2.1.1 and 9.14.2.1.2. For ease of understanding the synthesis process, the electrochemical synthesis of organic compounds has been differentiated as cathodic and anodic reactions.



Scheme 2 Cathodic reduction of quinones to 1,3-dioxolanes. Reproduced with permission from Sperry, J. B.; Wright, D. L. *Chem. Soc. Rev.* **2006**, *35*(7), 605–621.

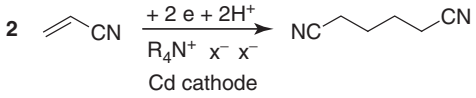
9.14.2.1.1 Cathodic reactions

The reduction reactions taking place on the cathode electrode have been utilized for the production of organic compounds, such as the reduction of phthalic acid to dihydrophthalic acid, electrocarboxylation of chloroethyldiphenyl ether, and electrohydrodimerization of acrylonitrile.[12] The focus of this section is on the synthesis of adiponitrile from acrylonitrile and the sequestration of CO_2 to form methanol and other valuable hydrocarbons.

9.14.2.1.1.1 Adiponitrile

In the field of electrochemical synthesis of organic compounds, adiponitrile is a very important compound because its synthesis using an electrochemical method takes up the largest production volume since the early 1960s.[19] Adiponitrile also plays a key role as an intermediate in the synthesis of nylon. In 1960, Manuel M. Baizer, working for Monsanto, developed the process for the hydrodimerization of acrylonitrile (AN) to form adiponitrile (ADN) using quaternary ammonium salt as supporting electrolyte, which resulted in 90% mass yield of adiponitrile.[12] Since then the electrochemical synthesis of ADN is also known as the 'Monsanto Process.' The Monsanto plant at Decatur, Alabama, in the USA produces at least 200 million kg yr^{-1} of adiponitrile using this electrochemical process.[2]

Scheme 3 illustrates the reduction reaction of hydrodimerization of acrylonitrile (CH_2CHCN) in the presence of quaternary ammonium salt for the formation of adiponitrile ($CNCH_2CH_2CH_2CH_2CN$) at a cadmium (Cd) cathode electrode. In 1960, Baizer found that using tetraethylammonium *p*-toluenesulfonate (quaternary ammonium salt) as the supporting electrolyte, gave 90% mass yield of adiponitrile.



Scheme 3 Hydrodimerization of acrylonitrile. Reproduced from Pütter, H. Industrial Electroorganic Chemistry. In *Organic Electrochemistry*, 4th ed.; Lund, H., Hammerich, O., Eds.; Marcel Dekker, Inc.: New York, **2001**, pp 1259–1308.

In the beginning, a divided cell was used for the synthesis of adiponitrile, where the cathode electrode was made of lead (Pb) and the anode electrode had 1% silver (Ag) in Pb as listed in Table 2. The aqueous solution used on the cathode side was a mix of acrylonitrile and adiponitrile in 40% tetraethylammonium ethyl sulfate, which was separated from the anode solution of dilute sulfuric acid by an ion exchange membrane (Ionics CR61). The divided cells were operated at a current density of 4.5 kA m^{-2} and it resulted in total voltage of 300 V for a 24 bipolar cell system.

Table 2 Comparison between different cell configurations for adiponitrile conversion

	Divided	*Undivided*
Cathode	Pb	Cd
Anode	Pb (1% Ag)	Steel
Membrane	Ionics CR61	None
Temperature	50 °C	55 °C
Current density	4.5 kA m^{-2}	2.0 kA m^{-2}
Electrode gap	7 mm	3 mm
Cell voltage	11.65 V	3.83 V
Power consumption	6.61 kWh g^{-1}	2.43 kWh g^{-1}
	Quaternary ammonium salt	
Cation	Tetraethylammonium	BisQat[a]
Anion	Ethyl sulfate	Phosphate
Concentration	40%	0.4%

[a]Hexamethylenebis(ethyltributyl)ammonium.

Source: Adapted from Pütter, H. Industrial Electroorganic Chemistry. In *Organic Electrochemistry*, 4th ed.; Lund, H., Hammerich, O., Eds.; Marcel Dekker, Inc.: New York, **2001**, pp 1259–1308.

The energy cost involved in operating the divided cells and also the related high cost associated with the repair and maintenance was responsible for the development of undivided cells. The cathode and anode used in the undivided cell were cadmium (Cd) and steel, respectively. The undivided cells were operated at a current density of 2 kA m^{-2} and its cell voltage was only 3.83 V in comparison with 11.65 V observed for the divided cell configuration utilized for ADN synthesis.

Figure 4 displays an undivided cell configuration used for the production of adiponitrile. The undivided cell is made of plastic-lined vessel with plastic filler material on the inner wall to hold the end electrodes. The undivided cell is operated with a series of bipolar electrodes and the electrodes are electrically connected at the end electrode. The electrolyte used for the production of adiponitrile is fed at the bottom of the undivided cell.

Using an undivided cell for the synthesis of adiponitrile requires safety precautions because oxygen gas is produced at the anode and hydrogen is also formed at the cathode; additionally, other volatile organic compounds are all present in single gas phase. Cadmium has high overpotential for hydrogen evolution, which helps to limit the generation of hydrogen at the cathode electrode. Moreover, the quaternary ammonium salt present in the electrolyte has a higher affinity to adsorb on Cd electrode than protons or water molecule, which increases the selectivity for the synthesis of adiponitrile. The electrolyte from the undivided cell

has a mixture of acrylonitrile, adiponitrile, quaternary ammonium salt, and other byproducts. This mixture was subjected to extraction columns and vacuum distillation to separate the product – adiponitrile (Figure 5). Employing these measures in the synthesis process for the undivided cell has resulted in the yield and current efficiencies close to 95%.

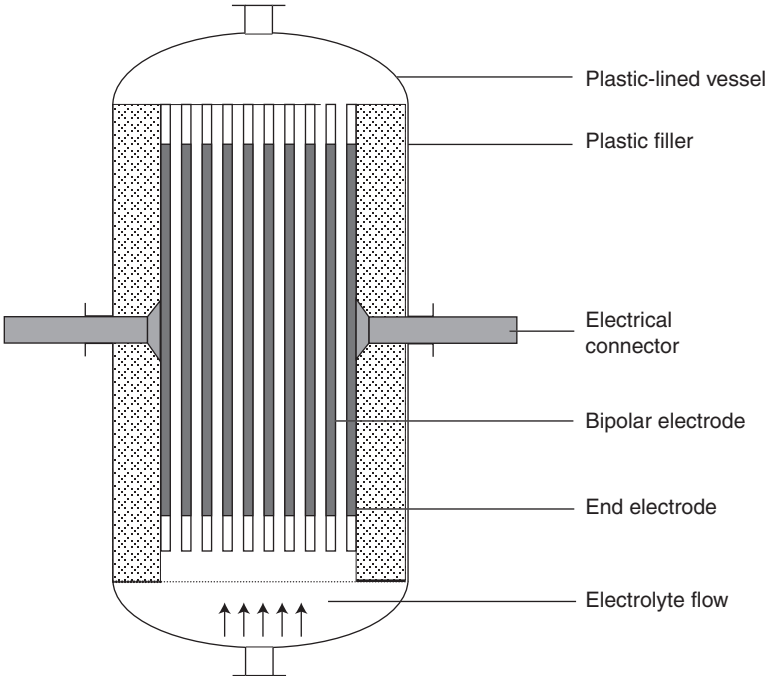


Figure 4 Schematic diagram of an undivided electrochemical cell for adiponitrile production. Reproduced from Pütter, H. Industrial Electroorganic Chemistry. In *Organic Electrochemistry*, 4th ed.; Lund, H., Hammerich, O., Eds.; Marcel Dekker, Inc.: New York, **2001**, pp 1259–1308.

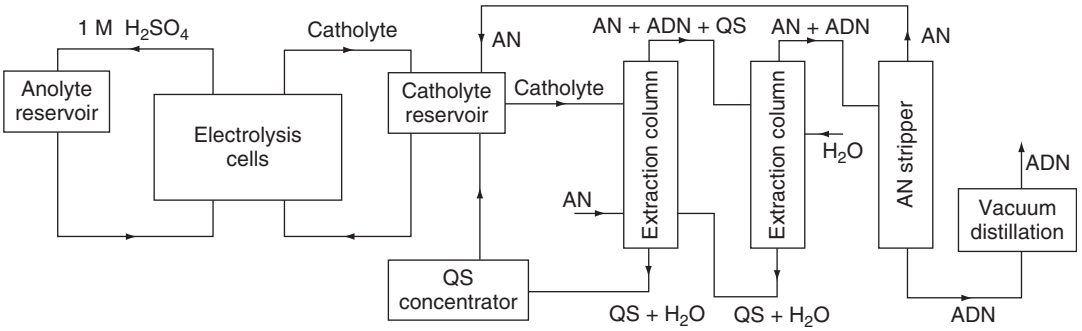


Figure 5 Monsanto flowsheet for the electrohydrodimerization of acrylonitrile to adiponitrile.[204]

9.14.2.1.1.2 Carbon dioxide

With fossil fuels as the most abundant source of power generation for both residential and vehicular operation, CO_2 is generated at rates that far outweigh its removal/conversion to raw materials, such as fuels and chemicals. The possibility of converting this abundant waste to a useful source has created an avenue of interest for both sustainable energy and environmental decontamination. The importance of this process is reflected in the developments of electrical methods for CO_2 and water conversion as one of the top priorities of the US Department of Energy.[20]

Although several chemical and catalytic methods have been tested for converting CO_2 to fuels including reaction with hydrogen, hydrocarbons, and organic carbonates, the use of energy from electricity provides a more sustainable approach, due to the possibility of renewable sources being used as the source of electricity.[21] Although alternative chemical routes for CO_2 reduction have shown disadvantages such as deactivation of typical catalysts due to the presence of water (methanol and ethanol formation) and high reaction temperatures (carbon monoxide (CO) formation from C–O dissociation), the use of electrochemical reduction can be performed under ambient conditions.[22,23] Of the metals tested, electrodes based on copper have

shown the best performance for conversion to hydrocarbons with considerable current densities and a high current efficiency in an aqueous electrolyte (Table 3).

Table 3 Effect of metal electrodes on the faradaic efficiencies (%) of products from CO_2 reduction as a function of potential vs. SHE (V) and current density (mA cm^{-2})[a]

Electrode	*Potential vs. SHE*	*Current Density*	*Faradaic Efficiency*							
			Methane	*Ethylene*	*Ethanol*	*Propanol*	*Carbon monoxide*	*Formate*	*Hydrogen*	*Total*
Pb	−1.63	5.0	0.0	0.0	0.0	0.0	0.0	97.4	5.0	102.4
Hg	−1.51	0.5	0.0	0.0	0.0	0.0	0.0	99.5	0.0	99.5
Tl	−1.60	5.0	0.0	0.0	0.0	0.0	0.0	95.1	6.2	101.3
In	−1.55	5.0	0.0	0.0	0.0	0.0	2.1	94.9	3.3	100.3
Sn	−1.48	5.0	0.0	0.0	0.0	0.0	7.1	88.4	4.6	100.1
Cd	−1.63	5.0	1.3	0.0	0.0	0.0	13.9	78.4	9.4	103.0
Bi	−1.56	1.2	–	–	–	–	–	77	–	–
Au	−1.14	5.0	0.0	0.0	0.0	0.0	87.1	0.7	10.2	98.0
Ag	−1.37	5.0	0.0	0.0	0.0	0.0	81.5	0.8	12.4	94.6
Zn	−1.54	5.0	0.0	0.0	0.0	0.0	79.4	6.1	9.9	95.4
Pd	−1.20	5.0	2.9	0.0	0.0	0.0	28.3	2.8	26.2	60.2
Ga	−1.24	5.0	0.0	0.0	0.0	0.0	23.2	0.0	79.0	102.0
Cu	−1.44	5.0	33.3	25.5	5.7	3.0	1.3	9.4	20.5	103.5[b]
Ni	−1.48	5.0	1.8	0.1	0.0	0.0	0.0	1.4	88.9	92.4[c]
Fe	−0.91	5.0	0.0	0.0	0.0	0.0	0.0	0.0	94.8	94.8
Pt	−1.07	5.0	0.0	0.0	0.0	0.0	0.0	0.1	95.7	95.8
Ti	−1.60	5.0	0.0	0.0	0.0	0.0	tr.	0.0	99.7	99.7

[a]Electrolyte is 0.1 M $KHCO_3$ and temperature is 18.5 ± 0.5 °C.
[b]Total also includes glycerol (1.4%), acetaldehyde (1.1%), and propaldehyde (2.3%).
[c]Total also includes ethane (0.2%).
Source: Reproduced with permission from Hori, Y.; Wakebe, H.; Tsukamoto, T.; Koga, O. *Electrochim. Acta* **1994**, *39*(11–12), 1833–1839.

As observed in the table, there are numerous products possible from CO_2 electrochemical reduction based on the number of electrons transferred in the reaction. In fact, one study has detected as many as 16 products in varying amounts (Table 4).[24]

Table 4 Detected products of CO_2 reduction, the number of electrons transferred and the standard reduction potentials (V) at a pH of 6.8 on a copper-based electrode

Product	*Number of electrons*	*Standard reduction Potential*
Formate	2	−0.02
Carbon Monoxide	2	−0.10
Methanol	6	0.03
Glyoxal	6	−0.16
Methane	8	0.17
Acetate	8	−0.26
Glycoaldehyde	8	−0.03
Ethylene Glycol	10	0.20
Acetaldehyde	10	0.05
Ethanol	12	0.09
Ethylene	12	0.08
Hydroxyacetone	14	0.46
Acetone	16	−0.14
Allyl alcohol	16	0.11
Propionaldehyde	16	0.14
1-Propanol	18	0.21

Source: Reproduced with permission from Kuhl, K.; Cave, E.; Abram, D.; Jaramillo, T. *Energy Environ. Sci.* **2012**, *5*(5), 7050–7059.

However, although the potentials shown (Table 4) indicate mostly favorable equilibrium thermodynamics, the kinetics have indicated that overpotentials upward of 1.0 V are required to produce these end-products (Table 3). These sluggish kinetics have suggested the bottleneck in CO_2 reduction to be due to the formation of a radical anion[25] (equation 1).

$$CO_2 + e^- \rightarrow CO_2^{\bullet -} \quad (-1.90\ \text{V vs. SHE}) \tag{1}$$

In addition to this limiting step, a competing reaction is hydrogen evolution due to the aqueous environment[25,26] (equation 2).

$$2H_2O + 2e^- \rightarrow 2OH^- + H_2 \ (-0.41 \text{ V vs. SHE}) \quad (2)$$

These issues with kinetics and the chemical environment as well as some of the issues associated with selectivity indicate that further understanding of this process is important to making further advances in this cathodic reaction. The significance of this reaction and the associated problems are one of the reasons why this study has been chosen for use in this chapter, especially as some exploratory industrial studies have been made in commercializing this process under nonaqueous conditions and high temperatures.[26,27]

9.14.2.1.2 Anodic reactions

In an electrochemical cell or process, the oxidation reaction happens on the surface of anode electrode. Electrooxidation of organic compounds can lead to the formation of valuable organic compounds and/or generate energy during that process. One of the well-known electrochemical technologies to produce power or electricity is fuel cells. Normally in a fuel cell, highly pure hydrogen gas is used as the fuel for power generation. But presently the availability of highly pure hydrogen in gaseous form depends on thermal decomposition of methane, commonly found in natural gas, or electrolysis of water or hydrogen containing inorganic compounds. The storage and transportation of hydrogen gas is been a key concern for applying fuel cells for practical use in addition to the high cost mainly associated with the catalysts.

However, the use of carbon-containing fuels in the fuel cell will eliminate the need for synthesizing high purity hydrogen; instead directly use the existing fuels or organic compounds, such as methanol, ethanol, propanol, and glycerol in the fuel cell to generate electricity. The two configurations of the fuel cell utilizing carbon-containing fuels are displayed in Figure 6, where the electrolyte can be either a cation exchange membrane or an anion exchange membrane.[28] For the fuel cell illustrated in Figure 6, oxygen from air is the oxidant, which is supplied to the cathode side and the electrooxidation of the carbon-containing fuel takes place at the anode. The electrochemical oxidation of carbon-containing fuel will produce CO_2 as one of the products at the anode electrode.

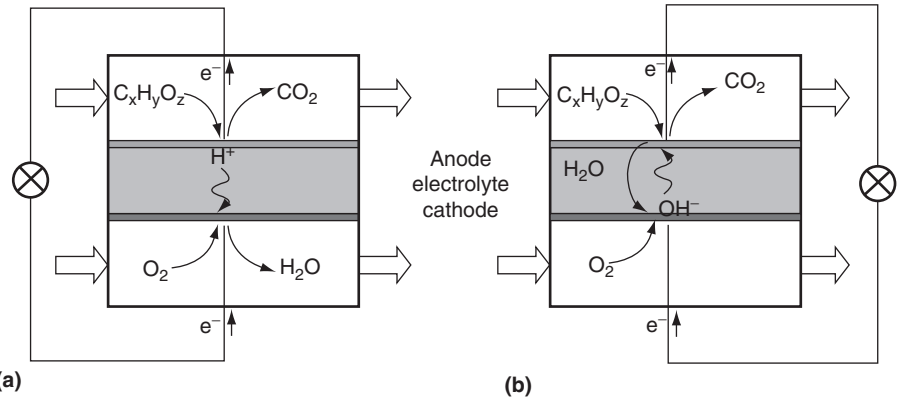


Figure 6 Working principle of low-temperature fuel cells with (a) cation exchange (e.g., H^+) or (b) anion exchange (e.g., OH^-); $C_xH_yO_z$ is any carbon-containing fuel, oxygen is the oxidant. Reproduced with permission from Krewer, U.; Vidakovic-Koch, T.; Rihko-Struckmann, L. *Chemphyschem.* **2011**, *12*(14), 2518–2544.

The thermodynamic values for the electrooxidation of various carbon-containing fuels and their corresponding cell voltages and energy density values are listed in Table 5.

9.14.2.1.2.1 Methanol

Among the carbon-containing fuels, methanol has been the most investigated fuel and extensively utilized in a fuel cell system, especially as direct methanol fuel cell (DMFC). The DMFC is a type of proton exchange membrane fuel cell (PEMFC), where liquid methanol is used as fuel instead of highly pure (>99.9%) hydrogen gas stream. The use of a liquid fuel, such as methanol, is beneficial for the management of energy and environment, because of the avoidance of rigorous energy-consuming processes for generating high purity hydrogen gas from fossil fuels. Additionally, liquid methanol can be transported with ease as opposed to the safety concerns associated with the movement of compressed hydrogen gas. These advantages, therefore, make the DMFC system a strong candidate for portable power generation system. The lightness, on the aspect of weight, of the direct methanol fuel cell system combined with liquid methanol gives DMFCs the possibility for military and defense applications.

The electrochemical reactions observed at the electrodes of a DMFC system are given below:

$$\text{Anode: } CH_3OH + H_2O \rightarrow CO_2 + 6H^+ + 6e^- \quad (3)$$

Table 5 Gibbs free energy change (kJ mol^{-1}), standard cell potential (V) and energy densities (MJ kg^{-1}) of low-temperature fuel cells with oxygen as the oxidant

Fuel	*Gibbs free energy change*[a]	*Standard cell potential*[a]	*Energy density*
Methanol[205]	702	1.213	21.9
Ethanol[205]	1325	1.145	28.7
1-Propanol[206]	1853	1.067	30.9
2-Propanol[205]	1948	1.122	32.4
n-Butanol[207]	2602	1.124	35.2
Dimethyl ether[205]	1387	1.198	30.3
Ethylene glycol[207]	1181	1.224	19
Formic acid[205]	270	1.400	5.6[b]
Glycerol	1622[b]	1.201	16.1[b]

[a]Calculated at standard conditions of 298 K and 101.325 Pa.
[b]Values calculated from other thermodynamic data.[208,209]
Source: Reproduced with permission from Krewer, U.; Vidakovic-Koch, T.; Rihko-Struckmann, L. *Chemphyschem.* **2011**, *12*(14), 2518–2544.

$$\text{Cathode: } 6H^+ + 6e^- + 3/2\ O_2 \rightarrow 3H_2O \tag{4}$$

Methanol (CH_3OH) is mixed with water and fed into the anode side of the fuel cell system. At the anode electrode, CH_3OH is electrochemically oxidized into CO_2, protons, and electrons using the Pt catalyst. The protons, produced during the oxidation reaction, are transferred to the cathode side via the proton exchange membrane, which also separates the anode electrode and its contents from the cathode compartment (**Figure 6(a)**). Typically, Nafion is used as the proton exchange membrane in the DMFC systems. The electrons, however, released at the anode electrode are transported through the external wire to the cathode electrode. This movement of electrons on the external wire constitutes the generation of power in a DMFC system. At the cathode electrode, the protons migrate through the membrane and the electrons from the external wire combine with the oxygen molecule, in the presence of Pt catalyst, to form water.

Pt catalyst is required to electrochemically oxidize methanol to its products. The electrooxidation of methanol undergoes multiple pathways and results in different end products. The complete oxidation of methanol should lead to the formation of CO_2; however, other soluble products such as formaldehyde and formic acid are also observed during the electrochemical oxidation of methanol. The illustration of different pathways undertaken by methanol to its products is shown in **Figure 7**.

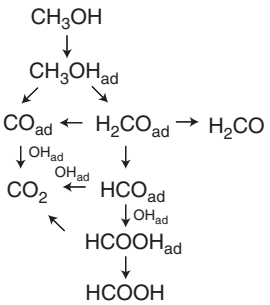


Figure 7 Mechanism for methanol oxidation in acidic media, indicating the reaction and conversion of species X adsorbed on the electrode surface (X_{ad}). Reproduced with permission from Krewer, U.; Vidakovic-Koch, T.; Rihko-Struckmann, L. *Chemphyschem.* **2011**, *12*(14), 2518–2544.

The total oxidation of methanol to CO_2 is observed when there is adsorption of CO and hydroxyl (OH) species on the surface of the Pt catalyst. However, the parallel reaction pathways for the oxidation of methanol results in the formation of formic acid (HCOOH) and formaldehyde (HCHO) species, which are soluble in the solution. The CO_2 yield or current efficiency for the oxidation process was observed to increase when the HCHO and HCOOH species were adsorbed back on the Pt catalyst, and then undergoes further electrooxidation to result in the formation of CO_2. During the methanol electrooxidation process, some of the methanol molecules will react with the formic acid, obtained from the parallel reaction, to form methyl formate, which also affects the yield and current efficiency for CO_2 formation.

The parameters that affect the yield and current efficiency in CO_2 production are potential of the electrode, temperature, pH, and flow rate of the electrolyte, morphology of the catalyst, thickness of the catalyst layer, particle size of the catalyst, and different metals used to form alloys with the Pt catalyst.[28] The parameters listed here have profound impact on the CO_2 current efficiency in an electrochemical cell during the methanol oxidation process. When the electrode potential of a Pt electrode is increased from 0.6 to 0.8 V versus reversible hydrogen electrode (RHE), the current efficiency for CO_2 was improved from 20% to 32%.[29] For the same electrode potential range, the Pt supported by nanoporous carbon electrodes displayed higher CO_2 current efficiency of 60% to 80% when compared with smooth Pt electrode.[30,31] One of the parameters that exhibited a major impact on the current efficiency is the

morphology of the Pt catalyst; the particle size of the catalyst is also important to attain complete oxidation of methanol to CO_2.[32] The size of the Pt nanoparticles has direct implication on the bond strengths of Pt–CO and Pt–OH bonds. The optimum Pt particle size ranging between 3 and 10 nm has been found to have positive impact on the methanol oxidation process.[33]

The CO_2 current efficiency and yield during the methanol oxidation process can be improved by increasing the electrode potential or the reaction overpotential at the electrode. But employing high overpotential also translates into high amount of energy being spent for the oxidation process. Using the knowledge on reaction mechanism for the methanol oxidation, operating with high overpotential on the Pt catalyst electrodes can be avoided. Bimetallic or Pt-based alloy catalysts are being investigated to facilitate the complete oxidation of methanol to CO_2 at low overpotentials. One of the elements added to the Pt as catalyst is ruthenium (Ru), for example, when Ru atoms were adsorbed on Pt single crystal – Pt(111)/Ru, the electrode was able to demonstrate nearly 100% oxidation of methanol to CO_2 via CO adatoms (adsorbed atoms).[29] The function of Ru in this Pt-based catalyst is to adsorb oxygen-containing species during the methanol oxidation reaction because of Ru's higher affinity, than Pt, toward oxygen-containing species. This helps in freeing or vacating Pt sites on the electrode for the adsorption of methanol for the oxidation reaction. Another explanation for the effectiveness of Pt–Ru catalyst in the methanol oxidation reaction is the electronic effect contributed by the Ru atoms, where Ru atom modifies the electronic structure of Pt, which in effect reduces the strength of the Pt–CO bond during the methanol oxidation reaction.[34–36]

The catalysts used for the electrooxidation of methanol process are expensive noble metals, such as Pt and Ru. There is extensive research being carried out to identify alternative and cheaper catalysts for the electrooxidation of methanol. Lead (Pb) and tin (Sn) have been combined with Pt to catalyze the methanol oxidation, especially to result in complete oxidation of methanol to CO_2 and also to avoid surface blockage of Pt catalyst by CO molecules.[37–40] The total oxidation of methanol to CO_2 was observed with tungsten carbide catalyst, which had comparable catalytic activity to Pt.[41] More research and investigations are being performed to increase the CO_2 current efficiency as well as its yield from the process of electrochemical oxidation of methanol. Controlling the parameters and choosing the appropriate catalyst will direct the reaction pathway in the methanol oxidation process to yield either CO_2 or formic acid or formaldehyde as the primary product.

9.14.2.2 Multiscale Modeling

Prediction of chemical properties across various time and length scales is referred to as multiscale modeling and covers calculations from the electronic scale to the macroscopic scale as depicted in Figure 8.

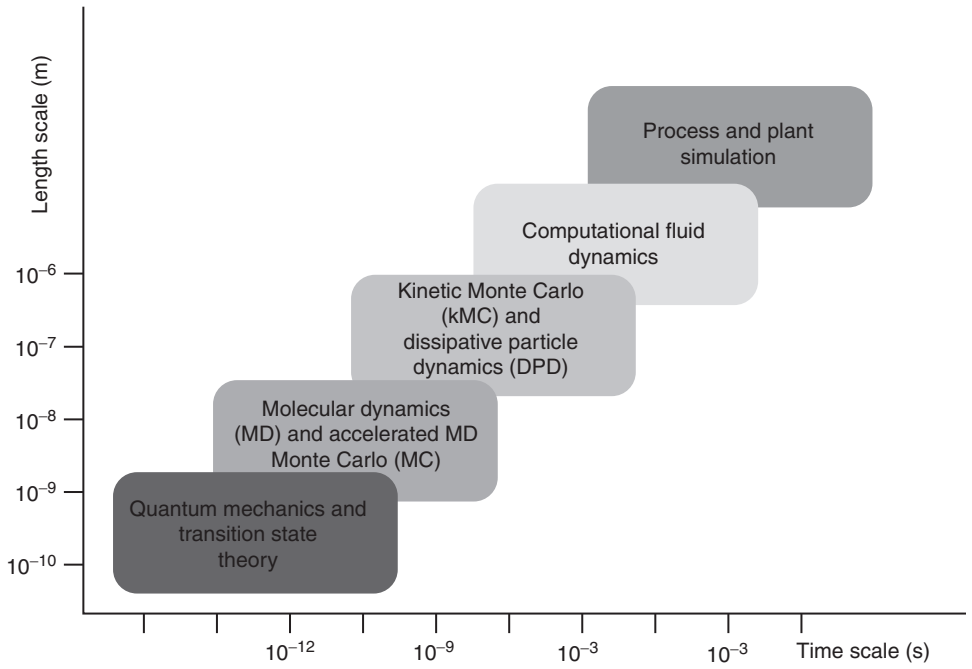


Figure 8 An illustration of multiscale modeling schemes along different time and length scales. Adapted from Keil, F. Multiscale Modelling in Computational Heterogeneous Catalysis. In *Multiscale Molecular Methods in Applied Chemistry*; Kirchner, B., Vrabec, J., Eds.; Springer: Berlin Heidelberg, **2012**, Vol. 307; pp 69–107, with permission from Springer Science+Business Media.

The growth in computational and processing power and development in the fields of quantum mechanics and molecular dynamics has allowed for the increased use of simulations in predicting properties such as vibrational and optical spectroscopies, reaction rates, diffusivity constants, and so on. In principle, calculations can be used to predict experimental results and thus serve

as an approach to fine-tuning the amount of experimental analyses required. However, in reality, experimental work is needed to verify/confirm theoretical conclusions. Conversely, theoretical predictions enhance experimental observation at levels where experimental observation is not currently possible. Thus, both theoretical and experimental approaches should be used in conjunction to create the complete picture of a chemical process. The development and applications of multiscale models is well documented in various books and reviews and a short summary of the methods and possibilities are provided in this section.

Elucidation of chemical properties begins at the electronic level and thus the foundation for multiscale models are based on the laws of Quantum Mechanics, describing the nature of the electronic interactions. Quantum Mechanical calculations are based on approaches that involve the use of *ab initio* models, semi-empirical methods and Density Functional Theory (DFT).[42] Although these methods are often better predictors for phenomena in the gas phase and at the solid–gas interface, that is, conditions similar to ultra-high vacuum experiments, the applications of quantum mechanics to electrochemical reactions – to include the effects of surface charge density and the solvent phases – have been an area of recent focus.[10,43] Electrochemical effects have been modeled in several ways including the use of point charges[44] and a finite electric field[45,46]; however, the methods developed by Norskov et al.[47,48] and Neurock et al.[49,50] have been the most common and are summarized in this section. These methods have been developed for use with systems that are periodic in two dimensions, that is, the electrode surface with the latter method being more computationally intensive because of the use of an internal reference.[51]

9.14.2.2.1 Computational hydrogen electrode

Norskov et al. uses the H_2/H^+ system as the reference potential and this has been referred to as the 'computational (standard) hydrogen electrode' (CHE).[52,53] This method for including electrochemical effects in the free energy has been successfully applied in describing the oxygen reduction reaction,[47,51] water electrolysis,[48,54] and nitrogen reduction.[52] For the H_2/H^+ system at a pressure of 1 bar, temperature of 298 K and pH 0,

$$H^+ + e^- \leftrightarrows {}^1/_2H_2 \text{ (0 V vs. SHE)} \tag{5}$$

the free energy change of the reaction is zero ($\Delta G = 0$) and as such,

$$G_{1/2H_2} = G_{H^+ + e^-} \tag{6}$$

Therefore, for a reaction at the surface of a catalyst and under the aforementioned conditions,

$$A_{ad} + H^+ + e^- \rightarrow AH_{ad} \text{ (0 V vs. SHE)} \tag{7}$$

The free energy for this reaction is,

$$\Delta G = G_{AH} - G_A - G_{H^+ + e^-} = G_{AH} - G_A - G_{1/2H_2} \tag{8}$$

Under nonstandard conditions, corrections will be added to equation 4 to approximate these effects and this is how the use of the CHE accounts for the electrochemical conditions.

With an applied potential, the free energy of the reaction can reflect this based on the Nernst equation, such that $\Delta G = -e\Phi$, where e is the elementary charge (1.60×10^{-19} C) and Φ is the applied potential. Consequently, the overall free energy of the reaction becomes

$$\Delta G = \Delta G_{\Phi = 0} + \Delta G_\Phi = G_{AH} - G_A - G_{1/2H_2} - e\Phi \tag{9}$$

To include the effect of pH on the free energy, this is based on the concentration of H^+,

$$\Delta G = -kT \ln[H^+] = kT \times \text{pH} \times \ln 10 \tag{10}$$

where k is Boltzmann's constant (1.38×10^{-23} J K^{-1}) and T is the temperature.

For solvent effects, free energy calculations can be performed by varying the coverage of water molecules on the surface[47] of the electrode or by semi-empirical approximations based on calculated dispersion effects due to hydrogen bonding.[52]

Finally, the effect of the electric field on the energy of the species in the reaction can be accounted for by the application of a finite field (in V Å^{-1}) and the assumption of an electrochemical layer of approximately 3 Å, thus providing a range of potentials.[45,46,51,55,56] The effect of the electric field has been found to be minimal in most cases and has been often excluded in the application of the CHE method.[48,51]

Overall, the free energy of the reaction can be estimated according to:

$$\Delta G = \Delta E + \Delta \text{ZPE} - T\Delta S + \Delta G_w + \Delta G_{pH} + \Delta G_\Phi + \Delta G_{field} \tag{11}$$

It is a combination of the electronic (ΔE), zero point energies (ΔZPE) and entropies (ΔS) calculated using electronic structure methods, solvation effects due to water coverage (ΔG_w), pH effects in the solution (ΔG_{pH}), applied potential effect (ΔG_Φ), and the local electric field (ΔG_{field}) of the electrochemical environment. A theoretical study[53] on the electrochemical pathways for CO_2

reduction to products found by Hori et al.[23] explains the application of equation 7 and provided insight into the use of CHE in an organic electrochemical reaction.

Initially, based on the reactants and products, the proposed intermediates formed can be combined into a suggested pathway (Figure 9). The purpose of the study was to investigate how copper catalyzed the CO_2 reduction to hydrocarbons and the potentials that would favor the production of certain products, for example, why hydrogen was generated before methane at less negative potentials.

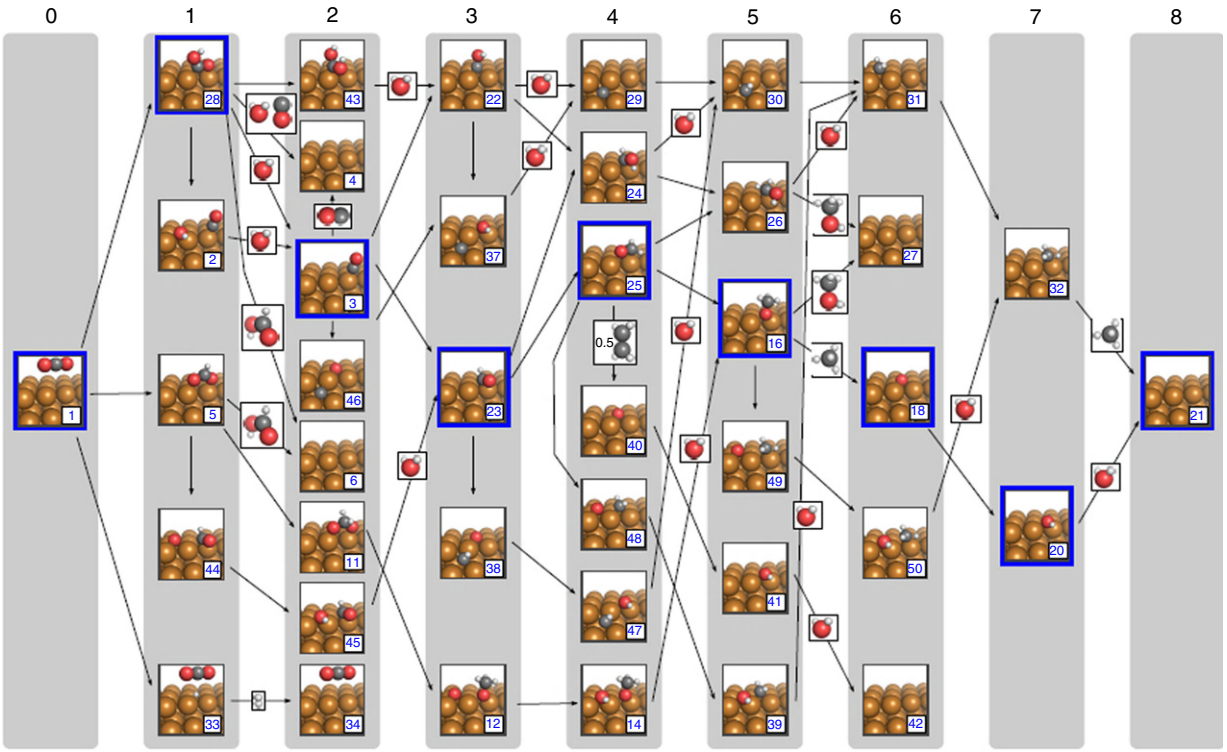


Figure 9 Reactants, Products, and Intermediates considered in the formation of H_2, H_2O, CO, CH_4, HCOOH, C_2H_4, and CH_3OH from CO_2. The surface considered is Cu(211) and the carbon, oxygen, hydrogen, and copper atoms are in gray, red, white, and orange, respectively. The numbers at the top of the column represent the number of proton–electron pairs transferred relative to CO_2. Reproduced with permission from Peterson, A.; Abild-Pedersen, F.; Studt, F.; Rossmeisl, J.; Norskov, J. *Energy Environ. Sci.* **2010**, *3*(9), 1311–1315.

For this system of species, the electronic energies can be calculated based on an electronic structure method and the accuracy of this calculation will be dependent on the type of method used. In the study by Peterson et al., DFT as applied in Dacapo[57] was used, although a variety of software is available.[58] The electronic energies were then combined with DFT-calculated zero point energies, heat capacities, and entropies to yield the chemical potential of the adsorbed molecules. Subsequent corrections were made for the effect of H_2O on the system by using calculated values of 0.5 eV for OH_{ad}, 0.25 eV for ROH_{ad} and 0.1 eV for CO_{ad} and CHO_{ad}. The point where the overall free energy change of the reaction becomes negative, determined the potential required for the reaction to occur. These potential values were calculated as -0.03, -0.41, -0.41, and -0.74 V for H_2, HCOOH, CO, and CH_4, respectively, using the CHE. This method also found that the step required in the formation of the hydrocarbons was the conversion of CO to CHO and suggested that materials that could bind CHO strongly would provide plausible consideration for use in CO_2 reduction.

9.14.2.2.2 Double reference method

The method developed by Filhol and Neurock is also referred to as the 'double reference method' (DRM) due to the use of a reference to a vacuum potential and a reference to an aqueous potential.[49,50]

In calculating the electronic properties of an adsorbate on an electrode surface, periodic boundary conditions are enforced such that the solid is defined by a fixed number of atomic layers separated by a vacuum layer typically >10 Å, with the adsorbate on one side of the surface (Figure 10).

In the DRM, this vacuum layer is filled with water molecules that are representative of the surface density of water. The structure of this aqueous phase is dependent on the metal structure and can be initially calculated by DFT. A vacuum of approximately 20 Å is inserted in the center of the aqueous phase to obtain an asymptotic potential at the center two slabs, with

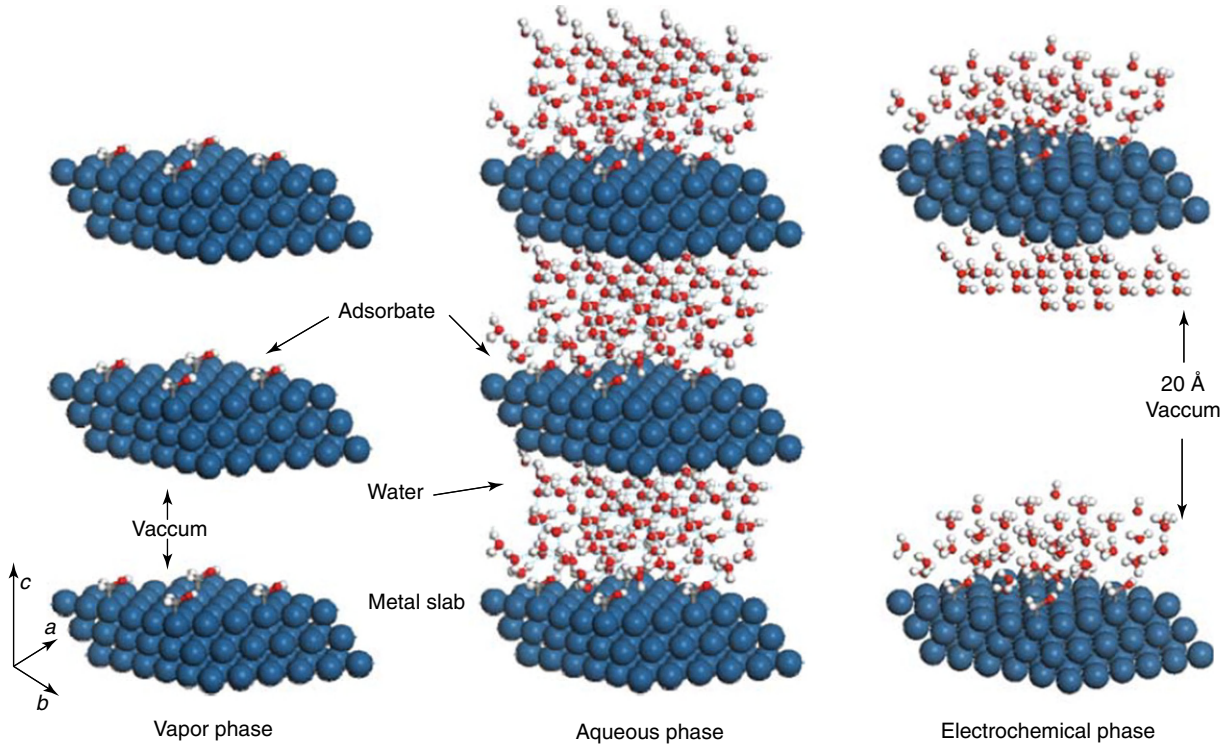


Figure 10 Illustration of an adsorbate present in the vapor, aqueous, and electrochemical phases. A vacuum has been inserted into the aqueous phase to depict the electrochemical phase and for calculation of the vacuum reference potential. The insertion of the vacuum and aqueous layers results in a slab distance of >30 Å. Reproduced from Wasileski, S.; Taylor, C.; Neurock, M. Modeling Electrocatalytic Reaction Systems from First Principles. In *Device and Materials Modeling in PEM Fuel Cells*; Paddison, S., Promislow, K., Eds.; Springer: Berlin, **2009**, Vol. 113; pp 551–574, with permission from Springer Science+Business Media.

the lower slab having the adsorbate on the surface (Figure 10). This vacuum, aqueous, adsorbate, and metal system thus become representative of the half-cell where the reaction of interest occurs.

If a potential *versus* the c-axis of Figure 10(c) is generated, the potentials obtained could be used to simulate the potentials in the vacuum (Φ_{vacuum}), aqueous (Φ_w), and metal (Φ_{metal}) layers as well as the potential at the Fermi level (Φ_{Fermi}) as shown in Figure 11.

The potential at the vacuum thus becomes the reference state when there is no charge present in the system and can be linearly shifted by a value of $\Delta\Phi_{shift}$ such that

$$\Phi_{vacuum} = 0V \tag{12}$$

Subsequently, the potential at the Fermi level can be calculated with respect to the reference by,

$$\Phi_{Fermi} = \frac{E_{Fermi}}{e} - \Delta\Phi_{shift} \tag{13}$$

where E_{Fermi} is the DFT-calculated Fermi level and e is the elementary charge.

To account for the effect of a charge density in the system, charges can be added to the system and a counter charge also. With this change, the potential at the center of the aqueous phase Φ_{water} experiences minimal change in potential and thus becomes the reference potential in the presence of a background charge. Its value in the absence of a charge, Φ_{water} $(q=0)$ can be calculated in reference to the vacuum reference from Figure 4 and subsequently the potential at all points in the charged system is shifted by a value $\Delta\Phi_{shift}$ (q), such that:

$$\Phi_{Water}(q) = \Phi_{Water}(q=0) \tag{14}$$

Consequently, the potential at the Fermi level in the charged system becomes:

$$\Phi_{Fermi}(q) = \frac{E_{Fermi}(q)}{e} - \Delta\Phi_{shift}(q) \tag{15}$$

A conversion to the standard hydrogen electrode is obtained by using the value of 4.8 V for the potential, although values between 4.4 and 4.8 V have been found in the literature.

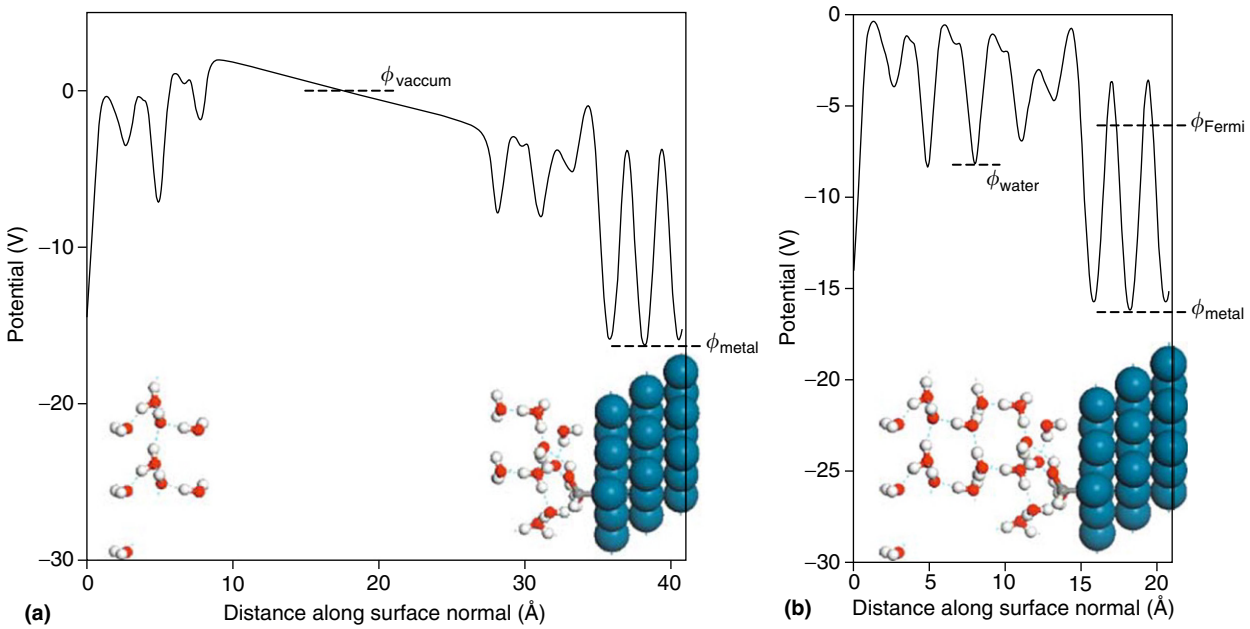


Figure 11 Potential vs. distance relationships for the (a) electrochemical and (b) aqueous phases illustrated in **Figure 10** indicating the differences in potential between the vacuum, aqueous, and metal layers in the solution. Reproduced from Wasileski, S.; Taylor, C.; Neurock, M. Modeling Electrocatalytic Reaction Systems from First Principles. In *Device and Materials Modeling in PEM Fuel Cells*; Paddison, S., Promislow, K., Eds.; Springer: Berlin, **2009**, Vol. 113; pp 551–574, with permission from Springer Science+Business Media.

The potential dependent free energy can thus be calculated by the following expression, which is fully defined by Neurock et al.[49]:

$$G = E_{DFT} + \int_0^Q \Delta\Phi_{shift}(q)dq - Q\Phi_{Fermi}(q=0) \tag{16}$$

where Q is used to account for the amount of background charge added.

This method was used to explain the effect of an electrochemical potential on methanol oxidation in a methanol fuel cell.[59] As mentioned in Section 9.14.2.1.2.1, methanol oxidation can occur through an indirect and a direct path to form CO and formaldehyde, respectively (**Figure 7**). CO formation, although indirect, is the primary path for methanol oxidation, whereas the formation of formaldehyde is the secondary path. Using the Neurock method, the two pathways were studied and reaction energies evaluated based on the following elementary reactions:

Indirect:

$$\begin{aligned} CH_3OH_{ad} &\rightarrow CH_2OH_{ad} + H^+ + e^- \\ &\rightarrow CHOH_{ad} + H^+ + e^- \\ &\rightarrow COH_{ad} + H^+ + e^- \\ &\rightarrow CO_{ad} + H^+ + e^- \end{aligned} \tag{17}$$

Direct:

$$\begin{aligned} CH_3OH_{ad} &\rightarrow CH_3O_{ad} + H^+ + e^- \\ &\rightarrow CH_2O_{ad} + H^+ + e^- \end{aligned} \tag{18}$$

As observed in these reactions, the formation of CO is based on an initial activation of the C–H bond, whereas the formation of formaldehyde is based on the initial activation of the O–H bond. The structure of the reactant, intermediate, and product molecules on the catalytic surface can be calculated (**Figure 12**), similar to the aforementioned method by Peterson et al.[53]; however, included in the calculation is the aqueous and electric charge of the system as opposed to an external correction. The calculations predicted that the secondary pathway would become facile when the potential exceeded 0.5 V versus SHE.

A closer examination of the figure is also indicative of one of the reasons why the electronic structure methods are useful. The number of catalytic atoms is lower in the secondary path than in the primary path. This suggested that this path would be

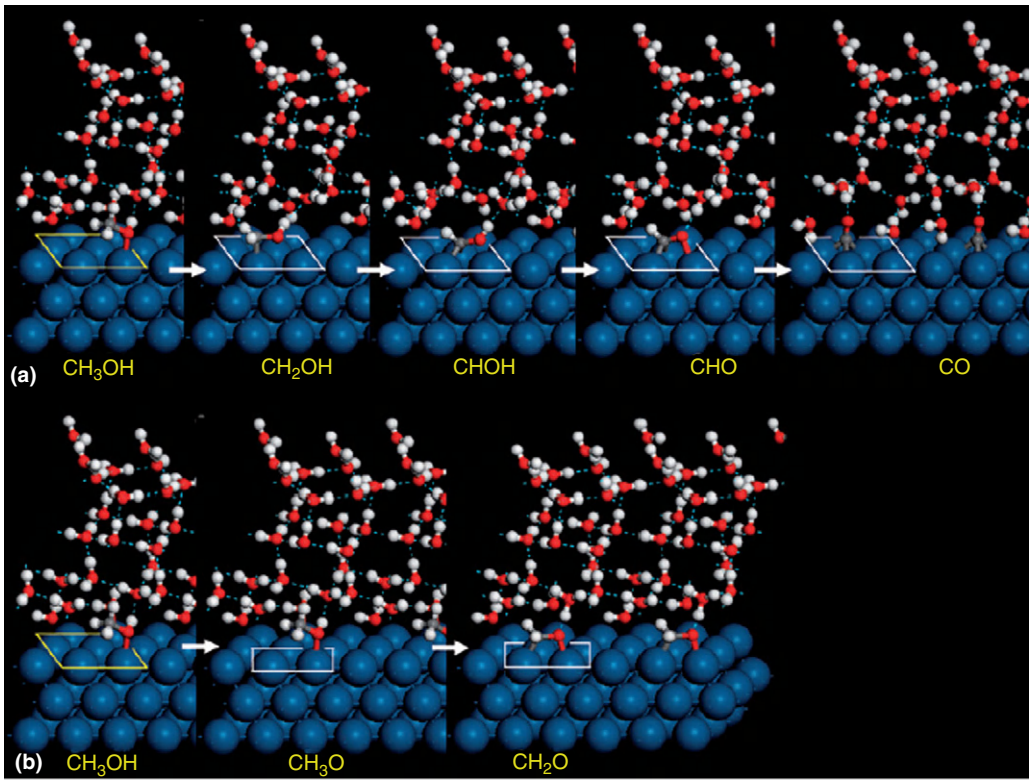


Figure 12 The oxidation of methanol through the activation of the C–H bond in the indirect path (A) and through the activation of the O–H bond in the direct path (B). Reproduced with permission from Neurock, M.; Janik, M.; Wieckowski, A. *Faraday Discuss.* **2008**, 140, 363–378.

independent of the catalyst structure and showed agreement with experimental observations. Subsequent calculations were able to predict that OH molecules (formed from the solution) were responsible for the CO oxidation at >0.6 V, with a reduction in activation energy of 0.52–0.38 eV from 0 to 1 V versus NHE.[59]

Other calculations[60] have been performed at the molecular dynamics level (as referenced in Figure 8), which evaluate the dynamics of organic electrochemistry including the redox potentials of tetrathiafulvalene, thianthrene, and benzoquinone[61,62] and the effect of acetonitrile coverage on the activity of anatase.[63,64]

Overall, the aims of these calculations and methods have been to expand on phenomena observed at the experimental level, which had been previously cumbersome to explain using experimental techniques. However, these examples also illustrate the possible steps that can be initiated in projecting the reactions that are possible on a particular surface and provide a pathway for initial estimates of plausible reactions before testing at the laboratory scale. Based on the fundamental electrochemistry considered and the simulations generated, an experimental setup at the bench scale can be performed.

9.14.3 Laboratory Research

Building on the ideas of Fundamental Electrochemistry (see Section 9.14.2), testing based on a bench scale model of the reaction is the next logical step in the development of an industrial process (Figure 1). These tests will be useful in investigating how well the predictions from the fundamental principles can be conveyed in reality. This section introduces combinatorial chemistry as the next logical step after multiscale modeling as multiple experiments will need to be performed on the hypothesis previously generated. The section also discusses the use of nanotechnology, which has helped in improving the kinetics observed in certain reactions and how this technology has aided in the feasibility of certain organic reactions. Further fundamental analyses through the introduction of *in situ* characterization in laboratory research have also been relevant in explaining phenomena occurring in real-time. The incorporation of these three separate and symbiotic techniques would prove successful in performing laboratory research.

9.14.3.1 Combinatorial Chemistry

Combinatorial Chemistry, as a literature term, was initiated in the early 1990s (although the methods date back to the 1980s) and is currently synonymous with High Throughput Chemistry.[65] As the names suggest, combinatorial and high throughput methods deal

with the ability to synthesize, characterize, and test a large array of chemical compounds simultaneously. These methods have been mostly used in the pharmaceutical field in drug design, where most medicines take 10–12 years to bring to market and a multi-pronged approach is required to facilitate production.[65] Recently, these methods have become more relevant in material science and electrochemistry, including catalysts, fuel cells, photoelectrics, optics, and parallel and serial electrosynthesis of organic compounds.[66–68] The establishment of the *ACS Combinatorial Synthesis* journal (formally the *Journal of Combinatorial Chemistry*), with its first issue in 1999, is a testament to the development and apparent importance of this field. As electrochemical science and technology involves both synthesis and characterization, the combinatorial approach as discussed here will examine both of these areas as well. The execution of combinatorial chemistry is dependent on the speed at which results (synthesis, characterization, or performance) can be obtained, thus automation is critical. With most electrochemical tests involving a measurement of current or voltage by a machine, these methods would prove especially useful when applied to electrochemical studies.

The first combinatorial electrochemistry study in the literature was performed by Reddington et al. in investigating methanol oxidation catalysts.[69] Although the testing was performed electrochemically, catalytic characterization was performed by optical measurements with a dye that detected the pH of the reaction. The study found that an electrode made up of $Pt_{44}Ru_{41}Os_{10}Ir_5$, in atomic compositions, performed better than a commercially available $Pt_{50}Ru_{50}$ electrode.[69] The study also provided a measure of the complexity involved in the application of combinatorial methods as an alloy made up of different compositions of Pt, Ru, Os, Ir, or Rh would yield 645 different compositions if primary, binary, ternary, and quaternary combinations of the five elements were used. Although the response measured was not quantitatively precise and posed a possible contamination due to the dye used, it served as a foray into combinatorial methods based on electrochemical testing. This study also indicated the importance of combinatorial electrochemistry in electrode development as neighboring compositions, such as Pt–Os and Pt–Rh, showed no activity for methanol oxidation and the most active catalyst may not have been found without the trial of varying compositions. Other electrochemical characterization studies also made use of an array of cells,[70–72] but potentiostatic experiments were conducted, which allowed for more quantitative analysis of the electrode performance; however, characterization was performed serially. Baeck et al. investigated possible electrodes for hydrogen generation for water electrolysis.[70] In the studies by Kulikov and Mirsky,[71,72] electrochemical synthesis and characterization of polymers was made using a 96-electrode electrochemical microarray with a single reference and auxiliary electrode, thus parallel synthesis was performed with serial characterization. As summarized by Muster et al., combinatorial electrochemical characterization can be performed in five configurations and these have been especially useful in investigating electrode performance for reactions (**Figure 13**). Essentially, studies by Reddington et al. and Baeck et al. were performed using the configurations in **Figures 13(c)** and **(e)**, respectively.

In combinatorial electrochemical synthesis, initial work by Yudin and Siu,[73–75] demonstrated parallel electrosynthesis of α-alkoxy compounds, hetero-bicyclic compounds, and 1,2-diamines (**Figure 14**).

Using a patented spatially addressable electrolysis platform of 16 cells,[76] current was applied in parallel, and identical conditions were created within each cell. The current density, temperature, and solvent conditions were optimized to generate and

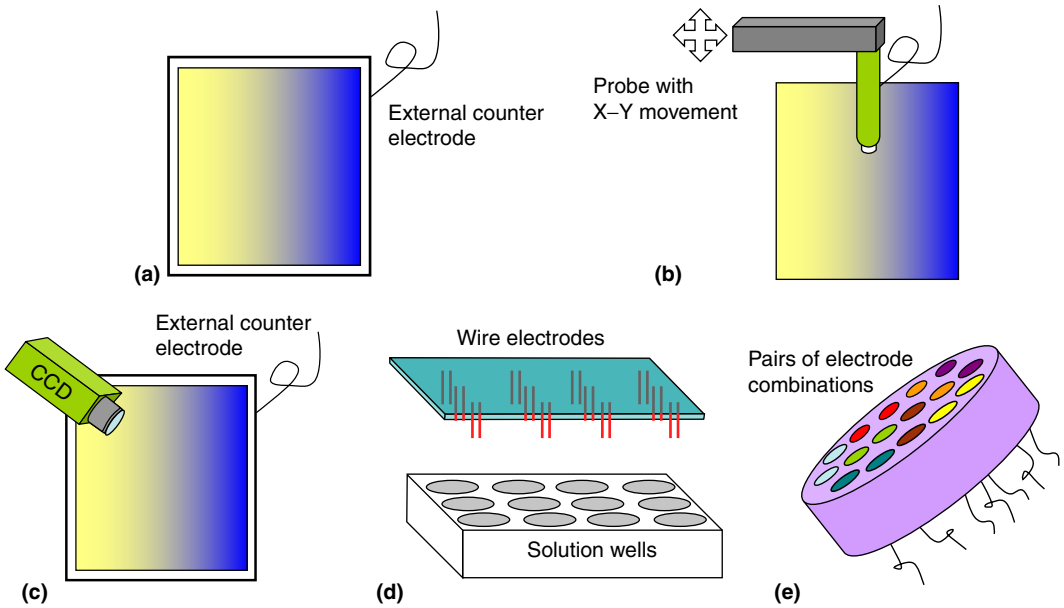


Figure 13 Common configurations for high-throughput electrochemical characterization. (a) compositional spread deposited over an electrode array and tested in a common solution, (b) sequential measurement of isolated regions across a compositional spread using a scanning capillary or probe, (c) a compositional spread placed under electrochemical control and monitored using optical responses, (d) parallel interrogation of electrodes of identical composition placed into varying electrolyte solution, and (e) parallel interrogation of electrodes of varying composition placed into a common electrolyte. Reproduced with permission from Muster, T. H.; Trinchi, A.; Markley, T. A.; *et al. Electrochim. Acta* **2011**, *56*(27), 9679–9699.

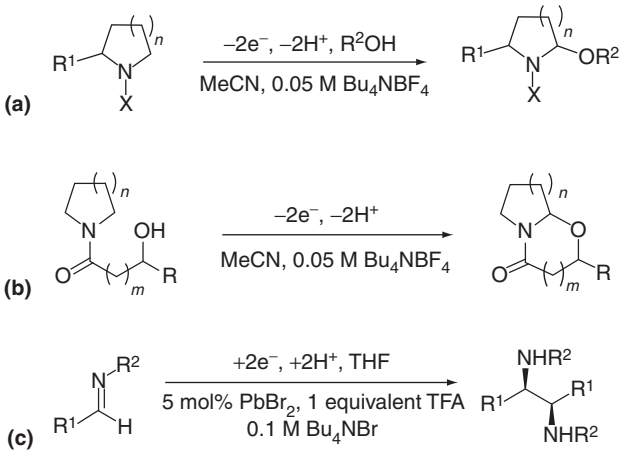


Figure 14 Series of parallel electrosynthesis of (a) α-alkoxy compounds, (b) hetero-bicyclic compounds, and (c) 1,2-diamines performed with the patented spatially addressable electrolysis platform.[76] Reproduced with permission from Yudin, A. K.; Siu, T. *Curr. Opin. Chem. Biol.* **2001**, *5*(3), 269–272.

increased yield of the products. Although this was a quantitative improvement over the initial work by Reddington et al., the method did not allow for parallel monitoring of the electrodes and thus the cells could not be optimized individually. A recent review by Yoshida et al. suggested that a temperature of $-78\ ^{\circ}C$ would help to further stabilize the carbocations and radicals generated as intermediates using the 'cation pool' method.[66] Although such low temperatures would further increase the energy consumption of the process, this energy sink could be offset by the advantages and importance of the product gained.

9.14.3.1.1 Combinatorial electrochemistry for methanol oxidation

As previously mentioned in Section 9.14.3.1, the first combinatorial electrochemical study was performed to analyze possible catalysts for methanol oxidation.[69] Subsequent studies have performed electrochemical analysis of the effects of catalytic preparation,[77,78] morphology,[79] and fuel composition[80] to name a few.

Research by Liu and Smotkin indicated that the optimum electrode previously predicted, $Pt_{44}Ru_{41}Os_{10}Ir_5$ (atomic compositions), did not perform better than a commercial $Pt_{50}Ru_{50}$ electrode when a different synthetic route was implemented.[78] This study also summarized the importance of high throughput analysis, especially for adopting electrochemistry on a large scale: the critical criteria of reproducibility and catalytic conditioning and preparation. The use of a 25-array cell[81] with 25 current followers (**Figure 10(e)**) provided a quantitative basis for comparison and confidence intervals and found that different commercial versions of PtRu catalysts showed differences between 10 and 60% in currents generated from methanol oxidation.[78]

Further work by Chan et al. combined both optical and electrochemical comparisons using the aforementioned 25-array cell and concluded that although the optical method served to eliminate candidates for methanol oxidation, it could not differentiate between activities.[77] It should be therefore noted that a combination of high throughput analyses would provide a platform for accelerating progress at the laboratory scale. The study by Guerin et al. used a 64-array of microscale cathodes to examine the effect of Pt loading and particle size on the electrode performance. The variability in performance (current density generated) within the same Pt loading was indicative of the variance in surface area with Pt loading, with standard deviations between 10 and 31% of the current densities. In addition, from an economic standpoint, a Pt loading of 30–40% would provide maximum performance per mass. These studies by Liu and Smotkin and by Guerin et al. are indicative of the complexity that would be involved in fabricating an electrode of maximum performance after molecular modeling has provided a foundation of possible components.

Another work by Jiang et al. used a serial connection of 40 individual fuel cells to investigate variability in performance with similarly fabricated cells, that is, catalytic loading, membrane type and area, and current collected.[80] It was found that at higher currents, the variability of the cell potential was larger, whereas an increase in fuel concentration increased the Tafel slope. The setup used in this cell could be similarly applied to evaluate the performance of the optimized composition previously tested by Reddington et al. as an initial foray into evaluating variability in the performance of quaternary alloys.

9.14.3.1.2 Combinatorial electrochemistry for carbon dioxide reduction

At this time, there hasn't been any literature found on combinatorial electrochemistry for testing the conversion of CO_2 to fuels, however this area appears to be a prime candidate for this analyses. It has been previously predicted that the most active catalyst for this conversion is copper[23,24] and there is also a surface structure[53] effect on performance. With other metals such as Ag, Au, and Zn active for CO_2 to CO reduction and Sn, Cd, and Ti active for CO_2 to formic acid reduction,[82] the use of combinatorial examination of catalytic morphology and composition effects could be performed. These examinations can be based on modified templates and arrays that have been used and developed for methanol synthesis from the aforementioned examples.

Overall, these studies represent a small sample size of the complexity in performing combinatorial electrosynthesis and electrochemical characterization, but suggest a plausible method for performing a large number of experiments where a combination of speed, repeatability, and precision is required. For preliminary analyses, based on results from multiscale modeling, qualitative analysis could be performed, where optical characterization could be implemented. Subsequent quantitative testing with a smaller dataset with higher-level characterization tools, including X-ray diffraction, infrared spectroscopy, mass spectroscopy, and potentiostatic tests can then be used. These structural techniques have become better improved for high throughput characterization and would provide a higher-level of precision with the tests obtained at the preliminary level.[67,83]

9.14.3.2 Nanotechnology

In the past decade, nanotechnology has gained prominence and admiration from the scientific community as well as the consumers of the devices containing this technology. The study of manipulating and engineering materials at atomic and molecular level is defined as nanotechnology. The atoms and molecules size ranges from 1 to 100 nm, where one nanometer is one billionth (10^{-9}) of a meter. According to experts, two important scientific events led to the emergence of nanotechnology as a separate field and discipline. In 1981, Gerd Binning and Heinrich Rohrer developed the scanning tunneling microscope (STM), an instrument to image surfaces at atomic scale, at IBM Zurich Research Laboratory, Switzerland.[84] Their invention and development of the STM instrument was recognized with the Nobel Prize in Physics in 1986.[85] In 1985, Sir Harold W. Kroto of the University of Sussex, UK, Richard E. Smalley and Robert F. Curl, Jr., from Rice University, USA, discovered fullerenes, a group of closed carbon structures, which includes the famous Buckminster fullerene or C_{60} or buckyball, and for this achievement they were awarded 1996 Nobel Prize in Chemistry.[86,87]

Today, the synthesis and use of carbon nanostructured materials play an important role in nanotechnology based systems. Nanostructures based on carbon such as carbon nanofiber, carbon nanotubes, and graphene are generally known for their improved morphological, optical, electrical, mechanical, and chemical properties, when compared with the macro- or micro-sized carbon-based materials, which is instrumental to include carbon nanostructures on various applications. The nanotechnology discipline is not limited to carbon-based nanostructures but it also includes nanomaterials made from other elements and compounds for applications in electronics and semiconductor industry, biomedical field, and energy sector.

Various types of structures were developed and investigated as nanomaterials such as nanoparticles used for catalytic reactions,[88–90] nanowires found in optoelectronics and sensors,[91] quantum dots (QDs) employed in solar cells and light-emitting diodes,[92,93] nanotubes especially carbon nanotube-based materials are used for biomolecule sensor, energy devices, and environmental applications,[94–97] as well as other forms in different applications.[98–103]

One of the interesting classes of organic compounds is photochromic compounds, which have the ability to change their chemical structure and/or property based on the frequency of the light. In 2003, Dulić et al. demonstrated a molecular switch based on photochromic class of molecules, namely, the dithienylcyclopentenes.[104] They studied the electronic property of a 1,2-bis[5′-(5″-acetylsulfanylthien-2″-yl)-2′-methylthien-3′-yl] cyclopentene attached to gold terminals by illuminating at different wavelengths. Figure 15 shows the molecular switch, where the photochromic molecule is in closed state (Figure 15(a)) and on exposure to wavelength of light in the range of 500–700 nm, it transforms to open state (Figure 15(b)). The electronic transport

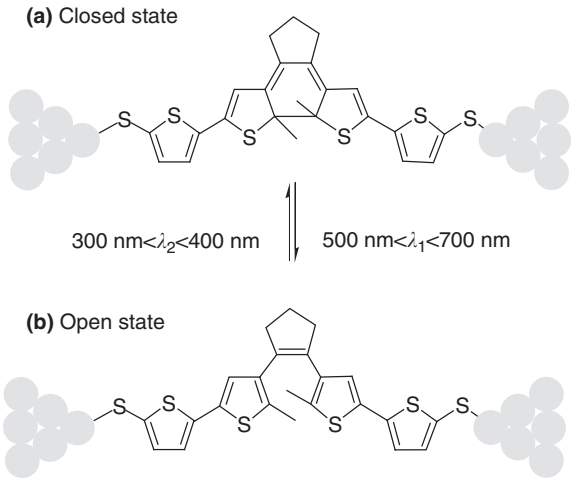


Figure 15 Photochromic molecular switch between two gold (Au) contacts in closed state (a) and open state (b). By exposing the molecule to light of wavelength in the range 500 nm $< \lambda_1 <$ 700 nm, the molecule will switch from (a) to (b). In solution the protected molecule can be switched back to the (a) state by exposing it to UV light with wavelength in the range 300 nm $< \lambda_2 <$ 400 nm. However, this is not possible if the molecules are connected to gold. Reprinted from Dulic, D.; van der Molen, S. J.; Kudernac, T.; *et al. Phys. Rev. Lett.* **2003**, *91*, 207402, with permission from American Physical Society.

through the closed state conformation of that molecule is referred as 'On' state, and the 'Off' state is when the photochromic molecule has the open state conformation.

The open state conformation of this molecule was not reversed to the closed state by using light of wavelength in the range of 300–400 nm. This behavior was attributed to the presence and interference of the electronic properties of the two gold contacts. If this molecule was in solution with no attachment to gold, then transition between closed and open state conformations is possible with appropriate wavelength of light. Other photoswitching molecules are being investigated as single-molecule junctions for optoelectronics application, where two-way switching is the expected outcome of the optoelectronic systems.[105–107]

A combination of different kinds of nanomaterials might be required to achieve the desired goal or advancement in a product. For example, cadmium sulfide (CdS) QDs are nanomaterials of an inorganic compound, which are used in solar cells to efficiently generate multiple electron–hole pairs, for size-tunable photon adsorption, and they can also help in exceeding the Shockley–Queisser limit on single-junction energy extraction from the solar spectrum.[92] The low photovoltaic efficiency of QD solar cells are due to the poor electron–hole separation and the associated inefficient transfer of photogenerated electrons to the electrodes, which are being eliminated with the use of single-walled carbon nanotubes (SWNTs) and graphene-based solar cells. In 2010, Guo et al. built QD solar cells consisting of multilayered graphene along with CdS QD layers (**Figure 16(a)**).[108]

This hybrid solar cell device (graphene–QD solar cells) was able to demonstrate incident photon-to-charge-carrier conversion efficiency (IPCE) as high as 16% and a photocurrent response of 10.8 A m^{-2} under 1000 W m^{-2} illumination (**Figure 16(b)**). The use of multiple layers of graphene in the QD solar cells provided high-specific surface area, tunable bandgap, helped in separating the electron–hole pair, and also improved the mobility of the electrons when compared with the SWNTs stacked in the SWNT–QD solar cells (**Figure 16(b)** and **(c)**).

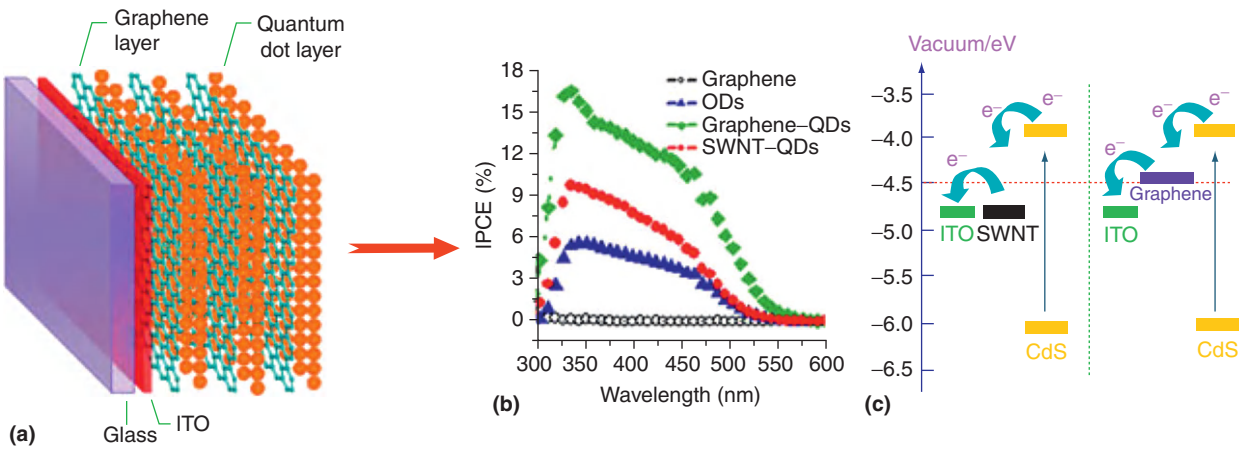


Figure 16 (a) Schematic representation of a layered graphene–CdS quantum dot (QD) solar cell. (b) Incident photon-to-charge-carrier conversion efficiency (IPCE) curves of devices with different photoelectrodes. (c) Energy level diagrams of devices based on (right) graphene–QD solar cells and (left) single-walled carbon nanotube (SWNT)–QD solar cells. The red dotted line highlights the easier transfer of electrons to indium tin oxide (ITO) from graphene compared with that from nanotubes. Reproduced with permission from Guo, C. X.; Yang, H. B.; Sheng, Z. M.; *et al. Angew. Chem. Int. Ed.* **2010**, *49*, 3014–3017 and Sperry, J. B.; Wright, D. L. *Chem. Soc. Rev.* **2006**, *35*(7), 605–621.

Nanomaterials have higher surface area especially catalysts with surface area larger than the corresponding macro- and micro-sized material is reflected on the product yield and cost. The use of nanocatalysts will not only increase the yield of the product but also reduce the catalyst cost by utilizing minimal amount. As an example, the Center for Electrochemical Engineering Research (CEER) at Ohio University has been investigating the electrochemical oxidation of urea in alkaline media with nickel electrodes.[109–114] Recent studies have shown that using one-dimensional nickel hydroxide ($Ni(OH)_2$) nanoribbons having dimensions of 15–20 nm thickness and several micrometers in length displayed 10 times higher current density for the electro-oxidation of urea than bulk $Ni(OH)_2$ powder electrodes.[115] However, on using the two-dimensional $Ni(OH)_2$ nanosheets as electrocatalyst for the oxidation of urea, the current density increased vastly by 170 times than the bulk nickel hydroxide powder.[116]

Another significance of the nanotechnology field is the development of small-sized devices for biological and analytical testing. In 2005, Popovtzer et al. built and tested a nano-biochip by integrating a microelectronic device with genetically modified *Escherichia coli* to electrochemically detect for toxicity in water.[117] This nano-biochip can be classified as a lab-on-a-chip device, where genetically modified *E. coli*, a living organism, on silicon substrate generated an electrical signal when it encountered toxicants present in the nanoliter volume of water.

The examples of various nanostructures for catalysts and the support material are illustrated in this section to give a broad overview and importance of the principles associated with the field of nanotechnology to attain highly efficient catalyst and higher yield for the desired product at a reasonable cost.

9.14.3.2.1 Nanotechnology in methanol oxidation

The electrochemical oxidation of methanol has been explained and discussed in Section 9.14.2.1.2.1. Pt is the electrocatalyst used for the oxidation of methanol in acidic media. The reaction yields soluble intermediates such as formic acid and formaldehyde as well as CO and CO_2. During the methanol oxidation process, the molecules of CO are adsorbed on the Pt surface, which prevents or hinders further oxidation of methanol over Pt catalyst. Complete oxidation of methanol results in the formation of CO_2, which diffuses off the Pt catalyst surface. The principles of nanotechnology are extensively used to develop efficient and advanced electrocatalyst with the help of Pt for the oxidation of methanol. Higher current density during methanol oxidation can be achieved by reducing the size of the Pt catalyst particles to the nanoscale. Nanoparticles or nanostructures of the catalyst increases the methanol oxidation current and it also helps in reducing the amount of noble metal catalysts required for this reaction.

Commercially, Pt nanoparticles are dispersed over carbon support, generally referred as Pt/C, which is used for methanol oxidation. The optimum particle size for Pt nanoparticles is $\sim$3 nm for these Pt/C catalysts.[118] The use of bimetallic catalyst has improved the oxidation reaction for methanol to result in the formation of CO_2 rather than soluble intermediates and eliminate the poisoning effect of CO over Pt catalyst. Ru is considered a good catalyst to be used in combination with Pt for the electrochemical oxidation of methanol. Different methods for the synthesis of the PtRu nanoparticles has been the focus of several research articles to develop an efficient catalyst over various carbon-based support materials (vulcanized carbon, mesoporous carbon thin film, carbon nanotubes), so that these nanoparticles can demonstrate higher catalytic activity toward the oxidation of methanol.[119–122]

Zhou et al. studied the synthesis of Pt nanoparticles over RuO_2–MnO_2 covered carbon nanotubes (CNTs) for the electro-oxidation of methanol.[123] The average particle size for Pt over RuO_2–MnO_2/CNTs support material was 2.0 nm. Using the high resolution transmission electron microscope (HRTEM), the authors were able to identify the crystalline nature of the nanoparticles. The distance between two lattice planes for most Pt nanoparticles was found to be $\sim$0.22$\dot{8}$ nm, which corresponds to Pt(111) crystal plane. The authors also observed an increase in methanol oxidation current with increase in the electrochemical active surface (EAS) area of the different catalysts synthesized. The EAS area for Pt/CNTs catalyst was only 78 $m^2\,g^{-1}$ Pt when compared with 104 and 137 $m^2\,g^{-1}$ Pt for Pt/RuO_2/CNTs and Pt/RuO_2–MnO_2/CNTs catalysts, respectively. The methanol oxidation current using the Pt/RuO_2–MnO_2/CNTs catalyst (865 A g^{-1} Pt) was more than four times the Pt/CNTs catalyst (187 A g^{-1} Pt), and at least one and half times higher than the Pt/RuO_2/CNTs catalyst (521 A g^{-1} Pt). According to Zhou et al., the presence of RuO_2 in the catalyst helps in the oxidation of adsorbed CO to CO_2, and the protons formed during this reaction is readily accepted by MnO_2 and effectively transported by the CNTs support material.

Cobalt (Co) can also be combined with Pt to form the bimetallic catalyst for the methanol oxidation. Qiu and Zou developed nanoporous PtCo (np-PtCo) catalyst using the selective dealloying method on a ternary PtCoAl alloy.[124] The scanning electron microscope (SEM), TEM, and HRTEM images of the PtCo catalyst are shown in Figure 17.

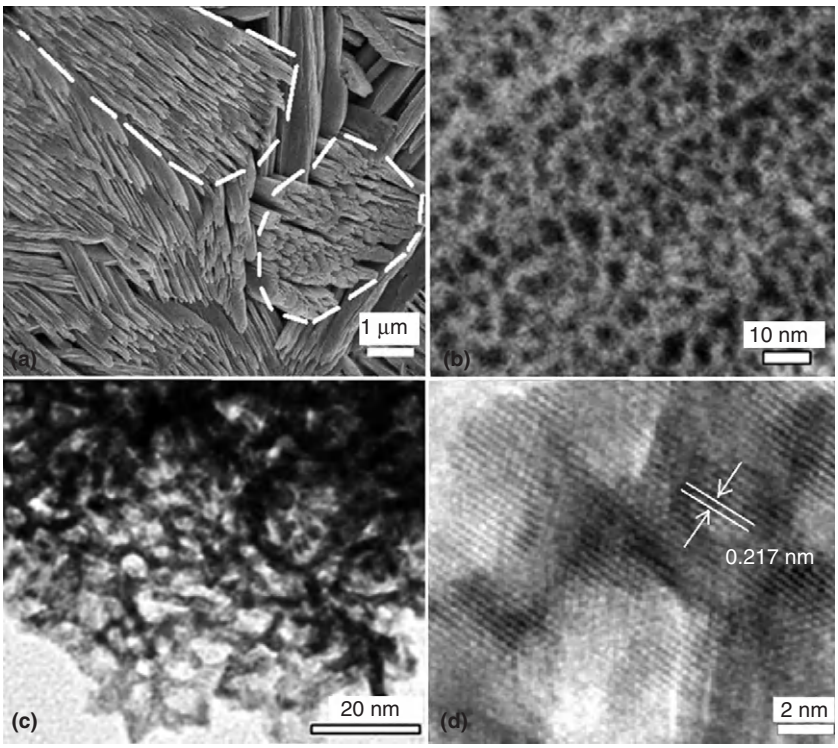


Figure 17 SEM (a and b), TEM (c), and HRTEM (d) images of np-PtCo. Reproduced from Qiu, H.; Zou, F. *ACS Appl. Mater. Interfaces* **2012**, *4*, 1404–1410.

Dealloying the ternary alloy PtCoAl resulted in several hundreds of PtCo nanorods; the dimension of these nanorods was hundreds of nanometer in diameter and several micrometers in length (Figure 17(a)). On closer look at the PtCo nanorods (Figure 17(c)), the authors were able to notice porous structure with an average pore size of ~3 nm, and therefore these nanostructures are referred as np-PtCo. The HRTEM image (Figure 17(d)) shows the distance between two lattice planes as 2.17 Å along the (111) crystal planes. Pt content in the np-PtCo nanostructure was measured to be ~65%. The porous nature of the np-PtCo catalyst improved the methanol oxidation peak current density by five times of the commercial Pt/C catalyst (Pt, 20 wt. %). The authors tested the stability of the np-PtCo nanostructure by performing cyclic voltammetry (CV) experiments between 0.6 and 0.9 V versus RHE in 0.5 M H_2SO_4 solution. After 5000 cycles of CV test, the np-PtCo catalyst retained more than 90% of its initial EAS area, whereas the EAS area of the commercial Pt/C catalyst dropped to ~74% of its initial value.

The stability of the catalyst support material in the acidic media for methanol electrooxidation is as important as the catalyst's stability. Gu et al. have investigated the use of cerium oxide or ceria (CeO_2) along with Vulcan XC-72 carbon black as support material for Pt nanoparticles.[125] The catalyst support material was made by mixing CeO_2 nanoparticles (average size, 5.3 nm) with carbon black. The optimum weight of CeO_2 in the Pt/CeO_2–C catalyst was found to be 20 wt.%, which helped creating a narrow Pt particle size distribution of 2.1 nm. This Pt/CeO_2–C catalyst displayed better catalytic activity with good structural stability for methanol oxidation.

Different nanostructures have been studied for the catalyst and support material for the methanol oxidation. One of those structures has been the core/shell configuration, where a mechanically stable material with good electrical conductivity is used as core material and the catalyst for the reaction covers the core material to form the shell. Guo and co-workers developed a novel material consisting of a gold (Au) core, which had a hollow cavity and Pt spikes covered the Au hollow spheres like a sponge.[126] The current for the methanol oxidation using the sponge-like Au/Pt core/shell nanomaterial was at least twice the commercial Pt/C catalyst. The core/shell structure has been combined with graphene to form a hybrid composite nanomaterial, which was investigated as catalyst for methanol oxidation.[127] The core of this hybrid nanomaterial is made of Au nanorod, which is covered with nanoislands of PtAg alloy along with graphene sheet to form the composite material. This hybrid material was highly stable in acidic media and demonstrated good catalytic activity toward methanol oxidation.

9.14.3.2.2 Nanotechnology in carbon dioxide reduction

The electrochemical reduction of CO_2 has implications on improving the environment by eliminating gaseous pollutant as well as producing liquid fuels, which will have positive impact on the energy industry. These reasons and features associated with the process of electrochemically converting CO_2 to liquid fuels have drawn tremendous interest from researchers around the world. The electrochemical approach of reducing CO_2 has resulted in the formation of various compounds, namely, CO, methane (CH_4), ethylene (C_2H_4), ethanol (C_2H_5OH), propanol (C_3H_7OH), formate ion ($HCOO^-$), and also hydrogen (H_2). Reducing CO_2 to its products has been electrochemically investigated in aqueous and nonaqueous solutions. In this chapter, we have limited the focus to only aqueous electrochemical reduction of CO_2 to liquid fuels.

Various metal electrodes have been explored for the electrochemical reduction of CO_2. The list of metal electrodes used for converting CO_2 to different organic compounds is given in Table 3. Among those metal electrodes, copper (Cu) is effective in producing CH_4, a high-value liquid fuel, at higher faradaic efficiency than synthesizing CO and formate. Recently, Tang et al. demonstrated the importance of the particle size of copper for the electroreduction of CO_2 and its selectivity toward hydrocarbons.[128] The authors prepared three samples of copper electrode, where Sample A was a Cu electrode electropolished in 1 M phosphoric acid solution at 2 V, Sample B was made of Cu nanoparticles (50–100 nm) covering the electropolished Cu electrode, and Sample C was a electropolished Cu electrode sputter cleaned with argon ions. Using SEM images, the authors were able to determine the surface area of Sample B, which has Cu nanoparticles, to be 2–3 times larger than the geometric surface area. The authors subjected the three Cu electrode samples to potentiostatic experiments in CO_2 saturated 0.1 M $KClO_4$ solution at −1.1 V versus RHE for 15 min. The faradaic efficiencies for the products obtained from the potentiostatic experiments are shown in Figure 18.

The products from the electroreduction of CO_2 are CH_4, C_2H_4, C_2H_6, and CO, which were produced with higher faradaic efficiencies by Sample B and C electrodes (rough electrodes). However, Sample A or smooth surfaced electrode had lower faradaic efficiency for these products. Selectivity for CO_2 reduced products were also higher for rough surface electrodes (Samples B and C) when compared with the smooth electrode (Sample A). As shown in Figure 18, Sample A displayed higher faradaic efficiency than other electrodes for generation of hydrogen gas.

Li and Kanan have recently developed a method to prepare Cu electrodes by electrochemically reducing micrometer thick Cu_2O films, which was used for the electroreduction of CO_2.[129] The authors report that the prepared Cu particles were able to reduce CO_2 to CO and formic acid (HCOOH) with high faradaic efficiency at low overpotentials (< -0.6 V vs. RHE). The Cu electrode also produced C2 hydrocarbons (C_2H_4 and C_2H_6) at high overpotentials (> -0.6 V vs. RHE). Li and Kanan were successful in developing the Cu electrode from Cu_2O films, which was resistant to deactivation due to electroreduction of CO_2 for several hours when compared with rapid deactivation of polycrystalline Cu under similar conditions. More information on the electrochemical reduction of CO_2 can be gathered from these literatures.[130,131]

In addition to the metals listed in Table 3 being used as catalysts for the electrochemical reduction of CO_2, metal organic frameworks have also been extensively studied and applied for CO_2 electroreduction. Metal organic frameworks are known to have high surface area (500–6240 $m^2\,g^{-1}$), wide range of pore size (3–3.5 Å), pore volume (0.4–3.6 $cm^3\,g^{-1}$), and many

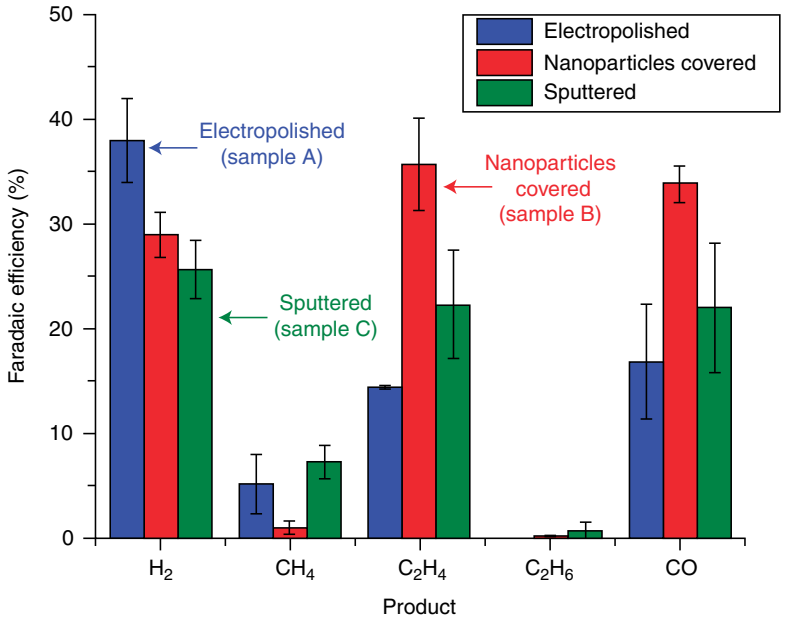


Figure 18 Faradaic efficiency for the products of electroreduction of CO_2 on three surfaces in CO_2-saturated 0.1 M $KClO_4$ upon –1.1 V vs. RHE, including Sample A (electropolished surface), Sample B (copper nanoparticle-covered surface), and Sample C (sputtered surface). Reproduced with permission from Tang, W.; Peterson, A. A.; Varela, A. S.; *et al. Phys. Chem. Chem. Phys.* **2012**, *14*(1), 76–81.

functionalities.[132] The recent reviews by Benson et al. and Inglis et al. give a detailed look at different types of metal ligand catalysts that are investigated to electrochemically convert CO_2 to liquid fuels.[133,134]

9.14.3.3 *In situ* Characterization

Investigation on the effect of electrochemical reactions over the physical structure and chemical composition of the electrode and catalyst using appropriate techniques is considered characterization of the electrode. Analysis for chemical composition of the solution and gaseous products, if any, also constitutes characterization of an electrochemical experiment. There are different types of characterization techniques and they can be classified as structural, chemical, electrical, optical, and electrochemical methods. Generally the components of the electrochemical cell, such as electrode, electrolyte, and membrane, are analyzed before and after the experiment to assess the effect of the electrochemical experiments; this procedure is known as *ex situ* analysis or characterization.

The idea or concept of monitoring the physical or chemical or any other parametrical change while the electrochemical experiment is taking place is known as an *in situ* characterization method. Among the available techniques for structural characterization of electrode material, scanning tunneling microscopy (STM), atomic force microscopy (AFM), and X-ray crystallography or commonly known as X-ray diffraction (XRD) have been combined with electrochemical systems to conduct *in situ* characterization of the electrode material.[135–140]

The chemical changes on the surface of the electrode have been studied using vibration spectroscopic techniques, such as Raman spectroscopy, Fourier transform-infrared spectroscopy (FT-IR), X-ray absorption spectroscopy, and UV–visible spectroscopy.[140–145] *In situ* characterization involving vibration spectroscopic techniques has been extensively used in the recent times to understand the electrode–electrolyte interactions. These techniques have helped in identifying the intermediate products during the electrochemical reactions, which has led to postulation of reaction mechanism for the electrochemical process. Since all the electrochemical reactions occur on the electrode surface, *in situ* characterization pertaining to the vibration spectroscopic techniques provides significant information.

9.14.3.3.1 In situ *characterization of methanol oxidation*

There are only a few research articles available in the open literature regarding *in situ* characterization for the electrochemical oxidation of methanol. Differential electrochemical mass spectrometry (DEMS) is considered an *in situ* characterization technique for methanol oxidation studies because DEMS has the capability to detect volatile products during electrochemical experiments.[29,140]

Herranz and co-workers have studied the effect of crystal structure of Pt_xSn catalyst on the electrooxidation of CO and methanol.[146] The authors evaluated the oxidation of CO and methanol with *in situ* techniques, namely, DEMS and electrochemically coupled–infrared reflection absorption spectroscopy (EC–IRAS). Herranz et al. synthesized nanoparticles of Pt_3Sn

(fcc phase) and PtSn (hcp phase) on carbon support. The catalytic activity for Pt_3Sn fcc phase was found to be better than the PtSn hcp phase for both CO and methanol electrooxidation.

Recently, Yang et al. studied the palladium (Pd) surface using *in situ* infrared spectroscopy to understand the self-dissociation of methanol molecule and its subsequent oxidation over the Pd surface in alkaline media.[147] The authors used two reflection modes, external reflection with thin layer of electrolyte structure and internal reflection with open electrolyte structure; and these reflection modes were denoted by IRAS and attenuated total reflection–surface enhanced infrared reflection absorption spectroscopy (ATR–SEIRAS). Figure 19(a) shows a 'dip' in the open circuit potential (OCP) of the Pd electrode when CH_3OH was added to 0.1 M NaOH solution. As an OCP value of –0.6 V versus Ag/AgCl was reached by the Pd electrode due to the addition of CH_3OH, the authors were assured, also based on cyclic voltammetry, that the CH_3OH molecule was dissociated into CO_{ad} and Pd–H. In the acid medium (0.1 M $HClO_4$), however, the OCP value of the Pd electrode increased to 0.57 V versus SCE with the addition of CH_3OH suggesting no dissociation of methanol in the acidic media over the Pd surface.

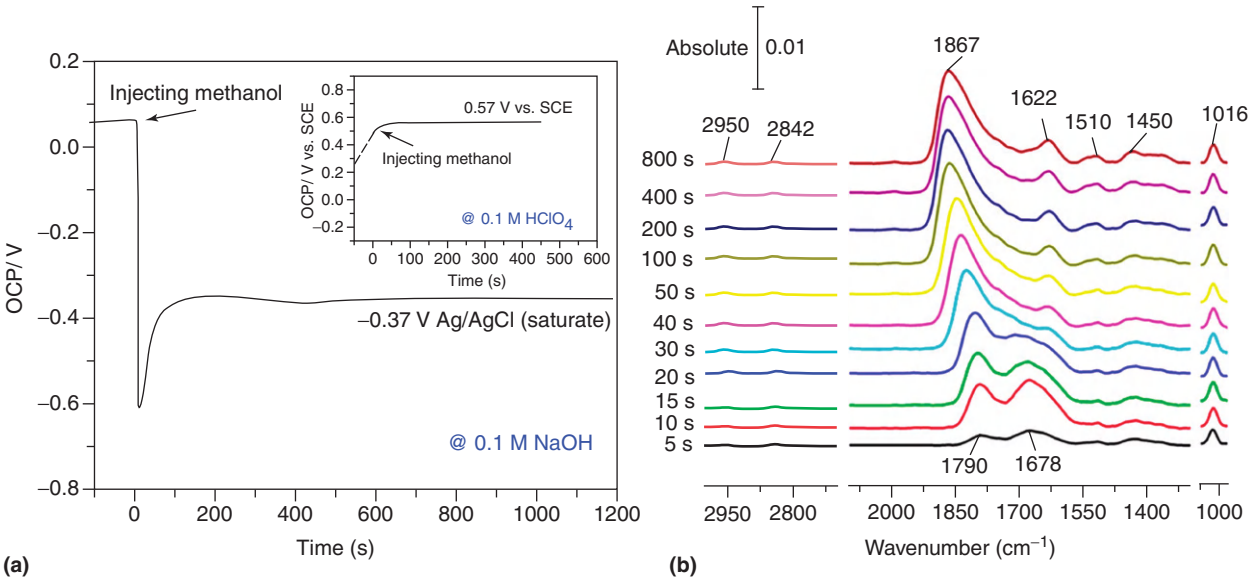


Figure 19 (a) Variation of open circuit potential (OCP) vs. time caused by injecting CH_3OH into 0.1 M NaOH solution, where the inset displayed a similar measurement taken in 0.1 M $HClO_4$. (b) Real-time ATR-SEIRAS spectra for a Pd film electrode in 0.1 M NaOH containing *c.* 0.5 M CH_3OH, employing the single-beam spectrum taken in 0.1 M NaOH as the reference spectrum. Reproduced from Yang, Y.-Y.; Ren, J.; Zhang, H.-X.; *et al. Langmuir* **2013**, *29*, 1709–1716.

In Figure 19(b), the real-time ATR–SEIRAS spectra of the Pd electrode after CH_3OH was injected to the alkaline solution (0.1 M NaOH) as illustrated. The spectra display the vibrations of different species, such as CH_3OH, adsorbed H_2O, and CO. The authors assigned the frequency range of 1678–1860 cm^{-1} to the adsorption of CO on the Pd electrode, which was denoted as ν(C–O) for the stretching vibration of CO_{ad}. The intensity of the CO band increased with time and the frequency of the band also had blue shifted in the time (approximately 200 s) the OCP value reached steady state (–0.37 V). This behavior along with the results from the *in situ* ATR–SEIRAS experiment led the authors to conclude that CH_3OH undergoes stepwise dehydrogenation on the Pd surface in alkaline media.

The soluble species formed during the electrooxidation of CH_3OH on the Pd surface was identified by the *in situ* IRAS spectra at different potentials as shown in Figure 20. In the *in situ* IRAS experiments, the authors obtained the spectra of the Pd electrode at a reference potential denoted by E_R and the sample potential was referred as E_S. The authors assigned the band at 1580 cm^{-1} from -0.35 V downward as the ν_{as}(OCO) band of dissolved formate, and the broad band at 1300–1500 cm^{-1} seen from –0.35 V was assigned to the dissolved CO_3^{2-}/ HCO_3^- and formate in the thin-layer electrolyte structure. The dissolved CO_2 band (ν_{as}(OCO)) was also observed at 2343 cm^{-1} from -0.15 to 0.05 V. Based on the *in situ* IRAS measurement, the authors confirmed the formation of formate and (bi)carbonate (and/or CO_2 depending on the local pH) species from the electrooxidation of CH_3OH.

9.14.3.3.2 In situ *characterization of carbon dioxide reduction*

The electrochemical reduction of CO_2 to produce liquid fuels and CO is an exciting and growing field. Unfortunately there is limited research work exploiting the benefits of the *in situ* characterization techniques to answer fundamental questions regarding the reaction pathways and product selectivity on different electrodes.

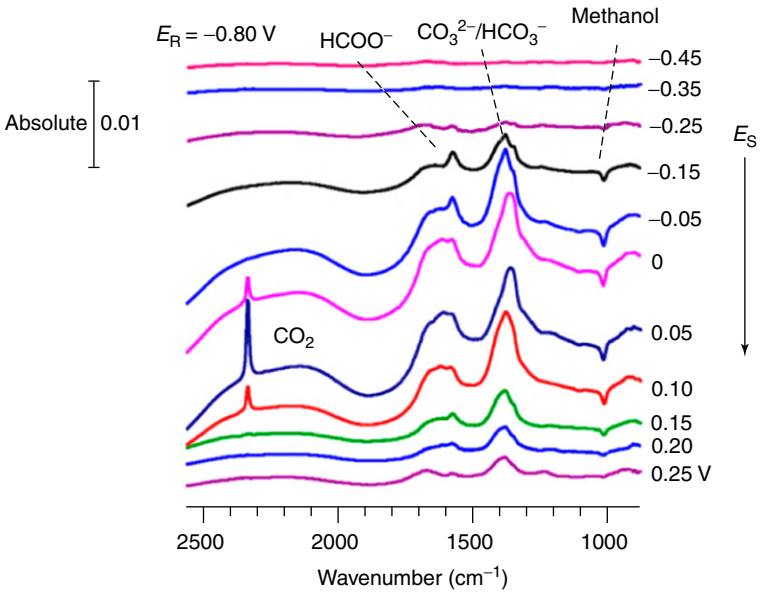


Figure 20 *In situ* IRAS spectra of CH_3OH electrooxidation at the Pd electrode at different potentials in 0.1 M NaOH + 0.1 M CH_3OH. E_s (sample potential) was varied from –0.45 to 0.25 V (vs. Ag/AgCl (sat)), and E_R (reference potential) is –0.8 V (vs. Ag/AgCl (sat)). Reproduced from Yang, Y.-Y.; Ren, J.; Zhang, H.-X.; *et al. Langmuir* **2013**, *29*, 1709–1716.

Innocent et al. performed *in situ* FT-IR spectroscopic studies to identify the intermediates formed during the electrochemical reduction of CO_2 on lead (Pb) electrode in aqueous and alkaline media.[148] The authors introduced CO_2, via bubbling, to a spectro-electrochemical cell containing a Pb electrode immersed in 0.5 M NaOH solution. While maintaining open circuit condition and continuously bubbling CO_2, the FT-IR spectra of the Pb electrode was measured every 5 s. Compilation of the FT-IR spectra of the Pb electrode in alkaline solution with CO_2 bubbling is shown in Figure 21. In this technique, the spectra were calculated based on the change in the absorbance value determined by $-\Delta A = \Delta R/R = (R_{ti} - R_{t=0})/R_{t=0}$, where $R_{t=0}$ is the 'reference' spectrum, which was recorded at $t = 0$. Figure 21(a) displays the FT-IR spectra for time span of 5–30 s from the beginning of CO_2 bubbling, where the intensity of the two negative bands, at 1394 and 1648 cm^{-1}, has increased with time. The authors assigned the 1394 cm^{-1} band to HCO_3^- ion and the 1648 cm^{-1} band to water molecules contained in the compound. Beyond 70s (Figure 21(b) and (c)), a band at 2346 cm^{-1} appeared in the FT-IR spectra. Innocent and co-workers ascribed this band at 2346 cm^{-1} to the interaction of the dissolved CO_2 with the Pb electrode in the alkaline solution.

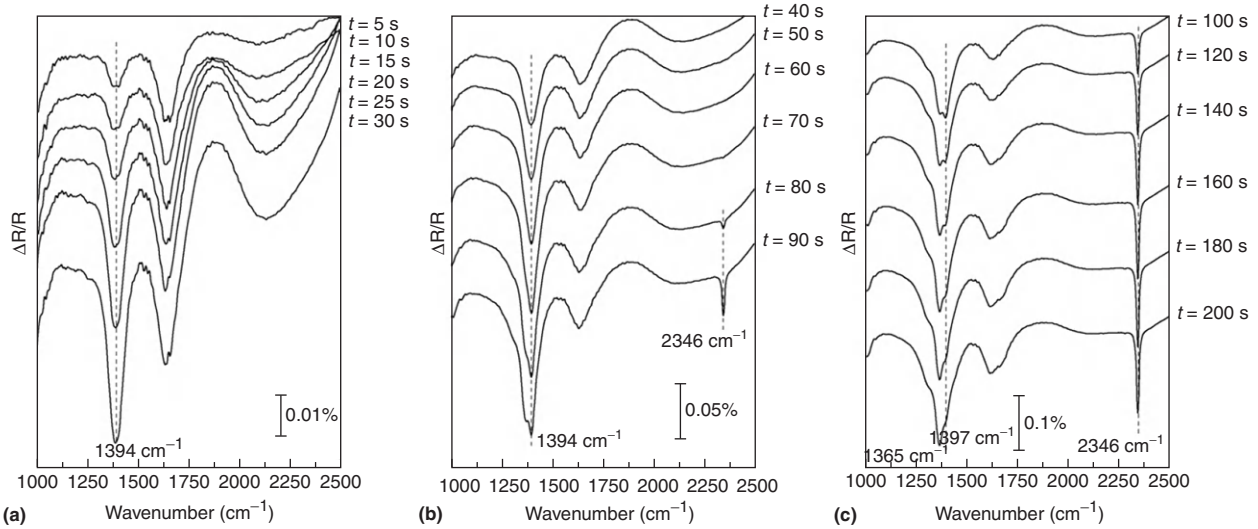


Figure 21 FT-IR spectra recorded in spectro-electrochemical cell without applied potential to a Pb electrode during CO_2 bubbling in 0.5 M NaOH; $\Delta R/R = (R_{ti} - R_{t=0})/R_{t=0}$, the 'reference' spectrum, $R_{t=0}$, was recorded at $t = 0$. (a) CO_2 bubbling between 5 and 30 s. (b) CO_2 bubbling between 40 and 90 s. (c) CO_2 bubbling between 100 and 200 s. Reproduced with permission from Innocent, B.; Pasquier, D.; Ropital, F.; *et al. Appl. Catal. B* **2010**, *94*(3–4), 219–224.

The effect of electrode potential on CO_2 reduction in alkaline solution was investigated, by the authors, using the *in situ* FT-IR spectroscopy. The *in situ* experiment was performed by measuring the spectra for Pb electrode using the single potential alteration infrared reflectance spectroscopy (SPAIRS). The presence of a new product or the disappearance of a product on the electrode surface was reported as variation of absorbance in each spectrum. The variation in absorbance for SPAIRS experiments is $-\Delta A = \Delta R/R = (R_{E2} - R_{E1})/R_{E1}$, where R_{E1} is the 'reference' spectrum recorded at chosen potential where no reduction of electroactive species was observed. The electrochemical cell was bubbled with CO_2 until before the appearance of the dissolved CO_2 band at 2346 cm^{-1} (Figure 21(b)). The SPAIR spectra collected at -1.8 V versus SCE was considered the 'reference' spectrum. The consumption of species is represented by a positive absorption band, in the SPAIR spectra, and the negative absorption band refers to the formation of species. In Figure 22, the SPAIR spectra of a Pb electrode in 0.1 M NaOH solution bubbled with CO_2 until the pH reached 8.6 is displayed.

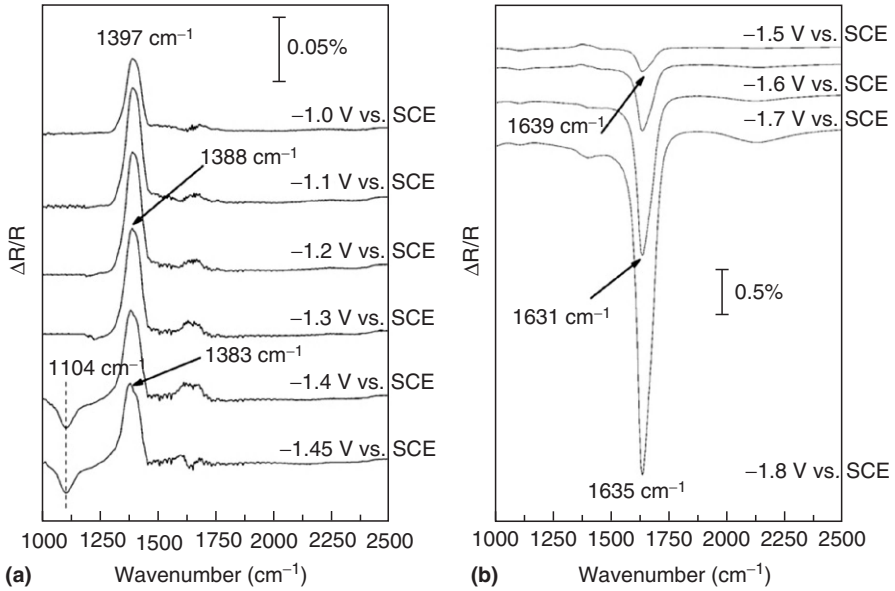


Figure 22 SPAIR spectra on a Pb electrode after bubbling CO_2 in 0.1 M NaOH until pH = 8.6; $\Delta R/R = (R_{E2} - R_{E1})/R_{E1}$, where the 'reference' spectrum, R_{E1}, was taken at –1.8 V vs. saturated calomel electrode (SCE). (a) Electrode potential from –1.0 V to –1.45 V vs. SCE. (b) Electrode potential from –1.5 V to –1.8 V vs. SCE. Reproduced with permission from Innocent, B.; Pasquier, D.; Ropital, F.; *et al. Appl. Catal. B* **2010**, *94*(3–4), 219–224.

The band for hydrogenocarbonate ions (HCO_3^-) was observed at 1397 cm^{-1} in Figure 22(a), for the electrode potential of -1.0 V versus SCE. With the increase in negative potential for the Pb electrode or otherwise known as reduction process, the intensity of the band at 1397 cm^{-1} reduced meaning disappearance of the HCO_3^- ions in the solution. At electrode potential of -1.4 V versus SCE, a band centered at 1104 cm^{-1} was noticed and it was assigned, by the authors, to the (ν_{CH}) bending vibration of $HCOO^-$. From the potential -1.5 V versus SCE, a major band was observed at 1633 cm^{-1} (Figure 22(b)), which was assigned to the symmetric stretching mode – ν_s(OCO) – from formate ($HCOO^-$). The intensity of this band, at 1633 cm^{-1}, increased from -1.5 to -1.7 V versus SCE, which confirmed the authors on the formation of formate ions with the electrochemical reduction of CO_2.

The advantage of combining traditional spectroscopic techniques with electrochemical experiments is illustrated in this section on *in situ* characterization for methanol oxidation and CO_2 reduction processes. The *in situ* characterization techniques are valuable methods in determining the intermediates and their interaction with electrode, and exploring reaction pathways to propose reaction mechanisms for the electrochemical process. This approach of using different techniques during electrochemical reaction has already started to attract several researchers to aide their quest.

9.14.4 Electrochemical Technology

The information obtained in bench scale tests are useful in characterizing the kinetics (current density) and the thermodynamics (cell potential) of the reaction and are thus a preamble to the scaling up of a process. As most industrial reactions are operated based on continuous flow systems rather than batch systems, the inclusion of flow reactors aid in engineering the process for both cost and conversion efficiency.[149] Consequently, the construction of reactors used in synthesis is crucial to the overall conversion of the raw materials, the yield of products, and the selectivity of one product over another when side reactions occur. Electrochemical organic processes are further complicated by the low conductivity of organic phases this bottleneck must be overcome in optimizing the process. Although the previous Sections 9.14.2 and 9.14.3 in this chapter have focused on reactions at one of the

electrodes, scale-up will require the consideration of reactions at both electrodes. In constructing an ideal organic electrochemical reactor, the product(s) at the anode and cathode should be coordinated to create a pair or couple.[150] This pairing/coupling of reactions will lower the costs related to energy consumption and potentially eliminate the need for a supporting electrolyte. However, this requires minimal separation as the diffusion layer can be approximated based on the Nernst diffusion model as[150,151]:

$$\delta = \frac{zFADC_{\text{bulk}}}{I_{\text{lim}}} \tag{19}$$

where δ is the diffusion layer thickness, z is the number of electrons transferred, F is Faraday's constant, D is the diffusion coefficient, A is the area of the electrode, C_{bulk} is the bulk concentration, and I_{lim} is the mass transport limited current. Therefore, a coupled reaction would be where the diffusion layers of both the anode and cathode overlap as shown in **Figure 23**, for two different electrode configurations.

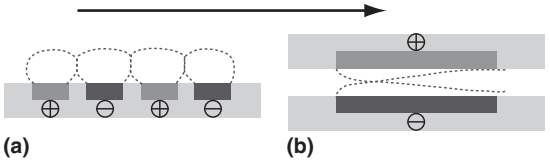


Figure 23 Diffusion layer thickness for an interdigitated (a) and channel (b) electrode configurations. The concentration profile of the product at each electrode is indicated by the dotted line, the + and – signs indicate the polarity of the electrode and the black arrow represents the direction of flow. If the distance between the electrodes is minimized on the order of the diffusion layer (δ), coupled reactions would be on the order of 2δ. Reproduced with permission from Paddon, C. A.; Atobe, M.; Fuchigami, T.; *et al. J. Appl. Electrochem.* **2006**, *36*(6), 617–634.

Configurations for pairing electroorganic reactions have been implemented in some of the processes from **Table 1**, including production of glyoxylic acid (**Figure 24(a)**)[152] and propylene oxide (**Figure 24(b)**).[153]

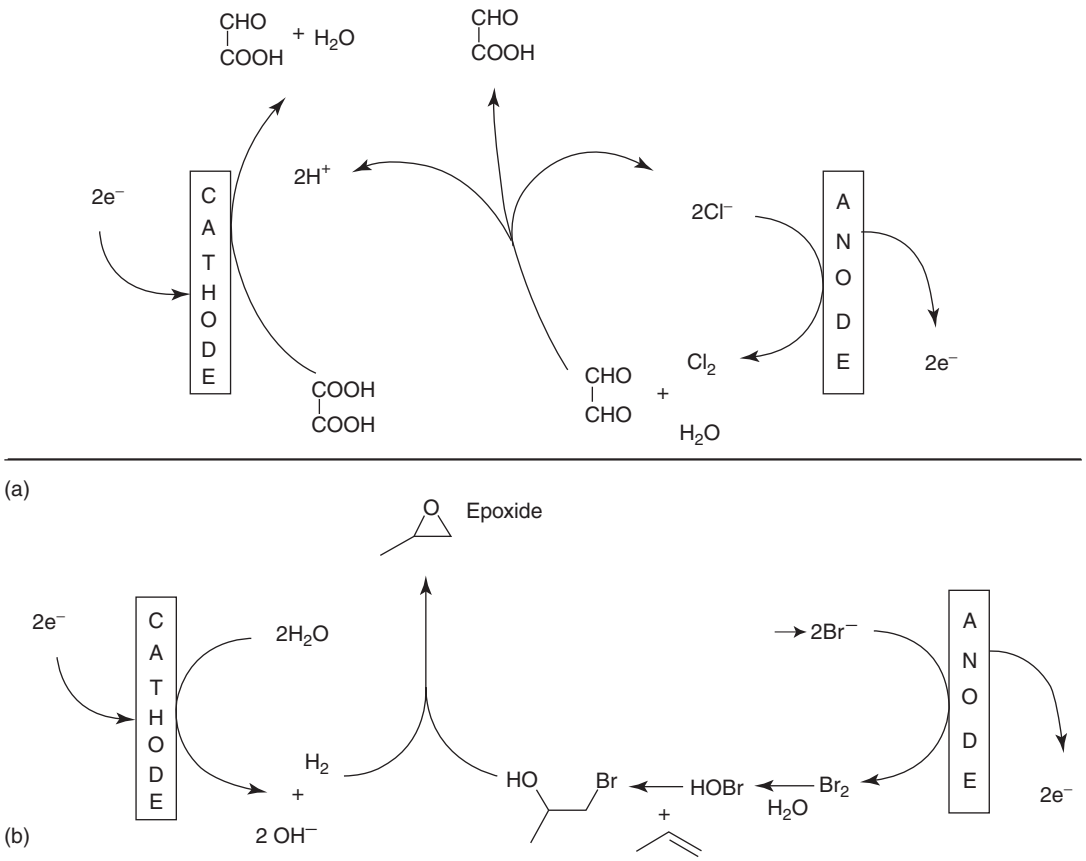


Figure 24 Paired electrosynthesis of glyoxylic acid (a) and propylene oxide (b) electrosynthesis. Both processes are indicative of a convergent paired electrosynthesis as the reactants produce a single product. Reproduced with permission from Paddon, C. A.; Atobe, M.; Fuchigami, T.; *et al. J. Appl. Electrochem.* **2006**, *36*(6), 617–634.

In a parallel configuration of electrodes (typical configuration in industry), the potential difference is related to the ohmic resistance by[154]:

$$\Delta U = IR = I\frac{d}{A\sigma} \tag{20}$$

where ΔU is the potential difference across the electrodes, I is the current generated (or applied), R is the electrolyte resistance, and σ is the conductivity of the solution. This equation shows the emphasis of reducing the electrode distance as the ionic conductivity of typical organic electrolytes is low and this can be counteracted by reducing the electrode distance. This also eliminates the need for a supporting electrolyte, used to enhance conductivity.

With a focus on minimizing the electrode distance to allow better control of the limiting conditions (equation 19), the use of microstructured cells have become more popular in advancing electroorganic reaction engineering as indicated in the literature related to construction of microreactors and electric field-influenced flow regimes.[154–159] This field is especially relevant considering how nanotechnology has been leveraged for improving reaction kinetics as previously discussed in Section 9.14.3.2. Subsequently, the use of nanotechnology along with microfluidic devices could combine the best characteristics of both nascent fields.

Microcells are based on dimensions between 10^{-6} and 10^{-3} m and can be classified based on the aspect ratio (S_R) defined by[154,160]:

$$S = \frac{d_x}{d_y} \tag{21}$$

where d_x and d_y are the width and height of the cell, respectively (Figure 25). Although these demarcations are arbitrary, they provide a guide for designing and specifying the reactor to be used.

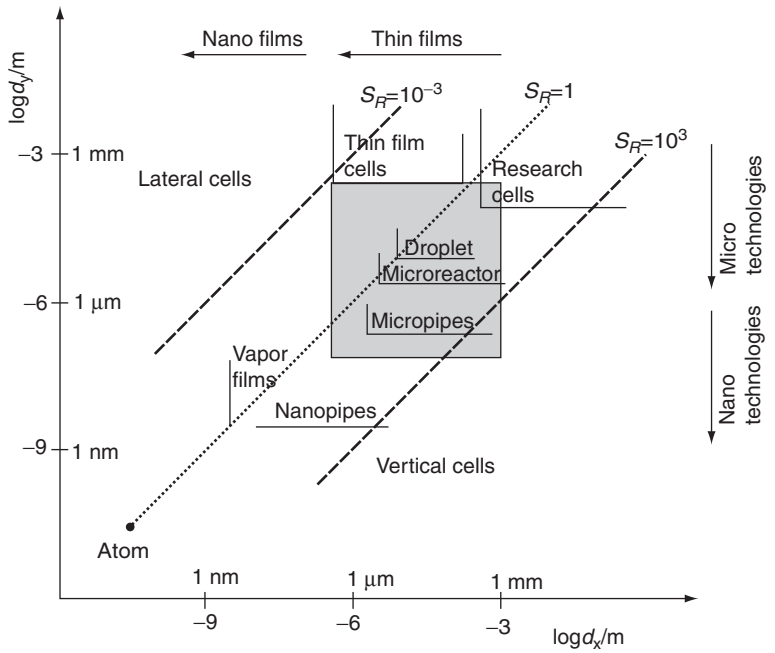


Figure 25 Classification of microreactors based on the aspect ratio S_R. Although the microscale is defined as 10^{-3}–10^{-6} m, scales below 10^{-3} can be included and thus the values are somewhat arbitrary. Reproduced with permission from Ziogas, A.; Kolb, G.; O'Connell, M.; *et al. J. of Appl. Electrochem.* **2009**, *39*(12), 2297–2313.

These cells have been tested in a variety of reactions, including oxidation of 4-methoxytoluene to 4-methoxy-benzaldehyde[161,162] and oxidation of furan to 2,5 dimethoxy-2,5-dihydrofurane.[163] To describe the performance of any flow reactor, the conversion (X), selectivity (S), and yield (Y) should be defined based on the primary reaction. If the electrochemical reaction is as follows (a cathodic reaction):

$$\mathrm{Ox} + \mathrm{ze}^- \rightarrow \mathrm{Re} \tag{22}$$

Then the conversion is described as:

$$X = \frac{n_{\mathrm{Ox}}^{\mathrm{in}} - n_{\mathrm{Ox}}^{\mathrm{out}}}{n_{\mathrm{Ox}}^{\mathrm{in}}} \tag{23}$$

The selectivity of the reaction is described as:

$$S = \frac{n_{\mathrm{Re}}^{\mathrm{out}}}{n_{\mathrm{Ox}}^{\mathrm{in}} - n_{\mathrm{O}x}^{\mathrm{out}}} \tag{24}$$

Whereas the yield is described as:

$$Y = \frac{n_{\mathrm{Re}}^{\mathrm{out}}}{n_{\mathrm{Ox}}^{\mathrm{in}}} \tag{25}$$

where n represents the molar flow rate of the species. With other possible reactions occurring, the goal of an optimal reaction is to maximize conversion, selectivity, and yield of the product of interest.

Further quantities have been developed by Rode et al. in describing the performance of a micro-electrochemical cell with a single pass, that is, no recycle stream.[154] They are the dimensionless current (I^*), the Wagner number (Wa), and the number of transfer units (NTU) and they are described as follows

$$I^* = \frac{I}{zFVC_{\mathrm{Ox}}^{\mathrm{in}}} \tag{26}$$

$$\mathrm{Wa} = \frac{\kappa}{zFk_{\mathrm{m}}C_{\mathrm{Ox}}^{\mathrm{in}}dk_{\mathrm{Ox}}} \tag{27}$$

$$\mathrm{NTU} = \frac{k_{\mathrm{m}}A}{V} \tag{28}$$

where V is the electrolyte volumetric flow rate, κ is the specific conductivity, k_m is the mass transfer coefficient, and k_{Ox} is the kinetic constant of the reaction (equation 22).

These expressions (equations 26–28) can be used to optimize the performance of a high conversion cell and influence the general properties for a reaction (equations 23–25). Ideal conditions require I^* (equation 26) to be close to 1 and is indicative of a maximum efficiency, that is, more of the current generated (or applied) is used in converting the reactants resulting in a higher yield. Values greater than 1 suggest an inefficient cell and could reduce the yield of the product in equation 22, because it is involved in other reactions.[154] However, NTU values (equation 27) higher than unity are preferred as they are related to high conversions, whereas low and high Wa (equation 28) are indicative of uniform distributions of current density and overpotential, respectively.[154]

These properties have been used to compare the performance of the conventional electrochemical conversion of 4-methoxytoluene to 4-methoxyaldehyde in comparison with two micro-electrochemical cells at different pressures (**Table 6**).

Table 6 Comparison of the performance of a conventional industrial cell and two micro-electrochemical cells with slightly different configurations

Process Parameters	Conventional cell[3]	Bipolar microcell[155]	High-pressure microcell[154]
Flow scheme	Continuous with recycle	Single pass high conversion	
Electrodes	Bipolar graphite rings	Glassy carbon	Glassy carbon anode Stainless steel cathode
Interelectrode gap (mm)	0.5–1	0.1	0.1
$C_{\mathrm{methoxytoluene}}^{\mathrm{in}}$ (%)[a]	10–25	1.4	7.5
$C_{\mathrm{electrolyte}}^{\mathrm{in}}$ (%)[a]	0.3–3 Potassium fluoride Sodium sulfonate	0.07 Potassium fluoride	0.07 Potassium fluoride
Pressure (bar)	Atmospheric	Atmospheric	5
Temperature (°C)	40–50	45	45
Current Density (mA mm^{-2})	0.3–0.5	0.01–0.4	0.51
Voltage per gap (V)	4–6	4–6	7
X (%)	90–99	99	90
S (%)	85	79	92
Y (%)	>80	78	82

[a]Concentrations are based on mass percentages.

Based on the overall reactor parameters, the microreactors show comparable performance to the industrial. This is especially significant considering the mass percentage of the supporting electrolyte is at least one order of magnitude less in the microcell than in the conventional cell. This was also observed in the conversion of furan, where the supporting electrolyte was eliminated while providing a yield of 98% in the microcell in comparison with 80–85% in the conventional electrochemical cell.[163] These studies indicate the possible advantages of the use of microreactors. However, electroorganic reactions can involve two-phase flow due to the production of gases at the opposing electrode or in side reactions, causing an increase in the potential difference between the electrodes. The complexity of hydrodynamics further complicated at this scale due to a shift in dominance from gravitational force to interfacial and viscous forces.[155] An illustration of this effect can be observed in Figure 26, where the variance of current density and liquid flow rate on the two-phase flow can be clearly observed.[155]

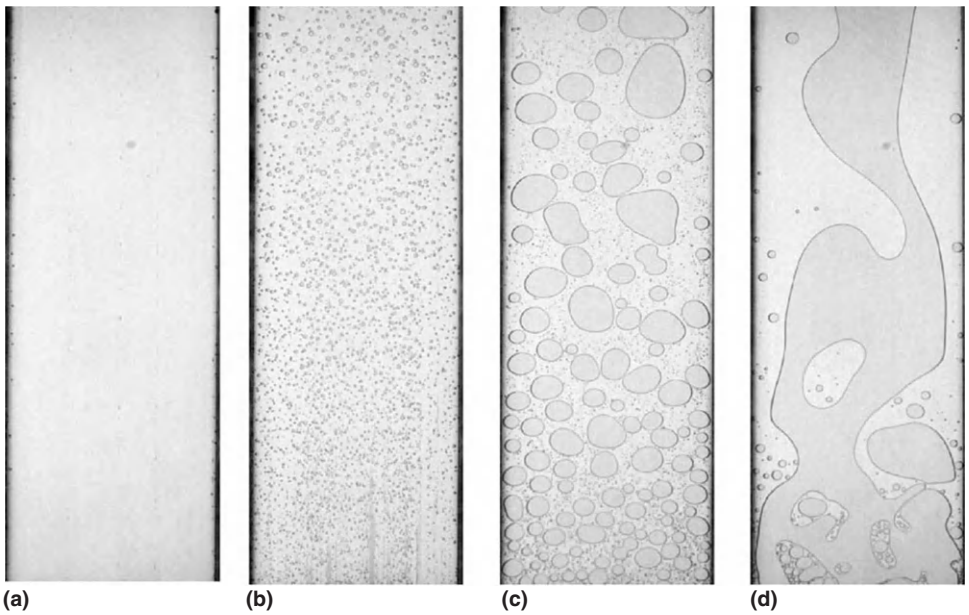


Figure 26 Flow patterns observed in the visualization cell for the 4-methylanisole methoxylation reaction. The experimental conditions for the visualized flow, current density (mA mm^{-2}) and flow velocity (m s^{-1}), respectively, are (a) no bubbles, 0.400 and 0.17; (b) dispersed bubbles, 1.500 and 0.17; (c) bubbly flow, 1.500 and 0.017; and (d) churn flow, 5.500 and 0.017. Reproduced with permission from Bouzek, K.; Jiricny, V.; Kodym, R.; Krist'al, J.; Bystron, T. *Electrochimica Acta* **2010**, *55*(27), 8172–8181.

This disruption of the cell characteristics (potential and current density) causes a decrease in the reaction parameters as the build-up of gas will decrease the rate of further liquid conversion due to lower electrode area and slower electron transfer. The use of a bipolar reactor has been suggested by Bouzek et al., as a configuration to decrease the effect of gas production, whereas operation at higher pressures has been used by Ziogas et al. (Table 6). Other hydrodynamic effects are related to the influence of an electric field on the motion of ions at this scale and heat transfer effects, as summarized by Zimmerman.[157] It can thus be surmised that the greater control of electrochemical properties on the microscale is not without drawbacks on the control of the flow dynamics.

9.14.4.1 Microfuel Cells for Methanol Oxidation

The use of microcells for the methanol oxidation reaction is especially relevant as the energy generated from this organic compound can be scaled from portable music devices requiring <1 W up to mobile military applications for up to 150 W.[158] As discussed in Section 9.14.4 (equation 26), the influence of flow at the cathode and anode plays a role in the efficiency of the cell, regardless of the scale considered.

The schematic of the direct methanol fuel cell previously discussed in Section 9.14.2.1.2 (Figure 6) shows that it is operated as a divided cell (Figure 3) and therefore the cathode and anode processes are separated by a membrane. However, this simplified schematic does not show the additional porous layers within the cell and the possible parasitic processes that occur (Figure 27).

The presence of the diffusion layers (DL), catalyst layers (CL), and the polymer electrolyte membrane (PEM) are associated with the mass transport of the reactants and products within the cell and influence the performance of the cell even after the optimal catalysts have been developed through computational models, combinatorial chemistry, and nanotechnology. These transport issues are therefore an important factor to be alleviated for the best performance of this fuel cell.

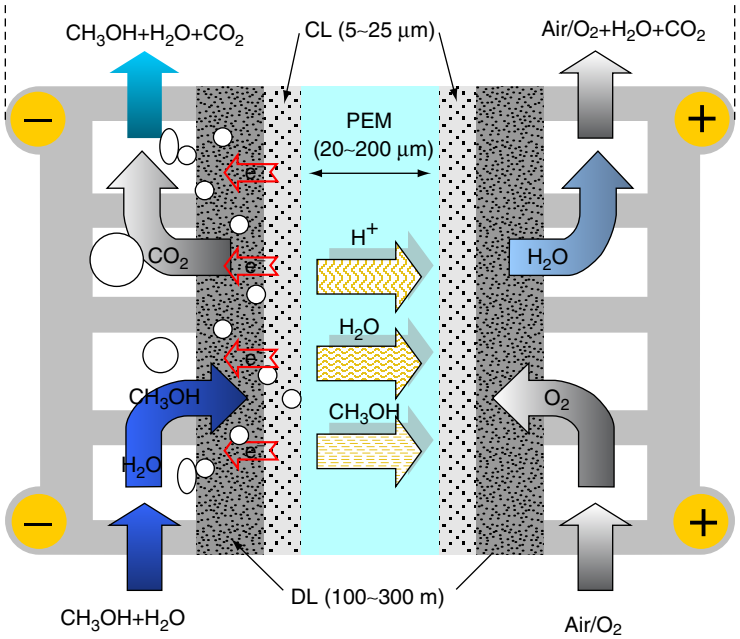


Figure 27 Schematic of an operating direct methanol fuel cell according to reactions 3–4 (depicted in Section 9.14.2.1.2.1) showing the diffusion layers (DL), catalyst layers (CL), and the polymer electrolyte membrane or proton exchange membrane (PEM) and their typical thicknesses. The diffusion of methanol and water across the PEM (called crossover) causes parasitic processes, which reduce the efficiency of operation. Reproduced with permission from Zhao, T. S.; Xu, C.; Chen, R.; Yang, W. W. *Prog. Energy Combust. Sci.* **2009**, *35*(3), 275–292.

In the review by Zhao et al.,[159] the critical issues have been fully discussed and summarized in this section. Aside from the effect of the two-phase flow previously discussed in Section 9.14.4 (liquid methanol and water with gaseous oxygen and CO_2), issues with the transport of methanol, water, and oxygen along and across the fuel cell layers are also relevant. Although an increase in methanol concentration will enhance the current generated in the fuel cell, this will increase the diffusion (methanol crossover) across the PEM leading to reactions at the cathode and a reduction on the cell performance. This has typically led to concentrations of 0.5–2.0 M being used, which conversely increase the concentration of water in the fuel. However, because water can also diffuse through the membrane, this lowered concentration trades one reactant crossover for another. Although work[164–166] is underway to substitute the typical PEM (Nafion) for a less-permeable membrane, Nafion is still the best membrane for proton transfer across the membranes. Transport issues at the anode are related to fuel transport through the cell so as to mitigate a significant drop in fuel concentration, while minimizing the effect of CO_2 bubbling during cell operation (equation 3). This has led to studies on the flow field effect (Figure 28) on the performance of the fuel cell.

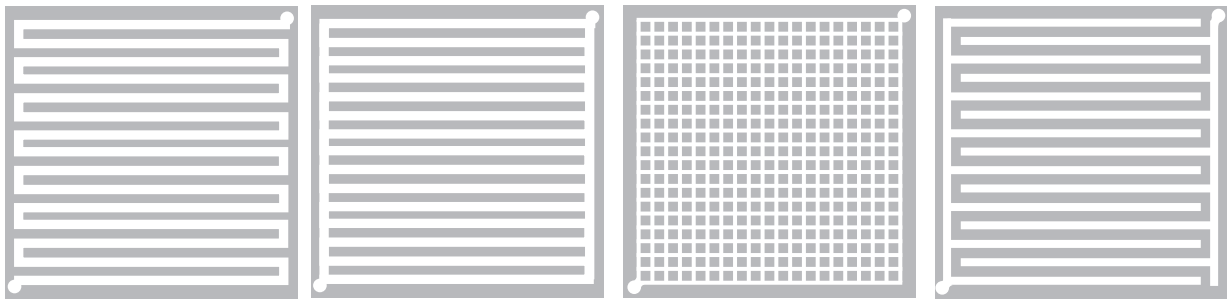


Figure 28 Flow fields studied in methanol fuel cells: (a) serpentine, (b) parallel, (c) spot, and (d) interdigitated. Reproduced with permission from Zhao, T. S.; Xu, C.; Chen, R.; Yang, W. W. *Prog. Energy Combust. Sci.* **2009**, *35*(3), 275–292.

Based on equation 28, an increase in the mass transfer coefficient will increase the NTU (a favorable condition for the electrochemical cell), and it has been observed that the use of serpentine flow field increases the mass transport coefficient, thus resulting in better performance (Figure 29).[167]

This change in mass transfer coefficient has been attributed to the difference in CO_2 bubble formation, where the bubbles in the parallel flow field and the serpentine flow field resulted in configurations similar to Figures 26(c) and (d), respectively.[168]

Other issues including flooding at the cathode due to water crossover and oxygen concentration and distribution on the cathode side have also been studied and provide ample areas for further improvement.

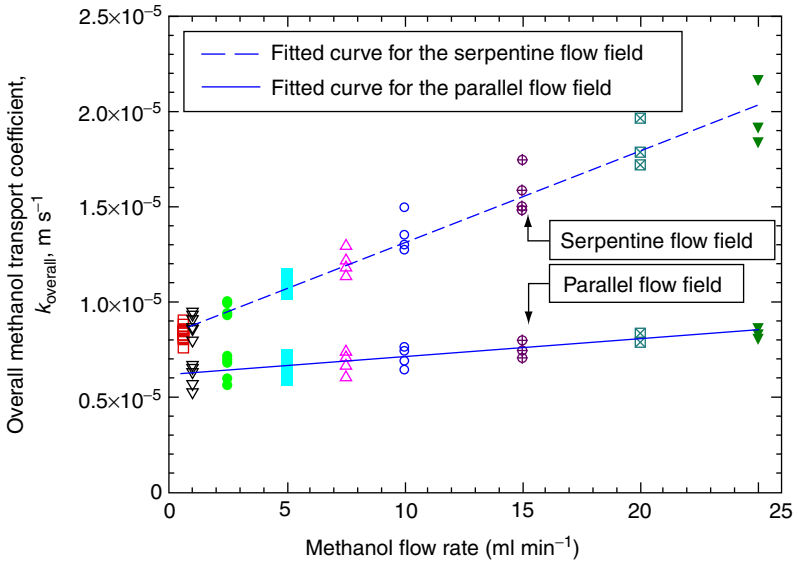


Figure 29 Effect of methanol flowrate and flow field on the mass transfer coefficient in a methanol fuel cell operated at different current densities. The increase in mass transport coefficient will cause an increase in the number of transfer units (27), thus increasing the conversion of methanol and the fuel cell performance. Reproduced with permission from Zhao, T. S.; Xu, C.; Chen, R.; Yang, W. W. *Prog. Energy Combust. Sci.* **2009**, *35*(3), 275–292.

9.14.4.2 Microfuel Cells for Carbon Dioxide Reduction

The use of microfluidics in the electroreduction of CO_2 to fuel is mitigated by the low solubility of CO_2 in water, which is 1.5 g l^{-1} under standard conditions.[169] This low solubility is influential in the poor performance of flow cells used for electrochemical reduction of CO_2, causing a diffusion limitation in the process. Alternative solvents including methanol and ionic liquids have been studied, with less than favorable results due to irreversible reactions with the ionic liquid and low current densities, suggesting that an aqueous environment (electrolyte) is still currently favored.[170] Consequently, in designing a flow cell, it would be crucial to increase the surface area of the electrode (through the use of nanotechnology) and also increase the pressure of operation.[171,172] As an example, Hara et al. quantified the effects of pressures up to 60 atm and current densities up to 900 mA cm^{-2}, finding that the most suitable conditions for hydrocarbon production were 375 mA cm^{-2} and 30 atm.[171] Although this high pressure condition is not as feasible, it is indicative of how the cell design is paramount in this nascent electrochemical technology.

Although there does not appear to be literature on the use of microfluidic cells in CO_2 reduction to fuels, examples of reactors designed for CO_2 to other chemicals, including formic acid and CO_2, have been used at the macro- and microscales.[173–176] A microfluidic cell design,[176] similar to the novel setup by Centi et al.,[174] fed CO_2 to the cell in the gas phase, whereas the electrolyte was directly in contact with the cathode and anode (**Figure 30**).

More recent studies by Cubaud et al.[177,178] have shown promise in the investigation of aqueous dissolution of CO_2 in microcells, which would provide further benefits for microfluidic cells operating in the aqueous phase. These studies have characterized the minimum liquid fraction for complete dissolution to be ≈ 0.55, a value that is relatively independent of pressure for the system studied. Such a high value for the ratio of water to CO_2 suggests a propensity for flooding of this electrolytic cell and therefore, the setup in **Figure 30** might still be the state of the art. As can be seen, the need for initial dissolution of CO_2 in water is eliminated, whereas the product formed was present in the electrolyte used. Although this cell setup will increase the cost of separation for aqueous chemicals, this setup will be particularly advantageous for the production of fuels as these hydrocarbons are immiscible with water. In conjunction with this study, a mathematical model of the microfluidic cell indicated that diffusion of CO_2 is still a major concern for improvement of this technology and further improvements can be made.[179]

In summary, while microfuel cells are possible improvements in flow cell configurations, two-phase hydrodynamics have been found to be drawbacks in this system. The design of the cell to overcome the transport issues is paramount in the feasibility of the technology and is an essential focus as it has to maintain the efficiency realized in bench scale tests where transport phenomena is often ignored. It should be noted that, although not a focus of this section, another avenue for understanding flow dynamics

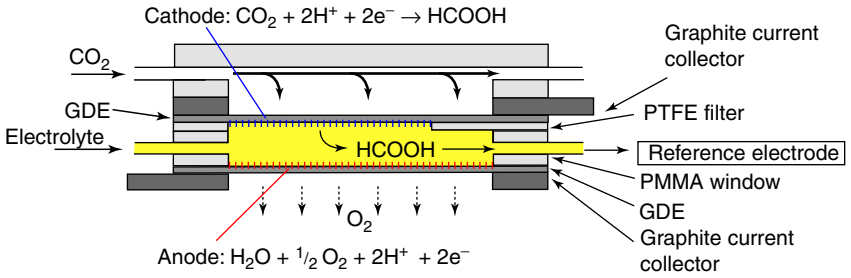


Figure 30 Schematic diagram of the microfluidic reactor for CO_2 conversion used in the production of formic acid. As observed, the aqueous phase is separated from carbon dioxide, which diffuses into the solution as opposed to dissolution before feeding into the cell. GDE, gas diffusion electrode; PTFE, polytetrafluoroethylene; PMMA poly(methyl methacrylate). Reproduced from Whipple, D. T.; Finke, E. C.; Kenis, P. J. A. *Electrochem. Solid State Lett.* **2010**, *13*, D109–D111.

within an electrochemical reactor is the use of numerical mathematical models including Computational Fluid Dynamics (Figure 8). These numerical methods solve the differential equations that describe the transport phenomena prevalent in chemical reactors, that is, heat, momentum, and mass transfer and are broadly divided into Taylor series formulation, Variational formulation, Method of weighted residuals, and Spectral Methods based on the estimation applied to the flow variables.[180] With the seminal work by Newman,[181] the transport principles used in designing chemical reactors can thus be extended to electrochemical reactors through inclusion of fields of electric potential.[182] These numerical methods have been implemented in certain commercial software including COMSOL® and FLUENT® and have been instrumental in understanding transport phenomena in fuel cells,[183–187] but other literature examples where cyclic voltamograms[188] and particle mobilities[189] have been studied provide a possible extension to simulations of electrosynthesis of organic compounds.

9.14.5 Pilot Plant Trials

Armed with atomic/molecular models, laboratory scale experiments and the flow profiles of the intended reaction and with the overall goal of industrial scale production, pilot plant trials represent a necessary intermediate. A definition of a pilot plant is a setup that mimics an operation (or set of operations) at the industrial scale.[190] Therefore, it is not only a smaller version of industrial equipment but also a small scale combination of interactions between different operating units. Although this might apply to laboratory scale research as well, some typical ratios have been defined to indicate the difference in sizes[191] (Table 7). It

Table 7 Correlation between system properties and typical scale-up ratios and scales of operation (kg hr^{-1})

System		*Scale of operation*		*Scale up ratio*[a]	
Reactant	Product	Laboratory	Pilot plant	Laboratory to pilot plant	Pilot plant to commercial
Gas	Gas	0.01–0.10	10–100	500–1000	200–1500
Gas	Liquid or solid	0.01–0.2	10–100	200–500	100–500
Liquid and gas	Liquid	0.01–0.2	1–30	100–500	100–500
Liquid	Solid or viscous liquid	0.005–0.2	1–20	20–200	20–250
Solid	Solid	0.10–1.0	10–200	10–100	10–200

[a]Scale-up ratio is defined as: commercial rate production rate ÷ pilot unit production rate.

Source: Reproduced from Bisio, A. Introduction to Scaleup. In *Scaleup of Chemical Processes: Conversion from Laboratory Scale Tests to Successful Commerical Size Design*; Bisio, A., Kabel, R. L., Eds.; Wiley: New York, **1985**, pp 1–33.

should be noted that while these values are typical for operations involving chemical reactions, electrochemical organic systems would be on a much smaller scale.[192]

The transition from laboratory to pilot to industrial scale is called scale-up, although the actual procedure begins with a scale down as the commercial production has to be the starting point of the study.[191] In other words, the commercial process is initially conceptualized and the pilot plant trials seek to lower the uncertainty in operating at a large scale. Consequently, for most chemical processes, pilot plant trials are not a necessary requirement. Some rules of thumb have been developed to consider the cases when a pilot plant would be essential[193] (Table 8).

Although most of this current chapter has focused on reactions in an electrochemical cell, Section 9.14.4 and Table 8 are a clear indication that the reactor is just one of the units present in commercial production. Therefore it is essential to consider how the electrochemical reactor will fit into the overall plant efficiency and economics. Although individual units may operate at optimal conditions, this may not be the case when these units are working in conjunction. As an example, consider the relationship between current density and heat generation: although an increased current density could potentially increase

Table 8 Rules of thumb for deciding what unit operations require pilot plant testing

Operation	*Pilot plant required?*	*Comments*
Distillation	Usually not. Sometimes needed to get tray efficiency or height equivalent to a theoretical plate data	Skipping pilot plant can sometimes produce surprises, for example, foaming
Fluid flow	Usually not, for single phase. Almost always, for two phase flow	Some polymer systems are also very difficult to predict
Reactors	Frequently	Scale-up from lab often justified for homogeneous systems, seldom for heterogeneous
Polymerizers	Almost always	
Evaporators, reboilers, heat exchangers, coolers, condensers	Usually not, unless there is a possibility of fouling	
Dryers	Yes – almost always	Usually done using commercial equipment
Solids handling		
Crystallization	Almost always	Should pilot in similar type of equipment proposed for industrial scale
Extraction		

Source: Reproduced from Aerstin, F. G.; Robbins, L. A.; Vogel, A. J. Gaining Experience Through Pilot Plants and Demonstration Units. In *Scaleup of Chemical Processes: Conversion from Laboratory Scale Tests to Successful Commercial Size Design*; Bisio, A.; Kabel, R. L., Eds.; Wiley: New York, **1985**, pp 655–676.

production (optimal reactor operation), the increased current density could result in increased current to side reactions and other irreversible processes in the cell. This could increase the complexity of mass and momentum transfer if the side reactions involve gas production. Simultaneously, the fact that most electrochemical systems are heterogeneous (solid electrodes, liquid electrolytes, and liquid/gaseous products) increased the complexity of heat transfer as well.[194] Overall, with the definition of a pilot plant and the rules of thumb mentioned, pilot scale trials would be unavoidable for electrochemical reactors.

One of the ways in which this difficulty is alleviated is by the extensive use of models available for unit operations. Commercial simulations used by chemical engineers include CHEMCAD® and Aspen Plus® and these simulators exist as the final stage in the scale of multiscale models introduced in Section 9.14.2.2 (**Figure 8**). As previously mentioned, although the reactor has been the focus of this chapter, this reactor is only one of multiple unit operations, which will have to fit in with other equipment for overall optimization. However, these commercial simulators mentioned are not currently optimized to handle electrochemical reactors. As a result, models for electrochemical reactors are added as separate routines written as computational code (using FORTRAN or Visual Basic) and then these codes are allowed to interface with the other unit operations within the simulator.[195,196] Essentially, the material and energy balances are performed within the simulator, whereas electrochemical phenomena are performed using a separate subroutine. The use of these subroutines has been especially useful in fuel cell-based plant simulations. In these simulations, the effect of different operating conditions, such as fuel humidity, purity, temperature, and pressure, on the efficiency and power generated have been examined. Although some simulations have used semi-empirical corrections to a reference voltage –current curve,[197,198] to reduce the amount of computational resources and complexity of the code, the use of a Taylor series formulation (Finite Difference Method)[199,200] has also been shown. These simulations are especially useful considering that they can provide information about cost estimates by sizing of the equipment used in heat exchanges, reactors, pumps, and others. In reality, it has been suggested that the cost of a pilot plant should not exceed the cost of 3 months of operation at the commercial level, else substantial technical or economic justification for constructing the pilot plant is required.[191]

9.14.6 Industrial Production

So far, the sections of this chapter have provided a broad and detailed overview of the different steps to systematically improve a conceptual idea of synthesizing an organic compound using electrochemical methods to pilot plant scale. As mentioned in Section 9.14.5, scale up of an electrochemical process involves transferring the reaction conditions from laboratory to pilot plant to industrial scale. Under the pilot plant trials, the production of the organic compound is accessed based on the rate of production, the yield of the desired product, efficiency of the different unit operations, energy consumption for the pilot plant, and economic assessment for the industrial scale production. Those electrochemical processes, which have demonstrated successful operation at pilot plant scale combined with the need for the organic compounds in the market, will result in scaling up the pilot plant to industrial scale production process. **Table 1** provides a list of organic compounds synthesized electrochemically at commercial and pilot plant scale operations.

The most successful organic compound synthesis process that has been commercialized via an electrochemical route is the electrosynthesis of adiponitrile from acrylonitrile. Adiponitrile (ADN) is a key intermediate for the production of nylon 6,6 polymers. It is used for the synthesis of hexamethylenediamine (HMD), which along with adipic acid are the raw materials for the production of nylon 6, 6 fibers and resins. In addition to the commercial electrochemical synthesis of adiponitrile using the Monsanto process, ADP has been produced in large quantity from the hydrocyanation of butadiene, which was developed and

commercialized by DuPont. The electrochemical route of synthesizing adiponitrile is employed by Solutia at Decatur, Alabama, in the USA, Asahi Chemical in Nobeoka, Japan, and by BASF at Seal Sands, UK. Chemically ADP is produced by DuPont in Texas, USA, and by Butachimie (joint venture between DuPont and Rhodia) in Chalampé, France.

According to the report from ICIS, a petrochemical market information provider, in 2000, world production of the adiponitrile was 1.375 million metric ton per year of which 32.8% was produced from an electrochemical route.[201] In a 2005 report, the global production increased to 1.564 million metric ton per year but the contribution from the electrochemical route dropped to 30.8% (0.481 million metric ton per year).[202] The assessment from the PCI Nylon, a market research consultancy, is that 1.197 million metric tons of ADP was produced in 2010 and only 29% of the ADP produced was from acrylonitrile.[203] The demand for nylon 6, 6 is the driving force for the production of HMD and ADP, which has remained fairly consistent over the past decade. However, the electrochemical synthesis of ADP has suffered slightly in its contribution toward global production mainly due to the reduced prices of the raw materials used in the butadiene route of ADP production. Natural gas is used in the butadiene route to synthesize ADP and in recent years the price for natural gas has come down.

The criteria to advance a synthesis process from pilot plant scale to industrial production level does not only depend on the scalability but it also involves economics, demand, and supply of the organic compound as well as the cost of the associated materials, such as the price of the raw materials used in the competing processes.

9.14.7 Summary

The use of electrochemistry in the synthesis of organic compounds has not been a widespread technique for varying reasons from education of scientists to the market for the products. However, the improvement in the current materials and methods used in the electrochemical cells indicates a direction that can yield positive benefits. This has been observed in the use of models, *in situ* characterization, and microfuel cells in improving the methanol and CO_2 conversion and these methods are transferrable to other current products as well.

Overall, although market economics will always play a larger role in the implementation of organic electrochemistry, the development of the field will be critical in ensuring that electroorganic chemistry can find avenues for use in chemical production.

References

1. Weinberg, N. L. Industrial Organic Electrosynthesis with Some Advice on Approaches to Scaleup. Available at: http://electrochem.cwru.edu/encycl/art-o01-org-ind.htm (accessed on 21 January 2013).
2. Sequeira, C. A. C.; Santos, D. M. F. *J. Braz. Chem. Soc.* **2009**, *20*, 387–406.
3. Pütter, H. Industrial Electroorganic Chemistry. In *Organic Electrochemistry*, 4th ed.; Lund, H., Hammerich, O., Eds.; Marcel Dekker, Inc.: New York, **2001**, pp 1259–1308.
4. Lorenz, W. J.; Plieth, W. *Electrochemical Nanotechnology: In Situ Local Probe Techniques at Electrochemical Interfaces*; Wiley-VCH: Weinheim, Germany; New York, **1998**.
5. Fleischmann, M.; Oliver, A.; Robinson, J. *Electrochim. Acta* **1986**, *31*, 899–906.
6. Ikai, A. *Surf. Sci. Rep.* **1996**, *26*, 263–332.
7. Weaver, M. *Top. Catal.* **1999**, *8*, 65–73.
8. Kirchner, B.; di Dio, P.; Hutter, J.; Vrabec, J. Real-World Predictions from Ab Initio Molecular Dynamics Simulations. In *Multiscale Molecular Methods in Applied Chemistry*; Kirchner, B., Vrabec, J., Eds.; Springer: Berlin and Heidelberg, **2012**, Vol. 307; pp 109–154.
9. Keil, F. Multiscale Modelling in Computational Heterogeneous Catalysis. In *Multiscale Molecular Methods in Applied Chemistry*; Kirchner, B., Vrabec, J., Eds.; Springer: Berlin and Heidelberg, **2012**, Vol. 307; pp 69–107.
10. Wasileski, S.; Taylor, C.; Neurock, M. Modeling Electrocatalytic Reaction Systems from First Principles. In *Device and Materials Modeling in PEM Fuel Cells*; Paddison, S., Promislow, K., Eds.; Springer: Berlin, **2009**, Vol. 113; pp 551–574.
11. Swenson, M.; Golden, J.; Languell, M., Modeling and Simulation: The Return on Investment in Materials Science – An IDC Chemicals Industry White Paper. International Data Corporation: Massachusetts, USA. (sponsored by Accelrys Inc.) **2004**.
12. Lund, H.; Hammerich, O. *Organic Electrochemistry*, 4th ed.; Marcel Dekker Inc.: New York, **2001**.
13. Shono, T. Oxidation by Electrochemical Methods. In *Comprehensive Organic Synthesis – Selectivity, Strategy and Efficiency in Modern Organic Chemistry*; Trost, B. M., Fleming, I., Eds.; Pergamon: Oxford, **1991**, Vol. 7; pp 789–813.
14. Sperry, J. B.; Wright, D. L. *Chem. Soc. Rev.* **2006**, *35*(7), 605–621.
15. Bard, A. J.; Faulkner, L. R. *Electrochemical Methods: Fundamentals and Applications*, 2nd ed.; John Wiley & Sons, Inc.: New York, **2001**.
16. Kochi, J. K. Electron-transfer Oxidation. In *Comprehensive Organic Synthesis – Selectivity, Strategy and Efficiency in Modern Organic Chemistry*; Trost, B. M., Fleming, I., Eds.; Pergamon: Oxford, **1991**, Vol. 7; pp 849–889.
17. Lund, H. *J. Solid State Electrochem.* **2011**, *15*, 1733–1751.
18. Schäfer, H. J. Comparison Between Electrochemical Reactions and Chemical Oxidations and Reductions. In *Organic Electrochemistry*, 4th ed.; Lund, H., Hammerich, O., Eds.; Marcel Dekker, Inc.: New York, **2001**, pp 207–221.
19. completely revised Weissermel, K., Arpe, H.-J., Eds. *Industrial Organic Chemistry Translated by Charlet R. Lindley and Stephen Hawkins,* 4th ed.; Wiley-VCH: Weinheim, **2003**.
20. Bell, A.T.; Gates, B.C.; Ray, D. *Basic Research Needs: Catalysis for Energy.* Office of Basic Energy Sciences, U.S. Department of Energy: Washington, DC, USA. **2007**; p 254.
21. Centi, G.; Perathoner, S. *Catal. Today* **2009**, *148*, 191–205.
22. Frese, K. W., Jr. Electrochemical Reduction of CO_2 at Solid Electrodes. In *Electrochemical and Electrocatalytic Reactions of Carbon dioxide*; Sullivan, B. P., Krist, K., Guard, H. E., Eds.; Elsevier: Amsterdam; New York, **1993**, xiii; p 299.
23. Hori, Y. Electrochemical CO_2 Reduction on Metal Electrodes. In *Modern Aspects of Electrochemistry*; Vayenas, C. G., White, R. E., Gamboa-Aldeco, M. E., Eds.; Springer Science and Business Media: New York, **2008**. Vol. 42.

24. Kuhl, K.; Cave, E.; Abram, D.; Jaramillo, T. *Energy Environ. Sci.* **2012**, *5*(5), 7050–7059.
25. Wenzhen, L. Electrocatalytic Reduction of CO_2 to Small Organic Molecule Fuels on Metal Catalysts. In *Advances in CO_2 Conversion and Utilization*; Hu, Y. H., Ed.; American Chemical Society: Washington, DC, USA. **2010**, Vol. 1056; pp 55–76.
26. Neelameggham, N. R. *JOM* **2008**, *60*, 36–41.
27. Hartvigsen, J.; Elangovan, S.; Frost, L.; *et al. ECS Trans.* **2008**, *12*, 625–637.
28. Krewer, U.; Vidakovic-Koch, T.; Rihko-Struckmann, L. *Chemphyschem.* **2011**, *12*(14), 2518–2544.
29. Wang, H. S.; Baltruschat, H. *J. Phys. Chem. C* **2007**, *111*, 7038–7048.
30. Jusys, Z.; Kaiser, J; Behm, R. J. *Langmuir* **2003**, *19*, 6759–6769.
31. Gao, L.; Huang, H. L.; Korzeniewski, C. *Electrochim. Acta* **2004**, *49*, 1281–1287.
32. Basri, S.; Kamarudin, S. K.; Daud, WRW; Yaakub, Z. *Intl. J. Hydrogen Energy* **2010**, *35*, 7957–7970.
33. Bergamaski, K.; Pinheiro, A. L. N.; Teixeira-Neto, E.; Nart, F. C. *J. Phys. Chem. B* **2006**, *110*, 19271–19279.
34. Lu, C.; Rice, C.; Masel, R. I.; *et al. J. Phys. Chem. B* **2002**, *106*, 9581–9589.
35. Park, K. W.; Choi, J. H.; Kwon, B. K.; *et al. J. Phys. Chem. B* **2002**, *106*, 1869–1877.
36. Sasaki, K.; Adzic, R. R. *J. Electrochem. Soc.* **2008**, *155*, B180–B186.
37. Belgsir, E. M.; Huser, H.; Leger, J. M.; Lamy, C. *J. Electroanal. Chem.* **1987**, *225*, 281–286.
38. Wang, H. S.; Alden, L.; DiSalvo, F. J.; Abruna, H. D. *Phys. Chem. Chem. Phys.* **2008**, *10*, 3739–3751.
39. Antolini, E.; Gonzalez, E. R. *Electrochim. Acta* **2010**, *56*, 1–14.
40. Antolini, E; Gonzalez, E. R. *Catal. Today* **2011**, *160*, 28–38.
41. Angelucci, C. A.; Deiner, L. J.; Nart, F. C. *J. Solid State Electrochem.* **2008**, *12*, 1599–1603.
42. Foresman, J. B.; Frisch, Æ. *Exploring Chemistry with Electronic Structure Methods*, 2nd ed; Gaussian, Inc.: Pittsburgh, PA, **1996**, p 302.
43. Koper, M. T. M. *Faraday Discuss.* **2009**, *140*, 11–24.
44. Crispin, X.; Geskin, V.; Bureau, C.; *et al. J. Chem. Phys.* **2001**, *115*, 10493–10499.
45. Wasileski, S.; Koper, M.; Weaver, M. *J. Chem. Phys.* **2001**, *115*, 8193–8203.
46. Blanco, R.; Orts, J. M. *Electrochim. Acta* **2008**, *53*, 7796–7804.
47. Norskov, J.; Rossmeisl, J.; Logadottir, A.; *et al. J. Phys. Chem. B* **2004**, *108*, 17886–17892.
48. Rossmeisl, J.; Logadottir, A.; Norskov, J. *Chem. Phys.* **2005**, *319*, 178–184.
49. Taylor, C. D.; Wasileski, S. A.; Filhol, J. S.; Neurock, M. *Phys. Rev. B* **2006**, *73*, 165402–165417.
50. Filhol, J. S.; Neurock, M. *Angew. Chem. Int. Ed.* **2006**, *45*, 402–406.
51. Karlberg, G.; Rossmeisl, J.; Norskov, J. *Phys. Chem. Chem. Phys.* **2007**, *9*, 5158–5161.
52. Skulason, E.; Bligaard, T.; Gudmundsdottir, S.; *et al. Phys. Chem. Chem. Phys.* **2012**, *14*, 1235–1245.
53. Peterson, A.; Abild-Pedersen, F.; Studt, F.; Rossmeisl, J.; Norskov, J. *Energy Environ. Sci.* **2010**, *3*(9), 1311–1315.
54. Rossmeisl, J.; Qu, Z. W.; Zhu, H.; Kroes, G. J.; Norskov, J. K. *J. Electroanal. Chem.* **2007**, *607*, 83–89.
55. Wasileski, S.; Koper, M.; Weaver, M. *J. Phys. Chem. B* **2001**, *105*, 3518–3530.
56. Wasileski, S.; Weaver, M.; Koper, M. *J. Electroanal. Chem.* **2001**, *500*, 344–355.
57. *CAMPOS*: Center for Atomic-Scale Materials Design –Wiki. Available at: http://wiki.fysik.dtu.dk/ (accessed on 22 January 2013).
58. O'Boyle, N.. Linux4Chemistry. Available at: http://www.redbrick.dcu.ie/~noel/linux4chemistry (accessed on 22 January 2013).
59. Neurock, M.; Janik, M.; Wieckowski, A. *Faraday Discuss.* **2008**, *140*, 363–378.
60. Kirchner, B.; di Dio, P.; Hutter, J. Real-World Predictions from Ab Initio Molecular Dynamics Simulations. In *Multiscale Molecular Methods in Applied Chemistry*; Kirchner, B., Vrabec, J., Eds.; Springer: Berlin, **2012**, Vol. 307; pp 109–154.
61. VandeVondele, J.; Lynden-Bell, R.; Meijer, E. J.; Sprik, M. *J. Phys. Chem. B* **2006**, *110*, 3614–3623.
62. Cheng, J.; Sulpizi, M.; Sprik, M. *J. Chem. Phys.* **2009**, *131*, 154504–154523.
63. Schiffmann, F.; Hutter, J.; VandeVondele, J. *J. Phys.: Condens. Matter* **2008**, *20*, 064206–064213.
64. Schiffmann, F.; VandeVondele, J.; Hutter, J.; *et al. Proc. Natl. Acad. Sci. USA* **2010**, *107*, 4830–4833.
65. Miertus, S.; Fassina, G. *Combinatorial Chemistry and Technology [electronic resource]: Principles, Methods, and Applications*; Marcel Dekker: New York, **1999**.
66. Yoshida, J.-i.; Kataoka, K.; Horcajada, R.; Nagaki, A. *Chem. Rev.* **2008**, *108*, 2265–2299.
67. Muster, T. H.; Trinchi, A.; Markley, T. A.; *et al. Electrochim. Acta* **2011**, *56*(27), 9679–9699.
68. Potyrailo, R.; Rajan, K.; Stoewe, K.; *et al. ACS Comb. Sci.* **2011**, *13*, 579–633.
69. Reddington, E.; Sapienza, A.; Gurau, B.; *et al. Science* **1998**, *280*, 1735–1737.
70. Baeck, S. H.; Jaramillo, T. F.; Brändli, C.; McFarland, E. W. *J. Comb. Chem.* **2002**, *4*, 563–568.
71. Kulikov, V.; Mirsky, V. M. *Meas. Sci. Technol.* **2004**, *15*, 49–54.
72. Kulikov, V.; Mirsky, V. M.; Delaney, T. L.; *et al. Meas. Sci. Technol.* **2005**, *16*, 95–99.
73. Siu, T.; Li, W.; Yudin, A. K. *J. Comb. Chem.* **2000**, *2*, 545–549.
74. Siu, T.; Li, W.; Yudin, A. K. *J. Comb. Chem.* **2001**, *3*, 554–558.
75. Yudin, A. K.; Siu, T. *Curr. Opin. Chem. Biol.* **2001**, *5*(3), 269–272.
76. Yudin, A. K.; Siu, T.; Li, W. Spatially addressable electrolysis platform and methods of use. WO200194666-A; EP1292388-A; US2004094407-A1; **2003**.
77. Chan, B. C.; Liu, R. X.; Jambunathan, K.; *et al. J. Electrochem. Soc.* **2005**, *152*, A594–A600.
78. Liu, R. X.; Smotkin, E. S. *J. Electroanal. Chem.* **2002**, *535*, 49–55.
79. Guerin, S.; Hayden, B. E.; Lee, C. E.; *et al. J. Comb. Chem.* **2004**, *6*, 149–158.
80. Jiang, R. Z.; Rong, C.; Chu, D. *J. Comb. Chem.* **2005**, *7*, 272–278.
81. Nayar, A.; Liu, R.; Willis, R.R.; Smotkin, E.S. Apparatus for screening e.g. catalysts in an array, Comprises fluid permeable array support aligned with a window of reaction cell, semipermeable membrane, and a location selective heat source. US6923939-B1.
82. Tornow, C. E.; Thorson, M. R.; Ma, S.; Gewirth, A. A.; Kenis, P. J. A. *J. Am. Chem. Soc.* **2012**, *134*, 19520–19523.
83. Kamerzell, T. J.; Esfandiary, R.; Joshi, S. B.; Middaugh, C. R.; Volkin, D. B. *Adv. Drug Delivery Rev.* **2011**, *63*, 1118–1159.
84. Binning, G.; Rohrer, H.; Gerber, C.; Weibel, E. *Phys. Rev. Lett.* **1982**, *49*, 57–61.
85. The Nobel Prize in Physics. Available at: http://www.nobelprize.org/nobel_prizes/physics/laureates/1986/ (accessed on 5 March 2013).
86. Kroto, H. W.; Heath, J. R.; Obrien, S. C.; Curl, R. F.; Smalley, R. E. *Nature* **1985**, *318*, 162–163.
87. The Nobel Prize in Physics. Available at: http://www.nobelprize.org/nobel_prizes/chemistry/laureates/1996/ (accessed on 5 March 2013).
88. Guo, S.; Wen, D.; Zhai, Y.; Dong, S.; Wang, E. *ACS Nano* **2010**, *4*, 3959–3968.
89. Wang, L.; Xu, L.; Kuang, H.; Xu, C.; Kotov, N. A. *Acc. Chem. Res.* **2012**, *45*, 1916–1926.
90. Cuenya, B. R. *Thin Solid Films* **2010**, *518*, 3127–3150.
91. Ramgir, N. S.; Yang, Y.; Zacharias, M. *Small* **2010**, *6*, 1705–1722.
92. Kamat, P. V. *J. Phys. Chem. C* **2008**, *112*, 18737–18753.
93. Kamat, P. V. *Acc. Chem. Res.* **2012**, *45*, 1906–1915.

94. Sgobba, V.; Guldi, D. M. *Chem. Soc. Rev.* **2009**, *38*, 165–184.
95. Tan, C. W.; Tan, K. H.; Ong, Y. T.; *et al. Environ. Chem. Lett.* **2012**, *10*, 265–273.
96. Jacobs, C. B.; Peairs, M. J.; Venton, B. J. *Anal. Chim. Acta* **2010**, *662*, 105–127.
97. Perez-Lopez, B.; Merkoci, A. *Microchim. Acta* **2012**, *179*, 1–16.
98. Dai, L.; Chang, D. W.; Baek, J.-B.; Lu, W. *Small* **2012**, *8*, 1130–1166.
99. Liu, J.; Xue, Y.; Zhang, M.; Dai, L. *MRS Bull.* **2012**, *37*, 1265–1272.
100. Reddy, A. L. M.; Gowda, S. R.; Shaijumon, M. M.; Ajayan, P. M. *Adv. Mater.* **2012**, *24*, 5045–5064.
101. Cullinan, M. A.; Panas, R. M.; DiBiasio, C. M.; Culpepper, M. L. *Sens. Actuators, A* **2012**, *187*, 162–173.
102. Liu, G.; Wang, K.; Hoivik, N.; Jakobsen, H. *Sol. Energy Mater. Sol. Cells* **2012**, *98*, 24–38.
103. Thiam, H. S.; Daud, W. R. W.; Kamarudin, S. K.; *et al. Int. J. Hydrogen Energy* **2011**, *36*, 3187–3205.
104. Dulic, D.; van der Molen, S. J.; Kudernac, T.; *et al. Phys. Rev. Lett.* **2003**, *91*, 207402–207405.
105. Kim, Y.; Hellmuth, T. J.; Sysoiev, D.; *et al. Nano Lett.* **2012**, *12*, 3736–3742.
106. Odell, A.; Delin, A.; Johansson, B.; Rungger, I.; Sanvito, S. *ACS Nano* **2010**, *4*, 2635–2642.
107. He, J.; Chen, F.; Liddell, P. A.; *et al. Nanotechnology* **2005**, *16*, 695–702.
108. Guo, C. X.; Yang, H. B.; Sheng, Z. M.; *et al. Angew. Chem. Int. Ed.* **2010**, *49*, 3014–3017.
109. Boggs, B. K.; King, R. L.; Botte, G. G. *Chem. Commun.* **2009**, *45*, 4859–4861.
110. Daramola, D. A.; Singh, D.; Botte, G. G. *J. Phys. Chem. A* **2010**, *114*, 11513–11521.
111. King, R. L.; Botte, G. G. *J. Power Sources* **2011**, *196*, 2773–2778.
112. King, R. L.; Botte, G. G. *J. Power Sources* **2011**, *196*, 9579–9584.
113. Yan, W.; Wang, D.; Botte, G. G. *Electrochim. Acta* **2012**, *61*, 25–30.
114. Vedharathinam, V.; Botte, G. G. *Electrochim. Acta* **2012**, *81*, 292–300.
115. Wang, D.; Yan, W.; Vijapur, S. H.; Botte, G. G. *J. Power Sources* **2012**, *217*, 498–502.
116. Wang, D.; Yan, W.; Botte, G. G. *Electrochem. Commun.* **2011**, *13*, 1135–1138.
117. Popovtzer, R.; Neufeld, T.; Biran, N.; *et al. Nano Lett.* **2005**, *5*, 1023–1027.
118. Gasteiger, H. A.; Kocha, S. S.; Sompalli, B.; Wagner, F. T. *Appl. Catal. B* **2005**, *56*, 9–35.
119. Carmo, M.; Dos Santos, A. R.; Poco, J. G. R.; Linardi, M. *J. Power Sources* **2007**, *173*, 860–866.
120. Lin, M.-L.; Huang, C.-C.; Lo, M.-Y.; Mou, C.-Y. *J. Phys. Chem. C* **2008**, *112*, 867–873.
121. Prabhuram, J.; Zhao, T. S.; Liang, Z. X.; Chen, R. *Electrochim. Acta* **2007**, *52*, 2649–2656.
122. Santasalo-Aarnio, A.; Borghei, M.; Anoshkin, I. V.; *et al. Int. J. Hydrogen Energy* **2012**, *37*, 3415–3424.
123. Zhou, C.; Peng, F.; Wang, H.; *et al. Fuel Cells* **2011**, *11*, 301–308.
124. Qiu, H.; Zou, F. *ACS Appl. Mater. Interfaces* **2012**, *4*, 1404–1410.
125. Gu, D.-M.; Chu, Y.-Y.; Wang, Z.-B.; *et al. Appl. Catal. B* **2011**, *102*, 9–18.
126. Guo, S.; Fang, Y.; Dong, S.; Wang, E. *J. Phys. Chem. C* **2007**, *111*, 17104–17109.
127. Feng, L.; Gao, G.; Huang, P.; *et al. Nanoscale Res. Lett.* **2011**, *6*, 551–560.
128. Tang, W.; Peterson, A. A.; Varela, A. S.; *et al. Phys. Chem. Chem. Phys.* **2012**, *14*(1), 76–81.
129. Li, C. W.; Kanan, M. W. *J. Am. Chem. Soc.* **2012**, *134*, 7231–7234.
130. Gattrell, M.; Gupta, N.; Co, A. *J. Electroanal. Chem.* **2006**, *594*, 1–19.
131. Spinner, N. S.; Vega, J. A.; Mustain, W. E. *Catal. Sci. Technol.* **2012**, *2*, 19–28.
132. Furukawa, H.; Ko, N.; Go, Y. B.; *et al. Science* **2010**, *329*, 424–428.
133. Benson, E. E.; Kubiak, C. P.; Sathrum, A. J.; Smieja, J. M. *Chem. Soc. Rev.* **2009**, *38*, 89–99.
134. Inglis, J. L.; MacLean, B. J.; Pryce, M. T.; Vos, J. G. *Coord. Chem. Rev.* **2012**, *256*, 2571–2600.
135. Itaya, K. *Prog. Surf. Sci.* **1998**, *58*, 121–247.
136. Tao, N. J.; Li, C. Z.; He, H. X. *J. Electroanal. Chem.* **2000**, *492*, 81–93.
137. Diez-Perez, I.; Sanz, F.; Gorostiza, P. *Curr. Opin. Solid State Mater. Sci.* **2006**, *10*, 144–152.
138. Borgese, L.; Zanola, P.; Bontempi, E.; Rossi, D.; Depero, L. E. *J. Coating. Tech. Res.* **2010**, *7*, 691–695.
139. De Marco, R.; Veder, J.-P. *Trends Analyt. Chem.* **2010**, *29*, 528–537.
140. Wasmus, S.; Kuver, A. *J. Electroanal. Chem.* **1999**, *461*, 14–31.
141. Tian, Z. Q.; Ren, B. *Annu. Rev. Phys. Chem.* **2004**, *55*, 197–229.
142. Li, J.-T.; Zhou, Z.-Y.; Broadwell, I.; Sun, S.-G. *Acc. Chem. Res.* **2012**, *45*, 485–494.
143. Nedoseykina, T.; Kim, M. G.; Park, S.-A.; *et al. Electrochim. Acta* **2010**, *55*, 8876–8882.
144. Kavan, L.; Dunsch, L. *ChemPhysChem* **2011**, *12*, 47–55.
145. Fernandez-Blanco, C.; Colina, A.; Heras, A.; Ruiz, V.; Lopez-Palacios, J. *Electrochem. Commun.* **2012**, *18*, 8–11.
146. Herranz, T.; Garcia, S.; Martinez-Huerta, M. V.; *et al. Int. J. Hydrogen Energy* **2012**, *37*, 7109–7118.
147. Yang, Y.-Y.; Ren, J.; Zhang, H.-X.; *et al. Langmuir* **2013**, *29*, 1709–1716.
148. Innocent, B.; Pasquier, D.; Ropital, F.; *et al. Appl. Catal. B* **2010**, *94*(3–4), 219–224.
149. Fogler, H. S. *Elements of Chemical Reaction Engineering*, 3rd ed.; Prentice Hall PTR: Upper Saddle River, N.J., **1999**, p 16.
150. Paddon, C. A.; Atobe, M.; Fuchigami, T.; *et al. J. Appl. Electrochem.* **2006**, *36*(6), 617–634.
151. Bard, A. J.; Faulkner, L. R. *Electrochemical Methods: Fundamentals and Applications*, 2nd ed.; Wiley: New York, **2001**, pp 28-30.
152. Jalbout, A. F.; Zhang, S. H. *Acta Chim. Slov.* **2002**, *49*, 917–923.
153. Belmont, C.; Girault, H. H. *Electrochim. Acta* **1995**, *40*, 2505–2510.
154. Ziogas, A.; Kolb, G.; O'Connell, M.; *et al. J. Appl. Electrochem.* **2009**, *39*(12), 2297–2313.
155. Bouzek, K.; Jiricny, V.; Kodym, R.; Krist'al, J.; Bystron, T. *Electrochim. Acta* **2010**, *55*(27), 8172–8181.
156. Krist'al, J.; Kodym, R.; Bouzek, K.; Jiricny, V.; Hanika, J. *Ind. Eng. Chem. Res.* **2012**, *51*, 1515–1524.
157. Zimmerman, W. B. *Chem. Eng. Sci.* **2011**, *66*, 1412–1425.
158. Grinberg, V. A.; Skundin, A. M. *Russ. J. Electrochem.* **2010**, *46*, 963–978.
159. Zhao, T. S.; Xu, C.; Chen, R.; Yang, W. W. *Prog. Energy Combust. Sci.* **2009**, *35*(3), 275–292.
160. Schultze, J. W.; Tsakova, V. *Electrochim. Acta* **1999**, *44*, 3605–3627.
161. Attour, A.; Rode, S.; Ziogas, A.; Matlosz, M.; Lapicque, F. *J. Appl. Electrochem.* **2008**, *38*, 339–347.
162. Attour, A.; Rode, S.; Lapicque, F.; Ziogas, A.; Matlosz, M. *J. Electrochem. Soc.* **2008**, *155*, E201–E206.
163. Horii, D.; Atobe, M.; Fuchigami, T.; Marken, F. *Electrochem. Commun.* **2005**, *7*, 35–39.
164. Neburchilov, V.; Martin, J.; Wang, H.; Zhang, J. *J. Power Sources* **2007**, *169*, 221–238.
165. Yunphuttha, C.; Bunjongpru, W.; Porntheeraphat, S.; *et al. Chem. Papers* **2012**, *66*, 1137–1145.
166. Majedi, F. S.; Hasani-Sadrabadi, M. M.; Emami, S. H.; *et al. Chem. Commun.* **2012**, *48*, 7744–7746.

167. Xu, C.; He, Y. L.; Zhao, T. S.; Chen, R.; Ye, Q. *J. Electrochem. Soc.* **2006**, *153*, A1358–A1364.
168. Yang, H.; Zhao, T. S. *Electrochim. Acta* **2005**, *50*, 3243–3252.
169. CRC. *Handbook of Chemistry and Physics*, 93rd ed.; Taylor & Francis: Boca Raton, FL, **2012**.
170. Mul, G.; Schacht, C.; van Swaaij, W. P. M.; Moulijn, J. A. *Chem. Eng. Process* **2012**, *51*, 137–149.
171. Hara, K.; Tsuneto, A.; Kudo, A.; Sakata, T. *J. Electrochem. Soc.* **1994**, *141*, 2097–2103.
172. Dufek, E. J.; Lister, T. E.; Stone, S. G.; McIlwain, M. E. *J. Electrochem. Soc.* **2012**, *159*, F514–F517.
173. Koleli, F.; Atilan, T.; Palamut, N.; *et al. J. Appl. Electrochem.* **2003**, *33*, 447–450.
174. Centi, G.; Perathoner, S.; Wine, G.; Gangeri, M. *Green Chem.* **2007**, *9*, 671–678.
175. Subramanian, K.; Asokan, K.; Jeevarathinam, D.; Chandrasekaran, M. *J. Appl. Electrochem.* **2007**, *37*, 255–260.
176. Whipple, D. T.; Finke, E. C.; Kenis, P. J. A. *Electrochem. Solid State Lett.* **2010**, *13*, D109–D111.
177. Sun, R.; Cubaud, T. *Lab Chip* **2011**, *11*, 2924–2928.
178. Cubaud, T.; Sauzade, M.; Sun, R. *Biomicrofluidics* **2012**, *6*, 022002–022010.
179. Wang, H.; Leung, D. Y. C.; Xuan, J. *Appl. Energy* **2013**, *102*, 1057–1062.
180. Kakac, S.; Pramuanjaroenkij, A.; Zhou, X. Y. *Intl. J. Hydrogen Energy* **2007**, *32*, 761–786.
181. Newman, J. S.; Thomas-Alyea, K. E. *Electrochemical Systems*, 3rd ed.; J. Wiley: Hoboken, NJ, **2004**.
182. Santhanagopalan, S.; White, R. E. Electrocatalytic reactor design. In *Electrocatalysis: Computational, experimental, and industrial aspects*; Zinola, C. F., Ed.; Taylor & Francis: Boca Raton, **2010**, pp 417–441.
183. Ma, L.; Ingham, D. B.; Pourkashanian, M.; Carcadea, E. *J. Fuel Cell Sci. Tech.* **2005**, *2*, 246–257.
184. Le, A. D.; Zhou, B. *J. Power Sources* **2008**, *182*, 197–222.
185. Le, A. D.; Zhou, B. *J. Power Sources* **2009**, *193*, 665–683.
186. Omran, M. P.; Farhadi, M.; Sedighi, K. *J. Fuel Cell Sci. Tech.* **2011**, *8*, 061004–061011.
187. DiGiuseppe, G.; Gowda, Y. J.; Honnagondanahalli, N. K.; Two-Dimensional, A. *J. Fuel Cell Sci. Tech.* **2012**, *9*, 011016–011027.
188. Stockmann, T. J.; Ding, Z. *Phys. Chem. Chem. Phys.* **2012**, *14*, 13949–13954.
189. Martinez-Lopez, J. I.; Moncada-Hernandez, H.; Baylon-Cardiel, J. L.; *et al. Anal. Bioanal. Chem.* **2009**, *394*, 293–302.
190. Euzen, J.-P.; Trambouze, P.; Wauquier, J.-P. *Scale-up Method for Chemical Processes*; Gulf Pub. Co.: Houston, TX, **1993**, pp 9-24.
191. Bisio, A. Introduction to Scaleup. In *Scaleup of Chemical Processes: Conversion from Laboratory Scale Tests to Successful Commerical Size Design*; Bisio, A., Kabel, R. L., Eds.; Wiley: New York, **1985**, pp 1–33.
192. Wendt, H.; Kreysa, G. *Electrochemical Engineering: Science and Technology in Chemical and Other Industries*; Springer: Berlin, **1999**, p 347.
193. Aerstin, F. G.; Robbins, L. A.; Vogel, A. J. Gaining Experience Through Pilot Plants and Demonstration Units. In *Scaleup of Chemical Processes: Conversion from Laboratory Scale Tests to Successful Commercial Size Design*; Bisio, A., Kabel, R. L., Eds.; Wiley: New York, **1985**, pp 655-676.
194. Prentice, G. *Electrochemical Engineering Principles*; Prentice Hall: Englewood Cliffs, NJ, **1991**, pp 261–262.
195. Chemstations Inc., CHEMCAD Version 6 User Guide. Chemstations, Inc.: Houston, Texas, USA **2011**, pp 109–110.
196. Aspen Technology Inc., Aspen Plus User Guide Version 10.2. Cambridge, MA: Aspen Technology, Inc., **2000**, pp 19-1–19-18.
197. Palsson, J.; Selimovic, A.; Sjunnesson, L. *J. Power Sources* **2000**, *86*, 442–448.
198. Barelli, L.; Bidini, G.; Gallorini, F.; Ottauiano, A. *Int. J. Hydrogen Energy* **2011**, *36*, 10434–10442.
199. Orecchini, F.; Bocci, E.; Di Carlo, A. *J. Fuel Cell Sci. Tech.* **2008**, *5*, 021015–021023.
200. Di Carlo, A.; Bocci, E.; Dell'Era, A. *Intl. J. Hydrogen Energy* **2011**, *36*, 7976–7984.
201. ICIS. Adiponitrile (ADN). Available at: http://www.icis.com/Articles/2000/05/01/112189/adiponitrile-adn.html (accessed on 22 March 2013).
202. ICIS. Adiponitrile. Available at: http://www.icis.com/Articles/2005/04/01/665143/adiponitrile.html (accessed on 22 March 2013).
203. PCI Nylon. Adiponitrile. Available at: http://pcinylon.com/index.php/markets-covered/adiponitrile (accessed on 22 March 2013).
204. Pletcher, D.; Walsh, F. C. *Industrial Electrochemistry*, 2nd ed.; Chapman and Hall: London, **1990**.
205. Qian, W. M.; Wilkinson, D. P.; Shen, J.; Wang, H. J.; Zhang, J. J. *J. Power Sources* **2006**, *154*, 202–213.
206. Lamy, C.; Lima, A.; LeRhun, V.; *et al. J. Power Sources* **2002**, *105*, 283–296.
207. Lamy, C.; Belgsir, E.; Leger, J. *J. Appl. Electrochem.* **2001**, *31*, 799–809.
208. Reid, R. C.; Prausnitz, J. M.; Poling, B. E. *The Properties of Gases and Liquids*, 4th ed.; McGraw-Hill: New York, **1987**.
209. Dean, J. A. *Lange's Handbook of Chemistry*, 15th ed.; McGraw-Hill: New York, **1999**.

9.15 Synthetic Biology Approaches for Organic Synthesis

PS Coelho and FH Arnold, California Institute of Technology, Pasadena, CA, USA
JC Lewis, University of Chicago, Chicago, IL, USA

© 2014 Elsevier Ltd. All rights reserved.

9.15.1	**Introduction**	390
9.15.2	**Enabling Technologies**	391
9.15.2.1	DNA Sequencing and Synthesis	391
9.15.2.2	Metagenomics and Bioinformatics	391
9.15.2.3	Protein Expression	393
9.15.3	**Enzyme Engineering**	393
9.15.3.1	Oxygenation	393
9.15.3.2	Halogenation	395
9.15.3.3	Dehydrogenation	395
9.15.3.4	Hydrogenation	397
9.15.3.5	Group Transfers	398
9.15.3.6	Hydrolysis and Condensation	399
9.15.3.7	Nonoxidative, Nonhydrolytic Bond Formation	400
9.15.3.8	Summary	403
9.15.4	**Metabolic Engineering**	403
9.15.4.1	Isoprenoids	403
9.15.4.1.1	Isoprene	404
9.15.4.1.2	Artemisinin	405
9.15.4.1.3	Taxol	407
9.15.4.1.4	Levopimaradiene	407
9.15.4.2	Steroids	410
9.15.4.3	Amino Acids	410
9.15.4.4	Diamines	412
9.15.4.5	Alcohols	412
9.15.4.6	Diols	414
9.15.4.7	Summary	415
9.15.5	**Beyond Nature: Design and Evolution of Artificial Function/Catalysis**	417
Acknowledgments		418
References		418

Glossary

Bioinformatics The study of methods for storing, retrieving, and analyzing biological data such as DNA, RNA, and protein sequence, structure, function, pathways, and genetic interactions.

Directed evolution A systematic algorithm of mutation and selection for improvements in the properties of a biological entity, such as an enzyme, a metabolic pathway, or a whole organism.

Heterologous protein expression Expression of a gene coding for a protein not natively produced by the production host.

Metabolic engineering Genetic alteration of metabolism to produce molecules of interest.

Metagenomics The study of genetic material recovered directly from environmental samples.

Operon A functioning unit of genomic DNA containing a cluster of genes under the control of a single promoter.

Recombinant (metabolic) pathway An artificial (metabolic) pathway created by combining one or more enzymes foreign to the host organism.

Synthetic biology Forward engineering of genetic material (genes, promoters, operons, genomes) encoding an artificial function.

9.15.1 Introduction

As the volumes of this collection illustrate, synthetic chemists have devised a powerful arsenal of chemical reactions – one that is often, if colloquially, claimed to enable the synthesis of any desired molecule given enough time. This factor, time, along with measures of material and energy economy, largely determines the efficiency, and thus utility, of chemical syntheses. Developing new catalysts, reactions, and functional molecules remains a time-intensive endeavor, and the costs of energy and material inputs along with waste from syntheses continue to increase as the global population swells and resources become more limited. Barring the removal of these pressures, advances in the ability to assemble molecules are essential.

 doi:10.1016/B978-0-08-097742-3.00931-9

Systematic and highly efficient approaches to the construction of molecular complexity have evolved in response to analogous supply and demand challenges over four billion years of natural selection. The emergence of myriad biocatalysts ultimately enabled the generation of the seemingly infinite array of natural products that inspire chemists (and provide immense human benefits). The efficiency of these evolved catalytic systems is typically far greater than that of any synthetic systems generated in the short 200 years of modern chemistry. This has driven extensive efforts to mimic these systems for synthetic applications, but stripping systems down to their simplest forms rarely replicates the levels of efficiency and selectivity that are the hallmarks of biology.

More recently, increased understanding of biology has allowed researchers to begin to harness the capabilities of biological catalysts, including enormous catalyst diversity, molecular recognition, selection, and evolution, for chemical synthesis. Furthermore, it is no longer limited to whole-cell or enzyme catalysts isolated from nature or cultured in the laboratory, but can readily modify these systems to suit the purposes. Efforts toward this end have taken many names over the course of their development, but are now encompassed by the umbrella term 'synthetic biology.' This review summarizes some key technologies and examples from this field, with the goal of illustrating how synthetic biology is already a powerful tool that can be used alongside and, increasingly, in place of conventional synthetic methods.

9.15.2 Enabling Technologies

9.15.2.1 DNA Sequencing and Synthesis

Since chemical function in biocatalysts is encoded and engineered at the DNA level, the ability to build systems for chemical synthesis is greatly influenced by technologies that enable efficient manipulation and analysis of genetic information. Reductions in the cost of DNA sequencing have outpaced Moore's law (a doubling in microprocessor computing power every 2 years), especially following the transition from Sanger-based (dideoxy chain termination sequencing) capillary electrophoresis sequencing to second-generation ('massively parallel') technologies in the mid-2000s.[1] Several competing massively parallel sequencing technologies have been brought to market, including but not limited to pyrosequencing (Roche/454), sequencing-by-ligation (Life Technologies), sequencing-by-synthesis (Illumina), optical single-molecule sequencing (Pacific Biosciences), and nanopore technology (Oxford Nanopore). All the massively parallel technologies differ significantly from Sanger capillary sequencing in that they occur in a nucleotide-by-nucleotide stepwise fashion, eliminating the need for discrete separation and detection of Sanger sequencing reaction products on a capillary instrument. An entire human genome can now be sequenced in a matter of hours for less than US $1000 (a dramatic reduction from US $700 000 000 in 2002).[2] This revolution in genomics has now made whole-genome sequencing experiments routine and has enabled initiatives to sequence entire ecosystems.[3]

The ability to chemically synthesize sequences of DNA greatly facilitates production and optimization of genetically encoded products. DNA synthesis capabilities have also improved at an exponential pace.[4] Synthetic oligonucleotides have been available for 20 years, and synthetic genes built commercially from those 'oligos' for the last 10 years. The ability to synthesize increasingly longer stretches of DNA is improving rapidly as evidenced from the following milestone 'firsts:' a synthetic gene in 1979 (207 base pairs, bp), a synthetic plasmid in 1990 (2100 bp), and a synthetic genome in 2008 (583 000 bp).[5] Because total chemical synthesis remains limited to relatively short DNA molecules (<200 nucleotides), novel enzymatic methods have been developed to assemble synthetic oligos into the desired DNA duplex length.[6] These methods can be broadly categorized as restriction enzyme-dependent or sequence-independent overlap techniques, either of which may be employed depending on the gene of interest.[7] *De novo* synthesis of entire genomes requires assembly at the chromosomal scale, which can be achieved by *in vivo* recombination in yeast or *Bacillus* by making use of native recombination mechanisms.[8] For example, in the 580 kb synthesis for the genome of *Mycoplasma genitalium*, *in vitro* recombination was used to assemble 101 overlapping cassettes each 5–7 kb in length into four DNA fragments of 144 kb, which were subsequently assembled into the complete genome by *in vivo* recombination in yeast.[5c] *De novo* DNA synthesis is a key enabling technology for synthetic biology because it permits access to arbitrary genes and even whole biosynthetic pathways directly from digital information (DNA sequences from databases), thus bypassing the need to clone genetic material from biological samples.

9.15.2.2 Metagenomics and Bioinformatics

Nature presents an immense collection of genes encoding biocatalysts that can be directly applied in chemical syntheses. The most diverse source of biocatalysts in nature is arguably the prokaryotes (archaea and bacteria), comprising millions of species that display an extraordinary diversity of niche, habitat range, and metabolisms.[9] However, genomic information for approximately 6000 prokaryotic species is only available in commercial culture collections, and it is estimated that 99% of all microorganisms may be recalcitrant to cultivation. Although it is not possible to characterize the enzymes and small molecules produced by uncultured bacteria using traditional microbiological methods, it is possible to extract microbial DNA directly from an environmental sample and clone this DNA into easily cultured bacteria. The utility of this approach for the discovery of novel biocatalysts and small molecules has been extensively reviewed.[10] In short, these 'metagenomic' libraries can be analyzed by the following two general strategies: (1) functional screening, which requires the heterologous expression of environmental DNA in a model cultured host to yield a phenotype of interest and (2) homology screening, which relies on DNA sequence similarity to identify genes of interest.

The first approach typically uses one of these three classes of functional screens: (1) direct readout assays, (2) reporter genes, and (3) complementation. Direct readout assays are applicable when the enzyme reaction product can be coupled to a spectroscopic signal or to the formation of a halo around the clone encoding the gene for the desired enzyme. For example, halo formation resulting from tributyrin ester hydrolysis in agar plates was used to screen a metagenomic library from the Antarctic desert soil that led to the discovery of a cold-active alkaliphilic esterase only distantly related to reported lipases.[11] Reporter genes may be used in special cases where the enzymatic product is known to elicit a response from a transcription factor. For example, a benzoate-sensitive transcription factor controlling green fluorescent protein expression was used to identify 11 amidases distantly related to known amidases from a wastewater sludge metagenomic library based on their activity on benzamide.[12] Genetic complementation assays may also be used, with very high throughput. Genencor–DuPont screened metagenomic libraries for a novel glycerol dehydratase that catalyzes the bottleneck reaction in the heterologous fermentation pathway to make 1,3-propanediol from sugars (see Section 9.15.4.6).[13] The complementation screen was based on an *Escherichia coli* strain that contained and expressed all genes necessary for anaerobic glycerol breakdown except the gene coding for glycerol dehydratase. The only way for such a strain to survive under anaerobic conditions with glycerol as the sole carbon and energy source is complementation by a gene that confers the glycerol or diol dehydratase activity. Out of the 560 000 *E. coli* clones tested two were found to contain active dehydratases with superior properties.[13]

Novel enzymes can also be identified from their sequence similarity to enzymes that possess the desired activity. This homology-based screening can be carried out *in vitro*, using polymerase chain reaction (PCR) and colony hybridization, or *in silico*, using bioinformatics. This approach is particularly suited for studying the production of secondary metabolites in prokaryotes, since the genes involved are typically clustered on the chromosomes. For example, homology screening was used to identify gene clusters associated with the biosynthesis of natural products derived from bacteria that exist in symbiosis with animals, including medicinally important pederins and patellamides.[14] Ultimately, heterologous expression of the gene clusters provides a renewable source of these compounds, which could not otherwise be isolated in sufficient quantities to permit extensive biological testing.

'Synthetic metagenomics' is another form of sequence-based screening that builds on advances in gene synthesis and bioinformatics. Several free web-based bioinformatics tools are available for aiding experimental design (**Table 1**). For example, the NCBI sequence database, which comprises both cultured and uncultured genomes, can be used to identify genes that are similar to a given enzyme gene. These genes can be optimized for expression in a particular heterologous host, chemically synthesized, cloned, and expressed in the selected host. This approach was used for the discovery and characterization of methyl halide transferases, which catalyze the transfer of a methyl group from the ubiquitous metabolite *S*-adenosyl methionine (SAM) to a halide ion.[15] A BLAST search of the NCBI database using known methyl chloride transferases yielded 89 putative methyl halide transferases from sources spanning the biological kingdoms, with a remarkable degree of sequence diversity (average of 28% amino acid identity between sequences). These genes were codon-optimized, expressed in *E. coli*, and analyzed for methyl halide

Table 1 A compilation of generally useful publicly available bioinformatic tools and resources

Database	*URL*	*Description*
Genbank – National Center for Biotechnology Information (NCBI)	http://www.ncbi.nlm.nih.gov/genbank/	Annotated collection of all publicly available DNA sequences
Basic Local Alignment Search Tool (BLAST) – NCBI	http://blast.ncbi.nlm.nih.gov/Blast.cgi	Compares a query sequence with a database of nucleotide or amino acid sequences
BRENDA Enzyme Database	http://www.brenda-enzymes.info/	Kinetic, thermodynamic, structural, and reaction information for enzymes
Kyoto Encyclopedia of Genes and Genomes(KEGG)	http://www.genome.jp/kegg/	Searchable metabolic pathway maps for various organisms
DR Nelson Cytochrome P450	http://drnelson.uthsc.edu/CytochromeP450.html	Reference for over 11 500 CYPs
eQuilibrator	http://equilibrator.weizmann.ac.il/	Computation of thermodynamic parameters for enzymatic reactions and metabolic pathways
Genome News Network (GNN)	http://www.genomenewsnetwork.org/	Updates on developments in genomics research
American Type Culture Collection (ATCC)	http://www.atcc.org/	Source of microbial strains, vectors, genomic, and cDNA libraries
FoldX	http://foldx.crg.es/	Estimates the contributions of mutations/interactions to the stabilities of proteins and protein complexes
Encyclopedia of *E. coli* K-12 genes and metabolism (EcoCyc)	http://ecocyc.org/	Transcriptional regulators, transporters, metabolic pathways; flux balance metabolic model
YeastCyc	http://pathway.yeastgenome.org/	152 metabolic pathways from *S. cerevisiae*
MetaCyc	http://biocyc.org/metacyc/index.shtml	1877 metabolic pathways from 2263 organisms
GLAMM	http://glamm.lbl.gov/	Regulation of metabolic pathways under a range of environmental conditions
Gene Designer (DNA 2.0)	https://www.dna20.com/genedesigner2/	Codon optimization of genes for heterologous expression

synthesis. More than half were active on halides ($X^- = Cl^-$, Br^-, and I^-), and subsequent engineering of the most active methyl halide transferase in *Sacchaoromyces cerevisiae* resulted in fermentative production of methyl halides from glucose with a volumetric productivity of 190 mg l^{-1} h^{-1}.[15]

9.15.2.3 Protein Expression

Once a gene encoding an enzyme of interest is identified, it must be expressed by some organism in a functional form. Expression level targets differ depending on whether the enzyme is used to catalyze a reaction in isolation or in the context of a well-balanced metabolic pathway. For example, metabolic engineering requires precise relative control of the expression of several enzymes (as opposed to the overexpression of a single enzyme) to prevent the accumulation of potentially toxic intracellular intermediates and to prevent the diversion of carbon and energy to other products. Expression levels must be carefully tuned rather than simply maximized to ensure high flux through the target pathway. This has been accomplished by varying the gene copy number, altering promoter sequences, and utilizing designer transcription factors.[16]

However, the production of isolated enzymes for single reactions is largely an exercise in maximizing expression of functional enzyme. This is often accomplished by optimizing culture conditions (e.g., time, temperature, media, aeration, etc.), but more recently gene modification has also been used to improve enzyme expression levels.[17] Modified leader sequences and optimization of codon choices have improved transcription and translation, respectively, but solubility (if dealing with a cytosolic enzyme) cannot generally be improved using these methods. This can be addressed in some cases by lowering the expression temperature, fusing a solubility-inducing protein to the target enzyme, or even expressing truncated soluble versions of the target enzyme.[18] Coexpressing target enzymes with chaperones has also been effective.[19] These are largely empirical techniques, and their mode of action remains the subject of active investigation, but they can be useful tools in the preparation of soluble enzymes.

The most important factor influencing protein expression is the host organism used. *E. coli* is often chosen due to the expansive set of genetic tools and relatively simple culturing requirements for this organism. However, *E. coli* is by no means appropriate for all enzymes and biosynthetic pathways, and one may choose from a wide range of organisms for a given application.[20] In general, a host organism must possess the ability not only to synthesize the gene product, which requires appropriate codon usage and GC content, but also to incorporate cofactors, form disulfide bonds, and perform any required posttranslational modifications. Many industrial enzymes are expressed in hosts with good secretion capabilities (e.g., filamentous fungi and *Bacillus* sp.), so that the enzyme can be precipitated or filtered directly from the supernatant, or even used without purification.

9.15.3 Enzyme Engineering

Enzymes produced using the methods outlined above are valuable catalysts for a range of chemical reactions. Extensive reviews on the utility of such catalysts[21] and the engineering of substrates[22] to suit those catalysts have been published. In many cases, however, enzymes themselves are not ideally suited to the task for which they are charged, and properties such as thermal stability, organic cosolvent, and pH tolerance, substrate scope, or selectivity may require improvement. Although some of these factors may be addressed through the use of specialized bioreactors, enzyme immobilization, or other process optimization,[23] modification of the enzyme itself has proven to be a powerful means of improving biocatalytic processes.[24] Indeed, the ability to engineer enzymes gives them a significant advantage over small molecule catalysts. For example, enzymes may be tuned for specific applications using a systematic process of mutation and selection known as directed evolution.[25]

The authors provide some examples of directed evolution of synthetically relevant enzymes,[24] to illustrate the types of improvements that have been made. Specific focus is laid on the use of directed evolution to alter substrate scope or reaction selectivity, rather than process-related properties such as thermal stability, solvent tolerance, or pH.[26] The choice of sequence modification approach depends on the problem; for example, how much is known about that enzyme? Is a crystal structure available or can a homology model be generated? Practical constraints also exist. Can libraries of mutant enzymes be generated readily, and is a high-throughput assay possible? Thus, the examples presented illustrate the results of various approaches and are grouped based on the type of reaction catalyzed rather than the methods employed.[24] Discussion of specific technologies and strategies for introducing sequence modifications (EP-PCR, DNA shuffling, site-directed recombination, ISM, circular permutation, etc.) are avoided, as they have been thoroughly discussed elsewhere.[27]

9.15.3.1 Oxygenation

Given the importance of oxygenation in synthetic organic chemistry, it is not surprising that several different classes of oxygenases have been engineered (*see* Chapter 7.04).[28] Of these, the cytochromes P450 (P450s) have been the subject of a particularly large volume of work due to their ability to hydroxylate unactivated C–H bonds and epoxidize olefins (**Figure 1**).[29] Several recent examples highlight the power of engineered P450s to hydroxylate a wide range of substrates whose structures differ significantly from the native substrates of these enzymes. The applications of engineered P450s in biocatalysis have been reviewed.[29,30]

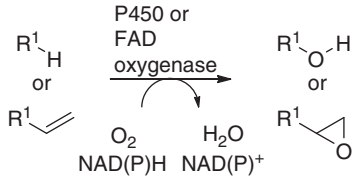


Figure 1 General scheme for oxygenase-catalyzed C–H hydroxylation and olefin epoxidation.

Cytochrome $P450_{BM3}$ from *Bacillus megaterium* (BM3) has been the subject of a large number of engineering efforts.[31] In this enzyme, the heme and diflavin reductase domains (FMN and FAD) are fused in a single polypeptide chain, rendering BM3 self-sufficient in generating the active oxidant from dioxygen and NAD(P)H. BM3 is soluble, readily overexpressed in a variety of heterologous hosts, and requires only atmospheric oxygen and a supply of nicotinamide adenine dinucleotide phosphate (NADPH) for monooxygenase activity. Arnold and coworkers have used directed evolution to alter the substrate scope of BM3, from long-chain fatty acids to gaseous alkanes, including propane and ethane.[32] Some of the intermediate mutants along the evolutionary lineage of the so-called BM3 propane monooxygenase (PMO) were found to have activity on a wide range of small organic molecules. These enzymes commonly catalyze both olefin epoxidation and C–H hydroxylation, and hydroxylation of secondary C–H bonds or those alpha to heteroatom substitution is particularly efficient. This activity has been enhanced to provide catalysts suitable for preparative-scale hydroxylation of drugs, protected sugars, steroids, alkaloids, and other small molecules (Figure 2). Others including Reetz et al., have described the directed evolution of BM3 for hydroxylation of substrates ranging from methane to aromatic heterocycles to steroids and terpenes.[29]

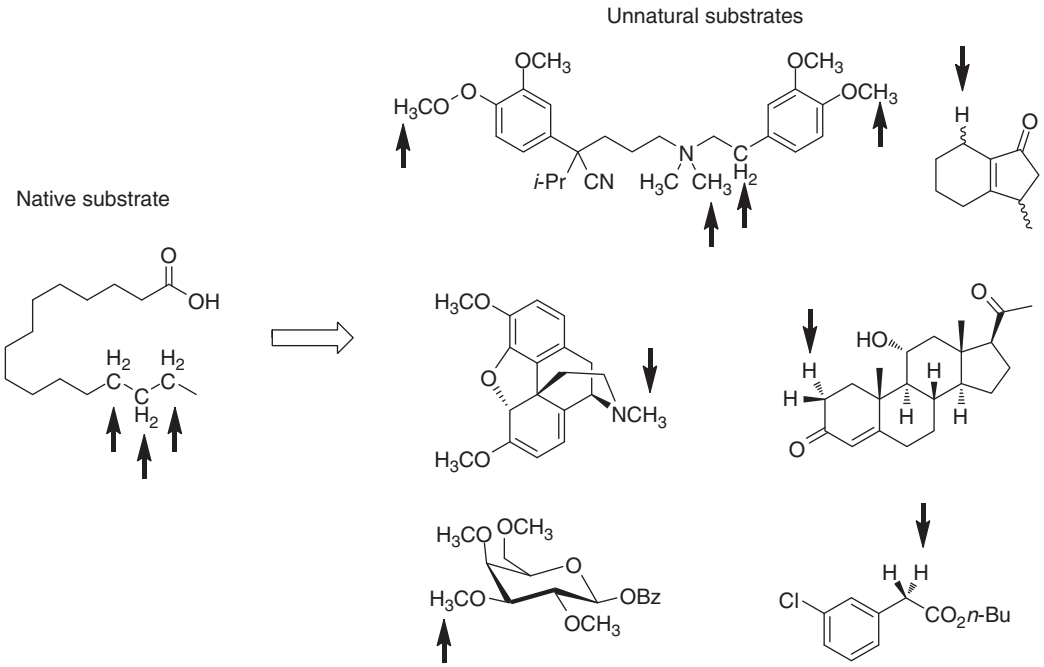


Figure 2 A native substrate for cytochrome $P450_{BM3}$ and representative substrates accepted by BM3 variants.[32] Arrows denote sites of hydroxylation. Block arrow denotes engineered activity on unnatural substrates.

Cytochrome P450 CAM from *Pseudomonas putida* has also been engineered as an oxygenation catalyst. Hydroxylations of substrates similar to those outlined above for BM3, including terpenes, arenes, polychlorinated arenes, and even ethane, have been accomplished using CAM variants.[29] Both cytochrome P450 CAM and BM3 accept small molecules (camphor and dodecanoic acid) as substrates, but significant sequence engineering effort is typically required to achieve high activity on larger substrates. In contrast, PikC, a P450 from *Streptomyces venezuelae* that catalyzes hydroxylation of an intermediate in the biosynthesis of the macrolactone YC-17 (22 carbon atoms),[33] can also hydroxylate a range of other macrocyclic compounds. Efforts are underway to expand this reactivity and enable hydroxylation of large substrates.

FAD-dependent oxygenases use an FAD hydroperoxide oxidant to catalyze oxygenation of activated substrates. Directed evolution of 2-hydroxybiphenyl 3-monooxygenase led to variants with improved activity on several substrates, including 2-*sec*-butylphenol, 2-methoxyphenol, and 2-*tert*-butylphenol (Figure 3(a)).[34] Similar efforts improved the hydroxylase activity of vanillyl-alcohol hydroxylase on cresol[35] and epoxidation activity of styrene monooxygenase from *P. putida* CA-3 on styrene, indene, and indole[36] (Figure 3(b) and (c)).

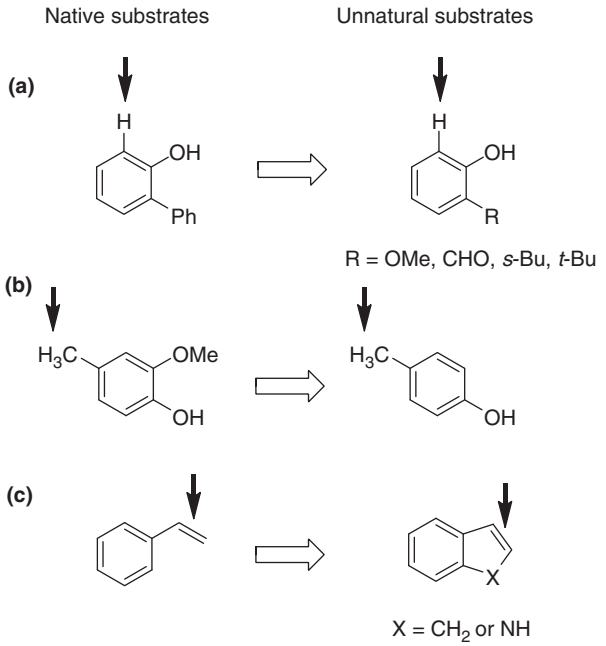


Figure 3 Native substrates and representative substrates accepted by variants of (a) 2-hydroxybiphenyl 3-monooxygenase,[34] (b) vanillyl-alcohol hydroxylase,[35] (c) styrene monooxygenase[36] from *P. putida* CA-3.

Extensive evolution of FAD-dependent Baeyer–Villiger monooxygenases,[37] which catalyze the eponymous chemical reaction on a range of native carbonyl- and thiocarbonyl-containing substrates (Figure 4(a)), has been reported. This work focused on improving activity and enantioselectivity on unnatural substrates, typically involving desymmetrization of prochiral ketones or kinetic resolution of racemic ketones.[38] For example, cyclohexanone monooxygenase (CHMO) was engineered to oxidize 4-hydroxycyclohexanone to either enantiomer of the corresponding lactone (Figure 4(b)), and related variants have been found to accept a wide range of substrates (Figure 4(c)). Many of these enzymes have been employed on large scales (e.g., 200 l), including the reactions of rac-bicyclo-[3.2.0]-hept-2-en-6-one and rac-2-phenylcyclohexanone, which provide near-quantitative conversion and high enantioselectivities (E-values > 100). Similarly high enantioselectivities are possible for the resolution of a range of substituted cyclohexanones using variants of phenylacetone monooxygenase (PAMO) (Figure 4(d)).

Finally, even multicomponent, nonheme iron oxygenases have been engineered by directed evolution. Mutations in the oxygenase subunit of these enzymes alter both their site selectivity and their substrate scope. Various arene dioxygenases have been engineered to accept unnatural substrates in order to make useful diene diols and phenols (Figure 5(a)).[39] For example, biphenyl dioxygenase variants were used to make the dioxygenated (and in some cases monooxygenated) products of a wide range of heterocycles and arenes (Figure 5(b)).[40]

Wood and others have made extensive efforts to expand the scope of toluene and xylene monooxygenases. Variants with improved activity and altered regioselectivity on indole[41] and naphthalene,[42] have been reported (Figure 6(a)). Furthermore, variants of toluene *p*-monooxygenase from *R. pickettii* PKO1 are capable of hydroxylating toluene at the *ortho*-, *meta*-, and *para*-positions (Figure 6(b)).[43]

9.15.3.2 Halogenation

Enzymatic halogenations typically involve oxidation of halide anion to an X^+ (X = halogen) equivalent that can react with electron-rich substrates. Directed evolution of heme-[44] and vanadium-dependent[45] haloperoxidases has improved the scope of biocatalytic halogenation. The site selectivity of halogenation reactions catalyzed by haloperoxidases has been questioned due to their release of free HOCl into solution.[46] However, FAD-dependent halogenases are known to catalyze site-specific halogenation of their native substrates. Thus, Van Pee and coworkers utilized site-directed mutagenesis to alter the site selectivity of tryptophan chlorination and bromination by the halogenase PrnA.[47] More recently, O'Connor and coworkers engineered the halogenase RebH to act on tryptamine, rather than its native substrate, tryptophan.[48]

9.15.3.3 Dehydrogenation

Dehydrogenases and a variety of oxidases catalyze the oxidation of organic substrates, including amines, alcohols, and sugars, via dehydrogenation (Figure 7(a)). The activities of these enzymes can also be reversed under suitable conditions to enable hydrogenation of unsaturated compounds (*vide infra*). The utility of the products of both modes of operation has motivated many successful examples of engineering these enzymes for synthetic applications.

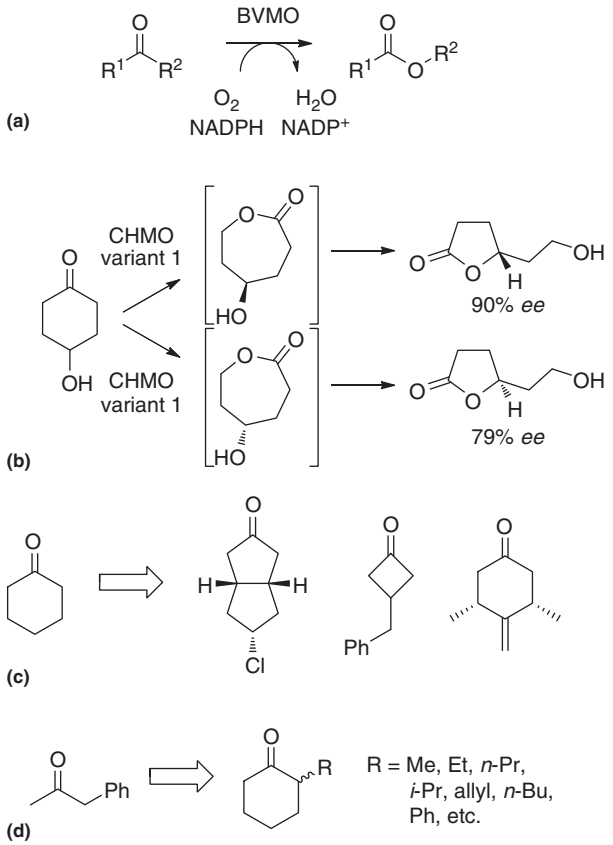


Figure 4 (a) General scheme for Baeyer–Villiger monooxygenase-catalyzed oxidation of carbonyl compounds. (b) Enantioselective oxidation of a *meso* ketone. (c) Native substrate and representative substrates accepted by variants of cyclohexanone monooxygenase. (d) Native substrate and representative substrates accepted by variants of PAMO.[37,38]

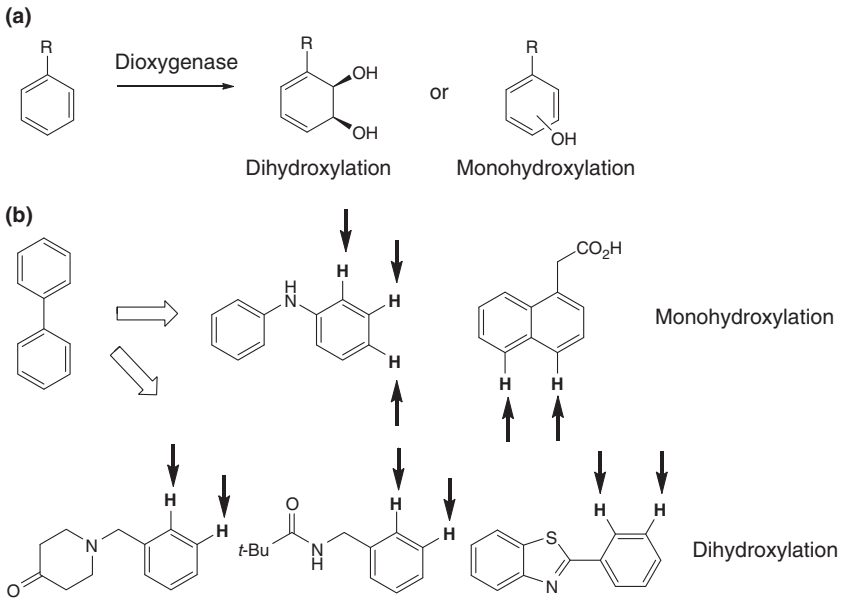


Figure 5 (a) General scheme for dioxygenase-catalyzed arene oxidation.[39] (b) Native substrate and representative substrates accepted by variants of biphenyl dioxygenase.[40] Arrows denote sites of oxygenation. Block arrow denotes engineered activity on unnatural substrates.

Amino acid dehydrogenases have been engineered to convert unnatural amino acids to the corresponding imines, which subsequently undergo hydrolysis to generate α-keto acids (**Figure 7(b)**).[49] Although not directly relevant to organic synthesis,

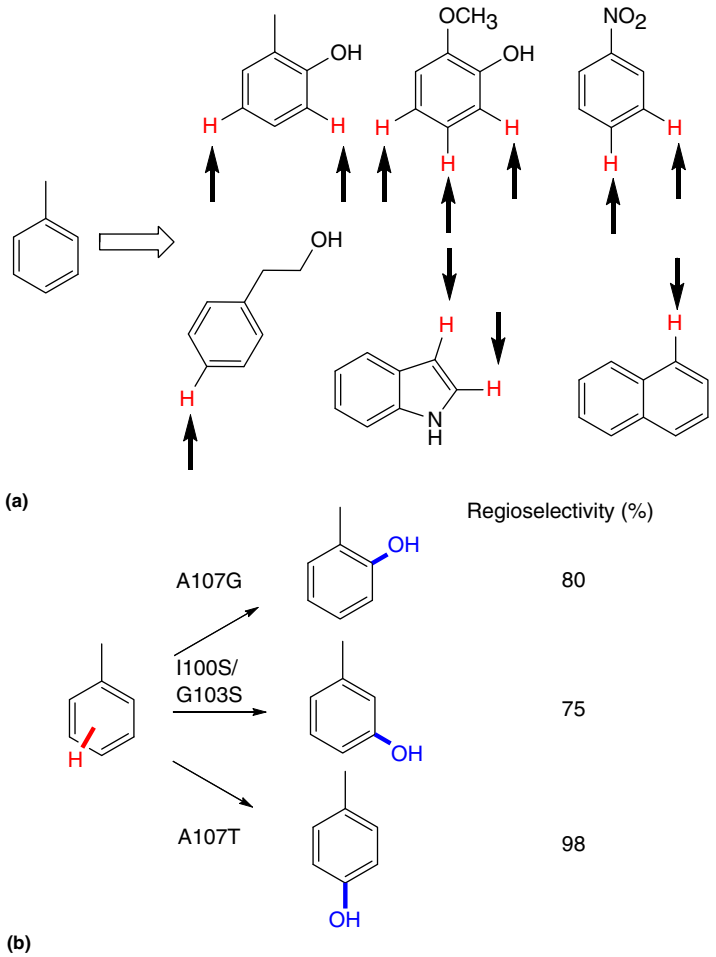


Figure 6 (a) Native substrate and representative substrates accepted by variants of toluene and xylene monooxygenases.[41,42] (b) Hydroxylation of ortho, meta, and para-positions of toluene using variants of a toluene monooxygenase.[43]

much work has also focused on improving alcohol, sugar, and other dehydrogenases for producing reducing equivalents needed by other redox enzymes.[50] Several oxidases also catalyze dehydrogenation of C–O and C–N bonds. Amino acids are also substrates for these enzymes, and directed evolution has been used to expand the range of amino acids that these enzymes accept.[51] Monoamine oxidase from *Aspergillus niger* has been studied as a catalyst for chemo-enzymatic deracemization of amines. In this process, the oxidase converts a single enantiomer of the racemic amine to an imine, which is subsequently reduced by a nonspecific reducing agent (**Figure 7(c)**).[52] Directed evolution has been used to expand the scope of this enzyme from several simple primary amines to a very large range of secondary amines (**Figure 7(d)**).[52] In a similar fashion, galactose oxidase, which naturally oxidizes the primary alcohol of galactose to the corresponding aldehyde, has been used to catalyze the oxidation of secondary alcohols to the corresponding ketones, enabling kinetic resolution of the alcohol enantiomers (**Figure 7(e)**).[53] Directed evolution of several other pyranose oxidase enzymes has also been described.[54]

9.15.3.4 Hydrogenation

As noted above, dehydrogenases can operate in 'reverse' to catalyze hydrogenation of unsaturated carbon–heteroatom bonds (i.e., the reverse of **Figure 7(a)**). This direction has significant importance due to the formation, rather than destruction or resolution, of a stereogenic center. Furthermore, these enzymes possess a remarkably broad substrate scope. For example, the S-selective dehydrogenase from *Rhodococcus erythropolis* and the R-selective dehydrogenase from *Lactobacillus kefir* have been used extensively as ketoreductases.[55] These enzymes accept a wide range of simple aldehydes and ketones as substrates for reduction and the corresponding alcohols as substrates for oxidation. In most cases, a specific cognate substrate for the wild-type enzyme is not known. Despite the utility of these enzymes, the desired selectivity is not always achieved, and directed evolution has been used to achieve highly selective reduction of a wide range of ketones, including aryl ketones, α-amino ketones, cyclic ketones, and β-dicarbonyl compounds, many on a commercial scale (**Figure 8**).[55] Importantly, both product enantiomers typically can be obtained using variants of one of the two aforementioned ketoreductases. Enolate reductases have also attracted much attention due to their ability to effect stereoselective hydrogenation of β-substituted α,β-unsaturated ketones.[56]

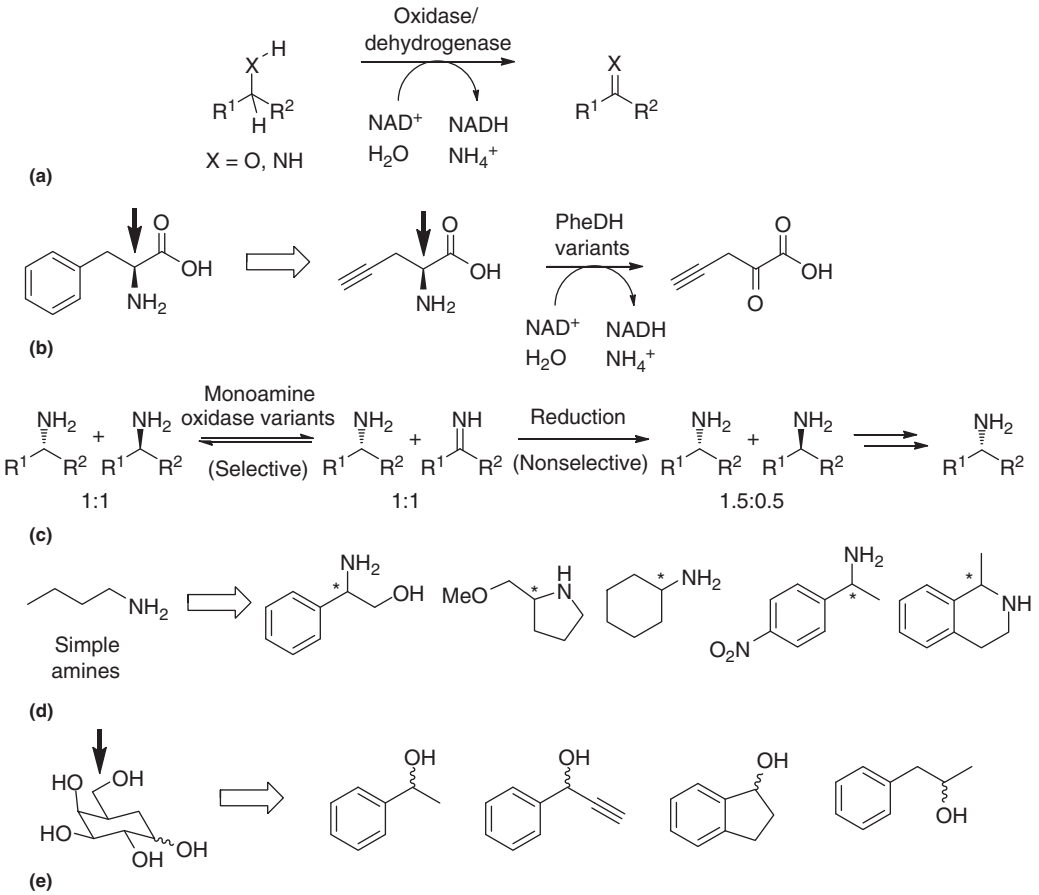


Figure 7 (a) General scheme for oxidase- and dehydrogenase-catalyzed reactions. (b) Native substrate and representative substrate accepted by a variant of phenylalanine dehydrogenase. The site of dehydrogenation is denoted by an arrow. Block arrows denote engineered activity on unnatural substrates.[49] (c) General scheme for oxidase-catalyzed deracemization of amines.[52] (d) Native substrate and representative substrates accepted by variants of a monoamine oxidase from *A. niger*. (e) Native substrate and representative substrates accepted by variants of a galactose oxidase.[53]

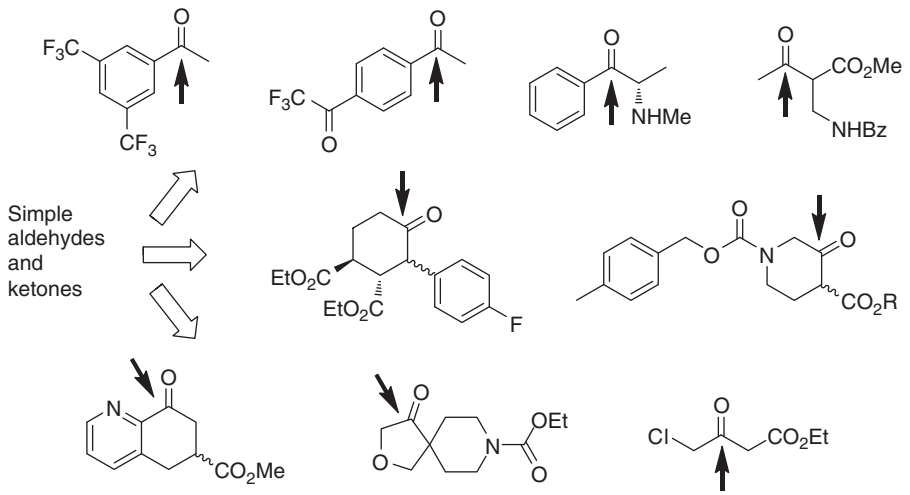


Figure 8 Representative substrates accepted by ketoreductase variants. The site of reduction is denoted by an arrow.[55] Block arrows denote engineered activity on unnatural substrates.

9.15.3.5 Group Transfers

Several different enzyme classes transfer functional groups and even entire molecular fragments from donor substrates to target substrates. Particularly notable in this regard are the pyridoxyl phosphate-dependent amino transferases, also known as

transaminases, which enable synthesis of chiral amines by exchanging amine and ketone functional groups on donor (typically amino acids or simple short-chain alkyl amines) and acceptor substrates, respectively (Figure 9(a)). The ω-transaminases have been the subject of the most engineering efforts due to the fact that they can accept a wide range of amine (rather than amino acid) donor substrates. These have been engineered to utilize simple amines as donor substrates with high efficiency. The reaction scope of the ketone acceptor substrate has been greatly expanded to enable the amination of a wide range of acyclic and cyclic ketones bearing a variety of functional groups (Figure 9(b)).[57] Variants capable of providing either enantiomer of the amine product have also been generated. Perhaps most impressively, as highlighted in Chapter 9.16 of this volume, researchers at Merck and Codexis engineered a transaminase capable of installing a chiral amine in the final step of the synthesis of the drug sitagliptin.[58]

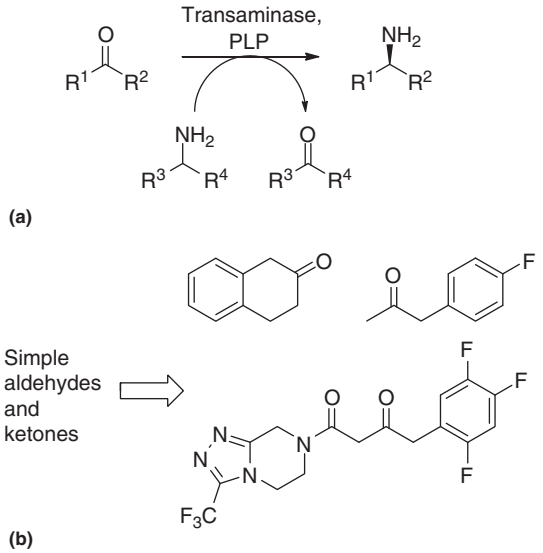


Figure 9 (a) General scheme for transaminase-catalyzed reductive amination. (b) Representative substrates accepted by transaminase variants.[57,58] Block arrow denotes engineered activity on unnatural substrates.

Glycotransferases have also benefited from directed evolution.[59] These enzymes transfer single sugar moieties to a range of aglycone (i.e., small molecule) substrates (Figure 10(a)), and directed evolution has been used to expand the scope of aglycones that may be utilized (Figure 10(b) and (c)). Glycosidases have also been used as glycotransferase catalysts. These enzymes possess transglycosidase activity in addition to hydrolytic activity, and the former has been improved through rational design of variants lacking a nucleophilic active site residue required for hydrolytic activity.[60] The resulting artificial transglycosidases enable glycosylation of a range of substrates, including sugars (to generate oligosaccharides) as well as aglycones (Figure 10(d)).

Directed evolution of sulfuryl-,[61] phosphoryl-,[62] glutathione,[63] and many other transferases has also been described. These enable highly selective tailoring of substrates with biologically important functional groups that are highly challenging to install using conventional synthetic methods.

9.15.3.6 Hydrolysis and Condensation

Hydrolases remain among the most commonly used enzymes in organic synthesis. In the forward direction, these enzymes hydrolyze a range of functional groups, including esters, amides, and nitriles, and many of these enzymes can be conveniently operated in the reverse direction to enable formation of these same functional groups. Directed evolution has been applied extensively to optimize hydrolase activity in both directions. Although not all of these can be covered here, the examples presented should provide readers with an idea of how these enzymes are typically used for chemical synthesis.

Lipases, which catalyze ester hydrolysis or formation (Figure 11(a)), were among the first enzymes to be evolved for improved organic solvent tolerance and enantioselectivity and have received extensive attention since these early efforts.[27] Engineered lipases enable efficient kinetic resolution of racemic esters and desymmetrization of meso diesters that are dramatically different, in many cases, from those accepted by the wild-type enzymes. Carboxyl esterases possess very similar hydrolytic activities[64] and have been engineered to improve enantioselectivity toward a range of substrates. Hydrolysis of carboxylic acid esters, including ibuprofen esters, 2-phenylalkanoic acid esters, and allene esters, has been achieved, and various alcohol leaving groups ranging from phenols to primary alcohols to tertiary alcohols can be used (Figure 11(b)). Among the most commonly used enzymes are those from *Pseudomonas aeruginosa* (PAL), *Bacillus subtilis* (BSLA), *Candida antarctica* (CALA/CALB),[65] and *Burkholderia cepacia* (BCL).

Epoxides have long been recognized as valuable synthetic intermediates, and epoxide hydrolases convert these compounds to enantioenriched diols (Figure 12(a)). These enzymes are typically used as catalysts for kinetic resolution of racemic epoxides, and

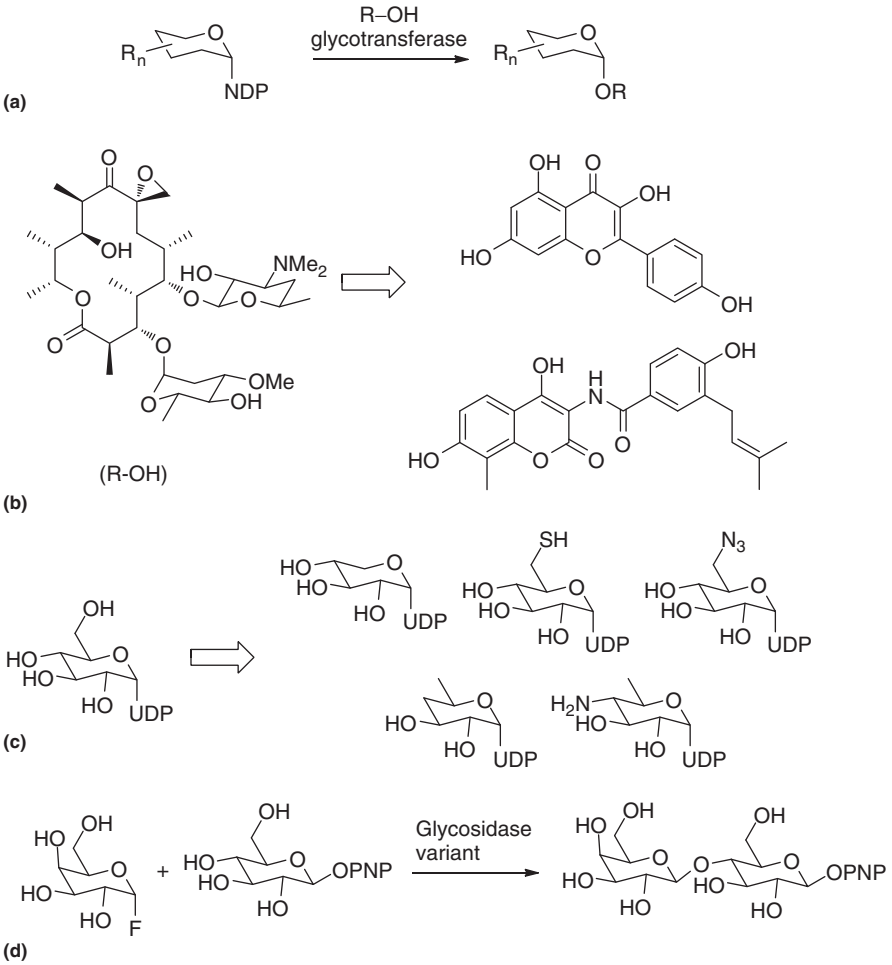


Figure 10 (a) General scheme for glycotransferase coupling of a nucleotide diphosphate (NDP) glycosyl donor and a glycosyl acceptor (R–OH). Block arrow denotes engineered activity on unnatural substrates. (b) Native glycosyl acceptor and acceptors accepted by glycotransferase variants.[59] (c) Native glycosyl donor and glycosyl donors accepted by glycotransferase variants.[59] (d) Representative glycosylation reaction catalyzed by an artificial transglycosidase.[60]

the epoxide hydrolase from *Aspergillus niger* has been a frequent target of engineering efforts (Figure 12(b)).[66] Halohydrin dehalogenases can also catalyze epoxide hydrolysis; however, these enzymes possess the added ability to resolve racemic halohydrins via epoxide formation before catalyzing epoxide opening with water (hydrolysis) and a range of additional nucleophiles, including azide, cyanide, and halide (Figure 12(c)). In a particularly notable example, directed evolution improved a halohydrin dehalogenase for production of the side chain of the commercial drug atorvastatin (Figure 12(c), Nu = CN, R = CH_2CO_2Et).[67] Several examples of similar efforts have been described, including engineering the halohydrin dehalogenase from *Agrobacterium radiobacter* for greater enantioselectivity on 2-chloro-1-phenethyl alcohol.[24]

9.15.3.7 Nonoxidative, Nonhydrolytic Bond Formation

Lyases catalyze nonoxidative, nonhydrolytic bond cleavage; when catalyzing the reverse direction (bond formation), these enzymes are called synthases. Perhaps among the most recognizable members of this class of enzymes to the synthetic chemist are the aldolases. Given the importance of the aldol reaction in synthetic organic chemistry, it is hardly surprising that enzymes capable of catalyzing this reaction on highly functionalized, unprotected substrates have received considerable attention. These enzymes utilize either an active site lysine (Class I aldolases) or zinc ion (Class II aldolases) to catalyze the cross aldol reaction between two carbonyl compounds (Figure 13(a)). Directed evolution has improved the utility of these enzymes, which typically have stricter requirements on at least one of the aldol partner substrates than many of the enzymes outlined above.[69]

For example, many aldolases require phosphorylated substrates, which are not typically desired by synthetic chemists. Reymond and coworkers removed this requirement by evolving a L-ramulose-1-phosphate (RhaD) aldolase to accept dihydroxyacetone as a substrate, which greatly improves the enzyme's utility (Figure 13(b)).[70] Similarly, 2-deoxyribose-5-phosphate aldolase (DERA), which naturally catalyzes the aldol reaction of acetaldehyde with D-glyceraldehyde-3-phosphate, was evolved to

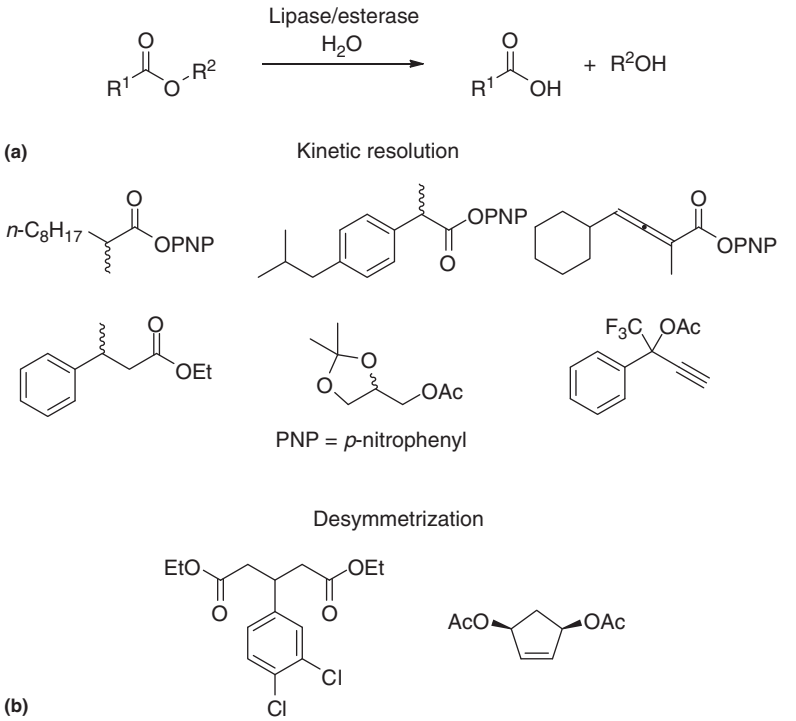


Figure 11 (a) General scheme for lipase- and esterase-catalyzed hydrolysis reactions. (b) Representative substrates accepted by lipase and esterase variants for either kinetic resolution or desymmetrization.[64,65]

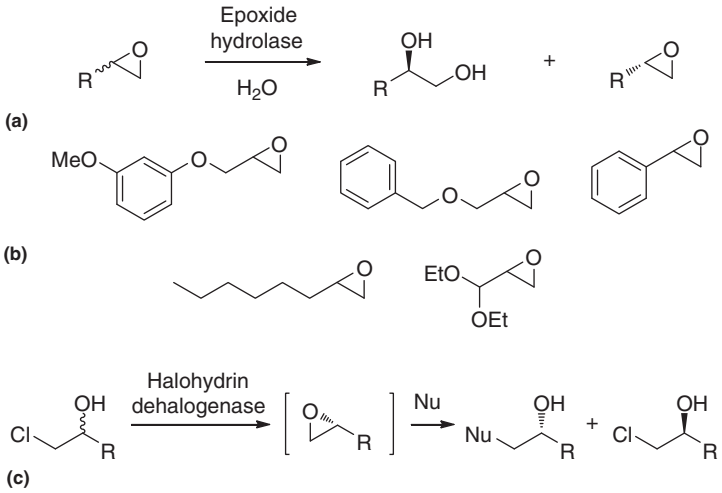


Figure 12 (a) General scheme for epoxide hydrolase-catalyzed reaction. (b) Representative substrates accepted by epoxide hydrolase variants.[66] (c) General scheme for halohydrin dehalogenase-catalyzed addition of nucleophiles to 2-halo alcohols.[68]

accept nonphosphorylated aldol acceptors.[71] Because this enzyme catalyzes the aldol reaction of two aldehydes, the product can in turn function as a substrate for a second aldol reaction (Figure 13(c)). Of course, not all aldolases require phosphorylated substrates, but expanding the substrate scope of these enzymes to include unnatural substrates remains highly desirable. For example, *N*-acetyl neuraminic acid lyase (NAL) catalyzes the aldol reaction between pyruvate and *N*-acetyl mannosamine and a variety of additional 5- and 6-carbon sugars. This scope has been extended by directed evolution to generate biologically relevant sialic acid derivatives (Figure 13(d)).[72]

As these examples highlight, aldolases can generate products containing a high degree of stereochemical information. Control of both the enantioselectivity and diastereoselectivity of these reactions is therefore crucial. For example, building upon the NAL-catalyzed reaction outlined above, researchers used directed evolution to generate variants capable of providing either the (4*S*)- or (4*R*)-enantiomer of the aldol product (Figure 13(d)).[73] Control over the diastereoselectivity of the aldol reaction requires that either enantiomer of the aldol acceptor function as a substrate for the aldolase. Indeed, D-2-keto-3-deoxy-6-phosphogluconate

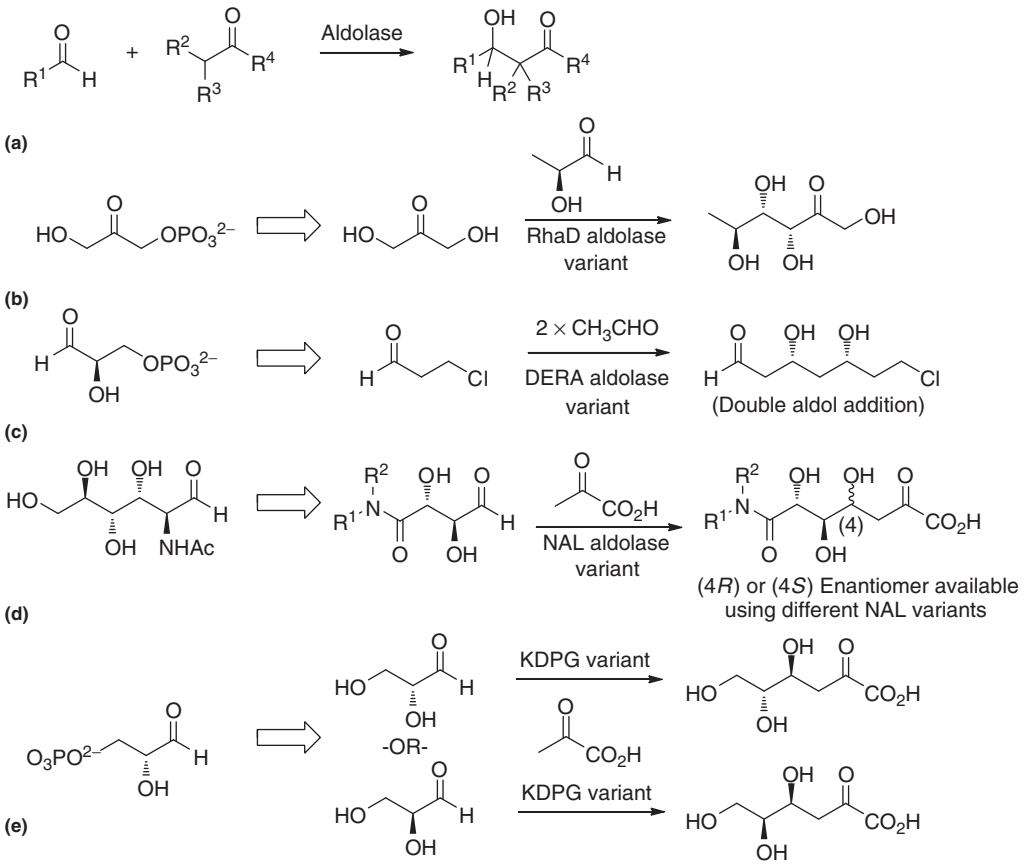


Figure 13 (a) General scheme for aldolase-catalyzed aldol reactions. (b, c) Native phosphorylated substrates and nonphosphorylated substrates accepted by DHAP and DERA aldolase variants.[70] Block arrow denotes engineered activity on unnatural substrates. (d) Native substrate and representative substrate accepted by an NAL aldolase variant. Different variants can be used to generate either the (4*R*) or (4*S*) product enantiomer.[72,73] (e) Native substrate and representative substrates accepted by KDPG aldolase variants to generate diastereomeric products.[74]

aldolase was evolved not only to accept nonphosphorylated substrates, including glyceraldehyde, but also to enable the reaction of either enantiomer of glyceraldehyde with pyruvate to provide diastereomeric products (**Figure 13(e)**).[74]

Hydroxynitrile lyases catalyze the addition of cyanide to aldehydes to generate synthetically valuable cyanohydrins. These enzymes have been the targets of several engineering efforts, including that of Glieder and coworkers, who were able to significantly improve the activity and enantioselectivity of a hydroxynitrile lyase from *Prunus amygdalus* to (*R*)-pantolactone (**Figure 14(a)**).[75] Amino acid lyases catalyze nonoxidative, reversible deamination of amino acids and hydroamination of α,β-unsaturated acids in the reverse direction. Altering the substrate scope of these enzymes has enabled the synthesis of unnatural amino acids (**Figure 14(b)**).[76] Directed evolution has been used to expand the scope of a number of naturally occurring synthase complexes, including those responsible for the biosynthesis of terpenes,[77] polyketides,[78] and nonribosomal peptides.[79]

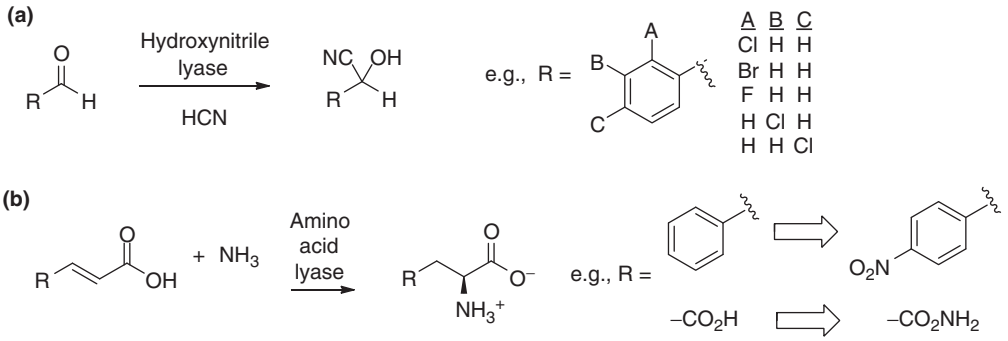


Figure 14 (a) General scheme for hydrocyanation of aldehydes using a hydroxynitrile lyase and representative substrates accepted by hydroxynitrile lyase variants.[75] (b) General scheme for hydroamination of α,β-unsaturated acids using an amino acid lyase and representative substrates accepted by amino acid lyase variants.[76]

9.15.3.8 Summary

Given that efforts to alter the properties of enzymes using directed evolution have only been underway for approximately 20 years,[80] and that the total range of enzymatic activities is far greater than those targeted for improvement thus far, much more progress can be expected in the tailoring of enzymes for synthetic applications. However, several general trends that have emerged are worth emphasizing, particularly to synthetic chemists.[81] The first is that many important transformations, including C–H bond functionalization (**Figure 2**),[82] hydroamination (**Figure 14(b)**),[76] and a wide range of carbon–carbon bond forming reactions, may be carried out in a preparative fashion using enzymes. Many chemists are comfortable with enzymatic hydrolysis reactions (see Section 9.15.3.6), but far greater synthetic power awaits early adopters of systems such as those described above. Second, many of these enzymes exhibit much broader substrate scope than is typically appreciated.[32] This renders enzymes similar to the 'general' catalysts typically employed by chemists. And, unlike those small molecule catalysts, which may be more or less applicable to a given target, enzymes can be systematically improved using directed evolution.

The examples outlined above show that changes in enzyme activity achieved using directed evolution can range from relatively minor, for example, increasing activity toward a known substrate, to surprisingly large, as exemplified by the commercial synthesis of sitagliptin using an enzyme evolved from a completely inactive parent enzyme.[58] Although the extent to which any given enzyme can be tuned appears to vary on a case-to-case basis, it is clear that for many enzymes, very large improvements can be realized. It should also be appreciated that in the course of evolving an enzyme for a given target, many additional enzymes with improved fitness on substrates not directly selected for are also obtained, which greatly expands the pool of catalysts available for synthesis.[32] This also provides starting points for rapid evolution of enzymes for new targets. Finally, although most work in this area has focused on improving enzymes for single reactions either *in vivo* or *in vitro*, the optimization of enzymes of inclusion in metabolic pathways, either natural or synthetic, holds great promise for the synthesis of a wide range of compounds. This will ultimately enable completely novel metabolic pathways to be developed for chemical production inside a cell.

9.15.4 Metabolic Engineering

Living organisms create molecular complexity under stringent limitations where cofactors are recycled and multiple catalysts coexist in the same medium without compromising efficiency and selectivity. This ability to catalyze multiple steps *in vivo*, without the need to isolate intermediates and change conditions (solvent, temperature, pH etc.),[83] underscores the tremendous potential of using metabolically engineered cells for efficient chemical synthesis. Natural selection has rarely acted to channel valuable energy and carbon toward production of a single compound. Thus, most organisms are suboptimally designed to convert a feedstock (i.e., glucose) to a desired product. Engineering organisms to become high-performance living factories is the ultimate goal of metabolic engineering.

Contemporary metabolic engineering utilizes various technologies (enzyme engineering, modeling, network analysis, manipulation of regulation, DNA synthesis, and careful analysis of genes, transcripts, and metabolites) to engineer organisms to synthesize chemical compounds of both native and heterologous origin.[84] This field has attracted intense industrial interest over the past decade, particularly to provide alternate, microbial sources of scarce compounds that are extracted from biological materials and cannot be synthesized economically by purely chemical means. Additionally, there is strong interest in fermentative processes to replace petrochemicals as a strategy to mitigate volatility in the price and supply of petroleum. The authors illustrate the state of the art by summarizing selected efforts directed at biomanufacturing commodities and specialty chemicals. The examples were selected based on diversity of methodology and are organized below according to natural product class.

9.15.4.1 Isoprenoids

Isoprenoids make up the most numerous and structurally diverse family of natural products, with more than 50 000 different compounds identified to date from all forms of life. Commonly isolated from plants (in which case they are also referred to as terpenoids), microbes, and marine organisms, these valuable compounds are used as flavors, fragrances, nutraceuticals, biodegradable pesticides, as well as potent anticancer and antimalarial drugs. Representative examples include limonene (responsible for the strong smell in oranges and used in many fragrances and artificial flavors), the anticancer drug taxol, the antimalarial agent artemisinin, and lycopene (the red pigment in tomatoes that is used as a nutraceutical). Due to their structural complexity, isoprenoids are difficult, expensive, and inefficient to synthesize chemically and have to be sourced from biological materials. However, these compounds are produced only in small quantities, and extraction and purification are costly as well. The biosynthesis of these complex targets directly from inexpensive carbon sources such as glucose by metabolic engineering in microbial hosts has provided an elegant alternative to chemical synthesis and extraction from natural sources.

All isoprenoids are biosynthesized from two precursors, isopentenyl pyrophosphate (IPP) and dimethyl allyl pyrophosphate (DMAPP), which undergo isomeric conversion catalyzed by the enzyme IPP isomerase. Elimination of pyrophosphate from DMAPP catalyzed by isoprene synthase forms isoprene, the simplest terpene (**Figure 15**). However, the nucleophilic methylene group of IPP can attack the electrophilic allylic CH_2 group of DMAPP to condense in a head-to-tail fashion to form geranyl pyrophosphate (GPP), the common precursor to all monoterpenes ($C_{10}H_{16}$, e.g., limonene). Chain elongation of GPP by addition of another IPP unit forms farnesyl pyrophosphate (FPP), the common precursor singular to all sesquiterpenes ($C_{15}H_{24}$, e.g., amorphadiene). Addition of

yet another IPP unit to FPP gives geranylgeranyl pyrophosphate (GGPP), from which all diterpenes are made ($C_{20}H_{32}$, e.g., taxadiene). The tail-to-tail condensation of two FPP molecules makes presqualene pyrophosphate, which is reduced to give squalene ($C_{30}H_{50}$), the precursor to steroids (see Section 9.15.4.2). The tail-to-tail linkage of two GGPP molecules makes the tetraterpene phytoene ($C_{40}H_{64}$, i.e., lycopene), which serves as a precursor to carotenoids. This collection of precursors provides starting points for a wide range of molecules of interest to chemists, some of which are shown in Figure 15.

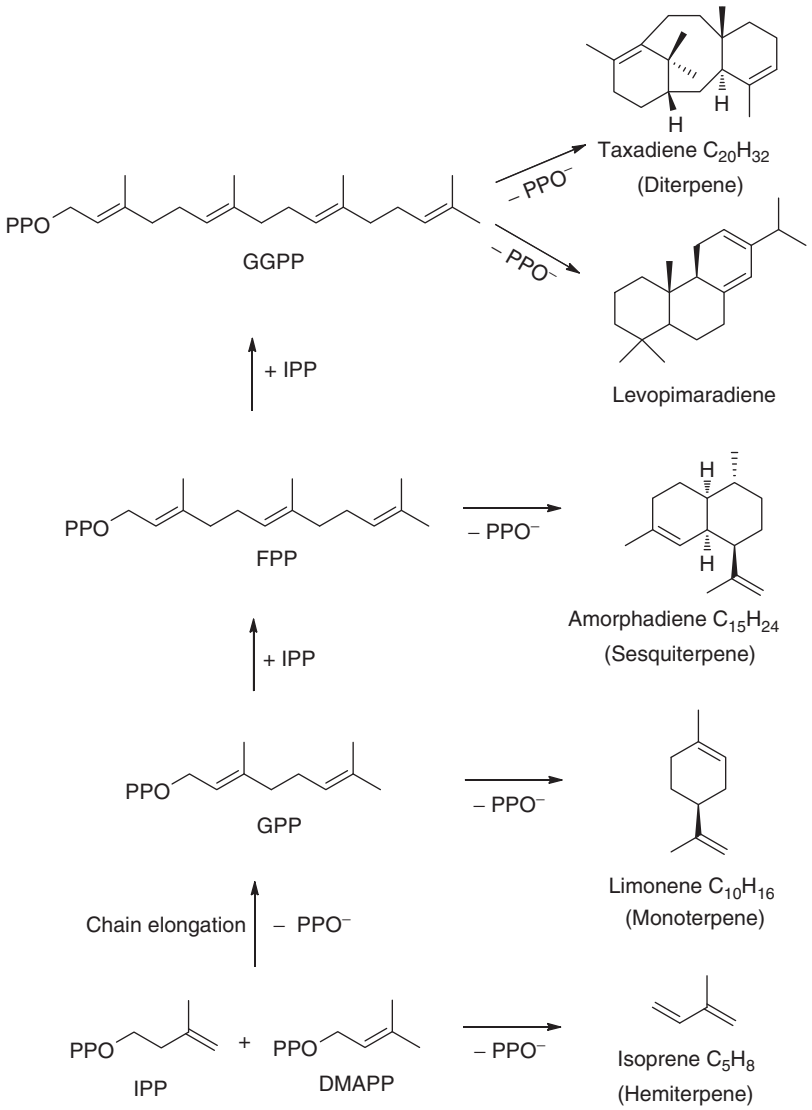


Figure 15 Terpene synthases make isoprenoids from pyrophosphate precursors derived from IPP and DMAPP.[85]

Given the importance of IPP and DMAPP in terpene biosynthesis, understanding the biosynthesis of these precursors is essential for any terpenoid engineering effort. In fact, IPP and DMAPP are produced by two distinct pathways that differ in their cofactor requirements and theoretical yields from glucose. The mevalonate (MVA) pathway converts the ubiquitous intermediate acetyl-coenzyme A (A-CoA) to IPP, whereas the 1-deoxy-D-xylulose-5-phosphate/2-C-methyl-D-erythritol-4-phosphate (DXP/MEP) pathway produces IPP and DMAPP from pyruvate and glyceraldehyde-3-phosphate derived from glycolysis. The MVA pathway offers a lower theoretical yield of conversion of glucose to isoprenoids ($0.252\ g\ g^{-1}$) compared with the DXP/MEP pathway ($0.302\ g\ g^{-1}$) due to its cofactor imbalance.[86] The choice of which pathway to engineer for maximizing flux toward IPP and DMAPP depends on the regulatory elements present in the host organism. It is important to note that accumulation of prenyl pyrophosphates has been found to be toxic to the host,[87] such that the metabolic engineering experiment has to go one step further and include the terpene synthase that will produce the hydrocarbon product.

9.15.4.1.1 Isoprene

Isoprene (2-methyl-1,3-butadiene) is an important commodity chemical used in a wide range of industrial applications, from production of synthetic rubber for tires and coatings to use in adhesives and specialty elastomers. Global industrial production of

synthetic isoprene from petrochemical feedstocks is approximately 1 million tons per year.[86] Isoprene is naturally produced by bacteria, animals, and plants, which are estimated to collectively release approximately 600 million tons per year into the atmosphere. Despite isoprene's pervasiveness in the environment, genetic approaches to identifying the genes encoding isoprene synthesis in prokaryotes have been pursued with limited success.[88] Thus far, only plant-derived isoprene synthases have been well characterized, and sequence data for isoprene synthases exist for only two plant families. Because the catalytic efficiencies of these enzymes are suboptimal for industrial applications ($K_M \sim 1$–10 mM and $k_{cat} \sim 1\ s^{-1}$),[86,89] protein engineering for superior kinetic parameters has been pursued by industrial groups.[89,90] As a proof of concept, recombinant production of isoprene in microbial hosts has been achieved by expressing plant isoprene synthases in *E. coli*, *S. cerevisiae*, and photosynthetic bacteria.[91]

Genencor–DuPont and The Goodyear Tire & Rubber Co. are developing a high-efficiency fermentative route for polymer-grade isoprene via heterologous expression of the MVA pathway and plant-derived isoprene synthases in *E. coli*.[86] The MVA pathway was chosen over the DXP/MEP pathway because it was better characterized and has been exploited industrially for the production of isoprenoids in both yeast and bacteria.[87,92] The volatile nature of isoprene (bp 34 °C) allows gas phase recovery, simplifying purification and eliminating potential feedback inhibition by virtue of product accumulation. This process is reported to have an isoprene yield of 0.11 g g^{-1}, volumetric productivity of 2.0 g l^{-1} h^{-1}, and a titer of 60 g l^{-1}.[86]

9.15.4.1.2 Artemisinin

Artemisinin, an endoperoxide sesquiterpene lactone, is an antimalarial drug produced in the leaves of *Artemisia annua*. Its biosynthesis comprises at least four enzymatic steps starting from FPP, the common precursor, to sesquiterpenes. The first committed step is the cyclization of FPP to amorpha-4,11-diene, catalyzed by amorphadiene synthase (ADS). The cytochrome P450 CYP71AV1 then oxidizes amorphadiene to artemisinic aldehyde and also makes artemisinic acid as a byproduct. Reduction to dihydroartemisinic aldehyde is catalyzed by artemisinic aldehyde Δ11 reductase, BDR2, and a specific aldehyde dehydrogenase is likely involved in the oxidation step to form hydroartemisinic acid, but the remaining steps in the pathway may be nonenzymatic.[93]

The semisynthesis of artemisinin via metabolic engineering is based on the *in vivo* overproduction of amorphadiene or artemisinic acid and their subsequent conversion to artemisinin through chemical reactions (**Figure 16**). Initial experiments aimed at improving the isoprenoid flux in *E. coli* focused on introducing the heterologous MVA pathway from *S. cerevisiae* to circumvent the regulatory elements found in *E. coli*'s native MEP pathway.[87] The recombinant eight-gene biosynthetic pathway was divided into two operons: a 'top' operon (MevT) that encodes the three enzymes required to convert the ubiquitous precursor acetyl-CoA to (*R*)-MVA and a 'bottom' operon (MBIS) that converts (*R*)-MVA to FPP (**Figure 16**). Coexpression of these operons with a synthetic ADS gene, optimized for expression in *E. coli*, resulted in the production of amorphadiene from glucose and glycerol with a final concentration of 0.5 g l^{-1} following optimization of process conditions.[87,94]

MVA supplementation studies suggested that the production of amorphadiene in this system was limited by the conversion of acetyl-CoA to MVA.[96] However, increased expression of the three enzymes in the top operon (MevT) – by increasing plasmid copy number and by replacing the promoter – resulted in cell growth inhibition. Gene titration studies and metabolite profiling using liquid chromatography mass spectrometry (LCMS) linked growth inhibition to the intracellular accumulation of the heterologous metabolite 3-hydroxy-3-methyl-glutarylcoenzyme A (HMG-CoA), which suggested that low activity of a single enzyme, HMG-CoA reductase (*tHMGR*), encoded in MevT, was the major bottleneck. This flux imbalance was alleviated by coexpressing the MevT operon with an additional medium-copy-number plasmid carrying an extra copy of *tHMGR*, effectively increasing the concentration of the catalyst in the bottleneck step and thereby achieving a threefold increase in MVA production. Further optimizations included replacing the yeast genes for HMG-CoA synthase and HMG-CoA reductase with equivalent genes from *Staphylococcus aureus* and improving the fermentation process under the restriction of carbon and nitrogen, so as to maximize flux toward the desired metabolic pathway, yielding commercially relevant titers of 27.4 g l^{-1} amorphadiene.[97]

The membrane-associated cytochrome P450 monooxygenase from *A. annua* (CYP71AV1) catalyzes the three-step oxidation of amorphadiene to artemisinic acid, producing the alcohol and aldehyde congeners of artemisinic acid as intermediates. To achieve the *in vivo* oxidation of amorphadiene to artemisinic acid, CYP71AV1 and its redox partner cytochrome P450 reductase (CPR), were codon-optimized for *E. coli* and coexpressed in the aforementioned strains. By engineering the N-terminal transmembrane sequence and using an expression plasmid suitable for P450 expression, artemisinic acid titers of 105 mg l^{-1} were achieved, when conducting the fermentation in the absence of a *n*-dodecane overlay.[98] Conversion of artemisinic acid to the drug artemisinin can be accomplished in just two *in vitro* chemical reactions, namely reduction to hydroartemisinic acid followed by a photooxidation cyclization reaction (**Figure 16**).[99]

Biosynthesis of artemisinic acid has also been achieved in the yeast *S. cerevisiae*, by upregulating the expression of several genes from the native MVA pathway and by heterologous expression, through chromosomal integration, of ADS, amorphadiene monooxygenase (CYP71AV1), and the reductase (CPR).[100] Since steroid biosynthesis in yeast competes with ADS for FPP availability, it was necessary to downregulate expression of squalene synthase, which catalyzes the first step downstream of FPP in the sterol pathway. Just as for *E. coli*, integration of an additional copy of *tHMGR* into the chromosome increased amorphadiene production, altogether producing >100 mg l^{-1} artemisinic acid. Interestingly, artemisinic acid was found to accumulate on the outer side of the cell membrane, allowing for a one-step purification following its 'total' synthesis in yeast. Artemisinic acid removed from the cell pellet by washing with alkaline buffer was extracted into ether and purified by silica gel chromatography to achieve greater than 95% purity.[100] Further strain engineering could not improve titers beyond 0.2 g l^{-1} for glucose-fed fermentations.[95b] However, strains that had been cloned with the pathway only up to amorphadiene achieved titers of greater than

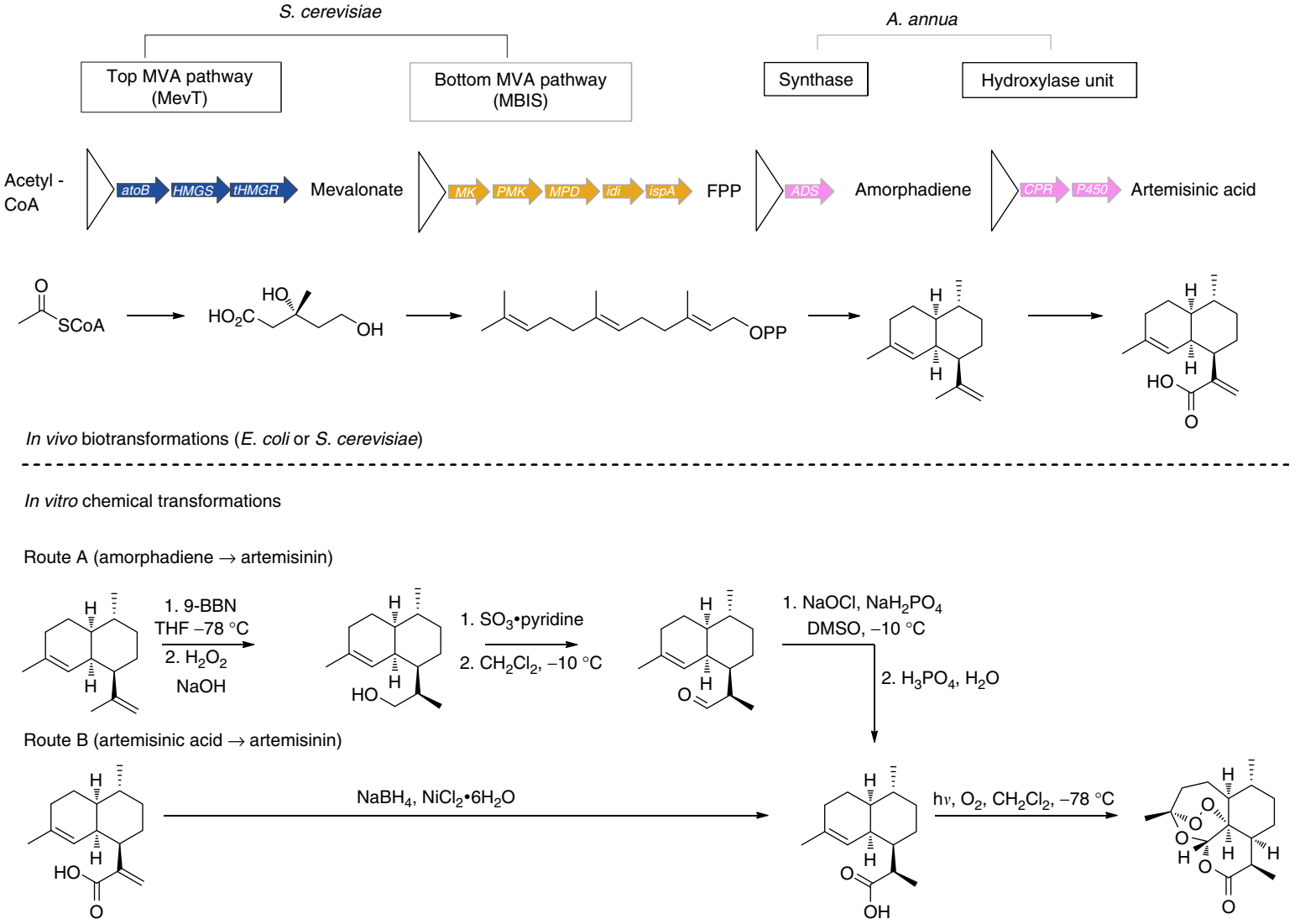


Figure 16 Semisynthetic scheme for artemisinin production. Enzymes encoded by the genes shown are: *atoB*, acetoacetyl-CoA thiolase; *HMGS*, HMG-CoA synthase; *tHMGR*, truncated HMG-CoA reductase (expressing only the C-terminal catalytic domain); *MK*, mevalonate kinase; *PMK*, phosphomevalonate kinase; *MPD*, mevalonate diphosphate decarboxylase; *idi*, IPP isomerase; *ispA*, farnesyl diphosphate synthase; *ADS*, amorphadiene synthase; *CPR*, cytochrome P450 reductase; *P450*, CYP71AV1.[95]

1.2 g l^{-1}. Subsequent improvements in the fermentation process for amorphadiene were able to significantly increase product titers up to the commercially relevant target of 37 g l^{-1}.[95b] Key developments included restricting phosphate in fed-batch fermentations – this is thought to limit growth and channel greater carbon flux to product – and replacing the restricted glucose feed with a restricted ethanol feed, which is thought to increase intracellular acetyl-CoA levels for the MVA pathway. Deletion of *GAL1 GAL10 GAL7* and Gal80p, a gene cluster required for the utilization of galactose, altogether eliminated the need to add expensive galactose for induction of amorphadiene production. The *S. cerevisiae*-based process has considerable advantages over the aforementioned *E. coli* process, most notably the absence of an expensive inducer such as IPTG and the lower oxygen uptake rate required for the restricted ethanol process, which reduces costs associated with aerating large fermentors.

In vitro chemical reactions are subsequently used to convert amorphadiene to dihydroartemisinic acid en route to artemisinin (**Figure 16**).[95b] Industrial production of semisynthetic artemisinin is being pursued by Amyris Biotechnologies in collaboration with Sanofi-Aventis.

9.15.4.1.3 Taxol

Taxol (paclitaxel) and its structural analogs are among the most potent and commercially successful anticancer drugs. Taxol comprises a highly oxygenated 6–8–6 tricyclic ring system, featuring a total of 11 stereogenic centers, an ester side chain, and a distinctive oxetane ring. Six independent total syntheses have been reported involving elaborate routes that require 37–51 steps, with yields too low for practical synthesis (highest yield of 0.4%).[83] Taxol was first isolated from the bark of *Taxus brevifolia* (Pacific Yew tree), and its biosynthetic pathway consists of approximately 20 enzymatic steps from the primary intermediate geranylgeranyl diphosphate (GGPP).[93] Taxadiene synthase catalyzes the cyclization of GGPP to taxa-4(5),11(12)-diene (**Figure 15**), the first committed step of the pathway, with remarkable fidelity generating the 6–8–6 tricycle with the correct chirality for the first three stereogenic centers. The diterpenoid core is further decorated by eight cytochrome P450-mediated oxygenations, four coenzyme A-dependent acylations, and a C13 side-chain assembly and attachment en route to taxol.

Metabolic engineering has been applied successfully to overproduce taxol precursors in *E. coli*.[101] Since the MEP pathway for making IPP and DMAPP (**Figure 17**, upstream module) is endogenous to *E. coli*, heterologous expression of only GGPP synthase and taxadiene synthase (**Figure 17**, downstream module) allows for the production of taxa-4(5), 11(12)-diene. The pathway was partitioned into two modules separated at IPP, the key intermediate in terpenoid biosynthesis. A total of 32 strains were constructed wherein eight native enzymes identified as bottlenecks in the upstream MEP pathway were expressed in one module and the two heterologous downstream enzymes were expressed in the other module. By systematically varying expression of each module, a nonlinear effect on taxadiene titers was observed for the relative dosage of the two pathways. Further optimizations such as chromosomal integration of the upstream operon, minimizing pathway inhibition by indole (a byproduct), and a two-phase fermentation to avoid air-stripping of taxadiene resulted in titers as high as 1.02 g l^{-1}.[101] Finally, the plant-derived cytochrome P450, taxadiene 5α hydroxylase, an unusual monooxygenase that catalyzes hydroxylation along with double-bond migration, was included in the pathway to generate taxadien-5α-ol (though this resulted in a much lower product titer of 50 mg l^{-1}).

9.15.4.1.4 Levopimaradiene

Levopimaradiene is the diterpenoid gateway precursor of the pharmaceutically important plant-derived ginkgolides. Heterologous production has been achieved in *E. coli* with a maximum titer of 700 mg l^{-1} using a combination of metabolic and protein engineering methods.[102] Introduction of plant-derived geranylgeranyl diphosphate synthase (GGPPS) and levopimaradiene synthase (LPS) codon-optimized for *E. coli* led to only marginal production of levopimaradiene (0.15 mg l^{-1}). Overexpression of the upstream MEP/DXP pathway for increasing the intracellular concentration of the isoprenoid precursors IPP and DMAPP led to a titer of 92 mg l^{-1}. However, further product amplification could not be achieved by continuing to increase the concentration of the bottleneck enzymes in the MEP/DXP pathway. This suggested that the inherently low-enzyme activity and specificity of the downstream steps had become rate limiting under high isoprenoid precursor flux. Thus, enzyme engineering at the key metabolic nodes was pursued in order to achieve substantial overproduction of the target diterpene.

LPS from *Ginkgo biloba* converts GGPP to levopimaradiene with approximately 87% selectivity, although also forming the isomers abietadiene (11%), sandaracopimaradiene (2%), and neoabietadiene (trace) (**Figure 18**).[102] This product mixture results from initial isomerization of GGPP in the first active site of LPS to form the intermediate copalyl diphosphate, which subsequently undergoes a poorly selective diphosphate-ionization cyclization in the second active site of LPS. This example illustrates how the poor selectivity of some terpene synthases can result in unwanted product formation, which leads to low metabolic fluxes and large product losses.

E. coli overexpressing the genes for the MEP/DXP pathway and expressing wild-type GGPPS was used to screen a library of LPS variants with mutations focused in the troublesome second active site. Mutations were selected to increase diterpene productivity and retain or improve the selectivity for levopimaradiene. Saturation mutagenesis at key residues and recombination of the top mutations improved productivity by 10-fold without significant changes in product distribution. Finally, the activity of GGPPS was improved 1.7-fold via random mutagenesis and an *in vivo* screen that utilized a lycopene biosynthetic pathway as a colorimetric reporter.[102] This example illustrates the utility of protein engineering in manipulating secondary metabolic pathways with poor selectivity to optimize microbial overproduction of desired chemicals.

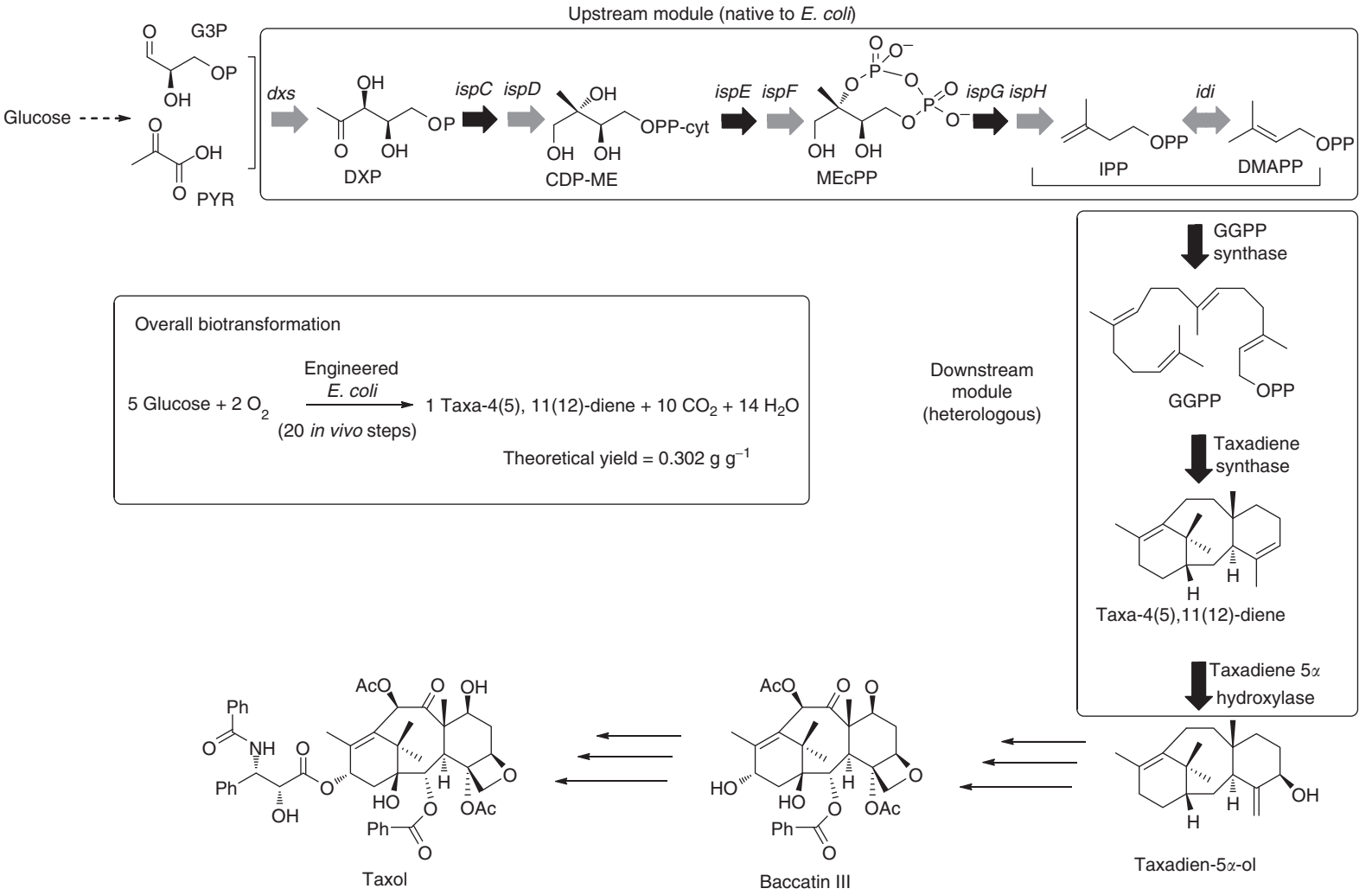


Figure 17 Biosynthesis of taxol precursors in *E. coli* via the DXP/MEP pathway (upstream module). Enzymes encoded by the genes shown are: *dxs*, 1-deoxy-D-xylulose-5-phosphate synthase; *ispC*, 1-deoxy-D-xylulose-5-phosphate reductoisomerase; *ispD*, 4-diphosphocytidyl-2-*C*-methyl-D-erythritol-2,4-cyclodiphosphate synthase; *ispE*, 4-diphosphocytidyl-2-*C*-methyl-D-erythritol kinase; *ispF*, 2-*C*-methyl-D-erythritol-2,4-cyclodiphosphate synthase; *ispG*, 1-hydroxy-2-methyl-2-(*E*)-butenyl-4- diphosphate synthase; *ispH*, 4-hydroxy-3-methyl-2-(*E*)-butenyl-4-diphosphate reductase; *idi*, IPP isomerase.[101]

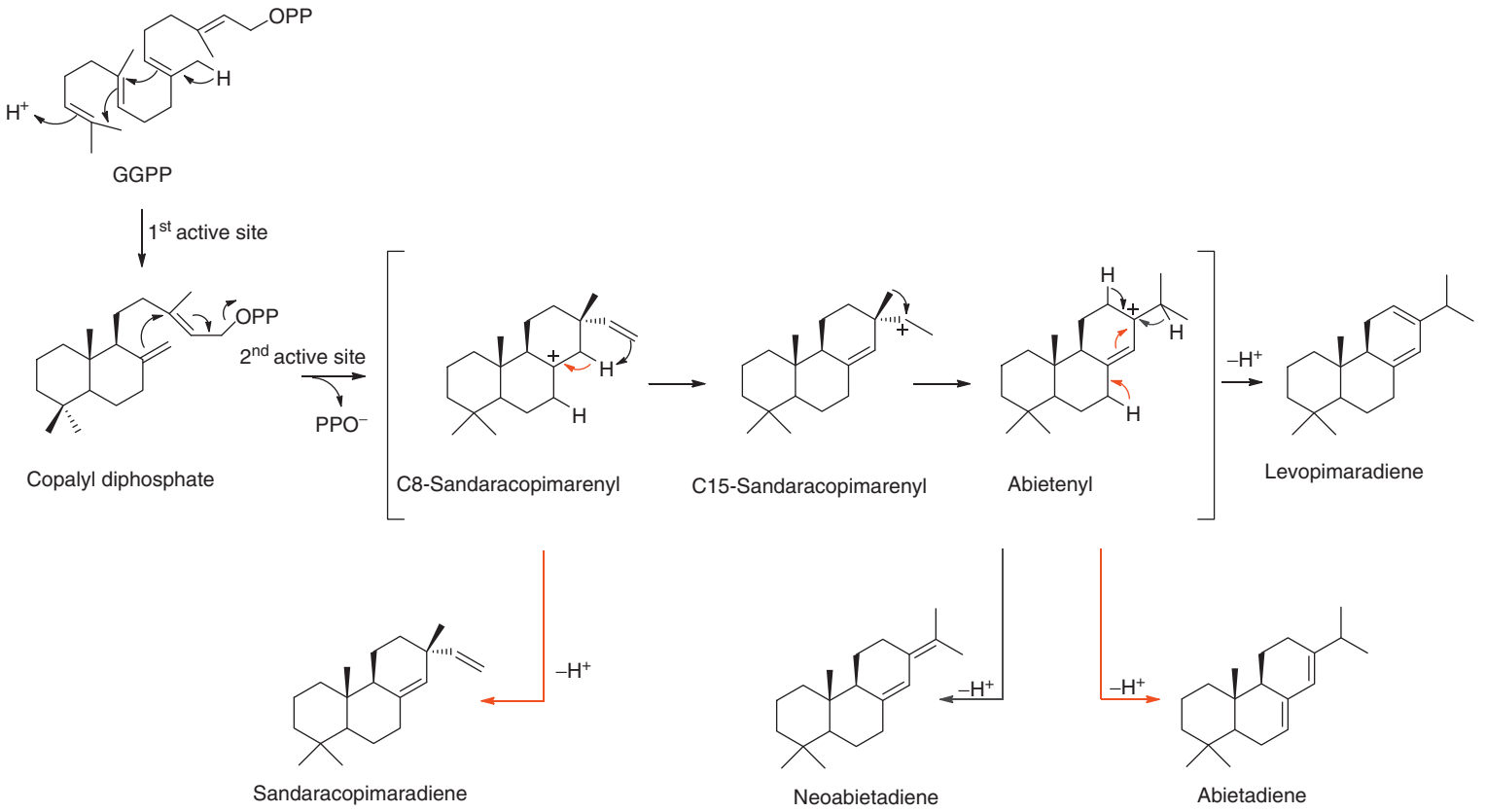


Figure 18 LPS catalyzes the cyclization of GGPP to levopimaradiene in two distinct active sites. In the first active site, deprotonation drives the formation of (+)-copalyl diphosphate (CPP). Reaction in a second active site leads to the formation of multiple products from GGPP with poor selectivity for levopimaradiene. CPP undergoes diphosphate-ionization cyclization to form the C8-sandaracopimarenyl cation, which can be deprotonated to release sandaracopimaradiene or undergo intramolecular proton transfer and 1,2-methyl migration to yield the abietenyl cation. Subsequent deprotonation of abietenyl cation at four possible sites produces abietadiene, levopimaradiene, neoabietadiene, and palustradiene (not shown).[102]

9.15.4.2 Steroids

Sterols are essential structural and regulatory components of eukaryotic cell membranes. Thus far, only a couple of members of this important class of natural products have been produced by engineered microbial hosts, most notably ergosterol and hydrocortisone. Ergosterol is the main sterol in yeast and is responsible for structural membrane features such as fluidity and permeability, similar to cholesterol in mammalian cells. Additionally, ergosterol is a precursor to vitamin D_2 and cortisone. Overproduction of ergosterol has been achieved in *S. cerevisiae* by overexpressing endogenous genes that are bottlenecks in the native ergosterol biosynthetic pathway (**Figure 19**).[103] Transformation of squalene, the polyisoprene precursor, to ergosterol requires the action of 12 different enzymes. Deregulated expression of HMG-CoA reductase leads to accumulation of squalene (due to higher isoprenoid flux via the MVA pathway) but not of ergosterol, suggesting that the steps downstream of squalene become rate limiting. Simultaneous overexpression of two genes along the *ERG* pathway led to a significant decrease of the squalene pool and concomitant increase in the amount of ergosterol.[103] With optimization in fermentation conditions, the final ergosterol titer has been reported to reach 1.98 g l^{-1}.[104]

Total biosynthesis of heterologous steroids in genetically programmed microorganisms has been pursued with limited success, with only modest titers reported. Notable advances include the overproduction of progesterone and hydrocortisone in yeast.[105,106] Hydrocortisone is the major steroid in mammals and an important intermediate of steroidal drug synthesis. Total biosynthesis of hydrocortisone in yeast involves 25 steps from acetyl-CoA (**Figure 19**), of which the first 19 are endogenous to *S. cerevisiae*. Conversion of ergosterol to hydrocortisone requires the introduction of one plant enzyme and five additional enzymatic steps catalyzed by eight mammalian proteins (**Figure 19**).[105] The heterologous genes were introduced by a combination of plasmid and genomic integration techniques. Elimination of competing pathways and balanced expression of the key enzymes resulted in the production of hydrocortisone as the major sterol (70% selectivity), albeit at low titers (<20 mg l^{-1}), reflecting the challenges in transferring a highly complex and mainly membrane-bound mammalian pathway into a microbial host.

9.15.4.3 Amino Acids

Amino acids are major industrial products of microbial fermentations, with a global market of greater than 3 million tons per year and applications ranging from animal feed to food and pharmaceutical products. The microbial hosts used in industry typically do not require foreign DNA for overproduction, and engineering efforts are instead directed toward bypassing native regulation mechanisms (i.e., feedback inhibition) that limit titer and productivity. Metabolic engineering applied to amino acid fermentation has been reviewed elsewhere.[107] Here, the discussion is limited to a summary of efforts to produce L-lysine and L-alanine in bacteria to illustrate approaches of genomic reconstruction and metabolic evolution.

More than 1 000 000 tons of L-lysine per year are produced from the Gram-positive bacterium *Corynebacterium glutamicum*.[108] Industrial strains of *C. glutamicum* have been developed by classical methods of whole-cell mutagenesis and selection. This technique generated many industrial fermentation strains, but has the serious disadvantage of accumulating uncharacterized secondary mutations that are detrimental to important properties such as growth, sugar consumption, and stress tolerance. For instance, *C. glutamicum* B-6 was constructed from the wild-type strain (ATCC 13032) by iterations of random mutation and selection, and is able to produce L-lysine to high titers (95 g l^{-1}) but with suboptimal rate (1.9 g l^{-1} h^{-1}), due to poor growth and sugar consumption.[109] It had been known for decades that the wild-type strain cannot accumulate L-lysine unless it is deficient in L-homoserine dehydrogenase, since this enzyme will divert flux toward the production of L-threonine, L-methionine, and L-isoleucine.[110] Comparative genomics of B-6 and the wild-type strain along the 16 proteins involved in the terminal pathway and the L-lysine efflux step revealed that only three enzymes had suffered amino acid mutations, with each differing from the wild-type copy by a single amino acid substitution.[109] Recombining the three evolved genes in the wild-type background leads to faster production of L-lysine (3.0 g l^{-1} h^{-1}) than in B-6, while retaining a high titer (80 g l^{-1}). This example of genome-based strain reconstruction shows how dissecting the genetic modifications responsible for phenotypic selection at the macroscopic level can lead to an industrially useful, genetically defined mutant without any foreign DNA.

In another effort to understand microbial metabolism at a systems biology level, in-depth profiling of intracellular metabolite concentrations, metabolic fluxes, and gene expression of lysine-producing *C. glutamicum* revealed that the phase shift from growth to lysine production is accompanied by a decrease in glucose uptake flux and the redirection of flux from the tricarboxylic acid (TCA) cycle toward lysine biosynthesis.[111] Additionally, metabolic engineering created an L-lysine hyper-producing *C. glutamicum* with impressive fermentation metrics: 120 g l^{-1} titer, 4.0 g l^{-1} h^{-1} volumetric productivity, and 0.55 g g^{-1} yield on glucose.[112] The engineered strain contained only 12 mutations, which were integrated into the genome without introducing foreign DNA and without requiring selection markers.

Production of L-alanine has been achieved in *E. coli* with industrially relevant parameters.[113] An *E. coli* strain that makes L-alanine as the major product was created by replacing the genomic lactic acid dehydrogenase gene in a strain already optimized for lactic acid fermentation with a heterologous alanine dehydrogenase (**Figure 20**). Alanine dehydrogenase produces alanine from pyruvate and ammonia using 1 equivalent of NADH (i.e., the biological equivalent of reductive amination, see Section 9.15.3.4). The engineered pathway is redox-balanced such that NADH oxidation (required for alanine biosynthesis) is coupled to ATP production and cell growth (**Figure 20**). This linkage provides a basis for metabolic evolution (i.e., serial or continuous cultivation) where selection for improvements in growth coselect for increased glycolytic flux and alanine production. Cells with increased growth rate due to spontaneous mutations will outcompete their parent strains and have increased alanine

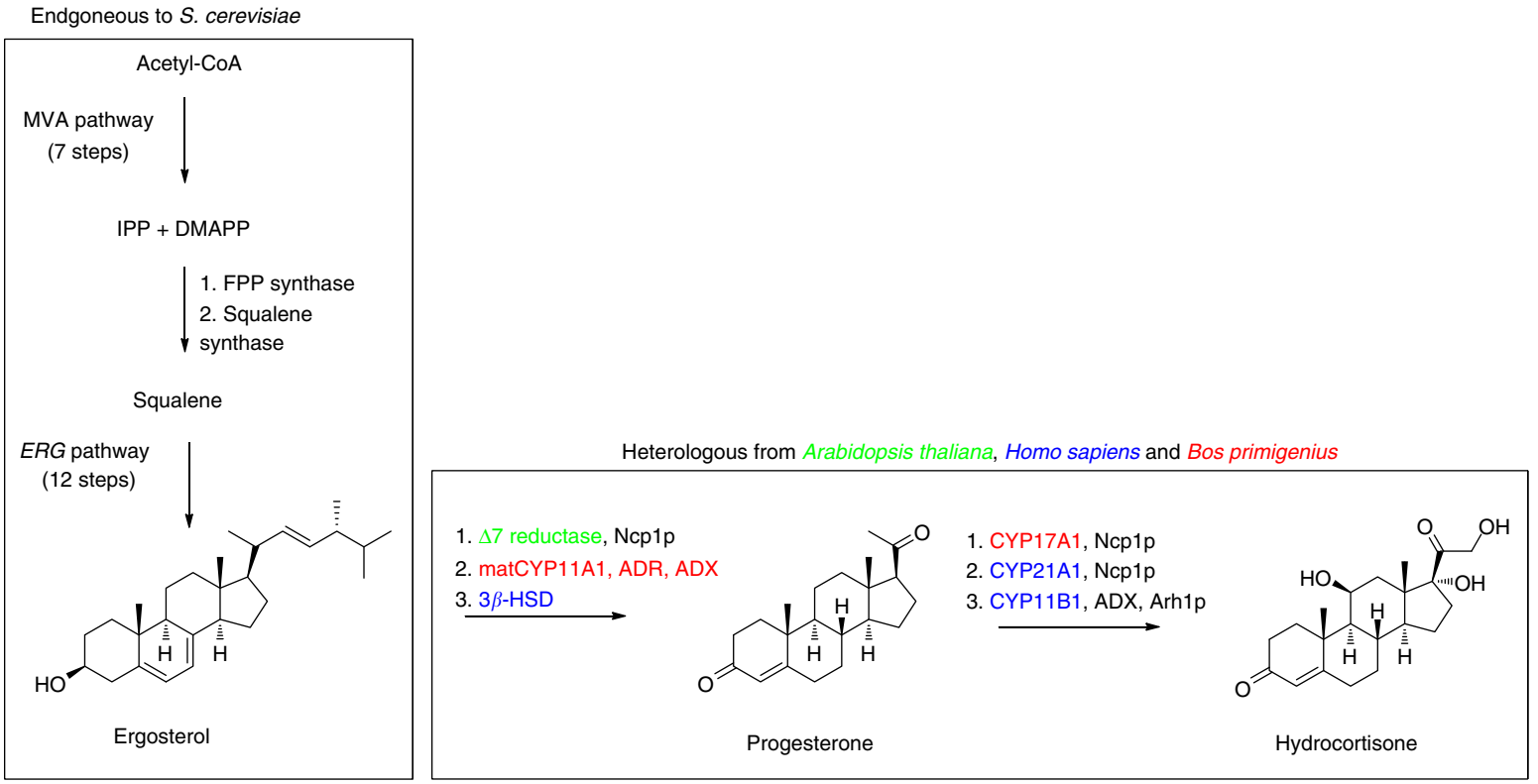


Figure 19 Endogenous biosynthesis of ergosterol in yeast and recombinant production of hydrocortisone involving mammalian and plant enzymes. Enzymes: matCYP11A1, mature form of CYP11A1 (P450 side chain cleaving); 3β-HSD, 3β-hydroxysteroid dehydrogenase-isomerase; ADX, bovine adrenodoxin (electron carrier); ADR, bovine adrenodoxin reductase; Δ7 reductase, Δ7 sterol reductase; Ncp1p, NADPH P450 reductase; Arh1p, adrenodoxin reductase homolog.[105]

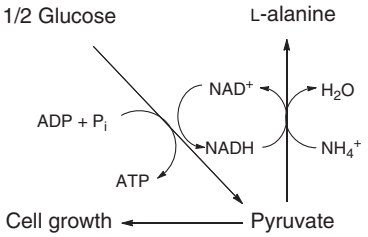


Figure 20 Fermentation of glucose to L-alanine generates a surplus of ATP allowing the pathway to be optimized by metabolic evolution.[113]

productivity. Deletion of other genes that divert metabolic flux away from the target pathway, optimizing fermentation conditions, and successive rounds of metabolic evolution achieved a final product titer of 114 g l^{-1}, 96% mass yield (with respect to glucose), 2.4 g l^{-1} h^{-1} average volumetric productivity, and product purity greater than 99.5%. In this example, chromosomal integration of a single heterologous gene provided sufficient levels of expression to support high levels of growth and product flux without the need for multicopy plasmids and selection agents for plasmid retention (thus obviating the need for expensive inducers and antibiotics). Impressively, the dried broth from batch fermentation in glucose mineral salts medium afforded, after cell removal, approximately 95% (w/w) L-alanine without further purification.

9.15.4.4 Diamines

Diamines have many industrial applications as components of polyamides, pharmaceuticals, agrochemicals, surfactants, and other materials. For example, putrescine (1,4-diaminobutane) is currently used to synthesize nylon-4,6 by polycondensation with adipic acid. Putrescine is naturally biosynthesized in *E. coli* and is thought to play a role in cell proliferation and normal cell growth; however, its intracellular concentration in *E. coli* is reported to be only ~30 mM, as it is elaborately regulated by biosynthesis, degradation, uptake, and excretion.[114] Accordingly, overproduction of putrescine in *E. coli* requires the concerted overexpression of bottleneck enzymes, deletion of competing degradation pathways, enhancing excretion, and hindering uptake back into cells. Amplification of putrescine biosynthesis in *E. coli* is based on seven enzymatic steps from the TCA cycle intermediate α-ketoglutarate (Figure 21).[115] The key step is decarboxylation of ornithine, a common precursor in arginine biosynthesis, to directly form putrescine. The putrescine importer (*puuP*) was deleted to prevent the cells from importing extracellular putrescine at the end of batch fermentations under conditions of carbon starvation. Arginine biosynthesis from ornithine requires the action of one of two ornithine carbamoyltransferases (*argI* and *argF*). The *argI argF* double knock-out is auxotrophic with respect to arginine, but arginine supplementation is undesirable since the pathway is feedback-inhibited by arginine at the level of *N*-acetylglutamate synthase. Deletion of just the *argI* gene, encoding the major carbamoyltransferase, results in increased production of putrescine and eliminates the requirement for arginine supplementation. Constitutive overexpression of the antiporter *potE*, responsible for putrescine excretion, was achieved by replacing its native promoter by a stronger promoter. Finally, high cell density fed-batch fermentations in glucose mineral salts medium allowed for a putrescine accumulation of 24.2 g l^{-1} at 0.75 g l^{-1} h^{-1}, with 0.168 g g^{-1} yield on glucose.[115]

Unlike putrescine, cadaverine is a minor polyamine found only in a few microorganisms.[116] In *E. coli*, cadaverine (1,5-pentanediamine) is biosynthesized from lysine in a single enzymatic step by the action of lysine decarboxylase. Accordingly, previously derived lysine-producing strains of *C. glutamicum* offer an excellent starting point for overproduction of this diamine. Toray Industries demonstrated that cadaverine accumulation can be achieved by chromosomal substitution of the native homoserine dehydrogenase gene (*hom*) in *C. glutamicum* for the lysine decarboxylase from *E. coli* (*cadA*).[117] Homoserine dehydrogenase deficiency is required for lysine accumulation (see Section 9.15.4.3) and thus is also important for improving flux toward cadaverine. Simultaneous *hom* removal and *cadA* expression resulted in a titer of 2.6 g l^{-1} cadaverine, with 0.052 g g^{-1} yield from glucose. Efficient secretion of cadaverine is important as its *in vivo* accumulation can inhibit lysine decarboxylase. Most cadaverine formed inside *C. glutamicum* is ionized (p*Ka* = 9.13) such that its secretion requires active transport across the cell membrane. Genome-wide transcription analysis of cadaverine-producing *C. glutamicum* was used to identify the key exporter, a permease with an undefined physiological role, which when overexpressed resulted in improved yields of cadaverine (0.136 g g^{-1} on glucose).[118] *E. coli* has also been engineered to overproduce cadaverine by overexpressing *cadA* and dihydrodipicolinate synthetase.[119] Deletion of genes involved in the utilization, degradation, and import of both putrescine and cadaverine was also required. Altogether, the engineered *E. coli* fermented sugars in mineral salts to a final cadaverine concentration of 9.61 g l^{-1}, at a volumetric productivity of 0.32 g l^{-1} h^{-1}, and a yield of 0.12 g g^{-1} on glucose.[119]

9.15.4.5 Alcohols

Alcoholic fermentation in *S. cerevisiae* is the largest-scale biotechnology process in operation (>70 million tons per year). Strains of *S. cerevisiae* have been developed over millennia of artificial selection for ethanol production, which is the end product of anaerobic fermentation in yeast. Intense academic and industrial research has been directed toward novel fermentation routes for higher chain alcohols with superior fuel properties and more versatile chemical applications. Isobutanol (2-methylpropan-1-ol), for example, is a precursor to C4 petrochemical building blocks as well as an excellent gasoline blend. Glucose to isobutanol

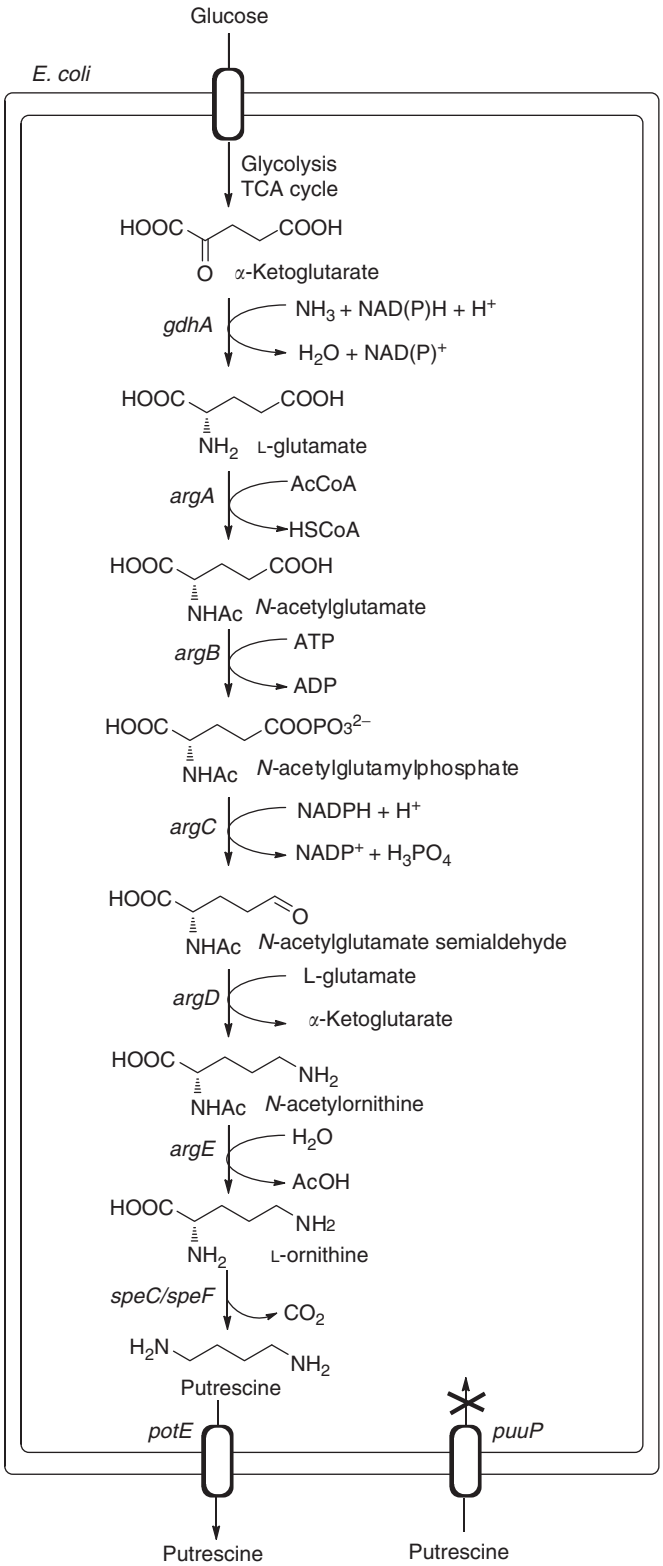


Figure 21 Putrescine biosynthesis in *E. coli*. Enzymes encoded by the genes shown are: *gdhA*, glutamate dehydrogenase; *argA*, *N*-acetylglutamate synthase; *argB*, *N*-acetylglutamate kinase; *argC*, *N*-acetylglutamyl phosphate reductase; *argD*, acetylornithine transaminase; *argE*, acetylornithine deacetylase; *speC/speF*, biosynthetic/degradative ornithine decarboxylase; *potE*, putrescine/ornithine antiporter; *puuP*, putrescine importer. TCA cycle, tricarboxylic acid cycle. Overall biotransformation: 1.03 glucose + 2 NH_3 putrescine + 2.18 CO_2 + NADH.[115]

conversion has been demonstrated in *E. coli* via a modified amino acid pathway that requires only two nonnative steps (KDC and ADH) and uses keto-isovalerate as a precursor (Figure 22).[120] Isobutanol titers of >20 g l^{-1} have been reached by using engineered strains with deletions in pathways competing for carbon and using cofactors that are available aerobically or microaerobically.[120] Anaerobic conditions are preferred, however, for lower operating costs, higher yields, and compatibility with existing ethanol plants. An anaerobic pathway that operates at nearly theoretical yield was achieved by engineering the KARI to switch cofactor preference (i.e., to use NADH instead of NADPH) and thereby consume NADH produced during glycolysis (Figure 22).[121]

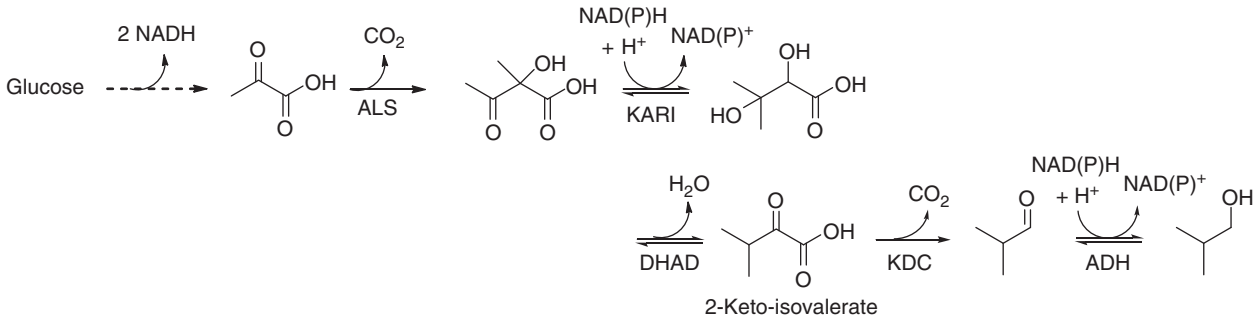


Figure 22 Glucose to isobutanol conversion via 2-keto-isovalerate. Enzymes: ALS, acetolactate synthase; KARI, ketol-acid reducto-isomerase; DHAD, dihydroxy-acid dehydratase; KDC, 2-ketoacid decarboxylase; ADH, alcohol dehydrogenase.[120]

9.15.4.6 Diols

1,3-Propanediol (PDO) is used in fiber polymers prepared from terephthalic acid and PDO that are produced in large volumes (e.g., for apparel and carpeting). PDO is naturally produced by a large number of bacteria, such as *Citrobacter*, *Clostridium*, *Enterobacter*, *Klebsiella*, and *Lactobacillus*, as the result of anaerobic growth on glycerol.[122] In these systems, glycerol is converted to PDO in just two steps, namely dehydration to 3-hydroxypropionaldehyde (3-HPA) followed by NAD(P)H-dependent reduction to PDO (Figure 23). The first reaction, which is rate limiting, proceeds via a free radical H-abstraction/rearrangement mechanism followed by spontaneous dehydration and is catalyzed by the coenzyme B_{12}-dependent glycerol dehydratase. This enzyme is eventually inactivated by a suicide reaction with glycerol, such that an ATP-dependent auxilliary reactivase (a chaperone-like

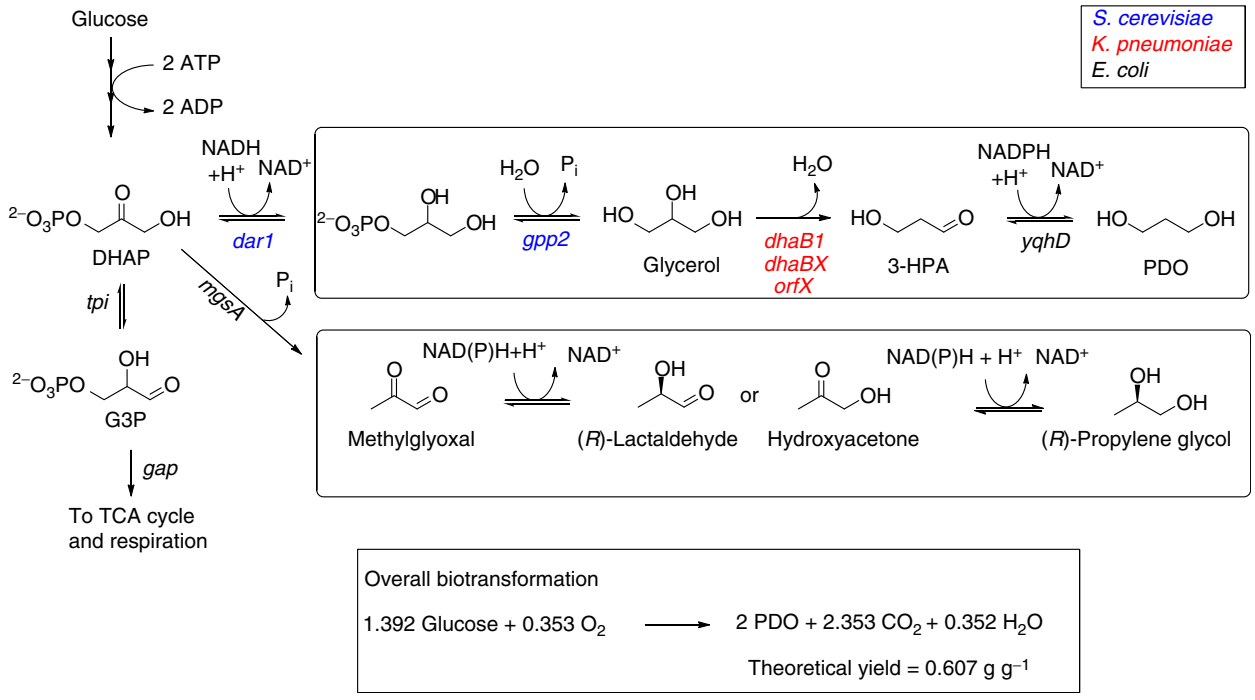


Figure 23 Recombinant pathways for the production of propanediols in *E. coli*. Enzymes encoded by the genes shown are: *dar1*, glycerol 3-phosphate dehydrogenase (*S. cerevisiae*); *gpp2*, glycerol 3-phosphate phosphatase (*S. cerevisiae*); *dhaB1*, glycerol dehydratase (*K. pneumoniae*); *dhaBX*, *orfX*, reactivating factors for glycerol dehydratase (*K. pneumoniae*); *yqhD*, oxidoreductase (*E. coli*); *mgsA*, methylglyoxal synthase (*E. coli*); *tpi*, triose phosphate isomerase (*E. coli*); *gap*, glyceraldehydes-3-phosphate dehydrogenase (*E. coli*). Calculations assumed that cellular respiration of 1 mol of glucose yields 12 mol NAD(P)H equivalents and 34 mol ATP.[124]

protein) is required to reestablish dehydratase activity. The high cost of supplementing vitamin B_{12} to the growth medium is an additional drawback of relying on a B_{12}-dependent enzyme in a metabolic pathway to PDO. Dehydratases with higher resistance to inactivation by glycerol and inhibition by PDO were identified in a metagenomics study, as described in Section 9.15.2.2.[13] Alternatively, B_{12}-independent glycerol dehydratases have been described and may find application in PDO bioproduction.[123]

No naturally occurring microbe has been reported to directly ferment glucose to PDO. In a landmark success of industrial metabolic engineering, Genencor–DuPont engineered *E. coli* to directly produce high levels of PDO from glucose.[122] The heterologous pathway imports two genes from *S. cerevisiae* (DAR1 and GPP2, **Figure 23**) to convert the glycolytic intermediate dihydroxyacetone phosphate (DHAP) to glycerol and the *K. pneumoniae* glycerol dehydratase (*dhaB1*) and its reactivating factors (*dhaBX*, *orfX*) that subsequently convert glycerol to 3-HPA. Reduction of 3-HPA to PDO is catalyzed by an oxidoreductase (*yqhD*) that is endogenous to *E. coli*. Since biosynthesis of the highly reduced product PDO from glucose requires additional inputs of NAD(P)H and ATP (equation 1, **Figure 23**), some glucose substrate needs to be oxidized through glycolysis and the TCA cycle to provide the necessary reducing equivalents and energy (equations 2 and 3 in **Figure 23**). This creates a branch point at triose phosphate isomerase (*tpi*), which interconverts DHAP and glyceraldehyde-3-phosphate (G3P). G3P is fed into the TCA cycle to produce reducing equivalents and energy required for the PDO pathway and cell growth. Downregulation of glyceraldehyde-3-phosphate dehydrogenase (*gap*) provides an improved flux control point while maximizing PDO yields. With additional modifications in the *E. coli* strain, the metabolically engineered organism provides PDO at a rate of 3.5 g l^{-1} h^{-1}, a titer of 135 g l^{-1} and a yield of 0.51 g g^{-1} in glucose-fed-batch aerobic fermentations.[122]

Fermentation of glucose to 1,2-propanediol (propylene glycol) in both homologous and heterologous hosts has also been investigated by various groups.[124,125] Major uses of propylene glycol are in unsaturated polyester resins, liquid laundry detergents, pharmaceuticals, cosmetics, antifreeze, and deicing formulations. Some microbes such as *Clostridium sphenoides* and *Thermoanaerobacterium thermosaccharolyticum* naturally ferment sugars to propylene glycol.[124] The pathways employed by these two organisms are very similar and have identical ATP and NAD(P)H cofactor requirements to the aforementioned PDO pathway (**Figure 23**). DHAP is first dephosphorylated to methylglyoxal by the action of methylglyoxal synthase (an enzyme which is also native to *E. coli*). In *C. sphenoides*, the methylglyoxal is reduced to (*R*)-lactaldehyde, whereas in *T. thermosaccharolyticum* the methylglyoxal is reduced to hydroxyacetone. Both of these intermediates are then reduced to (*R*)-1,2-propanediol. Propylene glycol production in these hosts is limited by low yields, a lack of genetic tools for rational biocatalyst improvement, and, in the case of *C. sphenoides*, by the requirement for phosphate-free media (it is both difficult and expensive to obtain commercial-grade medium components that are free of phosphate). Since *E. coli* naturally produces methylglyoxal, recombinant production of propylene glycol can be readily achieved by providing the appropriate reductase activities.[124]

1,4-Butanediol (BDO) is an important commodity chemical used to manufacture more than 2.5 million tons annually of valuable polymers. Current production is based on feedstocks of fossil origin such as acetylene, propane, butane, and butadiene. Because BDO is not produced naturally in any known organism, its production in *E. coli* required the establishment of a novel heterologous biochemical pathway.[126] Computational design was used to screen reaction classes (rather than actual enzyme-catalyzed reactions) that could intercept common metabolites in *E. coli* and convert those to BDO. This broader approach identified more than 10 000 putative pathways capable of converting common metabolites (i.e., acetyl-CoA, succinyl-CoA, α-ketoglutarate, and glutamate) to BDO in just four to six steps. Computational methods were used to rank the pathways according to maximum theoretical BDO yield, pathway length, number of nonnative steps, number of novel steps, and thermodynamic feasibility. Constraint-based modeling was then used to eliminate pathways that displayed unfavorable thermodynamics or low theoretical yield. The remaining 1000 pathways were ranked again according to the number of steps catalyzed by uncharacterized enzymes (based on KEGG and EcoCyc databases, see Section 9.15.2), the number of nonnative steps, and the total number of steps from central metabolism.

This process led to the selection of two artificial routes for BDO production from succinyl-CoA and α-ketoglutarate proceeding via 4-hydroxybutyrate as a common intermediate (**Figure 24**). The pathway was divided into an upstream module (succinyl-CoA/α-ketoglutarate to 4-hydroxybutyrate) and a downstream module (4-hydroxybutyrate to BDO) for experimental validation and metabolic engineering. Only two out of the seven enzymes are native to *E. coli*; the remaining enzymes have to be imported from other organisms, as shown in **Figure 24**. All enzymes act on their native substrates, with the exception of the aldehyde and alcohol dehydrogenases. A computational algorithm was used to predict gene knock-outs that couple BDO production to growth while preserving the maximum BDO theoretical yield. Knocking-out those genes eliminated *E. coli*'s ability to produce the usual fermentation products (ethanol, formate, lactate, succinate), thereby forcing production toward BDO to achieve redox balance. This led to improved BDO titers, but other intermediates were still formed preferentially, such as 4-hydroxybutyrate, succinate, and notably butyrolactone (likely formed spontaneously from 4-hydroxybutyrate-CoA, **Figure 24**). Finally, improvements in expression of TCA cycle enzymes under microaerobic conditions by lifting transcriptional repression and NADH inhibition of citrate synthase, as well as selecting an aldehyde dehydrogenase that acts on 4-hydroxybutyraldehyde but not on acetyl-CoA, led to formation of BDO as the main product with a final titer of 18 g l^{-1}.[126] This process is being commercialized by Genomatica in collaboration with BASF.

9.15.4.7 Summary

Designing new synthetic pathways into microbial hosts demands careful consideration of redox balance, ATP balance, product toxicity, feedback inhibition, and host selection, the last factor accounting for growth rate and ability to grow on simple media.

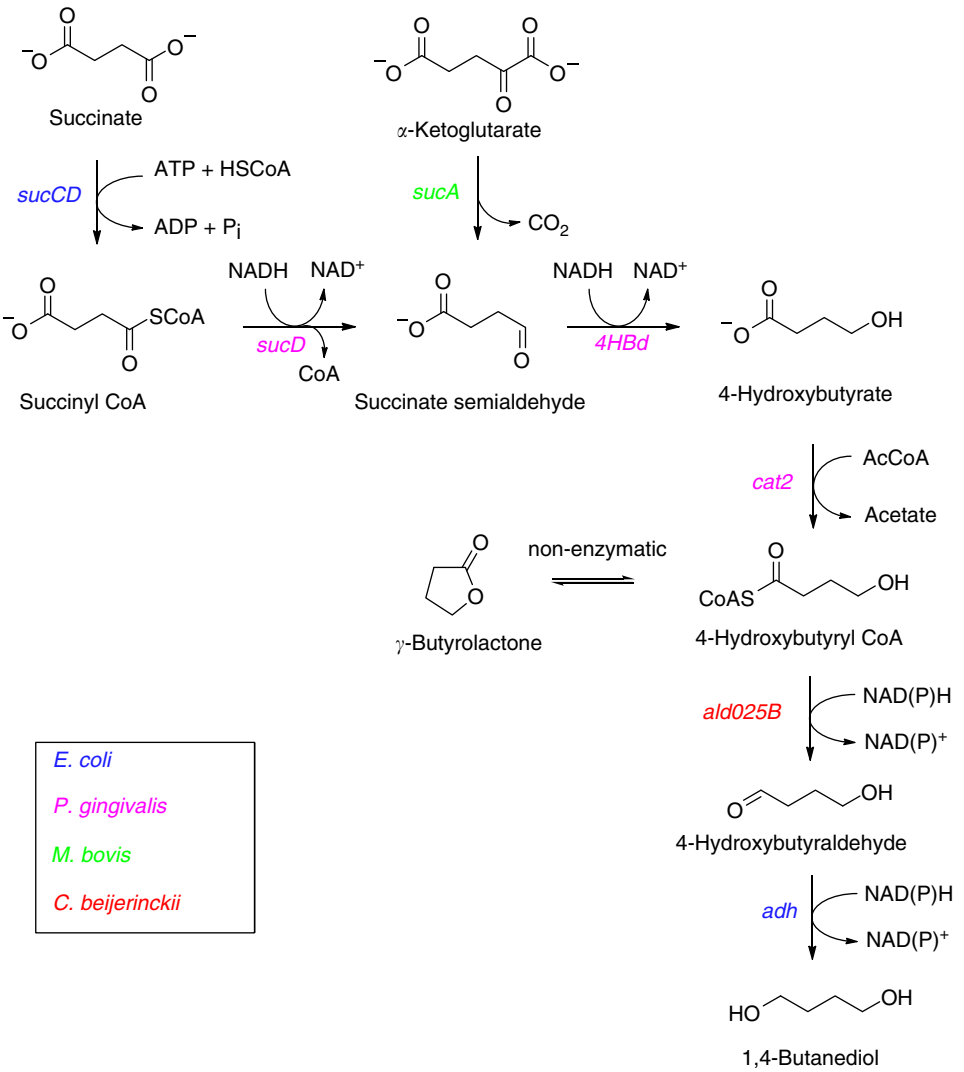


Figure 24 Computationally designed pathway for 1,4-butanediol production in *E. coli*. Enzymes encoded by the genes shown are: *sucCD*, succinyl-CoA synthetase (*E. coli*); *sucD*, semialdehyde dehydrogenase (*Porphyromonas gingivalis*); *4HBd*, 4-hydroxybutyrate dehydrogenase (*P. gingivalis*); *sucA*, α-keto acid decarboxylase (*Mycobacterium bovis*); *cat2*, 4-hydroxybutyryl-CoA transferase; *ald025B*, aldehyde dehydrogenase (*Clostridium beijerinckii*); *adh*, alcohol dehydrogenase (*E. coli*).[126]

There is no universal approach for engineering microbial metabolism, and successful efforts necessarily employ a range of technologies as outlined above. It is noteworthy that most case studies thus far have not involved extensive use of enzyme engineering, but focused instead on optimizing and balancing expression of naturally occurring enzymes in a convenient host. Notable exceptions include the engineered levopimaradiene and isobutanol pathways listed above (see Sections 9.15.4.1.4 and 9.15.4.5). Fine tuning of many recombinant pathways will likely involve more enzyme engineering to deliver enhanced kinetic parameters and substrate and product specificities at each catalytic node. However, the very possibility of such sensitive modulation should provide chemists with clear appreciation of the potential utility of biological catalysts relative to small molecule catalysts.

The three key metrics used to assess the utility of microbial processes – yield, volumetric productivity, and titer – are listed in Table 2 for some of the pathways discussed in Section 9.15.4. These examples developed over the last decade affirm the ability to manipulate microbial metabolism for industrial production of chemicals. However, most of these processes do not yet match the thermodynamic and kinetic efficiencies of yeast ethanol fermentations, adapted and improved over millennia by artificial selection. Process robustness is also an important consideration for large-scale implementation of these technologies. Ideally, the recombinant pathway should not require expensive inducers and selection markers (antibiotics), and the engineered strain should not require complex nutrients or ideally even sterile conditions for growth and should be tolerant to high product concentrations. This field is still in its infancy, and as techniques grow in sophistication and the understanding of metabolic control deepens, it is possible to look forward to enabling the vision of living factories for sustainable chemical production.

Table 2 Summary of key metrics for the pathways described in Section 9.15.4

Target product	*Host*	*Theoretical yield* ($g_{pdt}\ g_{Csource}^{-1}$)	*Practical yield* ($g_{pdt}\ g_{Csource}^{-1}$)	*Titer* ($g\ l^{-1}$)	*Volumetric productivity* ($g\ l^{-1}\ h^{-1}$)[a]
Isoprene[86]	*E. coli*	0.25[b]	0.11 (44%)	>60	2.0
Amorphadiene[95c]	*S. cerevisiae*	0.25	N/A	37	N/A
Taxadiene[101]	*E. coli*	0.30[c]	0.025 (7%)	1.00	N/A
L-Alanine[113]	*E. coli*	0.989	0.950 (96%)	114	2.37
L-Lysine[112]	*C. glutamicum*	0.75	0.55 (73%)	120	4.0
Putrescine[115]	*E. coli*	0.475	0.168 (35%)	24.2	0.75
Cadaverine[119]	*E. coli*	0.524	0.12 (23%)	9.61	0.32
Isobutanol	*S. cerevisiae*	0.41	0.41 (>95%)	N/A	2.0
1,3-Propanediol[122]	*E. coli*	0.607	0.51 (84%)	135	3.5
1,4-Butanediol[126]	*E. coli*	0.55	N/A	18.0	0.15
Ethanol	*S. cerevisiae*	0.51	~0.49 (96%)	~95	~8.0

[a]Average volumetric productivity was calculated based on total product produced per total fermentation time.
[b]Based on MVA pathway utilizing glucose as the carbon source.
[c]Based on MEP pathway utilizing glycerol as the carbon source.

9.15.5 Beyond Nature: Design and Evolution of Artificial Function/Catalysis

Given the rate at which the biotechnologies outlined above are being applied to chemical synthesis, it is reasonable to consider more recent advances that might soon have a similar impact. Although directed evolution of enzymes has clearly provided an extremely powerful tool to generate efficient catalysts, this process is only reliable once some initial activity is identified. Accordingly, researchers are starting to design enzymes *de novo* in order to reap the benefits of enzyme catalysis for reactions not found in nature; notable examples include designed enzymes for the Diels–Alder and retro-aldol reactions.[127] A range of non-natural transition metal-catalyzed reactions have also been enabled by incorporating metal catalysts into protein scaffolds.[128] The several different systems that have been devised can be classified generally according to how the metal catalyst is anchored into the protein, namely covalent, supramolecular, or dative attachment. Among the most well-studied systems are the (strep)avidin–biotin metalloenzymes (supramolecular anchoring) devised by Whitesides and greatly improved by Ward, which have been used for a range of transition metal-catalyzed reactions.[129]

Covalently linking a catalyst precursor (e.g., bisdiphenylphosphino rhodium) to a biotin anchor ensures that upon stoichiometric addition of (strept)avidin, the metal cofactor is quantitatively incorporated within the host protein. The resulting hybrid catalyst exhibits features of both homogeneous and enzyme catalysis. For example, features reminiscent of homogeneous catalysis include straightforward access to both enantiomers of the product, broad substrate scope, organic solvent tolerance, whereas acquired enzyme-like properties include access to genetic optimization, aqueous solubility and activity, and Michaelis–Menten behavior. This strategy has been used to create asymmetric systems for catalyzing rhodium-diphosphine hydrogenation of *N*-protected dehydroamino acids (Figure 25, up to 95% *ee*), palladium-diphosphine allylic alkylation (up to 95% *ee*), and vanadyl oxidation of sulfides (up to 93% *ee*).[129]

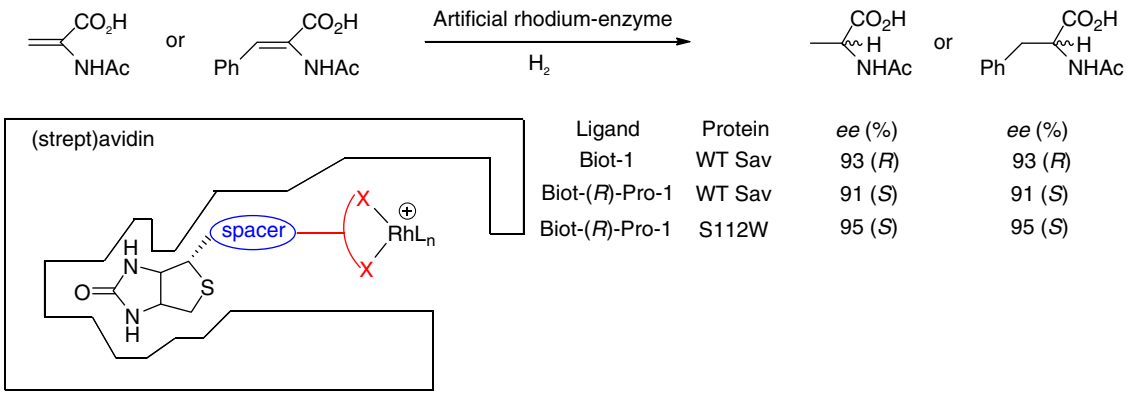


Figure 25 Reduction of *N*-acetamidoacrylic acid and *N*-acetamidocinnamic acid by artificial hydrogenases based on the biotin–avidin technology. The hybrid catalyst can be improved by chemogenetic optimization by varying the spacer (oval) or the chelating ligand, or by amino acid substitutions in the host protein [(strept)avidin].[129]

Nonnatural activities can also be installed into naturally occurring enzymes without the addition of synthetic cofactors. Taking advantage of the catalytic promiscuity of enzymes, panels of enzymes can be screened against synthetic reagents to discover

abiological reactions. For example, Purkarthofer et al. screened a hydroxynitrile lyase for nitro-aldol (Henry reaction) activity on nitromethane and various aldehydes and found that the wild-type enzyme could catalyze the carboligation of nitromethane to benzaldehyde with high enantioselectivity (92% *ee*).[130] Similarly, a panel of engineered cytochrome P450s was screened against diazoester and azide reagents for C=C and C–H functionalization by carbenoid and nitrenoid insertions.[131] P450 variants (with as few as one mutation from the wild type) could catalyze the cyclopropanation of styrene from ethyl diazoacetate with high enantioselectivity and exquisite diastereocontrol (Figure 26(a)) as well as the intramolecular C–H amination from arylsulfonyl azides (Figure 26(b)).[131]

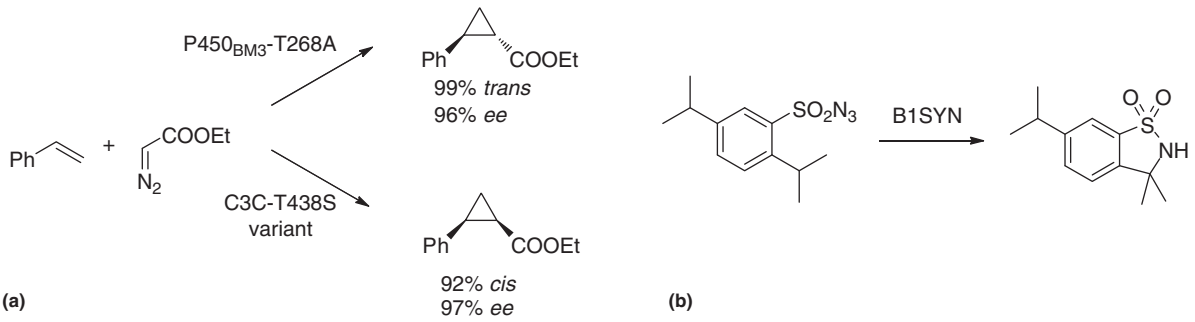


Figure 26 (a) $P450_{BM3}$-catalyzed cyclopropanation of styrene utilizing ethyl diazoacetate as a carbene precursor. Variant C3C-T438S has 14 mutations with respect to $P450_{BM3}$. (b) $P450_{BM3}$.-catalyzed intramolecular C–H amination from an arylsulfonyl azide. Variant B1SYN has 23 mutations with respect to $P450_{BM3}$.[131]

Evolution of *de novo* designed enzymes and artificial metalloenzymes will be useful for their optimization for synthetic applications.[132] As illustrated in Section 9.15.4, most metabolic engineering projects have aimed at establishing heterologous production of molecules with well-understood natural pathways. As protein engineering advances in installing nonnatural activities into enzymes, it can be expected that entirely artificial pathways will emerge for producing compounds of industrial relevance that are not synthesized naturally.

Of course both the catalysts and the format in which they are used can have a large impact on the utility and efficiency of a process. For example, some of the challenges associated with conducting reactions *in vivo* for metabolic engineering efforts were outlined in Section 9.15.4. Due to these challenges, researchers have sought to design cells with minimal genomes that might simplify metabolic networks to minimize undesired reactivity, divert more energy and materials toward target products, and simplify downstream bioprocessing.[133] Further simplifications have also been realized using cell-free biosynthetic systems in which cells are grown to provide the necessary cofactors and catalysts for a target process, then lysed to release these materials in a reactor. Substrates, cosolvents, and other reagents that may be detrimental to cell survival can then be utilized, and the concentration of these species in the reaction medium can be precisely controlled.[134] The relative concentrations of enzymes can be controlled by combining isolated enzymes in a single reactor to enable selective sequential reactions on a substrate via *in vitro* cascades.[135] Thus, in all of these cases, chemists are given increasing control over the complex milieu in living cells. As these processes are improved, chemists will thus have an increasing palette of systems to draw on to carry out target reactions with increased efficiency.

Acknowledgments

FHA and PSC were supported by the Gordon and Betty Moore Foundation for funding through the Caltech Programmable Molecular Technology Initiative and the Jacobs Institute for Molecular Engineering for Medicine. JCL was supported by an NIH Pathways to Independence Award (5R00GM087551-03).

References

1. Wetterstrand, K. A. DNA sequencing costs: data from the NHGRI large-scale genome sequencing program. Available at: http://www.genome.gov/sequencingcosts (accessed on 15 September 2012).
2. Life Technologies introduces the benchtop ion proton sequencer, designed to decode a human genome in one day for $1,000. Available at: http://www.lifetechnologies.com/us/en/home//about-us/news-gallery/press-releases/2012/life-techologies-itroduces-the-bechtop-io-proto.html.html (accessed on 1 September 2012).
3. (a) Venter, J. C.; Remington, K.; Heidelberg, J. F.; *et al. Science* **2004**, *304*(5667), 66–74. (b) Vogel, T. M.; Simonet, P.; Jansson, J. K.; *et al. Nat. Rev. Microbiol.* **2009**, *7*(4), 252.
4. Carlson, R. *Nat. Biotechnol.* **2009**, *27*(12), 1091–1094.
5. (a) Khorana, H. G. *Science* **1979**, *203*(4381), 614–625. (b) Mandecki, W.; Hayden, M. A.; Shallcross, M. A.; Stotland, E. *Gene* **1990**, *94*(1), 103–107. (c) Gibson, D. G.; Benders, G. A.; Andrews-Pfannkoch, C.; *et al. Science* **2008**, *319*(5867), 1215–1220.

6. Hughes, R. A.; Miklos, A. E.; Ellington, A. D. *Methods Enzymol.* **2011**, *498*, 277–309 (Synthetic Biology, Part B).
7. Ellis, T.; Adie, T.; Baldwin, G. S. *Integr. Biol.* **2011**, *3*(2), 109–118.
8. (a) Gibson, D. G.; Benders, G. A.; Axelrod, K. C.; *et al. Proc. Natl. Acad. Sci. USA* **2008**, *105*(51), 20404–20409. (b) Itaya, M.; Fujita, K.; Kuroki, A.; Tsuge, K. *Nat. Methods* **2008**, *5*(1), 41–43.
9. Torsvik, V.; Ovrebs, L.; Thingstad, T. F. *Science* **2002**, *296*(5570), 1064–1066.
10. (a) Lorenz, P.; Eck, J. *Nat. Rev. Microbiol.* **2005**, *3*(6), 510–516. (b) Iqbal, H. A.; Feng, Z.; Brady, S. F. *Curr. Opin. Chem. Biol.* **2012**, *16*(1–2), 109–116.
11. Hu, X. P.; Heath, C.; Taylor, M. P.; Tuffin, M.; Cowan, D. *Extremophiles* **2012**, *16*(1), 79–86.
12. Uchiyama, T.; Miyazaki, K. *Appl. Environ. Microbiol.* **2010**, *76*(21), 7029–7035.
13. Knietsch, A.; Bowien, S.; Whited, G.; Gottschalk, G.; Daniel, R. *Appl. Environ. Microbiol.* **2003**, *69*(6), 3048–3060.
14. (a) Piel, J. *Proc. Natl. Acad. Sci. USA* **2002**, *99*(22), 14002–14007. (b) Schmidt, E. W.; Nelson, J. T.; Rasko, D. A.; *et al. Proc. Natl. Acad. Sci. USA* **2005**, *102*(20), 7315–7320.
15. Bayer, T. S.; Widmaier, D. M.; Temme, K.; *et al. J. Am. Chem. Soc.* **2009**, *131*(18), 6508–6515.
16. Keasling, J. D. *ACS Chem. Biol.* **2008**, *3*(1), 64–76.
17. Welch, M.; Villalobos, A.; Gustafsson, C.; Minshull, J. *J. R. Soc. Interface* **2009**, *6*(Suppl. 4), S467–S476.
18. Esposito, D.; Chatterjee, D. K. *Curr. Opin. Biotechnol.* **2006**, *17*(4), 353–358.
19. Thomas, J. G.; Ayling, A.; Baneyx, F. *Appl. Biochem. Biotechnol.* **1997**, *66*(3), 197–238.
20. Makino, T.; Skretas, G.; Georgiou, G. *Microb. Cell Fact.* **2011**, *10*, 32.
21. Clouthier, C. M.; Pelletier, J. N. *Chem. Soc. Rev.* **2012**, *41*(4), 1585–1605.
22. Lairson, L. L.; Watts, A. G.; Wakarchuk, W. W.; Withers, S. G. *Nat. Chem. Biol.* **2006**, *2*(12), 724–728.
23. Kim, P.-Y.; Pollard, D. J.; Woodley, J. M. *Biotechnol. Prog.* **2007**, *23*(1), 74–82.
24. Strohmeier, G. A.; Pichler, H.; May, O.; Gruber-Khadjawi, M. *Chem. Rev.* **2011**, *111*(7), 4141–4164.
25. Tracewell, C. A.; Arnold, F. H. *Curr. Opin. Chem. Biol.* **2009**, *13*(1), 3–9.
26. Arnold, F. H. *Acc. Chem. Res.* **1998**, *31*(3), 125–131.
27. (a) Turner, N. J. *Nat. Chem. Biol.* **2009**, *5*(8), 567–573. (b) Reetz, M. T. *Angew. Chem. Int. Ed. Engl.* **2011**, *50*(1), 138–174.
28. Tee, K. L.; Schwaneberg, U. *Comb. Chem. High Throughput Screen.* **2007**, *10*(3), 197–217.
29. Fasan, R. *ACS Catal.* **2012**, *2*(4), 647–666.
30. Jung, S. T.; Lauchli, R.; Arnold, F. H. *Curr. Opin. Biotechnol.* **2011**, *22*(6), 809–817.
31. Warman, A. J.; Roitel, O.; Neeli, R.; *et al. Biochem. Soc. Trans.* **2005**, *33*(4), 747–753.
32. Lewis, J. C.; Arnold, F. H. *Chimia* **2009**, *63*(6), 309–312.
33. Li, S.; Chaulagain, M. R.; Knauff, A. R.; *et al. Proc. Natl. Acad. Sci. USA* **2009**, *106*(44), 18463–18468.
34. Meyer, A.; Wursten, M.; Schmid, A.; Kohler, H.-P. E.; Witholt, B. *J. Biol. Chem.* **2002**, *277*(37), 34161–34167.
35. van den Heuvel, R. H. H.; van den Berg, W. A. M.; Rovida, S.; van Berkel, W. J. H. *J. Biol. Chem.* **2004**, *279*(32), 33492–33500.
36. Gursky, L. J.; Nikodinovic-Runic, J.; Feenstra, K. A.; O'Connor, K. E. *Appl. Microbiol. Biotechnol.* **2010**, *85*(4), 995–1004.
37. Rehdorf, J.; Bornscheuer, U.T. Monooxygenases, Baeyer-Villiger Applications in Organic Synthesis. In *Encyclopedia of Industrial Biotechnology: Bioprocess, Bioseparation, and Cell Technology*; Rickinger, M. C. Ed.; John Wiley & Sons, Inc: Hoboken, **2010**, Vol. 5; pp 3572–3607.
38. Zhang, Z.-G.; Parra, L. P.; Reetz, M. T. *Chem. Eur. J.* **2012**, *18*(33), 10160–10172.
39. Boyd, D. R.; Bugg, T. D. H. *Org. Biomol. Chem.* **2006**, *4*(2), 181–192.
40. Furukawa, K.; Suenaga, H.; Goto, M. *J. Bacteriol.* **2004**, *186*(16), 5189–5196.
41. Rui, L.; Reardon, K. F.; Wood, T. K. *Appl. Microbiol. Biotechnol.* **2005**, *66*(4), 422–429.
42. Vardar, G.; Ryu, K.; Wood, T. K. *J. Biotechnol.* **2005**, *115*(2), 145–156.
43. Fishman, A.; Tao, Y.; Rui, L.; Wood, T. K. *J. Biol. Chem.* **2005**, *280*(1), 506–514.
44. Rai, G. P.; Sakai, S.; Florez, A. M.; Mogollon, L.; Hager, L. P. *Adv. Synth. Catal.* **2001**, *343*(6 + 7), 638–645.
45. Hasan, Z.; Renirie, R.; Kerkman, R.; *et al. J. Biol. Chem.* **2006**, *281*(14), 9738–9744.
46. Butler, A.; Sandy, M. *Nature* **2009**, *460*(7257), 848–854.
47. Lang, A.; Polnick, S.; Nicke, T.; *et al. Angew. Chem. Int. Ed. Engl.* **2011**, *50*(13), 2951–2953.
48. Glenn, W. S.; Nims, E.; O'Connor, S. E. *J. Am. Chem. Soc.* **2011**, *133*(48), 19346–19349.
49. Chen, S.; Engel, P. C. *J. Biotechnol.* **2009**, *142*(2), 127–134.
50. Wichmann, R.; Vasic-Racki, D. *Adv. Biochem. Eng. Biotechnol.* **2005**, *92*, 225–260, (Technology Transfer in Biotechnology).
51. Sacchi, S.; Rosini, E.; Molla, G.; Pilone, M. S.; Pollegioni, L. *Protein Eng. Des. Sel.* **2004**, *17*(6), 517–525.
52. Carr, R.; Alexeeva, M.; Enright, A.; *et al. Angew. Chem. Int. Ed. Engl.* **2003**, *42*(39), 4807–4810.
53. Escalettes, F.; Turner, N. J. *Chembiochem* **2008**, *9*(6), 857–860.
54. (a) Bastian, S.; Rekowski, M. J.; Witte, K.; Heckmann-Pohl, D. M.; Giffhorn, F. *Appl. Microbiol. Biotechnol.* **2005**, *67*(5), 654–663. (b) Sun, L.; Petrounia, I. P.; Yagasaki, M.; Bandara, G.; Arnold, F. H. *Protein Eng.* **2001**, *14*(9), 699–704.
55. Moore, J. C.; Pollard, D. J.; Kosjek, B.; Devine, P. N. *Acc. Chem. Res.* **2007**, *40*(12), 1412–1419.
56. Bougioukou, D. J.; Kille, S.; Taglieber, A.; Reetz, M. T. *Adv. Synth. Catal.* **2009**, *351*(18), 3287–3305.
57. Svedendahl, M.; Branneby, C.; Lindberg, L.; Berglund, P. *ChemCatChem* **2010**, *2*(8), 976–980.
58. Savile, C. K.; Janey, J. M.; Mundorff, E. C.; *et al. Science* **2010**, *329*(5989), 305–309.
59. Williams, G. J.; Zhang, C.; Thorson, J. S. *Nat. Chem. Biol.* **2007**, *3*(10), 657–662.
60. Shaikh, F. A.; Withers, S. G. *Biochem. Cell Biol.* **2008**, *86*(2), 169–177.
61. Koryakina, I.; Neville, J.; Nonaka, K.; Van Lanen, S. G.; Williams, G. J. *J. Biomol. Screen.* **2011**, *16*(8), 845–851.
62. Mihara, Y.; Utagawa, T.; Yamada, H.; Asano, Y. *Appl. Environ. Microbiol.* **2000**, *66*(7), 2811–2816.
63. Griswold, K. E.; Aiyappan, N. S.; Iverson, B. L.; Georgiou, G. *J. Mol. Biol.* **2006**, *364*(3), 400–410.
64. Schmidt, M.; Boettcher, D.; Bornscheuer, U. T. *Protein Pept. Lett.* **2009**, *16*(10), 1162–1171.
65. Lutz, S. *Tetrahedron Asymmetry* **2004**, *15*(18), 2743–2748.
66. Reetz, M. T.; Bocola, M.; Wang, L.-W.; *et al. J. Am. Chem. Soc.* **2009**, *131*(21), 7334–7343.
67. Ma, S. K.; Gruber, J.; Davis, C.; *et al. Green Chem.* **2010**, *12*(1), 81–86.
68. Tang, L.; Zhu, X.; Zheng, H.; Jiang, R.; Elenkov, M. M. *Appl. Environ. Microbiol.* **2012**, *78*(8), 2631–2637.
69. Bolt, A.; Berry, A.; Nelson, A. *Arch. Biochem. Biophys.* **2008**, *474*(2), 318–330.
70. (a) González-García, E.; Helaine, V.; Klein, G.; *et al. Chem. Eur. J.* **2003**, *9*, 893–899. (b) Sugiyama, M.; Greenberg, W.; Wong, C.-H. *Yuki Gosei Kagaku Kyokaishi* **2008**, *66*(6), 605–615.
71. Greenberg, W. A.; Varvak, A.; Hanson, S. R.; *et al. Proc. Natl. Acad. Sci. USA* **2004**, *101*(16), 5788–5793.
72. Woodhall, T.; Williams, G.; Berry, A.; Nelson, A. *Angew. Chem. Int. Ed. Engl.* **2005**, *44*(14), 2109–2112.
73. Williams, G. J.; Woodhall, T.; Farnsworth, L. M.; Nelson, A.; Berry, A. *J. Am. Chem. Soc.* **2006**, *128*(50), 16238–16247.

74. Fong, S.; Machajewski, T. D.; Mak, C. C.; Wong, C.-H. *Chem. Biol.* **2000**, *7*(11), 873–883.
75. Liu, Z.; Pscheidt, B.; Avi, M.; *et al. Chembiochem* **2008**, *9*(1), 58–61.
76. (a) Asano, Y.; Kira, I.; Yokozeki, K. *Biomol. Eng.* **2005**, *22*(1-3), 95–101. (b) Bartsch, S.; Bornscheuer, U. T. *Protein Eng. Des. Sel.* **2010**, *23*(12), 929–933.
77. Yoshikuni, Y.; Ferrin, T. E.; Keasling, J. D. *Nature* **2006**, *440*(7087), 1078–1082.
78. Lee, H. Y.; Harvey, C. J. B.; Cane, D. E.; Khosla, C. *J. Antibiot.* **2011**, *64*(1), 59–64.
79. Evans, B. S.; Chen, Y.; Metcalf, W. W.; Zhao, H.; Kelleher, N. L. *Chem. Biol.* **2011**, *18*(5), 601–607.
80. (a) Chen, K.; Arnold, F. H. *Proc. Natl. Acad. Sci. USA* **1993**, *90*(12), 5618–5622. (b) Stemmer, W. P. C. *Nature* **1994**, *370*(6488), 389–391.
81. Schoemaker, H. E.; Mink, D.; Wubbolts, M. G. *Science* **2003**, *299*(5613), 1694–1698.
82. Lewis, J. C.; Coelho, P. S.; Arnold, F. H. *Chem. Soc. Rev.* **2011**, *40*(4), 2003–2021.
83. Walji, A. M.; MacMillan, D. W. C. *Synlett* **2007**, *10*, 1477–1489.
84. Lee, J. W.; Kim, T. Y.; Jang, Y.-S.; Choi, S.; Lee, S. Y. *Trends Biotechnol.* **2011**, *29*(8), 370–378.
85. Christianson David, W. *Science* **2007**, *316*(5821), 60–61.
86. Whited, G. M.; Feher, F. J.; Benko, D. A.; *et al. Ind. Biotechnol.* **2010**, *6*(3), 152–163.
87. Martin, V. J. J.; Pitera, D. J.; Withers, S. T.; Newman, J. D.; Keasling, J. D. *Nat. Biotechnol.* **2003**, *21*(7), 796–802.
88. Julsing, M. K.; Rijpkema, M.; Woerdenbag, H. J.; Quax, W. J.; Kayser, O. *Appl. Microbiol. Biotechnol.* **2007**, *75*(6), 1377–1384.
89. Cervin, M. A.; Whited, G. M.; Miasnikov, A., *et al.* Plant isoprene synthase variants for improved microbial production of isoprene. US20100003716 A1, 2010.
90. Beck, Z. Q.; Estell, D. A.; Rife, C. L.; Wells, D. H.; Miller, J.V. Isoprene synthase variants for improved production of isoprene. WO2012058494 A3, 2012.
91. (a) Miller, B.; Oschinski, C.; Zimmer, W. *Planta* **2001**, *213*(3), 483–487. (b) Lindberg, P.; Park, S.; Melis, A. *Metab. Eng.* **2010**, *12*(1), 70–79. (c) Hong, S.-Y.; Zurbriggen Andreas, S.; Melis, A. *J. Appl. Microbiol.* **2012**, *113*(1), 52–65.
92. Anthony, J. R.; Anthony, L. C.; Nowroozi, F.; *et al. Metab. Eng.* **2009**, *11*(1), 13–19.
93. Ye, V. M.; Bhatia, S. K. *Biotechnol. J.* **2012**, *7*(1), 20–33.
94. Newman, J. D.; Marshall, J.; Chang, M.; *et al. Biotechnol. Bioeng.* **2006**, *95*(4), 684–691.
95. (a) Keasling, J. D. *Metab. Eng.* **2012**, *14*(3), 189–195. (b) Westfall, P. J.; Pitera, D. J.; Lenihan, J. R.; *et al. Proc. Natl. Acad. Sci. USA* **2012**, *109*(3), E111–E118.
96. Pitera, D. J.; Paddon, C. J.; Newman, J. D.; Keasling, J. D. *Metab. Eng.* **2007**, *9*(2), 193–207.
97. Tsuruta, H.; Paddon, C. J.; Eng, D.; *et al. PLoS One* **2009**, *4*(2), e4489.
98. Chang, M. C. Y.; Eachus, R. A.; Trieu, W.; Ro, D.-K.; Keasling, J. D. *Nat. Chem. Biol.* **2007**, *3*(5), 274–277.
99. Roth, R. J.; Acton, N. *J. Nat. Prod.* **1989**, *52*(5), 1183–1185.
100. Ro, D.-K.; Paradise Eric, M.; Ouellet, M.; *et al. Nature* **2006**, *440*(7086), 940–943.
101. Ajikumar, P. K.; Xiao, W.-H.; Tyo, K. E. J.; *et al. Science* **2010**, *330*(6000), 70–74.
102. Leonard, E.; Ajikumar, P. K.; Thayer, K.; *et al. Proc. Natl. Acad. Sci. USA* **2010**, *107*(31), 13654–13659.
103. Veen, M.; Stahl, U.; Lang, C. *FEMS Yeast Res.* **2003**, *4*(1), 87–95.
104. Shang, F.; Wen, S.; Wang, X.; Tan, T. *J. Biotechnol.* **2006**, *122*(3), 285–292.
105. Szczebara, F. M.; Chandelier, C.; Villeret, C.; *et al. Nat. Biotechnol.* **2003**, *21*(2), 143–149.
106. Duport, C.; Spagnoli, R.; Degryse, E.; Pompon, D. *Nat. Biotechnol.* **1998**, *16*(2), 186–189.
107. Park, J. H.; Lee, S. Y. *Biotechnol. J.* **2010**, *5*(6), 560–577.
108. Kind, S.; Jeong, W. K.; Schroeder, H.; Wittmann, C. *Metab. Eng.* **2010**, *12*(4), 341–351.
109. Ohnishi, J.; Mitsuhashi, S.; Hayashi, M.; *et al. Appl. Microbiol. Biotechnol.* **2002**, *58*(2), 217–223.
110. Kinoshita, S.; Nakayama, K.; Kitada, S. *J. Gen. Appl. Microbiol.* **1958**, *4*(2), 128–129.
111. Kromer Jens, O.; Sorgenfrei, O.; Klopprogge, K.; Heinzle, E.; Wittmann, C. *J. Bacteriol.* **2004**, *186*(6), 1769–1784.
112. Becker, J.; Zelder, O.; Häfner, S.; Schröder, H.; Wittmann, C. *Metab. Eng.* **2011**, *13*(2), 159–168.
113. Zhang, X.; Jantama, K.; Moore, J. C.; Shanmugam, K. T.; Ingram, L. O. *Appl. Microbiol. Biotechnol.* **2007**, *77*(2), 355–366.
114. Igarashi, K.; Kashiwagi, K. *Biochem. Biophys. Res. Commun.* **2000**, *271*(3), 559–564.
115. Qian, Z.-G.; Xia, X.-X.; Lee, S. Y. *Biotechnol. Bioeng.* **2009**, *104*(4), 651–662.
116. Tabor, C. W.; Tabor, H. *Microbiol. Rev.* **1985**, *49*(1), 81–99.
117. Mimitsuka, T.; Sawai, H.; Hatsu, M.; Yamada, K. *Biosci. Biotechnol. Biochem.* **2007**, *71*(9), 2130–2135.
118. Kind, S.; Kreye, S.; Wittmann, C. *Metab. Eng.* **2011**, *13*(5), 617–627.
119. Qian, Z.-G.; Xia, X.-X.; Lee, S. Y. *Biotechnol. Bioeng.* **2010**, *108*(1), 93–103.
120. Atsumi, S.; Hanai, T.; Liao, J. C. *Nature* **2008**, *451*(7174), 86–89.
121. Bastian, S.; Liu, X.; Meyerowitz, J. T.; *et al. Metab. Eng.* **2011**, *13*(3), 345–352.
122. Nakamura, C. E.; Whited, G. M. *Curr. Opin. Biotechnol.* **2003**, *14*(5), 454–459.
123. Raynaud, C.; Sarcabal, P.; Meynial-Salles, I.; Croux, C.; Soucaille, P. *Proc. Natl. Acad. Sci. USA* **2003**, *100*(9), 5010–5015.
124. Cameron, D. C.; Altaras, N. E.; Hoffman, M. L.; Shaw, A. J. *Biotechnol. Progr.* **1998**, *14*(1), 116–125.
125. (a) Altaras, N. E.; Cameron, D. C. *Biotechnol. Progr.* **2000**, *16*(6), 940–946. (b) Berrios-Rivera, S. J.; San, K.-Y.; Bennett, G. N. *J. Ind. Microbiol. Biotechnol.* **2003**, *30*(1), 34–40.
126. Yim, H.; Haselbeck, R.; Niu, W.; *et al. Nat. Chem. Biol.* **2011**, *7*(7), 445–452.
127. Richter, F.; Leaver-Fay, A.; Khare, S. D.; Bjelic, S.; Baker, D. *PLoS One* **2011**, *6*(5), e19230.
128. Kohler, V.; Wilson Yvonne, M.; Lo, C.; Sardo, A.; Ward Thomas, R. *Curr. Opin. Biotechnol.* **2010**, *21*(6), 744–752.
129. Ward, T. R. *Acc. Chem. Res.* **2011**, *44*(1), 47–57.
130. Purkarthofer, T.; Gruber, K.; Gruber-Khadjawi, M.; *et al. Angew. Chem. Int. Ed. Engl.* **2006**, *45*(21), 3454–3456.
131. (a) Coelho, P. S.; Brustad, E. M.; Kannan, A; Arnold, F. H. *Science* **2013**, *339*, 307–310. (b) Coelho, P. S.; Wang, Z. J.; Ener, M. E.; *et al. Nat. Chem. Biol.* **2013**, in press. (c) McIntosh, J. A.; Coelho, P. S.; Farwell, C. C.; *et al.* **2013**, in press.
132. Brustad, E. M.; Arnold, F. H. *Curr. Opin. Chem. Biol.* **2011**, *15*(2), 201–210.
133. Chiarabelli, C.; Stano, P.; Anella, F.; Carrara, P.; Luisi, P. L. *FEBS Lett.* **2012**, *586*(15), 2138–2145.
134. Hodgman, C. E.; Jewett, M. C. *Metab. Eng.* **2012**, *14*(3), 261–269.
135. Lopez-Gallego, F.; Schmidt-Dannert, C. *Curr. Opin. Chem. Biol.* **2010**, *14*(2), 174–183.

9.16 Enzyme Evolution as a Tool for Creating Improved Catalysts for Large-Scale Organic Synthesis

GW Huisman, Codexis, Inc., Redwood City, CA, USA

© 2014 Elsevier Ltd. All rights reserved.

9.16.1	**Introduction into Biocatalysis**	421
9.16.2	**The Need for Enzyme Evolution**	422
9.16.2.1	Adapting to the Differences Between a Biological Environment and that of a Chemical Manufacturing Plant	422
9.16.2.2	The Objective of Enzyme Evolution: Economic, Practical, and Green	423
9.16.3	**The Principles that Guide Enzyme Evolution**	425
9.16.3.1	Fitness Function	426
9.16.3.2	Diversity	427
9.16.3.3	Search Algorithm	427
9.16.4	**Tools Required for Effective Enzyme Evolution**	427
9.16.5	**Overview of Recently Developed Large-Scale Biocatalysis Processes that Involve Evolved Enzymes**	428
9.16.5.1	Atorvastatin	428
9.16.5.2	Ketoreductase Processes for Chiral Alcohols	430
9.16.5.3	Montelukast: Hydroxyester Intermediate	430
9.16.5.4	Duloxetine: Amino Alcohol Intermediate	431
9.16.5.5	Chiral Alcohol for Ezetimibe	432
9.16.5.6	Carbapenems: AOSA Precursor	432
9.16.5.7	Sitagliptin	433
9.16.5.8	Simvastatin	434
9.16.5.9	Boceprevir	435
9.16.6	**Anticipated Future Developments**	436
References		437

Glossary

Diversity Amino acid mutations in libraries of variants.

Diversity generation Applying methods to mutate a gene encoding the enzyme of interest to generate a library of variants that may contain new enzymes with improved properties for the desired function or may contain beneficial mutations for the desired process. Methods include random mutagenesis, site-directed mutagenesis, site saturation mutagenesis, etc.

DNA shuffling The original *in vitro* recombination technique, widely regarded as revolutionizing the field of directed molecular evolution [4,5]. DNA shuffling consists of random fragmentation of related parental DNA templates, followed by primerless polymerase chain reaction (PCR) recombination. The resulting libraries are composed of highly chimeric progeny. Variants with improved function are carried forward into subsequent rounds of evolution, fixing beneficial mutations in the population but discarding deleterious ones.

Fitness function The enzyme optimization objective expressed as the desired process.

ProSAR A bioinformatic tool that is used to determine protein sequence activity relationships, a technique inspired by quantitative structure activity relationships (QSAR), a machine-learning-based approach to small molecule drug design that is used extensively in medicinal chemistry to determine which molecular features correlate with improved drug activity and other machine learning applications, which is used to infer the effects of mutations in a combinatorial library of proteins on a function or property of interest. The models derived from the learning or training phase can be used to classify mutations as beneficial, deleterious, or neutral and these classifications can be used to design improved variants in subsequent rounds of evolution.[15]

Recombination The formation of new combinations of diversity in progeny sequences that is not present in the parents.

Search algorithm The methods used to efficiently sift through the available amino acid diversity to identifying variants with improved function: iterative error prone PCR, DNA shuffling via single gene, family, semisynthetic, and synthetic approaches amplified by bioinformatic tools such as ProSAR.

Semisynthetic shuffling A method of creating combinatorial libraries where DNA oligonucleotides are used to carry mutations that can freely recombine with a parental DNA template, giving significantly higher incorporation rates of mutations compared with traditional DNA shuffling.

9.16.1 Introduction into Biocatalysis

Biocatalysis entails the use of biological systems or parts thereof for the conversion of a substrate into a product of interest. This chapter focuses on the use of enzymes for the direct production of intermediates for the synthesis of complex active pharmaceutical ingredients. Specifically, the focus is on enzyme optimization tools that generate improved enzymes that enable practical biocatalysis.

Over 100 years ago, Rosenthaler used plant extracts to synthesis enantiomerically pure mandelonitrile. The use of nitrile hydratase for acrylamide manufacture, glycose isomerase (and others) for high-fructose corn syrup, and penicillin acylase for manufacture of semisynthetic penicillins were drivers toward further expansion of biocatalysts in chemical manufacture in the 1960s and 1970s.[1] Therefore, the advent of protein engineering in the 1980s promised to further increase the number of enzymatic process in the industry. Unfortunately, this structure-based rational design approach did not provide the breakthroughs that were anticipated. In hindsight, the reason for this relative lack of success in broadening the scope of biocatalysis is probably because of the fact that enzymatic catalysis proves to be substantially more complex than initially assumed, and the improved properties that were sought were not attainable with the small number of changes ($<1\%$) in an enzyme sequence that were experimentally tested.

Enzymes are typically composed of 200–400 amino acids (but sometimes as many as 1000) and their specific as well as bulk properties are a consequence of the nature and sequence of these amino acids. The site in enzymes where catalysis takes place, the so-called 'active site' (see schematic in Figure 1), is comprised of catalytic amino acid side chains held in a reactive configuration by neighboring amino acid residues. The nature of such neighboring residues also determines the size and the chemophysical environment of the active site. Hence, modification of residues in the active site may enhance the substrate range of the enzyme to include much larger substrates, or substrates that are more or less hydrophobic, charged, etc. Modification of active site residues may also alter the enantio- and regiospecificity of enzymes resulting in new nonnatural biocatalysts that have exquisite selectivity and are useful for large-scale application.

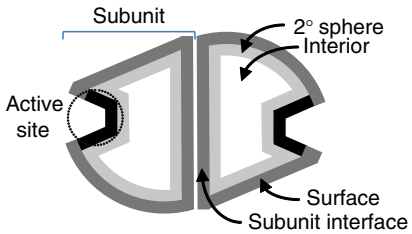


Figure 1 Schematic representation of a two-subunit enzyme, emphasizing the active site (black), secondary sphere (light gray), and surface (dark gray) that may interact with the external environment, or with other subunits.

Residues that are not in the active site, but interact with the active site residues, so-called secondary sphere amino acids, can be modified to modulate the activity of the enzyme through long-range effects. Finally, modification of residues at the surface of an enzyme may change the tolerance of the enzyme toward nonnatural conditions, such as the presence of solvents, extreme pH, increased temperature, etc. When surface residues are located at a subunit interface, mutations at these positions may lead to more stable enzymes by strengthening the quaternary structure of the enzyme.

9.16.2 The Need for Enzyme Evolution

9.16.2.1 Adapting to the Differences Between a Biological Environment and that of a Chemical Manufacturing Plant

For living cells it is crucial that enzymes perform the needed function on the appropriate substrate and under the right conditions.[2] Therefore, natural evolution has resulted in enzymes in which the sequence and type of the amino acids in the polypeptide are optimally organized to perform the required reaction in nature. The environment to which biological cells are exposed provides selective pressure to these cells and specifically to the enzymes of these cells. Therefore, it is important to realize that the evolutionary pressure that natural enzymes have been subject to only rarely (if at all) makes them exquisitely fit for a large-scale chemical process. In this context it is understandable that enzymes from natural sources are largely inadequate to function in a chemical process that includes high concentrations of feedstock and product, organic solvents, and elevated temperature or extreme pH. The relatively small number of mutations that were contemplated in the early protein engineering days, and the experimental challenge of making large sets of variants made the approach practically inefficient although great new insight in enzymatic catalysis were obtained.[3]

Ever since rational protein engineering approaches such as directed evolution were developed in the 1990s,[4,5] we see an upsurge in new practical biocatalytic processes. The substrate specificity of natural enzymes is a consequence of the specific role they fulfill in cellular metabolism; enantioselectivity of enzymes is crucial to ensure the reproducibility of cellular events that

involve chiral molecules, such as amino acids, and nucleosides; and feedback control mechanisms are necessary to regulate enzyme activity *in vivo*, by, for instance, substrate and product inhibition. All these facets limit the utility of enzymes in *in vitro* chemical manufacturing processes. Directed evolution not only aims at improving an enzyme for the specific conversion of interest, but also aims at removing the limitations that natural evolution may have introduced in the catalyst. As described before,[15,36] this may require changing up to 15% of the amino acids of a natural enzyme to generate practical biocatalysts. Further context of directed evolution of enzymes of interest to synthetic organic chemistry can be found in the chapter by Lewis et al. (COS 2012).

9.16.2.2 The Objective of Enzyme Evolution: Economic, Practical, and Green

Biocatalytic processes have been of interest for many years and are abundantly described in the scientific literature. Unfortunately, many articles related to biocatalysis discuss the conversion of substrates of interest with little consideration for practicality. For instance, identification of an enzyme that converts a ketone to a chiral alcohol with high selectivity in contrast to other enzymes does not make the process economic or practical if the substrate loading is low (20 g l^{-1}), the enzyme use high (S/C 5), and the cofactor use inefficient.[6]

Many enzyme evolution studies have shown that enzymes are highly adaptable. Recent reviews describe examples of evolved enzymes for use in organic synthesis.[1,7,8] Similarly, as for biocatalysis, in general, it is important to realize that the objective of scientific articles on enzyme evolution is not necessarily the development of a practical biocatalytic process and that in many instances the goal may just be to demonstrate that a particular enzyme can be improved to be more stable, to be more enantioselective, or to be better expressed in a heterologous host. For truly large-scale applications, several performance limitations of natural enzymes need to be overcome in order to enable that large-scale process. So, while a scientific paper may describe the generation of a more enantiospecific biocatalyst, if this catalyst still only converts rather low concentrations of starting material (1–2 g l^{-1}), the process is still dilute and not practical for large-scale implementation.[9]

Therefore, when optimizing enzymes for use in practical chemical synthesis, it is crucial to define the objective of the evolution approach as specifically as possible. The main driver for enzyme optimization when the application is its large-scale use is to minimize the cost of manufacture of the end product. Key enzyme evolution objectives therefore relate to: reaction yield, volumetric productivity, chemical purity (high conversion, efficient use of cosubstrates, high enantio- and chemical purity, etc.), and efficient use of biocatalyst. Typical reaction parameters and the corresponding performance targets used by Codexis scientists to guide enzyme evolution programs are listed in Table 1.

Table 1 Typical process design criteria applied to biocatalytic processes developed at Codexis

Parameter	*Target*
Product concentration	>75 g l^{-1}
Conversion	$>95\%$
Reaction time	<24 h
Enantiopurity of product	$>99\%$ *ee*
Purity of reaction product	$>98\%$
Enzyme loading	$<2\%$ (w/w)

Enzyme optimization for the process of interest allows for a complete design of the process before the initiation of enzyme optimization. Not only the process can be designed to be the most cost effective with respect to catalyst use and plant throughput, it can also be designed to be the most practical and the most environmentally friendly. Generally, biocatalytic reactions adhere very well to the 12 principles of green chemistry as illustrated in Table 2.

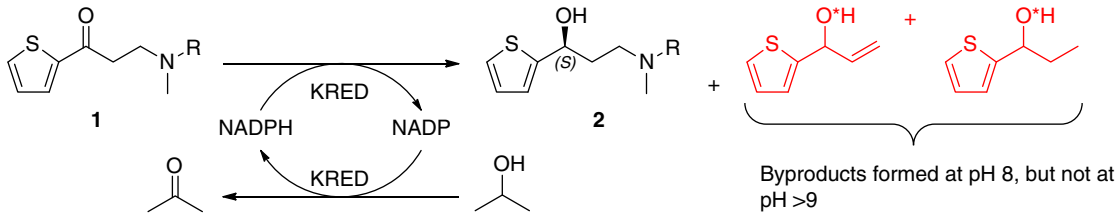
The choice of reaction conditions can affect the practicality of the process dramatically. This is illustrated for the biocatalytic reduction of a ketone precursor for duloxetine (the active pharmaceutical ingredient (API) in Cymbalta®, a serotonin –norepinephrine reuptake inhibitor) (Scheme 1). A practical process for the enantioselective, biocatalytic reduction of *N*,*N*-dimethyl-3-(2-thienyl)-3-ketopropanamine **1** (R is methyl) was enabled by first identifying reaction conditions under which the ketoamine was stable followed by evolution of the ketoreductase (KRED) to function efficiently under these conditions. By running the reaction at pH 9 and above, byproduct (red, Scheme 1) formation as seen at neutral pH is suppressed and the desired enantiomer is produced in high *ee* ($>99.0\%$) and yield.[10] In contrast, the biocatalytic reduction of the monomethyl analog, *N*-methyl-3-(2-thienyl)-3-ketopropanamine **1** (R is H), performs best at pH 6 in 85% isopropyl alcohol (IPA) as this substrate decomposes at basic pH.[11]

Choice of substrate may affect the greenness of the process. As described in the example Section 9.16.5.8, both the sodium and ammonium salt of monocolin J **3** are good substrates for the LovD enzyme in the synthesis of simvastatin **4**, a 3-hydroxy-3-methylglutaryl coenzyme A reductase inhibitor. The ammonium salt is more environmentally attractive; however, the NH_4-simvastatin reaction product precipitates from the reaction mixture, whereas the Na^+ salt does not (Scheme 2). Precipitation of the product directly from reaction mixture circumvented the need for an extractive workup, thereby decreasing the need for solvent and the potential for extra waste generation. This difference in properties was then used to evolve the LovD acylase to function optimally with the ammonium salt of monocolin J.

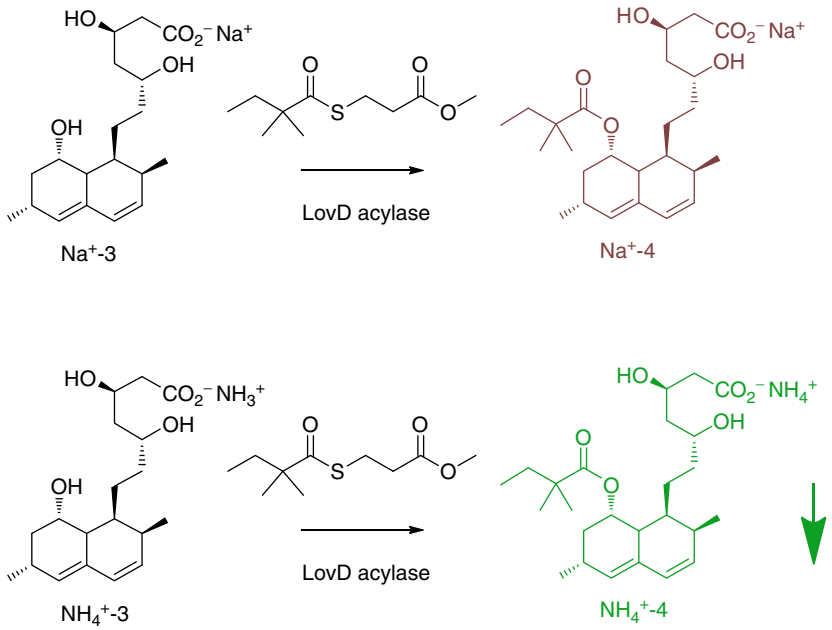
Table 2 Biocatalysis and the 12 principles of green chemistry[50]

Principle	*Biocatalysis relevance*
1. Prevention: It is better to prevent waste than to treat or clean up waste after it has been created.	Biocatalysts are usually highly selective for a given transformation and rarely produce byproducts. In addition, enzymes can be engineered to operate at high substrate loads under process-relevant concentrations to minimize solvent use.
2. Atom economy: Synthetic methods should be designed to maximize the incorporation of all materials used in the process into the final product.	Biocatalysts, particularly the widely used ketoreductases and emerging transaminases are more atom economical than many of the competing stochiometric reducing or aminating agents.
3. Less hazardous chemical syntheses: Wherever practical, synthetic methods should be designed to use and generate substances that possess little or no toxicity to human health and the environment.	Many traditional chemical transformations including reductions, reductive aminations, and oxidations use hazardous stochiometric redox agents (e.g., alkylboranes, metal borohydrides, pressurized hydrogen, and potent inorganic oxidants). In contrast, the stoichiometric agents used in biocatalysis are easily handled and considerably less hazardous (e.g., glucose, formate, isopropanol, isopropylamine, air/oxygen, and their products gluconate, CO_2, and acetone).
4. Designing safer chemicals: Chemical products should be designed to effect their desired function while minimizing their toxicity.	Biocatalysts are typically used to manufacture known molecules and this principle is not applicable.
5. Safer solvents and auxiliaries: The use of auxiliary substances (e.g., solvents, separation agents, etc.) should be made unnecessary wherever possible and innocuous when used.	Biocatalytic reactions are highly selective, giving high-purity products with low levels of byproducts, circumventing the need for auxiliary separation agents. In addition, enzymes operate effectively in aqueous environments (and water is an ideal green solvent) and can be engineered to perform in the presence of safe organic cosolvents such as isopropanol.
6. Design for energy efficiency: Energy requirements of chemical processes should be recognized for their environmental and economic impacts and should be minimized. If possible, synthetic methods should be conducted at ambient temperature and pressure.	Because biocatalysts operate efficiently under (close to) ambient temperatures, biocatalytic processes can avoid the requirements for extreme temperature and/or high pressure.
7. Use of renewable feedstocks: A raw material or feedstock should be renewable rather than depleting whenever technically and economically practical.	Enzymes are produced from renewable feedstocks via fermentation of a microbe overexpressing the corresponding gene. In contrast, many traditional metallic catalysts are derived from precious metals which are mined from finite resources.
8. Reduce derivatives: Unnecessary derivatization (use of blocking groups, protection/deprotection, and temporary modification of physical/chemical processes) should be minimized or avoided if possible, because such steps require additional reagents and can generate waste.	Owing to their exquisite selectivity, enzymes perform transformations with high accuracy at a specific reactive center in a molecule which may bear multiple reactive positions. This superb selectivity obviates the need for protecting groups.
9. Catalysis: Catalytic reagents (as selective as possible) are superior to stoichiometric reagents.	Enzymes are highly selective catalysts.
10. Design for degradation: Chemical products should be designed so that at the end of their function they break down into innocuous degradation products and do not persist in the environment.	Although the products they make may not be designed to degrade, enzymes themselves are proteins, made from natural amino acids that are readily degraded in standard waste treatment processes.
11. Real-time analysis for pollution prevention: Analytical methodologies need to be further developed to allow for real-time, in-process monitoring, and control before the formation of hazardous substances.	Some biocatalytic reactions can be monitored by real-time analysis: ketone reductions that use glucose/glucose dehydrogenase for cofactor recycling are run in pH-stat mode to maintain a neutral reaction pH with feeding of an appropriate base, addition of which is monitored continuously.
12. Inherently safer chemistry for accident prevention: Substances and the form of a substance used in a chemical process should be chosen to minimize the potential for chemical accidents, including releases, explosions, and fires.	Enzymatic reactions are run under benign conditions avoiding high temperatures and/or pressures, and use low-hazard donor molecules. For example, ketoreductases alcohols, such as isopropyl alcohol (IPA) as stoichiometric reducing agents, generating only acetone. This is in contrast to the hazard associated with high-pressure hydrogenations, or pyrophoric hydride-reducing agents. Similarly, transaminases utilize isopropylamine as an amine donor, avoiding the use of high-pressure reductive aminations, or the need to reduce imines with hydrides.

In some cases multiple biocatalytic routes to a product of interest each from different starting materials are practically feasible at least on paper (**Scheme 3**). For instance, for the manufacture of intermediates for atorvastatin, nitrilase-, KRED/halohydrin dehalogenase (HHDH)-, and aldolase-catalyzed processes have been described in the literature. Although the nitrilase-based process starts from inexpensive epichlorohydrin **5** and uses a single enzyme, the overall yield of hydroxynitrile **6** from the reaction (23%) and the chemical (97%) and chiral (98.8%) purity were too low for commercial use.[12]



Scheme 1



Scheme 2

The KRED/HHDH route starts from ethyl 4-chloroacetoacetate **7** and requires three different enzymes for manufacture of hydroxynitrile **6** and all were made highly efficient through enzyme evolution, minimizing the enzyme cost contribution and providing product of >99.9% *ee* and >98% chemical purity.[13] The practicality of this process is described in Section 9.16.5.1.

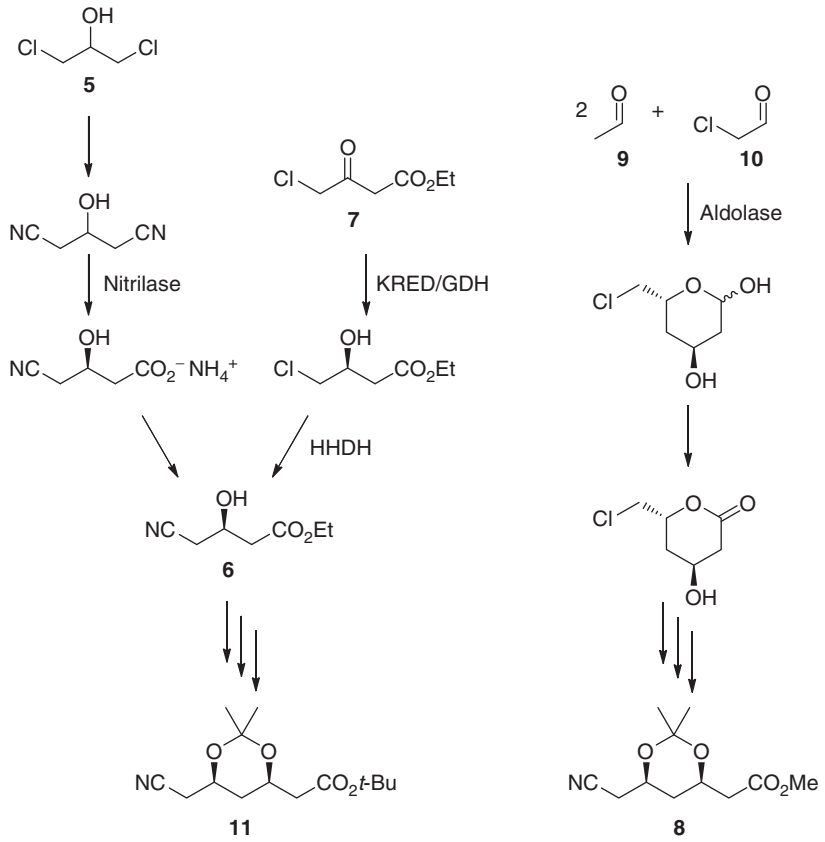
Similar to the nitrilase route, the aldolase route to the further advanced intermediate **8** uses a deoxyribose aldolase obtained from a metagenomic library as the only enzyme. Inexpensive acetaldehyde **9** and chloroacetaldehyde **10** are used as substrates. Although the aldolase sets both chiral centers, the chiral purity of the product (>99.9% *ee* and 96.6% *de*) is insufficient and requires upgrading. In addition, the subsequent chemistry is inefficient, involving a nonpractical recrystallization from chloroform, and uses trimethylsilyldiazomethane to generate the methyl ester **8**, an oil, rather than the commercial, crystalline *tert*-butyl ester **11** which is derived from hydroxynitrile **6**.[14]

These examples underscore that it is typical that multiple aspects of an enzymatic process need to be optimized in order to support large-scale manufacturing. Not only is the specific activity of a natural enzyme often insufficient, the enzyme may also need to be improved to function at nonnatural reaction conditions or with a different substrate and always needs to fit within the constraints of the overall process.

9.16.3 The Principles that Guide Enzyme Evolution

The objectives of an enzyme optimization program can only be accurately described if the target process is well understood. Often this is not the case and the designed biocatalytic process needs to be adapted as additional information becomes available on the potential scope of the process when process data obtained with improved enzyme variants becomes available. The development of a transaminase for manufacture of sitagliptin (described in more detail in the experimental Section 9.16.5.7) is a good example of how enzyme and process optimization go hand in hand.

The efficiency and outcome of enzyme evolution projects is determined by how well the three guiding principles of directed evolution are adhered to: the fitness function, diversity generation, and the search algorithm. If any of these guiding principles is



Scheme 3

compromised over the course of an enzyme evolution program, the end result will be suboptimal which in the worst case may mean that a practical enzyme and process cannot be developed. The fundamental scientific disciplines that support these guiding principles are chemical process development, molecular biology, microbiology, bioinformatics, analytical chemistry, and fermentation science as well as the overarching need for scientists in the respective disciplines to work closely together and to speak a common language.

9.16.3.1 Fitness Function

The fitness function for a given biocatalyst and more specifically the biocatalytic process is designed by process chemists. The fitness function describes as accurately as possible what the performance of the biocatalytic process needs to be. The key considerations relate to the economics of the process and its practicality at large scale. In addition, environmental considerations may have an effect on the definition of the fitness function.

Initially, the fitness function is often expressed as a definition of the desired process as described in Table 1. These criteria describe high reaction yield, high purity, high space-time yield, and effective use of the biocatalyst. Depending on the reaction, other criteria may be included, such as the concentration of cofactors (e.g., nicotinamide adenine dinucleotide phosphate (NADP) and NAD for ketone reductions catalyzed by ketoreductases), or cosubstrates (discussed for the sitagliptin example in Section 9.16.5.7).

It may be found during the course of biocatalytic process development as improved enzymes become available over the course of an optimization program that the process can be made more effective by including other solvents, different concentrations of solvent, changing to a more optimal pH, etc. Such factors have a direct impact on the quality of the process and how the designed fitness function may be reached. This freedom in process conditions provide an opportunity to steer the enzyme evolution toward a continuously improving process design.

Typically, it is desired to use the specific criteria of the fitness function in the high throughput (HTP) screening of enzyme libraries. The fitness of individual enzyme variants is determined via HTP screening where the enzyme variants expressed from the individual genes are tested under conditions that represent the desired process as closely as possible. Analytical methods used for the evaluation of individual enzyme variants range from colorimetric assays to more involving methods such as HPLC, GC, MS, CE, etc. For instance, when a process needs to run at 100 g l^{-1} it is often desirable to screen enzyme variants at a level as close as possible to 100 g l^{-1}, especially if the enzyme is inhibited by the reaction substrate. This is sometimes not possible, for instance,

because of the more difficult mixing of highly insoluble substrates within the small wells of microtiter plates. When an enzyme is severely product inhibited it may be necessary to screen variants under conditions that resemble 90% conversion (and sometimes even higher) by including the product in the HTP screen. For the evolution of an efficient HHDH-catalyzed process for the manufacture of an atorvastatin raw material, the enzyme libraries needed to be screened at 98% conversion.[15]

9.16.3.2 Diversity

Diversity encompasses the pool of alternative amino acids that can be introduced into the best available enzyme and by doing so may lead to improved function of the enzyme under study. This diversity is obtained by applying methods to mutate a gene encoding the starting enzyme thereby generating variants that may be improved for the desired function or may contain beneficial mutations for the desired process. Libraries of such variants are assessed in HTP screens for their activity with respect to the fitness function.

Methods for generating diversity include random mutagenesis, a method that introduces variation throughout the enzyme sequence without any preconceived notion on which residues might be important. Site-directed mutagenesis techniques have been used since the 1980s to introduce mutations at specific, predetermined sites, i.e., a small number of alternative amino acids were introduced at a single site in an enzyme sequence. This method is quite useful for obtaining information on the importance of a specific residue, but has seen limited utility in providing commercially relevant enzymes for chemical manufacturing processes. Site saturation mutagenesis involves generating all 19 possible variants at a specific residue in an enzyme. This approach is often used to identify the optimal amino acid at any given position. Another source of diversity is in closely related enzymes. Two 250 amino acid sequences that are 80% identical provide 50 positions where mutations have occurred naturally. This 'functional' diversity can be incorporated in enzyme libraries via molecular biology techniques, such as family shuffling[16] or semisynthetic shuffling.[17] When generating diversity it is crucial to control the level of mutagenesis as introduction of multiple new residues can easily result in outbalancing a beneficial mutation by deleterious ones.

9.16.3.3 Search Algorithm

Owing to the large number of possible enzyme variants, enzyme evolution requires efficient and robust search algorithms to rapidly sift through the countless possibilities. Before the invention of recombination-based DNA shuffling, directed evolution was limited to iterative rounds of random mutagenesis, where the best sequence of each round of evolution is used as a template for additional mutagenesis. Although this strategy is simple to execute and can provide a positive outcome, it has the two significant drawbacks: numerous beneficial mutations that are in improved but not the best hit are discarded at each round of evolution and deleterious mutations may be carried along as genetic hitchhikers. These asexual evolutionary methods are generally considered to be less efficient than algorithms, such as DNA shuffling that recombine beneficial mutations from multiple improved variants.

9.16.4 Tools Required for Effective Enzyme Evolution

The technologies for efficient evolution of enzymes for large-scale application can be divided into three main disciplines: molecular biology, high throughput screening, and process development.

Molecular biology tools are required for gene synthesis, diversity generation, and recombination of beneficial mutations. The genetic constructs are transformed into a microbial host, typically *Escherichia coli*, for HTP screening purposes. The development of appropriate HTP screens that resemble the process of interest requires experience with analytical chemistry, process chemistry, enzymology, automation, and bioinformatics. The best variants identified in HTP screening enter a phase of process development where process chemists evaluate the enzyme variants in scalable chemical systems, whereas biochemical engineers assess the fermentative production of the catalyst.

The molecular biology tools have been subject of many reviews and the reader is referred to recent overview articles that have been published in this area.[18–20]

With respect to HTP screening, the key consideration when developing practical enzymes is defining the fitness function, which dictates the appropriate screening conditions that mimic the desired commercial process.[21,22] Because the best variants are identified from enzyme libraries by their ability to perform under screening conditions, if these conditions are not truly representative of the desired process, variants may be selected that are improved for function under the screening conditions rather than the commercial-scale process conditions. Following this approach, iterative rounds of directed evolution can provide truly practical biocatalysts by repeatedly adding beneficial mutations to a parent enzyme. The approach to HTP screening for developing process-fit enzymes can be illustrated with the general conversion graph illustrated in **Figure 2**.

Development of biocatalytic processes is more straightforward than it may appear to chemists trained in traditional chemistry. Because enzymes work so well at ambient temperature and extreme pressure is rarely needed (only to distill off acetone which may be formed during enzymatic reduction or transamination reactions), the reaction vessels are simple stirred vessels ranging from low milliliter reactions in vials to 10 l glass vessels in a laboratory environment (**Figure 3**), up to thousands of liters reactions in stirred stainless steel, tank reactors. In fact, large-scale process conditions can be mimicked in 96-well microtiter plates with a 2 ml

well volume quite well as is done for HTP screening of enzyme libraries. Various practical examples of biocatalytic processes have recently been reviewed.[23]

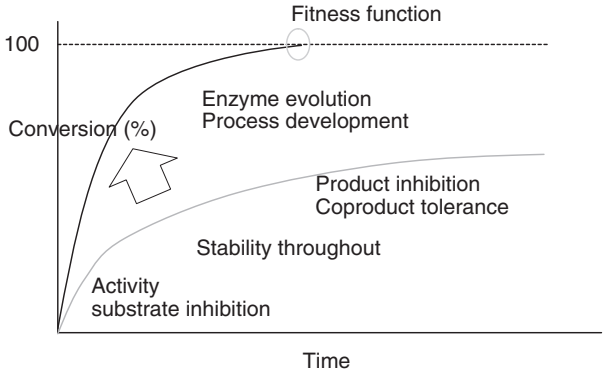


Figure 2 Natural enzymes are typically unable to catalyze industrially practical reactions. The gray reaction curve illustrates that while natural enzymes may have decent initial activity, this activity often tapers off quickly as a result to limited stability of the enzyme under the process conditions, or because of product inhibition. Enzyme evolution combined with process development allows for the rapid generation and identification of process-fit enzymes as illustrated by the black reaction curve that meets the desired fitness function (gray circle). Often such enzymes are highly stable and maintain a high activity throughout the reaction. Product inhibition and tolerance to other reaction components is increased.



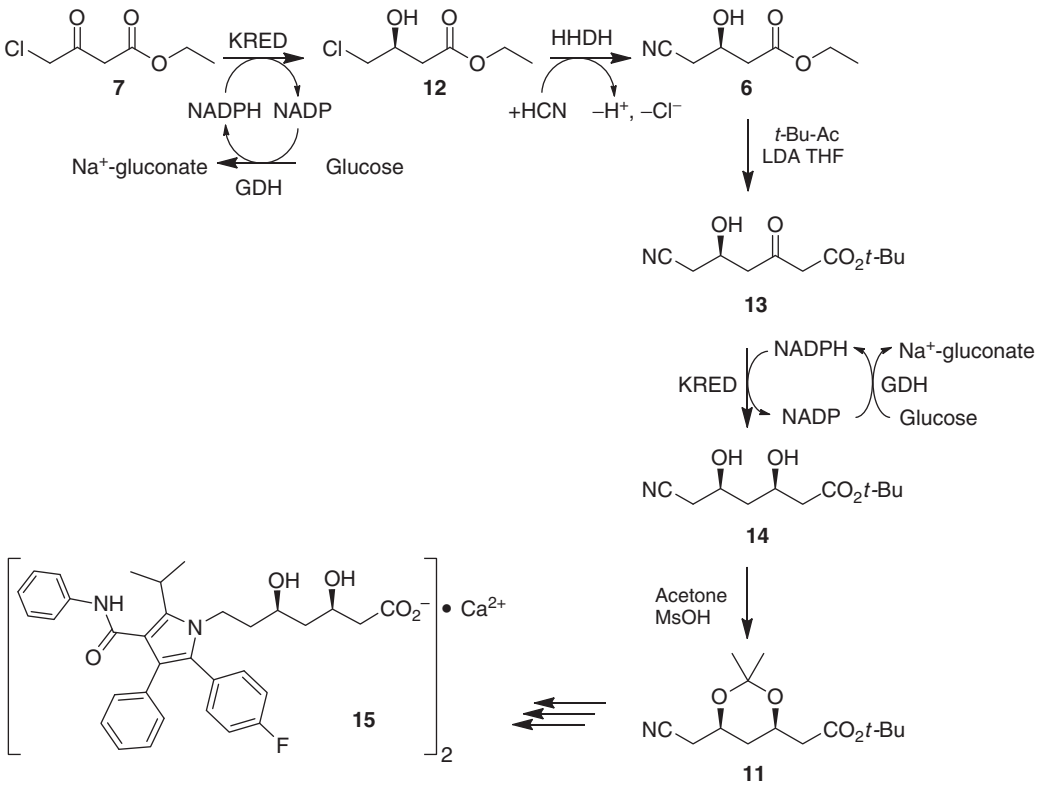
Figure 3 Photograph of a 10-l scale enzymatic reduction. A poorly soluble ketone precursor to montelukast (**15**) is reduced to the corresponding S-alcohol (**16**) under a mild vacuum to distill off acetone, a coproduct of the reaction.

9.16.5 Overview of Recently Developed Large-Scale Biocatalysis Processes that Involve Evolved Enzymes

9.16.5.1 Atorvastatin

Atorvastatin **15**, a blockbuster 'statin' drug developed by Pfizer, is used to treat hypercholesterolemia. Atorvastatin is a competitive inhibitor of HMG-CoA reductase and as such interferes with the rate limiting step in hepatic cholesterol biosynthesis. The key pharmacophore of the molecule is a synthetically challenging 3,5-dihydroxycarboxylic acid moiety. The key advanced

intermediate for atorvastatin, known as ATS8, **11**, bears all of the requisite chiral functionality (Scheme 4). Codexis developed an integrated biocatalytic process to **11** leveraging four enzymes over three key steps. The preferred synthetic approach to **11** starts with ethyl (*S*)-4-chloro-3-hydroxybutyrate **12**, and followed a sequence of cyanation, Claisen condensation, diastereoselective reduction, and protection. Currently more than 100 mT of **11** are produced per annum via this five enzyme biocatalytic process.



Scheme 4

The starting chiral hydroxyester **12** (4-chloro-3-hydroxybutyrate) is produced via enzymatic reduction of ethyl 4-chloro-acetoacetate **7**. Reducing equivalents are provided by the nicotinamide adenine dinucleotide phosphate reduced-form (NADPH) cofactor which is continuously regenerated by a second enzyme, glucose dehydrogenase (GHD), and a sacrificial cosubstrate, glucose. Both enzymes were evolved for activity and stability under the process conditions.[13] The KRED for this process was evolved by screening variants for the conversion of **7** to **12** in the presence of 108 g l^{-1} of both glucose and Na^+-gluconate, reaction conditions that represent the process at 60% conversion. In subsequent characterization of the resulting KREDs it was found that while the natural and final variant are similarly inhibited by ECAA in the absence of glucose/gluconate, the natural enzyme is significantly inhibited by **7** at 60% conversion, whereas the evolved variant is not (Codexis, unpublished results). With a space-time yield of 20 g l^{-1} h^{-1}, the process provides **12** of >99.9% *ee* in 95% isolated yield after continuous counter current extraction and removal of the butyl acetate cosolvent. The substrate-to-catalyst ratio is 180 on a weight basis and 44 000 on a molar basis.

The second step of the reaction sequence requires the nucleophilic displacement of the chlorine substituent in **12** with a cyanide group to give hydroxynitrile **6**. Typical methods of achieving this transformation required the use of high temperatures and basic conditions, which results in a range of undesired byproducts. This issue is compounded by the fact that the product is not crystalline and a tedious, high vacuum fractional distillation is required to obtain product of sufficient quality. An innovative biocatalytic solution was developed, that allows for the catalytic nucleophilic displacement at neutral pH (pH 7) and lower temperature (40 °C) using a highly regioselective evolved HHDH. This enzyme first catalyzes the closure of the chlorohydrin moiety of **12** to give the epoxide intermediate, and then aids the epoxide ring opening with cyanide rendering the overall reaction irreversible. The performance of the wild-type enzyme was improved approximately 4000-fold to enable a practical large-scale process.[21] At a S/C ratio of ~115 (w/w) **6** is produced with a space-time yield of 28 g l h^{-1} and is isolated in 92% yield after extraction and a wiped-film distillation.[13]

During the evolution of HHDH for manufacture of **6** ProSAR was implemented as a machine learning tool to distinguish beneficial, neutral, and deleterious mutations. This algorithm represented a step chance from hit shuffling[4,5] to mutation shuffling and has since been adopted in various enzyme evolution programs.

The achievements in the development of the enzyme-mediated process for the conversion of **12** into **6** were recognized with an EPA Presidential Green Chemistry Challenge Award in 2006.

The resulting hydroxynitrile **6** is subjected to a Claisen condensation with *tert*-butyl acetate to give the hydroxyketoester **13**. The key to the final part of the synthesis is in the ability to reduce the keto function with high stereoselectivity.

The difficult diastereoselective reduction of **13** using stoichiometric reagents is described in reference 24. The substrate solution is cooled to $-85\ ^{\circ}C$ and then treated with diethylmethoxyborane to form a chelated complex. The reduction of the ketone using $NaBH_4$ follows at an even lower temperature to give diol **14**. Even under such stringent conditions complete control of diastereoselectivity was not achieved. After quenching, the borate waste was removed using multiple vacuum distillations with methanol. The resulting dihydroxy ester **14** is not crystalline, and cannot be readily purified, so it is taken forward through to the crystalline intermediate **11**, which is upgraded. Although this valuable intermediate can be obtained in high purity, the route involves the use of hazardous stoichiometric borane reagents, generating substantial amounts of waste, which in turn demands large volumes of solvent to be used for removal. In addition, the difficulty in achieving the directed diastereoselective reduction requires that energy-intensive cryogenic conditions are needed.

Evolution of a natural KRED provided an enzyme capable of delivering the desired dihydroxy ester **14** in excellent diastereopurity.[25] The activity of the natural KRED was 100-fold lower than desired, and its stability was similarly insufficient. Using a combination of directed evolution techniques yielded a much improved variant capable of operating at very high substrate loads. Since the crude ketone substrate contains substantial amounts of *tert*-butyl acetoacetate ($\sim$30%) from the Claisen condensation step, screening of KRED variants could not be done with a HTP fluorescence screen that detects cofactor conversion as it would aberrantly identify enzymes improved for *tert*-butyl acetoacetate as hits. Instead, HTP HPLC was used.

The reaction proceeds to $>$98% conversion, giving the desired product **9** with unprecedented diastereopurity ($>$99.9% *de*), using the same glucose/GDH coupled cofactor recycling system that was developed for the reduction of **7** (13). In this process, crude ketone **13** at 300 g l^{-1} is completely converted to **14** in 22 h at a S/C ratio of 85. The green metrics of the biocatalytic reaction compare very favorably with the original chemical reduction: the substrate load is tripled over that reported in the patented process,[24] use of hazardous boron reagents is circumvented, cryogenic conditions are avoided, and the process gives an 85% reduction in organic solvent usage as it operates in a mainly aqueous medium. This process is now run at large scale, delivering $>$10 mT per month of high-quality intermediate.

9.16.5.2 Ketoreductase Processes for Chiral Alcohols

Chiral secondary alcohols are common intermediates in the manufacture of pharmaceutical APIs. Many commercial approaches to these intermediates use stoichiometric, hazardous, borane-based reagents. A second approach involves asymmetric hydrogenation for which heavy metal catalysts and chiral ligands are typically required. When these approaches do not provide a satisfactory route, a resolution is the common fallback with a potential loss of $>$50% in yield as the undesired stereoisomer. Biocatalytic reductions enabled by KREDs offer a practical, more sustainable alternative.[25,26]

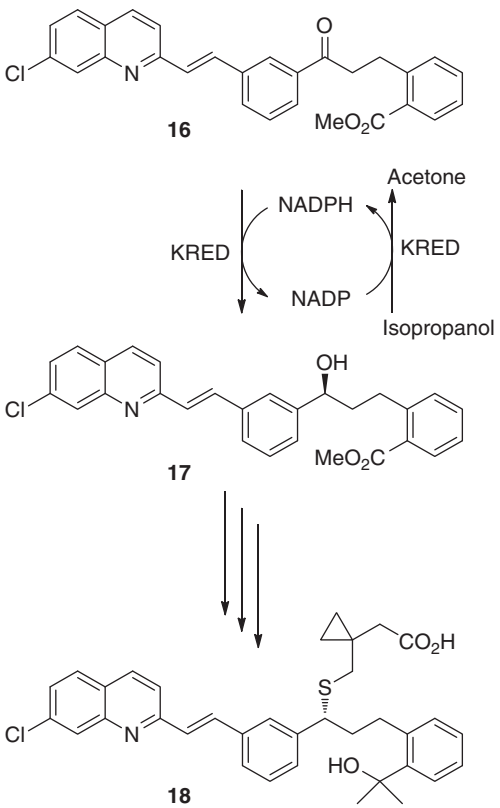
As discussed in Section 9.16.5.1, KRED-mediated reductions require the use of a cofactor (NADH or NADPH) to provide the reducing equivalents needed and enzymes are used for the efficient regeneration of these expensive cofactors. Cofactor regeneration is achieved through coupling of the desired reduction with GDH-catalyzed oxidation of glucose to gluconic acid (illustrated for reduction of **7** in Scheme 4), or through using a KRED that also accepts IPA as a substrate, giving acetone as the oxidized byproduct (illustrated for reduction of **16** in Scheme 5). In the latter case, the overall reaction is a coupled equilibrium (ketone + IPA gives chiral alcohol + acetone) where excess IPA can aid in driving the reaction toward high conversion. When high conversion is not achieved thermodynamically under ambient conditions, the equilibrium can be driven toward product by removal of the acetone coproduct via distillation. There are a number of published reviews focusing on KREDs, which include discussion of the mechanism and substrate range of KREDs,[27] applications in the fine chemical and pharmaceutical industries, and as part of more wide-ranging coverage of biocatalysts for pharmaceutically interesting targets.[28]

The use of KRED-catalyzed reductions is now an established strategy for catalytic ketone reduction to provide single enantiomers or diastereomers of a desired product in very high purity.[29,30] However, with some substrates natural enzymes are not sufficiently active or not capable of delivering the product in sufficient enantiomeric purity, in which case the product thus obtained requires upgrading with concomitant yield loss. The use of directed evolution technologies has enabled a large number of biocatalytic asymmetric reductions where previously no enzyme was available. These processes are briefly discussed.

9.16.5.3 Montelukast: Hydroxyester Intermediate

Montelukast **18** (developed and marketed by Merck as Singulair®) is an orally active leukotriene receptor antagonist used to control and relieve the symptoms of asthma and seasonal allergies. A biocatalytic alternative (Scheme 5) was developed to the original commercial route that uses excess DIP-Cl in tetrahydrofuran (THF) at low temperature to reduce ketone **15** to chiral alcohol **16**. Post reaction the crude product requires upgrading via crystallization to increase the chiral purity from 97.5% to 99.5% *ee* resulting in isolated yields of 65–87%.

Screening our collection of preevolved variants KRED variants for activity on **15** identified an enzyme that could deliver the required product with perfect enantiopurity. The activity of this variant was far from commercial utility and process development and enzyme optimization via directed evolution was initiated.



Scheme 5

In this process, 100 g l^{-1} **16** is converted into >99.5% *ee* **17** using 3.3% KRED. By running the reaction in 60% of a 1:5 toluene–IPA mixture, the solubilization of the poorly water-soluble ketone is sufficiently fast to enable complete conversion in a 24 h reaction. The product is then isolated via direct filtration. The process runs as a slurry-to-slurry reaction and is operated at 45 °C.

The biocatalyst was evolved for increased robustness to organic cosolvent, increased thermostability (up to 50 °C), and tolerance to the acetone coproduct which was a competitive inhibitor to the initial enzyme. The final enzyme variant was improved over 2000-fold compared to the initial enzyme variant that exhibited detectable activity. The process is used on manufacturing scale to supply the intermediate for generic montelukast manufacture.[31]

9.16.5.4 Duloxetine: Amino Alcohol Intermediate

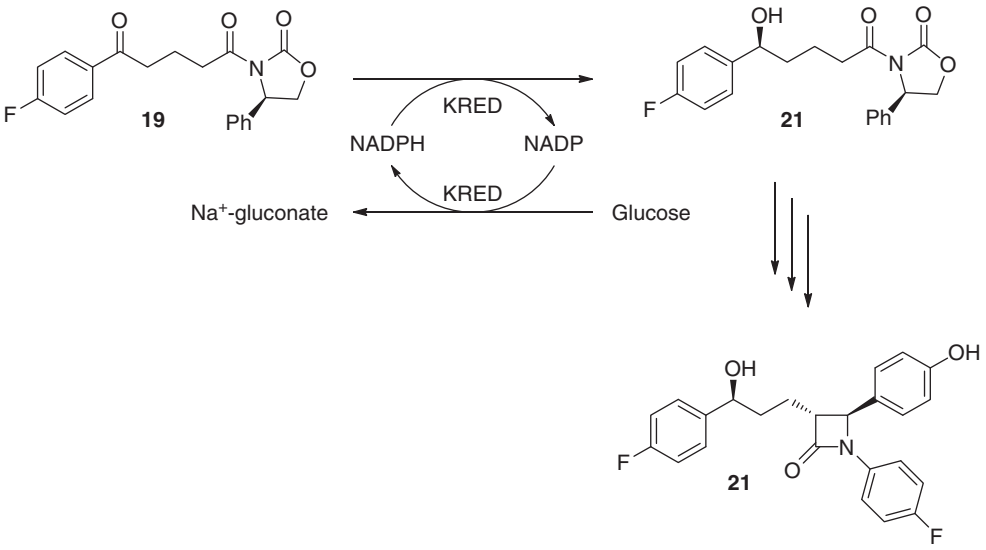
Duloxetine (developed by Lilly and marketed as Cymbalta™) is a dual serotonin and norepinephrine reuptake inhibitor and is used in the treatment of major depressive disorder. The (*S*)-thienylpropanolamine intermediate can be prepared as either the monomethyl amino alcohol, MMAA **1** (R=H) or dimethyl amino alcohol, DMAA **1** (R=Me) (Scheme 1). The route to the chiral amino alcohols **2** traditionally involved resolution of the racemic alcohol, which is inherently wasteful. A direct, asymmetric route to each amino alcohol would offer distinct advantages, and we screened our enzyme collection for variants capable of achieving this transformation using ketone **1, R=Me**. None of the natural enzymes in our collection had the desired activity, but a preengineered enzyme from a previous evolution program did exhibit the requisite activity and enantioselectivity.

Manufacture of both **2** (R=H) and **2** (R=Me) was targeted through enzyme evolution, using IPA as a stoichiometric reductant. Interestingly, the evolutionary path of the enzymes for the respective alcohols diverged because of the differing stabilities of the two substrates at different pHs. Dimethylaminoketone **1** (R=Me) was found to be unstable under neutral conditions, undergoing elimination of dimethylamine, and as such, it was required that the process be run at pH 9 or above with a large excess of IPA cosolvent to minimize decomposition (see Scheme 1). In contrast, the monomethyl aminoketone **1** (R=H) was unstable under basic and neutral conditions and the process required that an acidic buffer (pH 6) be used, and the enzyme was evolved to operate efficiently under these conditions. Thermostability was also required as it was necessary to distill off the acetone coproduct to drive the reactions to completion. In both cases, subjecting the KRED libraries to the required process conditions in parallel evolution programs allowed identification of relevant diversity to increase the activity and stability of the enzymes, and recombination of this respective diversity ultimately delivered different families of enzymes capable of operating under commercially viable conditions to give either **2**, R=Me (10) or **2**, R=H (11). The biocatalytic processes delivered the respective products with very high enantiopurity and the process to **2** (R=Me) is in commercial operation to supply manufacturers of generic duloxetine.

Reduction of either **2** (R=H) or **2** (R=Me) is achieved at a S/C of 100–150 giving product of >99.5% *ee*. Acetone is removed during the reaction via distillation to facilitate high conversion. As discussed earlier, because of instability of either substrate at pH 7–8, appropriate enzymes were evolved under conditions where substrate and product were most stable. For **2** (R=Me) these conditions were alkaline pH (>9), and 50% IPA, whereas for **2** (R=H), higher IPA concentration (>85%) and slightly acidic pH (<6) proved to be optimal.

9.16.5.5 Chiral Alcohol for Ezetimibe

Ezetimibe **21** is a cholesterol-lowering drug developed by Merck and marketed as a monotherapy under the trade name Zetia™, or in combination with Simvastatin as Vytorin™. The commercial route to ezetimibe proceeds via the chiral benzylic alcohol **20** which is typically prepared via asymmetric reduction of the corresponding ketone **19** using stoichiometric borane (as its THF complex) in the presence of a chiral boron catalyst, (*R*)-methyl-CBS (Scheme 6). Both the reagent and catalyst are hazardous materials, and post reaction large quantities of borate waste are produced. Furthermore, the product obtained from the reduction has less than perfect diastereopurity and requires upgrading.[32]



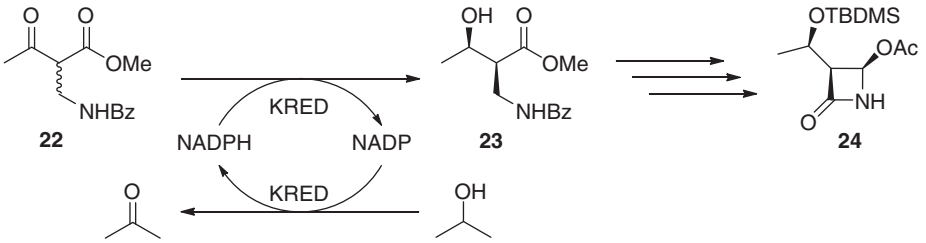
Scheme 6

Codexis investigated the potential for replacing the boron chemistry with a KRED-mediated reduction and screened the Codex™ panel plates for reduction of **18**. Although the wild-type parent of the panel enzymes had no detectable activity, active variants were found on the panel itself. Hits from this initial screen were further improved for both activity and stereoselectivity[33] until satisfactory enzyme performance was observed in the desired process. The process was designed to operate as a biphasic system as a mixture of toluene and buffered water, using a glucose/GDH-based cofactor recycling system. Evolution delivered a 12 000-fold improvement required to meet the fitness function, where 100 g l^{-1} ketone is converted at an S/C of 50 giving product of >99.9% *de* in >95% yield.

9.16.5.6 Carbapenems: AOSA Precursor

(3R,4R)-4-Acetoxy-3-[(R)-1-(*tert*-butyldimethylsilyloxy)ethyl]-2-azetidinone (AOSA) **24** is a key intermediate in the synthesis of many synthetic beta-lactam antibiotics including meropenem. One of the most successful approaches to this intermediate was developed by Takasago and proceeds via the *syn*-hydroxyester **23**, which is obtained using a reductive dynamic kinetic resolution of ketoester **22** (Scheme 7).[34] The reduction required very high pressure (100 atm H_2) and an Ru-(*R*)-BINAP catalyst in superheated (50 °C) dichloromethane. Despite these demanding conditions, the reaction gave product of imperfect stereopurity and a 96:4 *syn*:*anti* ratio of diastereoisomers was obtained requiring further upgrading.

We investigated the possibility of performing the diastereoselective reduction under milder reaction conditions to give **23** of high chiral purity in a KRED-based process. Screening of the Codex™ panel identified a wide range of variants that were active on **22**, and selection of the appropriate variant allowed predominant formation of any one of the four possible diastereoisomers. The best variant identified from the panel gave a 90:10 ratio of diastereoisomers, and was completely selective for the 3R-alcohol, but less specific for the 2S position. This variant required further evolution to improve its diastereoselectivity, and a ~250-fold activity improvement to meet the required process targets.



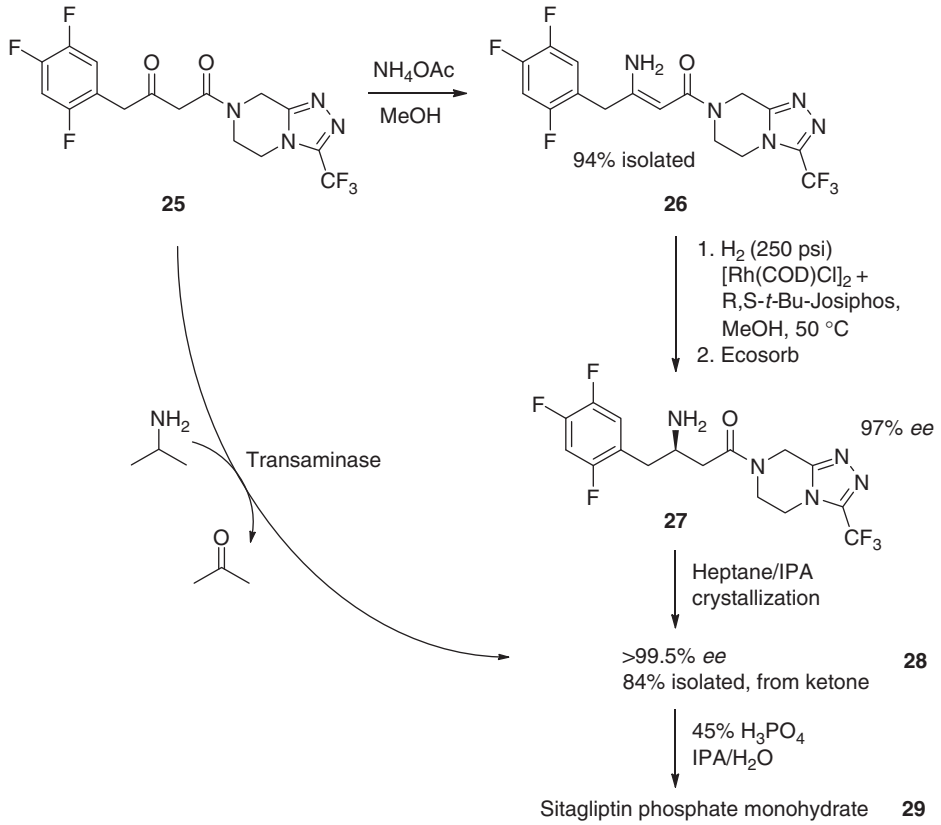
Scheme 7

With a space-time yield of $\sim 10\ g\ l^{-1}\ h^{-1}$, the desired diastereomer is obtained in >99.9% *ee*. The process runs at $250\ g\ l^{-1}$ **22** with an S/C of 250, using IPA for cofactor regeneration. The enzyme was evolved to use 10-fold less cosubstrate (NADP) than required by the natural enzyme.

The data from the initial Codex panel screen was analyzed using ProSAR to identify a series of important mutations that were used to prepare a new combinatorial library of enzyme variants. One of these variants provided the desired product in analytically perfect diastereoselectivity, and after incorporation of a further three mutations to improve stability, cofactor binding, and expression, the resulting variant exceeded all of the desired process targets.[35]

9.16.5.7 Sitagliptin

Sitagliptin **29** (marketed as Januvia® by Merck as monoformulated product and as Janumet® in coformulation with metformin) is an important new drug for the treatment of type II diabetes, a disease that affects over 240 million individuals worldwide. Demand for this drug is expected to increase significantly in the coming years, and a sustainable and more efficient manufacturing route was highly desirable. Sitagliptin contains a chiral amine moiety and the traditional approach to this intermediate involved an asymmetric hydrogenation of the corresponding enamine precursor **26** using a Rhodium–Josiphos catalyst, as shown in Scheme 8. Although this hydrogenation process provides the crude API **27** product with good chiral purity (97% *ee*) an upgrade through crystallization is necessary to meet the required enantiopurity for the free amine **28** of >99.5% *ee*. In addition, the hydrogenation requires specialized manufacturing equipment as the process is run at very high pressures (250 psi). Residual metal needs to be removed from the product so as to meet Food and Drug Administration (FDA) requirements.



Scheme 8

Merck and Codexis investigated the potential of a transaminase-based approach, which would allow direct conversion of the pro-sitagliptin ketone **25** into the high chirally pure amine **28**, thus removing the need to upgrade the chiral amine, the need for specialized equipment, and the use of heavy metal catalysts. In principle, this would be a highly attractive route to the amine product. Unfortunately, natural transaminases are limited to having activity only on ketones with at least one small substituent (methyl or alternatively small cyclic ketones).

In the absence of an enzyme with detectable activity, initial screening was conducted on a truncated analog of **25** in which a methyl group was substituted for the trifluorophenyl moiety. ATA117, an *R*-selective transaminase was found to have very low activity toward this substrate and *in silico* studies suggested that the heterocyclic side of the ketone docked into the large binding pocket but not perfectly. Significantly improved variants for the truncated substrate were identified and these served to start engineering of the active site to accommodate the full substrate **25**, which contains the bulky trifluorophenyl substituent of sitagliptin, rather than the methyl group. Following an *in silico* docking study, several active site residues were mutated alone or in combination to expand the small binding pocket. On screening these libraries, a variant containing three small pocket mutations provided the first detectable activity on **25** giving an estimated turnover of <1 per day. Once initial activity was found, albeit extremely low, this variant was optimized for commercial use over the course of 11 rounds of evolution.[36]

One of the components of the fitness function that was defined early on was the source of the amine functionality. Although the equilibrium of transaminase-based processes that use alanine as NH_2-donor can be pulled to completion by removal of the pyruvate coproduct, such schemes require additional enzymes that may not be functional under practical process conditions. It was therefore decided to use isopropylamine as NH_2-donor and evolve the enzyme to be tolerant to high concentrations of this donor as well as elevated temperature to facilitate stripping off of the acetone coproduct.

Evolution provided transaminase variants with increasing activity and once a reasonable activity was reached (four rounds provided a 1000-fold improvement over the first active variant), process development was initiated at Merck. As potential beneficial changes in the process were identified, they were used to adapt the fitness function and incorporated into the HTP screen. When the desired fitness function was solved through the combination of enzyme evolution and process development, the reaction conditions had changed dramatically with the reaction temperature increased from 25 to 45 °C, and the cosolvent concentration switched from methanol to dimethylsulfoxide (DMSO) and then increased from 5% to 50% DMSO. The equilibrium of the reaction was continuously shifted toward completion by increasing the concentration of isopropylamine in the reaction and removal of acetone via mild vacuum distillation and a nitrogen sweep. The reaction could be run at substrate loadings as high as 275 g l^{-1}, using 3 wt.% catalyst, completing in 24 h. The overall yield of sitagliptin **29** using this process was up to 13% higher than with the hydrogenation process. In addition, this biocatalytic process provided a 53% increase in productivity, a 19% decrease in total waste, elimination of all heavy metals and a reduction in total manufacturing cost.[36] The process has since been approved by the United States FDA.

Overall, the increase in biocatalyst activity was $>27\,000$-fold from the first enzyme variant with detectable activity on **25**, and the product was obtained in high yield with perfect enantiopurity (the *S*-enantiomer was never detected). Desai reflects on the three generations of sitagliptin manufacturing processes in a concise review.[37] Merck and Codexis jointly received the 2010 EPA Presidential Green Chemistry Challenge Award for this sitagliptin transaminase process.

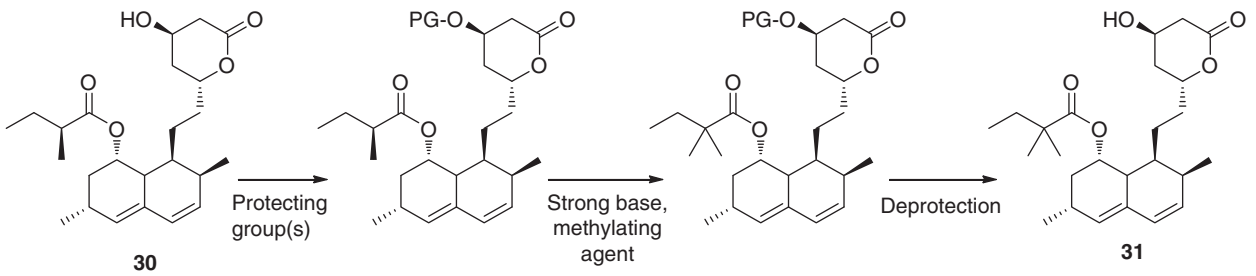
9.16.5.8 Simvastatin

Simvastatin **31** is a hypolipidemic drug developed by Merck and marketed as Zocor™. It is a potent HMG-CoA reductase inhibitor and blocks the biosynthetic pathway for cholesterol production. It is a synthetic derivative of lovastatin, a fermentation product from the fungus *Aspergillus terreus*, differing only by a single methyl group on the butyryl side chain. Simvastatin was the highest prescribed statin in 2010 with more than 94 million prescriptions filled according to IMS Health.

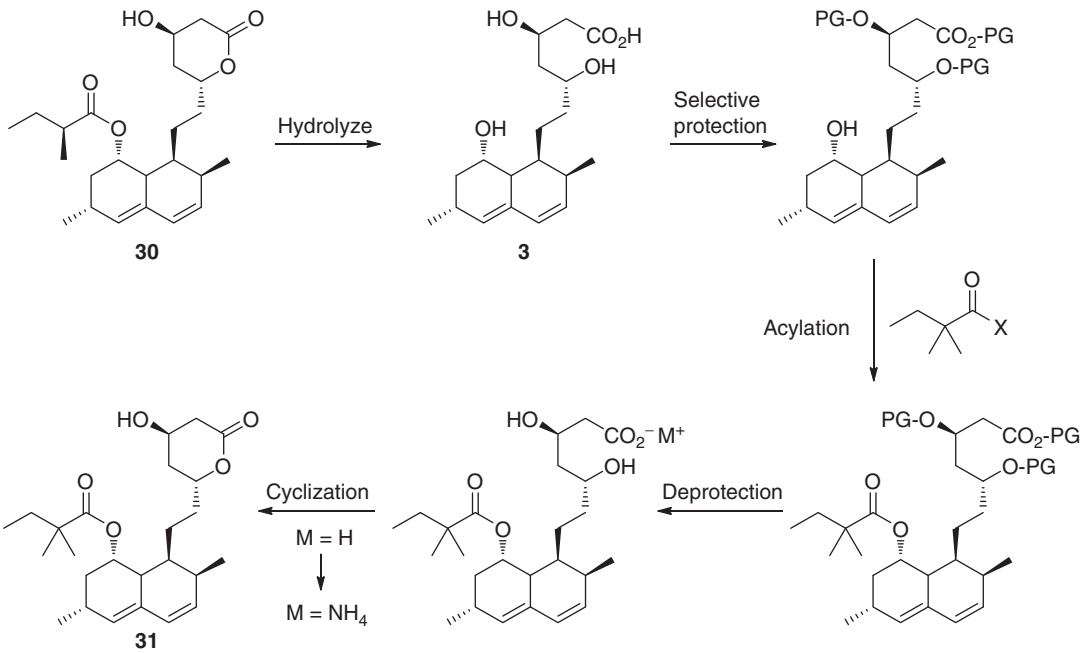
Simvastatin is generally manufactured by one of two main strategies, both starting with lovastatin. The first approach involves deprotonation of the side chain of lovastatin **24** after its protection, followed by direct methylation of the enolate (**Scheme 9**). The second approach involves removal of the side chain of **24** and replacement with the required dimethylbutyryl side chain. Both approaches require protecting group strategies, with the former also requiring cryogenic conditions and the use of a genotoxic alkylating agent (**Scheme 10**).

A conceptually more efficient approach is the regiospecific acylation of **3** without the need for protecting groups. Tang and coworkers at University of California, Los Angeles (UCLA) isolated and cloned the *lovD* gene which encodes the enzyme that catalyzes the final step of lovastatin biosynthesis in *A. terreus*. The UCLA scientists then demonstrated that this enzyme would accept a nonnatural dimethylbutyryl side chain donor, to give **4** (**Scheme 11**),[38] which is readily converted to the API **31**.

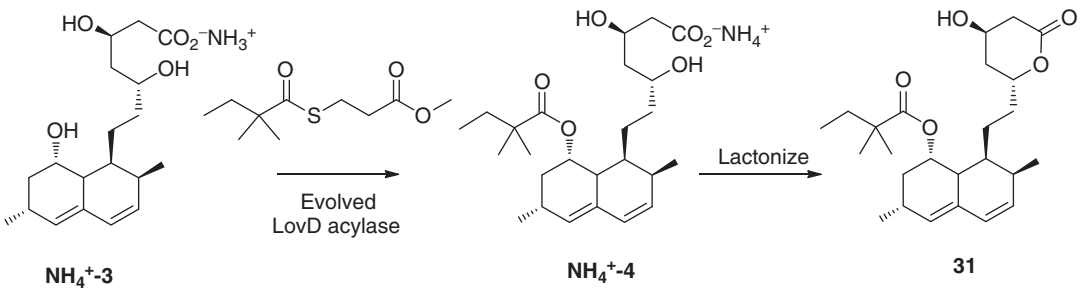
The activity and stability of the initial enzyme was poor and enzyme performance was improved by directed evolution with respect to enzyme activity, stability, and solubility, and to overcome substrate and product inhibition. In addition, the reaction was found to be an equilibrium reaction leading to incomplete conversion under typical reaction conditions. As described in Section 9.16.2.2, an innovative process was developed, in which the product is directly precipitated as the NH_4^+-salt during the process. This makes the biocatalytic acylation highly efficient and allows the isolation of the product in excellent purity via a simple direct drop process that removes up to three steps from the traditional acylation approach. The space-time yield for this reaction is ~ 2.5 g l^{-1} h^{-1} with a final product concentration of 100 g l^{-1}. By producing the product as the NH_4^+-salt, the amount of side-chain donor can be minimized to 1.1 equivalents.[39,40] The process has been scaled-up for commercial manufacture and received the 2012 EPA Presidential Green Chemistry Challenge Award.



Scheme 9



Scheme 10



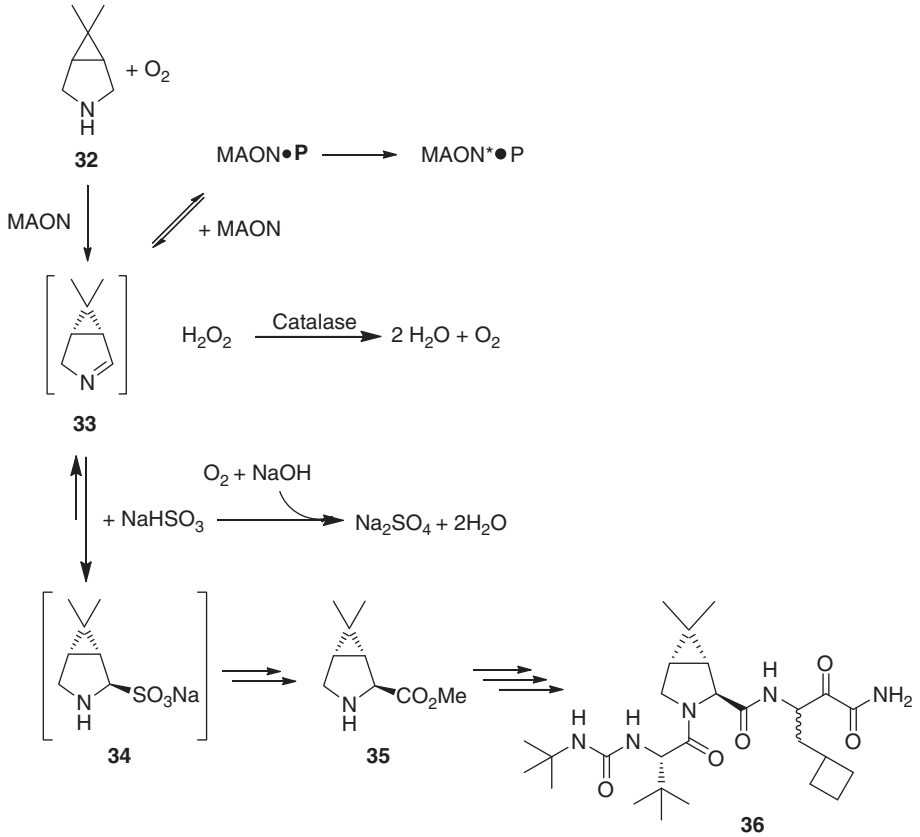
Scheme 11

9.16.5.9 Boceprevir

Boceprevir **36** is the API in Victrelis™, a recently approved peptidomimetic inhibitor of NS3 serine protease in the Hepatitis C virus. Boceprevir is manufactured from four building blocks including a chiral dimethylcyclopropylproline analog, P2 **35**.

35 was prepared by cyclopropanation of a Δ^3-pyrroline derivative of pyroglutamic acid for medicinal chemistry studies, and from caronic anhydride for large-scale synthesis. Initially, hydrolytic desymmetrization of caronic anhydride was used to set up the two chiral centers followed by installing of the third center via diastereospecific cyanation. This procedure is long and in the next process caronic anhydride was converted into 6,6-dimethyl-3-azabicyclo[3.1.0]hexane **32** which after oxidation, cyanation, and methanolysis provided *rac*.-**35**, which was resolved.

Using an evolved monoamine oxidase, Merck and Codexis scientists developed a process for the enantiospecific oxidation of **32**, providing the chiral imine **33** which was then further telescoped to **35** as shown in Scheme 12.[41]



Scheme 12

Over the course of the evolution program several challenges were addressed to enable the asymmetric biocatalytic oxidation of **32**. Owing to the volatility of **33** and its inhibitory effect on the enzyme, it was captured as the highly water-soluble bisulfate adduct **34**. The bisulfate adduct is readily converted into **35** in subsequent chemical steps. The coproduct of the oxidation of **32** is enzyme-inhibiting H_2O_2 and this is decomposed using commercially available catalase. Finally, bisulfite is readily oxidized to sulfate under the reaction conditions and hence accurate control over the process is required as bisulfate oxidation results in accumulation of **33**, yield loss through stripping of **33**, and irreversible enzyme inhibition. Over the course of four rounds of evolution using diversity obtained through random mutagenesis, family shuffling using a homologous monoamine oxidase, and site-directed mutagenesis, the monoamine oxidase from *Aspergillus niger* was evolved toward the desired fitness. The final enzyme was more active, more thermally stable and more soluble on expression in *E. coli* compared to the natural enzyme.

Compared to the resolution process, incorporation of the biocatalytic step increased the yield of **35** by 150%, whereas reducing the use of raw material and water by 60%. This process has been used for commercial production of **35**.

9.16.6 Anticipated Future Developments

Enzyme evolution has provided significant momentum to the application of biocatalysis for commercial-scale manufacturing processes.[1,22] As pharmaceutical molecules become more complex and the number of chiral compounds in clinical development increases, the use of enzymes in their synthesis will continue to increase. With increased availability of practical biocatalysts, enzymes will find their way from the process laboratories to earlier phases of development including medicinal chemistry.

The cost contribution of enzymes will continue to be a barrier to wide-scale adoption of this technology and while development of robust enzyme becomes less expensive, the cost of enzyme to the overall manufacturing cost will drive biocatalysis toward further intensification. Enzyme immobilization, long practiced for the manufacture of bulk chemical products such as 6APA and 7ACA for semisynthetic penicillins, and also for manufacture of high-fructose corn syrup, will increasingly be adopted to increase efficiency even further. Recent developments in this area for the synthesis of a nonnatural amino acid for odanacatib[42] and sitagliptin[43] provide the first glimpses of where this expansion may lead. Ultimately, directed evolution will emerge to parallel the biosynthetic reaction assemblies used in nature in order to accomplish multiple transformations in series.[44]

Improvements in enzyme evolution will continuously be sought.[45,46] This should not be confused with alternative methods, which are encountered in the literature, but not necessarily more efficient. Improvements in diversity generation and in HTP screening should reduce the time of the evolution cycle, ultimately culminating in complete *in silico* design of a final catalyst. Until now the computational design of enzymes has provided activities that still need orders of magnitude improvement, but as the effect of mutations in evolved enzymes can be understood and rationalized in general engineering concepts, this learning should yield first improved library design and ultimately more predictive computational tools.

Finally, new enzymes for complex reactions will be identified and made practically useful for chemical manufacture.[47,48] Given that enzymes can now be developed to withstand unprecedented harsh conditions, for instance, carbonic anhydrase to function in 4.2 M methyldiethanolamine at pH 11.8 and 75 °C,[49] it is without a doubt that extremely robust biocatalysts will have a major impact on how complex chemicals are manufactured in the future.

References

1. Bornscheuer, U. T.; Huisman, G. W.; Kazlauskas, R. J.; *et al. Nature* **2012**, *485*, 185–195.
2. Huisman, G. W.; Lalonde, J. J. Enzyme Evolution for Chemical Process Applications. In *Biocatalysis in the Pharmaceutical and Biotechnology Industries*; Patel, R., Ed.; CRC Press, **2006**, pp 717–742.
3. Estell, D. A.; Graycar, T. P.; Miller, J. V.; *et al. Science* **1986**, *233*, 659–663.
4. Stemmer, W. P. C. *Nature* **1994**, *370*, 389–391.
5. Stemmer, W. P. *Proc. Natl. Acad. Sci. USA* **1994**, *91*, 10747–10751.
6. Calvin, S. J.; Mangan, D.; Miskelly, I.; *et al. Org. Proc. Res. Dev.* **2012**, *16*, 82–86.
7. Strohmeier, G. A.; Pichler, H.; May, O.; Gruber-Khadjawi, M. *Chem. Rev.* **2011**, *111*, 4141–4164.
8. Clouthier, C. M.; Pelletier, J. N. *Chem. Soc. Rev.* **2012**, *41*, 1585–1605.
9. Reetz, M. T.; Bocola, M.; Wang, L.-W.; *et al. J. Am. Chem. Soc.* **2009**, *131*, 7334–7343.
10. Savile, C.; Gruber, J. M.; Mundorff, E.; Huisman, G. W.; Collier, S. J., Ketoreductase polypeptides for the production of a 3-aryl-3-hydroxypropanamine from a 3-aryl-3-ketopropanamine. WO2010025238, 2010.
11. Savile, C.; Gruber, J. M.; Mundorff, E.; Huisman, G. W.; Collier, S. J., Ketoreductase polypeptides for the production of a 3-aryl-3-hydroxypropanamine from a 3-aryl-3-ketopropanamine. WO2010025287, 2010.
12. Bergeron, S.; Chaplin, D. A.; Edwards, J. H.; *et al. Org. Proc. Res. Dev.* **2006**, *10*, 661–665.
13. Ma, S. K.; Gruber, J.; Davis, C.; *et al. Green Chem.* **2010**, *12*, 81–86.
14. Greenberg, W. A.; Varvak, A.; Hanson, S. R.; *et al. Proc. Natl. Acad. Sci. USA* **2004**, *101*, 5788–5793.
15. Fox, R. J.; Davis, S. C.; Mundorff, E.; *et al. Nat. Biotechnol.* **2007**, *25*, 338–344.
16. Crameri, A.; Raillard, S. A.; Bermudez, E.; Stemmer, W. P. *Nature* **1998**, *391*, 288–291.
17. Stutzman-Engwall, K.; Conlon, S.; Fedechko, R.; *et al. Metab. Eng.* **2005**, *7*, 27–37.
18. Nannemann, D. P.; Birmingham, W. R.; Scism, R. A.; Bachmann, B. O. *Future Med. Chem.* **2011**, *3*(7), 809–819.
19. Dalby, P. A. *Curr. Opin. Struct. Biol.* **2011**, *21*, 473–480.
20. Bornscheuer, U.; Kazlauskas, R. J. *Curr. Protocol. Protein Sci.* **2011**, *66*, 26.7.1–26.7.14.
21. Fox, R. J.; Clay, M. D. *Trends Biotechnol.* **2009**, *27*, 137–140.
22. Turner, N. J. *Nat. Chem. Biol.* **2009**, *5*, 567–573.
23. Whittal, J.; Sutton, P. *Practical Methods for Biocatalysis and Biotransformations*, 2nd ed.; Wiley: New York, **2012**.
24. Butler, D. E.; Le, T. V.; Millar, A.; Nanninga, T. N. Process for the synthesis of (5R)-1,1-dimethylethyl-6-cyano-5-hydroxy-3-oxo-hexanoate. US5,155,251, 1992.
25. Giver, L. J.; Newman, L. M.; Mundorff, E.; *et al.* Ketoreductase enzymes and uses thereof. US7,879,585, 2011.
26. Huisman, G. W.; Liang, J.; Krebber, A. *Curr. Opin. Chem. Biol.* **2010**, *14*, 122–129.
27. Matsuda, T.; Yamanaka, R.; Nakamura, K. *Tetrahedron Asym.* **2009**, *20*, 513–557.
28. Patel, R. *Biocatalysis in the Pharmaceutical and Biotechnology Industries*; CRC Press, **2006**.
29. DeWildeman, S. M. A.; Sonker, T.; Schoemaker, H. E.; *et al. Acc. Chem. Res.* **2007**, *40*, 1260–1266.
30. Moore, J. C.; Pollard, D. J.; Kosjek, B.; *et al. Acc. Chem. Res.* **2007**, *4*, 1412–1419.
31. Liang, J.; Lalonde, J.; Borup, B.; *et al. Org. Proc. Res. Dev.* **2010**, *14*, 193–198.
32. Fu, X.; McAllister, T. L.; Thiruvengadam, T. K.; Tann, C.-H.; Su, D. *Tetrahedron Lett.* **2003**, *44*, 801–804.
33. Mundorff, E.; de Vries, E. Ketoreductase polypeptides for the stereoselective production of 9(4S)-3[(5S-5-(4-fluorophenyl)-5-hydroxypentanoyl]-4-phenyl-1,2-oxazolidin-2-one. WO2010025085, 2010.
34. Noyori, R.; Ikeda, T.; Ohkuma, T.; *et al. J. Am. Soc. Chem.* **1989**, *111*, 9134–9135.
35. Campopiano, O.; Mundorff, E.; Borup, B.; Voladri, R. Ketoreductase polypeptides for the production of azetidinone. US7,883,879, 2011.
36. Savile, C. K.; Janey, J. M.; Mundorff, E. C.; *et al. Science* **2010**, *329*, 305–309.
37. Desai, A. A. *Angew. Chem. Int. Ed. Engl.* **2011**, *50*, 1974–1976.
38. Xie, X.; Watanabe, K.; Wojcicki, W. A.; *et al. Chem. Biol.* **2006**, *13*, 1161–1169.
39. Gilson, L.; Collier, S. J.; Sukumaran, J.; *et al.* Variant LovD polypeptides and their uses. WO2011041231, 2011.
40. Collier, S. J.; Teo, E. L.; Sukumaran, J.; Wilson, R. J.; Xu, J. Improved Lov-D acyltransferase mediated acylation. WO2011041233, 2011.
41. Li, T.; Liang, J.; Ambrogelly, A.; *et al. J. Am. Chem. Soc.* **2012**, *134*, 6467–6472.
42. Truppo, M. D.; Hughes, G. *Org. Proc. Res. Dev.* **2011**, *15*, 1033–1035.
43. Truppo, M. D.; Strotman, H.; Hughes, G. *Chem. Cat. Chem.* **2012**, doi:10.1002/cctc.201200228.
44. Davies, I. W.; Welch, C. J. *Science* **2009**, *325*, 701–704.
45. Goldsmith, M.; Tawfik, D. S. *Curr. Opin. Struct. Biol.* **2011**, *21*, 1–7.
46. Kazlauskas, R. J.; Bornscheuer, U. T. *Nat. Chem. Biol.* **2009**, *5*, 526–529.
47. Vick, J. E.; Schmidt-Dannert, C. *Angew. Chem. Int. Ed.* **2011**, *50*, 7476–7478.
48. Nestl, B. M.; Nebel, B. A.; Hauer, B. *Curr. Opin. Chem. Biol.* **2011**, *15*, 187–193.
49. Savile, C. K.; Lalonde, J. J. *Curr. Opin. Biotechnol.* **2011**, *22*, 818–823.
50. Anastas, P.; Warner, J. *Green Chemistry: Theory and Practice*; Oxford University Press: New York, **1998**.

9.17 Chemistry of Antibody–Small Molecule Drug Conjugates

RM Garbaccio, Merck & Co., Inc., West Point, PA, USA

© 2014 Elsevier Ltd. All rights reserved.

9.17.1	**Introduction – Brief Antibody–Drug Conjugates (ADCs) Backgrounder and Scope**	439
9.17.2	**Antibody Chemistry**	439
9.17.2.1	Natural Amino Acid	439
9.17.2.2	Nonnatural Amino Acid	442
9.17.3	**Conjugation Chemistry**	443
9.17.3.1	Heterogeneous Conjugation	443
9.17.3.1.1	Cysteine	443
9.17.3.1.2	Lysine (amides, Traut's reagent, reductive amination)	444
9.17.3.2	Homogeneous Conjugation of Natural Antibodies	445
9.17.3.2.1	Glycans	445
9.17.3.2.2	*N*-terminal conjugation	445
9.17.3.2.3	Enzymatic conjugation	447
9.17.3.3	Homogeneous Conjugation of Engineered/Unnatural Antibodies	447
9.17.3.3.1	Engineered cysteine/selenocysteine	447
9.17.3.3.2	Unnatural amino acid	448
9.17.4	**Linker Chemistry**	449
9.17.4.1	Chemically Labile	450
9.17.4.1.1	Disulfides	450
9.17.4.1.2	Hydrazones	451
9.17.4.2	Enzymatically Labile	451
9.17.4.2.1	Lysosomal proteases (cathepsin, plasmin)	451
9.17.4.2.2	β-Glucuronidase substrates	455
9.17.4.3	Nonlabile	455
9.17.5	**Loading Chemistry**	457
9.17.5.1	Dendrimers	459
9.17.5.2	Others	459
9.17.6	**Small Molecule Chemistry**	459
9.17.6.1	Payloads	461
9.17.6.2	Recognition of SAR Tolerability	461
9.17.7	**Conclusions and Future for Organic Synthesis in ADCs**	461
References		461

Glossary

Antibody-drug conjugate (ADC) A therapeutic modality that combines the targeting ability of an antibody with the potency of a small molecule through their conjugation.

Catabolism A metabolic pathway for degradation, as an example – the metabolism of an antibody into its constitutive amino acids.

Chemoselectivity The selective reactivity of one functional group in the presence of others.

Cytotoxic A molecule that elicits cell death, as an example – a tubulin-binder or DNA-damaging agent.

Drug antibody ratio (DAR) The stoichiometry between a small molecule and an antibody in an ADC.

Linker The chemical compound connecting two moieties, for example – connecting a payload to an antibody in an ADC.

Lysosome A cytosolic organelle that metabolizes molecules, for example – catabolizes antibodies.

Monoclonal antibody (mAb) An antibody made from a unique parent immune cell that recognizes a single epitope; targets that epitope on a desired cell.

NHS ester *N*-hydroxy succinimidyl ester, a commonly used functional group for making amide bonds.

Payload The small molecule attached to an antibody through a linker in an ADC.

Pharamcokinetics The study of the absorption, distribution, metabolism, and excretion of substances introduced into a living system.

Protease An enzyme responsible for protein catabolism, often found in lysosomes.

Regioselectivity The selective reactivity at one functional group in a molecule versus another identical functional group generating constitutional isomers.

Self-immolative A linker that on release results in a second chemical reaction that eliminates all atoms of the linker from the payload.

Unnatural amino acid (UAA) Any amino acid not naturally encoded by a living organism.

 doi:10.1016/B978-0-08-097742-3.00942-3

9.17.1 Introduction – Brief Antibody–Drug Conjugates (ADCs) Backgrounder and Scope

Antibody–drug conjugates (ADCs) are an emerging class of targeted therapeutics that has generated impressive results in oncology clinical trials highlighted by the recent approval of Adcetris® (brentuximab vedotin) for Hodgkin's lymphoma.[1–3] The strategy for this platform relies on the targeting ability of an antibody to specifically deliver a cytotoxic agent to the tumor and to minimize exposure in healthy tissue, thus increasing the therapeutic index relative to dosing the untargeted cytotoxic agent alone.[4,5] From a structural standpoint and to define the scope of this chapter, an ADC consists of a small molecule cytotoxic agent (payload) that is conjugated to a monoclonal antibody (mAb) through covalent linkage. Thus the three components of an ADC are the antibody, linker, and payload (Figure 1). Within these structural components, highlighted by three well-known ADCs in Figure 1, chemistry has played an important role in the evolution of this approach to its current state and is poised to spur progress toward next-generation ADCs.

A chemist new to the field may view the antibody conjugation as something outside the scope of traditional organic chemistry. In reality, the difference between antibody conjugation and standard small molecule chemistry is an appreciation for the size and complexity of the antibody-reacting partner, along with the analytical/purification methods required to characterize it. The same principles of chemoselectivity that apply to conventional synthesis are equally critical here, but the options are fewer in the current state-of-the-art. Methods for conjugating small molecules to large proteins have evolved over the years; from nonspecific to specific and from simply connective linkers to linkers that are triggered to release under specific physiological conditions. The ADC field has harnessed these chemistry developments and leveraged them to synergize with advances in the expression and humanization of mAbs.

In order to delineate the roles for synthetic chemistry in construction and optimization of this platform, a graphic for the general steps in ADC assembly and delivery is presented here (Scheme 1). In ADC assembly, a cytotoxic small molecule (payload) is appended to a bifunctional linker that may bring an important set of properties to the conjugate including the potential ability of the linker to be cleaved under certain physiological conditions. This small molecule linker is then conjugated to an antibody via different chemistries and stoichiometry. In delivery, following subcutaneous (s.c.) or intravenous dosing, the ADC must be stable in circulation until it encounters and binds to its cell-surface antigen (step 1). After binding to its receptor, the ADC is internalized through endocytosis and trafficked into a lysosome (step 2) where the antibody and/or linker are degraded releasing the small molecule into the cytosol where it can engage its target (step 3). The chemistry used to define the conjugation between antibody, linker, and small molecule, as well as the stability of the linker itself has been shown to have a significant effect on the *in vivo* performance of the ADC. A practicing chemist in the field will need to recognize the interdependent nature of their chemistry selections for this multicomponent therapeutic platform.

This chapter is written to survey the current state of organic synthesis in the production of antibody–drug conjugates providing examples of the chemistries used in standard techniques as well as emerging new approaches. As a primer for chemists entering this field, each section will make note of desired properties for each component: antibody, linker, and small molecule as well as the critical bonds that connect them.

9.17.2 Antibody Chemistry

At first glance, antibody production would appear to be out of scope for this chapter as hybridoma cell production and recombinant engineering are dominant state-of-the-art technologies for antibody production. However, direct chemical conjugation to natural amino acid-comprised antibodies has several limitations including: restriction to lysine and cysteine (Cys) conjugation, heterogeneity of conjugation site, and tight control of stoichiometry of drug loading. As an alternative to this, methods to incorporate orthogonal reactivity (chemoselectivity) in a site-specific manner are being developed. These technologies continue to rely on genetic engineering for mutant antibody production, but chemistry has played a key role in the identification of chemical and enzymatic reactions that leverage the mutant antibody sequence and structure. Beyond the scope of this chapter is the use of antibody fragments as targeting moieties as this does not currently expand the scope of chemistry to be discussed.

9.17.2.1 Natural Amino Acid

For the majority of published ADC chemistry, heterogeneous conjugation to available lysines or reduced cysteine disulfides is the preferred method. In this section, antibody production methods employing natural amino acids either as substitutes for natural unreactive residues, or as peptide tags, are summarized as they dictate and facilitate subsequent chemoselective conjugations with improved access to homogeneous conjugates. Beyond the scope of this review are the wealth of outstanding protein-modification chemistries that have been extensively reviewed[6] but have yet to find standard use in the preparation of ADCs.

The ability to enable site-specific chemoselectivity carries not only the benefit of minimizing conjugate heterogeneity, but also has the potential to minimize payload–linker interference with antibody–receptor recognition, effector function, and pharmacokinetic behavior by ensuring conjugation occurs at nonfunctional regions of the antibody primary sequence. Thus, protein engineers have considered the sequence and nature of reactivity of the amino acids in the strategies discussed here (Table 1). As a primary example, mAbs contain 32 Cys that are tethered through 4-interchain and 12-intrachain disulfide bridges, thus the

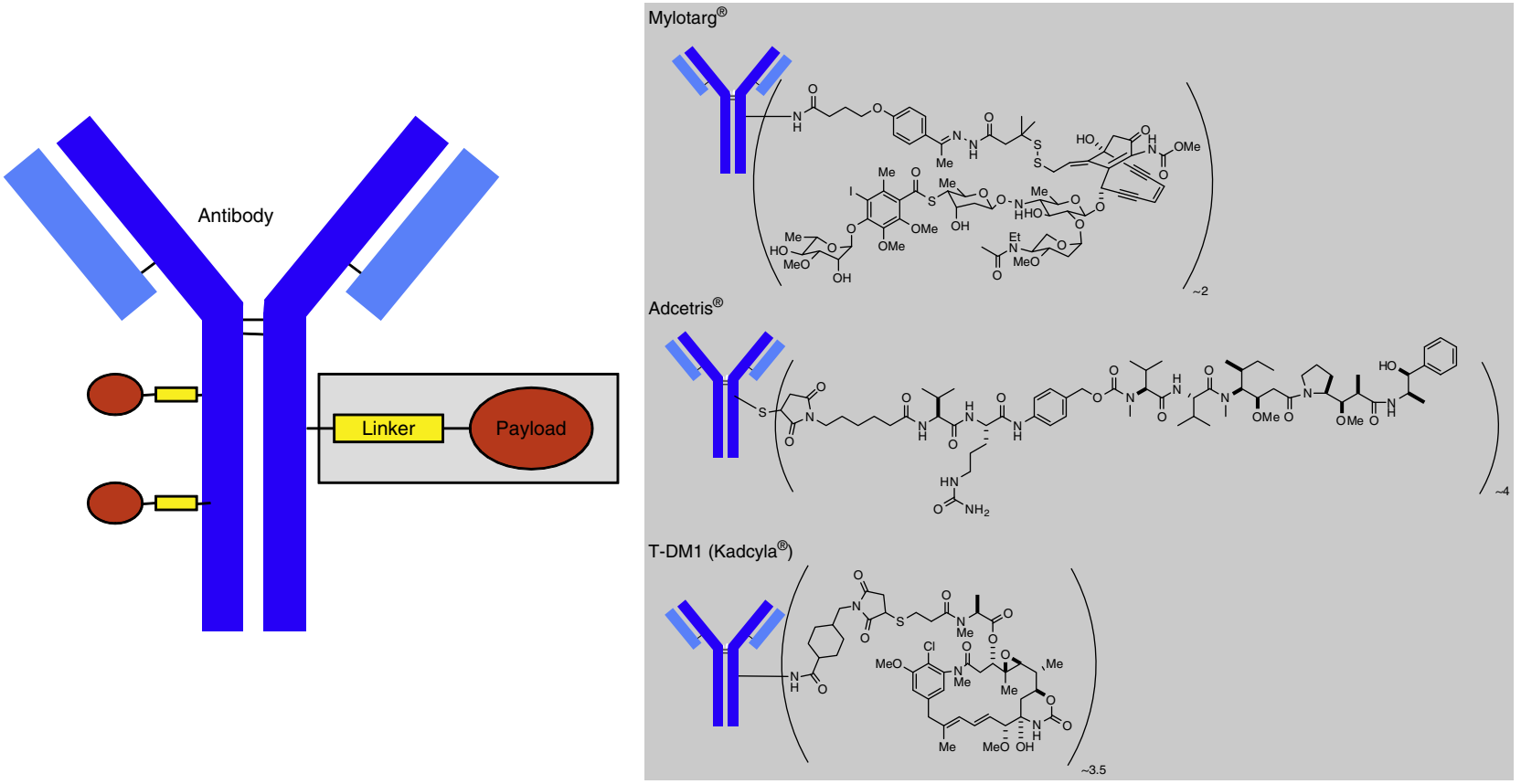
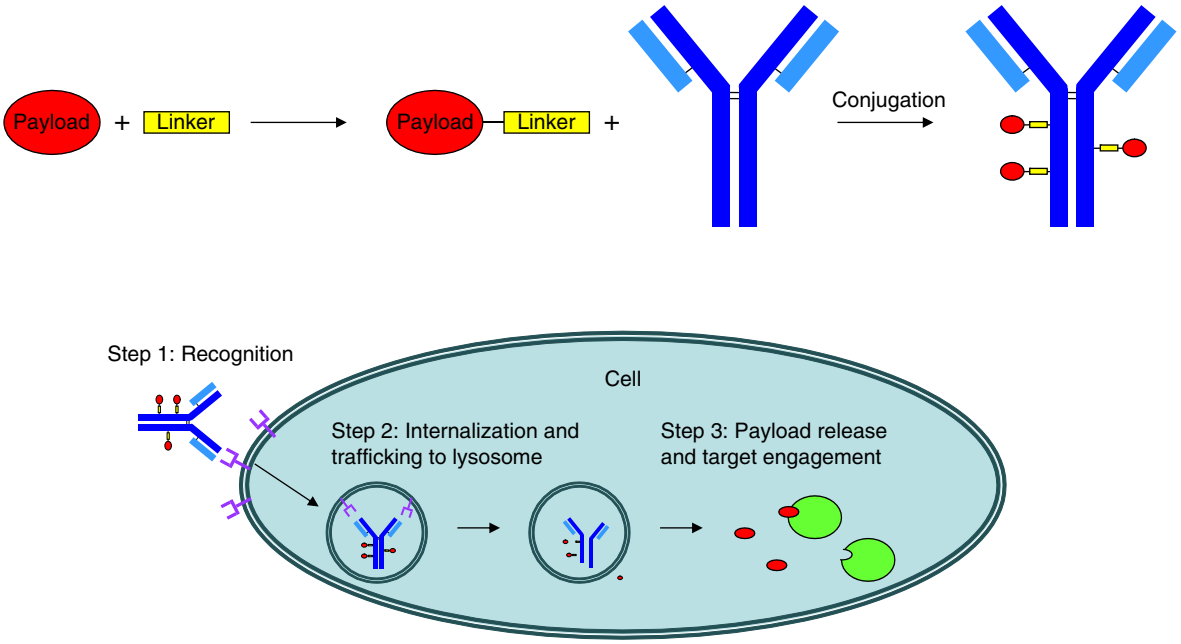
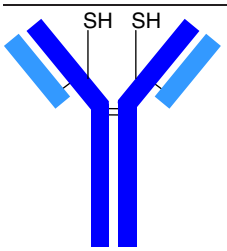
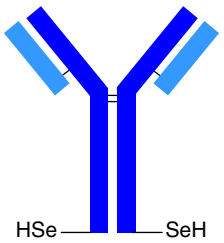
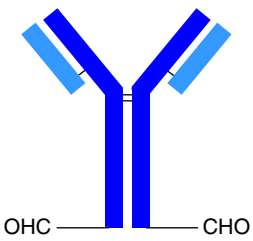


Figure 1 General structure of an antibody–drug conjugate and structures of Mylotarg®, Adcetris®, and T-DM1 (Kadcyla®).



Scheme 1 General assembly and pathway of delivery for an antibody–drug conjugate.

Table 1 Methods to enable chemo- and site-selective conjugation to the antibody using natural amino acids

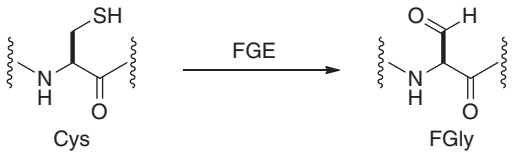
Structure	*Technology*	*Rationale*	*Positional flexibility or C-terminus*
	THIOMAB	Encoding of free cysteine residues for site-specific thiol conjugation	Flexible
	*C*-terminal selenocysteine	Cotranslational insertion of *C*-terminal selenocysteine for site-specific selenocysteine conjugation	*C*-terminus
	Aldehyde tagging	Introduction of a peptide sequence recognized by FGE into antibody primary sequence	Demonstrated for *C*- and *N*-terminus

introduction of additional Cys residues provides unique sites of chemical reactivity.[7] Termed THIOMABs, these antibodies were engineered to contain reactive Cys at specific sites within the antibody that minimized interference with the antibody function.[8] Various linkers are enabled by these Cys as described in Section 9.17.3. From seminal publications in the field, the authors have demonstrated that the choice of the conjugation site modulates both the *in vivo* stability and therapeutic activity of the

conjugate [9,10] providing the most compelling evidence that site-specific conjugation will be integral for future-generation ADCs. One potential drawback to this approach is the requirement that the activation of the engineered Cys for conjugation requires three additional steps (reduction, dialysis, and reoxidation of bridging disulfides).

As an alternative to the THIOMABs, selenocysteine (Sec)-incorporation at the *C*-terminal position has been developed to allow for site-selective conjugation.[11] Selenols have higher nucleophilicity than thiols, and do not require subsequent activation steps before conjugation. Currently, a drawback to this approach is the requirement for *C*-terminal placement of the selenocysteine in light of the possibility that an alternative location may provide superior properties to the ADC. In addition, this approach may be limited to a 1:1 drug:antibody ratio (DAR) as termination at the UGA stop codon-dominated Sec insertion.

A third approach for antibody engineering is the installation of a recognition sequence for the formyl glycine-generating enzyme (FGE) which can convert the recognized Cys into a formyl glycine (FGly) residue (**Scheme 2**). The resulting aldehyde provides the opportunity for chemoselective and site-specific conjugation and this method has been termed 'aldehyde tagging.'[12,13] Advantages of this approach include that the surrounding peptide recognition sequence for FGE was reduced to six amino acids, and that mammalian cells used for recombinant expression can also efficiently effect the Cys to FGly transformation. A potential disadvantage of this approach is that the requirement for an unmodified Cys in the FGE recognition sequence may impact protein folding although this was not observed for the IgG antibody examined.



Scheme 2 FGE conversion of Cys to FGly.

9.17.2.2 Nonnatural Amino Acid

For exquisite orthogonal reactivity and site-specificity, methods for the generation of antibodies with genetically encoded unnatural amino acids (UAAs) are a compelling direction for the next generation of ADCs. The challenge of achieving this in *Escherichia coli*, yeast, and mammalian cells was significant: how to cotranslationally introduce an UAA into machinery evolved for the natural 20 amino acids? The solution required three components that provide the necessary orthogonality and efficiency: A unique tRNA–codon pair, a specific aminoacyl-tRNA synthetase, and sufficient intracellular levels of the UAA.[14,15] Although more than 30 UAAs have been incorporated by this technology, of highest value to the ADC field are three UAAs with chemical handles that facilitate conjugation in the presence of other reactive natural amino acids (i.e., lysine, glutamate) and an aqueous environment. The most extensively used UAA in this regard is *para*-acetyl phenylalanine (**1**) that enables selective oxime formation with hydroxylamine nucleophiles (**Figure 2**).[16] Alternatively, the popular [3 + 2] Huisgen cycloaddition or 'click' reaction can be utilized with *para*-azido phenylalanine (**2**) or propynyl-tyrosine (**3**)-containing proteins.[17] The repertoire of UAAs incorporated into proteins continues to expand[18] the opportunities for this chemistry strategy.

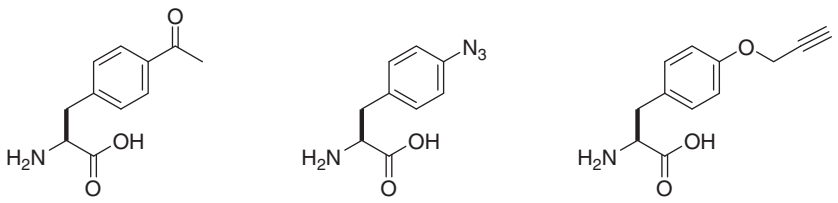


Figure 2 Selection of commonly employed nonnatural amino acids.

There are few publications on the application of UAA incorporation into antibodies,[19,20] even though it is being practiced extensively within the industry at companies like Ambrx, Redwood Biosciences, and Sutro Biopharma. Given the ability to control the site of incorporation and provide powerful chemoselectivity, it is anticipated that this approach will be more widely adopted as the ADC field grows in popularity.

The selection of a natural or mutated antibody for ADC assembly dictates the options for conjugation chemistry in the next section. Some of the aforementioned engineered systems will be revisited, while direct chemical conjugation on unmodified antibodies has also been explored.

9.17.3 Conjugation Chemistry

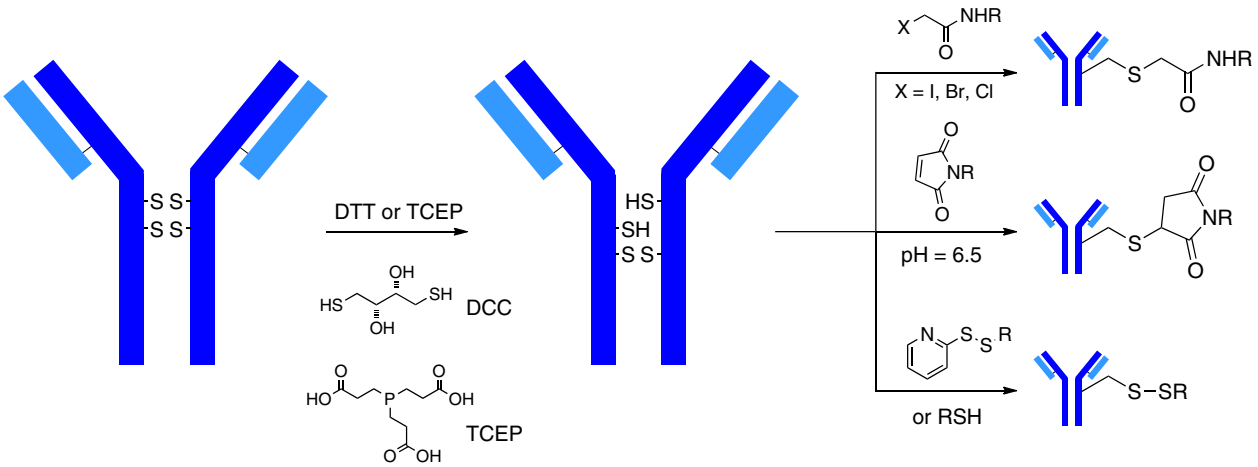
Covalent modification of an antibody presents several challenges including: competition among hundreds of reactive sites, aqueous media, low- to ambient temperature, and narrow pH range. As a result, the chemical reactions utilized are highly efficient and insensitive to water. The nature of this chemistry between the antibody and a linker–small molecule is dictated to a great degree by the functional groups available on the antibody. Section 9.17.2 highlighted the available functional groups on the mAb, and this section details the reacting partner that enables connection of the linker–small molecule to the mAb. As a goal, conjugation to the antibody should maintain the pharmacokinetics and physicochemical properties of the mAb while having sufficient stability to endure systemic circulation. There is evidence that suggests the location[10] and loading[11] (the number of drug–linker molecules attached to an antibody is called the drug:antibody ratio (DAR)) may have a significant impact on these parameters – thus conjugation chemistry needs to be tightly controlled. First-generation ADCs have relied on the heterogeneous conjugation to available lysines or reduced interchain disulfides (Cys) and remarkable progress has been made using these approaches including nearly all of the current ADC clinical candidates. With the purpose of increasing uniformity in ADC assembly, alternative approaches using genetic engineering, nonnatural amino acids, and chemical/enzymatic approaches have been devised to allow for site-specific conjugation. If these new methods can overcome potential scalability and regulatory concerns, it is likely that this evolution toward uniform conjugates will result in second generation ADCs with improved properties and performance. The chemistry in this section relies heavily on robust and orthogonal bond-forming reactions that can be conducted in aqueous environments to facilitate reactivity and thus high levels of conversion to a well-defined conjugate.

9.17.3.1 Heterogeneous Conjugation

Much of the published literature around antibody–drug conjugates uses a direct conjugation strategy of a linker–payload electrophile with the natural nucleophilic amino acids (i.e., Cys, Lys) in the antibody primary sequence. This approach inevitably results in a heterogeneous distribution of conjugates, given the number and placement of these amino acids throughout the primary sequence. Thus potentially important properties like location of conjugation and DAR are difficult to control, and purification is sometimes required to eliminate subpopulations of conjugates that have higher loading, or no drug loading at all. Despite these hurdles, more than 30 ADCs have been advanced into clinical development using these conjugation approaches.

9.17.3.1.1 Cysteine

Given the high nucleophilicity of its sulfhydryl, and its low natural abundance in proteins, Cys is a common choice for a conjugation handle.[21] Importantly, a full-length antibody contains no free thiol groups as the 16 or more Cys in the conserved region are tethered in inter- and intrachain disulfide bridges. Thus, to enable conjugation through Cys, the antibody must be subjected to a partial reduction to selectively break the interchain disulfide bridges (Scheme 3).[22] The free sulfhydryls can then be conjugated with a linker–small molecule through several chemistries including: α-halo carbonyl alkylations, Michael additions, and disulfide formation. In the case of α-halo carbonyl alkylations, concomitant lysine alkylation has been observed and minimized with the use of α-chloro carbonyls.[23] Alternatively, Michael additions to maleimides are effective if careful control of pH between 6.5 and 7.5 is maintained to ensure lysine protonation and avoid N-alkylation (will occur at pH > 7.5). The disulfide approach has been frequently used to impart cleavability in the linker, and this will be discussed in greater detail in the linkers section.



Scheme 3 Antibody conjugation through Cys.

Conjugation to form a disulfide is often conducted with an activated disulfide-containing linker–small molecule. However, a recent application of the disulfide conjugation strategy in the form of 'traceless' linkers has been demonstrated which alternatively activates the antibody thiol with Ellman's reagent.[24] In addition to the moderate heterogeneity of these conjugates (Figure 3), the risk in this general approach is that antibody stability and/or biodistribution may be adversely impacted by perturbation of these disulfide bridges. Nevertheless, Adcetris® assembled via Cys conjugation, has navigated commercial production, and earned FDA approval.[25]

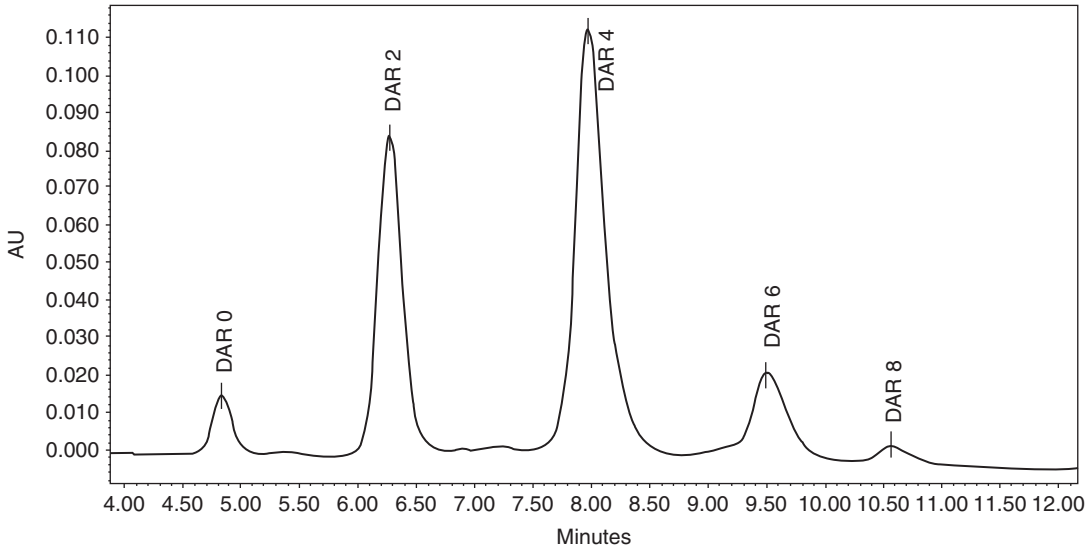
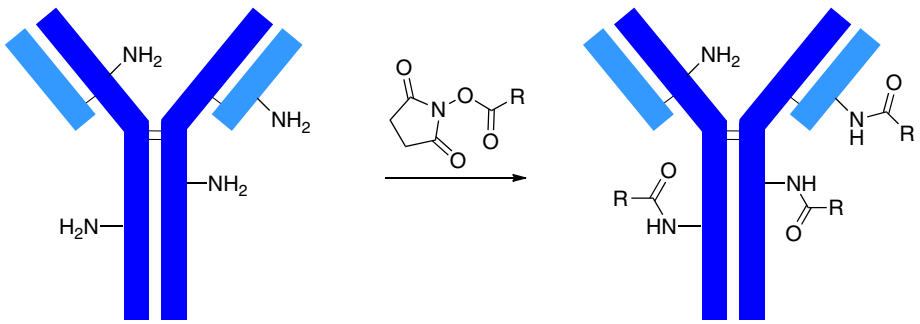


Figure 3 Representative hydrophobic interaction chromatography (HIC) of *anti*-STEAP1 ADC with average DAR of approximately 3.5. The peak assignments are consistent with the conjugation of the linker–drug being primarily limited to the interchain Cys of the antibody and leading to a DAR distribution of mainly 0, 2, 4, 6 or 8. Representative chromatogram for Cys conjugation. Reprinted from Boswell, C. A.; Mundo, E. E.; Zhang, C.; *et al. Bioconjug. Chem.* **2010**, *10*, 1994–2004, with permission from American Chemical Society.

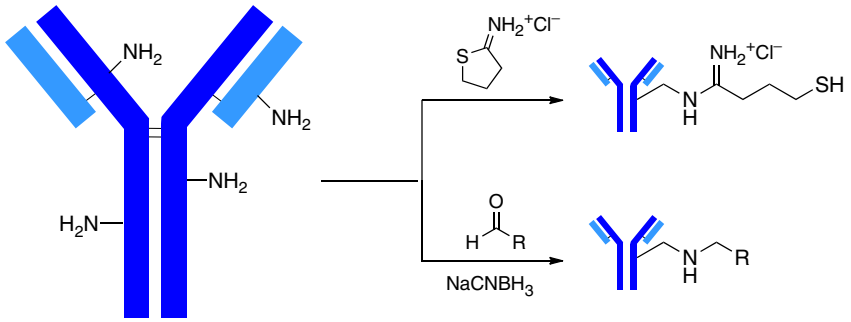
9.17.3.1.2 Lysine (amides, Traut's reagent, reductive amination)

Lysine provides a nucleophilic ε-amine that is abundant in antibodies ($n \sim 86$)[26] and requires no manipulation before conjugation. Direct lysine conjugation is often the alternative to Cys modification particularly in instances where a stable amide linkage is preferred or when the increased conjugate heterogeneity is not a concern. Antibody lysine residues have been conjugated most frequently through amide formation with *N*-hydroxysuccinimidyl (NHS) esters and a number of commercial linkers rely on this chemistry (Scheme 4). Analysis of this antibody conjugation method demonstrates that up to 20 different lysines are modified by this protocol[27] and that low levels of Cys and tyrosine modification can also occur.[28] In addition, careful stoichiometry and reaction monitoring are helpful in maintaining the target DAR, although a distribution of products is inevitable.



Scheme 4 Antibody conjugation through lysine using NHS esters.

An alternative conjugation chemistry that preserves the positive charge of a lysine residue uses 2-imiothiolane (Traut's reagent)[29] to make an amidine with a pendant thiol for connection to a linker or payload (Scheme 5). This method has the advantage of accessing thiol-based conjugation without having to reduce the antibody. Reductive aminations of antibody lysines have also been achieved and these reactions also retain the positive charge of the lysine residue. Maintenance of positive charge may have the benefit of reducing the risk for antibody aggregation following conjugation.



Scheme 5 Antibody conjugation through lysine using Traut's reagent and reductive amination.

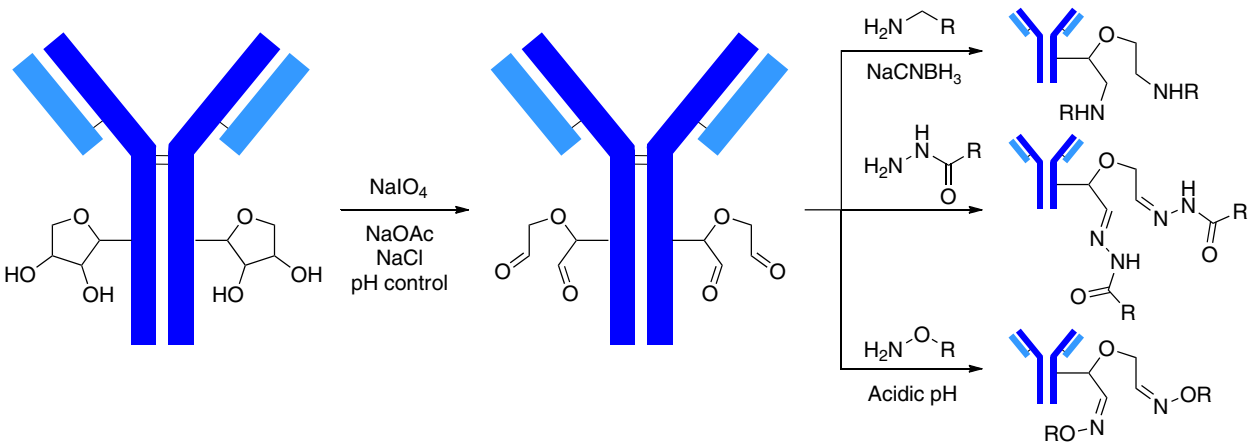
Lysine conjugation bears the risk of heterogeneous conjugations described in Section 9.17.3.1.2, but is undoubtedly the most reliable method for robust attachment where this heterogeneity is not a significant concern. In addition, the field generally agrees that lysine and Cys conjugations with moderate DAR[2–4] have been achieved with no loss in antibody affinity.[30]

9.17.3.2 Homogeneous Conjugation of Natural Antibodies

For the purposes of this chapter, homogeneous (regiospecific) conjugation methods are those that provide the chemical control to react at a single site on an antibody (either natural or engineered). In the strictest terms, due to local heterogeneity of expressed antibodies in their sequence and glycan – many of the methods do not produce a true single entity. These conjugations do, however, afford greater homogeneity than the conjugation methods mentioned in Section 9.17.3.2, and some can be directly applied to natural antibodies. The recent success of engineered (mutant) antibodies often affords even greater control over the final ADC.

9.17.3.2.1 Glycans

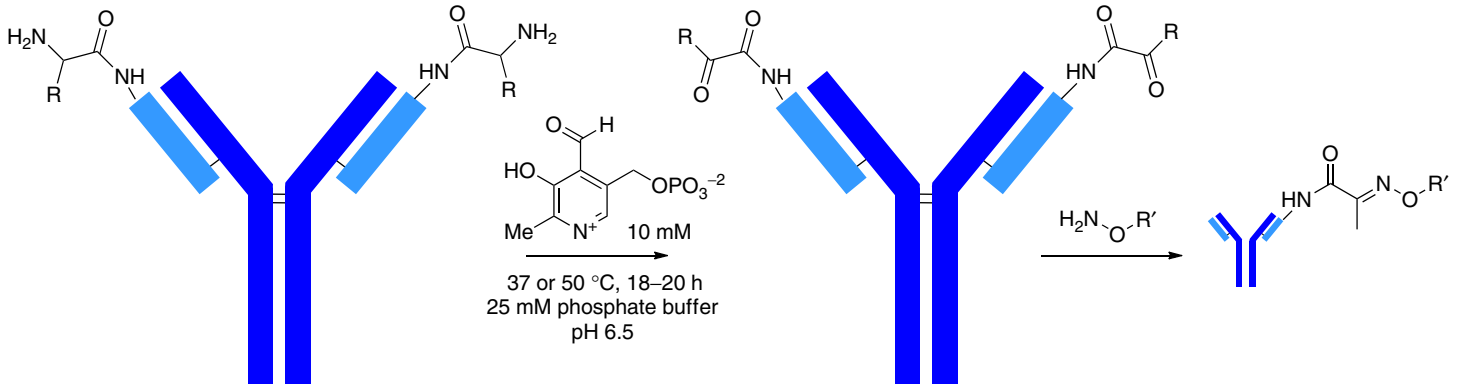
One of the earliest homogeneous conjugation strategies takes advantage of carbohydrate chains that are located in the Fc region of the antibody.[31] Periodate-oxidation of these carbohydrates produces aldehydes under mild conditions that are reactive to amine, hydrazide, and hydroxyl amine-based nucleophiles (Scheme 6).[32] The conditions for this oxidation have been carefully studied to reduce heterogeneity and control loading.[33] An advantage to this approach is that it can be used directly on natural antibodies, and that the carbohydrates are distant from the binding regions needed for antigen recognition. Although this approach has found significant early use in the conjugation of fluorescent labels, it has not found as much use in the preparation of antibody –drug conjugates. In addition, although conjugation does occur specifically at sites that contain carbohydrates, the products are not homogeneous due to nonhomogeneous natural oligosaccharide decoration and number of potential aldehydes. A risk to this approach is the disruption of the role the carbohydrate has in antibody structure stabilization and propensity for aggregation.



Scheme 6 Antibody conjugation through periodate cleavage of glycans.

9.17.3.2.2 N-terminal conjugation

In an impressive example of leveraging differences in pKa, the α-amine of an *N*-terminal amino acid (pKa ~8) in the light chain of an antibody can preferentially undergo transamination with pyridoxal-5′-phosphate (PLP) to produce a ketone and avoid reaction with the ε-amines of the lysine side chains (pKa ~10).[34] This ketone undergoes smooth conjugation with oximes to form hydroxylamines (Scheme 7). Whereas this chemistry takes place in the antigen-binding region, it does not appear to impact

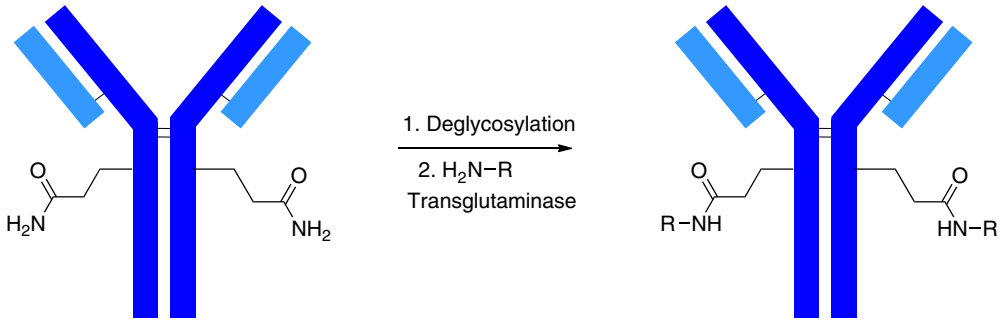


Scheme 7 Antibody conjugation through *N*-terminal transamination.

epitope recognition. One limitation of this approach is that the reaction is sensitive to the nature of the terminal amino acid and works best for A, G, D, E, and N. However, some antibodies may not tolerate the elevated temperature required for transamination.

9.17.3.2.3 Enzymatic conjugation

A bioorganic conjugation method that allows site-specific attachment at glutamines flanked by a consensus recognition sequence for a bacterial transaminase has been reported for the synthesis of radioimmunoconjugates.[35] Deglycosylation of the antibody is required before transamination, and a 2:1 conjugate was obtained with exclusive attachment to Q295 within the heavy chain (Scheme 8). The homogeneous conjugate has the advantage of chemical attachment at a location distant from the antigen-binding site, but requires deglycosylation which may impact overall properties and performance of the ADC.



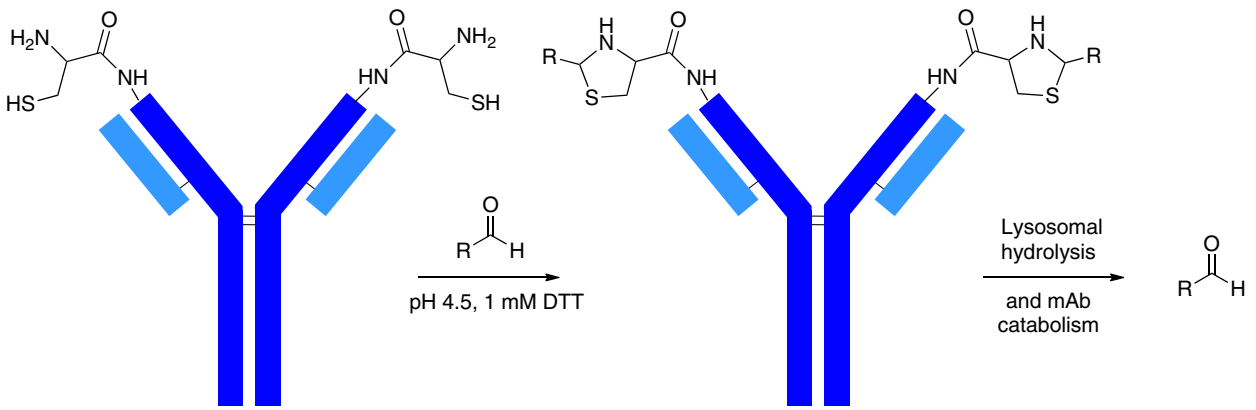
Scheme 8 Site-specific antibody conjugation through transamination.

9.17.3.3 Homogeneous Conjugation of Engineered/Unnatural Antibodies

Site-specific conjugation of natural antibodies is challenging, made more so by the variable incorporation of diverse amino acids in the hypervariable antigen-binding region. Recombinant expression is the tool of choice for this strategy due to its ability to site-specifically incorporate orthogonal amino acids that impart the highest level of chemical control over conjugation. As discussed Section 9.17.3.3, the advantages for site-specific conjugation include homogeneity of the conjugate for optimization and Chemistry, Manufacturing and Controls (CMC) purposes, conjugation to conserved locations distal to the antigen- and Fc-binding regions, and control of DAR which has been demonstrated to impact the therapeutic window.

9.17.3.3.1 Engineered cysteine/selenocysteine

As described in Section 9.17.2.1, the THIOMAB antibodies incorporate free Cys residues capable of single-site attachment as all naturally incorporated cysteines are in their oxidized forms as disulfide bridges.[8–11] Site-specific conjugation to these unique cysteines relies on the same chemistry for heterogeneous Cys conjugation – α-halo carbonyl alkylations, Michael additions, and disulfide formation. *C*-terminal selenocysteine-containing antibodies[12] have been conjugated through similar Michael-addition chemistry with maleimides. A recent report that utilizes an antibody expressed with an *N*-terminal Cys on the heavy chain enables a thiazolidine ligation between the 1,2-amino thiol and an aldehyde-containing payload (Scheme 9).[36] Following internalization



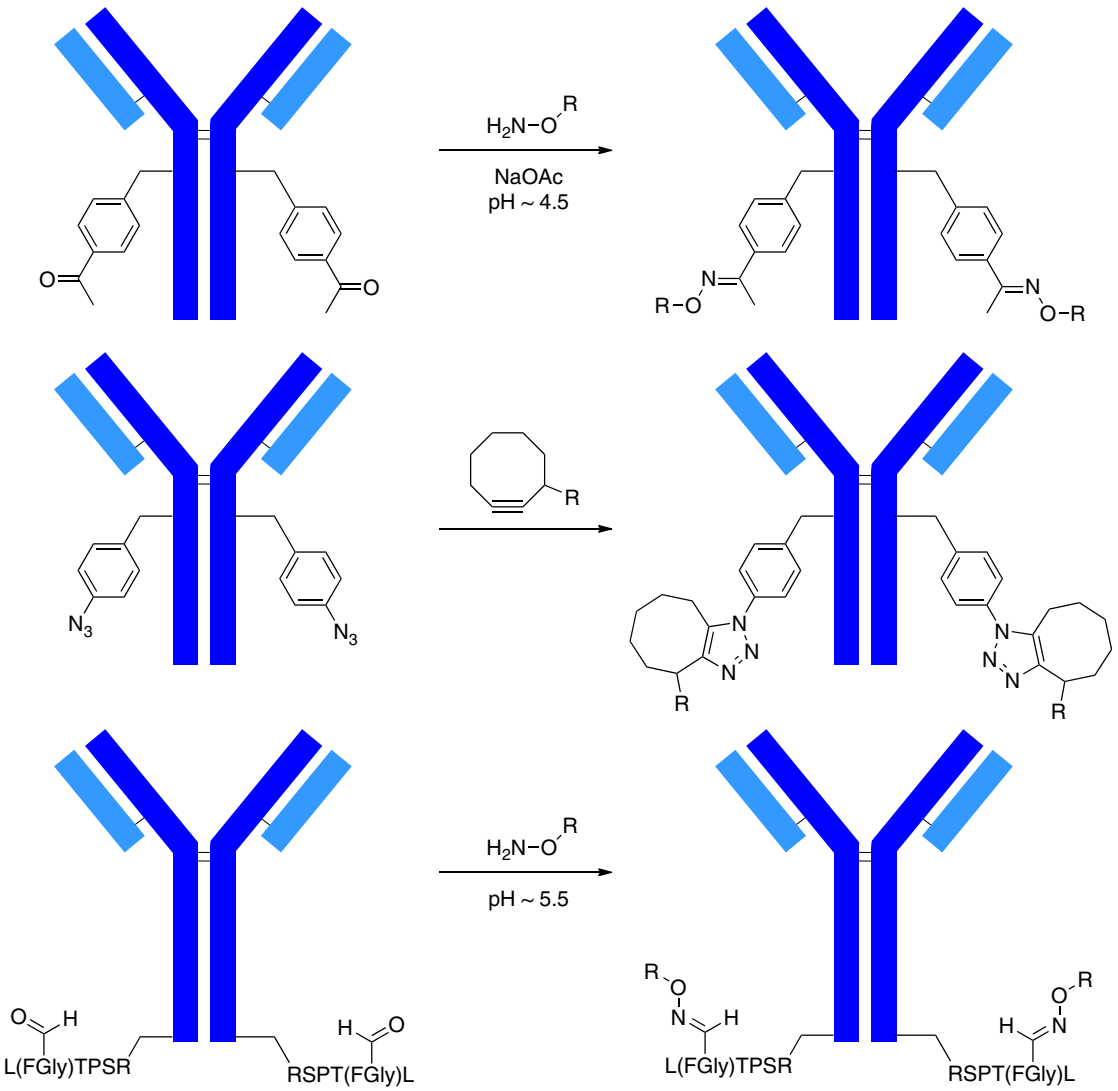
Scheme 9 Antibody conjugation through *N*-terminal thiazolidination.

into the target cell and hydrolysis of the thiazolidine, the parent payload and unmodified antibody are produced. This traceless conjugation may have unique advantages for cytotoxic payloads with aldehyde functionality.

9.17.3.3.2 Unnatural amino acid

Antibodies with genetically encoded unnatural amino acids enable the application of unique orthogonal chemistry to effect site-specific conjugation. As detailed in Section 9.17.2.2, three of the UAA functional groups that have been successfully utilized are the ketone, azide, and aldehyde (Scheme 10). With these functional handles, oxime and [3 + 2] cycloaddition ('click') chemistry are finding increasing use due to their aqueous compatibility, mild nature, and rates of conversion. For ketone-containing proteins, hydroxylamines were found to react more efficiently than hydrazides, and thus are the preferred functionality for this strategy. Oxime formation optimally proceeds at acidic pH (~4.5)[20] and this may be a limitation for some antibodies. Alternatively, click chemistry has found application in homogeneous conjugates of engineered antibodies, but use of 'copper-free' conditions is recommended.[37] By taking advantage of strained cycloalkynes, which react with azides in the absence of copper, chemists can avoid the potentially challenging problem of separating copper from their antibody conjugate. The copper-free strained-cycloalkyne strategy for antibody conjugation is yet to be documented in peer-reviewed literature, whereas variants of this cycloaddition chemistry including *trans*-cyclooctenes/norbornenes with tetrazines as reacting partners [18,38,39] are being practiced on proteins and are easily applicable in preparing antibody–drug conjugates. Given the scope of UAA incorporation possible through genetic encoding, further expansion of the menu for conjugation reactions is likely.

Alternatively, antibodies with genetically encoded aldehyde tags (Scheme 10) can also participate in site-specific oxime conjugation with hydroxylamine linker–payload molecules.[12,13,40] With an aldehyde rather than a ketone as one of the reacting



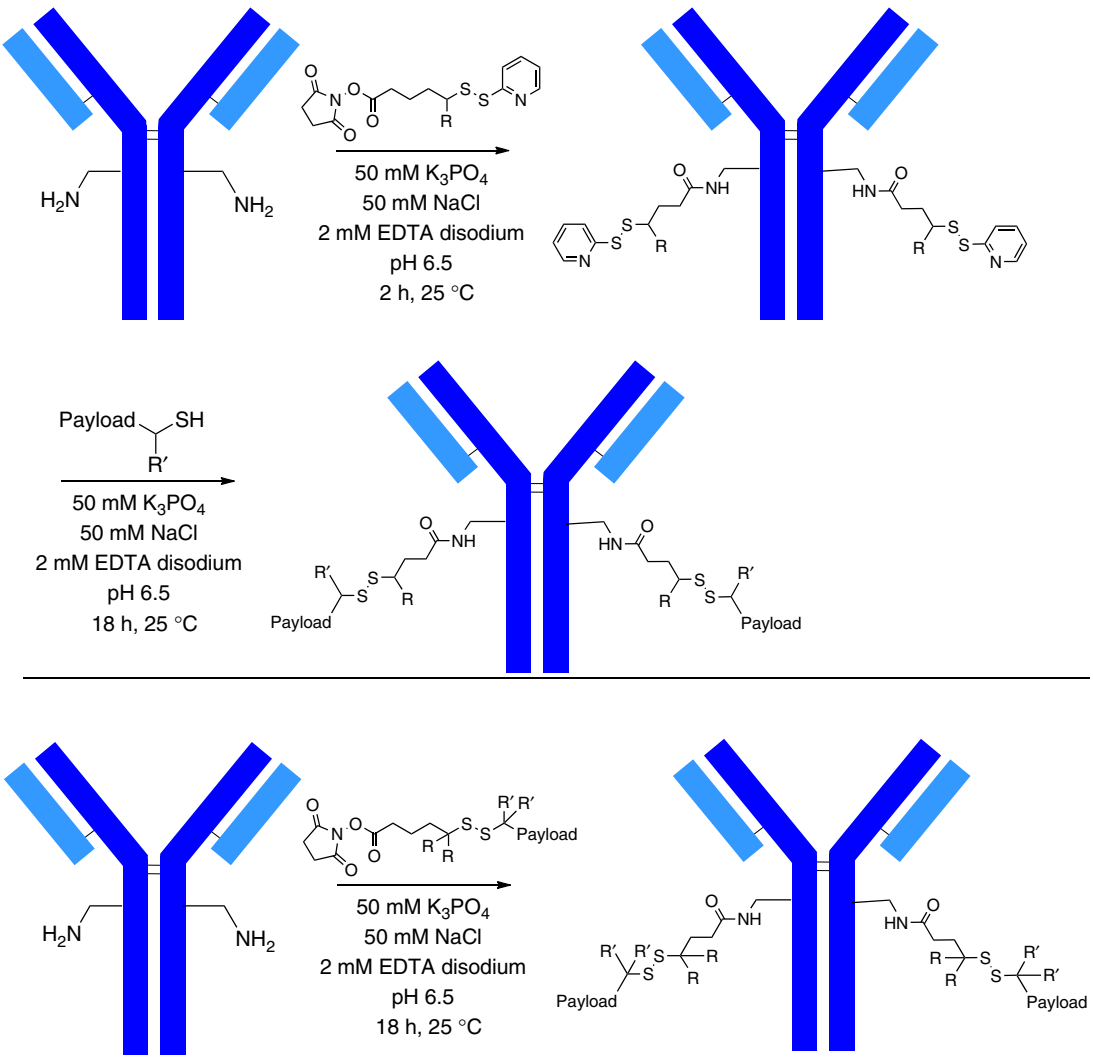
Scheme 10 Site-specific antibody conjugation through unnatural amino acids.

partners the reaction conditions are more mild (pH 5.5), but, to date, the aldehyde-tagging method has only been shown for *C*- and *N*-terminal loci of antibodies. Given that the natural substrates for the FGE enzyme have internal consensus sequences, it is possible that this strategy will be expanded to other locations on the antibody.

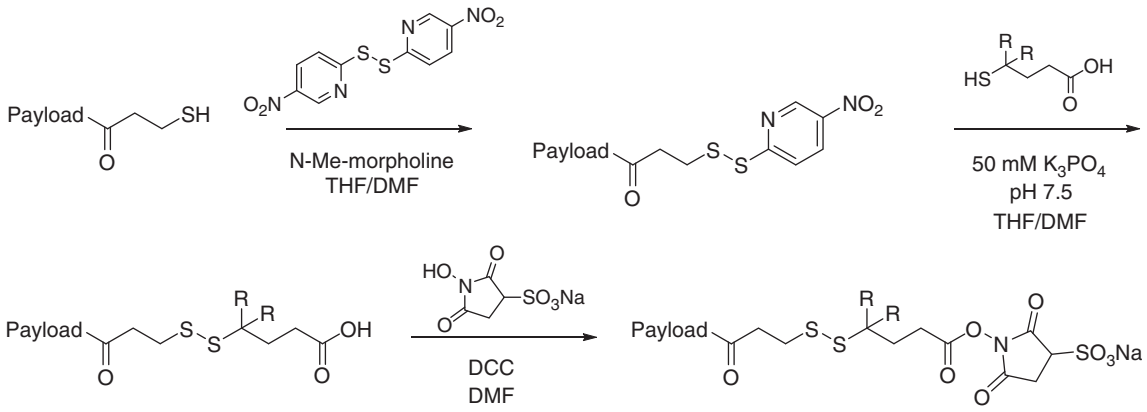
9.17.4 Linker Chemistry

One of the more exciting and dynamic areas of chemistry focus within the ADC field has been that of linker design and synthesis.[4] Simply stated, the goal of the linker is to arrive at the right balance between plasma stability required for prolonged circulation and efficient payload release at or within the target cell. An important selection of linker type is made based on the chemist's knowledge of structure-activity relationship (SAR) for the payload. If the payload will be pharmacologically active with a residual linker fragment, noncleavable linker designs may be superior as the antibody catabolism still allows for linker–payload release from the lysosome. However, if the payload has restrictive SAR and must be delivered as a parent drug to be active, cleavable and self-immolative designs are preferred creating an unusual challenge for the practicing chemist.

Selection of the environmental trigger for release within the target cell is used here to organize linker types. Cleavable linkers that depend on chemical and enzymatic differences in the intracellular environment have been investigated, as have noncleavable linkers that rely on antibody catabolism in the lysosome for release. As the field has matured, so has the understanding of the properties that can be imparted by the linker on both the physicochemical attributes of the conjugate as well as the pharmacological profile of the payload including limiting efflux from the cell following delivery. The chemistry used here is more straightforward in that the linker is typically appended to the small molecule before antibody conjugation and thus predictably relies on protecting group manipulation and standard small molecule methods to manage the sequence assembly.



Scheme 11 Alternative sequences for ADC assembly with disulfide linkers.



Scheme 12 Synthesis of disulfide-containing linker–payload molecules.

9.17.4.1 Chemically Labile

Much of the early chemistry used to construct ADCs installed linkers had chemical reactivity that would be greater in an intracellular environment than in circulation. Two important physiological differences between these environments were leveraged: the increased concentration of glutathione inside cells for disulfide cleavage and the acidification of the endosomal–lysosomal trafficking pathway for acyl hydrazone cleavage.

9.17.4.1.1 Disulfides

As the concentration of glutathione is approximately 1000-fold greater in the cytoplasm than in blood, chemists have utilized disulfides as a linker strategy for ADC delivery. In one example, plasma stability of these disulfides was found to be insufficient, and hindered disulfides were employed to address this potential liability.[41] The synthesis of these ADCs can either be accomplished by final conjugation of an NHS-ester bearing linker–payload molecule with the available lysines on an antibody, or by final disulfide formation between a thiol-containing linker–payload molecule and an antibody conjugated with a pyridylthiol-terminating

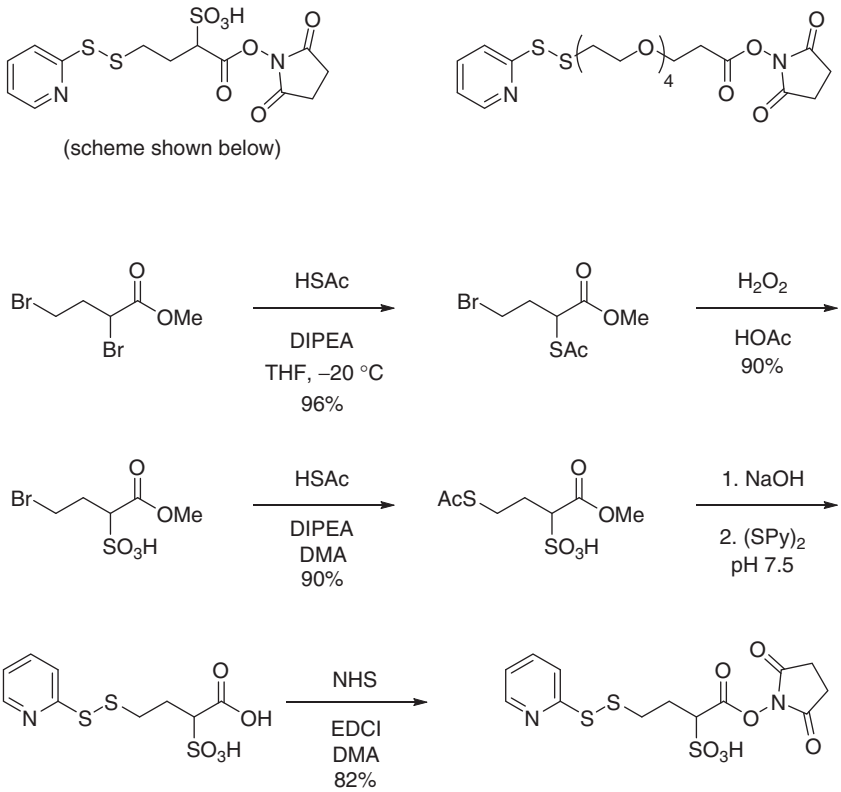


Figure 4 Synthesis of hydrophilic disulfide linkers.

linker (Scheme 11). The chemistry described below will focus on the disulfide formation as the common key step; antibody conjugation using an NHS ester has been described in Section 9.17.3.1.2.

Disulfides can generally be synthesized through the combination of an activated pyridyl disulfide and a free thiol, but require additional steps to set up the linker–payload molecule that is ready for conjugation to the lysines of an antibody (Scheme 12). Careful pH control is generally required for the disulfide formation, and a water-solubilized NHS ester was used for more hydrophobic linkers.

The hydrophobic nature of the disulfide linkers described earlier is thought to be limiting in the amount of payload that can be loaded onto an antibody, and can result in aggregation, loss of affinity, and rapid clearance. Hydrophilic polyethylene glycol and sulfate-containing linkers (Figure 4) have been synthesized and demonstrated to enable higher loading (DAR 6–8) without compromising ADC aggregation or pharmacokinetics (PK).[42] Notably, these polar linkers are also thought to slow the efflux of the payloads following delivery into the cell resulting in increased accumulation of payload within the target cell. Noncleavable alternatives to these linkers were also reported. Incorporation of these linkers follows the chemistry described in Schemes 11 and 12.

An extension of the disulfide concept has recently been reported in which thiol-containing payloads can directly be conjugated to noninternalizing antibodies.[24] This design relies on the antibody to colocalize the labile disulfide-linker payload to the reducing environment of the tumor, and allow for targeted release of a permeable molecule in a traceless fashion (no additional linker functionality required).

9.17.4.1.2 Hydrazones

Most ADCs internalize following antigen binding via an endocytic process. As the resulting endosome matures and ultimately fuses with a lysosome, there is an increasing acidification of the compartment down to approximately pH 4. Thus, a linker design that is stable at neutral physiological pH but reactive at pH 4 was one of the first successful designs employed. This design was incorporated into Mylotarg® which relied on the selective hydrolysis of an acyl hydrazone in the lysosomal compartment of the targeted CD33-positive cells (Figure 5).[43,44]

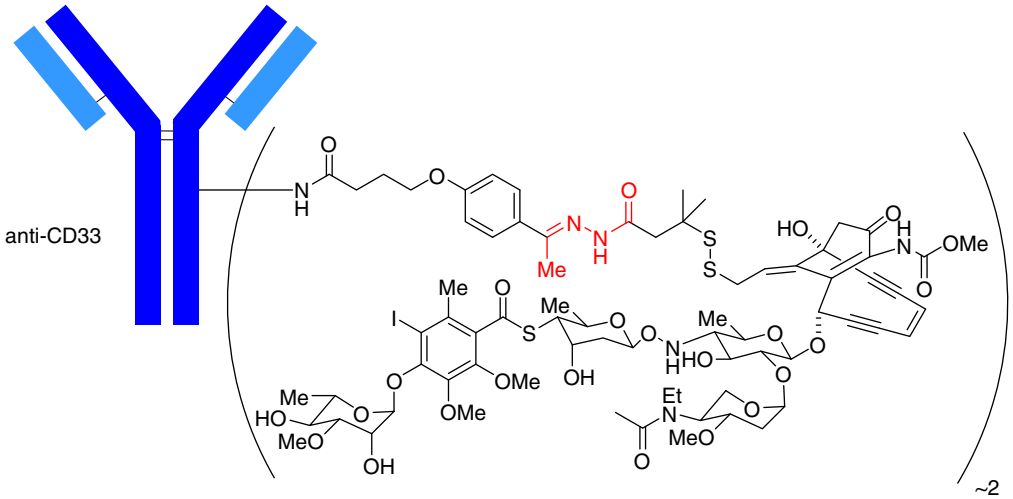


Figure 5 Mylotarg®.

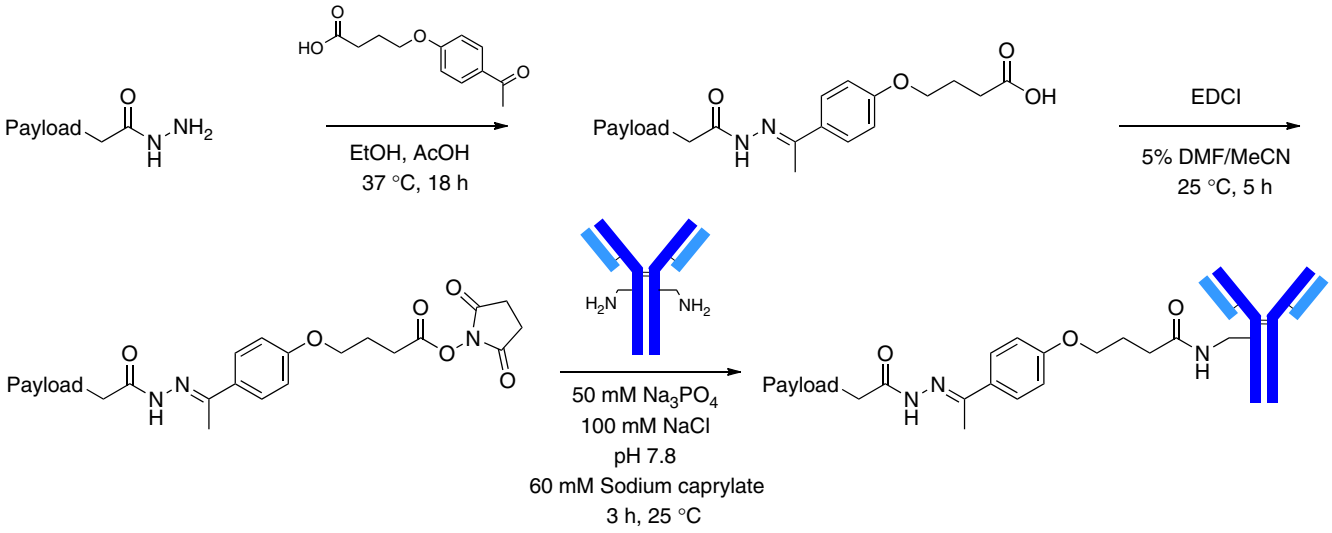
The synthesis of the acyl hydrazone containing linker–payload molecule requires acid-catalyzed hydrazone formation, 1-(3-dimethylaminopropyl)-3-ethylcarbodiimide (EDCI) coupling, and buffered conjugation to the available lysines on an antibody (Scheme 13).

9.17.4.2 Enzymatically Labile

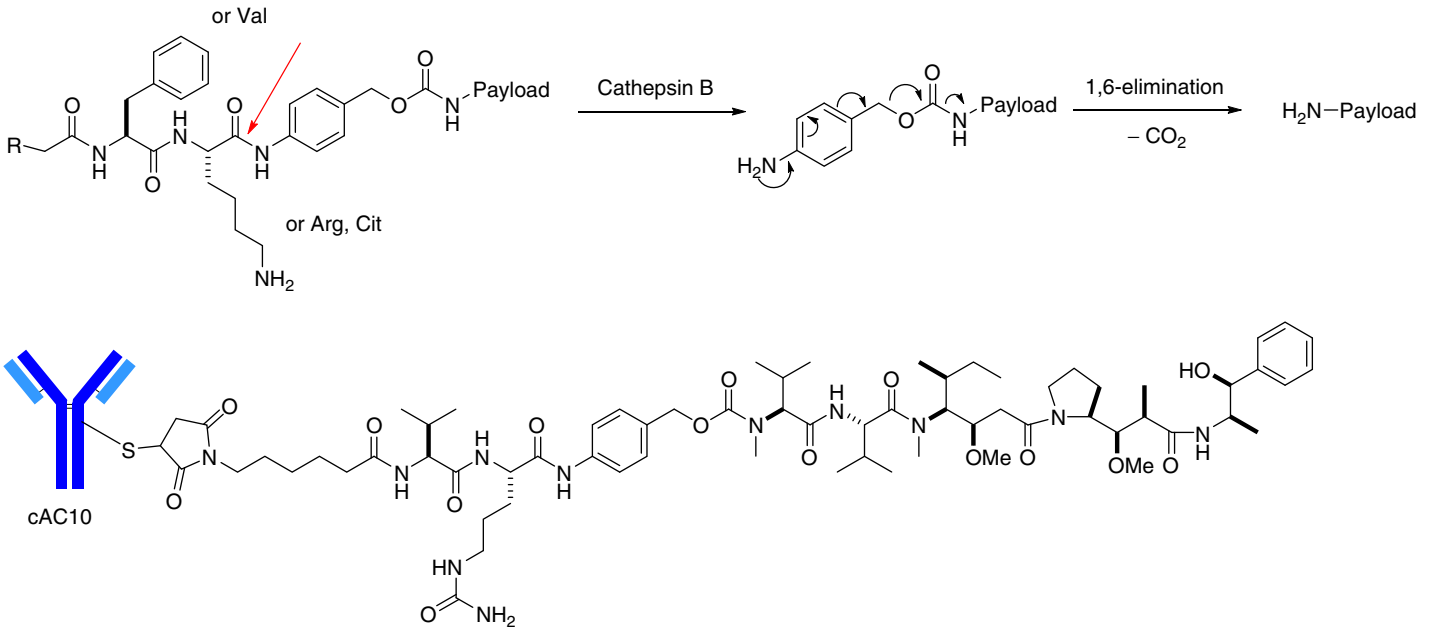
The alternative to leveraging chemical differences between the blood and lysosomal compartment is to take advantage of the numerous hydrolytic enzymes that are restricted to the lysosome due to their capacity to degrade biopolymers such as peptides and carbohydrates. These enzymes have specific recognition of peptide sequences or carbohydrate patterns that enable a well-designed ADC to undergo cleavage only in their lysosomal vicinity. This promising enzyme–labile linker platform is still being developed, and is exemplified further for proteases and glucuronidases.

9.17.4.2.1 Lysosomal proteases (cathepsin, plasmin)

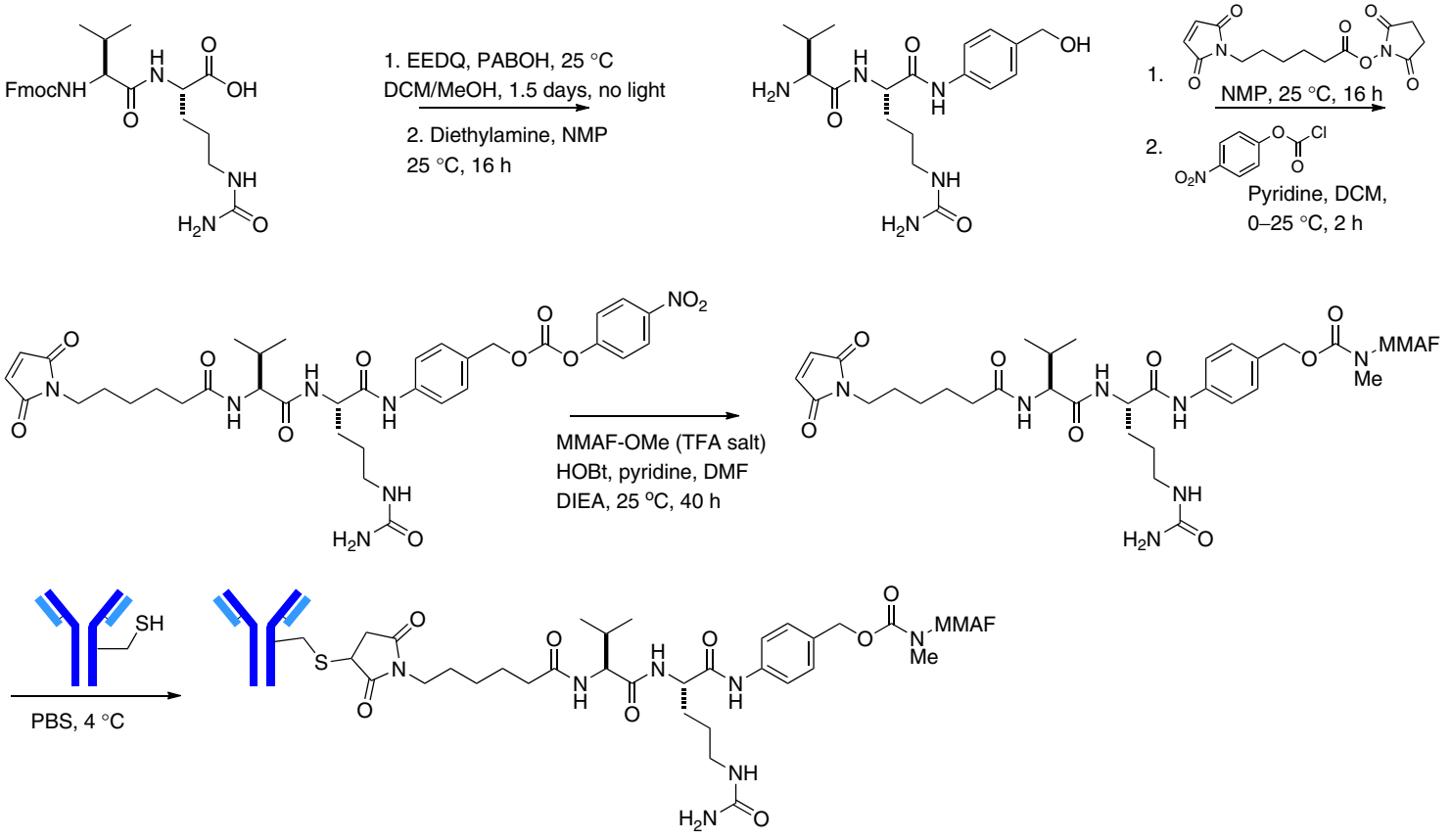
Proteases such as cathepsin B are highly active only at the acidic pH of a lysosomal environment (pH ~4) and have restricted activity in blood due to the neutral pH and presence of serum protease inhibitors. Thus, linkers that act as substrates for these enzymes may provide the ideal balance between serum stability and lysosomal degradation. The recognition peptide sequence for



Scheme 13 General assembly of an acyl hydrazone-linked ADC.



Scheme 14 Cathepsin B-sensitive linker strategy.



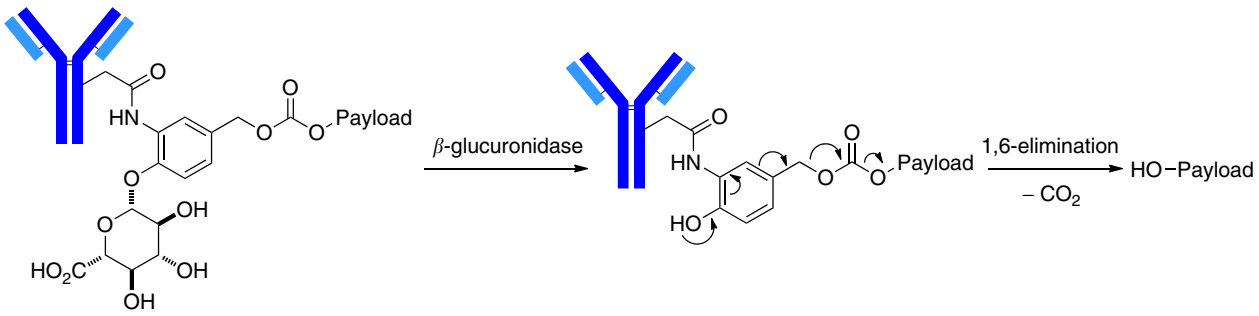
Scheme 15 Cathepsin B-sensitive linker synthesis.

the protease is broad, but for reactivity and solubility purposes, Phe(or Val) and Lys(or Arg/Cit) are favored, respectively, as they have the requisite hydrophobic and hydrophilic sequence residues.[45,46] However, these linkers must also be designed to accommodate the cathepsin B active site, and some payloads like doxorubicin have been observed to be too bulky to be accommodated.[47] Thus, a self-immolative spacer, para-aminobenzylcarbonyl (PABC)[48] is generally used to ensure enzymatic cleavage and return parent drug following degradation (Scheme 14). The enzyme cleaves specifically at the amide bond connecting the polar residue to the PABC group. This strategy is utilized for the approved ADC Adcetris®.[45,49]

The synthesis of these cathepsin B-sensitive linkers is initiated with the commercially available dipeptide followed by coupling with the self-immolative PABC group and protecting group manipulation (Scheme 15). The 6-maleimidohexanoic acid NHS ester is appended to the valine end of the dipeptide for eventual conjugation to the antibody. Payload attachment is then facilitated by use of the *p*-nitrophenyl carbonate. The final linker–payload molecule is conjugated to the antibody through partially reduced disulfides on the antibody backbone.

9.17.4.2.2 β-Glucuronidase substrates

Glucuronidase activity in a lysosome can also be leveraged as a strategy to promote linker degradation only within a target cell. β-Glucuronidase is normally expressed in lysosomes and has peak enzymatic activity at pH 4. Thus a linker strategy that relies on deglycosylation of a β-glucuronide may achieve the ideal properties for an ADC. This strategy has been applied to several payload types and utilizes a similar PABC self-immolative linker to allow return of the parental payload with no linker residue (Scheme 16).[50–52]An added advantage of this approach is the hydrophilic nature of the carbohydrate, which may provide advantages in solubility and aggregation properties of the resulting ADC.



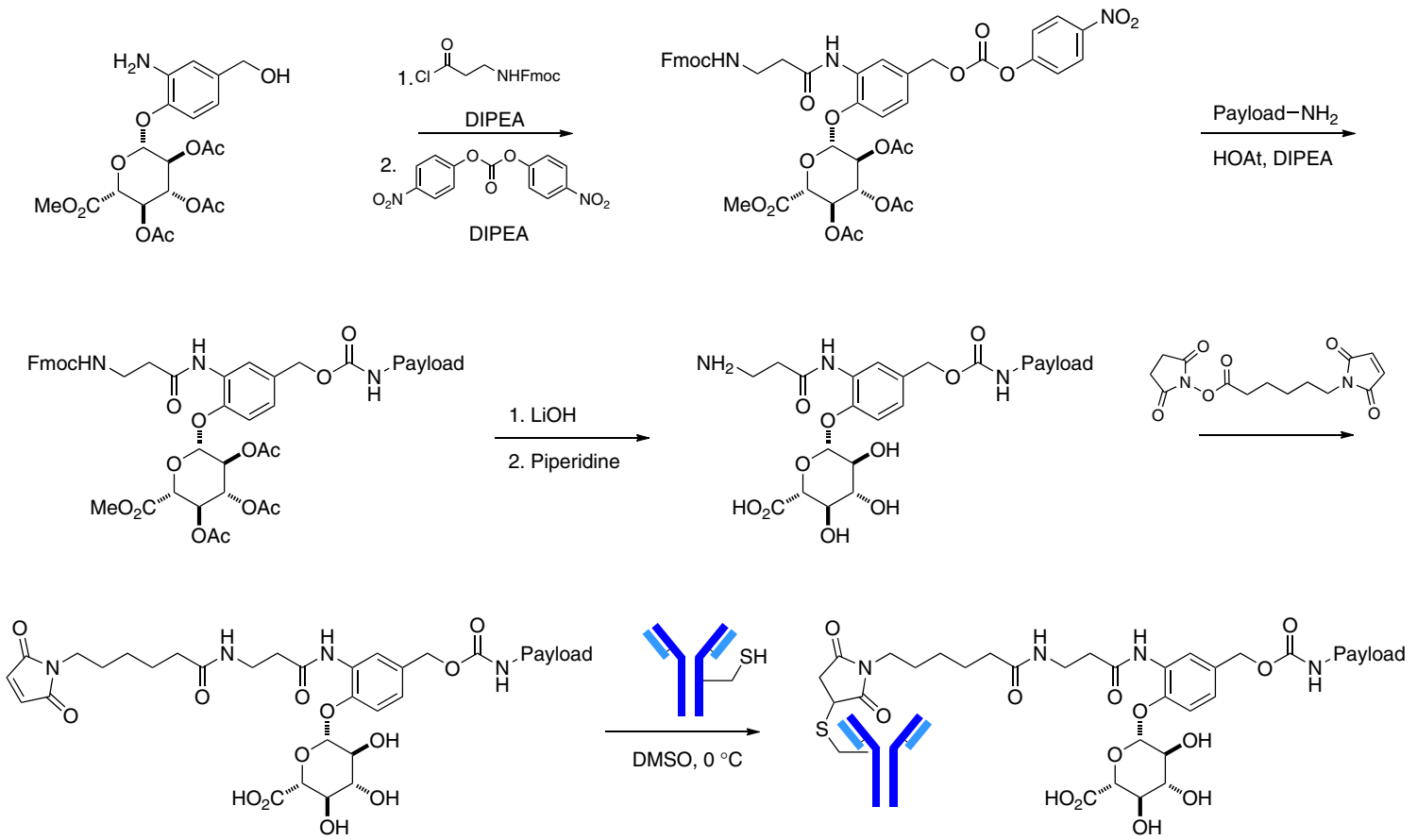
Scheme 16 β-Glucuronide linker strategy.

The synthesis of this linker requires several steps including orthogonal protecting group manipulation.[50] Antibody conjugation is typically the final step in the sequence (Scheme 17).

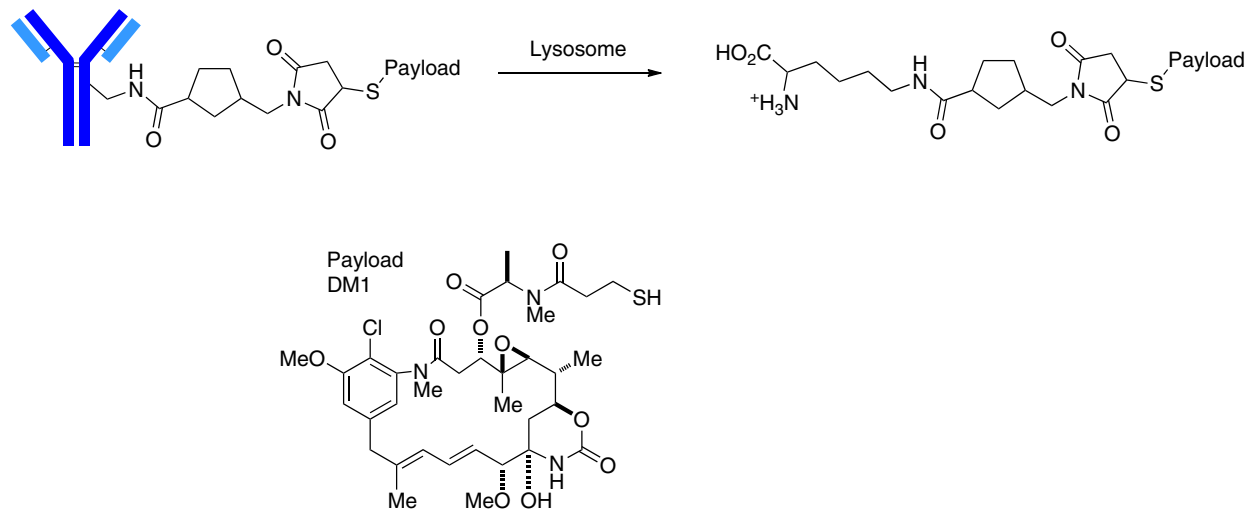
9.17.4.3 Nonlabile

An important and unexpected observation with several examples in the ADC field is that noncleavable linkers can effectively deliver payload, and may offer wider therapeutic margins for cytotoxics due to their superior stability in circulation and lack of a bystander effect.[53–55] It has been demonstrated that lysosomal catabolism of the antibody will free the linker–payload still attached to the cysteine- or lysine residue through which it was conjugated.[54,56] If the payload SAR can tolerate this residual linker and charged amino acid, this polarized payload may be retained in the cell for a longer duration, and will not easily pass into a neighboring cell (perhaps a healthy one) through passive permeability (bystander effect). This strategy may represent an optimal approach for the assembly of a cytotoxic ADC. This strategy has been employed for trastuzumab-DM1 (T-DM1) for HER2-positive metastatic breast cancer[53](Scheme 18).

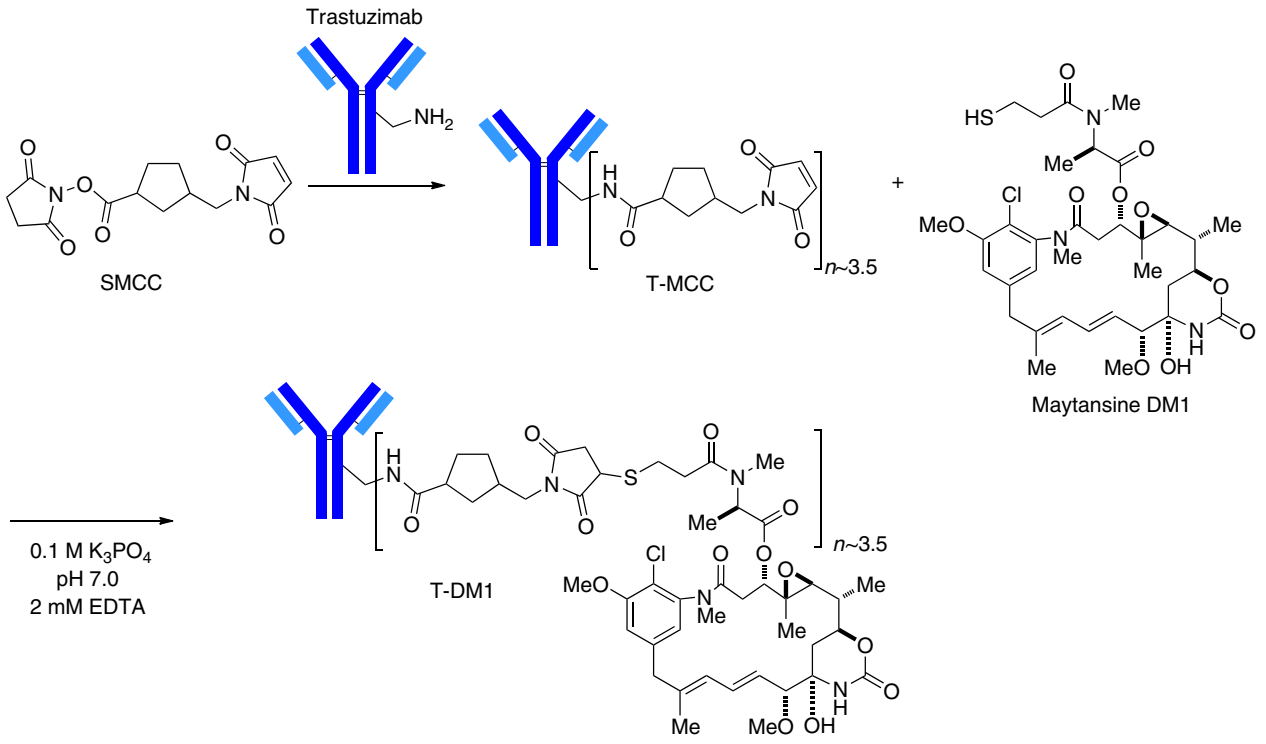
The synthesis of these linkers is straightforward. Combination of the linker with the payload, followed by standard conjugation to the antibody, produces noncleavable ADCs with little protecting group manipulation (Scheme 19).[57] Conjugation can be through lysine or Cys using the range of electrophiles described in Section 9.17.3. A potential advantage of the noncleavable linker strategy is that the efflux potential of the payload may be modulated by the properties of the residual linker (often the cysteine- or lysine linker adduct of the catabolized ADC). Payloads with polar linkers emerging from the lysosome may be slow to escape the target cell, and also slow to enter a nontarget neighboring cell through passive permeability thus prolonging the desired effect only in a target cell. Simply stated, if a charged linker remains attached to the payload – it limits the ability of the payload to kill nearby nontargeted cells.[53,58] The benefits and drawbacks of this 'bystander effect' are highly dependent on tumor biology and vasculature, and is likely a subject of empirical testing with the current knowledge.



Scheme 17 β-Glucuronide linker synthesis.



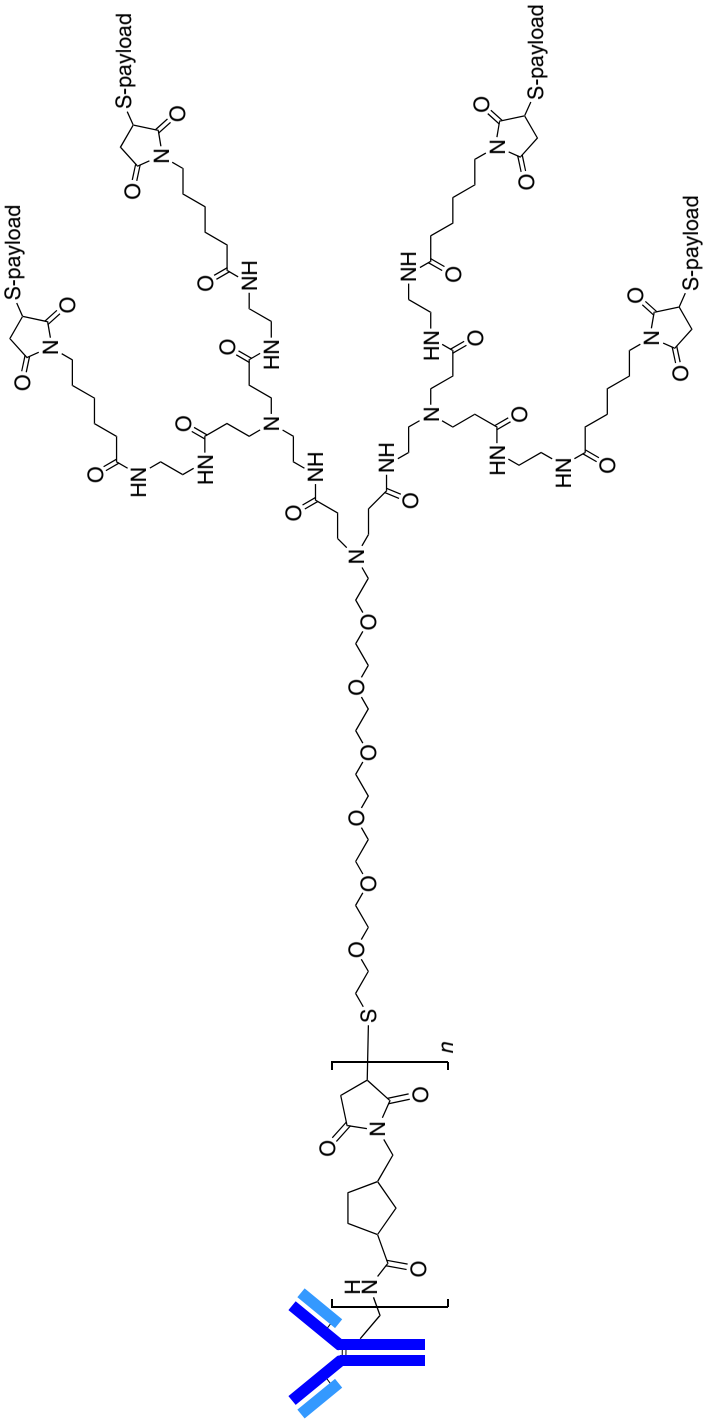
Scheme 18 Noncleavable linker strategy.



Scheme 19 Noncleavable linker synthesis.

9.17.5 Loading Chemistry

The DAR is a measurement of drug loading in the ADC field that is recognized as an important parameter with measurable impact on antibody properties and performance. Most advanced ADCs have settled on a DAR of 2 ~ 4 as the optimal balance between getting enough small molecule into the target cell and having too much drug on the antibody such that affinity, aggregation, and PK are negatively impacted.[5,30] A recent publication has data that suggest more soluble linkers may increase the useable DAR up to ~ 8.[42] Despite these advances, a key limitation of ADCs in general is that, given the molecular weight difference between an mAb (150 000) and a small molecule payload (400), only a limited amount of small molecule (< 1 mg total) can be delivered with a maximum conventional s.c. mAb dose volume. For this reason, the payloads currently in clinical development are exquisitely potent (sub-nM). This limitation can directly be addressed by identifying methods for increasing loading beyond a DAR of 8



Scheme 20 Dendrimers as a strategy to increase drug loading.

without compromising the mAb properties. The chemistry described in this section is still nascent, and a general solution has not been achieved. Such a solution may enable the ADC strategy to be applied to payloads beyond the exquisitely cytotoxic variety covered in this review.

9.17.5.1 Dendrimers

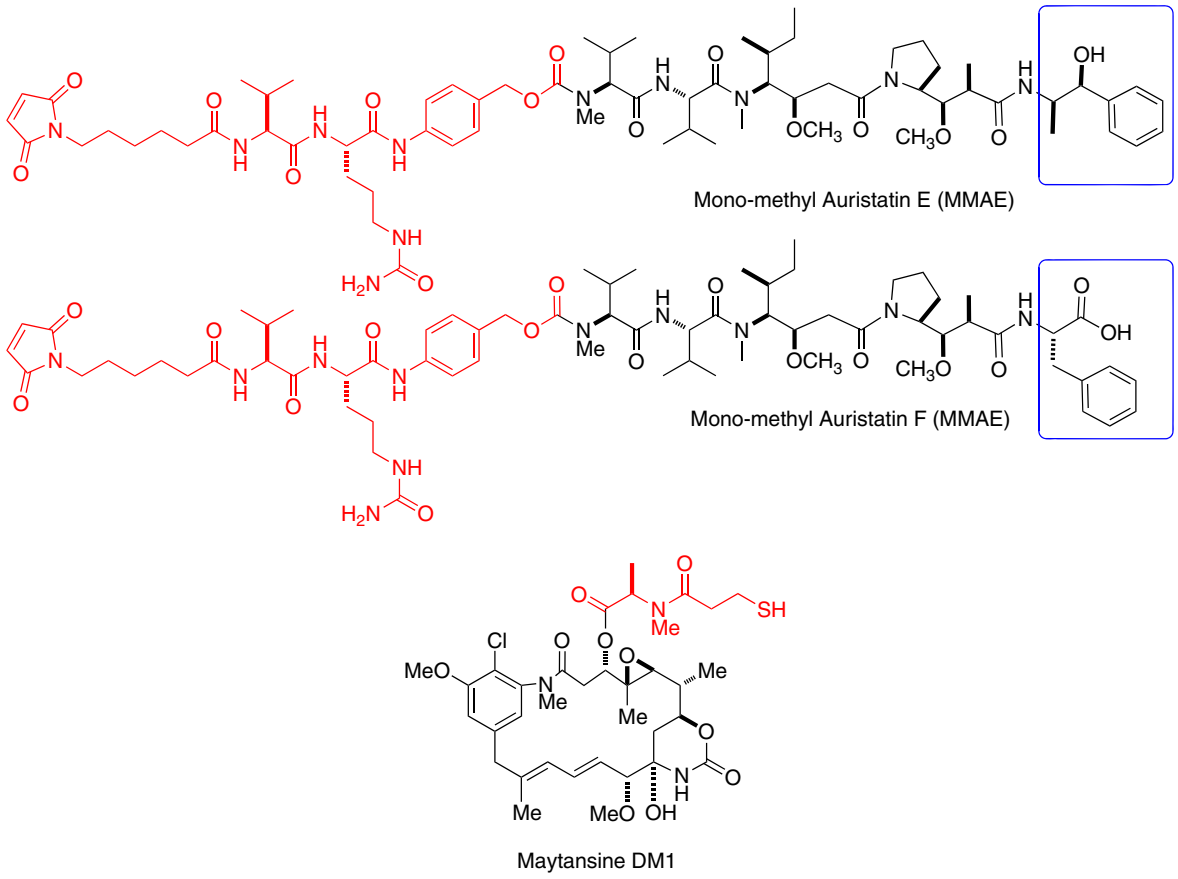
The use of dendrimers offers a potential solution to the loading problem for ADCs described in Section 9.17.5. As delivery vehicles, dendrimers offer high loading capacity for payloads with reduced polydispersity relative to polymers. In the ADC field, dendrimers like the polyamidoamine (PAMAM) system have been explored for their ability to deliver radiotherapeutic (i.e., DOTA[59]) and traditional payloads (i.e., methotrexate[60]) (**Scheme 20**). In one report, it was determined that the number and not the size of the dendrimers was the primary determinant of the ADC immunoreactivity. The authors concluded that dendrimers that could carry up to 128 chelating agents per site could be loaded up to ~1.7 derivatizations per antibody molecule and a majority of the antibody–antigen binding could still be retained.[59]

9.17.5.2 Others

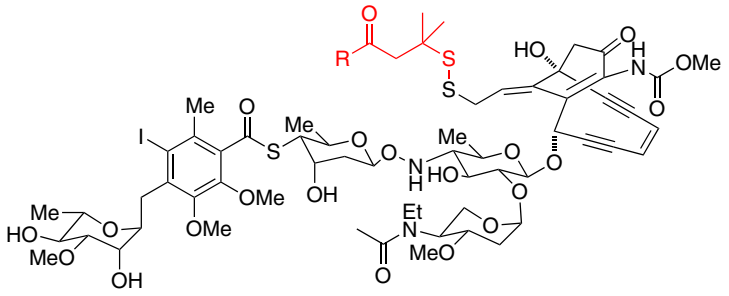
Currently, there are few other publications in the area of ADC-specific loading strategies within the scope of this review. Very recently, Mersana Therapeutics has partnered with both Adimab and Endo Pharmaceuticals to bring its Fleximer® platform (biodegradable and carbohydrate-based) to the ADC field with the promise of achieving increased drug loading but publications employing this strategy are currently unavailable.[61] Beyond the scope of this review, immunoliposomes are an alternative approach that leverage the capacity of lipid nanoparticles that can also be targeted with antibodies attached to their surface.

9.17.6 Small Molecule Chemistry

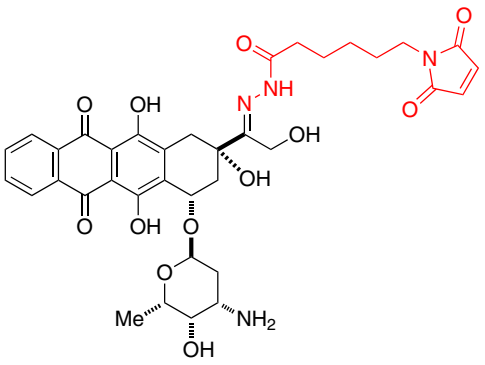
Attachment of a linker to the small molecule falls within the standard set of chemical transformations that do not require review here and are dependent on the context of the small molecule structure. However, from a delivery standpoint, one must determine



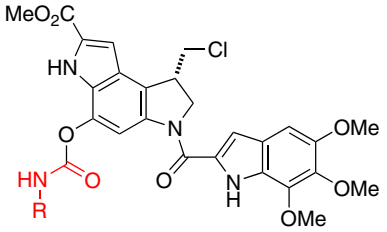
Scheme 21 Payload linkers targeting tubulin. Payloads in black, linker in red.



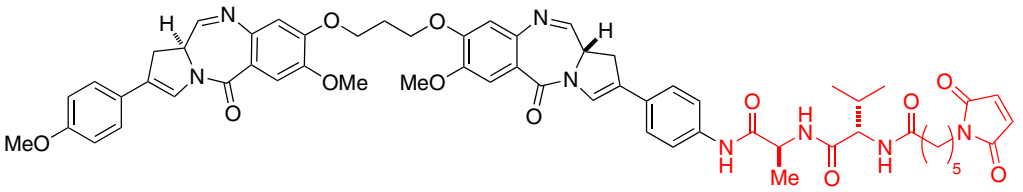
Calicheamicin



Doxorubicin



Duocarmycin



Pyrrolobenzodiazepine dimer (PDB)

Scheme 22 Payload linkers targeting DNA. Payloads in black, linker in red.

whether or not their small molecule pharmacology can tolerate the presence of a strategically located linker, or if the linker needs to 'self-immolate' in order to preserve the small molecule function. This matching process between linker properties and site of attachment on the small molecule should dictate chemistry selection. Examples provided in Section 9.17.6.1 are representative, but this process must be performed in every case.

9.17.6.1 Payloads

Antibody–drug conjugates currently in the clinic carry two classes of highly potent cytotoxic payloads: those directed at tubulin as antimitotics (Scheme 21), and those directed at DNA as damaging agents (Scheme 22). While other payloads have been surveyed in the literature, the scope of chemistry utilized to append them to an antibody is not extended beyond that described in Section 9.17.3.

9.17.6.2 Recognition of SAR Tolerability

In an ideal situation, the SAR for the payload is sufficiently understood and tolerant that placement of a linker will not adversely impact its potency. In this preferred case, as with the maytansines and auristatins, a chemist can select either cleavable (i.e., protease- or acid-sensitive) or noncleavable linkers to deliver payload after either linker degradation or antibody catabolism in the lysosome. Alternatively, some payloads like calicheamycin and duocarmycin require a very specific cleavage to promote their pharmacological mechanism of action and thus require cleavable linkers. In Schemes 21 and 22, the payloads are identified in black and a representative linker design and location are highlighted in red.

An understanding of the SAR for the payload molecule is important not only for the selection and location of the linker, but also for the modulation of other properties of the ADC such as solubility and propensity for cellular efflux following delivery. As discussed in Section 9.17.6.1, the efflux properties of the payload may determine its ability to enter neighboring cells (bystander effect) and thus chemists have introduced functional analogs that impact membrane permeability. As a premier example, MMAE and MMAF (Scheme 21) are permeable and nonpermeable, respectively due to the inclusion of a carboxylic acid moiety in MMAF (in the blue box).[49]

For the chemist entering the ADC field, a careful balance between understanding the desired pharmacology and the properties of the cytotoxic agent should be the first step in the selection of a payload.

9.17.7 Conclusions and Future for Organic Synthesis in ADCs

ADCs are an emerging therapeutic platform that has evolved into a clinically validated approach in oncology with the help of synthetic chemistry. The chemical methods that have been developed to date are only now bridging into second generation ADC designs that confer increased homogeneity, environment-dependent stability, and the potential for improved properties. Analogous to the role that chemistry plays in the development of small molecule therapeutics, chemists in this field should continue to seek new structural control over each optimizable parameters of an ADC: conjugation, linkers, payload loading, and even the antibody itself. With recent clinical success, the ADC field will continue to grow as will the need for chemists to contribute to novel and differentiated ADCs.

References

1. Sapra, P.; Hooper, A. T.; O'Donnell, C. J.; Gerber, H. P. *Expert Opin. Investig. Drugs* **2011**, *20*, 1131–1149.
2. Polson, A. G.; Ho, W. Y.; Ramakrishnan, V. *Expert Opin. Investig. Drugs* **2011**, *20*, 75–85.
3. Carter, P. J.; Senter, P. D. *Cancer* **2008**, *14*, 154–169.
4. Ducry, L.; Stump, B. *Bioconjug. Chem.* **2010**, *21*, 5–13.
5. Chari, R. V. J. *Acc. Chem. Res.* **2008**, *41*, 108–119.
6. Stephanopoulos, N.; Francis, M. B. *Nat. Chem. Biol.* **2011**, *7*, 876–884.
7. Stimmel, J. B.; Merrill, B. M.; Kuyper, L. F.; *et al. J. Biol. Chem.* **2000**, *275*, 30445–30450.
8. Junutula, J. R.; Raab, H.; Clark, S.; *et al. Nat. Biotechnol.* **2008**, *8*, 925–932.
9. Boswell, C. A.; Mundo, E. E.; Zhang, C.; *et al. Bioconjug. Chem.* **2010**, *10*, 1994–2004.
10. Shen, B. Q.; Xu, K.; Liu, L.; *et al. Nat. Biotechnol.* **2012**, *30*, 184–189.
11. Hofer, T.; Skeffington, L. R.; Chapman, C. M.; Rader, C. *Biochemistry* **2009**, *48*, 12047–12057.
12. Carrico, I. S.; Carlson, B. L.; Bertozzi, C. R. *Nat. Chem. Biol.* **2007**, *3*, 321–322.
13. Wu, P.; Shui, W.; Carlson, B. L.; *et al. Proc. Natl. Acad. Sci.* **2009**, *106*, 3000–3005.
14. Cornish, V. W.; Hahn, K. M.; Schultz, P. G. *J. Am. Chem. Soc.* **1996**, *118*, 8150–8151.
15. Wang, L.; Xie, J.; Schultz, P. G. *Annu. Rev. Biophys. Biomol. Struct.* **2006**, *35*, 225–249.
16. Wang, L.; Zhang, Z.; Brock, A.; Schultz, P. G. *Proc. Natl. Acad. Sci. USA* **2003**, *100*, 56–61.
17. Miles, S.; Tyagi, S.; Banterle, N.; *et al. J. Am. Chem. Soc.* **2012**, *134*, 5187–5195.
18. Lang, K.; Davis, L.; Torres-Kolbus, J.; *et al. Nat. Chem.* **2012**, *4*, 298–304.
19. Kazane, S. A.; Sok, D.; Cho, E. H.; *et al. Proc. Natl. Acad. Sci. USA* **2012**, *109*, 3731–3736.
20. Axup, J. Y.; Bajjuri, K. M.; Ritland, M.; *et al. Proc. Natl. Acad. Sci. USA* **2012**, *109*, 16101–16106.

21. Chalker, J. M.; Bernardes, G. J. L.; Lin, Y. A.; Davis, B. G. *Chem. Asian. J.* **2009**, *4*, 630–640.
22. Sun, M. M. C.; Beam, K. S.; Cerveny, C. G.; *et al. Bioconjug. Chem.* **2005**, *16*, 1282–1290.
23. Nielsen, M. L.; Vermeulen, M.; Bonaldi, T.; *et al. Nat. Methods* **2008**, *5*, 459–460.
24. Bernardes, G. J. L.; Casi, G.; Trussel, S.; *et al. Angew. Chem. Int. Ed.* **2012**, *51*, 941–944.
25. Doronina, S. O.; Toki, B. E.; Torgov, M. Y.; *et al. Nat. Biotechnol.* **2003**, *21*, 778–784.
26. Wellman, A. A.; Meares, C. F. *Nucleic Acids Res.* **1990**, *18*, 5281.
27. Wang, L.; Amphlett, G.; Blattler, W. A.; Lambert, J. M.; Zhang, W. *Protein Sci.* **2005**, *14*, 2436–2446.
28. Chih, H. W.; Gikanga, B.; Yang, Y.; Zhang, B. *J. Pharm. Sci.* **2011**, *100*, 2518–2525.
29. Mandler, R.; Kobayashi, H.; Davis, M. Y.; Waldmann, T. A.; Brechbiel, M. W. *Bioconjug. Chem.* **2002**, *13*, 786–791.
30. Hamblett, K. J.; Senter, P. D.; Chace, D. F.; *et al. Clin. Cancer Res.* **2004**, *10*, 7063–7070.
31. O'Shannessy, D. J.; Quarles, R. H. *J. Immunol. Methods* **1987**, *99*, 153–161.
32. Laguzza, B. C.; Nichols, C. L.; Briggs, S. L.; *et al. J. Med. Chem.* **1989**, *32*, 548–555.
33. Hage, D. S.; Wolfe, C. A. C.; Oates, M. R. *Bioconjug. Chem.* **1997**, *8*, 914–920.
34. Scheck, R. A.; Dedeo, A. T.; lavorone, M. T.; Francis, M. B. *J. Am. Chem. Soc.* **2008**, *130*, 11762–11770.
35. Jeger, S.; Zimmerman, K.; Blanc, A.; *et al. Angew. Chem. Int. Ed.* **2010**, *49*, 9995–9997.
36. Casi, G.; Huguenin-Dezot, N.; Zuberbuhler, K.; Scheuermann, J.; Neri, D. *J. Am. Chem. Soc.* **2012**, *134*, 5887–5892.
37. Agard, N. J.; Baskin, J. M.; Prescher, J. A.; Bertozzi, C. R. *ACS Chem. Biol.* **2006**, *1*, 644–648.
38. Kaya, E.; Vrabel, M.; Deiml, C.; *et al. Angew. Chem. Int. Ed.* **2012**, *51*, 4466–4469.
39. Wang, Y. S.; Fang, X.; Wallace, A. L.; Wu, B.; Liu, W. R. *J. Am. Chem. Soc.* **2012**, *134*, 2950–2953.
40. Rabuka, D.; Rush, J. S.; deHart, G. W.; Wu, P.; Bertozzi, C. R. *Nat. Protoc.* **2012**, *7*, 1052–1067.
41. Kellogg, B. A.; Garret, L.; Kovtun, Y.; *et al. Bioconjug. Chem.* **2012**, *22*, 717–727.
42. Zhao, R. Y.; Wilhelm, S. D.; Audette, C.; *et al. J. Med. Chem.* **2011**, *54*, 3606–3623.
43. Hamann, P. R.; Hinman, L. M.; Beyer, C. F.; *et al. Bioconjug. Chem.* **2002**, *13*, 40–46.
44. Hamann, P. R.; Hinman, L. M.; Hollander, I.; *et al. Bioconjug. Chem.* **2002**, *13*, 47–58.
45. Dubowchik, G. M.; Firestone, R. A.; Padilla, L.; *et al. Bioconjug. Chem.* **2002**, *13*, 855–869.
46. Cezari, M. H. S.; Puzer, L.; Juliano, M. A.; Carmona, A. K.; Juliano, L. *Biochem. J.* **2002**, *368*, 365–369.
47. Dubowchik, G. M.; Firestone, R. A. *Bioorg. Med. Chem. Lett.* **1998**, *8*, 3341–3346.
48. Carl, P. L.; Chakravarty, P. K.; Katzenellenbogen, J. A. *J. Med. Chem.* **1981**, *24*, 479–480.
49. Doronina, S. O.; Bovee, T. D.; Meyer, D. W.; *et al. Bioconjug. Chem.* **2008**, *19*, 1960–1963.
50. de Graff, M.; Boven, E.; Scheeren, H. W.; Haisma, H. J.; Pinedo, H. M. *Curr. Pharm. Des.* **2002**, *8*, 1391–1403.
51. Jeffrey, S. C.; Andreyka, J. B.; Bernhardt, S. X.; *et al. Bioconjug. Chem* **2006**, *17*, 831–840.
52. Jeffrey, S. C.; De Brabander, J.; Miyamoto, J.; Senter, P. D. *J. Med. Chem. Lett.* **2010**, *1*, 277–280.
53. Erickson, H. K.; Park, P. U.; Widdison, W. C.; *et al. Cancer Res.* **2006**, *66*, 4426–4433.
54. Phillips, G. L.; Li, G.; Dugger, D. L.; *et al. Cancer Res.* **2008**, *68*, 9280–9290.
55. Doronina, S. O.; Mendelsohn, B. A.; Bovee, T. D.; *et al. Bioconjug. Chem.* **2006**, *17*, 114–124.
56. Erickson, H. K.; Widdison, W. C.; Mayo, M. F.; *et al. Bioconjug. Chem.* **2010**, *21*, 84–92.
57. Wakankar, A. A.; Feeney, M. B.; Rivera, J.; *et al. Bioconjug. Chem.* **2010**, *21*, 1588–1595.
58. Kovtun, Y. V.; Audette, C. A.; Ye, Y.; *et al. Cancer Res.* **2006**, *66*, 3214–3221.
59. Wangler, C.; Moldenhauer, G.; Eisenhut, M.; Haberkorn, U.; Mier, W. *Bioconjug. Chem.* **2008**, *19*, 813–820.
60. Wu, G.; Barth, R. F.; Yang, W.; *et al. Mol. Cancer Ther.* **2006**, *5*, 52–57.
61. MacDougall Biomedical Communications. Press release from Mersana on ADCs, **2012**. Available at: http://www.mersana.com/news-events/news-events-pr-2012-03-07-php.php (accessed on 09 August 2013).

9.18 Post-Synthetic Chemical Functionalization of Oligonucleotides

Yu Yuan, University of Central Florida, Orlando, FL, USA
Weimin Wang, Merck Research Laboratories, West Point, PA, USA

© 2014 Elsevier Ltd. All rights reserved.

9.18.1	**Introduction**	463
9.18.2	**Strategies for Oligonucleotide Postsynthetic Modification**	465
9.18.2.1	Conjugation Through Thioether Linkage	465
9.18.2.1.1	Thioether formation by Michael reaction	465
9.18.2.1.2	Thioether formation by nucleophilic substitution reaction	468
9.18.2.2	Conjugation Through Disulfide Linkage	468
9.18.2.3	Conjugation Through Amide Linkage	471
9.18.2.4	Conjugation by Cycloaddition Reaction	473
9.18.2.4.1	Conjugation by [3 + 2] cycloaddition	473
9.18.2.4.2	Conjugation by [4 + 2] cycloaddition	473
9.18.2.4.3	Conjugation by [4 + 1] cycloaddition	478
9.18.2.5	Conjugation Through Imine, Hydrazone, and Oxime Linkages	478
9.18.2.6	Conjugation Through Other Linkages	481
9.18.3	**Conclusion and Future Perspective**	484
References		492

Glossary

Conjugation A process that covalently links two or more chemical entities together. In the case of oligonucleotide conjugation, it refers to the covalent modification of an oligonucleotide.

Copper(I)-catalyzed azide–alkyne cycloaddition (CuAAC) A 1,3-dipolar cycloaddition reaction between azide and alkyne catalyzed by Cu(I) species to generate 1,2,3-triazole. The cycloaddition proceeds with remarkable efficiency and selectivity, and it is often referred as the 'click chemistry.'

Green fluorescent protein (GFP) A protein that is originally isolated from jellyfish *Aequorea victoria*. GFP emits green fluorescence when it is exposed to light in the blue to ultraviolet range.

Intein A protein segment that can excise itself from the protein backbone and mediate the peptide bond formation between the two flanking fragments.

Native chemical ligation (NCL) A native amide bond-forming reaction between the C-terminal thioester of one peptide and the N-terminal Cys residue of a second peptide.

Oligonucleotide (ON) A short nucleic acid polymer, typically with less than 50 nucleotide residues.

Positron emission tomography (PET) A 3D nuclear imaging technique that detects the gamma rays produced by the annihilation of electron and positron.

Transferase An enzyme that transports a specific functional group from one molecule to another. Transferase is classified as EC 2 in the enzyme commission number system.

9.18.1 Introduction

Synthetic oligonucleotides (ONs) have been extensively investigated in recent years as a class of promising compounds for therapeutic and diagnostic applications.[1–5] As shown in **Figure 1(a)**, ONs are linked through phosphodiester bonds of 5′ and 3′ hydroxyls on the adjacent pentose sugars. They are composed of either ribonucleotides (A, G, C, and U) or deoxyribonucleotides (dA, dG, dC, and dT). To overcome the intrinsic poor stability and unfavorable pharmacokinetics, many of these ONs are chemically modified. Chemical modifications have been introduced to major components of ONs, including phosphate backbone, pentose sugar, and nucleobase.[6–8] Several typical modifications are shown in **Figure 1(b)**. Many phosphate variants such as phosphorothioate,[9–11] boranophosphate,[12–14] phosphoramidate,[15] methylphosphate, and phosphates transiently protected by *S*-acyl-2-mercaptoethyl groups[16,17] are used to increase the nuclease resistance. The 2′-position of pentose sugars is another common place for modification,[18] for example, 2′-fluoro,[19] 2′-*O*-methyl,[20] and locked nucleic acid (LNA)[21–25] are popular substitution groups. These modifications not only increase the nuclease resistance but also increase the binding affinity to the complementary target.[26] More dramatic but rather unconventional modifications change the ON backbone structures.

The backbone modifications include phosphorodiamidate morpholino ONs[27–29] and peptide nucleic acids (PNAs).[30,31] These modifications impart better stability, although maintaining the high affinity for their targets.[32] The neutral backbone also gives opportunity to tune the pharmacokinetics of ONs. All of the above-mentioned modifications are achieved through stepwise solid-phase synthesis. Although the solid-support approach can provide convenient removal of more reagents, and may resolve

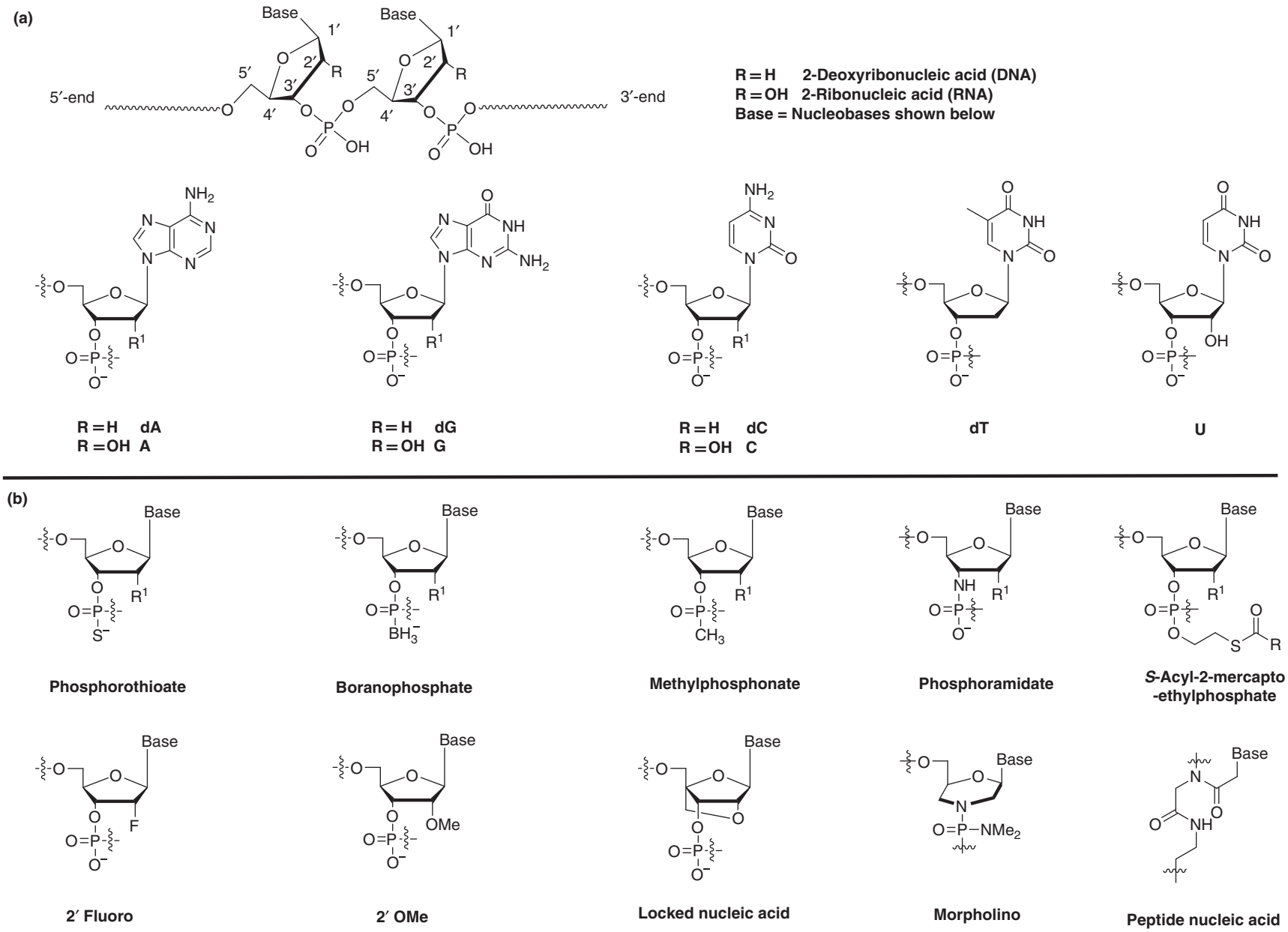


Figure 1 (a) Structures of natural nucleic acids and nucleotide residues; (b) structures of selected chemically modified nucleotide residues.

incompatible solubility problem between the canonical ONs and the modifiers, it requires customized synthesis for each individual building block. In addition, the scope of the modifications may be limited by the restrictions of solid phase synthesis chemistry, for example, the orthogonality of the protective groups as well as the harsh final deprotective conditions.

A complementary strategy for chemical modification of ONs, to be detailed in this chapter, is the postsynthetic modification (Figure 2).[33] In this approach, the ON and the modifier are prepared separately with functionalized linkages (X and Y), and the final conjugation is performed in a buffer solution, such as 4-(2-hydroxyethyl)-1-piperazineethanesulfonic acid buffer (HEPES) or phosphate buffered saline (PBS). Given the vast repertoire of bio conjugation chemistry, a variety of modifiers, ranging from small molecules such as lipids, peptides, fluorescent dyes, and small targeting ligands to macromolecules, such as polymers, saccharides, proteins, and monoclonal antibodies,[33] have been incorporated into ONs to achieve better therapeutic properties. Therefore, the postsynthetic approach not only greatly broadens the chemical space of ON modifications, but also endows the ON conjugates with novel physical properties. This protocol offers potential solution to the challenges in ON therapy such as chemical stability, plasma pharmacokinetics, biodistribution, tissue targeting, cellular uptake, endosomal escape, and target engagement. ON postsynthetic modification is also advantageous from a medicinal chemistry point of view, because the late-stage modification is preferred for efficient and systematic structure–activity relationship studies.

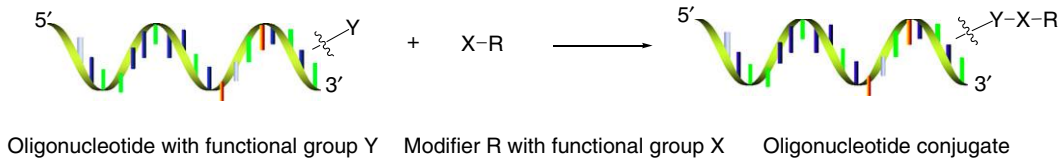


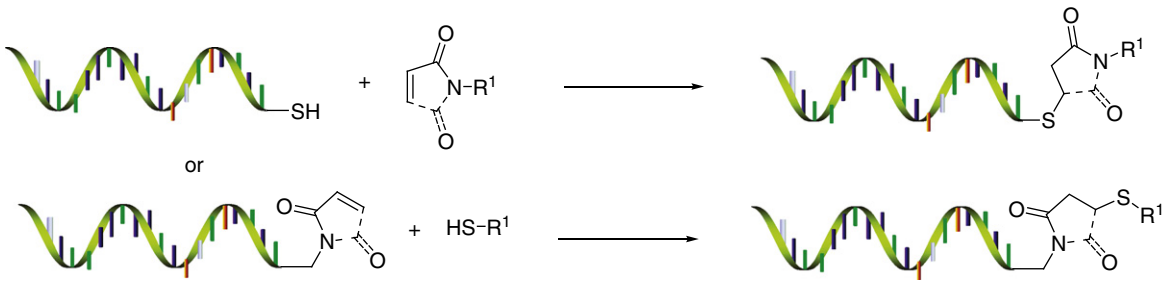
Figure 2 Generic scheme of postsynthetic functionalization of oligonucleotide.

9.18.2 Strategies for Oligonucleotide Postsynthetic Modification

In this section, we will discuss strategies for ON postsynthetic modifications in solution phase. Even though the 5′ and 3′ termini are the most common positions for ON conjugation, the reported precedents have extended the conjugation sites to 2′ positions of ribose sugars, various nucleobases and phosphate backbones. Because significant amount of work has been presented in the literature, we will only focus on representative examples which highlight the scope and the application within each reaction category. Several other reviews on the topics addressed herein have been published in the past, and detailed examples can be found in these accounts.[33–40]

9.18.2.1 Conjugation Through Thioether Linkage

A thioether linkage can be prepared by conjugate addition or by nucleophilic substitution reactions. It is a relatively stable linkage, even though thioether can be converted to sulfoxide or sulfone under oxidative conditions. The thiol group is more nucleophilic than amino and hydroxyl groups and this property is frequently used to differentiate sulfur atom from other nucleophilic elements (Scheme 1).

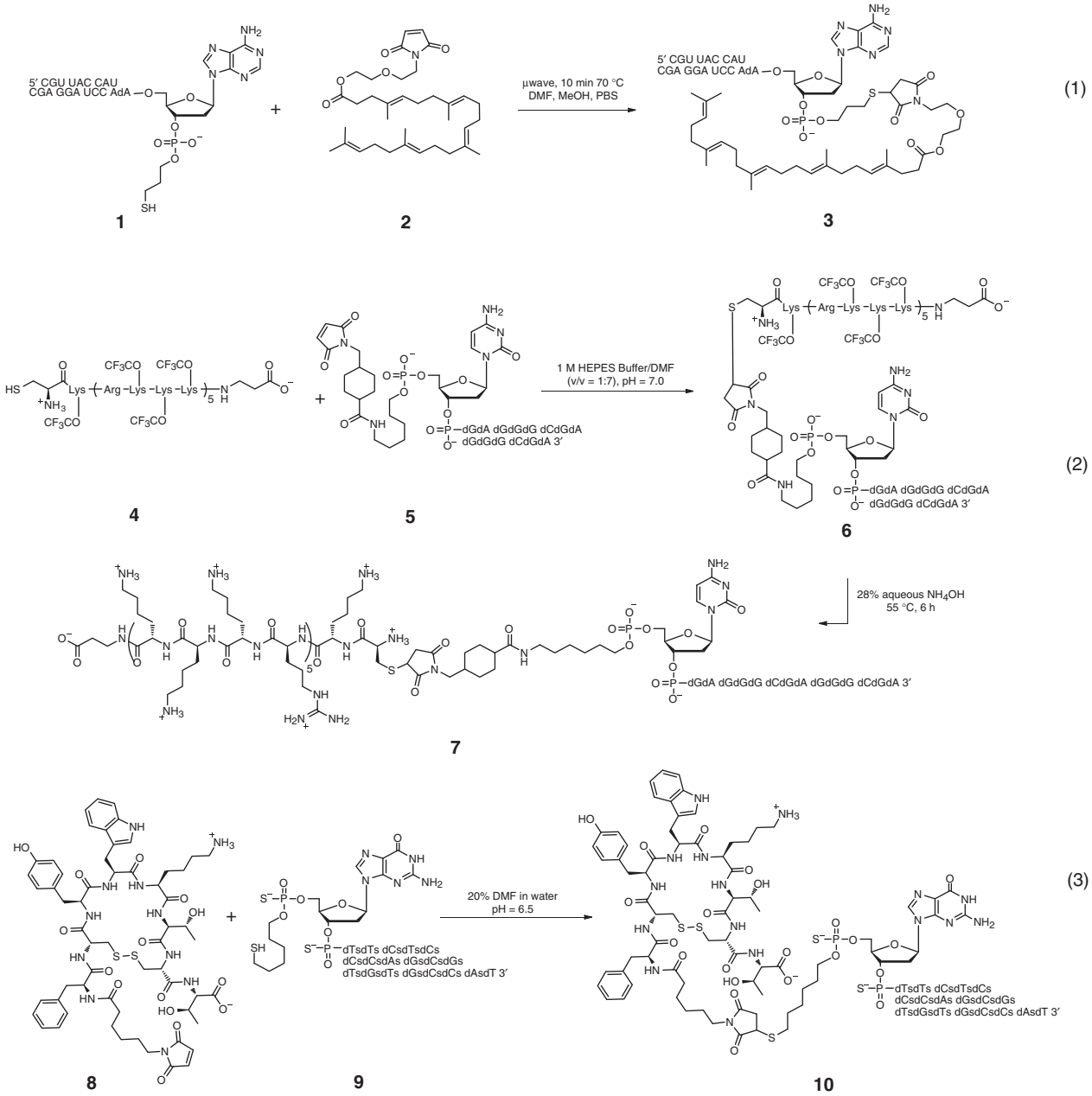


Scheme 1 Thioether formation by Michael reaction.

9.18.2.1.1 Thioether formation by Michael reaction

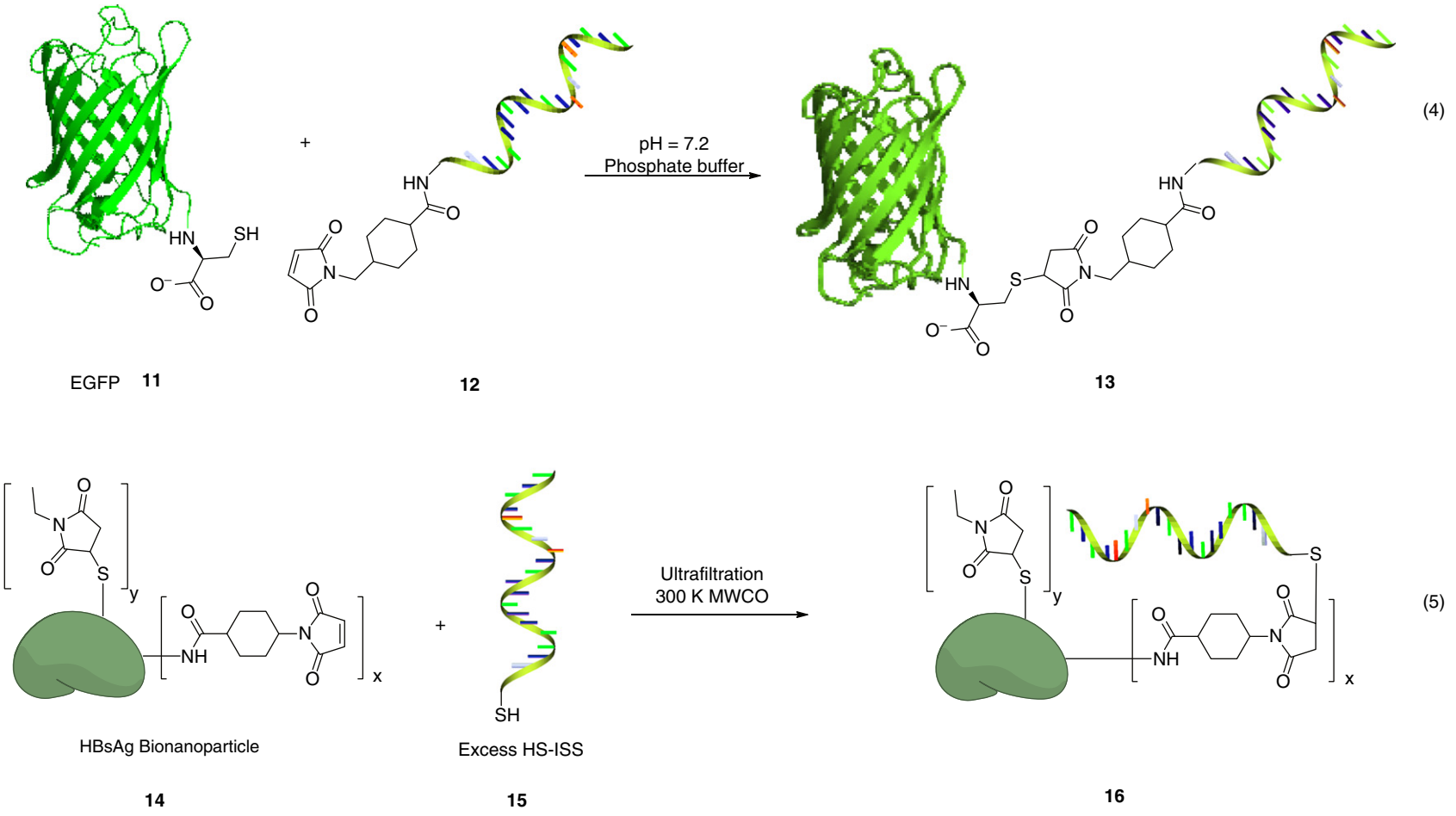
The Michael reaction is one of the most widely used strategies for ON conjugation. Small molecules, peptides, and proteins all have been attached to ONs by this protocol. The superior nucleophilicity of the thiol group under neutral or slightly acidic conditions provides excellent chemoselectivity for ON conjugation. Depending on the ease of installation and chemical

compatibility, the ON can be equipped with either a Michael donor or a Michael acceptor, as highlighted in the following text (Scheme 2).



Scheme 2 ON conjugation by thiol addition to maleimide.

Massaad-Massade and Couvreur demonstrated that siRNA sense strand **1** could be efficiently conjugated to a squalene derivative **2** by maleimide–sulfhydryl chemistry to afford a lipid siRNA conjugate **3** (equation 1).[41] On hybridization with the antisense strand, the siRNA–lipid conjugate self-organized in water as nanoparticles. Peptide–ON conjugates can be prepared by thioether formation as well. The anionic nature of ON poses significant synthetic challenges for the conjugation involving cationic peptides due to aggregation caused by the strong charge–charge interaction. To overcome the unfavorable effect, Zuber and coworkers used trifluoroacetamide protected peptides for the initial conjugation, followed by removal of the masking group to give the desired conjugates (equation 2).[42] The protected cationic peptide **4** was conjugated to a 15-mer deoxyribonucleic acid (DNA) **5** and the resulting product **6** was treated with aqueous ammonia to liberate conjugate **7**. To further highlight the elegant chemoselectivity, an example of conjugation between a cyclic peptide with disulfide bond and maleimide is shown in equation 3.



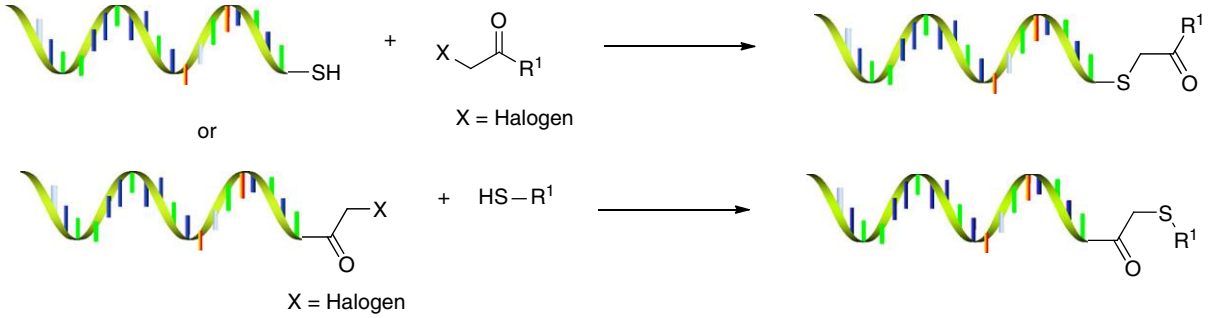
Scheme 3 ON–protein conjugate prepared by Michael reaction.

Somatostatin analog Tyr^3-octreotate–maleimide **8** was successfully attached to all-phosphorothioate antisense ON **9** via 5′ thiol group. Conjugate **10** retained nanomolar affinity toward somatostatin receptors.[43]

In addition to small molecules and peptides, proteins have been attached to ONs. Depending on their tertiary structures, proteins can conjugate to single or multiple copies of ONs. Niemeyer and coworkers ligated a single copy of ON to six different recombinant fluorescent proteins including the enhanced green fluorescent protein (EGFP) **11**. Such selectivity was attributed to the greater accessibility of the C-terminal Cys residue (equation 4).[44] In contrast, the development of a potent hepatitis B virus (HBV) vaccine requires conjugation of multiple copies of an immunostimulatory sequence (ISS) to HBV surface antigens. Polyvalent conjugate **16** was prepared by thioether formation between maleimide **14** and multicopies of thiol-modified C-phosphate-G ON **15** (equation 5)[45] (Scheme 3).

9.18.2.1.2 Thioether formation by nucleophilic substitution reaction

Thioether formation by nucleophilic substitution is also broadly used for ON postsynthetic modification. Although bromo- or iodoacetamides are popular electrophiles, other functional groups bearing reasonable leaving groups have been used in conjugation reactions. To improve the chemoselectivity, the S_N2 substitution reaction may be conducted in slightly acidic conditions to mitigate the competition from the free amino groups in the reaction mixture (Scheme 4).



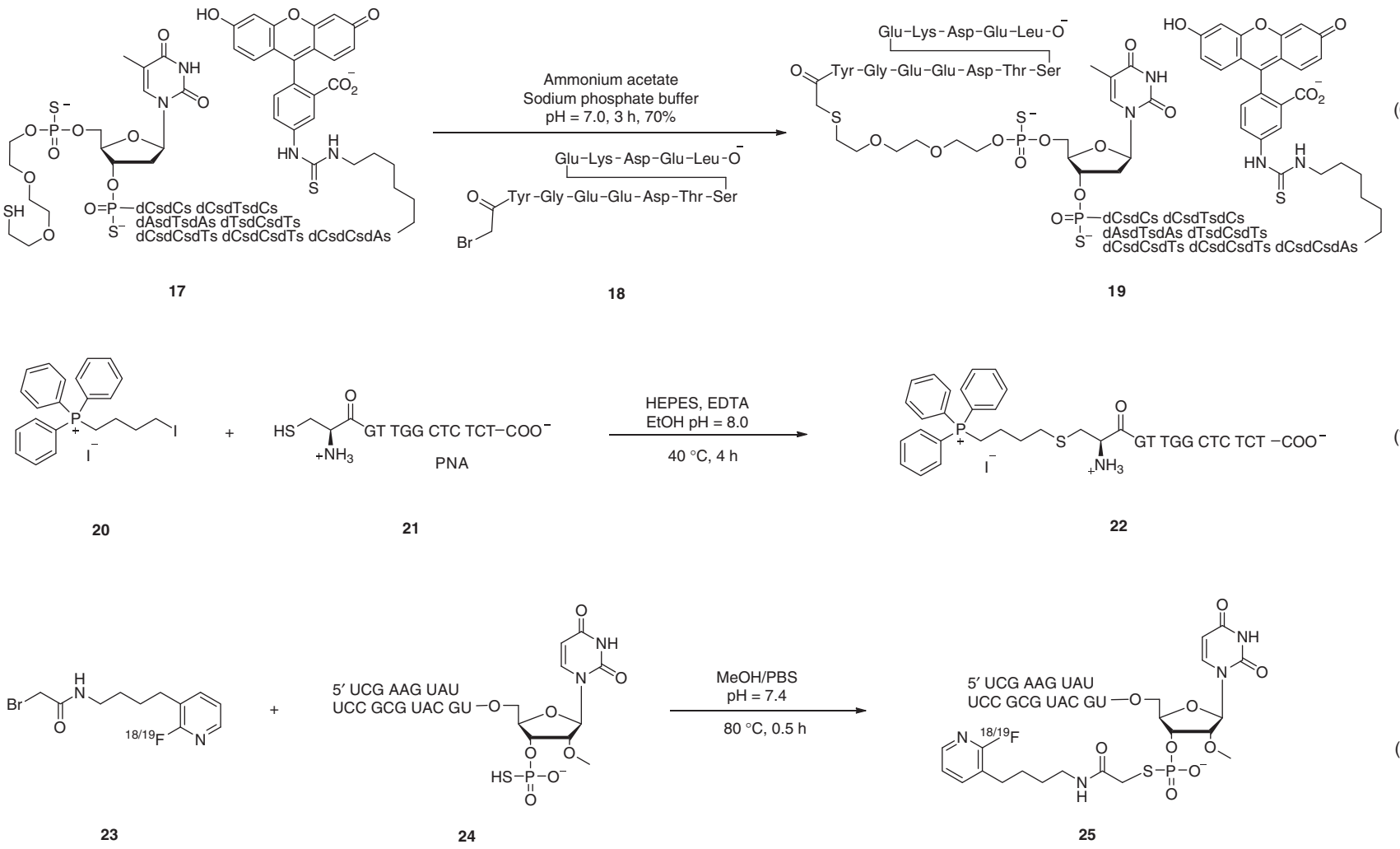
Scheme 4 Thioether formation by nucleophilic substitution reaction.

Examples of thioether formation at terminal and internal positions are shown in Schemes 5 and 6 respectively. As shown in equation 6, the free thiol group at terminal position generally exhibits better reactivity toward electrophiles than that of internal phosphorothioates. In this case, signal peptide **18** bearing a KDEL sequence with pendant N-terminal bromoacetamide was selectively conjugated to the 5′ position of ON **17** leaving the internal phosphorothioates intact (equation 6).[46] Similarly, in equation 7, a Cys thiol group at the terminal of PNA **21** was alkylated by iodide **20**, which was tethered to a lipophilic phosphonium cation.[47] Phosphorothioates are not always innocent in ON conjugation, as both terminal and internal phosphorothioates have been employed for thioether formation, with the terminal phosphorothioate displaying greater nucleophilicity. For instance (equation 8), positron emission tomography (PET) probe **23** was attached to the 3′ position of antisense strand **24** to study the biodistribution of siRNA *in vivo*.[48,49] Slightly elevated temperature was applied to the fluorine-18 conjugation reaction, which provided practical kinetics to synthesize the short-life ^{18}F conjugate.

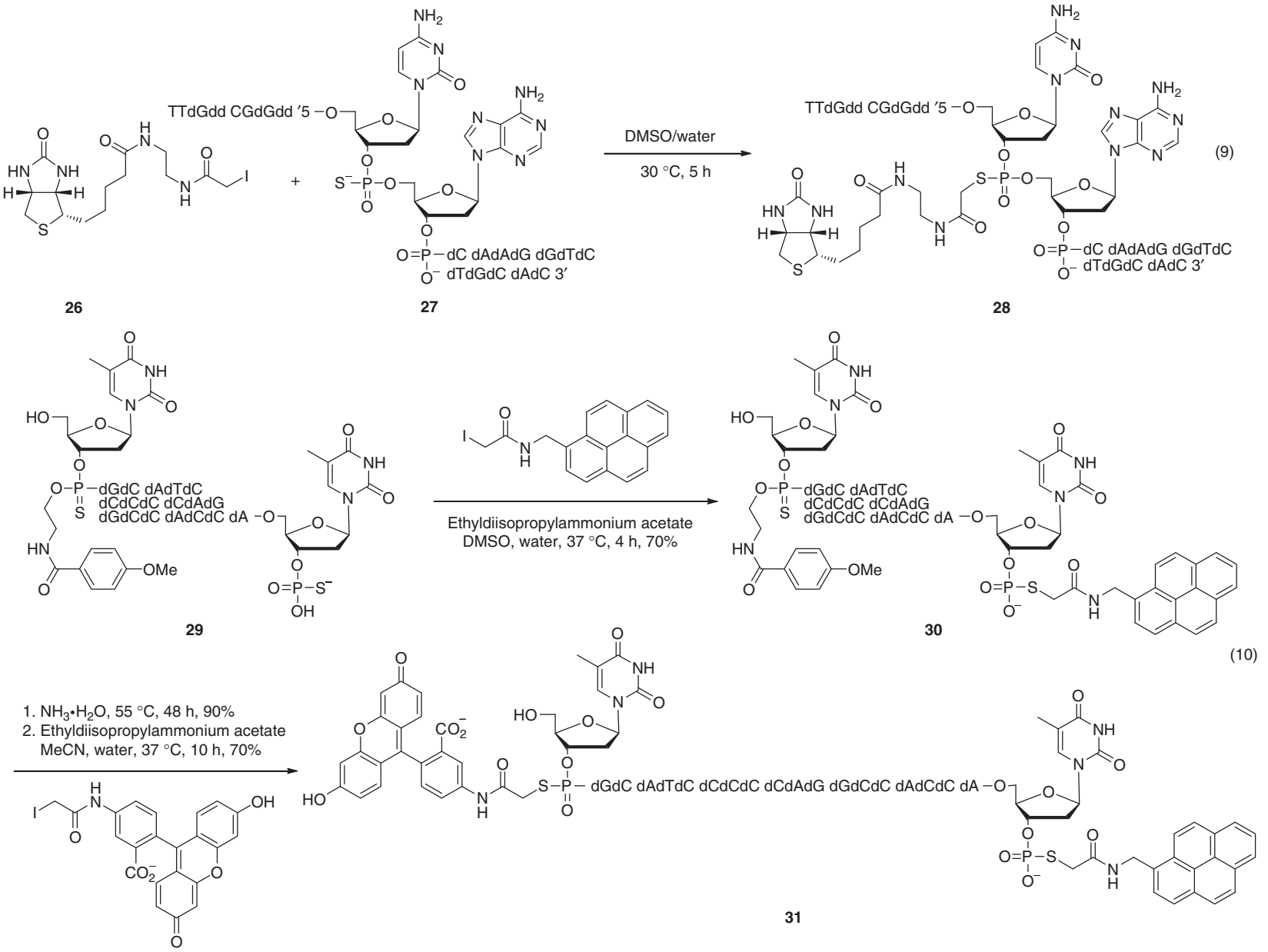
As illustrated in equation 9, when the more reactive iodoacetamide **26** was employed as an electrophile, the internal phosphorothioate in ON **27** could be modified by a biotin derivative and the resulting conjugate was used to control the alignment of multiple proteins with nanometer resolution.[11] Scientists from Isis Pharmaceuticals placed a novel protective group on the phosphorothioate during the solid phase synthesis, which enabled double labeling of ON **29** (equation 10).[50] The 3′ phosphorothioate was first labeled with a pyrene reporter and a second dye reporter was then introduced to ON **30** after the internal phosphorothioate was released by aminolysis.

9.18.2.2 Conjugation Through Disulfide Linkage

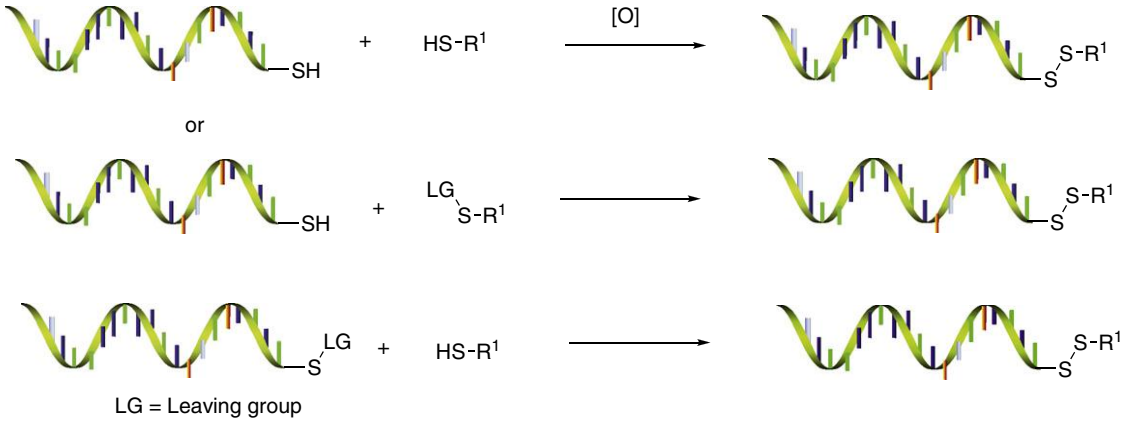
ON conjugation through a disulfide linkage has been applied to a diverse range of thiol-containing substrates. The cleavable nature of disulfide bond under a reductive environment provides a unique advantage for each component to exert its own function once the conjugate reaches the target location. This is particularly important for ON-based therapeutics; although a peptide is used to facilitate the delivery of siRNA to the cytosol, the free siRNA (rather than the peptide conjugate) is still the preferred loading substrate for the RNA-induced silencing complex (RISC). A disulfide-linked siRNA–peptide conjugate can be reduced in the cytosol by glutathione and the active siRNA is released for target engagement. The general methods are summarized in Scheme 7 for disulfide bond formation. Two free thiols are joined together by oxidation or one free thiol reacts with a preactivated sulfur derivative. The most common preactivation method for a thiol group is the installation of a pyridylsulfenyl or 3-nitropyridylsulfenyl disulfide bond. The activation step can be carried out separately or in the same spot as the conjugation reaction, thus offering greater flexibility and selectivity when compared with the direct oxidation method (Scheme 8).



Scheme 5 Thioether formation by nucleophilic substitution at terminal position.



Scheme 6 Thioether formation by nucleophilic substitution at internal position.



Scheme 7 ON conjugation through disulfide linkage.

As shown in equation 11, peptide **32** with a C-terminal cysteamide and ON **33** with a 5′ free thiol were coupled under oxidative conditions.[51] This type of conjugation is not frequently used, as the homodimer byproduct is unavoidable and the peptide or protein may not be stable toward oxidation. On the contrary, preactivation strategy has much broader application and better selectivity. Peptides with a Cys residue at either C- or N-terminus can be treated with pyridyl disulfide to generate the electrophile (e.g., **35**) and the subsequent reaction with thiol-containing ON will furnish a peptide–ON conjugate (equation 12).[52] Alternatively, the ON can be preactivated as well. Park and coworkers demonstrated that cysteamine-modified hyaluronic acid **38** could be effectively conjugated to ON **39** and afforded protamine **40**, a conjugate that produced good gene inhibition (equation 13).[53]

9.18.2.3 Conjugation Through Amide Linkage

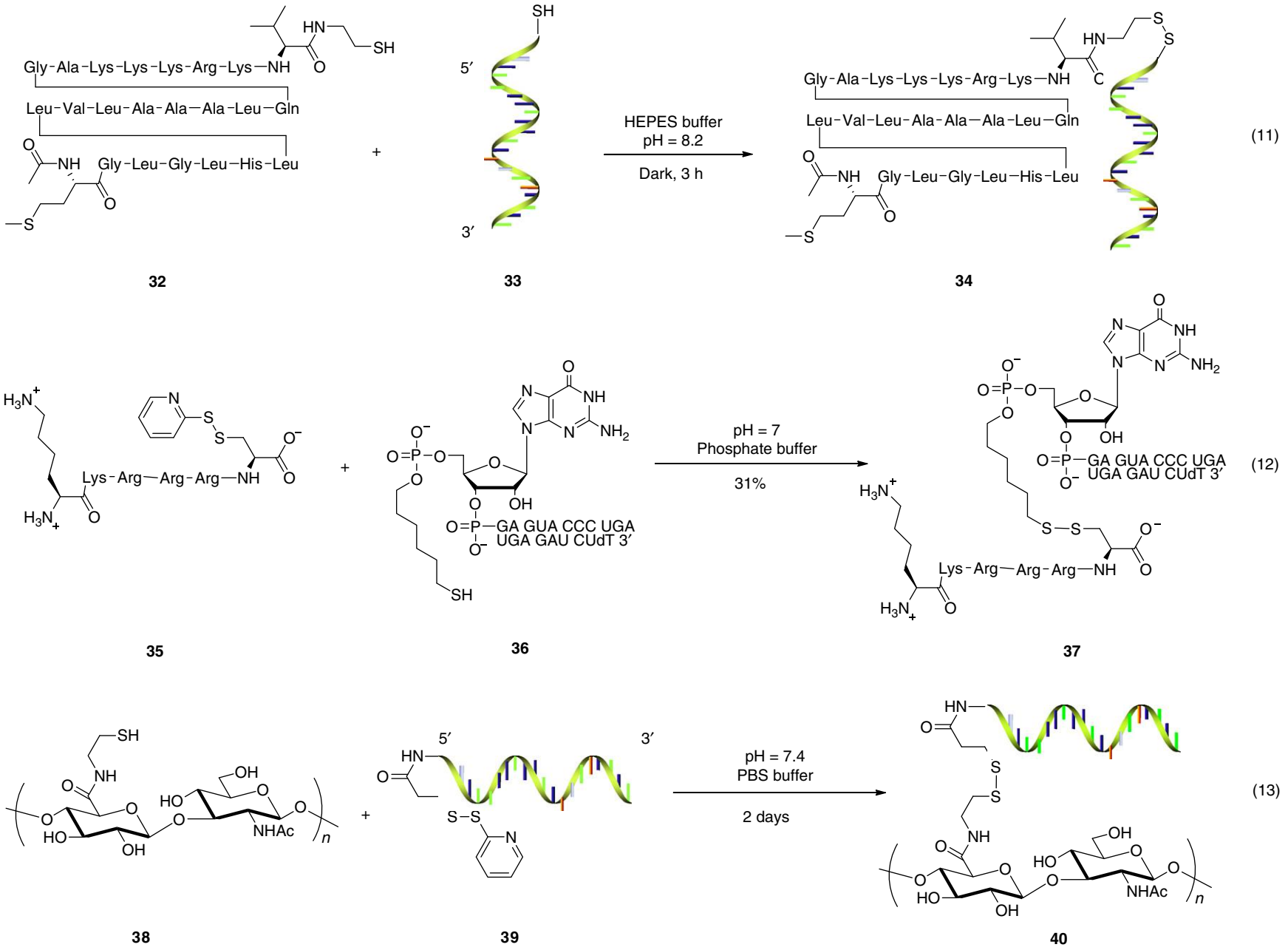
Amide formation is another strategy for ON conjugation. In Scheme 9, the free carboxylic acid and amino group are shown as the generic structures; in analogy to peptide synthesis, such amide formation requires external coupling reagents. In practice, free carboxylic acids may be present in both coupling partners; therefore, the activated esters derived from *N*-hydroxysuccinimide (NHS), pentafluorophenol (PFP), and *para*-nitrophenol (PNP) are more commonly used than the free acids (Scheme 10). Similar transformations, involving phosphoramide, urea, and thiourea formation, have also been proven to be effective in ON conjugation (Scheme 11).

As demonstrated in equation 14, the 3′ amino group on ON **41** and aliphatic carboxylic acid **42** were joined together under the effect of 2-(7-aza-1*H*-benzotriazole-1-yl)-1,1,3,3-tetramethyluronium hexafluorophosphate (HATU).[54] ON **45** with a preinstalled NHS ester selectively reacted with C-terminal amine of peptide **44** bearing an RGD sequence (equation 15).[55] In this case, direct activation by an external coupling reagent would be difficult because peptide **44** also possessed free carboxylic acid groups on the Asp and Pro residues.

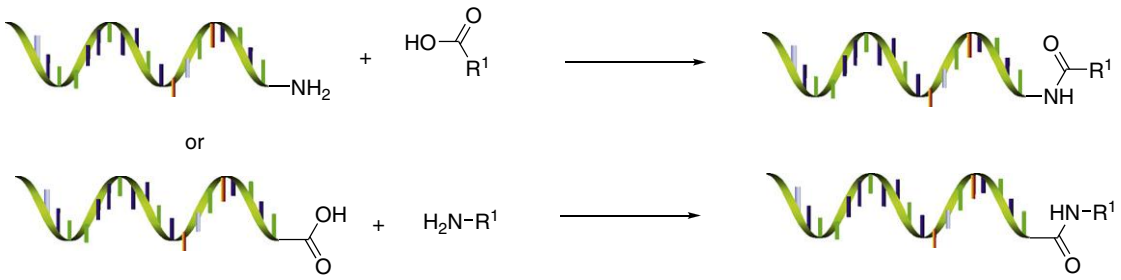
The difficulty in activating phosphate groups makes phosphoramidate formation less common in ON conjugation. However, Wang and coworkers optimized a 1-ethyl-3-(3-dimethylaminopropyl) carbodiimide (EDC)-based coupling protocol and successfully prepared conjugate **49** between biotin derivative **47** and an 87-mer RNA molecule with a remarkable 80% yield (equation 16).[56] The temperature was carefully controlled at 41 °C to balance the reaction kinetics and the phosphorimidazolide hydrolysis. Thiourea formation has been applied to ON conjugation. Aptamer **51** was conjugated to copper chelator **50** by thiourea formation and the product **52** was used for PET imaging application with ^{64}Cu (equation 17).[57]

The most abundant biomolecules containing carboxamide backbones are peptides and proteins. From a synthetic point of view, it is not surprising that the methodologies developed for peptide coupling and protein modifications have been extended to ON conjugation (Scheme 12). Native chemical ligation (NCL) is a powerful strategy for large peptide and protein chemical synthesis, as it offers exquisite selectivity and very high yield.[58] NCL employs a thioester as acyl donor and an N-terminal Cys as acyl acceptor. This allows the amide bond to be exclusively formed at the Cys residue. As shown in equation 18, Cys-modified ON **54** was ligated to peptide thioester **53** under the NCL conditions to afford the peptide–ON conjugate in excellent yield.[59] Expressed proteins can be ligated to N-terminal Cys residue as well if the expressed protein is equipped with a C-terminal thioester. Expressed protein ligation (EPL) takes advantage of the protein splicing mechanism to express a fused intein fragment at the C-terminus of the protein of interest.[60] Under appropriate conditions, the carboxamide linkage between the protein and the intein is converted to a thioester, and the protein of interest becomes suitable for NCL. As shown in equation 19, enhanced cyan fluorescent protein (ECFP) **56** fused with an intein domain and a chitin-binding domain (CBD, not shown) was ligated to a Cys residue at the 5′ end of ON **57**.[61]

Staudinger ligation (SL)[62,63] employs phosphine and azide as coupling partners. ON **60** with a 5′ azido group was site-specifically labeled with fluorescent molecule **59** possessing an *ortho*-diphenylphosphinyl benzoate functional group (equation 20). This reaction proceeded via an aza-ylide intermediate and was accompanied by concomitant oxidation of the phosphorus.[64] Enzyme-mediated ligation (EML) is another important approach for site-selective modification. One recent



Scheme 8 ON conjugation through disulfide linkage.



Scheme 9 ON conjugation through amide linkage.

example is illustrated in equation 21. Under the effect of microbial transglutaminase (MTG), chimeric protein **62**, an EGFP tethered a short substrate peptide of MTG, was transferred to ON acyl donor **63** with good efficiency[65] (Scheme 13).

9.18.2.4 Conjugation by Cycloaddition Reaction

9.18.2.4.1 Conjugation by [3 + 2] cycloaddition

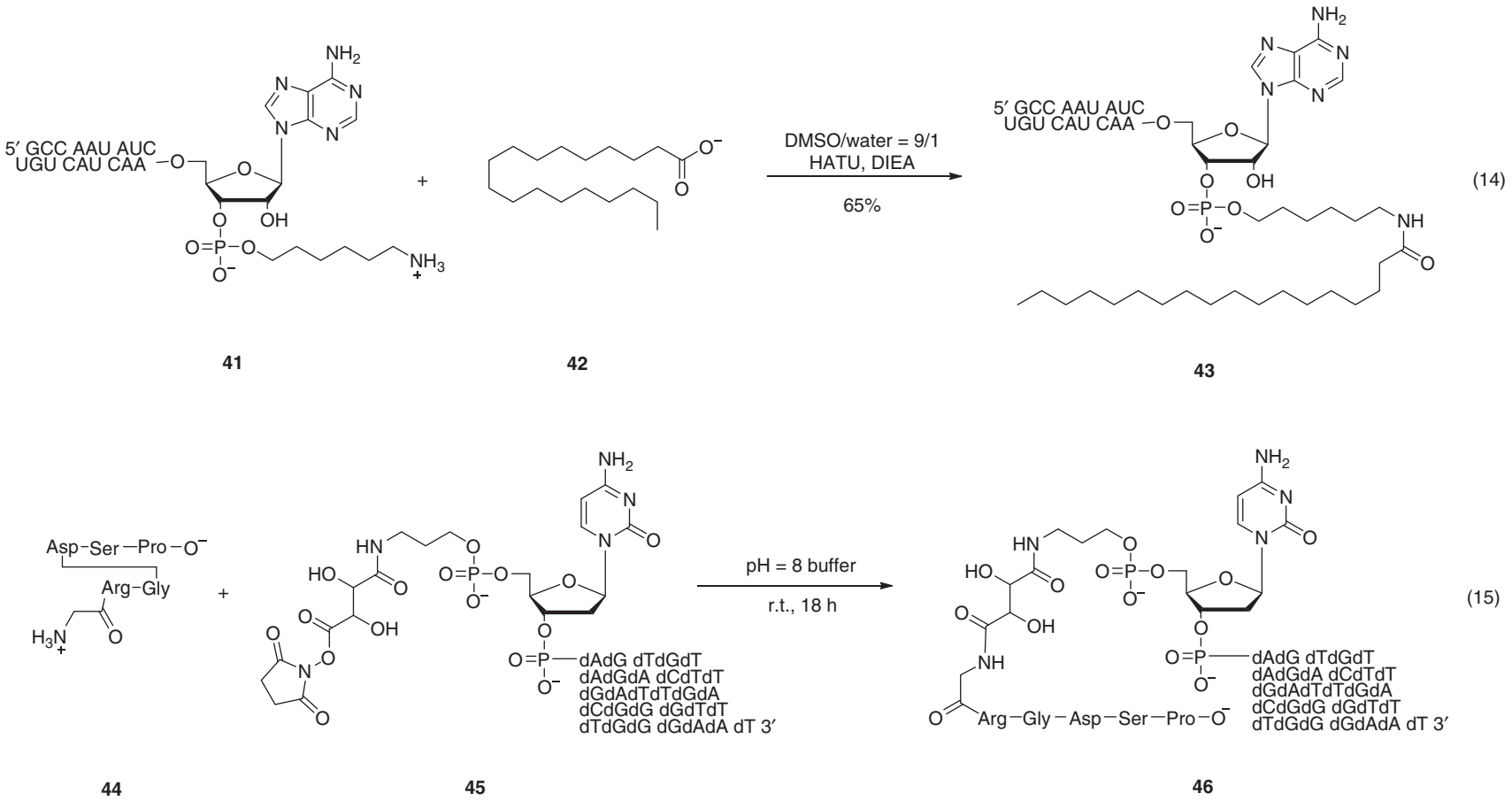
The cycloaddition between a 1,3-dipole and a dipolarophile offers a unique connectivity between the conjugation components (Scheme 14). Depending on the functional group, polarity, catalyst, and other reaction conditions, the cycloadduct can adopt different bond configuration and atom arrangement. The increased interest in using [3 + 2] dipolar addition reaction for ON conjugation is due to the recent development in the copper(I)-catalyzed azide–alkyne cycloaddition (CuAAC) or the "click reaction."[66,67] Because of its superior selectivity, excellent kinetics, and functional group tolerability, CuAAC is recognized as an extremely useful tool for biomolecular modification and numerous ONs have been modified by CuAAC with multiple chemical entities including small molecule reporters, peptides, proteins, polyethylene glycols (PEGs), and other ONs (Scheme 15). However, oxidative degradation of ONs and proteins in the presence of copper and molecular oxygen is a major concern for CuAAC applications. In addition, the replacement of the sulfur atom by an oxygen atom in phosphorothioate is also observed in some click reactions. To address the above mentioned problems, several laboratories have introduced copper-free conditions, in particular, the strain-promoted azide–alkyne cycloadditions,[68] for ON conjugation (Scheme 16).[69] Under copper-free conditions, cyclooctynes are often used as dipolarophiles and the cycloadducts are formed in the absence of the metal catalyst, albeit in lower efficiency compared to copper catalyzed reactions. The metal-free conditions reduce the liability of unspecific modifications of ONs and allow for biological applications where copper is prohibited due to its high toxicity.

Because of its compatibility with phosphoramidite chemistry, the alkyne group is typically installed on the ON at the flank ends or at the internal positions. In equation 22, ON **66** with a pendent 5′ alkyne group underwent CuAAC reaction with a galactose derived azide **65** to generate desired triazole conjugate **67**.[70] Although many different copper(I) catalysts, such as CuBr and $[Cu(MeCN)_4]PF_6$, have been applied to the CuAAC reaction, the *in situ* generation of the copper(I) species from copper sulfate and sodium ascorbate is the most widely used protocol. In many cases, an external ligand is not critical for the cycloaddition to proceed, but under certain conditions, an external ligand can greatly enhance the reaction rate. In equations 23 and 24, two ONs with alkyne groups on the nucleobase and on the phosphate backbone, respectively, were smoothly modified by azide-containing small molecules under copper catalysis.[71,72] In both transformations, the tris-(benzyltriazolyl)methylamine (TBTA)[73] was used as an external ligand to accelerate the cycloadditions. The incorporation of an internal azido group in an ON by solid phase synthesis poses significant challenges due to the potential reactions between azide and phosphoramidite. A rare example, illustrated in equation 25, an ON **74** possessing an internal 2′ azido cytidine was successfully synthesized by the phosphodiester strategy. The subsequent labeling of **74** by CuAAC reaction provided an important probe molecule to study the physico- and biochemical properties of 2′ azido modifications.[74]

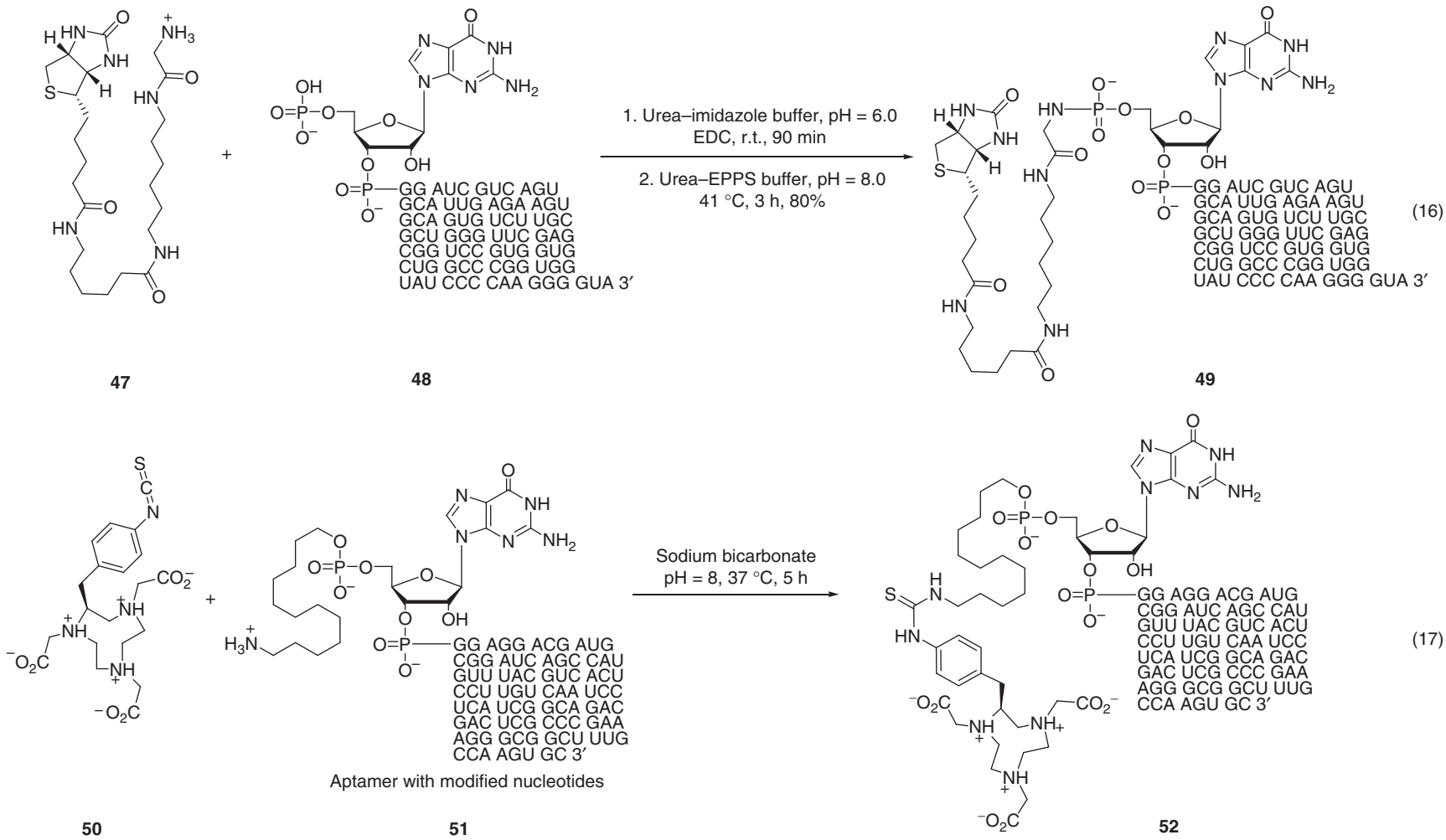
The generality of CuAAC stretches well beyond ON and small molecule cycloadditions. As illustrated in equation 26, peptide propiolic amide **78** was subjected to CuAAC reaction in the presence of TBTA ligand producing cycloadduct **79** in 56% yield.[75] In a different event (equation 27), an intramolecular cycloaddition was achieved by using bi-functional ON **80**.[76] Many of the ON conjugates prepared by CuAAC are intended for biological and medical applications, which warrants stringent scrutiny of the residual copper content in the final products. Given the toxicity concern, in conjunction with the chelation effect of peptide, protein, and ON, it is not surprising to see the application of the strain-promoted alkyne–azide cycloaddition to ON conjugate synthesis. As a representative example, shown in equation 28, polyT ON **82** with a tethered cyclooctyne moiety at 3′ end reacted with azido oligosaccharide **83** in water to furnish adduct **84** in the absence of any metal catalyst.[77] The copper-free condition is considered bio-compatible and its high promise in biomedical research has promoted the commercialization of several cyclooctyne-derived phosphoramidites.

9.18.2.4.2 Conjugation by [4 + 2] cycloaddition

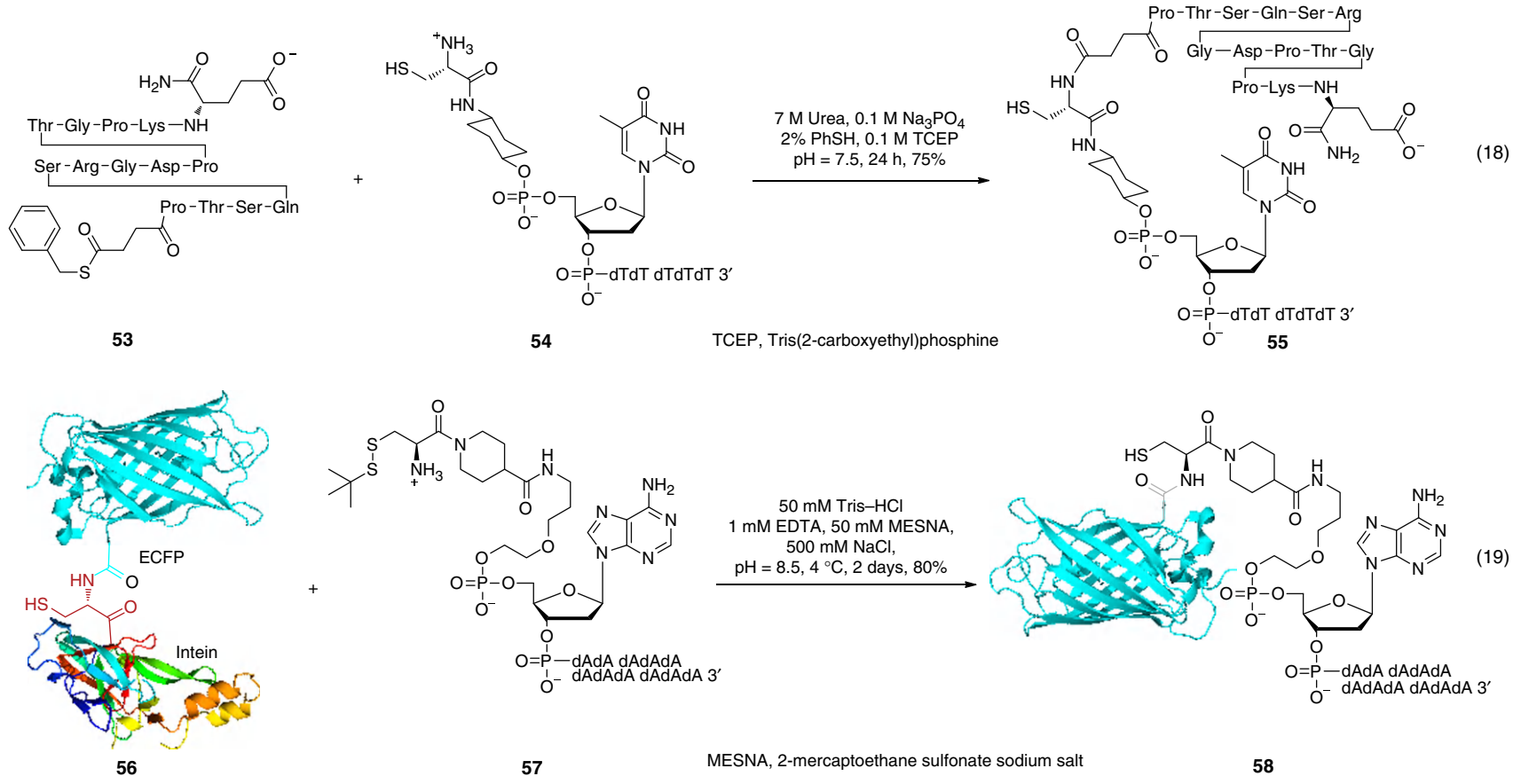
It is difficult to overstate the historical status of the Diels–Alder reaction[78] in the field of chemical synthesis. The [4 + 2] cycloaddition is an extremely versatile reaction to construct polycyclic structures, and its extensive application in natural product



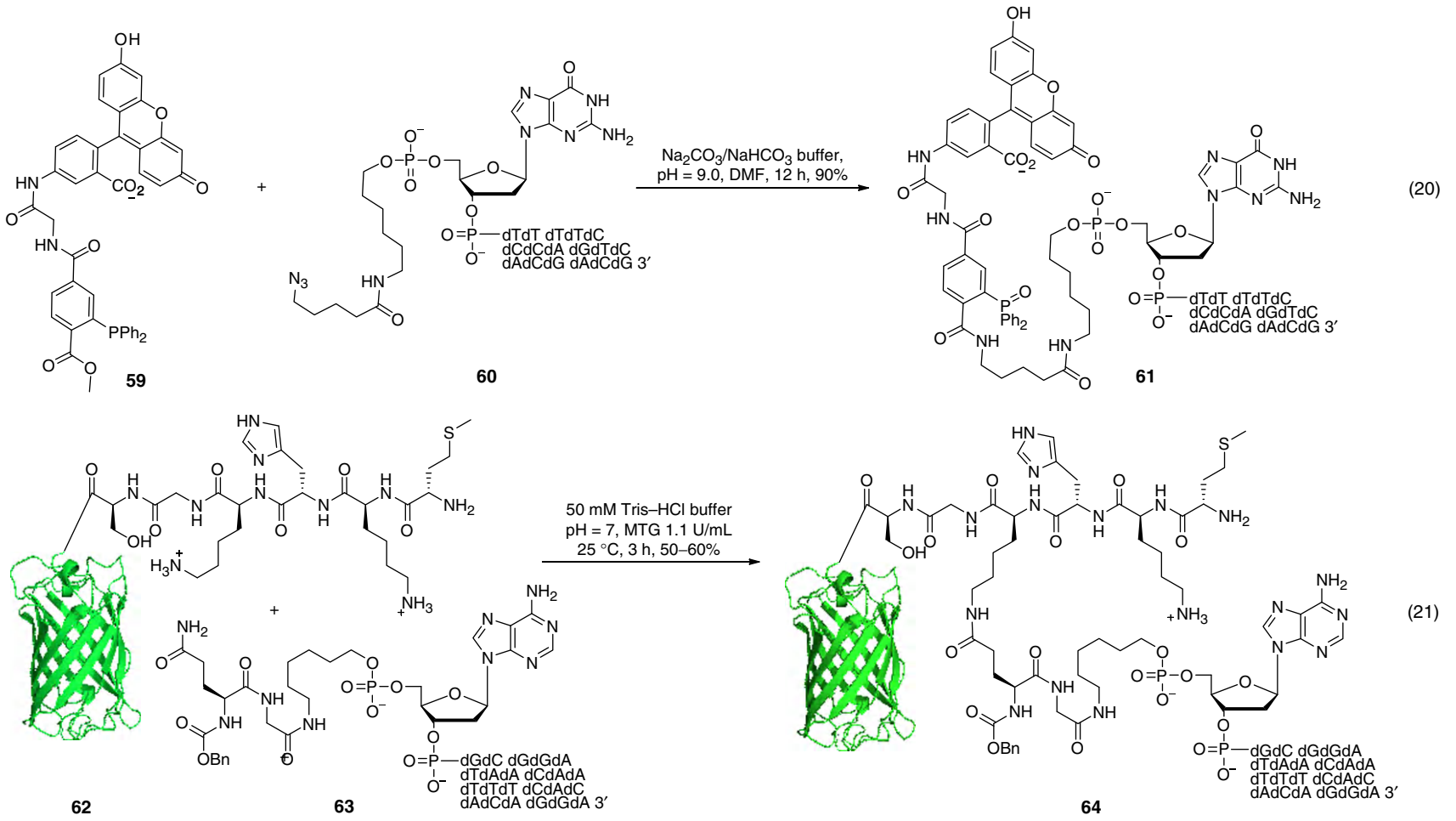
Scheme 10 ON conjugation through amide linkage.



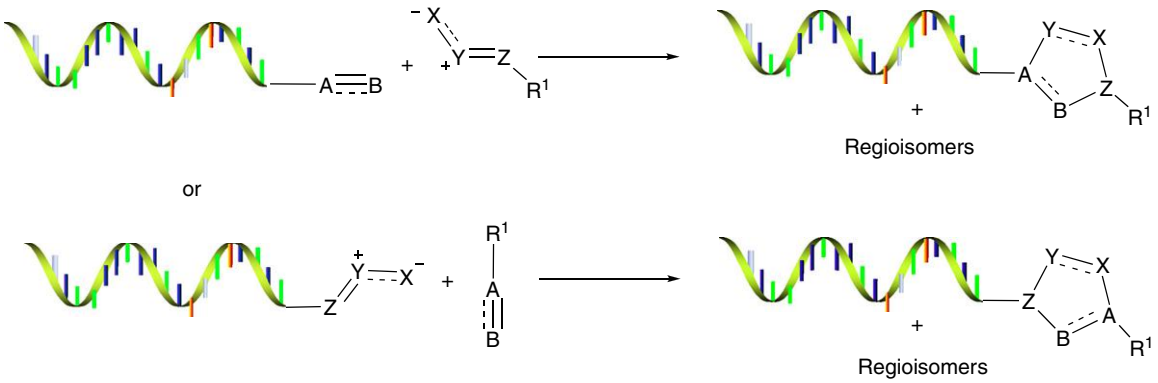
Scheme 11 ON conjugation through phosphoramidate and thiouea linkages.



Scheme 12 ON conjugation by NCL and EPL.



Scheme 13 ON conjugation by SL and EML.



Scheme 14 ON conjugation through [3 + 2] cycloadditon.

synthesis[79] represents the great advancement of modern organic chemistry. However, [4 + 2] cycloaddition between inactivated diene and dienophile proceeds at a modest rate. To make the cycloaddition reaction suitable for ON conjugation (Scheme 17), various activation strategies have been applied to the diene and dienophile to minimize the energy gap between the highest occupied molecular orbital (HOMO) and the lowest unoccupied molecular orbital (LUMO). Among the strategies, Lewis acid activation, substitution with electron-donating or -withdrawing groups, and addition of ring strain to diene or dienophile are frequently used methods to improve the kinetics of ON conjugation. Aqueous media offer another advantage for such [4 + 2] reactions in ON conjugation. In the 1980s, Breslow and coworkers reported that reaction rate and diastereoselectivity of Diels–Alder reactions were significantly improved when it was carried out in water.[80,81]

The diene moieties are generally more stable toward automated ON synthesis, therefore, they are often installed on the ONs (Scheme 18). In many cases, the dienophiles are strained cyclic molecules attached to the ON modifiers such as maleimide. As demonstrated in equations 29 and 30, phosphorothioate-containing ON **86** bearing a 5′ hexadiene fragment underwent Diels–Alder reaction with biotin-derived maleimide **85** and peptide maleimide **88,** respectively, in near quantitative yields at 37 °C.[82] The phosphorothioate is inert to maleimide under these conditions, likely due to steric reasons, but can be reactive toward maleimide when it is located at the terminal positions.

Furan is compatible to ON synthesis and provides high lying HOMO states because of its high electron density (Scheme 19). As shown in equation 31, ON **90** with an internal furan moiety was labeled by various dye-derived maleimides, and the fluorescence emission of the conjugate was studied in detail.[83] The [4 + 2] cycloaddition has been used to investigate the conformational changes of higher order ON structures. Self-complementary ON **93** forms a stable, hairpin-like secondary structure. On modification of the loop region by Diels–Alder reaction, a pronounced destabilization of the hairpin structure was observed in **95** (equation 32).[84] An inverse electron-demand Diels–Alder reaction between norbornene-labeled ON **97** and water-soluble tetrazine derivative **96** is shown in equation 33.[85] It was postulated that this reaction was entropically driven, as the adduct releases a molecule of nitrogen as it rearranged to final dihydrodiazene conjugate **98**.

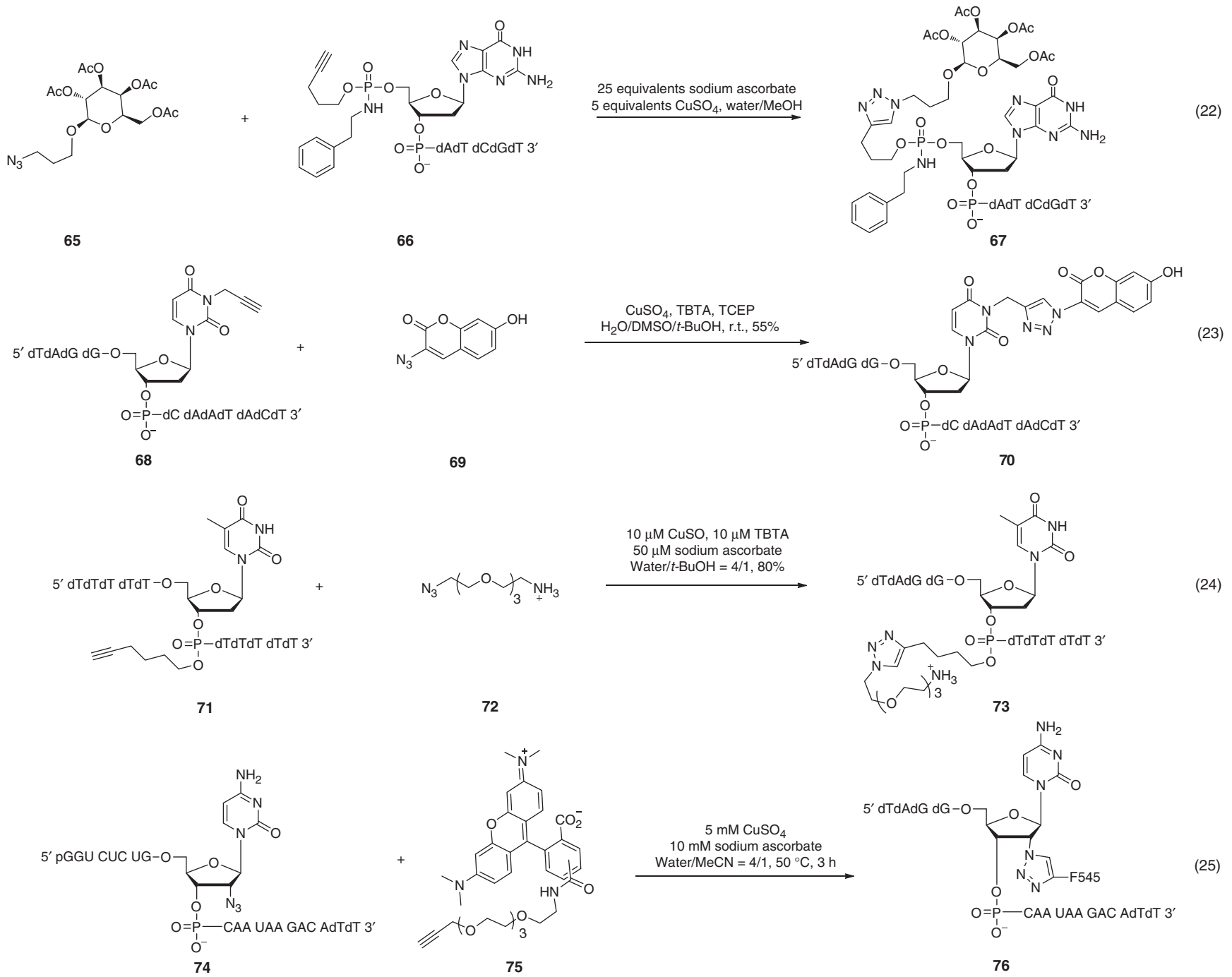
9.18.2.4.3 Conjugation by [4 + 1] cycloaddition

The [4 + 1] cycloaddition in this section refers to condensation reaction between an aldehyde and vicinal XH and YH groups (Scheme 20). Mature chemistry is available for producing 1,2-diols; 1,2-aminoalcohols; 1,2-diamines; and natural amino acids, such as Ser, Thr, and Cys, are readily accessible in free or protected forms. The condensation reaction generates a water molecule; therefore, aqueous media for ON conjugation drives the equilibrium in the unproductive direction. For this reason, only the Cys-based [4 + 1] reaction has been studied in detail and the examples given in the following scheme are focused on thiazolidine formation.

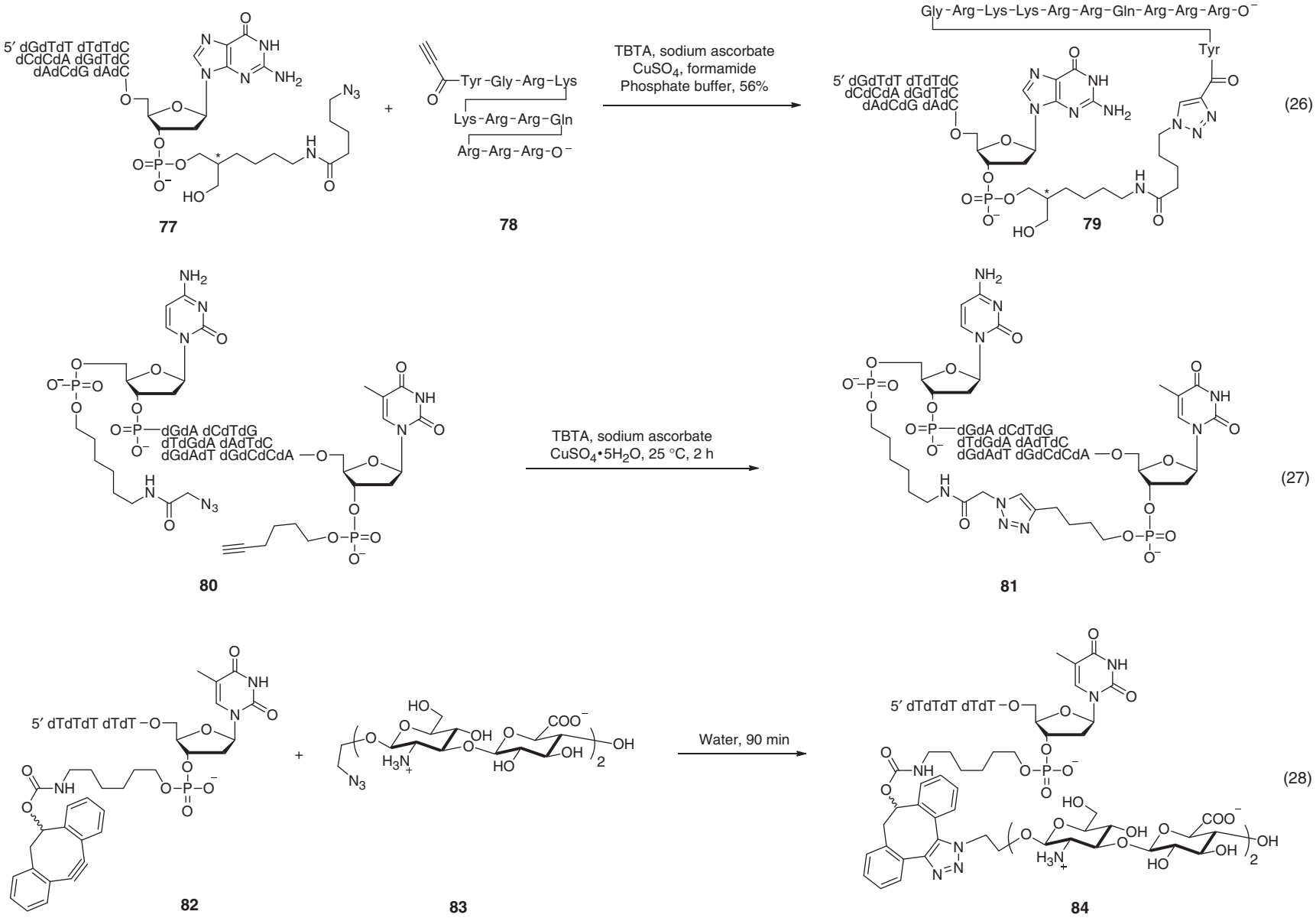
As illustrated in Scheme 21, a formyl group at either terminal position (equations 34 and 35)[86,87] or internal postions (equation 36)[88] was converted to thiazolidine in the presence of a Cys residue. The pH of the reaction buffer was adjusted between 4 and 6 to maintain a favorable equilibrium. The stability of thiazolidine is indeed a concern for its broader application. For example, the condensation between ON **105** and peptide **106** proceeded with 90% conversion, however, the isolated yield for thiazolidine was only 25%.[88]

9.18.2.5 Conjugation Through Imine, Hydrazone, and Oxime Linkages

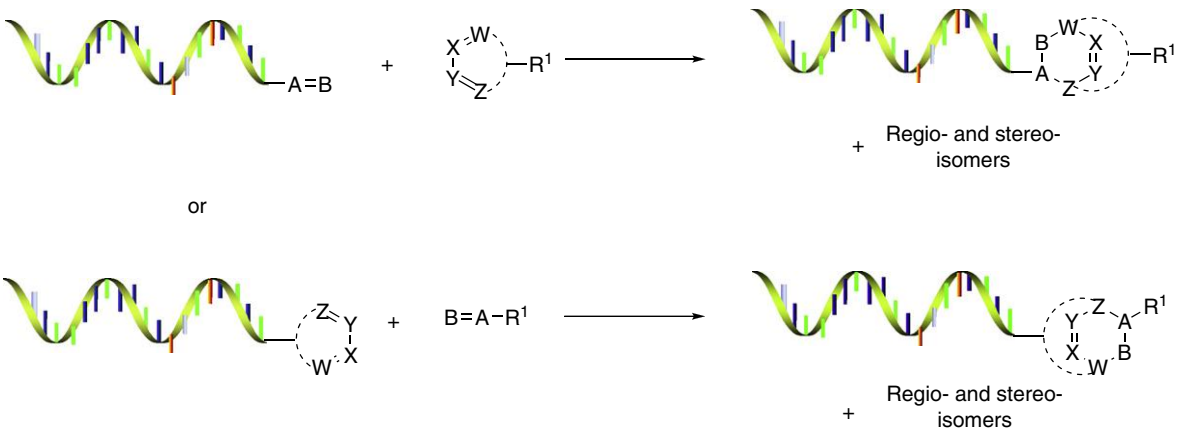
As shown in Scheme 22, the condensation between a nitrogen atom and an aldehyde represents another important category of ON postsynthetic modifications. Depending on the nature of the X group, imine ($X{=}CR^2R^3$), hydrazone ($X{=}NR^2$), or oxime ($X{=}O$) conjugates can be produced under appropriate conditions. Although the C=N double bonds are present in all three adducts, their stabilities are only remotely related. Imine or Schiff base is the least stable linkage among the three around neutral pH, therefore the C=N double bond of imine is often reduced by borohydride to give a stable amine linkage. In contrast, the hydrazone and oxime linkages display far greater hydrolytic stability, which is attributed to the resonance structures that can



Scheme 15 ON conjugation by [3 + 2] cycloaddition.



Scheme 16 ON conjugation through inter-, intramolecular, and strain-promoted [3 + 2] cycloaddition reactions.



Scheme 17 ON conjugation by [4 + 2] cycloaddition reaction.

delocalize the positive charge on the carbon atom of the C═N double bond. However, the discovery of the exceptional stability of trimethylhydrazonium, along with the fact that oximes are generally more stable than hydrazones under hydrolytic conditions, leads to the proposal that the stability of imine, hydrazone, and oxime is correlated with the level of resistance to C═N double bond protonation.[89]

Metal-coordinated phthalocyanines are excellent near-infared fluorescent tags for biomedical analysis. In equation 37, PEG-modified mono-zinc phthalocyanine **108** was ligated to ON **109** by sodium cyanoborohydride-mediated *in situ* Schiff base reduction[90] (Scheme 23).

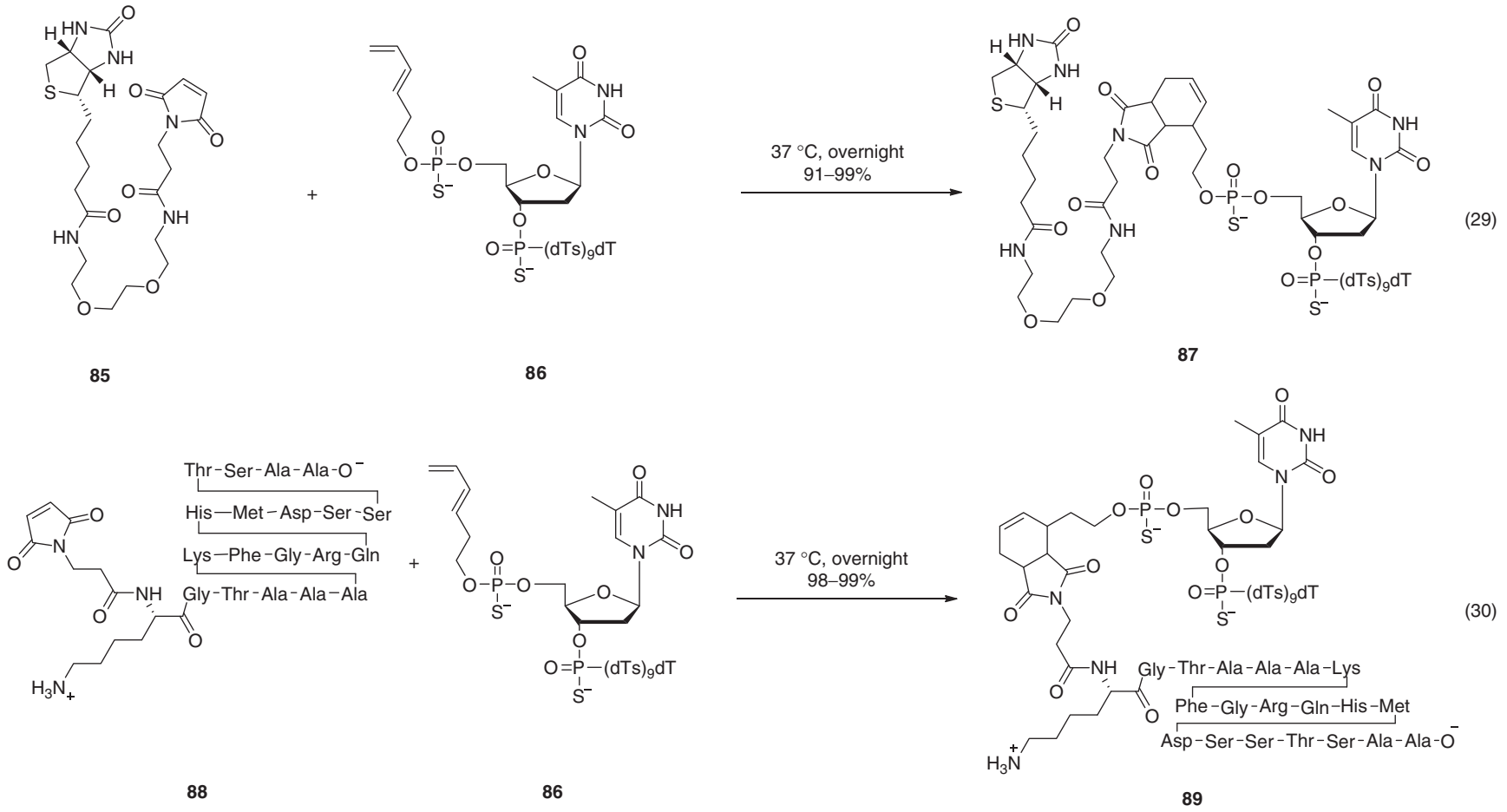
Instead of forming hydrazone derivatives with simple aldehydes and ketones, hydrazine offers the flexibility to generate condensed heterocycles with polycarbonyl compounds (Scheme 24). For example (equation 38), ON **111** with a tethered hydrazine group at an internal position was converted to the corresponding pyrazole via sequential dehydration of 1,3-dicarbonyl compound **112**.[91] Alternatively, the same ON **111** can form a hydrazone adduct **115** by reacting with glyoxylamide-terminated peptide **114** (equation 39).[91] As the nucleophilicity of hydrazine is higher than that of primary amine, the competition of Lys side chain is negligible. Although the option is still available to reduce the C═N double to a more stable C–N single bond, such transformation is not necessary because the hydrazone provides sufficient stability as a linkage. In the ON hydrazone or oxime-forming reactions, glyoxylic aldehydes, and aromatic aldehydes are the choices of preferred carbonyl compounds, because they have no α protons and the conjugations are substantially cleaner than that of their aliphatic aldehyde counterparts. Not only peptides, but also large proteins, such as antibodies, have been attached to ONs by hydrazone or oxime-formation. One example to demonstrate the power of hydrazone conjugation is shown in equation 40. Primary amine groups on an antibody were functionalized by an NHS ester of hydrazinonicotinic acid, and the resulting hydrazino–antibody hydrazine was efficiently coupled with ON **116** after overnight incubation.[92] Despite a chemoseletive hydrazone formation, this ON conjugation is not site-specific owing to the existence of multiple primary amines on the antibody. The homogeneous protein conjugate has tremendous advantages over the heterogenic analog in terms of purification, characterization, and systematic structure–activity investigation. The recent development of amber codon manipulation and the evolution of aminoacyl t-RNA synthetase has enabled site-selective incorporation of unnatural amino acids bearing ketone or aldehyde side chains.[93] This genetic protocol should allow for the preparation of homogeneous ON–protein conjugates.

The ON conjugation by oxime formation shares many similarities with that of the hydrazone formation (Scheme 25). In equations 41 and 42, oxyamino sugar **119** and oxyamino cyclic peptide **123** were joined to ONs **120** and **122,** respectively, by oxime formation under acidic conditions.[94,95]

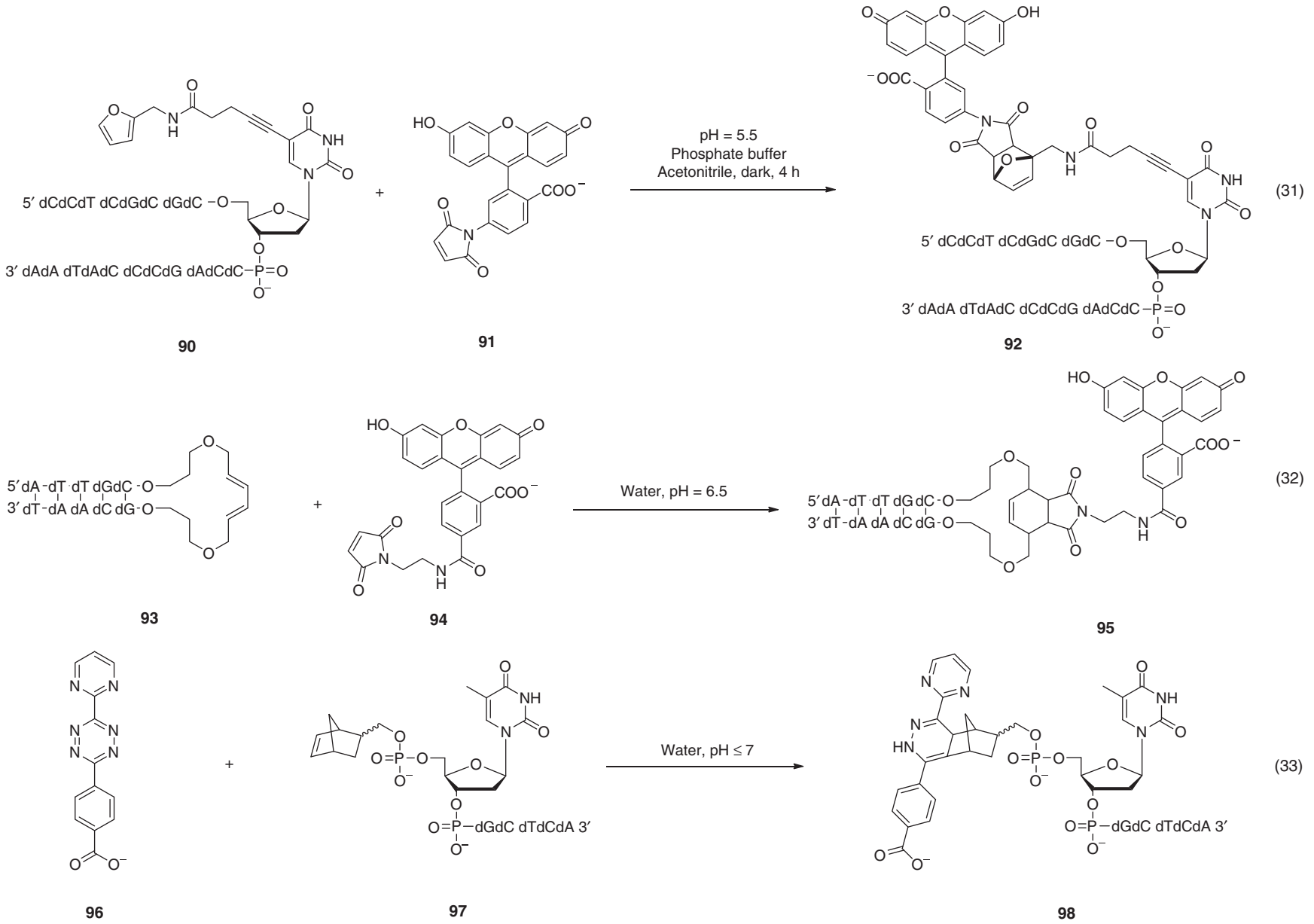
9.18.2.6 Conjugation Through Other Linkages

To date, thiol, amine, carbonyl, and cycloaddition chemistry are the most commonly used methods for ON postsynthetic modifications and their popularity roots from the availability of these functional groups as well as the overall efficiency for ON conjugation. However, as the application of ONs becomes increasingly broad and sophisticated, we predict a strong demand for more diverse organic transformations that enable thorough structure–activity relationship studies on the nucleobases and ON backbones (Scheme 26).

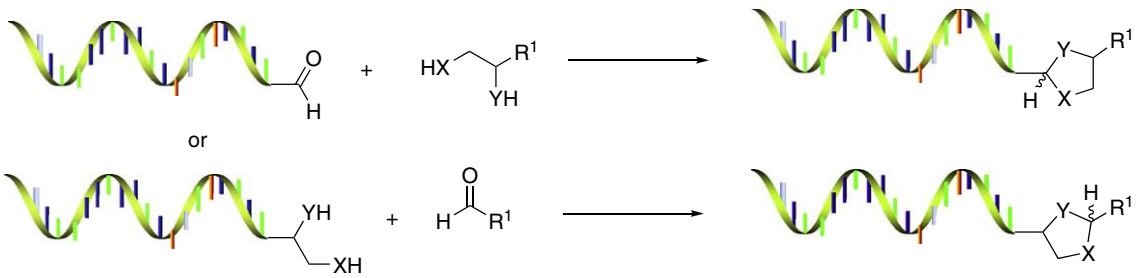
Transition metal-catalyzed cross-coupling reactions have been explored for nucleobase postsynthetic modifications. As shown in equation 43, Manderville and coworkers reported a postsynthetic guanine arylation by Pd-catalyzed Suzuki–Miyaura reaction.[96] A bromo guanine containing ON **125** was coupled with arylboronic acid **126** in aqueous acetonitrile under the effect of Pd and a water-soluble tris(2-sulfophenyl)phosphine trisodium (TPPTS) ligand to give aryl guanine **127** in excellent yield. They found that the coupling conditions were applicable to a series of boronic acids and the reactions were insensitive to flanking residues on the ON.



Scheme 18 ON conjugation by [4 + 2] cycloaddition reaction.



Scheme 19 ON conjugation by [4 + 2] cycloaddition reaction at internal positions.



Scheme 20 Conjugation by [4 + 1] cycloaddition reaction.

Photo-induced cross-linking reactions have also been applied to ON modification. As shown in equation 44, ON **128** with a tethered photo-reactive Ru(II) species could induce electron transfer between the Ru(II) ligand and the guanine residue on complementary strand **129**. The resulting radical intermediates recombined to afford cross-linked ON **130**.[97] As expected, the degree of cross-linking is influenced by the ligand type, the position and the length of the tether, and the light exposure time. Another type of photo-induced modification is shown in equation 45: azidobenzene **131** was transformed to a reactive species under irradiation and the union of ON **132** with the transient species afforded labeled ON **133** with up to 20% radiolabeling efficiency in approximately 2 h.[98]

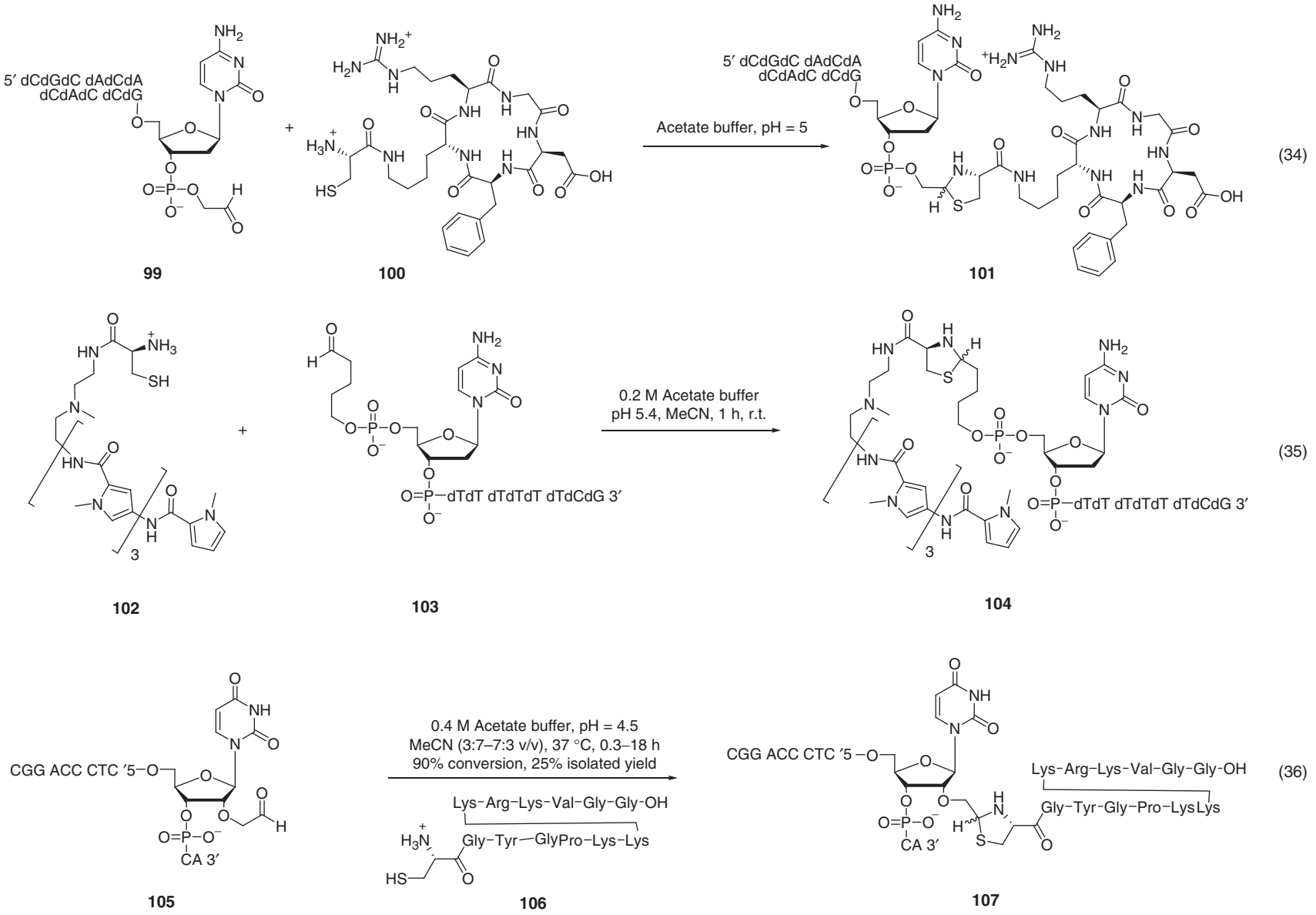
Other well-established organic transformations, such as diazo transfer reaction and amine addition to olefin, have found applications in ON modification (Scheme 27). Diazo transfer reagent **135** was employed to convert pendent amino groups on ONs to azido groups by M^{2+} (M = Zn, Co, Cu) catalysis (equation 46).[99] This transformation is useful as the resulting azide can either participate in [3 + 2] cycloaddition for further modifications or act as temporary protective group for the amines. An example of amine addition to an electron-deficient double bond is illustrated in equation 47. In the absence of other nucleophilic functional groups, ON **137** with an internal guanine analog reacted with the N-terminal amino group of peptide **138** under acidic conditions with a remarkable yield. This guanine analog has proved to be effective toward Cys-containing peptides as well.[100] In Section 9.18.2.5, we discussed transaminase MTG-mediated ON modifications. In theory, the majority of the EC 2 enzymes are capable of performing similar reactions under optimized conditions if the ONs are appropriately functionalized. For example (equation 48), Sheppard and coworkers used *N*-acetylglucosamine (GlcNAc)-ON **140** as substrate for glycosyl transferase to synthesize Lewis X (LeX)-ON conjugate **141**.[101] Sequential treatment of **140** with β-1,4-galactosyl transferase and α-1,3-fucosyl-transferase in the presence of uridine diphosphate galactose (Gal-UDP) and guanosine diphosphate fucose (Fuc-GDP) afforded the desire conjugate in quantitative yield.

9.18.3 Conclusion and Future Perspective

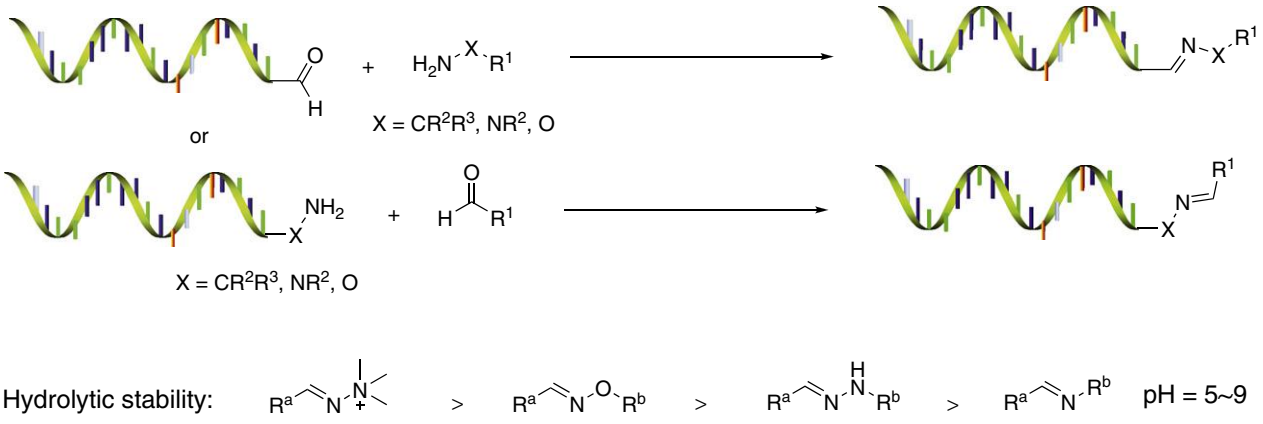
As described in this chapter, many powerful protocols have been developed for ON postsynthetic conjugation. The large repertoire of conjugation chemistry, flexible choice of conjugation sites, and a diverse selection of modifier groups provide great opportunities for ONs to mature as a new therapeutic means. However, such diversity also poses challenges in making appropriate choice. Conjugation chemistry, conjugation sites, activation groups on the coupling partners, connection linkages (e.g., cleavable, noncleavable, enzymatically active), and type of applications all have to be taken into account to make the best decision. For this reason, rational design with the goal of tailoring molecules to particular purposes is essential for successful ON conjugate applications. Indeed, much of the excitement in this field is coming from the clinical trials of the carefully engineered ON conjugates.

As the field continues to grow, the development of more orthogonal coupling reactions with high efficiency will be necessary for ON therapy development. In particular, there is an imminent demand for chemistry that allows for selective coupling of multiple fragments to the ON, including small molecules, lipids, peptides, fluorescent labels, and macromolecules such as PEG, saccharides, and proteins. It is needless to say that such coupling reactions must be able to offer high purity products without tedious purification. Although not detailed in this chapter, development in the purification methods should be pursued in parallel to address the separation problems associated with the less ideal conjugation reactions.

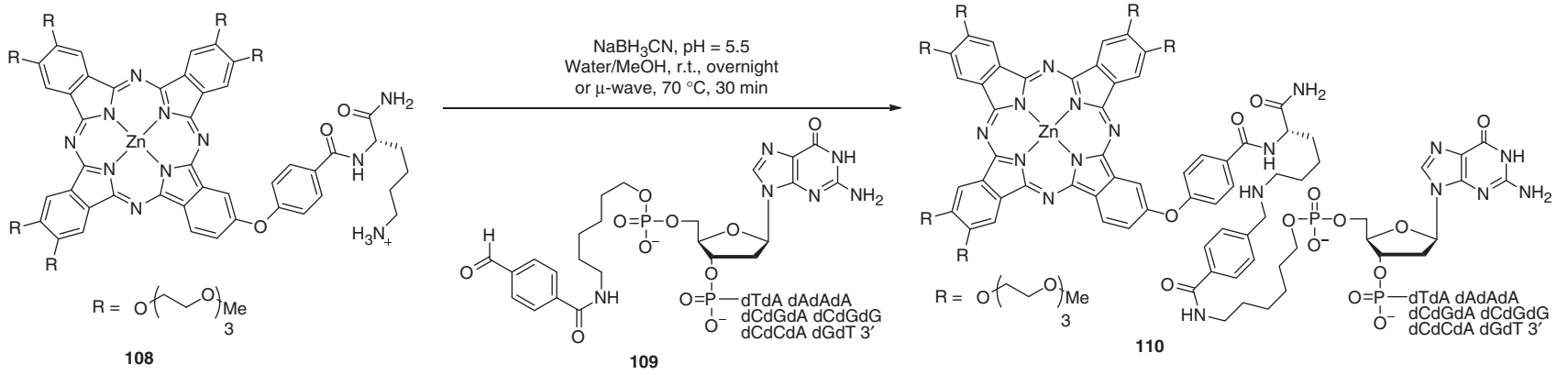
In the past two decades, we have witnessed tremendous progress of clinical applications of ON conjugates; but challenges remained in the delivery of the conjugates to the appropriate compartments where the therapeutic targets reside. Compared with other techniques for ON delivery such as cationic based lipid nanoparticles and polymers, ON conjugates offer unique advantages in terms of defined composition and stoichiometry, ease of purification and characterization, potential multiple routes of administration, and the opportunity for systematic structure–activity studies. The increasing interests in ON conjugation as an effective way to tackle delivery challenges is evident from the fact that more conjugate-based ON drug candidates are entering clinical trials. For example, an exon-skipping morpholino antisense ON conjugated with a cell penetrating peptide is now in phase II trial (AVI-4658) for the treatment of Ducheme muscular dystrophy. Alnylam recently announced their plan to file an investigational new drug (IND) application for the treatment of transthyretin-mediated amyloidosis (ATTR), utilizing a



Scheme 21 ON conjugation by [4 + 1] cycloaddition reaction.

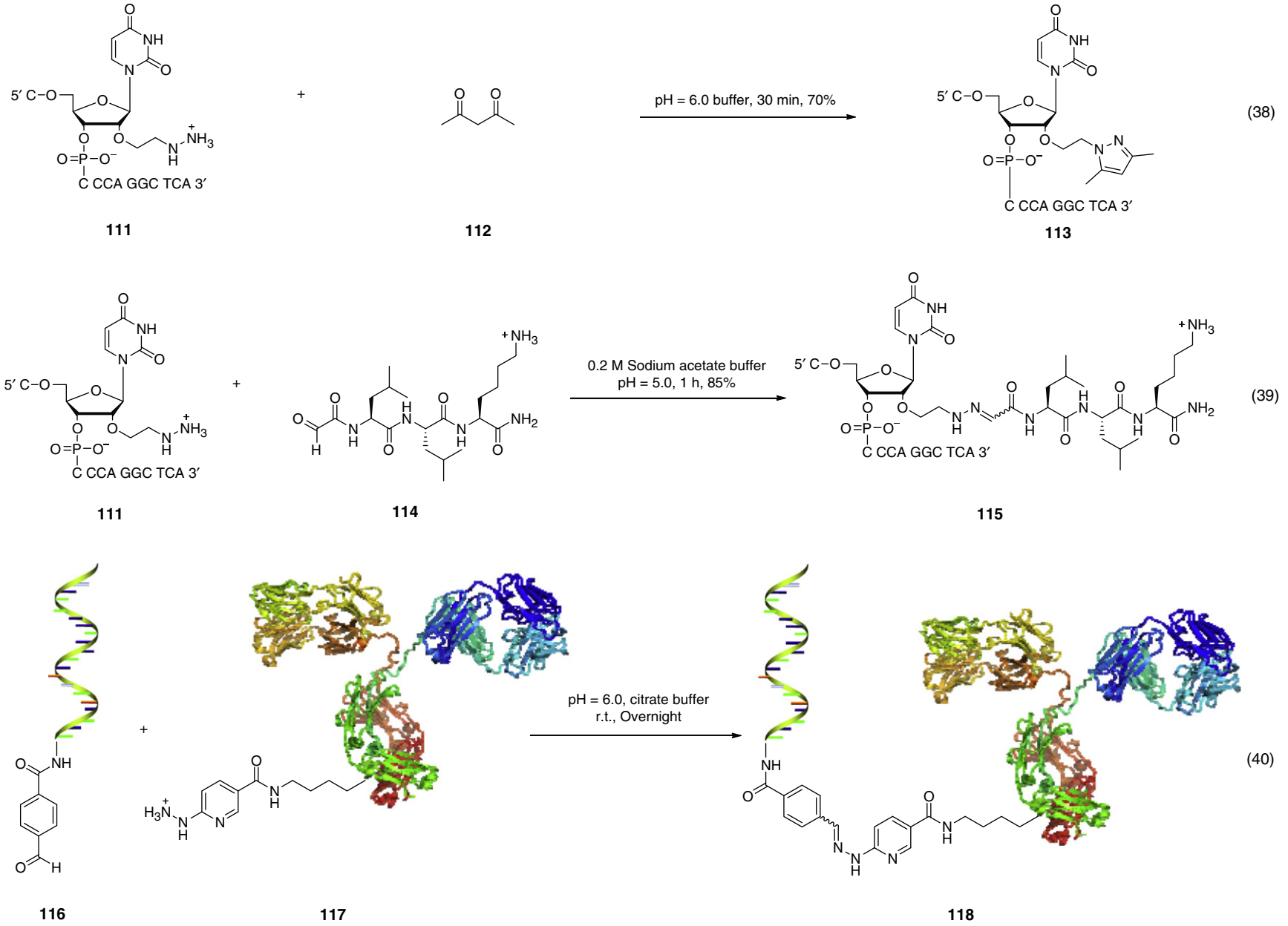


Scheme 22 Conjugation through imine, hydrazone, and oxime linkages.

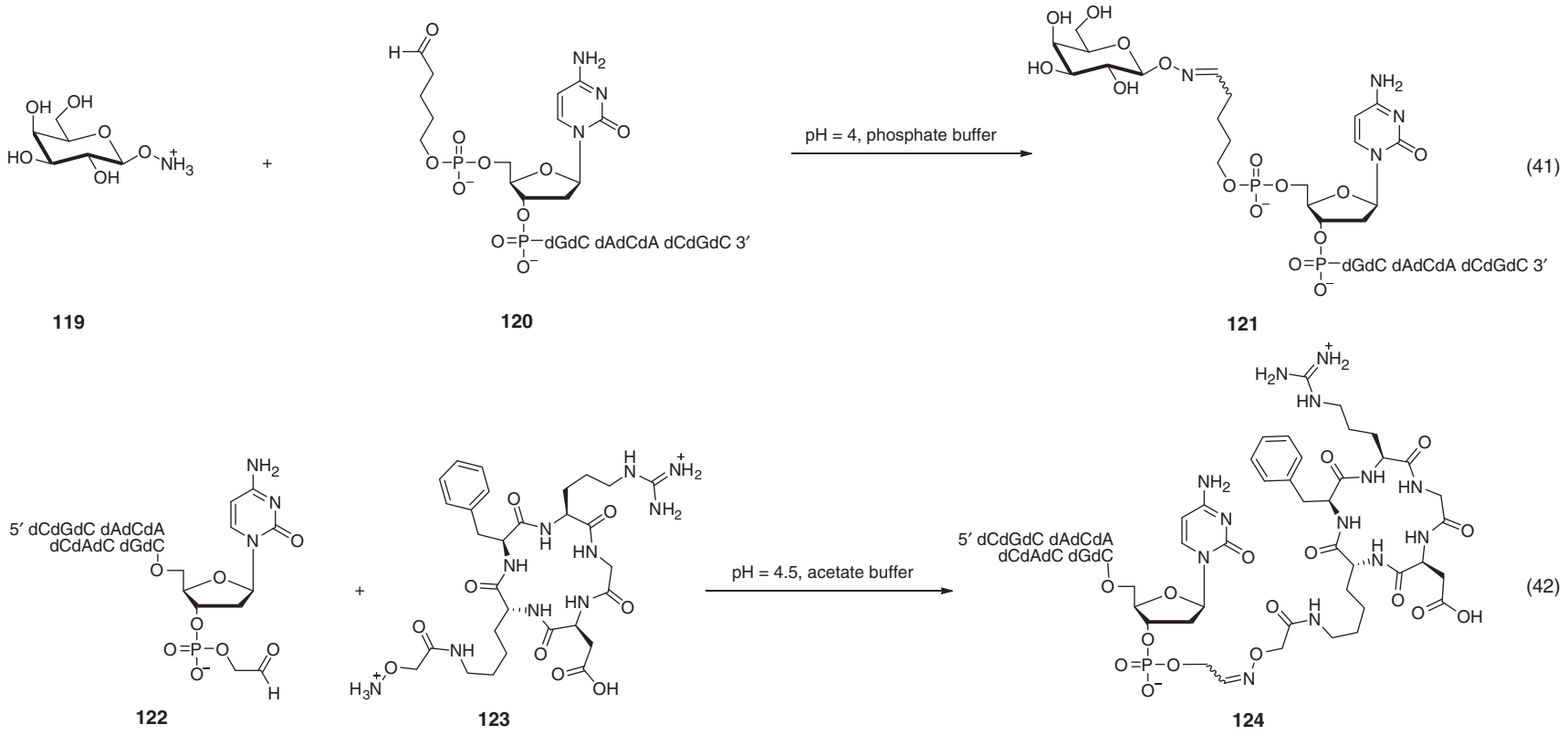


108 109 110 (37)

Scheme 23 ON conjugation by reductive amination reaction.



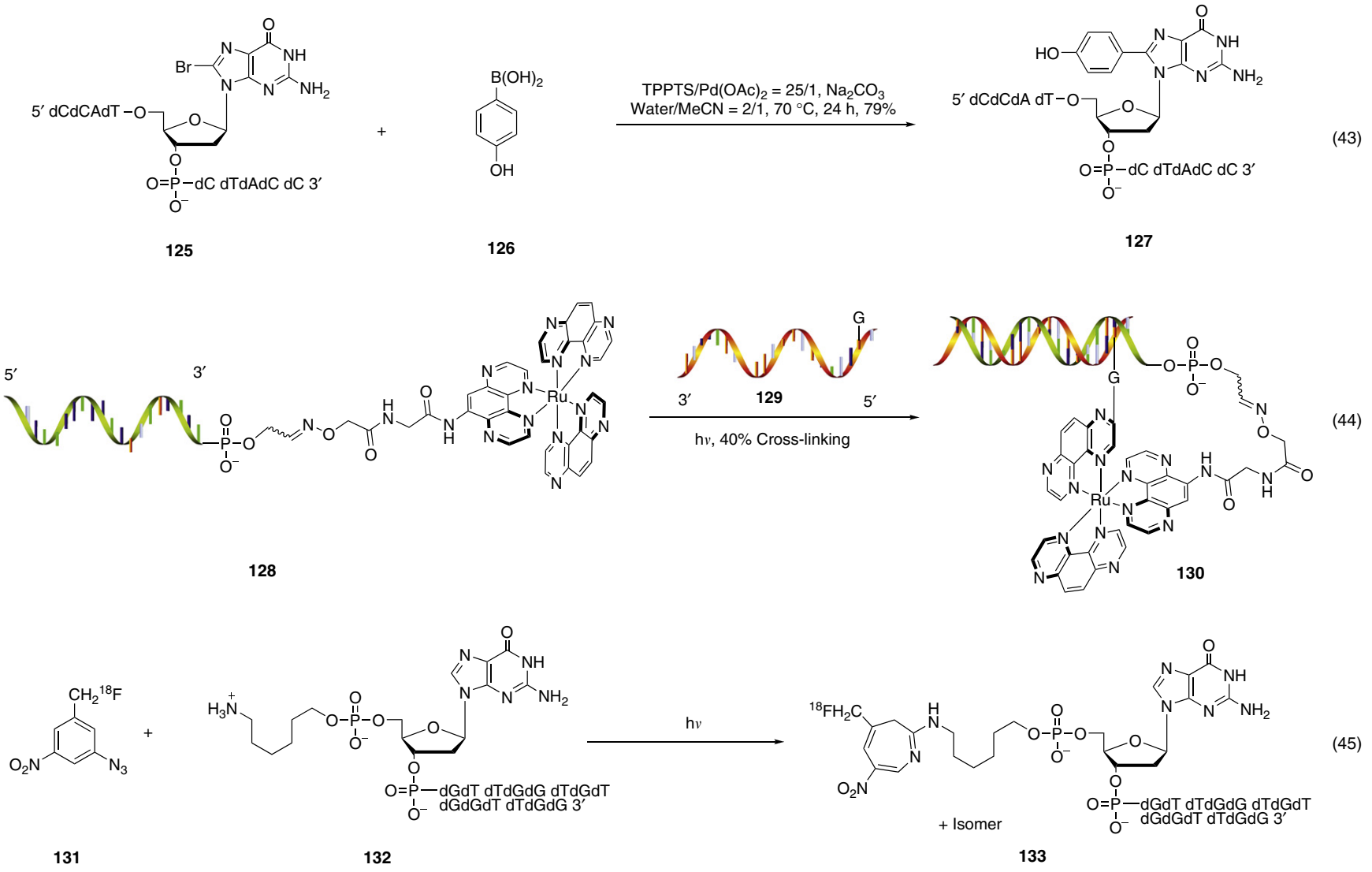
Scheme 24 ON conjugation through hydrazone linkage.



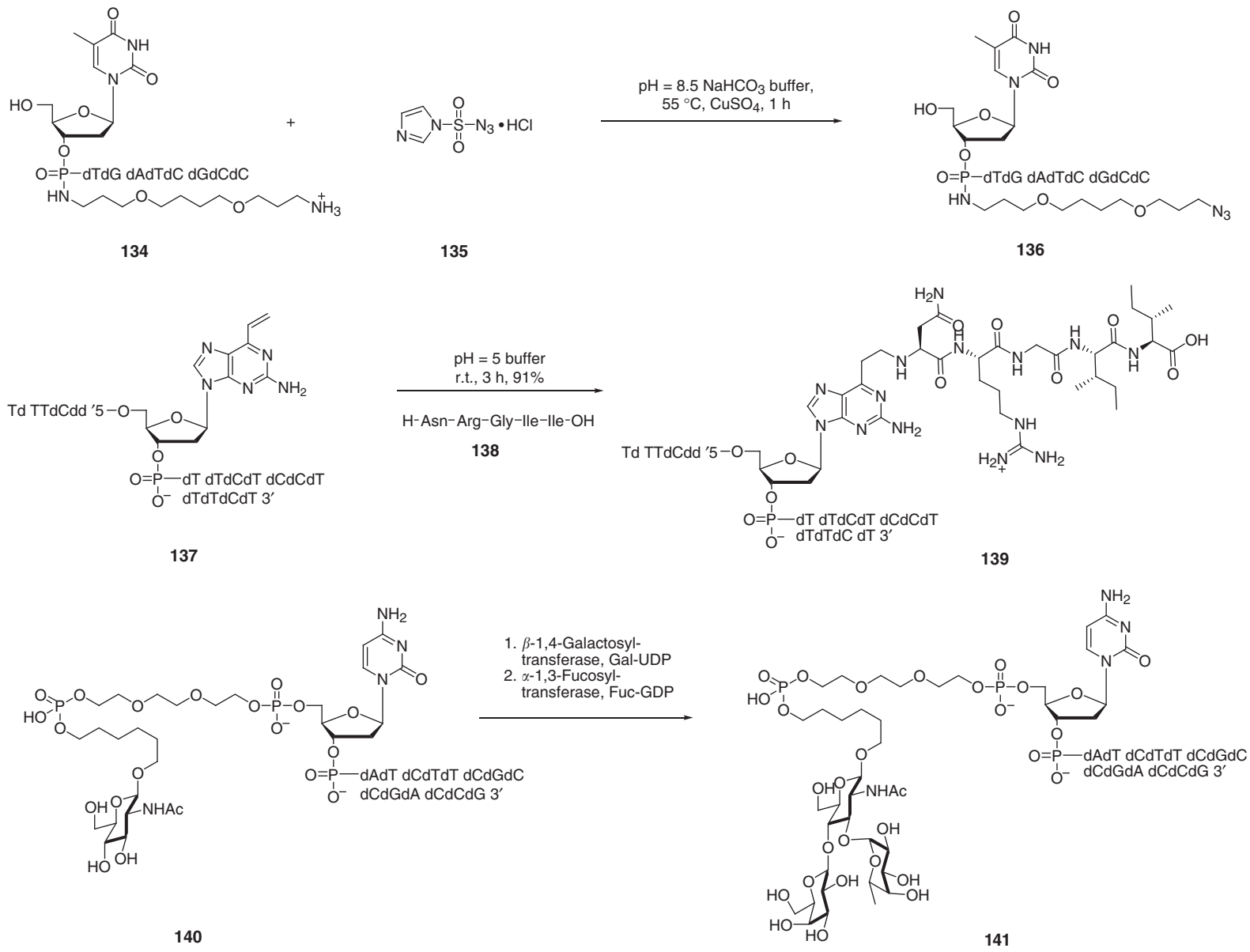
119 120 121 (41)

122 123 124 (42)

Scheme 25 ON conjugation through oxime linkage.



Scheme 26 ON conjugation by Pd catalysis and photochemistry.



Scheme 27 ON modification by other miscellaneous methods.

GalNAc–siRNA conjugate delivery approach and subcutaneous dose administration. We envision that ON postsynthetic conjugates will be broadly used as a new modality for therapeutics and diagnostics. This will undoubtedly be coupled to new developments in chemical strategies that facilitate the investigation of pharmacokinetics, metabolites, and subcellular trafficking.

References

1. Opalinska, J. B.; Gewirtz, A. M. *Nat. Rev. Drug Discov.* **2002**, *1*, 503–514.
2. Kim, D. H.; Rossi, J. J. *Nat. Rev. Genet.* **2007**, *8*, 173–184.
3. Dorsett, Y.; Tuschl, T. *Nat. Rev. Drug Discov.* **2004**, *3*, 318–329.
4. Manoharan, M. *Antisense Nucleic Acid Drug Dev.* **2002**, *12*, 103–128.
5. Chan, J. H. P.; Lim, S.; Wong, W. S. F. *Clin. Exp. Pharmacol. Physiol.* **2006**, *33*, 533–540.
6. Bell, N. M.; Micklefield, J. *ChemBioChem* **2009**, *10*, 2691–2703.
7. Eckstein, F. *Biochimie* **2002**, *84*, 841–848.
8. Harborth, J.; Elbashir, S. M.; Vandenburgh, K.; *et al. Antisense Nucleic Acid Drug Dev.* **2003**, *13*, 83–105.
9. Choung, S.; Kim, Y. J.; Kim, S.; Park, H.-O.; Choi, Y.-C. *Biochem. Biophys. Res. Commun.* **2006**, *342*, 919–927.
10. Geary, R. S.; Yu, R. Z.; Levin, A. A. *Curr. Opin. Invest. Drugs* **2001**, *2*, 562–573.
11. Lee, J. H.; Wong, N. Y.; Tan, L. H.; Wang, Z.; Lu, Y. *J. Am. Chem. Soc.* **2010**, *132*, 8906–8908.
12. Hall, A. H. S.; Wan, J.; Shaughnessy, E. E.; Ramsay, S. B.; Alexander, K. A. *Nucleic Acids Res.* **2004**, *32*, 5991–6000.
13. Hall, A. H. S.; Wan, J.; Spesock, A.; *et al. Nucleic Acids Res.* **2006**, *34*, 2773–2781.
14. Li, P.; Sergueeva, Z. A.; Dobrikov, M.; Shaw, B. R. *Chem. Rev.* **2007**, *107*, 4746–4796.
15. Froehler, B.; Ng, P.; Matteucci, M. *Nucleic Acids Res.* **1988**, *16*, 4831–4839.
16. Alvarez, K.; Vasseur, J.-J.; Beltran, T.; Imbach, J.-L. *J. Org. Chem.* **1999**, *64*, 6319–6328.
17. Spinelli, N.; Meyer, A.; Hayakawa, Y.; Imbach, J.-L.; Vasseur, J.-J. *Eur. J. Org. Chem.* **2002**, *2002*, 49–56.
18. Prakash, T. P.; Allerson, C. R.; Dande, P.; *et al. J. Med. Chem.* **2005**, *48*, 4247–4253.
19. Muhonen, P.; Tennila, T.; Azhayeva, E.; *et al. Chem. Biodivers.* **2007**, *4*, 858–873.
20. Kraynack, B. A.; Baker, B. F. *RNA* **2006**, *12*, 163–176.
21. Gruenweller, A.; Wyszko, E.; Bieber, B.; *et al. Nucleic Acids Res.* **2003**, *31*, 3185–3193.
22. Koshkin, A. A.; Singh, S. K.; Nielsen, P.; *et al. Tetrahedron* **1998**, *54*, 3607–3630.
23. Obika, S.; Nanbu, D.; Hari, Y.; *et al. Tetrahedron Lett.* **1997**, *38*, 8735–8738.
24. Vester, B.; Wengel, J. *Biochemistry* **2004**, *43*, 13233–13241.
25. Wahlestedt, C.; Salmi, P.; Good, L.; *et al. Proc. Natl. Acad. Sci. USA* **2000**, *97*, 5633–5638.
26. Allerson, C. R.; Sioufi, N.; Jarres, R.; *et al. J. Med. Chem.* **2005**, *48*, 901–904.
27. Zhang, N.; Tan, C.; Cai, P.; *et al. Bioorg. Med. Chem.* **2009**, *17*, 2441–2446.
28. Summerton, J. *Biochim. Biophys. Acta Gene Struct. Expression* **1999**, *1489*, 141–158.
29. Summerton, J.; Weller, D. *Antisense Nucleic Acid Drug Dev.* **1997**, *7*, 187–195.
30. Nielsen, P. E.; Egholm, M.; Berg, R. H.; Buchardt, O. *Science* **1991**, *254*, 1497–1500.
31. Hanvey, J. C.; Peffer, N. J.; Bisi, J. E.; *et al. Science* **1992**, *258*, 1481–1485.
32. Potenza, N.; Moggio, L.; Milano, G.; *et al. Int. J. Mol. Sci.* **2008**, *9*, 299–315.
33. Singh, Y.; Murat, P.; Defrancq, E. *Chem. Soc. Rev.* **2010**, *39*, 2054–2070.
34. Goodchild, J. *Bioconjug. Chem.* **1990**, *1*, 165–187.
35. Zatsepin, T. S.; Oretskaya, T. S. *Chem. Biodivers.* **2004**, *1*, 1401–1417.
36. Zatsepin, T. S.; Stetsenko, D. A.; Gait, M. J.; Oretskaya, T. S. *Bioconjug. Chem.* **2005**, *16*, 471–489.
37. Venkatesan, N.; Kim, B. H. *Chem. Rev.* **2006**, *106*, 3712–3761.
38. Lu, K.; Duan, Q.-P.; Ma, L.; Zhao, D.-X. *Bioconjug. Chem.* **2010**, *21*, 187–202.
39. Ustinov, A. V.; Stepanova, I. A.; Dubnyakova, V. V.; *et al. Russ. J. Bioorg. Chem.* **2010**, *36*, 401–445.
40. Raouane, M.; Desmaële, D.; Urbinati, G.; Massaad-Massade, L.; Couvreur, P. *Bioconjug. Chem.* **2012**, *23*, 1091–1104.
41. Raouane, M.; Desmaele, D.; Gilbert-Sirieix, M.; *et al. J. Med. Chem.* **2011**, *54*, 4067–4076.
42. Fraley, A. W.; Pons, B.; Dalkara, D.; *et al. J. Am. Chem. Soc.* **2006**, *128*, 10763–10771.
43. Mier, W.; Eritja, R.; Mohammed, A.; Haberkorn, U.; Eisenhut, M. *Bioconjug. Chem.* **2000**, *11*, 855–860.
44. Lapiene, V.; Kukolka, F.; Kiko, K.; Arndt, A.; Niemeyer, C. M. *Bioconjug. Chem.* **2010**, *21*, 921–927.
45. Raja, K.; McDonald, R.; Tuck, S.; *et al. Bioconjug. Chem.* **2007**, *18*, 285–288.
46. Aubert, Y.; Bourgerie, S.; Meunier, L.; *et al. Nucleic Acids Res.* **2000**, *28*, 818–825.
47. Muratovska, A.; Lightowlers, R. N.; Taylor, R. W.; *et al. Nucleic Acids Res.* **2001**, *29*, 1852–1863.
48. Viel, T.; Kuhnast, B.; Hinnen, F.; *et al. J. Labelled Comp. Radiopharm.* **2007**, *50*, 1159–1168.
49. Viel, T.; Boisgard, R.; Kuhnast, B.; *et al. Oligonucleotides* **2008**, *18*, 201–212.
50. Guzaev, A. P.; Manoharan, M. *Org. Lett.* **2001**, *3*, 3071–3074.
51. Chaloin, L.; Vidal, P.; Lory, P.; *et al. Biochem. Biophys. Res. Commun.* **1998**, *243*, 601–608.
52. Park, J. W.; Bang, E.-K.; Jeon, E. M.; Kim, B. H. *Org. Biomol. Chem.* **2012**, *10*, 96–102.
53. Mok, H.; Park, J. W.; Park, T. G. *Bioconjug. Chem.* **2007**, *18*, 1483–1489.
54. Aaronson, J. G.; Klein, L. J.; Momose, A. A.; *et al. Bioconjug. Chem.* **2011**, *22*, 1723–1728.
55. Michael, J.; Schoenzart, L.; Israel, I.; *et al. Bioconjug. Chem.* **2009**, *20*, 710–718.
56. Wang, T.-P.; Chiou, Y.-J.; Chen, Y.; *et al. Bioconjug. Chem.* **2010**, *21*, 1642–1655.
57. Rockey, W. M.; Huang, L.; Kloepping, K. C.; *et al. Bioorg. Med. Chem.* **2011**, *19*, 4080–4090.
58. Dawson, P. E.; Muir, T. W.; Clarklewis, I.; Kent, S. B. H. *Science* **1994**, *266*, 776–779.
59. Stetsenko, D. A.; Gait, M. J. *J. Org. Chem.* **2000**, *65*, 4900–4908.
60. Muir, T. W.; Sondhi, D.; Cole, P. A. *Proc. Natl. Acad. Sci. USA* **1998**, *95*, 6705–6710.
61. Takeda, S.; Tsukiji, S.; Nagamune, T. *Bioorg. Med. Chem. Lett.* **2004**, *14*, 2407–2410.
62. Saxon, E.; Armstrong, J. I.; Bertozzi, C. R. *Org. Lett.* **2000**, *2*, 2141–2143.
63. Saxon, E.; Bertozzi, C. R. *Science* **2000**, *287*, 2007–2010.
64. Wang, C. C. Y.; Seo, T. S.; Li, Z. M.; Ruparel, H.; Ju, J. Y. *Bioconjug. Chem.* **2003**, *14*, 697–701.

65. Tominaga, J.; Kemori, Y.; Tanaka, Y.; *et al. Chem. Commun.* **2007**, *43*, 401–403.
66. Rostovtsev, V. V.; Green, L. G.; Fokin, V. V.; Sharpless, K. B. *Angew. Chem. Int. Ed.* **2002**, *41*, 2596–2599.
67. Tornoe, C. W.; Christensen, C.; Meldal, M. *J. Org. Chem.* **2002**, *67*, 3057–3064.
68. Agard, N. J.; Prescher, J. A.; Bertozzi, C. R. *J. Am. Chem. Soc.* **2004**, *126*, 15046–15047.
69. Jayaprakash, K. N.; Peng, C. G.; Butler, D.; *et al. Org. Lett.* **2010**, *12*, 5410–5413.
70. Meyer, A.; Pourceau, G.; Vasseur, J.-J.; Morvan, F. *J. Org. Chem.* **2010**, *75*, 6689–6692.
71. Sirivolu, V. R.; Chittepu, P.; Seela, F. *ChemBioChem* **2008**, *9*, 2305–2316.
72. Tanabe, K.; Ando, Y.; Nishimoto, S.-I. *Tetrahedron Lett.* **2011**, *52*, 7135–7137.
73. Chan, T. R.; Hilgraf, R.; Sharpless, K. B.; Fokin, V. V. *Org. Lett.* **2004**, *6*, 2853–2855.
74. Fauster, K.; Hartl, M.; Santner, T.; *et al. ACS Chem. Biol.* **2012**, *7*, 581–589.
75. Brown, S. D.; Graham, D. *Tetrahedron Lett.* **2010**, *51*, 5032–5034.
76. Grajkowski, A.; Cieslak, J.; Kauffman, J. S.; *et al. Bioconjug. Chem.* **2008**, *19*, 1696–1706.
77. van Delft, P.; van Schie, E.; Meeuwenoord, N. J.; *et al. Synthesis* **2011**, *43*, 2724–2732.
78. Diels, O.; Alder, K. *Justus Liebigs Ann. Chem.* **1928**, *460*, 98–122.
79. Takao, K.; Munakata, R.; Tadano, K. *Chem. Rev.* **2005**, *105*, 4779–4807.
80. Rideout, D. C.; Breslow, R. *J. Am. Chem. Soc.* **1980**, *102*, 7816–7817.
81. Breslow, R.; Maitra, U.; Rideout, D. *Tetrahedron Lett.* **1983**, *24*, 1901–1904.
82. Sanchez, A.; Pedroso, E.; Grandas, A. *Bioconjug. Chem.* **2012**, *23*, 300–307.
83. Graham, D.; Grondin, A.; McHugh, C.; Fruk, L.; Smith, W. E. *Tetrahedron Lett.* **2002**, *43*, 4785–4788.
84. Tona, R.; Haner, R. *Bioconjug. Chem.* **2005**, *16*, 837–842.
85. Schoch, J.; Wiessler, M.; Jaeschke, A. *J. Am. Chem. Soc.* **2010**, *132*, 8846–8847.
86. Villien, M.; Defrancq, E.; Dumy, P. *Nucleosides Nucleotides Nucleic Acids* **2004**, *23*, 1657–1666.
87. Ghosh, S.; Defrancq, E.; Lhomme, J. H.; Dumy, P.; Bhattacharya, S. *Bioconjug. Chem.* **2004**, *15*, 520–529.
88. Zatsepin, T. S.; Stetsenko, D. A.; Arzumanov, A. A.; *et al. Bioconjug. Chem.* **2002**, *13*, 822–830.
89. Kalia, J.; Raines, R. T. *Angew. Chem. Int. Ed.* **2008**, *47*, 7523–7526.
90. Erdem, S. S.; Nesterova, I. V.; Soper, S. A.; Hammer, R. P. *J. Org. Chem.* **2009**, *74*, 9280–9286.
91. Zatsepin, T. S.; Gait, M. J.; Oretskaya, T. S.; Stetsenko, D. A. *Tetrahedron Lett.* **2006**, *47*, 5515–5518.
92. Kozlov, I. A.; Melnyk, P. C.; Stromsborg, K. E.; *et al. Biopolymers* **2004**, *73*, 621–630.
93. Wang, L.; Xie, J.; Schultz, P. G. *Annu. Rev. Biophys. Biomol. Struct.* **2006**, *35*, 225–249.
94. Forget, D.; Renaudet, O.; Defrancq, E.; Dumy, P. *Tetrahedron Lett.* **2001**, *42*, 7829–7832.
95. Forget, D.; Renaudet, O.; Boturyn, D.; Defrancq, E.; Dumy, P. *Tetrahedron Lett.* **2001**, *42*, 9171–9174.
96. Omumi, A.; Beach, D. G.; Baker, M.; Gabryelski, W.; Manderville, R. A. *J. Am. Chem. Soc.* **2011**, *133*, 42–50.
97. Deroo, S.; Le Gac, S.; Ghosh, S.; *et al. Eur. J. Inorg. Chem.* **2009**, *2009*, 524–532.
98. Lange, C. W.; VanBrocklin, H. F.; Taylor, S. E. *J. Labelled Comp. Radiopharm.* **2002**, *45*, 257–268.
99. Lartia, R.; Murat, P.; Dumy, P.; Defrancq, E. *Org. Lett.* **2011**, *13*, 5672–5675.
100. Ali, M.; Nagatsugi, F.; Sasaki, S.; Nakahara, R.; Maeda, M. *Nucleosides Nucleotides Nucleic Acids* **2006**, *25*, 159–169.
101. Wang, Y. L.; Sheppard, T. L. *Bioconjug. Chem.* **2003**, *14*, 1314–1322.